Provenance and Diagenesis of the Lower Cetaceous to Middle Jurassic Sandstones in the Slope Well Newburn H-23, Scotian Slope

By
Christopher R. Sangster

A Thesis Submitted to
Saint Mary's University, Halifax, Nova Scotia
in Partial Fulfillment of the Requirements for
a Bachelor of Science, Honours Geology.

April, 2016, Halifax, Nova Scotia

Approved:	Dr. Georgia Pe-Piper Supervisor
Approved:	Dr. Basilios Tsikouras External Reader
Date:	April 14, 2016

Provenance and Diagenesis of the Lower Cretaceous to Middle Jurassic Sandstones in the Slope Well Newburn H-23, Scotian Slope

Christopher Sangster

Abstract

Newburn H-23 is one of seven deep wells drilled on the Scotian Slope. These wells are new and thus in the early stages of research. As such it is important to determine the history of the detrital and diagenetic minerals found in this well and to draw comparisons between them and their shallower age equivalents on the shelf. Sandy intervals from the Early Cretaceous have been analyzed dominantly using various methods to observe chemical and textural relationships between diagenetic and detrital minerals.

The detrital mineralogy of these sandstone intervals is similar to other wells in the Sable Sub-basin, suggesting that they are sourced by the Sable River with minor input from Meguma Group metasediments and an increased supply of sodic volcanic clasts, probably from Scatarie Bank. The diagenetic history of this well, however, contains several mineralogical occurrences which are have not yet been identified elsewhere in the Scotian basin, including probable diagenetic zircon and fluorine rich ferroan-calcite. These minerals, along with diagenetic titania minerals suggest: **a)** low pH, a high organic content, and a high fluoride content in circulating basinal fluids during mesodiagenesis; and **b)** a supply of zirconium, increased salinity in basinal fluids, and higher than expected temperatures during mesodiagenesis. These findings are consistent with evidence from other wells for high salinities and temperatures late in the history of the Scotian Basin.

Porosity values in these sandstones are similar to those of the Alma and Glenelg fields in the Scotian basin, contain gas shows, and are above the cut off permeability for gas reservoirs. These sandstones are therefore potentially economic reservoirs in the Scotian basin. However, they may not be of high quality since the sandy intervals in which potential sources are located in are thin with late diagenetic minerals filling some of the secondary porosity.

April 14th 2016

Acknowledgements

This project has been an incredible opportunity for me to learn and grow both as a scientist and a person. Over the course of this project I have had help from, and been given advice from many people including friends, family, and professors, some of whom played a larger role in this project than others but all of whom helped me during the course of this project. So thank you to everyone who has helped me in any way over the course of this thesis. Like I mentioned there are some people who have been instrumental to this project and I would like to thank them below.

I would like to thank Georgia for not only sharing with me her vast knowledge and experience, but also for her continuing encouragement, feedback, patience (which I'm sure I tested at times), and the countless hours spent guiding me throughout this project, without which none of this would be possible. She has helped me set the framework for future endeavors in science and has been a major source of inspiration for me throughout this project on a personal and professional level. Thank you for allowing me this incredible opportunity to learn from you and for everything else you have done for me. I look forward to continuing to work with you over the coming years.

I would like to thank Yuanyuan Zhang, who taught me almost every program I used during the course of this project and showed me (at times by force) how to present my ideas and data clearly and professionally, all while keeping a smile on my face. She provided me with the encouragement and support that I needed to complete this project and taught me so much about every aspect of research.

I would like to thank Dr. Basilios Tsikouras for the feedback he provided as external reader. His comments were detailed, constructive, and allowed me the opportunity to further improve on the project.

I would like to thank the Canada Nova-Scotia Offshore Petroleum Board (CNSOPB) for providing all the samples used through this project.

I would particularly like to thank Andrew MacRae for his help in securing the sidewall core samples, without which this project would not have been possible. He along with the rest of the faculty here at Saint Mary's has been extremely helpful during this thesis and I would like to thank them for all they have done. Thank you Xiang Yang, for guiding me through the process of taking SEM analyses and taking the time to answer my questions and help with any issues that I encountered along the way. I would like to thank Randy Corney, for his help with point counting and for always taking the time to help me with my many tech. related questions and problems. I would like to thank Mitch Kerr, for his help with Raman Laser analyses which we performed on several samples.

I would also like to thank David Piper, for his help collecting the cuttings samples from the CNSOPB as well as the comments and corrections over the course of the thesis, and Dan-Cezar Dutuc and Isabel Chavez Gutierrez for their work in preparing the cuttings samples used in this project.

Funding for this project was provided by Encana, (administered by the Offshore Energy Research Association (OERA)), and the Natural Sciences and Engineering Research Council of Canada (NSERC).

Of course I would like to thank my family, particularly my mother and father, for their absolute and unwavering support throughout this project, and for their patience while they waited for me to finish it. You showed interest in what I was doing (even though I wasn't always forthcoming with details), put up with me through all the late nights and grumpy mornings, and helped me maintain focus on what was important. I cannot thank you enough for your support and understanding.

Thank you again to everyone else who has listened to me ramble about my samples, helped me with questions and problems, and supported me throughout this journey. I look forward to continuing my research at Saint Mary's University over the coming years.

Table of Contents

List of Tables

List of Figures

List of Appendices

Chapter 1: Introduction

The Scotian Basin (Fig 1.1) is a passive continental margin basin formed by the rifting of the North Atlantic Ocean in the Late Triassic (McIver, 1972; Given, 1977; Wade and Maclean, 1990). The sandstones of this basin (particularly those of the Missisauga Formation (Fig. 1.2) are known to be potential oil and gas reservoirs. In the period between 2002 and 2004 seven deepwater wells were drilled off of the Scotian slope, including Annapolis B-24 and G-24, Newburn H-23, Torbrook C-15, Balvenie B-79, Weymouth A-45, and Crimson F-81, following up on previous work done between 1982 and 1987 (Fig 1.1). These new wells were prompted by the success in other passive margins of the Atlantic Ocean such as West Africa, Brazil and the Gulf of Mexico.

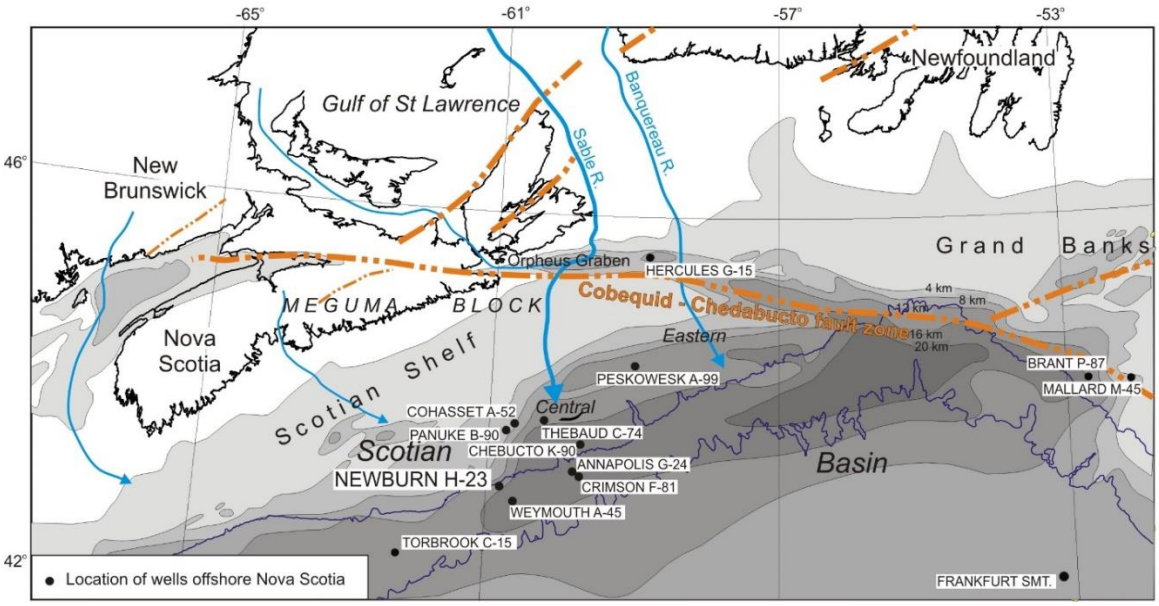

Fig. 1.1: Isopach map showing distribution of wells in the offshore of Nova Scotia as well as paleoriver paths. Map modified from Wade and MacLean 1990.

These deepwells are all located within the same basin and are thought to have been sourced by the Sable paleo-river (Fig. 1.1). The Newburn H-23 well is the only one of these deepwells with available sidewall cores which are representative of the

stratigraphic levels of interest, and so it has been selected as the first of these wells to be studied in detail.

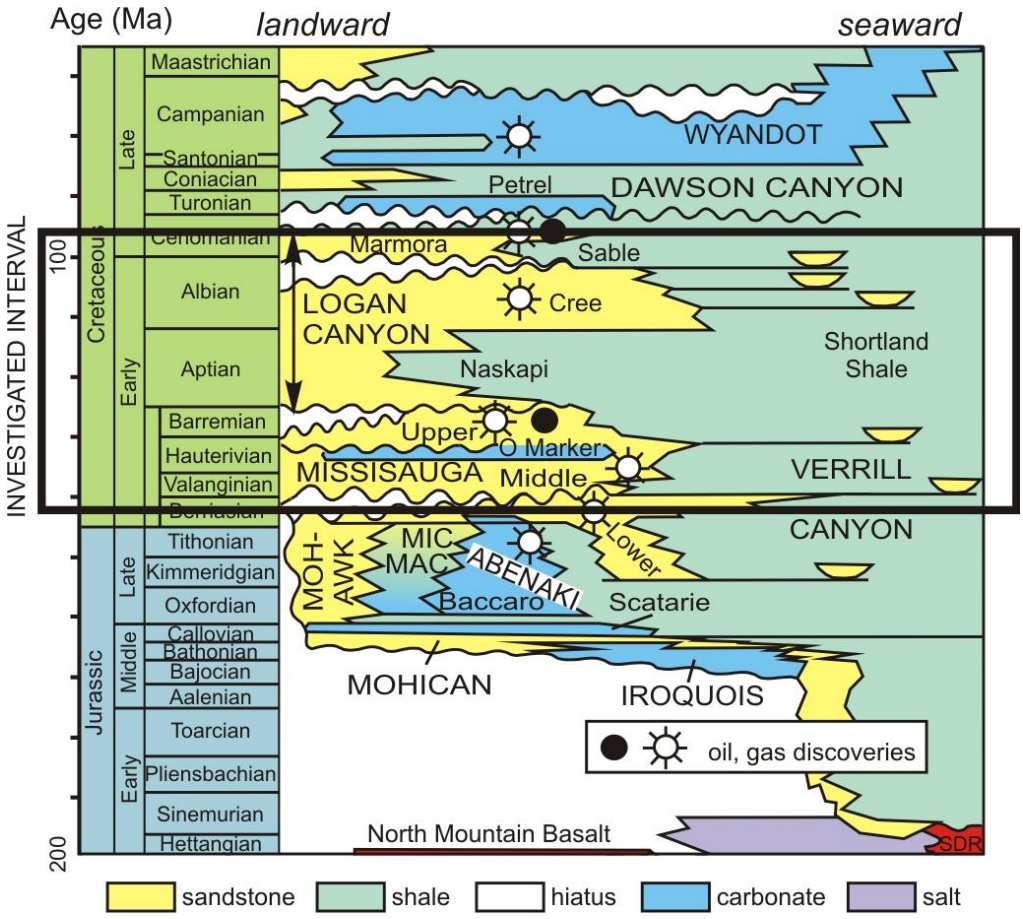

Fig. 1.2: Stratigraphic column of the Scotian basin. Modified from Weston et al., (2012).

1.1 Objectives

The project objective is to determine the provenance and diagenesis of the lower Cretaceous sandstone intervals in the Newburn H-23 well, observe how they change with increasing depth, and to draw comparisons between this "deep well" off the slope and its shallower shelf age equivalent sandstones.

1.2 Regional Geological Setting

The early stages of rifting in the Scotian basin produced clastic successions and salt deposits. As rifting continued into the Jurassic the deposition became dominated by carbonate rocks. This was followed by fluvial, deltaic, and shelf deposition of the sandstones and shales of the Upper Jurassic and Lower Cretaceous Missisauga and Logan Canyon Formations (Fig 1.2) (Pe-Piper et al., 2014). Later deposits in the Upper Cretaceous and Cenozoic are shales and to a lesser extent chalks (Fig 1.2).

Underlying the Scotian Basin shelf and slope (Fig 1.1) are several interconnected depocenters (Wade & MacLean, 1990). One of these depocenters is the Sable Sub-basin. The center of the Sable Sub-basin is underlain by syn-rift salt and the Sub-basin itself contains many growth faults and salt tectonic features (Cummings, Arnott 2005). In the Jurassic and early Cretaceous the Sable Sub-basin underwent rapid subsidence resulting in accumulation of more than 10 km of Mesozoic and Cenozoic sediments (Wade & MacLean, 1990; Wade, MacLean, & Williams, 1995). In the same Sub-basin the Missisauga Formation fluvial sandstones are overlain by the mudstones of the Logan Canyon Formation (Cummings, Arnott 2005).

It has been suggested that the detritus for the Late Jurassic and Early Cretaceous sedimentary rocks in the Scotian basin was supplied by the Banquereau river in the eastern portion of the basin and the Sable river in the central portion of the basin (Pe-Piper et al., 2014). It is believed that these rivers supplied sediments sourced from the Labrador rift, crystalline bedrock, and late Paleozoic sedimentary basins from the Appalachian orogen (Zhang et al., 2014). Middle Jurassic sediments were sourced from the Meguma terrain in southern Nova Scotia and Carboniferous sandstones (Li et al., 2012).

1.3 Well history

The Newburn H-23 well was drilled by the Chevron Corporation between May 22, 2002 and August 21, 2002 by the Deepwater Millennial drillship. It was spudded in 977 m of water and drilled to a depth of 6070 m. The drilling stopped 330 m shallower than originally intended as a result of formation tops being encountered 200 m earlier than expected.

The Newburn H-23 well was drilled into turbiditic sandstones generated in the Early Cretaceous by adjacent salt withdrawal (Kidston et al., 2007). These sandstones are the lowstand equivalents of the top Missisauga formation and are part of a large detachment fault at the toe of the slope.

A series of tests and analysis have been run on the samples extracted from this well including permeability and porosity measurements and X-ray diffraction (XRD) during the initial drilling and are included in the post drill report provided by the Chevron Corporation.

In this report samples from the depths of 4305.5 m to 4325.7 m are Early Albian in age and correspond to the Logan Canyon Formation, these sandstones have been classified as Sand 1. This interval appears to be a 20 m thick fining upwards channel sand with quartz and lithic fragment conglomerates at the base. It displays no gas and has an average porosity of 18% (Kidston et al., 2007).

Samples from a depth of 4348.5 m to 4357.5 m are also Early Albian in age and belong to the lateral equivalent of the Logan Canyon Formation. These sediments have been classified as Sand 2, and are very fine to fine-grained shaley sandstones. This sand interval has a significant gas show and an average porosity of 13.5% (Kidston et al., 2007).

Samples from depths of 5402 m to 5408 m are Mid Hauterivian in age and belong to the Upper Missisauga Formation. These are classified as Sand 3, and are composed of very fine to fine grained sandstones with a substantial gas show. These sands are suggested to be channel sand deposits with 19 % porosity (Kidston et al., 2007).

Samples from depths of 5957.5 m to 5963.5 m are Middle Hauterivian in age and correspond to the base of the Upper Missisauga Formation. These are classified as Sand 4, a 3 m thick succession of very fine to fine grained sandstone with a weak gas show and an average porosity of 14% (Kidston et al., 2007).

Several of the collected samples are not included in the reported sand units: these are samples from 5965 m to 5975 m in depth. They belong to the lateral equivalent of the Missisauga Formation, as they are Middle Hauterivian in age.

Chapter 2: Methods

2.1 Sampling

Samples from the wells drilled in the Scotian Basin are stored at the Geoscience Research Center of the Canada Nova Scotia Offshore Petroleum Board (CNSOPB) in Dartmouth, Nova Scotia. No conventional core was taken in this well during drilling. The only available samples are cuttings and sidewall cores. In total 14 cuttings samples and 21 sidewall core samples were taken.

Cuttings samples within the targeted stratigraphic levels were researched in the well reports and inspected to find intervals with maximum sand proportions. The weight of each of the cuttings samples provided by the CNSOPB was not permitted to be more than 30 g and the size of each of the sidewall core samples was only enough to make one

polished thin section The chosen samples were selected based on stratigraphic level to provide representative information about the well. The selected samples are summarized in Table 2.1.

Table 2.1: Sample summary indicating sample type and stratigraphic level of the studied samples.

Well	Depth (m)	Sample Type	Stratigraphic Level
Newburn H-23	4300	cutting, grain mount	Cree
Newburn H-23	4313.5	sidewall core, thin section	Cree
Newburn H-23	4315	cutting, grain mount	Cree
Newburn H-23	4318.5	sidewall core, thin section	Cree
Newburn H-23	4353.5	sidewall core, thin section	Cree
Newburn H-23	4913.8	sidewall core, thin section	Upper Missisauga
Newburn H-23	5213.5	sidewall core, thin section	Middle Missisauga
Newburn H-23	5403.6	sidewall core, thin section	Middle Missisauga
Newburn H-23	5406.5	sidewall core, thin section	Middle Missisauga
Newburn H-23	5407.0	sidewall core, thin section	Middle Missisauga
Newburn H-23	5408.5	sidewall core, thin section	Middle Missisauga
Newburn H-23	5950	cutting, grain mount	Middle Missisauga
Newburn H-23	5957.8	sidewall core, thin section	Middle Missisauga
Newburn H-23	5961.7	sidewall core, thin section	Middle Missisauga
Newburn H-23	5962	sidewall core, thin section	Middle Missisauga
Newburn H-23	5965	cutting, grain mount	Middle Missisauga
Newburn H-23	5975	cutting, grain mount	Middle Missisauga

2.2 Sample Preparation

2.2.1 Cuttings Samples

The cleaning and processing of the cuttings samples was performed at the Geology Lab in the Department of Geology at Saint Mary's University. The samples had been stored at the CNOSPB for over ten years and as a result of this storage some of the samples had compacted into aggregates. In addition the samples had an oily smell to them suggesting either the presence of an oil show or the use of oil based drilling muds. To

break down the aggregates and clean the samples they were immersed in a solution of natural water and mild dishwasher liquid detergent in individual graduated glass beakers. The samples were then allowed to soak in this solution for three days, allowing for the mud which was the main component of the cement to be dissolved freeing the sand grains. After the sediments were removed from the solution they were washed in de-ionized water and sieved through a 53 μm sieve to remove the mud component.

To prepare the samples for heavy mineral separation the samples need to be completely dry. Methanol was added to the sediments in order to accomplish this quickly. After the application of methanol the samples were uncovered and exposed to fresh air in a fume-hood for two to three days in order to dry them.

The heavy mineral separation was performed at the Sediment Laboratory in the Bedford Institute of Oceanography (BIO) in Dartmouth. The first step in this process was passing the samples through a 250 μm sieve in order to remove any remaining aggregates or large lithic clasts and thus concentrate individual mineral grains. The remaining sediment from each sample was then immersed with sodium polytungstate in plastic tubes that were inserted into a Fisherbrand 50 ml concentric base centrifuge. Sodium polytungstate in aqueous solution is a non-toxic heavy liquid with a density of 2.9 g/cm^3, which can be used for heavy mineral separation. These tubes were then placed in a Thermo Fisher SorvalXR Floor model centrifuge with 750 ml swinging buckets with inserts for 50 ml conical base centrifuge tubes and rotated for 30 minutes.

After the minerals with a density > 2.9 g/cm^3 were separated from the less dense minerals, the bottom portion of the tube, where the heavy minerals had sank to, was frozen using liquid nitrogen so that the lighter minerals could be removed without remixing them with the heavy minerals. The heavy minerals were then washed in de-

ionized water to remove the sodium polytungstate and then placed in an oven for three days at a temperature of 60ºC to remove the water from the samples.

Some of the samples had a very small proportion of heavy minerals in them and so they returned very little sediment from the heavy mineral separation. In order to have enough material to analyze some samples were combined (Table 2.2).

The heavy mineral separates were sent to Vancouver Petrographics to produce the 30 µm thickness polished thin sections. These samples were inspected under a petrographic microscope to select grains of interest for analysis under the Scanning Electron Microscope (SEM). To prepare the samples for analysis under the SEM they were carbon coated using a Leica EM CED030 desktop carbon coater.

Table 2.2: Summary of combined cuttings samples.

Well	Depth (m)	Mixture (m)	Weight (g)
Newburn H-23	4300	4300	0.39
		4305	
		4310	
Newburn H-23	4315	4315	0.71
		4320	
		4325	
		4345	
		4350	
Newburn H-23	5950	-	1.55
Newburn H-23	5955	-	1.34
Newburn H-23	5960	-	1.82
Newburn H-23	5965	-	1.5
Newburn H-23	5970	-	1.71
Newburn H-23	5975	-	1.56

2.3 Analytical Techniques

The samples were analyzed using a variety of techniques: firstly using a Scanning Electron Microscope (SEM) for chemical analyses and the textural relationships of minerals in the samples; secondly using an Electron Microprobe (EMP) for more precise

chemical analyses; and thirdly using a Laser Raman Microspectrometer (LRM) to look for specific mineral occurrences. The various analytical techniques used to analyze each sample is summarized in Table 2.3.

Table 2.3: Summary table detailing analytical techniques performed on the studied samples from Newburn H-23.

Well	Depth (m)	Sample Type	Microscope	SEM	EMP	LMS	Point Counting
Newburn H-23	4300	cuttings	×	×			
Newburn H-23	4313.5	sidewall core	×	×			×[1,3]
Newburn H-23	4315	cuttings	×	×			
Newburn H-23	4317.5	sidewall core					
Newburn H-23	4318.5	sidewall core	×	×			×[1,2,3]
Newburn H-23	4319.8	sidewall core					
Newburn H-23	4323.0A	sidewall core					
Newburn H-23	4323.0B	sidewall core					
Newburn H-23	4349.7	sidewall core					
Newburn H-23	4353.5	sidewall core	×	×	×		×[1,3]
Newburn H-23	4354.5	sidewall core					
Newburn H-23	4913.8	sidewall core	×	×			×[1]
Newburn H-23	5213.5	sidewall core	×	×	×		×[1,3]
Newburn H-23	5403.6	sidewall core	×	×	×		×[1,3]
Newburn H-23	5406.5	sidewall core	×	×		×	×[1,2]
Newburn H-23	5407.0	sidewall core	×	×	×		×[1,3]
Newburn H-23	5408.5	sidewall core	×	×	×		×[1,2,3]
Newburn H-23	5950	cuttings	×	×			
Newburn H-23	5955	cuttings	×				
Newburn H-23	5957.8	sidewall core	×	×			
Newburn H-23	5960	cuttings	×				
Newburn H-23	5960.5	sidewall core					
Newburn H-23	5961.2	sidewall core					
Newburn H-23	5961.7	sidewall core	×	×			×[1,2,3]
Newburn H-23	5962.0	sidewall core	×	×			×[1,3]
Newburn H-23	5962.8	sidewall core					
Newburn H-23	5965	cuttings	×	×			
Newburn H-23	5970	cuttings	×				
Newburn H-23	5975	cuttings	×	×			

[1] point counted using the method outlined in 2.6.1
[2] point counted using the method outlined in 2.6.2
[3] point counted using the method outlined in 2.6.3

2.3.1 Scanning Electron Microscope (SEM)

SEM analysis was completed in the Regional Analytical Centre at Saint Mary's University using a LEO 1450 VP SEM acquiring the back-scattered electron (BSE) images and energy dispersive spectroscopy (EDS) chemical analyses of minerals. This SEM has a maximum resolution of up to 3.5 nm at 30 kV, it is equipped with an INCA X-max 80mm^2 silicon-drift detector (SDD) EDS system that has a detection limit > 0.1%. A tungsten filament is also used to produce a BSE of the grains on the polished thin section. A pure cobalt standard was used to calibrate the beam for use in analysis. The average beam diameter is approximately 10 μm and has an interactive volume which can extends into the sample to varying depths depending on the composition of the material analyzed, this leads to analyses of mineral mixtures in grain smaller than the beam.

Elemental mapping of quantitative compositional data is processed by the QuantMap package in Oxford Instrument's INCA program. The colour bar at the bottom of each elemental mapping image is scaled to EDS analysis (volatile free). X-ray mapping of oxides instead of element is presented in this study, because the oxide concentrations are more useful and informative when identifying mineral phases compared with element concentrations.

2.3.2 Electron Microprobe (EMP)

Samples found to contain calcite with fluorine where taken for analysis at the Regional Electron Microprobe Center at Dalhousie University, in Halifax Nova Scotia. Analysis was performed with a JEOL-8200 electron microprobe (EMP) which uses a Noran 133 eV energy dispersive spectrometer and five wavelength spectrometers. The EMP uses wavelength dispersive spectroscopy (WDS) and gives more accurate analyses.

Since the mineral to be analyzed were thought to be a carbonate mineral rich in fluorine, mostly higher than 10 wt.%, fluorite (~49 wt.% F) was chosen to be the standard of fluorine, rather than fluorapatite (~4.5 wt.%). Meanwhile, fluorapatite was also analyzed as a control. Diffracting crystal LDE1 is more sensitive than other crystals in the microprobe spectrometers and is thus chosen for F analysis. The measured elements and different standards for calibration of each element are listed in Table 2.4. The element distribution for each channel (spectrometer) with different diffracting crystal is also listed in Table 2.5.

Table 2.4: Standards used during EMP analyses of F-rich calcite.

Element		Standard
Major elements	Ca	Calcite
	F	Fluorite; Fluorapatite as a control
Minor and Trace elements (mostly <5%)	Fe	Garnet
	Mg	Dolomite
	Mn	Pyrolusite
	S	Pyrrhotite
	Si	Sanidine
	Al	
	K	
	Na	jadeite

Table 2.5: Element distribution for each channel (spectrometer) with different diffracting crystals for the analyses of Table 2.3.

CH-1 LDE1	CH-2 PETJ	CH-3 TAP	CH-4 TAPH	CH-5 LIFH
F	S			
	Ca	Na	Si	Fe
	K	Mg	Al	Mn

2.3.3 Laser Raman Microspectrometry (LRM)

Raman laser spectroscopy analysis was completed in the Regional Atlantic Centre at Saint Mary's University using a Horiba Jobin-Yvon LabRam HR confocal instrument. The LRM uses a 100mW 532 nm Nd-YAG diode laser from Toptica Phonotics and a Synapse charge-coupled device from Horiba Jobin-Yvon. The LRM also uses a 100x Olympus MPlanN objective for images and analysis.

The detector is cooled to -50 ^{o}C, and a minimal working distance between the objective and sample is used to reduce interference. A 25 µm confocal hole diameter, and 600 grooves/mm grating was used for all analyses, yielding a spectral resolution of approximately,2 cm. Spectra were collected using an accumulation of three, ten second acquisitions with a laser spot size of approximately 1 µm at 50% laser power. The spectra were collected in two spectral windows 200 – 4000 cm^{-1} and 200 – 2600 cm^{-1}.

The analyzed polished thin section had all carbon coating removed using methanol to increase the intensity of the peaks of the minerals and insure more accurate results.

2.4 Point counting

A transmitted and reflected light petrographic microscope was used to look at all 21 polished thin sections from the sidewall cores. After brief examination, 12 representative polished thin sections were selected for further detailed study. A Nikon Eclipse E 400 polarizing microscope equipped with a Pixlink digital camera and an automatic stepping stage controlled by software from Conwy Valley Systems was used to point count these twelve samples. The point counting analyses were used in the Folk and Dickinson diagrams for sandstone classification and probable provenance type. Four selected samples received additional point counting for heavy minerals to help determine provenance (samples 4318.5 m, 5406 m, 5408.5 m, and 5961.7 m).

2.4.1 Standard point counting

To determine the modal composition of all twelve samples the point counted grains are assigned to the following groups: Quartz (monocrystalline quartz and polycrystalline quartz), lithic clasts (igneous lithic clasts, metamorphic lithic clasts, and sedimentary lithic clasts), total lithic clasts (polycrystalline quartz, igneous lithic clasts, metamorphic lithic clasts, and sedimentary lithic clasts), feldspars (plagioclase and K-feldspars), stable heavy minerals (detrital rutile, apatite, tourmaline, fluorite, zircon, and spinel), unstable detrital minerals (chlorite, muscovite, epidote, and biotite) (Table 3.1). For each pts 600 grains were counted. Four of the samples received a second round of point counting in order to establish the reproducibility of the point counting results (Table 3.2).

2.4.2 Detailed mineral point counting by petrographic microscope

Four samples (4318.5 m, 5406 m, 5408.5 m, and 5961.7 m) were counted again in order to collect better data of the heavy minerals in these samples (Table 4.4). They were selected on the basis of stratigraphic level, abundance and variability of non-quartz detrital minerals in both BSE images and from the initial point counting. Only monocrystalline quartz, alkali feldspars, plagioclase, muscovite, detrital titania, detrital zircon, spinel, and tourmaline were counted. 600 grains were counted to ensure representative sampling. In subsequent drawn diagrams the quartz was removed to better show how the remainder of the detrital minerals changed with depth.

2.4.3 Heavy mineral point counting based on BSE images

Point counting was also performed using BSE images (Table 4.2). All of the analyzed detrital heavy mineral grains from all sites in the samples were counted and plotted later on pie diagrams.

2.5 Chemical fingerprinting

The chemical analyses for several detrital minerals of all the samples were used for provenance determination. The selected minerals include tourmaline, muscovite, biotite, and spinels. These are common detrital heavy minerals in these samples and have been plotted to characterize the sediment source. The chemical analyses were screened to insure only pure mineral analyses were used. Such analyses were then recalculated and plotted using the Minpet software.

2.6 Stratigraphic column

In order to better understand how the individual samples from this well relate to one another and change with increasing depth they have been plotted on a stratigraphic column (Fig. 2.1). LogPlot software was used to generate this stratigraphic column (Fig. 2.1) and includes data on the depth, lithology, age, formation, gamma ray logging, and detrital mineral point counting of all the samples collected from this well.

The lithology is based on the detailed cuttings log in the post drill report from The Chevron Corporation and supplemented in areas where no cuttings reports are available using data from the post drill analysis (Kidston et al., 2007). The formations and age columns were generated using data from the Play Fairway Analysis (PFA) report on formation tops and biostratigraphy, as well as the predrill interpretation. The gamma ray log is an Environmentally Corrected Gamma Ray Log (ECGR) conducted during well operation. Pie diagrams generated from detrital mineral point counting (Table 4.4) were also added to the stratigraphic column. All polished thin sections produced from the sidewall cores as well as all of the grain mounts from the cuttings samples have been plotted on the stratigraphic column (Fig. 2.1) to show the distribution of sampling in this well.

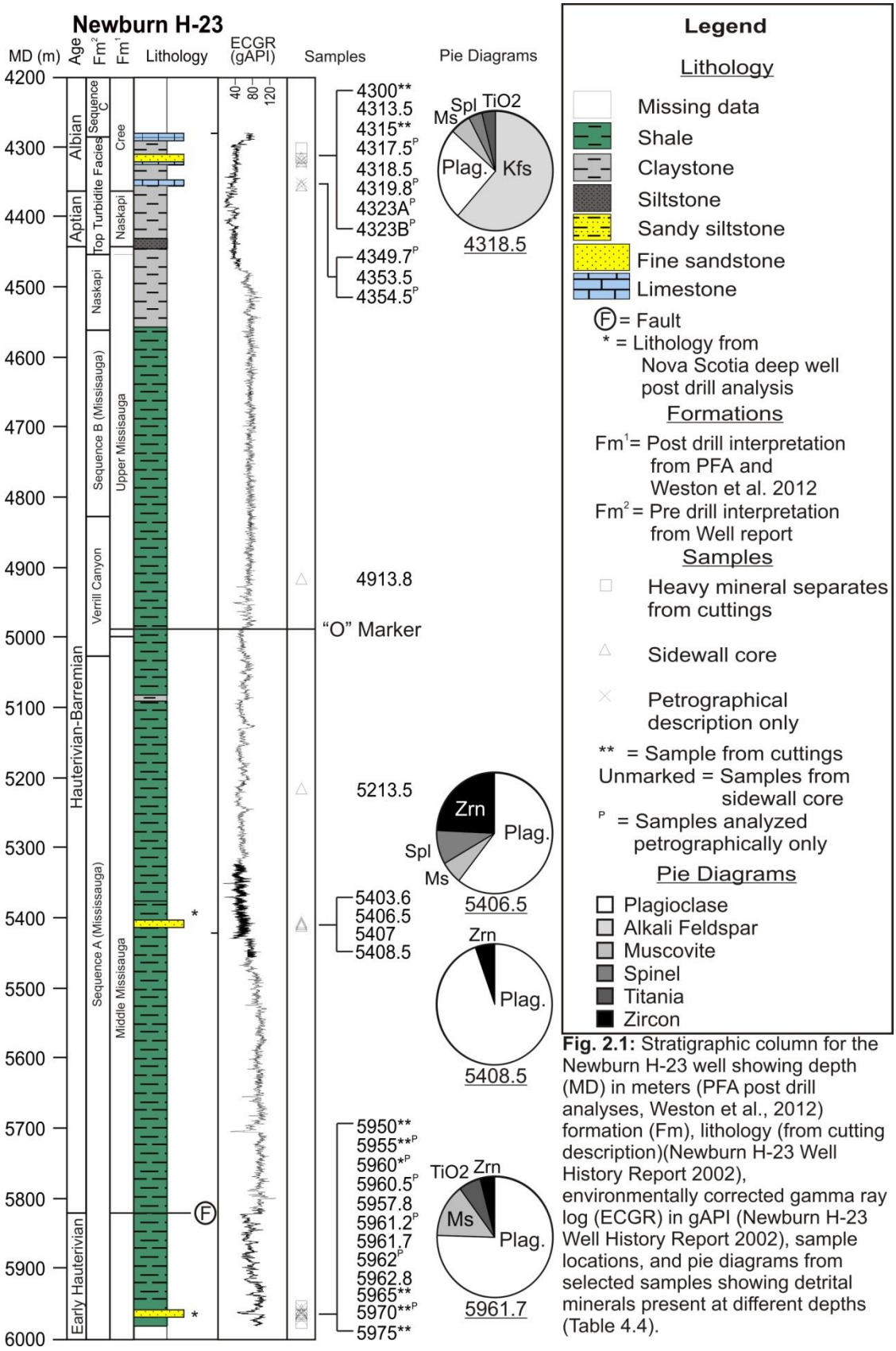

Fig. 2.1: Stratigraphic column for the Newburn H-23 well showing depth (MD) in meters (PFA post drill analyses, Weston et al., 2012) formation (Fm), lithology (from cutting description)(Newburn H-23 Well History Report 2002), environmentally corrected gamma ray log (ECGR) in gAPI (Newburn H-23 Well History Report 2002), sample locations, and pie diagrams from selected samples showing detrital minerals present at different depths (Table 4.4).

Chapter 3: Data presentation

A total of 17 samples (cuttings and sidewall cores) have been analyzed from this well. All of which have been analyzed using the SEM to produce BSE images and chemical analyses (App. 1 and 2). Point counting has also been performed on the 12 pts from the sidewall cores to determine their modal composition (Table 3.1). Data presented in this chapter was collected using the methods outlined in chapter 2.

3.1 Modal composition

Modal composition is the percentage of various detrital minerals in a sample. For the Newburn H-23 well it has been determined using point counting methods the results of which are listed in Table 3.1. The modal composition can be used for a variety of purposes including classification of sedimentary rocks and the reconstruction of paleotectonic environments giving information about the environments and sources of sedimentary rocks.

Table 3.1: Summary table of standard point counting by petrographic microscope used to determine modal composition (Figs. 3.1-4).

% of total rock											
Sample	**Sorting**	**Average grain size (μm)**	**Wentworth scale classification**	**Monocrystalline Quartz**	**Polycrystalline Quartz**	**Feldspar**	**Lithic Clasts**	**Heavy Minerals**	**Unstable Minerals**	**Total Quartz**	**Total Lithic Clasts (Polycrystalline Quartz + Lithic Clasts)**
H-23 4313.5	Well sorted	188	Fine upper sand	78	5.5	8.8	6.6	0.3	0.7	90.5	12.1
H-23 4318.5	Poorly sorted	395	Medium upper sand	71.8	9.3	12.5	6.2	0	0.2	88.7	15.5
H-23 4353.5	Well sorted	220	Fine upper sand	78.8	2.8	9	9.3	0	0	83.5	12.1
H-23 4353.5 Repeat				81.7	1.7	6.8	9.7	0	0.2	83.4	11.4
H-23 4913.8	Well sorted	177	Fine upper sand	82.7	4.5	1.3	10	0.4	1.2	87.2	14.5
H-23 5213.5	Well sorted	118	Fine lower sand	89.7	1.5	2.3	6	0	0.5	91.2	7.5
H-23 5213.5 Repeat				89.5	0.7	2.3	6.6	0.5	0.3	90.2	7.3
H-23 5403.6	Well sorted	126	Fine lower sand	93.7	0.8	2.6	2	0.2	0.7	81.1	2.8
H-23 5406.5	Well sorted	240	Fine upper sand	85.3	5.2	4.3	3.8	1.1	0.2	96.8	9
H-23 5407	Well sorted	96	Fine lower sand	91.3	1.2	1.5	5.2	0.2	0.7	92.5	6.4
H-23 5408.5	Well sorted	140	Fine lower sand	95.5	1.3	1.2	1.8	0	0.2	81.6	3.1
H-23 5408.5 Repeat				89	1.7	3.8	5.3	0.2	0	90.7	7
H-23 5957.8	Well sorted	84	Very fine upper sand	87.7	2.8	2.8	6.7	0	0	90.5	9.5
H-23 5961.7	Well sorted	100	Fine lower sand	93	0.7	2.8	2	0	1.5	94.5	2.7
H-23 5961.7 Repeat				85.7	2.8	3.2	7.4	0.2	0.8	88.5	10.2
H-23 5962	Well sorted	160	Fine lower sand	85.2	3.5	3.7	6.8	0.3	0.5	93.7	10.3

3.1.1 Sandstone classification

The results from the point counting are plotted on QFL diagrams to classify the sandstones on the basis of modal composition. The QFL diagram from Folk (1968) (Fig. 3.1 and 3.2) is a ternary diagram which uses (Q) total quartz (monocrystalline and polycrystalline), (F) feldspars (alkali feldspar and plagioclase), and (L) lithic clasts (igneous, metamorphic and sedimentary) as parameters to classify various types of sandstones as outlined by Folk (1968).

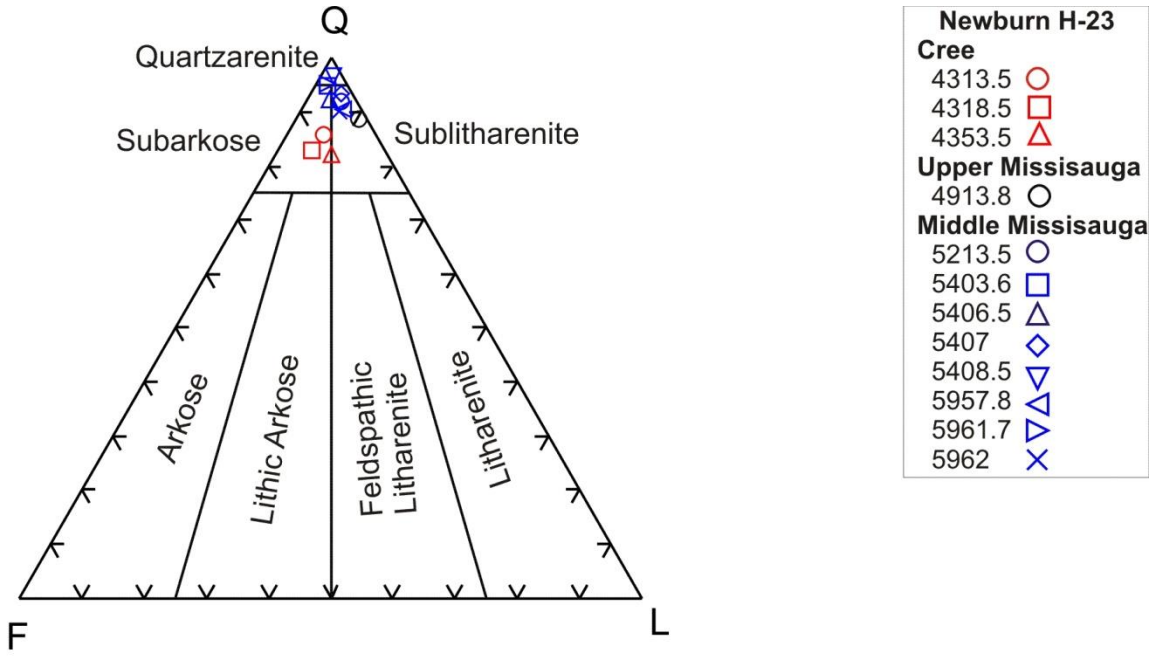

Fig. 3.1: QFL plot showing modal composition of sandstone using nomenclature and fields from Folk (1968).

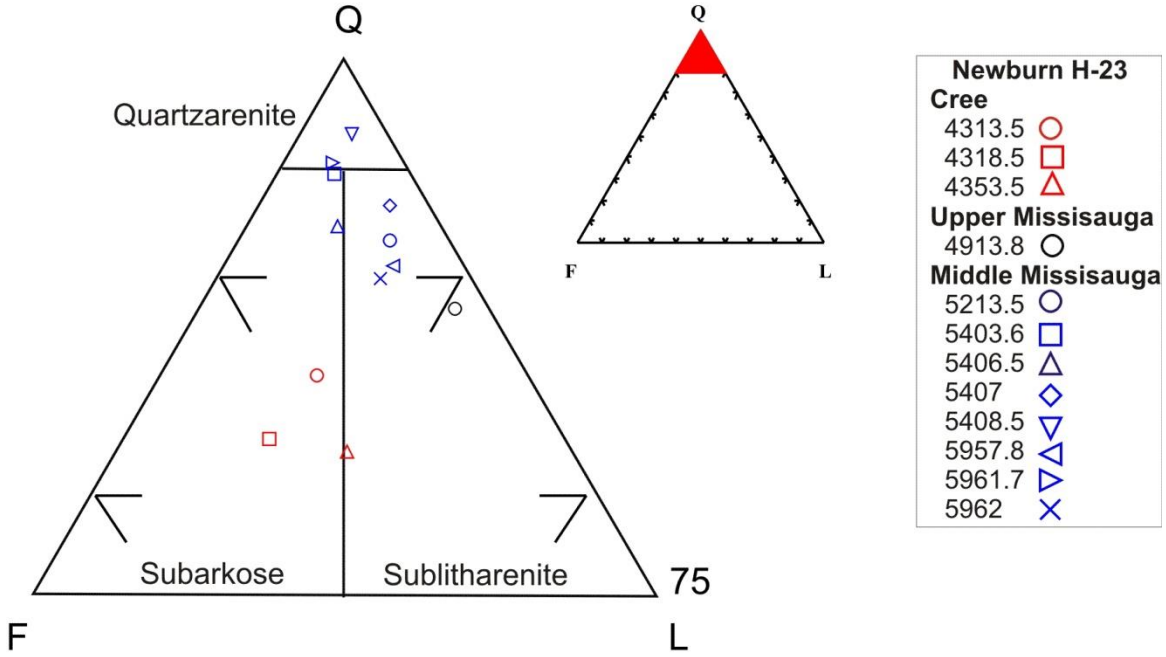

Fig. 3.2: QFL plot showing modal composition of sandstone above 75% quartz, using nomenclature and fields from Folk (1968).

3.1.1.1 Cree Member

Samples from the Cree Member are dominantly subarkose with two of the three samples (samples 4313.5 m and 4318.5 m) falling within that field on the QFL diagram (Fig. 3.2). The remaining sample (4353.5 m) plots as a sub-litharenite which is very close to the division between the two fields (Fig. 3.2).

3.1.1.2 Upper Mississauga Formation

There is only one sample from the Upper Missisauga Formation (sample 4913.8 m) and it falls within the sub-litharenite field (Fig. 3.2).

3.1.1.3 Middle Mississauga Formation

The middle Mississauga has the most samples of any of the formations in this study. The samples are spread across subarkose (samples 5403.6 m and 5406.5 m), quartzarenite (samples 5408.5 m and 5961.7 m), and sublitharenite (samples 5213.5 m, 5407 m, 5957.8 m, and 5962 m) on the QFL diagram (Fig. 3.2). The trend appears to be a decrease in feldspars and increasing in lithic clast content with depth, although not all samples follow this trend.

3.1.2 Paleotectonic environment

Dickinson et al. (1983) have introduced two classification diagrams, the QFL and Q_mFL_t. The QFL diagram identifies paleotectonic environments (Fig. 3.3) and classify possible source areas on a continental block (in dark grey), a recycled orogen (in light grey), and a magmatic arc (in white). The Q_mFL_t diagram (Fig. 3.4) uses (Q_m) monocrystalline quartz, (F) feldspars, and (L_t) total lithic clasts (polycrystalline quartz, igneous, metamorphic, and sedimentary lithic clasts). This diagram also identifies

paleotectonic environments and identifies sediment sources from a continental block (in dark grey), a recycled orogen (in light grey), and a magmatic arc (in white).

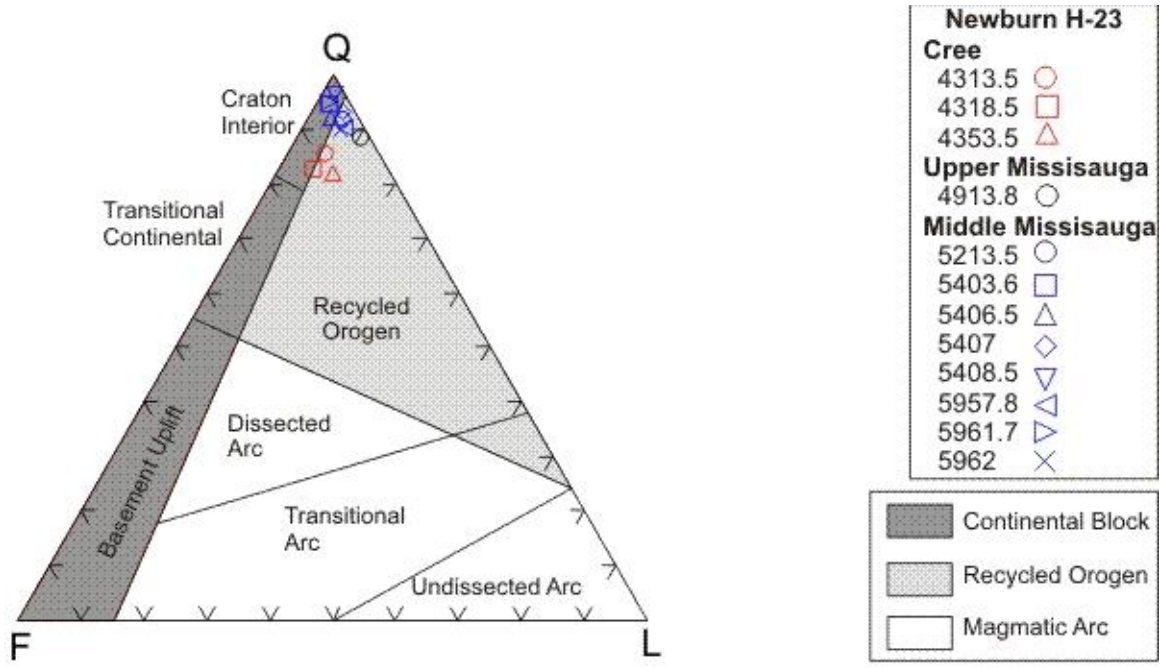

Fig. 3.3: QFL plot for framework modes using paleotectonic fields from Dickinson et al. (1983).

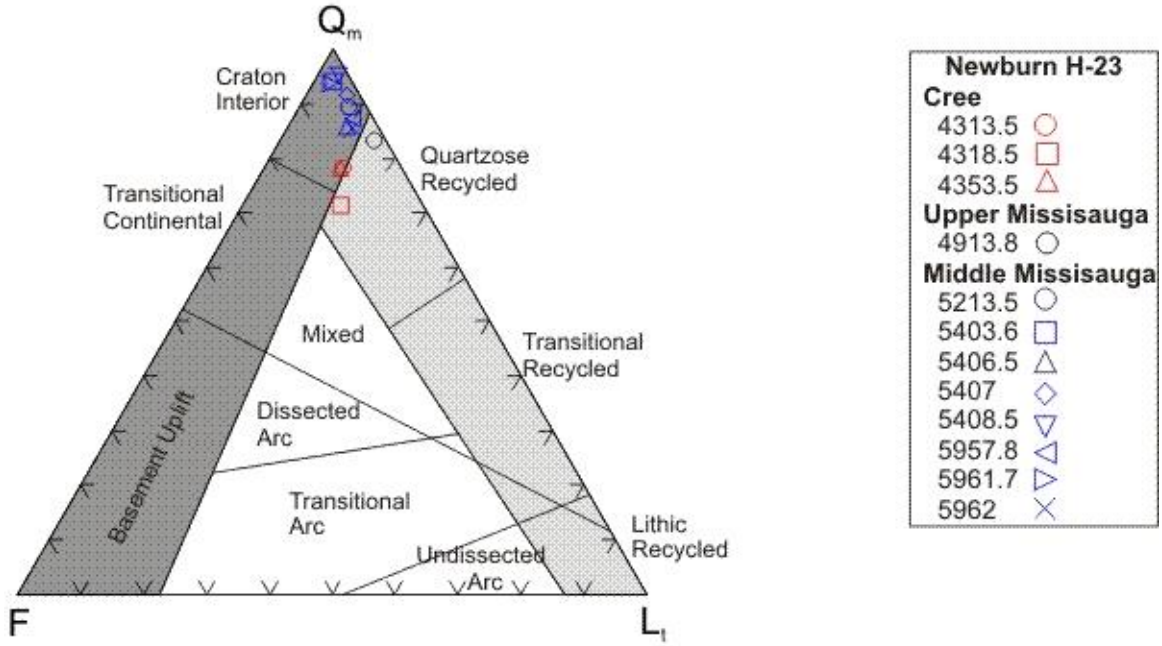

Fig. 3.4: Q_mFL_t (Q_m = monocrystalline quartz. L_t = lithic clasts plus polycrystalline quartz) for framework modes using paleotectonic fields from Dickinson et al. (1983).

3.1.2.1 Cree Member

All three samples (samples 4313.5m, 4318.5m, and 4353.5m) plot in a cluster in the boundary between the recycled orogen field and the craton interior segment of the continental block field on the QFL diagram (Fig. 3.3). In The Q_mFL_t diagram all three samples again plot in a cluster in the boundary between the same two fields, but with a minor shift in their relative positions (Fig. 3.4).

3.1.2.2 Upper Mississauga Formation

There is only one sample from the Upper Missisauga (sample 4913.8m) and it falls within the recycled orogen field on the QFL diagram (Fig. 3.3) and on the Q_mFL_t diagram (Fig. 3.4) it plots in the quartzose recycled segment of the recycled orogen field.

3.1.2.3 Middle Mississauga Formation

On the QFL diagram the samples are divided evenly between the craton interior (samples 5403.6 m, 5406.5 m, 5408.5 m, and 5961.7 m) and recycled orogen (samples 5213.5 m, 5407 m, 5957.8 m, and 5962 m) fields. All studied samples fall within the craton interior field on the Q_mFL_t diagram.

3.1.3 Reproducibility

Four samples were point counted a second time in order to determine the reproducibility of their results. The standard deviation between original and repeated data was calculated in excel (Table 3.2). The most significant differences are related to the counts of lithic clasts which have increased in all samples. The standard deviations which were returned are small with the largest being 6.4 which indicates that the data is reproducible.

Table 3.2: Summary table of results from repeated standard point counting by petrographic microscope of 4353.5m, 5213.5m, 5408.5m, and 5961.7m.

Sample	4353.5m			5213.5m			5408.5m			5961.7m		
	Original %	Repeat %	Std Dev	Original %	Repeat %	Std Dev	Original %	Repeat %	Std Dev	Original %	Repeat %	Std Dev
Monocrystalline Quartz	78.8	81.7	2.1	89.7	89.5	0.1	95.5	89.0	4.6	93.0	85.7	5.2
Polycrystalline Quartz	2.8	1.7	0.8	1.5	0.7	0.6	1.3	1.7	0.3	0.7	2.8	1.5
Lithic Clasts	9.3	9.7	0.3	6.0	6.6	0.4	1.8	5.3	2.5	2.0	7.4	3.8
Heavy Minerals	0.0	0.0	0.0	0.0	0.5	0.4	0.0	0.2	0.1	0.0	0.2	0.1
Unstable Minerals	0.0	0.2	0.1	0.5	0.3	0.1	0.2	0.0	0.1	1.5	0.8	0.5
Feldspar	9.0	6.8	1.6	2.3	2.3	0.0	1.2	3.8	1.8	2.8	3.2	0.3
Total Quartz	83.5	83.4	0.1	91.2	90.2	0.7	81.6	90.7	6.4	94.5	88.5	4.2
Total Lithic Clasts	12.1	11.4	0.5	7.5	7.3	0.1	3.1	7.0	2.8	2.7	10.2	5.3

3.2 Petrographic changes with stratigraphy: Detrital and diagenetic minerals in polished grain mounts from the cuttings samples

Five grain mounts of heavy mineral separates have been analyzed as a part of this project. In several cuttings samples there was insufficient sand fraction to make grain mounts and thus there are only grain mounts available from the Cree Member of the Logan Canyon and the Middle Missisauga formations. These samples contain several minerals which may be the result of contamination from the drilling muds used in this well. Synthetic Oil Based Drilling Muds were used (SOBM) which can contain “metals” (presumably metal ores) that have been added to the mud (Enyiegbulam and Iheaturu 2007). Several sulfides and metal oxides are present in the grain mounts, but absent in polished thin sections from equivalent depths, and as a result we are treating them as possible contaminants. Such minerals include psilomelane, magnetite, chalcopyrite, and covelite. BSE images and chemical analyses from the grain mounts are provided in appendix 1.

3.2.1 Cree Member

Sample 4300: This sample is made from the combined cuttings from depth intervals 4300 m to 4310 m (Table 2.2). Detailed cuttings description provided by the post drill analysis (Kidston et al., 2007) for this range suggests that the lithology is a combination of claystone, sandstone and limestone. The claystone is the most dominant lithology and is present from 4300m-4305m. It is off white to grey-white in colour, silty and rarely sandy, becoming locally chalky limestone with occasional dead oil. The sandstone is the second most dominant lithology and is present from 4310m-4315m. It is off-white in colour and fine grained containing medium grains. The sands are well sorted and sub-rounded with common limestone interbeds. The limestone is off-white to greyish white in colour, argillaceous, contains trace carbonaceous flakes, and silty white clay interbeds. Detrital minerals identified in the grain mount in this sample are albite, biotite, spinel, diopside, epidote, hornblende, ilmenite, K-feldspar, muscovite, quartz, titania, tourmaline, and zircon. The diagenetic minerals include barite, chlorite, F-apatite, fluorite, Fe-dolomite, goethite, hematite, limonite, pyrite, siderite, and titania. The suspected drilling mud contaminants include chalcopyrite, magnetite, and psilomelane.

Summary: Detrital minerals in this sample are albite, biotite, spinel, diopside, epidote, hornblende, ilmenite, K-feldspar, muscovite, quartz, titania, tourmaline, and zircon. The diagenetic minerals barite, chlorite, F-apatite, fluorite, Fe-dolomite, goethite, hematite, limonite, pyrite, siderite, and titania. Possible contaminants are chalcopyrite, magnetite, and psilomelane.

Sample 4315: This sample is made from the combined cuttings from depth intervals 4315m to 4350m (Table 2.2). Detailed cuttings description provided by the post drill analysis (Kidston et al., 2007) for this range suggests that the lithology is sandstone,

limestone, claystone, and calcareous marlstone. Limestone is present at the most levels spanning from 4315m-4325m and 4345m-4355m. It is off-white and light-brown in parts. These limestones are sandy and silty grading into calcareous sandstone; they are also argillaceous becoming marly containing trace glauconite and minor grey claystone lamellae. The sandstone is present from 4315m-4320m and is off-white in colour and fine grained with rare medium size grains. The sands are sub-rounded and well-rounded with rare limestone interbeds. The claystone is present from 4325m-4330m and from 4350m-4355m. It is grey brown in colour, silty, and shows carbonaceous flakes. The calcareous marlstone is only present from 4325m-4330m. It is light tan to grey and argillaceous. Detrital minerals identified in the grain mount from this sample are albite, spinel, muscovite, quartz, and zircon. The diagenetic minerals are apatite, barite, goethite, kaolinite, limonite, pyrite, and siderite. Suspected drilling mud contaminants include psilomelane.

Summary: Detrital minerals in this sample are albite, spinel, muscovite, quartz, and zircon. The diagenetic minerals are apatite, barite, goethire, kaolinite, limonite, pyrite, and siderite. Psilomelane is a possible contaminant.

3.2.2 Middle Missisauga

Sample 5950: The detailed cuttings description provided by the post drill analysis (Kidston et al., 2007) for this sample suggests that the lithology is 50% shale and 50% siltstone. The shale is medium grained, grey in colour, and slightly silty and calcareous with light-grey coarse silt laminae and carbonaceous laminations as well as nodular pyrite. The siltstone component is light-grey to off-white in colour. It grades from coarse silt to very fine grained sand, is slightly calcareous and arenaceous. It also contains trace

carbonaceous laminations. Detrital minerals identified in the grain mount from this sample are actinolite, biotite, K-feldspar, labradorite, magnetite, muscovite, quartz, titania, and zircon. The diagenetic minerals are barite, chlorite, dolomite, fluorite, limonite, pyrite, siderite, and titania. Suspected drilling mud contaminants are magnetite and psilomelane.

Summary: Detrital minerals in this sample are actinolite, biotite, K-feldspar, labradorite, magnetite, muscovite, quartz, titania, and zircon. The diagenetic minerals are barite, chlorite, dolomite, fluorite, limonite, pyrite, siderite, and titania. Possible contaminants include magnetite and psilomelane.

Sample 5965: The detailed cuttings description provided by the post drill analysis for this sample suggests that the lithology is medium brown shale, which is slightly silty and calcareous with traces of pyrite and brown calcareous stringers. Detrital minerals identified in the grain mount from this sample are albite, ilmenite, magnetite, muscovite, quartz, titania, and tourmaline. The diagenetic minerals are ankerite, barite, calcite, chlorite, fluorite, hematite, limonite, pyrite, and siderite. Suspected drilling mud contaminants include arsenopyrite, covelite, and psilomelane.

Summary: Detrital minerals in this sample are albite, ilmenite, magnetite, muscovite, quartz, titania, and tourmaline. The diagenetic minerals are ankerite, barite, calcite, chlorite, fluorite, hematite, limonite, pyrite, and siderite. Possible contaminants include arsenopyrite, covelite, and psilomelane.

Sample 5975: The detailed cuttings description provided by the post drill analysis (Kidston et al., 2007) for this sample suggests that the lithology is grey-brown shale, which is slightly silty and calcareous with traces of pyrite and white calcareous lamellae. Detrital minerals identified in the grain mount for this sample are albite, hornblende, K-

feldspar, muscovite, quartz, titania, and tourmaline. The diagenetic minerals are ankerite, apatite, barite, calcite, chlorite, dolomite, F-apatite, fluorite, limonite, pyrite, and siderite. Suspected drilling mud contaminants include chalcopyrite, magnetite, and psilomelane.

Summary: Detrital minerals in this sample are albite, hornblende, K-feldspar, muscovite, quartz, titania, and tourmaline. The diagenetic minerals are ankerite, apatite, barite, calcite, chlorite, dolomite, F-apatite, fluorite, limonite, pyrite, and siderite. Possible contaminants include chalcopyrite, magnetite, and psilomelane.

3.3 Petrographic changes with stratigraphy: Detrital and Diagenetic minerals in polished thin section from sidewall core samples.

There are 12 polished thin sections from the Newburn H-23 well which range from the Cree Member to the Middle Missisauga (Fig. 2.1). Along with the representative figures provided in this chapter, additional BSE images and chemical analyses are provided in appendix 2.

The analyzed polished thin sections from the Middle Missisauga Formation range in sample depths from 5213.5 m to 5962 m, these polished thin sections appear to be in two separate groups of sample depths, one above 5410 m and the other below 5950 m. Since the samples from the Middle Missisauga Formation show such a large distribution in depths they have been separated into two groups, within which the distribution of sample depths is smaller and the samples within the group better relate to one another in terms of mineralogy and diagenetic conditions. Group 1 includes samples 5213.5 m, 5403.6 m, 5406.5 m, 5407 m, and 5408.5 m, and Group 2, includes samples 5957.8 m, 5961.2 m, and 5962 m.

3.3.1 Cree Member

Sample 4313.5: The sidewall core description provided by the post drill analysis (Kidston et al., 2007) is of a grey, poorly sorted, and very fine to fine grained sandstone with carbonaceous shale micro-laminations and calcareous cement. Petrographic analysis of this sample suggests that this is a well sorted fine grained subarkose (Fig. 3.2) with an average grain size of 188 µm (Table 3.1.). Core analysis gives a porosity of 0.175 and a maximum permeability of 0.4 mD.

The identified detrital grains in this sample are albite, K-feldspar, muscovite, monazite, oligoclase, quartz, titania, zircon, and lithic clasts. The diagenetic minerals are ankerite, apatite, barite, calcite, chlorite, F-apatite, illite, kaolinite, magnesian siderite, siderite, sphalerite, titania, and zircon. Lithic clasts in this sample are composed of ragged titania, quartz and muscovite (Fig. 3.5A), and fine grained lithic clasts composed mainly of albite laths (Fig., 3.5D). This lithology is termed trachytic lithic clasts in subsequent samples. There are also mudstone intraclasts composed of illite and chlorite cemented by siderite (App 2-1 Fig. 16 and 18) present in this sample.

The porosity along intergranular boundaries is filled by titania, pyrite, chlorite, kaolinite, and siderite. Diagenetic titania also forms along the cleavage planes of muscovite in a lithic clast and also fills dissolution voids within it (Fig. 3.5A position a). Illite and kaolinite fill dissolution voids within albite (Fig. 3.5B). Diagenetic F-apatite has straight crystal outlines towards pore and engulfs quartz (Fig. 3.5C). Siderite forms along intergranular boundaries (Fig. 3.5C) and fills dissolution voids in a trachytic lithic clast (Fig. 3.5D). Barite forms along the intergranular boundaries of albite (Fig. 3.5B). Sphalerite forms in porosity that is rimmed by chlorite (Fig. 3.5E). Quartz overgrowths are also present in this sample forming in open porosity.

Summary: The detrital minerals in this sample are albite, K-feldspar, muscovite, monazite, oligoclase, quartz, titania, and zircon. Lithic clasts are granitoid rocks composed of either titania and muscovite, or quartz and muscovite, and trachytes. Mudstone intraclasts are also present. The diagenetic minerals are ankerite, apatite, barite, calcite, chlorite, F-apatite, illite, kaolinite, magnesian siderite, siderite, sphalerite, titania, and zircon. The paragenetic sequence for this sample is tentatively interpreted as: Quartz overgrowths → Kaolinite + Illite → Calcite → Ankerite → Apatite + Chlorite → Siderite + Mg-Siderite → Pyrite,* Titania, Sphalerite, Zircon.

* Note: Minerals separated by a comma (,) indicates that their age relative to one another is unknown.

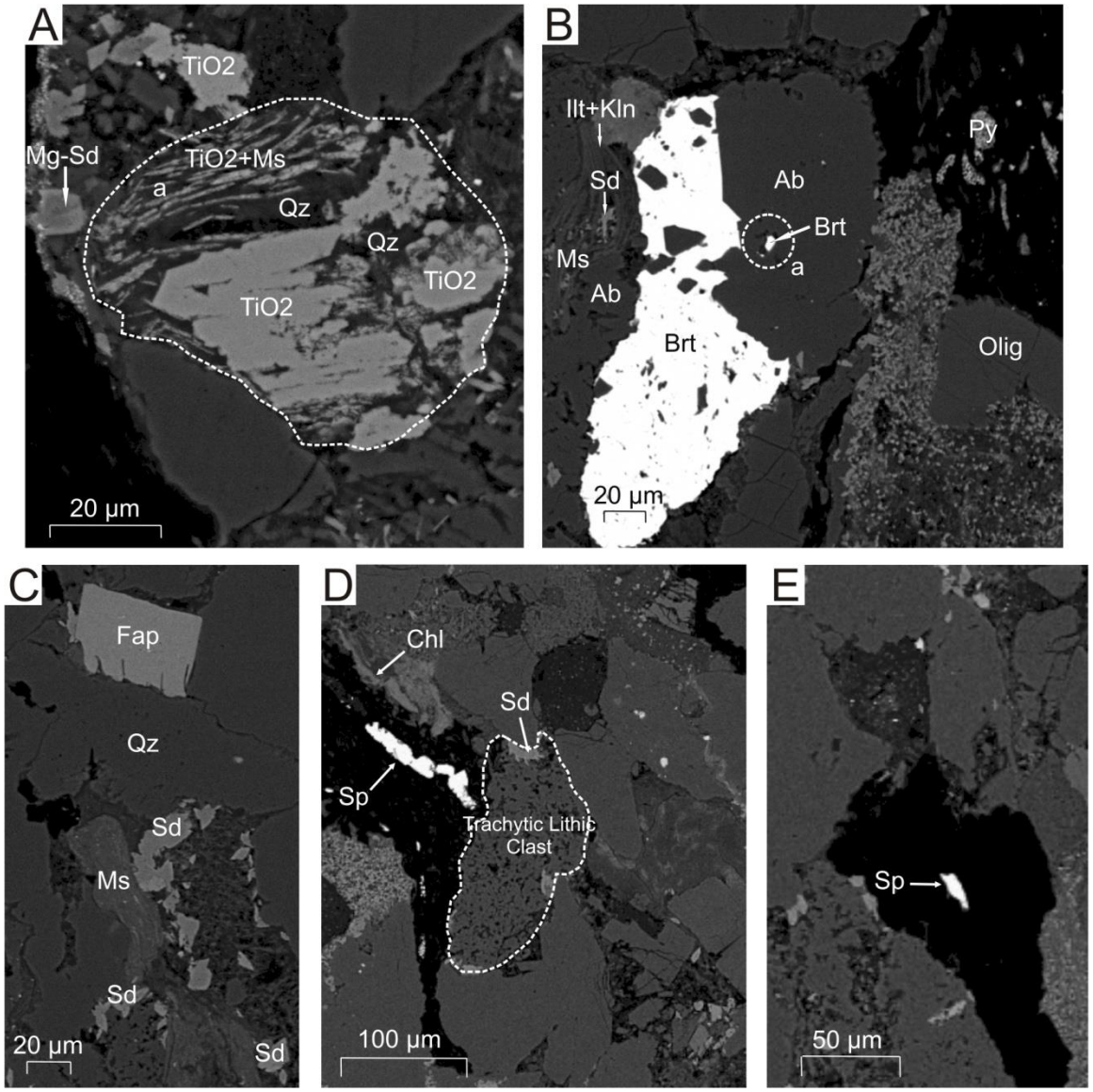

Fig. 3.5: Representative BSE images of textures and minerals from the Cree member in the Newburn H-23 well (Sample 4313.5m).
A: Sample 4313.5m (App. 2-1, Fig. 10). Lithic clast comprised of ragged titania, muscovite, and quartz. Diagenetic titania forms along the cleavage planes of detrital muscovite (position a).
B: Sample 4313.5m (App. 2-1, Fig. 20). Diagenetic barite forms along intergranular boundary of albite grains as well as filling dissolution voids within albite (position a). Illite and kaolinite also fill dissolution voids within albite.
C: Sample 4313.5m (App. 2-1, Fig. 12).Diagenetic fluorapatite with straight crystal outlines towards pore engulfs quartz. Siderite fills pore along intergranular boundary between quartz grains.
D: Sample 4313.5m (App. 2-1, Fig. 7). Diagenetic sphalerite has formed in a vein. Trachytic lithic clast comprised of albite has dissolution voids filled by siderite.
E: Sample 4313.5m (App. 2-1, Fig. 7). Diagenetic sphalerite has formed in a pore.

Sample 4318.5: The sidewall core description provided by the post drill analysis is of a grey poorly sorted fine to medium grained sandstone with carbonaceous shale micro-laminations and calcareous cement. Petrographic analysis of this sample suggests that this is a poorly sorted medium grained subarkose (Fig. 3.2) with an average grain size of 395 µm (Table 3.1). Core analysis gives porosity of 0.165 and a maximum permeability of 2.65 mD.

The detrital grains identified in this sample are albite, spinel, K-feldspar, muscovite, oligoclase, quartz, and lithic clasts. The diagenetic minerals apatite, barite, chlorite, F-apatite, hematite, illite, kaolinite, pyrite, titania, siderite, and zircon. Lithic clasts in this sample are composed of trachytic lithic clasts, granitoid lithic clasts made up of K-feldspar, quartz, albite, and muscovite (Fig. 3.7A), thes sample also contains intraclasts that consist of muscovite, chlorite, albite, and quartz cemented by siderite (Fig. 3.6C).

This sample contains abundant K-feldspar with extensive dissolution, some of these dissolution pores have been filled by drilling mud during the drilling process (Fig. 3.6A), others remained as abundant secondary porosity throughout the sample. Kaolinite and chlorite form along intergranular boundaries between quartz and K-feldspar with chlorite replacing kaolinite (Fig. 3.6A position a). There are abundant intraclasts which have plastically deformed around framework grains (Fig. 3.6D). Diagenetic F-apatite (3.7E position a) zircon (Fig. 3.6D) with sharp crystal outlines fill porosity which may have been generated by dissolution of K-feldspar. Siderite (Fig. 3.7C), kaolinite, and illite (Fig. 3.6B) fill dissolution voids in trachytic lithic clasts. Chlorite and apatite fills dissolution voids in albite and hematite forms in a pore (Fig. 3.6B). Chlorite, titania, and

siderite fill dissolution voids in trachytic lithic clasts. Quartz overgrowths are also present partially filling secondary porosity predating kaolinite (App. 2-2, Fig. 11).

Summary: The detrital minerals in this sample are albite, spinel, K-feldspar, muscovite, oligoclase, and quartz. Lithic clasts are granitoid rocks and trachytes. The diagenetic minerals include apatite, barite, chlorite, F-apatite, hematite, illite, kaolinite, pyrite, titania, siderite, and zircon. There are also abundant intraclasts. The paragenetic sequence for this sample is tentatively interpreted as: Quartz overgrowths → Kaolinite +Illite → Siderite (cement in intraclasts) → Chlorite + Apatite + Fluorapatite→ Titania, Barite, Pyrite, Zircon.

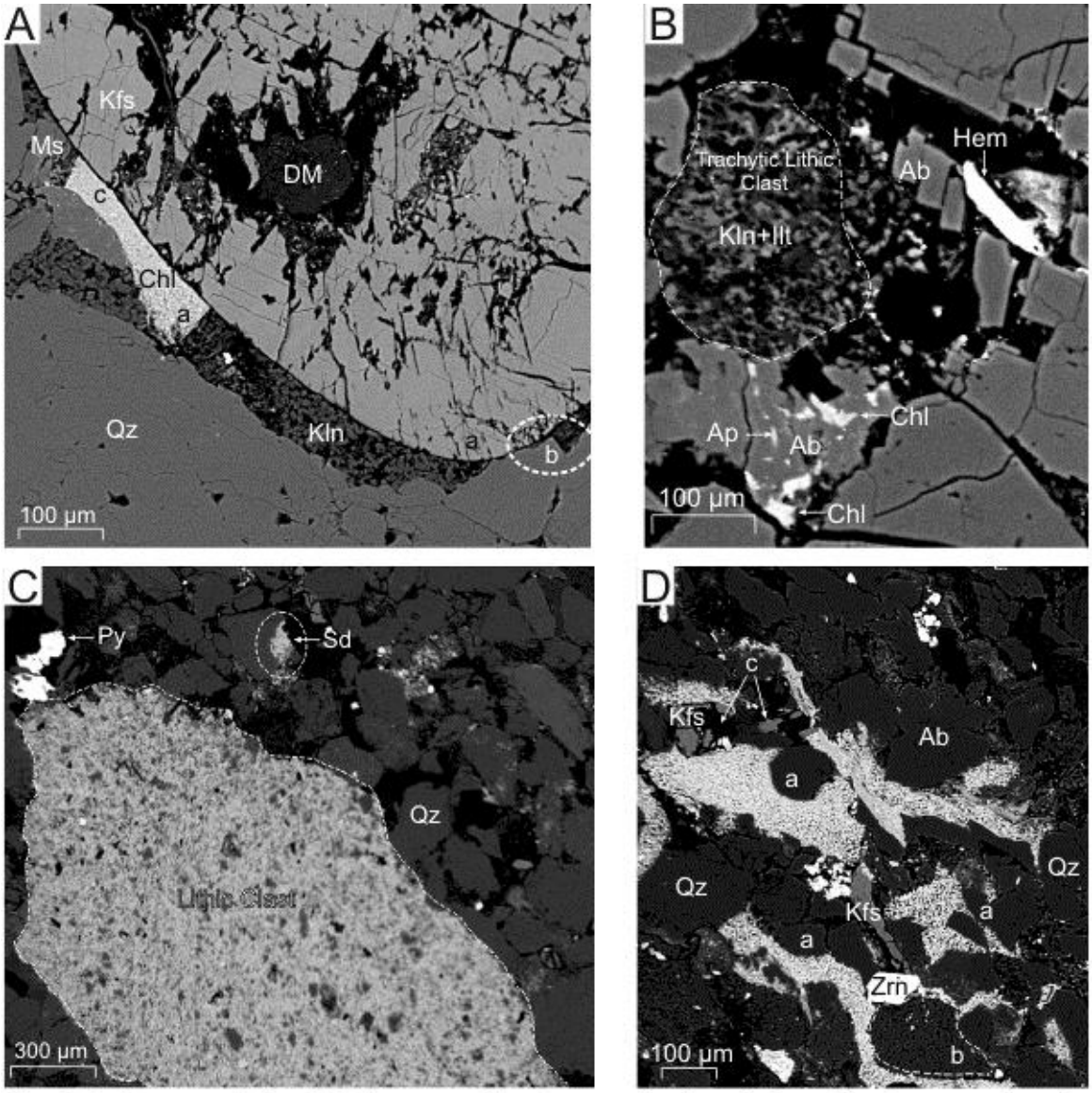

Fig. 3.6: Representative BSE images of textures and minerals from the Cree member in the Newburn H-23 well (Sample 4318.5m).
A: Sample 4318.5m (App. 2-2, Fig. 10). K-feldspar grain with dissolution voids partially filled by drilling mud (DM). Kaolinite filling pore space between detrital K-feldspar and quartz. Chlorite engulfs kaolinite(position a) and seems to invade quartz overgrowths (position b) displacing kaolinite. Muscovite grain replaced by chlorite (position c).
B: Sample 4318.5m (App. 2-2, Fig. 6).Chlorite and apatite fill dissolution voids in albite. Diagenetic hematite cuts albite. Kaolinite and illite fill dissolution voids in partially dissolved trachytic lithic clast.
C: Sample 4318.5m (App. 2-2, Fig. 9). Lithic clast made up of muscovite, chlorite, quartz and albite cemented by early siderite. Diagenetic siderite along intergranular boundaries.
D: Sample 4318.5m (App. 2-2, Fig. 3). Muscovite completely replaced by chlorite. Plastically deformed intraclast of siderite and chlorite rims quartz grains (positions a) and fill pores. Chlorite and siderite intraclast fill pore with detrital K-feldspar relics. Trachytic lithic clast (position b). Partially dissolved K-feldspar generates secondary porosity (positions c). Probable diagenetic zircon has straight crystal outlines and cuts framework grains such as quartz, K-feldspar, and trachytic lithic clasts (position b).

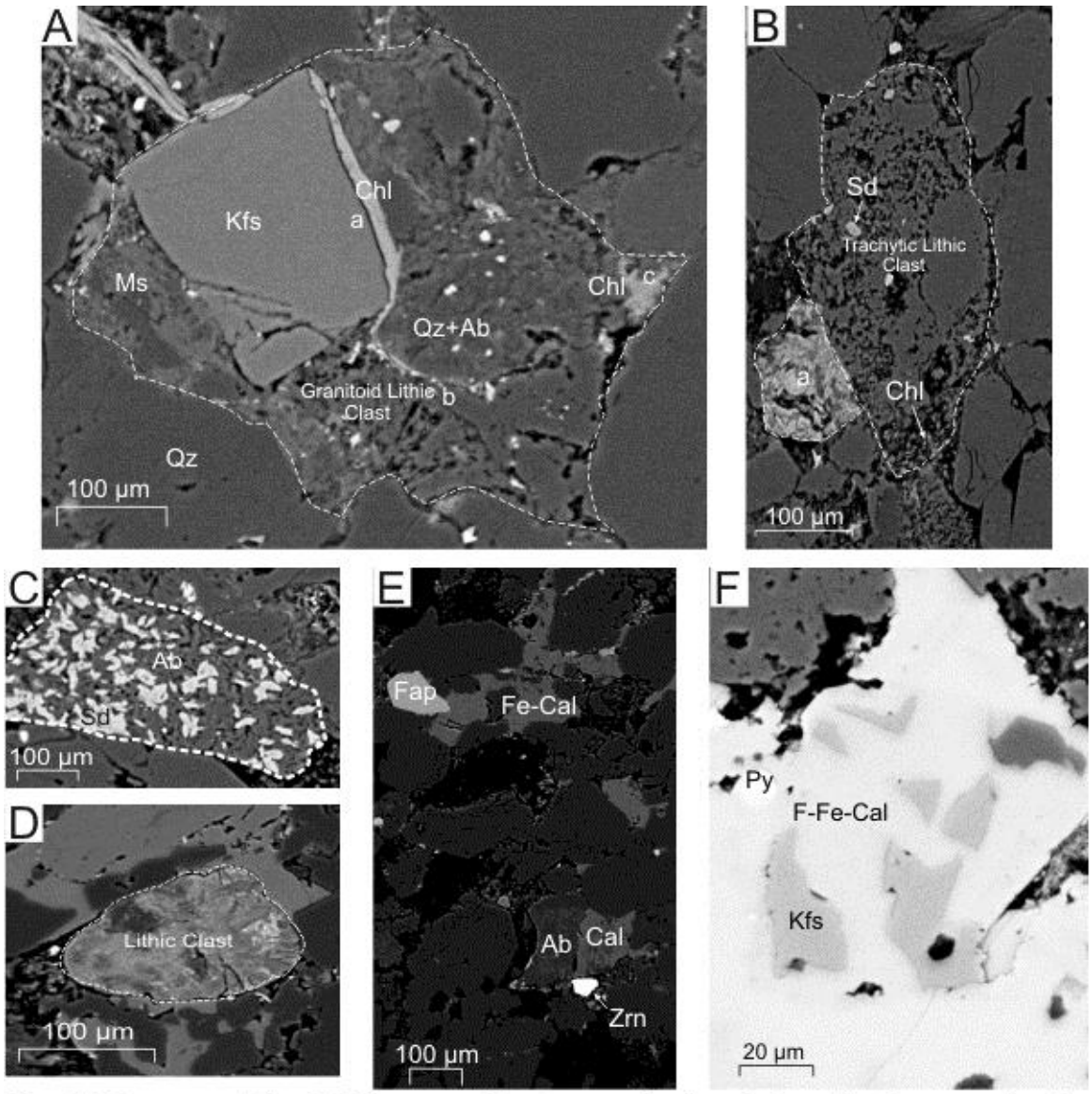

Fig. 3.7: Representative BSE images of textures and minerals from the Cree member in the Newburn H-23 well (Samples 4318.5m and 4353.5m).
A: Sample 4318.5m (App. 2-2, Fig. 12). Plastically deformed chloritized muscovite (position a) in contact with K-feldspar grain (position a). Chlorite fills secondary porosity along intergranular boundary (position b). Granitoid lithic clast with chlorite filling porosity (position c).
B: Sample 4318.5m (App. 2-2, Fig. 15). Trachytic lithic clast with chlorite and siderite filling dissolution voids. Fluorapatite with some fibrous chlorite fills secondary porosity (position a).
C: Sample 4318.5m (App. 2-2, Fig. 12). Siderite filling dissolution voids in trachytic lithic clast.
D: Sample 4353.5m (App. 2-3, Fig. 12). Lithic clast composed of fluorapatite, apatite and quartz, partly replaced by chlorite.
E: Sample 4353.5m (App. 2-3, Fig. 14). Diagenetic fluorapatite cuts Fe-calcite. Diagenetic zircon with straight crystal outline fills pore.
F: Sample 4353.5m (App. 2-3, Fig. 17). F-Fe-calcite engulfs K-feldspar. Pyrite fills dissolution voids in F-Fe-calcite.

Sample 4353.5: The sidewall core description provided by the post drill analysis is of a grey, poorly sorted very fine to fine grained sandstone with calcareous cement. Petrographic analysis of this sample suggests that this is a well sorted fine grained sublitharenite (Fig. 3.2) with an average grain size of 220 μm (Table 3.1). Core analysis gives a porosity of 0.121 and a maximum permeability of 0.28 mD.

The identified detrital grains in this sample are albite, spinel, K-feldspar, muscovite, quartz and lithic clasts. The diagenetic minerals are ankerite, calcite, chlorite, F-apatite, F-calcite, Fe-calcite, F-Fe-calcite, glauconite, kaolinite, pyrite, titania, and zircon. The lithic clasts in this sample are granitoid lithic clasts containing F-apatite, apatite, and quartz (Fig. 3.7D), as well as trachytes (Fig. 3.8A).

This sample is cemented by F-Fe-, F-, and Fe-calcite. The F-Fe-calcite has engulfed K-feldspar and contains relics of the engulfed K-feldspar, and also has dissolutions voids filled by pyrite (Fig. 3.7F). Diagenetic F-apatite cuts F-calcite (Fig. 3.7E). This sample also contains diagenetic zircon with sharp crystal outlines that fill porosity (Fig. 3.7E). Siderite replaces F-calcite (Fig. 3.8A). Preserved glauconite pellet is surrounded by calcite (Fig. 3.8B). Titania fills an open pore rimmed by chlorite near detrital spinel (Fig. 3.8D). There are also abundant quartz overgrowths into Fe-calcite (Figs. 3.8C and E position a).

Summary: The detrital minerals in this sample are albite, spinel, K-feldspar, muscovite, and quartz. The lithic clasts are granitoids with apatite, F-apatite, and quartz, and trachytes. The diagenetic minerals are ankerite, calcite, chlorite, F-apatite, F-calcite, Fe-calcite, F-Fe-calcite, glauconite, kaolinite, pyrite, titania, and zircon. The paragenetic sequence for this sample is tentatively interpreted as: Glauconite → Quartz overgrowths?

Kaolinite, Illite → Calcite → Ankerite → Fe-Calcite → F-Calcite + F-Fe-Calcite → Chlorite + Fluorapatite → Pyrite, Siderite, Titania, Zircon.

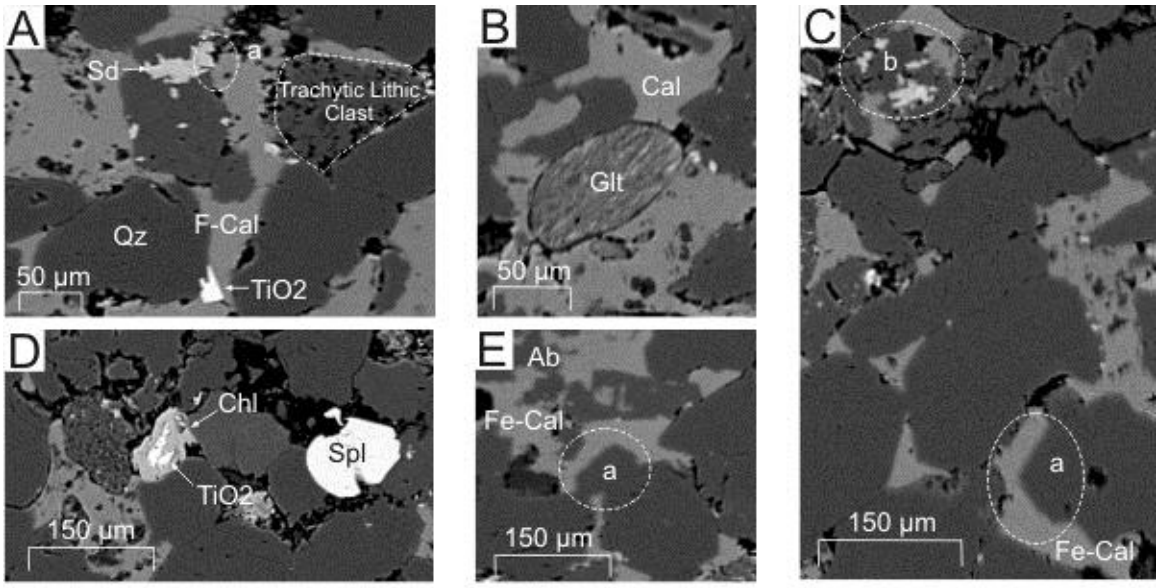

Fig. 3.8: Representative BSE images of textures and minerals from the Cree member in the Newburn H-23 well (Sample 4353.5m).
A: Sample 4353.5m (App. 2-3, Fig. 8). Siderite appears to replace F-calcite (position a). Trachytic lithic clast.
B: Sample 4353.5m (App. 2-3, Fig. 8). Glauconite pellet.
C: Sample 4353.5m (App. 2-3, Fig. 3). Quartz overgrowths surrounded by Fe-calcite (position a). Siderite (position b) fills dissolution voids in quartz grain.
D: Sample 4353.5m (App. 2-3, Fig. 8). Titania fills open porosity rimmed by chlorite. Detrital spinel grain.
E: Sample 4353.5m (App. 2-3, Fig. 3). Quartz overgrowths surrounded by Fe-calcite (position a).

3.3.2 Upper Mississauga formation

Sample 4913.8: The sidewall core description provided by the post drill analysis is of a medium grey siltstone with a shaley fraction. Petrographic analysis of this sample suggests that this is a well sorted fine grained sublitharenite (Fig. 3.2) with an average grain size of 177 µm (Table 3.1). Core analysis gives a porosity of 0.094 and a maximum permeability of 0.09 mD.

The detrital minerals in this sample are albite, muscovite, oligoclase, quartz, and lithic clasts. The diagenetic minerals are ankerite, apatite, barite, calcite, chlorite, F-

apatite, kaolinite, pyrite, siderite, sphalerite, titania, xenotime, and zircon. Lithic clasts in this sample include granitoid lithic clasts (Fig. 3.9C) composed of albite and muscovite, trachytic lithic clasts. There are also mudstone intraclasts (Fig. 3.9E) composed of chlorite, apatite, and siderite.

This sample contains diagenetic zircons with sharp crystal outlines that fill pores in muddy matrix (Fig. 3.9A). Diagenetic xenotime also fills pores and shows dissolution as well as fracturing (Fig. 3.9B). Titania with irregular engulfs ankerite filling porosity (Fig. 3.9F) it may also be replacing barite (Fig. 3.9F position a) and filling dissolution voids in trachytic lithic clasts (Fig. 3.9D). Barite engulfs kaolinite and fills porosity (Fig. 3.9D). This sample has a fine grained matrix composed of fine grained silicates including clays which are in contact with quartz overgrowths (App. 2-4, Fig. 15).

Summary: The detrital minerals in this sample are albite, muscovite, oligoclase, and quartz. The lithic clasts are granitoids and trachytes. There are also mudstone intraclasts. The diagenetic minerals are ankerite, apatite, barite, calcite, chlorite, F-apatite, kaolinite, pyrite, siderite, sphalerite, titania, xenotime, and zircon. The paragenetic sequence for this sample is tentatively interpreted as: Quartz overgrowths → Illite + Kaolinite → Ankerite → Chlorite + Apatite + Fluorapatite → Barite, Sphalerite, Titania, Pyrite, Siderite, Xenotime, Zircon.

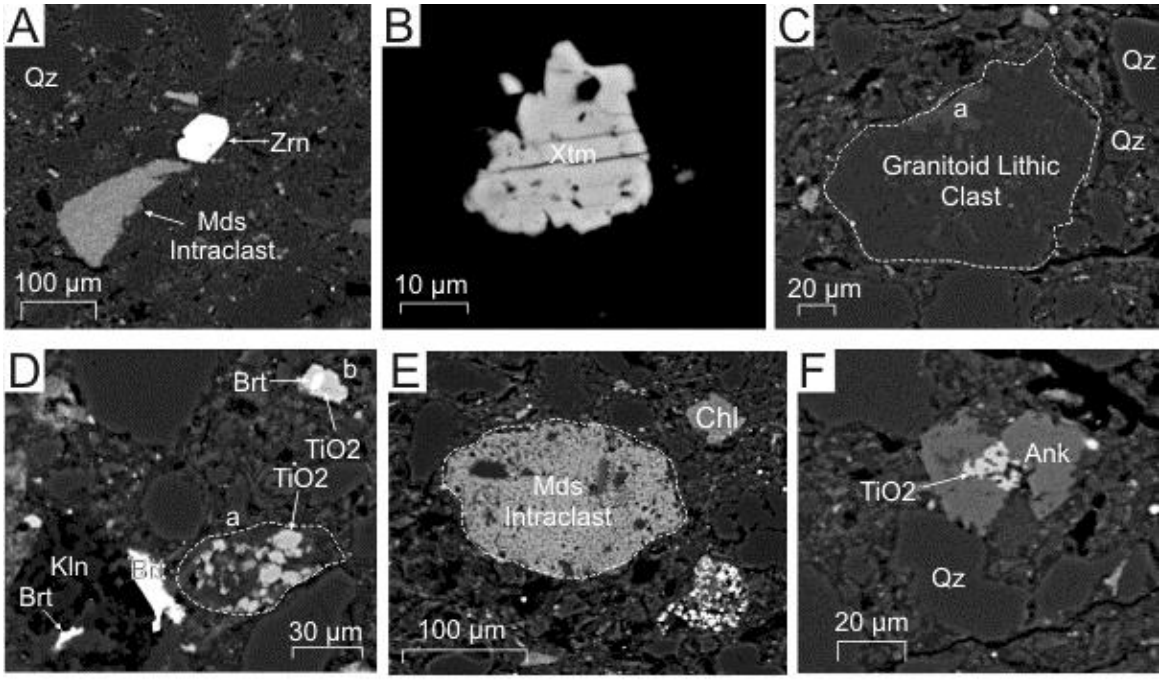

Fig. 3.9: Representative BSE images of textures and minerals from the Upper Missisauga Formation in the Newburn H-23 well (Sample 4913.8m).
A: Sample 4913.8m (App. 2-4, Fig. 13). Probably diagenetic zircon fills pore.
B: Sample 4913.8m (App. 2-4, Fig. 11). Probably diagenetic xenotime with fractures.
C: Sample 4913.8m (App. 2-4, Fig. 16). Granitoid lithic clast composed of albite and muscovite. Some of the muscovite has also been chloritized (position a).
D: Sample 4913.8m (App. 2-4, Fig 12). Diagenetic barite fills open porosity and engulfs kaolinite booklets. Titania fills dissolution voids in trachytic lithic clast (position a). Titania surrounds barite (position b).
E: Sample 4913.8m (App. 2-4, Fig 9). Mudstone intraclast composed of chlorite, apatite, and siderite.
F: Sample 4913.8m (App. 2-4, Fig. 14). Titania engulfs ankerite.

3.3.3 Middle Mississauga formation (Group 1)

Sample 5213.5: The sidewall core description provided by the post drill analysis is of a grey-white limestone and shale. Petrographic analysis of this sample suggests that this is a well sorted, fine grained sublitharenite (Fig. 3.2) with an average grain size of 118 µm (Table 3.1). No core analysis was performed on this sample.

The detrital minerals in this sample are albite, spinel, muscovite, quartz, zircon, and lithic clasts. The diagenetic minerals are ankerite, apatite, barite, calcite, chlorite, F-apatite, F-calcite, Fe-calcite, F-Fe-calcite, kaolinite, pyrite, titania, and zircon. Lithic clast

are granitoids composed of quartz, albite, and muscovite (Fig. 3.10E) and trachytes (Fig. 3.11A).

This sample is cemented by ankerite, F-calcite, Fe-calcite, and F-Fe-calcite. These cements interact with each other commonly throughout the sample often appearing as patches of differently coloured patches. Ankerite appears to have been replaced by F-calcite, and later both were corroded to form secondary porosity (Fig. 3.10A) which is later filled by pyrite (Fig. 3.11C). The F-calcite appears to predate and replaced by F-Fe-calcite (Fig. 3.11C). Diagenetic zircon has straight crystal outlines and cuts framework grains and cement (Fig. 3.10B). Quartz overgrowths appear to be corroded and thus predate F-calcite (Fig. 3.10B). Preserved bedding appears to be cut by subhedral titania (Fig. 3.10C). Titania rims a pore filled with chlorite (Fig. 3.10D) suggesting that chlorite post-dates titania. Framboidal pyrite fills dissolution voids in quartz (Fig. 3.10E position b) and is surrounded by calcite (Fig. 3.10E position c). Barite fills porosity (Fig. 3.10F). An ankerite rhombohedra is partly replaced by F-calcite or Fe-calcite (Fig. 3.11A). Chlorite forms along dissolution along intergranular boundary between F-calcite and quartz (Fig. 3.11A position b).

Summary: The detrital minerals in this sample are albite, spinel, muscovite, quartz, and zircon. The lithic clasts are granitoids and trachytes. The diagenetic minerals are ankerite, apatite, barite, calcite, chlorite, F-apatite, F-calcite, Fe-calcite, F-Fe-calcite, kaolinite, pyrite, titania, and zircon. The paragenetic sequence for this sample is tentatively interpreted as: Pyrite (framboidal) → Quartz overgrowth → Fe-Calcite, Calcite, Ankerite → F-Calcite, Calcite, Ankerite → F-Fe-Calcite, Calcite, Ankerite → Titania → Chlorite → Apatite + Fluorapatite → Siderite, Barite, Pyrite, Zircon.

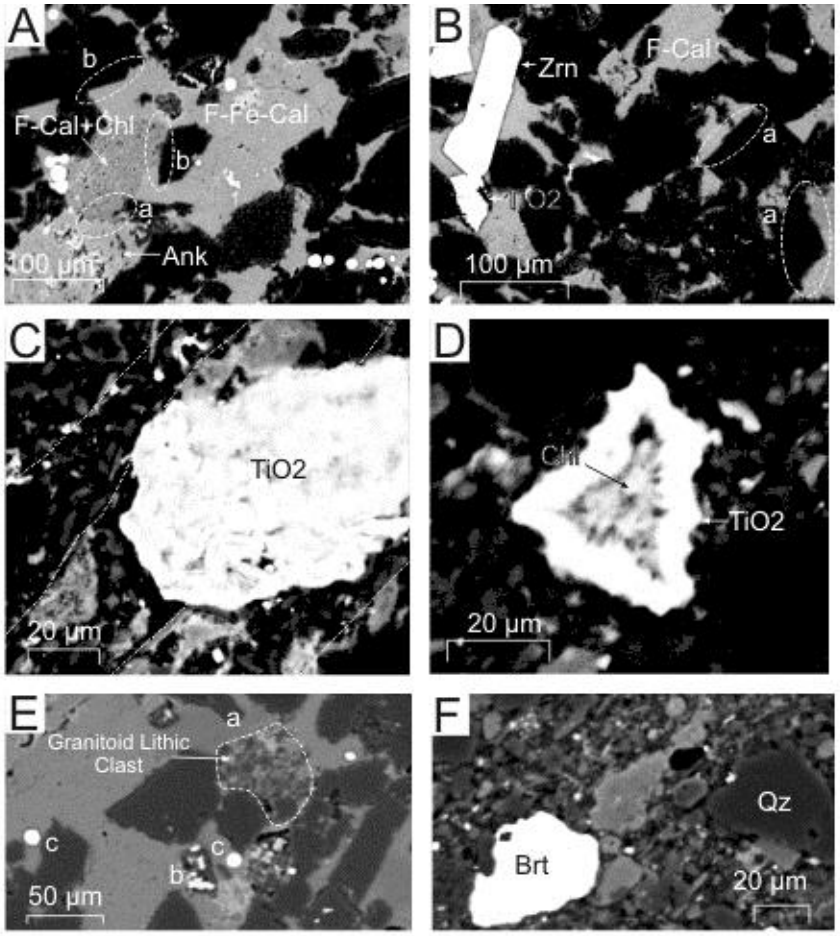

Fig. 3.10: Representative BSE images of textures and minerals from the Middle Missisauga Formation in the Newburn H-23 well (Sample 5213.5m).
A: Sample 5213.5m (App. 2-5, Fig. 5). Ankerite is replaced by low iron F-calcite and both were subsequently corroded forming secondary porosity (position a) and both postdate quartz overgrowth (positions b).
B: Sample 5213.5m (App. 2-5, Fig. 6). Probable diagenetic zircon cuts framework grains and F-calcite. Quartz overgrowth (positions a) appears corroded in contact with F-calcite.
C: Sample 5213.5m (App. 2-5, Fig. 7). Subhedral titania appears to cut bedding.
D: Sample 5213.5m (App. 2-5, Fig. 7). Titania rims pore filled with chlorite.
E: Sample 5213.5m (App. 2-5, Fig. 12). Granitoid lithic clast composed of quartz, albite and muscovite partially replaced by chlorite (position a). Framboidal pyrite in quartz (position b) and is surrounded by calcite (positions c).
F: Sample 5213.5m (App. 2-5, Fig. 13). Barite fills porosity.

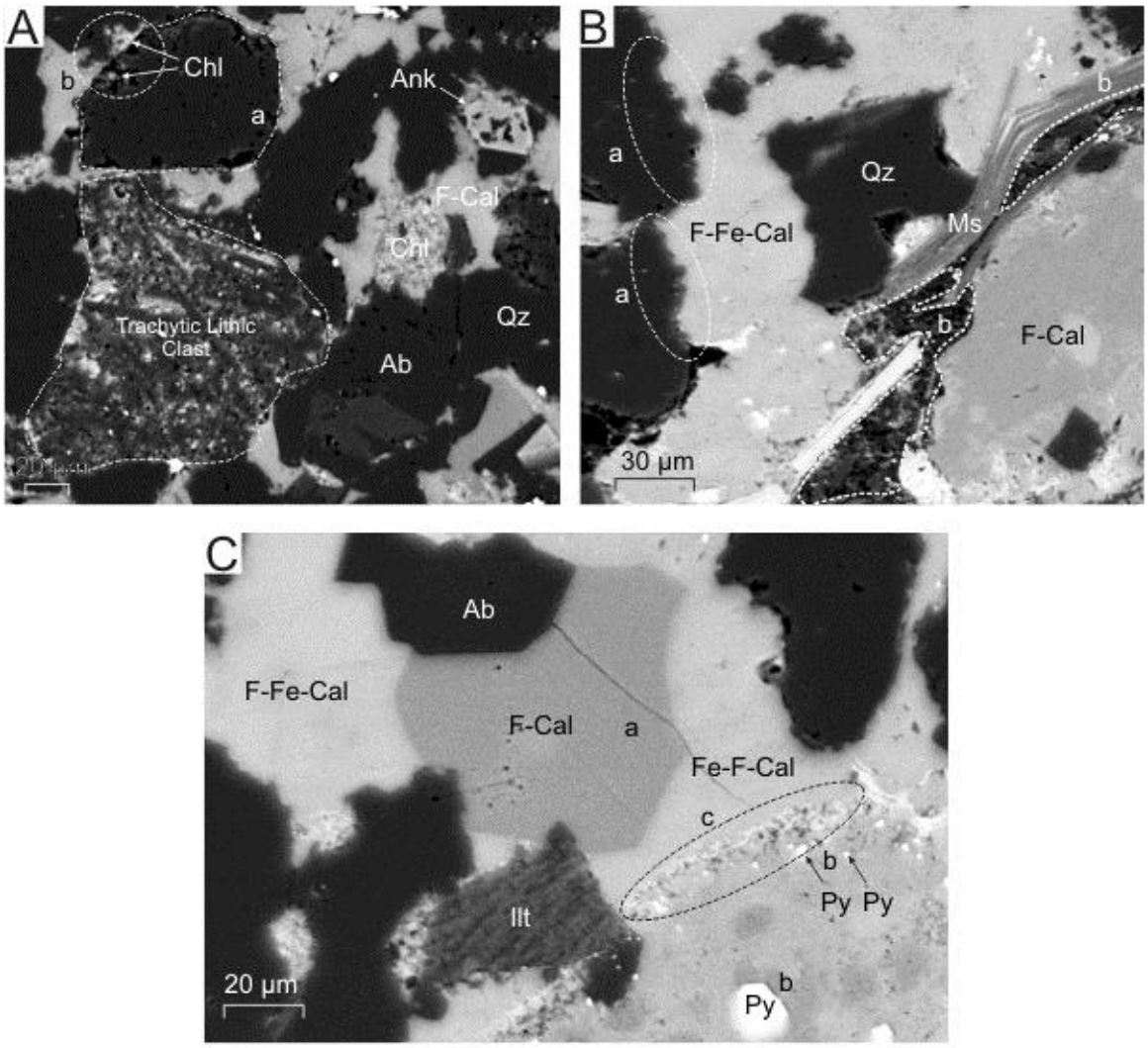

Fig. 3.11: Representative BSE images of textures and minerals from the Middle Missisauga Formation in the Newburn H-23 well (Sample 5213.5m).
A: Sample 5213.5m (App. 2-5, Fig. 9). Trachytic lithic clast with chlorite filling dissolution voids within albite. Dissolution of quartz grain along intergranular boundary shared with F-calcite (position a), and chlorite partially fills void (position b). Ankerite rhombohedron engulfs albite and is replaced by F-calcite/Fe-calcite.
B: Sample 5213.5m (App. 2-5, Fig. 18). F-calcite corrodes quartz overgrowths (positions a). The occurrence of quartz between the cleavage planes of muscovite (position b) has three possible interpretations: mechanically fractured quartz, a granitoid lithic clast, or silty matrix, within which titania and chlorite partially fill dissolution voids.
C: Sample 5213.5m (App. 2-5, Fig. 17). Dark patch of low iron F-calcite (position a) being replaced by F-calcite with higher iron levels. Pyrite fills dissolution in F-calcite (position b), and pyrite and chlorite (position c) also rim F-calcite which is surrounded by F-Fe-calcite.

Sample 5403.6: The sidewall core description provided by the post drill analysis is of a light-brownish-white, fairly well sorted silty to very fine grained sandstone with siliceous cement. Petrographic analysis of this sample suggests that this is a well sorted fine grained subarkose (Fig. 3.2) with an average grain size of 126 μm (Table 3.1). Core analysis gives a porosity of 0.072 and a maximum permeability of less than 0.01 mD.

The detrital grains identified from this sample are albite, K-feldspar, muscovite, quartz, titania, zircon, and lithic clasts. The diagenetic minerals are ankerite, barite, calcite, chlorite, F-apatite, F-calcite, F-Fe-calcite, illite, kaolinite, pyrite, titania, siderite, sphalerite, and zircon. This sample contains trachytic lithic clasts (Fig. 3.12E) as well as mudstone intraclasts composed of chlorite and siderite (Fig. 3.13B).

This sample has a muddy matrix composed of muscovite, chlorite, and quartz (Fig. 3.12D position a) which has siderite rims surrounding part of it (Fig. 3.12D). Kaolinite fills porosity and is rimmed by chlorite (Fig. 3.12B). Chlorite also fills porosity between grains of fractured quartz (Fig. 3.12A position c). Diagenetic titania cuts the kaolinite and chlorite (Fig. 3.12B) and diagenetic zircon cuts quartz and probably engulfs chlorite (Fig. 3.12C). Albite is engulfed by calcite which is in turn engulfed by barite (Fig. 3.12E). Barite engulfs F-calcite as well (Fig. 3.12F position b). F-calcite engulfs chlorite (Fig. 3.12G position a). Chlorite crosscuts kaolinite (Fig. 3.13A position b), rims quartz (Fig. 3.13A position c), and is crosscut by a vein filled pyrite and F-calcite (Fig. 3.13A position a). Ankerite engulfs albite and chlorite (Fig. 3.13B). Quartz overgrowths predate chlorite (Fig. 3.12A).

Summary: The detrital minerals in this sample are albite, K-feldspar, muscovite, quartz, titania, and zircon. The lithic clasts are trachytes. There are also mudstone intraclasts. The diagenetic minerals are ankerite, barite, calcite, chlorite, F-apatite, F-calcite, F-Fe-calcite,

illite, kaolinite, pyrite, titania, siderite, sphalerite, and zircon. The paragenetic sequence for this sample is tentatively interpreted as: Quartz overgrowth → Fracture → Kaolinite → Chlorite, Siderite, F-Calcite, F-Fe-Calcite, Calcite, Ankerite, Pyrite, Fluorapatite → Titania, Barite, Siderite (rims), Zircon

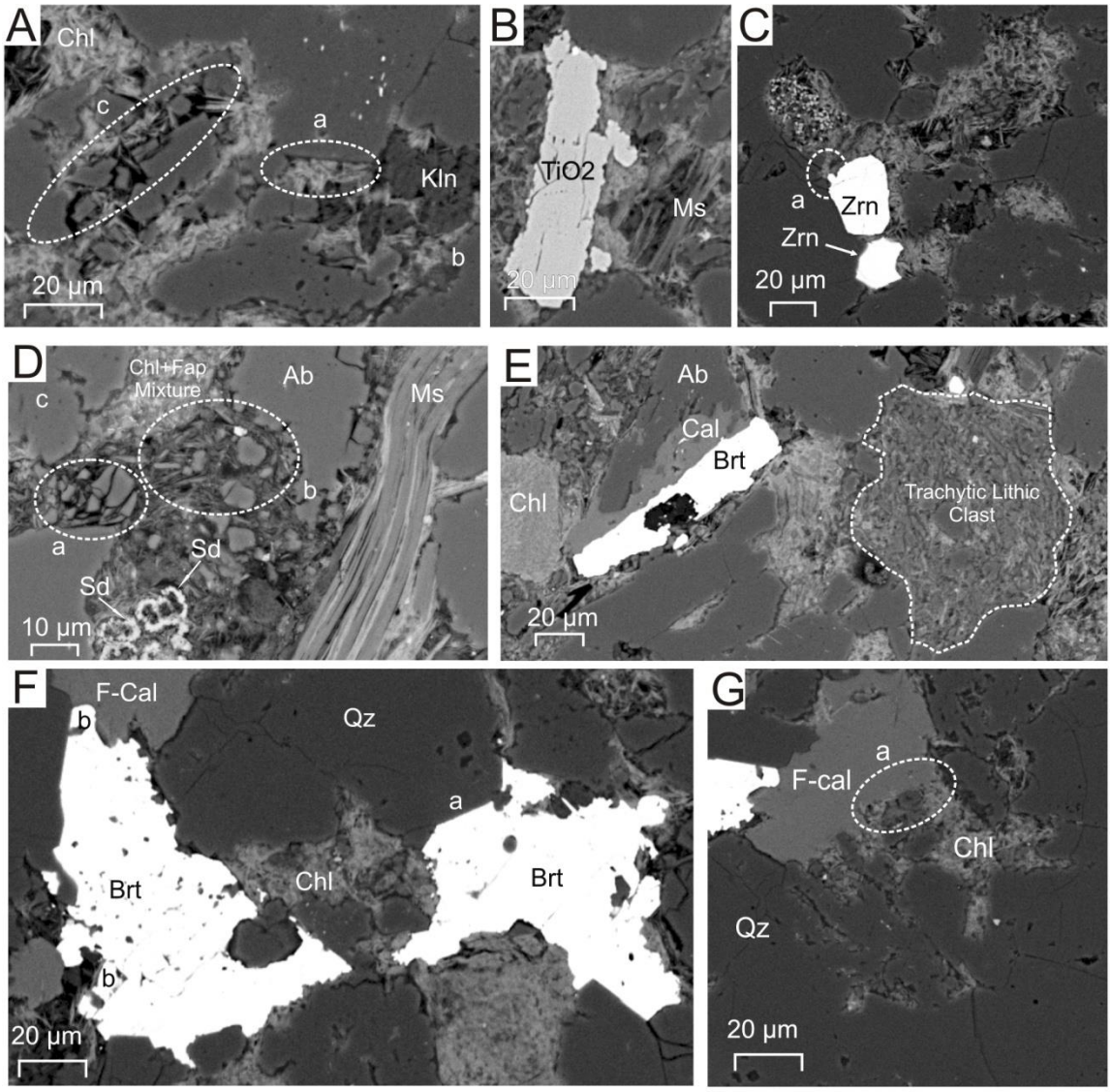

Fig. 3.12: Representative BSE images of textures and minerals from the Middle Missisauga Formation in the Newburn H-23 well (Sample 5403.6m).
A: Sample 5403.6m (App. 2-6, Fig. 3). Quartz overgrowth (position a) predates chlorite. Kaolinite fills porosity and is rimmed by chlorite (position b).Fractured quartz with fibrous chlorite partially filling voids (position c).
B: Sample 5403.6m (App. 2-6, Fig. 3). Diagenetic titania.
C: Sample 5403.6m (App. 2-6, Fig. 12). Zircon cuts quartz and probably engulfs chlorite (position a) and with euhedral crystal outlines towards both.
D: Sample 5403.6m (App. 2-6, Fig. 5). Mechanically fractured quartz (position a). Muddy matrix (position b) composed of muscovite, chlorite and quartz with late siderite rims surrounding part of this matrix. In places (position c) detrital quartz has a moderate amount of secondary porosity.
E: Sample 5403.6m (App. 2-6, Fig. 6). Albite is engulfed by calcite, which appears to be engulfed by barite. Trachytic lithic clast consists of chlorite and alkali feldspar.
F: Sample 5403.6m (App. 2-6, Fig. 10). Diagenetic barite engulfs quartz (position a) and engulfs F-calcite (position b).
G: Sample 5403.6m (App. 2-6, Fig. 10). F-calcite engulfs chlorite (position a).

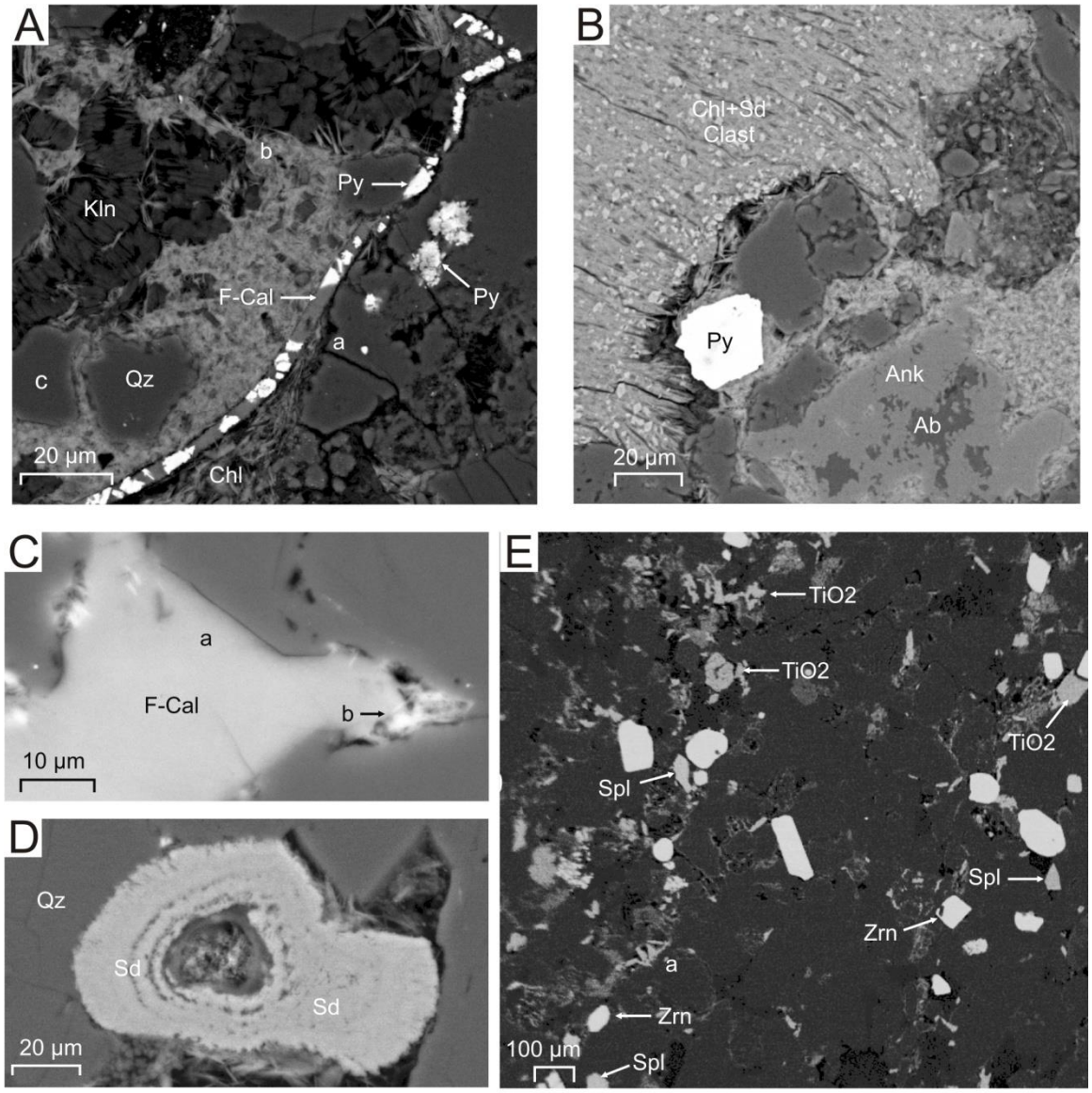

Fig. 3.13: Representative BSE images of textures and minerals from the Middle Missisauga Formation in the Newburn H-23 well (Samples 5403.6m and 5406.5m).
A: Sample 5403.6m (App. 2-6, Fig. 13). Vein filled with pyrite and F-calcite cutting through chlorite (position a). Chlorite cross-cut porous kaolinite (position b) and rims quartz grains (position c).
B: Sample 5403.6m (App. 2-6, Fig. 7). Ankerite engulfs albite and chlorite. Siderite intermixed with chlorite in a lithic clast or an intraclast.
C: Sample 5403.6m (App. 2-6, Fig. 18). F-calcite is in contact with quartz overgrowth (position a). F-calcite seems to engulf chlorite (position b).
D: Sample 5406.5m (App. 2-7, Fig. 2). Siderite concretion with a hole in the center.
E: Sample 5406.5m (App. 2-7, Fig. 10). Detrital zircon, titania, and spinel in relatively straight lines, probably along original bedding picked out by heavy minerals.

Sample 5406.5: The sidewall core description provided by the post drill analysis is of a light-brownish-white moderately well sorted very fine grained sandstone with siliceous cement. Petrographic analysis of this sample suggests that this is a well sorted fine upper subarkose (Fig. 3.2) with an average grain size of 240 μm (Table 3.1). Core analysis gives a porosity of 0.091 and a maximum permeability of 0.04 mD.

The detrital minerals in this sample are albite, spinel, muscovite, quartz, titania, tourmaline, zircon, and lithic clasts. The diagenetic minerals are ankerite, apatite, calcite, chlorite, F-apatite, glauconite, illite, kaolinite, pyrite, siderite, titania, xenotime, and zircon. The lithic clasts in this sample are trachytes.

This sample contains laminae of heavy minerals such as spinel, zircon, and titania which mark the original bedding (Fig. 3.13E). Siderite concretion fills porosity and contains a hole at its center (Fig. 3.13D). Detrital tourmaline inhibits both quartz overgrowth and the formation of diagenetic titania (Fig 3.14A). Kaolinite in this sample post-dates a major compaction event, quartz suturing (Fig. 3.14B position a), and fills pore probably near the end of the formation of quartz overgrowths (Fig. 3.14B).

Summary: The detrital minerals in this sample are albite, spinel, muscovite, quartz, titania, tourmaline, and zircon. The lithic clasts are trachytes. The diagenetic minerals are ankerite, apatite, calcite, chlorite, F-apatite, glauconite, illite, kaolinite, pyrite, siderite, titania, and zircon. The paragenetic sequence for this sample is tentatively interpreted as: Siderite (concretion.) + Glauconite → Quartz overgrowth → Kaolinite → Calcite → Chlorite → Apatite → Ankerite → Siderite (rhombohedra), Xenotime, Titania, Pyrite, Zircon.

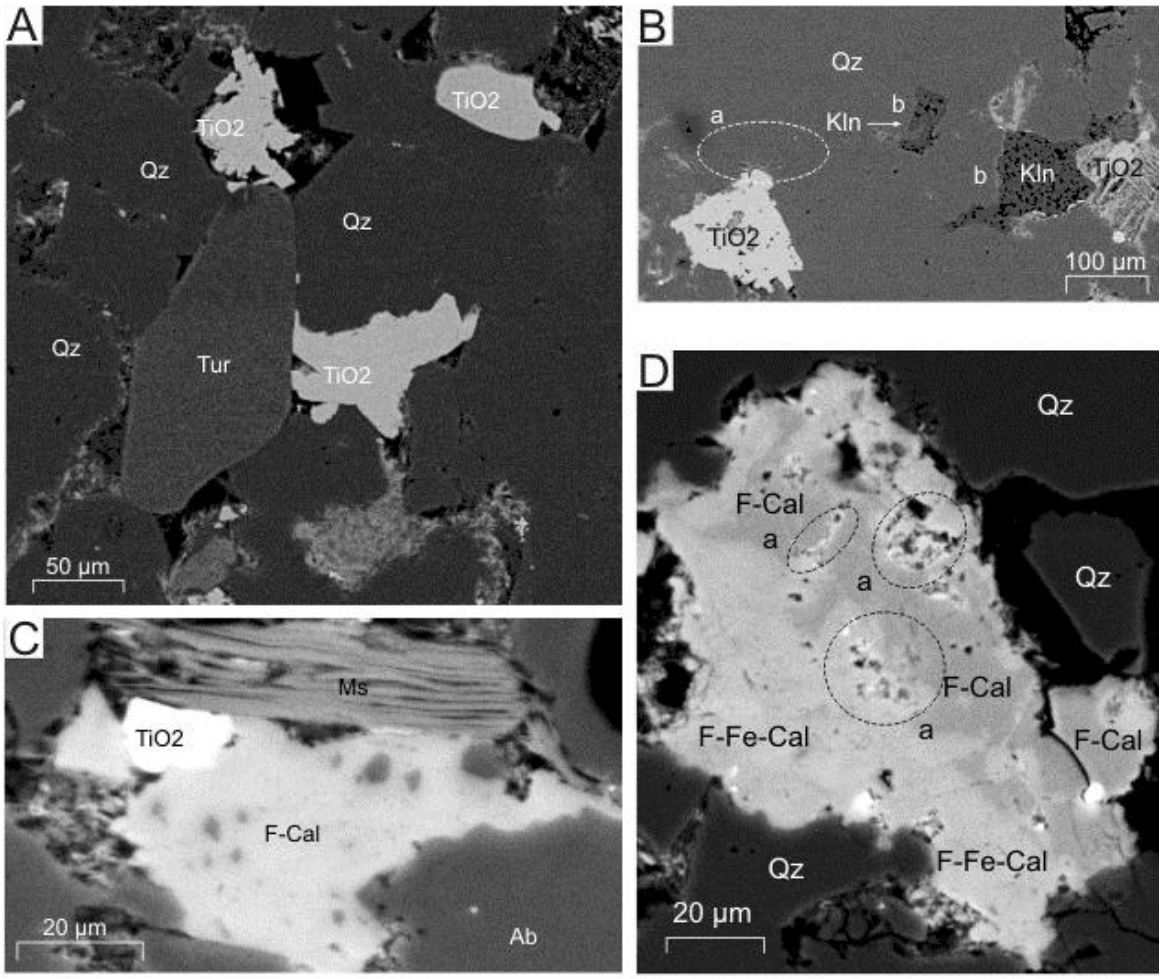

Fig. 3.14: Representative BSE images of textures and minerals from the Middle Missisauga Formation in the Newburn H-23 well (Sample 5406.5m and 5407m).
A: Sample 5406.5m (App. 2-7, Fig. 8). Detrital tourmaline grain inhibits quartz overgrowth as well as the growth of titania. Diagenetic titania with straight crystal outlines partially filling pore. Diagenetic titania engulfs quartz.
B: Sample 5406.5m (App. 2-7, Fig. 6). Kaolinite post-dates major compaction event (quartz suturing (position a)) and fills pores probably near the end of the formation of quartz overgrowths (positions b). Subhedral titania forms along intergranular boundary (or replaces framework grain), engulfs chlorite and replaces quartz.
C: Sample 5407m (App. 2-8, Fig. 14). F-calcite engulfs albite. Titania cuts F-calcite.
D: Sample 5407m (App. 2-8, Fig. 18). F-calcite replaced by lighter F-Fe-calcite. Chlorite (positions a) fills dissolution voids in F-calcite.

Sample 5407: The sidewall core description provided by the post drill analysis is of a light-brownish well sorted silty to very fine grained sandstone with silica cement. Petrographic analysis of this sample suggests that this is a well sorted fine lower sublitharenite (Fig. 3.2) with an average grain size of 96 μm (Table 3.1). Core analysis gives a porosity of 0.170 and a maximum permeability of 0.15 mD.

The detrital minerals in this sample are albite, muscovite, quartz and lithic clasts. The diagenetic minerals are ankerite, apatite, calcite, chlorite, F-apatite, F-calcite, F-Fe-calcite, illite kaolinite, pyrite, siderite, sphalerite, titania, and zircon. Lithic clasts in this sample are dominantly trachytic lithic clasts that are composed of albite.

This sample is cut by kaolinite a vein which locally corresponds to quartz overgrowths or grain boundaries (position a), kaolinite booklets (position b) are later cut by chlorite (Fig. 3.15A). F-calcite engulfs albite and is cut by titania (Fig. 3.14C). There are two types of F-calcite in this sample, F-Fe-calcite and F-calcite. The F-calcite is partially replaced by F-Fe-calcite (Fig. 3.14D). In the same figure (positions a) chlorite fills dissolution voids in F-calcite.

Summary: The detrital minerals in this sample are albite, muscovite, and quartz. The lithic clasts are trachytes. The diagenetic minerals are ankerite, apatite, calcite, chlorite, F-apatite, F-calcite, F-Fe-calcite, illite kaolinite, pyrite, siderite, sphalerite, titania, and zircon. The paragenetic sequence for this sample is tentatively interpreted as: Quartz overgrowth → Fracture → Kaolinite → Illite → F-Calcite, Calcite, Ankerite → F-Fe-Calcite, Calcite, Ankerite → Chlorite → Fluorapatite, Titania, Siderite, Sphalerite, Pyrite, Zircon.

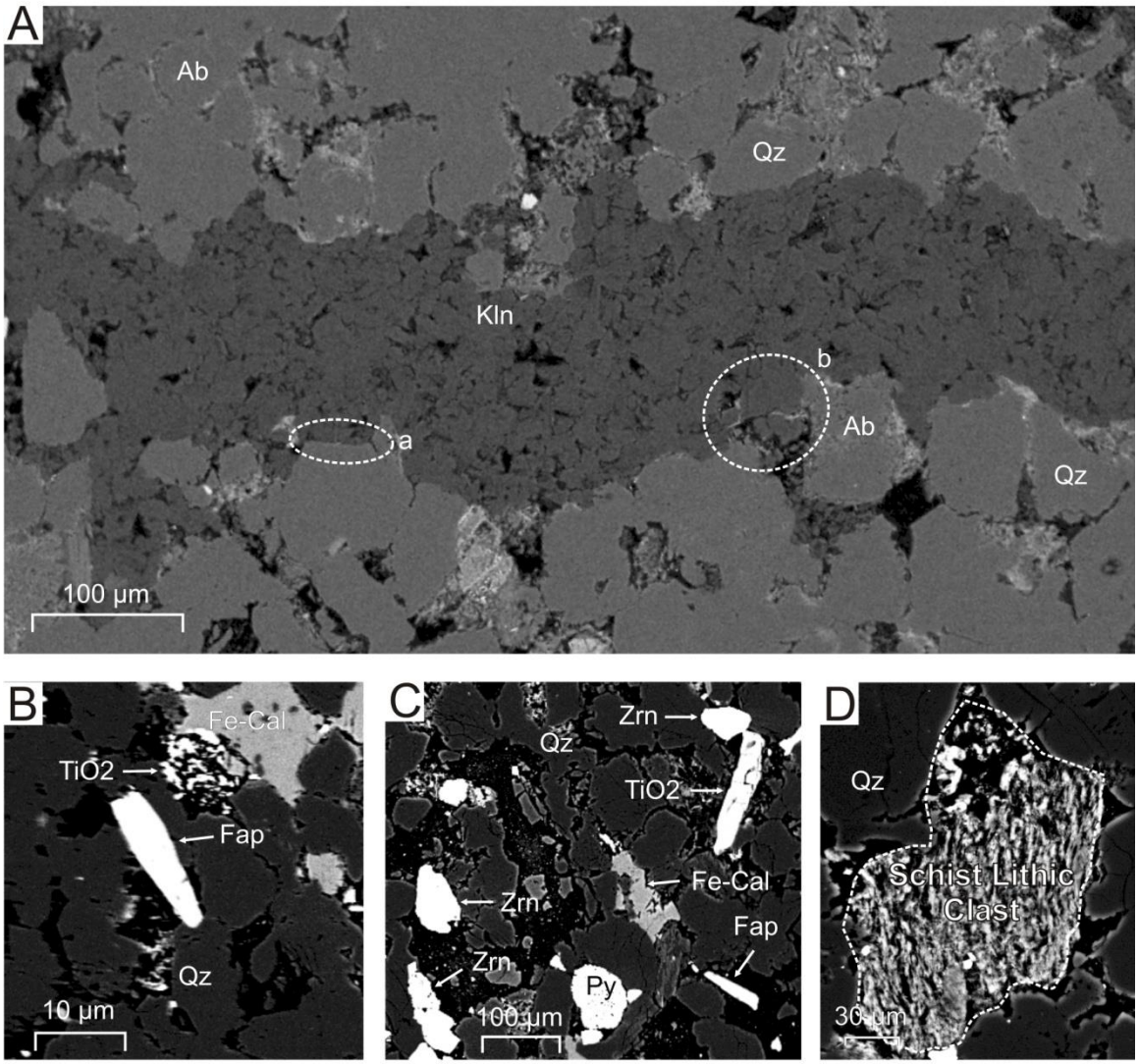

Fig. 3.15: Representative BSE images of textures and minerals from the Middle Missisauga Formation in the Newburn H-23 well (Samples 5407m and 5408.5m).
A: Sample 5407m (App. 2-8, Fig. 1). Kaolinite vein fills fracture cutting framework quartz grains. Fracture locally corresponds to quartz overgrowth or grain boundary (position a). Chlorite cuts through kaolinite booklets in vein (position b).
B: Sample 5408.5m (App. 2-9, Fig. 16). Subhedral fluorapatite cuts quartz grain and partly fills pore.
C: Sample 5408.5m (App. 2-9, Fig. 11). Diagenetic zircon fills pore and engulfs quartz. Subhedral fluorapatite partly fills pore.
D: Sample 5408.5m (App. 2-9, Fig. 14). Schist lithic clast composed of quartz, albite, and chlorite. Titania later fills dissolution voids in the clast.

Sample 5408.5: The sidewall core description provided by the post drill analysis is of a light-brownish to off-white moderately well sorted very fine to fine grained sandstone. Petrographic analysis of this sample suggests that this is a well sorted, fine grained quartz arenite (Fig. 3.2) with an average grain size of 140 μm (Table 3.1). Core analysis gives a porosity of 0.179 and a maximum permeability of 6.43 mD.

The detrital minerals in this sample are albite, spinel, oligoclase, quartz, and tourmaline. The diagenetic minerals in this sample are ankerite, apatite, barite, calcite, chlorite, Fe-calcite, F-Fe-calcite, fluorite, illite, kaolinite, pyrite, siderite, titania, and zircon. Lithic clasts in this sample include trachytes and schists composed of quartz, albite, and chlorite (Fig. 3.15F).

This sample contains diagenetic F-apatite, zircon, and titania all of which fill porosity, cut framework grains and have straight crystal outlines (Fig. 3.15B and C). Quartz overgrowths abut ankerite (App. 2-9, Fig. 4) and form in open porosity (App. 2-9, Fig. 10).

Summary: The detrital minerals in this sample are albite, chromian spinel, oligoclase, quartz, and tourmaline. The lithic clasts are trachytes and schists. The diagenetic minerals in this sample are ankerite, apatite, barite, calcite, chlorite, Fe-calcite, F-Fe-calcite, F-apatite, fluorite, illite, kaolinite, pyrite, siderite, titania, and zircon. The paragenetic sequence for this sample is tentatively interpreted as: Kaolinite + Quartz overgrowths? → Illite → Fe-Calcite (Calcite + Ankerite??) → F-Calcite (Calcite + Ankerite??) → F-Fe-Calcite (Calcite + Ankerite??) → Chlorite → Fluorapatite, Apatite, Fluorite → Siderite, Barite, Pyrite, Titania, Zircon.

3.3.4 Middle Mississauga formation (Group 2)

Sample 5957.8: The sidewall core description provided by the post drill analysis is of a grey very fine grained sandstone with calcareous cement interbedded with grey black shale. Petrographic analysis of this sample suggests that this is a well sorted very fine grained sublitharenite (Fig. 3.2) with an average grain size of 84 μm (Table 3.1). Core analysis gives a porosity fraction of 0.099 and a maximum permeability value of 0.02 mD.

The detrital minerals in this sample are albite, spinel, muscovite, quartz, titania, zircon, and lithic clasts. The diagenetic minerals in this sample are ankerite, apatite, calcite, chlorite, F-apatite, Fe-calcite, illite, kaolinite, pyrite, siderite, and titania. Lithic clasts in this sample are granitoids composed of quartz and chlorite laths (Fig. 3.16D), schists composed of chloritized muscovite and albite, later engulfed by titania (Fig. 3.16E). The mudstone intraclasts are composed of chlorite plastically deformed around framework silicates (Fig. 3.16A).

A trachytic lithic clast has illite filling dissolution voids, the illite grains appear to have formed with a preferential orientation, left to right (position a), and along crystal boundaries (position b) (Fig. 3.17E). Chlorite cuts possible coated calcite grain (Fig. 3.17F position a). Calcite fills porosity (Fig. 17A) and forms in pores and along intergranular boundaries. Calcite is rimmed by fibrous chlorite (Fig. 3.16B), and siderite engulfs chlorite and rims a pore (Fig. 16C position a). Detrital spinel grain shows corrosion and possible recrystallization forming a straight crystal edge (position c) is rimmed by chlorite (Fig. 3.17D).

Summary: The detrital minerals in this sample are albite, spinel, muscovite, quartz, titania, and zircon. The lithic clasts are trachytes and schists. The diagenetic minerals in

this sample are ankerite, apatite, calcite, chlorite, F-apatite, Fe-calcite, illite, kaolinite, pyrite, siderite, and titania. The paragenetic sequence for this sample is tentatively interpreted as: Fe-Calcite (coated grain) → Illite, Kaolinite → Ankerite, Calcite → Chlorite, Apatite + Fluorapatite → Titania, Pyrite, Siderite.

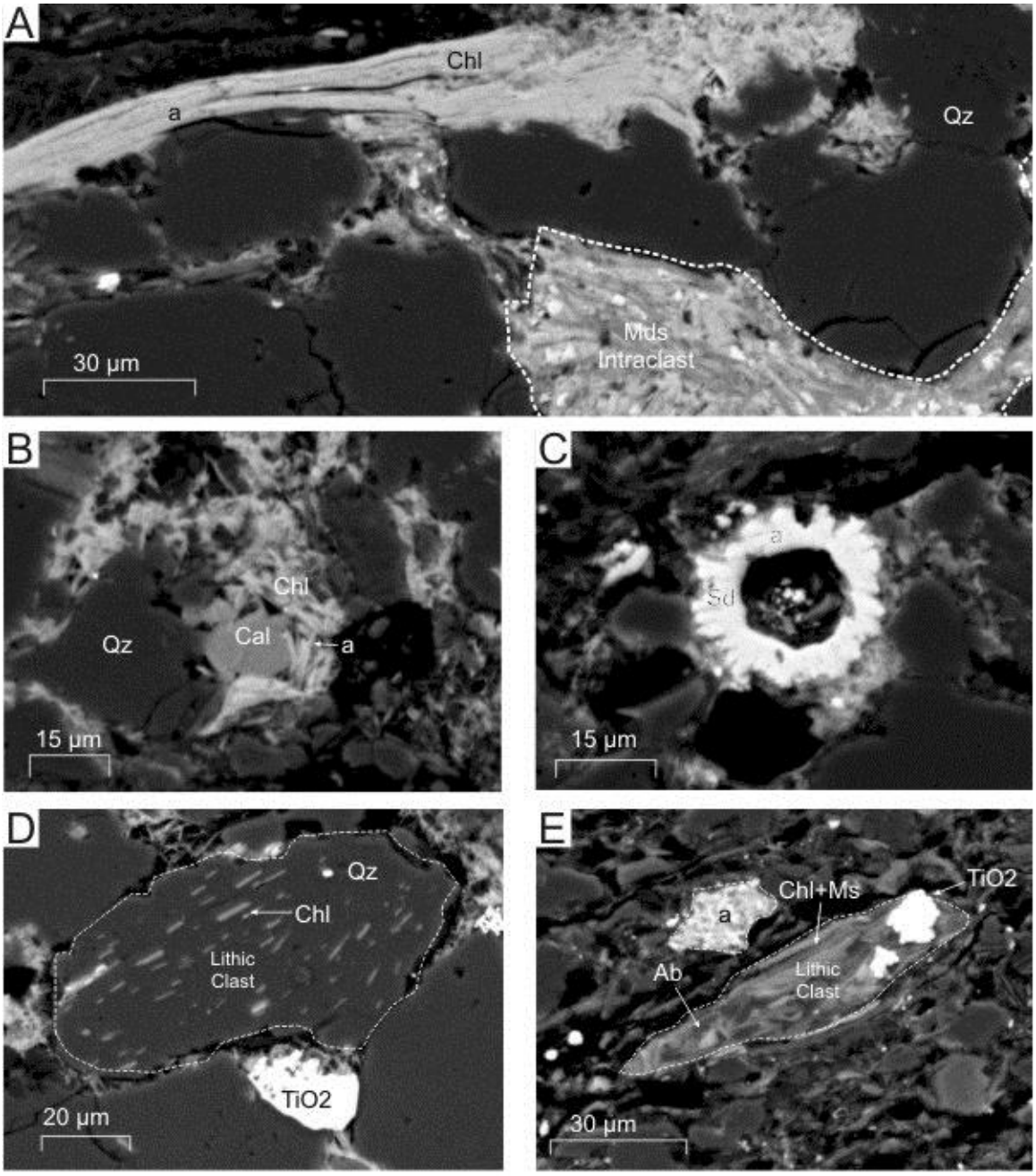

Fig. 3.16: Representative BSE images of textures and minerals from the Middle Missisauga Formation in the Newburn H-23 well (Sample 5957.8m).
A: Sample 5957.8m (App. 2-10, Fig. 4). Mudstone intraclast comprised of chlorite plastically deformed around quartz grains. Fully chloritized muscovite (position a).
B: Sample 5957.8m (App. 2-10, Fig. 4). Calcite appears to fill secondary porosity. Fibrous chlorite rims sparry calcite grain (position a).
C: Sample 5957.8m (App. 2-10, Fig. 11). Siderite engulfs chlorite, and rims a pore (position a).
D: Sample 5957.8m (App. 2-10, Fig. 8). Lithic clast composed of quartz and very minor chlorite laths.
E: Sample 5957.8m (App. 2-10, Fig. 15). Lithic clast originally composed of albite and muscovite; the muscovite has been chloritized and the albite has been partially engulfed by titania. Mud intraclast (position a).

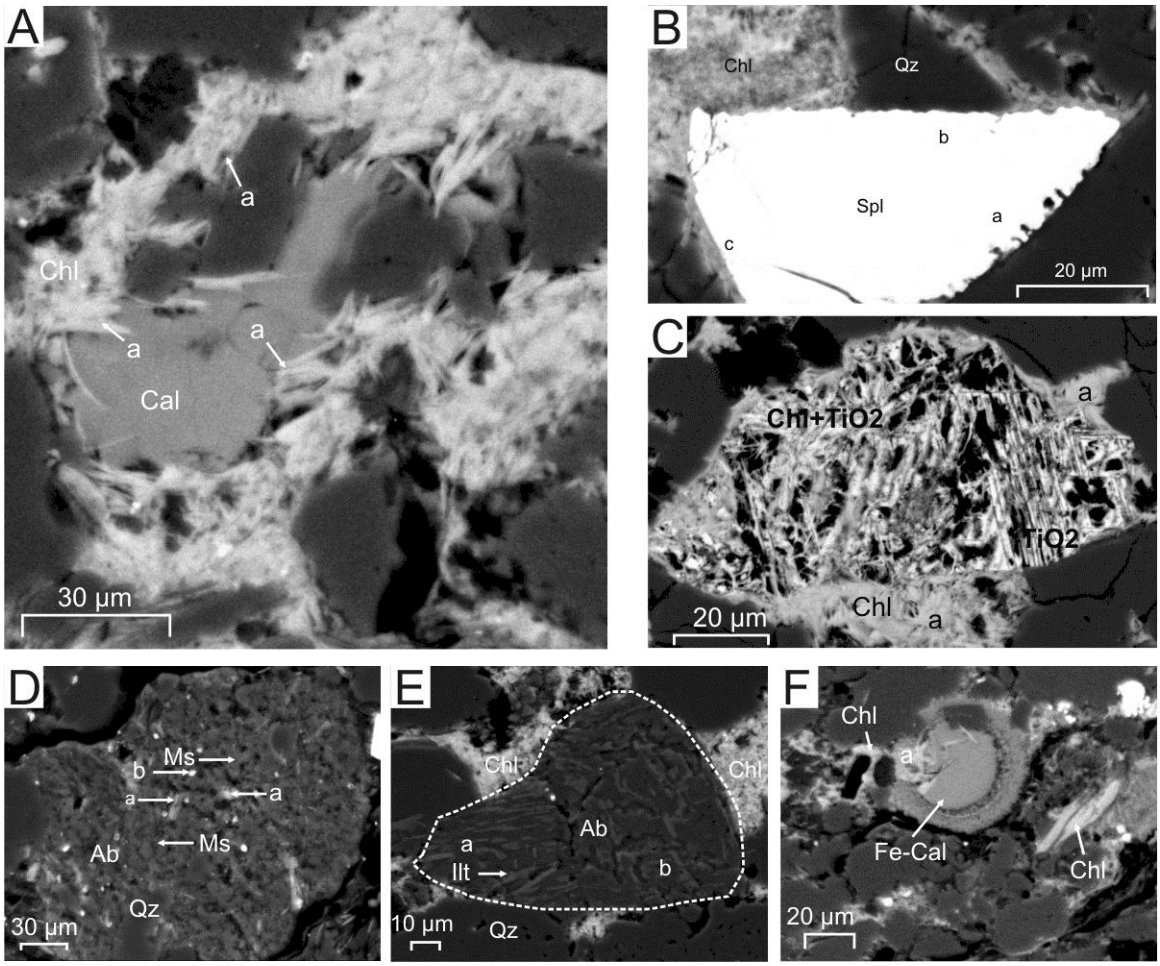

Fig. 3.17: Representative BSE images of textures and minerals from the Middle Missisauga Formation in the Newburn H-23 well (Sample 5957.8m).
A: Sample 5957.8m (App. 2-10, Fig. 7). Fibrous chlorite engulfs calcite (position a).
B: Sample 5957.8m (App. 2-10, Fig. 5). Chlorite fills pores and intergranular boundaries. Detrital spinel grain has been corroded (position a,b). Straight euhedral edge, probably protected from corrosion, is rimmed by chlorite (position c).
C: Sample 5957.8m (App. 2-10, Fig. 10). Chlorite rims (position a) and cuts detrital titania which has been partly dissolved, leaving high secondary porosity.
D: Sample 5957.8m (App. 2-10, Fig. 18). Granitic lithic clast composed of albite, quartz and muscovite. The muscovite appears to have altered to produce chlorite (positions a) and illite (position b).
E: Sample 5957.8m (App. 2-10, Fig. 6). Trachytic lithic clast composed of albite laths with dissolution voids filled by illite with what appears to be a preferential orientation left to right (position a) and along crystal boundaries (position b).
F: Sample 5957.8m (App. 2-10, Fig. 19). Possible coated grain of Fe-calcite cut by chlorite (position a).

Sample 5961.7: The sidewall core description provided by the post drill analysis is of a grey sandstone with calcareous cement and shale stringer. Petrographic analysis of this sample suggests that this is a well sorted fine grained quartzarenite (Fig. 3.2) with an average grain size of 100 μm (Table 3.1).Core analysis gives a porosity of 0.127 and a maximum permeability of 0.03 mD.

The detrital minerals in this sample are albite, muscovite, quartz, titania, zircon, and lithic clasts. The diagenetic minerals in this sample are Al-phosphate, ankerite, apatite, calcite, chlorite, Fe-calcite, F-apatite, pyrite, siderite, sphalerite, titania, and zircon. The lithic clasts in this sample are trachytes and probable pumice clasts which are later altered to chlorite, and rarely contain albite with later siderite infilling preserved porosity (Fig. 3.18C and D).

This sample contains detrital zircon which has dissolution and straight crystal outline recrystallized in contact with kaolinite filling pore (Fig. 3.18A and 18F) and is slightly lobate (Fig. 3.18F position a). Pyrite and chlorite have formed along the cleavage planes of a possibly plucked out muscovite grain (Fig. 3.18A position a). Ankerite replacing quartz, with calcite either as replacement, relic, or filling of a dissolution void (Fig. 3.18A position a). Another grain of ankerite contains Fe-calcite with another unclear age relationship (Fig. 3.19A). The sample also contains framboidal pyrite (Fig. 3.19B), as well as pyrite which appears to pseudomorph muscovite (Fig. 3.19C). Al-phosphate inhibits quartz overgrowth and fills porosity (Fig. 3.18E) although it may be contamination. A grain of detrital titania is ragged and rimmed by chlorite (Fig. 3.18B).
Summary: The detrital minerals in this sample are albite, muscovite, quartz, titania, and zircon. The lithic clasts are mostly trachytes with probable altered pumice clasts. The diagenetic minerals in this sample are Al-phosphate, ankerite, apatite, calcite, chlorite, Fe-

calcite, F-apatite, pyrite, siderite, sphalerite, titania, and zircon. The paragenetic sequence for this sample is tentatively interpreted as: Al-phosphate? → Quartz overgrowth → Kaolinite → Chlorite → Apatite + Fluorapatite → Calcite → Ankerite → Fe-Calcite → Siderite, Titania, Sphalerite, Pyrite, Zircon.

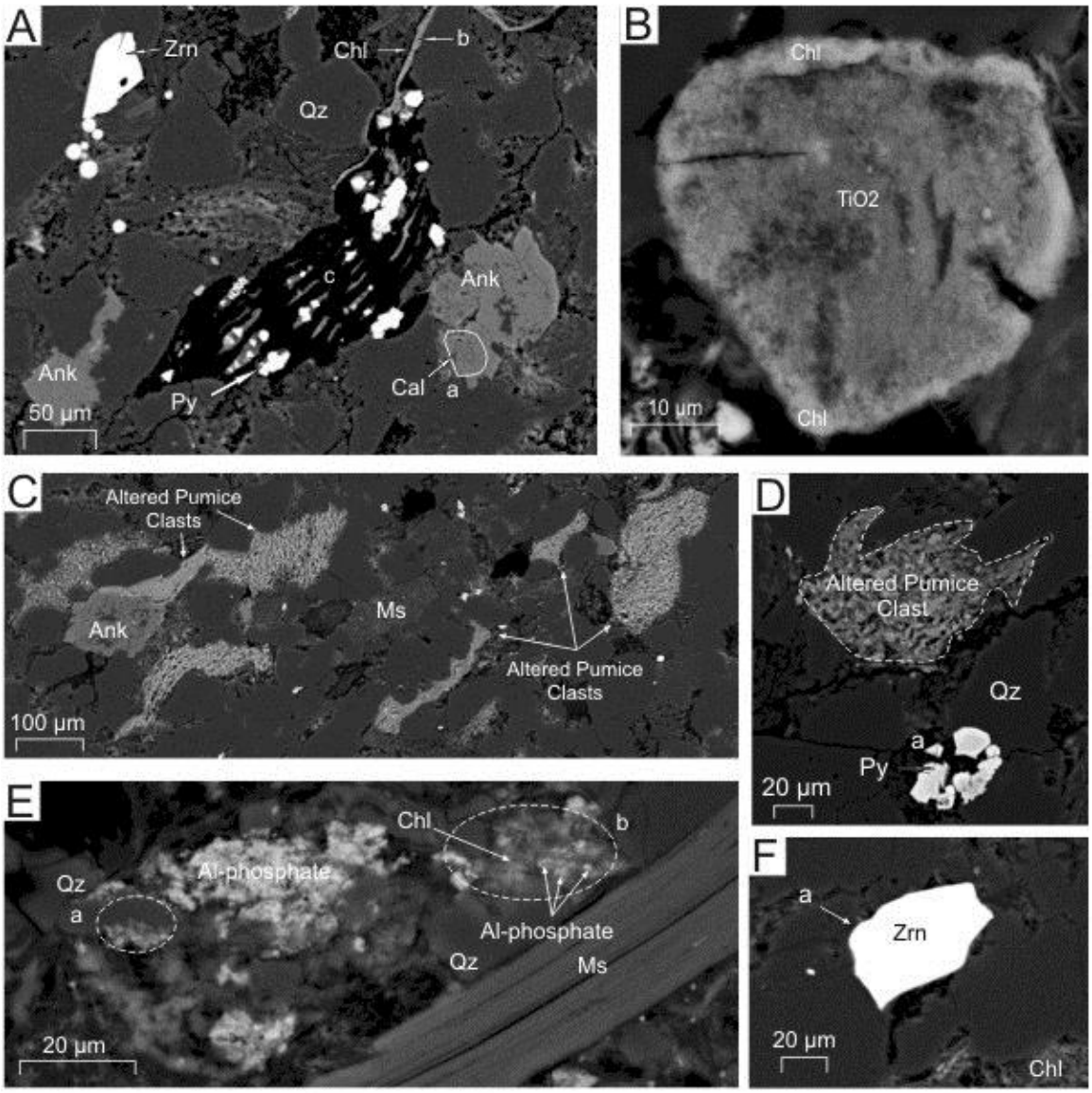

Fig. 3.18: Representative BSE images of textures and minerals from the Middle Missisauga Formation in the Newburn H-23 well (Sample 5961.7m).
A: Sample 5961.7m (App. 2-11, Fig. 4). Probably a detrital zircon with dissolution void and straight crystal outline recrystalized in contact with kaolinite filling pore. Ankerite associated with quartz and calcite (position a). Plastically deformed muscovite which has been completely chloritized (position b). Pyrite and chlorite form along cleavage planes of probably plucked out muscovite grain (position c).
B: Sample 5961.7m (App. 2-11, Fig. 21). Ragged detrital titania partially dissolved and is rimmed by later chlorite.
C: Sample 5961.7m (App. 2-11, Fig. 2). Probable pumice clasts which have altered, producing chlorite and have later been deformed. .
D: Sample 5961.7m (App. 2-11, Fig. 14). Probably an altered pumice clast, comprised of chlorite and albite, and with later siderite filling open preserved porosity. Pyrite crystalites partially fill a pore (position a).
E: Sample 5961.7m (App. 2-11, Fig. 8). Al-phosphate appears to inhibit quartz overgrowth (position a) and to be cut by chlorite (position b), however it may be contamination.
F: Sample 5961.7m (App. 2-11, Fig. 9). Zircon appears to be diagenetic with straight crystal outlines in contact with quartz and pore and is slightly lobate (position a).

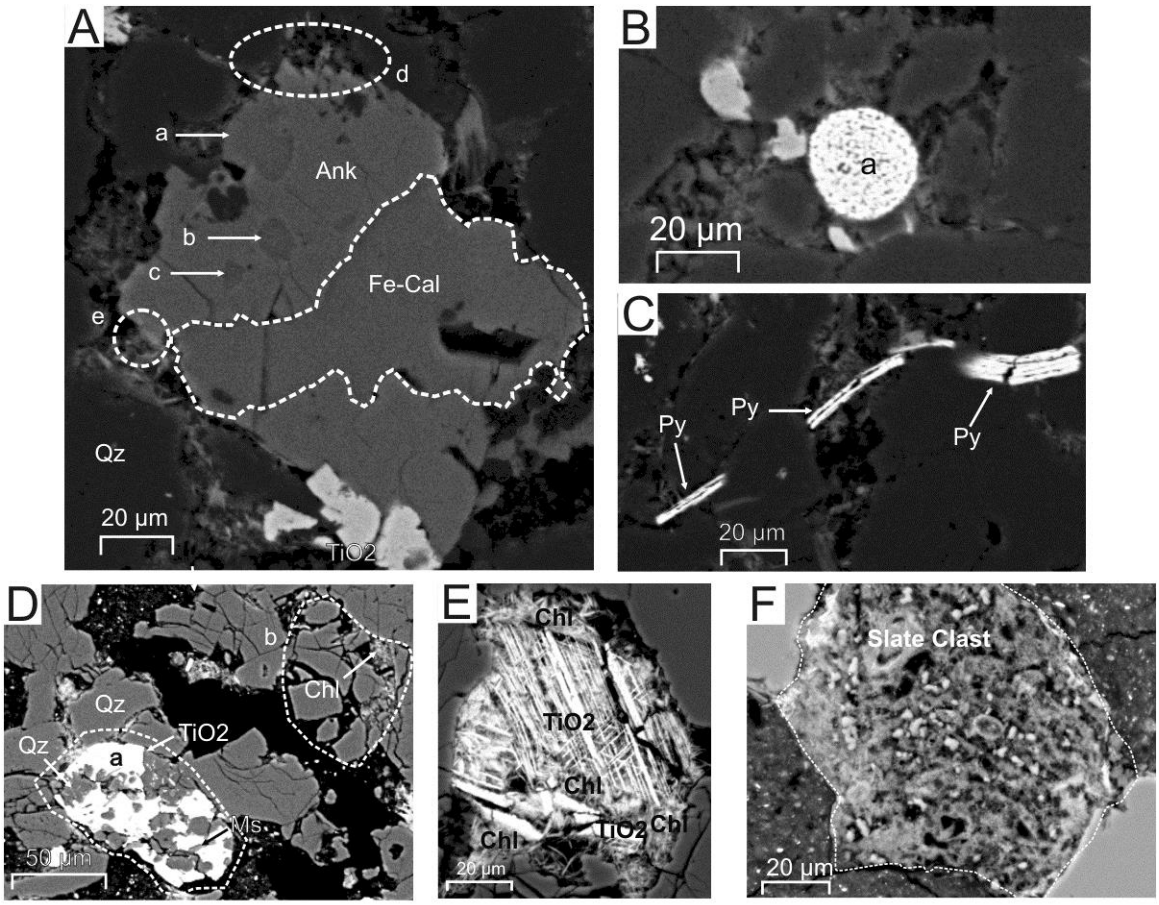

Fig. 3.19: Representative BSE images of textures and minerals from the Middle Missisauga Formation in the Newburn H-23 well (Samples 5961.7m and 5962m).
A: Sample 5961.7m (App. 2-11, Fig. 15). Fe-calcite (positions a,b,c) in ankerite with unclear age relationship. Ankerite engulfs kaolinite (position d) and chlorite (position e) fills pore.
B: Sample 5961.7m (App. 2-11, Fig. 12). Framboidal pyrite (position a).
C: Sample 5961.7m (App. 2-11, Fig. 13). Pyrite appears to have pseudomorphed muscovite.
D: Sample 5962m (App. 2-12, Fig. 1). Lithic clast (position a) composed of quartz muscovite and titania. Mechanically fractured quartz (position b) with chlorite filling pore.
E: Sample 5962m (App. 2-12, Fig. 10). Detrital Titania with trellis structure surrounded by chlorite.
F: Sample 5962m (App. 2-12, Fig. 21). Slate clast composed of muscovite, quartz, and chlorite.

Sample 5962: The sidewall core description provided by the post drill analysis is of a grey, very fine to fine grained sandstone with calcareous and siliceous cement and minor carbonaceous laminations. Petrographic analysis of this sample suggests that this is a well sorted fine lower sublitharenite (Fig. 3.2) with an average grain size of 160 μm (Table 3.1). Core analysis gives a porosity of 0.088 and a maximum permeability of less than 0.01 mD.

The detrital grains in this sample are albite, spinel, K-feldspar, muscovite, quartz, titania, zircon, probably monazite, and lithic clasts. The diagenetic minerals in this sample are ankerite, apatite, barite, calcite, chlorite, Fe-calcite, F-apatite, fluorite, illite, kaolinite, Mg-calcite, pyrite, siderite, titania, and zircon. Lithic clasts in this sample are composed of titania and quartz (Fig. 3.19D), quartz and muscovite as slate (Fig. 3.19F), and albite in trachytes. There is also a probable pumice clast, which has altered producing fibrous chlorite and was later compacted (Fig. 3.22A-C).

This sample contains a possible pellet that consists of sparry calcite and Fe-calcite which has partially recrystallized and engulfed illite, chlorite, and kaolinite (Fig. 3.20A position a). It also contains a detrital titania grain with a trellis structure that has been surrounded by later chlorite (Fig. 3.19E). Porosity in this sample is filled by ankerite (Fig. 3.20E), kaolinite, and chlorite (Fig. 3.20D). A rosset of siderite has a central pore and engulfs chlorite and ankerite (Fig. 3.20E). There is abundant diagenetic zircon which cuts framework silicate grains and fills porosity (Fig. 3.20B and C). There is evidence of mechanically fractured quartz with fibrous chlorite filling pores generated by the fracturing grains (Fig. 3.22A position c). Ankerite which fills porosity is partially replaced by Fe-calcite and contains dissolution voids (Fig. 3.21B). Fe-calcite surrounds dissolution voids filled with chlorite and illite, the relative age however is unclear (Fig.

3.21B position a). Kaolinite forms along intergranular boundaries of framework grains and contains traces of monazite (Fig. 3.21A), it is indeterminate whether this monazite is detrital or diagenetic however, since monazite has been observed to be detrital in another sample in this well (Sample 4353.5m) it is probably also detrital in this sample.

Summary: The detrital minerals in this sample are albite, spinel, K-feldspar, probable monazite, muscovite, quartz, titania, and zircon. The lithic clasts are trachytes, slate, and an altered pumice clast. The diagenetic minerals in this sample are ankerite, apatite, barite, calcite, chlorite, Fe-calcite, F-apatite, fluorite, illite, kaolinite, Mg-calcite, pyrite, siderite, titania, and zircon. The paragenetic sequence for this sample is tentatively interpreted as: Quartz overgrowth + Fracture → Kaolinite, Illite → Chlorite → Fluorapatite + Apatite + Fluorite + Ankerite → Calcite → Fe-Calcite → Barite, Titania, Pyrite, Siderite, Calcite (Sparry), Zircon.

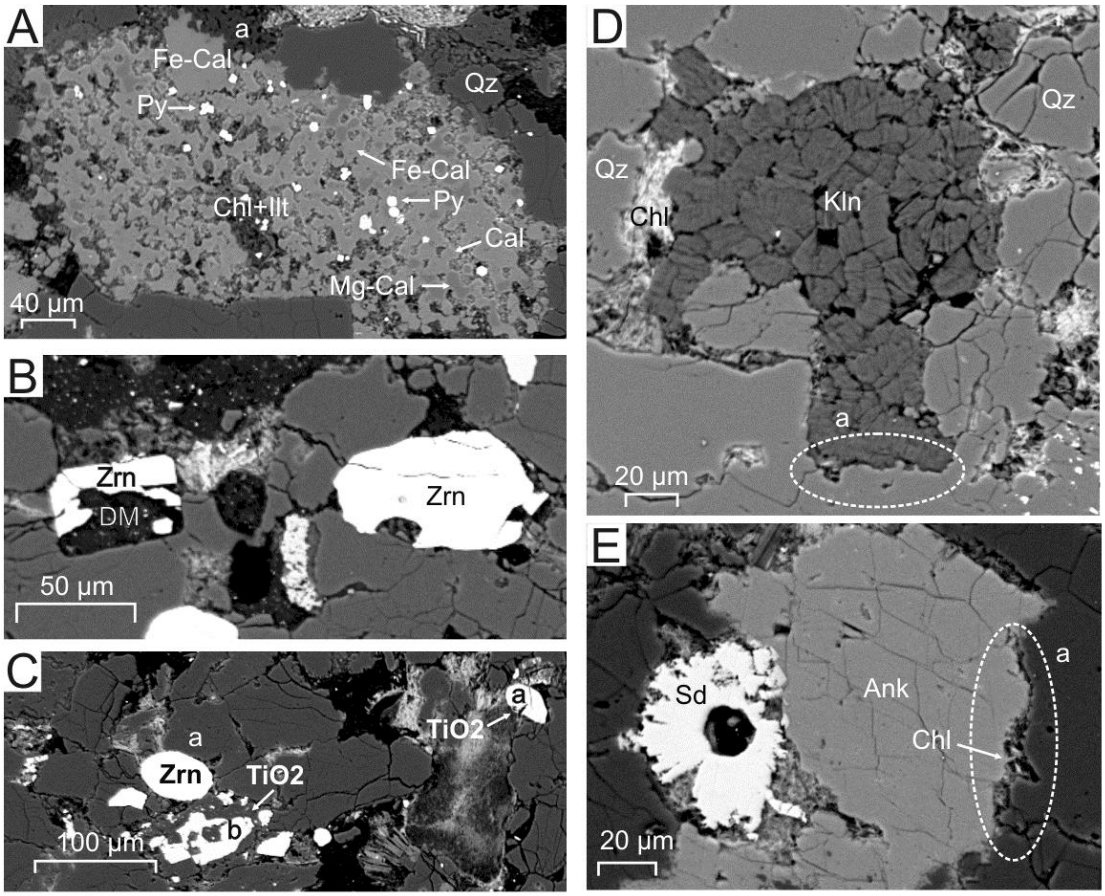

Fig. 3.20: Representative BSE images of textures and minerals from the Middle Missisauga Formation in the Newburn H-23 well (Sample 5962m).
A: Sample 5962m (App. 2-12, Fig. 6). Sparry calcite and Fe-calcite engulf chlorite and illite as well as kaolinite (position a). This may be an original pellet.
B: Sample 5962m (App. 2-12, Fig. 2). Diagenetic zircon and drilling mud fill porosity.
C: Sample 5962m (App. 2-12, Fig. 12). Detrital titania and zircon (positions a). Diagenetic titania engulfs quartz (position b).
D: Sample 5962m (App. 2-12, Fig. 14). Kaolinite booklets fill pore and engulf quartz (position a).
E: Sample 5962m (App. 2-12, Fig. 17). Rosette of siderite has a central pore and engulfs chlorite and ankerite. Fibrous chlorite fills intergranular boundary between ankerite and quartz (position a).

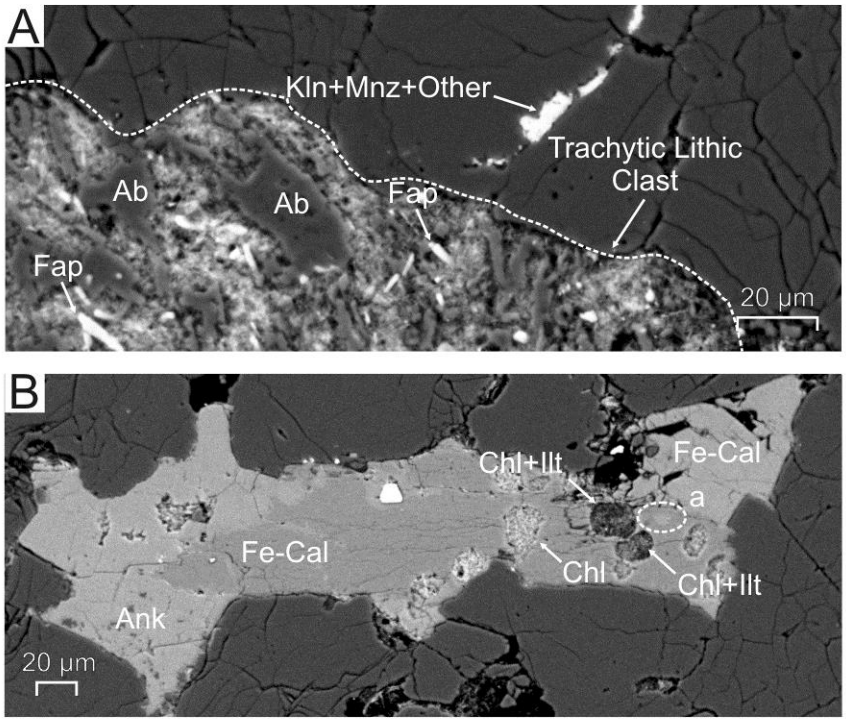

Fig. 3.21: Representative BSE images of textures and minerals from the Middle Missisauga Formation in the Newburn H-23 well (Sample 5962m).
A: Sample 5962m (App. 2-12, Fig. 11). Kaolinite forms along an intergranular boundary and contains traces of monazite. Trachytic lithic clast is composed mostly of albite. Chlorite and fluorapatite fills dissolution voids in this clast.
B: Sample 5962m (App. 2-12, Fig. 8). Ankerite has been partially replaced by Fe-calcite and contains dissolution voids. Fe-calcite surrounds dissolution voids filled with chlorite and illite (position a) but relative age is unclear.

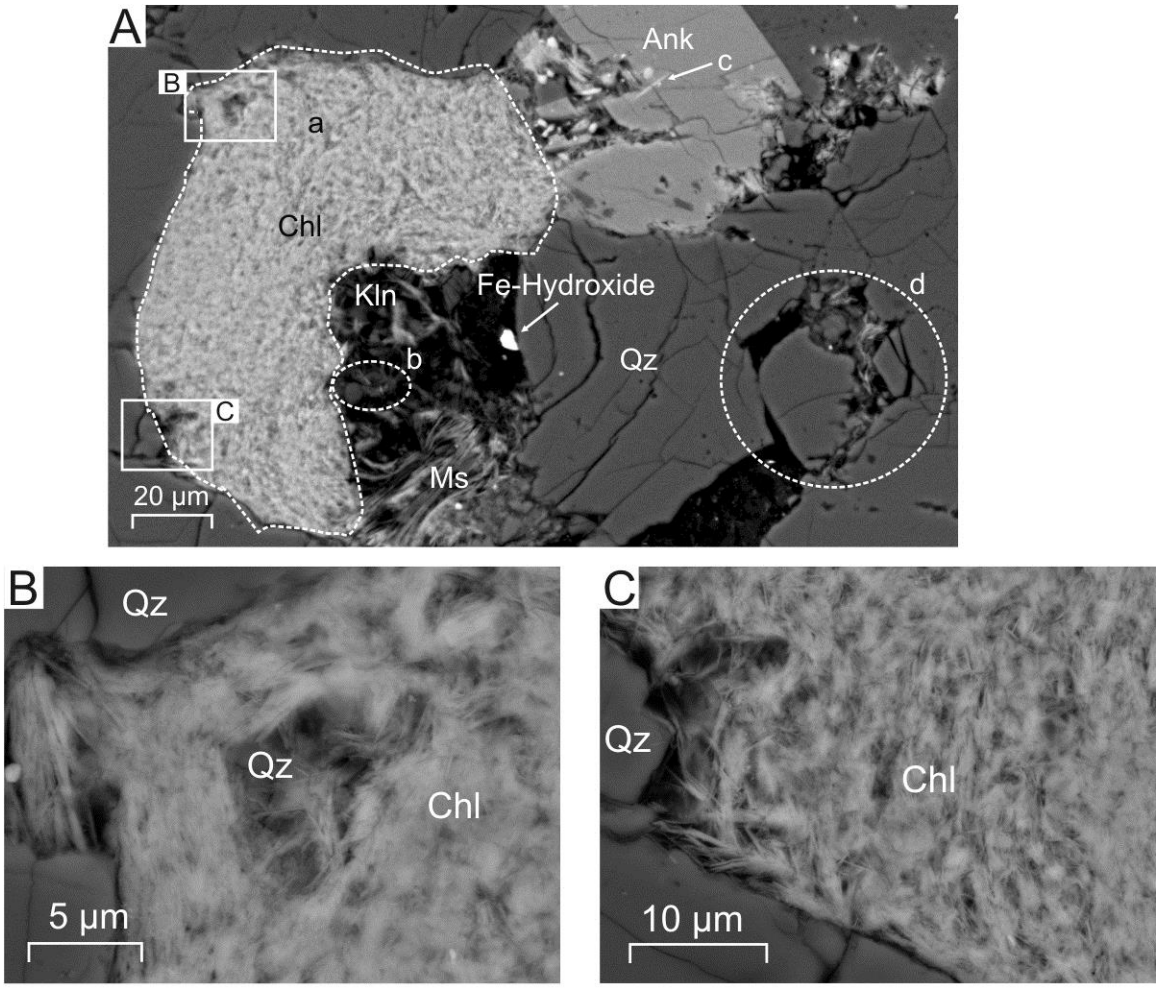

Fig. 3.22: Representative BSE images of textures and minerals from the Middle Missisauga Formation in the Newburn H-23 well (Sample 5962m).
A: Sample 5962m (App. 2-12, Fig. 5). Probable pumice clast (position a) which has altered to fibrous chlorite. Fe-Hydroxide in void surrounded by drilling mud. Chlorite cuts kaolinite booklets (postion b) and ankerite (position c). Mechanically fractured quartz (position d). Fibrous chlorite fills pore generated after fracturing of quartz (position d).
B: Sample 5962m (App. 2-12, Fig. 24). Fibrous chlorite from an altered pumice clast appears to engulf a fragment from the surrounding quartz grains.
C: Sample 5962m (App. 2-12, Fig. 25) Magnified BSE image of App. 2-12, Fig. 5. Fibrous chlorite appears to be from an altered pumice clast, which was later compacted.

Chapter 4: Discussion

4.1 Provenance

The study of provenance uses detrital minerals and lithic clasts to attempt to determine the source of sedimentary rocks. To this end detrital minerals and lithic clasts from the Newburn H-23 well have been compared to other wells in the Sable Sub-basin to determine potential sources.

4.1.1 Detrital minerals

The data obtained from SEM BSE images and EDS chemical analyses of the cuttings samples using polished mounts of heavy mineral separation (pmhm) and polished thin sections (pts) from sidewall cores are summarized in Table 4.1, and have been used to determine detrital mineral assemblages for the Newburn H-23. Additionally heavy minerals grains have been counted in SEM BSE images (Table 4.2), during bulk rock point counting (Table 2.1), and as independent detrital mineral point counting (Table 4.4A) to show how the proportions of heavy detrital minerals change with depth. The heavy detrital minerals in this well include spinel, zircon, titania, and tourmaline. The analyzed samples from this well are quartz rich sandstones and so the majority of point counted grains are quartz, to better observe the heavy detrital mineralogy in the samples, the results of the bulk rock point counting (Table 2.1) have been recalculated to exclude quartz, feldspars, and muscovite (Table 4.3). The independent detrital mineral point counting (Table 4.4A) has only been recalculated to exclude quartz so that feldspars and muscovite can also be observed with depth (Table 4.4B).

It should be noted that the counts represented in figures 4.1-4.3, based on tables 4.2-4.4, are based on only the small number of certain specific heavy minerals

encountered during point counting. Because of the small numbers, differences between samples may not be significant.

The different types of lithic clasts have also been recorded, their lithologies identified, and the detrital mineral assemblages have been compared with other assemblages found in wells drilled in the Sable Sub-basin.

Table 4.1: Summary of petrography from all samples (Sidewall cores and cuttings) based on BSE images.

Well	Depth (m)	Sample Type	Stratigraphic Level	Appendix	Detrital Mineral Present[1]	Diagenetic Mineral Present[1]	Contaminants
Newburn H-23	4300	cutting, grain mount	Cree	1-1	Ab, Bt, Spl, Di, Hbl, Ilm, Kfs, Ms, Qz, TiO2, Tur, Zrn	Brt, Chl, Ep, Fap, Fe-Dol, Fl, Gth, Hem, Lm, Py, Sd	Cpy, Mag, Ps
Newburn H-23	4315	cutting, grain mount	Cree	1-2	Ab, Spl, Ms, Qz, Zrn	Ap, Brt, Gth, Kln, Lm, Py, Sd	Ps
Newburn H-23	5950	cutting, grain mount	Middle Missauga	1-3	Act, Bt, Kfs, Lbd, Mag, Ms, Qz, TiO2, Zrn	Brt, Chl, Dol, Fl, Lm, Py, TiO2, Sd	Mag, Ps
Newburn H-23	5965	cutting, grain mount	Middle Missauga	1-4	Ab, Ilm, Mag, Ms, Qz, TiO2, Tur	Ank, Brt, Cal, Chl, Fl, Hem, Lm, Py, Sd	Apy, Cv, Ps
Newburn H-23	5975	cutting, grain mount	Middle Missauga	1-5	Ab, Hbl, Kfs, Ms, Qz, TiO2, Tur	Ank, Ap, Brt, Cal, Chl, Dol, Py, Fap, Fl, Lm, Sd	Cpy, Mag, Ps
Newburn H-23	4313.5	core thin section	Cree	2-1	Ab, Kfs, Ms, Mzn, Oli, Qz, TiO2, Zrn	Ank, Ap, Brt, Cal, Chl, Fap, Ilt, Kln, Mg-Sd, Sd, Sp, TiO2, Zrn	
Newburn H-23	4318.5	core thin section	Cree	2-2	Ab, Spl, Kfs, Ms, Oli, Qz, Zrn	Ap, Brt, Chl, Fap, Hm, Ilt, Kln, Py, TiO2, Sd, Zrn	
Newburn H-23	4353.5	core thin section	Cree	2-3	Ab, Spl, Kfs, Ms, Qz,	Ank, Cal, Chl, Fap, F-Cal, Fe-Cal, F-Fe-Cal, Glt, Kln, Py, TiO2, Zrn	
Newburn H-23	4913.8	core thin section	Upper Missisauga	2-4	Ab, Ms, Oli, Qz	Ank, Ap, Brt, Cal, Chl, Fap, Kln, Py, Sd, Sp, TiO2, Xtm, Zrn	
Newburn H-23	5213.5	core thin section	Middle Missauga	2-5	Ab, Spl, Ms, Qz, Zrn	Ank, Ap, Brt, Cal, Chl, Fap, F-Cal, Fe-Cal, F-Fe-Cal, Kln, Py, TiO2, Zrn	
Newburn H-23	5403.6	core thin section	Middle Missauga	2-6	Ab, Kfs, Ms, Qz, TiO2, Zrn	Ank, Brt, Cal, Chl, Fap, F-Cal, F-Fe-Cal Ilt, Kln, Py, TiO2, Sd, Sp, Zrn	
Newburn H-23	5406.5	core thin section	Middle Missauga	2-7	Ab, Spl, Ms, Qz, TiO2, Tur, Zrn	Ank, Ap, Cal, Chl, Fap, Glt, Ilt, Kln, Py, Sd, TiO2, Zrn	
Newburn H-23	5407.0	core thin section	Middle Missauga	2-8	Ab, Ms, Qz	Ank, Ap, Cal, Chl, Fap, F-Cal, F-Fe-Cal, Ilt, Kln, Py, Sd, Sp, TiO2, Zrn	
Newburn H-23	5408.5	core thin section	Middle Missauga	2-9	Ab, Cr-Spl, Oli, Qz, Tur	Ank, Ap, Brt, Cal, Chl, Fap, Fe-Cal, F-Fe-Cal, Fl, Ilt, Kln, Py, Sd, TiO2, Zrn	
Newburn H-23	5957.8	core thin section	Middle Missauga	2-10	Ab, Spl, Ms, Qz, TiO2, Zrn	Ank, Ap, Cal, Chl, Fap, Fe-Cal, Ilt, Kln, Py, Sd, TiO2	
Newburn H-23	5961.7	core thin section	Middle Missauga	2-11	Ab, Ms, Qz, TiO2, Zrn	Al-PO4, Ank, Ap, Cal, Chl, Fe-Cal, Fap, Py, Sd, Sp, TiO2, Zrn	
Newburn H-23	5962	core thin section	Middle Missauga	2-12	Ab, Spl, Kfs, Mnz?, Ms, Qz, TiO2, Zrn	Ank, Ap, Brt, Cal, Chl, Fe-Cal, Fap, Fl, Ilt, Kln, Mg-Cal, Py, Sd, TiO2, Zrn	

Note: 1 Ab=ablite, Al-PO4=aluminophosphate, Ank=ankerite, Ap=apatite, Apy=arsenopyrite, Brt=barite, Bt=biotite, Cal=calcite, Chl=chlorite, Cpy=chalcopyrite, Cr-Spl=chromian spinel, Cv=covelite, Di=diopside, Dol=dolomite, Ep=epidote, Fap=fluorapatite, F-Cal=fluorine calcite, Fe-Cal=ferroan calcite, F-Fe-Cal=ferroan flourine calcite Fl=fluorite, Glt=glauconite, Gth=goethite, Hbl=hornblende, Hem=hematite, Ilm=ilmanite, Ilt=illite, Kfs=k-feldspar, Kln=kaolinite, Lbd=labrodorite, Mag=magnetite, Mg-Sd=Mg-siderite, Ms=muscovite, Mzn=monazite, Oli=oligoclase, Ps=psilomelane, Py=pyrite, Qz=quartz, Sd=siderite, Spl=spinel, TiO2=titania, Tur=tourmaline, Xtm=xenotime, Zrn=zircon

Table 4.2: Detrital heavy mineral point counting based on BSE images from Pts. Table shows counts of detrital spinel, titania minerals, tourmaline, and zircon from BSE images. Counts have been normalized to show percentages.

Well Name		Total heavy minerals grains	Titania	Zircon	Spinel	Tourmaline
H-23 4313.5	Count	5	3	2		
	Percentage	100	60	40		
H-23 4318.5	Count	8	1	4	3	
	Percentage	100	12.5	50	37.5	
H-23 4353.5	Count	1			1	
	Percentage	100			100	
H-23 4913.8	Count	0				
	Percentage	0				
H-23 5213.5	Count	4	1	2	1	
	Percentage	100	25	50	25	
H-23 5403.6	Count	0				
	Percentage	0				
H-23 5406.5	Count	61	8	33	16	4
	Percentage	100	13	54	26	7
H-23 5407	Count	4		4		
	Percentage	100		100		
H-23 5408.5	Count	6	2	1	2	1
	Percentage	100	33	17	33	17
H-23 5957.8	Count	3	1	1	1	
	Percentage	100	33	33	33	
H-23 5961.7	Count	5	3	2		
	Percentage	100	60	40		
H-23 5962	Count	6	3	2	1	
	Percentage	100	50	33	17	

Table 4.3: Normalized data from standard point counting of 600 grains using the petrographic microscope for modal composition (Table 3.1) to show only heavy minerals point counted.

Sample Depth		Total % HM grains	Spinel	Titania	Tourmaline	Zircon
4313.5	Total %	0.3				0.3
	Normalized %	100				100
4318.5	Total %	0				
	Normalized %	0				
*4353.5	Total %	0				
	Normalized %	0				
4353.5 Repeat	Total %	0				
	Normalized %	0				
4913.8	Total %	0.4			0.2	0.2
	Normalized %	100			50	50
*5213.5	Total %	0				
	Normalized %	0				
5213.5 Repeat	Total %	0.5		0.2		0.3
	Normalized %	100		40		60
5403.6	Total %	0.2				0.2
	Normalized %	100				100
5406.5	Total %	1.1	0.3	0.5		0.3
	Normalized %	100	27	45		27
5407	Total %	0.2			0.2	
	Normalized %	100			100	
*5408.5	Total %	0				
	Normalized %	0				
5408.5 Repeat	Total %	0.2		0.2		
	Normalized %	100		100		
5957.8	Total %	0				
	Normalized %	0				
*5961.7	Total %	0				
	Normalized %	0				
5961.7 Repeat	Total %	0.2		0.2		
	Normalized %	100		100		
5962	Total %	0.3		0.3		
	Normalized %	100		100		

* indicates that the sample data was not plotted. The data gathered from the repeated point counting of the sample, which represents increased experience, was plotted to insure that only the most accurate counts were plotted.

Table 4.4A: Detailed mineral point counting for selected samples for Newburn H-23 well using a petrographic microscope. The samples were selected on the basis of: stratigraphic level, and the abundance of non-quartz detrital minerals.

Well Name	Sample Depth (m)	# of Grains	Mean Grain Size (µm)	Sorting	% Quartz	% Alkali Feldspars	% Plagioclase	% Muscovite	% Biotite	% Chlorite	% Spinel	% Titania	% Tourmaline	% Zircon
Newburn H-23	4318.5	600	395	Poor	94.8	3.2	1.3	0.3			0.2	0.2		
Newburn H-23	5406.5	600	240	Moderate	96.7		2	0.2			0.3			0.8
Newburn H-23	5408.5	600	140	Well	94.5		5.2							0.3
Newburn H-23	5961.7	600	100	Well	95.2		3.7	0.7				0.3		0.2

Table 4.4B: Detrital mineral point counting from Table 4.4A normalized to exclude quartz.

Well Name	Sample Depth (m)		% Total	% Alkali Feldspars	% Plagioclase	% Muscovite	% Biotite	% Chlorite	% Spinel	% Titania	% Tourmaline	% Zircon
Newburn H-23	4318.5	Total %	5.2	3.2	1.3	0.3			0.2	0.2		
		Normalized %	100	61.5	25.0	5.8			3.8	3.8		
Newburn H-23	5406.5	Total %	3.3		2.0	0.2			0.3			0.8
		Normalized %	100		60.6	6.1			9.1			24.2
Newburn H-23	5408.5	Total %	5.5		5.2							0.3
		Normalized %	100		94.5							5.5
Newburn H-23	5961.7	Total %	4.9		3.7	0.7				0.3		0.2
		Normalized %	100		75.5	14.3				6.1		4.1

4.1.1.1 Cree Member

The detrital mineral assemblage from the Cree Member of the Newburn H-23 well is the most diverse. It contains albite, Al-chromite and chromian spinel (henceforth referred to as spinel), K-feldspar, muscovite, quartz, titania, and zircon with minor biotite, diopside, hornblende, ilmenite, monazite, oligoclase, and tourmaline (Table 4.1).

At the maximum depth from which a sample is available in the Cree Member (sample 4353.5 m) the only recorded detrital heavy mineral during point counting is

spinel which is joined by zircon and titania at 4318.5 m and disappears at the most shallow depth of 4313.5 m. No grains of tourmaline have been observed in this interval during point counting (Fig. 4.1).

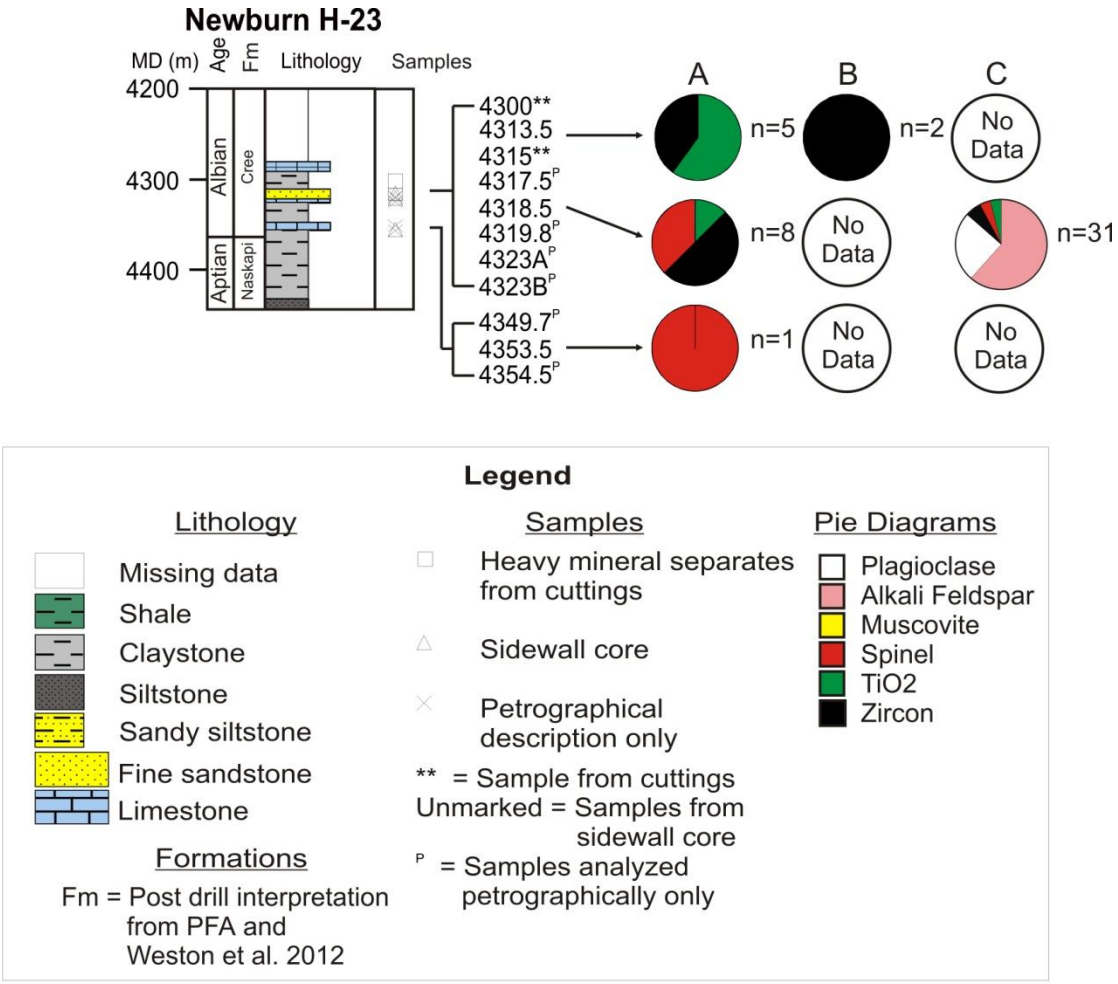

Fig. 4.1: Stratigraphic column for the Cree Member in the Newburn H-23 well showing depth (MD) in meters, formation (Fm), lithology (from cutting description), sample locations, and pie diagrams of detrital minerals present using three methods **A:** Pie diagrams generated from point counting of heavy minerals in SEM BSE images from Pts (Table 4.2). **B:** Pie diagrams generated from point counting using Petrog software and stepping stage on Pts. The data has been renormalized to include only heavy minerals (Table 4.3). **C:** Pie diagrams generated from point counting using Petrog software and stepping stage on selected samples (Table 4.4A) and data has been renormalized to exclude quartz

4.1.1.2 Upper Missisauga Formation

The detrital mineral assemblage from the Upper Missisauga Formation includes albite, muscovite, oligoclase, quartz, tourmaline, and zircon. There is only one sample from the Upper Missisauga Formation and as a result no comments can be made on how the heavy mineral abundances change with depth in this unit, however standard point counting suggests that they are split evenly between tourmaline and zircon (Fig 4.2).

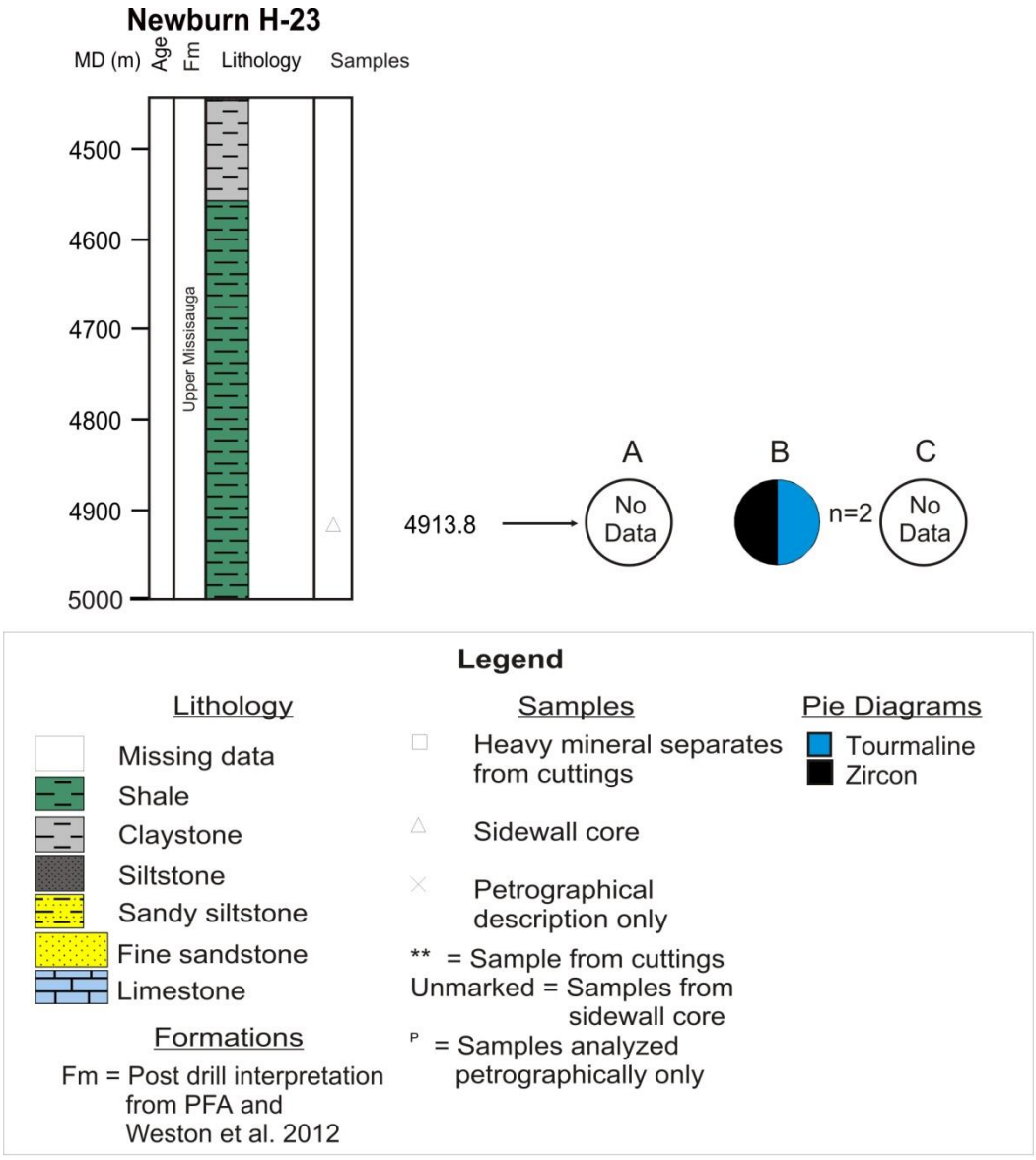

Fig. 4.2: Stratigraphic column for the Upper Missisauga Formation in the Newburn H-23 well showing depth (MD) in meters, formation (Fm), lithology (from cutting description), sample locations, and pie diagrams of detrital minerals present using three methods **A:** Pie diagrams generated from point counting of heavy minerals in SEM BSE images from Pts. (Table 4.2) **B:** Pie diagrams generated from point counting using Petrog software and stepping stage on Pts. The data has been renormalized to include only heavy minerals. (Table 4.3) **C:** Pie diagrams generated from point counting using Petrog software and stepping stage on selected samples (Table 4.4A) and data has been renormalized to exclude quartz

4.1.1.3 Middle Missisauga Formation (Group 1)

The detrital mineral assemblage from the Middle Missisauga Formation contains albite, spinel, K-feldspar, muscovite, quartz, titania, and zircon with minor oligoclase and tourmaline.

Detrital heavy minerals in the Middle Missisauga Formation are dominantly zircon with a maximum percentage of 100% at several depth intervals (5403.6 m and 5407 m). The next most prevalent detrital minerals are titania, spinel, and tourmaline respectively. This interval contains the majority of the tourmaline grains from this well being present at three depths (5406 m, 5407 m, and 5408 m) and is the major mineral at a depth of 5407 m (Table 4.3).

Zircon is the only mineral which has been point counted from this stratigraphic level which is present in all samples (Fig. 4.3). Sample 5408 m contains detrital zircon, tourmaline, spinel, and titania, but in the overlying sample (5407 m) titania and spinel are absent, leaving zircon and tourmaline. The next sample (5406.5 m) contains all these heavy detrital minerals, but sample 5403.6 m contains only zircon. At the most shallow sample (5213.5 m) of the Middle Missisauga the spinel, titania, and zircon are present but tourmaline is not. Interestingly in this unit neither spinel nor titania are present without the other.

Sample 5406 m contains lineations of heavy minerals and as a result contains the most heavy detrital minerals of all of the sidewall core samples (Table 4.2) and gives the most representative data for the Middle Missisauga. The proportions from 5406 m mostly agree with the overall trend from this interval with zircon as the major component; however, the proportion of detrital spinel is elevated compared to titania.

4.1.1.4 Middle Missisauga Formation (Group 2)

The detrital mineral assemblage from this group of the Middle Missisauga Formation contains albite, spinel, K-feldspar, muscovite, quartz, titania, and zircon with minor actinolite, biotite, hornblende, ilmenite, labradorite, magnetite, and tourmaline. Titania is the dominant detrital heavy mineral in the Middle Missisauga Formation followed by zircon and spinel.

In the Middle Missisauga Formation the deepest sample (5962 m) contains detrital spinel, titania, and zircon, but in shallower samples (e.g. 5961.7 m) spinel disappears, returning in sample 5957.8 m.

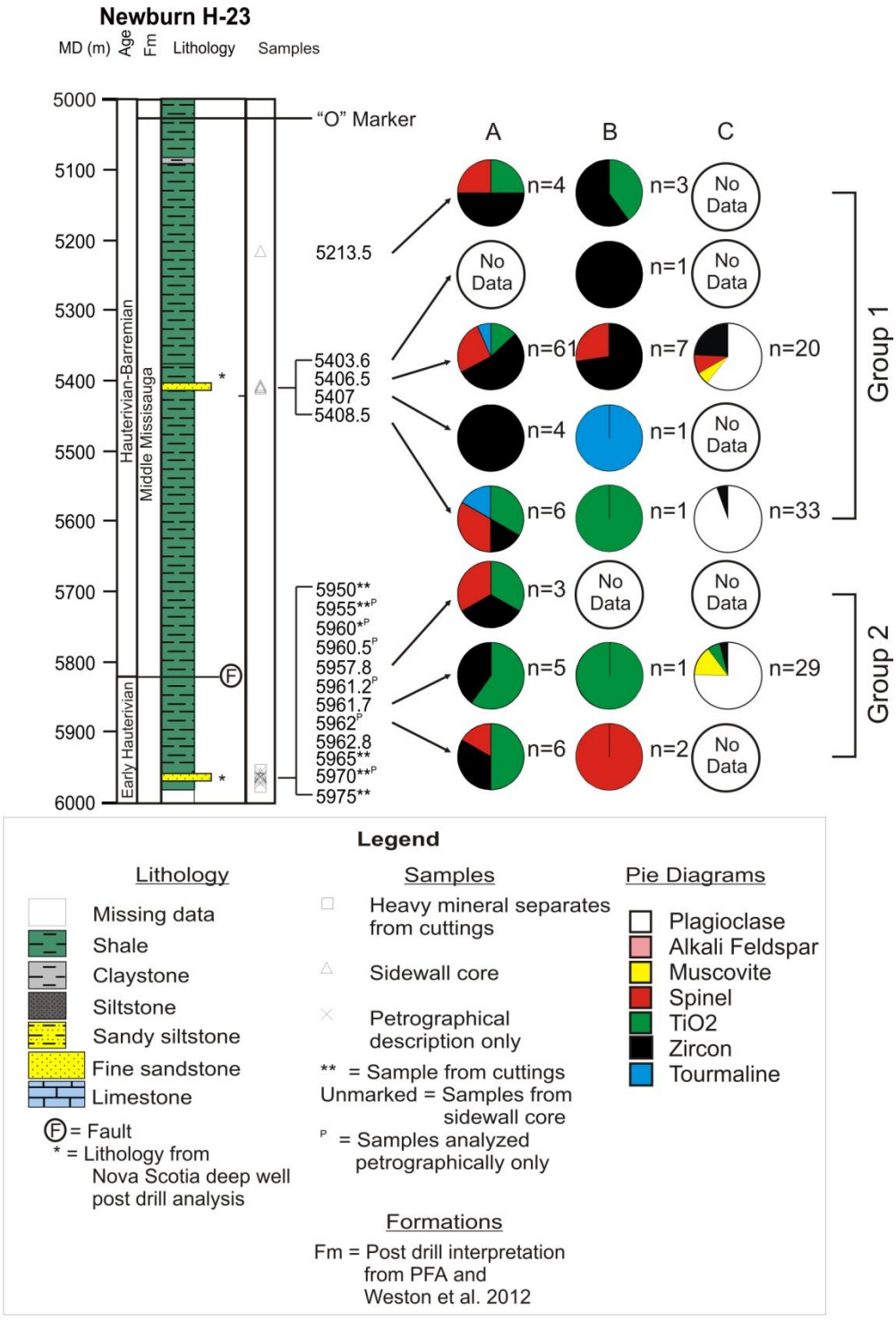

Fig. 4.3: Stratigraphic column for the Middle Missisauga Formation in the Newburn H-23 well showing depth (MD) in meters, formation (Fm), lithology (from cutting description), sample locations, and pie diagrams of detrital minerals present using three methods **A:** Pie diagrams generated from point counting of heavy minerals in SEM BSE images from Pts (Table 4.2). **B:** Pie diagrams generated from point counting using Petrog software and stepping stage on Pts. The data has been renormalized to include only heavy minerals (Table 4.3). **C:** Pie diagrams generated from point counting using Petrog software and stepping stage on selected samples (Table 4.4A) and data has been renormalized to exclude quartz

4.1.2 Lithic Clasts

Lithic clasts provide information about the sources of the sediments present since they are small preserved fragments of the original source rock. As a result they are often a more accurate tool for determining the source of sediments than the detrital minerals which are contained within the samples.

4.1.2.1 Cree Member

The Cree Member of the Logan Canyon Formation in this well contains granitoid lithic clasts and trachytic lithic clasts. The granitoid lithic clasts are fragments of felsic igneous rocks that contain **a)** quartz, muscovite, and titania (Fig. 3.5A) **b)** K-feldspar, quartz, and albite (Fig. 3.7A) and **c)** quartz, apatite, and F-apatite (Fig. 3.7D) and indicate that there was a felsic igneous rock source (granite and rhyolite). The trachytic lithic clasts are very similar to the sodic volcanic rocks that have been documented from the Lower Cretaceous volcanic rocks of the South-West Grand Banks (Pe-Piper et al., 1994) suggesting that the trachytic lithic clasts in this well may have also been sourced from this area. Mudstone intraclasts are also present and consist of illite, chlorite, and siderite; and muscovite, chlorite, albite, quartz, and siderite (Fig. 3.6C) and plastically deform around framework grains.

4.1.2.2 Upper Missisauga Formation

The Lithic clasts in this stratigraphic level are similar to those in the Cree Member sandstones.

4.1.2.3 Middle Missisauga Formation (Group 1)

The Middle Missisauga Formation (Group 1) contains lithic clasts similar to those in the Cree Member sandstones, but additionally contains schist clasts. These schist clasts contain quartz, albite, and chlorite (Fig. 3.15F) and indicate input from a metamorphic rock source.

4.1.2.4 Middle Missisauga Formation (Group 2)

The Middle Missisauga Formation (Group 2) contains lithic clasts similar to those in the Middle Missisauga Formation (Group 1) sandstones, but additionally contains slate clasts and a probable altered pumice clast. The slate contains quartz and muscovite (Fig. 3.19F) and indicates input from a metamorphic rock source and the altered pumice clast has produced fibrous chlorite and supports input from a volcanic source.

4.1.3 Comparison with other wells in the Scotian basin

4.1.3.1 Detrital mineral overview for the Newburn H-23 well

Albite, spinel, muscovite, quartz, titania, and zircon are detrital minerals which are present in all stratigraphic units present in this well.

Plagioclase other than albite is found rarely as oligoclase in all units except for the Middle Missisauga (Group 2) which contains a single analyzed grain of labradorite. K-feldspar is present in all but the Upper Missisauga Formation and is most prevalent in the Cree Member. Amphiboles are present as hornblende in the Cree Member and Middle Missisauga Formation (Group 2) and actinolite in the Middle Missisauga Formation (Group 2). Pyroxenes (diopside) are found only in the Cree Member. Tourmaline if found in the Cree Member and Middle Missisauga formation. Ilmenite is present in the Cree

Member and the Middle Missisauga Formation (Group 2) and magnetite is found in the Middle Missisauga Formation (Group 2). Glauconite is present as preserved pellets in the Cree Member and Middle Missisauga Formation. Rare earth bearing minerals are found in the Cree Member and Middle Missisauga Formation (Group 2) as monazite.

K-feldspar, spinel, and tourmaline occur together and are absent in the Upper Missisauga formation. Similarly amphiboles, biotite, and ilmenite only occur together and are found in the Cree Member and the Middle Missisauga Formation (Group 2) and are found with diopside in the Cree Member.

4.1.3.2 Lithic clast overview for the Newburn H-23 well

All stratigraphic units contain trachytic lithic clasts suggesting a continuous input. These trachytic clasts can be found in several other wells in the Scotian basin notably the Alma K-85 and Glenelg N-49 well, which have documented clasts in the Cree Member (Bowman et al., 2012). These are sodic volcanic lithic clasts which are composed of aligned albite laths. Magnetic data suggests that the volcanic centers are located on the Scatarie Bank and eastward along the northern edge of the Laurentian Sub-basin (Bowman et al., 2012). The trachytic lithic clasts present throughout this well and the basin are most likely the result of the erosion of these volcanoes. Trachytic lithic clasts have been reported to be most common throughout the lower Cree Member (Bowman et al., 2012), however trachytic lithic clasts in this well have been found to have similar concentrations throughout the well suggesting that there was a near constant input from sodic volcanic rocks. The presence of probable altered pumice clasts in the Middle Missisauga Formation (Group 2) also suggests volcanic input. The Cree Member and Upper Missisauga formation are both sourced from felsic igneous rocks and sodic

volcanic rocks while the Middle Missisauga Formation is sourced from felsic igneous rocks, sodic volcanic rocks, and metamorphic rocks.

4.1.3.3 Detrital minerals from other wells in the Sable Sub-basin

There have been many wells drilled in the Scotian basin which have been studied since exploration began. The Newburn H-23 is in the Sable Sub-basin which also contains the Alma K-85, Glenelg N-49, North Triumph B-52 (Pe-Piper et al., 2004), and Musquodoboit E-23 wells (Pe-Piper et al., 2011). The detrital mineral assemblages have been compared to these other wells in the Sable Sub-basin to determine mineral variation within the Sub-basin.

4.1.3.3.1 Logan Canyon Formation

The major mineral assemblages in the Alma K-85, Glenelg N-49 (Pe-Piper et al., 2004), and Musquodoboit E-23 wells (Pe-Piper et al., 2011) from the Scotian basin include apatite, biotite (except for Musquodoboit E-23), spinel, ilmenite, K-feldspar, garnet, muscovite, plagioclase (albite, andesine, and oligoclase), titania (except for Musquodoboit E-23), tourmaline (except in Glenelg N-49), and zircon. Additionally minor chloritoid from Glenelg N-49, monazite from the Alma K-85 well, and diopside, magnetite, and staurolite from the Musquodoboit E-23 well are present.

Of the major minerals from these assemblages garnet and andesine are the only minerals which separate the Newburn H-23 well from the other wells of the Sable subbasin. In terms of minor minerals it is lacking chloritoid, and staurolite which are metamorphic minerals. Of these wells however Newburn H-23 is the only one to contain amphiboles (hornblende) (Table 4.1).

4.1.3.3.1 Missisauga Formation

The major mineral assemblages in the Alma K-85, Glenelg N-49, North Triumph B-52 (Pe-Piper et al., 2004), and Musquodoboit E-23 wells (Pe-Piper et al., 2011) from the Scotian basin are less continuous in the Missisauga Formation compared to the Logan Canyon Formation, however some shared assemblages persist. These minerals include spinel, garnet (except for Glenelg N-49), K-feldspar, muscovite (except for Alma K-85), plagioclase (albite and oligoclase) and titania (except for Musquodoboit E-23), tourmaline, and zircon. Additionally minor ilmenite from the Alma K-85 well, amphiboles (tremolite), diopside, and magnetite from the Musquodoboit E-23 well, biotite from the Glenelg N-49 and Musquodoboit E-23 wells, apatite from the Glenelg N-49 and North Triumph B-52 wells, and monazite from the Alma K-85 and North Triumph B-52 wells.

Of these major mineral assemblages the Newburn H-23 well does not contain garnet. It is lacking diopside, magnetite, and tremolite but contains actinolite, hornblende, and labradorite (Table 4.1) which are not seen elsewhere in the Sable Sub-basin.

4.1.4 Overall Interpretation

The sandstone intervals from the Newburn H-23 well largely share detrital mineralogy with others wells nearby in the central Scotian Basin, lacking mostly minor detrital minerals. This suggests that they share a source during the Early Cretaceous, during this time period the source was dominantly from the Sable River with minor input from the Meguma Group, a continuous supply of sodic volcanic rocks, and pumice, probably from the Scatarie Bank and nearby volcanoes. Garnet is notably absent and has been documented in other wells to become less frequent with burial depths over 3.5 km

owing to dissolution (Morton and Hallsworth 1999). Given that current depths in Newburn H-23 are over 4 km it is likely that the majority of the garnet from the studied intervals have been dissolved.

4.2 Geochemical fingerprinting

Heavy mineral assemblages are widely used to determine the provenance of sediments owing to their relative stability and distinct chemical ranges which can be traced to specific sources. The chemical analyses of four detrital minerals (muscovite, tourmaline, biotite, and spinel) have been plotted to determine probable provenance of the different stratigraphic intervals of the Newburn H-23 well.

4.2.1 Muscovite

Muscovite is a common detrital mineral in this well at depths in all stratigraphic levels of interest and is therefore an excellent mineral to help in identifying of a source area. Unfortunately muscovite is easily altered to chlorite, illite, and hydromuscovite and as a result the analyses of muscovite in this well had to be screened to insure that only the freshest grains were plotted for provenance. Analyses containing more than 3% combined FeO, MgO, and F were omitted from provenance diagrams. Analyses were plotted on a total aluminum versus potassium graph (in atomic formula units (a.f.u.), recalculated using Si = 8) with fields from Reynolds et al., 2010 (Fig. 4.4).

4.2.1.1 Cree Member

Muscovite grains from the Cree Member plot in and around both the igneous and metasedimentary fields of Reynolds et al. (2010) (Fig. 4.4B). However, the majority of the analyzed grains does not fall within these fields but do overlap with outlier values for

the Meguma metasediments (Fig. 4.5D) that may show partial alteration to illite. EMP analyses of muscovite grains from the Alma K-85 well (Fig. 4.5A) and Glenelg field (Fig. 4.5C), however, plot strongly within the igneous muscovite field (Pe-Piper et al., 2009b) with rare analyses from the Glenelg field also plotting around the metasedimentary field (Fig. 4.5C).

4.2.1.2 Missisauga Formation

The analyzed grains from the Upper Missisauga formation plot in and around the metasedimentary field (Fig. 4.4C). Muscovite grains from the Middle Missisauga formation however plot in both the igneous and metasedimentary fields with the majority of analyses plotting in and around the metasedimentary field, with three falling in the igneous field and the remainder falling between the two fields (Fig. 4.4D). Analyses from the LaHave platform (Naskapi N-30 and Sambro I-29 wells) (Fig. 4.5B), Orpheus Graben (Fox I-22, Crow F-52, Argo F-38, and Jason C-20) (Fig. 4.5B), and the Glenelg field (Fig. 4.5C) also plot in both the igneous and Meguma metasedimentary fields (Pe-Piper et al., 2009b).

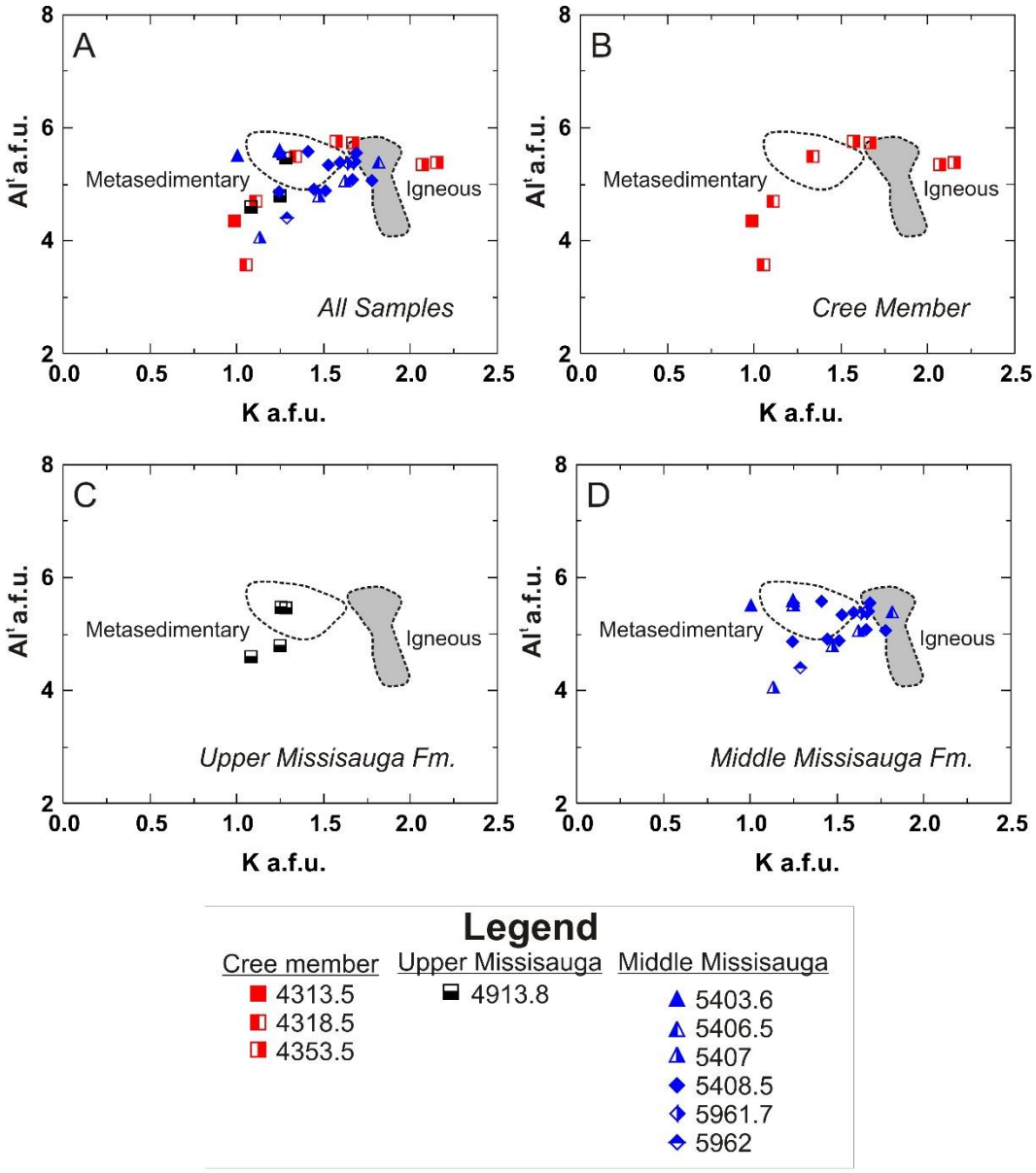

Fig. 4.4: Al^t a.f.u. vs K a.f.u. variation in muscovite. Fields generated from electron microprobe analyses of muscovites. Grey field shows Meguma terrane igneous muscovites, the dashed field includes 85% of the Meguma Group metasedimentary muscovite analyses. Data from Reynolds et al. 2010. **A:** All the analyses of muscovite from the Newburn H-23 well. **B:** Analyses of muscovite grains from the Cree Member of the Logan Canyon Formation. **C:** Analyses of muscovite grains from the Upper Missisauga Formation. **D:** Analyses of muscovite grains from the Middle Missisauga Formation.

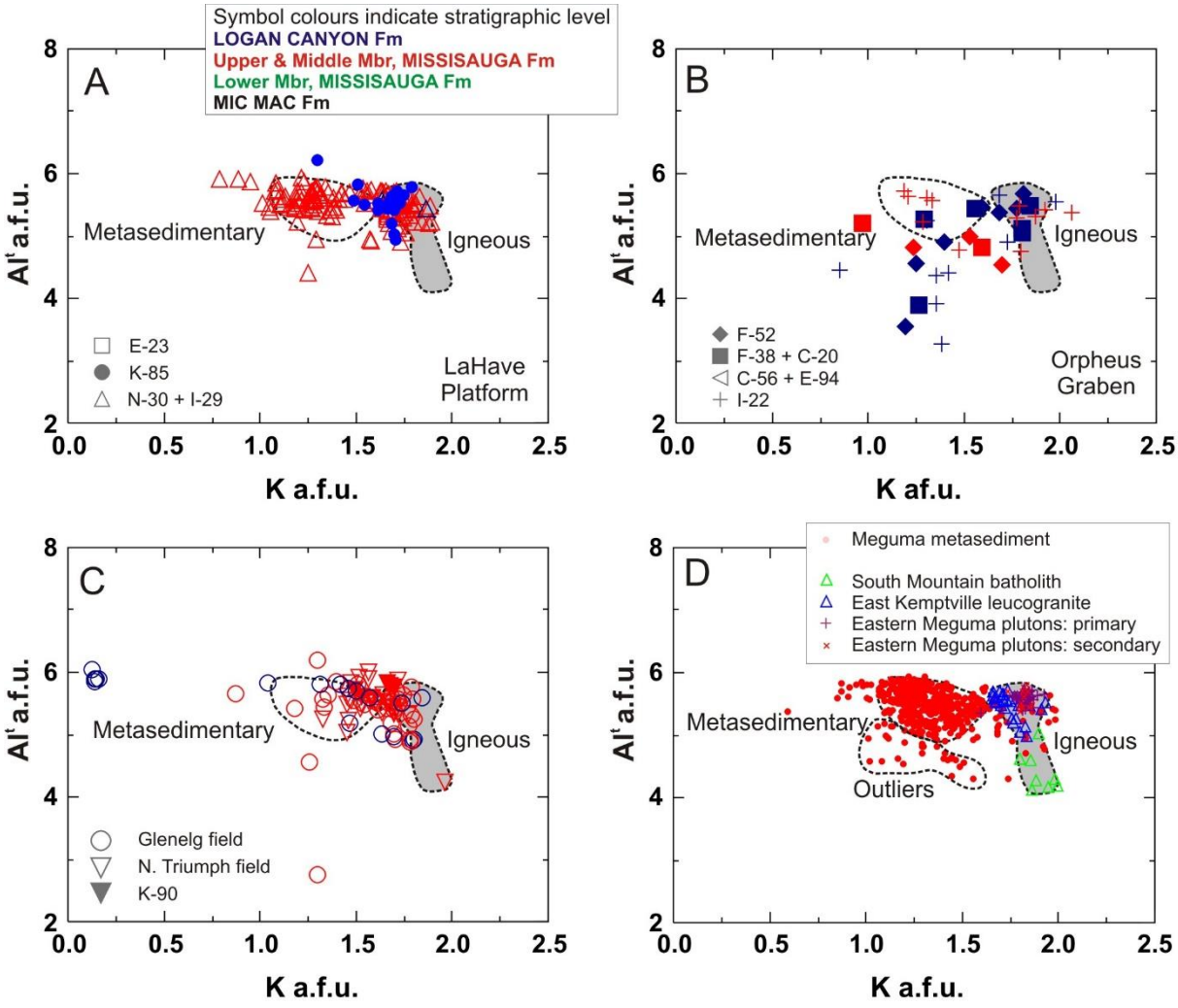

Fig. 4.5: Modified plots from Pe-Piper 2009. Al^t a.f.u. vs K a.f.u. variation in muscovite. Fields generated from electron microprobe analyses of muscovites. Grey field shows Meguma terrane igneous muscovites, the dashed field includes 85% of the Meguma Group metasedimentary muscovite analyses. Data from Reynolds et al. 2010. Analyses of muscovite grains from the Logan Canyon, Upper Missisauga, Middle Missisauga, Lower Missisauga, and Mic Mac formations from the **A:** Lahave Platform **B:** Orpheus Graben **C:** Glenelg and North Triumph fields **D:** South Mountain batholith, Eastern Meguma plutons, and Meguma metasedimentary rocks, outlier analyses for the Meguma metasediments are also indicated.

4.2.2 Tourmaline

Tourmaline is a highly stable detrital mineral and is common throughout the Scotian Basin and as a result is widely used as an indicator for sediment sources. Tourmaline is plotted on a ternary diagram using Al-Fe^{2+}-Mg (in a.f.u. recalculated using O=23.5) with four distinct fields (Pe-Piper et al., 2009b) (Fig. 4.6).

The tourmaline analyses from this well are of grains from both the Cree Member and the Middle Missisauga Formation and dominantly plot as type 4 tourmalines on the ternary plot with rare analyses falling within the type 1 field from both the Cree Member and the Middle Missisauga Formation, and in field 6 from the Cree Member (Fig. 4.6). Type 4tourmalines represent a metapelitic and psammitic source while type 1 is granitic and field 6 tourmalines are from a metapelitic calc-silicate rocks. These analyses are similar to those obtained from the Alma K-85 well (Pe-Piper et al., 2010), Musquodoboit E-23 well (Pe-Piper et al., 2009a), and Glenelg field (Pe-Piper et al., 2009b) for both the Cree Member and the Middle Missisauga Formation.

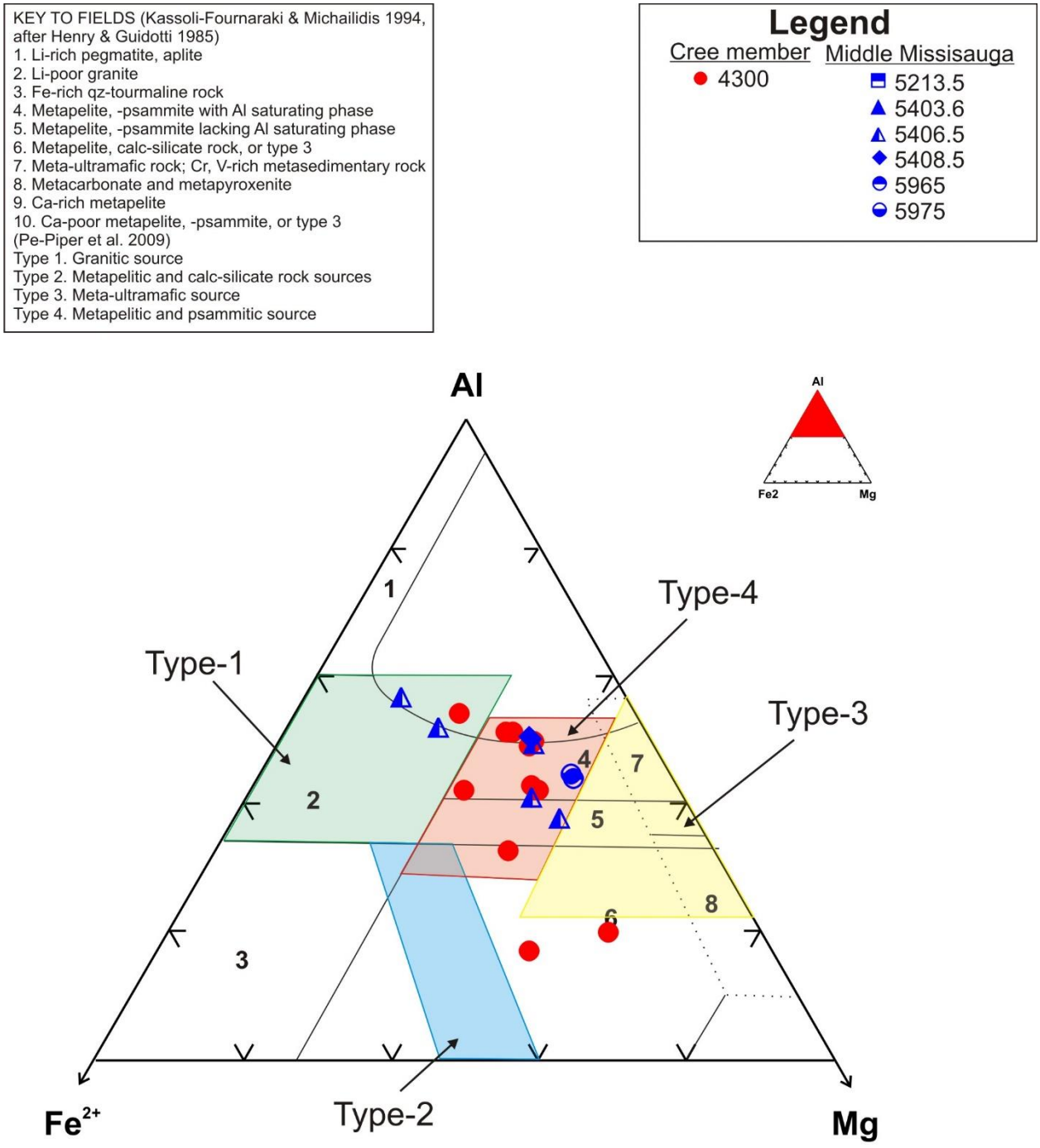

Fig. 4.6: Chemical variation in tourmaline based on Al - Mg - Fe^{2+} showing fields from Henry and Guidotti (1994), Kassoli-Fournaki and Michalaidas (1994), and Pe-Piper et al. (2009).

4.2.3 Biotite

Biotite suffers from the same issues as muscovite in terms of alteration, and organized data in regards to sources in the Scotian basin are scarce. As a result biotite chemistry is used dominantly to determine the rock type of their source (Fig. 4.7B) and to further discriminate igneous sources (Fig. 4.7C). Analyses have been plotted on an aluminium versus iron over iron and magnesium plot (in a.f.u. recalculated using Si=8) to determine the nomenclature of the analyses after Deer et al., 1992 (Fig. 4.7A); titanium oxide versus aluminum oxide (in wt. %) to determine source rock type after Fleet 2003 (Fig. 4.7B), and finally on an iron oxide – magnesium oxide – aluminum oxide diagram after Rahmen 1994 (Fig. 4.7C), using only the analyses that plotted within the igneous field in Fig. 4.7B to further classify the source rock.

There are only three analyzed grains of biotite from this well. Two of which plot as phlogopite (Samples 4300m and 5950m) and one as biotite (Sample 5975m) (Fig. 4.7B). The biotite from the Cree Member plots in the igneous field, while the analyses from the Middle Missisauga formation plot in and around the metamorphic field (Fig. 4.7C). The igneous biotite falls within the calcalkali field (Fig. 4.7E). Biotite from the Alma K-85 well has biotite analyses which plot as both igneous and metamorphic grains in the Logan Canyon Formation. The biotite classified as igneous falls within the peraluminous field. The Glenelg biotites are the most similar to the biotite found in Newburn H-23 and fall mostly within the metamorphic field in the Middle Missisauga Formation with a single igneous calkaline analysis (Pe-Piper et al., 2009b).

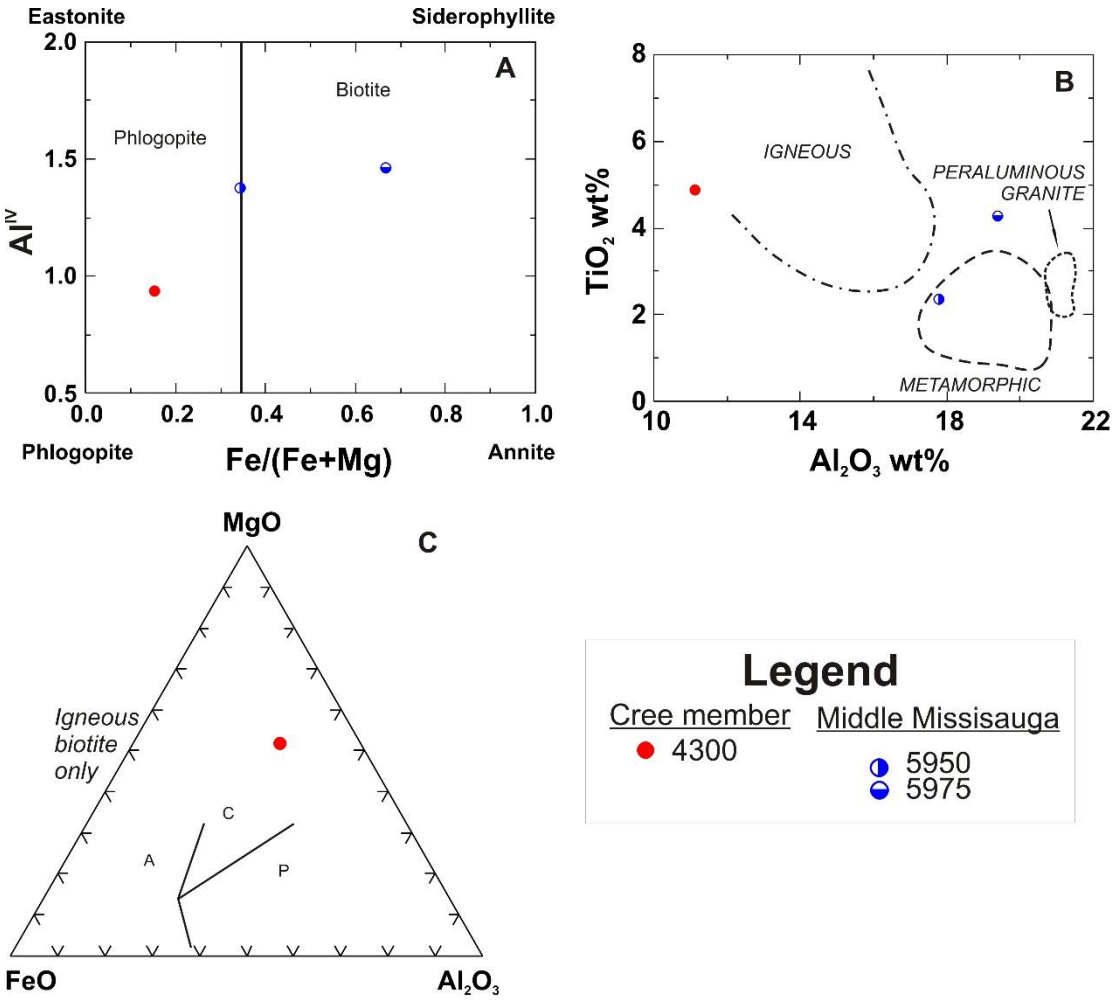

Fig. 4.7: Chemical variation in biotite and phlogopite. Nomenclature in A) from Deer et al. (1992). Fields in B) from Fleet (2003). Fields in C) apply to igneous biotite only (from Abdel Rahmen, 1994): A = alkali, C = calcalkali, P = peraluminous.

4.2.4 Spinel

Spinel is a detrital mineral known for being stable during diagenesis and being easily traced back to its source area as a result of its widely ranging in composition from locality to locality. However due to its stability it is prone to be polycyclic, and this may be indicated by common occurrence of both spinel and zircons (Zhang et al., 2014). Spinel analyses have been classified using bi-plots of chromium number (100*Cr/Cr+Al) vs magnesium number (100*Mg/Mg+Fe^{2+}) (Fig. 4.8) and chromium number vs TiO_2 (Fig.

4.9) to show potential source areas. The chromium number vs TiO_2 plot (Fig. 4.9) uses fields defined by EMP data, the spinel analyses from Newburn H-23 well however, were taken using an SEM. Due to the differences in detection limits between the EMP and SEM, analyses with less than 0.2 wt%TiO_2 have been omitted from the plot, since they are below accurate detection limits for the SEM and therefore do not necessarily represent the sources which the analyses plot as.

Spinel analyses from this well are dominantly chromite with lesser Chromian-spinels and rare boninitic-type chromites (Fig. 4.8). They are almost entirely chromites in the Cree Member and show a greater diversity in the Middle Missisauga Formation (Fig. 4.8). The analyses from the Newburn H-23 well plot mostly within the field representing spinel analyses from other wells in the Sable Sub-basin (Fig. 4.8).

The spinels from the Newburn H-23 plot mainly within the boninite field from both the Cree Member and the Middle Missisauga Formation. Additionally one analysis from the Cree Member plots as an island arc tholeiitic source (sample 4318.5 m) and analyses from the Middle Missisauga plot as MORB (Samples 5406.5 m and 5408.5 m) and island arc tholeiitic environments (sample 5406.5 m and 5962 m) (Fig. 4.9). The signature of these spinels most closely resembles the Newfoundland Appalachians Ophiolitic source (Fig. 4.9).

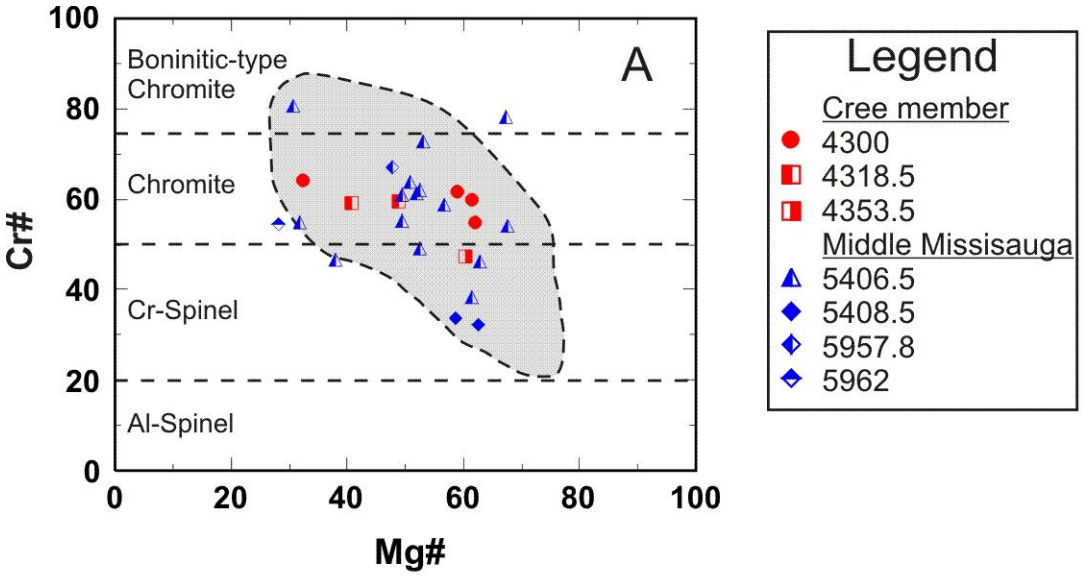

Fig. 4.8: Chemical variation in spinel/chromite analyses from the Newburn H-23 well with fields from Tsikouras et al. (2011). The grey field shows analyses from Glenelg, N.Triumph, and Alma K-90 (Pe-Piper et al. 2009).

Spinel analyses from the Alma K-85 well from Pe-Piper et al. (2011) plot dominantly as chromian-spinels, particularly in the Middle Missisauga, with rare chromites when plotted using the fields from Tsikouras et al. (2011). These spinels are mostly island arc basalt and MORB sources for the Middle Missisauga and MORB sources for the Logan Canyon Formation. Spinel analyses from the Musquodoboit E-23 well range widely in the Middle Missisauga Formation and Cree Member from a boninites source to island-arc tholeiites to MORBs (Pe-Piper et al., 2009b). The Glenelg field and North Triumph spinels plot in a similar fashion in the Middle Missisauga Formation and Logan Canyon Formation as in Newburn H-23 (Fig. 4.9) (Pe-Piper et al., 2009b). The range of the sources for the Glenelg Field however appears to be more widespread than that of the Newburn H-23 well.

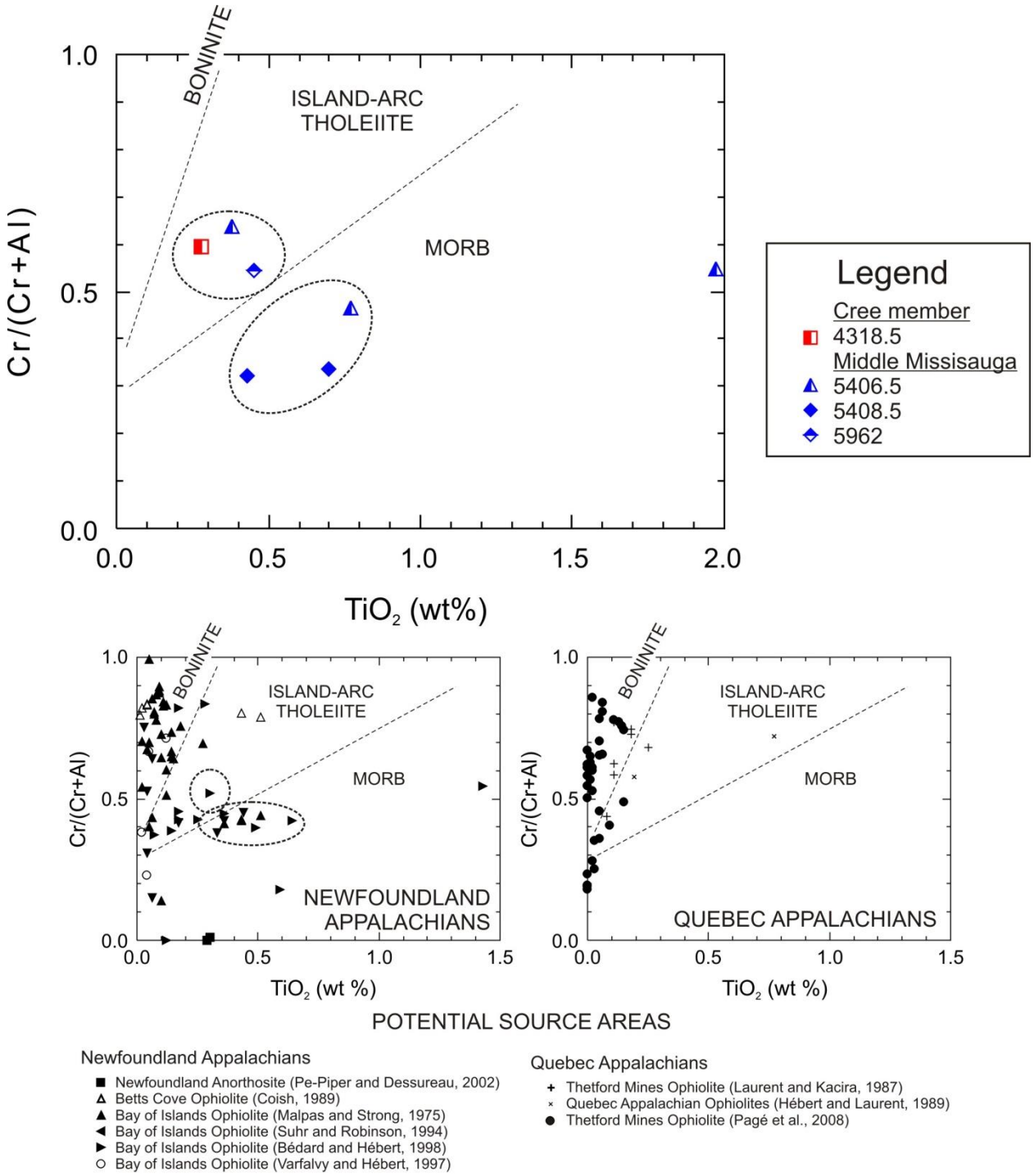

Fig. 4.9: Chemical variation in spinel in the Newburn H-23 well (above) and potential source rocks (below). Fields after Pearce et al. (2000).

4.2.5 Summary

Cree Member

The Cree Member contains **a)** muscovite grains from igneous and metasedimentary fields (Fig. 4.4B) **b)** tourmaline from a mostly metapelitic and psammitic source with some from a granitic and metapelitic calc silicate source (Fig. 4.6) **c)** phlogopite (Fig. 4.6B) from a calcalkali igneous source (Fig. 4.7E) and **d) C**hromites and a single chromian-spinel with a single grain from an island arc tholeiitic ophiolite.

Upper and Middle Missisauga Formation

The Upper Missisauga formation only has a sufficient number of muscovite grains to be able to determine their potential sources. These muscovite analyses plot in the field of metasedimentary source (Fig. 4.4B). The Middle Missisauga Formation contains **a)** muscovite grains which plot as igneous and metamorphic (Fig. 4.4B) **b)** tourmaline is mostly from metapelitic and psammitic sources with minor amounts from a granitic source (Fig. 4.6) **c)** the biotite and phlogopite are from a metamorphic source (Fig. 4.7C) and **d)** the chromite and chromian-spinel grains seem to be dominantly from a MORB ophiolite with a minor amount from island arc tholeiitic ophiolite.

4.2.6 Overall Interpretation

The detrital minerals analyzed in the Newburn H-23 well show the most similarity to wells from the Glenelg field suggesting that they probably share a similar source. The Glenelg field was sourced by a paleo-St. Lawrence River (Pe-Piper et al., 2005) now known as the Sable River (Zhang et al., 2014). This river carried sediments partially sourced from the northern Appalachians and Labrador (Zhang et al., 2014). This confirms the conclusion from the detrital mineralogy of the Newburn H-23 well which suggests

that these sandstones share a sediment source with other wells from the Sable Sub-basin and were deposited by the Sable River in the Early Cretaceous.

4.3 Diagenesis

Diagenesis is a process which sedimentary rocks undergo during burial. During burial basinal fluids interact with sediments with increasing temperature at depth, these fluids have variable salinities, dissolved species, and pH. As fluids interact with the sediments they dissolve framework grains which are unstable, generating secondary porosity, and precipitate diagenetic minerals which become cements which may also be dissolved as burial continues. The order in which these diagenetic minerals form and are dissolved is called a paragenetic sequence and gives insight into the conditions present during the burial of sedimentary rocks and records temperature, chemical composition, and pH changes in the circulating fluids.

4.3.1 Fluorine Rich Ferroan-Calcite

Calcite grains with elevated fluorine content have been identified using SEM EDS analyses and are present in five samples in the Newburn H-23 well, fluorine bearing calcite is a carbonate species which has not been identified in previously studied wells in the Scotian Basin. It is therefore an interesting mineralogical discovery. The F-calcite bearing samples are present in one sample from the Cree Member (sample 4353.5 m) and the remaining four samples are all from the Middle Missisauga Formation (Group 1) (samples 5213.5 m, 5403.6 m, 5407 m, and 5408.5 m) (Table 4.1). Fluorine is a light element and as a result is difficult to detect using the SEM, which often overestimates the proportion of fluorine during analysis. Fluorine levels from these samples based on EDS analyses, range from 2 to 27 weight percent.

In order to determine the true concentration of fluorine in these samples they were also analyzed using the electron microprobe (EMP) (Appendix 3). In the EMP analyses fluorine totals range between 1 wt% and 2.5 wt% in F-Fe-calcite. This may reflect the difficulty of accurately analyzing fluorine. Fluorine has also been reported in chlorite analyses with concentrations as high as 6.9 wt%, suggesting that fluorine is not limited to calcite.

The presence of fluoride (F-) in carbonates has been accredited to a variety of sources including the advection of hydrothermal fluids through sediments, Al-silicate reactions, degradation of sea grass, and carbonate mineral diagenesis (Rude and Aller 1991). Sea water contains on average between 1200 and1400 ppm fluoride and has been shown to be preferentially removed by calcium carbonate (Carpenter 1969).

Aragonite can contain up to 1000 ppm of fluorine, which is high compared to the typical 75-550 ppm commonly contained in calcite from marine calcareous skeletons and oolites (Kitano et al., 1973). Fluoride tends to concentrate in aragonite when the parent solution is depleted in magnesium, while it concentrates in calcite when the parent solution is enriched in magnesium (Rude and Aller 1991), and as magnesium concentrations rise so too does the concentration of fluorine in calcite (Kitano et al., 1973). Aragonite and Mg-calcite are easily dissolved during diagenesis and the calcium carbonate is reprecipitated as low Mg-calcite, since aragonite can contain a greater concentration of fluoride than calcite this process releases fluoride into pore waters (Rude and Aller 1991).

The released fluoride has several possible fates, some of it can be lost to overlying water by exchange, some may be consumed during the formation of fluorapatite, and

some may be adsorbed during the reprecipitation of calcium carbonate, Fe-oxyhydroxides, and Mn-oxides (Rude and Aller 1991).

The method in which fluoride has been thus shown to be removed from solution is: **a)** by adsorption onto the surface of calcite, demonstrated in calcite nano particles, at low fluoride concentrations (<5 ppm) (Budyanto et al., 2015) and high pH (Padhi and Tokunaga 2015) and **b)** from the precipitation of fluorite on the surface of the calcite at concentrations greater than 10 ppm (Budyanto et al., 2015) and low pH (Padhi and Tokunaga 2015).

Since aragonite and calcite are polymorphs, they cannot be distinguished using chemical analyses. The fluorine content in these carbonates are very high and since aragonite is so much better at concentrating fluorine compared to calcite, it is possible that the $CaCO_3$ in these samples could be aragonite rather than calcite. However aragonite is a metastable mineral which is stable at high pressures and low temperatures (Fyfe and Bischoff 1964). In order for aragonite to be stable at a temperature of 180°C, a burial depth of 10-15 km is required (Johannes and Puhan 1971). Assuming a geothermal gradient of 40°C/km during the Cretaceous (Karim et al., 2011) the estimated depth at which this temperature is achieved is 4.5 km which is not deep enough for aragonite to be stable. Based on this geothermal gradient used by Karim et al. (2011) pressure and temperature conditions are never within the aragonite stability field and as a result it remains metastable throughout diagenesis in this well and is easily replaced by calcite. This suggests that the $CaCO_3$ in this well is calcite and not aragonite despite the elevated fluorine concentrations.

In the studied samples F-carbonates interact with silicate framework grains and other carbonates within the well. Albite, K-feldspar, and quartz grains are engulfed by Fe-

calcite (Fig. 4.10A) and ankerite engulfs albite (Fig. 4.10C). Fe-calcite and F-Fe-calcite engulf quartz overgrowths (Figs. 4.10C,D,E positions A) and Fe-calcite surrounds and replaces ankerite (Fig. 4.10C). Calcite is replaced by later F-Fe-calcite (Fig 1F) and Fe-calcite (Figs. 1B,), which also replaces Mg-calcite (Fig. 4.10B). Chlorite fills dissolution voids in F-Fe-calcite and calcite (Fig. 4.10F), cuts F-Fe-calcite (Fig. 4.10D and E), and engulfs silt sized quartz (Fig. 4.10E). Late siderite rims (Fig. 4.10A) and also fills dissolution voids (Fig. 4.10B) in Fe-calcite. The paragenetic sequence for the minerals which interact with F-Fe-calcite is: Albite + Quartz + K-feldspar → Quartz overgrowths → Ankerite + Calcite + Mg-Calcite → Fe-Calcite + F-Fe-calcite → Dissolution → Fibrous Chlorite → Siderite (late).

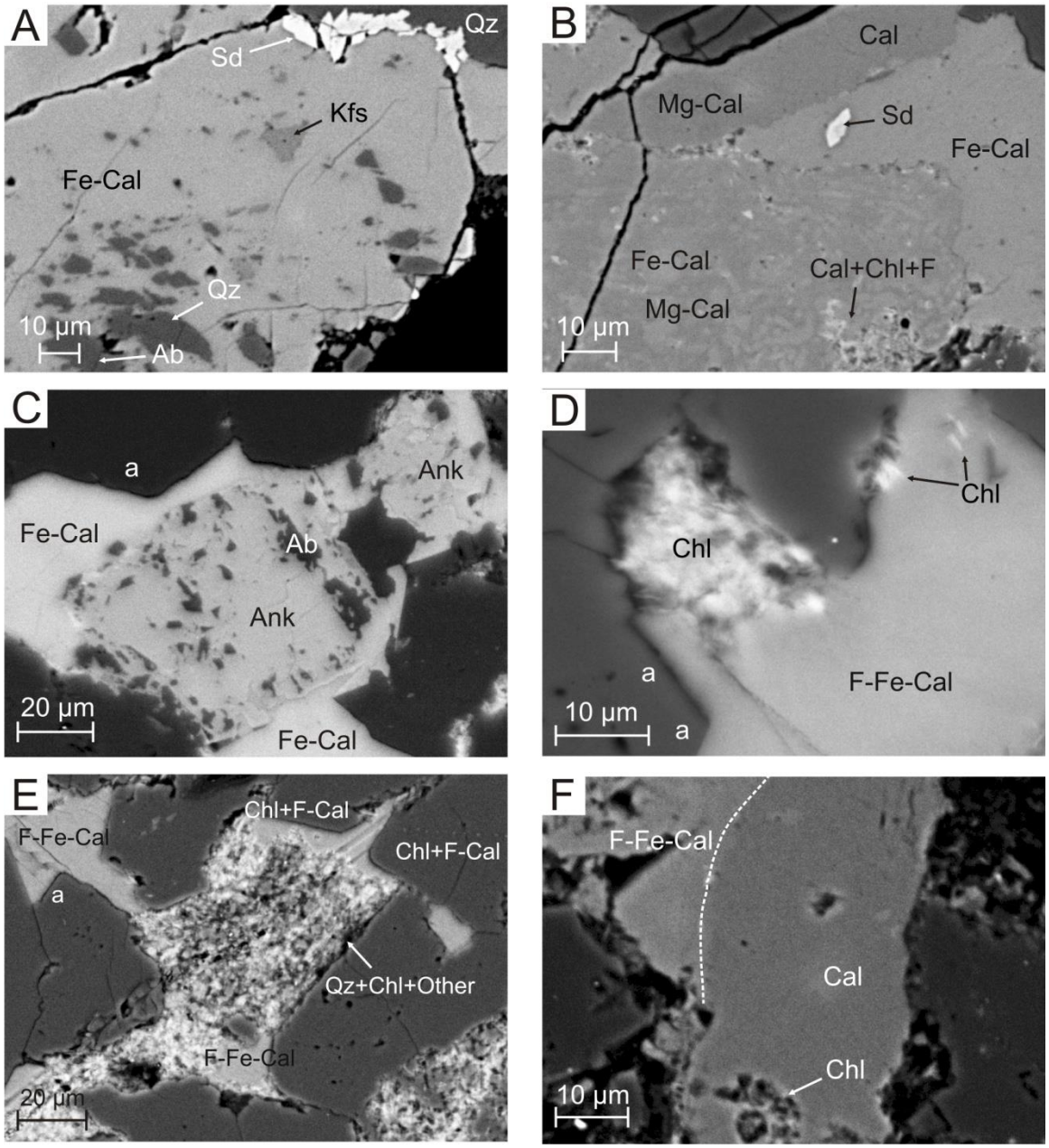

Fig. 4.10: Representative BSE images of textures of F-calcite and other carbonates from the Newburn H-23 well.
A: Sample 4353.5m (App. 3-1, Fig. 2a). Fe-calcite engulfs albite, K-feldspar, and quartz and is partly replaced by siderite.
B: Sample 5213.5m (App. 3-2, Fig. 2a). Calcite and Mg-calcite are replaced by Fe-calcite. Siderite fills a dissolution void in Fe-calcite.
C: Sample 5213.5m (App. 3-2, Fig. 3). Ankerite engulfs albite. Fe-calcite surrounds and replaces ankerite and engulfs quartz overgrowths (position a).
D: Sample 5403.6m (App. 3-3, Fig. 2). Fibrous chlorite cuts F-Fe-calcite. F-Fe-calcite engulfs quartz overgrowths (position a).
E: Sample 5403.6m (App. 3-3, Fig. 3). F-Fe-calcite engulfs quartz overgrowths (position a). Chlorite cuts F-Fe-calcite and engulfs silt-sized quartz.
F: Sample 5407m (App. 3-4, Fig. 2a). Calcite and F-Fe-calcite have dissolution voids filled by chlorite. Calcite has been partly replaced by F-Fe-calcite.The contact between calcite and F-Fe-calcite is marked by the dashed line.

The EMP data has been recalculated from weight percent oxides to weight percent of elements (wt. %) and are plotted on bi-plots (Fig. 4.11) and ternary diagrams (Fig. 4.12). In the studied samples there is a linear relationship between Fe_t and Mg in the Fe-calcite (Fig. 4.11A). This suggests that a small amount of Fe substitutes for Mg, and this results in the presence of two types of calcite in these samples: Mg-calcite and Fe-calcite (Fig. 4.11A). The Mg content of Fe-calcite increases steadily from 0.1 to 0.3 wt. % as Fe increases, whereas fluorine increases from 0 up to 2.5 wt. % in the Fe-calcite (Fig. 4.11A) and shows no correlation with Fe content. There is no fluorine in the Mg-calcite and there is no correlation between Mg and fluorine in the Fe-calcite (Fig. 4.11B), despite the relationship suggested by several studies that a higher Mg content increases the adsorption of fluoride onto calcite (Rude and Aller 1991). High fluorine Fe-calcite and low fluorine Fe-calcite plot in overlapping groups on the carbonate classification plot (Fig. 4.12B). The fluorine content in the Fe-calcite does not show any correlation with their Fe_t content (Fig. 4.11C), which suggests that the availability of the fluoride may be more important in the presence of F-Fe-calcite than the crystal structure of the Fe-calcite in a sandstone sample.

Although rare F-Fe-calcite has been seen among Fe-calcites in both the Logan Canyon and the Middle Missisauga Formation (Group 1) studied samples, most of the fluorine enrichment is in two samples from the Middle Missisauga (Group 1)(Samples 5403.6m and 5407m) (Fig. 4.11C). This may suggest that depth influences either the availability of fluoride or the mechanism of association of fluoride with Fe-calcite. It may also be important that the F-Fe-calcite is late in the diagenetic paragenesis of these samples and it seems to be associated with dissolution, fibrous chlorite lining secondary

porosity, and late siderite. These observations also suggest changes in the composition of circulating basinal fluids.

Fluid inclusion studies (Karim et al., 2012) show that in the western Sable Sub-basin (Glenelg, Thebaud, and Chebucto fields) fluid inclusions may have > 20% NaCl equivalent salinity. Based on Koritnig (1951) such brines might contain 20-40ppm fluoride.

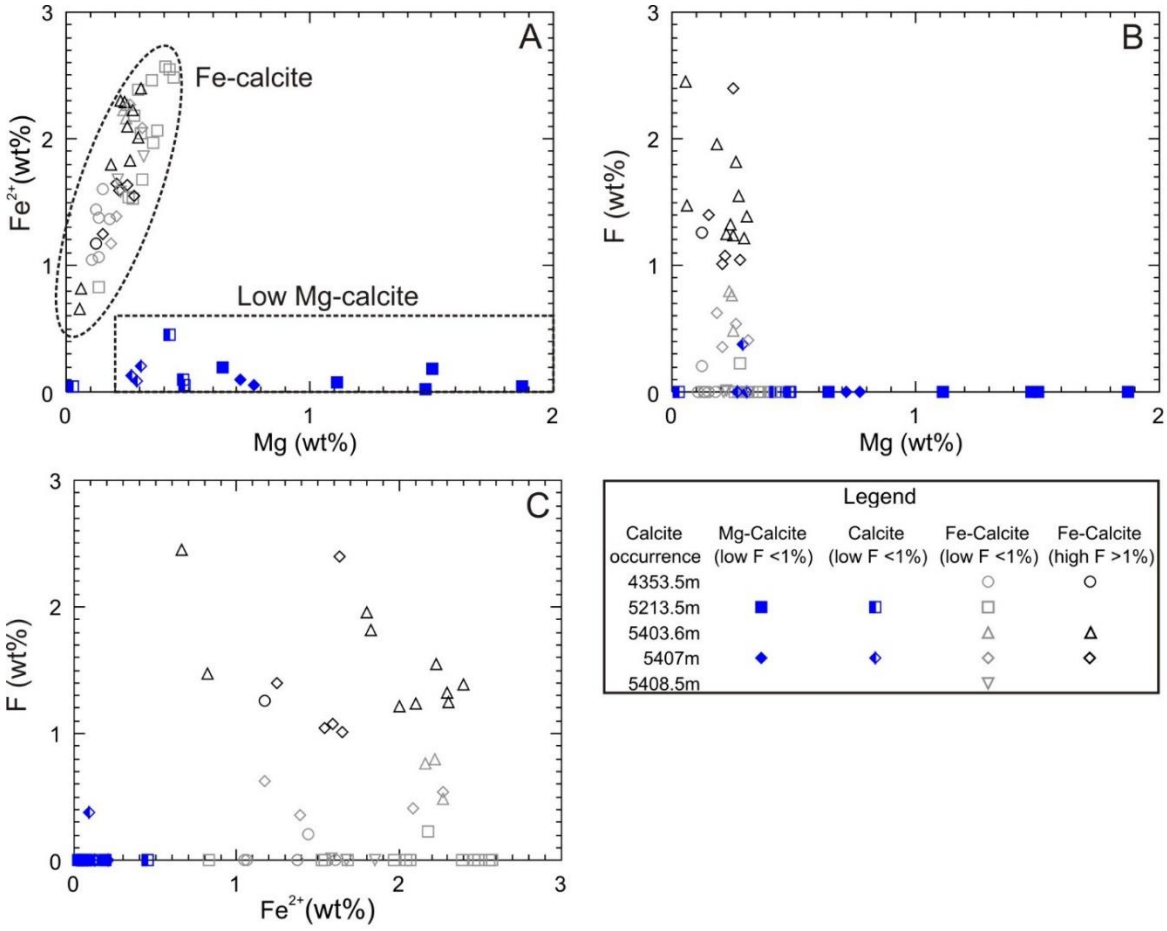

Fig. 4.11: Bi-plots of calcite analyses using EMP data from the Newburn H-23 well. **A:** Analyses plotted on a fluorine versus iron graph in element wt%. **B:** Analyses plotted on a fluorine versus magnesium graph in element weight percent (wt%). **C:** Analyses plotted on an iron versus magnesium graph in element wt%.

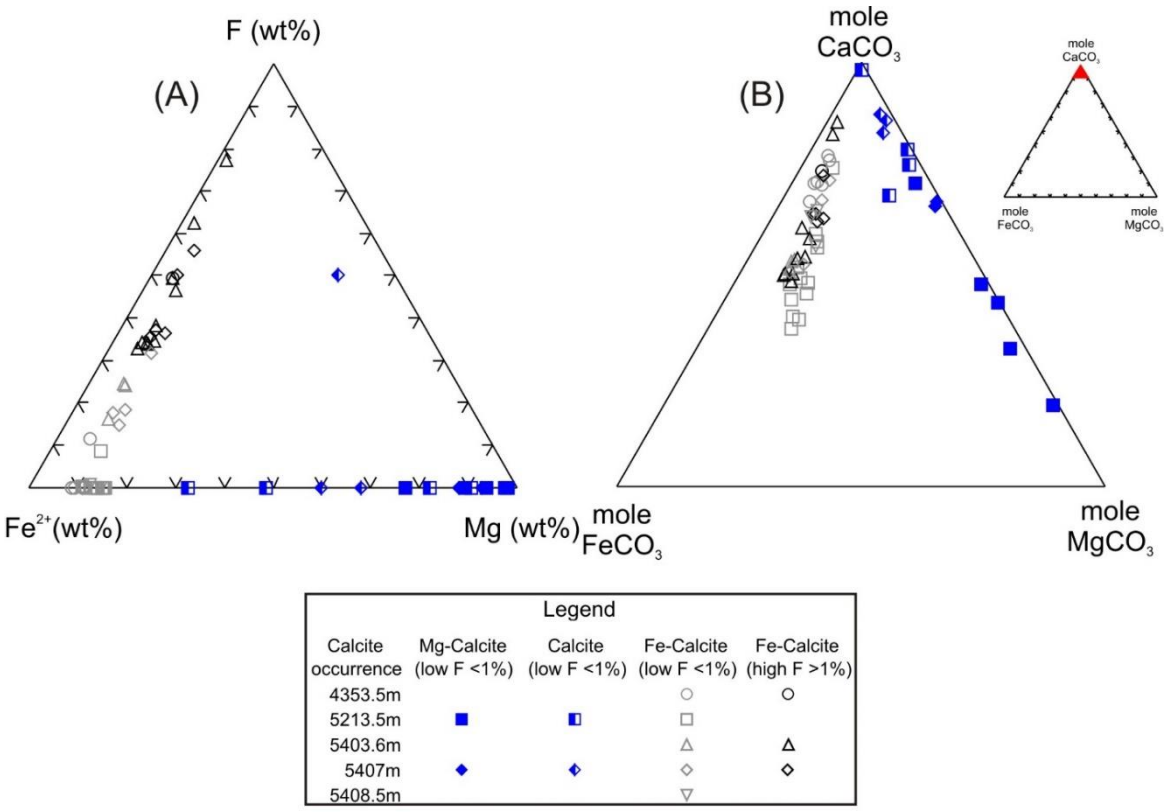

Fig. 4.12: Ternary diagram of calcite EMP data from the Newburn H-23 well. **A:** Analyses plotted on a fluorine, iron, and magnesium ternary diagram in element wt%. **B:** Analyses plotted on a $CaCO_3$, $FeCO_3$, and $MgCO_3$ ternary diagram in mole%.

The question of how fluoride is incorporated in calcite has been further investigated by elemental mapping of a sandstone sample (5408.5m) with apparent F-Fe-calcite cement. In the literature, both fluoride adsorption and surface precipitation of fluorite on calcite have been proposed (Budyanto et al., 2015). In this study, the elemental mapping was also used to determine if a) fluorite microcrystals can be seen; b) if minerals other than calcite were hosts for fluorine; and c) if textural distribution of fluorine provides evidence for timing of fluoride enrichment.

In the studied sample framework grains comprise quartz, lithic clasts, albite and muscovite (Figs. 4.13A, 4.14). Quartz grains have overgrowths that have resulted in complete silica cementation in many areas, but with some porosity bounded by euhedral

quartz crystal faces (a in Fig. 4.13A). Albite and muscovite have been partly engulfed by the silica overgrowths with variable fluorine, up to 3 wt. %, in other samples with similar lithic clasts (Fig. 4.10E). Porosity was partly filled by massive (?sparry) ferroan calcite after quartz overgrowths (b in Fig. 4.13A). There is some secondary porosity formed by dissolution along crystal boundaries in the silicate mineral framework (c in Fig. 4.13A).

An area (Fig. 4.13) now principally of calcite and chlorite appears morphologically to have been a lithic clast partly deformed during compaction (Figs. 4.13B and C). This lithic clast includes a few 5–10 mm quartz grains, a 40 mm long muscovite flake, a 10 mm grain of titania, and (from EDS analysis) some phosphate (Fig. 4.13A). Most of the chlorite is fibrous or platy and it appears porous and diagenetic (4.13C). Secondary porosity has delicate chlorite fibers, suggesting that the porosity formed by volume reduction from a precursor, rather than by dissolution of chlorite. This late chlorite contains also variable fluorine (up to 3 wt. % in another sample with similar lithic clast, Fig. 4.10E). The calcite appears sparry with abundant secondary porosity particularly along crystal boundaries (Fig. 4.13C). Neither figure 4.13B or 4.13C shows any microcrystalline fluorite present.

To determine how the fluorine was distributed within this deformed lithic clast an element map was taken using the SEM. Fluorine is strongly positively correlated with the presence of calcite. Lower levels of fluorine are present in the chlorite and in the outermost few mm at the edge of the framework silicate minerals (Fig. 4.14B, where the white line marks the edge of quartz and albite). In many cases, especially in the albite, the high fluorine is related to the presence of secondary porosity, but this is not the case on the right side of the image. Fluorine is present beyond the edge of the lithic clast and appears to coat the edges of surrounding framework grains.

In conclusion, the resolution of the elemental mapping is not sufficient to distinguish between surface adsorption of fluoride and surface precipitation of fluorite. There is no evidence at the scale of resolution for precipitation of fluorite. However it seems that fluoride is also adsorbed on to chlorite and the margins of framework quartz. In the case of chlorite (Fig. 4.13B), the fluoride may be in the micron-scale porosity, but image resolution is insufficient to determine if there is nano-scale porosity in the quartz (Figs. 4.13A and 4.14D).

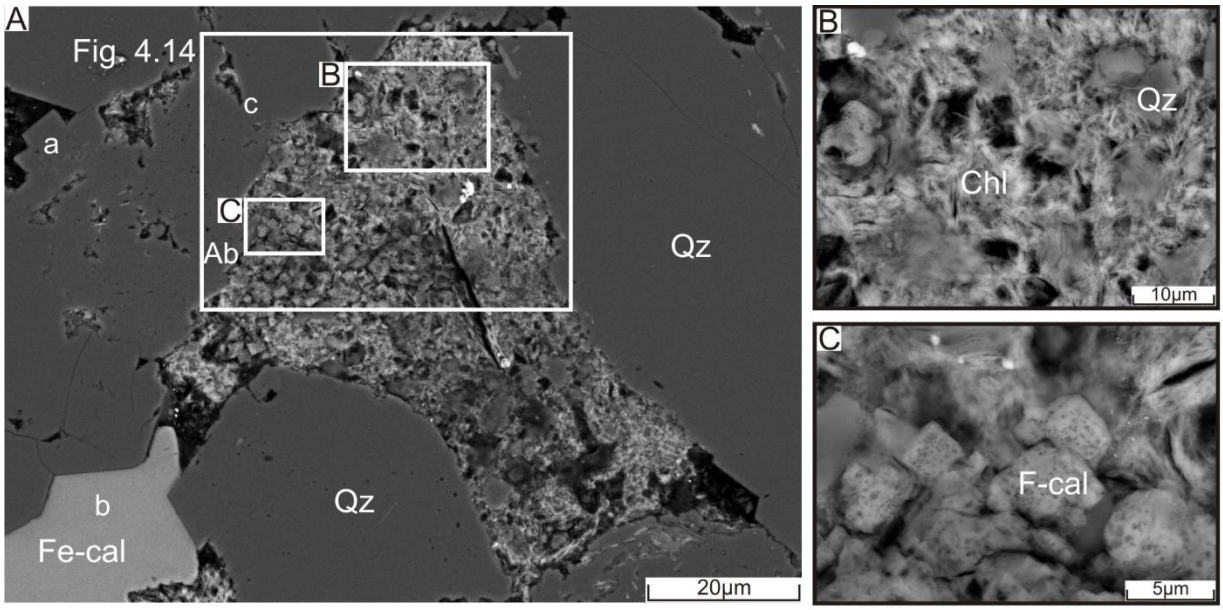

Fig. 4.13: BSE images from sample H-23 5408.5 m showing a lithic clast which has been affected by late cementation of F-calcite and chlorite (see details in Fig. 2-9.18, Appendix 2-9). The location of the elemental mapping of Fig. 4.14 is shown.

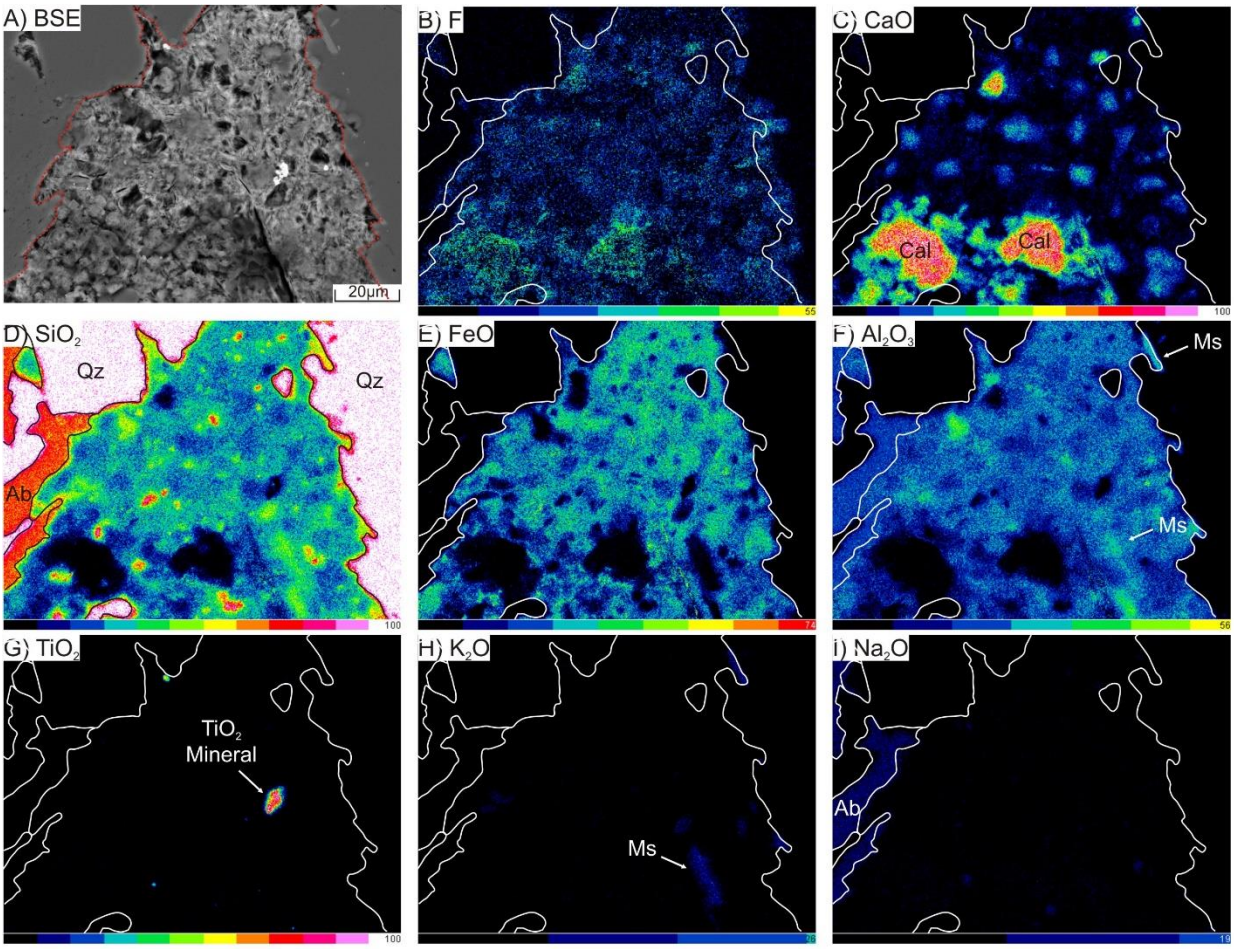

Fig. 4.14: BSE image (A) and quantitative element mapping images (B-I) from SEM-EDS analysis of sample H-23 5408.5 showing the distributions of F, CaO, SiO_2, FeO, Al_2O_3, TiO_2, K_2O and Na_2O. See location in Fig. 4.13. The colour bar in the elemental maps is scaled to the quantitative EDS analysis (wt%). The intergranular boundary is marked by solid white line.

Raman spectral analyses were also performed on F-Fe-calcites from sample 5403.6 m in order to determine how fluorine behaved during the formation of the F-Fe-calcite, specifically if fluorite has precipitated on the F-Fe-calcite surface. All of the analyses returned calcite as the major mineral phase (Figs. 4.15-4.17), however two analyses, ~2µm apart, showed minor "shoulder" peaks (Figs. 4.17A and 4.17B) which correspond to two peaks from a pure fluorite analyses (Figs 4.17A and 4.17B). These shoulder peaks are not present in all analyses from this grain. They are only present in the right vertex of the F-Fe-calcite grain (Figs 4.15D and 4.16D). When compared to the

EMP analyses (App. 3-3.2), no relationship was found between areas which have a high fluorine content and those areas which have shoulder spectral lines. This suggests that fluorite surface precipitation probably occurred as patches in the F-Fe-calcite and that it was not the only method by which fluorine was incorporated into the F-Fe-calcite analyses. Additionally, since no shoulder peaks were found in the other analyzed grains it seems that fluoride adsorption onto Fe-calcite was predominant, and the conditions which favored the surface precipitation of fluorite did not persist throughout the entire period of formation of the F-Fe-calcite.

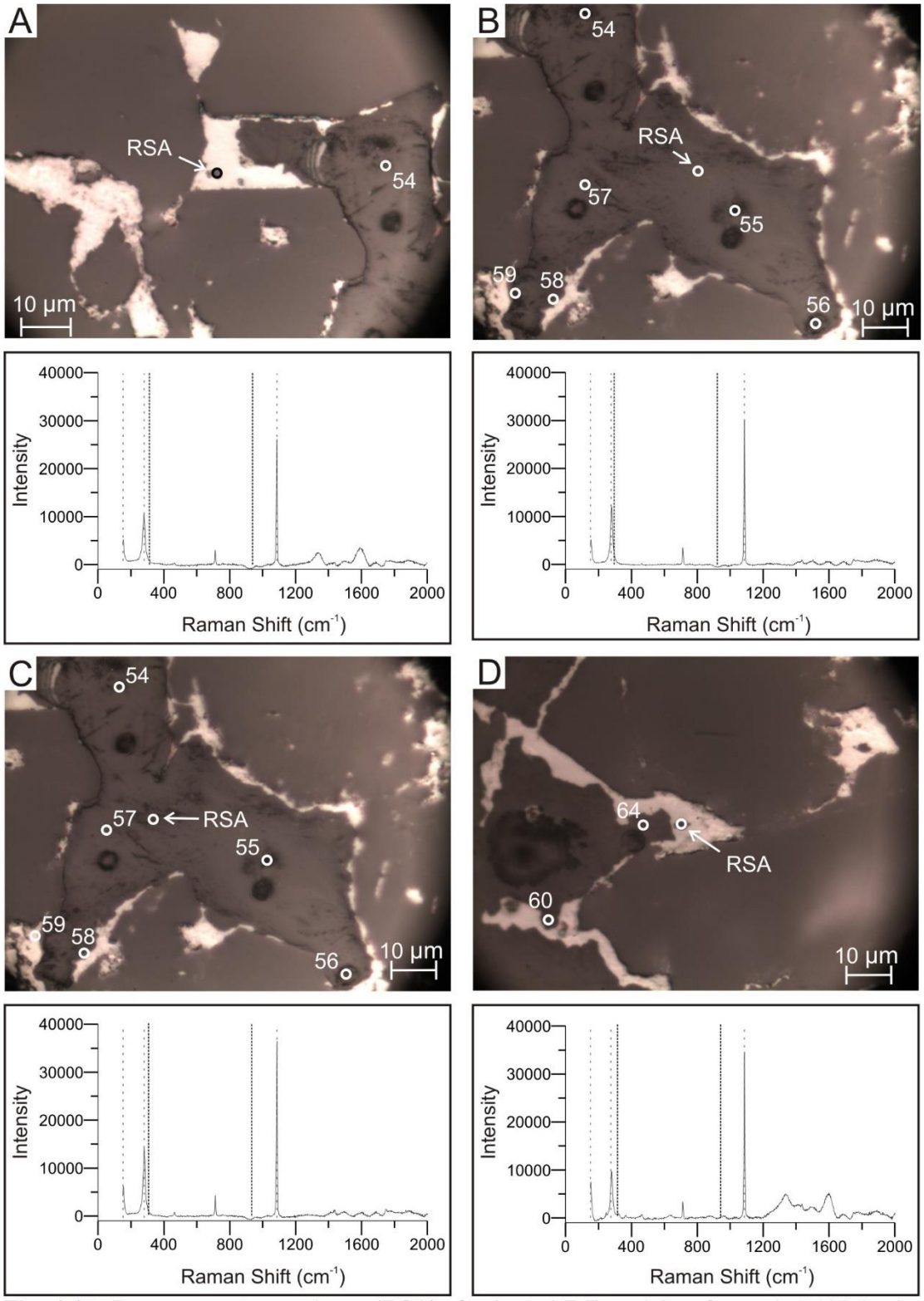

Fig. 4.15: Raman spectra analyses (RSA) of selected F-Fe-calcite of sample 5403.6m in the Newburn H-23 well, with reference spectral lines for calcite (dashed grey lines) and fluorite (dashed black lines), as well as the locations of EMP analyses (Figs 1 and 2 App. 3-3) that also have been used for RSA. **A-D:** Location of spots used for RSA. Note that a second spectrum from location D is shown in Fig. 4.16D.

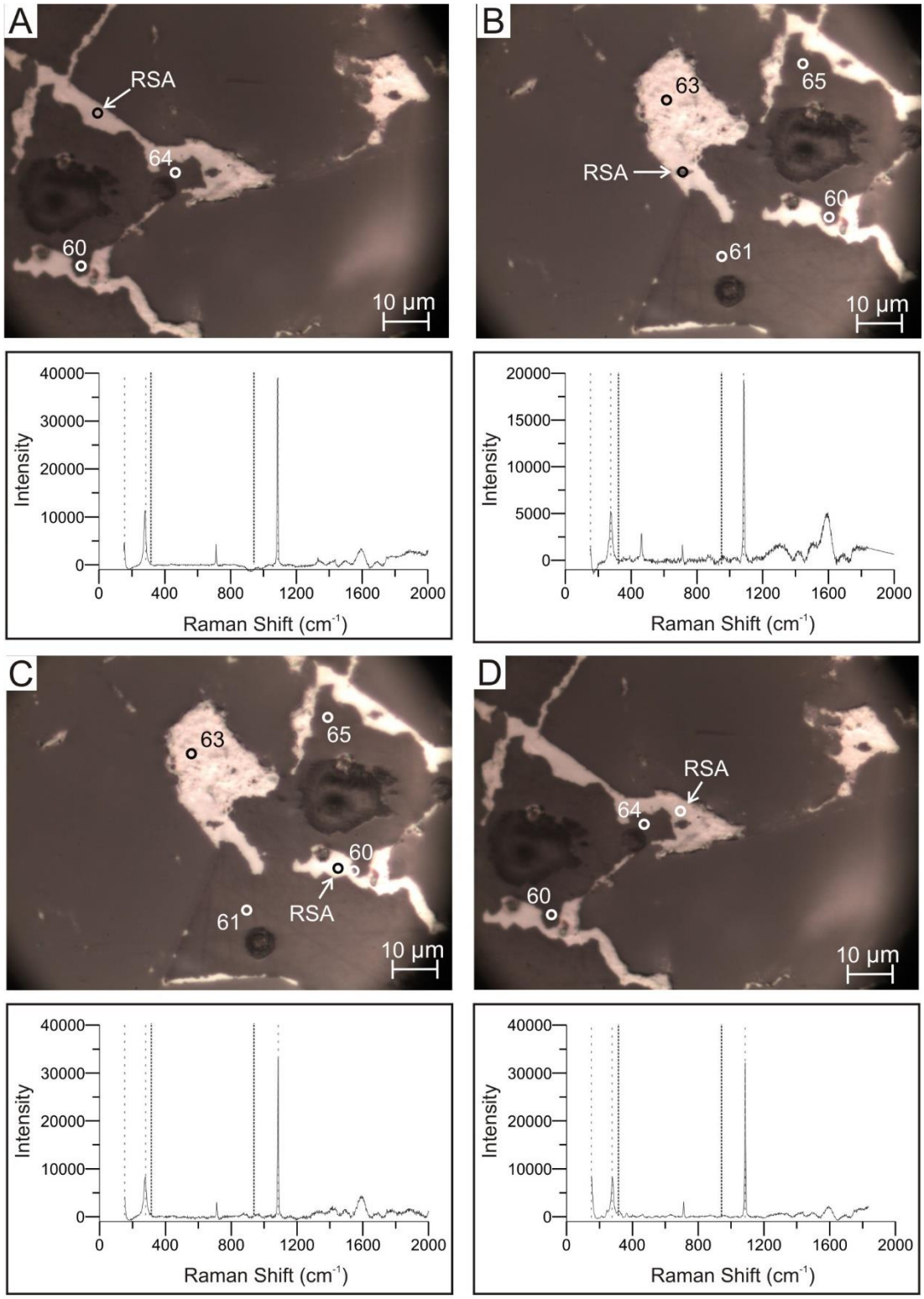

Fig. 4.16: Raman spectra analyses (RSA) of selected F-Fe-calcite of sample 5403.6m in the Newburn H-23 well, with reference spectral lines for calcite (dashed grey lines) and fluorite (dashed black lines), as well as the locations of EMP analyses (App. 3-3, Fig. 2) that also have been used for RSA. **A-D:** Location of spots used for RSA.

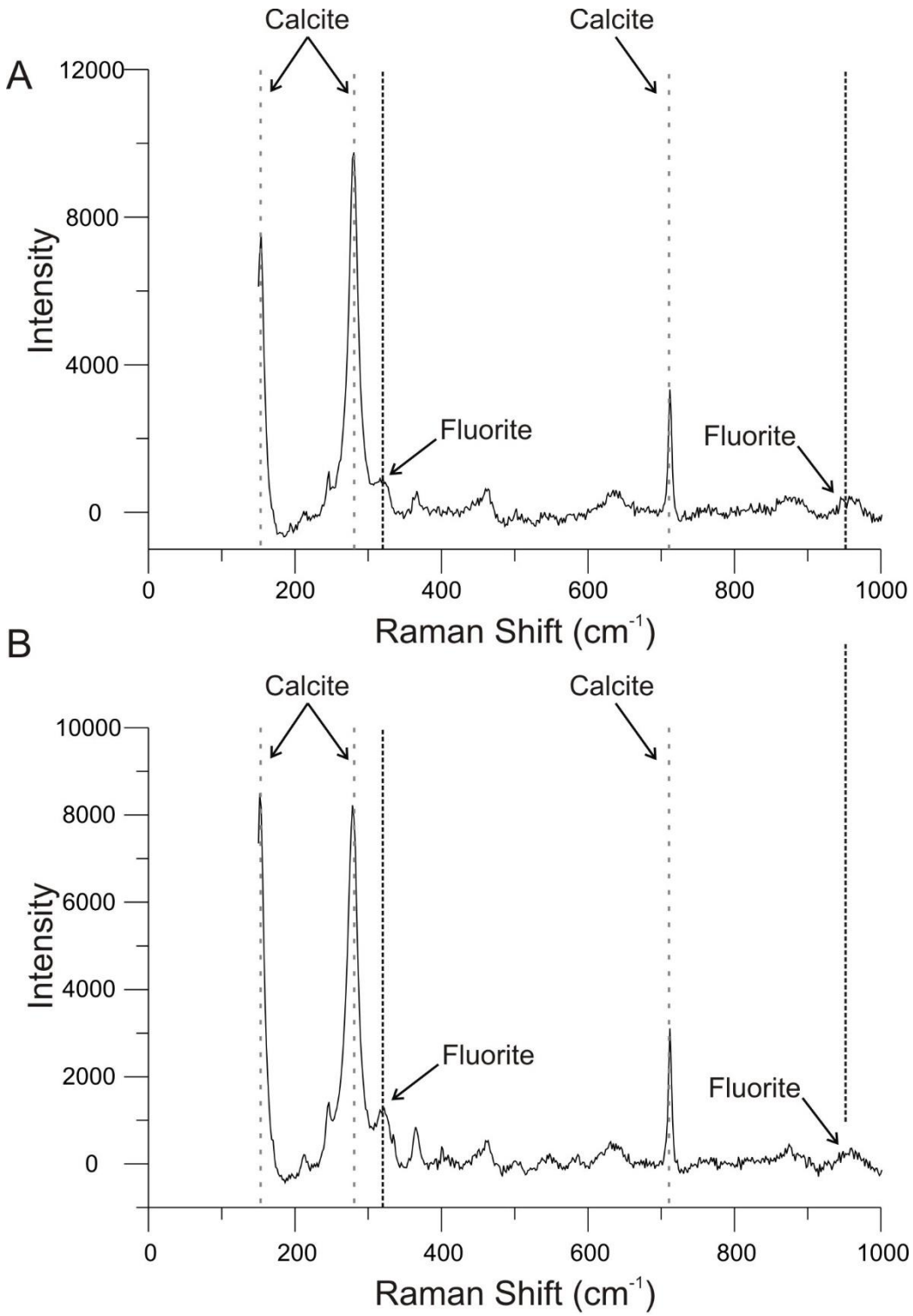

Fig. 4.17: Magnified Raman spectra from Figs. 4.15D and 4.16D from sample 5403.6m in the Newburn H-23 well, with reference spectral lines for calcite (dashed grey lines) and fluorite (dashed black lines). **A:** From Fig. 4.15D: shows small peaks which probably correspond to fluorite peaks. **B:** From Fig. 4.16D shows small peaks which probably correspond to fluorite peaks.

4.3.1.1 Summary

Carbonate cements in the Newburn H-23 well show a complex history of formation, dissolution, and reprecipitation. Ankerite, calcite, and Mg-calcite are the earliest species which are then later replaced by Fe-calcite and F-Fe-calcite and finally by siderite (Fig. 4.10). No aragonite, high fluorine Mg-calcite, or high fluorine calcite were observed in these samples to suggest the initial source of fluorine in this well. Of these minerals only Fe-calcite has been shown to contain fluorine >1 wt. %, and of the five samples analyzed high fluorine levels are only demonstrated in three samples, two of which are from the Middle Missisauga (Group 1) and range in fluorine content between 0.36 and 2.4 wt. %. X-ray mapping of a lithic clast from sample 5408.5m, which contains high fluorine in Fe-calcite, showed: no evidence of fluorite precipitation, variable fluorine content in chlorite, and a zone of elevated fluorine which extends into surrounding framework silicate grains. These observations suggest that the fluoride is also adsorbed onto the surfaces of the minerals of the analyzed lithic clast. Raman spectral analyses showed that some minor fluorite had precipitated on the surface of the Fe-calcite. It seems that this precipitation of fluorite occurred as rare patches, due probably to local physicochemical conditions. This data thus confirms that the majority of fluorine present in the F-Fe-calcite is the result of surface adsorption.

4.3.1.2 Overall Interpretation

The F-Fe-calcite in this study is most common in the deepest studied samples, late in their paragenesis and seems to be associated with dissolution, fibrous chlorite lining secondary porosity and late siderite. These observations suggest: **a)** The depth probably influenced either the availability of fluoride or the mechanism of association of fluoride

with Fe-calcite, **b)** changes in the composition of circulating basinal fluids, and **c)** an environment with low pH and F concentrations locally >10 ppm.

4.3.2 Titania minerals

Titania minerals are considered to be those which have a chemical composition of TiO_2. Such minerals form diagenetically under several different environmental conditions. The most common of these minerals include anatase, brookite, and rutile. Due to the fact that all of these titania minerals are polymorphs they cannot be distinguished chemically, however they have distinguishing optical and morphological features which can be used to identify them. Rutile and anatase crystallize in the tetragonal system (Nesse 2013), while brookite crystallizes in the orthorhombic system (Anthony et al., 2005). In thin section all three polymorphs show extreme positive relief, but have several diagnostic features: **a)** rutile is uniaxial positive, reddish brown, pale brown, or sometimes opaque in colour with weak pleochroism and generally forms as elongated tetragonal prisms or as slender, acicular, or hair like crystals (Nesse 2013); **b)** brookite is biaxial positive, brown, yellowish brown, reddish brown, dark brown to iron-black, yellowish brown to dark brown in colour with weak pleochroism, and it typically forms as tabular or pyramidal crystals (Nesse 2013); **c)** anatase is uniaxial negative pale brown, red brown, or deep brown in colour with weak pleochroism and generally forms as elongated dipyramids (Nesse 2013). Despite these differences it is still often difficult to differentiate between the three polymorphs using a petrographic microscope, however, several techniques have been developed to help with this issue of which Raman Laser Spectrometry has been used in this study.

Titanium is typically considered to be an immobile element and has been used in chemical discrimination plots specifically designed to minimize the effects of alteration on igneous rocks. It has however, been demonstrated that titanium is mobile in some sedimentary rocks.

The titanium which forms authigenic anatase, brookite, and rutile has been suggested to be sourced from detrital Fe-Ti-oxides, titanite, and biotite (Morad 1986). In general titanium minerals are resistant to weathering. However rutile and anatase have to been shown to be dissolved in ferrasols (Fe-rich soils) and later reprecipitated as anatase (Cornu et al., 1999) and detrital rutile as well can be dissolved during deep burial (Schulz et al., 2016), so dissolution of detrital titania minerals may also source diagenetic titania.

Titanium is increasingly mobile in solutions with a pH below 2 (Brookins 1988) and titanium forms complexes with a variety of organic compounds (Cornu et al., 1999) including ligands (Hays et al., 1994), orthotitanic acid (Fitzpatrick et al., 1978), and phosphate (Pe-Piper et al., 2011), which increase the solubility of titanium. Organic acids form "organo-titanium" complexes (Hays et al., 1994) which play a later role during the precipitation of titania minerals. In natural water conditions titanium becomes hydrated forming $TiO(OH)_2$ as a titanium hydrate which can be transported in pH conditions above 2 as colloidal particles (Skrabal 1995). This liberated titanium can be removed from solution as a result of flocculation of colloidal material, adsorption, and from scavenging by Mn and Fe oxides (Skrabal et al., 1995) reducing titanium available for titania minerals.

The precipitation of titania has been linked to the alteration of ilmenite under reducing conditions (Morad and Aldahan 1986), the "replacement" of feldspars (Morad and Aldahan 1987a), and the breakdown of organo-titanium complexes (Hays et al.,

1994). Titania minerals also form at temperatures below 150°C as a result of the presence of organic compounds and media (Chang et al., 2009, Ismagilov et al., 2009, Wang et al., 2012) and so the breakdown of organo-titanium complexes may play a pivotal role in precipitating titania minerals in systems in which organic material is widely available and temperatures are characteristic of deep burial diagenesis. So the formation of titania minerals may be largely controlled by the ability of organic compounds to complex with titanium.

Authigenic titania minerals form initially as nano-particles, < 100 nm in size in more than one dimension (Nowak and Bucheli 2007), which later aggregate into clusters several microns in size (Hotze et al., 2010). The ability of titania species to aggregate is promoted by an increase in the ionic strength of the solution in which titanium is being held (Chen et al., 2012). However increasing ionic strength also promotes the adsorption of organic matter onto the nano-particles (Chen et al., 2012). The adsorption of some organic acids, such as humic acid which occurs at pH below 6 (Yang et al., 2009), and organic matter onto the surface of the nano-particles decreases the ability of the titania nano-particles to aggregate (Domingos et al., 2009 and Keller et al., 2010).

The initial formation of brookite over anatase is favored by a pH of < 2 (Bhave and Lee 2007) and concentrations of $TiCl_4$ below $0.05 mol/dm^3$ at 100°C are required for it to form over rutile (Pottier et al., 2001). However synchronous crystallization of all three titania minerals (anatase, brookite, and rutile) has been shown to occur between 70°C and 100°C (Bhave and Lee 2007).

Since rutile is the most stable phase and anatase and brookite are metastable, the end product studied in the majority of research is rutile and as a result the typical path of precipitation has been found to be first hydrous oxide which converts to anatase and then

to rutile (Fitzpatrick and Chittleborough 2002). However brookite has a surface enthalpy which is larger than that of anatase and as the particle size of anatase increases its enthalpy changes very slightly while brookite has an enthalpy which increases quickly as its size increases (Benning and Waychunas 2008). As a result of this enthalpy difference, titania which first forms crystals of anatase may later change to brookite as crystal size continues to increase (Benning and Waychunas 2008). This means that the full path of precipitation may well be hydrous oxide which converts to anatase, then to brookite, and finally to rutile, a process which occurs at 475°C (Hu et al., 2003), as aggregation of nano-particles proceeds. Anatase may survive the aggregation process as long as the crystallization process of titania nano-particles is rapid, which promotes the nucleation and maintains crystallization of anatase (Bennings and Waychunas 2008).

Diagenetic titania has been observed in organic rich sedimentary rocks ranging in thermal maturity from immature to gas-window maturity (Schulz et al., 2016). These authors found that brookite occurs independent of total organic content (TOC) and thermal maturity. Anatase was found to form in samples from oil-water contacts and along faults. Brookite was further shown to require low pH and temperatures to precipitate from solution, whereas anatase requires higher temperatures. Brookite also forms in closed “micro-environments”, where conditions that allow the continuing formation of brookite occur.

Diagenetic titania minerals in this well cut and engulf early diagenetic minerals such as chlorite (Fig. 4.19A) and calcite (Fig. 4.19C), however their age relationship with high temperature, late forming minerals such as barite, sphalerite, and siderite is uncertain, as there is no textural evidence of relative age. Diagenetic titania crystals range in size from < 5 μm to ~120 μm with several major modes of occurrence in this well:

a) filling dissolution voids in framework lithic clasts with titania being around 1 µm in size (Fig. 4.18A). **b)** Along the cleavage planes of muscovite ranging from <1 µm to 10 µm in size (Figs. 18B and C). **c)** Along intergranular boundaries as single grains ranging from 2 µm to 50µm in size (Fig. 4.18D). **d)** Filling porosity cutting other diagenetic minerals (Figs. 4.19A and B). **e)** As aggregates composed of subhedral (typically 20 µm) to anhedral grains (<1 µm) which can be as large as ~120 µm (Figs. 4.19C and D).

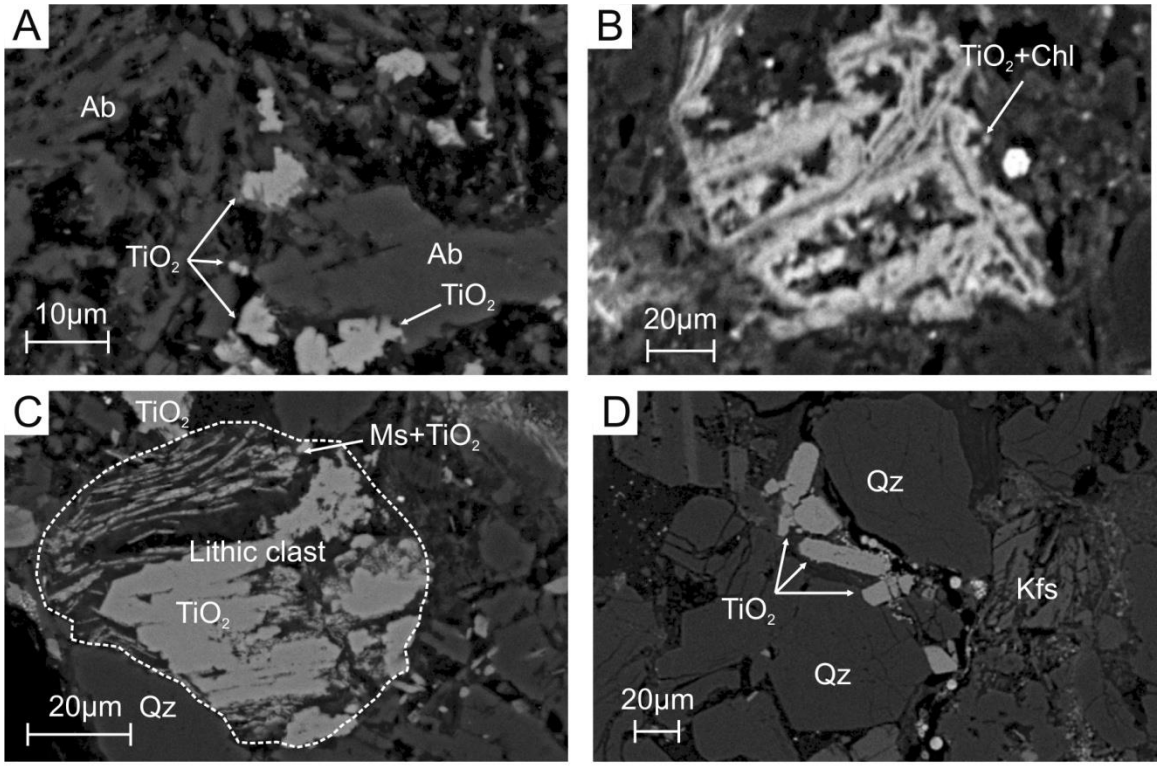

Fig. 4.18: Representative BSE images of titania minerals in the Newburn H-23 well.
A: Sample 4313.5m (App. 2-1, Fig. 21). Original albite-rich lithic clast has dissolution voids partly filled with titania.
B: Sample 4913.8m (App. 2-4, Fig. 7). Titania forms along the cleavage planes of chloritized muscovite, and appears to engulf it.
C: Sample 4313.5m (App. 2-1, Fig. 10). Lithic clast comprised of ragged titania, muscovite, quartz and siderite. Diagenetic titania forms along the cleavage planes of detrital muscovite.
D: Sample 4313.5m (App. 2-1, Fig. 14). Diagenetic titania forms along intergranular boundaries of framework grains.

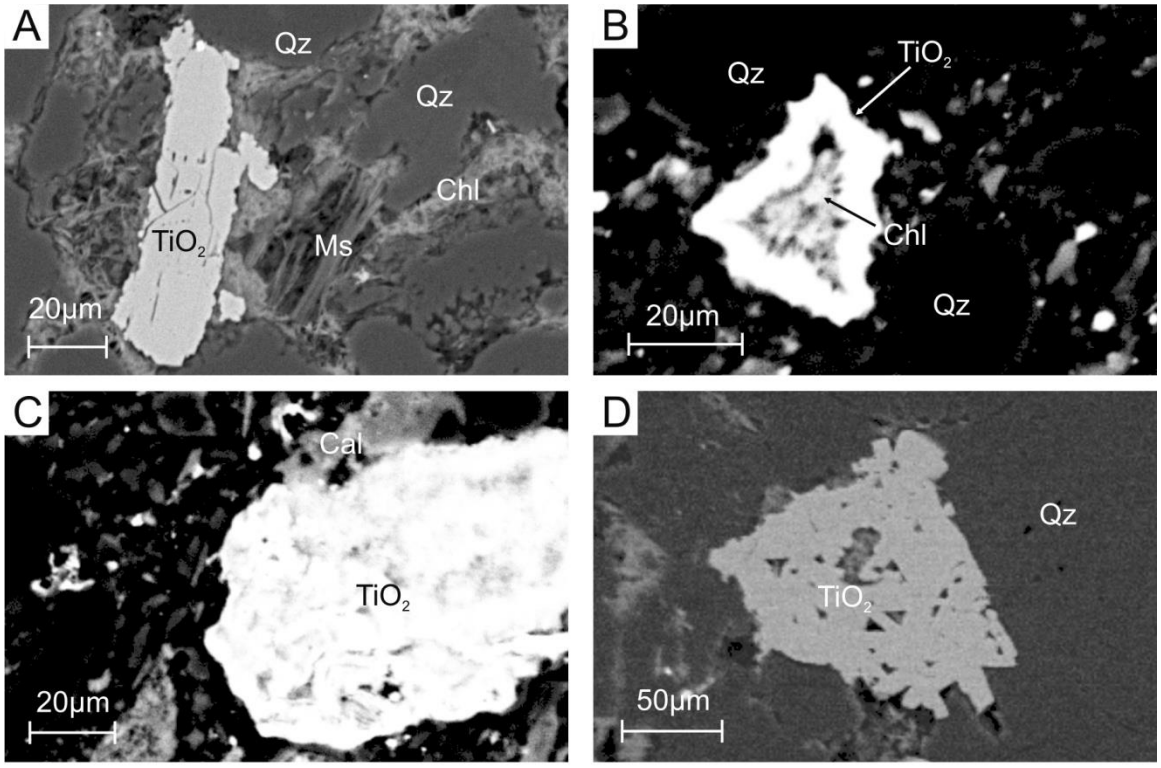

Fig. 4.19: Representative BSE images of titania minerals in the Newburn H-23 well.
A: Sample 5403.6m (App. 2-6, Fig. 3). Diagenetic titania cuts fibrous chlorite.
B: Sample 5213.5m (App. 2-5, Fig. 7). Titania rims pore filled with chlorite.
C: Sample 5213.5m (App. 2-5, Fig. 7). Subhedral titania appears to cut bedding.
D: Sample 5406.5m (App. 2-7, Fig. 6). Subhedral aggregate of titania.

To identify the types of titania minerals present in these samples titania grains have been analyzed using a Raman Laser Spectrometer (RLS). Diagenetic titania grains from sample 5406.5 m were analyzed due to the abundance of diagenetic titania present in the sample. The analyzed grains were chosen to represent anhedral and subhedral occurrences of titania. Spectra obtained from the Raman spectrometer of diagenetic titania minerals in sample 5406.5m indicate that there are at least two species of titania minerals present in this sample, two grains of anatase (Figs. 4.20A and B), and two grains of brookite (Figs. 20C and D).

The analyzed grains of anatase show two different forms: anhedral anatase which appearing to surround framework grains (Fig. 4.20A) and subhedral anatase with sharp

crystal outlines (Fig. 4.20B). Brookite also shows similar forms with one analyzed grain being anhedral filling porosity (Fig. 4.20C) and a second one which is subhedral in a cluster of several titania minerals between framework grains (Fig. 4.20D). All analyzed grains appear to be clean crystals with no apparent evidence that they are agglomerations or detrital grains.

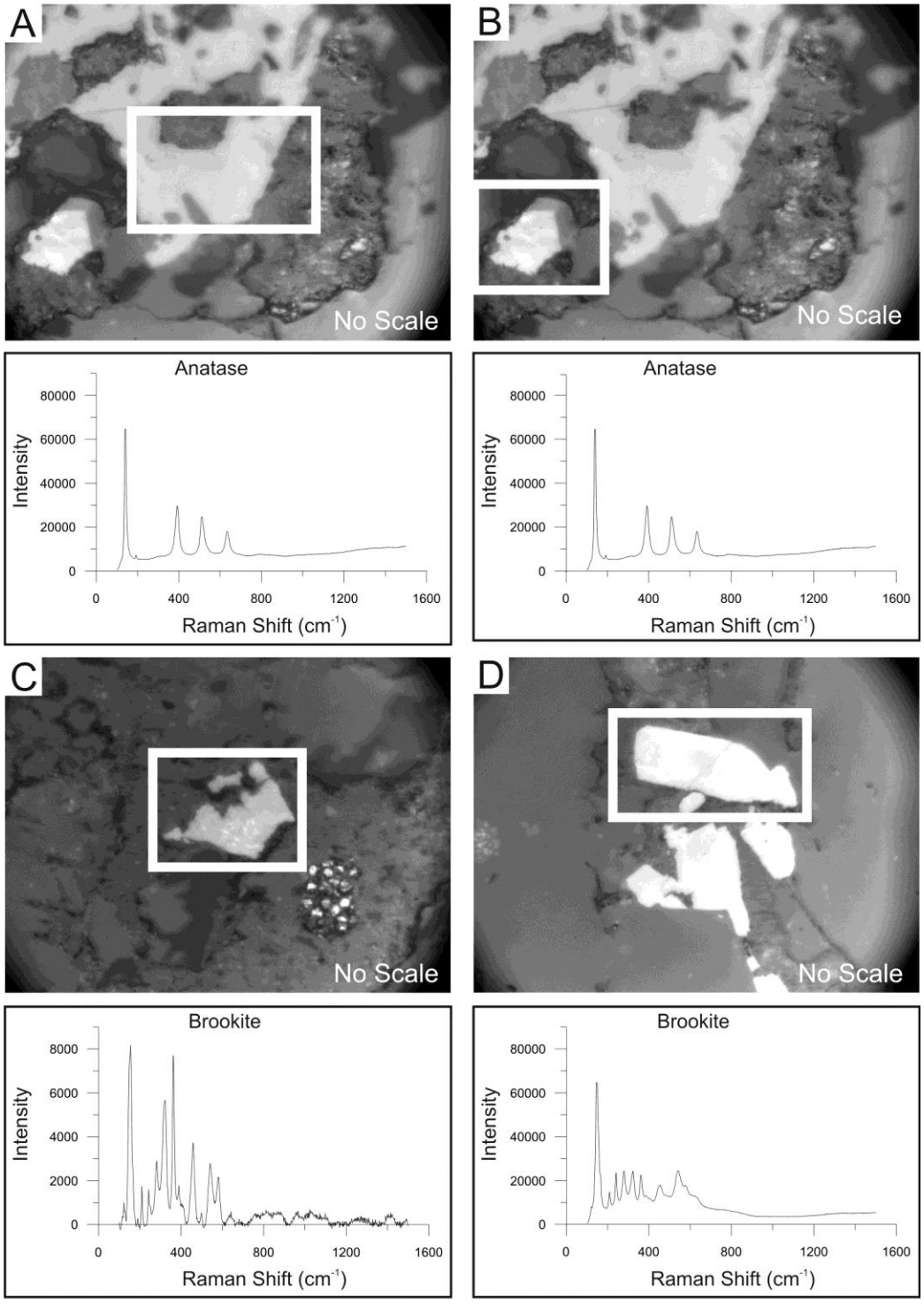

Fig. 4.20: Raman spectra of selected titania grains from sample 5406.5m. **A)** Analysis of anhedral authigenic anatase grain. **B)** Analysis of sub-hedral authigenic anatase grain. **C)** Analysis of anhedral authigenic brookite. **D)** Analysis of sub-hedral authigenic brookite.

4.3.2.1 Overall Interpretation

It is difficult to determine the conditions that allowed the formation of both anatase and brookite in the same sample. However there are several possible interpretations: **a)** co-precipitation of both phases; **b)** anatase formed first at which point some nano-particles aggregated sufficiently to be converted to brookite, while the remainder did not, possibly due to non-uniform supply of titania nano-particles throughout the sample; **c)** changing conditions of titanium bearing fluids, i.e. pH, titanium content, organic acid content, and temperature, resulting in different species of titania minerals forming locally in the sample or as the fluids, responsible for their formation, evolved with depth and time. A possible scenario in this case could be that initial brookite precipitation was followed by hydrocarbon migration that caused the system to become an oil-water contact environment which favored the formation of later anatase.

4.3.3 Diagenetic Zircon

Zircon is typically thought of as being a refractory mineral which endures all the stages of diagenesis with minimal effect on its composition and crystal structure. However papers published recently suggest that zircon may be more susceptible to dissolution and overgrowths than previously thought.

The textures and occurrences of multiple zircon grains in the Newburn H-23 well display crystal outlines which suggest that they may not be entirely detrital in nature. These features include crystal outlines which are straight in contact with porosity (Figs. 4.21A,B,E,F,G,H,I and 4.22E,H), partially lobate (Fig. 3.18F), appearing to partly fill porosity (Figs. 4.21D and 4.22A-C,G-I), and cross cutting other framework and cement minerals including chlorite (Figs. 4.21F,G and 4.22D,F), calcite (Figs. 4.21C,E), kaolinite

(Fig. 4.22H), K-feldspar (Fig. 4.21B), and quartz (Figs. 4.21B,E,G and 4.22A-D,G). Thus the textural relationships zircon shows with other minerals in the studied samples strongly suggest that these grains are partly or wholly diagenetic in origin.

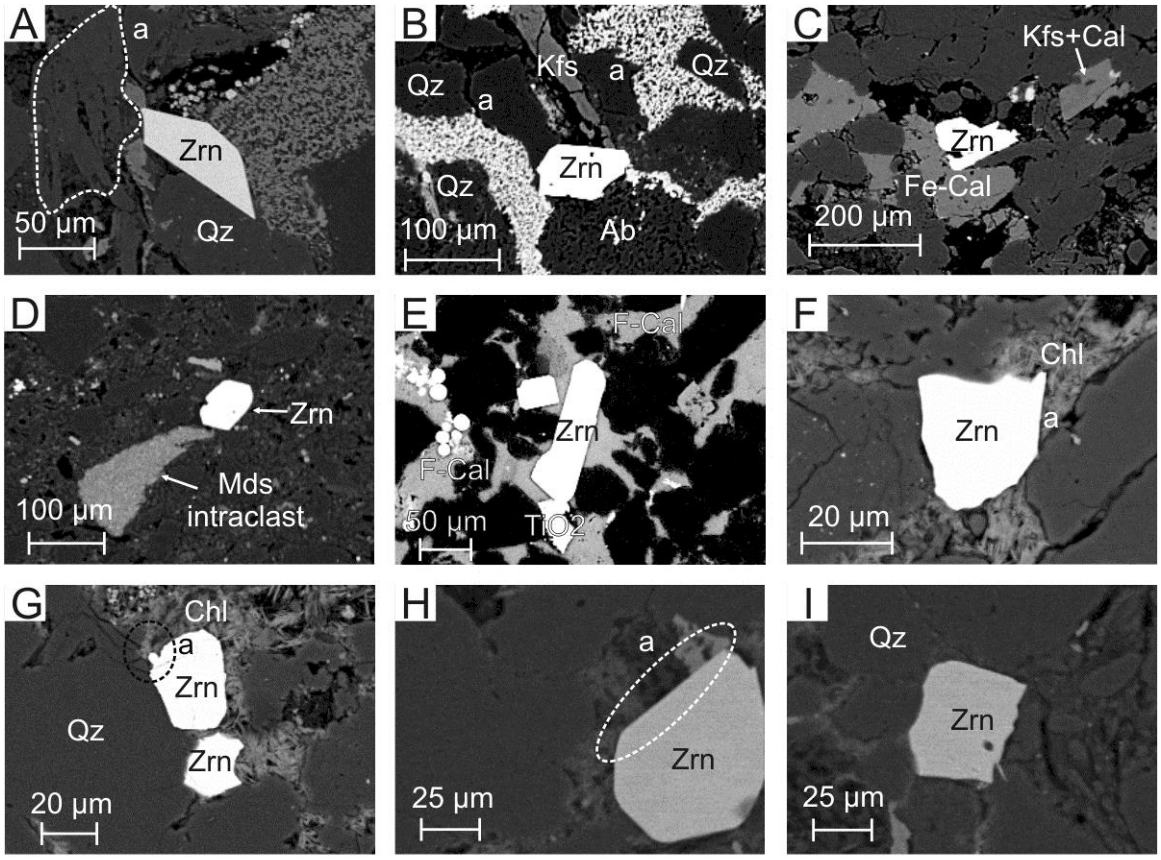

Fig. 4.21: Representative BSE images of textures in diagenetic zircon from the Newburn H-23 well.
A: Sample 4313.5m (App. 2-1, Fig. 1). Probable diagenetic zircon with sharp crystal outlines against silicate mineral and a dissolution void. Trachytic lithic clast (position a).
B: Sample 4318.5m (App. 2-2, Fig. 3). Plastically deformed intraclast of siderite and chlorite rims on quartz grains (positions a). Diagenetic zircon has straight crystal outlines and cuts framework grains, quartz and K-feldspar.
C: Sample 4353.5m (App. 2-3, Fig. 9). Euhedral face of diagenetic zircon in contact with Fe-calcite.
D: Sample 4913.8m (App. 2-4, Fig. 13). Diagenetic zircon fills pores. Mudstone (Mds) intraclast consisting of chlorite and siderite.
E: Sample 5213.5m (App. 2-5, Fig. 6). Diagenetic zircon cuts framework grains and F-calcite.
F: Sample 5403.6m (App. 2-6, Fig. 11). Zircon with straight crystal outlines towards chlorite (position a).
G: Sample 5403.6m (App. 2-6, Fig. 12). Euhedral faces of zircon in contact with quartz and probably engulfs chlorite (position a) and with euhedral crystal outlines towards both.
H: Sample 5406.5m (App. 2-7, Fig. 16). Euhedral faces of zircon appear to post-date filling of a pore (position a).
I: Sample 5406.5m (App. 2-7, Fig. 16). Diagenetic zircon with straight crystal outlines towards voids.

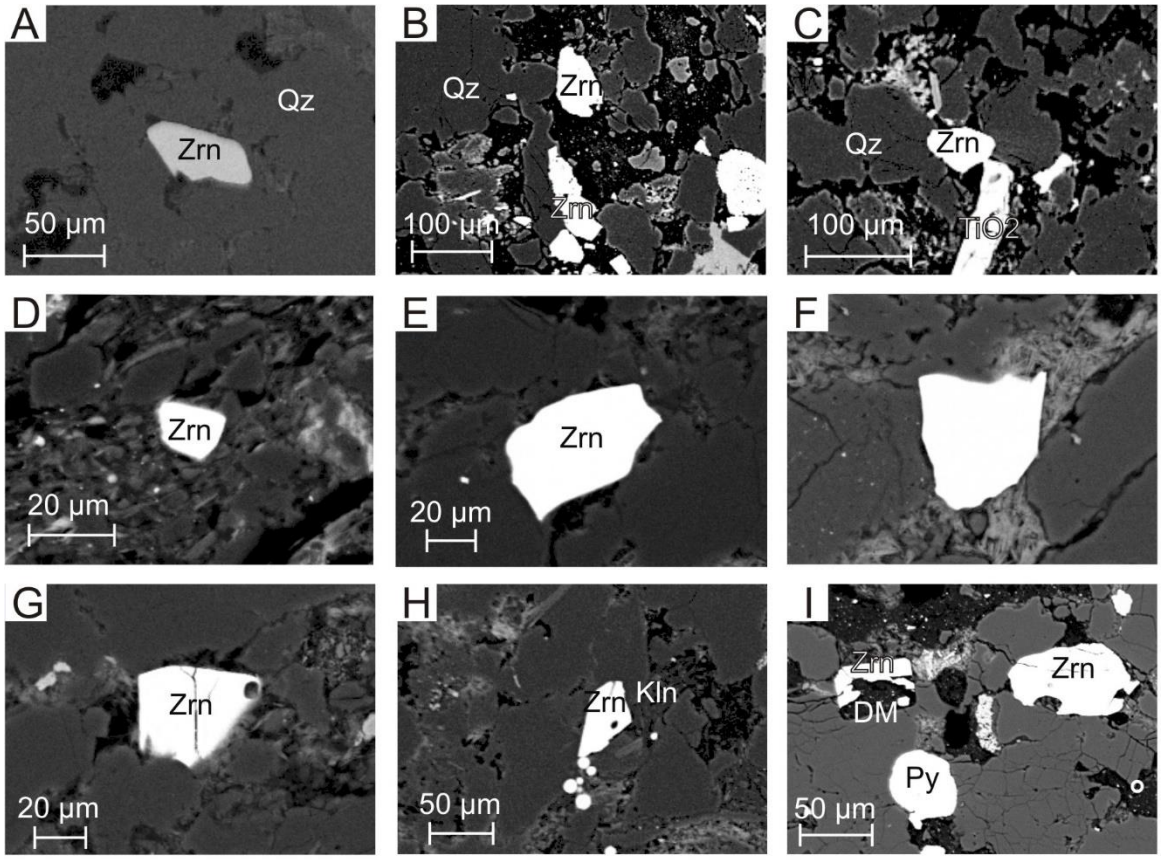

Fig. 4.22: Representative BSE images of textures in diagenetic zircon from the Newburn H-23 well.
A: Sample 5407m (App. 2-8, Fig. 12). Diagenetic zircon fills pore and cuts quartz.
B: Sample 5408.5m (App. 2-9, Fig. 11). Diagenetic zircon fills pore and engulfs quartz.
C: Sample 5408.5m (App. 2-9, Fig. 11). Diagenetic zircon fills pore and engulfs quartz.
D: Sample 5957.8m (App. 2-10, Fig. 17). Zircon cross cuts framework grains, quartz and muscovite.
E: Sample 5961.7m (App. 2-11, Fig. 9). Zircon appears to be diagenetic with straight crystal outlines in contact with quartz and pore.
F: Sample 5961.7m (App. 2-11, Fig. 11). Diagenetic Zircon cuts chlorite and is euhedral against porosity.
G: Sample 5961.7m (App. 2-11, Fig. 19). Diagenetic zircon fills pore and engulfs quartz.
H: Sample 5961.7m (App. 2-11, Fig. 4). Diagenetic zircon with dissolution void and straight crystal outline in contact with kaolinite filling pore.
I: Sample 5962m (App. 2-12, Fig. 2). Diagenetic zircon and drilling mud (DM) fill porosity.

The zircon grains from this well range in size from 20 μm (Fig. 4.19E) to ~140 μm (Fig. 4.19E) and appear to be well formed and clean, with rare dissolution voids and fractures. However high magnification images of the zircon grains (Fig. 4.23) show outgrowths (Figs 4.23A-C), dissolution accompanied by dark patches (Fig 4.23D), and zoning (Fig. 4.23A). This suggests that zircon grains which appear to be wholly diagenetic may in fact be the result of outgrowths or even detrital grains.

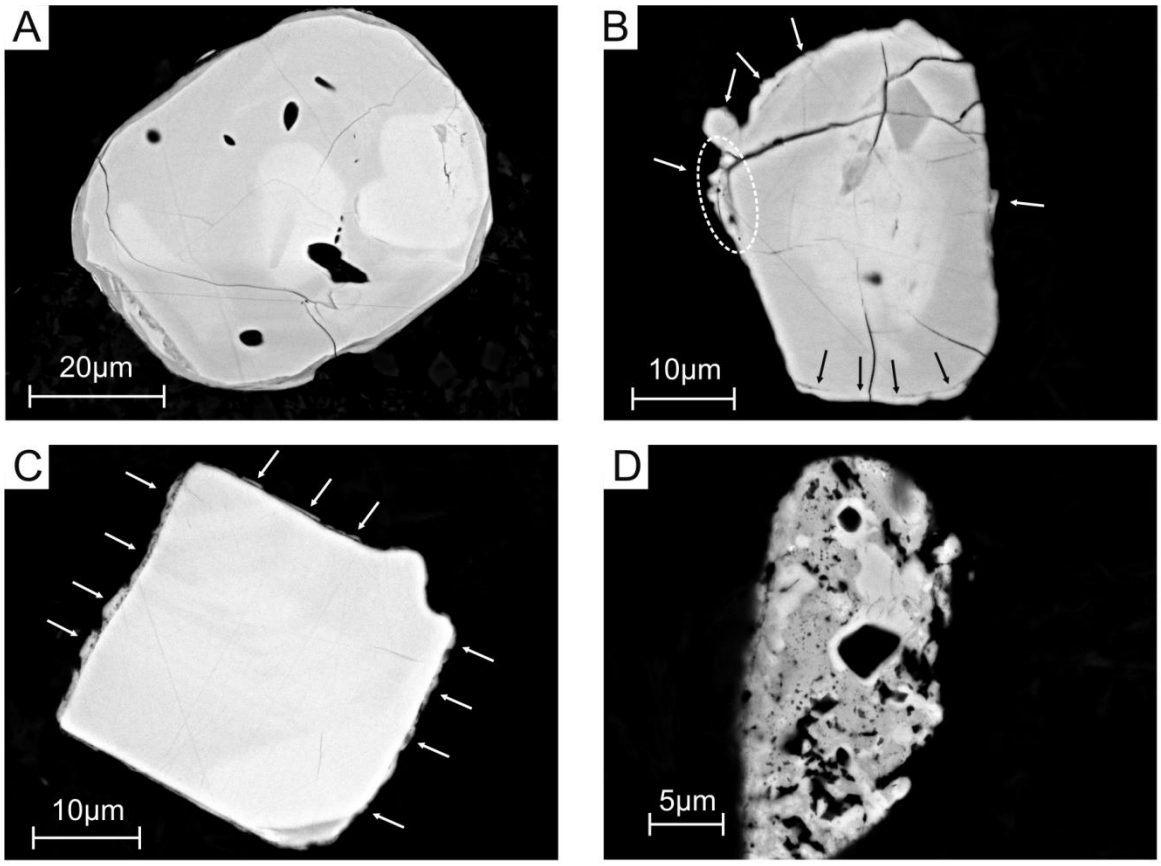

Fig. 4.23: High magnification BSE images of zircon grains from the Newburn H-23 well.
A: Sample 4313.5m (App. 2-1, Fig. 12). Zircon grain showing a dark rim which is probably an outgrowth of diagenetic zircon.
B: Sample 5403.6m (App. 2-6, Fig. 12). Zircon grain showing outgrowths (arrows), some of which are in contact with quartz (dashed line).
C: Sample 5961.7m (App. 2-11, Fig. 6). Zircon grain showing abundant outgrowths (arrows).
D: Sample 5961.7m (App. 2-11, Fig. 6). Zircon grain with abundant dissolution voids and dark patches which correspond to areas with dissolution voids.

The diagenetic zircon described in the literature shows varying morphologies. Outgrowths have been shown to form as minute irregular crystals attached to detrital zircon grains (Rasmussen 2005, figs. 3 and 4). These irregular crystals are typically less than 3μm in size and are commonly in "frilly rims" that partly surround detrital zircon, and can also line the surface of fragments of detrital zircon (Rasmussen 2005, figs. 5 and 6).

Zircon has also been shown to form in voids and fractures in coprolites in three forms **a)** amorphous zircon which fills pores in the coprolite, these are the largest of the diagenetic zircon which are described by Bojanowski et al. (2012) as up to 40 μm; **b)** bladed, saw tooth like, zoned crystals which line the walls of fractures in a coprolite; **c)** spherical zircon which is similar to bladed zircon and is formed by aggregates of prismatic zircon in radiating arrangements. These aggregates form a homogenous blanket on the walls of cracks (Bojanowski et al., 2012).

Zircon from low grade metamorphic rocks has been shown to have darker patches in BSE images that represent zones of low temperature dissolution-reprecipitation of metamict zircon within detrital zircon grains. These dark zircons are highly porous, resulting from volume changes during alteration, and have a distinct brightness contrast from the unaltered zircon, often forming along zoning and at the core of the detrital zircon where radiation damage has accumulated (Hay and Dempster 2009).

Zircon grains studied from a variety of rocks, which range in metamorphic grade, reveal that the accumulation of radiation damage (forming metamict zircon), followed by fluid access at low temperature result in alteration and replacement of metamict zircon. Zircon alteration appears to be pervasive in low grade metasedimentary rocks which contain metamict zircon (Hay and Dempster 2009). As metamict zircon is dissolved

during alteration it supersaturates the fluids in contact with the zircon with zirconium, this supersaturated zirconium is later re-precipitated as dark zircon where metamict zircon has been dissolved. The lowest reported temperature suite, from the Easdale slates, had a maximum temperature of 300-350°C. The new low temperature zircon crystals from the metamorphic rocks are porous, inclusion rich, probably nano-crystalline, hydrous, and enriched in non-formula elements (e.g. Fe, Al) and grow as a result of dissolution-reprecipitation processes (Hay and Dempster 2009). Increasing metamorphic grade and higher temperatures appear to enhance dissolution. The liberated zirconium is mobilized from areas of low temperature alteration and forms outgrowths on the margins of unmodified zircon crystals.

Metamorphic grade temperatures are not the only method of dissolution and reprecipitation of existing zircon grains; this process has been suggested to occur even in sedimentary rocks (Bojanowski et al., 2012). The dissolution and reprecipitation of zircon is facilitated by a combination of high concentrations of fluorine, phosphate, and carbonate in hydrothermal fluids in contact with zircon (Bojanowski et al., 2012). This process can occur at temperatures as low as 270° C (Bojanowski et al., 2012), and irregular outgrowths have been shown to form in prehnite-pumpellyite grade shales at 250° C (Rasmussen 2004).

The mobility of Zr is promoted by the presence of ligands in solution, F^- and PO_4^{3-} anions are major ligands (Giere 1990) forming complexes with Zr which allow for the typically immobile element to be transported in solution. F^- in particular is an important during this process, as a content of between 0 and 6 wt% F^- in solution increases the solubility of Zr by its square (Rubin et al., 1992). Since these ligands are so important to the mobility of Zr it follows that the deposition of Zr is heavily related to their behaviour

within the fluids. Decreases in ligand activity within solution facilitates the removal of Zr from solution (Giere 1990), particularly during the formation of minerals which contain the complexing elements (Giere 1990).

In the Newburn H-23 well there are several diagenetic minerals which contain fluorine and phosphorus including apatite, fluorapatite, fluorite, and F-Fe-calcite. Since these are considered to be major ligands for Zr it is likely that the fluids responsible for the formation of these minerals may well have also transported the Zr which sourced diagenetic zircon in this well, and that their formation may have resulted in the formation of diagenetic zircon.

The characteristics of the fluids responsible for the mobilization of Zr vary. High concentrations of Zr have been documented in alkaline fluids with pH values of ~10 (Vard and William-Jones 1993) and ~12 (Kraynov et al., 1969). Solubility experiments performed by Aja et al. (1995) on Zr bearing minerals showed that $Zr(OH)_{4(aq)}$ is the dominant form in which Zr is transported in solution over a wide variety of pH conditions. However, due to the abundance of F bearing minerals in these samples and that F^- is a major ligand for Zr it is more likely that Zr has been transported in a F^- complex. According to the model of Zr solubility used by Aja et al. (1995), F^- complexes cannot form under alkaline conditions, and so the fluids responsible for the transport of Zr were probably not alkaline.

The conditions proposed by Bojanowski et al. (2012) and Rasmussen (2004) are not too far removed from the ones that may be suggested for the Scotian Basin. High temperature diagenetic minerals, sphalerite and barite, are present in all stratigraphic levels in the Newburn H-23 well. Sphalerite (samples 4315.5 m, 4913.8 m, 5403.6 m, 5407 m, 5961.2 m), which forms between 140 and 200°C (Karim et al., 2008), and barite

(samples 4315.5 m, 4318.5 m, 4913.8 m, 5213.5 m, 5403.6 m, 5408.5 m, 5962 m), which forms hydrothermally between 70 and 250°C, although is also known to form from seafloor seeps (Pe-Piper et al., 2015).

A widespread thermal event in the Scotian Basin during the Aptian-Albian may be recorded by high trapping temperature of primary fluid inclusions in quartz overgrowths and carbonate cements, volcanism in the Orpheus graben and enhanced heat flow in terrestrial basins (Bowman et al., 2012), and by strongly negative δC^{13} in carbonate cements of that age (Karim et al., 2012). This event increased the temperature of circulating brines, as shown in trapping temperatures in quartz overgrowths which are as high as 228°C and in carbonate cements as high as 189°C in the Lower Missisauga Formation in the Thebaud well (Karim et al., 2012). Entrapment temperatures have been shown to be at least 20-40°C higher than present down-hole temperatures. It has been suggested that this thermal event is the result of a regional process in the mantle, probably related to the rifting of Iberia and the Grand Banks (Pe-Piper et al., 2007). This event increased the regional geothermal gradient to 55°C/km (Karim et al., 2012). The presence of diagenetic sphalerite in the Glenelg field post-dating carbonate cements was correlated with Albian-Cenomanian movement on the Balvenie salt Roho system. However sphalerite and high temperature fluid inclusions in Albian sandstones at Peskwesk A-99 (Pe-Piper at al., 2015) and apatite fission track data from Albian aged sandstones in several wells (Li et al., 1995) indicate younger hot fluid flow in the basin, likely in the Late Cretaceous or Paleogene. This inferred hot fluid flow at Peskwesk A-99 correlates with latest Cretaceous or Paleogene movement on the Banquereau salt detachment (Pe-Piper et al., 2015).

4.3.3.1 Summary

Zircon grains in the Newburn H-23 well are formed with sharp edges against porosity and cutting framework grains, have outgrowths, and show dissolution voids. Diagenetic zircons in the literature have been documented to form at temperatures of approximately 270°C and form outgrowths at around 250°C. In such cases, zirconium has been shown to be mobilized during the alteration of zircons during low grade metamorphism and may have been the source for these diagenetic zircon crystals. The presence of diagenetic sphalerite and the documented high temperature fluid flow events in the Scotian Basin indicate conditions which could have been suitable for the formation of diagenetic zircon in this well by a mechanism similar to that described by Bojanowski et al. (2012).

4.3.3.2 Overall Interpretation

If the zircon grains which have displayed crosscutting relationships and pore filling textures are wholly diagenetic, then the euhedral form of these grains may suggest **a)** a large supply of complexing ligands, particularly F^-, in parent solutions which formed the zircon, **b)** a large supply of zirconium from altered and dissolved metamict zircon, **c)** temperatures above 270°C which formed diagenetic outgrowths on detrital zircon grains.

However these euhedral grains may represent airborne volcanic ash from Cretaceous volcanic eruptions in the Scotian Basin or relative hardness of adjacent framework grains. U/Pb dating of small (<50 μm), euhedral, inclusion free zircon crystals with or without outgrowths is suggested to determine if the formation of wholly, or largely diagenetic zircon grains has occurred in the Newburn H-23 well or if they are of detrital origin.

The morphologies observed in high magnification BSE images (Fig. 4.23) suggest that precipitation of diagenetic zircon occurred dominantly in the form of outgrowths on probably detrital zircon grains, and that it is possible that conditions required to alter metamict zircon were also present within this well. The presence of outgrowths on detrital zircon grains as well as apparent dissolution of diagenetic zircon grains suggests temperatures of at least 250°C, along with a large supply of both complexing elements, such as fluorine and phosphorus, and zirconium from dissolved detrital zircon and lithic clasts. However, further work is required to determine the extent of diagenetic zircon formation on the Newburn H-23 well.

4.3.4 Paragenetic sequences

Paragenetic sequences are used to reconstruct the evolution of sedimentary rocks during burial. These sequences have been generated from observations made in chapter 3.3 and use several textural criteria including: **a)** replacement of one mineral by another with the replaced mineral being older; **b)** engulfment of one mineral by another with the engulfed mineral being older; **c)** one mineral impeding the growth of another with the impeding mineral being older; **d)** one mineral deforming around another with the deformed mineral being older. The majority of the paragenetic sequences, which have been generated (Figs. 4.24-4.27) for this well, are generally similar with mostly minor differences related to the presence of several minerals. Such as glauconite and F-calcite, which are only present in the Cree Member and the Middle Missisauga Formation (Group 1). The paragenetic sequences from this well indicate the following: **a)** F-Fe-calcite in the Cree Member and Middle Missisauga Formation (Group 1) suggests increased fluoride concentration and salinity in circulating basinal fluids at those intervals during

eodiagenesis; **b)** diagenetic zircon from all intervals suggests increased temperatures of at least 250°C , and a supply of complexing elements and zirconium during mesodiagenesis; **c)** diagenetic sphalerite from the Cree Member and Middle Missisauga Formation suggests high salinity in the well during mesodiagenesis; and **d)** the presence of diagenetic titania minerals at all intervals suggests low pH and high organic content in pore waters during eodiagenesis to mesodiagenesis.

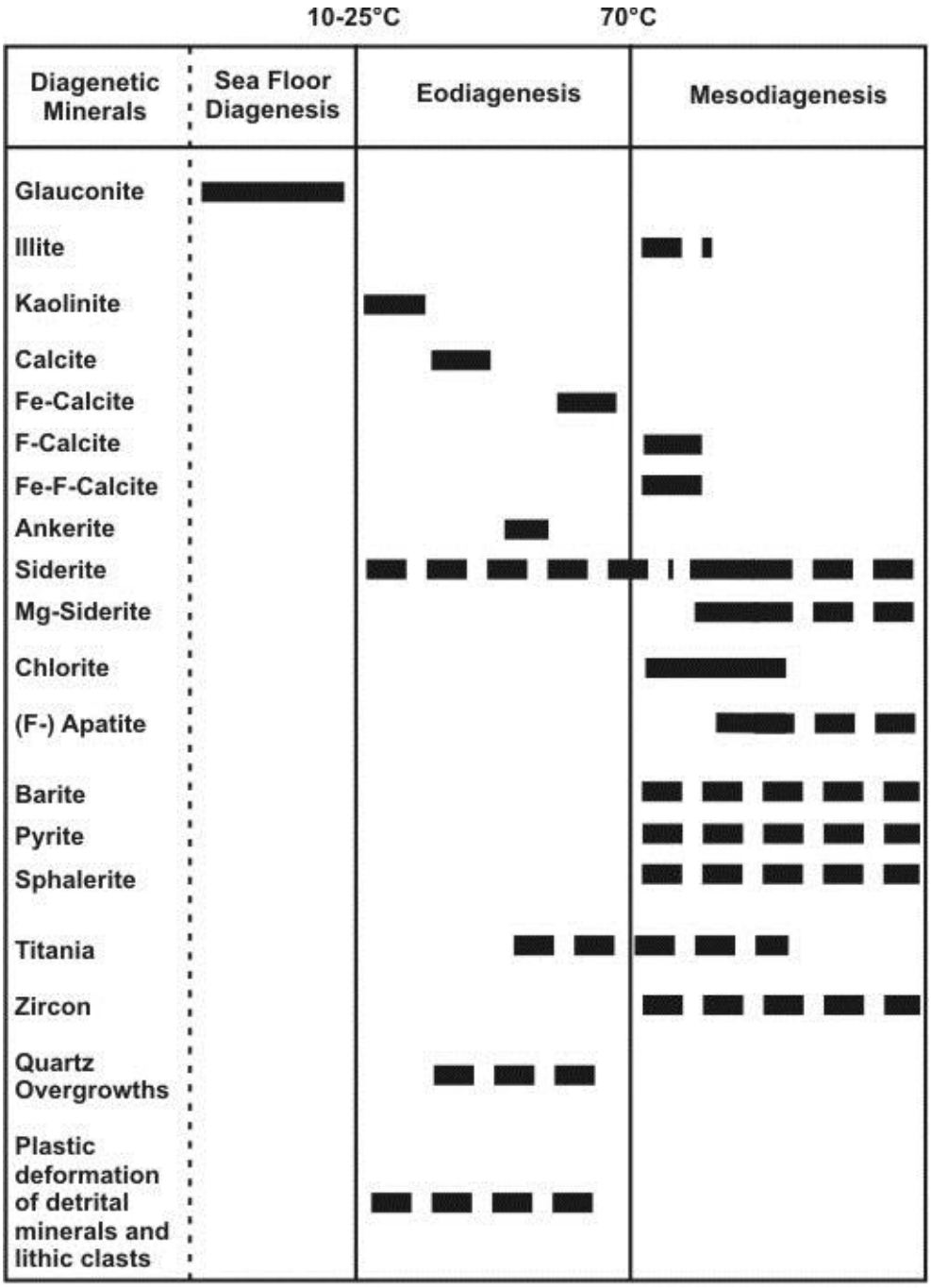

Fig. 4.24: Interpreted paragenetic sequences generated using textural relationships shared between samples from the Cree Member of the Logan Canyon Formation in the Newburn H-23 well. The boundary between eodiagenesis and mesodiagenesis was taken from Morad et al. (2000) and El Ghali et al. (2006).

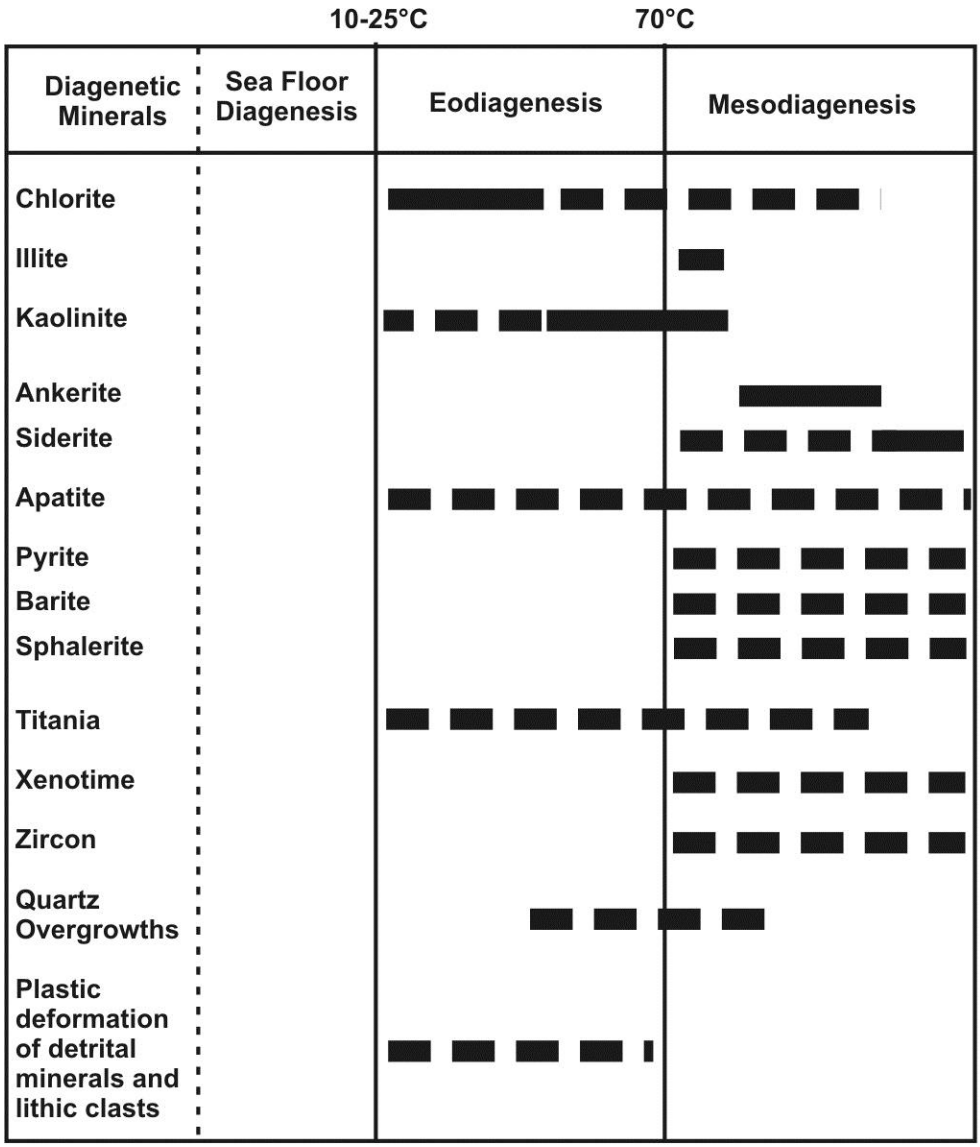

Fig. 4.25: Interpreted paragenetic sequences generated using textural relationships shared between samples from the Upper Missisauga Formation in the Newburn H-23 well. The boundary between eodiagenesis and mesodiagenesis was taken from Morad et al. (2000) and El Ghali et al. (2006).

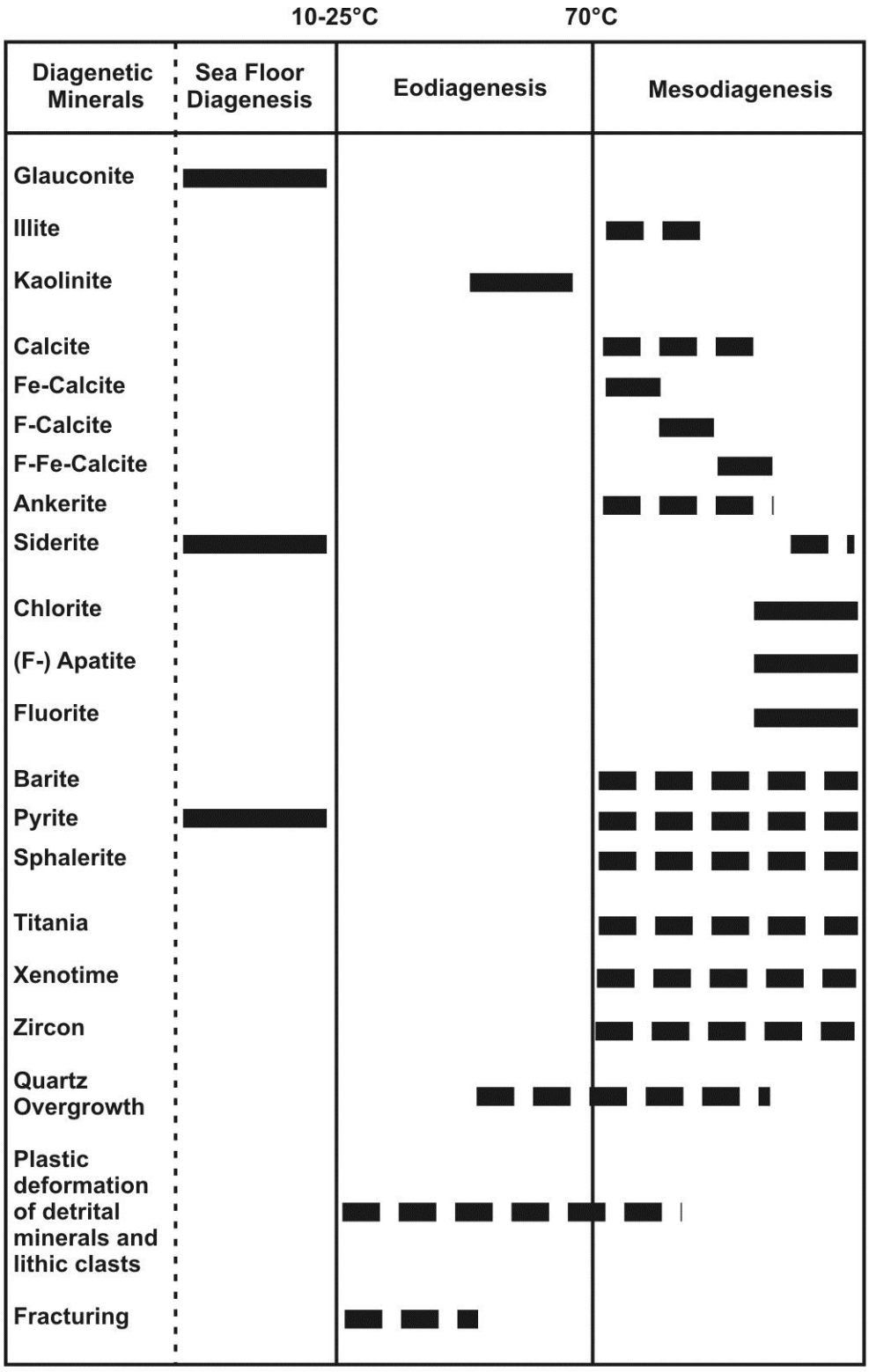

Fig. 4.26: Interpreted paragenetic sequences generated using textural relationships shared between samples from the Middle Missisauga Formation (Group 1) in the Newburn H-23 well. The boundary between eodiagenesis and mesodiagenesis was taken from Morad et al. (2000) and El Ghali et al. (2006).

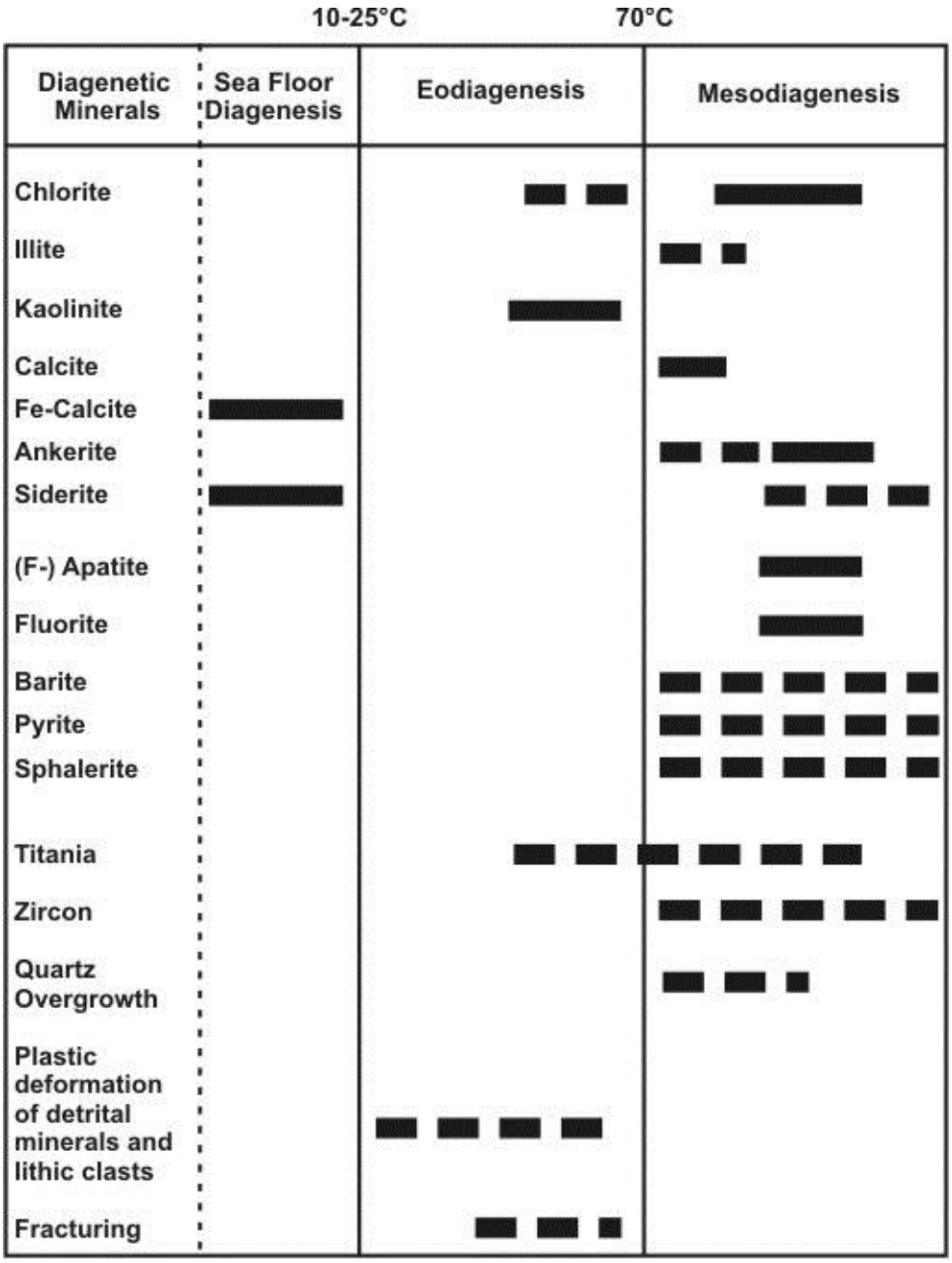

Fig. 4.27: Interpreted paragenetic sequences generated using textural relationships shared between samples from the Middle Missisauga Formation (Group 2) in the Newburn H-23 well. The boundary between eodiagenesis and mesodiagenesis was taken from Morad et al. (2000) and El Ghali et al, (2006).

4.4 Reservoir quality

The sandstone intervals of the Newburn H-23 well have displayed gas shows at several levels (Table 4.5) (Kidston et. al. 2007). The intervals which contain hydrocarbons are in the Cree Member (sand 2) and the Middle Missisauga Formation (both groups 1 and 2) (sands 3 and 4 respectively). Additional potential reservoir sands have been identified in this well, but they have been classified as non-commercial due to the thin nature of the intervals (Kidston et al., 2007). The identified reservoir sands are very-fine to fine grained sandstones and sand 3 in the Middle Missisauga (Group 1) has been suggested to be channel sands (Kidston et al., 2007). Porosity in these sands range between 13.5% and 19% with the largest gas show present where porosity is the greatest (sand 3).

Table 4.5: Modified table from Kidston et al. 2007 showing reservoir properties in the Newburn H-23 well.

Sand #	Stratigraphic Level	Top (m)	Base (m)	Net Pay (m)	Porosity (%)	SW (%)	SWC Porosity (%)	SWC k (mD)	Lithology
Sand 1	Cree Member	4305.5	4325.7	Wet?	18.0	Wet	8.9-18.1	<0.01-42.4	Fining upward channel sand with a lag deposit
Sand 2	Cree Member	4348.5	4357.5	2.00	13.5	60.0	12.1-12.9	0.28-0.80	Very-fine to fine grained shaly sandstone
Sand 3	Middle Missisauga Formation (Group 1)	5402.0	5408.0	3.00	19.0	23.0	7.2-18.9	<0.01-6.43	Channel sand deposit
Sand 4	Middle Missisauga Formation (Group 2)	5957.5	5963.5	2.50	14.0	28.0	8.8-13.3	<0.01-0.03	Very-fine to fine grained shaly sandstone

Reservoir sandstone intervals in the Alma field are found within the Upper Missisauga Formation and are coarsening upwards well sorted, subangular, and very-fine to fine grained sandstones. The cements tend to be siliceous with some calcareous and

minor sideritic intervals. The porosity in this field range from 23% to 11.4% (CNSOPB 2000).

Reservoir sandstone intervals in the Glenelg field have been identified in the Logan Canyon and Missisauga Formations which are gas and oil bearing respectively. The Logan Canyon formation contains sheet like, laterally continuous, fluvial and shallow marine sandstones with porosity ranging between 30% at the top and 20% at the bottom (CNSOPB 2000).

The Upper Missisauga Formation reservoir sands are sheet like and about 200 m thick. The Middle Missisauga Formation are also about 200 m thick and are fluvial channel deposits. The average porosity in the Missisauga Formation is about 15% (CNSOPB 2000).

Reservoir sands from the Newburn H-23 well have average porosities ranging from 13.5% to 19% (Table 4.5) similar to the Alma and Glenelg fields and the majority of them also have gas shows. The majority of sand intervals have permeability measurements from sidewall core (SWC) which are above the "rule of thumb" permeability cut off for gas reservoirs of 0.1 mD (Kidston et al., 2007). The only identified reservoir which doesn't have a gas show is the sand 1 interval which has the second highest porosity and is a fining upward channel sand and possible lag deposit. The entire Cretaceous has been deposited in an outer shelf environment (Kidston et al., 2007). The sand 3 has the highest average porosity, largest gas show, and thickest net pay making it the most economically viable of the intervals (Table 4.5), it is contained within the Middle Missisauga Formation (Group 1).

Table 4.6: Measured porosity and permeability values from the well history report (The Chevron Corporation et al., 2002)

Stratigraphic Unit	Sample Depth (m)	Porosity (%)	Permiability (mD)
Cree Member	4307.8	11.6	0.01
	4312.8	10.1	0.01
	4313.5	17.5	0.4
	4317.5	18.1	42.4
	4318.5	16.5	2.65
	4319.8	8.9	0.06
	4323	13.1	0.18
	4325.5	9.3	0.31
	4349.7	12.4	0.42
	4353.5	12.1	0.28
	4354.5	12.9	0.8
Upper Missisauga Formation	4913.8	9.4	0.09
Middle Missisauga Formation (Group 1)	5403.6	7.2	0.01
	5406.5	9.1	0.04
	5407	17	0.15
	5407.5	18.9	5.73
	5408.5	17.9	6.43
	5422.5	9.9	0.02
Middle Missisauga Formation (Group 2)	5957.8	11.7	0.02
	5960.5	13.3	0.02
	5961.2	8.8	0.03
	5961.7	12.7	0.03
	5962	8.8	0.01
	5962.8	10.2	0.01

When the porosity and permeability values are plotted from the analyses of SWC from the Newburn H-23 well give relationships which follow a similar trend as the Abenaki subbasin (Gould et al., 2011). The values from the Newburn H-23 well do not extend as far as from the Abenaki subbasin as they max out around 20% porosity and a maximum of 42 mD permeability compared to the Abenaki subbasin which can extend to 30% porosity and around 10000 mD permeability. However the Cree Member in the Newburn H-23 well has a steeper trend (Fig. 4.28) than in the Abenaki subbasin meaning that the permeability rises faster in Newburn than in the Abenaki subbasin. The

Missisauga formation in Newburn has similar limit as the Cree Member but has a slightly shallower trend.

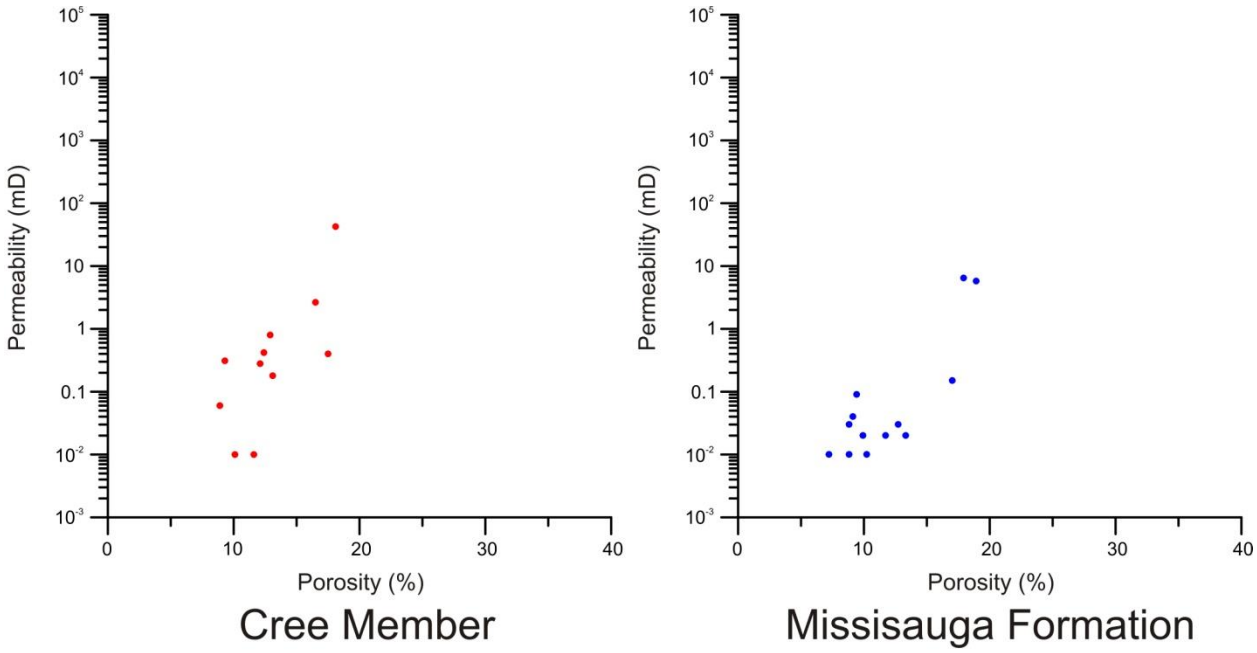

Fig. 4.28: Permeability versus Porosity plot of analysed side wall cores from the Cree Member and Missisauga Formation from the Newburn H-23 well.

Samples from Sand 1 (samples 4313.5 m and 4318.5 m) contain rare carbonate cements and have porosity mostly filled by early kaolinite. Secondary porosity is formed as the result of partly dissolved K-feldspars. Kaolinite forms in eodiagenesis and due to this early formation would have prevented the flow and retention of hydrocarbons early in the sands burial, however the dissolution of feldspars has resulted in secondary porosity. The majority of the porosity in this sand is probably related to the dissolution of feldspars.

Sand 2 (sample 4353 m) contains a large portion of carbonate cements including calcite and later Fe-calcite. Calcite forms in eodiagenesis, while Fe-calcite forms later in mesodiagenesis. The carbonate cement is widespread in the sample and secondary porosity within the cement is rare.

Samples from Sand 3 (samples 5403.6 m, 5406.5 m, 5407 m) have kaolinite filling porosity which is either synchronous or predates quartz over growths. Kaolinite forms in eodiagenesis and due to this early formation would have prevented the flow and retention of hydrocarbons early in the sands burial.

Samples from Sand 4 (samples 5957.8 m, 5961.7 m, and 5962 m) show a high degree of compaction in the framework grains along with plastically deformed intraclasts. High compaction lowers porosity and permeability by decreasing the space between grains, similarly deformed intraclasts conform to contours and grain boundaries lowering porosity. However at the greatest depth (5962 m) the sample shows high secondary porosity which has been filled by drilling mud, this probably lowered the average porosity of the sand layer.

4.4.1 Overall Interpretation

In summary the CNSOPB play adequacy for the Newburn H-23 well is the highest of the deep wells in the Scotian Basin (Kidston et al., 2007) with 80% adequacy for reservoir and 100% source. The porosity values are similar to that of the Alma and Glenelg fields in the Scotian basin, contain gas shows, and is above the cut off permeability for gas reservoirs. These sandstones are therefore potentially economic reservoirs in the Scotian basin. However since the sandy intervals in which these potential sources are located in are thin, and contain abundant early diagenetic minerals which fill part of the porosity they may not be of high quality.

Chapter 5: Conclusion

The project objective was to determine the provenance and diagenesis of the lower Cretaceous sandstone intervals in the Newburn H-23 well, how they change with increasing depth, and to draw comparisons between this "deep well" off the slope and its shallower shelf age equivalent sandstones. The findings of this study are:

1) The sandstone intervals from the Newburn H-23 well largely share detrital mineralogy with others wells nearby in the central Scotian Basin, lacking mostly minor detrital minerals. The detrital minerals analyzed in the Newburn H-23 well show the most similarity to wells from the Glenelg field. This suggests that they share a source during the Early Cretaceous, and that during this time period the source was dominantly the Sable River with minor input from Meguma Group metasediments and a constant supply of sodic volcanic rocks probably from the Scatarie Bank. .
2) The Newburn H-23 well has several distinct diagenetic minerals which have not been reported elsewhere in the Scotian Basin. These minerals include fluorine rich ferroan-calcite and diagenetic zircon.
3) F-Fe-calcite, diagenetic sphalerite, and diagenetic zircon support previous studies which suggest high salinity and temperatures late in the history of the Scotian Basin.
4) The presence of both diagenetic brookite and anatase suggest low pH, high organic content in pore waters, high titanium content in porewaters, and possibly an oil-water contact zone in the Middle Missisauga Formation (Group 1) which favoured the formation of anatase.

5) The majority of the paragenetic sequences which have been generated for this well are generally similar with mostly minor differences related to the presence of several minerals. The paragenetic sequences suggest: **a)** increased salinity, low pH, and a high organic content in circulating basinal fluids during eodiagenesis and mesodiagenesis; and **b)** increased fluoride content in basinal fluids during mesodiagenesis.
6) The porosity values from Newburn H-23 are similar to that of the Alma and Glenelg fields in the Scotian basin, contain gas shows, and is above the cut off permeability for gas reservoirs. These sandstones are therefore potentially economic reservoirs in the Scotian basin. However since the sandy intervals in which these potential sources are located in are thin, and contain abundant early diagenetic minerals they may not be of high quality.

References

Aja, S. U., Wood, S. A., and Williams-Jones, A. E., 1995, The aqueous geochemistry of Zr and the solubility of some Zr-bearing Minerals, Applied Geochemistry, v. 10, p. 603-620.

Anthony, J.W., Bideaux, R.A., Bladh, K.W., and Nichols, M.C., Eds., Handbook of Mineralogy, Mineralogical Society of America, Chantilly, VA 20151-1110, USA. http://www.handbookofmineralogy.org/. (Accessed February 19 2016).

Bédard, J.H. and Hebert, R., 1998, Formation of chromitites by assimilation of crustal pyroxenites and gabbros into peridotitic intrusions: North Arm Mountain massif, Bay of Islands ophiolite, Newfoundland, Canada: Journal of Geophysical Research, v. 103, p. 5165–5184.

Benning, L.G., and Waychunas, G.A., 2008, Nucleation, growth, and aggregation of mineral phases: mechanisms and kinetic controls, in Brantley, S.L., Kubicki, J.D., and White, A.F., eds., Kinetics of Water–Rock Interaction: New York, Springer, p. 259–333.

Bhave, R.C., and Lee, B.I., 2007, Experimental variables in the synthesis of brookite phase TiO2 nanoparticles: Materials Science and Engineering, v. A 467, p. 146–149.

Bojanowski, M.J., Bagin´ski, B., Clarkson, E., Macdonald, R., Marynowski, L., 2012, Low-temperature zircon growth related to hydrothermal alteration of siderite concretions in Mississippian shales, Scotland, Contributions to Mineral Petrology, v. 164, p. 245–259.

Bowman, S. J., Pe-Piper, G., Piper, D. J., Fensome, R. A., and King, E. L., 2012. Early Cretaceous volcanism in the Scotian Basin. This article is one of a series of papers

published in this CJES Special Issue on the theme of Mesozoic–Cenozoic geology of the Scotian Basin. Canadian Journal of Earth Sciences, v. 49(12), p. 523-1539.

Brookins, D.G., 1988, Eh–pH Diagrams for Geochemistry: New York, Springer-Verlag, 176 p

Budyanto, S., Kuo, Y., Liu, J.C., 2015, Adsorption and precipitation of fluoride on calcite nanoparticles: A spectroscopic study, Separation and Purification Technology, v. 150, p. 325–331.

Canada-Nova Scotia Offshore Petroleum Board (CNSOPB), 2000, Technical Summaries of Scotian Shelf Significant and Commercial Discoveries

Carpenter, R., 1969, Factors controlling marine geochemistry of fluorine, Geochimica et Cosmochimica Acta, v. 33, p. 1153-1167.

Chang, J.A., Vithal, M., Baek, C., and Seok, S., 2009, Morphological and phase evolution of TiO2 nanocrystals prepared from peroxotitanate complex aqueous solution: Influence of acetic acid: Journal of Solid State Chemistry, v. 182, p. 749-756.

Chen, G., Liu, X., and Su, C., 2012, Distinct effects of humic acid on transport and retention of TiO2 rutile nanoparticles in saturated sand columns: Environmental Science and Technology, v. 46, p. 7142-7150.

The Chevron Corporation et al., 2002, Well History Report For Newburn H-23 At Exploration Licence Area 2359 Off the Scotian Shelf Offshore, Nova Scotia

Coish, R.A., 1989: Boninitic lavas in Appalachian ophiolites: a review. In: Boninites and related rocks, 264-. Edited by A.J. Crawford. Unwin Hyman, London.

Cornu, S., Lucas, Y., Lebon, E., Ambrosi, J.P., Luizao, F., Rouiller, J., Bonnay, M., and Neal, C., 1999, Evidence of titanium mobility in soil profiles, Manaus, central Amazonia: Geoderma, v. 91, p. 281–295.

Cummings, D.I., and Arnott., R.W.C., 2005, Growth-faulted shelf-margin deltas: a new (but old) play type, offshore Nova Scotia, Bulletin of Canadian Petroleum Geology, v. 53, p. 211-236.

Domingos, R.F., Tufenkji, N., and Wilkinson, K.J., 2009, Aggregation of titanium dioxide nanoparticles: role of a fulvic acid: Environmental Science and Technology, v. 43, p. 1282–1286.

Enyiegbulam, M.E., Iheaturu, N.C., 2007, Effect of Spent Oil Base Drilling Mud Solids on the Mechanical Properties of UPR Composites: Journal of Polymer Engineering, v. 27(2), p. 149–63.

Fitzpatrick, R.W., and Chittleborough, D.J., 2002, Titanium and zirconium minerals, in Soil Science Society of America, ed., Soil Mineralogy with Environmental Applications: Soil Science Society of America, Book Series 7, p. 667–690.

Folk, R. L., 1968, Petrology of Sedimentary Rocks: Austin, University of Texas Publication, 170 p.

Fyfe, W.S., and Bischoff, J.L., 1964, The Calcite-Aragonite Problem.

Gieré, R., 1990, Hydrothermal Mobility of Ti, Zr and REE: Examples from the Bergell and Adamello Contact Aureoles (Italy), Terra nova, v. 2, p. 60-67.

Given, M. M., 1977. Mesozoic and early Cenozoic geology of offshore Nova Scotia. Bulletin of Canadian Petroleum Geology, v. 25(1), p. 63-91.

Hay, D.C., and Dempster, T.J., 2009, Zircon Behaviour during Low-temperature Metamorphism, Journal of Petrology, v. 50, p. 571-589.

Hays, P.D., James, W.D., and Tieh, T.T., 1994, The role of NAA in studies of organic diagenesis of rocks: Journal of Radioanalytical and Nuclear Chemistry, v. 180, p. 15–23

Hebert, R., and Laurent, R.,1989: Mineral chemistry of ultramafic and mafic plutonic rocks of the Appalachian ophiolites, Quebec, Canada: Chemical Geology, v. 77, p. 265–285.

Hotze, E.M., Phenrat, T., and Lowry, G.V., 2010, Nanoparticle Aggregation: Challenges to Understanding Transport and Reactivity in the Environment: Journal of Environmental Quality, v. 39(6), p. 1909-1924.

Hu, Y., Tsai, H.-L., and Huang, C.-L., 2003, Effect of brookite phase on the anatase-rutile transition in the titania nanoparticles: Journal of the European Ceramic Society, v. 23, p. 691-696.

Ismagilov, Z.R., Tsykoza, L.T., Shikina, N.V., Zarytova, V.F., Zinoviev, V.V., and Zagrebelnyi, S.N., 2009, Synthesis and stabilization of nano-sized titanium dioxide: Russion Chemical Reviews, v. 78 (9), p. 873-885.

Johannes, W., and Puhan, D., The Calcite-Aragonite Transition, Reinvestigated: Contr. Mineral. and Petrol.: v. 31, p. 28-38.

Karim, A., Hanley, J.J., Pe-Piper, G., and Piper, D.J.W., 2012, Paleohydrogeological and thermal events recorded by fluid inclusions and stable isotopes of diagenetic minerals in Lower Cretaceous sandstones, offshore Nova Scotia, Canada: AAPG Bulletin, v. 96(6), p. 1147-1169.

Karim, A., Pe-Piper, G., Piper, D.J.W., and Hanley, J.J., 2011, Thermal and hydrocarboncharge history and the relationship between diagenesis and reservoir connectivity: Venture field, offshore Nova Scotia, eastern Canada. Canadian Journal of Earth Sciences, v. 48, p. 1293–1306.

Keller, A.A., Wang, H., Zhou, D., Lenihan, H.S., Cherr, G., Cardinale, B.J., Miller, R., and Ji, Z., 2010, Stability and aggregation of metal oxide nanoparticles in natural aqueous matrices: Environmental Science and Technology, v. 44 , p. 1962–1967.

Kidston, A.G., Smith, B., Brown, D.E., Makrides, C. and Altheim, B., 2007, Nova Scotia Deep Water Offshore Post-Drill Analysis – 1982-2004. Canada-Nova Scotia Offshore Petroleum Board, Halifax, Nova Scotia, 181p.

Kitano, Y., and Okumura, M., 1973, Coprecipitation of fluoride with calcium carbonate: Geochem, v. 7, p. 37-49.

Koritnig, S., 1951, Ein beitrag zur geochemie des fluor:(Mit besonderer Berücksichtigung der Sedimente): Geochimica et Cosmochimica Acta, v. 1(2), p. 89-116.

Kraynov, S. R., Mer'kov, A. N., Petrova, N. G., Baturinskaya, I. V., and Zharikova V. M., 1969, Highly alkaline (pH 12) fluosilicate waters in the deeper zones of the Lovozero massif, Geochem. Int., v. 6/4, p. 635-640.

Laurent, R., and Kacira, N., 1987, Spinel deposits in the Appalachian Ophiolites. In: Evolution of chromium ore fields, p. 169–193. Edited by C.W. Stowe. Van Nostrand Reinhold Co., New York.

Li, G., Pe-Piper, G., and Piper, D.J.W., 2012. The provenance of Middle Jurassic sandstones in the Scotian Basin: petrographic evidence of passive margin tectonics: Canadian Journal of Earth Sciences, v. 49, p. 1463-1477.

Malpas, J., and Strong, D.F., 1975. A comparison of chrome-spinels in ophiolites and mantle diapirs of Newfoundland: Geochimica et Cosmochimica Acta, v. 39, p. 1045–1060.

McIver, N. L., 1972. Cenozoic and Mesozoic stratigraphy of the Nova Scotia shelf. Canadian Journal of Earth Sciences, v. 9(1), p. 54-70.

Morad, S., 1986, Pyrite–chlorite and pyrite–biotite relations in sandstones: Sedimentary Geology, v. 49, p. 177–192

Morad, S., and Aldahan, A.A., 1986, Alteration of detrital Fe-Ti oxides in sedimentary rocks: Geological Society of America, Bulletin, v. 97, p. 567–578.

Morad, S., and Aldahan, A.A., 1987, Diagenetic "replacement" of feldspars by titanium ox- ides in sandstones: Sedimentary Geology, v. 51, p. 147–153.

Morton, A., and Hallsworth C.R., 1999. Processes controlling the composition of heavy mineral assemblages in sandstones. Sedimentary Geology, 124, 3-29.

Nesse, W.D., 2013, Introduction to Optical Mineralogy (4th ed.), New York, New York, USA: Oxford University Press, Inc.

Nowack, B., and Bucheli, T.D., 2007, Occurrence, behavior, and effects of nanoparticles in the environment: Environmental Pollution, v. 150, p. 5-22.

OETR (Offshore Energy Technical Research), 2011, Atlas: Play Fairway Analysis, Offshore Nova Scotia, Canada. Available from http://www.novascotiaoffshore.com/analysis#atlas (Accessed November 2011).

Padhi, S., Tokunaga, T., 2015, Surface complexation modeling of fluoride sorption onto calcite, Journal of Environmental Chemical Engineering, v. 3, p. 1892–1900.

Page, P., Bedard, J.H., Schroetter, J.-M and Tremblay, A., 2008. Mantle petrology and mineralogy of the Thetford Mines ophiolite complex: Lithos, v. 100, p. 255-292.

Pearce, J. A., Barker, P. F., Edwards, S. J., Parkinson, I. J., and Leat, P. T., 2000, Geochemistry and tectonic significance of peridotites from the South Sandwich arc–basin system, South Atlantic: Contributions to Mineralogy and Petrology, v. 139(1), p. 36-53.

Pe-Piper, G., and Yang, X., 2014. Albitisation of detrital feldspars in the Scotian Basin: implications for the thermal evolution of the basin. Open file report 7117.

Pe-Piper, G., Jansa, L.F. and Palacz, Z., 1994, Geochemistry and regional significance of the early Cretaceous bimodal basalt-felsic associations on Grand Banks, eastern Canada: Bulletin of Geological Society of America, v. 106, p. 1319-1331.

Pe-Piper, G., Karim, A., amd Piper, D.J.W., 2011, Authigenesis of Titania Minerals and the Mobility of Ti: New Evidence From Pro-Deltaic Sandstones, Cretaceous Scotian Basin, Canada: Journal of Sedimentary Research, v. 81, p. 762-773.

Pe-Piper, G., MacKie, H., and Piper, D. J.W., 2009a, Petrology, Mineralogy and Geochemistry of the Musquodoboit E-23 well, Scotian Shelf, Open file report 6281.

Pe-Piper, G., Piper, D.J.W., Lefort, D., and Ledger-Piercey, S., 2011, Sediment provenance and diagenesis, Lower Cretaceous of the Alma K-85 well, Scotian Shelf, Open file report 6837.

Pe-Piper, G., Tsikouras, B., Piper, D.J.W., and Triantaphyllidis, S., 2009b. Chemical fingerprinting of detrital minerals in the Upper Jurassic-Lower Cretaceous sandstones, Scotian Basin. Geological Survey of Canada open file 6288.

Pettibone, J.M., Cwiertny, D.M., Scherer, M., and Grassian, V.H., 2008, Adsorption of organic acids on TiO2 nanoparticles: effects of pH, nanoparticle size, and nanoparticle aggregation: Langmuir, v. 24, p. 6659–6667

Piper, D.J.W., Pe-Piper, G., and Ingram, S., 2004, Early Cretaceous sediment failure in the southeastern Sable sub-basin, offshore Nova Scotia: Bulletin of the American Association of Petroleum Geologists, v. 88, p. 991-1006.

Pottier, A., Chane, C., Tronc, E., Mazerolles, L., and Jolivet, J.-P., 2011, Synthesis brookite TiO2 nanoparticles by thermolysis of TiCL4 in strongly acidic aqueous media: J. Mater. Chem, v. 11, p. 1116-1121.

Rasmussen, B., 2005, Zircon growth in very low grade metasedimentary rocks: evidence for zirconium mobility at ~250˚C, Contributions to Mineral Petrology, v. 150, p. 146–155.

Reynolds, P. H., Pe-Piper, G., and Piper, D. J., 2010. Sediment sources and dispersion as revealed by single-grain 40Ar/39Ar ages of detrital muscovite from Carboniferous and Cretaceous rocks in mainland Nova Scotia. Canadian Journal of Earth Sciences, v. 47(7), p. 957-970.

Rubin, J. N. , Henry, C. D., and Price, J. G., 1993, The mobility of zirconium and other "immobile" elements during hydrothermal alteration, Chemical Geology, v. 110, pg. 29-47.

Rude, P.D, and Aller, R.C., 1991, Fluorine mobility during early diagenesis of carbonate sediment: An indicator of mineral transformations, Geochimica et Cosmochimica Acta, v. 55, p. 2491-2509.

Schulz, H.-M., Biermann, S., Van Berk, W., Krüger, M., Straaten, N., Bechtel, A., Wirth, R., Lüders, V., Schovsbo, N.H., and Crabtree, S., 2015, From shale oil to biogenic shale gas: retracing organic–inorganic interactions in the Alum Shale (Furongian–Lower Ordovician) in southern Sweden: American Association of Petroleum Geologists, Bulletin, v. 99, p. 927–956.

Skrabal, S.A., 1995, Distributions of dissolved titanium in Chesapeake Bay and the Amazon River Estuary: Geochimica et Cosmochimica Acta, v. 59, p. 2449–2458.

Stevens, R.E., 1944. Composition of some spinels of the western Hemisphere: American Mineralogist, v. 29, p. 1-34.

Suhr, G., and Robinson, P.T., 1994. Origin of mineral chemical stratification in the mantle section of the Table Mountain massif (Bay of Islands Ophiolite, Newfoundland, Canada): Lithos, v. 31, p. 81–102.

Tsikouras, B., Pe-Piper, G., Piper, D. J. W., and Schaffer, M., 2011, Varietal heavy mineral analysis of sediment provenance, Lower Cretaceous Scotian Basin, eastern Canada, Sedimentary Geology, v. 237, p. 150-165.

Vard E. and Williams-Jones A. E., 1993, A fluid inclusion study of vug minerals in dawsonite phonolite sills, Mont&al, Quebec: Implications for HFSE mobility. Contrib. Mineral. Petrol., v. 113, p. 410-423.

Varfalvy, V. and Hebert, R., 1997. Petrology and geochemistry of pyroxenite dykes in upper mantle peridotites of the North Arm Mountain massif, Bay of Islands ophiolite, Newfoundland: implications for the genesis of boninitic and related magmas: Canadian Mineralogist, v. 35, p. 543-570.

Wade, J. A., Williams, G. L., and MacLean, B. C., 1995. Mesozoic and Cenozoic stratigraphy, eastern Scotian Shelf: new interpretations. Canadian Journal of Earth Sciences, v. 32(9), p. 1462-1473.

Wade, J.A. and MacLean, B.C., 1990. Aspects of the geology of the Scotian Basin from recent seismic and well data. Geology of Canada, v. 2, p. 190-238.

Wang, C., Deng, Z.-X., and Li, Y., 2001, Synthesis of Nanocrystalline Anatase and Rutile Titania in Mixed Organic Media: Inorg. Chem., v. 40, p. 5210-5214.

Wentworth, C.K., 1922, A Scale of Grade and Class Terms for Clastic Sediments: The Journal of Geology, v. 30, p. 377-392.

Weston, J.F., MacRae, R.A., Ascoli, P., Cooper, M.K.E., Fensom, R.A., Shaw, D., and Williams, G.L., 2012. A revised biostratigraphic and well-log sequencestratigraphic framework for the Scotian Margin, offshore eastern Canada: Canadian Journal of Earth Sciences, v. 49, p. 1417-1462.

Yang, K., Lin, D., and Xing, B., 2009, Interactions of humic acid with nanosized inorganic oxides: Langmuir, v. 25, p. 3571–3576.

Zhang, Y., Pe-Piper, G., and Piper, D. J., 2014. Sediment geochemistry as a provenance indicator: unravelling the cryptic signatures of polycyclic sources, climate change, tectonism and volcanism: Sedimentology, v. 61(2), p. 383-410.

Appendix 1: Scanning electron microscope (SEM) backscatter electron (BSE) images for heavy mineral grain mounts from Newburn H-23 well with EDS mineral analyses.

Appendix 1-1: SEM-BSE images and EDS mineral analyses for sample Newburn H-23 4300m.

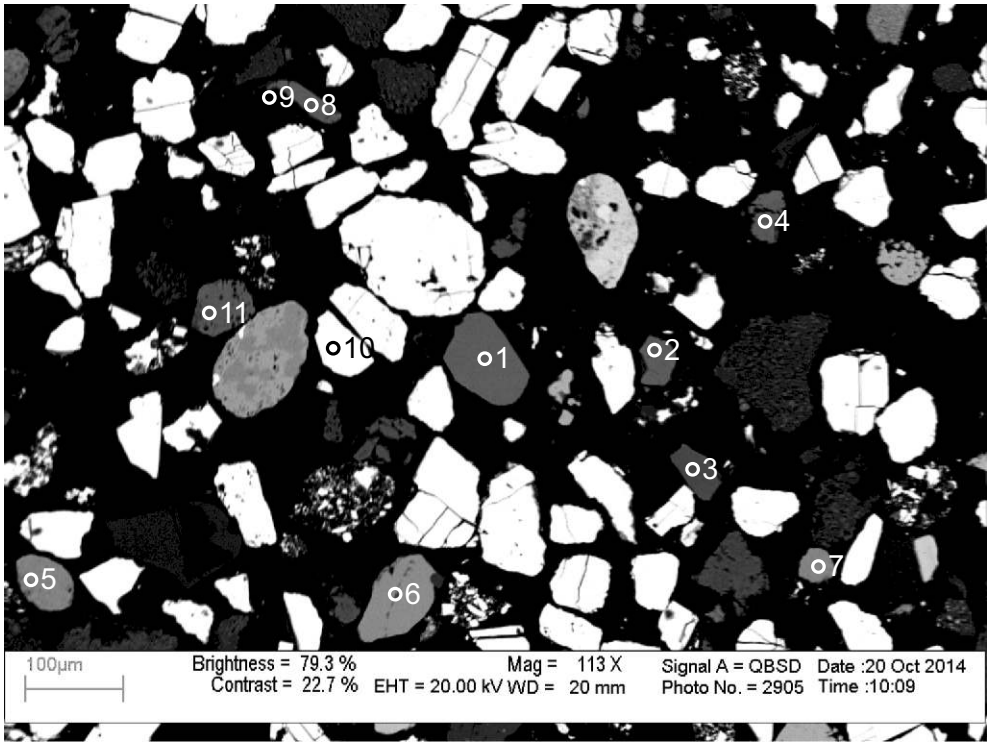

1: Titania
2: Titania
3: Fluorapatite
4: Titania
5: Siderite
+Quartz
6: Ilmenite
7: Siderite
+Quartz
8: Titania
9: Quartz
10: Barite
11: Titania

Figure 1-1.1: Sample Newburn 4300m site 2 (SEM).

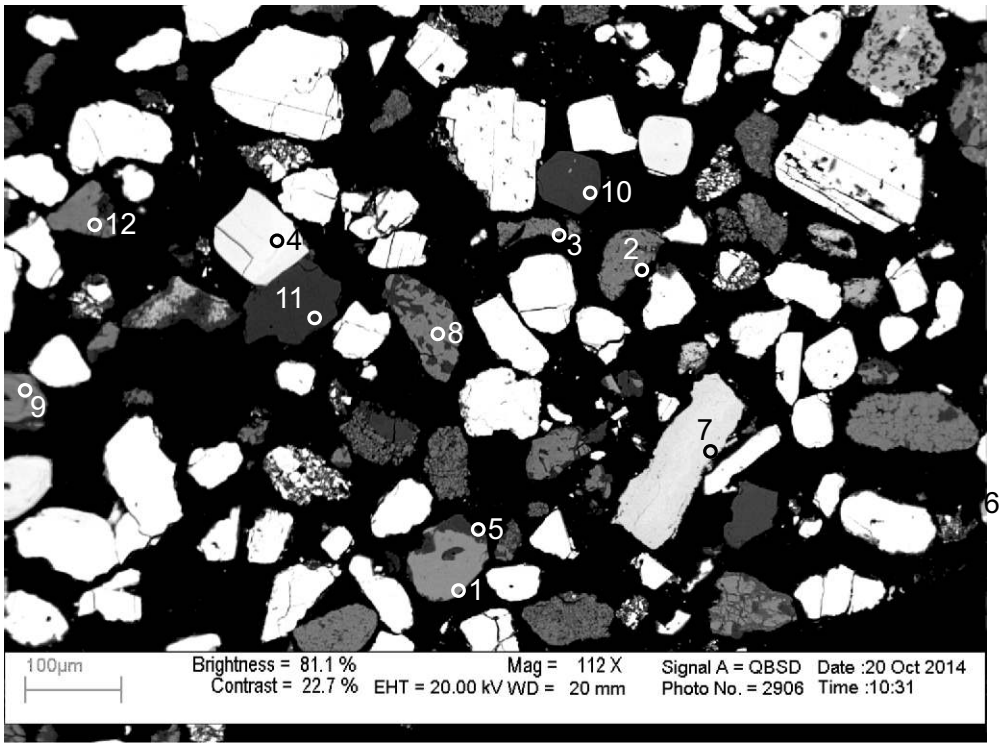

1: Titania
2: Siderite
+Albite
+Other
3: Chlorite
+K-feldspar
4: Zircon
5: Quartz
+Titania
+Muscovite
6: Siderite
+Quartz
7: Limonite
8: Albite
+Siderite
9: Siderite
10: Tourmaline
11: Quartz
12: Siderite
+Muscovite

Figure 1-1.2: Sample Newburn 4300m site 3 (SEM).

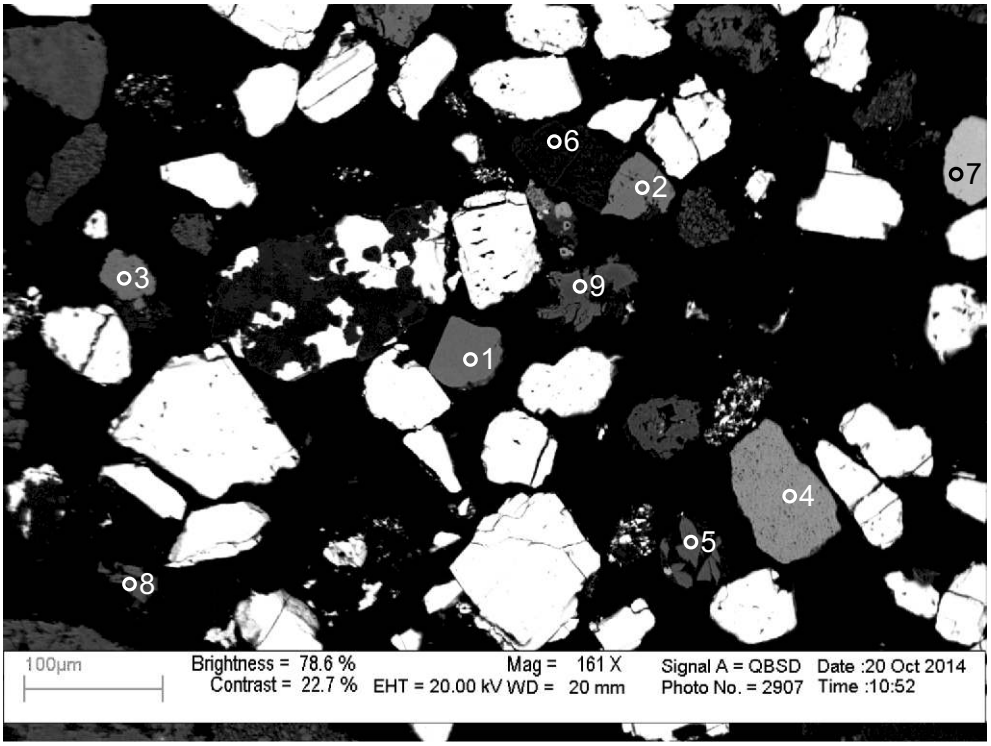

1: Titania
2: Titania
3: Titania
4: Limonite
+Other
5: Siderite
+K-feldspar
6: Hole
7: Pyrite
8: Ilmenite
9: Siderite

Figure 1-1.3: Sample Newburn 4300m site 4 (SEM).

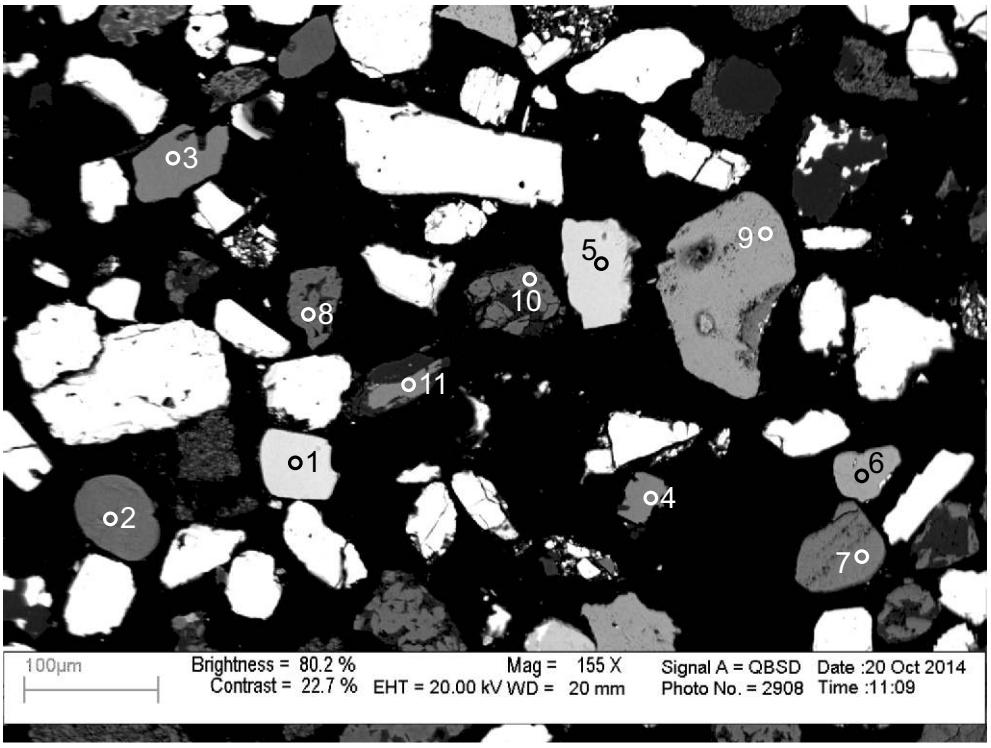

1: Zircon
2: Titania
3: Titania
4: Titania
5: Zircon
6: Limonite
+Quartz
7: Titania
8: Siderite
+Other
9: Limonite
+Quartz
10: Siderite
+Albite
+K-feldspar
11: Titania

Figure 1-1.4: Sample Newburn 4300m site 5 (SEM).

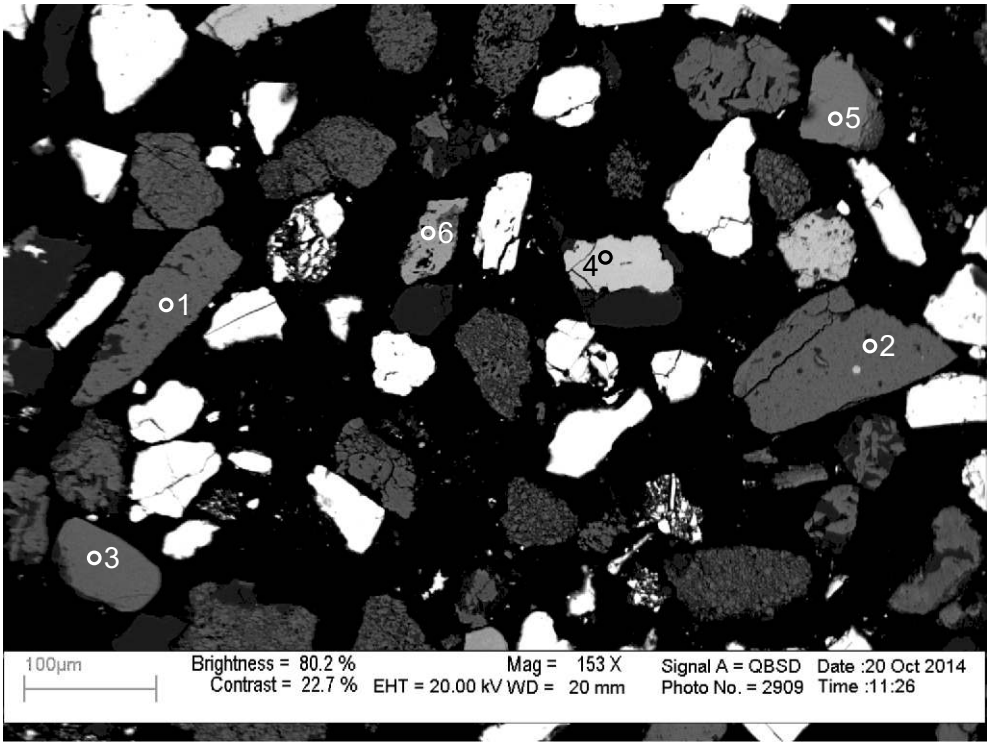

1: Siderite
2: Siderite
3: Fluorapatite
4: Pyrite
5: Titania
6: Limonite
+Other

Figure 1-1.5: Sample Newburn 4300m site 6 (SEM).

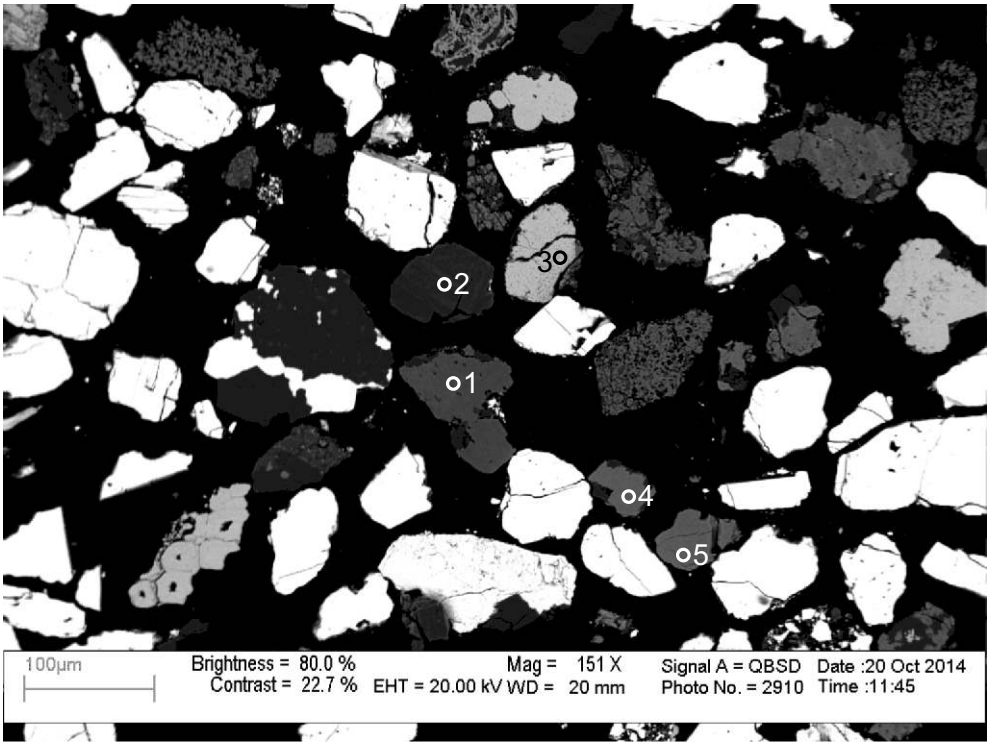

1: Epidote
2: Ankerite
3: Pyrite
4: Fluorapatite
5: Fluorapatite

Figure 1-1.6: Sample Newburn 4300m site 7 (SEM).

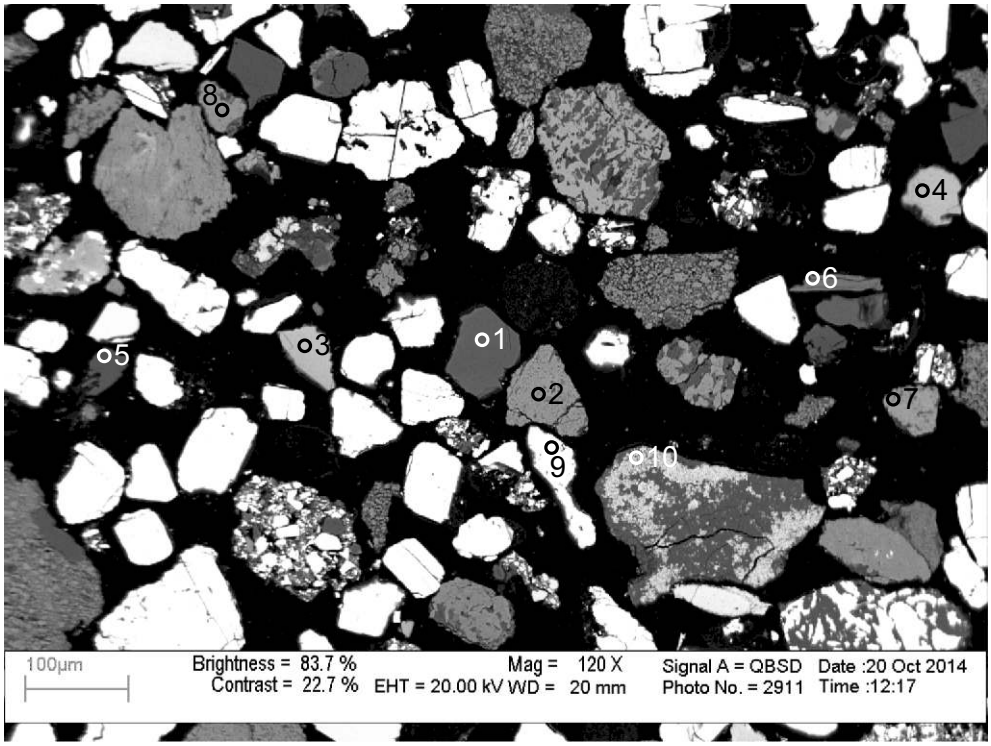

1: Tourmaline
2: Siderite
+Apatite
3: Spinel
4: Spinel
5: Albite
6: Biotite
7: Siderite
+Chlorite
8: Siderite
+Chlorite
9: Barite
10: Pyrite
+Albite
+K-feldspar

Figure 1-1.7: Sample Newburn 4300m site 8 (SEM). 9 10

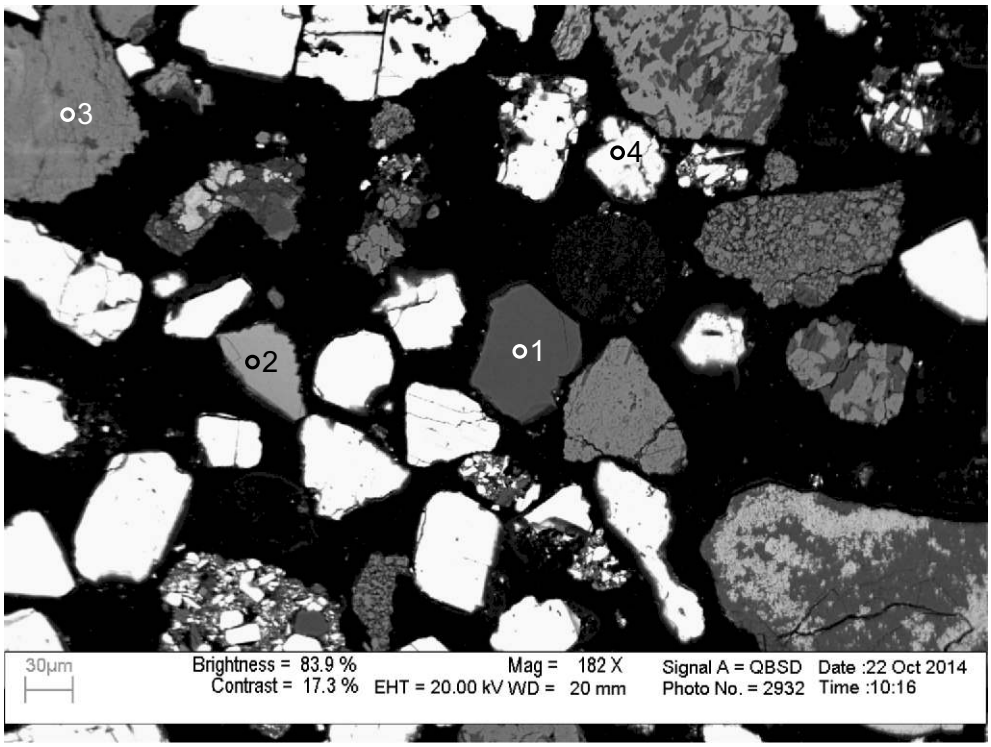

1: Tourmaline
2: Spinel
3: Siderite
+Albite
+Chlorite
4: Barite

Figure 1-1.8: Sample Newburn 4300m site 9 (SEM).

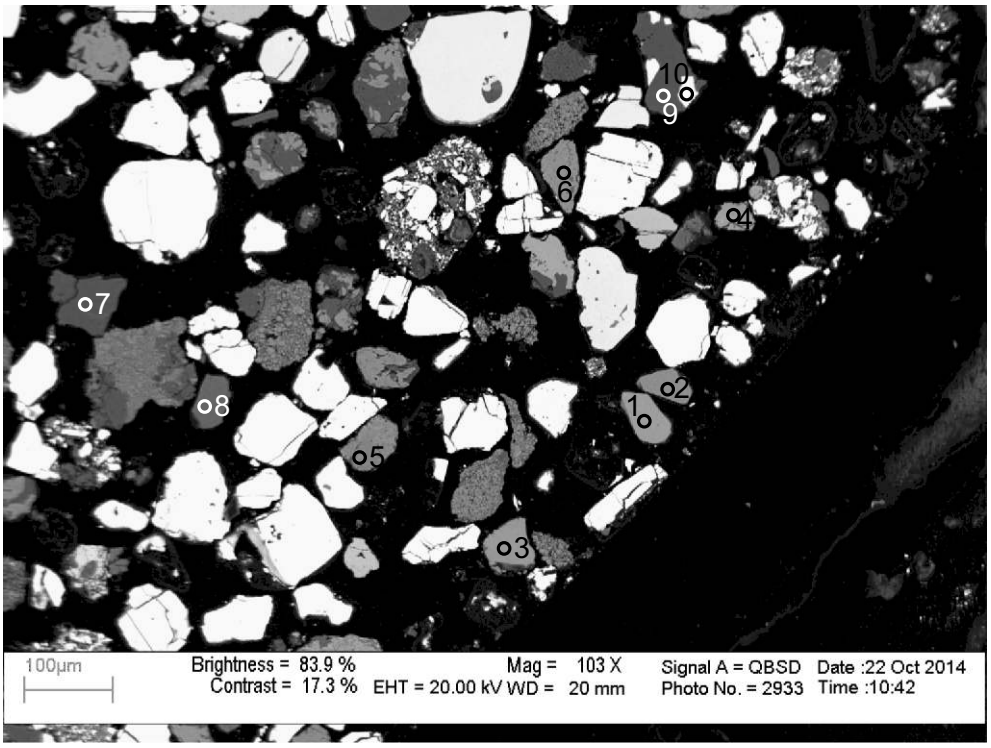

1: Titania
2: Fluorite
3: Siderite
4: Titania
5: Siderite +K-feldspar
6: Siderite +Other
7: Quartz
8: Tourmaline
9: Quartz
10: Barite

Figure 1-1.9: Sample Newburn 4300m site 10 (SEM).

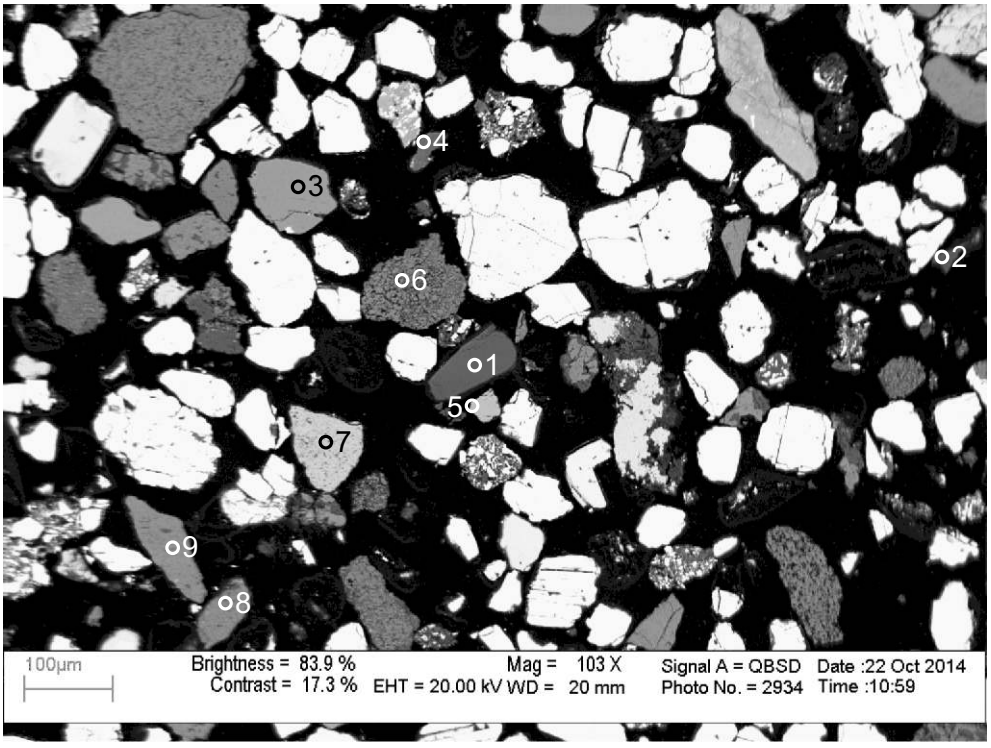

1: Tourmaline
2: Quartz
3: Siderite
4: K-feldspar
5: Spinel
6: Siderite +Chlorite
7: Limonite +Other
8: Siderite +Apatite +Quartz
9: Siderite +Apatite +Quartz

Figure 1-1.10: Sample Newburn 4300m site 11 (SEM).

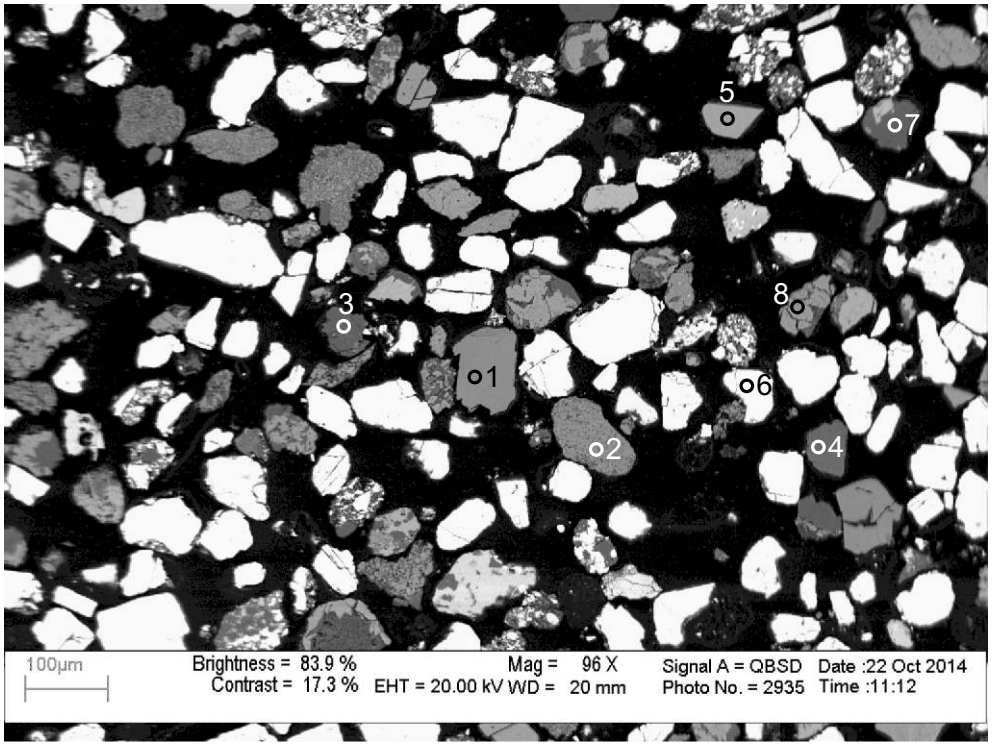

1: Hornblende
2: Siderite +Quartz
3: Albite
4: Ankerite
5: Fluorapatite
6: Barite
7: Albite
8: Siderite

Figure 1-1.11: Sample Newburn 4300m site 12 (SEM).

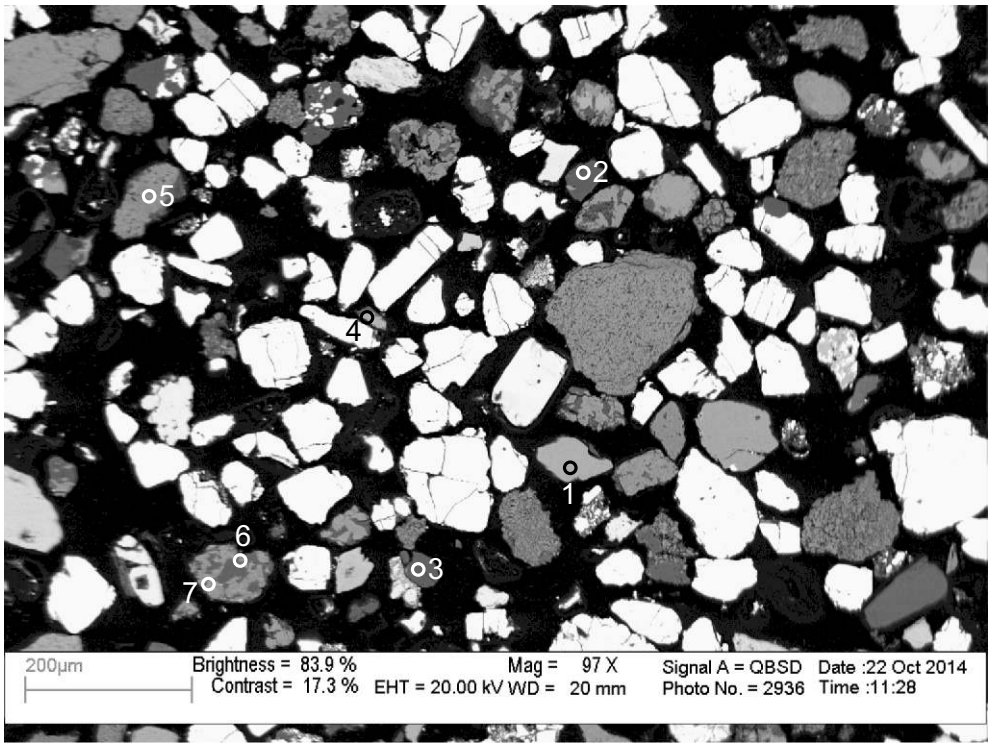

1: Titania
2: Albite
3: Quartz
4: Titania
5: Siderite +Albite
6: Albite
7: Siderite +Chlorite

Figure 1-1.12: Sample Newburn 4300m site 13 (SEM).

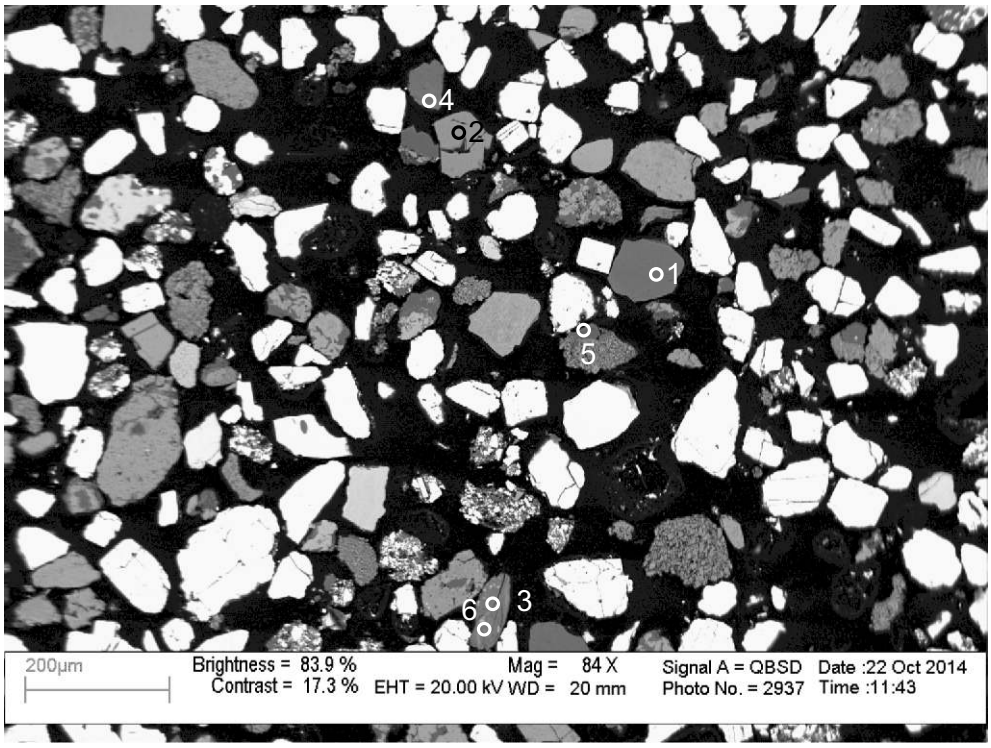

1: Tourmaline
2: Diopside
3: Titania +Chlorite
4: Fe-Dolomite
5: Quartz
6: Chlorite

Figure 1-1.13: Sample Newburn 4300m site 14 (SEM).

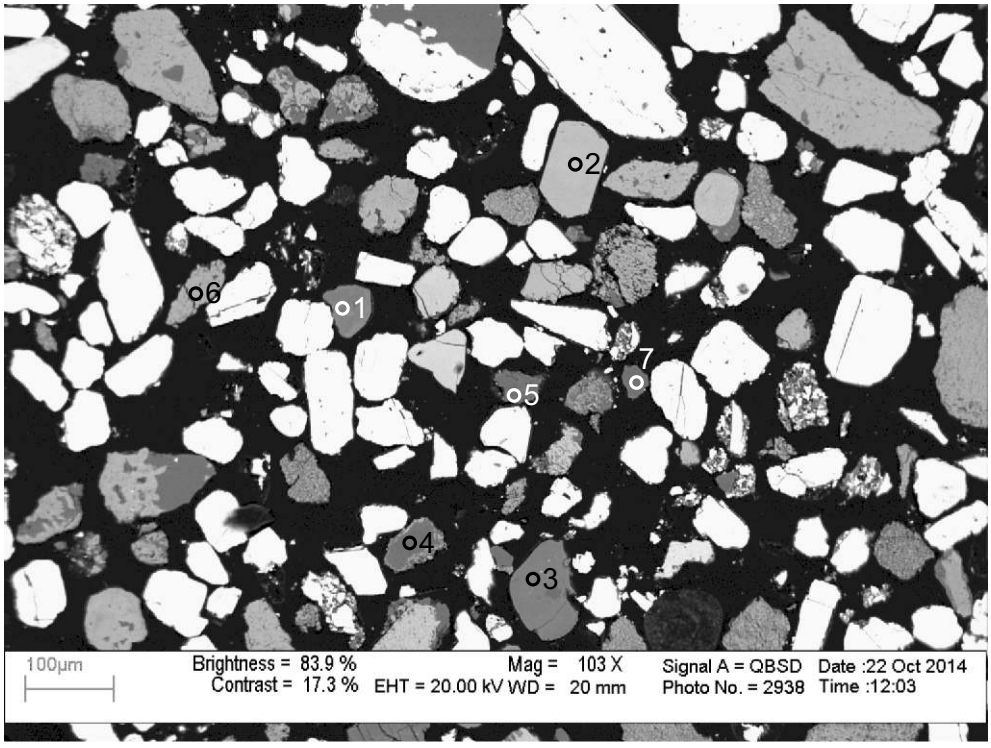

1: Tourmaline
2: Fluorapatite
3: Tourmaline
4: Quartz
5: Quartz
6: Siderite
7: Quartz

Figure 1-1.14: Sample Newburn 4300m site 15 (SEM).

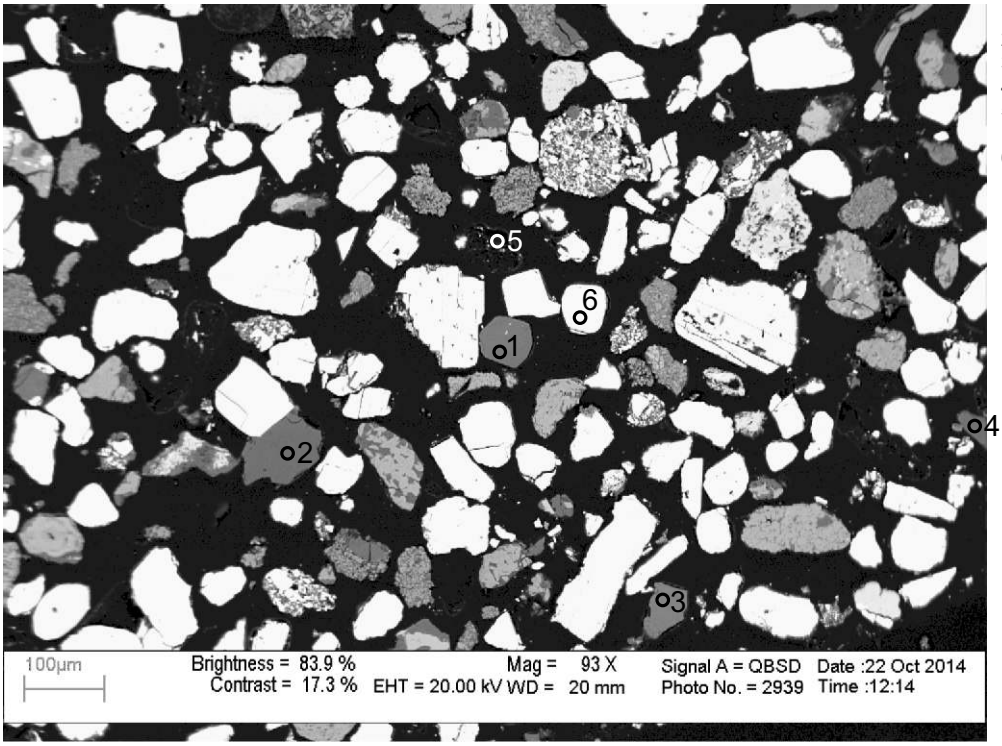

Figure 1-1.15: Sample Newburn 4300m site 16 (SEM).

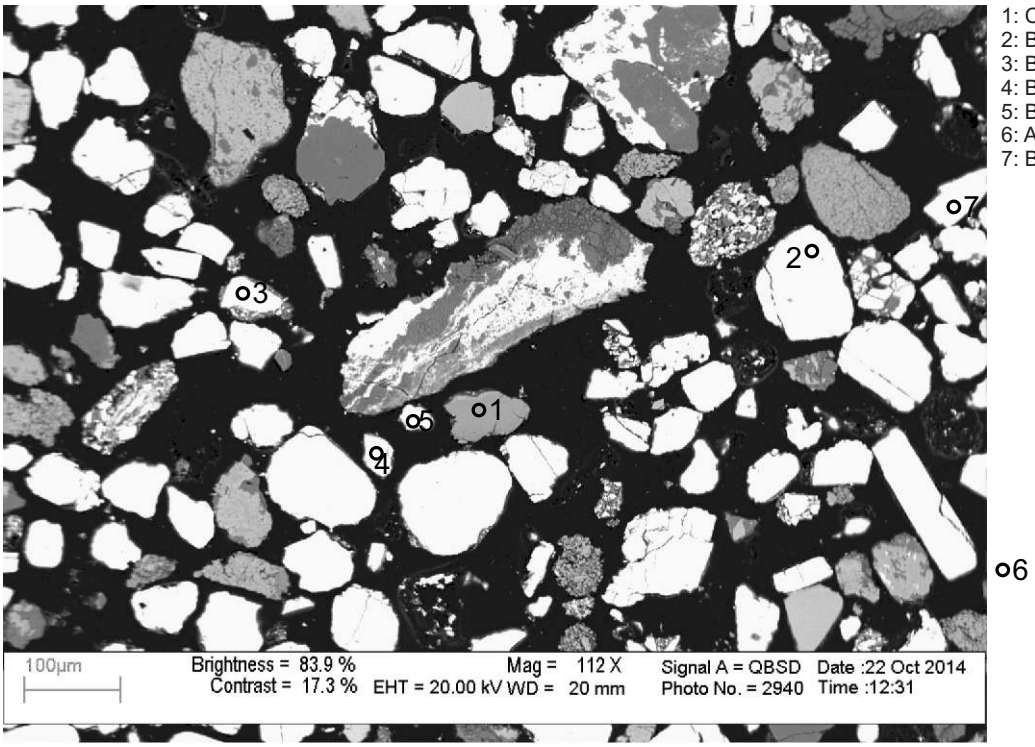

Figure 1-1.16: Sample Newburn 4300m site 17 (SEM).

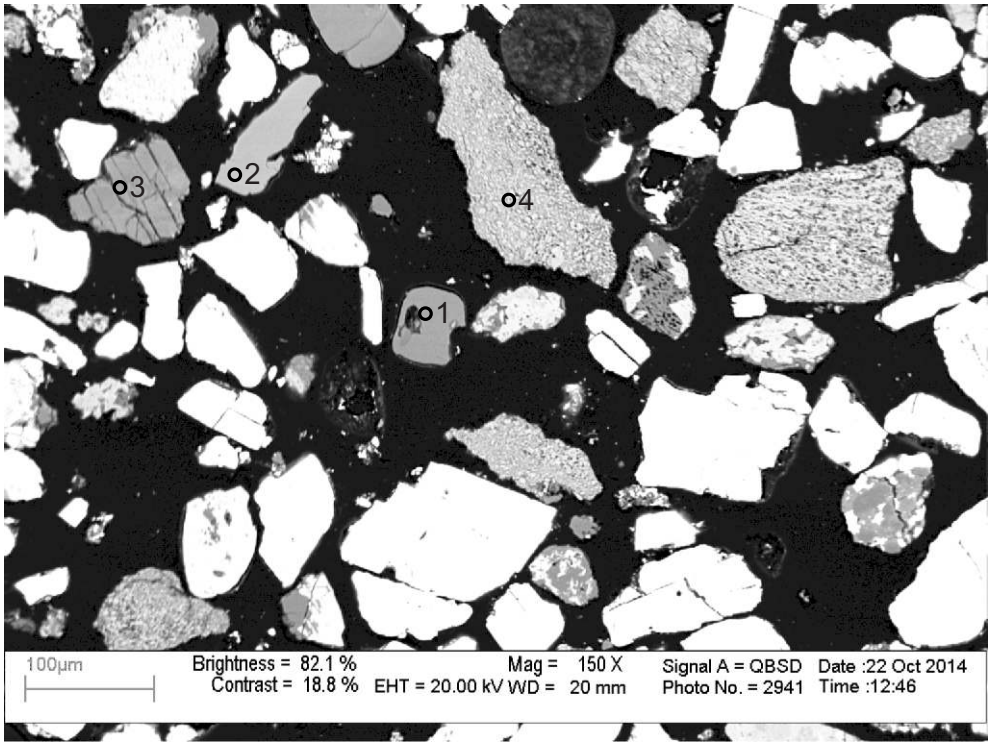

1: Tourmaline
2: Diopside
3: Fe-Dolomite +Chlorite
4: Siderite +Muscovite

Figure 1-1.17: Sample Newburn 4300m site 18 (SEM).

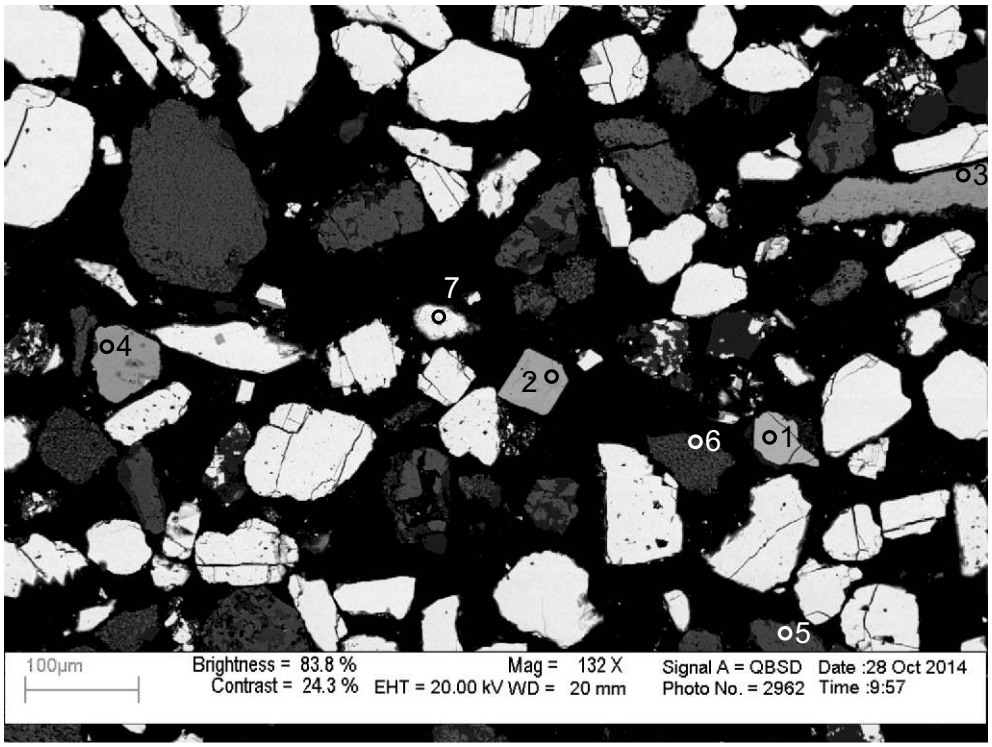

1: Chlalcopyrite
2: Zircon
3: Hematite +Goethite
4: Psilomelane
5: Siderite +Muscovite
6: Siderite +Muscovite
7: Barite

Figure 1-1.18: Sample Newburn 4300m site 19 (SEM).

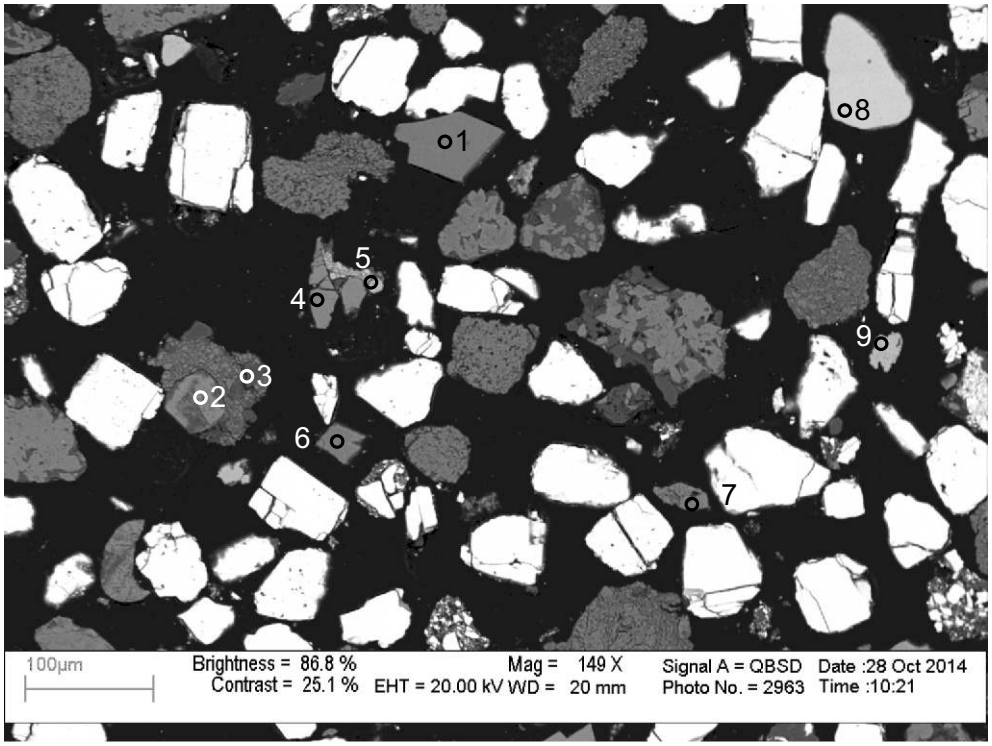

1: Fluorite
2: Titania +Quartz
3: Quartz
4: Titania
5: Pyrite
6: Fluorapatite
7: Titania +Chlorite
8: Zircon
9: Limonite +Other

Figure 1-1.19: Sample Newburn 4300m site 20 (SEM).

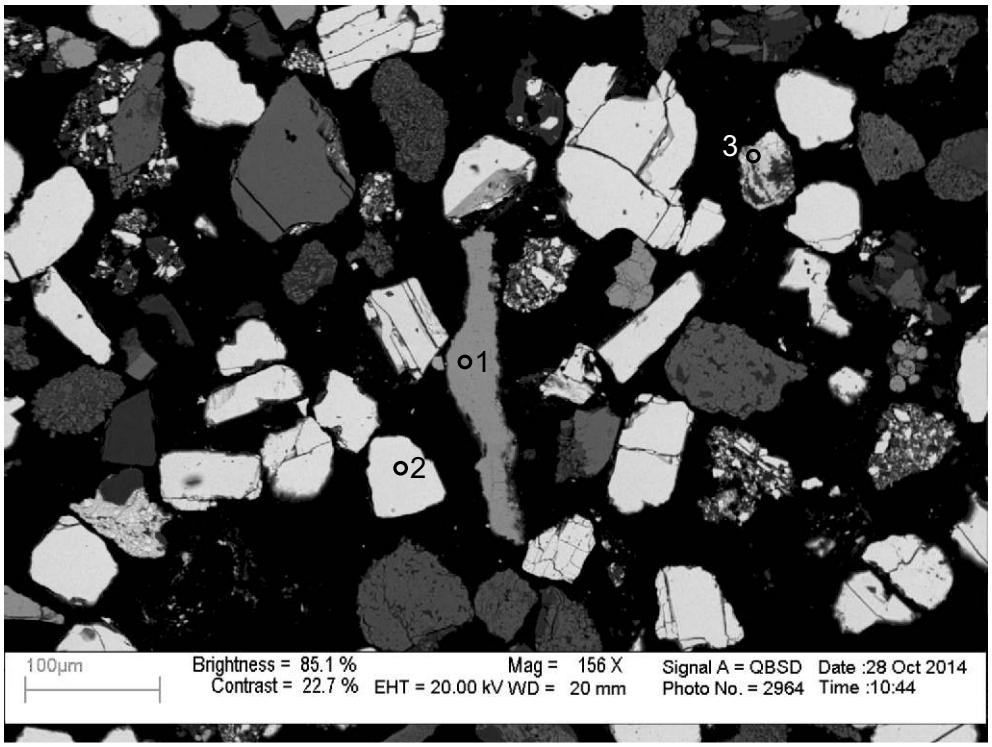

1: Limonite +Other
2: Barite
3: Barite

Figure 1-1.20: Sample Newburn 4300m site 21 (SEM).

Table 1-1: Scaning Electron Microscope chemical analyses of sample 4300m from Newburn H-23 well.

Sample	Site	Position	Mineral	SiO_2	TiO_2	Al_2O_3	FeO	MnO	MgO	CaO	Na_2O	K_2O	P_2O_5	SO_3	F	Cl	Cr_2O_3	CoO	NiO	CuO	ZnO	As_2O_3	SrO	ZrO_2	BaO	Ce_2O_3	WO_3	Total	Total Actual
H-23 4300m	2	1	TiO_2		99.12		0.89																					100	100
H-23 4300m	2	2	TiO_2		99.68		0.32																					100	99
H-23 4300m	2	3	Fap				0.31			44.21	0.39		43.81	0.92	8.86	0.38											1.12	100	122
H-23 4300m	2	4	TiO_2		99.55		0.45																					100	100
H-23 4300m	2	5	Sd+Qz	8.41		3.70	83.78			0.67										2.52	0.92							100	60
H-23 4300m	2	6	Ilm	2.78	51.93		41.60	1.34		2.34																		100	88
H-23 4300m	2	7	Sd+Qz	3.68			95.86			0.46																		100	68
H-23 4300m	2	8	TiO_2		100.00																							100	91
H-23 4300m	2	9	Qz	99.99																								100	119
H-23 4300m	2	10	Brt											39.48				-0.17							60.68			100	103
H-23 4300m	2	11	TiO_2	0.66	96.50	2.85																						100	87
H-23 4300m	3	1	TiO_2		99.47																							99	96
H-23 4300m	3	2	Sd+Ab+Other	15.19		4.29	53.81	0.80	16.37	5.34	2.08	1.10		1.05														100	66
H-23 4300m	3	3	Chl+Kfs	40.35		21.54	27.56		3.08	2.56		1.61		1.05											2.27			100	45
H-23 4300m	3	4	Zrn	30.78																				69.22				100	113
H-23 4300m	3	5	Qz+TiO_2+Ms	71.73	20.12	6.41					0.30	1.43																100	102
H-23 4300m	3	6	Sd+Qz	6.48			92.95	0.57																				100	66
H-23 4300m	3	7	Lm				100.00																					100	76
H-23 4300m	3	8	Ab+Sd	25.14		8.16	46.69	1.17	6.98	3.30	8.55																	100	71
H-23 4300m	3	9	Sd				42.00	0.68	10.75	2.57																		56	45
H-23 4300m	3	10	Tur	38.72	0.42	33.72	5.43		6.13	0.52	2.05																	87	101
H-23 4300m	3	11	Qz	99.99																								100	112
H-23 4300m	3	12	Sd+Ms	5.54		1.38	67.18	1.69	18.24	5.51		0.46																100	51
H-23 4300m	4	1	TiO_2		99.05												0.96											100	94
H-23 4300m	4	2	TiO_2	3.02	93.68	1.34	1.98																					100	92
H-23 4300m	4	3	TiO_2	3.49	92.89	1.47	1.35				0.80																	100	91
H-23 4300m	4	4	Lm+Other	9.24		1.19	83.83			0.42											5.32							100	68
H-23 4300m	4	5	Sd+Kfs	5.22		1.57	72.62	1.30	14.72	3.79		0.76																100	55
H-23 4300m	4	6	Hole	91.45		6.18	0.40		0.48			1.47																100	114
H-23 4300m	4	7	Py				25.24							74.76														100	223
H-23 4300m	4	8	Ilm	5.54	67.44	1.89	19.86		3.18	0.94	1.15																	100	76
H-23 4300m	4	9	Sd	1.51		1.11	38.98	0.95	9.78	3.67																		56	53
H-23 4300m	5	1	Zrn	30.70																				69.30				100	118
H-23 4300m	5	2	TiO_2	0.73	97.50	0.59	1.20																					100	78
H-23 4300m	5	3	TiO_2		100.00																							100	88
H-23 4300m	5	4	TiO_2		97.97		2.03																					100	89
H-23 4300m	5	5	Zrn	31.06																				68.93				100	118
H-23 4300m	5	6	Lm+Other	5.01			92.97			0.43											1.58							100	65
H-23 4300m	5	7	TiO_2	2.52	95.53	1.30	0.66																					100	88
H-23 4300m	5	8	Sd+Other	5.07	0.68	1.23	68.61	1.50	16.18	4.83		0.53	1.35															100	53
H-23 4300m	5	9	Lm+Qz	8.90			90.02	1.10																				100	65
H-23 4300m	5	10	Sd+Ab+Kfs	7.47		2.46	70.40	1.24	13.60	3.15	1.29	0.41																100	54
H-23 4300m	5	11	TiO_2		98.32		1.69																					100	83
H-23 4300m	6	1	Sd	3.49		2.63	38.13	0.41	5.37	4.22		0.27	1.48															56	56
H-23 4300m	6	2	Sd	1.23		0.76	41.07	0.45	7.06	4.08			1.35															56	55
H-23 4300m	6	3	Fap							46.19			45.62		8.20													100	101
H-23 4300m	6	4	Py				25.78							74.21														100	197
H-23 4300m	6	5	TiO_2		98.52		1.49																					100	87

Table 1-1: Scaning Electron Microscope chemical analyses of sample 4300m from Newburn H-23 well.

Sample	Site	Position	Mineral	SiO_2	TiO_2	Al_2O_3	FeO	MnO	MgO	CaO	Na_2O	K_2O	P_2O_5	SO_3	F	Cl	Cr_2O_3	CoO	NiO	CuO	ZnO	As_2O_3	SrO	ZrO_2	BaO	Ce_2O_3	WO_3	Total	Total Actual
H-23 4300m	6	6	Lm+Other	1.69		2.82	93.30			0.88				0.95		0.37												100	59
H-23 4300m	7	1	Ep	37.41		21.88	8.84			18.87																		87	100
H-23 4300m	7	2	Ank				10.38	1.16	17.54	26.91																		56	52
H-23 4300m	7	3	Py	2.55		0.83	24.75					0.33		71.54														100	194
H-23 4300m	7	4	Fap							45.91			46.20		6.88												1.02	100	109
H-23 4300m	7	5	Fap				0.28		0.53	44.97			45.28	0.60	7.11												1.26	100	109
H-23 4300m	8	1	Tur	38.63	0.89	31.54	6.10		6.59	0.82	2.43																	87	94
H-23 4300m	8	2	Sd+Ap	1.65		1.49	52.89	0.57	5.39	21.24			16.77															100	62
H-23 4300m	8	3	Spl			20.24	18.87		12.55								48.35											100	90
H-23 4300m	8	4	Spl			22.60	23.13		13.40								40.88											100	99
H-23 4300m	8	5	Ab	68.41		18.52					13.08																	100	108
H-23 4300m	8	6	Bt	37.64	4.87	11.09	5.90		18.23		1.00	6.84			10.43													96	120
H-23 4300m	8	7	Sd+Chl	10.67		9.50	70.77	1.02	5.26	2.78																		100	54
H-23 4300m	8	8	Sd+Chl	5.03		1.42	71.57	1.16	17.05	3.79																		100	49
H-23 4300m	8	9	Brt											39.75				-0.15					3.10		57.32			100	99
H-23 4300m	8	10	Py+Ab+Kfs	12.62		1.02	21.78				0.44	0.34		63.50					0.32									100	174
H-23 4300m	9	1	Tur	39.01	0.90	31.34	5.94		6.82	0.74	2.25																	87	101
H-23 4300m	9	2	Spl			21.11	18.83		13.17								46.91											100	96
H-23 4300m	9	3	Sd+Ab+Chl	22.85		16.97	48.68	0.67	6.42	3.37	1.05																	100	64
H-23 4300m	9	4	Brt											39.08											60.94			100	107
H-23 4300m	10	1	TiO_2		100.00																							100	103
H-23 4300m	10	2	Fl							41.61					58.38													100	205
H-23 4300m	10	3	Sd				52.42	1.71		1.87																		56	56
H-23 4300m	10	4	TiO_2	0.66	97.51		1.84																					100	107
H-23 4300m	10	5	Sd+Kfs	12.51	0.75	3.29	54.38	0.96	19.95	6.18		2.00																100	63
H-23 4300m	10	6	Sd+Other	7.51		4.91	65.53	0.74	7.35	8.94		0.53	4.49															100	61
H-23 4300m	10	7	Qz	99.99																								100	116
H-23 4300m	10	8	Tur	38.86	0.42	25.41	10.07		8.57	1.44	2.23																	87	100
H-23 4300m	10	9	Qz	99.99																								100	131
H-23 4300m	10	10	Brt											39.20											60.80			100	116
H-23 4300m	11	1	Tur	37.72	0.55	34.25	6.10		5.42	0.83	2.13																	87	110
H-23 4300m	11	2	Qz	99.99																								100	139
H-23 4300m	11	3	Sd				49.34	3.99	1.76	0.91																		56	52
H-23 4300m	11	4	Kfs	67.26		17.74	0.55					14.44																100	121
H-23 4300m	11	5	Spl			17.74	28.39		6.45								47.42											100	97
H-23 4300m	11	6	Sd+Chl	7.62	4.70	6.95	53.41	0.89	19.14	7.28																		100	58
H-23 4300m	11	7	Lm+Other	6.37		2.99	79.23													0.94	6.77	3.70						100	62
H-23 4300m	11	8	Sd+Ap+Qz	17.65		2.53	36.79	0.61	4.23	22.93			15.26															100	68
H-23 4300m	11	9	Sd+Ap+Qz	4.02		3.23	61.35	0.99	9.43	14.40			6.55															100	55
H-23 4300m	12	1	Hbl	47.16	1.67	10.18	15.90		9.80	9.68	1.78	0.84																97	124
H-23 4300m	12	2	Sd+Qz	12.19		10.43	56.15	0.77	15.37	5.05																		100	69
H-23 4300m	12	3	Ab	65.74		21.20	0.46			0.85	10.76	0.96																100	129
H-23 4300m	12	4	Ank				6.84	0.73	20.44	27.99																		56	64
H-23 4300m	12	5	Fap							43.54	0.51		44.52	0.65	9.69											1.08		100	129
H-23 4300m	12	6	Brt											39.38				-0.01							60.66			100	119
H-23 4300m	12	7	Ab	68.52		18.56					12.93																	100	145
H-23 4300m	12	8	Sd	1.69			39.82	0.96	10.53	3.00																		56	61
H-23 4300m	13	1	TiO_2		99.30		0.69																					100	106
H-23 4300m	13	2	Ab	68.60		18.56					12.85																	100	144

Table 1-1: Scaning Electron Microscope chemical analyses of sample 4300m from Newburn H-23 well.

Sample	Site	Position	Mineral	SiO_2	TiO_2	Al_2O_3	FeO	MnO	MgO	CaO	Na_2O	K_2O	P_2O_5	SO_3	F	Cl	Cr_2O_3	CoO	NiO	CuO	ZnO	As_2O_3	SrO	ZrO_2	BaO	Ce_2O_3	WO_3	Total	Total Actual
H-23 4300m	13	3	Qz	99.73			0.27																					100	125
H-23 4300m	13	4	TiO_2	1.13	97.75	0.62	0.50																					100	98
H-23 4300m	13	5	Sd+Ab	6.70		2.83	65.24	1.08	17.00	5.26	1.90																	100	58
H-23 4300m	13	6	Ab	68.18		3.46	22.89	0.49	2.52	1.58		0.89																100	91
H-23 4300m	13	7	Sd+Chl	4.90		1.66	73.88	1.33	15.54	2.69																		100	57
H-23 4300m	14	1	Tur	39.48		34.18	7.49		3.90		1.96																	87	121
H-23 4300m	14	2	Di	54.89		3.16	10.23	0.45	11.16	19.16	0.97																	100	131
H-23 4300m	14	3	TiO_2+Chl	20.17	43.89	13.34	8.71		13.17			0.71																100	104
H-23 4300m	14	4	Fe-Dol				10.78	1.90	37.89	49.43																		100	62
H-23 4300m	14	5	Qz	99.99																								100	141
H-23 4300m	14	6	Chl	32.27	0.66	19.10	12.40		17.83			2.74																85	100
H-23 4300m	15	1	Tur	37.31	0.30	25.89	6.32		10.11	2.04	1.63				3.40													87	131
H-23 4300m	15	2	Fap	0.88						44.76			44.71		8.93											0.73		100	141
H-23 4300m	15	3	Tur	39.09	0.32	30.56	8.90		4.89		3.24																	87	122
H-23 4300m	15	4	Qz	99.99																								100	138
H-23 4300m	15	5	Qz	98.98		0.79						0.23																100	139
H-23 4300m	15	6	Sd	0.76			37.47	0.52	11.64	5.62																		56	58
H-23 4300m	15	7	Qz	99.99																								100	145
H-23 4300m	16	1	Tur	38.62	0.48	34.14	5.12		6.25	0.34	2.05																	87	134
H-23 4300m	16	2	Qz	99.99																								100	143
H-23 4300m	16	3	Tur	38.43	0.84	28.81	8.60		6.77	1.90	1.65																	87	126
H-23 4300m	16	4	Qz	99.99																								100	156
H-23 4300m	16	5	Brt+Ms	36.64		13.06	2.11			1.86		1.75		20.00											24.58			100	19
H-23 4300m	16	6	Zrn	31.13																				68.88				100	156
H-23 4300m	17	1	Chl	27.84		21.38	20.56	0.68	14.54																			85	132
H-23 4300m	17	2	Brt											39.28				-0.08					2.60		58.21			100	155
H-23 4300m	17	3	Brt											39.08				0.05					2.09		58.77			100	138
H-23 4300m	17	4	Brt											39.85				-0.13							60.30			100	136
H-23 4300m	17	5	Brt											39.23				0.13							60.66			100	142
H-23 4300m	17	6	Ab	68.43		18.57					13.00																	100	183
H-23 4300m	17	7	Brt											39.90				-0.01					2.09		58.03			100	163
H-23 4300m	18	1	Tur	42.57	0.83	34.07	5.75		5.51	0.37	2.30																	91	137
H-23 4300m	18	2	Di	54.42		6.12	1.49		17.00	20.95																		100	157
H-23 4300m	18	3	Fe-Dol+Chl	3.32		1.64	11.06	1.91	35.30	46.76																		100	71
H-23 4300m	18	4	Sd+Ms	7.94		5.29	59.18	0.97	18.70	7.37		0.57																100	72
H-23 4300m	19	1	Cpy				22.01							54.41						23.57								100	206
H-23 4300m	19	2	Zrn	31.02																				68.99				100	128
H-23 4300m	19	3	Hem+Gth				99.48	0.52																				100	110
H-23 4300m	19	4	Ps					76.92		1.26															21.81			100	77
H-23 4300m	19	5	Sd+Ms	6.33		3.70	70.42	0.74	10.65	6.42		0.60	1.15															100	70
H-23 4300m	19	6	Sd+Ms	3.66		2.21	69.69	0.99	14.99	8.09		0.37																100	57
H-23 4300m	19	7	Brt											37.61				0.05							62.36			100	107
H-23 4300m	20	1	Fl							43.74					56.26													100	158
H-23 4300m	20	2	TiO_2+Qz	32.37	67.16		0.48																					100	96
H-23 4300m	20	3	Qz	99.39			0.60																					100	98
H-23 4300m	20	4	TiO_2		99.45		0.55																					100	89
H-23 4300m	20	5	Py		0.30		27.85							71.84														100	192
H-23 4300m	20	6	Fap				0.54			45.91			43.95	0.80	7.72												1.10	100	106
H-23 4300m	20	7	TiO_2+Chl	11.10	76.21	4.99	4.84		2.87																			100	90

Table 1-1: Scaning Electron Microscope chemical analyses of sample 4300m from Newburn H-23 well.

Sample	Site	Position	Mineral	SiO_2	TiO_2	Al_2O_3	FeO	MnO	MgO	CaO	Na_2O	K_2O	P_2O_5	SO_3	F	Cl	Cr_2O_3	CoO	NiO	CuO	ZnO	As_2O_3	SrO	ZrO_2	BaO	Ce_2O_3	WO_3	Total	Total Actual
H-23 4300m	20	8	Zrn	30.74																				69.26				100	110
H-23 4300m	20	9	Lm+Other				95.93	0.66									3.41											100	76
H-23 4300m	21	1	Lm+Other				100.00																					100	76
H-23 4300m	21	2	Brt											37.56				-0.01					1.73		60.72			100	92
H-23 4300m	21	3	Brt											37.46				0.05							62.51			100	93

Appendix 1-2: SEM-BSE images and EDS mineral analyses for sample 4315m.

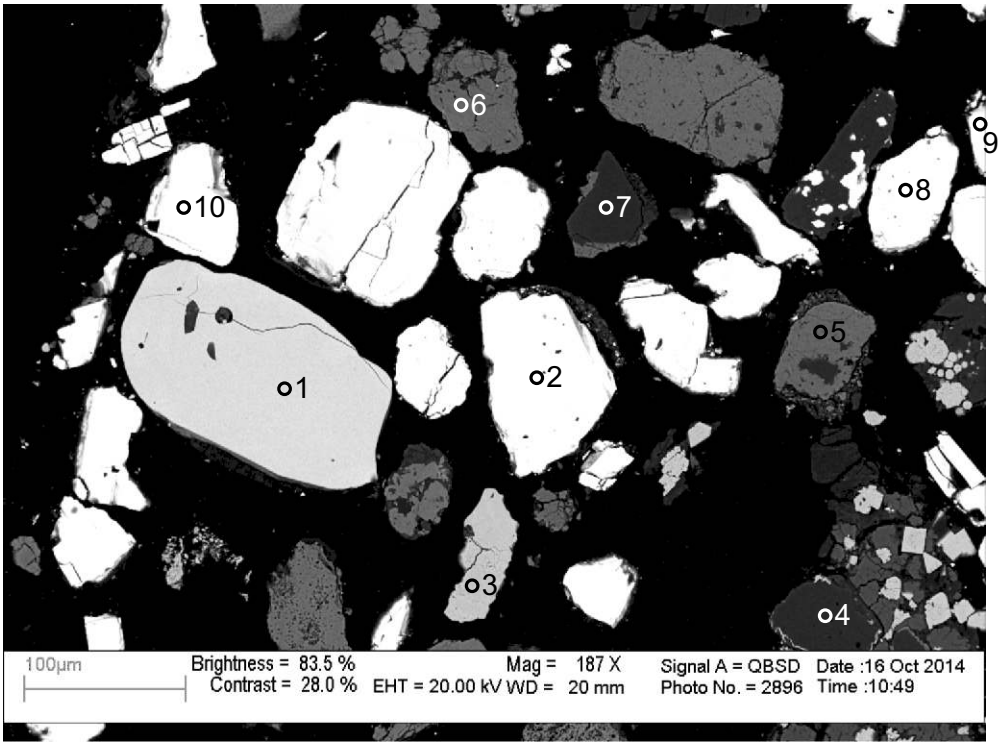

1: Zircon
2: Barite
3: Pyrite
4: Quartz
5: Siderite
+Apatite
+Albite
6: Siderite
+Albite
7: Quartz
8: Barite
9: Barite
10: Barite

Figure 1-2.1: Sample Newburn 4315m site 1 (SEM).

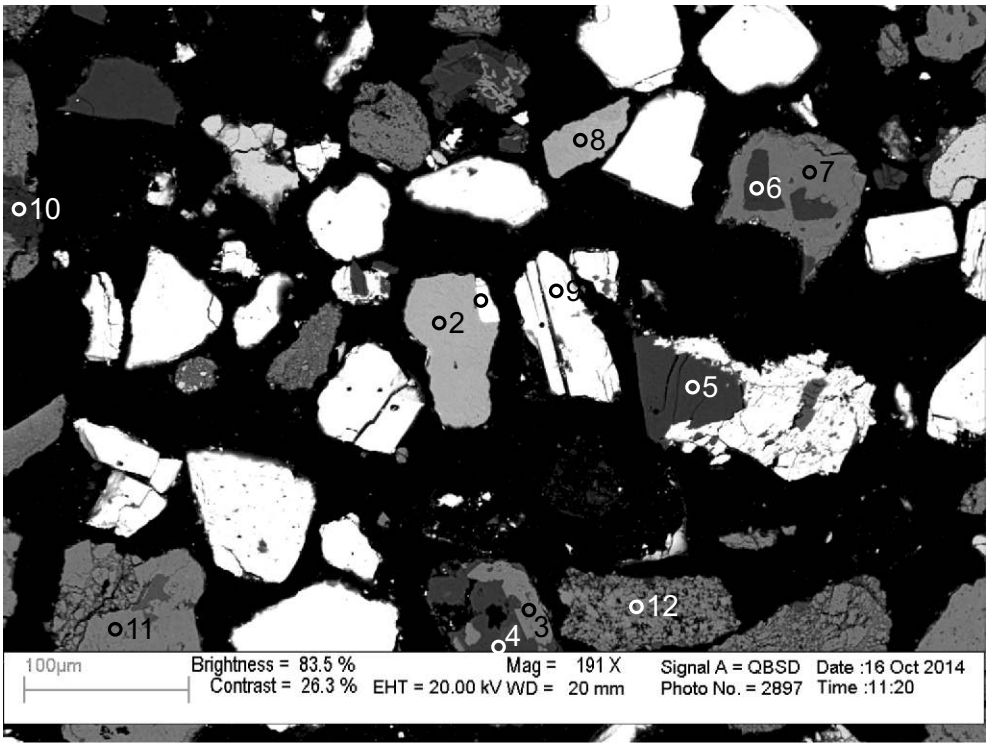

1: Barite
2: Limonite
+Other
3: Siderite
+Chlorite
4: Albite
5: Albite
6: Quartz
7: Siderite
8: Limonite
+Other
9: Barite
10: Kaolinite
11: Siderite
+Muscovite
12: Siderite
+Muscovite

Figure 1-2.2: Sample Newburn 4315m site 2 (SEM).

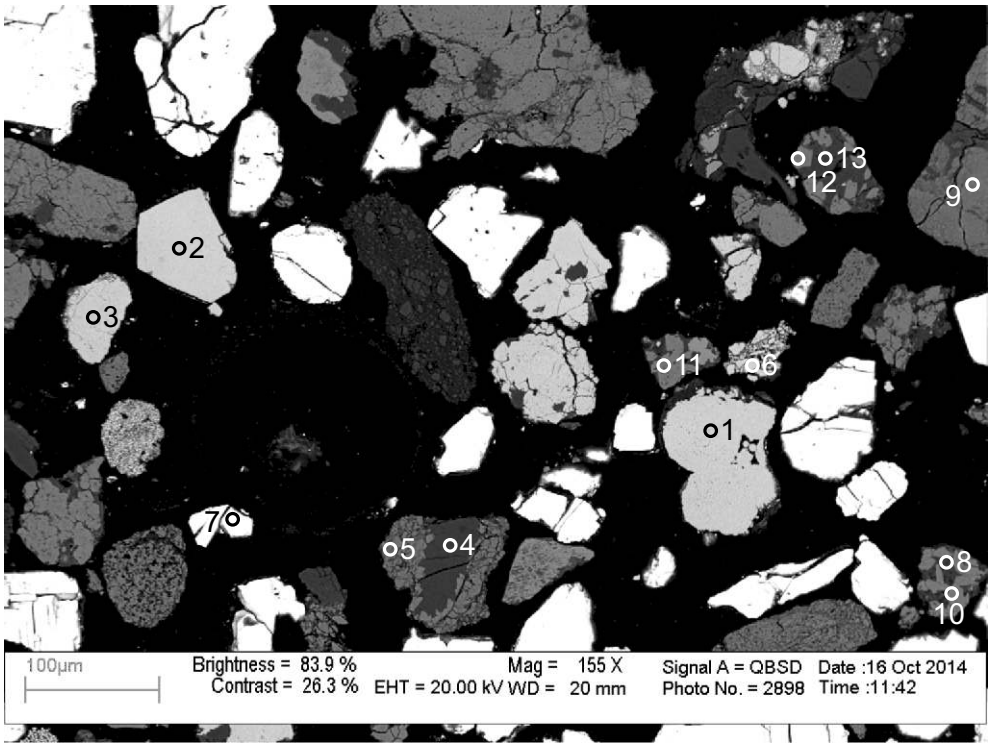

1: Pyrite
2: Pyrite
3: Pyrite
4: Albite
5: Siderite
+Chlorite
6: Pyrite
7: Barite
8: Albite
9: Siderite
10: Siderite
+Chlorite
11: Siderite
+Chlorite
12: Siderite
13: Albite

Figure 1-2.3: Sample Newburn 4315m site 3 (SEM).

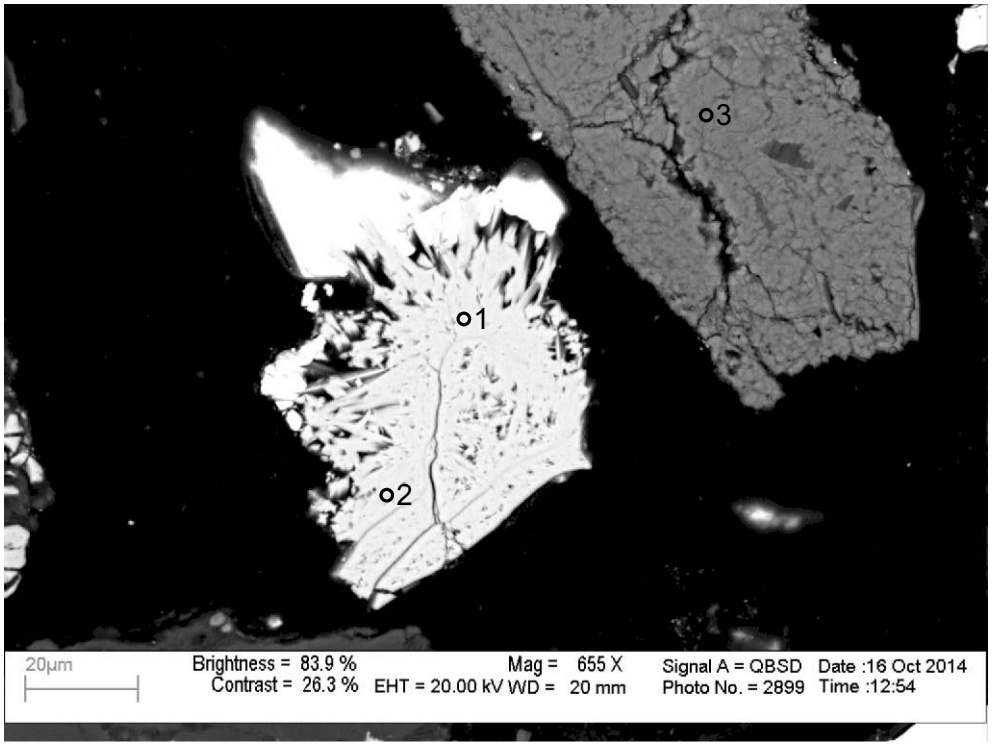

1: Psilomelane
2: Psilomelane
3: Siderite
+Albite
+Chlorite

Figure 1-2.4: Sample Newburn 4315m site 4 (SEM).

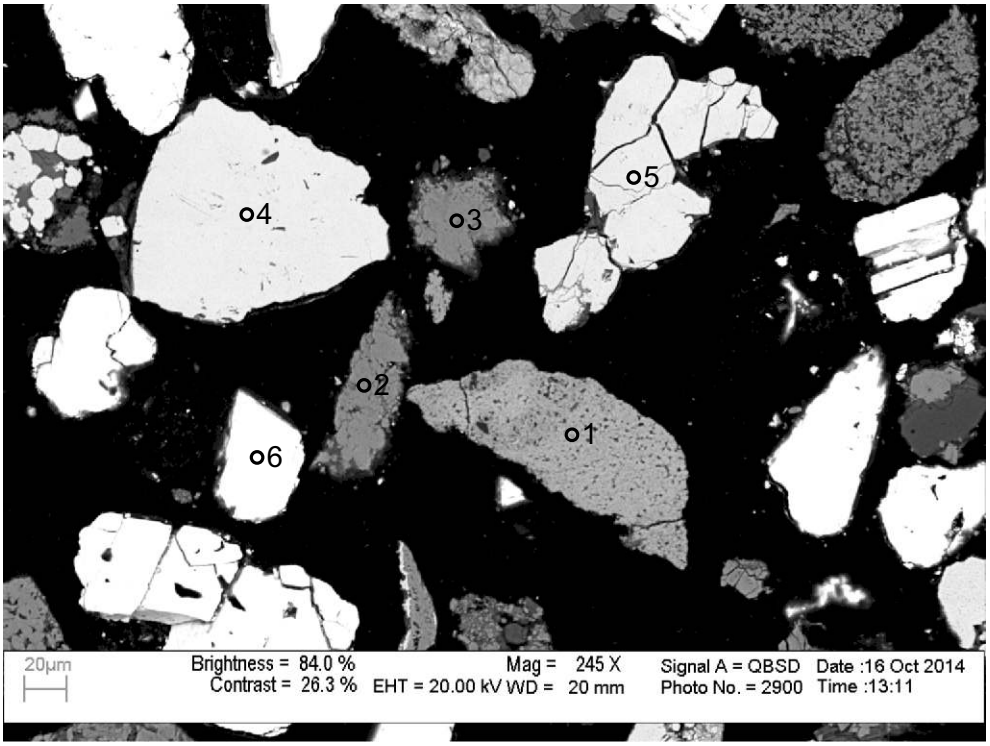

Figure 1-2.5: Sample Newburn 4315m site 5 (SEM).

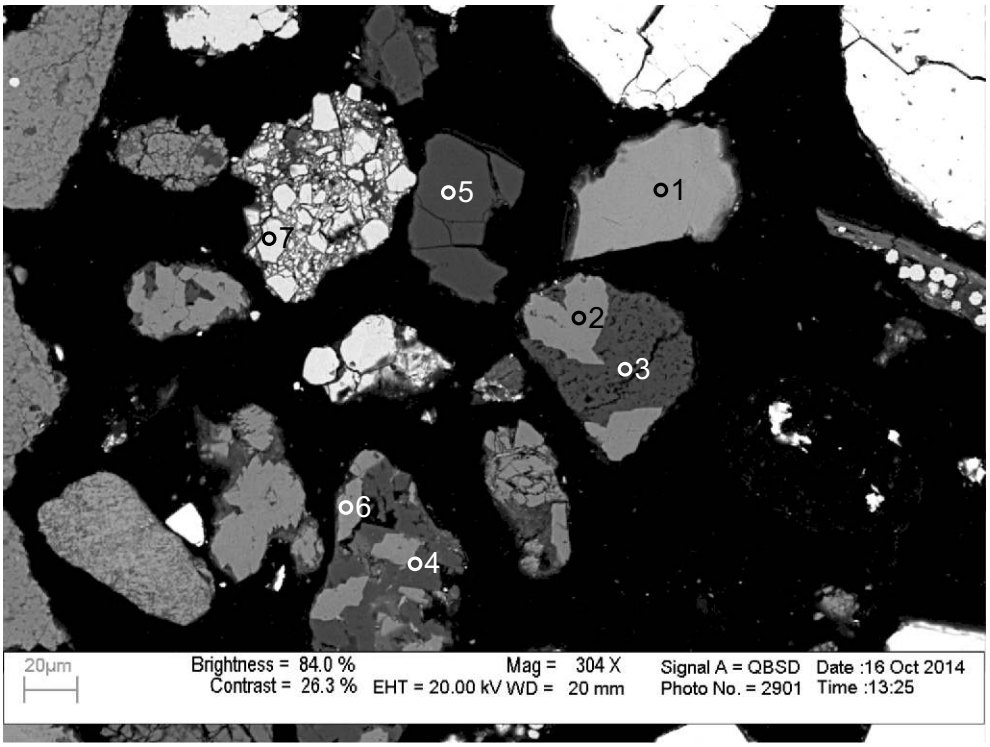

Figure 1-2.6: Sample Newburn 4315m site 6 (SEM).

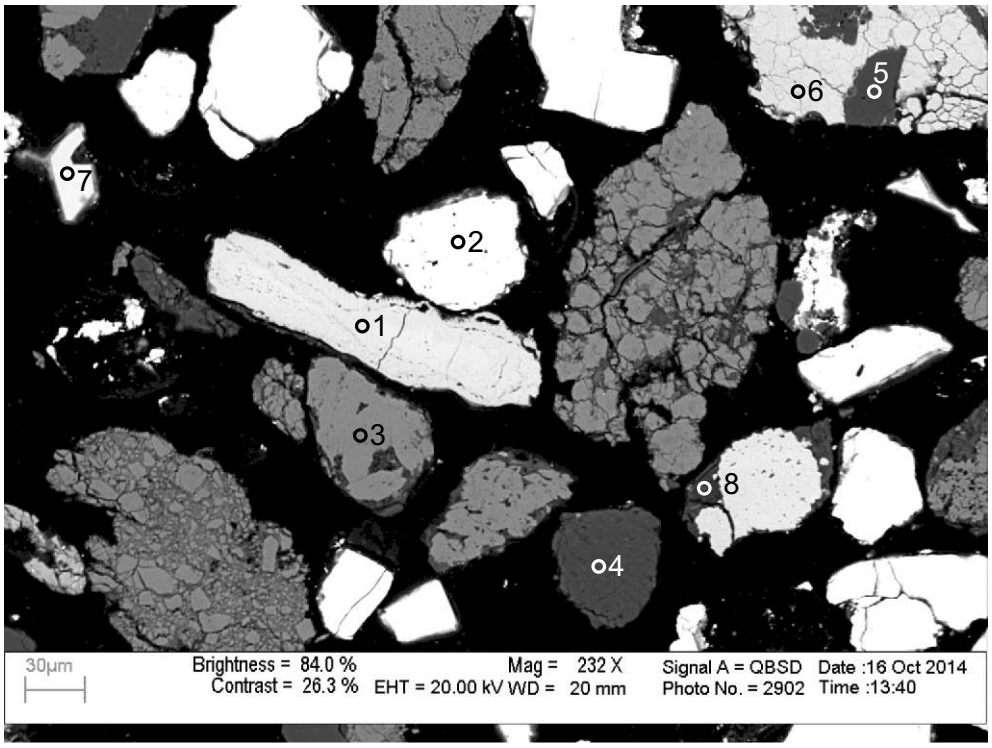

1: Goethite
+Limonite
2: Barite
3: Siderite
4: Quartz
5: Quartz
6: Pyrite
7: Zircon
8: Muscovite
+Chlorite
+Pyrite

Figure 1-2.7: Sample Newburn 4315m site 7 (SEM).

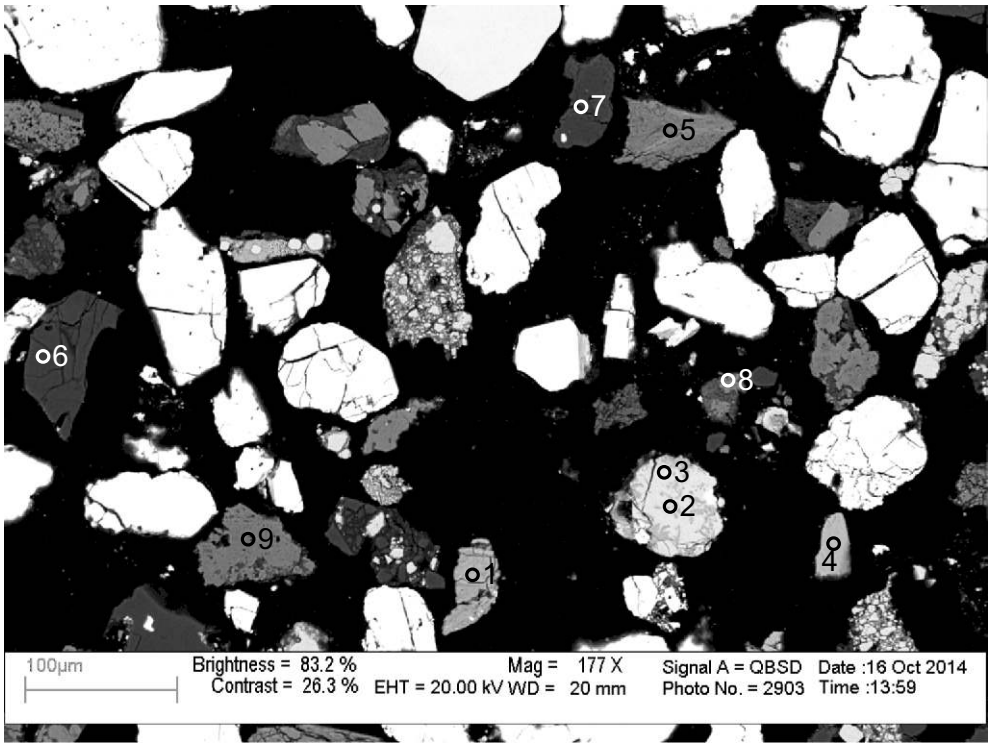

1: Contaminant
2: Psilomelane
3: Psilomelane
4: Limonite
5: Siderite
+Apatite
+Albite
6: Quartz
7: Quartz
+Muscovite
8: Siderite
+Chlorite
9: Siderite
+Muscovite

Figure 1-2.8: Sample Newburn 4315m site 8 (SEM).

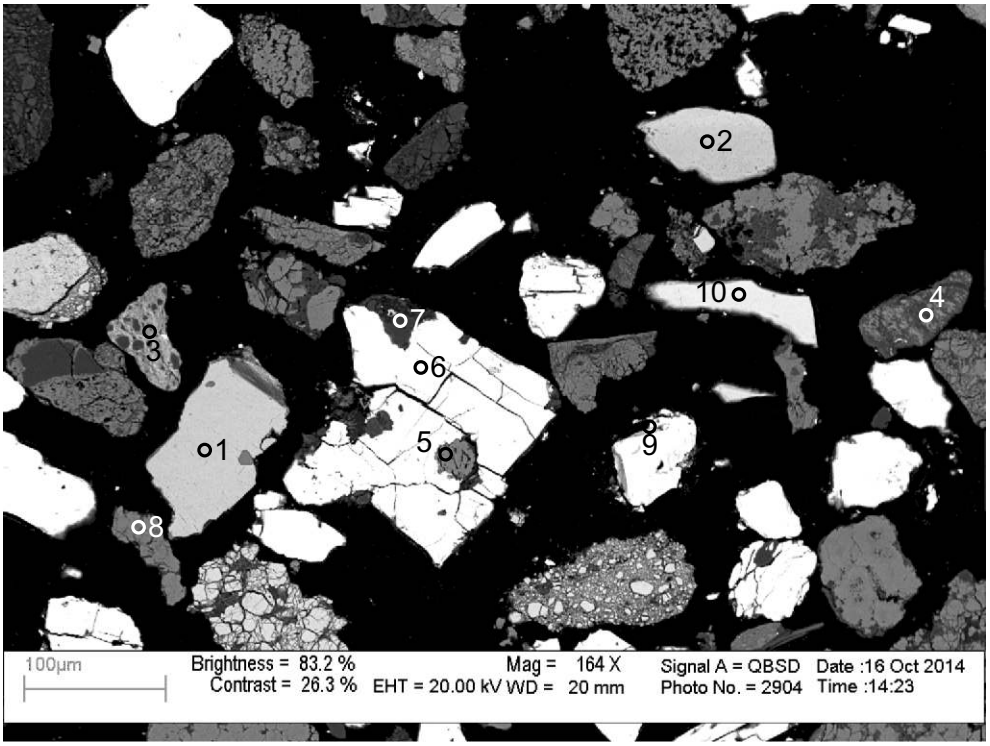

1: Limonite
2: Limonite +Other
3: Psilomelane
4: Quartz +Titania
5: Siderite +Chlorite
6: Barite
7: Quartz
8: Siderite +Apatite +Chlorite
9: Barite
10: Zircon

Figure 1-2.9: Sample Newburn 4315m site 9 (SEM).

Table 1-2: Scanning Electron Microscope chemical analyses of sample 4315m from Newburn H-23 well.

Sample	Site	Position	Mineral	SiO_2	TiO_2	Al_2O_3	FeO	MnO	MgO	CaO	Na_2O	K_2O	P_2O_5	SO_3	F	Cl	Cr_2O_3	CoO	NiO	CuO	ZnO	As_2O_3	SrO	ZrO_2	MoO_3	Sb_2O_3	BaO	Total	Actual Total
H-23 4315m	1	1	Zrn																									100	121
H-23 4315m	1	2	Brt											37.33									1.48				61.20	100	118
H-23 4315m	1	3	Py				28.73							71.27														100	227
H-23 4315m	1	4	Qz	99.75			0.24																					100	131
H-23 4315m	1	5	Sd+Ap+Ab	2.27		1.23	75.21	0.83	12.60	6.62			1.26															100	67
H-23 4315m	1	6	Sd+Ab	2.48		1.44	73.43		12.27	10.38																		100	64
H-23 4315m	1	7	Qz	99.73			0.26																					100	125
H-23 4315m	1	8	Brt											36.88													63.11	100	121
H-23 4315m	1	9	Brt											37.53									2.09				60.39	100	123
H-23 4315m	1	10	Brt											37.51									2.20				60.31	100	115
H-23 4315m	2	1	Brt				1.47							36.28				0.01									62.24	100	115
H-23 4315m	2	2	Lm+Other	4.60			94.93	0.48																				100	78
H-23 4315m	2	3	Sd+Chl	1.80		0.72	80.77	1.33	11.62	3.76																		100	60
H-23 4315m	2	4	Ab	67.96		18.46	0.31			1.30	11.95																	100	119
H-23 4315m	2	5	Ab	69.29		18.67					12.04																	100	124
H-23 4315m	2	6	Qz	99.54			0.45																					100	126
H-23 4315m	2	7	Sd		0.30		39.61	0.87	8.99	6.23																		56	62
H-23 4315m	2	8	Lm+Other	3.36			92.38			2.57			1.28			0.41												100	82
H-23 4315m	2	9	Brt											37.78				0.09					1.71				60.43	100	118
H-23 4315m	2	10	Kln	46.81		36.14	0.36				0.29				2.40													86	95
H-23 4315m	2	11	Sd+Ms	5.41		3.57	68.45	0.54	14.59	6.91		0.52																100	62
H-23 4315m	2	12	Sd+Ms	14.01		7.56	62.48	1.05	9.10	4.41		1.39																100	65
H-23 4315m	3	1	Py				28.38							71.62														100	232
H-23 4315m	3	2	Py				27.81							72.19														100	226
H-23 4315m	3	3	Py				28.32							71.69														100	214
H-23 4315m	3	4	Ab	66.29		21.22	0.32			0.90	10.95	0.34																100	122
H-23 4315m	3	5	Sd+Chl	2.67		1.51	75.23	0.63	12.57	7.37																		100	57
H-23 4315m	3	6	Py				28.38							71.62														100	239
H-23 4315m	3	7	Brt											38.01				0.06									61.93	100	115
H-23 4315m	3	8	Ab	66.42		18.10	2.91			0.28	12.28																	100	135
H-23 4315m	3	9	Sd	0.52			39.98	0.34	8.59	6.57																		56	68
H-23 4315m	3	10	Sd+Chl	2.31		1.10	79.14	1.54	11.31	4.60																		100	66
H-23 4315m	3	11	Sd+Chl	2.89		1.19	78.62	1.10	12.20	4.00																		100	67
H-23 4315m	3	12	Sd				45.26	0.83	8.02	1.90																		56	70
H-23 4315m	3	13	Ab	67.21		19.07	1.62				11.84	0.25																100	140
H-23 4315m	4	1	Ps	0.66			2.86	73.54																			22.92	100	89
H-23 4315m	4	2	Ps				2.35	74.69																			22.95	100	89
H-23 4315m	4	3	Sd+Ab+Chl	2.63		1.27	71.32	0.57	12.15	12.06																		100	69
H-23 4315m	5	1	Lm+Other	11.27	0.50	17.16	69.06			0.39		0.33		0.70			0.58											100	98
H-23 4315m	5	2	Sd+Other	60.58		1.02	32.19	0.49	2.45	3.27																		100	91
H-23 4315m	5	3	Sd+Ap				79.43	1.48	9.05	8.72			1.31															100	64
H-23 4315m	5	4	Py				28.06							71.94														100	242
H-23 4315m	5	5	Py				27.90							72.09														100	248
H-23 4315m	5	6	Brt											37.31													62.71	100	120
H-23 4315m	6	1	Cr-Sp			28.40	19.17		10.25								42.19											100	121
H-23 4315m	6	2	Sd				45.30	0.85	7.12	2.73																		56	68
H-23 4315m	6	3	Ab	69.01		18.50	0.24				11.81	0.43																100	126
H-23 4315m	6	4	Ab	68.71		18.84	0.58				11.88																	100	134

Table 1-2: Scanning Electron Microscope chemical analyses of sample 4315m from Newburn H-23 well.

Sample	Site	Position	Mineral	SiO_2	TiO_2	Al_2O_3	FeO	MnO	MgO	CaO	Na_2O	K_2O	P_2O_5	SO_3	F	Cl	Cr_2O_3	CoO	NiO	CuO	ZnO	As_2O_3	SrO	ZrO_2	MoO_3	Sb_2O_3	BaO	Total	Actual Total
H-23 4315m	6	5	Qz	99.99																								100	135
H-23 4315m	6	6	Sd			0.44	45.58	0.85	6.87	2.26																		56	66
H-23 4315m	6	7	Py				28.10							71.92														100	256
H-23 4315m	7	1	Gth+Lm				100.00																					100	105
H-23 4315m	7	2	Brt	1.45										34.86				0.01									63.70	100	118
H-23 4315m	7	3	Sd				45.29	0.90	6.84	2.96																		56	69
H-23 4315m	7	4	Qz	99.37		0.40	0.23																					100	133
H-23 4315m	7	5	Qz	99.39			0.60																					100	147
H-23 4315m	7	6	Py				28.50							71.49														100	267
H-23 4315m	7	7	Zrn	30.87																				69.13				100	138
H-23 4315m	7	8	Ms+Chl+Py	54.61	0.52	27.70	4.25		2.16	0.87	0.40	4.78		2.72	2.01													100	116
H-23 4315m	8	1	Contaminant	2.87			81.77			2.28							8.42								4.65			100	90
H-23 4315m	8	2	Ps				33.86	53.88		0.49																	11.76	100	93
H-23 4315m	8	3	Ps				1.25	80.08		0.43										0.63							17.61	100	100
H-23 4315m	8	4	Lm	0.92			99.08																					100	92
H-23 4315m	8	5	Sd+Ap+Ab	5.86		2.95	64.57	0.75	7.13	12.13	0.89		5.73															100	83
H-23 4315m	8	6	Qz	99.99																								100	136
H-23 4315m	8	7	Qz+Ms	94.87		3.10	0.22					0.69			1.12													100	143
H-23 4315m	8	8	Sd+Chl	2.40		1.44	76.58	0.65	10.38	8.55																		100	71
H-23 4315m	8	9	Sd+Ms	3.06		1.27	74.45	1.33	14.48	5.09		0.35																100	69
H-23 4315m	9	1	Lm	0.64	4.55	0.68	94.11																					100	96
H-23 4315m	9	2	Lm+Other	2.63		1.66	87.22			2.15						0.45				1.25		1.74				2.86		100	94
H-23 4315m	9	3	Ps	24.29		14.09		40.30	0.91	0.71	0.58	4.53							0.65	2.89	1.19						9.88	100	100
H-23 4315m	9	4	Qz+TiO_2	90.53	9.19		0.27																					100	134
H-23 4315m	9	5	Sd+Chl	1.73		0.91	82.27	1.52	6.53	7.05																		100	60
H-23 4315m	9	6	Brt											37.23									1.61				61.20	100	125
H-23 4315m	9	7	Qz	99.99																								100	135
H-23 4315m	9	8	Sd+Ap+Chl	2.01		1.38	77.56	0.90	11.38	5.72			1.03															100	69
H-23 4315m	9	9	Brt											38.48				-0.05									61.59	100	131
H-23 4315m	9	10	Zrn	31.08																				68.92				100	133

Appendix 1-3: SEM-BSE images and EDS mineral analyses for sample Newburn H-23 5950m.

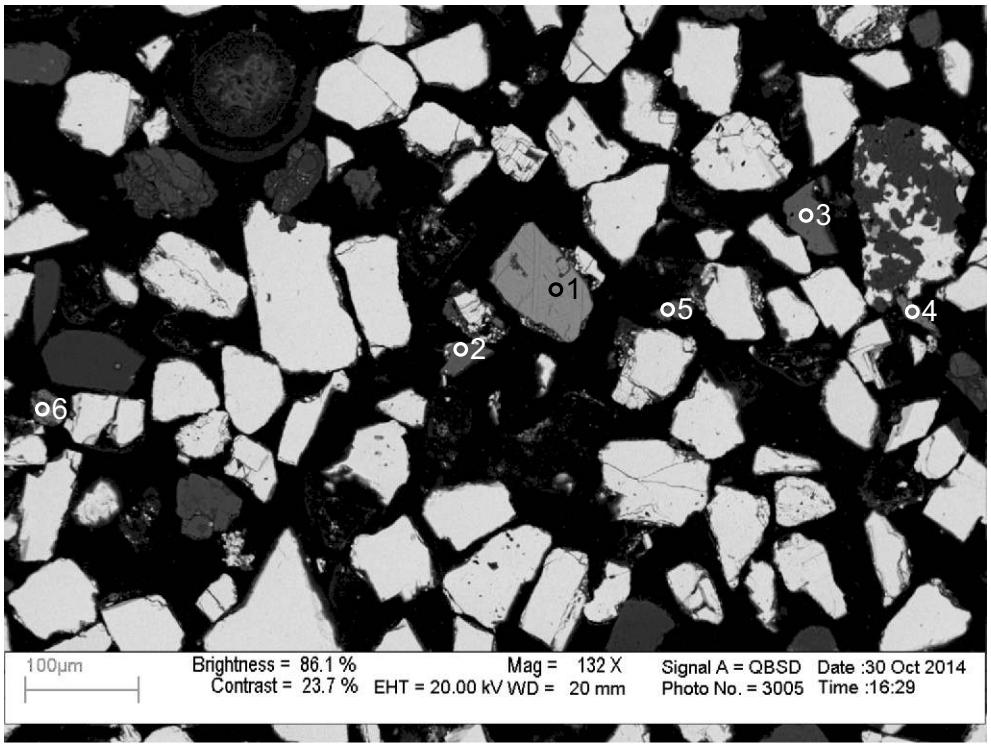

1: Limonite +Other
2: Chlorite
3: Fluorite
4: Pyrite
5: Fluorite
6: Pyrite

Figure 1-3.1: Sample Newburn 5950m site 2 (SEM).

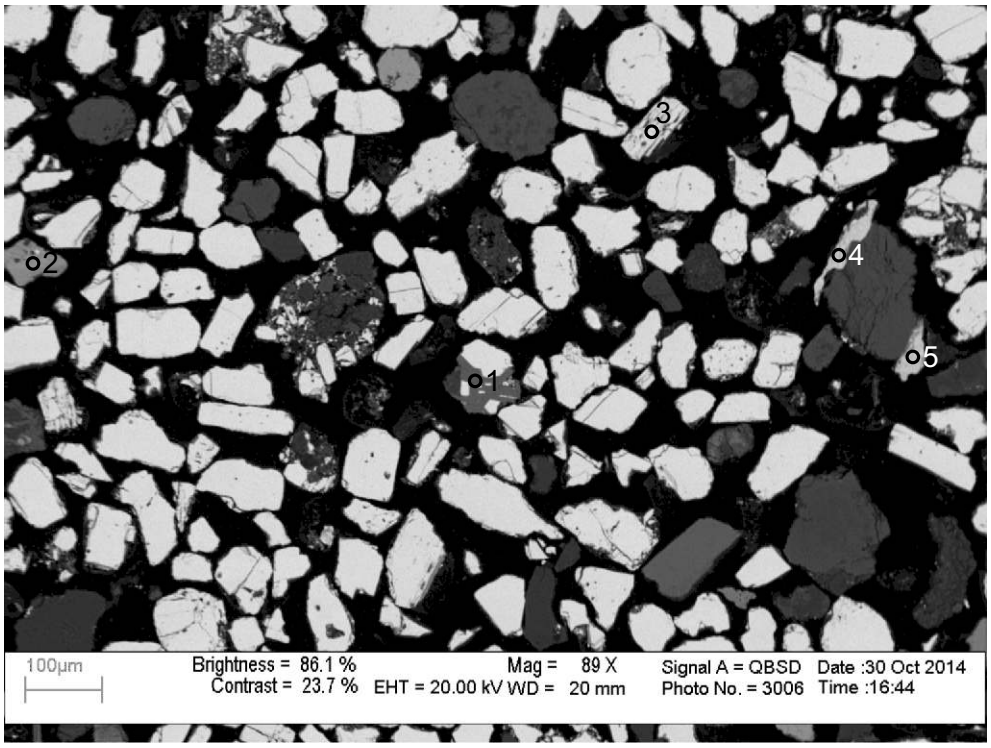

1: Chlorite
2: Psilomelane
3: Barite
4: Barite
5: Barite

Figure 1-3.2: Sample Newburn 5950m site 3 (SEM).

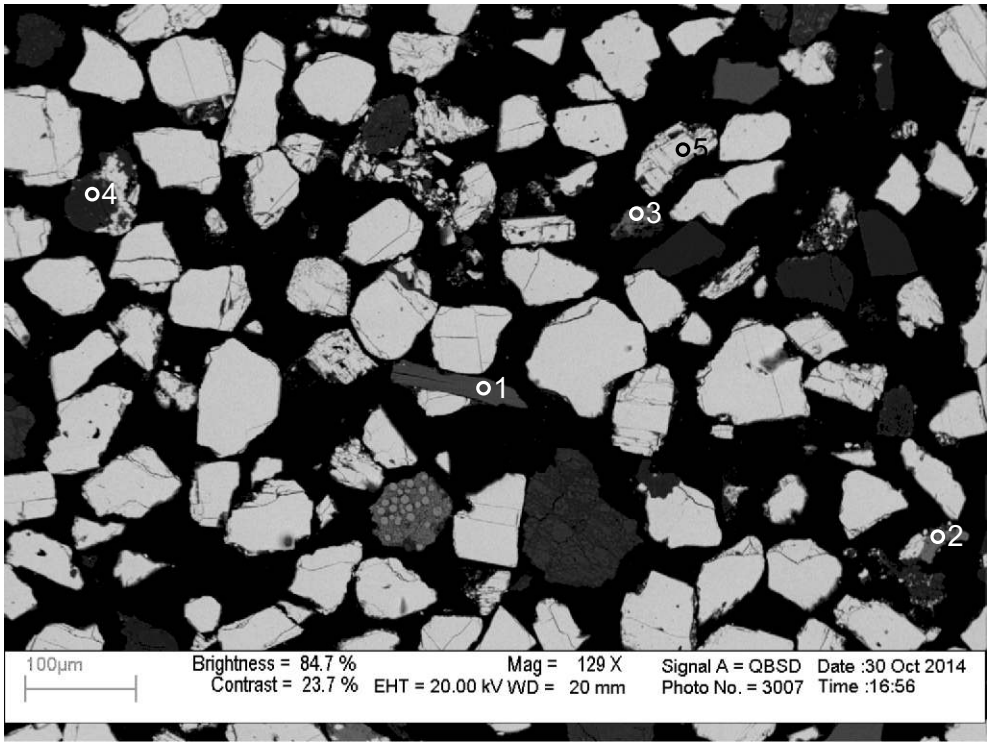

Figure 1-3.3: Sample Newburn 5950m site 4 (SEM).

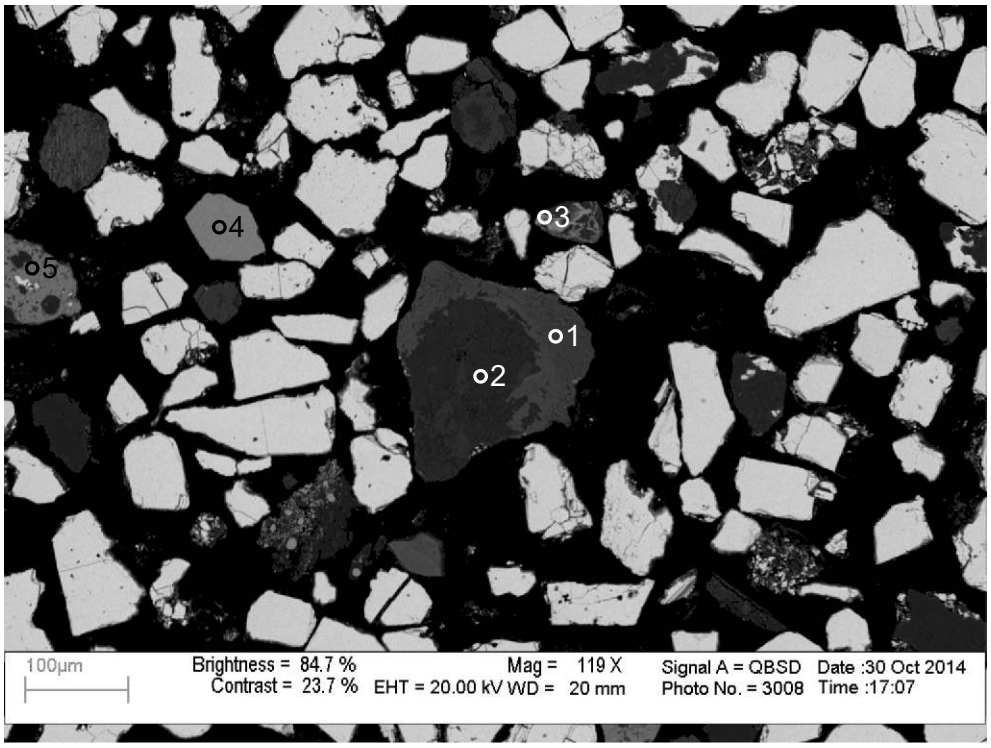

Figure 1-3.4: Sample Newburn 5950m site 5 (SEM).

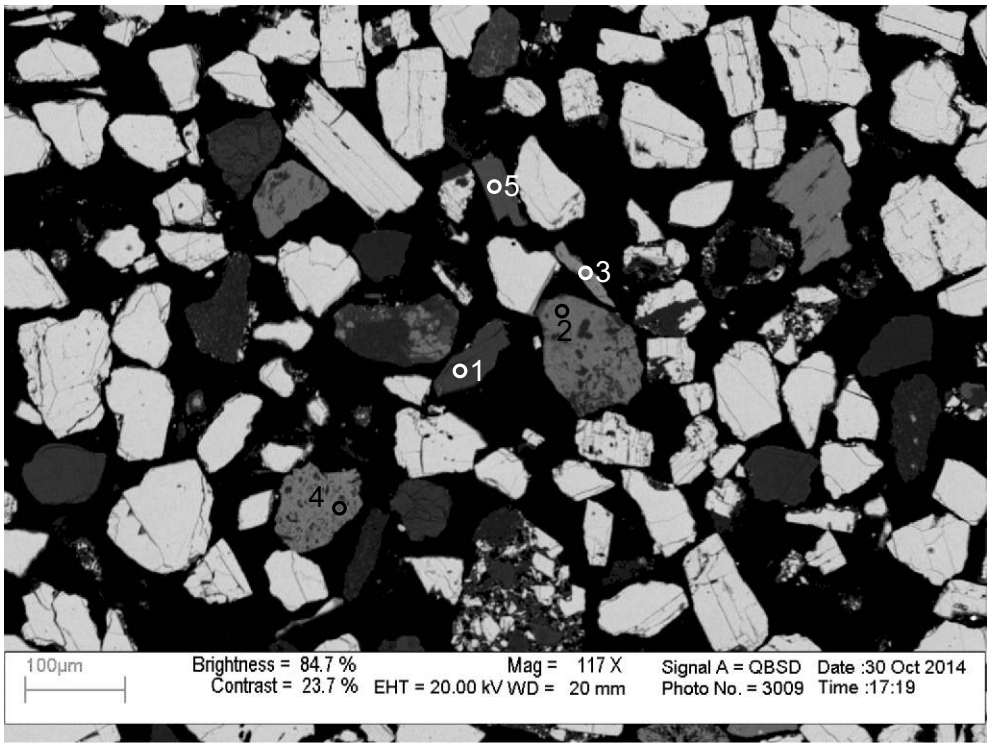

1: Biotite
2: Siderite +Quartz
3: Limonite +Quartz
4: Siderite +Quartz
5: Fluorite

Figure 1-3.5: Sample Newburn 5950m site 6 (SEM).

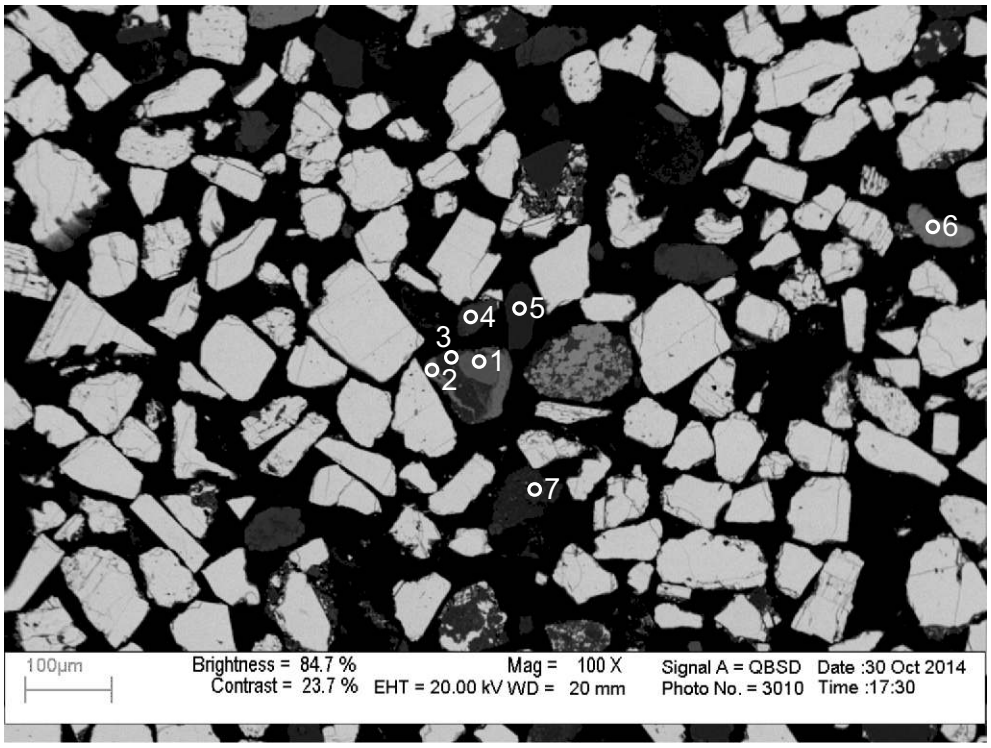

1: Titania
2: Siderite +Quartz
3: Muscovite +Chlorite
4: Chlorite
5: Quartz
6: Limonite +Quartz
7: Calcite +Chlorite

Figure 1-3.6: Sample Newburn 5950m site 7 (SEM).

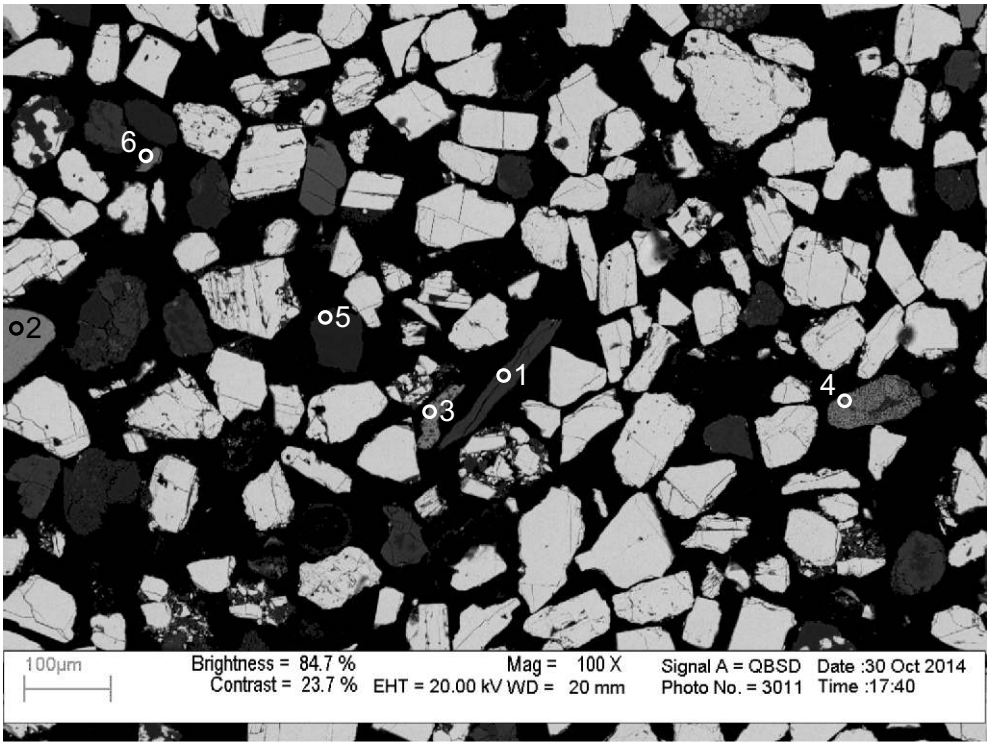

Figure 3.7: Sample Newburn 5950m site 8 (SEM).

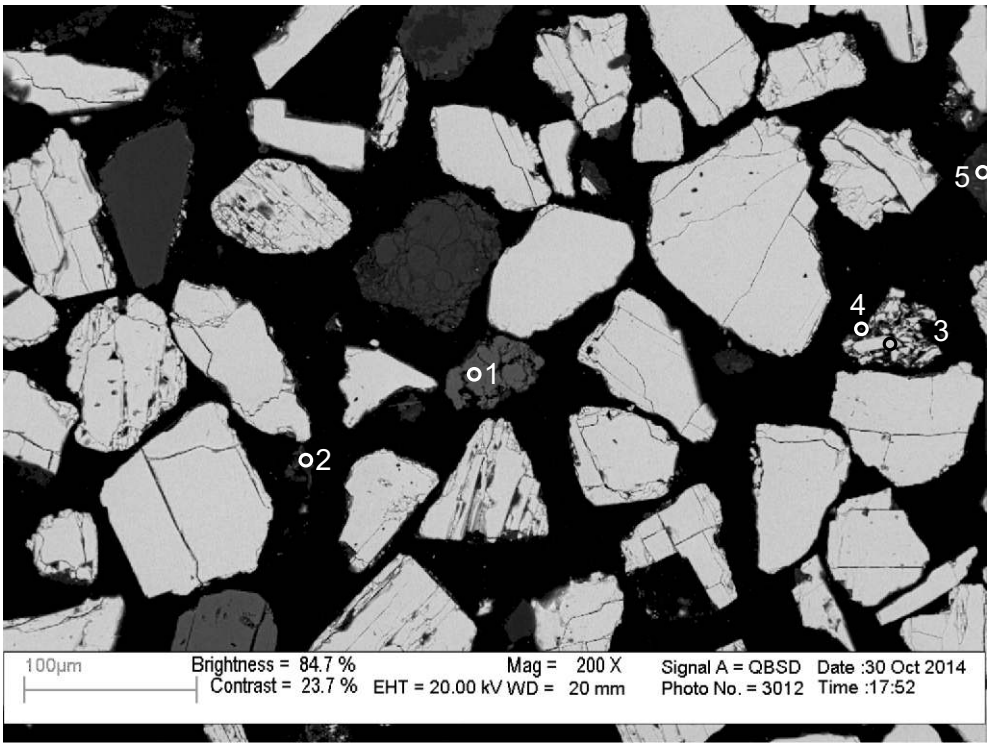

Figure1-3.8: Sample Newburn 5950m site 9 (SEM).

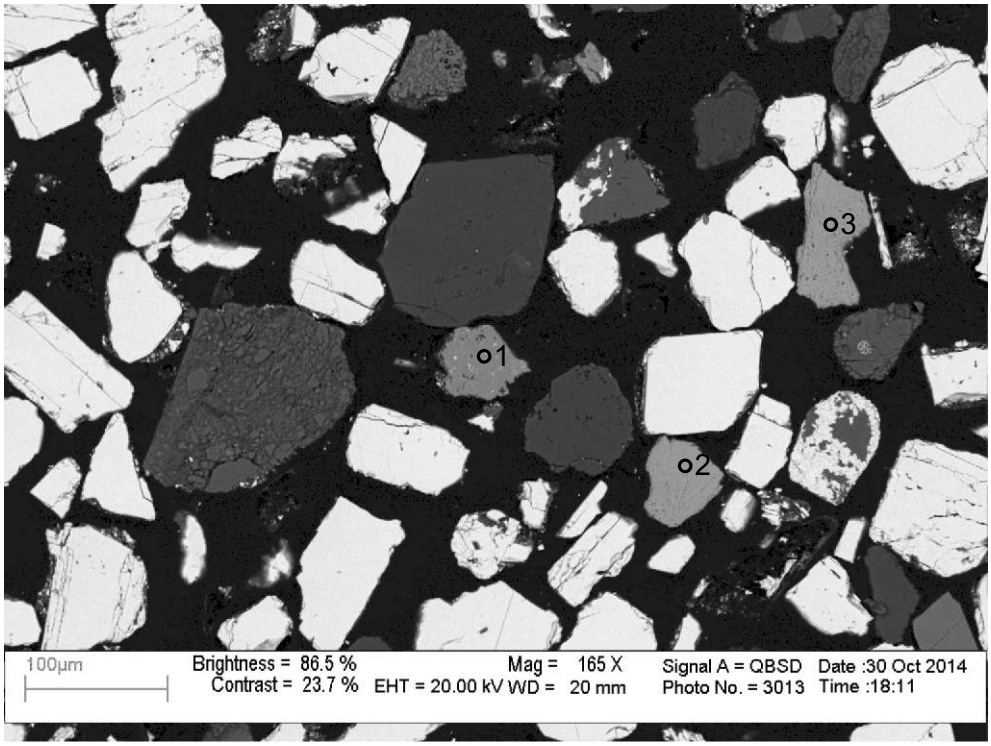

1: Contaminant
2: Limonite
3: Limonite

Figure 1-3.9: Sample Newburn 5950m site 10 (SEM).

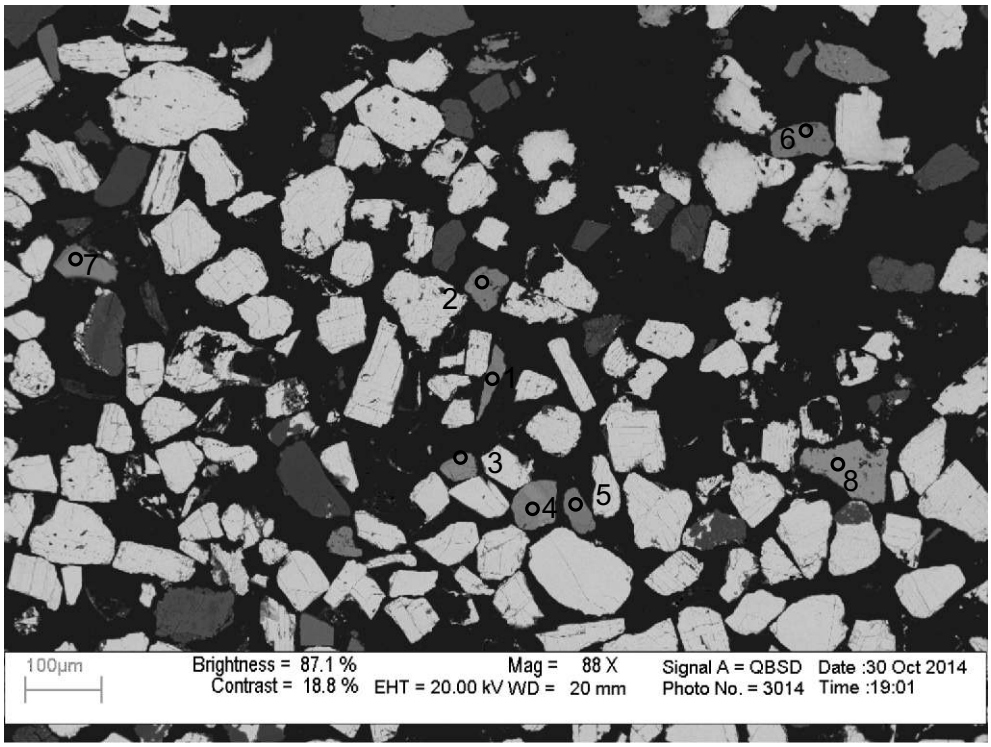

1: Limonite +Other
2: Limonite +Chlorite
3: Limonite +Quartz
4: Limonite +Psilomelane
5: Limonite +Quartz
6: Limonite +Other
7: Limonite +Other
8: Pyrite

Figure 1-3.10: Sample Newburn 5950m site 11 (SEM).

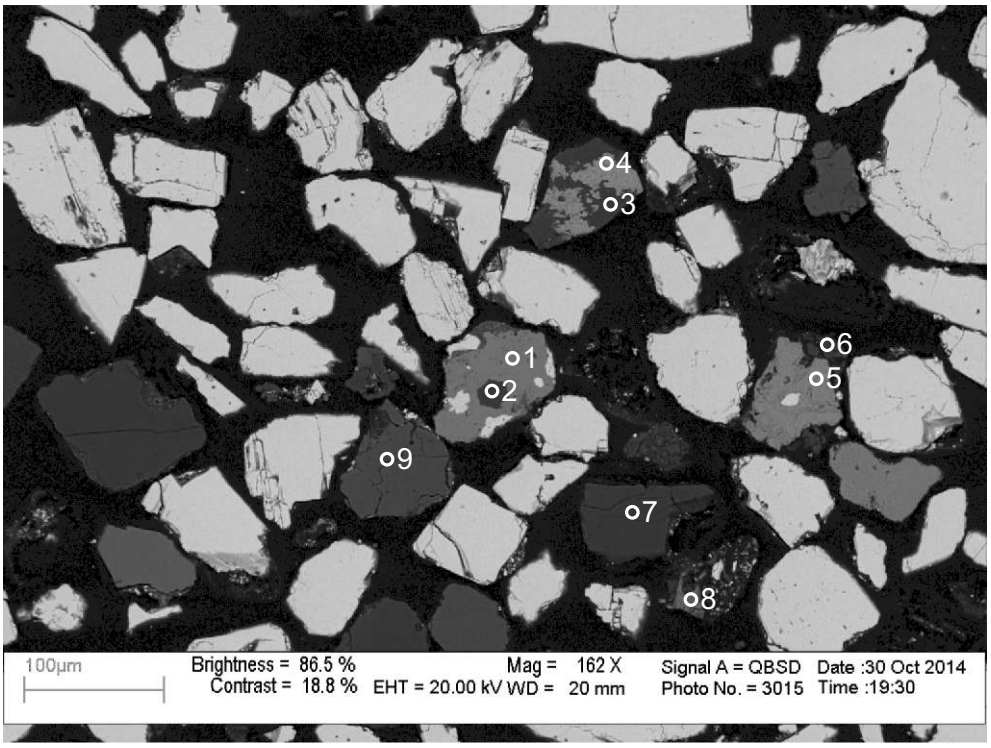

1: Siderite +Chlorite
2: Quartz +Muscovite
3: Quartz
4: Limonite +Chlorite
5: Limonite +Other
6: Quartz
7: Quartz
8: Mix
9: Calcite

Figure 1-3.11: Sample Newburn 5950m site 12 (SEM).

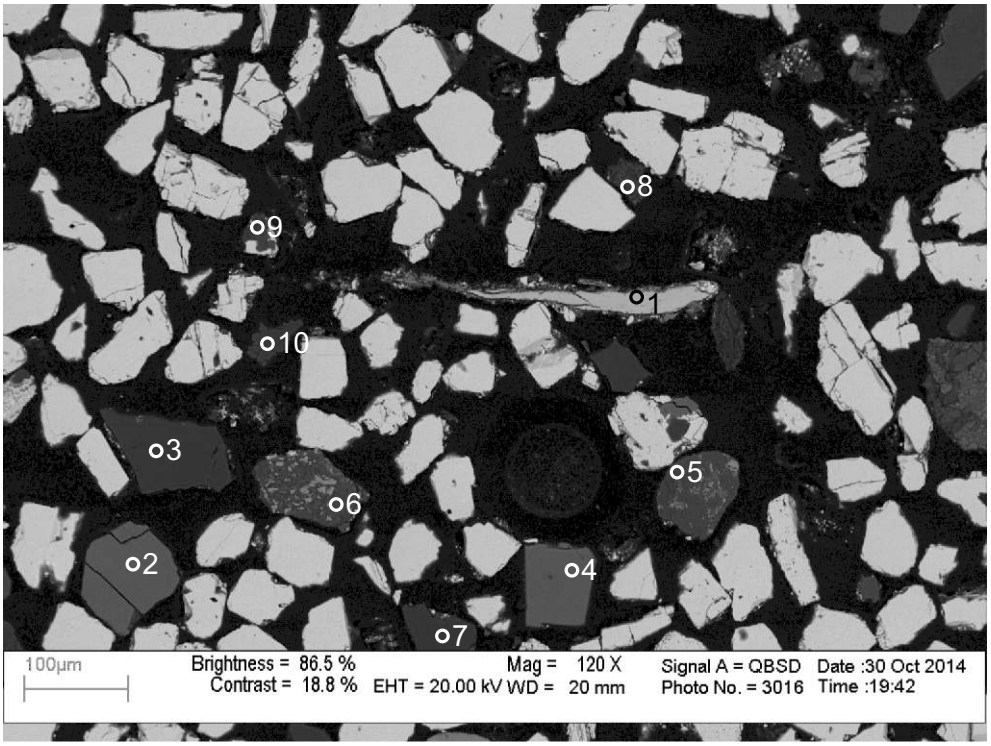

1: Magnetite
2: Fluorite
3: Quartz
4: Fluorite
5: K-feldspar
6: Mix
7: Quartz
8: Mix
9: Quartz +K-feldspar
10: Dolomite

Figure 1-3.12: Sample Newburn 5950m site 13 (SEM).

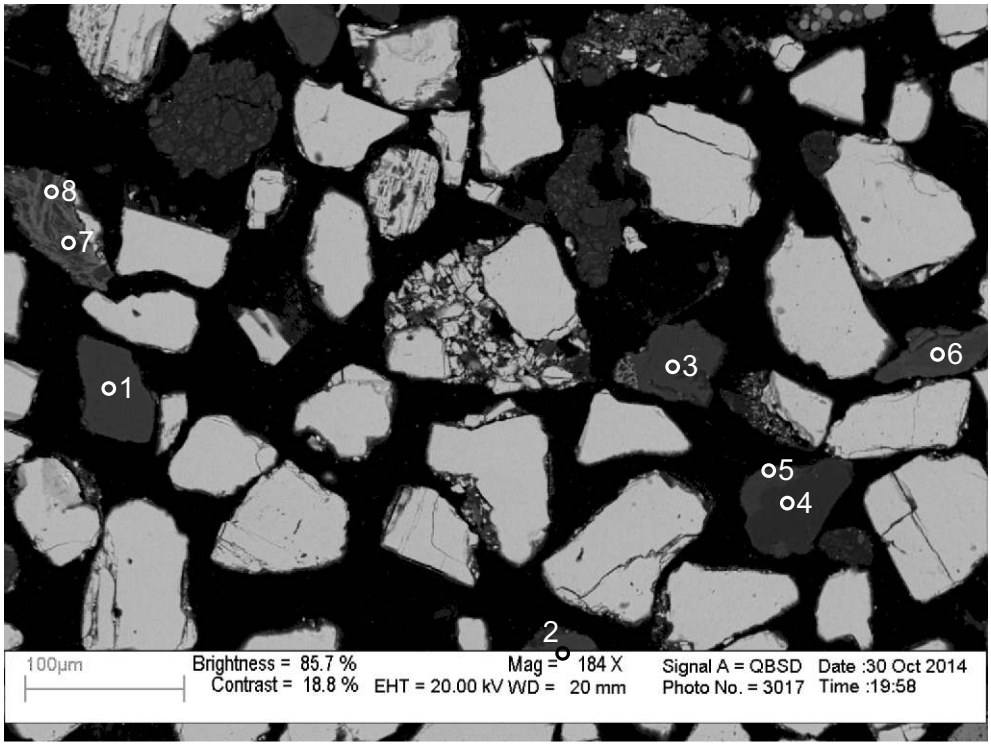

1: Calcite
2: Siderite
3: K-feldspar
4: Quartz
5: K-feldspar
6: Muscovite +Other
7: Quartz
8: Chlorite +Muscovite

Figure 1-3.13: Sample Newburn 5950m site 14 (SEM).

Table 1-3: Scanning Electron Microscope chemical analyses of 5950m from Newburn H-23 well.

Sample	Site	Position	Mineral	SiO_2	TiO_2	Al_2O_3	FeO	MnO	MgO	CaO	Na_2O	K_2O	P_2O_5	SO_3	F	Cl	Cr_2O_3	CoO	CuO	ZnO	As_2O_3	SrO	Sb_2O_3	BaO	WO_3	PbO	Total	Actual Total
H-23 5950m	2	1	Lm+Other	0.83	2.60	1.17	94.76	0.63																			100	86
H-23 5950m	2	2	Chl	25.25		21.11	36.16		2.48																		85	96
H-23 5950m	2	3	Fl							42.40					57.61												100	185
H-23 5950m	2	4	Py	2.97		2.42	28.41		0.60					64.92										0.68			100	173
H-23 5950m	2	5	Fl							42.54					57.46												100	180
H-23 5950m	2	6	Py				27.11							72.89													100	203
H-23 5950m	3	1	Chl	25.75		20.30	35.66		2.33															0.97			85	88
H-23 5950m	3	2	Ps	4.83		9.69	2.68	60.11		1.74		0.72							1.11					14.74		4.37	100	70
H-23 5950m	3	3	Brt											38.58										58.77	2.66		100	106
H-23 5950m	3	4	Brt							0.50				38.26								1.57		59.67			100	108
H-23 5950m	3	5	Brt											39.15										58.94	1.93		100	114
H-23 5950m	4	1	Chl	25.07		20.40	36.97		2.57																		85	93
H-23 5950m	4	2	Qz+Sd	48.80		1.25	49.00	0.56		0.39																	100	101
H-23 5950m	4	3	Py	0.56			28.24			0.20				70.22										0.80			100	179
H-23 5950m	4	4	Qz+Chl	96.54		0.85	1.02		1.61																		100	110
H-23 5950m	4	5	Brt											39.15										60.86			100	119
H-23 5950m	5	1	Act	53.68	1.02	3.15	14.43		13.32	11.40																	97	122
H-23 5950m	5	2	Lbd	59.49		25.36	0.51			6.90	7.74																100	128
H-23 5950m	5	3	Lm+Ms	19.42	3.39	10.15	62.43		0.98			3.64															100	97
H-23 5950m	5	4	Ps+Other					81.12		0.69		1.75												16.45			100	79
H-23 5950m	5	5	Sd+Other	7.25			88.42													4.32							100	76
H-23 5950m	5	6	Mix	32.24	4.92	14.25	16.65	0.44	2.17	23.51				0.92	4.89												100	98
H-23 5950m	6	1	Bt	39.86	2.35	17.76	12.90		13.88			9.24															96	120
H-23 5950m	6	2	Sd+Qz	8.36			90.20			0.46									0.98								100	84
H-23 5950m	6	3	Lm+Qz	2.65			91.16	0.85									5.34										100	98
H-23 5950m	6	4	Sd+Qz	11.81			73.27			0.97									0.95	5.94	3.38					3.72	100	79
H-23 5950m	6	5	Fl							43.50					56.49												100	194
H-23 5950m	7	1	TiO_2		100.00																						100	95
H-23 5950m	7	2	Sd+Qz	8.32		6.93	84.30			0.43																	100	69
H-23 5950m	7	3	Ms+Chl	47.11	3.92	26.40	14.27		1.08			6.54		0.70													100	72
H-23 5950m	7	4	Chl	28.13		21.28	20.68		14.91																		85	95
H-23 5950m	7	5	Qz	99.99																							100	113
H-23 5950m	7	6	Lm+Qz	3.94			95.66			0.39																	100	76
H-23 5950m	7	7	Cal+Chl	9.63		6.48	6.18		1.92	75.78																	100	48
H-23 5950m	8	1	Cal				1.47			54.53																	56	53
H-23 5950m	8	2	Lm				100.00																				100	83
H-23 5950m	8	3	Lm+Other	2.52	2.70	1.66	92.79					0.31															100	92
H-23 5950m	8	4	Py	2.74		2.46	27.29		0.76					66.75													100	224
H-23 5950m	8	5	Qz	99.99																							100	126
H-23 5950m	8	6	Sd+Qz	7.85			91.17			0.98																	100	72
H-23 5950m	9	1	TiO2		100.00																						100	102
H-23 5950m	9	2	Qz+Chl	88.78		2.40	3.25		2.93							2.64											100	9
H-23 5950m	9	3	Brt			0.55								37.28										62.19			100	114

Table 1-3: Scanning Electron Microscope chemical analyses of 5950m from Newburn H-23 well.

Sample	Site	Position	Mineral	SiO_2	TiO_2	Al_2O_3	FeO	MnO	MgO	CaO	Na_2O	K_2O	P_2O_5	SO_3	F	Cl	Cr_2O_3	CoO	CuO	ZnO	As_2O_3	SrO	Sb_2O_3	BaO	WO_3	PbO	Total	Actual Total
H-23 5950m	9	4	Brt+Other	44.86		2.63	0.93			0.77		0.55		18.85	4.00									27.39			100	68
H-23 5950m	9	5	Ms	51.62	0.92	26.94	3.59		2.15			9.78															95	117
H-23 5950m	10	1	Contaminant						4.97	1.19										93.84							100	62
H-23 5950m	10	2	Lm				100.00																				100	91
H-23 5950m	10	3	Lm	0.96			97.58														1.44						100	92
H-23 5950m	11	1	Lm+Lm+Other	7.06			89.63			0.78			1.44							1.08							100	74
H-23 5950m	11	2	Lm+Lm+Chl	4.92		1.00	93.10	0.97																			100	75
H-23 5950m	11	3	Lm+Qz	2.37			95.86																1.77				100	83
H-23 5950m	11	4	Lm+Ps	2.10			76.62	15.85		0.78						0.33								4.32			100	76
H-23 5950m	11	5	Lm+Lm+Qz	7.64			91.58			0.78																	100	76
H-23 5950m	11	6	Lm+Lm+Other	8.06			88.97	0.62		1.15			1.19														100	72
H-23 5950m	11	7	Lm+Other	17.09		0.94	67.15			5.82						0.85				1.49						6.67	100	76
H-23 5950m	11	8	Py				27.13							72.86													100	247
H-23 5950m	12	1	Sd+Chl	5.71		1.04	92.12	0.77		0.36																	100	88
H-23 5950m	12	2	Qz+Ms	93.93		3.70	1.13					1.23															100	138
H-23 5950m	12	3	Qz	98.57		0.85	0.27					0.30															100	143
H-23 5950m	12	4	Lm+Chl	4.49	0.58	1.72	93.22																				100	102
H-23 5950m	12	5	Lm+Other	4.83			87.89			1.27						0.62				5.35							100	95
H-23 5950m	12	6	Qz	99.99																							100	144
H-23 5950m	12	7	Qz	99.99																							100	142
H-23 5950m	12	8	Mix	8.58	2.45	23.11	15.75	0.50	3.96	45.66																	100	123
H-23 5950m	12	9	Cal							56.00																	56	58
H-23 5950m	13	1	Mag	0.58			97.49	0.63									1.32										100	158
H-23 5950m	13	2	Fl							43.89					56.11												100	191
H-23 5950m	13	3	Qz	99.99																							100	133
H-23 5950m	13	4	Fl							44.51					55.49												100	199
H-23 5950m	13	5	Kfs	66.81		17.72						15.47															100	139
H-23 5950m	13	6	Mix	48.47		22.66	15.01		2.47			8.44		1.20										1.73			100	114
H-23 5950m	13	7	Qz	97.53		1.53						0.63				0.32											100	136
H-23 5950m	13	8	Mix	61.93	0.70	15.61	4.99		1.96	5.19	1.16	2.19		1.65	1.96									2.68			100	128
H-23 5950m	13	9	Qz+Kfs	85.40		7.46	0.32				0.36	6.46															100	132
H-23 5950m	13	10	Dol						23.57	30.43																	54	62
H-23 5950m	14	1	Cal						0.92	55.08																	56	62
H-23 5950m	14	2	Sd				15.86	0.41	10.85	28.87																	56	69
H-23 5950m	14	3	Kfs	66.74		17.84						15.41															100	137
H-23 5950m	14	4	Qz	99.99																							100	146
H-23 5950m	14	5	Kfs	67.13		17.78						15.10															100	141
H-23 5950m	14	6	Ms+Other	47.90	0.60	33.65	0.63		1.82		0.55	9.08			1.33									4.43			100	131
H-23 5950m	14	7	Qz	98.49		0.85	0.41					0.24															100	133
H-23 5950m	14	8	Chl+Ms	49.76		14.53	31.66		0.48			3.55															100	103

Appendix 1-4: SEM-BSE images and EDS mineral analyses for sample 5965m.

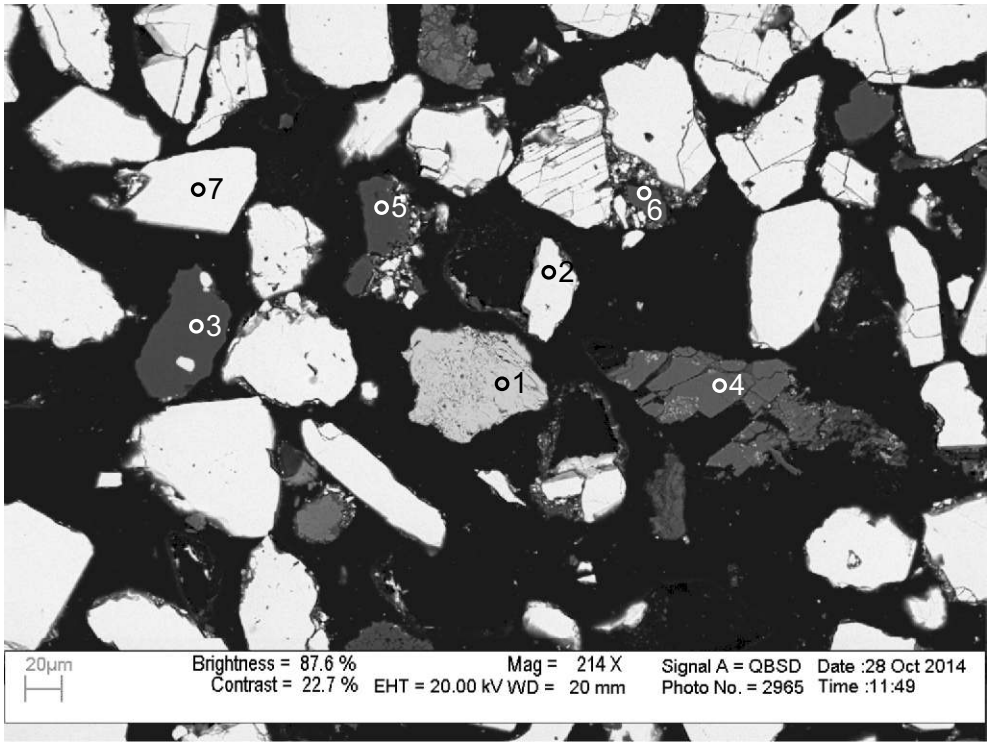

Figure 1-4.1: Sample Newburn 5965m site 2 (SEM).

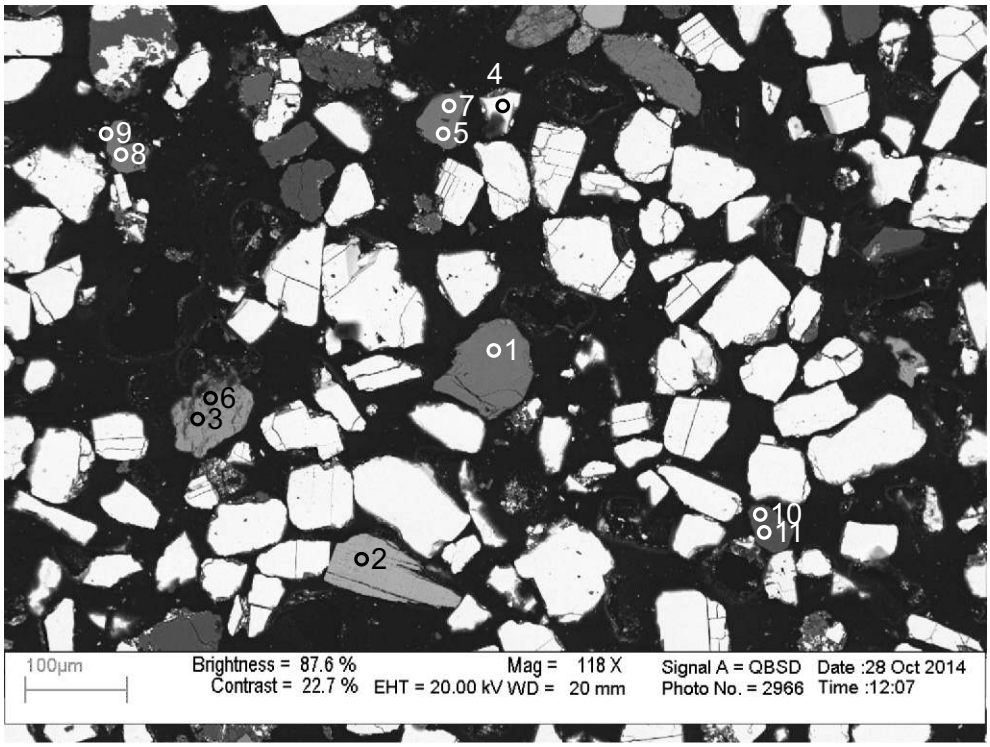

Figure 1-4.2: Sample Newburn 5965m site 3 (SEM).

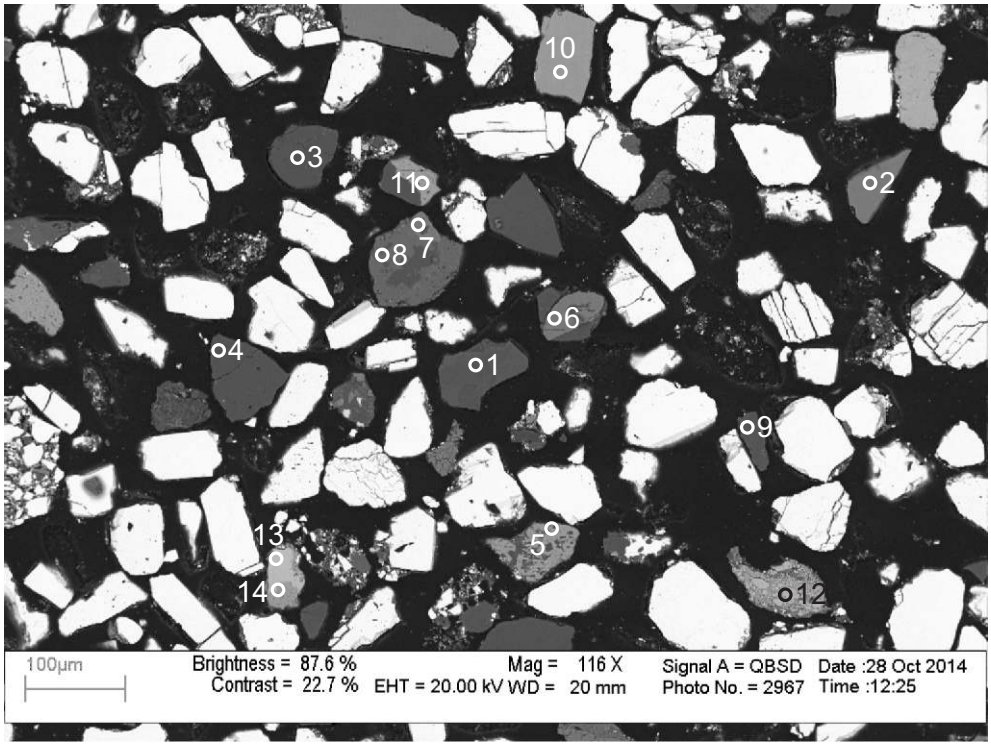

1: Tourmaline
2: Fluorite
3: Quartz
4: Quartz
5: Ilmenite
6: Siderite
7: Siderite +Quartz
8: Ankerite
9: Dolomite
10: Limonite +Quartz
11: Limonite +Other
12: Pyrite
13: Psilomelane
14: Limonite +Quartz

Figure 1-4.3: Sample Newburn 5965m site 4 (SEM).

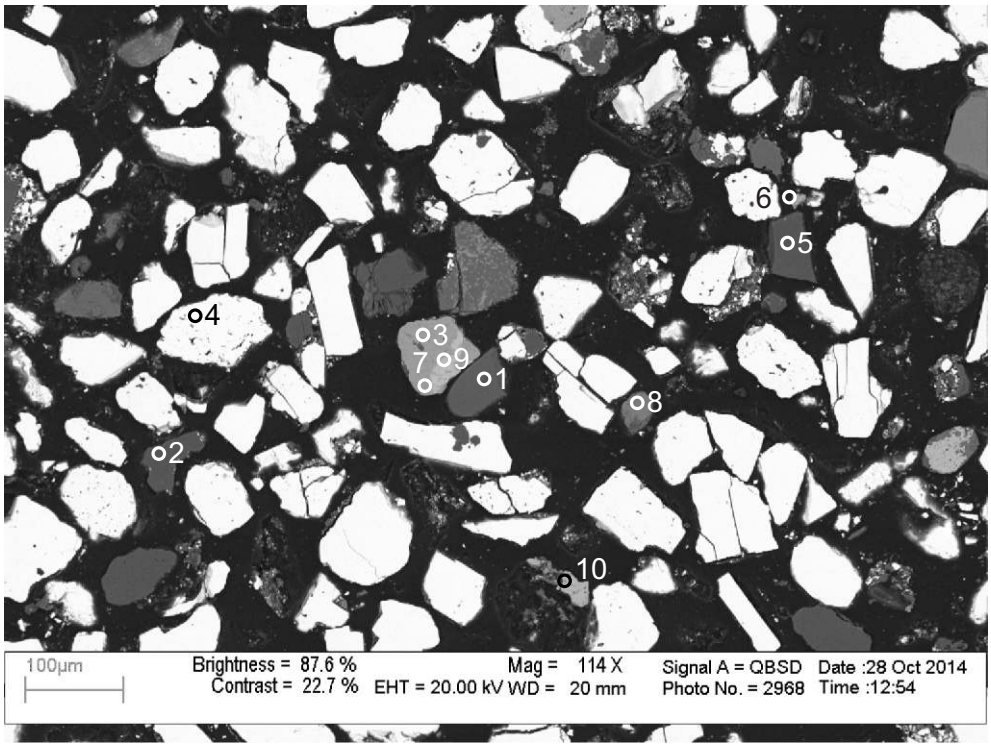

1: Quartz +Others
2: Quartz
3: Siderite +Other
4: Barite
5: Quartz
6: Limonite +Other
7: Limonite +Quartz
8: Siderite
9: Psilomelane +Siderite
10: Pyrite

Figure 1-4.4: Sample Newburn 5965m site 5 (SEM).

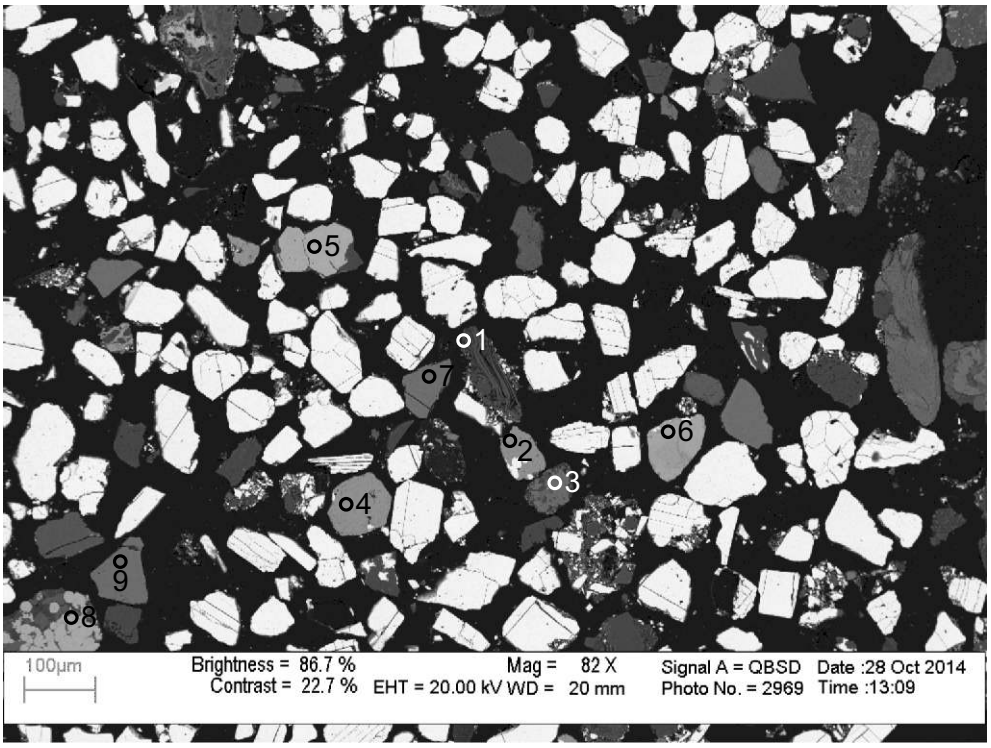

1: Albite
2: Limonite +Other
3: Siderite
4: Limonite +Other
5: Pyrite
6: Psilomelane
7: Fluorite
8: Pyrite+Other
9: Fluorite

Figure 1-4.5: Sample Newburn 5965m site 6 (SEM).

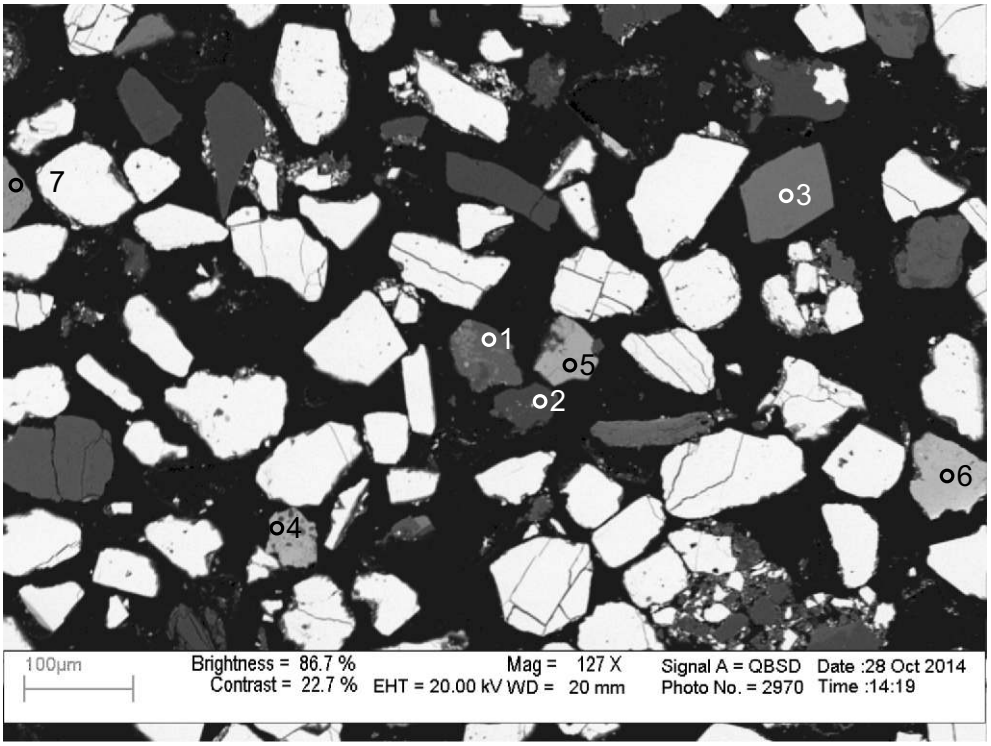

1: Chlorite
2: Quartz
3: Fluorite
4: Psilomelane +Muscovite +Other
5: Pyrite
6: Pyrite+Other
7: Limonite +Quartz

Figure 1-4.6: Sample Newburn 5965m site 7 (SEM).

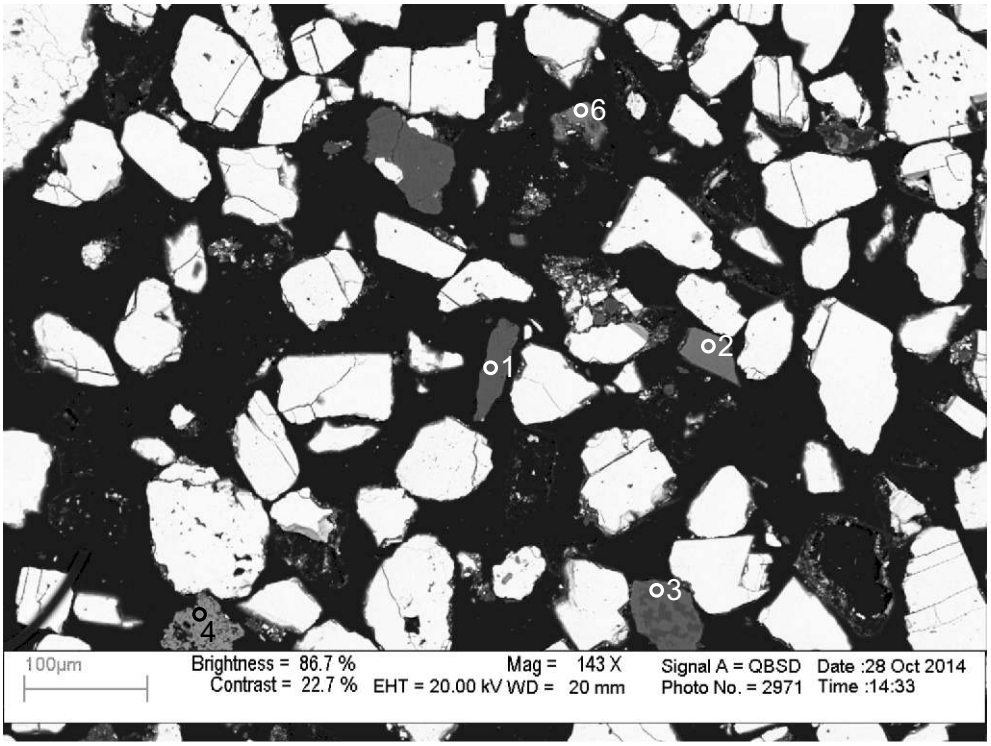

Figure 1-4.7: Sample Newburn 5965m site 8 (SEM).

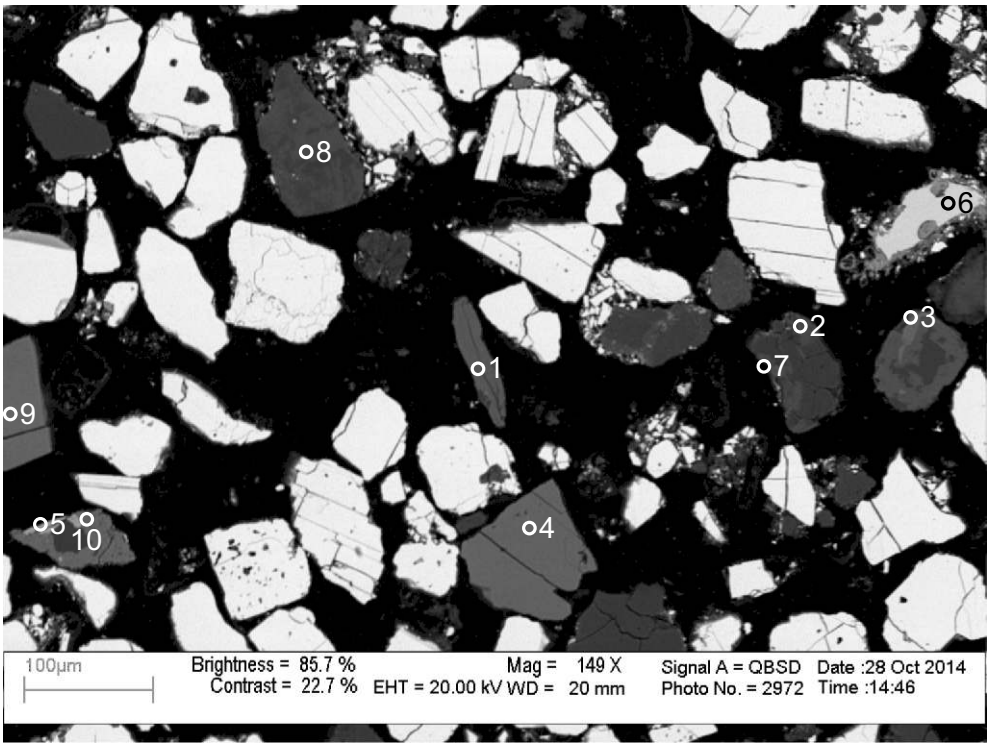

Figure 1-4.8: Sample Newburn 5965m site 9 (SEM).

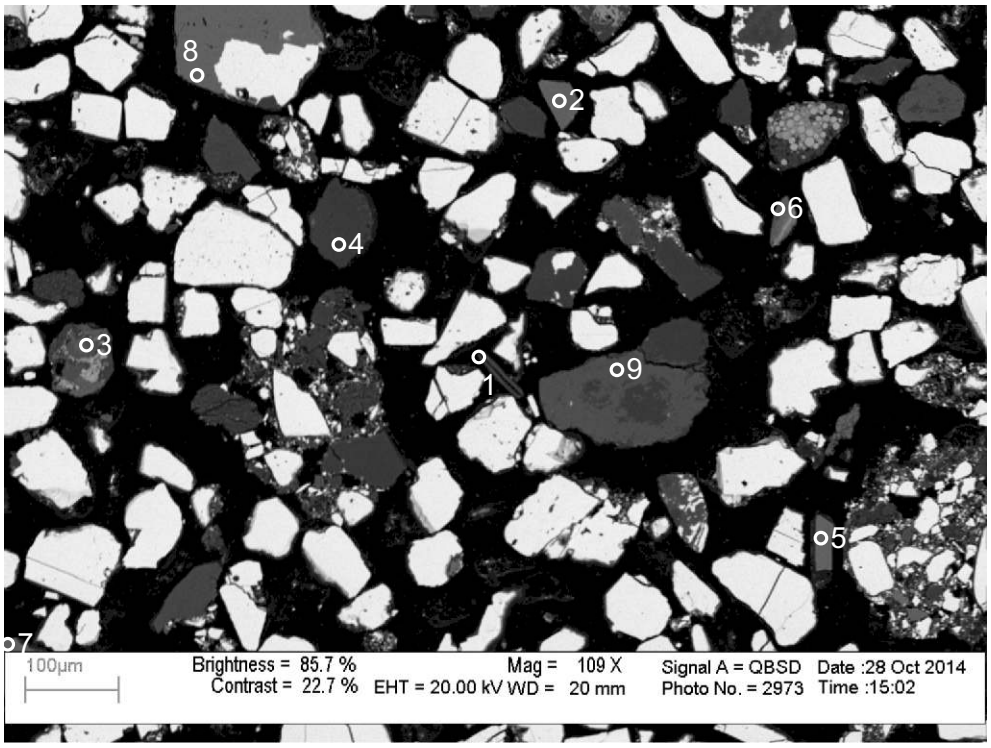

1: Albite
+Muscovite
2: Fluorite
3: Fe-Calcite
4: Quartz
5: Fluorite
6: Siderite
+Apatite
+Albite
7: Fluorite
8: Fluorite
9: Ankerite

Figure 1-4.9: Sample Newburn 5965m site 10 (SEM).

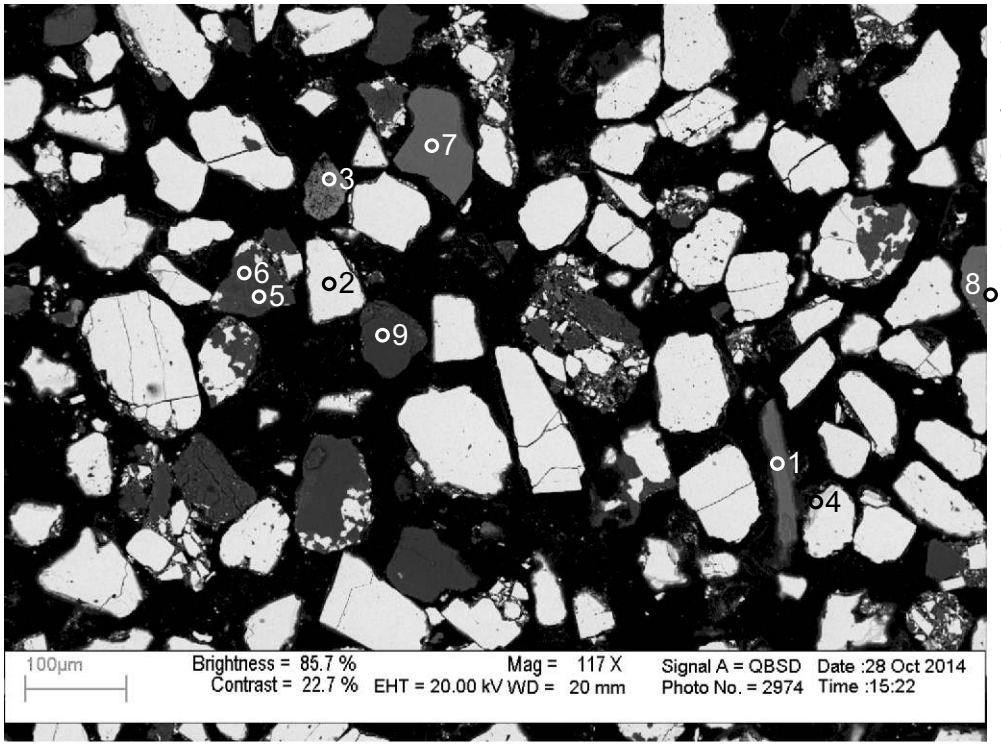

1: Fluorite
2: Barite
3: Limonite
+Other
4: Barite
5: K-feldspar
6: Quartz
+K-feldspar
7: Fluorite
8: Siderite
9: Quartz

Figure 1-4.10: Sample Newburn 5965m site 11 (SEM).

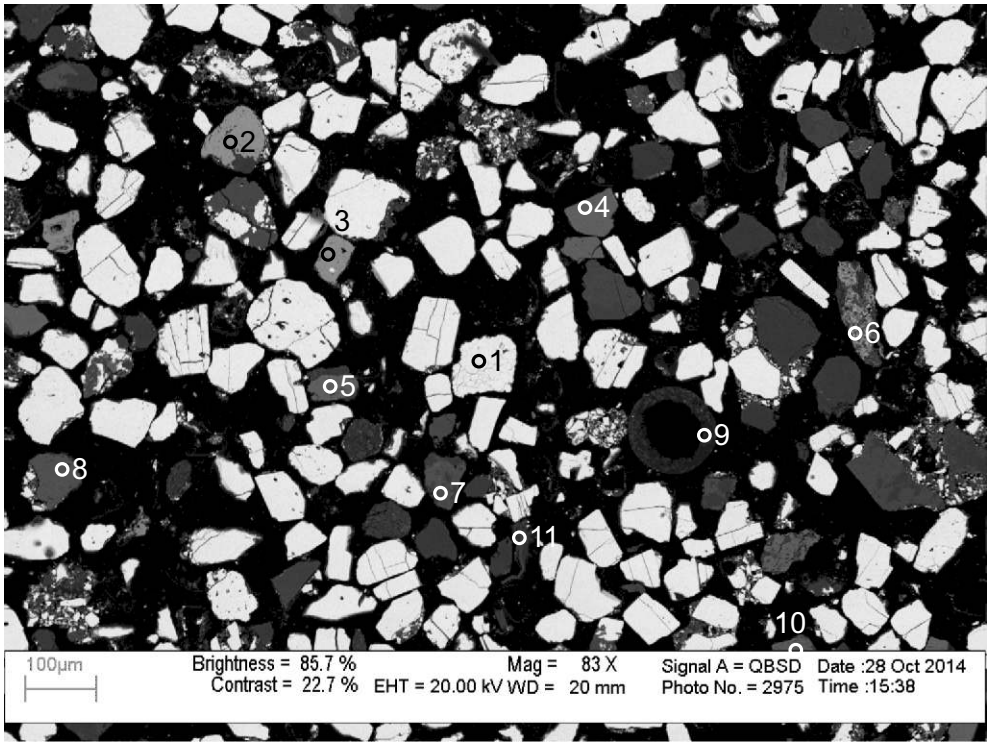

1: Barite
2: Limonite +Chlorite
3: Limonite +Other
4: Fluorite
5: Siderite
6: Pyrite+Other
7: Ankerite +Quartz
8: Andalusite +Other
9: Barite+Other
10: Chlorite
11: Muscovite

Figure 1-4.11: Sample Newburn 5965m site 12 (SEM).

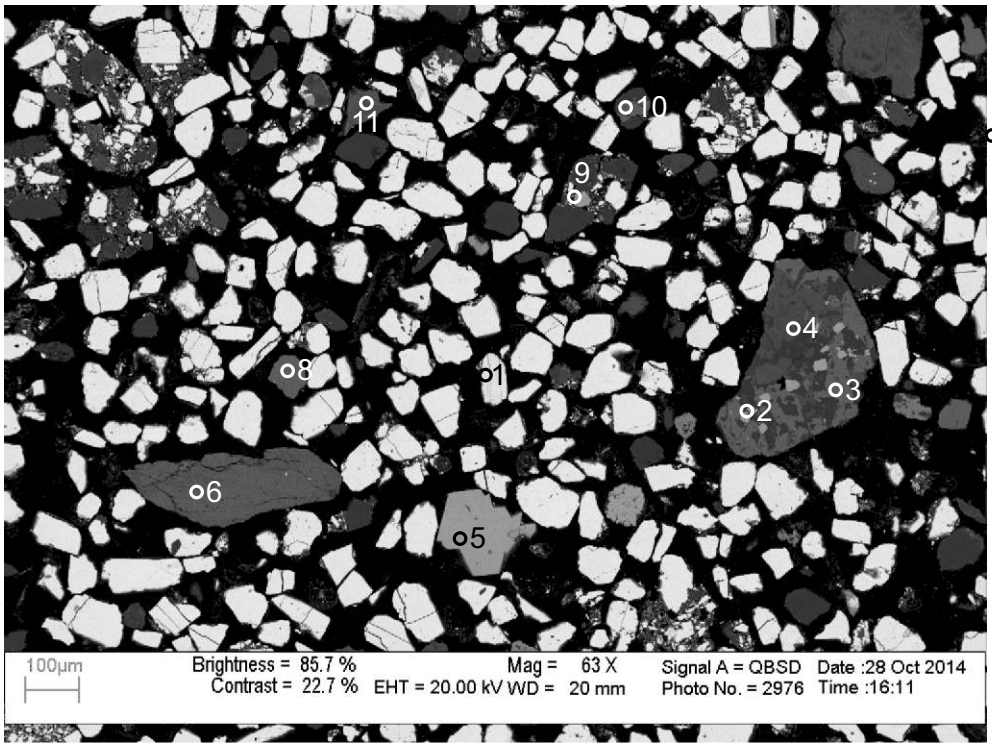

1: Barite
2: Pyrite
3: Siderite
4: Ankerite +Albite
5: Fluorite
6: Siderite +Albite +Apatite
7: Siderite +Albite
8: Fluorapatite
9: Pyrite
10: Siderite
11: Siderite +Other

Figure1-4.12: Sample Newburn 5965m site 13 (SEM).

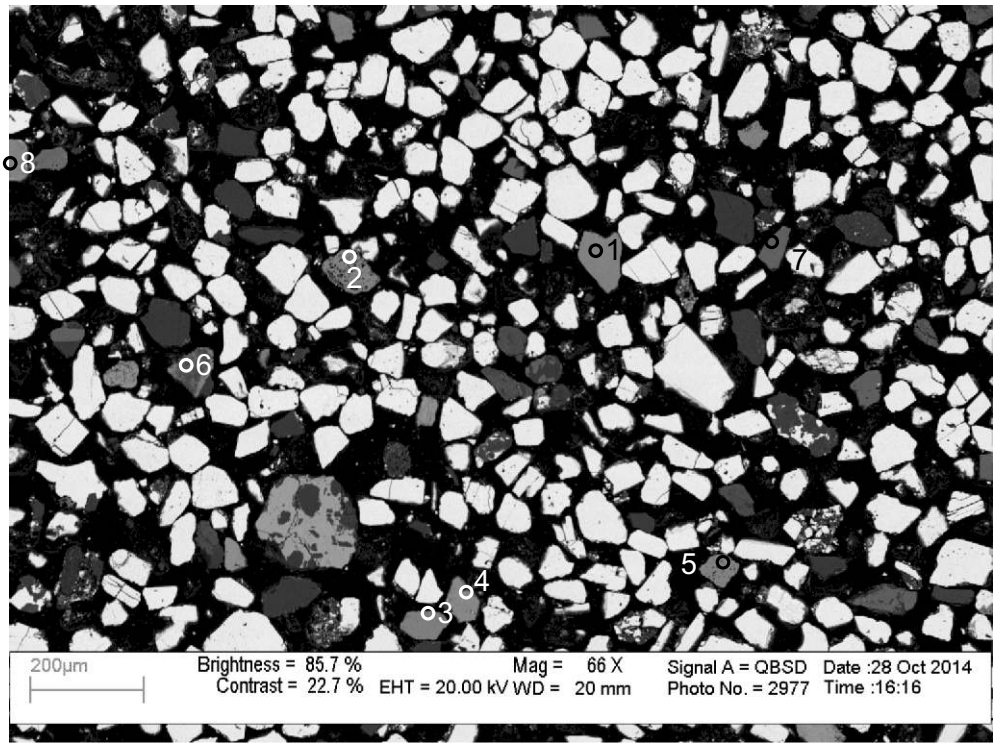

1: Limonite +Quartz
2: Limonite +Apatite +Other
3: Limonite +Apatite +Other
4: Limonite +Apatite +Other
5: Limonite +Quartz
6: Muscovite +Hem
7: Fluorite
8: Cuprite +Limonite +Other

Figure 1-4.13: Sample Newburn 5965m site 14 (SEM).

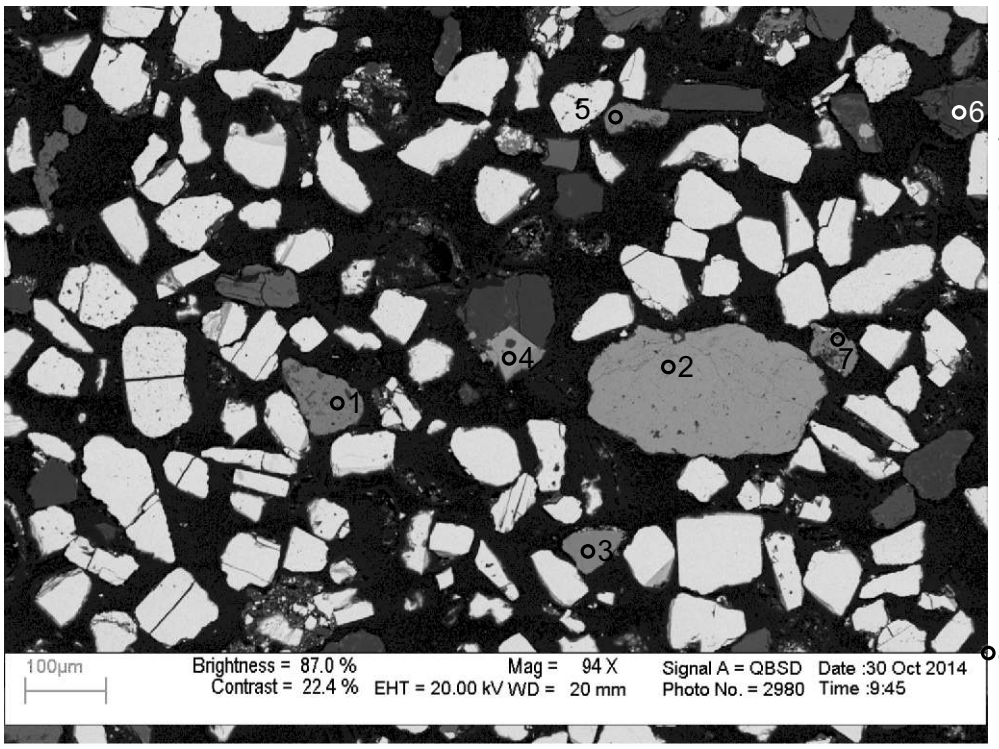

1: Limonite +Other
2: Fluorite
3: Limonite +Quartz
4: Fluorite
5: Limonite +Quartz
6: Albite
7: Siderite +Chlorite
8: Siderite +Quartz

Figure 1-4.14: Sample Newburn 5965m site 15 (SEM).

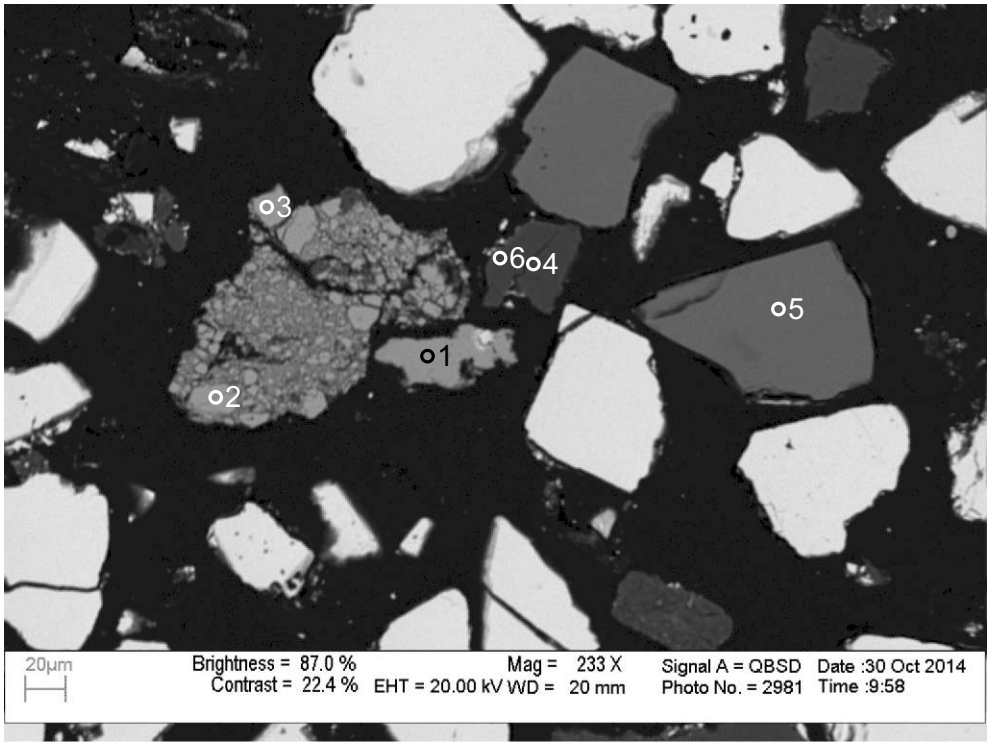

Figure 1-4.15: Sample Newburn 5965m site 16 (SEM).

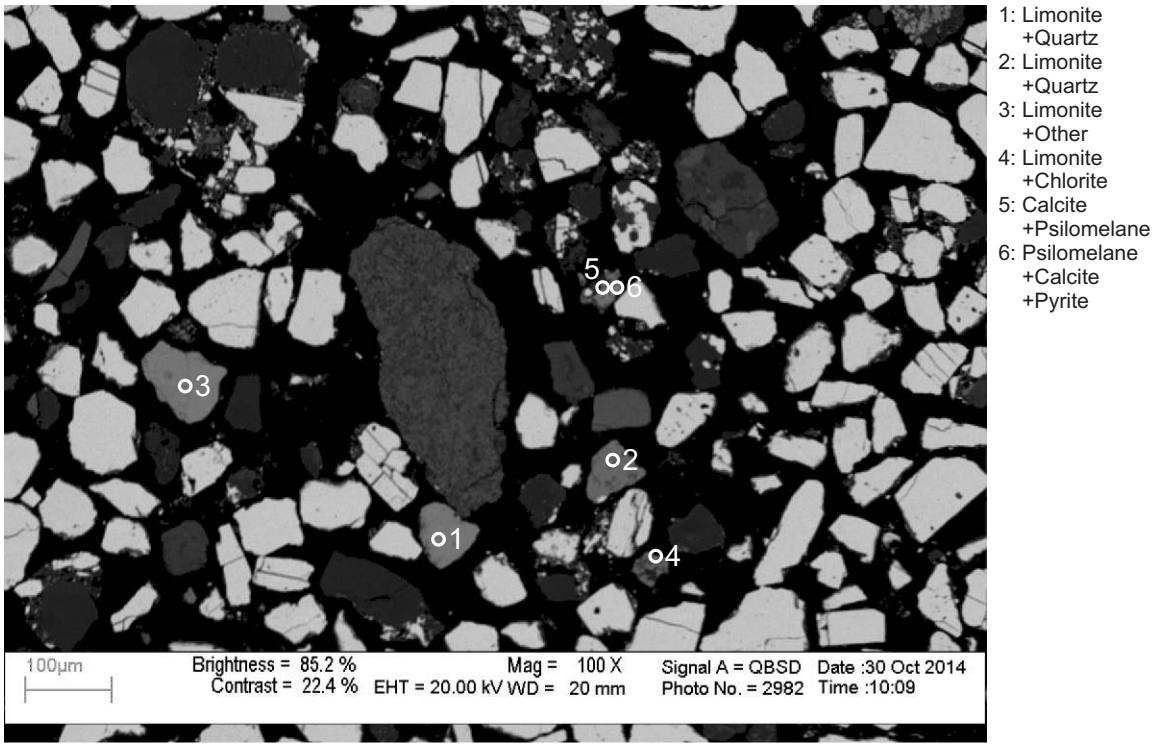

Figure 1-4.16: Sample Newburn 5965m site 17 (SEM).

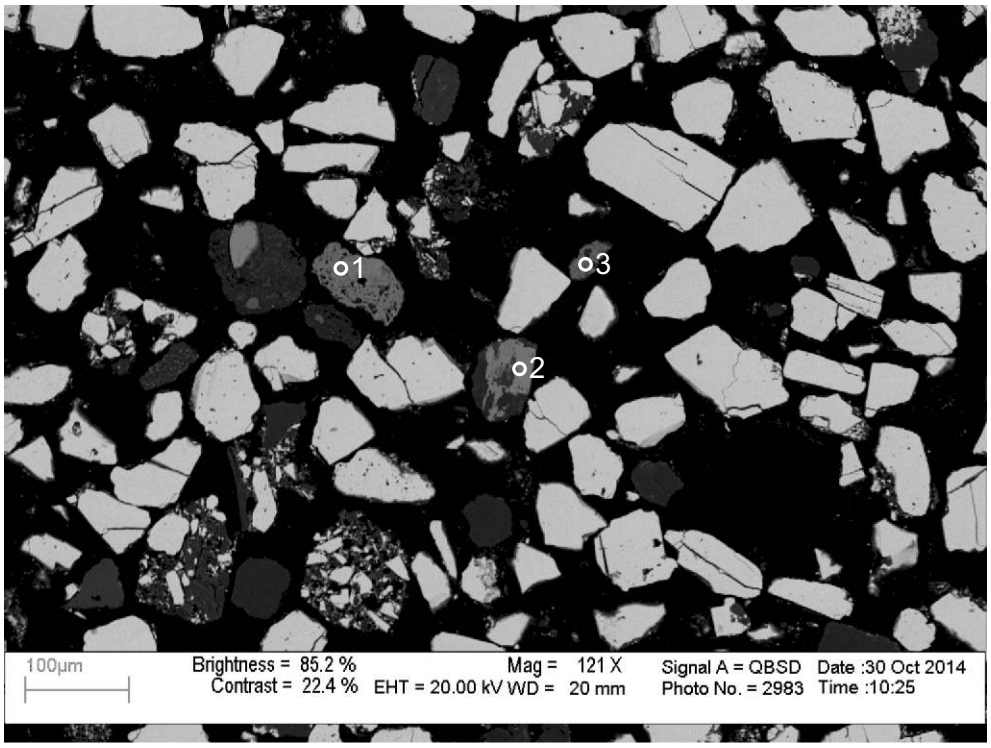

1: Limonite +Other
2: Limonite +Other
3: Limonite +Muscovite

Figure 1-4.17: Sample Newburn 5965m site 18 (SEM).

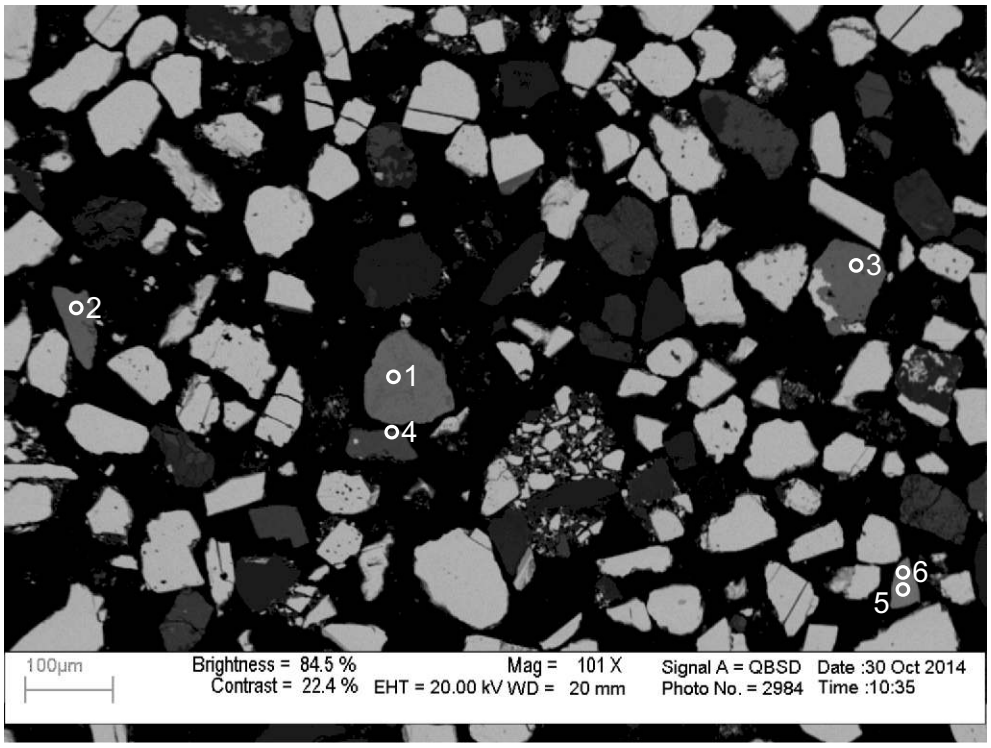

1: Limonite +Quartz
2: Limonite +Other
3: Limonite +Other
4: Limonite +Calcite
5: Psilomelane
6: Psilomelane

Figure 1-4.18: Sample Newburn 5965m site 19 (SEM).

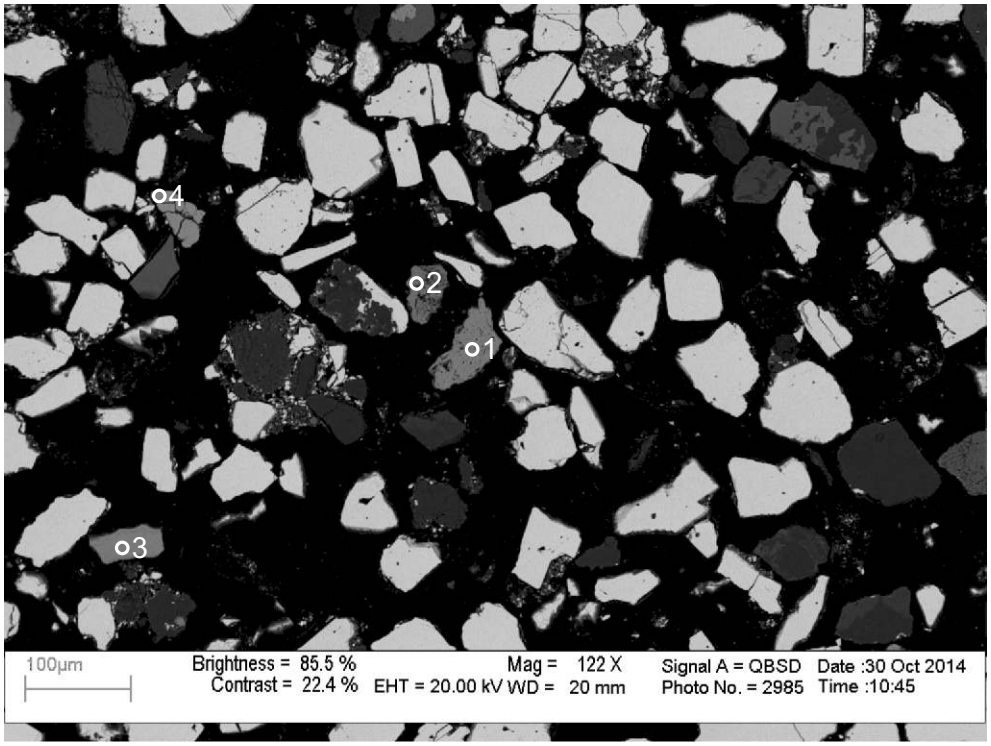

1: Limonite +Quartz
2: Limonite +Quartz
3: Limonite +Quartz
4: Pyrite

Figure 1-4.19: Sample Newburn 5965m site 20 (SEM).

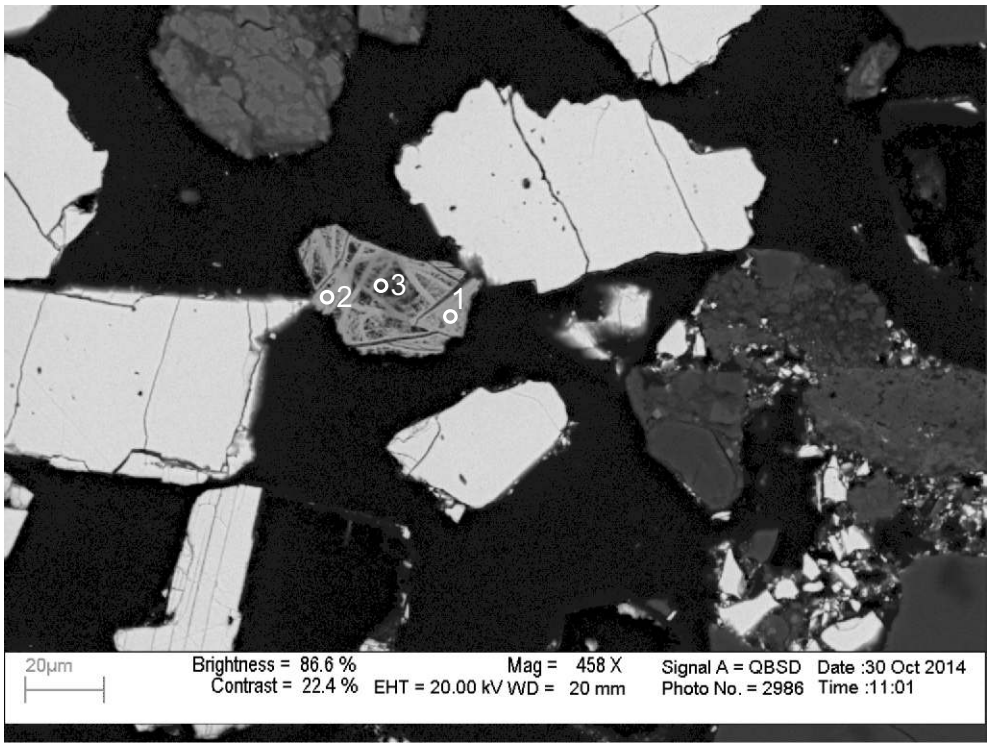

1: Psilomelane
2: Psilomelane
3: Psilomelane

Figure 1-4.20: Sample Newburn 5965m site 21 (SEM).

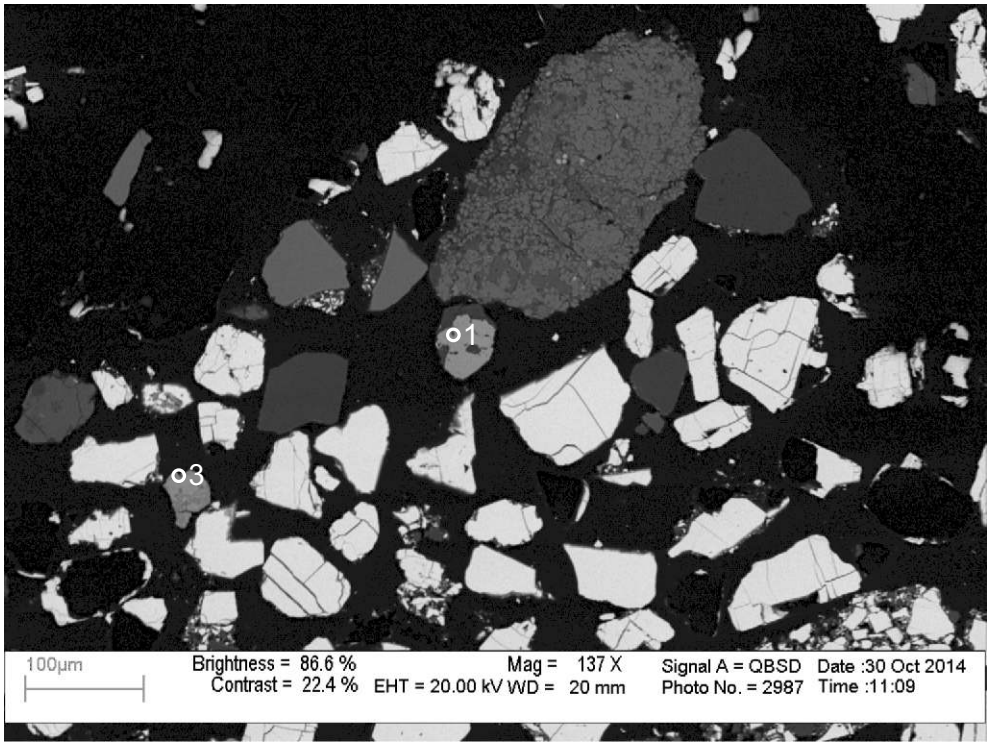

Figure 1-4.21: Sample Newburn 5965m site 22 (SEM).

Table 1-4: Scanning Electron Microscope chemical analyses of sample 5965m from Newburn H-23 well.

Sample	Site	Position	Mineral	SiO_2	TiO_2	Al_2O_3	FeO	MnO	MgO	CaO	Na_2O	K_2O	P_2O_5	SO_3	F	Cl	Cr_2O_3	CoO	NiO	CuO	ZnO	As_2O_3	SrO	Sb_2O_3	BaO	Ce_2O_3	WO_3	PbO	Total	Actual Total
H-23 5965m	2	1	Cv											53.19						46.82									100	192
H-23 5965m	2	2	Brt											38.08				-0.10					1.94		60.11				100	119
H-23 5965m	2	3	Qz	99.99																									100	121
H-23 5965m	2	4	Ank				15.64	1.00	9.09	30.28																			56	60
H-23 5965m	2	5	Qz	99.11		0.89																							100	123
H-23 5965m	2	6	Dol				5.58	1.11	19.38	27.93																			54	59
H-23 5965m	2	7	Brt											37.61				0.11					1.17		61.11				100	114
H-23 5965m	3	1	Chl	26.81		19.09	32.36		6.74																				85	102
H-23 5965m	3	2	Lm				92.94															7.06							100	82
H-23 5965m	3	3	Lm+Ms+Other	20.84		14.38	60.39		0.78	0.74		2.88																	100	85
H-23 5965m	3	4	Brt											37.91				0.08					1.60		60.42				100	118
H-23 5965m	3	5	Fl							44.10					55.89														100	178
H-23 5965m	3	6	Lm+Ms	8.79		6.08	83.42			0.70		1.00																	100	76
H-23 5965m	3	7	Fl							43.85					56.16														100	178
H-23 5965m	3	8	Fl							44.51					55.50														100	166
H-23 5965m	3	9	Fl							43.61					56.39														100	169
H-23 5965m	3	10	Qz	99.43		0.57																							100	125
H-23 5965m	3	11	Qz	99.99																									100	126
H-23 5965m	4	1	Tur	38.48	0.72	33.07	4.33		7.60	0.77	2.02																		87	110
H-23 5965m	4	2	Fl							43.86					56.13														100	197
H-23 5965m	4	3	Qz	99.99																									100	126
H-23 5965m	4	4	Qz	99.99																									100	123
H-23 5965m	4	5	Ilm		62.70		35.76	1.52																					100	100
H-23 5965m	4	6	Sd				44.68	1.57	8.57	1.18																			56	64
H-23 5965m	4	7	Sd+Qz	1.65			79.20	2.66	14.49	2.01																			100	63
H-23 5965m	4	8	Ank				15.42	1.08	9.72	29.78																			56	61
H-23 5965m	4	9	Dol				0.43		22.62	30.73						0.22													54	59
H-23 5965m	4	10	Lm+Qz	7.25			90.18	0.58		0.69												1.29							100	81
H-23 5965m	4	11	Lm+Other	8.43		1.42	81.29			0.66											8.20								100	82
H-23 5965m	4	12	Py				27.60							72.41															100	251
H-23 5965m	4	13	Ps					76.64		0.66															22.69				100	81
H-23 5965m	4	14	Lm+Qz	5.88			91.37	1.60																	1.16				100	76
H-23 5965m	5	1	Qz+Others	96.93		2.44	0.64																						100	129
H-23 5965m	5	2	Qz	99.13		0.87																							100	122
H-23 5965m	5	3	Sd+Other	4.62		0.93	88.65	3.83		1.44						0.52													100	81
H-23 5965m	5	4	Brt											37.71				0.05					1.57		60.68				100	117
H-23 5965m	5	5	Qz	99.99																									100	137
H-23 5965m	5	6	Lm+Other	5.09		3.10	90.17																		1.64				100	86
H-23 5965m	5	7	Lm+Qz	4.04			91.67	3.78		0.50																			100	79
H-23 5965m	5	8	Sd				44.42	1.67	8.64	1.28																			56	65
H-23 5965m	5	9	Ps+Sd				9.62	68.62		0.83										0.96					19.97				100	87
H-23 5965m	5	10	Py				27.72			0.18				72.12															100	230
H-23 5965m	6	1	Ab	68.41		18.99	0.32				12.27																		100	130
H-23 5965m	6	2	Lm+Other	2.87		0.79	95.33	0.56		0.46																			100	78
H-23 5965m	6	3	Sd				43.05	1.73	9.41	1.81																			56	61
H-23 5965m	6	4	Lm+Other	2.08		1.13	95.69			0.45											0.65								100	74
H-23 5965m	6	5	Py				27.65							72.37															100	228
H-23 5965m	6	6	Ps					84.43		0.84		0.99								1.93					11.81				100	84
H-23 5965m	6	7	Fl							44.75					55.26														100	176
H-23 5965m	6	8	Py+Other	0.34			26.99			0.43				72.24															100	194
H-23 5965m	6	9	Fl							43.63					56.37														100	161
H-23 5965m	7	1	Chl	29.59		18.37	21.34	0.44	15.02			0.25																	85	117
H-23 5965m	7	2	Qz	99.99																									100	140
H-23 5965m	7	3	Fl							44.06					55.94														100	213

Table 1-4: Scanning Electron Microscope chemical analyses of sample 5965m from Newburn H-23 well.

Sample	Site	Position	Mineral	SiO_2	TiO_2	Al_2O_3	FeO	MnO	MgO	CaO	Na_2O	K_2O	P_2O_5	SO_3	F	Cl	Cr_2O_3	CoO	NiO	CuO	ZnO	As_2O_3	SrO	Sb_2O_3	BaO	Ce_2O_3	WO_3	PbO	Total	Actual Total
H-23 5965m	7	4	Ps+Ms+Other	6.65		4.35	2.61	64.40		1.40		1.11													19.50				100	92
H-23 5965m	7	5	Py				27.81							72.19															100	255
H-23 5965m	7	6	Pyro+Other	11.08		15.40	7.58	37.88		1.29		1.39														2.19		23.18	100	106
H-23 5965m	7	7	Lm+Qz	3.55			95.37	1.08																					100	80
H-23 5965m	8	1	Chl	28.72		19.56	18.11		18.62																				85	114
H-23 5965m	8	2	Fl							43.57					56.42														100	204
H-23 5965m	8	3	Ank				15.27	1.11	9.09	30.53																			56	64
H-23 5965m	8	4	Lm+Other	3.96		2.29	81.51	9.79		1.97						0.49													100	75
H-23 5965m	8	5	Qz	99.99																									100	142
H-23 5965m	8	6	Sd				50.28	3.41	1.94	0.37																			56	65
H-23 5965m	9	1	Chl	24.57		22.87	28.04	1.37	7.77	0.38																			85	100
H-23 5965m	9	2	Ms	49.52	0.90	27.80	4.60		1.99			10.19																	95	125
H-23 5965m	9	3	Sd				44.81	1.74	7.64	1.81																			56	72
H-23 5965m	9	4	Fl							43.80					56.21														100	199
H-23 5965m	9	5	Py+Other	0.41		0.34	28.59			0.21				70.44															100	222
H-23 5965m	9	6	Lm+Qz	0.62			97.68	1.68																					100	160
H-23 5965m	9	7	Ms+Py+Brt	62.38		18.39	1.60		1.14			5.54		3.42	2.74										4.81				100	103
H-23 5965m	9	8	Kfs+Qz	72.16		14.74						13.11																	100	134
H-23 5965m	9	9	Fl							43.42					56.58														100	188
H-23 5965m	9	10	Sd+Other	6.12		4.93	73.38	0.84	7.03	6.03			1.70																100	66
H-23 5965m	10	1	Ab+Ms	50.01	1.32	35.28	0.91		0.56		1.56	10.36																	100	104
H-23 5965m	10	2	Fl							43.71					56.28														100	206
H-23 5965m	10	3	fe cal				7.71	0.81	1.56	89.93																			100	59
H-23 5965m	10	4	Qz	99.99																									100	137
H-23 5965m	10	5	Fl							43.95					56.06														100	206
H-23 5965m	10	6	Sd+Ap+Ab	3.96		2.46	71.19		8.32	10.66	1.12		2.27																100	72
H-23 5965m	10	7	Fl							43.28					56.73														100	181
H-23 5965m	10	8	Fl							43.40					56.59														100	196
H-23 5965m	10	9	Ank				15.66	1.00	9.55	29.79																			56	70
H-23 5965m	11	1	Fl							44.06					55.95														100	187
H-23 5965m	11	2	Brt											37.71				-0.06					2.31		60.05				100	115
H-23 5965m	11	3	Lm+Other	3.44			94.57														1.99								100	71
H-23 5965m	11	4	Brt							0.49				40.33									2.09		57.11				100	128
H-23 5965m	11	5	Kfs	66.55		18.03						15.43																	100	119
H-23 5965m	11	6	Qz+Kfs	97.29		1.63						1.07																	100	122
H-23 5965m	11	7	Fl							44.76					55.23														100	184
H-23 5965m	11	8	Sd				48.14	3.61	3.50	0.75																			56	66
H-23 5965m	11	9	Qz	99.99																									100	126
H-23 5965m	12	1	Brt											37.98				-0.05					1.77		60.30				100	127
H-23 5965m	12	2	Lm+Chl	3.38	4.60	1.68	87.87		2.47																				100	94
H-23 5965m	12	3	Lm+Other	3.66		0.72	94.26															1.36							100	87
H-23 5965m	12	4	Fl							43.50					56.51														100	196
H-23 5965m	12	5	Sd				44.03	1.48	8.79	1.70																			56	63
H-23 5965m	12	6	Py+Other	0.94		0.30	29.46			0.41	0.03			68.89															100	213
H-23 5965m	12	7	Ank+Qz	1.78			27.41	1.60	17.78	51.43																			100	64
H-23 5965m	12	8	And+Other	29.29		44.10	19.00	6.69	0.95																				100	103
H-23 5965m	12	9	Brt+Other	13.90			10.16							34.33											41.61				100	12
H-23 5965m	12	10	Chl	27.42	0.36	19.98	30.28		6.27	0.69																			85	113
H-23 5965m	12	11	Ms	48.94		36.25	1.20		0.39		0.67	7.54																	95	117
H-23 5965m	13	1	Brt											37.36				-0.06					2.11		60.61				100	110
H-23 5965m	13	2	Py				27.18							72.84															100	272
H-23 5965m	13	3	Sd				46.70	1.53	7.16	0.61																			56	71
H-23 5965m	13	4	Ank+Ab	23.00		5.57	16.58	1.14	10.88	39.92	2.90																		100	84
H-23 5965m	13	5	Fl				27.62							72.39															100	239

Table 1-4: Scanning Electron Microscope chemical analyses of sample 5965m from Newburn H-23 well.

Sample	Site	Position	Mineral	SiO_2	TiO_2	Al_2O_3	FeO	MnO	MgO	CaO	Na_2O	K_2O	P_2O_5	SO_3	F	Cl	Cr_2O_3	CoO	NiO	CuO	ZnO	As_2O_3	SrO	Sb_2O_3	BaO	Ce_2O_3	WO_3	PbO	Total	Actual Total
H-23 5965m	13	6	Sd+Ab+ap	7.25		4.25	65.30	0.99	10.83	8.76	1.08		1.54																100	60
H-23 5965m	13	7	Sd+Ab	15.36		4.16	38.16	1.87	14.13	23.94	2.40																		100	87
H-23 5965m	13	8	Fap							45.68			44.00		8.21								2.11						100	128
H-23 5965m	13	9	Py				27.25							72.76															100	255
H-23 5965m	13	10	Sd				42.69	1.74	9.93	1.64																			56	68
H-23 5965m	13	11	Sd+Other	2.01		1.19	73.51	0.94	14.11	8.24																			100	62
H-23 5965m	14	1	Lm+Qz	1.26			98.21	0.54																					100	91
H-23 5965m	14	2	Lm+Apy+Other	2.65		3.48	90.03							1.05								2.80							100	84
H-23 5965m	14	3	Lm+Ap+Other	7.59		0.87	88.11	0.61		1.72			1.10																100	83
H-23 5965m	14	4	Lm+Ap+Other	4.49	0.97	0.98	89.84			0.59			1.12						1.02	0.98									100	85
H-23 5965m	14	5	Lm+Qz	3.04			96.95																						100	90
H-23 5965m	14	6	Ms+Lm	42.27	0.78	27.63	20.70		0.99			6.77									0.85								100	113
H-23 5965m	14	7	Fl							44.26					55.74														100	214
H-23 5965m	14	8	Cpr+Lm+Other	8.60			62.90			1.16			1.76	2.12		0.91				22.56									100	80
H-23 5965m	15	1	Lm+Other	9.31		2.66	88.03																						100	81
H-23 5965m	15	2	Fl				27.65							72.37															100	253
H-23 5965m	15	3	Lm+Qz	4.11			95.91																						100	83
H-23 5965m	15	4	Fl				27.45							72.54															100	249
H-23 5965m	15	5	Lm+Qz	2.89			94.62	1.19		1.30																			100	86
H-23 5965m	15	6	Ab	68.56		18.82				0.25	12.38																		100	149
H-23 5965m	15	7	Sd+Chl	6.14		0.98	79.31	8.68	0.93	1.68															2.30				100	77
H-23 5965m	15	8	Sd+Qz	1.24			95.77	1.21		1.79																			100	85
H-23 5965m	16	1	Lm				100.00																						100	97
H-23 5965m	16	2	Py				27.40							72.61															100	245
H-23 5965m	16	3	Py				27.38							72.64															100	249
H-23 5965m	16	4	Qz	99.43		0.57																							100	140
H-23 5965m	16	5	Fl							43.85					56.16														100	203
H-23 5965m	16	6	Qz	99.15		0.83																							100	145
H-23 5965m	17	1	Lm+Qz	1.09			98.90																						100	101
H-23 5965m	17	2	Lm+Qz	5.48			91.87			0.39											2.27								100	86
H-23 5965m	17	3	Lm+Other	2.44		0.76	95.60																	1.22					100	97
H-23 5965m	17	4	Lm+Chl	11.40		4.18	82.77		1.16	0.50																			100	93
H-23 5965m	17	5	Cal+Ps		1.38	1.11	4.97	56.53		27.91					4.13												3.95		100	112
H-23 5965m	17	6	Ps+Cal+Py	1.88		2.14	8.37	35.28		27.59				3.50	5.52										7.60		8.11		100	51
H-23 5965m	18	1	Lm+Other	6.70			88.03			0.71	0.73									2.74	1.08								100	82
H-23 5965m	18	2	Lm+Other	1.90	1.40		95.80		0.88																				100	97
H-23 5965m	18	3	Lm+Ms	17.28		14.08	65.82			0.77		2.05																	100	105
H-23 5965m	19	1	Lm+Qz	4.06			95.93																						100	76
H-23 5965m	19	2	Lm+Other	4.94		1.11	93.05													0.88									100	66
H-23 5965m	19	3	Lm+Other	2.80			95.03	1.21		0.59						0.38													100	78
H-23 5965m	19	4	Lm+Cal				85.60	4.44		1.92											8.04								100	54
H-23 5965m	19	5	Ps					76.16		0.46										1.79					21.58				100	82
H-23 5965m	19	6	Ps					77.31												0.84					21.83				100	81
H-23 5965m	20	1	Lm+Qz	1.16			98.84																						100	95
H-23 5965m	20	2	Lm+Qz	3.32			90.11	5.20		1.39																			100	65
H-23 5965m	20	3	Lm+Qz	5.35			92.94															1.70							100	85
H-23 5965m	20	4	Py				27.12							72.89															100	234
H-23 5965m	21	1	Ps			0.87		76.87		0.60		0.63								2.77					18.27				100	80
H-23 5965m	21	2	Ps					76.78												2.52					20.70				100	79
H-23 5965m	21	3	Ps					76.52		0.74		0.90								2.54					16.12		3.15		100	54
H-23 5965m	22	1	Qz+Lm	1.18	5.02		93.27										0.54												100	100
H-23 5965m	22	2	Lm+Qz	1.35			97.54																	1.10					100	103
H-23 5965m	22	3	Brt+Lm+Other	8.94		2.21	67.13			1.37				8.37							1.44				10.53				100	83

Appendix 1-5: SEM-BSE images and EDS mineral analyses for sample 5975m.

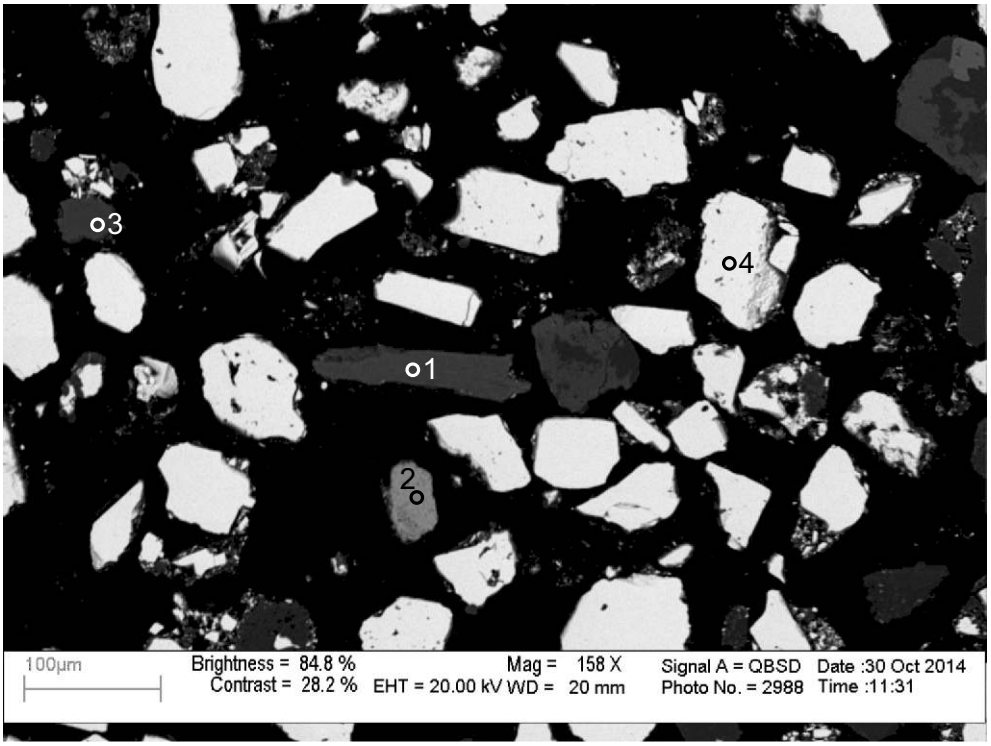

1: Hornblende
2: Limonite
3: Calcite
4: Barite

Figure 1-5.1: Sample Newburn 5975m site 2 (SEM).

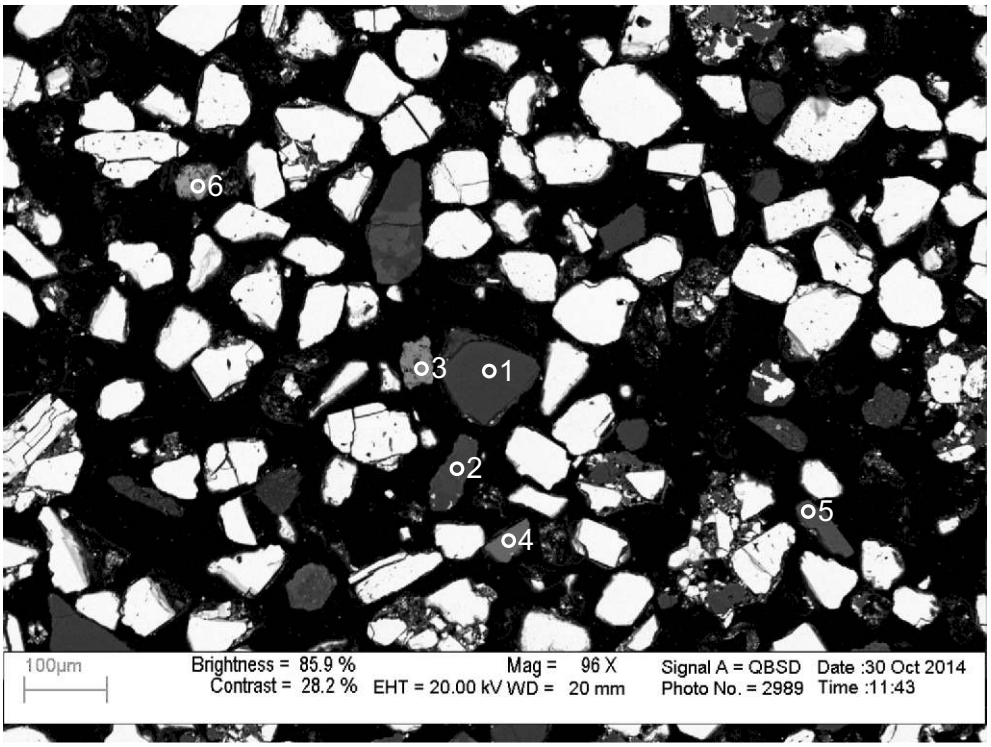

1: Tourmaline
2: Quartz
+K-feldspar
3: Siderite
+Apatite
+Quartz
4: Fluorite
5: Calcite
6: Limonite
+K-feldspar

Figure 1-5.3: Sample Newburn 5975m site 3 (SEM).

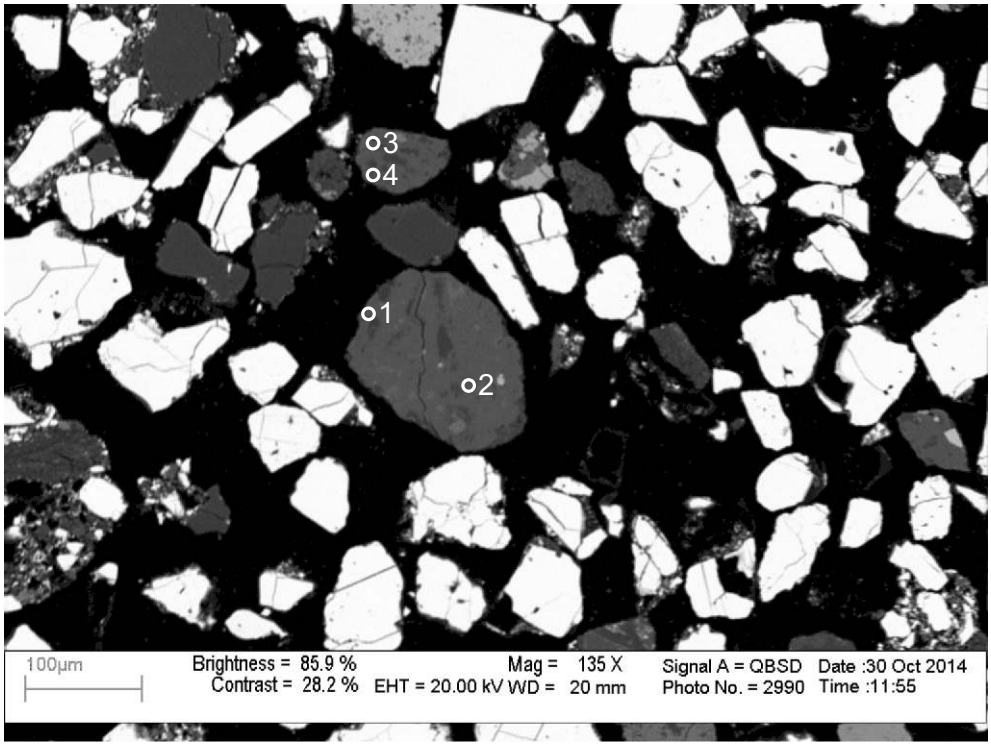

1: Albite +Ankerite
2: Albite +Ankerite
3: Albite +Ankerite
4: Muscovite +Ankerite

Figure 1-5.3: Sample Newburn 5975m site 4 (SEM).

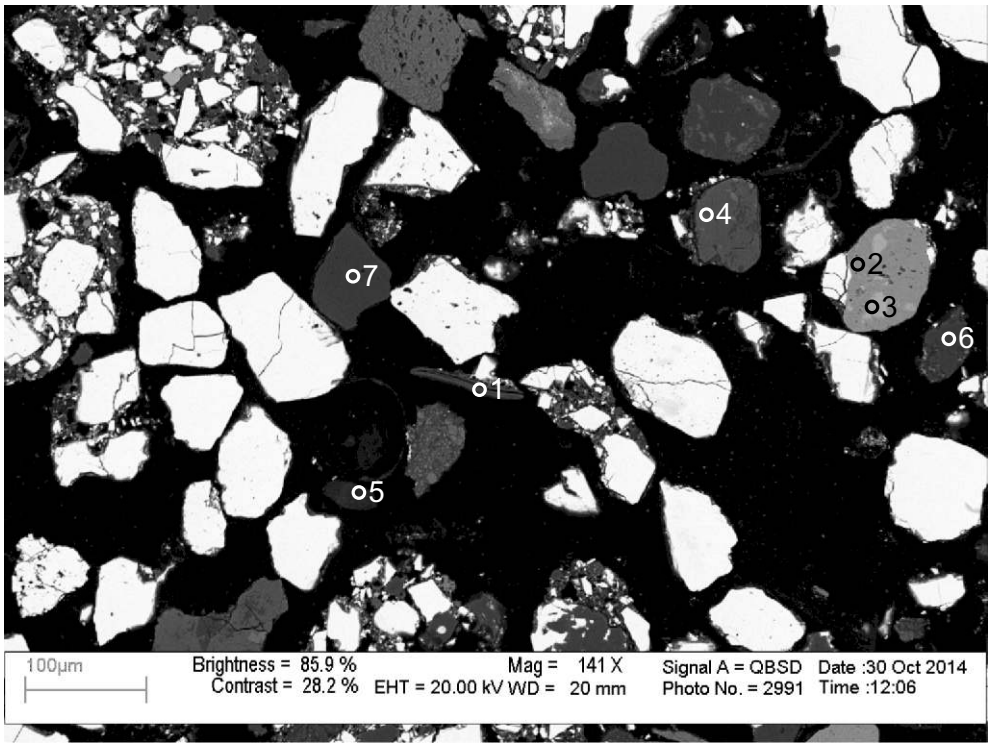

1: Muscovite
2: Limonite +Chlorite
3: Psilomelane
4: Ankerite
5: Fluorite
6: Quartz
7: Quartz

Figure 1-5.4: Sample Newburn 5975m site 5 (SEM).

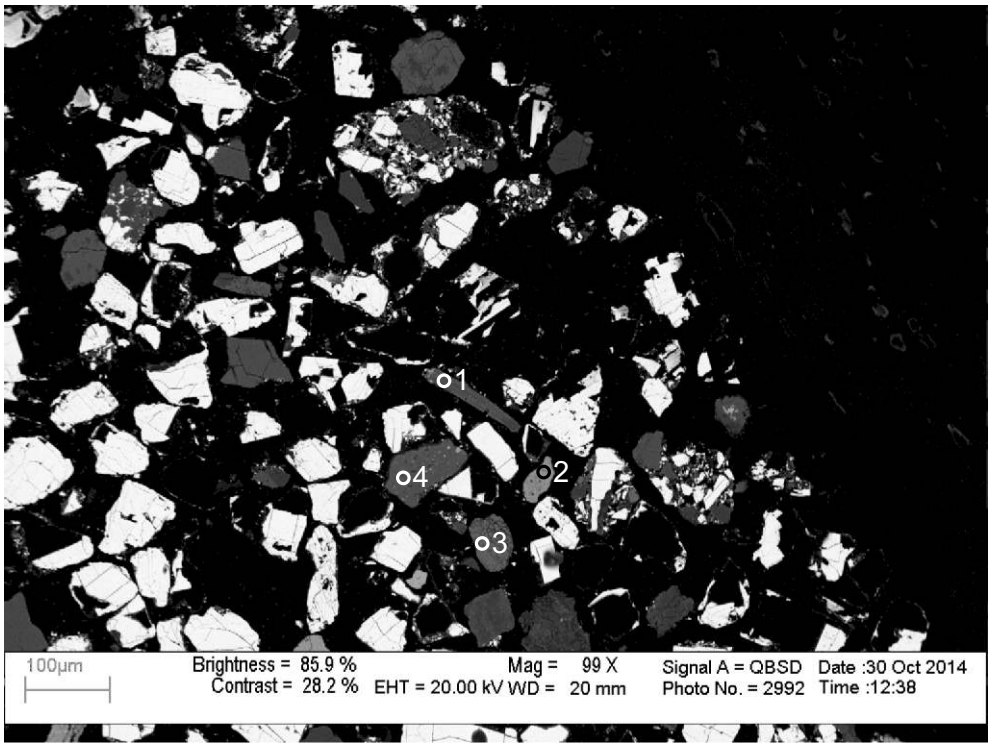

1: Biotite
2: Limonite
+Quartz
3: Fluorapatite
4: Quartz
+Chlorite

Figure 1-5.5: Sample Newburn 5975m site 6 (SEM).

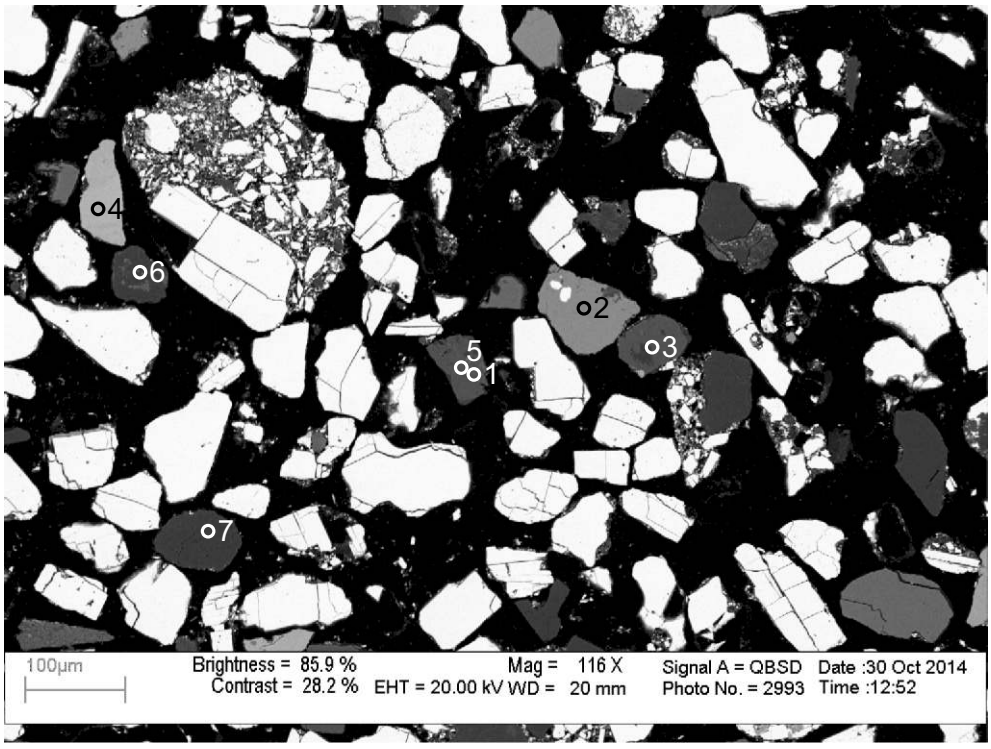

1: Ankerite
+Chlorite
2: Limonite
+Quartz
3: Ankerite
4: Psilomelane
5: Ankerite
6: Albite
+Apatite
7: Dolomite

Figure 1-5.6: Sample Newburn 5975m site 7 (SEM).

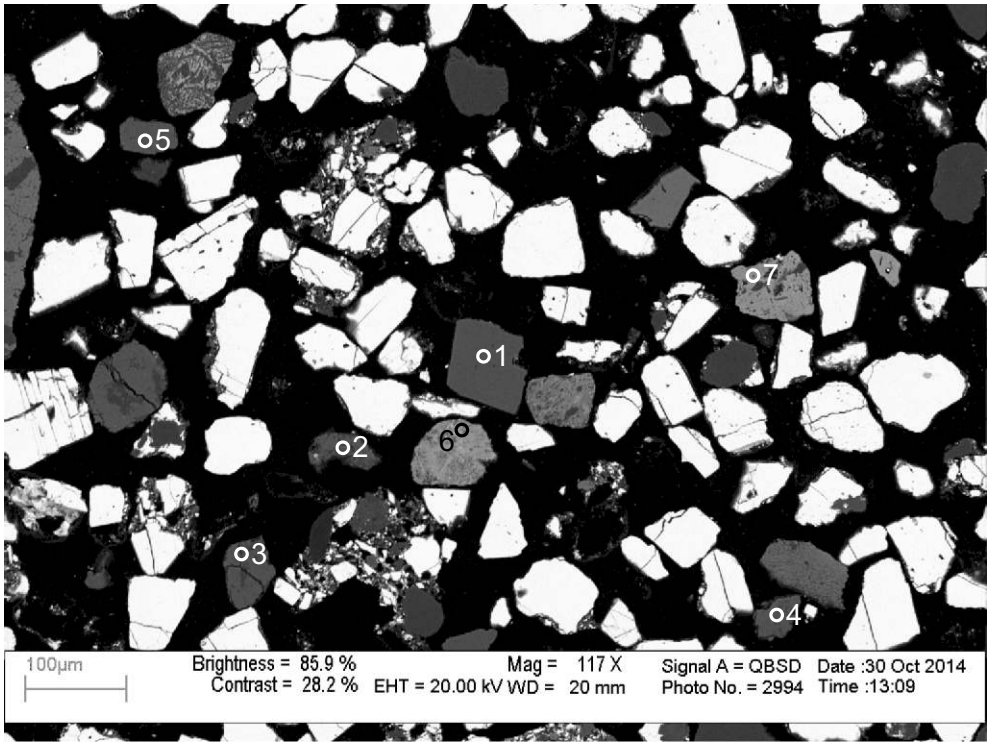

1: Calcite
2: Ankerite +Chlorite
3: Ankerite +Quartz
4: Ankerite
5: Ankerite +Other
6: Limonite +Other
7: Limonite +Other

Figure 1-5.7: Sample Newburn 5975m site 8 (SEM).

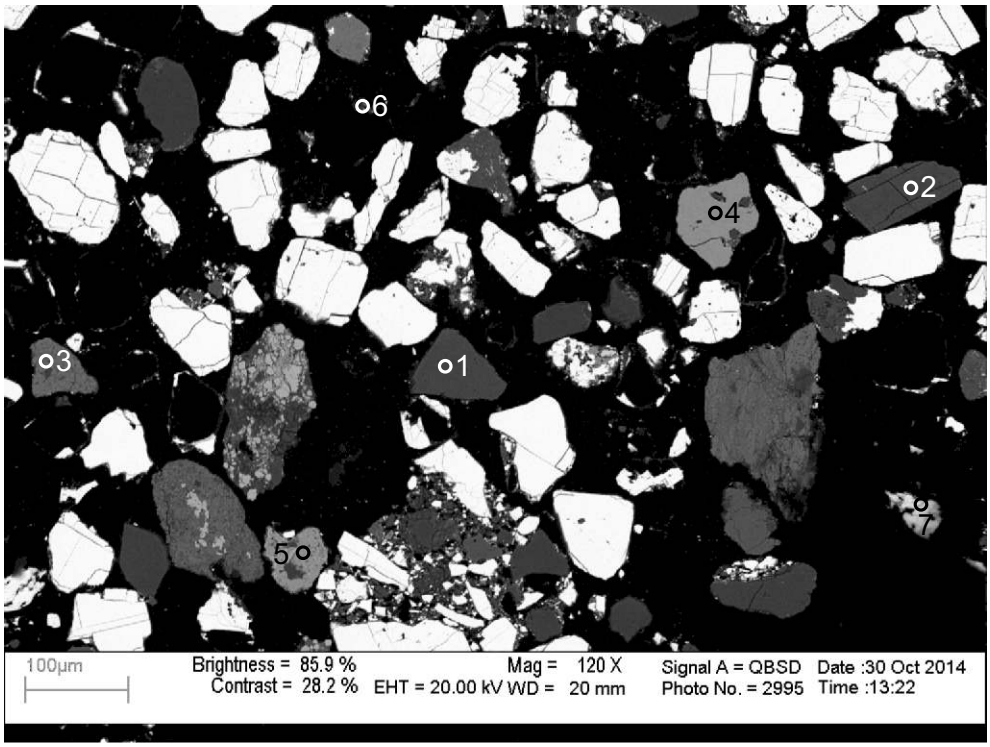

1: Dolomite
2: Dolomite
3: Siderite +Other
4: Limonite +Other
5: Limonite +Quartz
6: Barite +Quartz +Other
7: Barite

Figure 1-5.8: Sample Newburn 5975m site 9 (SEM).

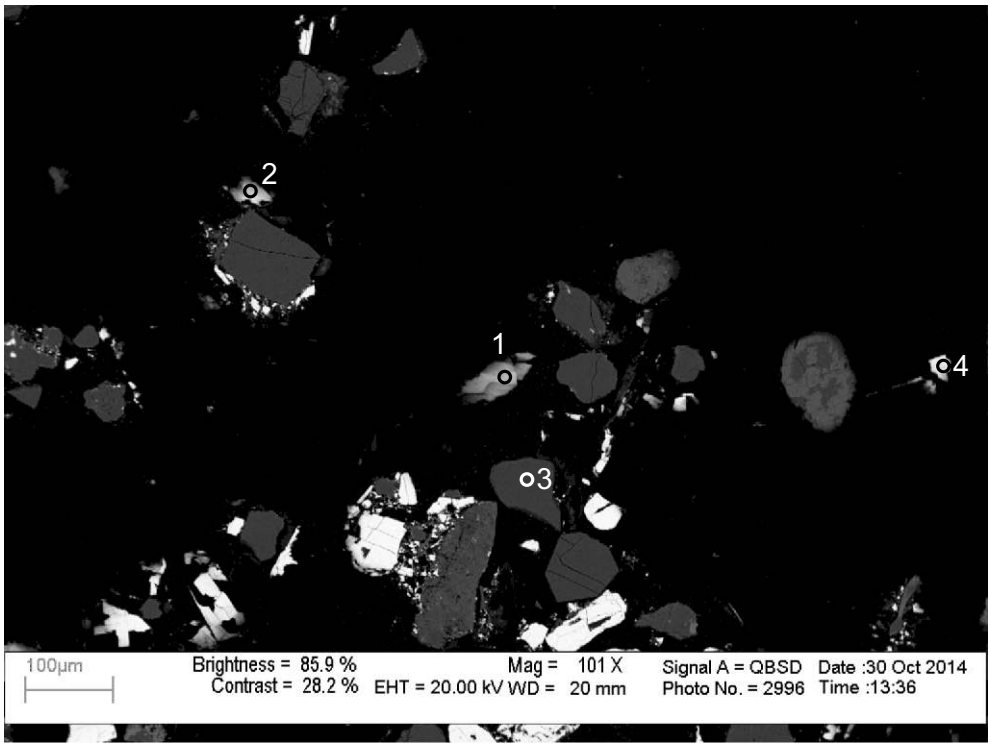

Figure 1-5.9: Sample Newburn 5975m site 10 (SEM).

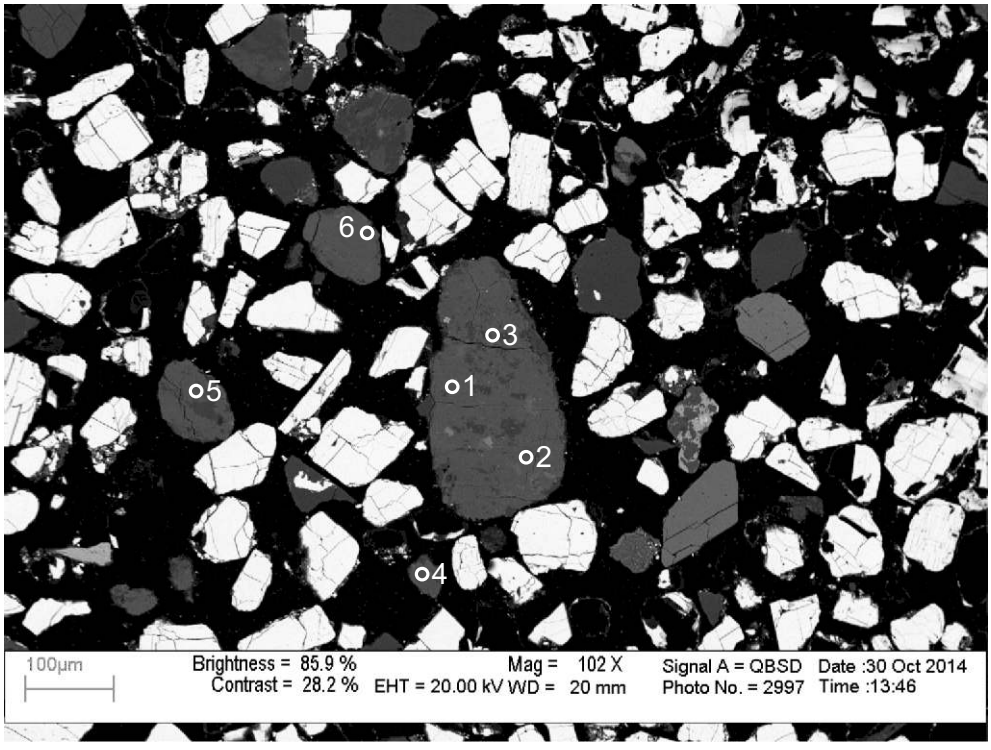

Figure 1-5.10: Sample Newburn 5975m site 11 (SEM).

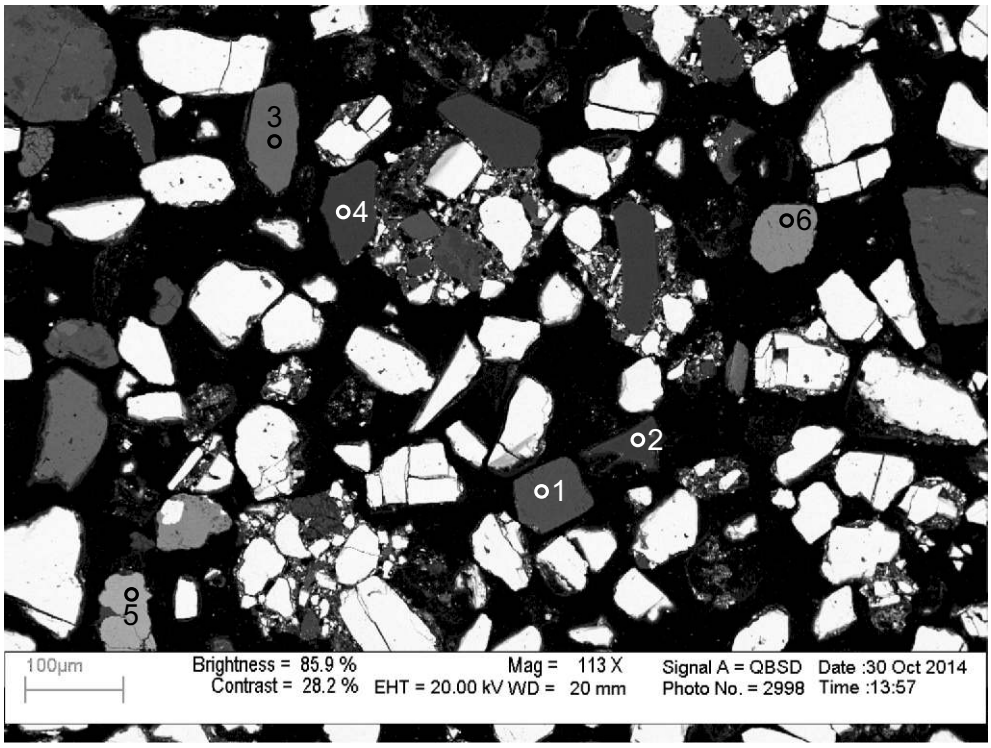

Figure 1-5.11: Sample Newburn 5975m site 12 (SEM).

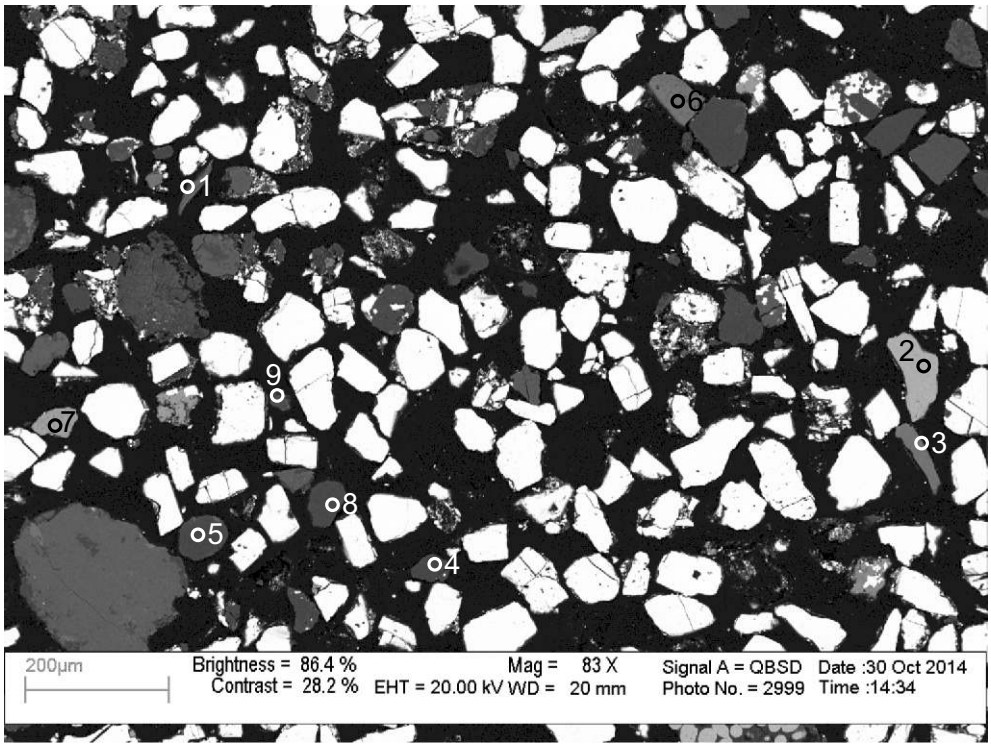

Figure 1-5.12: Sample Newburn 5975m site 13 (SEM).

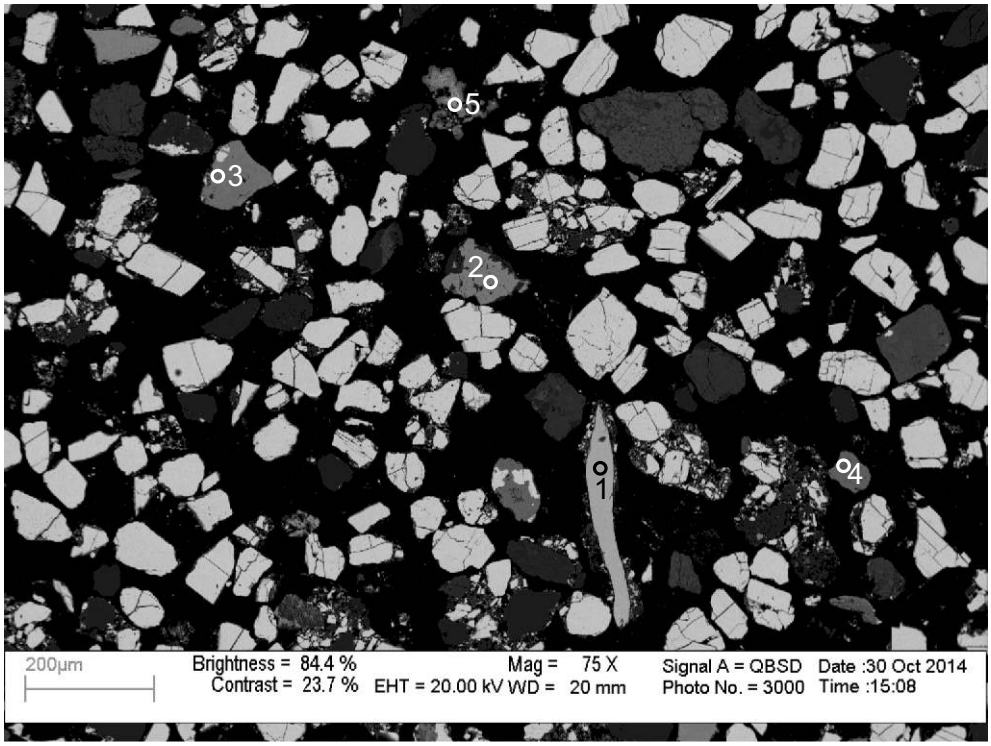

1: Magnetite +Other
2: Pyrite
3: Siderite +Muscovite
4: Siderite +Quartz
5: Psilomelane

Figure 1-5.13: Sample Newburn 5975m site 14 (SEM).

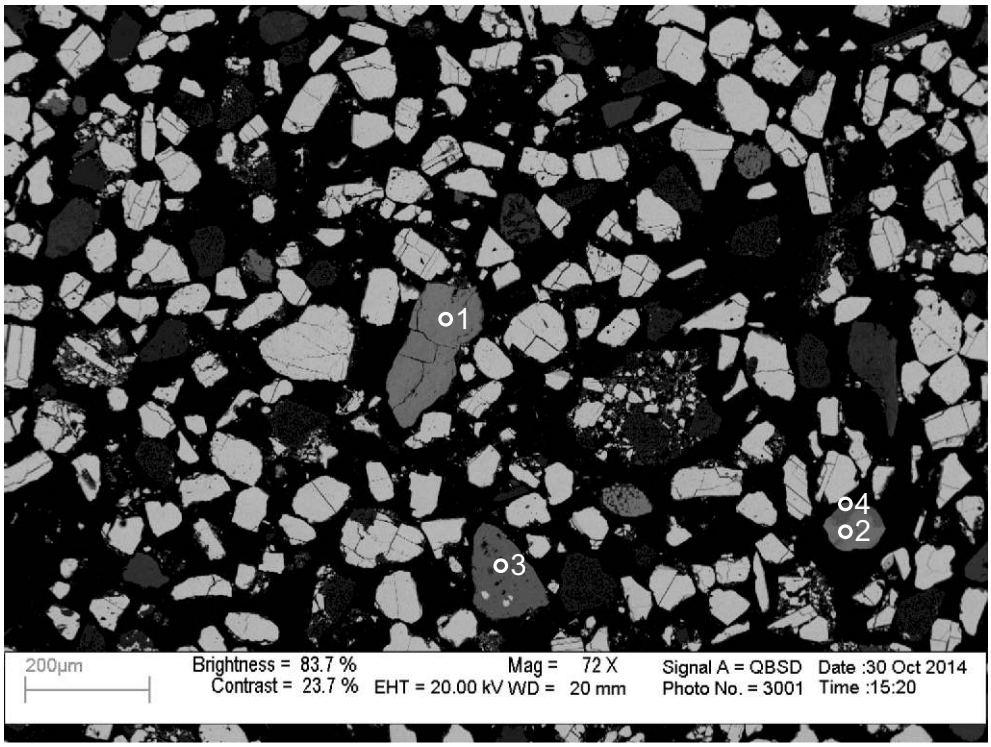

1: Limonite
2: Psilomelane
3: Limonite +Quartz
4: Limonite +Quartz

Figure 1-5.14: Sample Newburn 5975m site 15 (SEM).

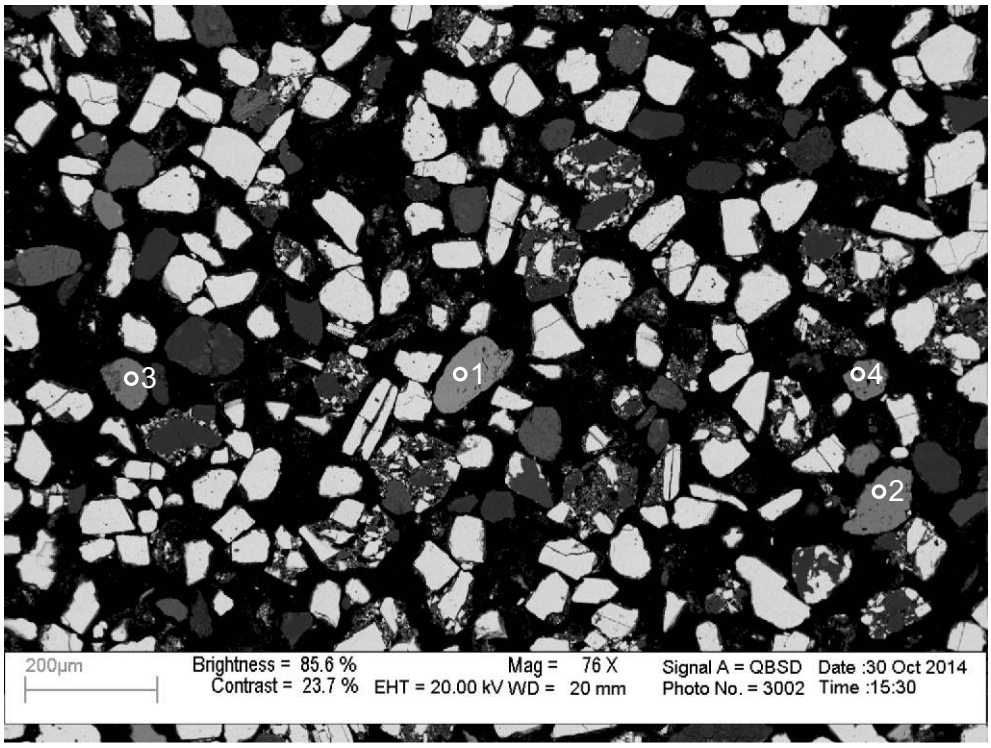

Figure 1-5.15: Sample Newburn 5975m site 16 (SEM).

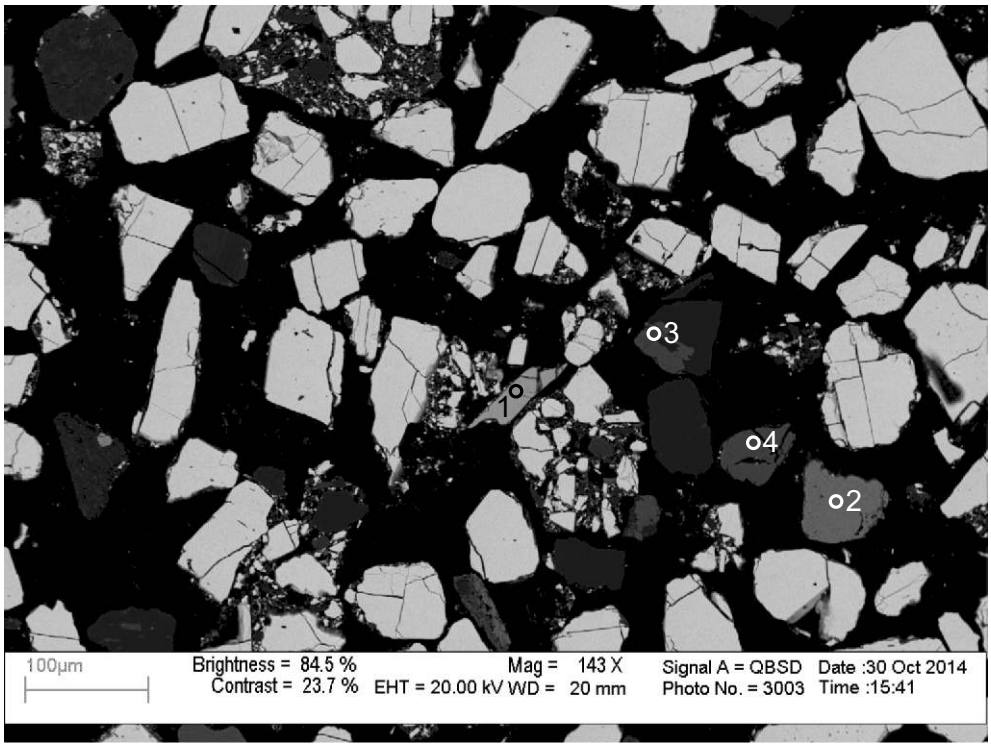

Figure 1-5.16: Sample Newburn 5975m site 17 (SEM).

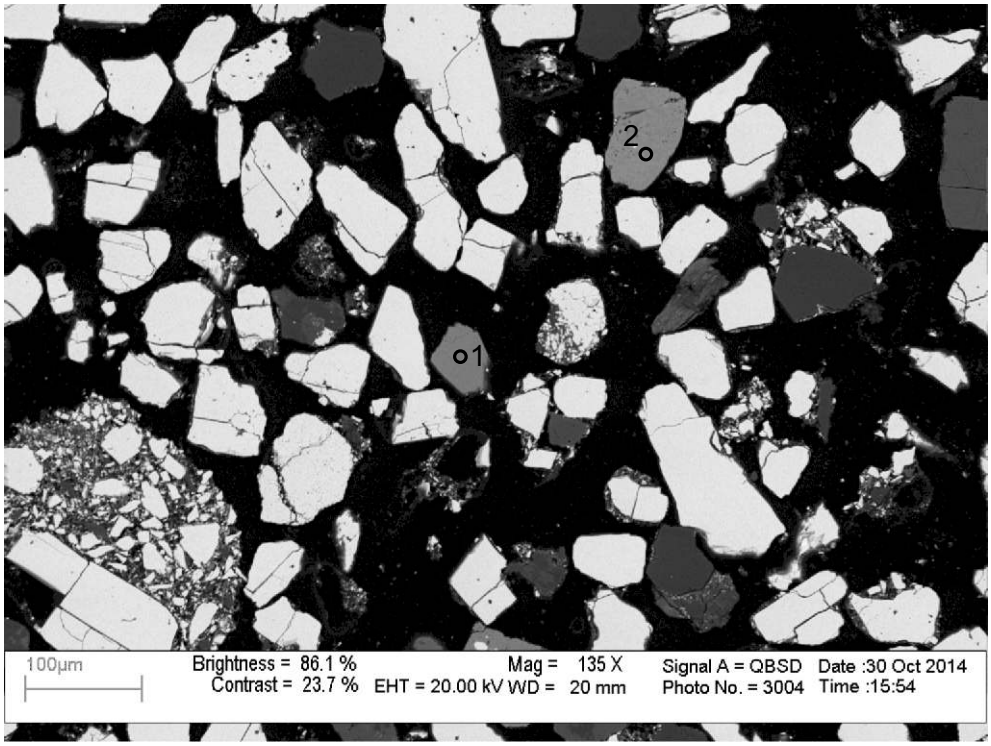

Figure 1-5.16: Sample Newburn 5975m site 17 (SEM).

Table 1-5: Scanning Electron Microscope chemical analyses of sample 5975m from Newburn H-23 well.

Sample	Site	Position	Mineral	SiO_2	TiO_2	Al_2O_3	FeO	MnO	MgO	CaO	Na_2O	K_2O	P_2O_5	SO_3	F	Cl	Cr_2O_3	CoO	CuO	ZnO	As_2O_3	SrO	BaO	Total	Actual Total
H-23 5975m	2	1	Hb	50.37		7.33	12.48	0.35	13.88	11.49	0.73	0.38												97	129
H-23 5975m	2	2	Lm	1.37			98.63																	100	96
H-23 5975m	2	3	Cal							53.72					2.28									56	63
H-23 5975m	2	4	Brt											37.41									62.61	100	139
H-23 5975m	3	1	Tur	38.12	0.89	32.87	4.38		7.73	1.06	1.95													87	116
H-23 5975m	3	2	Qz+Kfs	84.41		7.92	0.59					7.08												100	132
H-23 5975m	3	3	Sd+Ap+Qz	9.46			87.83			1.48			1.24											100	85
H-23 5975m	3	4	Fl							43.85					56.15									100	195
H-23 5975m	3	5	Cal				0.50		1.90	53.59														56	65
H-23 5975m	3	6	Lm+Kfs	41.35	1.88	4.42	49.99					2.36												100	121
H-23 5975m	4	1	Ab+Ank	31.19		8.43	16.38	1.05	9.52	28.10	5.35													100	91
H-23 5975m	4	2	Ab+Ank	41.14		10.83	11.51	0.75	5.99	22.57	7.21													100	99
H-23 5975m	4	3	Ab+Ank	43.77		13.09	10.75	0.68	5.57	19.49	6.65													100	104
H-23 5975m	4	4	Ms+Ank	13.13	1.20	6.12	23.74	1.10	13.83	38.84		1.25		0.80										100	78
H-23 5975m	5	1	Ms	49.54	0.65	30.12	1.96		1.99		0.73	10.01												95	119
H-23 5975m	5	2	Lm+Chl	6.18		4.38	88.02	1.41																100	89
H-23 5975m	5	3	Ps				1.51	80.81				0.37											17.30	100	92
H-23 5975m	5	4	Ank				15.69		11.30	29.01														56	66
H-23 5975m	5	5	Fl	1.09						76.35				1.07	19.61	1.87								100	41
H-23 5975m	5	6	Qz	99.99																				100	141
H-23 5975m	5	7	Qz	99.99																				100	133
H-23 5975m	6	1	Bt	46.87	4.27	19.39	12.52		3.51			9.43												96	106
H-23 5975m	6	2	Lm+Qz	23.21		1.44	75.36																	100	82
H-23 5975m	6	3	Fap	15.62		12.06	25.52		3.35	19.76		0.67	19.09		3.96									100	89
H-23 5975m	6	4	Qz+Chl	48.99	0.63	28.40	13.59	6.08	2.32															100	114
H-23 5975m	7	1	Ank+Chl	9.01		1.30	25.01	1.65	15.95	47.08														100	69
H-23 5975m	7	2	Lm+Qz	6.46			92.88	0.66																100	83
H-23 5975m	7	3	Ank				16.43		10.47	29.10														56	67
H-23 5975m	7	4	Ps					76.91		0.73													22.36	100	83
H-23 5975m	7	5	Ank				14.87	1.02	9.96	30.16														56	65
H-23 5975m	7	6	Ab+Ap	57.67		15.74	1.26			7.02	9.41		8.91											100	124
H-23 5975m	7	7	Dol				0.59	0.32	23.21	29.88														54	58
H-23 5975m	8	1	Cal				0.62	0.79		52.68					1.90									56	62
H-23 5975m	8	2	Ank+Chl	2.59		1.61	29.50	1.29	14.58	50.44														100	58
H-23 5975m	8	3	Ank+Qz	17.93		1.08	21.74	1.39	16.63	40.87		0.35												100	70
H-23 5975m	8	4	Ank				15.82	0.97	9.17	30.04														56	67
H-23 5975m	8	5	Ank+Other	4.09		1.30	25.36	1.38	19.27	48.62														100	65
H-23 5975m	8	6	Lm+Other	1.80		1.10	96.46	0.65																100	76
H-23 5975m	8	7	Lm+Other	6.95		2.29	89.35	1.02		0.39														100	92
H-23 5975m	9	1	Dol				5.70	1.88	18.23	28.18														54	64
H-23 5975m	9	2	Dol				5.28	0.86	19.78	28.08														54	69
H-23 5975m	9	3	Sd+Other	63.81		0.81	22.22	0.43	2.21	6.97			3.55											100	98

Table 1-5: Scanning Electron Microscope chemical analyses of sample 5975m from Newburn H-23 well.

Sample	Site	Position	Mineral	SiO_2	TiO_2	Al_2O_3	FeO	MnO	MgO	CaO	Na_2O	K_2O	P_2O_5	SO_3	F	Cl	Cr_2O_3	CoO	CuO	ZnO	As_2O_3	SrO	BaO	Total	Actual Total
H-23 5975m	9	4	Lm+Other	6.40		2.31	88.92			0.87										1.52				100	89
H-23 5975m	9	5	Lm+Qz	7.23			92.77																	100	80
H-23 5975m	9	6	Brt+Qz+Other	21.50		12.32	3.11		1.48	1.67		1.63		19.53	4.75	0.85							33.19	100	48
H-23 5975m	9	7	Brt											40.38		0.47						2.72	56.44	100	57
H-23 5975m	10	1	Cpy				20.82							54.99					24.18					100	121
H-23 5975m	10	2	Brt											40.80		0.61		0.04					58.56	100	41
H-23 5975m	10	3	Qz	99.99																				100	126
H-23 5975m	10	4	Brt											39.65				-0.03				1.98	58.41	100	71
H-23 5975m	11	1	Ank				16.34	0.89	9.38	29.39														56	61
H-23 5975m	11	2	Ank				15.28	0.90	9.71	30.11														56	61
H-23 5975m	11	3	Ank+Ab+Py	5.22		1.63	27.17	1.42	15.54	45.71	1.64			1.67										100	66
H-23 5975m	11	4	Ank+Ap				26.84	1.45	19.43	49.52			2.77											100	60
H-23 5975m	11	5	Ab+Ank	34.61		8.52	15.81	0.99	9.88	27.37	2.82													100	72
H-23 5975m	11	6	Ank	3.57		3.01	15.17	0.78	7.78	25.69														56	63
H-23 5975m	12	1	Cal						0.65	55.35														56	59
H-23 5975m	12	2	Qz	99.99																				100	131
H-23 5975m	12	3	Fl							44.69					55.31									100	178
H-23 5975m	12	4	Qz	99.99																				100	127
H-23 5975m	12	5	Py				27.85							72.14										100	212
H-23 5975m	12	6	Lm+Other	7.23			89.85	1.12		1.79														100	84
H-23 5975m	13	1	Chl+Ms	35.79		29.82	27.61		4.11			2.66												100	100
H-23 5975m	13	2	Lm+Qz	2.33			97.66																	100	104
H-23 5975m	13	3	Cal	0.83			1.00			44.42				0.92	8.82									56	37
H-23 5975m	13	4	Qz	99.99																				100	129
H-23 5975m	13	5	Qz	99.99																				100	122
H-23 5975m	13	6	Ap+Sd+Chl	2.01		1.47	70.76	1.14	12.83	10.26			1.56											100	70
H-23 5975m	13	7	Lm+Qz	7.47			91.96			0.57														100	80
H-23 5975m	13	8	Qz	99.99																				100	125
H-23 5975m	13	9	Qz+Brt	94.17		0.55				0.46				1.22	2.32								1.30	100	105
H-23 5975m	14	1	Mag+Other	0.53			97.94	0.44									1.08							100	143
H-23 5975m	14	2	Py	0.98			27.11							71.92										100	231
H-23 5975m	14	3	Sd+Ms	4.51		2.23	68.97	21.21				0.52											2.53	100	81
H-23 5975m	14	4	Sd+Qz	5.78			93.28			0.94														100	86
H-23 5975m	14	5	Ps			1.53	8.67	57.08		4.04					5.62					0.73			22.33	100	77
H-23 5975m	15	1	Lm				99.21										0.79							100	96
H-23 5975m	15	2	Ps				1.48	76.79		1.68													20.04	100	87
H-23 5975m	15	3	Lm+Qz	1.75			98.25																	100	77
H-23 5975m	15	4	Lm+Qz	8.32			90.38	0.88		0.42														100	86
H-23 5975m	16	1	Lm+Qz	2.42			97.58																	100	92
H-23 5975m	16	2	Lm+Other	4.66			93.76	0.79		0.78														100	87
H-23 5975m	16	3	Lm+Qz	2.35			97.66																	100	71
H-23 5975m	16	4	Lm+Other	6.65		0.79	90.44	1.34		0.78														100	84

Table 1-5: Scanning Electron Microscope chemical analyses of sample 5975m from Newburn H-23 well.

Sample	Site	Position	Mineral	SiO_2	TiO_2	Al_2O_3	FeO	MnO	MgO	CaO	Na_2O	K_2O	P_2O_5	SO_3	F	Cl	Cr_2O_3	CoO	CuO	ZnO	As_2O_3	SrO	BaO	Total	Actual Total
H-23 5975m	17	1	Cpy				21.51							55.09					23.42					100	202
H-23 5975m	17	2	Lm+Qz	4.04			92.38			0.84											2.75			100	83
H-23 5975m	17	3	Sd				43.10	1.69	9.89	1.32														56	64
H-23 5975m	17	4	Fl							44.75					55.26									100	184
H-23 5975m	18	1	Lm+Qz+Ap	7.85			89.15			1.30			1.72											100	84
H-23 5975m	18	2	Lm+Other	3.25		1.04	95.70																	100	85

Appendix 2: Scanning electron microscope (SEM) backscattered electron (BSE) images for sidewall core from Newburn H-23 well with EDS mineral analyses

Appendix 2-1: SEM-BSE images and EDS mineral analyses for sample Newburn H-23 4313.5m

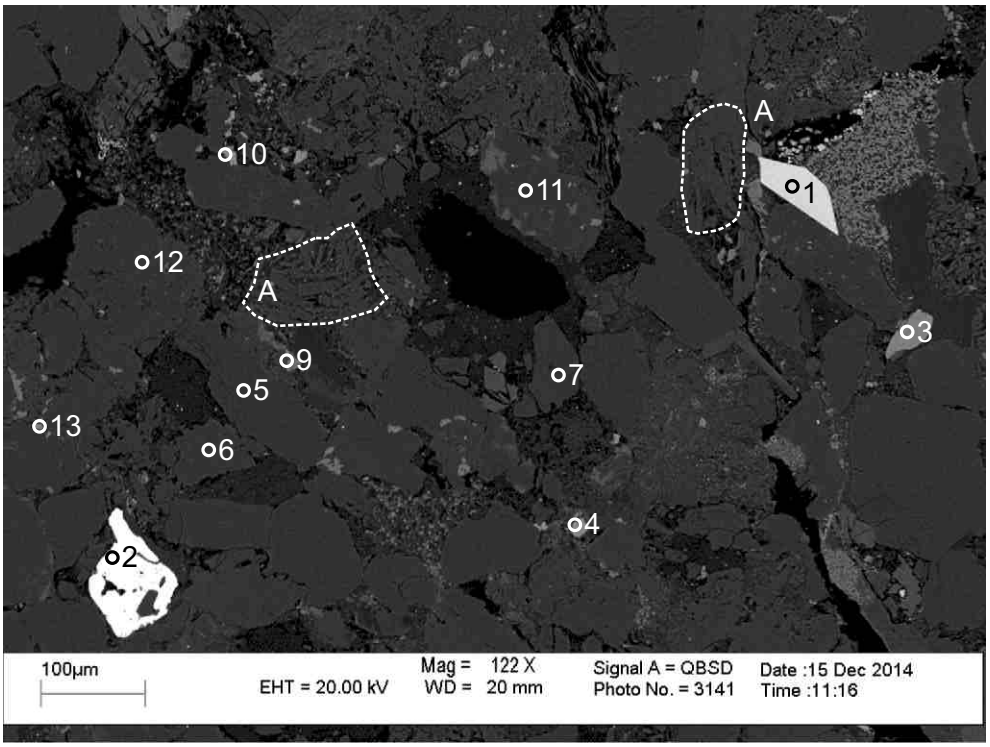

1: Zircon
2: Barite
8
3: Titania
4: Titania
5: Quartz
6: Albite
7: Albite
8: Titania
9: Fluorapatite +Chlorite
10: Titania+ Other
11: Albite
12: Albite
13: Albite

Figure 2-1.1: Sample Newburn 4313.5m site 1 (SEM). Diagenetic zircon (1) with sharp crystal outlines against silicate mineral and a dissolution void. Diagenetic barite (2) apparently engulfing silicate minerals and open porosity. Trachytic lithic clast (position A).

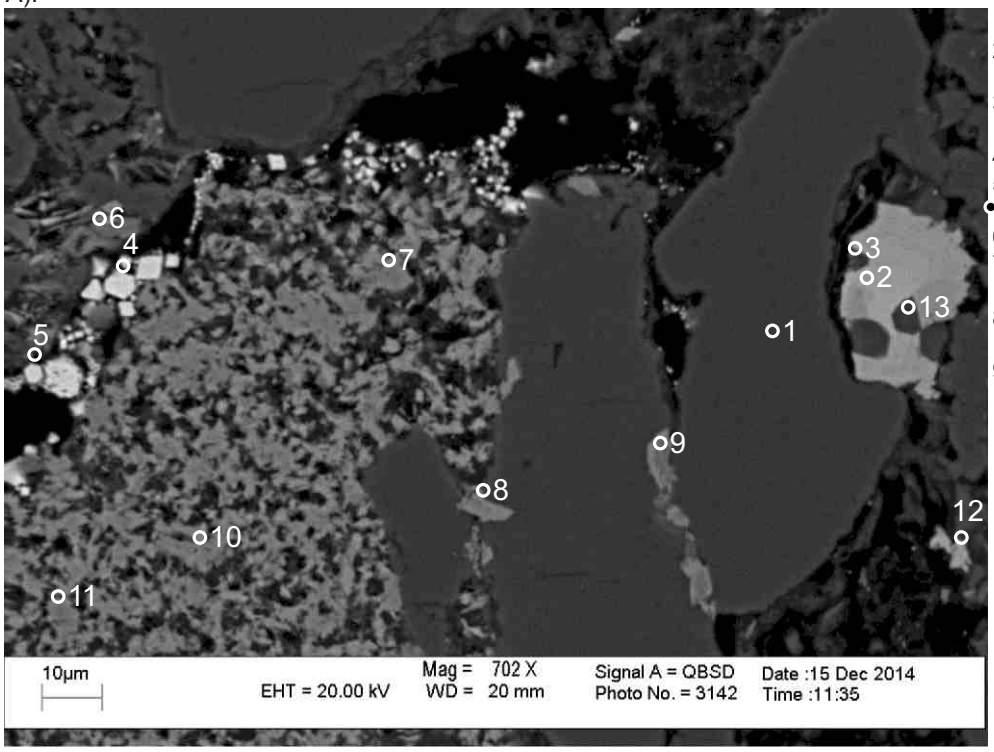

1: Quartz
2: Titania+ Other
3: Albite+ Titania
4: Pyrite
5: Mix
14
6: Mix
7: Siderite+ Chlorite
8: Siderite+ K-Feldspar
9: Siderite+ Other
10: Siderite+ Quartz
11: Siderite+ Chlorite
12: Titania+ Albite+ K-Feldspar
13: Albite+ Titania
14: Quartz

Figure 2-1.2: Sample Newburn 4313.5m site 2 (SEM). Pore space rimmed by early euhedral pyrite (4) and filled by siderite (7,10,11) and chlorite (7,11). Diagenetic titania (2,3) engulfing albite (13) and is separated from quartz (14) by a crystal boundary enlarged by dissolution.

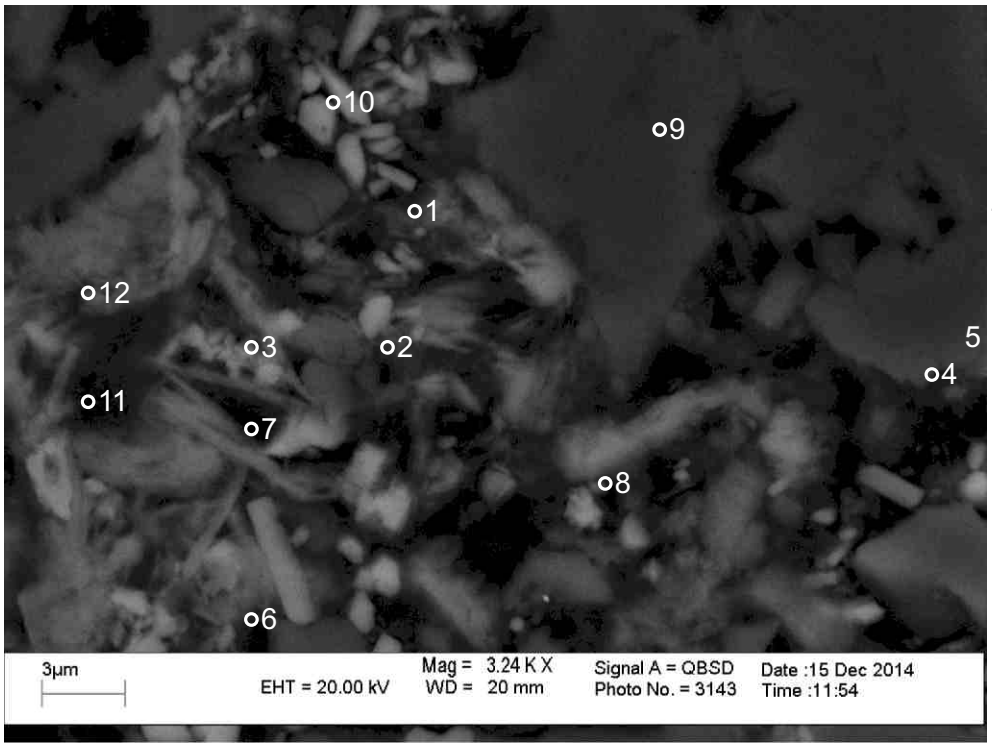

1: Fluorapatite +Illite
2: Illite+ Siderite+ Apatite
3: Chlorite+ Illite
4: Albite+ Apatite+Illite
5: Albite+ Apatite+Illite
6: Fluorapatite +Albite +Other
7: Chlorite+ Other
8: Albite+Illite
9: Albite
10: Apatite+ Other
11: Albite+ Illite+ Apatite+ Other
12: Chlorite+ Apatite

Figure 2-1.3: Sample Newburn 4313.5m site 3 (SEM). Albite (4,9) has dissolution voids partly filled by apatite or fluorapatite and illite (4,1). Early euhedral apatite (10) and chlorite (7) have formed in the pore.

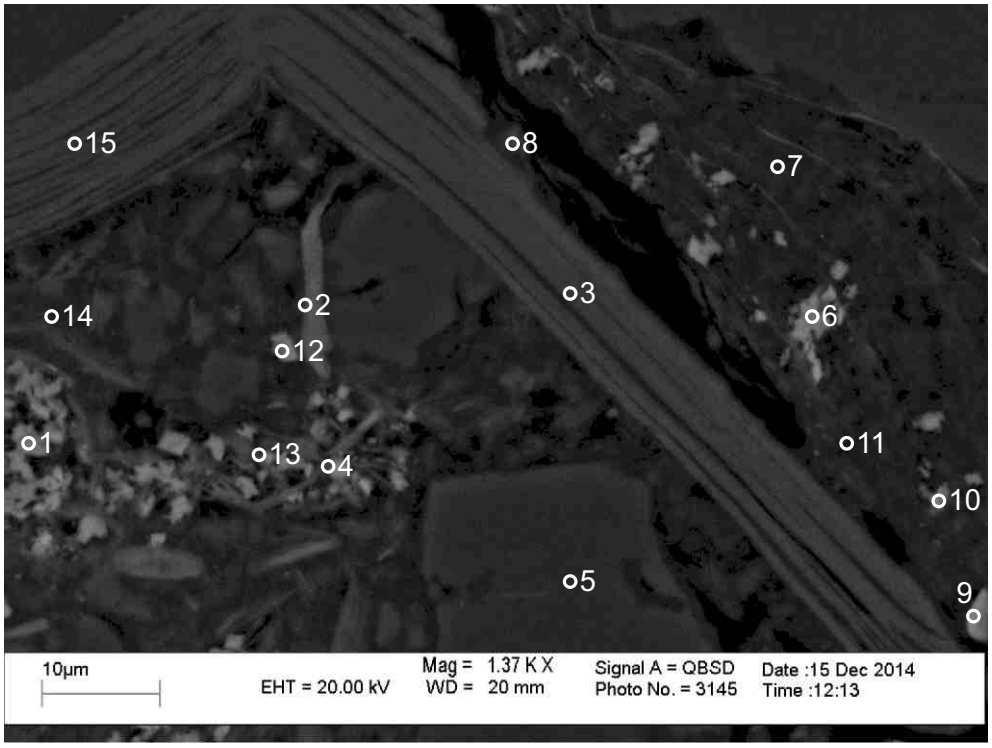

1: Siderite+ Other
2: Chlorite+ Illite
3: Muscovite
4: Chlorite
5: Quartz
6: Siderite+ Chlorite
7: Kaolinite
8: Muscovite+ Chlorite
9: Siderite+ Chlorite
10: Kaolinite+ Chlorite
11: Kaolinite+ Illite
12: Siderite+ Other
13: Chlorite
14: Illite+ Quartz
15: Muscovite

Figure 2-1.4: Sample Newburn 4313.5m site 4 (SEM). Detrital muscovite (3,15) partly replaced by chlorite (8). Siderite (6,9,10) partly fills dissolution voids in aligned kaolinite and illite (7,11). Euhedral chlorite (13,14) and siderite (1) fill a pore.

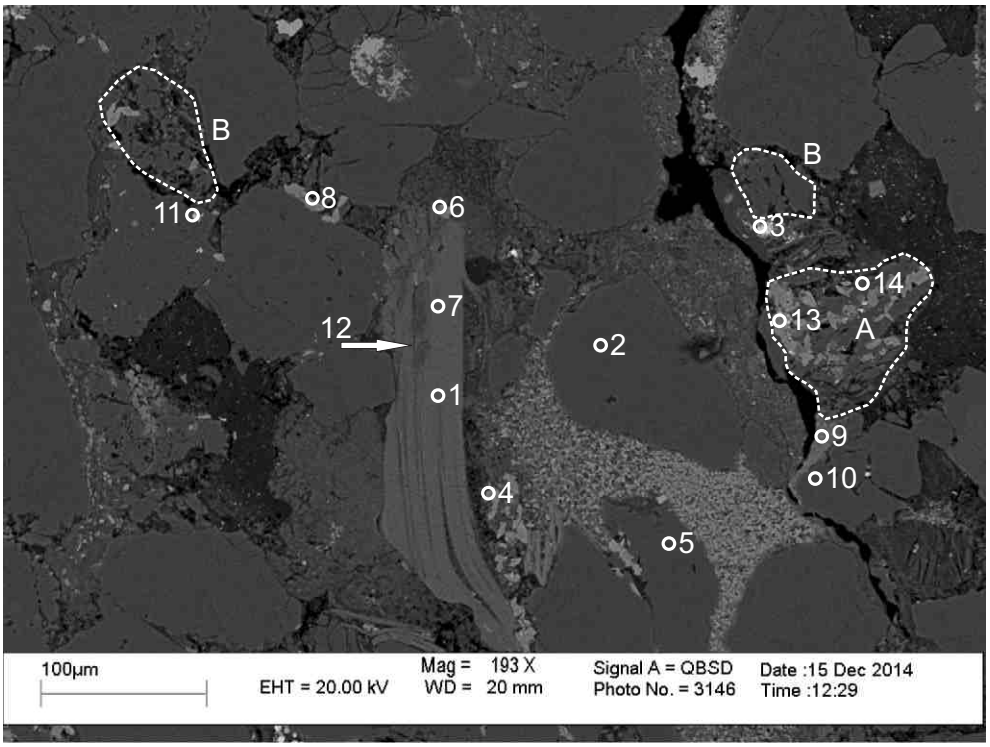

1: Muscovite
2: Quartz
3: Pyrite+ Muscovite
4: Siderite+ Apatite+ Other
5: Quartz
6: Siderite+ Muscovite
7: Siderite+ Muscovite
8: Albite
9: Chlorite+ Titania
10: Quartz
11: Albite+ Pyrite+ Quartz
12: Quartz+ Albite
13: Siderite+ Other
14: Albite

Figure 2-1.5: Sample Newburn 4313.5m site 5 (SEM). Detrital muscovite (1) with siderite (6,7) between the cleavage planes as well as quartz and albite (12) in a hole within the crystal. Pyrite (11) partly occupies a dissolution void within albite (11). Albite-rich lithic clast (position A) with dissolution voids filled with siderite (13). Trachytic lithic clast (position B).

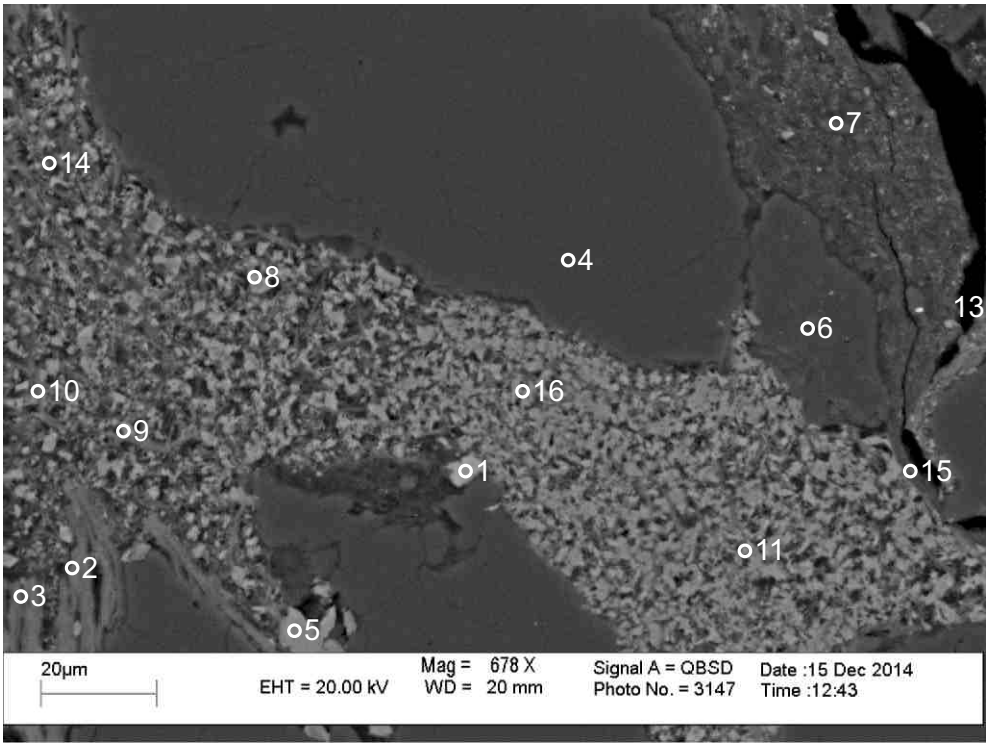

1: Titania+ Other
2: Chlorite+ Other
3: Chlorite+ Other
4: Quartz
5: Siderite+ Quartz
6: Quartz+Illite
7: Quartz+Illite
8: Siderite+ Kaolinite
9: Siderite+ Illite
10: Chlorite
11: Mg-Siderite +Kaolinite
12: Chlorite+ Titania
13: Titania+ Chlorite
14: Mg-Siderite +Kaolinite
15: Muscovite
16: Mg-Siderite +Kaolinite

Figure 2-1.6: Sample Newburn 4313.5m site 6 (SEM). Chloritized muscovite (2,3) bounds a pore filled with titania (1), siderite (8,9), kaolinite (8,14,16) , chlorite (10), and ilite (9).

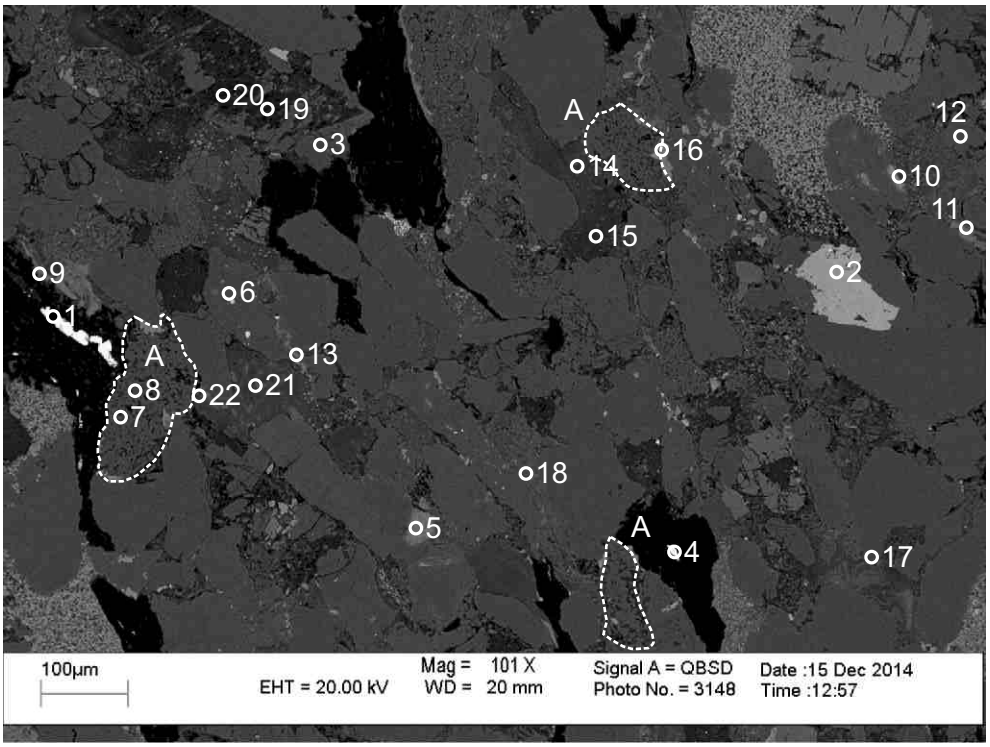

1: Sphalerite
2: Titania
3: Illite+ Kaolinite
4: Sphalerite
5: Siderite+Illite
6: Quartz+ Albite
7: Albite
8: Albite
9: Chlorite
10: Illite+ Kaolinite
11: Mg-Siderite +Illite
12: Albite
13: Albite+Illite
14: Quartz+ Illite
15: Albite+ Other
16: Mg-Siderite +Quartz
17: Quartz
18: Mix
19: Albite
20: Albite
21: Muscovite+ Titania
22: Titania+ Illite

Figure 2-1.7: Sample Newburn 4313.5m site 7 (SEM). Diagenetic sphalerite (1,4) has formed in a vein as well as in a pore. Trachytic lithic clast (position A) comprised of albite (7,8).

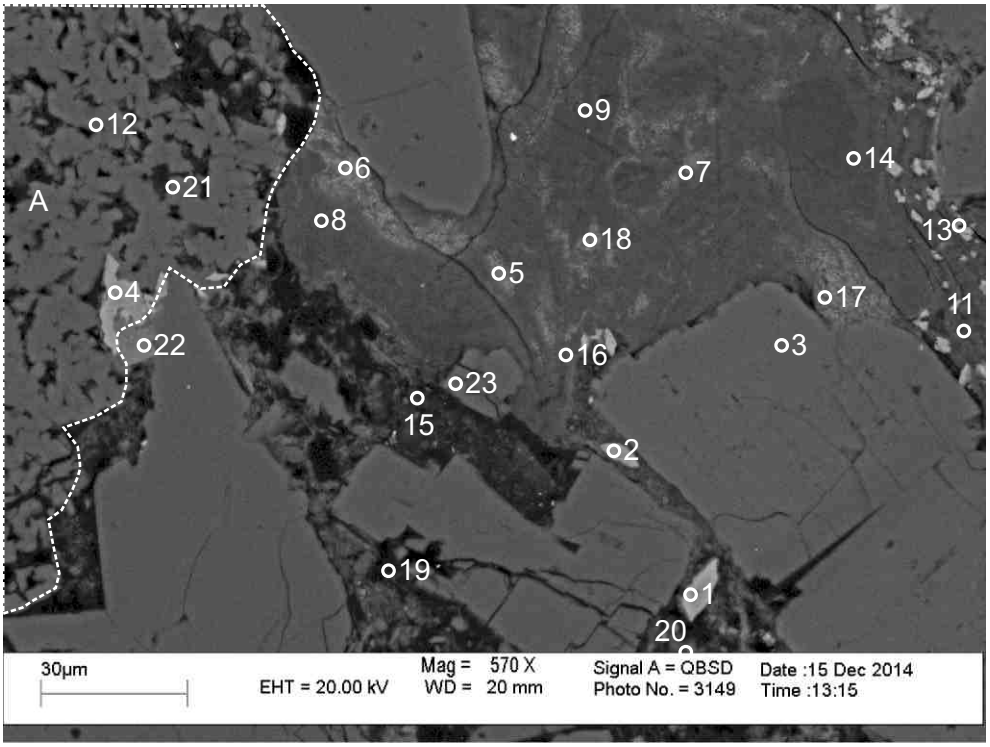

1: Mg-Siderite +Chlorite
2: Mg-Siderite +Other
3: Albite
4: Mg-Siderite +Quartz
5: Titania+Illite
6: Titania+Illite
7: Titania+Illite
8: Muscovite
9: Muscovite
10: Siderite+ Kaolinite
11: Kaolinite+ Quartz+ Other
12: Albite
13: Kaolinite+ Chlorite
14: Illite
15: DrillingMud
16: Muscovite+ Other
17: Titania+ Illite+Other
18: Titania+ Illite+Other
19: Albite+Illite
20: Muscovite+ Other
21: Albite
22: Ankerite+ Illite
23: Albite

Figure 2-1.8: Sample Newburn 4313.5m site 8 (SEM). Close up of site 21 Figure 2-1.7 Trachytic lithic clast (position A) comprised of albite (12,21) and with siderite (4) in dissolution void.

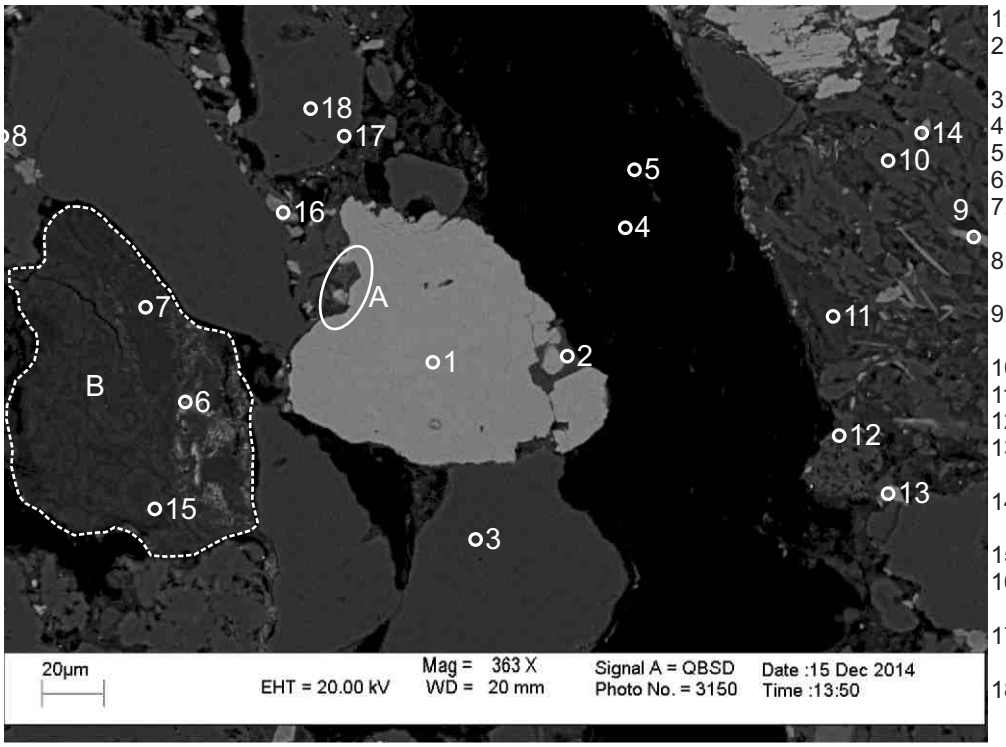

Figure 2-1.9: Sample Newburn 4313.5m site 9 (SEM). Detrital titania (1,2) showing dissolution (position A) and embays quartz (2). Lithic clast (position A) of albite (7), titania (6) and illite (6,7,15).

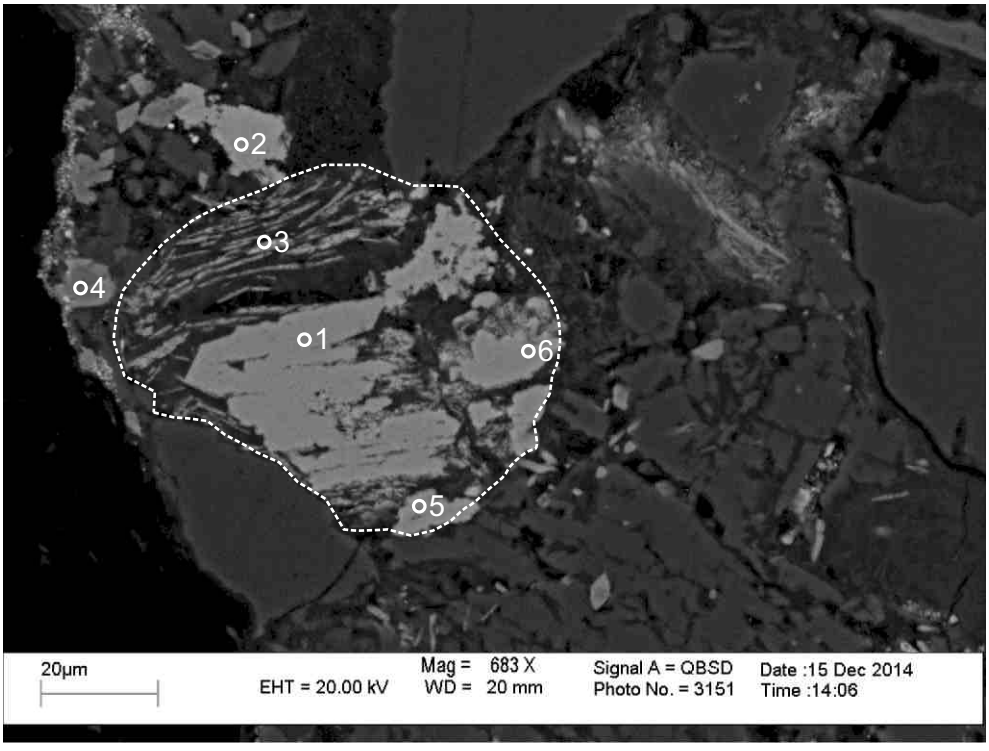

Figure 2-1.10: Sample Newburn 4313.5m site 10 (SEM). Lithic clast comprised of ragged titania (1,5,6), muscovite (3), quartz and siderite. Diagenetic titania (3) forms along the cleavage planes of detrital muscovite.

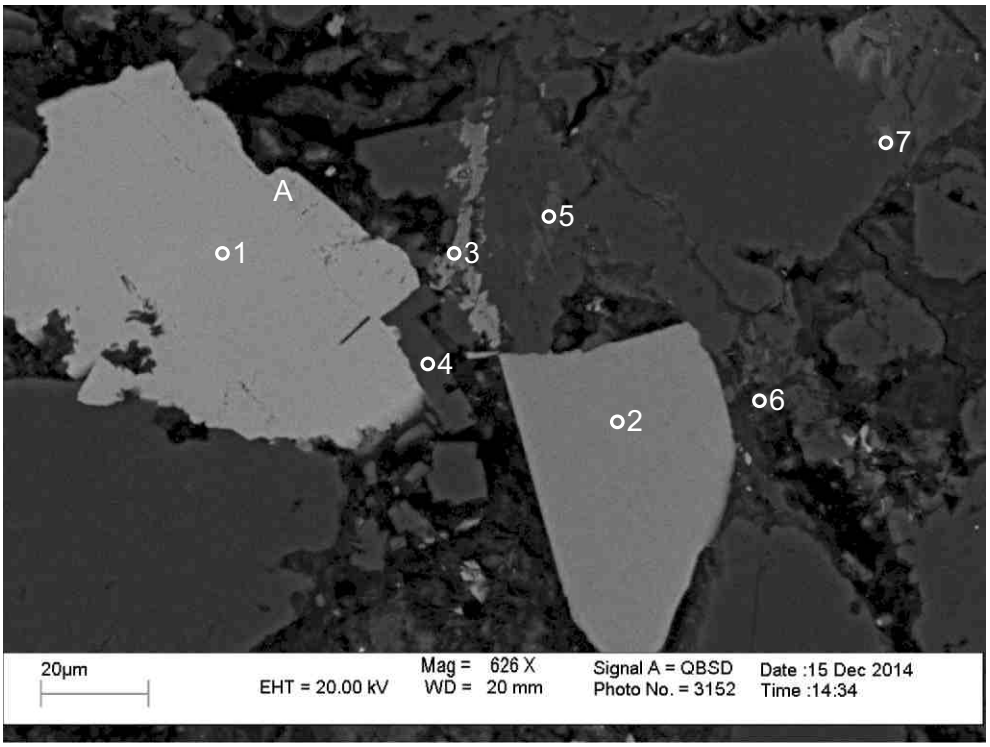

1: Titania+ Chlorite
2: Fluorapatite
3: Siderite+ Albite
4: Albite
5: Muscovite+ Albite
6: Albite+ K-Feldspar
7: Chlorite+ Albite+Illite

Figure 2-1.11: Sample Newburn 4313.5m site 11 (SEM). Detrital titania (1) with dissolution voids and probably diagenetic overgrowth (position A). Fluorapatite (2) with long flat face towards void probably diagenetic grain. Patches of albite (4) Diagenetic siderite (3), chlorite (7) and probably illlite.

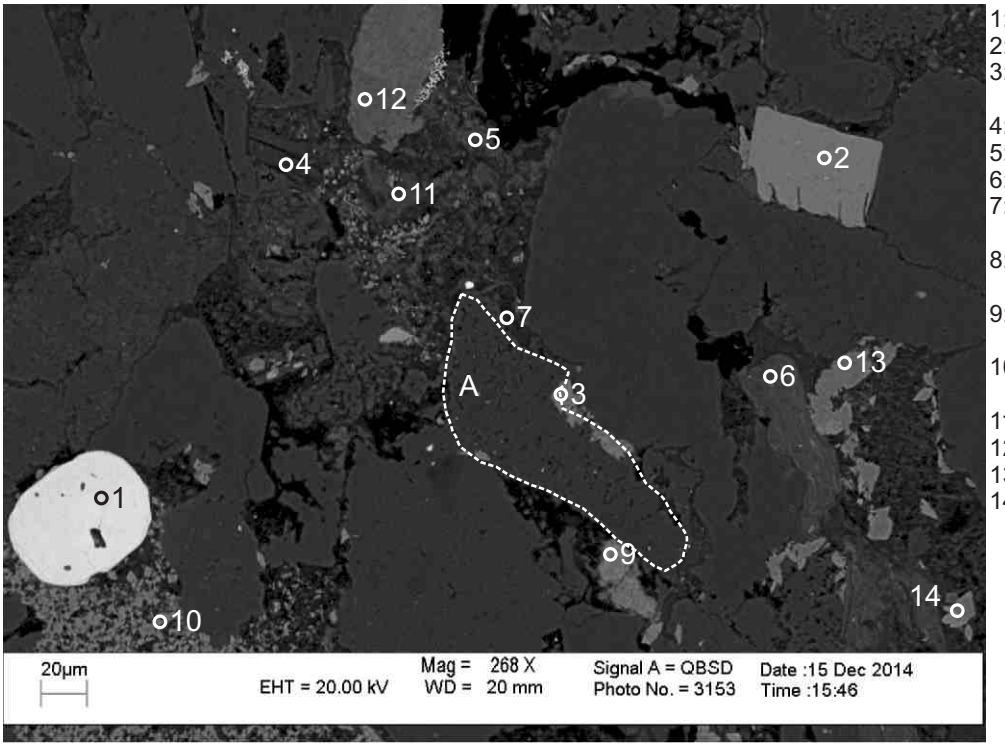

1: Zircon
2: Fluorapatite
3: Siderite+ Quartz
4: Muscovite
5: Illite
6: Muscovite
7: Kaolinite+ Illite
8: Siderite+ Quartz
9: Titania+ Other
10: Chlorite+ Siderite
11: Illite+Other
12: Chlorite
13: Mg-Siderite
14: Siderite+ Other

Figure 2-1.12: Sample Newburn 4313.5m site 12 (SEM). Rounded detrital zircon (1) with dissolution voids. Diagenetic fluorapatite (2) with straight crystal outlines towards pore and probably engulfing quartz. Siderite (3,13) fills pore along intergranular boundary between quartz grains. Trachytic lithic clast (position A).

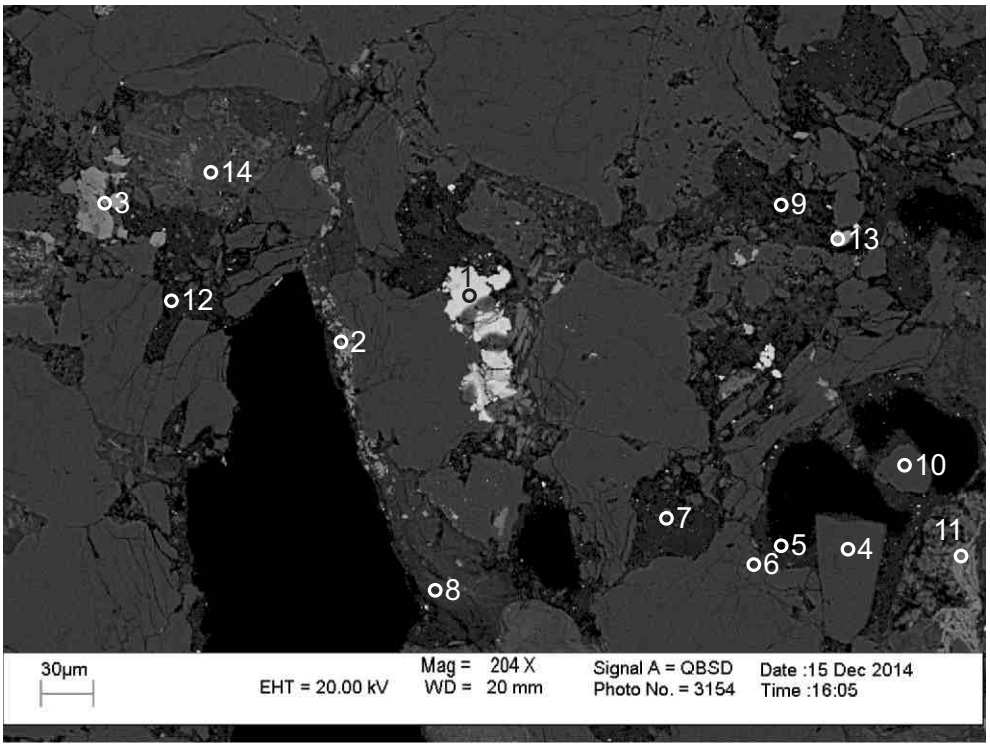

1: Pyrite
2: Chlorite+ Calcite
3: Titania+ Siderite
4: Quartz
5: DrillingMud+ Siderite
6: Quartz
7: DrillingMud+ Siderite
8: Kaolinite+ Other
9: Kaolinite
10: Quartz
11: Chlorite+ Siderite
12:DrillingMud +Calcite
13: Titania
14: Illite+ Titania

Figure 2-1.13: Sample Newburn 4313.5m site 13 (SEM). Kaolinite (9) fills pore. Pyrite and calcite (2) rim pore as well.

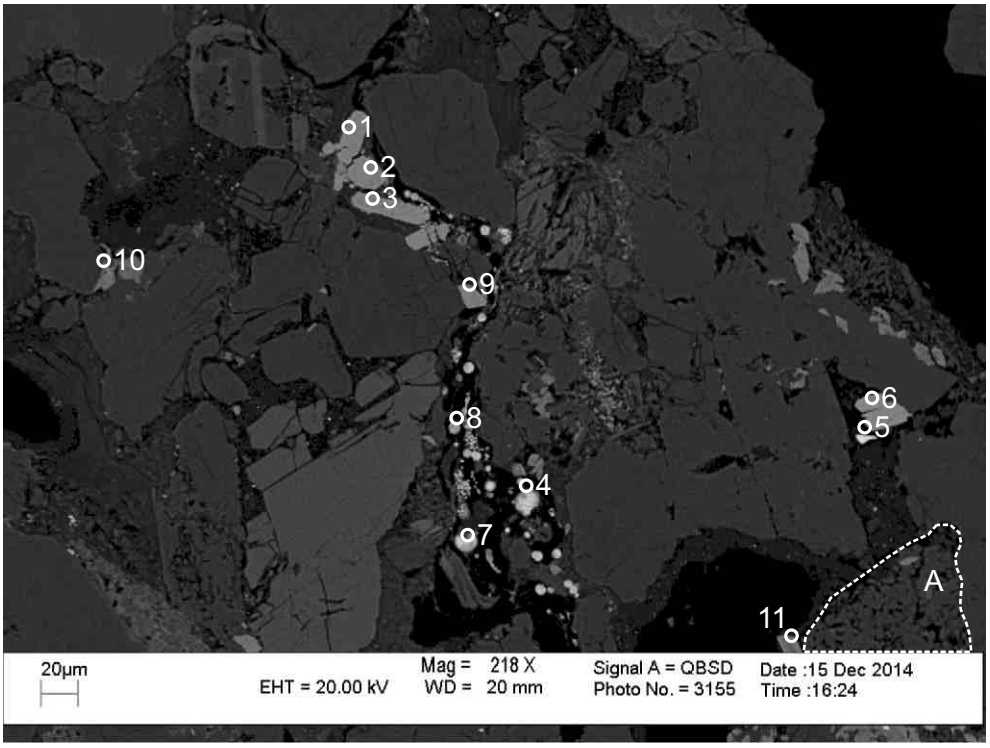

1: Kaolinite+ Chlorite+ Titania
2: Titania
3: Titania
4: Pyrite+ Chlorite
5: Chlorite+ Titania
6: Titania
7: Pyrite+Other
8: Pyrite+Other
9: Titania+ Quartz
10: Siderite+ Chlorite
11: Siderite+ Quartz
12
12: Siderite+ Quartz

Figure 2-1.14: Sample Newburn 4313.5m site 14 (SEM). Diagenetic titania (1,2,3,9), pyrite (8,4,7) and late chlorite (1), kaolinite (1) and siderite (10) form along intergranular boundaries. Trachytic lithic clast (positionA).

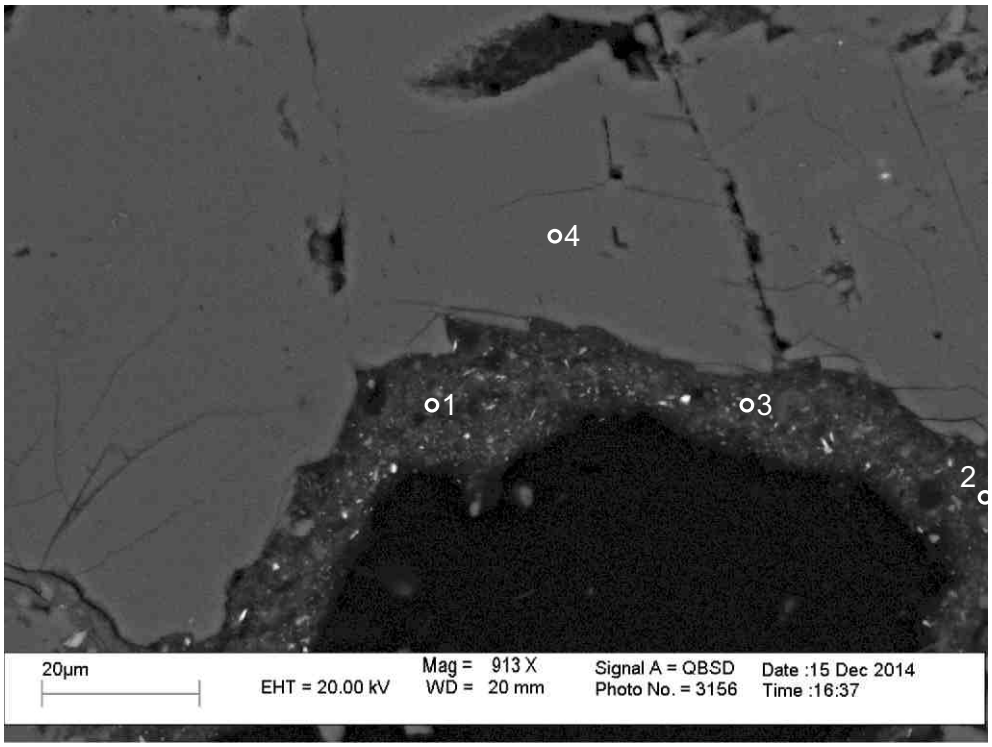

Figure 2-1.15: Sample Newburn 4313.5m site 15 (SEM). Drilling mud (1,2,3) filling a large pore. Large grains of detrital albite (4).

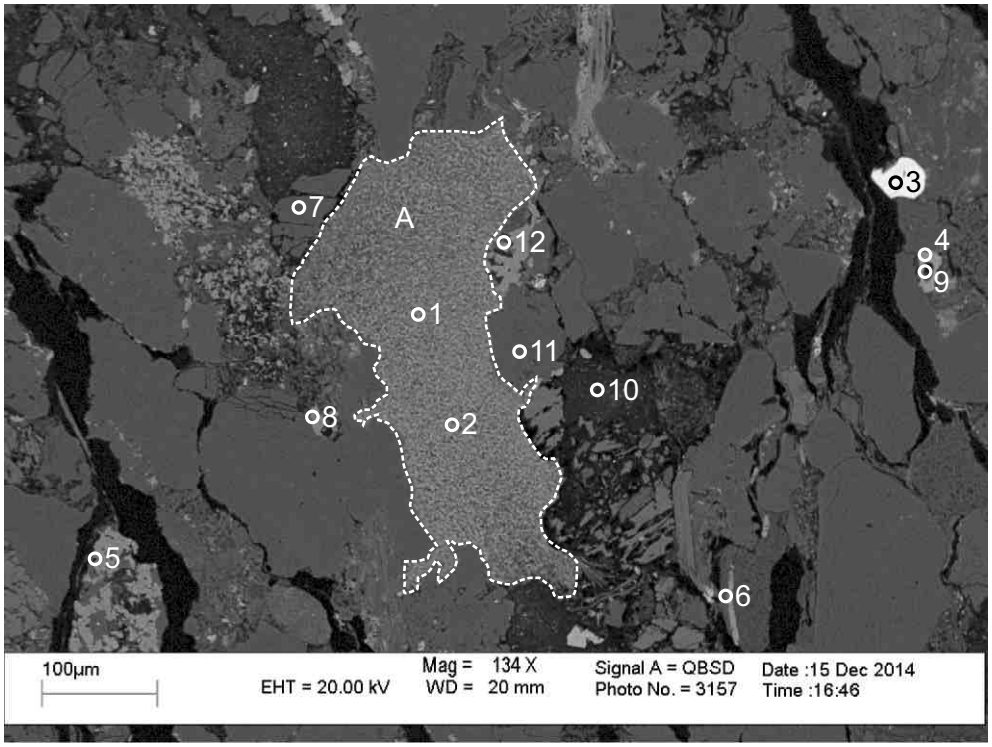

Figure 2-1.16: Sample Newburn 4313.5m site 16 (SEM). Siderite (5) fills dissolution voids within and embays albite (5). Mudstone intraclast (position A) cemented by early siderite (1,2).

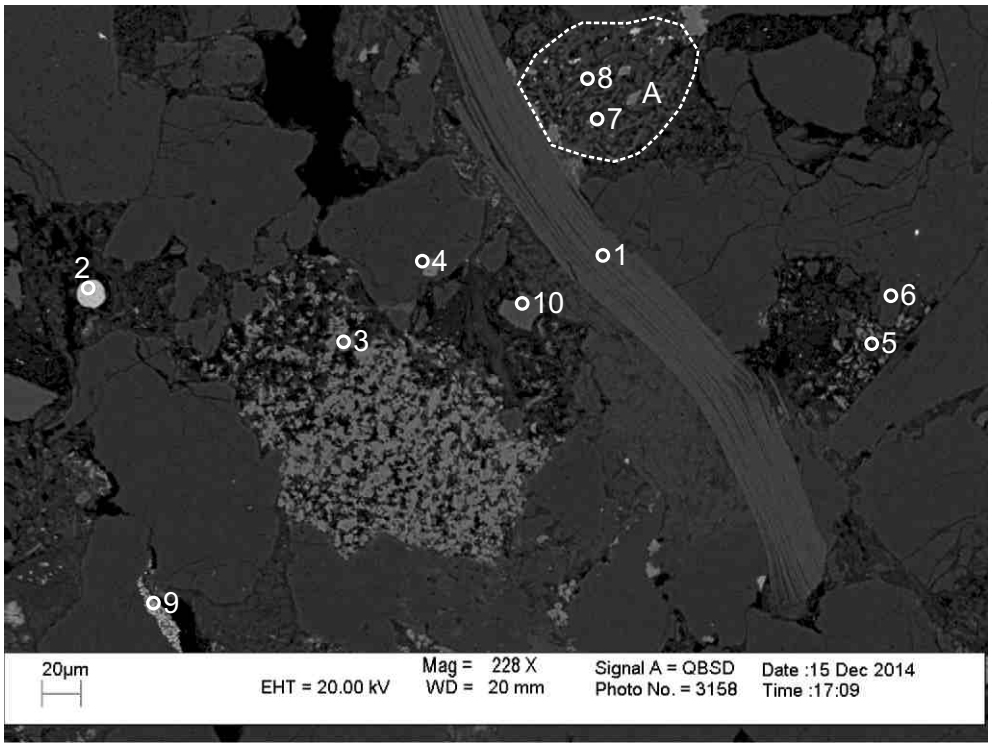

1: Muscovite
2: Pyrite+Other
3: Siderite
4:Fluorapatite+ Quartz
5: Siderite+ Albite+ Pyrite
6: Quartz
7: Illite
8: Albite+Other
9: Pyrite+ Albite+Other
10: K-Feldspar

Figure 2-1.17: Sample Newburn 4313.5m site 17 (SEM). Detrital muscovite (1) grain with some plastic deformation. Siderite (3) cement filling pore probably postdates kaolinite. Trachytic lithic clast (position A).

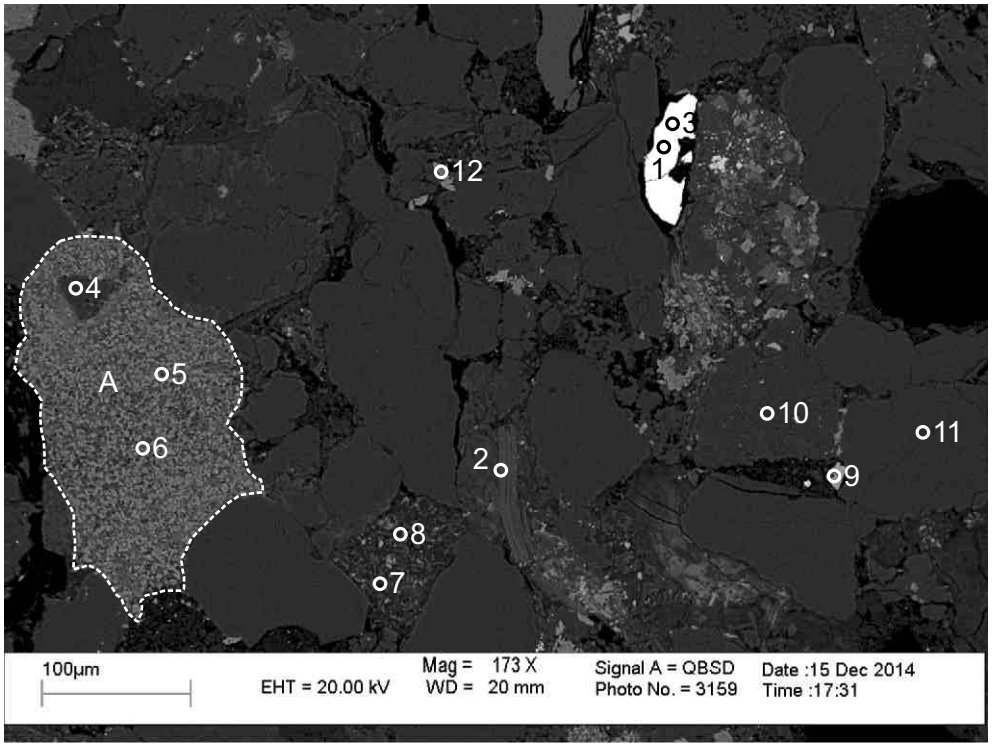

1: Monazite
2: Muscovite+ Other
3: Monazite
4: Quartz+ Albite
5: Chlorite+ Illite
6: Siderite+ Chlorite
7: Chlorite+ Illite
8: Albite
9: Titania+ Kaolinite
10: Quartz+ Albite
11: Quartz
12: Siderite

Figure 2-1.18: Sample Newburn 4313.5m site 18 (SEM). Detrital monazite (1,3) with recrystalized faces towards pore. Mudstone intraclast (position A) made up of chlorite (5,6), quartz (4), albite (4) and illite (5) cemented by early siderite (6). Albite (8) is partially replaced by illite and chlorite (7). kaolinite and titania (9) fill secondary porosity. Detrital muscovite grain (2).

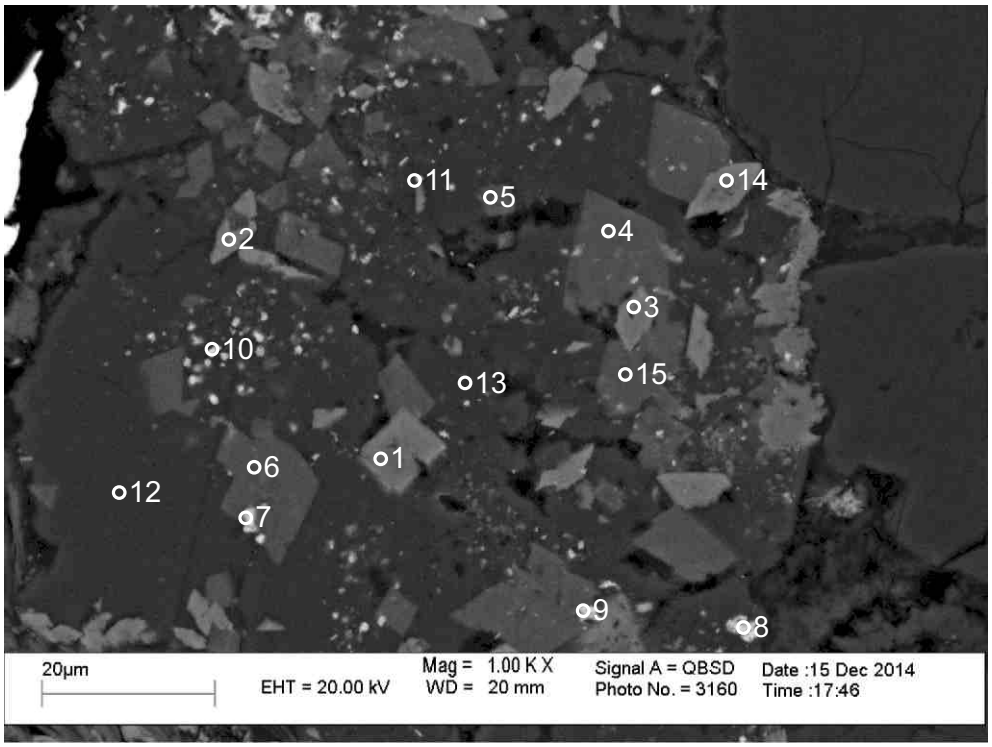

1: Siderite+ Chlorite
2: Siderite+ Albite
3: Siderite+ Chlorite
4: Ankerite+ Apatite
5: Fluorite+ Albite+ Other
6: Ankerite+ Quartz
7: Pyrite+ Dolomite
8: Pyrite+Other
9: Pyrite+Other
10: Albite+ Pyrite
11: Albite+ Pyrite
12: Albite
13: Albite
14: Mg-Siderite +Quartz
15: Ankerite

Figure 2-1.19: Sample Newburn 4313.5m site 19 (SEM). Original albite-rich lithic clast (13) has dissolution voids partly filled with siderite rhombohedrons (1,2,3,14) and ankerite (4,6,15). Siderite rhombohedrons (1,2) also rim albite (12).

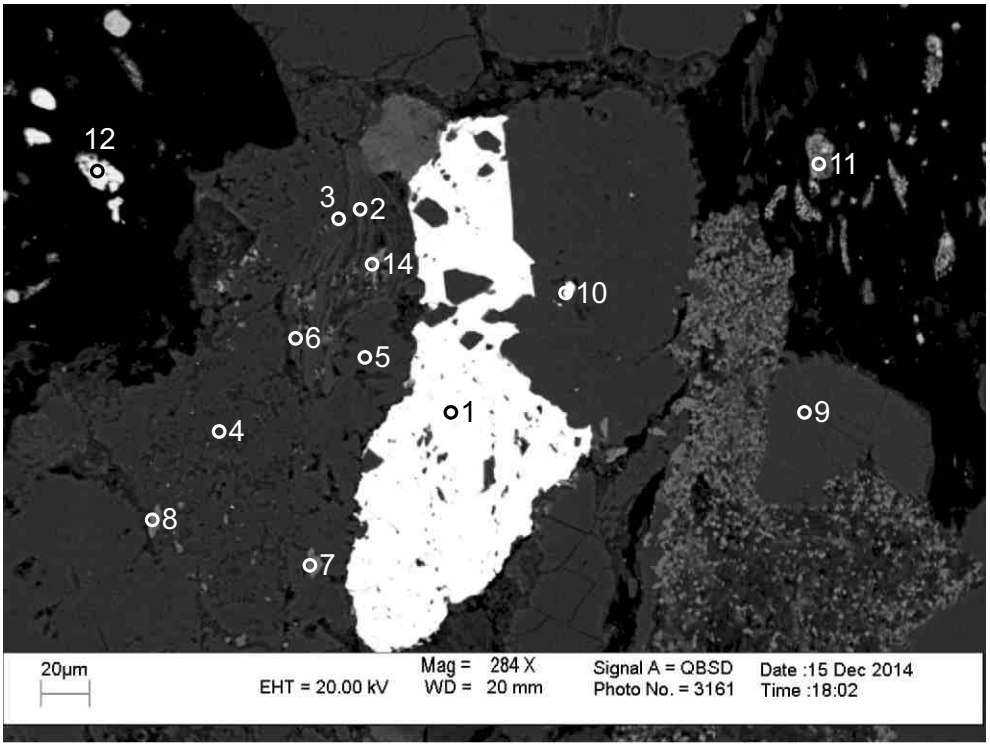

1: Barite
2: Illite+ Kaolinite
3: Illite+ Kaolinite
4: Quartz+ Albite
5: Albite
6: Muscovite+ Albite
7: Siderite+ Chlorite
8: Siderite+ Quartz
9: Oligoclase
10: Barite+ Albite
11: Pyrite+Illite
12: Sphalerite
13: Pyrite+ Other
14: Siderite+ Quartz

Figure 2-1.20: Sample Newburn 4313.5m site 20 (SEM). Diagenetic barite (1) forms along intergranular boundary of albite grains (5,10) as well as filling dissolution voids within albite (10). Illite and kaolinite (2,3,6) also fill dissolution voids within albite. Probably diagenetic sphalerite (12) fills pore.

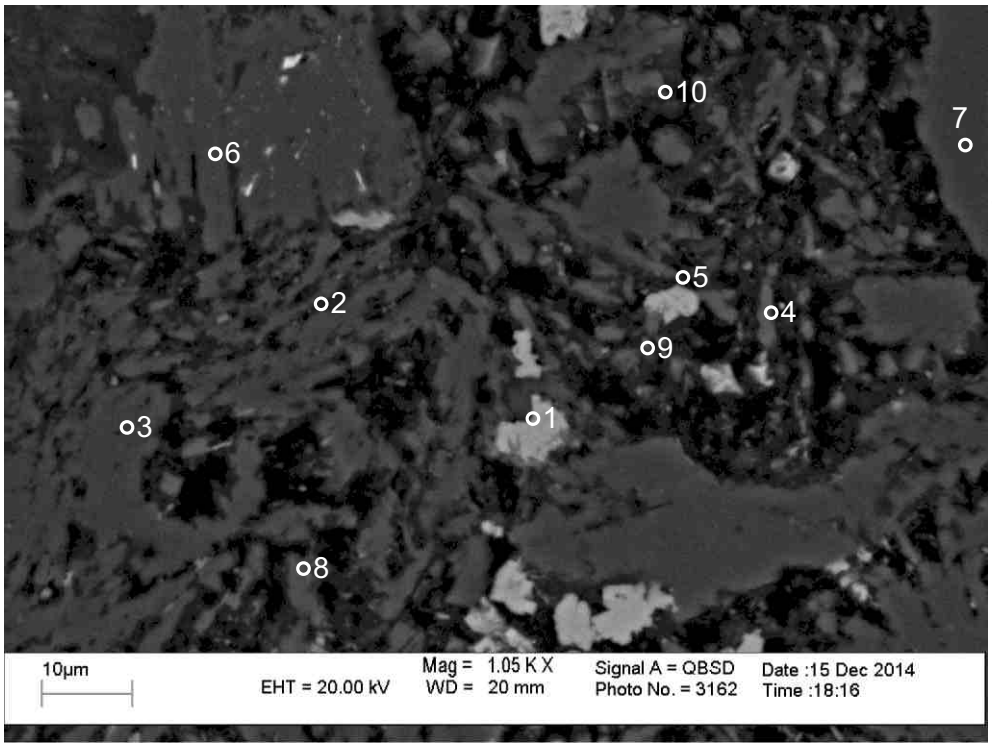

Figure 2-1.21: Sample Newburn 4313.5m site 21 (SEM). Original albite-rich lithic clast (2-6,8-9) has dissolution voids partly filled with titania (1)

Table 2-1: Scaning Electron Microscope chemical analyses of sample 4313.5m from Newburn H-23 well.

Sample	Site	Position	Mineral	SiO_2	TiO_2	Al_2O_3	FeO	MnO	MgO	CaO	Na_2O	K_2O	P_2O_5	SO_3	F	Cl	CoO	NiO	CuO	ZnO	SrO	ZrO_2	Nb_2O_5	MoO_3	Ag_2O	BaO	La_2O_3	Ce_2O_3	Nd_2O_3	Total	Actual Total
H-23 4313.5m	1	1	Zrn	31.49																		68.51								100	149
H-23 4313.5m	1	2	Brt											37.66												62.34				100	125
H-23 4313.5m	1	3	TiO_2		99.00		1.00																							100	132
H-23 4313.5m	1	4	TiO_2		97.58	1.23	1.18																							100	123
H-23 4313.5m	1	5	Qz	99.99																										100	139
H-23 4313.5m	1	6	Ab	69.27		18.65					12.08																			100	142
H-23 4313.5m	1	7	Ab	69.07		18.86					12.05																			100	147
H-23 4313.5m	1	8	TiO_2	1.90	94.80		3.31																							100	119
H-23 4313.5m	1	9	Fap+Chl	2.97		3.25	4.01		0.61	42.69			41.41		5.05															100	134
H-23 4313.5m	1	10	TiO_2+Other	0.66	97.01	0.77	1.53																							100	118
H-23 4313.5m	1	11	Ab	68.52		19.44				0.45	11.58																			100	146
H-23 4313.5m	1	12	Ab	79.81		12.43					7.77																			100	135
H-23 4313.5m	1	13	Ab	64.07	0.62	18.22	5.98		0.81		9.10	1.22																		100	107
H-23 4313.5m	2	1	Qz	99.99																										100	138
H-23 4313.5m	2	2	TiO_2+Other	0.73	84.00		3.14																12.15							100	119
H-23 4313.5m	2	3	Ab+TiO_2	38.66	38.52	10.96	2.53				9.33																			100	136
H-23 4313.5m	2	4	Py	1.26		0.38	29.38							68.99																100	178
H-23 4313.5m	2	5	Mix	39.98		17.16	13.92		1.21	2.53	2.60	1.59	2.25	18.75																100	95
H-23 4313.5m	2	6	Mix	41.46	0.53	18.99	24.40		4.68	2.71	3.69	0.93	2.59																	100	111
H-23 4313.5m	2	7	Sd+Chl	2.18		1.70	67.30	0.94	19.72	8.19																				100	68
H-23 4313.5m	2	8	Sd+Kfs	13.07		4.02	64.02	1.59	10.98	3.51	2.82																			100	79
H-23 4313.5m	2	9	Sd+Other	11.06		1.91	62.74	0.96	19.32	4.00																				100	72
H-23 4313.5m	2	10	Sd+Qz	1.56			75.40	0.90	12.87	9.26																				100	64
H-23 4313.5m	2	11	Sd+Chl	6.01		4.16	63.85		18.77	7.22																				100	69
H-23 4313.5m	2	12	TiO_2+Ab+Kfs	35.47	43.47	14.13	1.02				4.29	1.64																		100	119
H-23 4313.5m	2	13	Ab+TiO_2	38.33	36.68	11.47	0.80				9.75												2.99							100	141
H-23 4313.5m	2	14	Qz	97.03		1.87					0.62	0.48																		100	138
H-23 4313.5m	3	1	Fap+Ilt	24.39		14.38	7.60		2.37	19.90	1.15	2.08	21.36		6.81															100	129
H-23 4313.5m	3	2	Ilt+Sd+Ap	37.33		19.12	22.17		2.75	8.75	2.59	2.58	4.72																	100	86
H-23 4313.5m	3	3	Chl+Ilt	35.55		22.62	32.06		5.67	1.96		2.13																		100	88
H-23 4313.5m	3	4	Ab+Ap+Ilt	52.75		18.56	6.91		0.65	6.98	6.65	1.36	6.14																	100	89
H-23 4313.5m	3	5	Ab+Ap+Ilt	50.66		13.47	7.22		0.83	13.91	2.83	1.00	10.08																	100	61
H-23 4313.5m	3	6	Fap+Ab+Other	15.55		7.90	5.78		1.19	28.01	1.75	0.57	30.54		8.69															100	134
H-23 4313.5m	3	7	Chl+Other	34.16		23.05	33.09		6.14	1.62	0.73	1.23																		100	102
H-23 4313.5m	3	8	Ab+Ilt	45.71		21.88	19.84		3.88	2.99	3.25	2.45																		100	104
H-23 4313.5m	3	9	Ab	68.26		18.84	0.63				12.03	0.25																		100	140
H-23 4313.5m	3	10	Ap+Other	10.82		4.76	1.97			35.75	1.94	0.57	36.14		8.03															100	131
H-23 4313.5m	3	11	Ab+Ilt+Ap+Other	48.60	7.16	25.15	6.87		2.04	2.48	1.01	4.77	1.90																	100	91
H-23 4313.5m	3	12	Chl+Ap	34.55		22.09	27.54		4.44	4.88	1.15	0.71	4.65																	100	101
H-23 4313.5m	4	1	Sd+Other	11.94		7.22	57.13	0.92	16.60	5.58		0.61																		100	77
H-23 4313.5m	4	2	Chl+Ilt	45.35		24.73	17.56	0.53	9.25		0.65	1.92																		100	129
H-23 4313.5m	4	3	Ms	50.04	0.74	29.28	2.13		2.32		0.45	10.05																		95	126
H-23 4313.5m	4	4	Chl	31.83		19.24	19.89		12.88	0.54		0.61																		85	105
H-23 4313.5m	4	5	Qz	99.99																										100	140
H-23 4313.5m	4	6	Sd+Chl	3.38		2.80	67.62	0.92	16.52	8.77																				100	72
H-23 4313.5m	4	7	Kln	48.07	0.45	36.09	1.38																							86	115
H-23 4313.5m	4	8	Ms+Chl	53.99	0.98	27.72	7.05		4.56		0.62	5.06																		100	90
H-23 4313.5m	4	9	Sd+Chl	18.82	0.93	16.51	52.51	1.23	7.26	1.92		0.81																		100	92
H-23 4313.5m	4	10	Kln+Chl	50.42		37.83	9.04		1.36	0.92		0.45																		100	110
H-23 4313.5m	4	11	Kln+Ilt	53.63	1.25	38.96	3.81		0.85			1.52																		100	100
H-23 4313.5m	4	12	Sd+Other	24.71		13.94	41.05	0.83	10.46	3.85	1.54	1.99	1.65																	100	99
H-23 4313.5m	4	13	Chl	31.27		20.08	20.27		11.91	0.71		0.76																		85	106
H-23 4313.5m	4	14	Ilt+Qz	78.49		15.14	1.56		1.59			3.22																		100	124
H-23 4313.5m	4	15	Ms	49.79	0.76	31.07	2.00		2.08			9.30																		95	124
H-23 4313.5m	5	1	Ms	48.62		28.35	5.46		1.99			10.58																		95	127
H-23 4313.5m	5	2	Qz	99.99																										100	144
H-23 4313.5m	5	3	Py+Ms	16.22	9.54	7.71	16.80		0.55	0.66	1.17	1.78		43.75								1.82								100	163
H-23 4313.5m	5	4	Sd+Ap+Other	3.68		0.96	49.16	0.80	17.13	15.98			10.38	1.92																100	83
H-23 4313.5m	5	5	Qz	99.99																										100	141
H-23 4313.5m	5	6	Sd+Ms	18.03		8.33	52.39	0.83	14.71	4.25		1.46																		100	85

Table 2-1: Scaning Electron Microscope chemical analyses of sample 4313.5m from Newburn H-23 well.

Sample	Site	Position	Mineral	SiO_2	TiO_2	Al_2O_3	FeO	MnO	MgO	CaO	Na_2O	K_2O	P_2O_5	SO_3	F	Cl	CoO	NiO	CuO	ZnO	SrO	ZrO_2	Nb_2O_5	MoO_3	Ag_2O	BaO	La_2O_3	Ce_2O_3	Nd_2O_3	Total	Actual Total
H-23 4313.5m	5	7	Sd+Ms	51.38		30.18	5.25		1.71		0.46	11.03																		100	130
H-23 4313.5m	5	8	Ab	61.69		19.63	5.96		0.76	0.70	9.41	1.87																		100	98
H-23 4313.5m	5	9	Chl+TiO_2	33.41	6.97	21.13	23.94		14.54																					100	116
H-23 4313.5m	5	10	Qz	99.99																										100	148
H-23 4313.5m	5	11	Ab+Py+Qz	51.06	0.50	3.68	10.12				3.06			31.54																100	155
H-23 4313.5m	5	12	Qz+Ab	87.86		7.01				1.09	4.04																			100	149
H-23 4313.5m	5	13	Sd+Other	1.71	2.39		59.20		24.13	6.44				6.12																100	78
H-23 4313.5m	5	14	Ab	68.28	0.47	18.95					12.31																			100	148
H-23 4313.5m	6	1	TiO_2+Other	1.90	96.15	0.60	1.02			0.34																				100	116
H-23 4313.5m	6	2	Chl+Other	38.46	1.85	26.17	23.11		9.97			0.45																		100	118
H-23 4313.5m	6	3	Chl+Other	36.71	3.60	25.92	24.30		8.19		0.66	0.63																		100	106
H-23 4313.5m	6	4	Qz	99.99																										100	142
H-23 4313.5m	6	5	Sd+Qz	3.17			80.34	1.36	13.07	2.07																				100	70
H-23 4313.5m	6	6	Qz+Ilt	94.25		3.70	0.63					1.42																		100	137
H-23 4313.5m	6	7	Qz+Ilt	92.61		5.01	0.81		0.43			1.14																		100	137
H-23 4313.5m	6	8	Sd+Kln	5.18		2.97	61.87		18.41	11.59																				100	69
H-23 4313.5m	6	9	Sd+Ilt	27.30		16.80	40.45		11.74	3.18		0.55																		100	89
H-23 4313.5m	6	10	Chl	26.09		15.02	31.94		10.47	1.49																				85	89
H-23 4313.5m	6	11	Mg-Sd+Kln	16.81		11.07	51.90	0.79	14.51	4.94																				100	79
H-23 4313.5m	6	12	Chl+TiO_2	33.99	6.66	21.18	22.10		16.05																					100	121
H-23 4313.5m	6	13	TiO_2+Chl	19.06	51.58	12.17	13.43		2.90			0.87																		100	109
H-23 4313.5m	6	14	Mg-Sd+Kln	25.67		17.76	44.78	0.62	8.94	2.24																				100	86
H-23 4313.5m	6	15	Ms+Chl	49.67	0.93	25.94	13.19		2.98	0.77	0.81	5.69																		100	103
H-23 4313.5m	6	16	Mg-Sd+Kln	6.67		4.50	63.76		19.05	6.02																				100	71
H-23 4313.5m	7	1	Sp				3.41							53.39					2.64	40.57										100	201
H-23 4313.5m	7	2	TiO_2		96.28	1.93	1.80																							100	126
H-23 4313.5m	7	3	Ilt+Kln	56.77		35.67	1.24		1.06			5.24																		100	101
H-23 4313.5m	7	4	Sp				5.12							50.57					3.82	40.50										100	177
H-23 4313.5m	7	5	Sd+Ilt	9.95		4.97	65.96	1.19	11.44	5.40		1.07																		100	68
H-23 4313.5m	7	6	Qz+Ab	94.47		3.04					2.48																			100	131
H-23 4313.5m	7	7	Ab	69.93		18.88					10.73	0.46																		100	110
H-23 4313.5m	7	8	Ab	68.90		19.42					10.99	0.69																		100	121
H-23 4313.5m	7	9	Chl	31.08		22.15	26.06		4.56		0.63	0.52																		85	102
H-23 4313.5m	7	10	Ilt+Kln	56.52	1.83	34.81	1.51		0.60	0.84	0.53	3.37																		100	114
H-23 4313.5m	7	11	Mg-Sd+Ilt	27.60	2.87	11.41	37.99	0.77	12.25	2.64		4.48																		100	96
H-23 4313.5m	7	12	Ab	69.10		18.50					12.40																			100	156
H-23 4313.5m	7	13	Ab+Ilt	67.21		19.31	0.89			0.43	11.88	0.29																		100	138
H-23 4313.5m	7	14	Qz+Ilt	90.64	1.15	6.88						1.34																		100	139
H-23 4313.5m	7	15	Ab+Other	61.05	3.15	26.51	1.43		1.53		1.08	4.70				0.54														100	96
H-23 4313.5m	7	16	Mg-Sd+Qz	25.33			54.70		15.85	4.10																				100	83
H-23 4313.5m	7	17	Qz	99.19		0.81																								100	146
H-23 4313.5m	7	18	Mix	54.14	2.09	23.71	10.54		2.70	0.84	3.75	2.25																		100	119
H-23 4313.5m	7	19	Ab	68.78		17.69					11.76			1.27		0.52														100	58
H-23 4313.5m	7	20	Ab	67.66		18.46					12.90			0.97																100	120
H-23 4313.5m	7	21	Ms+TiO_2	44.47	23.79	23.03	1.60		1.41		0.94	4.77																		100	99
H-23 4313.5m	7	22	TiO_2+Ilt	32.71	42.94	17.38	1.31		1.01	0.57	0.84	3.26																		100	104
H-23 4313.5m	8	1	Mg-Sd+Chl	5.84		1.51	63.82		22.80	5.25		0.79																		100	71
H-23 4313.5m	8	2	Mg-Sd+Other	16.77		8.86	49.95		17.53	4.49	1.27	1.13																		100	83
H-23 4313.5m	8	3	Ab	66.19		20.97				2.27	10.57																			100	142
H-23 4313.5m	8	4	Mg-Sd+Qz	6.40		1.68	64.49	1.43	21.46	4.53																				100	72
H-23 4313.5m	8	5	TiO_2+Ilt	27.49	50.68	15.38	1.26		1.03	0.63	0.69	2.85																		100	107
H-23 4313.5m	8	6	TiO_2+Ilt	24.54	57.45	13.09	1.56			0.53	0.77	2.07																		100	107
H-23 4313.5m	8	7	TiO_2+Ilt	38.61	33.46	20.31	1.65		1.18		0.97	3.81																		100	106
H-23 4313.5m	8	8	Ms	56.41		28.81	1.96		1.77		0.73	5.33																		95	105
H-23 4313.5m	8	9	Ms	55.73	0.84	28.70	1.61		1.24		0.88	6.00																		95	102
H-23 4313.5m	8	10	Sd+Kln	7.06		7.39	62.66	1.23	14.91	6.76																				100	79
H-23 4313.5m	8	11	Kln+Qz+Other	54.61	1.30	39.89	2.88		0.66			0.65																		100	105
H-23 4313.5m	8	12	Ab	69.48		18.50					12.01																			100	135
H-23 4313.5m	8	13	Kln+Chl	50.83		35.16	10.41		1.49	0.78		1.32																		100	79

Table 2-1: Scaning Electron Microscope chemical analyses of sample 4313.5m from Newburn H-23 well.

Sample	Site	Position	Mineral	SiO_2	TiO_2	Al_2O_3	FeO	MnO	MgO	CaO	Na_2O	K_2O	P_2O_5	SO_3	F	Cl	CoO	NiO	CuO	ZnO	SrO	ZrO_2	Nb_2O_5	MoO_3	Ag_2O	BaO	La_2O_3	Ce_2O_3	Nd_2O_3	Total	Actual Total
H-23 4313.5m	8	14	Ilt	53.42	0.54	26.39	1.93		1.47		0.80	5.45																		90	110
H-23 4313.5m	8	15	Dm	49.46		3.72	5.11		27.36	2.90	0.97	0.79			9.30	0.41														100	79
H-23 4313.5m	8	16	Ms+Other	54.12	7.87	27.78	1.89		1.56		1.28	5.50																		100	108
H-23 4313.5m	8	17	TiO_2+Ilt+Other	29.56	46.14	17.46	1.30		0.85	0.66	0.88	3.14																		100	105
H-23 4313.5m	8	18	TiO_2+Ilt+Other	33.18	41.65	17.95	1.20		1.01	0.57	1.21	3.24																		100	109
H-23 4313.5m	8	19	Ab+Ilt	63.88		24.41	2.34		1.26		4.85	2.54				0.71														100	95
H-23 4313.5m	8	20	Ms+Other	52.03	2.34	29.34	2.10		1.19	2.20	1.74	5.61		2.97		0.50														100	84
H-23 4313.5m	8	21	Ab	68.84		18.61					12.54																			100	149
H-23 4313.5m	8	22	Ank+Ilt	11.06		3.25	23.62	0.75	14.04	44.97	1.75	0.55																		100	75
H-23 4313.5m	8	23	Ab	68.95		18.76					12.27																			100	149
H-23 4313.5m	9	1	TiO_2		100.00																									100	117
H-23 4313.5m	9	2	Qz+TiO_2	87.07	12.93																									100	131
H-23 4313.5m	9	3	Qz	99.99																										100	139
H-23 4313.5m	9	4	Hole	45.01		22.07								32.91																100	6
H-23 4313.5m	9	5	Hole	49.97		24.13						5.78		20.13																100	11
H-23 4313.5m	9	6	TiO_2+Ilt	29.22	48.09	16.42	0.96		0.88	0.49	0.88	3.08																		100	110
H-23 4313.5m	9	7	Ms+Ab	56.92	4.15	28.15	1.61		1.66		1.12	6.09				0.29														100	103
H-23 4313.5m	9	8	Sd+Other	8.64		1.21	56.37		19.57	13.47		0.72																		100	67
H-23 4313.5m	9	9	Fap+Ab	20.17		5.84				31.64	2.32		33.66		6.36															100	142
H-23 4313.5m	9	10	Ab	68.43		19.42				0.48	11.65																			100	142
H-23 4313.5m	9	11	Ms	54.91		27.66	1.54		1.84		0.89	5.48			2.40	0.27														95	115
H-23 4313.5m	9	12	Ab	66.94		20.20	1.78		0.56	0.56	8.68	1.29																		100	120
H-23 4313.5m	9	13	Sd+Chl	5.43		1.21	70.19	1.25	17.21	4.70																				100	69
H-23 4313.5m	9	14	Mg-Sd+Ab	22.76		7.92	47.23	1.28	12.14	3.97	4.72																			100	93
H-23 4313.5m	9	15	Ms	55.55	0.71	27.46	1.80		1.92	0.79	0.95	5.82																		95	103
H-23 4313.5m	9	16	Sd+Ab	21.73		4.52	54.34	0.89	13.00	3.57	1.95																			100	79
H-23 4313.5m	9	17	Qz+Kln	92.37		6.93						0.69																		100	121
H-23 4313.5m	9	18	Qz	99.99																										100	137
H-23 4313.5m	10	1	TiO_2	0.71	99.28																									100	114
H-23 4313.5m	10	2	TiO_2	1.26	96.38	0.76	1.58																							100	113
H-23 4313.5m	10	3	TiO_2+Ms	25.56	51.39	19.03	2.77					1.24																		100	110
H-23 4313.5m	10	4	Mg-Sd+Other	2.87		1.25	61.51		23.51	9.08				1.80																100	71
H-23 4313.5m	10	5	TiO_2	1.37	97.97	0.66																								100	116
H-23 4313.5m	10	6	TiO_2		100.00																									100	116
H-23 4313.5m	11	1	TiO_2+Chl	1.37	95.81	1.61	1.21																							100	121
H-23 4313.5m	11	2	Fap							46.82			45.51		6.58													1.09		100	144
H-23 4313.5m	11	3	Sd+Ab	23.12		7.05	46.97	1.12	15.27	2.81	3.67																			100	91
H-23 4313.5m	11	4	Ab	69.44		18.40					12.16																			100	147
H-23 4313.5m	11	5	Ms+Ab	58.25		28.21	2.89				2.60	8.03																		100	138
H-23 4313.5m	11	6	Ab+Kfs	61.12	1.12	25.21	0.46		0.73		8.09	3.26																		100	155
H-23 4313.5m	11	7	Chl+Ab+Ilt	36.73		27.04	24.11		9.62		1.29	1.22																		100	132
H-23 4313.5m	12	1	Zrn	30.33						1.41												68.26								100	129
H-23 4313.5m	12	2	Fap							46.73			44.55		8.73															100	136
H-23 4313.5m	12	3	Sd+Qz	12.54			72.07	1.47	10.70	3.25																				100	69
H-23 4313.5m	12	4	Ms	54.55		29.73	2.00		1.36		0.82	6.54																		95	101
H-23 4313.5m	12	5	Ilt	52.24		22.54	3.95		3.69			7.59																		90	118
H-23 4313.5m	12	6	Ms	51.96	0.57	26.67	2.85		3.56			9.39																		95	122
H-23 4313.5m	12	7	Kln+Ilt	63.47		31.37	1.52		0.61	0.52		2.52																		100	102
H-23 4313.5m	12	8	Sd+Qz	1.50			64.62		26.66	7.22																				100	68
H-23 4313.5m	12	9	TiO_2+Other	4.41	89.93	2.32	3.33																							100	104
H-23 4313.5m	12	10	Chl+Sd	24.81		18.25	47.01		5.60	3.74		0.58																		100	61
H-23 4313.5m	12	11	Ilt+Other	58.83		24.00	3.74		4.06			9.37																		100	121
H-23 4313.5m	12	12	Chl	32.02		16.88	23.24		12.87																					85	104
H-23 4313.5m	12	13	Mg-Sd	0.98			37.49		13.05	4.47																				56	65
H-23 4313.5m	12	14	Sd+Other	5.52			71.59	1.15	16.93	4.10		0.72																		100	68
H-23 4313.5m	13	1	Py				27.03	1.25						71.74																100	234
H-23 4313.5m	13	2	Chl+Cal	29.59		24.64	35.61		6.10	4.06																				100	81
H-23 4313.5m	13	3	TiO_2+Sd	1.86	84.47		11.42		1.44	0.83																				100	91
H-23 4313.5m	13	4	Qz	99.99																										100	132

Table 2-1: Scaning Electron Microscope chemical analyses of sample 4313.5m from Newburn H-23 well.

Sample	Site	Position	Mineral	SiO_2	TiO_2	Al_2O_3	FeO	MnO	MgO	CaO	Na_2O	K_2O	P_2O_5	SO_3	F	Cl	CoO	NiO	CuO	ZnO	SrO	ZrO_2	Nb_2O_5	MoO_3	Ag_2O	BaO	La_2O_3	Ce_2O_3	Nd_2O_3	Total	Actual Total
H-23 4313.5m	13	5	Dm+Sd	54.49		6.22	14.20		21.26	1.87						1.96														100	27
H-23 4313.5m	13	6	Qz	99.99																										100	134
H-23 4313.5m	13	7	Dm+Sd	40.88		4.88	25.69		23.13	2.60	1.35	0.70				0.78														100	51
H-23 4313.5m	13	8	Kln+Other	55.06		38.32	3.72		0.78		0.58	1.55																		100	103
H-23 4313.5m	13	9	Kln	50.34		35.66																								86	109
H-23 4313.5m	13	10	Qz	99.99																										100	134
H-23 4313.5m	13	11	Chl+Sd	24.37		18.44	44.55		8.90	3.75																				100	80
H-23 4313.5m	13	12	Dm+Cal	49.09		4.44	8.01		21.14	12.72	1.46	1.12		2.02																100	62
H-23 4313.5m	13	13	TiO_2		98.35		1.65																							100	111
H-23 4313.5m	13	14	Ilt+TiO_2	58.51	1.77	26.72	3.20		3.15			6.64																		100	107
H-23 4313.5m	14	1	Kln+Chl+TiO_2	0.66	99.33																									100	105
H-23 4313.5m	14	2	TiO_2		98.38		1.62																							100	103
H-23 4313.5m	14	3	TiO_2		100.00																									100	105
H-23 4313.5m	14	4	Py+Chl	1.33		0.93	24.46		3.12					70.19																100	199
H-23 4313.5m	14	5	Chl+TiO_2	43.98	9.94	17.50	17.25		8.69			1.49				1.15														100	28
H-23 4313.5m	14	6	TiO_2		100.00																									100	106
H-23 4313.5m	14	7	Py+Other				26.87		1.61		0.51			70.99																100	207
H-23 4313.5m	14	8	Py+Other	2.05		1.11	26.76			0.63	1.69	0.29		67.47																100	180
H-23 4313.5m	14	9	TiO_2+Qz	5.37	94.63																									100	99
H-23 4313.5m	14	10	Sd+Chl	8.49		4.08	77.64	1.82	4.23	3.75																				100	40
H-23 4313.5m	14	11	Sd+Qz	3.10			81.61	1.46	11.54	2.29																				100	61
H-23 4313.5m	14	12	Sd+Qz	3.04			77.70	1.64	13.75	3.86																				100	63
H-23 4313.5m	15	1	Dm+Other	47.40		6.88	14.55		20.15	1.92	2.02	1.22			5.43	0.44														100	70
H-23 4313.5m	15	2	Dm+Other	47.32		7.22	9.15		23.43	3.12		0.99		1.25	6.94	0.60														100	66
H-23 4313.5m	15	3	Dm+Other	45.65		4.86	13.42		23.36	1.90	1.08	0.61		1.37	7.11	0.64														100	70
H-23 4313.5m	15	4	Ab	69.33		18.78					11.89																			100	132
H-23 4313.5m	16	1	Sd+Ilt	27.66		19.31	41.62		7.79	2.98		0.63																		100	76
H-23 4313.5m	16	2	Sd+Chl	9.60		6.31	64.65	0.89	13.15	5.39																				100	61
H-23 4313.5m	16	3	Zrn	31.19																		68.81								100	128
H-23 4313.5m	16	4	Sd				48.34	2.78		4.87																				56	60
H-23 4313.5m	16	5	Ab+Sd	27.75		8.71	42.58	0.97	7.49	2.87	7.33			2.30																100	78
H-23 4313.5m	16	6	Fap+Other	0.98		0.70				46.31	0.69	0.23	43.29		7.79															100	124
H-23 4313.5m	16	7	Ab	69.29		18.76					11.96																			100	123
H-23 4313.5m	16	8	Mg-Sd+Qz	1.86			64.75	0.89	24.79	7.72																				100	61
H-23 4313.5m	16	9	Sd+Ilt	46.72		8.77	29.83	1.54	2.69	7.37		1.42		1.67																100	42
H-23 4313.5m	16	10	Dm+Other	47.25		4.67	7.82		19.68	6.35	1.67	1.22			10.69	0.65														100	70
H-23 4313.5m	16	11	Qz	99.99																										100	124
H-23 4313.5m	16	12	Sd+Ilt	28.00		16.59	41.33		7.71	3.68		2.69																		100	78
H-23 4313.5m	17	1	Ms	47.22	0.52	31.60	3.62		1.07		0.77	9.89				0.30														95	112
H-23 4313.5m	17	2	Py+Other	0.30			28.11				0.74			70.87																100	213
H-23 4313.5m	17	3	Sd				42.26	0.66	9.56	3.53																				56	61
H-23 4313.5m	17	4	Fap+Qz	36.37						26.82	0.62		28.64	0.67	6.63	0.24														100	137
H-23 4313.5m	17	5	Sd+Ab+Py	12.88		8.09	57.80		8.13	4.95	2.63			1.87		3.65														100	34
H-23 4313.5m	17	6	Qz	99.99																										100	129
H-23 4313.5m	17	7	Ilt	52.74		22.14	1.91		1.22		4.84	4.36			2.38	0.41														90	126
H-23 4313.5m	17	8	Ab+Other	63.94		18.69	1.33				10.49	0.82		2.07	2.39	0.28														100	122
H-23 4313.5m	17	9	Py+Ab+Other	4.60		1.47	26.99				1.02	0.23		65.67																100	179
H-23 4313.5m	17	10	Kfs	66.79		18.01					0.75	14.44																		100	124
H-23 4313.5m	18	1	Mzn							1.32			37.69		-0.83										3.28		16.02	32.65	9.88	100	110
H-23 4313.5m	18	2	Ms+Other	50.29	1.05	32.42	4.30		1.19			10.73																		100	116
H-23 4313.5m	18	3	Mzn							1.06			37.33		-1.01										3.78		16.24	31.36	11.24	100	110
H-23 4313.5m	18	4	Qz+Ab	87.32		8.30					4.40																			100	119
H-23 4313.5m	18	5	Chl+Ilt	36.64	0.83	24.15	29.25		5.41	1.13	1.09	1.48																		100	86
H-23 4313.5m	18	6	Sd+Chl	10.18		8.62	61.84		13.60	5.76																				100	63
H-23 4313.5m	18	7	Chl+Ilt	53.52	0.77	24.26	10.24		5.06	0.83	2.86	2.46																		100	88
H-23 4313.5m	18	8	Ab	61.99	1.57	20.43	4.07		1.38		9.61	0.94																		100	114
H-23 4313.5m	18	9	TiO_2+Kln	4.02	93.08	2.89																								100	107
H-23 4313.5m	18	10	Qz+Ab	91.07		5.84					2.82	0.28																		100	134
H-23 4313.5m	18	11	Qz	99.99																										100	134
H-23 4313.5m	18	12	Sd				43.06	1.23	8.54	3.18																				56	62

Table 2-1: Scaning Electron Microscope chemical analyses of sample 4313.5m from Newburn H-23 well.

Sample	Site	Position	Mineral	SiO_2	TiO_2	Al_2O_3	FeO	MnO	MgO	CaO	Na_2O	K_2O	P_2O_5	SO_3	F	Cl	CoO	NiO	CuO	ZnO	SrO	ZrO_2	Nb_2O_5	MoO_3	Ag_2O	BaO	La_2O_3	Ce_2O_3	Nd_2O_3	Total	Actual Total
H-23 4313.5m	19	1	Sd+Chl	3.36		1.19	67.33	1.20	21.61	5.32																				100	65
H-23 4313.5m	19	2	Sd+Ab	13.76		4.76	60.93	1.28	11.49	4.20	3.59																			100	77
H-23 4313.5m	19	3	Sd+Chl	5.35	0.85	1.49	67.86	1.42	17.33	5.69																				100	67
H-23 4313.5m	19	4	Ank+Ap				26.44		18.11	51.73			3.74																	100	64
H-23 4313.5m	19	5	Fl+Ab+Other	23.89		7.01	10.02		5.85	25.84	5.66		1.28		20.42															100	109
H-23 4313.5m	19	6	Ank+Qz	1.78			27.62		18.97	51.63																				100	60
H-23 4313.5m	19	7	Py+Dol	0.96			27.80		5.19	14.05				51.99																100	135
H-23 4313.5m	19	8	Py+Other	8.02		2.44	23.29			1.04	2.01	0.22		62.68				0.33												100	218
H-23 4313.5m	19	9	Py+Other	6.44		1.76	27.74		1.81	4.24	1.87			54.69				1.50												100	169
H-23 4313.5m	19	10	Ab+Py	24.86		7.20	17.07			0.62	5.80			44.45																100	193
H-23 4313.5m	19	11	Ab+Py	52.60		14.68	5.85			1.39	10.00			15.46																100	143
H-23 4313.5m	19	12	Ab	68.86		19.05					12.09																			100	130
H-23 4313.5m	19	13	Ab	68.95	0.60	18.10				0.32	11.68	0.37																		100	127
H-23 4313.5m	19	14	Mg-Sd+Qz	3.87			67.57	1.51	20.64	6.41																				100	65
H-23 4313.5m	19	15	Ank	2.41			15.33	0.49	10.44	27.32										0.01										56	66
H-23 4313.5m	20	1	Brt											37.86			0.06				1.53					60.57				100	120
H-23 4313.5m	20	2	Ilt+Kln	52.54	0.58	33.09	2.96		1.76		0.90	5.53			2.62															100	107
H-23 4313.5m	20	3	Ilt+Kln	55.45	0.55	28.55	4.18		2.52		1.08	4.99			2.67															100	108
H-23 4313.5m	20	4	Qz+Ab	97.33		1.25					0.75			0.65																100	123
H-23 4313.5m	20	5	Ab	68.82		19.10					12.08																			100	124
H-23 4313.5m	20	6	Ilt+Ab	45.37	0.57	25.96	16.47		3.50	1.68	1.01	5.44																		100	86
H-23 4313.5m	20	7	Sd+Chl	13.33		4.29	61.02	0.93	13.98	3.36	3.10																			100	69
H-23 4313.5m	20	8	Sd+Qz	12.04	0.82		68.54	1.42	13.76	3.44																				100	65
H-23 4313.5m	20	9	Oli	65.91		21.18				2.73	10.17																			100	126
H-23 4313.5m	20	10	Brt+Ab	15.64		5.67					4.44			28.37			-0.11									46.02				100	140
H-23 4313.5m	20	11	Py+Ilt	4.06		2.19	26.01					0.36		67.37																100	172
H-23 4313.5m	20	12	Sp				4.01							52.96						43.04										100	187
H-23 4313.5m	20	13	Py+Other	2.37		0.83	26.76				0.57			69.47																100	233
H-23 4313.5m	20	14	Sd+Qz	2.03			80.84		11.13	5.99																				100	59
H-23 4313.5m	21	1	TiO_2+Other	2.10	92.01	1.04	1.27			1.76			1.81																	100	112
H-23 4313.5m	21	2	Ab+Ap	65.29		17.57				2.63	11.77	0.34	2.41																	100	132
H-23 4313.5m	21	3	Ab+Other	68.39		18.42				0.73	12.15	0.31																		100	132
H-23 4313.5m	21	4	Ab+Ap	65.35	0.70	18.95	0.77			1.44	8.37	1.11	0.87											2.43						100	100
H-23 4313.5m	21	5	Ab+Other	59.13	6.27	17.02	0.94			4.07	8.05	0.66	3.00	0.85																100	78
H-23 4313.5m	21	6	Ab	68.45		19.31			0.46		11.23	0.55																		100	131
H-23 4313.5m	21	7	Qz	99.99																										100	135
H-23 4313.5m	21	8	Ab+Ap	65.03		18.01				3.27	11.16		2.54																	100	126
H-23 4313.5m	21	9	Ab+Other	66.42	1.42	18.40				1.36	10.49	0.60	1.31																	100	108
H-23 4313.5m	21	10	Ab+Ap	49.71		16.67	0.63		0.81	12.48	5.08	0.92	13.70																	100	82

Appendix 2-2: SEM-BSE images and EDS mineral analyses for sample Newburn H-23 4318.5m

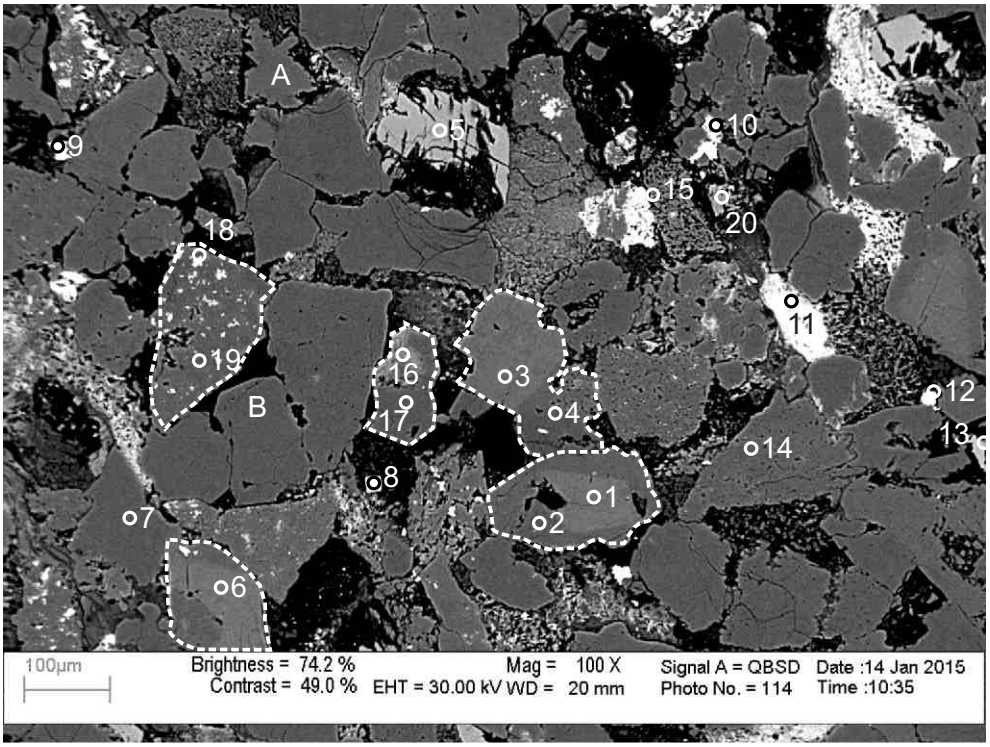

1: Albite
2: Quartz
3: Albite
4: Quartz
5: K-Feldspar
6: Albite
7: Quartz
8: Titania
9: Titania
10: Chlorite+ Titania+ Other
11: Titania+ Quartz+ Other
12: Albite
13: K-Feldspar
14: Albite+ Quartz
15: Albite
16: K-Feldspar
17: Quartz
18: Albite+ Quartz
19: Quartz+ Albite
20: Muscovite

Figure 2-2.1: Sample Newburn 4318.5m site 1 (SEM). Detrital K-feldspar (5,13) partially dissolved. Titania in dissolution voids (8,9,11). Trachytic lithic clast (15). Detrital muscovite partially dissolved (20). Granitoid lithic clasts (1,2,3,4,6,16,17,18,19) some of which are partially dissolved (16,17) and composed of albite, quartz and K-feldspar.

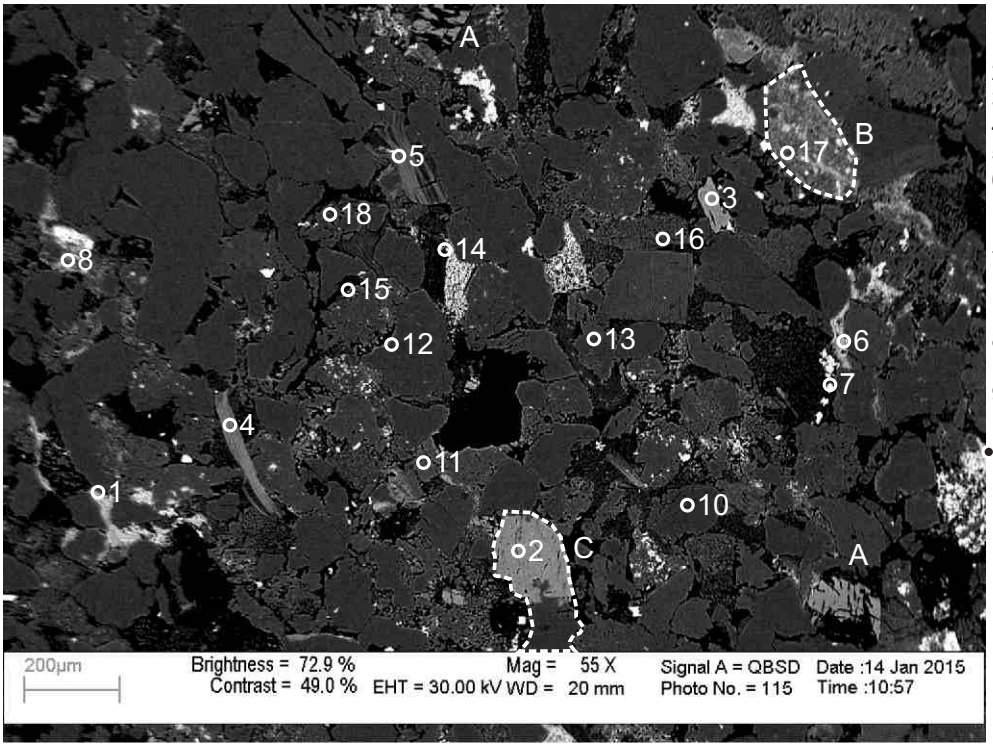

1: Chlorite+ Other
2: K-Feldspar
3: K-Feldspar
4: Muscovite
5: Muscovite
6: Quartz+ Chlorite+ Pyrite
7: Quartz+ Titania+ Other
8: Muscovite+ Chlorite
9: Chlorite+ Siderite
10: Quartz
11: Albite
12: Quartz
13: Albite
14: Chlorite+ Hole
15: Albite
16: Albite
17: Quartz+ Chlorite+ Muscovite
18: Quartz+ Other

Figure 2-2.2: Sample Newburn 4318.5m site 2 (SEM). Partially dissolved K-feldspar (positions A) generates secondary porosity. Titania (7) cuts through pore filled by kaolinite. Chlorite and pyrite (6) form along the intergranular boundry between quartz grains. Shale clast (position B) containing chloritized muscovite (17), and quartz. Chlorite partially fills pore possibly replacing lithic clast. Granitoid lithic clast (position C) composed of partially dissolved K-feldspar (2) and quartz.

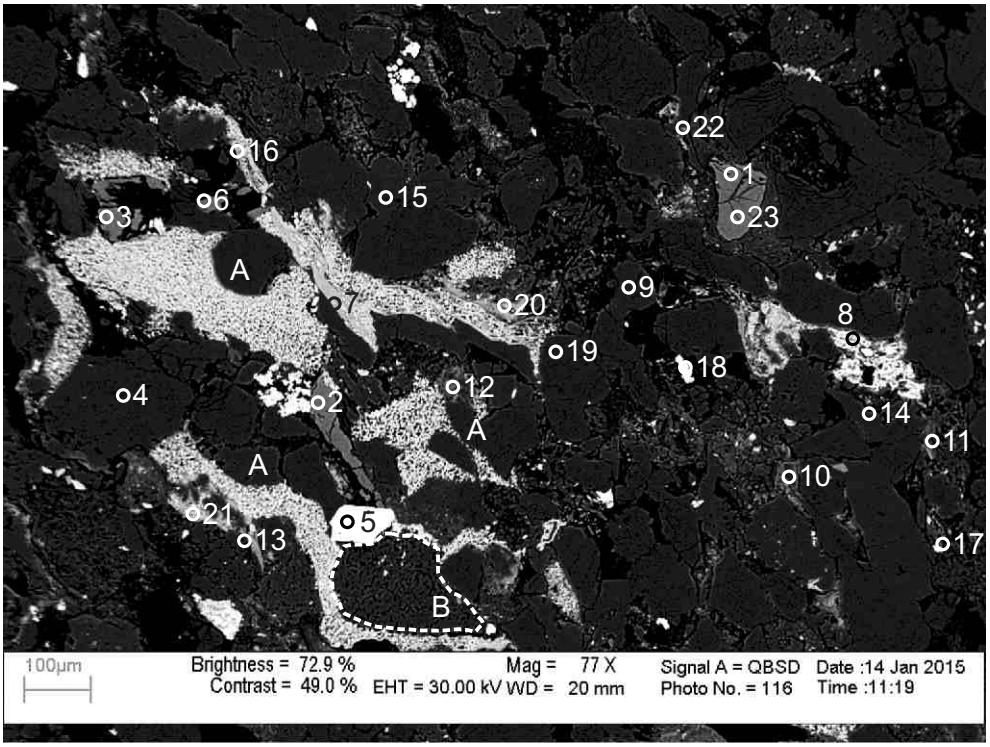

1: K-Feldspar
2: K-Feldspar
3: K-Feldspar
4: Quartz
5: Zircon
6: K-Feldspar
7: Chlorite
8: Titania+ Other
9: Albite
10: Muscovite+ Chlorite
11: Muscovite+ Chlorite
12: K-Feldspar +Chlorite
13: Muscovite+ Chlorite
14: Albite
15: Albite
16: Chlorite+ Siderite
17: Albite
18: Titania+ Muscovite+ Other
19: Quartz
20: Chlorite
21: Chlorite
22: Quartz+ Other
23: K-Feldspar

Figure 2-2.3: Sample Newburn 4318.5m site 3 (SEM). partially dissolved K-feldspar (3). Muscovite completely replaced by chlorite (7). Plastically deformed intraclast of siderite and chlorite rims quartz grains (positions A) and fill pores. Chlorite and siderite intraclast (16) fill pore with detrital K-feldspar relics. Trachytic lithic clast (position B). Partially dissolved K-feldspar (3) generates secondary porosity. Titania (8) cuts chlorite in pore. Diagenetic zircon (5) has straight crystal outlines cuts and framework grains such as quartz and K-feldspar (2).

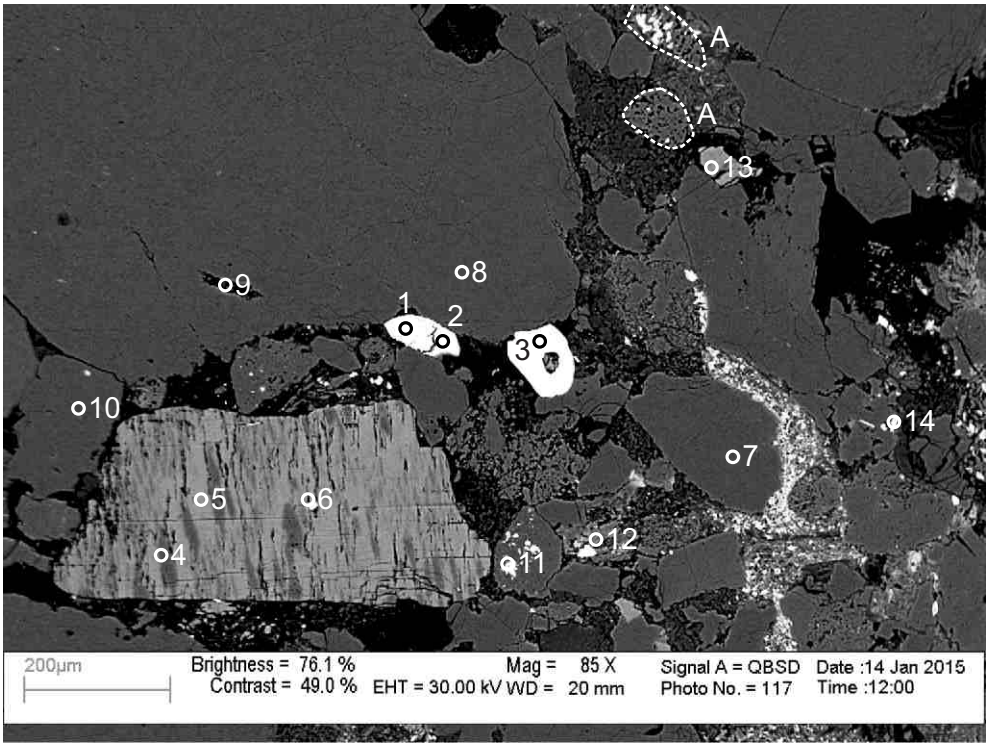

1: Spinel
2: Spinel
3: Zircon
4: Albite
5: K-Feldspar
6: K-Feldspar
7: Quartz
8: Quartz
9: Quartz+ Kaolinite
10: Quartz
11: Pyrite+ Albite
12: Muscovite+ Chlorite
13: K-Feldspar
14: Quartz+ Kaolinite+ Titania

Figure 2-2.4: Sample Newburn 4318.5m site 4 (SEM). Perthite grain (4-6). Detrital spinel (1,2) and zircon (3) with dissolution void. Chloritized muscovite (12). Kaolinite and titania fill porosity. Pyrite (11) fills dissolution in albite. Trachytic lithic clast (positions A).

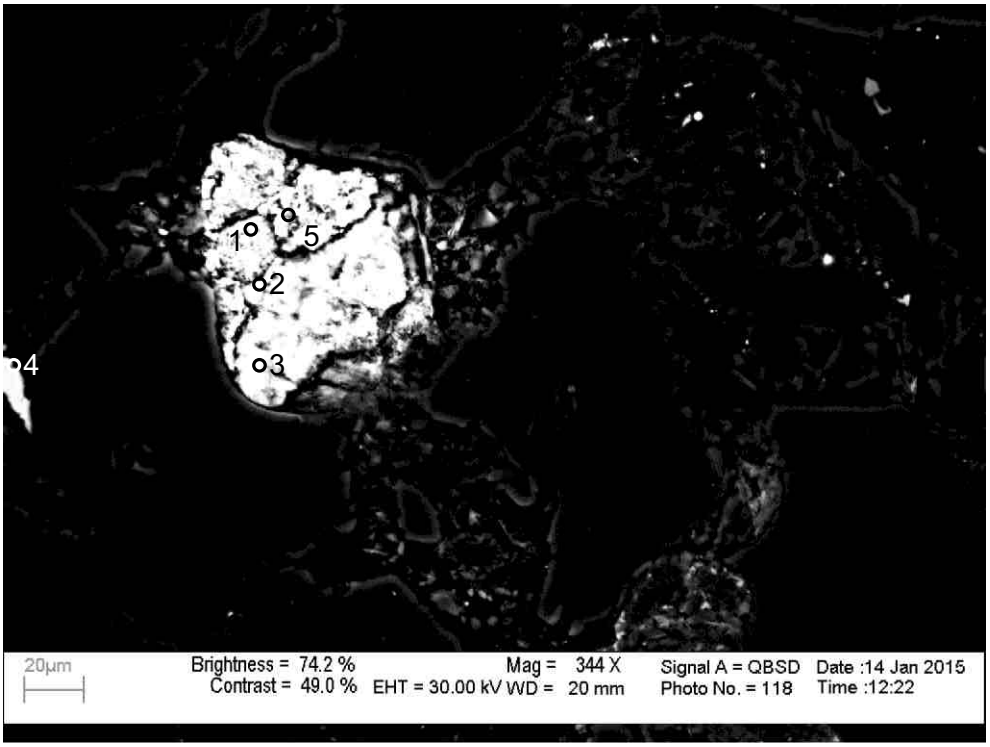

1: Spinel+ Other
2: Spinel+ Other
3: Spinel+ Other
4: Titania
5: Spinel+ Other

Figure 2-2.5: Sample Newburn 4318.5m site 5 (SEM). Detrital spinel grain with dissolution voids (1,2,3,5).

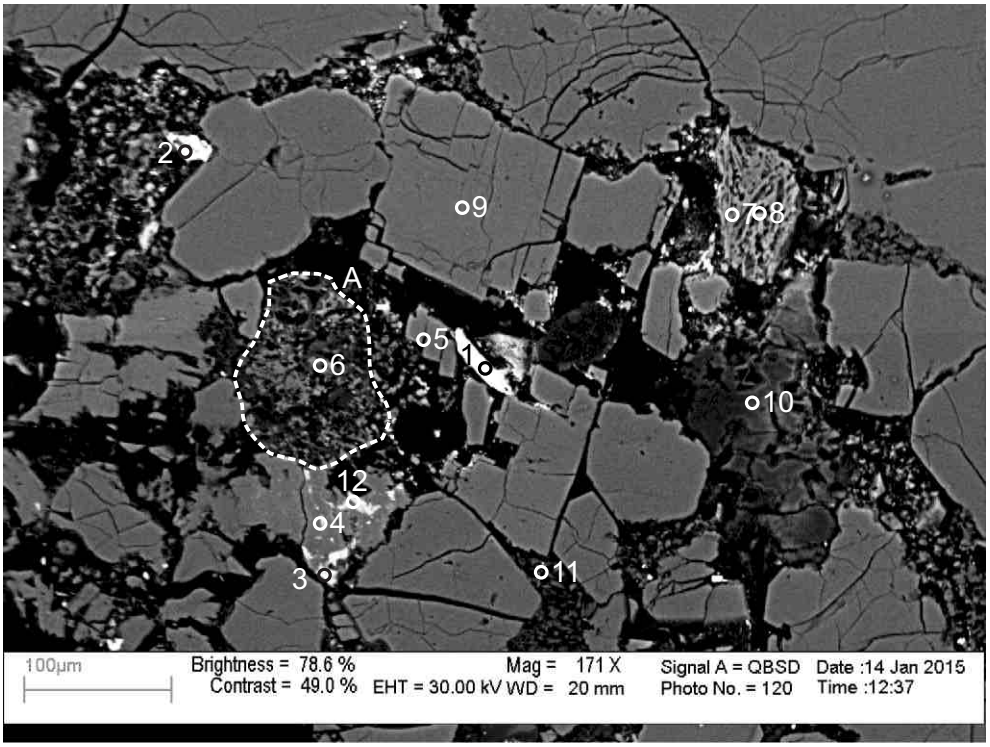

1: Hematite+ Quartz
2: Titania+ Kaolinite
3: Chlorite
4: Albite+ Apatite
5: Albite
6: Albite+ Kaolinite+ Illite
7: Albite+ Apatite
8: Albite+ Apatite
9: Albite
10: Muscovite
11: Kaolinite
12: Chlorite

Figure 2-2.6: Sample Newburn 4318.5m site 6 (SEM). Chlorite (3,12) and apatite (4) fill dissolution voids in albite (4). Titania (2) cuts kaolinite which filling a pore. Diagenetic hematite (1) cuts albite (5). Kaolinite and illite (6) fill dissolution voids in partially dissolved trachytic lithic clast (position A). Apatite engulfs albite grain (7,8).

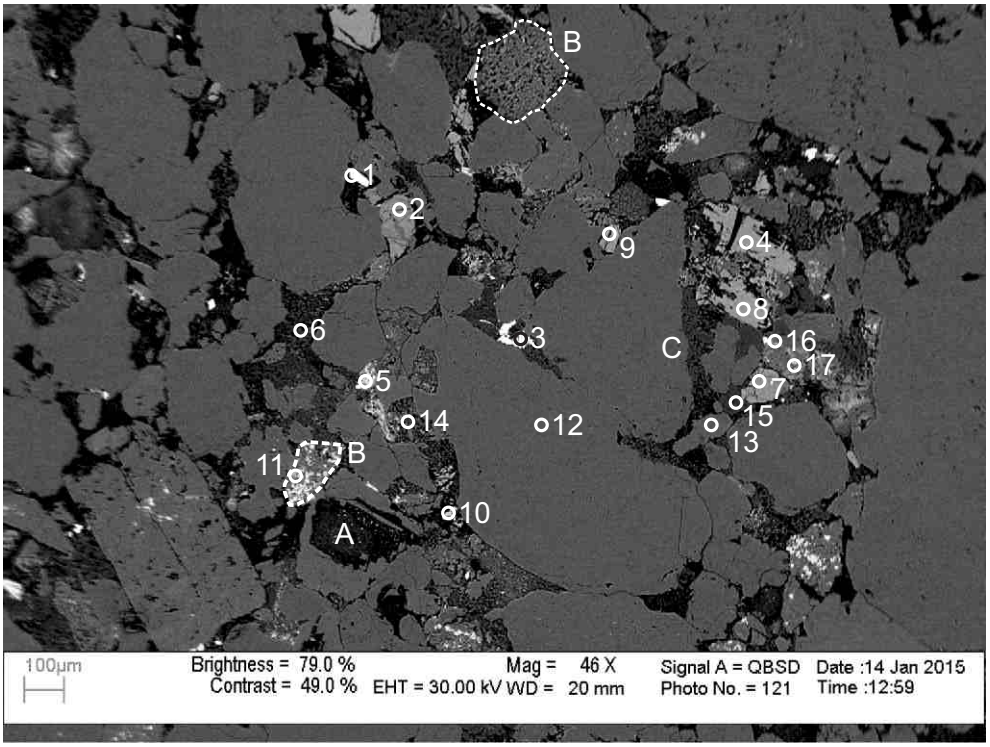

1: Titania+ Chlorite
2: K-Feldspar+ Albite
3: Titania+ Chlorite
4: K-Feldspar
5: Chlorite
6: Kaolinite
7: K-Feldspar
8: K-Feldspar
9: K-Feldspar
10: Chlorite+ Hole
11: Albite+ K-Feldspar +Mix
12: Albite
13: Albite
14: Muscovite+ Hole
15: Kaolinite
16: Quartz
17: Muscovite+ Chlorite

Figure 2-2.7: Sample Newburn 4318.5m site 7 (SEM). Perthite (2). Secondary porosity has been filled by drilling mud (position A). Trachytic lithic clast (positions B) with dissolution filled by chlorite, titania and siderite (11). Kaolinite shows irregular contact with quartz (position C). Titania and chlorite (3) crosscut kaolinite booklets.

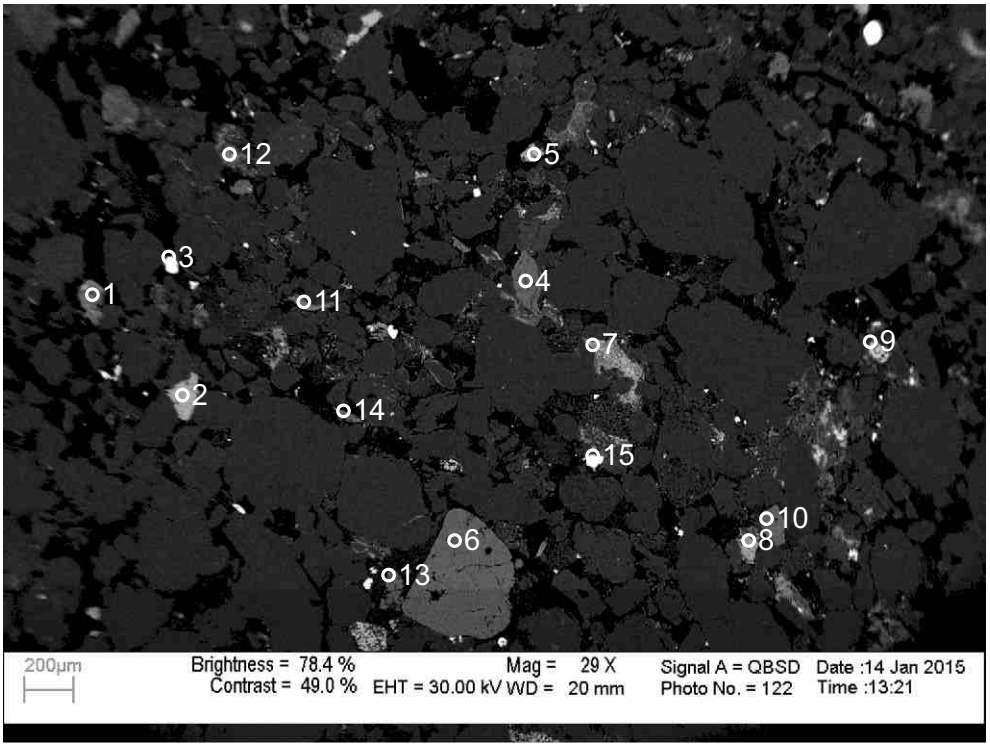

1: Quartz+ Chlorite
2: Chlorite
3: Spinel+ Quartz
4: K-Feldspar
5: Hematite+ Albite+ Apatite
6: K-Feldspar
7: Chlorite+ Calcite
8: Chlorite
9: Albite+ Titania+ Other
10: K-Feldspar
11: Chlorite+ Muscovite
12: Chlorite+ Calcite
13: Albite
14: K-Feldspar
15: Zircon

Figure 2-2.8: Sample Newburn 4318.5m site 8 (SEM). Chloritized muscovite (11). K-feldspar (6) with dissolution voids. Chlorite and calcite interaclast (7). Titania fills dissolution in albite (9). Plastically deformed chloritized muscovite (11).

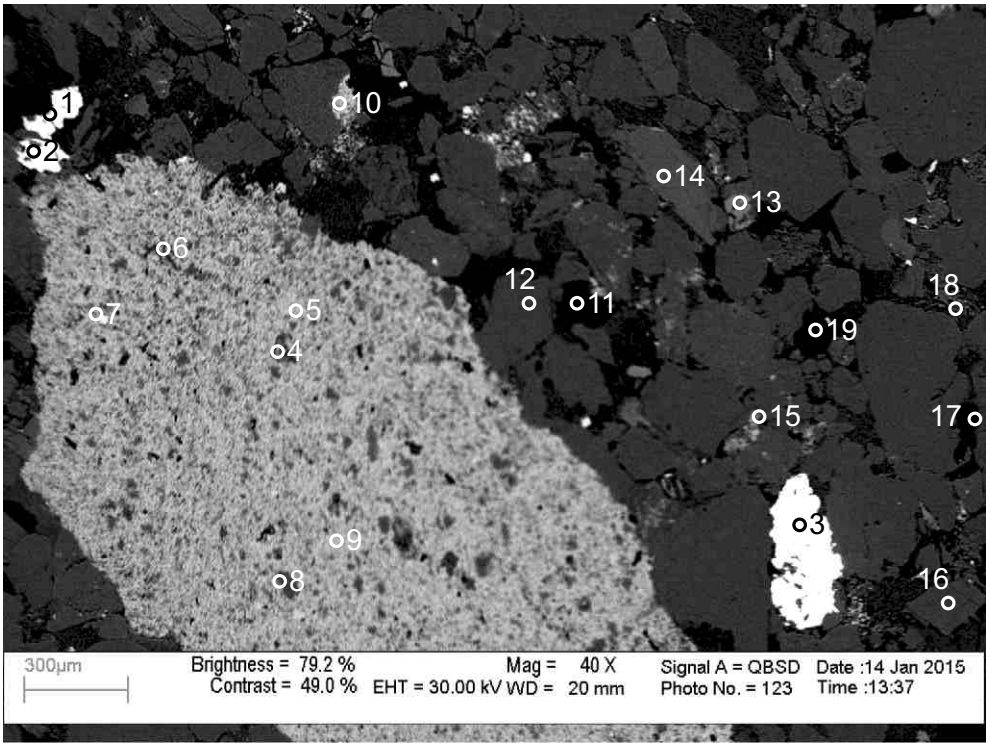

1: Pyrite
2: Pyrite
3: Barite
4: Muscovite+ Chlorite+ Siderite
5: Chlorite+ Siderite+ Muscovite
6: Muscovite+ Chlorite+ Siderite
7: Titania+ Chlorite+ Siderite
8: Albite+ Other
9: Siderite+ Muscovite
10: Siderite+ Albite+ Hole
11: Hole
12: Quartz
13: K-Feldspar
14: Albite
15: Quartz+ Other
16: Albite
17: Hole
18: Muscovite
19: Hole

Figure 2-2.9: Sample Newburn 4318.5m site 9 (SEM). Lithic clast made up of muscovite, chlorite, quartz and albite cemented by early siderite (4-9). Diagenetic barite (3) filling pore space between quartz grains. Diagenetic siderite (10) along intergranular boundaries.

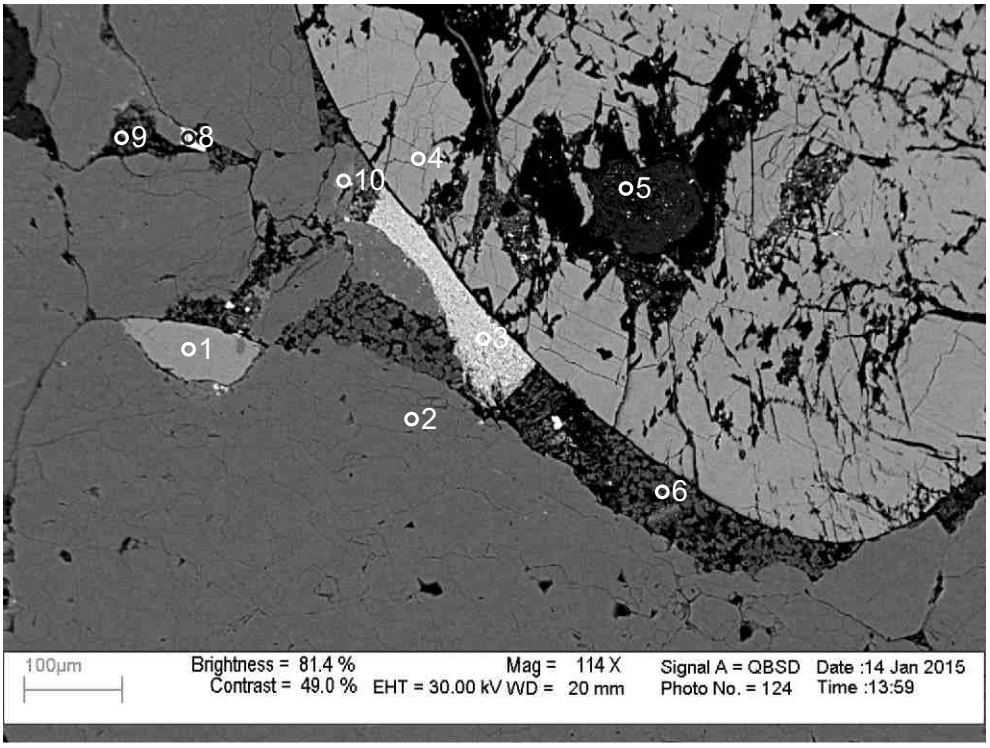

1: K-Feldspar
2: Quartz
3: Chlorite+ Other
4: K-Feldspar
5: Drilling Mud
6: Kaolinite
7: Quartz+ Kaolinite
8: Titania+ Chlorite
9: Kaolinite
10: Muscovite

Figure 2-2.10: Sample Newburn 4318.5m site 10 (SEM). K-feldspar (4) grain with dissolution voids partially filled by drilling mud (5). Muscovite grain replaced by chlorite (3). Kaolinite (6,7,9) filling pore space between detrital K-feldspar (4) and quartz (2). Chlorite (3) engulfs kaolinite (6).

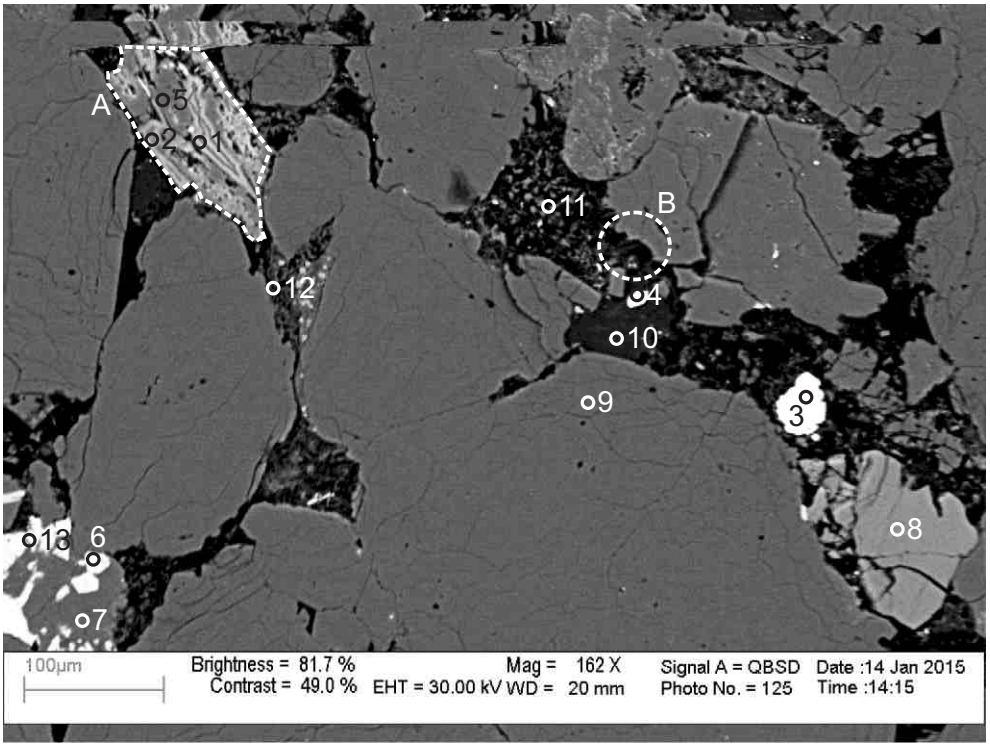

1: Chlorite
2: Chlorite
3: Pyrite
4: Contaminant
5: Albite
6: Titania+ Kaolinite
7: Quartz+ K-Feldspar
8: K-Feldspar
9: Quartz
10: Hole
11: Kaolinite
12: Muscovite+ Other
13: Titania+ Chlorite

Figure 2-2.11: Sample Newburn 4318.5m site 11 (SEM). Detrital quartz (7) is engulfed by Titania (6,13) minerals. Albite or trachytic lithic clast (position A) is cut by, and has dissolution voids partly filled by chlorite (1,2). Kaolinite (11), pyrite (3) with displacive texture and quartz overgrowth (position B) fill secondary porosity where relics of K-feldspar (8) remain.

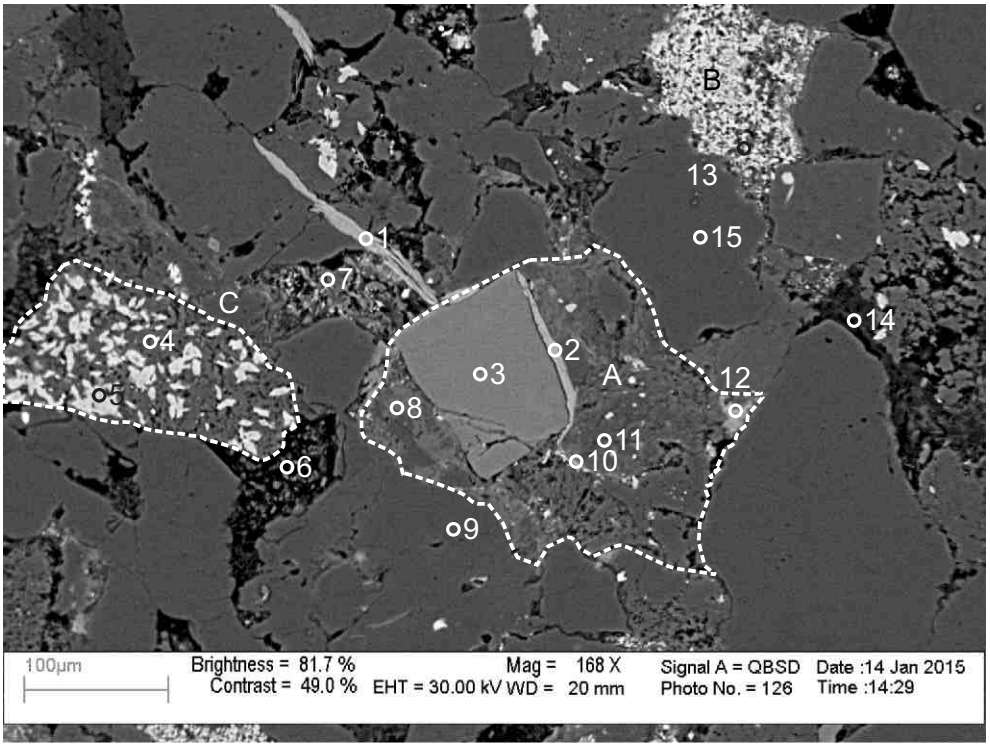

1: Chlorite+ Muscovite+ Titania
2: Chlorite+ Muscovite+ Titania
3: K-Feldspar
4: Albite
5: Siderite+ Albite
6: Kaolinite
7: Albite+Other
8: Muscovite
9: Quartz
10: K-Feldspar +Chlorite
11: Quartz+ Albite+ K-Feldspar
12: Chlorite
13: Chlorite
14: Quartz+ Kaolinite+ K-Feldspar
15: Quartz

Figure 2-2.12: Sample Newburn 4318.5m site 12 (SEM). Siderite (5) filling dissolution voids in trachytic lithic clast (4) (position C). Plastically deformed chloritized muscovite (2) in contact with K-feldspar (3) grain. Kaolinite (6) fills porosity some of which may be due to dissolution of K-feldspar (14). Chlorite (12) fills secondary porosity along intergranular boundary. Granitoid lithic clast (position A) with cholrite filling porosity. Chlorite (13) fills large pore (position B) possibly replacing lithic clast.

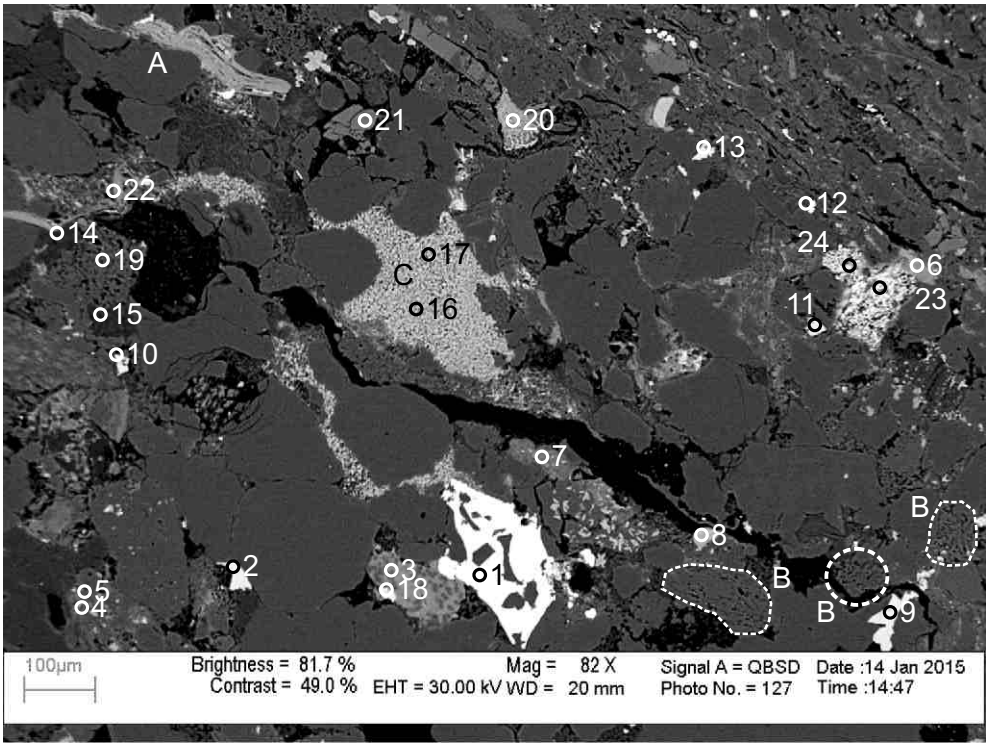

1: Pyrite
2: Titania+ Chlorite
3: Quartz+ Chlorite
4: Quartz+ Muscovite+ Apatite+ Other
5: Muscovite+ Chlorite
6: Chlorite+ Muscovite
7: Chlorite
8: Chlorite
9: Titania+ Chlorite
10: Titania+ Albite
11: Titania+ Chlorite
12: Chlorite+ Pyrite
13: Titania+ Kaolinite
14: Kaolinite+ Other
15: Kaolinite+ Other
16: Chlorite+ Siderite
17: Chlorite+ Siderite
18: Titania+ Chlorite
19: Quartz+ Muscovite
20: Fe-Chlorite
21: K-Feldspar
22: Chlorite+ Illite+ Titania
23: Titania+ Chlorite
24: Titania+Other

Figure 2-2.13: Sample Newburn 4318.5m site 13 (SEM). Diagenetic pyrite (1) with straight crystal outline. Plastically deformed chloritized muscovite (20, position A). Quartz over growth into pore (position B). Original intraclast of siderite intermixed with chlorite partly or completely recrystalized to fill pore (position C).

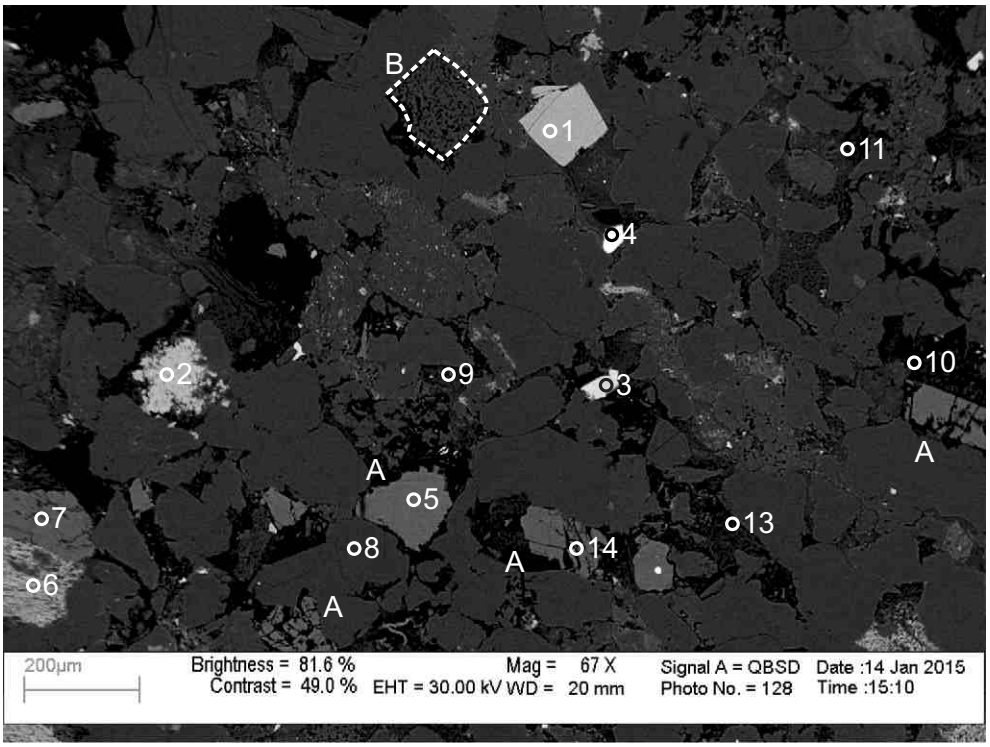

1: Fluorapatite
2: Siderite
3: Titania+ Chlorite
4: Zircon+Other
•12
5: K-Feldspar
6: Siderite+ Chlorite
7: K-Feldspar
8: Quartz
9: Muscovite+ Apatite
10: Muscovite+ Other
11: Muscovite+ Other
12: Muscovite+ Other
13: Muscovite+ Other
14: K-Feldspar

Figure 2-2.14: Sample Newburn 4318.5m site 14 (SEM). Diagenetic fluorapatite (1) with sharp crystal faces cutting into surrounding quartz grains. Chlorite and siderite (6) engulf K-feldspar (7). Siderite (2) engulfs kaolinite and fills open porosity. Abundant partially dissolved K-feldspar (positions A) form secondary porosity. Trachytic lithic clast (position B).

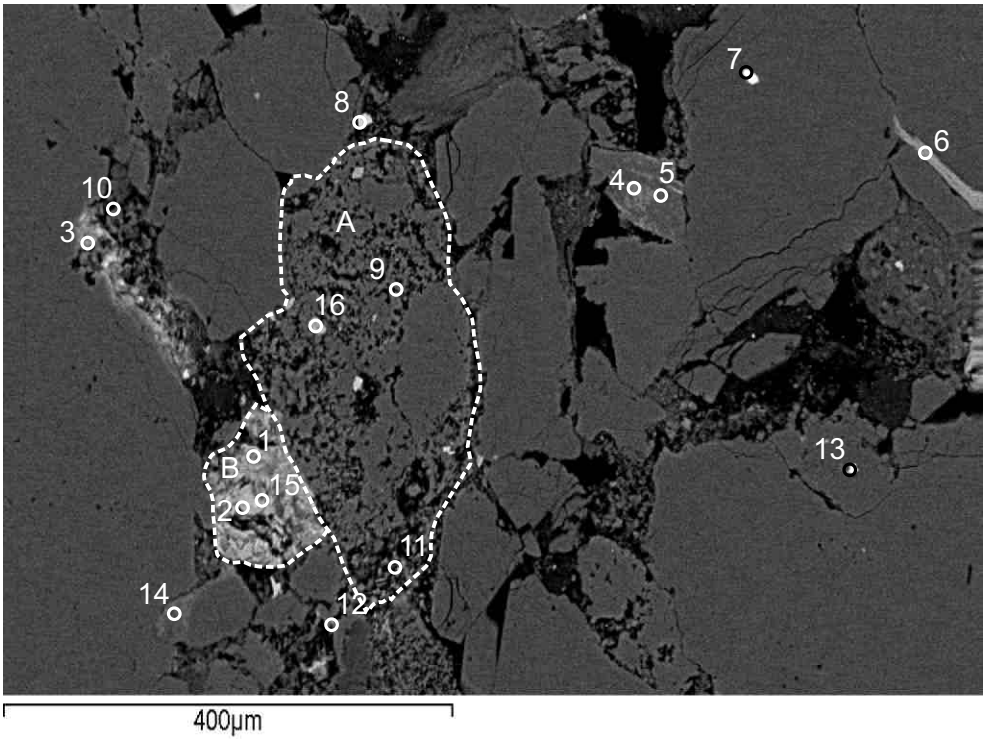

1: Fluorapatite +Chlorite
2: Fluorapatite +Chlorite
3: Titania+ Chlorite
4: Chlorite+ Albite
5: Albite+Other
6: K-Feldspar+ Chlorite
7: Zircon
8: Titania+ Chlorite
9: Albite
10: Kaolinite
11: Albite+ Chlorite
12: Albite+ Apatite
13: Pyrite+ Quartz
14: Muscovite+ Chlorite
15:Fluorapatite
16: Siderite

Figure 2-2.15: Sample Newburn 4318.5m site 15 (SEM). Trachitic lithic clast (9,11,12) with chlorite (8) and siderite (16) filling dissolution voids (position A). Fluorapatite with some fibrous chlorite (1,2,15) fill secondary porosity (position B).

Table 2-2: Scaning Electron Microscope chemical analyses of sample 4318.5m from Newburn H-23 well.

Sample	Site	Position	Mineral	SiO_2	TiO_2	Al_2O_3	FeO	MnO	MgO	CaO	Na_2O	K_2O	P_2O_5	SO_3	F	Cl	Sc_2O_3	Chr_2O_3	NiO	ZnO	SrO	Y_2O_3	ZrO_2	MoO_3	BaO	Ce_2O_3	HfO_2	WO_3	PbO	Total	Actual Total
H-23 4318.5m	1	1	Ab	65.20		21.54				2.85	10.25	0.16																		100	97
H-23 4318.5m	1	2	Qz	99.99																										100	93
H-23 4318.5m	1	3	Ab	66.61		20.50				1.13	11.19	0.58																		100	97
H-23 4318.5m	1	4	Qz	99.99																										100	95
H-23 4318.5m	1	5	Kfs	66.51		18.29					0.62	14.60																		100	92
H-23 4318.5m	1	6	Ab	64.60		21.75				2.99	10.52	0.12																		100	91
H-23 4318.5m	1	7	Qz	99.99																										100	87
H-23 4318.5m	1	8	TiO_2	0.43	99.20		0.37																							100	72
H-23 4318.5m	1	9	TiO_2	1.24	96.66	0.72	1.38																							100	68
H-23 4318.5m	1	10	Chl+TiO_2+Other	47.77	11.18	24.66	9.10		2.75	1.19		2.07	0.57	0.55		0.17														100	67
H-23 4318.5m	1	11	TiO_2+Qz+Other	33.65	62.85	1.00	2.17			0.32																				100	74
H-23 4318.5m	1	12	Ab	69.61		17.84	0.21				11.89					0.47														100	63
H-23 4318.5m	1	13	Kfs	65.84		17.19					2.80	11.00			2.63	0.54														100	33
H-23 4318.5m	1	14	Ab+Qz	78.55		13.32					8.02	0.12																		100	104
H-23 4318.5m	1	15	Ab	68.07		19.18					12.35	0.40																		100	111
H-23 4318.5m	1	16	Kfs	65.69	0.57	21.94	1.40		1.76		0.47	6.94		1.22																100	90
H-23 4318.5m	1	17	Qz	99.99																										100	92
H-23 4318.5m	1	18	Ab+Qz	83.41		9.07	0.14				6.81	0.13		0.42																100	91
H-23 4318.5m	1	19	Qz+Ab	97.50		1.34					1.13																			100	91
H-23 4318.5m	1	20	Ms	51.81	0.40	28.07	2.69		2.66		0.66	8.72																		95	93
H-23 4318.5m	2	1	Chl+Other	54.27		17.06	23.70		3.03	1.32		0.61																		100	55
H-23 4318.5m	2	2	Kfs	66.72		17.99						15.29																		100	89
H-23 4318.5m	2	3	Kfs	66.79		18.03					0.61	14.57																		100	98
H-23 4318.5m	2	4	Ms	49.34	0.48	34.08	2.23		0.96		0.42	7.49																		95	73
H-23 4318.5m	2	5	Ms	48.57	0.68	35.74	0.56		0.41		1.03	8.02																		95	83
H-23 4318.5m	2	6	Qz+Chl+Py	56.65		5.33	10.32		0.73	0.17	0.53	0.41		25.84																100	128
H-23 4318.5m	2	7	Qz+TiO_2+Other	74.51	22.62	2.46	0.22					0.19																		100	74
H-23 4318.5m	2	8	Ms+Chl	43.38	13.58	24.00	8.80		6.42	0.66		3.17																		100	65
H-23 4318.5m	2	9	Chl+Sd	24.39		19.33	39.64	0.58	12.57	3.50																				100	68
H-23 4318.5m	2	10	Qz	99.99																										100	94
H-23 4318.5m	2	11	Ab	66.06		20.71				1.79	11.32	0.13																		100	92
H-23 4318.5m	2	12	Qz	99.99																										100	88
H-23 4318.5m	2	13	Ab	74.40		15.42					10.17																			100	102
H-23 4318.5m	2	14	Chl+hole	33.37	0.78	20.05	32.61	0.46	8.62	2.59		1.52																		100	61
H-23 4318.5m	2	15	Ab	69.22		20.52					9.01	1.05				0.20														100	46
H-23 4318.5m	2	16	Ab	68.54		18.93					12.21	0.31																		100	99
H-23 4318.5m	2	17	Qz+Chl+Ms	83.51		9.13	1.99		0.76		2.86	1.73																		100	104
H-23 4318.5m	2	18	Qz+Other	94.30		3.84	0.14				1.27	0.46																		100	86
H-23 4318.5m	3	1	Kfs	66.57		18.06					0.55	14.83																		100	92
H-23 4318.5m	3	2	Kfs	66.72		18.14					0.86	14.29																		100	85
H-23 4318.5m	3	3	Kfs	66.61		18.08	0.18				0.73	14.39																		100	81
H-23 4318.5m	3	4	Qz	99.11			0.89																							100	80
H-23 4318.5m	3	5	Zrn	30.78						2.50													66.72							100	83
H-23 4318.5m	3	6	Kfs	66.72		18.14					0.59	14.53																		100	83
H-23 4318.5m	3	7	Chl	20.53	0.54	14.94	33.27	0.48	11.82	3.43																				85	58
H-23 4318.5m	3	8	TiO_2+Other	1.95	93.59	2.17	0.72			0.87			0.71																	100	68
H-23 4318.5m	3	9	Ab	68.26		19.07					12.67																			100	94
H-23 4318.5m	3	10	Ms+Chl	56.47		31.86	2.52		1.92	0.74	1.36	5.13																		100	81
H-23 4318.5m	3	11	Ms+Chl	63.51	0.23	24.34	3.77		1.92	0.42	0.42	5.37																		100	78
H-23 4318.5m	3	12	Kfs+Chl	75.68		16.72	1.24		1.58			4.78																		100	88
H-23 4318.5m	3	13	Ms+Chl	51.58	0.22	28.46	9.87		4.69		0.49	4.69																		100	73
H-23 4318.5m	3	14	Ab	67.60		20.29				0.20	11.92																			100	95
H-23 4318.5m	3	15	Ab	68.50		18.93					12.57																			100	89
H-23 4318.5m	3	16	Chl+Sd	34.18	0.93	22.43	31.74	0.40	7.68	1.82		0.83																		100	61
H-23 4318.5m	3	17	Ab	68.07		19.22					12.23	0.48																		100	93
H-23 4318.5m	3	18	TiO_2+Ms+Other	31.19	40.47	17.59	1.53		1.74	0.49	0.62	2.82			3.32	0.24														100	60

Table 2-2: Scaning Electron Microscope chemical analyses of sample 4318.5m from Newburn H-23 well.

Sample	Site	Position	Mineral	SiO_2	TiO_2	Al_2O_3	FeO	MnO	MgO	CaO	Na_2O	K_2O	P_2O_5	SO_3	F	Cl	Sc_2O_3	Chr_2O_3	NiO	ZnO	SrO	Y_2O_3	ZrO_2	MoO_3	BaO	Ce_2O_3	HfO_2	WO_3	PbO	Total	Actual Total
H-23 4318.5m	3	19	Qz	99.99																									100	87
H-23 4318.5m	3	20	Chl	33.53		18.40	24.16		7.52	0.44	0.55	0.39																	85	66
H-23 4318.5m	3	21	Chl	29.86		19.13	26.03		8.91	1.08																			85	62
H-23 4318.5m	3	22	Qz+Other	94.15		4.29	0.63					0.94																	100	80
H-23 4318.5m	3	23	Kfs	67.04		17.95					0.49	14.53																	100	88
H-23 4318.5m	4	1	Spl		0.28	20.29	24.82		10.20									44.42											100	65
H-23 4318.5m	4	2	Spl			21.56	22.94		8.39									46.79		0.35									100	64
H-23 4318.5m	4	3	Zrn	31.83																			67.58				0.60		100	79
H-23 4318.5m	4	4	Ab	68.09		19.41				0.21	12.30																		100	73
H-23 4318.5m	4	5	Kfs	66.68		17.99					0.81	14.51																	100	71
H-23 4318.5m	4	6	Kfs	57.54		15.53	11.39		1.97		0.61	12.96																	100	62
H-23 4318.5m	4	7	Qz	99.99																									100	80
H-23 4318.5m	4	8	Qz	99.99																									100	77
H-23 4318.5m	4	9	Qz+Kln	60.95	1.32	34.69	0.28				0.43	0.84			1.51														100	62
H-23 4318.5m	4	10	Qz	99.99																									100	69
H-23 4318.5m	4	11	Py+Ab	7.85		3.10	22.38				1.25	0.64		64.47					0.29										100	126
H-23 4318.5m	4	12	Ms+Chl	59.51	0.65	28.87	1.84		2.54			6.58																	100	63
H-23 4318.5m	4	13	Kfs	66.64		17.97						14.94													0.45				100	76
H-23 4318.5m	4	14	Qz+Kln+TiO_2	53.35	10.53	35.50	0.21				0.42																		100	55
H-23 4318.5m	5	1	Spl+Other	9.60	0.58	9.92	37.39	6.73	8.90									23.48		3.40									100	55
H-23 4318.5m	5	2	Spl+Other	5.80	0.95	3.70	38.57	10.35	2.84	0.42								29.79		7.57									100	48
H-23 4318.5m	5	3	Spl+Other	8.56	1.00	6.41	29.38	6.74	1.36	0.74								30.29		15.55									100	49
H-23 4318.5m	5	4	TiO_2	4.60	91.78	2.99	0.63																						100	56
H-23 4318.5m	5	5	Spl+Other	8.49	0.67	4.40	34.66	9.04	7.21	0.28								26.40		8.86									100	55
H-23 4318.5m	6	1	Hm+Qz	7.19			92.29	0.52																					100	69
H-23 4318.5m	6	2	TiO_2+Kln	10.93	77.15	10.28	1.13				0.51																		100	60
H-23 4318.5m	6	3	Chl	28.36	5.16	17.07	24.59		6.17	0.38	0.89	0.44		1.15						0.78									85	52
H-23 4318.5m	6	4	Ab+Ap	50.74		15.51	1.96			10.14	11.35	0.23	8.50	1.10						0.47									100	72
H-23 4318.5m	6	5	Ab	69.07		18.59					12.34																		100	72
H-23 4318.5m	6	6	Ab+Kln+Ilt	63.77	0.28	23.01	0.54		0.68	0.91	5.47	2.72			2.60														100	43
H-23 4318.5m	6	7	Ab+Ap	65.93	0.70	19.08				1.15	11.34	0.55	1.26																100	71
H-23 4318.5m	6	8	Ab+Ap	56.80	4.04	19.59	0.63		0.65	4.56	6.11	1.96	5.66																100	56
H-23 4318.5m	6	9	Ab	68.52		19.08					12.39																		100	69
H-23 4318.5m	6	10	Ms	55.36		27.83	1.59		2.06	1.56		6.39				0.22													95	49
H-23 4318.5m	6	11	Kln	50.65	0.28	33.72								1.05		0.31													86	35
H-23 4318.5m	6	12	Chl	37.31	0.98	19.53	17.01		6.75	0.18	3.06	0.19																	85	61
H-23 4318.5m	7	1	TiO_2+Chl	2.12	94.48	1.74	1.67																						100	49
H-23 4318.5m	7	2	Kfs+Ab	67.11		18.16					3.24	11.50																	100	56
H-23 4318.5m	7	3	TiO_2+Chl	2.12	93.39	2.87	1.61																						100	51
H-23 4318.5m	7	4	Kfs	66.57		17.88					0.67	14.88																	100	69
H-23 4318.5m	7	5	Chl	26.13	12.97	20.85	20.34		4.07	0.20		0.43																	85	49
H-23 4318.5m	7	6	Kln	49.60		36.40																							86	48
H-23 4318.5m	7	7	Kfs	66.66		18.06					0.39	14.88																	100	67
H-23 4318.5m	7	8	Kfs	66.74		17.95					0.40	14.90																	100	67
H-23 4318.5m	7	9	Kfs	66.51		18.18					0.75	14.56																	100	66
H-23 4318.5m	7	10	Chl+hole	36.97		18.74	32.02	0.57	5.17	3.64		2.88																	100	35
H-23 4318.5m	7	11	Ab+Kfs+Mix	59.49	1.17	19.29	5.94		1.76	2.17	8.43	1.75																	100	47
H-23 4318.5m	7	12	Ab	99.99																									100	63
H-23 4318.5m	7	13	Ab	72.69		16.34					10.95																		100	69
H-23 4318.5m	7	14	Ms+Hole	57.91		34.18	2.53		1.13	0.57		3.66																	100	39
H-23 4318.5m	7	15	Kln	49.00		37.00																							86	55
H-23 4318.5m	7	16	Qz	97.74		1.40	0.46					0.39																	100	64
H-23 4318.5m	7	17	Ms+Chl	50.87	0.67	25.43	11.06		4.03	1.96		5.96																	100	53
H-23 4318.5m	8	1	Qz+Chl	57.29	0.87	14.80	13.97		12.52	0.57																			100	41
H-23 4318.5m	8	2	Chl	29.58	0.30	21.20	27.91		5.72	0.30																			85	37
H-23 4318.5m	8	3	Spl+Qz	23.77	1.30	29.61	11.44		4.10			0.35						29.45											100	36

Table 2-2: Scaning Electron Microscope chemical analyses of sample 4318.5m from Newburn H-23 well.

Sample	Site	Position	Mineral	SiO_2	TiO_2	Al_2O_3	FeO	MnO	MgO	CaO	Na_2O	K_2O	P_2O_5	SO_3	F	Cl	Sc_2O_3	Chr_2O_3	NiO	ZnO	SrO	Y_2O_3	ZrO_2	MoO_3	BaO	Ce_2O_3	HfO_2	WO_3	PbO	Total	Actual Total
H-23 4318.5m	8	4	Kfs	66.85		17.99					0.74	14.42																		100	62
H-23 4318.5m	8	5	Hm+Ab+Ap	16.64		4.35	46.84	0.94	15.17	7.63	2.68	0.83	4.03	0.90																100	37
H-23 4318.5m	8	6	Kfs	66.44		18.18					1.12	14.26																		100	55
H-23 4318.5m	8	7	Chl+Cal	30.10		23.60	34.14	0.48	6.63	5.07																				100	43
H-23 4318.5m	8	8	Chl	29.18	6.86	18.42	21.91		7.90	0.21	0.52																			85	51
H-23 4318.5m	8	9	Ab+TiO_2+Other	41.95	34.05	14.44	0.53			1.08	7.02	0.95																		100	61
H-23 4318.5m	8	10	Kfs	66.66		17.78					0.38	15.17																		100	64
H-23 4318.5m	8	11	Chl+Ms	43.55	2.07	25.62	17.33		8.41	1.27		1.75																		100	43
H-23 4318.5m	8	12	Chl+Cal	30.40		19.58	33.00	0.54	9.55	6.16		0.79																		100	31
H-23 4318.5m	8	13	Ab	67.56		18.91					11.54	1.99																		100	53
H-23 4318.5m	8	14	Kfs	66.83		17.95					0.63	14.57																		100	52
H-23 4318.5m	8	15	Zrn	31.51																			68.11				0.38			100	62
H-23 4318.5m	9	1	Py	0.34			26.90							72.76																100	92
H-23 4318.5m	9	2	Py	0.51			25.37		3.40					70.72																100	87
H-23 4318.5m	9	3	Brt	1.75										38.38											59.90					100	62
H-23 4318.5m	9	4	Ms+Chl+Sd *	45.09		26.85	16.52		5.22	2.95		3.07				0.31														100	44
H-23 4318.5m	9	5	Chl+Sd+Ms *	21.88	0.35	11.55	50.82	0.74	6.63	5.32	0.98	1.76																		100	33
H-23 4318.5m	9	6	Ms+Chl+Sd *	65.48		18.01	9.35		1.82	1.12	1.17	3.04																		100	45
H-23 4318.5m	9	7	TiO_2+Chl+Sd *	20.75	55.31	9.83	9.97		1.79	1.02		1.32																		100	40
H-23 4318.5m	9	8	Ab+Other *	77.89		13.13	0.21				8.55	0.23																		100	57
H-23 4318.5m	9	9	Sd+Ms *	17.03		9.50	56.59	0.77	7.69	5.68	1.54	1.17																		100	32
H-23 4318.5m	9	10	Sd+Ab+hole	6.52		4.16	61.49	0.79	15.30	10.54	1.20																			100	30
H-23 4318.5m	9	11	Hole	54.66	0.47	2.74	7.09		25.97	2.64		0.64			5.43	0.36														100	39
H-23 4318.5m	9	12	Qz	99.99																										100	64
H-23 4318.5m	9	13	Kfs	67.02		18.23					1.71	13.01																		100	66
H-23 4318.5m	9	14	Ab	64.82		21.96				2.87	10.06	0.29																		100	67
H-23 4318.5m	9	15	Qz+Other	93.10		5.23	1.25					0.42																		100	67
H-23 4318.5m	9	16	Ab	68.75		18.65					12.61																			100	68
H-23 4318.5m	9	17	Hole	54.49	0.62	3.34	8.13		29.03	3.06		0.82				0.50														100	36
H-23 4318.5m	9	18	Ms	53.47	0.36	30.86	1.41		1.45		0.71	6.74																		95	61
H-23 4318.5m	9	19	Hole	53.39	0.50	3.72	8.47		28.19	2.53		0.82		1.22		0.66		0.48												100	31
H-23 4318.5m	10	1	Kfs	66.34		18.22					0.74	14.72																		100	49
H-23 4318.5m	10	2	Qz	99.99																										100	52
H-23 4318.5m	10	3	Chl+Other	31.32	0.30	23.79	34.57	0.32	7.38	1.94		0.39																		100	41
H-23 4318.5m	10	4	Kfs	66.21		18.31					0.65	14.84																		100	50
H-23 4318.5m	10	5	DM	42.18		5.65	18.73		28.79	1.27		0.94		1.55		0.88														100	19
H-23 4318.5m	10	6	Kln	49.81		36.19																								86	46
H-23 4318.5m	10	7	Qz+Kln	57.16		37.62	2.83		0.75	0.35		0.75				0.54														100	28
H-23 4318.5m	10	8	TiO_2+Chl	7.25	86.29	4.84	1.14					0.47																		100	40
H-23 4318.5m	10	9	Kln	50.16		35.54						0.30																		86	28
H-23 4318.5m	10	10	Ms	58.21		25.52	1.61		2.15			7.50																		95	46
H-23 4318.5m	11	1	Chl	31.39		22.33	25.76		5.16	0.37																				85	38
H-23 4318.5m	11	2	Chl	31.89		21.33	24.97		5.61	0.41	0.79																			85	36
H-23 4318.5m	11	3	Py	0.62			26.41		0.83					72.14																100	92
H-23 4318.5m	11	4	Contaminant	28.28		2.34	4.27		2.77	1.34		0.59								0.70									59.71	100	54
H-23 4318.5m	11	5	Ab	67.83		19.03	1.33				11.81																			100	48
H-23 4318.5m	11	6	TiO_2+Kln	2.91	94.93	2.15																								100	39
H-23 4318.5m	11	7	Qz+Kfs	98.79	0.28	0.64						0.29																		100	48
H-23 4318.5m	11	8	Kfs	66.59		17.95					0.90	14.56																		100	52
H-23 4318.5m	11	9	Qz	99.99																										100	51
H-23 4318.5m	11	10	Hole	56.39	0.42	3.29	6.99		28.44	2.76		0.66		0.80		0.27														100	29
H-23 4318.5m	11	11	Kln	51.00		34.86						0.15																		86	49
H-23 4318.5m	11	12	Ms+Other	56.43		33.43	1.05		1.14	0.94		5.35	1.35			0.30														100	28
H-23 4318.5m	11	13	TiO_2+Chl	7.17	92.23		0.62																							100	39
H-23 4318.5m	12	1	Chl+Ms+TiO_2	38.36	8.29	17.61	17.79		14.49			3.47																		100	42
H-23 4318.5m	12	2	Chl+Ms+TiO_2	43.08	8.66	17.65	15.06		12.10			3.43																		100	43

Table 2-2: Scaning Electron Microscope chemical analyses of sample 4318.5m from Newburn H-23 well.

Sample	Site	Position	Mineral	SiO_2	TiO_2	Al_2O_3	FeO	MnO	MgO	CaO	Na_2O	K_2O	P_2O_5	SO_3	F	Cl	Sc_2O_3	Chr_2O_3	NiO	ZnO	SrO	Y_2O_3	ZrO_2	MoO_3	BaO	Ce_2O_3	HfO_2	WO_3	PbO	Total	Actual Total
H-23 4318.5m	12	3	Kfs	66.61		17.99					0.70	14.70																		100	48
H-23 4318.5m	12	4	Ab	62.02	0.55	17.72	2.29			0.20	11.07	0.57		5.59																100	51
H-23 4318.5m	12	5	Sd+Ab	10.76		3.48	63.85	1.42	11.19	4.88	2.62		1.81																	100	25
H-23 4318.5m	12	6	Kln	52.18		31.37	1.63			0.36		0.22				0.25														86	39
H-23 4318.5m	12	7	Ab+Other	61.35		20.18	0.30			3.26	9.91	1.42	3.57																	100	53
H-23 4318.5m	12	8	Ms	62.29	0.26	23.84	1.27		0.84			6.51																		95	48
H-23 4318.5m	12	9	Qz	99.99																										100	47
H-23 4318.5m	12	10	Kfs+Chl	51.00	3.79	19.22	14.25		6.80	0.45	0.69	3.82																		100	40
H-23 4318.5m	12	11	Qz+Ab+Kfs	78.98		13.47	1.00		0.86		2.76	2.93																		100	46
H-23 4318.5m	12	12	Chl	32.90		20.77	22.70		7.71	0.32		0.60																		85	40
H-23 4318.5m	12	13	Chl	19.51		16.43	36.40	0.46	8.05	3.88		0.28																		85	31
H-23 4318.5m	12	14	Qz+Kln+Kfs	58.10		36.35	0.69		0.75	0.70	0.75	2.66																		100	37
H-23 4318.5m	12	15	Qz	99.99																										100	48
H-23 4318.5m	13	1	Py				27.43							72.59																100	79
H-23 4318.5m	13	2	TiO_2+Chl	2.59	94.78	1.34	1.31																							100	35
H-23 4318.5m	13	3	Qz+Chl	55.96	0.73	17.06	17.39		8.84																					100	36
H-23 4318.5m	13	4	Qz+Ms+Ap+Other	55.60	0.40	29.76	4.32		2.09		0.84	5.87	1.12																	100	37
H-23 4318.5m	13	5	Ms+Chl	69.61	0.27	22.18	0.95		0.85		0.81	5.32																		100	41
H-23 4318.5m	13	6	Chl+Ms	39.04	2.42	22.11	23.22	0.23	10.02	0.52	0.67	1.77																		100	42
H-23 4318.5m	13	7	Chl	33.88	0.24	22.16	15.90		11.97	0.44		0.41																		85	36
H-23 4318.5m	13	8	Chl	33.86		18.44	23.22	0.79	6.53		0.56	1.60																		85	38
H-23 4318.5m	13	9	TiO_2+Chl	1.86	95.10	1.32	1.72																							100	38
H-23 4318.5m	13	10	TiO_2+Ab	25.35	56.21	8.86	0.80				8.79																			100	46
H-23 4318.5m	13	11	TiO_2+Chl	2.59	94.78	1.25	1.38																							100	39
H-23 4318.5m	13	12	Chl+Py	26.25	0.67	17.71	15.26		0.95	0.35	0.67	2.02		36.13																100	66
H-23 4318.5m	13	13	TiO_2+Kln	18.70	63.77	15.66	0.89				0.77	0.20																		100	44
H-23 4318.5m	13	14	Kln+Other	57.14		40.68	1.17				0.55	0.46																		100	33
H-23 4318.5m	13	15	Kln+Other	56.45		42.65	0.42				0.49																			100	34
H-23 4318.5m	13	16	Chl+Sd	9.97		7.12	60.62	0.96	15.09	6.25																				100	24
H-23 4318.5m	13	17	Chl+Sd	3.14		1.70	67.94	1.07	17.91	8.23																				100	22
H-23 4318.5m	13	18	TiO_2+Chl	5.82	84.94	4.08	3.36		1.81																					100	36
H-23 4318.5m	13	19	Qz+Ms	89.16		7.33	0.57		0.41		0.67	1.85																		100	42
H-23 4318.5m	13	20	Fe-Chl	25.88		20.39	43.66	0.53	7.16	1.43	0.96																			100	30
H-23 4318.5m	13	21	Kfs	66.27		18.23					0.58	14.90																		100	44
H-23 4318.5m	13	22	Chl+Ilt+TiO_2	37.78	4.57	18.90	19.90	0.28	14.91			3.67																		100	34
H-23 4318.5m	13	23	TiO_2+Chl	2.89	93.58	1.19	2.07			0.28																				100	33
H-23 4318.5m	13	24	TiO_2+Other	6.48	90.29	1.87	0.66				0.69																			100	37
H-23 4318.5m	14	1	Fap							47.07			45.12		7.82															100	45
H-23 4318.5m	14	2	Sd				46.50	1.02	4.55	3.93																				56	19
H-23 4318.5m	14	3	TiO_2+Chl	0.73	96.90	1.28	1.09																							100	36
H-23 4318.5m	14	4	Zrn+Other	30.08		1.38	0.85			1.12							0.74					0.29	65.54							100	40
H-23 4318.5m	14	5	Kfs	66.61		17.97					0.62	14.79																		100	41
H-23 4318.5m	14	6	Sd+Chl	5.22	3.37	3.70	62.77	1.02	15.62	8.31																				100	19
H-23 4318.5m	14	7	Kfs	67.06		17.71						15.23																		100	37
H-23 4318.5m	14	8	Qz	99.99																										100	41
H-23 4318.5m	14	9	Ms+Ap	54.16	2.19	27.42	1.07		1.99	2.08	1.12	4.93	1.54		3.51															100	34
H-23 4318.5m	14	10	Ms+Other	56.50	3.82	33.16	1.11		0.76	0.34	0.90	2.96				0.45														100	29
H-23 4318.5m	14	11	Ms+Other	59.34		28.97	2.02		1.64	0.97	0.85	5.76				0.46														100	31
H-23 4318.5m	14	12	Ms+Other	54.89		28.68	1.16		1.82	2.28	0.85	5.17			4.76	0.39														100	41
H-23 4318.5m	14	13	Ms+Other	53.39	8.61	26.45	1.31		1.63	1.54	0.80	5.71				0.57														100	26
H-23 4318.5m	14	14	Kfs	67.04		17.91					0.57	14.48																		100	45
H-23 4318.5m	15	1	Fap+ Chl	16.56	4.89	17.31	0.99		0.63	19.52		1.65	28.83	1.22	2.97						3.73					1.70				100	38
H-23 4318.5m	15	2	Fap+ Chl	4.62	1.05	4.55		0.43	0.83	38.94		0.45	40.44		8.69															100	41
H-23 4318.5m	15	3	TiO_2+Chl	26.21	54.85	17.54	1.39																							100	14
H-23 4318.5m	15	4	Chl+Ab	46.87		20.48	14.40	0.43	15.34		2.47																			100	38
H-23 4318.5m	15	5	Ab+Other	65.01		19.29	1.67		1.33	0.57	10.87	0.34		0.92																100	43

Table 2-2: Scaning Electron Microscope chemical analyses of sample 4318.5m from Newburn H-23 well.

Sample	Site	Position	Mineral	SiO_2	TiO_2	Al_2O_3	FeO	MnO	MgO	CaO	Na_2O	K_2O	P_2O_5	SO_3	F	Cl	Sc_2O_3	Chr_2O_3	NiO	ZnO	SrO	Y_2O_3	ZrO_2	MoO_3	BaO	Ce_2O_3	HfO_2	WO_3	PbO	Total	Actual Total
H-23 4318.5m	15	6	Kfs+Chl	59.60	2.14	13.19	16.09		5.46			3.52																		100	34
H-23 4318.5m	15	7	Zrn	37.97																			58.61				3.41			100	42
H-23 4318.5m	15	8	TiO_2+Chl	1.97	95.88	1.45	0.71																							100	33
H-23 4318.5m	15	9	Ab	68.39		19.14					12.13	0.34																		100	45
H-23 4318.5m	15	10	Kln	49.38		36.62																								86	34
H-23 4318.5m	15	11	Ab+Chl	60.65		21.67	3.27		0.61	0.73	9.60	1.36												2.10						100	37
H-23 4318.5m	15	12	Ab+Ap	56.73		16.95				7.26	11.32	0.59	7.15																	100	44
H-23 4318.5m	15	13	Py+Qz	31.83			15.86				0.65			51.66																100	77
H-23 4318.5m	15	14	Ms+Chl	52.69		29.17	7.27		4.78			6.11																		100	34
H-23 4318.5m	15	15	Fap	2.63		2.72		0.39	0.70	41.89			41.57		7.01											1.18		1.92		100	36
H-23 4318.5m	15	16	Sd	3.58		1.24	38.44	0.99	9.00	2.74																				56	20

* = Lithic Clast

Appendix 2-3: SEM-BSE images and EDS mineral analyses for sample Newburn H-23 4353.5m

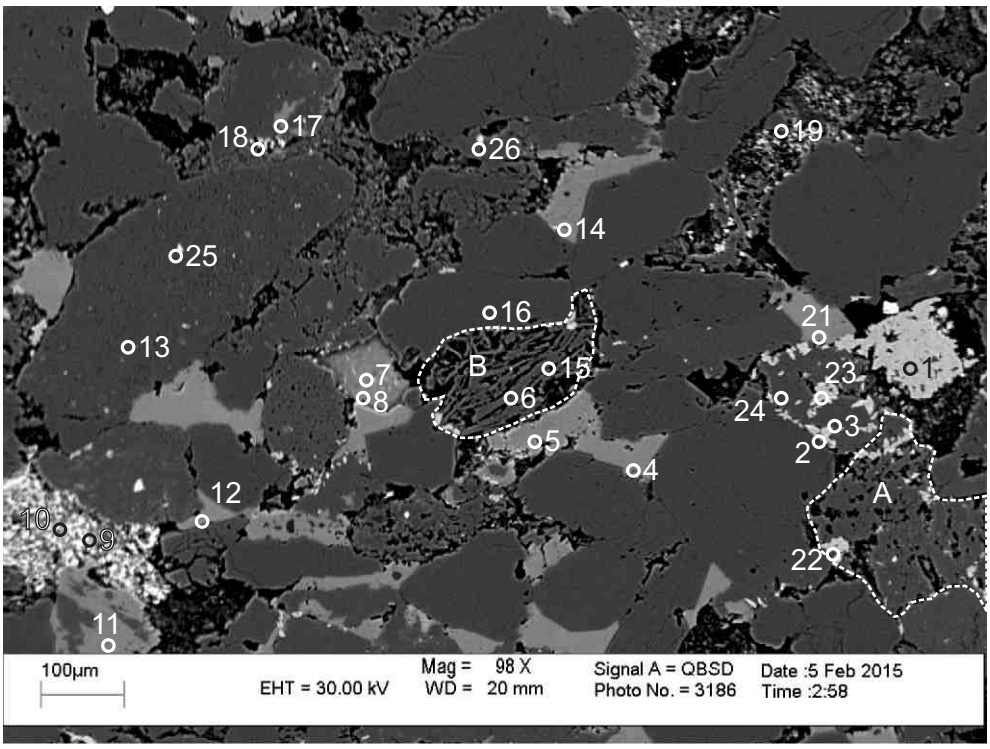

1: Siderite+ Other
2: Mix
3: Albite+ Pyrite
4: Fe-Calcite+ Kaolinite
5: Calcite+ Chlorite
6: Albite+Illite
7: Chlorite
8: Chlorite+ Calcite
9: Titania+ Chlorite
10: Titania+ Chlorite
11: Fe-Calcite+ Quartz
12: Albite
13: Quartz
14: Calcite
15: Albite+ Illite
16: Quartz
17: Albite+Calcite
18: Muscovite +Titania
19: Chlorite
20: Albite+ Calcite
21: Ankerite+Albite
22: Siderite+Albite
23: Albite
24: Albite
25: Quartz
26: Albite

Figure 2-3.1: Sample Newburn 4353.5m site 1 (SEM). Table 2-3A. Siderite (1) replaces ankerite (21). Trachytic lithic clast (position A) with siderite (22) filling voids between albite grains. Trachytic lithic clast (position B) composed primarily of albite with some illite (6,15).

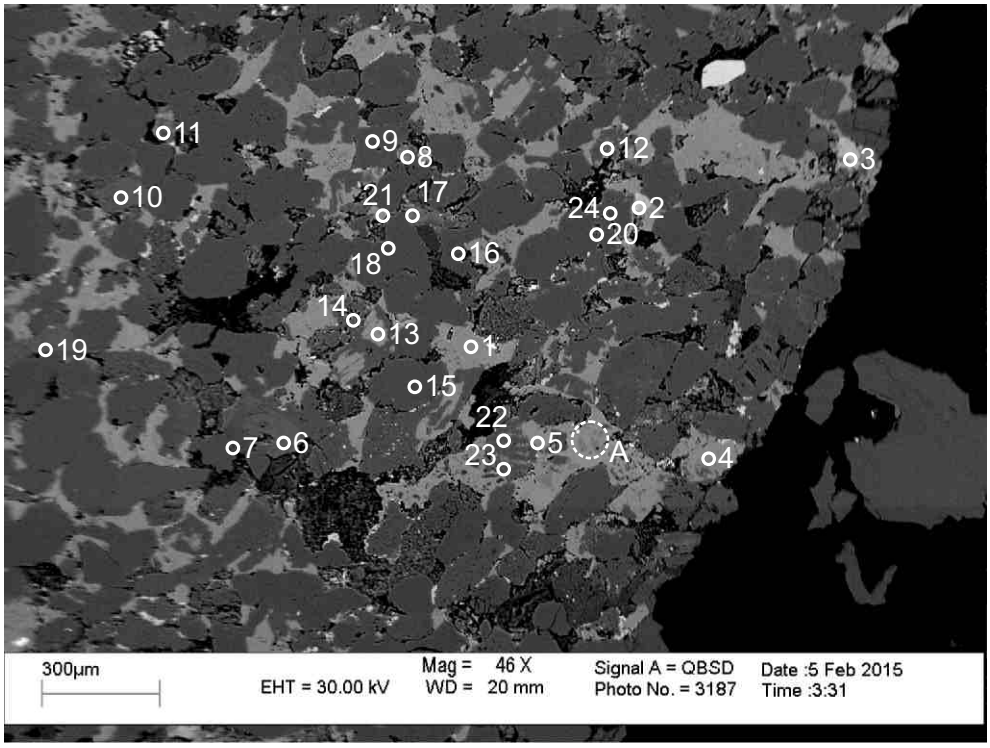

1: Calcite+ Other
2: Chlorite
3: Chlorite
4: F-Calcite+ Chlorite
5: F-Calcite
6: Oligoclase
7: Quartz
8: Quartz+ Chlorite
9: Albite
10: Oligoclase
11: Albite
12: Albite
13: Fe-Calcite +Albite
14: Albite
15: Quartz
16: Quartz
17: Muscovite
18: Quartz
19: Oligoclase
20: Quartz
21: F-Calcite+ Other
22: Albite
23: Albite
24: Quartz

Figure 2-3.2: Sample Newburn 4353.5m site 2 (SEM) Table 2-3A. Framework grains of quartz (7,15,16,18,20), oligoclase (6,10,19), and albite (11,12,14,22,23) cemented by F-calcite (1,4,5,21) and Fe-calcite (13). F-calcite (5) engulfs Fe-calcite (position A).

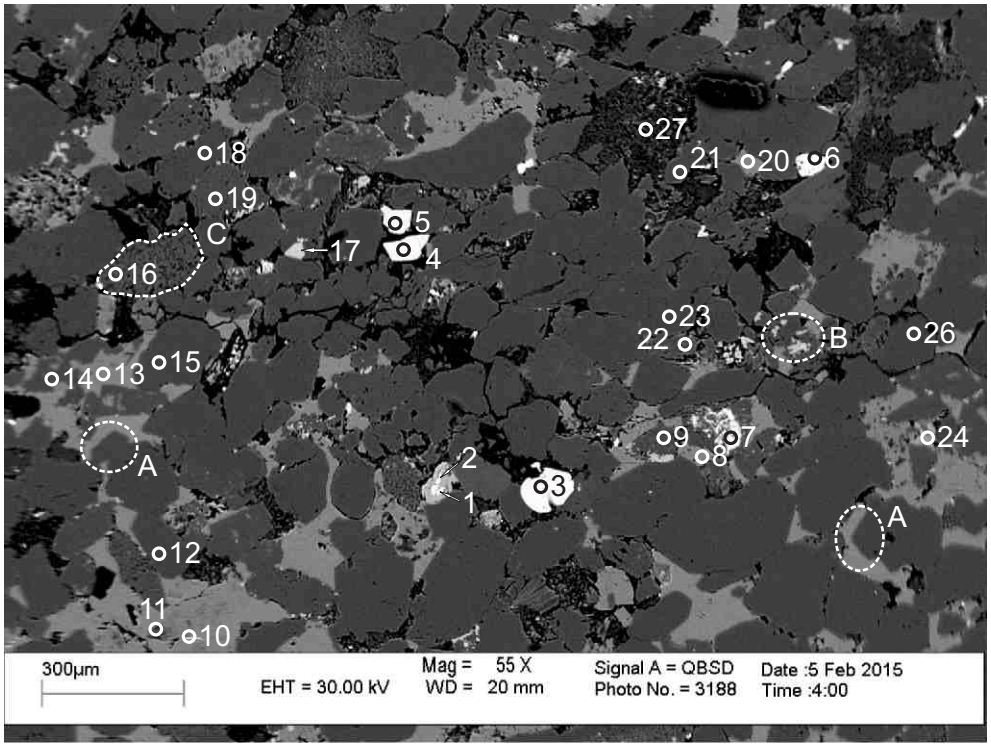

1: Titania+ Chlorite
2: Chlorite
3: Spinel
4: Titania
5: Titania
6: Titania
7: Pyrite+ Quartz
8: Fe-Calcite
9: Quartz
10: Fe-Calcite
11: Albite
12: Quartz
13: Fe-Calcite +Muscovite
14: Albite
15: Quartz
16: Albite+ Other
17: Fluorapatite
18: Quartz
19: Albite
20: Fe-Calcite
21: Quartz
22: Albite
23: Quartz
24: Chlorite
25: Chlorite
26: Quartz
27: Kaolinite

Figure 2-3.3: Sample Newburn 4353.5m site 3 (SEM). Table 2-3A. Kaolinite (27) fills pore with irregular contact with quartz grains. Titania appears to fill porosity rimmed by chlorite (1,2). Pyrite (7) fills dissolution voids in quartz grain. Quartz overgrowths into Fe-calcite (positions A). Siderite (position B) fills dissolution voids in quartz grain. Diagenetic fluorapatite with sharp crystal outline forms along intergranular boundary. Trachytic lithic clast (position C).

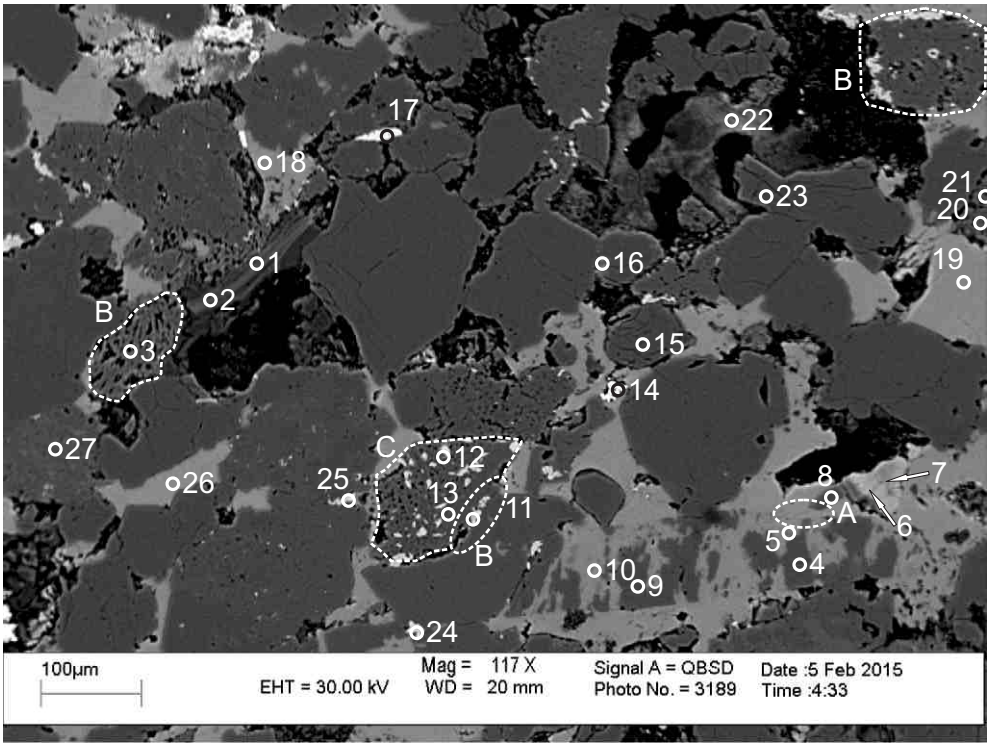

1: Muscovite
2: Muscovite
3: Albite
4: Albite
5: Calcite+ Muscovite
6: Chlorite
7: Chlorite
8: Quartz+ Calcite
9: Albite
10: Fe-Calcite+ Albite
11: Albite
12: Albite
13: Albite
14: Pyrite+ Calcite
15: Quartz
16: Quartz+ Muscovite
17: Titania+ Muscovite
18: Fe-Calcite
19: Fe-Calcite
20: Quartz+ Other
21: Muscovite +Other
22: Titania+ Other
23: Quartz
24: Albite
25: Fe-Calcite+ Albite
26: Calcite+ Other
27: Albite

Figure 2-3.4: Sample Newburn 4353.5m site 4 (SEM). Table 2-3A. Plastically deformed chloritized muscovite (1,2). Calcite (5,10) engulfs albite (4,9). Pyrite (14) fills dissolution void in calcite. Titania (17) forms along intergranular boundary. Possible detrital chlorite (6,7) with fracture. Fe-calcite appears to replace and surround calcite (position A). Siderite forms in dissolution voids formed along intergranular boundaries shared by quartz and Fe-calcite (positions B) as well as in voids within trachytic lithic clasts (positions B and C).

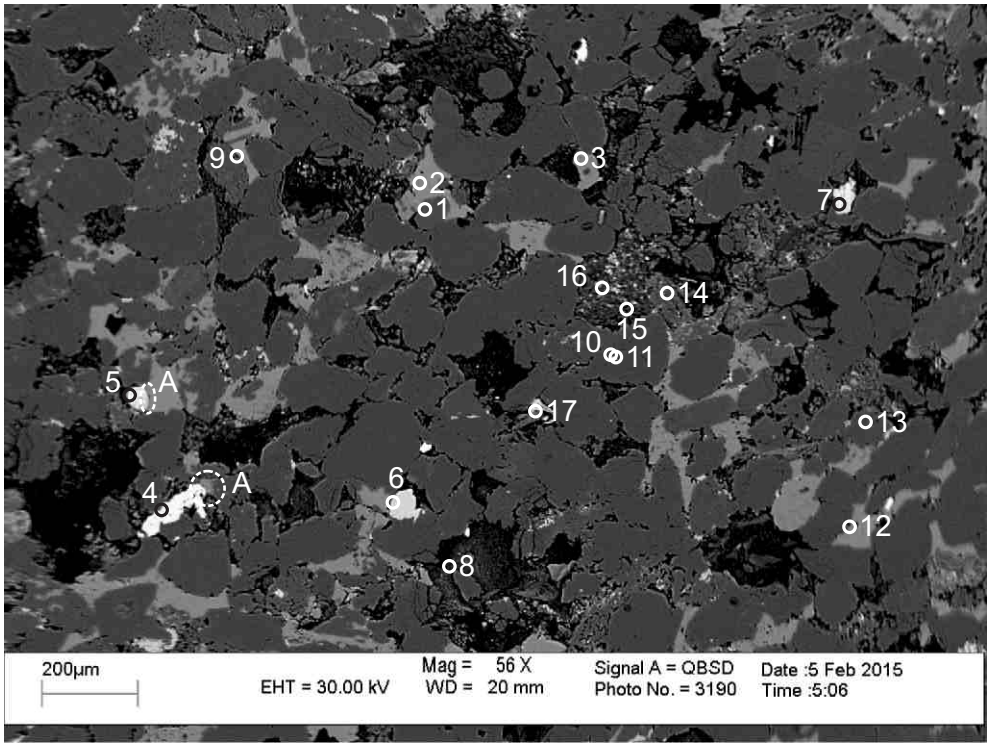

1: Kaolinite+ Albite
2: Calcite
3: Calcite
4: Titania
5: Titania+ Chlorite
6: Fluorapatite
7: Titania+ Chlorite
8: Hole
9: Calcite+ Quartz
10: Quartz
11: Quartz
12: Calcite+ Chlorite
13: Albite
14: Mix
15: Kaolinite
16: Illite +Fluorapatite +Titania
17: Illite+ Chlorite+ Titania

Figure 2-3.5: Sample Newburn 4353.5m site 5 (SEM). Table 2-3A. Illite, fluorapatite and Titania (16) fill voids between books of kaolinite (15) filling pore. Diagenetic fluorapatite (6) engulfs quartz. Titania (4) appears to engulf calcite (positions A).

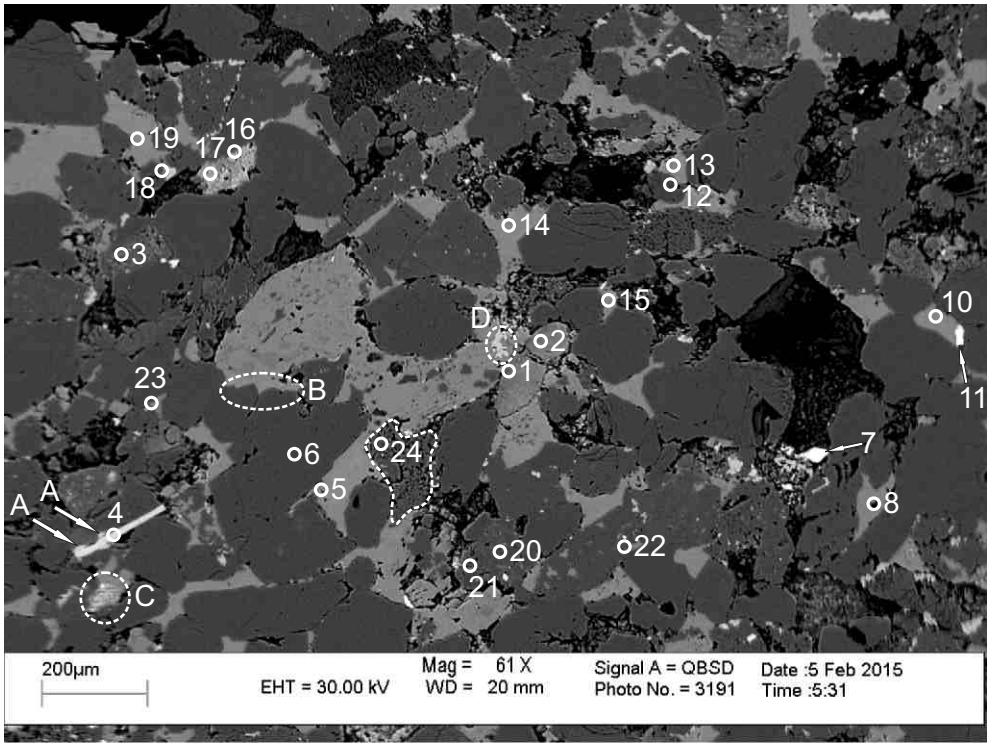

1: K-Feldspar+ Chlorite
2: K-Feldspar+ Chlorite
3: Albite+ Chlorite
4: Fluorapatite
5: Fe-Calcite
6: Quartz
7: Zircon
8: Calcite+ Other
9: Calcite
10: Fe-Calcite
11: Titania+ Quartz
12: Quartz
13: Calcite
14: Calcite
15: Calcite
16: Chlorite
17: Chlorite
18: Siderite+ Quartz
19: Calcite
20: Albite
21: Quartz
22: Albite+ Calcite
23: Calcite+ Chlorite
24: Albite+ Illite

Figure 2-3.6: Sample Newburn 4353.5m site 6 (SEM).Table 2-3A. Detrital K-feldspar (1,2) is associated with chlorite. Euhedral diagenetic fluorapatite (4) cuts chlorite (position A) and framework grain. Fe-calcite (5) surrounds quartz (6) (position B). Titania (11) forms along the along pore boundary of Fe-calcite (10). Fe-Calcite (22) fills dissolution voids in albite/quartz. Chlorite appears to fill secondary porosity in Fe-calcite (position C). Fine grained chlorite (16,17) fills pore. Diagenetic zircon (7) fills void between kaolinite booklets. Siderite replaces Fe-calcite (position D). Trachytic lithic clast (24).

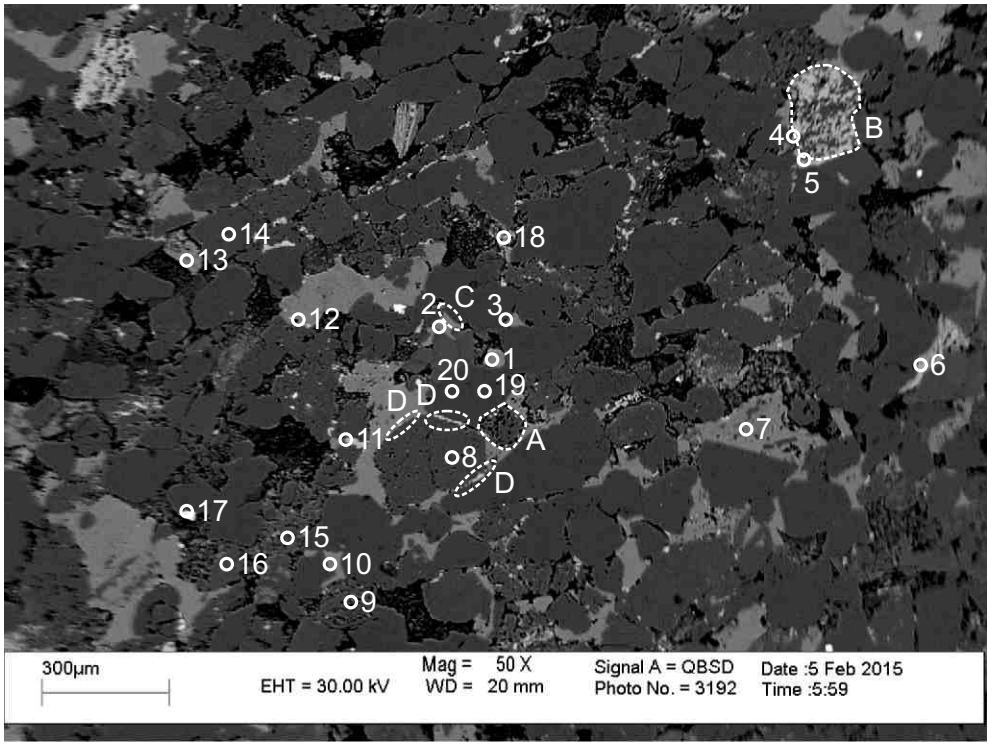

1: K-Feldspar+ Chlorite
2: Calcite
3: Calcite+ Chlorite
4: Albite+ Siderite+ Calcite
5: Albite+ Siderite+ Calcite
6: Albite+ Chlorite+ Calcite
7: Calcite
8: Albite
9: Albite+ Fluorapatite +Titania
10: Quartz+ Calcite
11: Albite+ Chlorite+ Ankerite
12: Calcite
13: Calcite
14: Albite+ Quartz
15: Muscovite
16: Albite
17: Titania+ Chlorite
18: Chlorite
19: Quartz
20: Quartz

Figure 2-3.7: Sample Newburn 4353.5m site 7 (SEM).Table 2-3A. Trachytic lithic clast (position A). Siderite (4,5) fills voids in trachytic lithic clast (position B) composed of albite and replaces calcite which surrounds the clast. Corroded quartz overgrowth into F-calcite (position C). Siderite (positions D) surrounds albite (8).

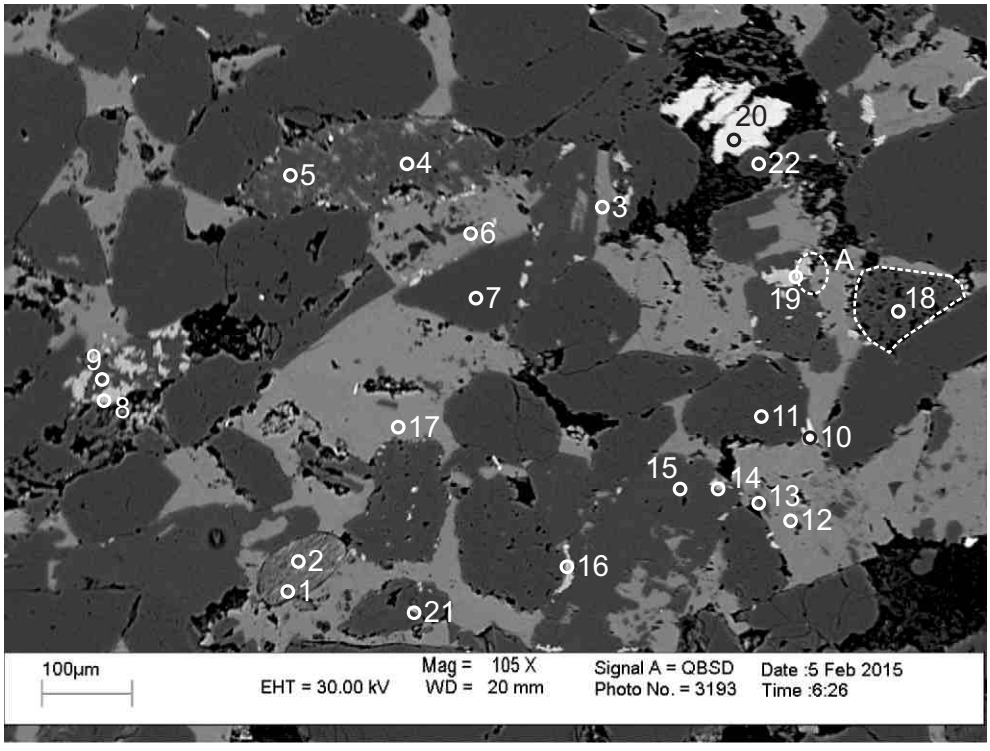

1: Glauconite
2: Glauconite
3: Calcite
4: Albite
5: Albite
6: Calcite+ Albite
7: Quartz
8: Siderite+ Illite
9: Calcite+ Albite
10: Titania
11: Quartz
12: F-Calcite+ Illite
13: Albite
14: Albite
15: Albite
16: Albite+ Chlorite+ Ankerite
17: Calcite
18: Albite
19: Siderite+ Albite
20: Siderite
21: Quartz+ Other
22: Quartz

Figure 2-3.8: Sample Newburn 4353.5m site 8 (SEM).Table 2-3A. Siderite (19) appears to replace F-calcite (position A). Glauconite pellet (1,2). Trachytic lithic clast (18). Siderite (20) fills pore.

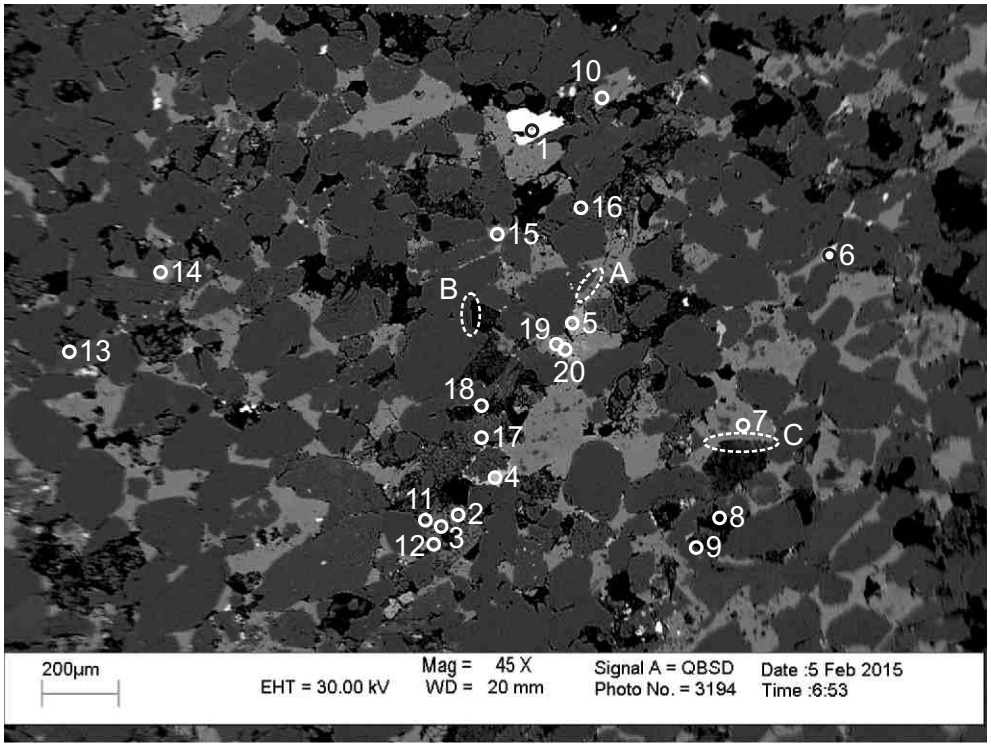

1: Zircon+ Other
2: K-Feldspar+ Chlorite
3: K-Feldspar+ Chlorite
4: Siderite+ Quartz
5: Chlorite
6: Titania+ Quartz
7: Calcite+ K-feldspar
8: Kaolinite
9: Kaolinite
10: K-Feldspar +Calcite
11:K-Feldspar +Chlorite
12: K-Feldspar +Chlorite
13: Albite
14: Calcite
15: Calcite
16: Albite
17: Illite+ Chlorite
18: Illite+ Chlorite
19: Chlorite
20: Calcite+ Chlorite

Figure 2-3.9: Sample Newburn 4353.5m site 9 (SEM).Table 2-3A. Diagenetic zircon (1) appears to cut Fe-calcite. Siderite (4) rims quartz. Straight crystal boundary against pore (position C) which is filled by kaolinite and it is possibly a relic crystal outline from replaced K-feldspar (7). Chlorite fills dissolution voids in detrital K-feldspar grain (2,3,11,12). Kaolinite fills pore (8,9).

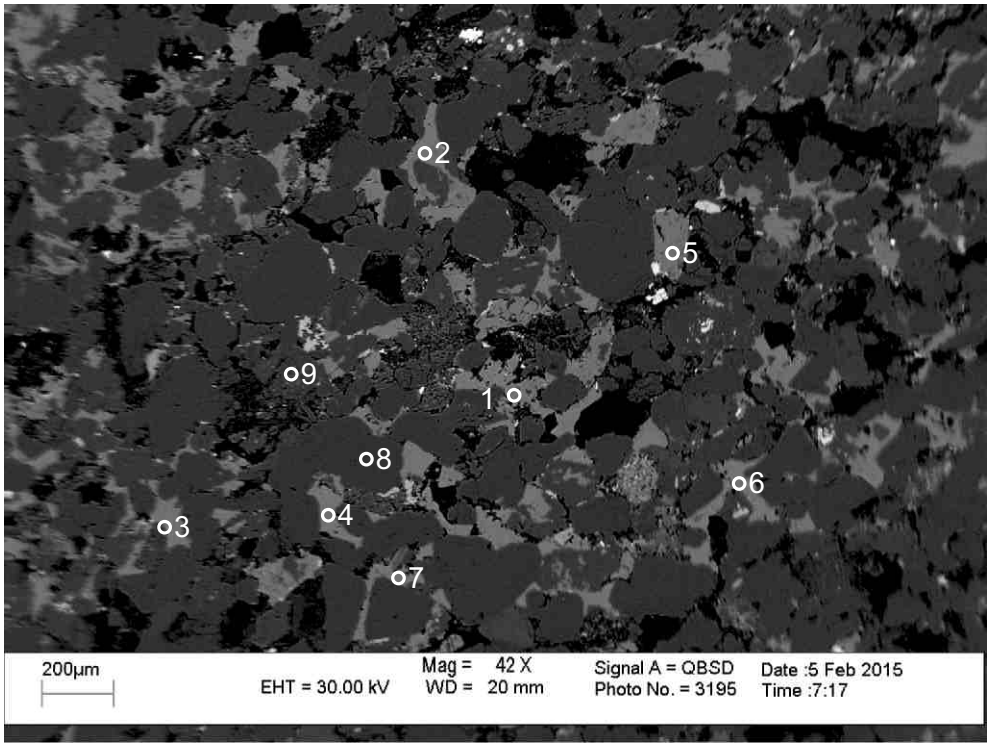

1: Calcite
2: Calcite+ K-Feldspar
3: Calcite
4: Fe-Calcite
5: Calcite
6: Fe-Calcite
7: Calcite
8: Quartz
9: Quartz+ Albite+ Pyrite

Figure 2-3.10: Sample Newburn 4353.5m site 10 (SEM).Table 2-3A. Pyrite (9) fills dissolution voids in quartz and albite. Calcite (1,2,3,5,7) and Fe-calcite (4,6) cement framework grains of quartz (8,9) and albite (9) and engulf K-feldspar (2).

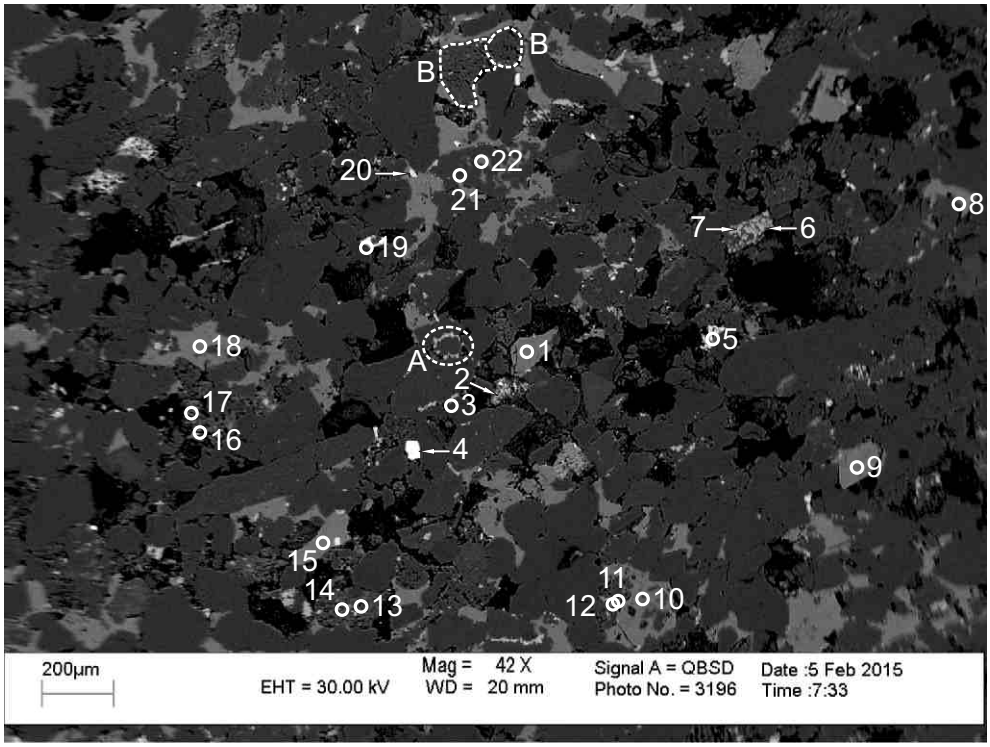

1: Calcite+ K-feldspar
2: Chlorite+ Muscovite+ Pyrite
3: Quartz
4: Zircon
5: Quartz+ Chlorite+Titania
6: Albite+Siderite+ Chlorite
7: Albite+Chlorite+ Siderite
8: Calcite
9: Calcite
10: Calcite+ Muscovite
11: Mix
12: Albite+Other
13: Muscovite+ Chlorite
14: Muscovite+ Chlorite
15: Calcite
16: Muscovite+ Chlorite
17: Muscovite+ Chlorite
18: Calcite
19: Quartz+ Titania+ Hole
20: Titania+ Muscovite+ Calcite
21: Albite
22: Calcite+ Chlorite

Figure 2-3.11: Sample Newburn 4353.5m site 11 (SEM). Table 2-3A. Titania (20) fills dissolution void in calcite. Siderite rims quartz grain (position A). Diagenetic zircon (4) with straight crystal outlines cuts quartz and partly fills porosity. Siderite and chlorite (6,7) fill dissolution voids in albite. Pyrite fills dissolution voids and forms along cleavage plains of chloritized muscovite (2). Trachytic lithic clast (positions B).

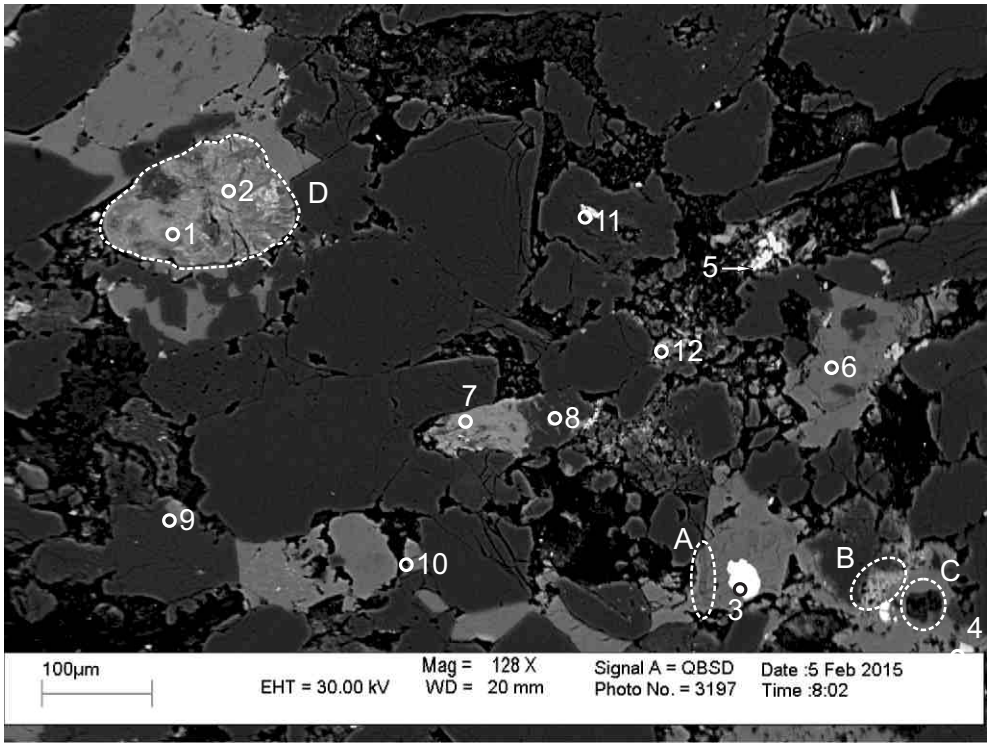

1: Fluorapatite +Chlorite
2: Chlorite+ Apatite
3: Pyrite
4: Titania+ Calcite
5: Titania+ Chlorite
6: Albite+ Muscovite+ Calcite
7: Chlorite
8: Albite
9: Albite+ Calcite
10: Calcite+ Quartz
11: Quartz+ Other
12: Albite+ Chlorite

Figure 2-3.12: Sample Newburn 4353.5m site 12 (SEM).Table 2-3A. Possible remnant K-feldspar is engulfed by calcite (position A). Pyrite (3) forms in a dissolution void in calcite. Lithic clast (position D) composed of fluorapatite, apatite, quartz, and chlorite (1,2). Titania cuts fibrous chlorite (5). Chlorite engulfs calcite (position B). Calcite engulfs kaolinite (position C).

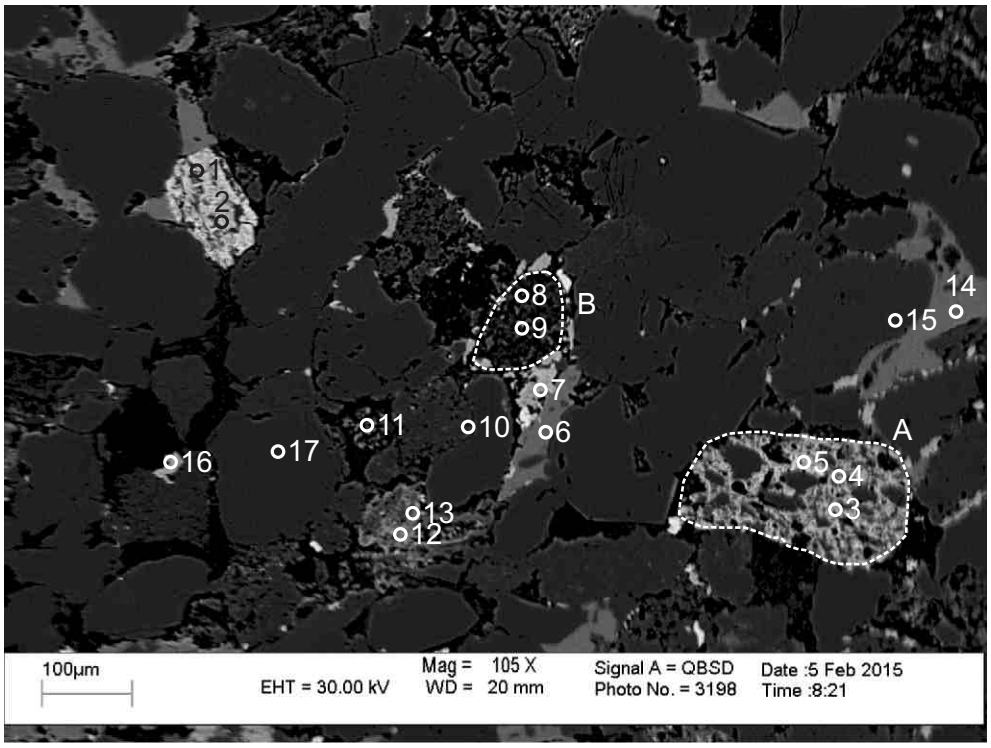

1: Titania+ Chlorite
2: Titania+ Chlorite
3: Titania+ Quartz+ Other
4: Muscovite+ Titania
5: Titania+ Muscovite
6: Calcite
7: Siderite+ Chlorite+ Other
8: Albite+ Muscovite
9: Albite+ Muscovite
10: Quartz+ Muscovite
11: Albite
12: Chlorite
13: Chlorite
14: Calcite
15: Albite
16: Siderite+ Chlorite+ Other
17: Quartz

Figure 2-3.13: Sample Newburn 4353.5 site 13 (SEM). Table 2-3A. Schist lithic clast composed of quartz and muscovite (3-5), the muscovite has been cut by titania (position A). Siderite (7) rims lithic clast composed of albite (8,9) and muscovite (position B). Fibrous chlorite fills pore (12,13). Titania and chlorite (1,2) engulf calcite.

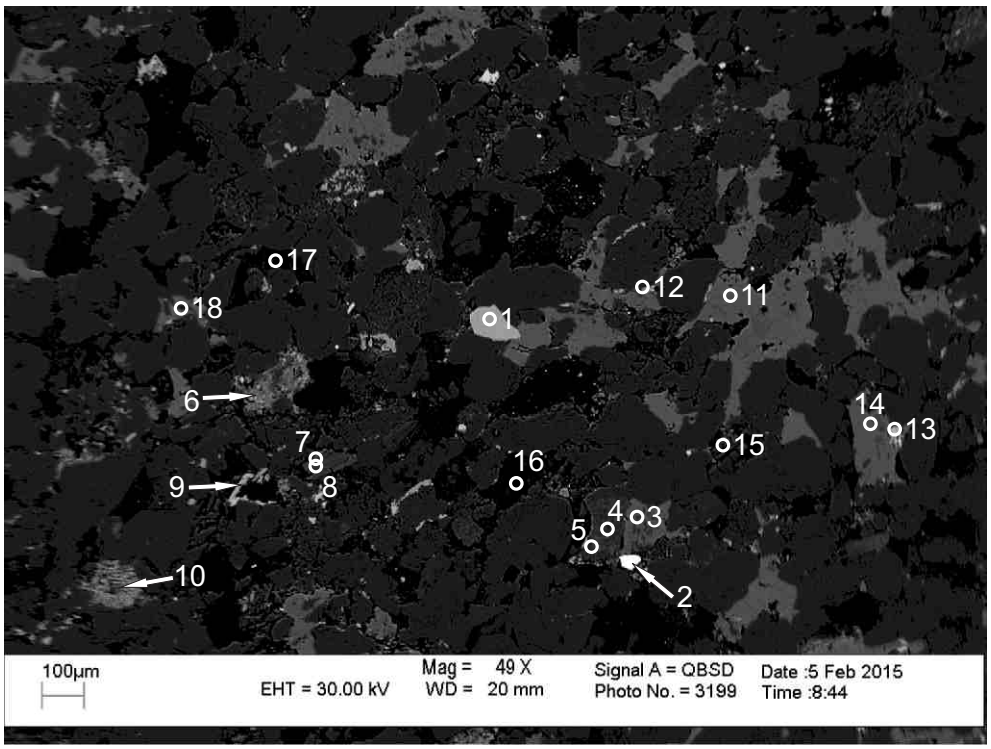

1: Fluorapatite
2: Zircon
3: Calcite+ Albite
4: Albite+ Muscovite+ Chlorite
5: Albite
6: Siderite+ Chlorite+ Other
7: Muscovite
8: Muscovite
9: Fluorapatite
10: Chlorite+ Muscovite +Calcite
11: Fe-Calcite +K-Feldspar
12: Albite+ Siderite+ Chlorite
13: Titania+ Albite
14: K-Feldspar +Calcite
15: Muscovite
16: Muscovite
17: Hole
18: Albite+ Calcite

Figure 2-3.14: Sample Newburn 4353.5m site 14 (SEM).Table 2-3A. Diagenetic fluorapatite (1) engulfs Fe-calcite (11). Diagenetic zircon (2) with straight crystal outline fills pore. Diagenetic fluorapatite (9) rims pore. Chlorite (10) replaces muscovite along cleavage planes. Chlorite cuts albite and muscovite (4,5).

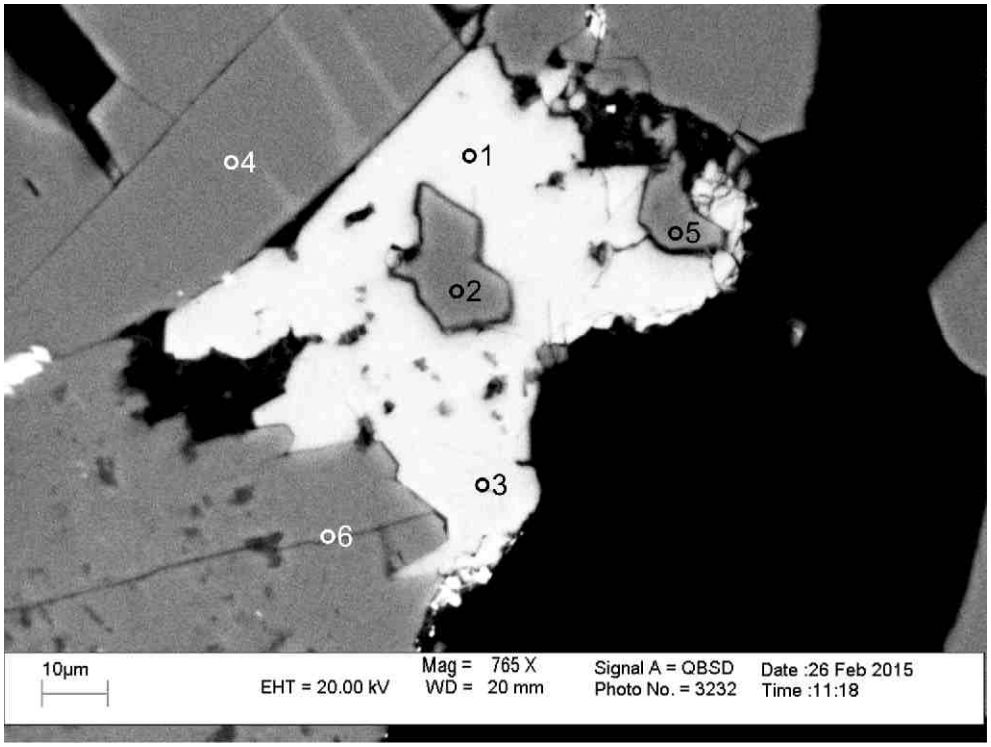

1.Fe- F-Calcite
2. Quartz
3. F-Caclite
4. Albite
5. Quartz
6. Albite

Figure 2-3.15: Sample Newburn 4353.5m site 1 (SEM). Table 2-3B. F-Fe-calcite (1) and F-calcite (3) engulf quartz (2,5).

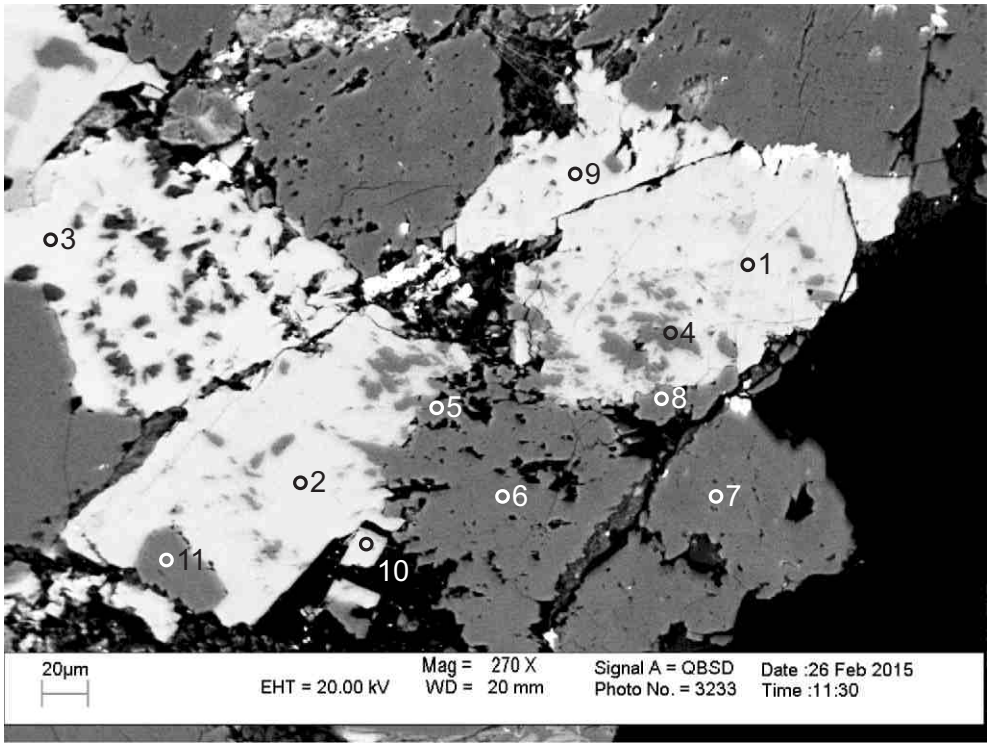

1. F-Calcite
2. F-Calcite
3. F-Fe-Calcite
4. Albite+ Quartz
5. Albite+ Quartz
6. Albite
7. Albite
8. Albite
9. F-Fe-Calcite
10. F-Calcite
11. Albite

Figure 2-3.16: Sample Newburn 4353.5m site 2 (SEM). Table 2-3B. F-calcite (1,2,10) and F-Fe-calcite (3,9) engulf albite (6-8,11) and quartz (4,5).

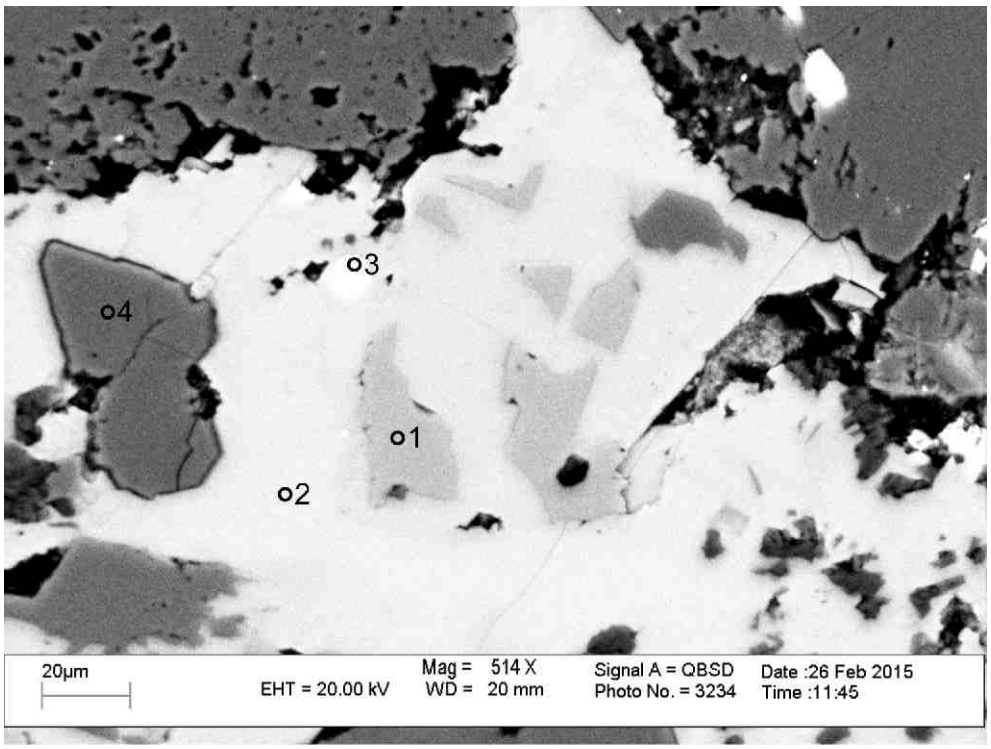

1. K-Feldspar
2. F-Fe-Calcite
3. Pyrite
4. Quartz

Figure 2-3.17: Sample Newburn 4353.5m site 3 (SEM). Table 2-3B. F-Fe-calcite (2) engulfs K-feldspar (1). Pyrite (3) fills dissolution voids in F-Fe-calcite (2).

Table 2-3A: Scaning Electron Microscope chemical analyses of sample 4353.5m from Newburn H-23 well.

Sample	Site	Position	Mineral	SiO_2	TiO_2	Al_2O_3	FeO	MnO	MgO	CaO	Na_2O	K_2O	P_2O_5	SO_3	F	Cl	Sc_2O_3	Cr_2O_3	NiO	CuO	ZnO	Y_2O_3	ZrO_2	Ce_2O_3	HfO_2	WO_3	Total	Actual Total
H-23 4353.5m	1	1	Sd+Other	9.37	0.38	3.02	58.79	0.63	18.32	7.22	0.73	0.66	0.87														100	73
H-23 4353.5m	1	2	Mix	47.30	0.67	2.23	35.53	0.48	8.95	4.17		0.65															100	92
H-23 4353.5m	1	3	Ab+Py	66.42		19.59	0.82				10.53			2.62													100	124
H-23 4353.5m	1	4	Fe-Cal+Kln	7.40		7.69	1.17			83.73																	100	69
H-23 4353.5m	1	5	Cal+Chl	5.13		4.10	7.67	0.31	1.59	80.90		0.31															100	65
H-23 4353.5m	1	6	Ab+Ilt	66.94		21.69	0.46			0.43	9.05	1.43															100	100
H-23 4353.5m	1	7	Chl	29.00		23.51	26.09		4.78	1.19		0.20				0.24											85	82
H-23 4353.5m	1	8	Chl+Cal	29.24		24.41	29.07		5.07	11.99						0.20											100	77
H-23 4353.5m	1	9	TiO_2+Chl	3.12	90.63	3.04	1.08		0.55	1.15	0.42																100	62
H-23 4353.5m	1	10	TiO_2+Chl	3.32	88.84	4.88	0.82			0.90			0.99			0.27											100	58
H-23 4353.5m	1	11	Fe-Cal+Qz	1.22			1.56			97.22																	100	54
H-23 4353.5m	1	12	Ab	67.86		20.58				1.08	10.22	0.28															100	107
H-23 4353.5m	1	13	Qz	98.40		1.17						0.41															100	105
H-23 4353.5m	1	14	Fe-Cal	0.88			1.25	0.27		53.45		0.15															56	62
H-23 4353.5m	1	15	Ab+Ilt	66.83	0.22	21.50	0.31			0.35	9.67	1.14															100	109
H-23 4353.5m	1	16	Qz	99.99																							100	113
H-23 4353.5m	1	17	Ab+Cal	56.11		17.50	0.30			16.47	9.40	0.20															100	106
H-23 4353.5m	1	18	Ms+TiO_2	52.52	5.22	26.79	3.32		3.12	0.94	0.66	7.20				0.23											100	90
H-23 4353.5m	1	19	Chl	29.91	0.30	19.91	21.44	0.26	8.72	2.56		0.52		0.68		0.70											85	76
H-23 4353.5m	1	20	Ab+Fe-Cal	52.62	1.17	18.97	3.02		0.83	14.29	7.40	1.71															100	107
H-23 4353.5m	1	21	Ank+Ab	15.34		5.65	39.57	0.76	9.90	26.68	1.79	0.29															100	73
H-23 4353.5m	1	22	Sd+Ab	39.85		12.75	30.63	0.57	5.82	2.91	7.48																100	88
H-23 4353.5m	1	23	Ab	68.73		20.03	0.54				10.70																100	120
H-23 4353.5m	1	24	Ab	64.50		19.44	4.82			0.32	10.91																100	121
H-23 4353.5m	1	25	Qz	99.26		0.55						0.19															100	108
H-23 4353.5m	1	26	Ab	68.60		20.60	0.23				10.39	0.19															100	116
H-23 4353.5m	2	1	F-Cal+Other	2.72		0.68	1.56	0.31		88.53		1.23			5.00												100	65
H-23 4353.5m	2	2	Chl	28.38		19.75	25.19	0.57	10.57	0.54																	85	107
H-23 4353.5m	2	3	Chl	23.56	0.30	17.77	31.76		7.92	3.30	0.39																85	101
H-23 4353.5m	2	4	F-Cal+Chl	2.82		1.19	1.67			86.44		0.20			7.68												100	71
H-23 4353.5m	2	5	F-Cal				0.93			52.46					2.61												56	60
H-23 4353.5m	2	6	Oli	62.79		23.92	0.14			4.60	8.28	0.28															100	102
H-23 4353.5m	2	7	Qz	99.99																							100	94
H-23 4353.5m	2	8	Qz+Chl	68.39		9.83	12.92		7.83	0.64	0.39																100	96
H-23 4353.5m	2	9	Ab	70.02		19.48					10.50																100	110
H-23 4353.5m	2	10	Oli	64.60		22.90				3.27	8.98	0.25															100	98
H-23 4353.5m	2	11	Ab	65.63		20.60	0.95			0.62	10.06	0.29		1.87													100	102
H-23 4353.5m	2	12	Ab	65.12	0.40	19.90	3.76		0.63	0.24	9.65	0.31															100	114
H-23 4353.5m	2	13	Fe-Cal+Ab	3.53		1.47	2.01	0.32		91.77	0.89																100	58
H-23 4353.5m	2	14	Ab	67.19		21.33	1.90		0.60	0.31	8.26	0.39															100	87
H-23 4353.5m	2	15	Qz	99.99																							100	105
H-23 4353.5m	2	16	Qz	99.99																							100	108
H-23 4353.5m	2	17	Ms	46.60		33.48	1.62		0.81		0.87	10.01			1.62												95	108

Table 2-3A: Scaning Electron Microscope chemical analyses of sample 4353.5m from Newburn H-23 well.

Sample	Site	Position	Mineral	SiO_2	TiO_2	Al_2O_3	FeO	MnO	MgO	CaO	Na_2O	K_2O	P_2O_5	SO_3	F	Cl	Sc_2O_3	Cr_2O_3	NiO	CuO	ZnO	Y_2O_3	ZrO_2	Ce_2O_3	HfO_2	WO_3	Total	Actual Total
H-23 4353.5m	2	18	Qz	99.99																							100	107
H-23 4353.5m	2	19	Oli	63.85		23.28				3.93	8.61	0.33															100	93
H-23 4353.5m	2	20	Qz	96.52		1.80	0.85		0.46	0.20		0.16															100	116
H-23 4353.5m	2	21	F-Cal+Other	8.00		3.08	1.75			83.67		0.41			3.08												100	63
H-23 4353.5m	2	22	Ab	66.55		19.54	3.00		0.73	0.18	9.84	0.17															100	114
H-23 4353.5m	2	23	Ab	66.42		20.69	1.58		0.63	0.36	10.12	0.20															100	111
H-23 4353.5m	2	24	Qz	99.41		0.40	0.18																				100	117
H-23 4353.5m	3	1	TiO_2+Chl	4.88	82.17	4.02	8.09		0.85																		100	91
H-23 4353.5m	3	2	Chl	28.62	0.64	17.25	27.79		10.71																		85	93
H-23 4353.5m	3	3	Spl	0.45		30.57	14.87		13.35									40.77									100	110
H-23 4353.5m	3	4	TiO_2		100.00																						100	98
H-23 4353.5m	3	5	TiO_2		100.00																						100	98
H-23 4353.5m	3	6	TiO_2	3.94	93.21	1.55	0.39		0.40	0.52																	100	111
H-23 4353.5m	3	7	Py+Qz	22.06		1.63	20.11				0.74	0.46		54.86					0.15								100	186
H-23 4353.5m	3	8	Fe-Cal	0.48			1.15			54.37																	56	63
H-23 4353.5m	3	9	Qz	91.62		1.72	1.22			0.88	0.81		0.44	3.30													100	121
H-23 4353.5m	3	10	Fe-Cal	1.55			3.62	0.21	0.54	49.44		0.65															56	52
H-23 4353.5m	3	11	Ab	68.90		19.92				0.39	10.79																100	92
H-23 4353.5m	3	12	Qz	99.99																							100	96
H-23 4353.5m	3	13	Fe-Cal+Ms	3.85		1.53	1.45			92.71		0.46															100	54
H-23 4353.5m	3	14	Ab	67.79		20.05				1.50	10.66																100	98
H-23 4353.5m	3	15	Qz	99.99																							100	101
H-23 4353.5m	3	16	Ab+Other	64.82	0.18	20.33	0.18		0.76	1.62	9.80	1.29	1.01														100	101
H-23 4353.5m	3	17	Fap				0.19		0.41	50.79			40.72	0.55	5.81	0.21										1.34	100	120
H-23 4353.5m	3	18	Qz	99.99																							100	104
H-23 4353.5m	3	19	Ab	68.86		20.33					10.66	0.14															100	108
H-23 4353.5m	3	20	Fe-Cal				1.13			54.87																	56	64
H-23 4353.5m	3	21	Qz	99.99																							100	121
H-23 4353.5m	3	22	Ab	67.81		21.05	0.55			0.34	10.25																100	123
H-23 4353.5m	3	23	Qz	99.99																							100	119
H-23 4353.5m	3	24	Chl	32.91		22.46	17.68		8.63	0.68	0.33	2.31															85	107
H-23 4353.5m	3	25	Chl	27.33		8.94	0.79			42.81	5.13																85	97
H-23 4353.5m	3	26	Qz	99.99																							100	126
H-23 4353.5m	3	27	Kln	47.68		37.54	0.42			0.15		0.21															86	105
H-23 4353.5m	4	1	Ms	45.83	0.41	36.64	0.63		0.44		1.22	9.84															95	105
H-23 4353.5m	4	2	Ms	46.11	0.41	37.04	0.57		0.43		1.11	9.33															95	102
H-23 4353.5m	4	3	Ab	65.59		19.58	0.44			2.18	10.44		1.79														100	118
H-23 4353.5m	4	4	Ab	69.10		20.10					10.79																100	116
H-23 4353.5m	4	5	Cal+Ms	37.09		11.34	0.42			45.67	2.29	3.19															100	85
H-23 4353.5m	4	6	Chl	28.08		22.52	28.35		4.76	0.72	0.57																85	91
H-23 4353.5m	4	7	Chl	28.42		23.40	27.25		4.47	0.78	0.48					0.19											85	92
H-23 4353.5m	4	8	Qz+Cal	84.11			0.31			15.57																	100	108
H-23 4353.5m	4	9	Ab	68.63		20.07				0.78	10.52																100	110

Table 2-3A: Scaning Electron Microscope chemical analyses of sample 4353.5m from Newburn H-23 well.

Sample	Site	Position	Mineral	SiO_2	TiO_2	Al_2O_3	FeO	MnO	MgO	CaO	Na_2O	K_2O	P_2O_5	SO_3	F	Cl	Sc_2O_3	Cr_2O_3	NiO	CuO	ZnO	Y_2O_3	ZrO_2	Ce_2O_3	HfO_2	WO_3	Total	Actual Total
H-23 4353.5m	4	10	Cal+Ab	22.20		6.08	0.94			68.25	1.85	0.66															100	71
H-23 4353.5m	4	11	Ab	66.02		19.01	3.86			0.21	10.91																100	100
H-23 4353.5m	4	12	Ab	65.59		19.50	3.65			0.35	10.66	0.25															100	108
H-23 4353.5m	4	13	Ab	69.20		20.20					10.58																100	111
H-23 4353.5m	4	14	Py+Cal	1.80		0.66	17.47	0.30	0.66	30.91				48.22													100	117
H-23 4353.5m	4	15	Qz	99.99																							100	114
H-23 4353.5m	4	16	Qz+Ms	87.56		7.60	1.54		0.98			2.31															100	109
H-23 4353.5m	4	17	TiO_2+Ms	17.73	73.61	5.59	0.96					1.53	0.55														100	95
H-23 4353.5m	4	18	Fe-Cal				1.14			54.86																	56	57
H-23 4353.5m	4	19	Fe-Cal				1.08			54.92																	56	63
H-23 4353.5m	4	20	Qz+Other	95.52		2.89	0.60					0.99															100	115
H-23 4353.5m	4	21	Ms+Other	78.98		13.38	1.96		0.80	0.48	0.31	4.08															100	109
H-23 4353.5m	4	22	TiO_2+Other	26.03	53.81	14.08	0.98		1.11	0.88		2.78				0.33											100	78
H-23 4353.5m	4	23	Qz	99.99																							100	117
H-23 4353.5m	4	24	Ab	64.84		18.61	5.00			0.45	11.10																100	96
H-23 4353.5m	4	25	Fe-Cal+Ab	25.69		10.35	4.26			54.43	4.79	0.49															100	63
H-23 4353.5m	4	26	Cal+Other	3.98			2.33	0.31		93.38																	100	57
H-23 4353.5m	4	27	Ab	66.98		21.37	0.22			0.24	9.94	1.25															100	107
H-23 4353.5m	5	1	Kln+Ab	43.10	0.73	39.51	4.30		9.25	0.98	2.12																100	102
H-23 4353.5m	5	2	Cal				1.04	0.21		54.76																	56	59
H-23 4353.5m	5	3	Cal	1.65		0.46	0.94	0.20		52.51		0.24															56	66
H-23 4353.5m	5	4	TiO_2	0.77	98.83		0.40																				100	84
H-23 4353.5m	5	5	TiO_2+Chl	6.85	88.77	2.61	0.76		0.46			0.58															100	87
H-23 4353.5m	5	6	Fap				0.27		0.58	51.46			40.93		5.26	0.28										1.25	100	116
H-23 4353.5m	5	7	TiO_2+Chl	3.42	92.18	2.06	1.27			0.39		0.25						0.42									100	104
H-23 4353.5m	5	8	Hole	49.97	0.30	5.50	16.34	0.19	16.66	2.62	0.75	0.96		0.72	5.45	0.51											100	73
H-23 4353.5m	5	9	Fe-Cal+Qz	8.09			1.85		0.61	89.45																	100	59
H-23 4353.5m	5	10	Qz	96.50			0.63							2.87													100	117
H-23 4353.5m	5	11	Qz	99.99																							100	116
H-23 4353.5m	5	12	Cal+Chl	1.62		1.90	1.14	0.20		51.14																	56	66
H-23 4353.5m	5	13	Ab	71.32		18.76					9.94																100	127
H-23 4353.5m	5	14	Mix	69.05	0.40	15.25	3.05		7.79		0.30	4.14															100	112
H-23 4353.5m	5	15	Kln	47.12		36.99	0.42		0.77	0.27		0.30						0.13									86	110
H-23 4353.5m	5	16	Ilt+Fap+TiO_2	46.63	5.42	30.61	1.08		1.53	2.14	0.82	5.48	3.02	0.50	1.75	0.27								0.75			100	98
H-23 4353.5m	5	17	Ilt+Chl+TiO_2	56.56	6.69	19.44	7.59		4.64		0.57	4.22				0.27											100	84
H-23 4353.5m	6	1	Kfs+Chl	54.68		18.74	12.34		2.95	0.95	0.42	9.93															100	98
H-23 4353.5m	6	2	Kfs+Chl	55.34		17.08	13.08		3.10	0.70	0.47	10.01				0.23											100	102
H-23 4353.5m	6	3	Ab+Chl	56.95	0.22	21.30	8.99		4.88	0.43	6.96	0.30															100	90
H-23 4353.5m	6	4	Fap	1.86		0.91		0.17		48.55	0.75		39.09		8.09									0.59			100	107
H-23 4353.5m	6	5	Fe-Cal				1.25			54.75																	56	54
H-23 4353.5m	6	6	Qz	99.99																							100	103
H-23 4353.5m	6	7	Zrn	29.99																			70.01				100	127
H-23 4353.5m	6	8	Cal+Other	30.78		21.82	4.25		1.63	39.26	0.39	1.67				0.21											100	74

Table 2-3A: Scaning Electron Microscope chemical analyses of sample 4353.5m from Newburn H-23 well.

Sample	Site	Position	Mineral	SiO_2	TiO_2	Al_2O_3	FeO	MnO	MgO	CaO	Na_2O	K_2O	P_2O_5	SO_3	F	Cl	Sc_2O_3	Cr_2O_3	NiO	CuO	ZnO	Y_2O_3	ZrO_2	Ce_2O_3	HfO_2	WO_3	Total	Actual Total
H-23 4353.5m	6	9	Cal				0.48			55.52																	56	67
H-23 4353.5m	6	10	Fe-Cal				1.34			54.66																	56	65
H-23 4353.5m	6	11	TiO_2+Qz	24.41	73.51	0.87	0.73			0.46																	100	121
H-23 4353.5m	6	12	Qz	99.99																							100	117
H-23 4353.5m	6	13	Fe-Cal				1.20			54.80																	56	63
H-23 4353.5m	6	14	Cal				0.98			55.02																	56	59
H-23 4353.5m	6	15	Fe-Cal	3.39			1.15			51.46																	56	60
H-23 4353.5m	6	16	Chl	26.00		20.48	30.76		6.23	1.13	0.40																85	82
H-23 4353.5m	6	17	Chl	26.95		22.12	29.67		4.58	1.16	0.54																85	76
H-23 4353.5m	6	18	Sd+Qz	19.47		1.06	54.86	0.67	16.85	7.09																	100	63
H-23 4353.5m	6	19	Fe-Cal				1.22	0.22		54.56																	56	53
H-23 4353.5m	6	20	Ab	69.27		17.14	3.06		1.48		9.07																100	120
H-23 4353.5m	6	21	Qz	95.47		3.10	0.40				0.85	0.19															100	106
H-23 4353.5m	6	22	Ab+Fe-Cal	34.38		12.06	1.17			45.24	7.16																100	83
H-23 4353.5m	6	23	Fe-Cal+Chl	8.09		2.04	1.76	0.30		87.04	0.77																100	55
H-23 4353.5m	6	24	Ab+Ilt	66.38	1.13	21.13				1.67	7.29	1.05	1.35														100	65
H-23 4353.5m	7	1	Kfs+Chl	55.94		13.47	15.36		3.63		0.42	11.02				0.17											100	96
H-23 4353.5m	7	2	Fe-Cal				1.31			54.69																	56	54
H-23 4353.5m	7	3	Cal+Chl	8.96		2.12	1.83			87.09																	100	58
H-23 4353.5m	7	4	Ab+Sd+Cal	42.63	0.45	14.23	25.38	0.37	4.28	3.50	8.56	0.61															100	97
H-23 4353.5m	7	5	Ab+Sd+Cal	40.60	0.75	10.75	30.76	0.54	7.01	3.67	5.35	0.57															100	83
H-23 4353.5m	7	6	Ab+Chl+Cal	48.50	0.75	22.39	16.65	0.18	4.48	1.05	5.15	0.88															100	111
H-23 4353.5m	7	7	Cal	4.18		0.93	0.61			50.14		0.14															56	63
H-23 4353.5m	7	8	Ab	69.01		20.29					10.54					0.15											100	101
H-23 4353.5m	7	9	Ab+Fap+TiO_2	55.62	5.14	20.44	0.42		0.53	3.95	6.28	1.42	3.99		2.20												100	85
H-23 4353.5m	7	10	Qz+Cal	82.66			0.40			16.93																	100	87
H-23 4353.5m	7	11	Ab+Chl+Ank	44.58		15.72	24.61	0.37	4.28	2.36	7.50	0.35				0.22											100	78
H-23 4353.5m	7	12	Cal	0.42		0.41	1.13			54.04																	56	52
H-23 4353.5m	7	13	Cal	2.13		0.63	0.92			51.65		0.66															56	52
H-23 4353.5m	7	14	Ab+Qz	82.27		11.07					6.66																100	102
H-23 4353.5m	7	15	Ms	49.35	0.19	30.15	3.42		2.71		0.34	8.85															95	82
H-23 4353.5m	7	16	Ab	68.99		20.43					10.60																100	91
H-23 4353.5m	7	17	TiO_2+Chl	3.53	91.84	2.65	1.70			0.28																	100	75
H-23 4353.5m	7	18	Chl	29.31		23.74	24.42		5.74	0.69	0.37	0.36				0.37											85	76
H-23 4353.5m	7	19	Qz	99.99																							100	103
H-23 4353.5m	7	20	Qz	99.99																							100	102
H-23 4353.5m	8	1	Glt	54.09	0.59	19.00	5.44		2.54		0.27	6.07															88	103
H-23 4353.5m	8	2	Glt	52.14	0.70	20.52	4.87		2.23			7.52															88	102
H-23 4353.5m	8	3	Cal	1.26			0.78			53.96																	56	62
H-23 4353.5m	8	4	Ab	65.50		20.71	3.22				10.39	0.18															100	115
H-23 4353.5m	8	5	Ab	67.86		20.52	0.76			0.27	10.34	0.25															100	111
H-23 4353.5m	8	6	Cal+Ab	23.34		10.03	0.99			59.97	5.66																100	76
H-23 4353.5m	8	7	Qz	99.99																							100	111

Table 2-3A: Scaning Electron Microscope chemical analyses of sample 4353.5m from Newburn H-23 well.

Sample	Site	Position	Mineral	SiO_2	TiO_2	Al_2O_3	FeO	MnO	MgO	CaO	Na_2O	K_2O	P_2O_5	SO_3	F	Cl	Sc_2O_3	Cr_2O_3	NiO	CuO	ZnO	Y_2O_3	ZrO_2	Ce_2O_3	HfO_2	WO_3	Total	Actual Total
H-23 4353.5m	8	8	Sd+Ilt	13.73		4.80	56.04	0.53	18.06	5.86		0.99															100	61
H-23 4353.5m	8	9	Fe-Cal+Ab	43.62		14.46	7.10	0.19	2.30	23.18	9.13																100	92
H-23 4353.5m	8	10	TiO_2	2.27	92.68	1.51	1.43			2.11																	100	99
H-23 4353.5m	8	11	Qz	99.28		0.72																					100	113
H-23 4353.5m	8	12	F-Cal+Ilt	17.76		11.70	1.40			64.95		1.22			2.98												100	66
H-23 4353.5m	8	13	Ab	68.05		19.12				2.59	10.23																100	116
H-23 4353.5m	8	14	Ab	65.25		19.46	4.39			0.35	10.54																100	110
H-23 4353.5m	8	15	Ab	69.31		20.05					10.64																100	114
H-23 4353.5m	8	16	Ab+Chl+Ank	43.36		12.06	27.57	0.46	7.43	2.59	6.54																100	76
H-23 4353.5m	8	17	Fe-Cal				1.30	0.19		54.51																	56	56
H-23 4353.5m	8	18	Ab	69.31		20.05					10.65																100	116
H-23 4353.5m	8	19	Sd+Ab	12.26		4.44	56.52	0.80	14.96	7.07	2.64	0.29	1.03														100	71
H-23 4353.5m	8	20	Sd				54.17	0.32		0.39			1.11														56	55
H-23 4353.5m	8	21	Qz+Other	91.00		0.96	6.38		0.90	0.36	0.40																100	99
H-23 4353.5m	8	22	Qz	98.66		0.98	0.18					0.18															100	115
H-23 4353.5m	9	1	Zrn+Other	27.75		1.53	0.32			1.40							1.09					2.71	65.22				100	95
H-23 4353.5m	9	2	Kfs+Chl	55.04		20.01	11.39		2.97		0.38	10.21															100	89
H-23 4353.5m	9	3	Kfs+Chl	55.30		22.07	9.25		2.67		0.58	9.96				0.18											100	86
H-23 4353.5m	9	4	Sd+Qz	2.44			65.26	0.67	20.59	11.01																	100	55
H-23 4353.5m	9	5	Chl	29.08		21.20	24.65		9.78	0.29																	85	90
H-23 4353.5m	9	6	Qz+TiO_2	58.49	40.85		0.66																				100	107
H-23 4353.5m	9	7	Cal+Ms	6.08		1.81	1.44			89.16		1.51															100	67
H-23 4353.5m	9	8	Kln	49.12		36.12	0.18					0.24				0.34											86	77
H-23 4353.5m	9	9	Kln	53.10		31.56	0.39		0.34	0.21		0.22				0.17											86	71
H-23 4353.5m	9	10	Kfs+Cal	35.00		11.30	0.66	0.18		43.60	0.69	8.59															100	95
H-23 4353.5m	9	11	Kfs+Chl	54.89		23.32	8.74		2.92		0.53	9.61															100	85
H-23 4353.5m	9	12	Kfs+Chl	54.66		25.72	6.05		2.57	0.77	0.67	9.38				0.17											100	88
H-23 4353.5m	9	13	Ab	65.18		21.84	0.46			1.19	9.56	0.99		0.77													100	89
H-23 4353.5m	9	14	Fe-Cal				1.22			54.78																	56	47
H-23 4353.5m	9	15	Fe-Cal				1.19		0.32	54.49																	56	57
H-23 4353.5m	9	16	Ab	68.09		21.28	0.33				10.31																100	113
H-23 4353.5m	9	17	Ilt+Chl	70.81	1.43	13.87	6.19		2.14	0.88	0.31	4.37															100	89
H-23 4353.5m	9	18	Ilt+Chl	75.09	1.45	14.66	2.41		1.09		0.24	5.05															100	71
H-23 4353.5m	9	19	Chl	26.02		23.24	29.20		4.85	1.70																	85	89
H-23 4353.5m	9	20	Cal+Chl	9.56		9.32	12.03		2.27	66.83																	100	69
H-23 4353.5m	10	1	Cal	1.27		0.44	0.44			53.85																	56	56
H-23 4353.5m	10	2	Cal+Kfs	20.86		7.26	1.24	0.23		66.29		4.12															100	73
H-23 4353.5m	10	3	Cal				0.45			55.55																	56	43
H-23 4353.5m	10	4	Fe-Cal	0.96		0.68	1.06			53.31																	56	48
H-23 4353.5m	10	5	Cal	2.81		1.14	0.90			50.61	0.54																56	64
H-23 4353.5m	10	6	Fe-Cal				1.23			54.77																	56	57
H-23 4353.5m	10	7	Cal				0.70			55.30																	56	48
H-23 4353.5m	10	8	Qz	99.99																							100	93

Table 2-3A: Scaning Electron Microscope chemical analyses of sample 4353.5m from Newburn H-23 well.

Sample	Site	Position	Mineral	SiO_2	TiO_2	Al_2O_3	FeO	MnO	MgO	CaO	Na_2O	K_2O	P_2O_5	SO_3	F	Cl	Sc_2O_3	Cr_2O_3	NiO	CuO	ZnO	Y_2O_3	ZrO_2	Ce_2O_3	HfO_2	WO_3	Total	Actual Total
H-23 4353.5m	10	9	Qz+Ab+Py	88.07	0.27	5.20	0.85				2.80	0.20		2.60													100	93
H-23 4353.5m	11	1	Cal+Kfs	7.40		2.34	1.39	0.28		87.04		1.54															100	65
H-23 4353.5m	11	2	Chl+Ms+Py	28.43	10.69	21.60	22.84		3.40	2.69	0.58	1.24	1.74	4.79							2.02						100	77
H-23 4353.5m	11	3	Qz	99.99																							100	102
H-23 4353.5m	11	4	Zrn	31.92																			67.28		0.80		100	107
H-23 4353.5m	11	5	Qz+Chl+TiO_2	46.04	11.21	22.81	9.39		5.59	0.50	0.49	3.97															100	110
H-23 4353.5m	11	6	Ab+Sd+Chl	33.01	2.02	7.61	33.09	0.39	16.63	3.64	2.60	0.79				0.22											100	73
H-23 4353.5m	11	7	Ab+Chl+Sd	50.04	0.58	16.14	19.18	0.31	2.06	1.47	9.94	0.31															100	111
H-23 4353.5m	11	8	Cal	1.78			0.96	0.17		53.09																	56	69
H-23 4353.5m	11	9	Cal				1.18	0.18		54.64																	56	63
H-23 4353.5m	11	10	Cal+Ms	17.78		6.29	1.14	0.23		71.33	0.77	2.43															100	70
H-23 4353.5m	11	11	Mix	57.48		3.97	1.98		0.65	35.22		0.72															100	81
H-23 4353.5m	11	12	Ab+Other	66.79		18.23	4.08		3.08	0.38	6.12	1.31															100	95
H-23 4353.5m	11	13	Ms+Chl	56.41	0.43	28.12	3.71		1.96		0.44	8.93															100	76
H-23 4353.5m	11	14	Ms+Chl	53.48	1.27	31.27	2.37		1.59		0.39	9.62															100	90
H-23 4353.5m	11	15	Fe-Cal				1.34	0.20		54.47																	56	48
H-23 4353.5m	11	16	Ms+Chl	52.32	1.48	31.88	2.51		1.58			9.99				0.24											100	67
H-23 4353.5m	11	17	Ms+Chl	48.82	0.65	32.61	4.13		1.56			12.23															100	61
H-23 4353.5m	11	18	Fe-Cal	0.97		0.38	1.44	0.20		53.01																	56	48
H-23 4353.5m	11	19	Qz+TiO_2+Hole	56.05	28.09	10.00	0.57		0.95	0.27					4.08												100	91
H-23 4353.5m	11	20	TiO_2+Ms+Cal	8.86	79.32	6.63	0.67			3.64		0.90															100	92
H-23 4353.5m	11	21	Ab	69.12		20.14					10.75																100	108
H-23 4353.5m	11	22	Cal+Chl	4.71		1.72	1.53	0.31		91.35		0.37															100	60
H-23 4353.5m	12	1	Fap+Chl	15.19	1.03	12.43	11.09	0.19	4.78	27.91	0.49	0.76	20.85		5.28												100	94
H-23 4353.5m	12	2	Chl+Ap	35.28	0.37	24.64	16.62	0.21	6.60	7.54	0.53	2.69	5.55														100	90
H-23 4353.5m	12	3	Py				21.43			0.34				55.83						22.41							100	166
H-23 4353.5m	12	4	TiO_2+Fe-Cal	0.62	93.21	0.83	1.57			3.79																	100	93
H-23 4353.5m	12	5	TiO_2+Chl	5.52	81.62	6.41	4.93		1.31	0.22																	100	99
H-23 4353.5m	12	6	Ab+Ms+Cal	49.18		14.70	0.36			24.70	5.39	5.67															100	96
H-23 4353.5m	12	7	Chl	28.55		19.19	23.33		13.75	0.17																	85	88
H-23 4353.5m	12	8	Ab	65.97		20.20	2.59		0.93	0.24	10.08																100	101
H-23 4353.5m	12	9	Ab+Cal	51.28		16.16	0.46			22.43	9.68																100	90
H-23 4353.5m	12	10	Fe-Cal+Qz	27.49		1.11	2.83	0.36	3.68	64.35		0.20															100	60
H-23 4353.5m	12	11	Qz+TiO_2	92.41	7.41		0.18																				100	103
H-23 4353.5m	12	12	Ab+Chl	59.60		20.60	9.70		2.09	0.60	5.69	1.72															100	95
H-23 4353.5m	13	1	TiO_2+Chl	5.88	87.94	4.48	0.78			0.38	0.55																100	82
H-23 4353.5m	13	2	TiO_2+Chl	11.00	75.15	8.58	3.16		0.93	0.32	0.59	0.28															100	83
H-23 4353.5m	13	3	TiO_2+Qz+Other	35.08	62.99	1.59	0.32																				100	99
H-23 4353.5m	13	4	Ms+TiO_2	42.51	48.26	7.12	0.31					1.79															100	100
H-23 4353.5m	13	5	TiO_2+Ms	18.29	77.43	3.00	0.30					0.99															100	92
H-23 4353.5m	13	6	Cal	1.26			0.56			54.18																	56	53
H-23 4353.5m	13	7	Sd+Chl+Other	10.67	0.37	4.08	58.48	0.96	15.93	6.98	2.12	0.39															100	58
H-23 4353.5m	13	8	Ab+Ms	65.54	0.17	21.64	0.26		0.38	0.41	8.95	1.25			1.25	0.13											100	98

Table 2-3A: Scaning Electron Microscope chemical analyses of sample 4353.5m from Newburn H-23 well.

Sample	Site	Position	Mineral	SiO_2	TiO_2	Al_2O_3	FeO	MnO	MgO	CaO	Na_2O	K_2O	P_2O_5	SO_3	F	Cl	Sc_2O_3	Cr_2O_3	NiO	CuO	ZnO	Y_2O_3	ZrO_2	Ce_2O_3	HfO_2	WO_3	Total	Actual Total
H-23 4353.5m	13	9	Ab+Ms	62.72	2.35	23.13	0.36		0.70	0.42	8.12	2.22															100	98
H-23 4353.5m	13	10	Qz+Ms	92.07	0.20	5.06	0.41		0.61			1.64															100	89
H-23 4353.5m	13	11	Ab	71.41		18.61	0.49		0.40	0.17	8.53	0.41															100	104
H-23 4353.5m	13	12	Chl	26.78		21.33	26.98		5.33	2.47	0.39		1.56			0.16											85	74
H-23 4353.5m	13	13	Chl	34.18		23.32	19.58		6.44	0.56		0.91															85	76
H-23 4353.5m	13	14	Cal	0.88		0.39	0.63			53.95		0.14															56	57
H-23 4353.5m	13	15	Ab	68.90		20.37					10.73																100	104
H-23 4353.5m	13	16	Sd+Chl+Other	10.95		3.50	58.23	0.61	19.32	6.06		1.35															100	52
H-23 4353.5m	13	17	Qz	99.99																							100	90
H-23 4353.5m	14	1	Fap				0.18	0.18		52.01			40.21		6.63	0.32								0.47			100	107
H-23 4353.5m	14	2	Zrn	30.01																			69.30		0.68		100	103
H-23 4353.5m	14	3	Cal+Ab	23.89		7.58	1.26			62.40	4.89																100	71
H-23 4353.5m	14	4	Ab+Ms+Chl	61.72		22.64	4.77		1.77	0.36	7.56	1.17															100	93
H-23 4353.5m	14	5	Ab	58.21		21.41	9.07		2.22	0.22	8.45	0.42															100	90
H-23 4353.5m	14	6	Sd+Chl+Other	10.44		7.84	53.50	0.36	20.51	7.33																	100	51
H-23 4353.5m	14	7	Ms	45.93	1.12	33.72	0.83		1.08		0.28	12.04															95	81
H-23 4353.5m	14	8	Ms	45.35	1.24	33.79	0.77		0.96		0.41	12.49															95	86
H-23 4353.5m	14	9	Fap	9.41	0.48	9.49	1.94	0.61	0.51	43.19			32.22		2.17												100	54
H-23 4353.5m	14	10	Chl+Ms+Cal	29.91		19.22	32.65		11.97	4.44	0.77	1.02															100	54
H-23 4353.5m	14	11	Fe-Cal+Kfs	4.24		1.42	1.31			91.76		1.26															100	58
H-23 4353.5m	14	12	Ab+Sd+Chl	43.08		4.12	40.64	0.65	5.87	2.98	2.66																100	75
H-23 4353.5m	14	13	TiO_2+Ab	6.05	84.45	4.69	2.32		0.65	0.83	1.02																100	86
H-23 4353.5m	14	14	Kfs+Cal	32.02		9.86	0.67			48.59		8.85															100	80
H-23 4353.5m	14	15	Ms	48.55	1.90	28.29	2.72		2.28			11.26															95	58
H-23 4353.5m	14	16	Ms	54.40	0.68	27.08	1.69		1.72	1.27	0.80	6.44				0.91											95	37
H-23 4353.5m	14	17	Hole	57.05		39.19	1.11			0.87		1.53				0.25											100	61
H-23 4353.5m	14	18	Ab+Cal	65.89		19.50				4.14	10.48																100	65

Table 2-3B: Scaning Electron Microscope chemical analyses of sample 4353.5m from Newburn H-23 well (re-annalysis of fluorine-calcite).

Sample	Site	Position	Mineral	SiO_2	Al_2O_3	FeO	MnO	MgO	CaO	Na_2O	K_2O	SO_3	F	Total	Actual Total
H-23 4353.5	1	1	F-Fe-Cal			1.16			49.04				5.79	56	57
H-23 4353.5	1	2	Qz	99.99										100	118
H-23 4353.5	1	3	F-Cal			0.74			46.33				8.93	56	61
H-23 4353.5	1	4	Ab	68.71	18.65				0.25	12.4				100	119
H-23 4353.5	1	5	Qz	99.79					0.2					100	116
H-23 4353.5	1	6	Ab	67.77	20.05	0.21			0.25	11.73				100	117
H-23 4353.5	2	1	F-Cal			0.87	0.25		49.31				5.56	56	59
H-23 4353.5	2	2	F-Cal			0.93			51.11				3.96	56	54
H-23 4353.5	2	3	F-Fe-Cal			1.30			51.74				2.95	56	52
H-23 4353.5	2	4	Ab+Cal	62.81	17.18				8.34	11.69				100	113
H-23 4353.5	2	5	Ab+Cal	67	18.01				2.69	12.32				100	115
H-23 4353.5	2	6	Ab	68.92	18.67					12.4				100	120
H-23 4353.5	2	7	Ab	78.72	12.36					8.93				100	121
H-23 4353.5	2	8	Ab	68.63	18.16				0.98	12.24				100	121
H-23 4353.5	2	9	F-Fe-Cal			1.11			51.54				3.34	56	55
H-23 4353.5	2	10	F-Fe-Cal	0.59		1.18			50.75				3.49	56	54
H-23 4353.5	2	11	Ab	67.86	19.37				0.78	12				100	117
H-23 4353.5	3	1	Kfs	66.7	17.91					0.67	14.72			100	117
H-23 4353.5	3	2	F-Fe-Cal			1.25			52.65				2.11	56	53
H-23 4353.5	3	3	Py			25.9			4.09			70.02		100	183
H-23 4353.5	3	4	Qz	99.99										100	118

Appendix 2-4: SEM-BSE images and EDS mineral analyses for sample Newburn H-23 4913.8m

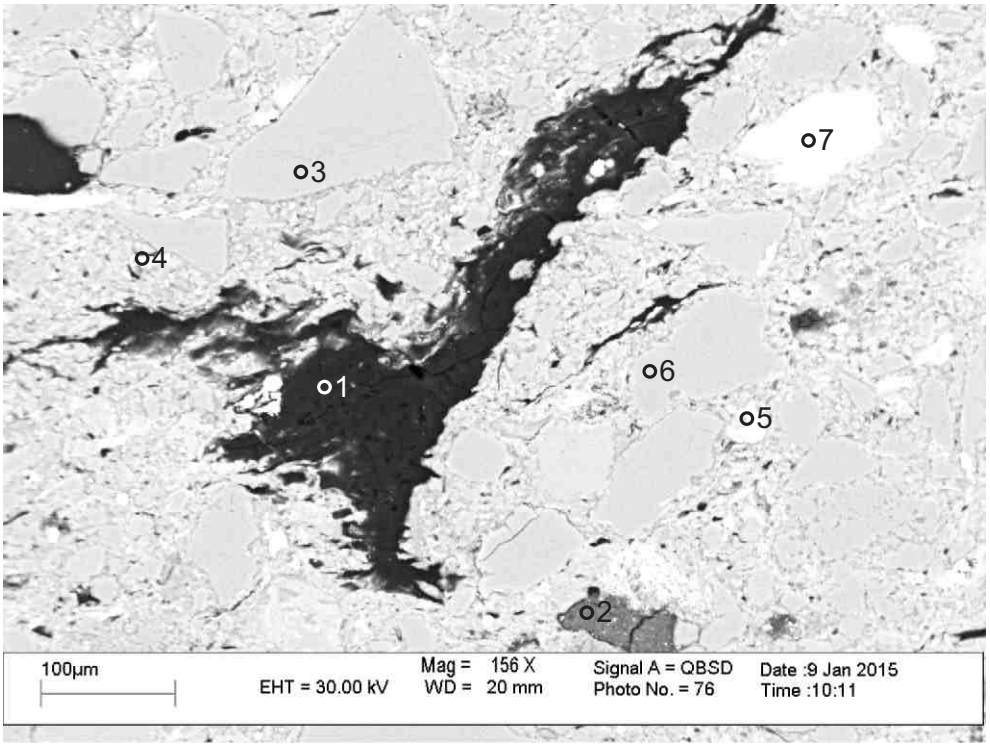

Figure 2-4.1: Sample Newburn 4913.8m site 1 (SEM). Barren pore (1) and pore space filled by drilling mud (2), diagenetic pyrite (4), and siderite (5).

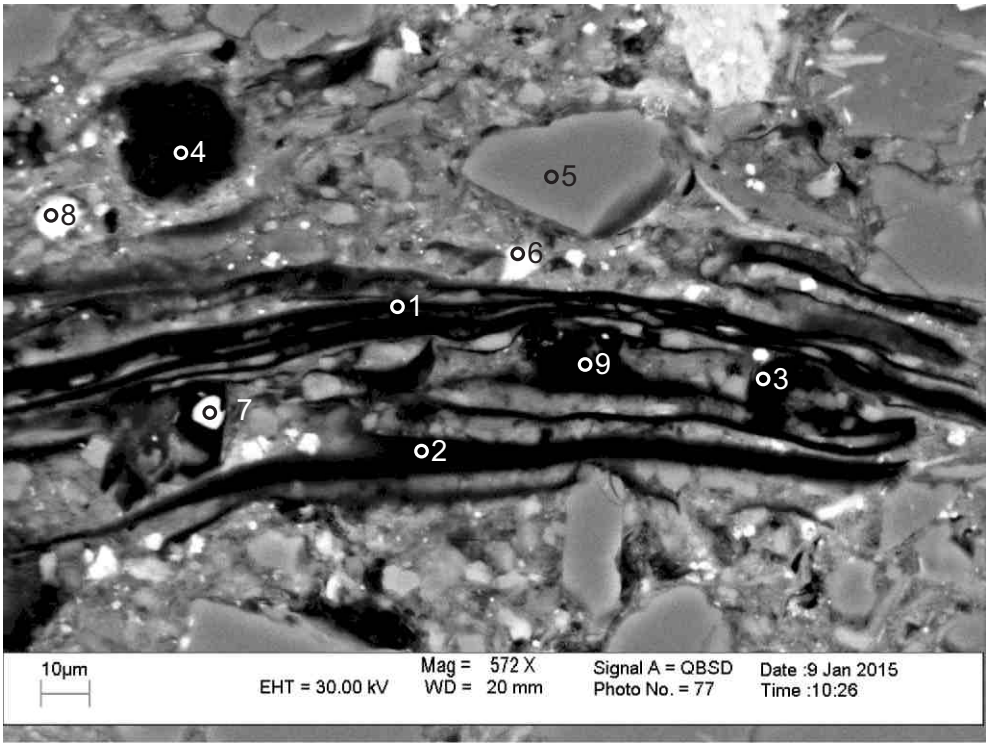

Figure 2-4.2: Sample Newburn 4913.8m site 2 (SEM). Detrital muscovite (1) with sphalerite (3,9) along its cleavage planes.

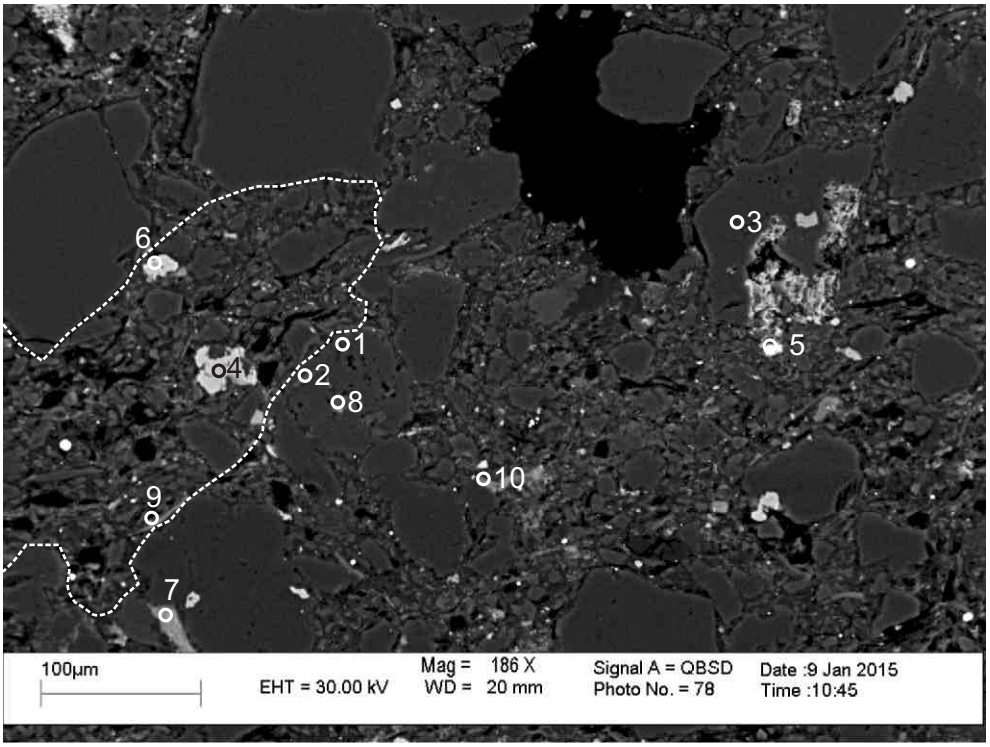

Figure 2-4.3: Sample Newburn 4913.8m site 3 (SEM). Titania (4,6) and fibrous chlorite (9) fill dissolution voids in probably partially dissolved or mechanically shattered trachytic lithic clasts.

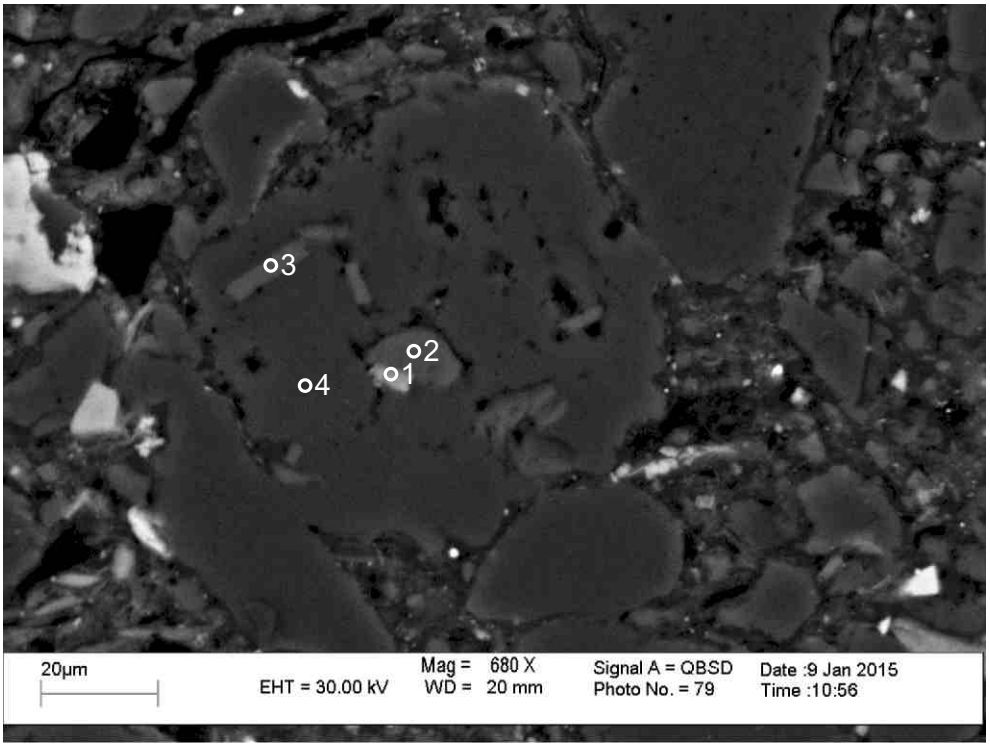

Figure 2-4.4: Sample Newburn 4913.8m site 4 (SEM). Close up of analysis 1,2,8 Figure 2-4.3. Muscovite (2,3) and fluorapatite (1) occupying dissolution voids within albite (4).

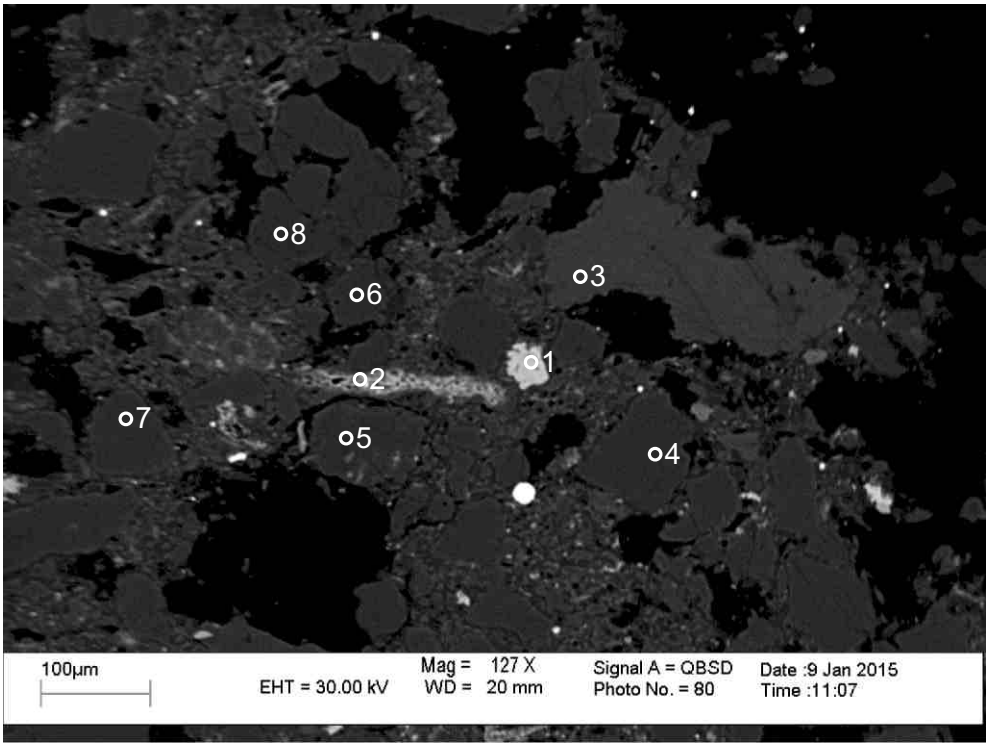

1: Titania+ Chlorite
2: Pyrite+ Chlorite
3: Oligoclase
4: Quartz
5: Quartz
6: Quartz
7: Quartz
8: Quartz

Figure 2-4.5: Sample Newburn 4913.8m site 5 (SEM). Mud intraclast composed of chlorite and pyrite (2). Abundant porosity.

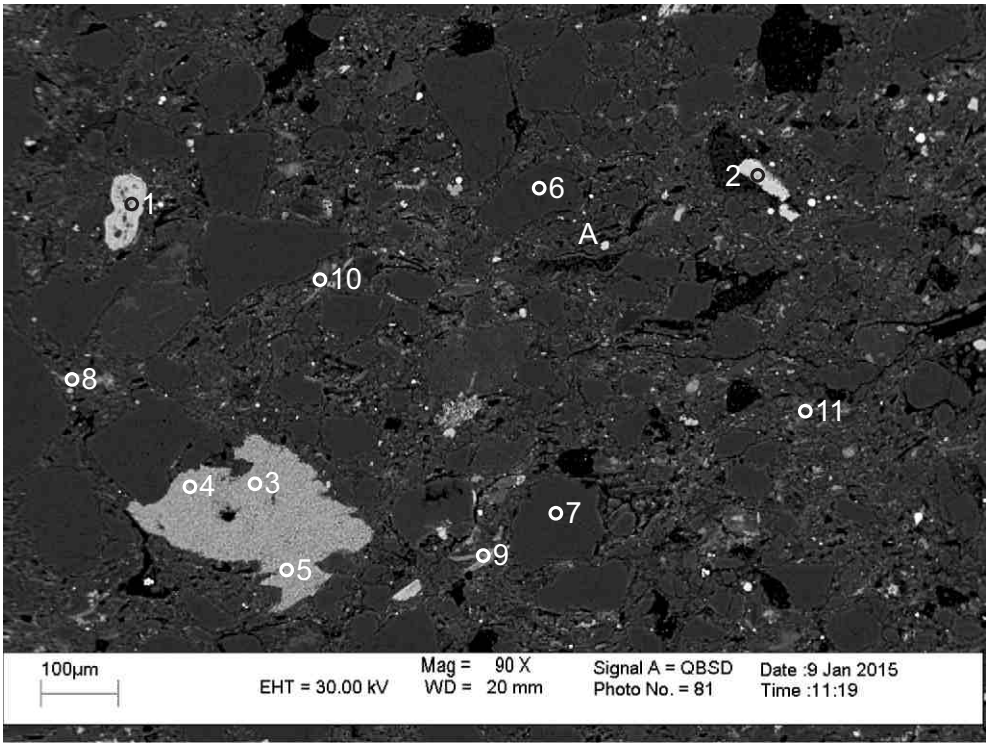

1: Titania+ Chlorite
2: Titania+ Chlorite
3: Siderite+ Chlorite
4: Siderite+ Chlorite
5: Siderite+ Chlorite
6: Quartz
7: Quartz
8: Chlorite
9: Chlorite
10: Chlorite+ Muscovite
11: Quartz+ Muscovite

Figure 2-4.6: Sample Newburn 4913.8m site 6 (SEM). Mud intraclast composed of chlorite and siderite (3-5). Titania and chlorite (1) engulf muddy matrix composed of quartz, muscovite and chlorite. Plastically deformed muscovite bounds pore filled by kaolinite (postition A).

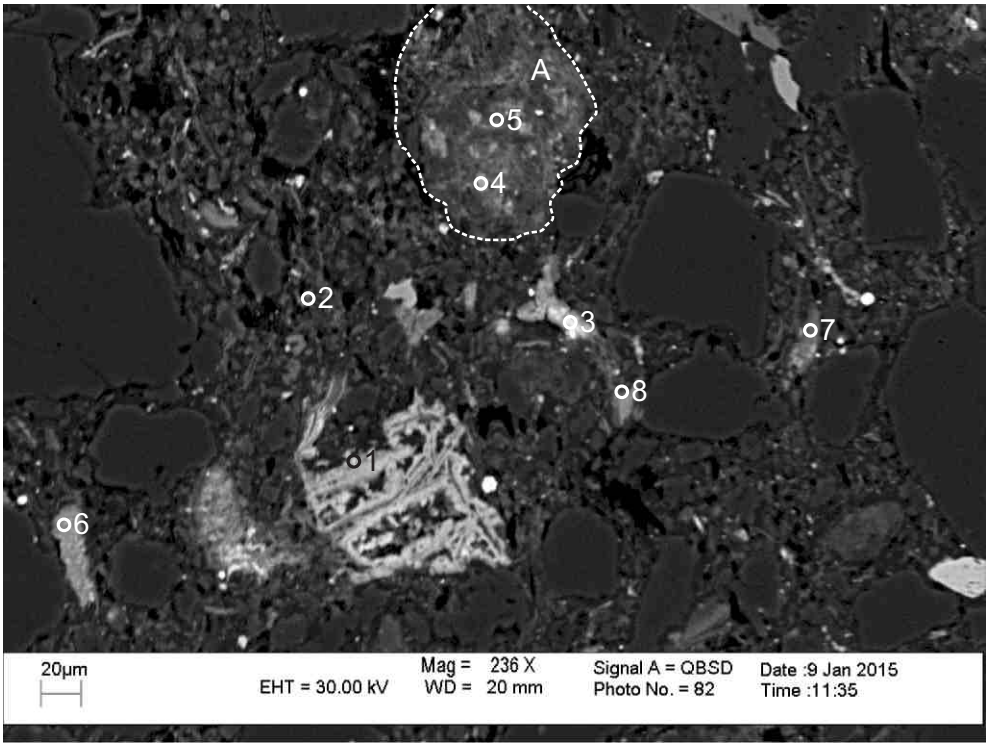

1: Titania+ Chlorite
2: Muscovite+ Chlorite
3: Contaminant
4: Chlorite+ Contaminant
5: Chlorite+ Albite
6: Chlorite+ Other.
7: Chlorite
8: Chlorite+ Apatite

Figure 2-4.7: Sample Newburn 4913.8m site 7 (SEM). Chlorite (4,5) fills dissolution in trachytic lithic clast (position A). Titania (1) forms along the cleavage planes of muscovite. Chlorite and apatite (8) fill pore.

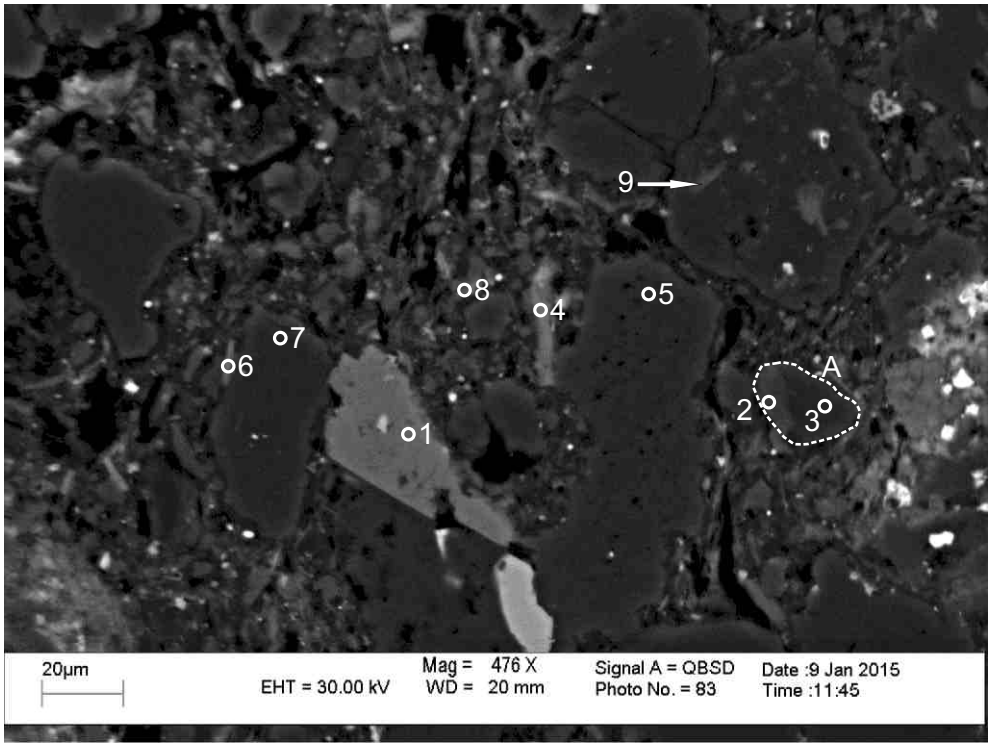

1: Ankerite
2: Muscovite
3: Quartz
4: Chlorite
5: Albite
6: Quartz+ Muscovite+ Chlorite
7: Quartz
8: Quartz+ Muscovite+ Chlorite
9: Quartz+ Muscovite+ Chlorite

Figure 2-4.8: Sample Newburn 4913.8m site 8 (SEM). Muscovite (9) inclusion in quartz (9) is partially replaced by chlorite (9). Ankerite (1) engulfs quartz. Granitoid lithic clast composed of quartz (3) and muscovite (2) (position A) in muddy matrix.

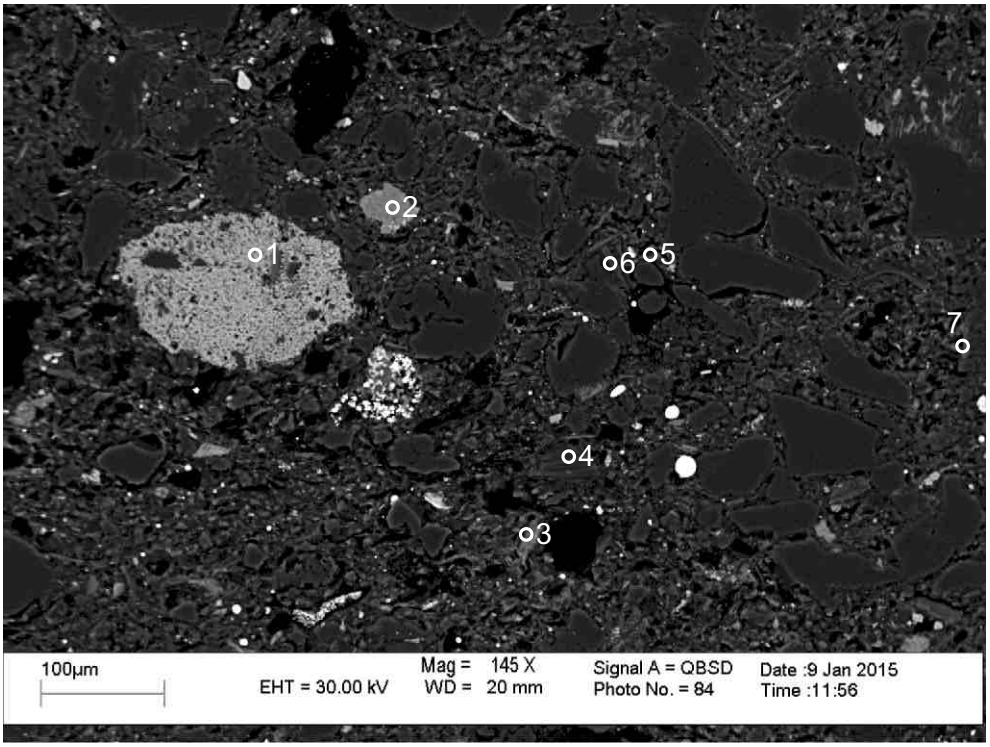

1: Siderite+ Chlorite+ Apatite
2: Chlorite
3: Chlorite
4: Muscovite
5: Muscovite+ Chlorite
6: Muscovite+ Chlorite
7: Muscovite+ Chlorite

Figure 2-4.9: Sample Newburn 4913.8m site 9 (SEM). Mud intraclast composed of chlorite, apatite, and siderite (1) .

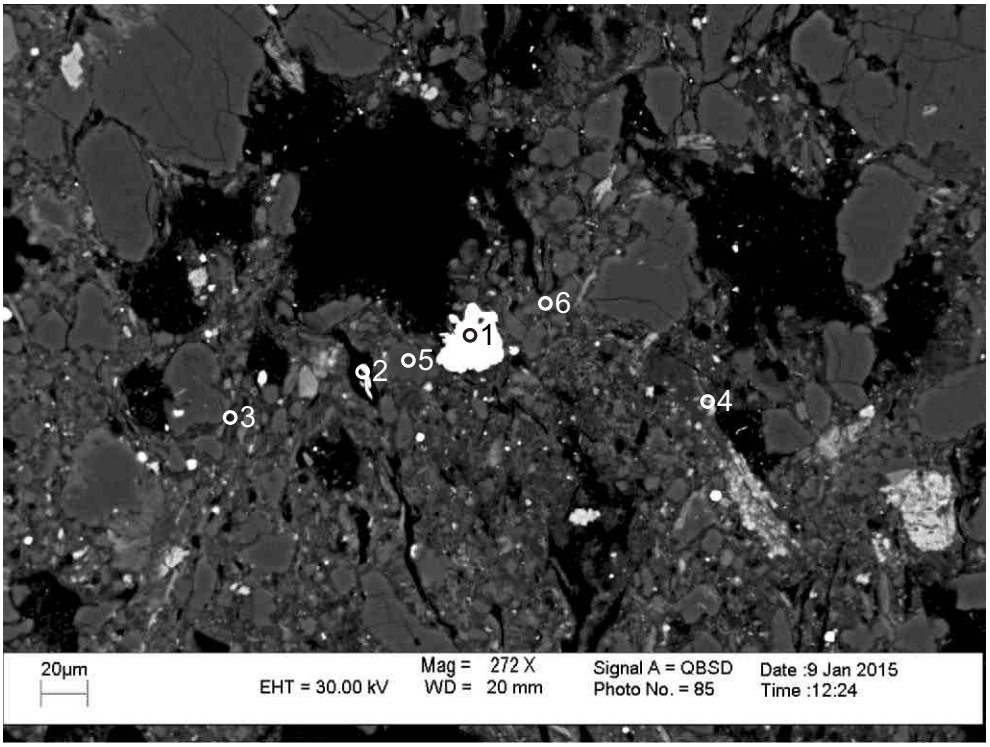

1: Xenotime
2:Contaminant
3: Muscovite+ Chlorite
4: Chlorite
5: Albite
6: Oligoclase

Figure 2-4.10: Sample Newburn 4913.8m site 10 (SEM). Diagenetic xenotime (1) probably fills porosity. Muddy matrix consists of albite (5), oligoclase (6), quartz, chlorite (3) and muscovite (3).

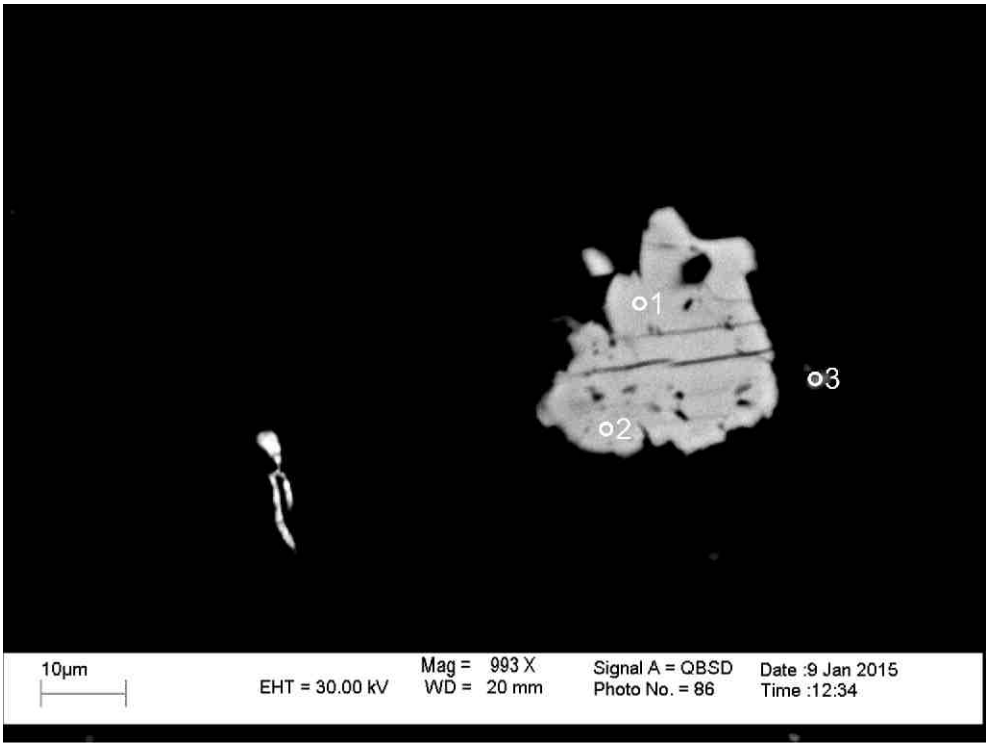

1: Xenotime
2: Xenotime
3: Pyrite

Figure 2-4.11: Sample Newburn 4913.8m site 11 (SEM). Close up of analysis 1 Figure 2-4.10. diagenetic xenotime with fractures.

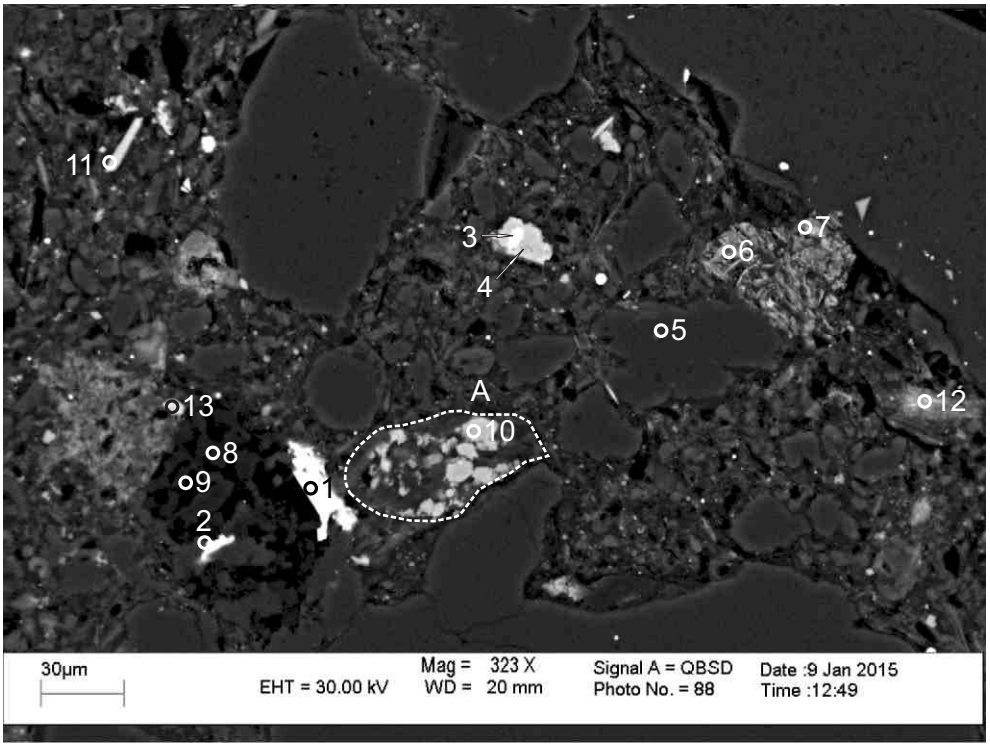

1: Barite
2: Barite+ Albite
3: Titania+ Barite
4: Titania+ Chlorite
5: Quartz
6: Titania+ Quartz
7: Quartz+ Titania
8: Kaolinite
9: Kaolinite+ Albite
10: Titania+ Other
11: Titania+ Other
12: Titania+ Other
13: Titania+ Other

Figure 2-4.12: Sample Newburn 4913.8m site 12 (SEM). Diagenetic barite (1) fills open porosity and engulfs kaolinite (8,9) booklets. Titania (4) probably engulfs barite (3). Titania (10) fills dissolution voids in trachytic lithic clast (position A). Titania (6,7) fills pore in very fine matrix.

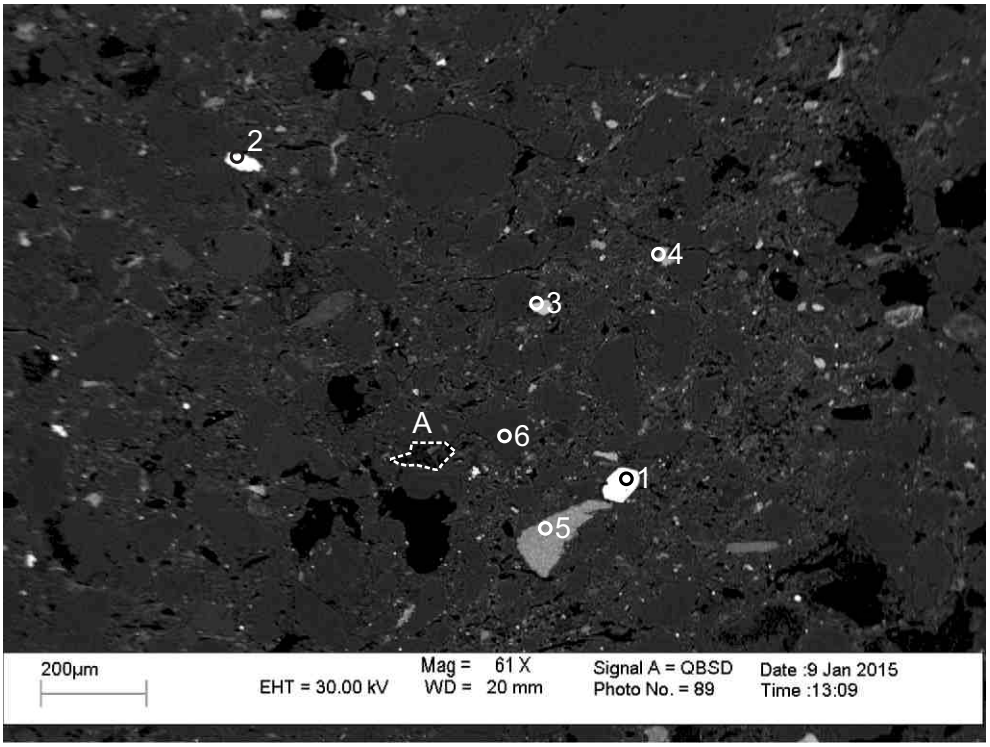

1: Zircon
2: Pyrite
3: Titania
4: Siderite+ Other
5: Siderite+ Chlorite
6: Quartz

Figure 2-4.13: Sample Newburn 4913.8m site 13 (SEM). Diagenetic zircon (1) fills pore. Mud intraclast containing chlorite and siderite (5). Titania (3), pyrite (2), and siderite (4) fill open porosity in, and engulf the muddy matrix. Kaolinite fills pore (position A).

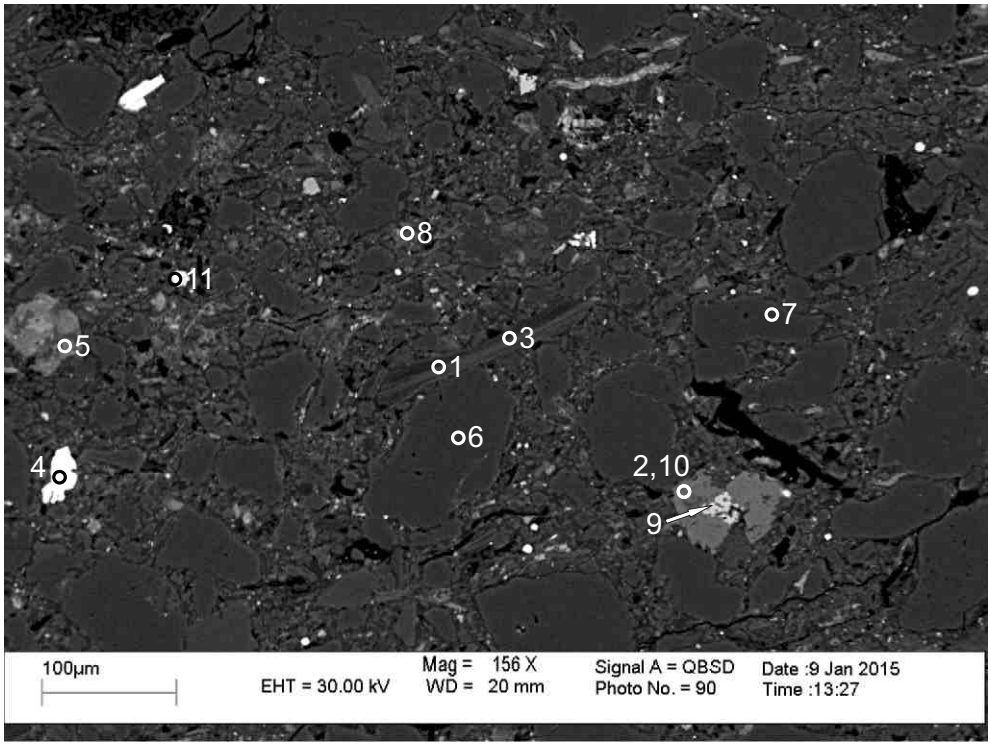

1: Muscovite
2: Ankerite
3: Muscovite
4: Barite
5: Quartz+ Chlorite
6: Quartz
7: Quartz
8: Quartz+ Chlorite+ Other
9: Titania+ Other
10: Ankerite
11: Pyrite

Figure 2-4.14: Sample Newburn 4913.8m site 14 (SEM). Ankerite (2,10) engulfs quartz. Titania (9) engulfs ankerite (2,10). Diagenetic barite (4) fills open porosity in the muddy matrix. Chlorite engulfs quartz grain (5).

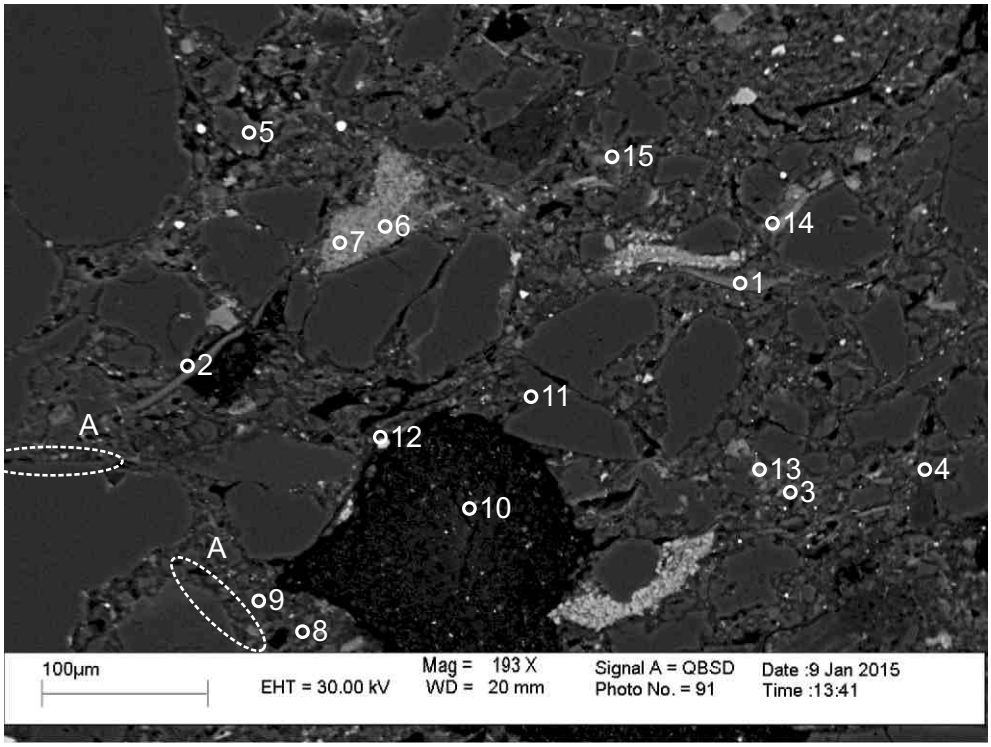

1: Chlorite
2: Muscovite
3: Muscovite+ Chlorite
4: Muscovite +Chlorite
5: Albite
6: Chlorite+ Apatite
7: Chlorite+ Apatite
8: Muscovite+ Chlorite
9: Quartz+Illite
10: DrillingMud
11: Quartz
12: Titania+ Chlorite
13: Albite+ Chlorite
14: Chlorite+ Muscovite
15: Chlorite+ Muscovite

Figure 2-4.15: Sample Newburn 4913.8m site 15 (SEM). Drilling mud (10) occupying pore space. Mud intraclast containing chlorite and apatite (6,7). Plastically deformed chloritized muscovite (1,14). Quartz overgrowths (positions A) in contact with matrix.

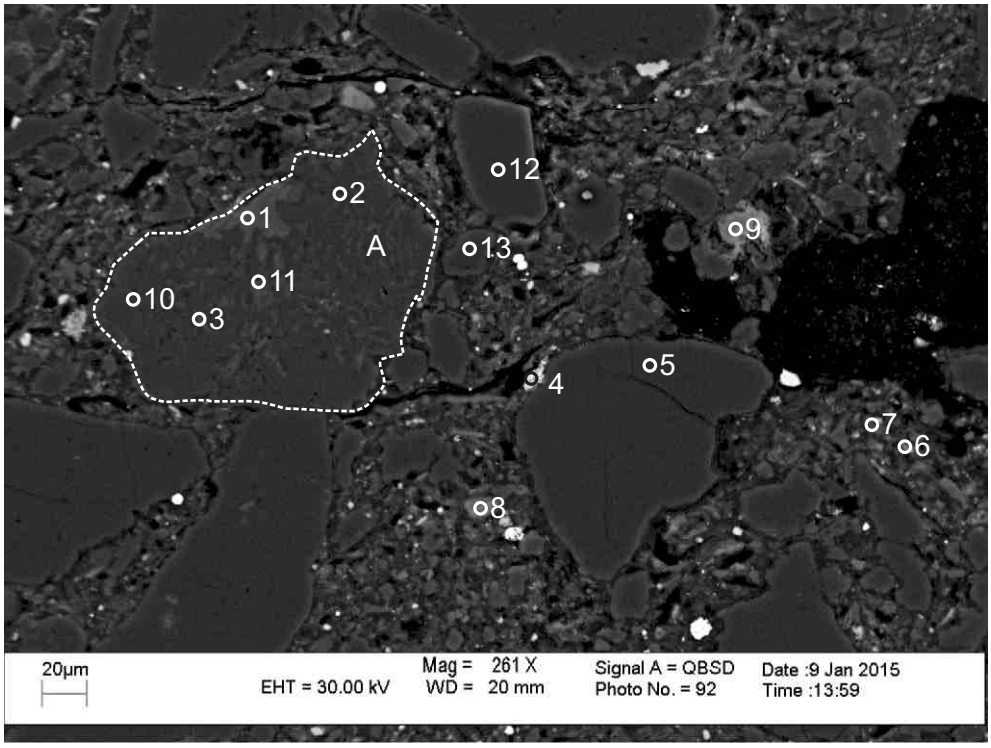

1: Muscovite+ Chlorite
2: Albite
3: Albite+ Illite
4: Pyrite
5: Quartz
6: Muscovite+ Titania+ Chlorite
7: Quartz
8: Chlorite
9: Ankerite+ Other
10: Albite
11: Chlorite+ Muscovite
12: Quartz
13: Quartz

Figure 2-4.16: Sample Newburn 4913.8m site 16 (SEM). Granitoid lithic clast composed of albite (2,3,10) and muscovite (1,3,11) some of which has been cloritized.

Table 2-4: Scaning Electron Microscope chemical analyses of sample 4913.8m from Newburn H-23 well.

Sample	Site	Position	Mineral	SiO_2	TiO_2	Al_2O_3	FeO	MnO	MgO	CaO	Na_2O	K_2O	P_2O_5	SO_3	F	Cl	Sc_2O_3	Cr_2O_3	CoO	NiO	CuO	ZnO	As_2O_3	SrO	Y_2O_3	ZrO_2	BaO	Gd_2O_3	Dy_2O_3	Yb_2O_3	Ta_2O_5	WO_3	PbO	Total	Actual Total
H-23 4913.8m	1	1	Hole		25.60									62.18		12.22																		100	2
H-23 4913.8m	1	2	DM	51.13		3.80	8.77		23.02	4.48		0.95			6.84	1.03																		100	50
H-23 4913.8m	1	3	Qz	99.99																														100	116
H-23 4913.8m	1	4	Py+Other	8.34		3.25	22.81					0.34		65.27																				100	169
H-23 4913.8m	1	5	Sd+Other	1.93			86.49	4.65		6.94																								100	56
H-23 4913.8m	1	6	Qz	99.99																														100	121
H-23 4913.8m	1	7	TiO_2+Other	7.98	82.95	4.44	3.78			0.46		0.37																						100	96
H-23 4913.8m	2	1	Ms+Other	68.01		25.06	2.73					2.04		2.17																				100	45
H-23 4913.8m	2	2	Mix	66.36	0.93	21.71	3.37		1.72			4.53		1.37																				100	52
H-23 4913.8m	2	3	Sp+Other	52.45	2.50	23.79	3.24							13.26								4.77												100	12
H-23 4913.8m	2	4	Mix	59.45		13.32	13.21		2.45	3.18	1.56	3.76		2.32		0.75																		100	18
H-23 4913.8m	2	5	Qz	99.99																														100	119
H-23 4913.8m	2	6	Sd+Other	15.23		7.92	58.65	1.07	5.01	7.88	1.62	0.53	2.09																					100	72
H-23 4913.8m	2	7	TiO_2+Chl	4.41	90.31	3.61	1.69																											100	92
H-23 4913.8m	2	8	Py	1.26		0.93	26.39							71.44																				100	214
H-23 4913.8m	2	9	Sp+Other	34.51		24.90	3.49							28.32		1.92						6.87												100	12
H-23 4913.8m	3	1	Ab	71.00		16.95	0.28				11.74																							100	121
H-23 4913.8m	3	2	Ms	51.07	0.36	30.59	2.31		1.01		0.81	8.85																						95	114
H-23 4913.8m	3	3	Qz	99.99																														100	123
H-23 4913.8m	3	4	TiO_2+Chl	4.28	92.54	2.19	0.99																											100	104
H-23 4913.8m	3	5	Py+Other	6.59		4.53	25.42		0.63			0.46		62.40																				100	216
H-23 4913.8m	3	6	TiO_2+Kln	3.02	94.66	2.32																												100	99
H-23 4913.8m	3	7	Chl	31.11	0.62	22.51	24.95		4.78	0.57		0.47																						85	89
H-23 4913.8m	3	8	Ms+Other	51.02	0.38	31.86	2.69		1.04	0.71	0.94	10.15	1.19																					100	109
H-23 4913.8m	3	9	Chl+Other	43.04	0.77	27.02	17.01		10.05		0.62	1.52																						100	112
H-23 4913.8m	3	10	Chl+Ab	46.63		25.00	20.83		3.96	0.34	2.29	0.94																						100	94
H-23 4913.8m	4	1	Fap+Other	24.15	0.28	14.55	1.39			20.74	1.91	4.94	25.60		6.44																			100	121
H-23 4913.8m	4	2	Ms	57.43	0.45	25.83	1.93		0.67		1.48	7.21																						95	109
H-23 4913.8m	4	3	Ms	54.90		29.92	0.48		0.67		0.77	6.50			1.75																			95	121
H-23 4913.8m	4	4	Ab	69.48		18.76					11.74																							100	123
H-23 4913.8m	5	1	TiO_2+Chl	1.86	96.46	1.15	0.54																											100	94
H-23 4913.8m	5	2	Py+Chl	4.13		2.49	55.63	2.54	4.59	5.99				24.62																				100	68
H-23 4913.8m	5	3	Oli	64.30		22.15				3.58	9.34	0.61																						100	113
H-23 4913.8m	5	4	Qz	99.99																														100	113
H-23 4913.8m	5	5	Qz	99.99																														100	110
H-23 4913.8m	5	6	Qz	99.99																														100	111
H-23 4913.8m	5	7	Qz	99.99																														100	106
H-23 4913.8m	5	8	Qz	99.99																														100	107
H-23 4913.8m	6	1	TiO_2+Chl	3.70	89.67	1.83	4.21											0.58																100	89
H-23 4913.8m	6	2	TiO_2+Chl	2.25	95.76	0.89	1.08																											100	109
H-23 4913.8m	6	3	Sd+Chl	16.09		12.53	60.30	0.81	7.89	2.38																								100	69
H-23 4913.8m	6	4	Sd+Chl	25.97	0.40	15.72	46.12	0.63	7.51	1.62		2.01																						100	66
H-23 4913.8m	6	5	Sd+Chl	23.57		17.19	50.22	0.58	6.22	1.90		0.31																						100	75
H-23 4913.8m	6	6	Qz	99.99																														100	121
H-23 4913.8m	6	7	Qz	99.99																														100	120
H-23 4913.8m	6	8	Chl	28.04		16.54	24.33		5.83	3.66		0.28	6.31																					85	81
H-23 4913.8m	6	9	Chl	31.76		20.08	18.79		13.83		0.54																							85	91
H-23 4913.8m	6	10	Chl+Ms	43.00	0.40	22.35	9.53		10.35	5.81		3.28	5.29																					100	102
H-23 4913.8m	6	11	Qz+Ms	85.87	0.37	9.33	1.67		0.58	0.24	0.40	1.53																						100	131
H-23 4913.8m	7	1	TiO_2+Chl	2.67	92.18	2.36	2.32			0.46																								100	85
H-23 4913.8m	7	2	Ms+Chl	54.12	1.63	28.21	7.18		3.25	0.50	0.59	4.52																						100	102
H-23 4913.8m	7	3	Contaminant	4.77		2.72	7.17				2.40	1.55		37.61		0.21			6.98	27.02	0.71												8.90	100	119
H-23 4913.8m	7	4	Chl+Contaminant	29.56		18.33	18.58		5.94	1.53	0.82	0.72		12.54										9.84								2.17		100	102
H-23 4913.8m	7	5	Chl+Ab	41.93	0.28	23.54	25.09		5.36	0.48	2.86	0.47																						100	98
H-23 4913.8m	7	6	Chl+Other.	29.24		22.30	40.02		6.05	1.06				1.32																				100	88
H-23 4913.8m	7	7	Chl	36.55		23.49	15.31		5.83	1.56	0.49	0.90	0.88																					85	105

Table 2-4: Scaning Electron Microscope chemical analyses of sample 4913.8m from Newburn H-23 well.

Sample	Site	Position	Mineral	SiO_2	TiO_2	Al_2O_3	FeO	MnO	MgO	CaO	Na_2O	K_2O	P_2O_5	SO_3	F	Cl	Sc_2O_3	Cr_2O_3	CoO	NiO	CuO	ZnO	As_2O_3	SrO	Y_2O_3	ZrO_2	BaO	Gd_2O_3	Dy_2O_3	Yb_2O_3	Ta_2O_5	WO_3	PbO	Total	Actual Total
H-23 4913.8m	7	8	Chl+Ap	38.63	0.38	25.72	21.87		6.86	2.67		1.31	2.57																					100	108
H-23 4913.8m	8	1	Ank	3.81		2.35	14.61	0.47	9.35	25.41																								56	58
H-23 4913.8m	8	2	Ms	49.35	0.30	37.40	0.55				1.69	5.70																						95	117
H-23 4913.8m	8	3	Qz	99.99																														100	116
H-23 4913.8m	8	4	Chl	30.95		17.09	27.67		8.25	0.37	0.50	0.19																						85	95
H-23 4913.8m	8	5	Ab	69.03		18.65	0.33				11.99																							100	120
H-23 4913.8m	8	6	Qz+Ms+Chl	80.01	0.40	8.60	7.96		1.92			1.12																						100	114
H-23 4913.8m	8	7	Qz	99.19		0.66						0.16																						100	116
H-23 4913.8m	8	8	Qz+Ms+Chl	50.59	1.15	21.69	17.32		6.10	0.32	1.42	1.39																						100	111
H-23 4913.8m	8	9	Qz+Ms+Chl	72.78		19.16	2.37		0.75			4.96																						100	118
H-23 4913.8m	9	1	Sd+Chl+Ap	9.39		5.86	70.05	0.74	4.69	7.44		0.42	1.42																					100	59
H-23 4913.8m	9	2	Chl	31.08	0.74	20.80	19.75		11.57	0.50		0.57																						85	94
H-23 4913.8m	9	3	Chl	27.71	0.32	18.20	29.48	0.39	6.32	1.46		0.84				0.27																		85	94
H-23 4913.8m	9	4	Ms	49.06	0.45	35.68	0.61				1.65	7.55																						95	103
H-23 4913.8m	9	5	Ms+Chl	58.21	0.83	28.63	4.44		2.09	0.57	0.47	4.77																						100	109
H-23 4913.8m	9	6	Ms+Chl	49.33	0.25	36.00	0.98		0.51		1.60	7.94			3.40																			100	111
H-23 4913.8m	9	7	Ms+Chl	63.85		18.44	6.51		6.82	0.45		3.91																						100	114
H-23 4913.8m	10	1	Xtm										40.74						1.25						45.59			2.34	7.40	2.70				100	97
H-23 4913.8m	10	2	Contaminant	9.39		5.95	2.30		1.18			0.55		22.65					2.03	11.95													43.98	100	63
H-23 4913.8m	10	3	Ms+Chl	61.52	1.68	29.33	1.51		1.11		0.67	4.19																						100	81
H-23 4913.8m	10	4	Chl	32.18	2.51	22.86	21.41		4.11	0.43	0.59	0.92																						85	69
H-23 4913.8m	10	5	Ab	72.16		16.87					10.97																							100	109
H-23 4913.8m	10	6	Oli	63.15		22.90	0.39			3.47	9.59	0.51																						100	106
H-23 4913.8m	11	1	Xtm										47.80						1.50						35.60			3.05	7.90	3.34	0.82			100	87
H-23 4913.8m	11	2	Xtm	2.29									45.44						1.37						37.97			2.18	7.76	2.98				100	89
H-23 4913.8m	11	3	Py	7.77		4.95	23.43		0.55		0.50	0.42		62.40																				100	173
H-23 4913.8m	12	1	Brt											40.93										6.54			52.54							100	105
H-23 4913.8m	12	2	Brt+Ab	18.85		9.16	0.26				3.86			29.72										8.27			29.90							100	116
H-23 4913.8m	12	3	TiO_2+Brt		35.11	0.68	0.62							26.59										6.65			30.35							100	106
H-23 4913.8m	12	4	TiO_2+Chl	1.97	95.80	0.89	1.35																											100	96
H-23 4913.8m	12	5	Qz	99.19	0.35					0.46																								100	111
H-23 4913.8m	12	6	TiO_2+Qz	42.93	55.30	1.47	0.28																											100	115
H-23 4913.8m	12	7	Qz+TiO_2	48.50	47.02	3.27	0.71					0.48																						100	104
H-23 4913.8m	12	8	Kln	51.99		31.24					2.32					0.46																		86	90
H-23 4913.8m	12	9	Kln+Ab	60.45		36.32					2.70					0.53																		100	39
H-23 4913.8m	12	10	TiO_2+Other	1.78	97.03	0.53	0.42					0.26																						100	95
H-23 4913.8m	12	11	TiO_2+Other	7.21	85.85	5.61	0.87					0.46																						100	99
H-23 4913.8m	12	12	TiO_2+Other	8.04	78.85	4.18	5.61		1.03	0.78		0.76		0.77																				100	78
H-23 4913.8m	12	13	TiO_2+Other	10.35	79.03	5.86	2.80				1.52	0.43																						100	95
H-23 4913.8m	13	1	Zrn	29.99		2.02	0.66			0.83							1.37								4.78	60.37								100	89
H-23 4913.8m	13	2	Py	0.28			26.94				0.77			72.02																				100	177
H-23 4913.8m	13	3	TiO_2	1.52	96.21	0.81	1.48																											100	91
H-23 4913.8m	13	4	Sd+Other	1.54		1.30	82.80	5.31		6.55			2.50																					100	55
H-23 4913.8m	13	5	Sd+Chl	19.17	0.52	14.98	54.46	0.57	7.36	2.60		0.36																						100	69
H-23 4913.8m	13	6	Qz	99.99																														100	109
H-23 4913.8m	14	1	Ms	48.88	0.52	35.48	0.66				1.78	7.69																						95	100
H-23 4913.8m	14	2	Ank	4.16		2.39	14.63	0.55	9.25	25.03																								56	61
H-23 4913.8m	14	3	Ms	50.67	0.86	28.96	3.57		1.48		0.55	8.90																						95	104
H-23 4913.8m	14	4	Brt											40.00										10.12			49.88							100	98
H-23 4913.8m	14	5	Qz+Chl	45.31		17.86	22.68		13.33	0.24	0.59																							100	88
H-23 4913.8m	14	6	Qz	99.99																														100	111
H-23 4913.8m	14	7	Qz	99.99																														100	115
H-23 4913.8m	14	8	Qz+Chl+Other	42.25	8.64	25.91	16.09		3.22	0.49	0.57	2.41				0.42																		100	80
H-23 4913.8m	14	9	TiO_2+Other	6.97	83.42	7.20	1.38			1.04																								100	103
H-23 4913.8m	14	10	Ank	2.82		1.67	15.28	0.59	9.95	25.69																								56	61
H-23 4913.8m	14	11	Py	0.98			27.80							71.22																				100	188

Table 2-4: Scaning Electron Microscope chemical analyses of sample 4913.8m from Newburn H-23 well.

Sample	Site	Position	Mineral	SiO_2	TiO_2	Al_2O_3	FeO	MnO	MgO	CaO	Na_2O	K_2O	P_2O_5	SO_3	F	Cl	Sc_2O_3	Cr_2O_3	CoO	NiO	CuO	ZnO	As_2O_3	SrO	Y_2O_3	ZrO_2	BaO	Gd_2O_3	Dy_2O_3	Yb_2O_3	Ta_2O_5	WO_3	PbO	Total	Actual Total
H-23 4913.8m	15	1	Chl	38.16	0.32	18.25	17.25		9.32			0.76		0.53								0.42												85	88
H-23 4913.8m	15	2	Ms	53.36		31.37	0.85				1.88	7.53																						95	92
H-23 4913.8m	15	3	Ms+Chl	62.08	0.47	23.83	7.68		2.14	0.46		3.32																						100	96
H-23 4913.8m	15	4	Ms+Chl	71.38	0.83	18.39	3.91		1.38	1.08		3.05																						100	97
H-23 4913.8m	15	5	Ab	67.60		19.27	0.94				11.97	0.22																						100	105
H-23 4913.8m	15	6	Chl+Ap	33.26		22.67	25.74		4.28	5.79	1.04	0.54	5.59	1.07																				100	90
H-23 4913.8m	15	7	Chl+Ap	31.70		22.73	27.02		4.05	7.01	0.90	0.41	6.16																					100	86
H-23 4913.8m	15	8	Ms+Chl	65.12	1.88	23.30	3.76		1.97	0.41	0.50	3.07																						100	91
H-23 4913.8m	15	9	Qz+Ilt	96.73		2.57	0.33					0.37																						100	101
H-23 4913.8m	15	10	DM	43.83		3.55	11.40		22.30	2.98	1.17	0.96			13.79																			100	71
H-23 4913.8m	15	11	Qz	99.99																														100	112
H-23 4913.8m	15	12	TiO_2+Chl	15.36	73.13	7.88	1.52		1.41			0.69																						100	92
H-23 4913.8m	15	13	Ab+Chl	64.84		12.72	13.17		4.10	0.22	4.71	0.25																						100	99
H-23 4913.8m	15	14	Chl+Ms	45.42	0.50	24.07	19.39		8.22	0.43		1.96																						100	92
H-23 4913.8m	15	15	Chl+Ms	48.58	0.57	27.72	14.79		3.58	1.08	0.61	3.05																						100	80
H-23 4913.8m	16	1	Ms+Chl	49.91		35.37	2.66		0.91		0.46	10.70																						100	99
H-23 4913.8m	16	2	Ab	67.66		20.20				0.35	11.32	0.47																						100	106
H-23 4913.8m	16	3	Ab+Ms	62.19		25.64	0.58				8.09	3.51																						100	103
H-23 4913.8m	16	4	Py	3.53		1.40	27.30				1.27	0.17		66.32																				100	158
H-23 4913.8m	16	5	Qz	99.99																														100	109
H-23 4913.8m	16	6	Ms+TiO_2+Chl	43.23	19.97	25.94	3.86		1.63	1.15	0.66	2.55	1.03																					100	115
H-23 4913.8m	16	7	Qz	94.27		3.38	1.13		0.70			0.52																						100	107
H-23 4913.8m	16	8	Chl	39.64		21.25	17.71		3.37	0.29	1.95	0.80																						85	87
H-23 4913.8m	16	9	Ank+Other	5.03		2.99	27.29	1.05	17.78	45.88																								100	57
H-23 4913.8m	16	10	Ab	66.96		20.22				1.60	11.23																							100	107
H-23 4913.8m	16	11	Chl+Ms	54.12	1.63	28.21	7.18		3.25	0.50	0.59	4.52																						100	94
H-23 4913.8m	16	12	Qz	99.99																														100	108
H-23 4913.8m	16	13	Qz	99.99																														100	107

Appendix 2-5: SEM-BSE images and EDS mineral analyses for sample Newburn H-23 5213.5m

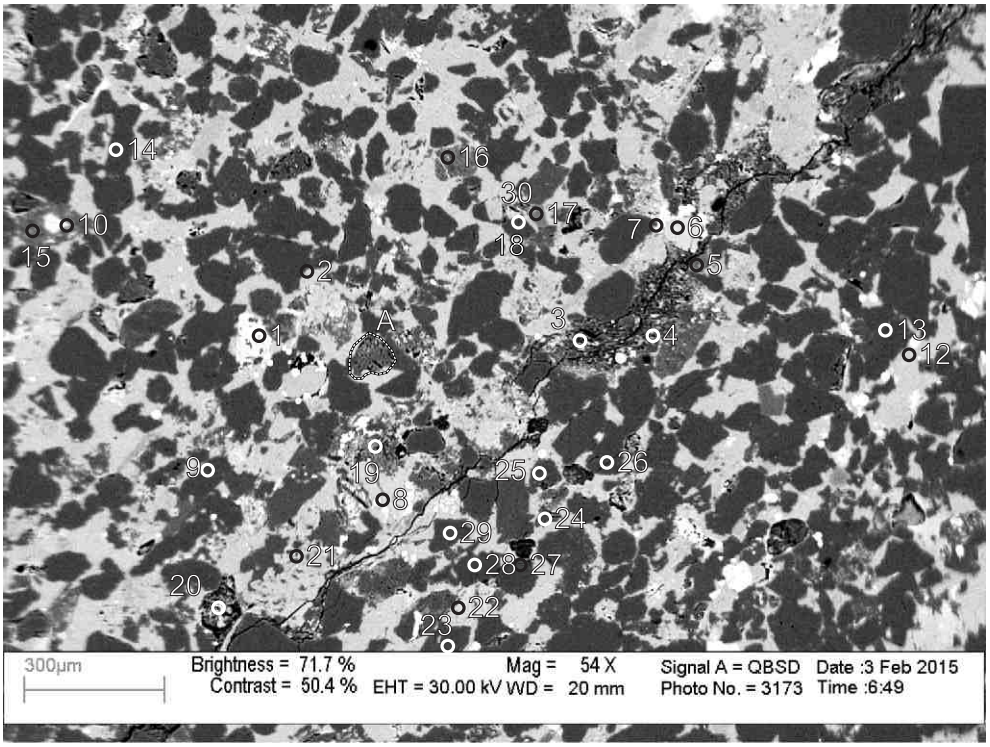

1: Titania
2: Fe-Calcite
3: Quartz+Other
4: Quartz+ Chlorite+ Calcite
5: Albite+Chlorite
6: Ankerite
7: Pyrite
8: Ankerite
9: Quartz
10: Albite
11: Titania+ Chlorite
12: Fe-Calcite
13: Quartz
14: Quartz
15: Albite
16: Muscovite+ Chlorite+ Quartz
17: Chlorite+ Albite
18: Quartz
19: Muscovite+ Chlorite+ Titania
20: Chlorite
21: F-Calcite+ Albite
22: Ankerite+ Pyrite+ Apatite
23: Quartz
24: Quartz+ Other
25: Quartz
26: Quartz
27: Quartz
28: Quartz
29: Quartz
30: Albite+ Chlorite

Figure 2-5.1: Sample Newburn 5213.5m site 1 (SEM). Table 2-5A. Framework grains of quartz (3,4,9,13,14,18,23-29) and albite (5,15,17,21,30) cemented by Fe-calcite (2,4,12), F-calcite (21) and ankerite (6,8,22). Trachytic lithic clast (position A).

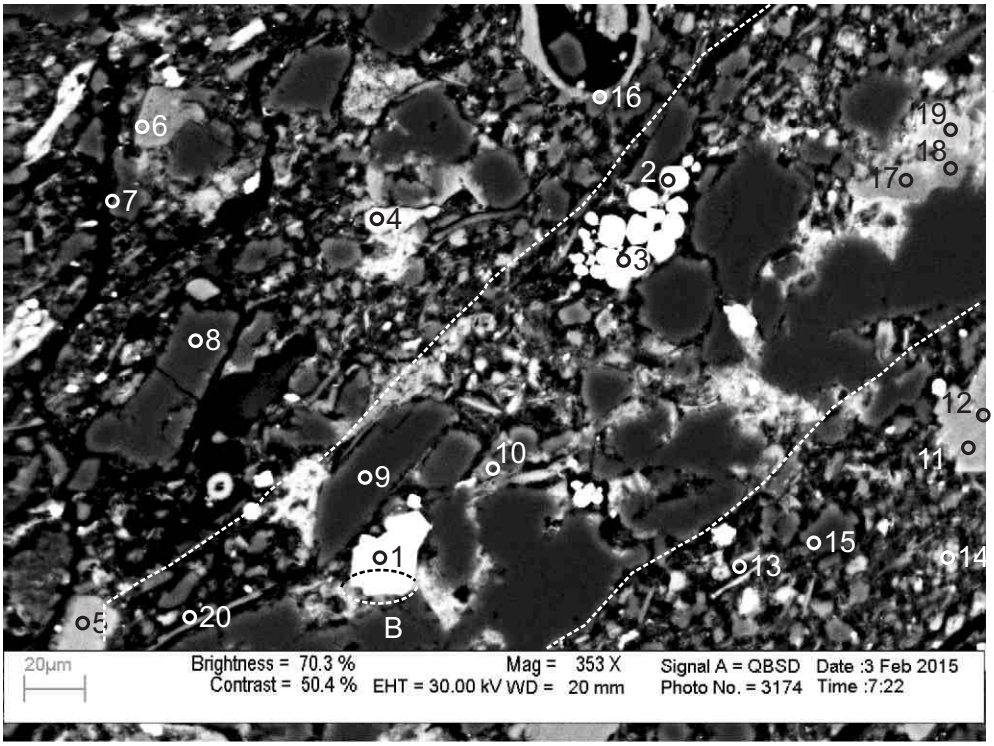

1: Pyrite
2: Pyrite
3: Pyrite
4: Chlorite+ Apatite
5: F-Calcite
6: F-Calcite+ Chlorite
7: Quartz
8: Albite
9: Quartz
10: Albite+ Pyrite+ Calcite
11: Ankerite+ Quartz
12: Ankerite+ Chlorite
13: Muscovite+ Ankerite
14: F-Calcite+ Muscovite
15: Quartz+ Other
16: F-Calcite+ Quartz
17: F-Calcite
18: F-Calcite+ Quartz
19: F-Fe-Calcite
20: Muscovite+ Chlorite

Figure 2-5.2: Sample Newburn 5213.5m site 2 (SEM). Table 2-5A. Sandy layer interbedded with silty matrix. F-calcite (16) rims pore. Euhedral pyrite (1) cuts chlorite (position B). Silty matrix composed of quartz (7,15,16), muscovite (13,14,20) and chlorite (20). Chlorite and apatite (4) partly fill pore in muddy matrix.

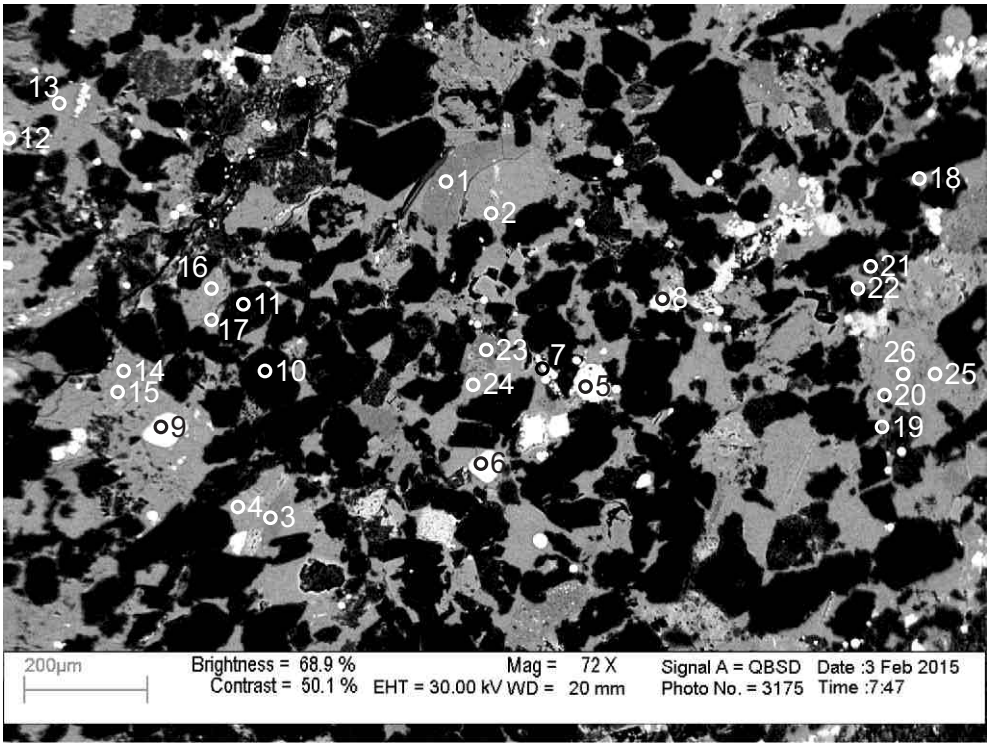

1: F-Calcite
2: F-Calcite+ Chlorite
3: F-Calcite
4: F-Calcite+ Chlorite
5: Pyrite
6: Zircon
7: Quartz+Titania
8: Pyrite+ Chlorite+ Calcite
9: Titania+Illite
10: Quartz
11: Quartz
12: Chlorite
13: F-Fe-Calcite
14: Ankerite+ Kaolinite
15: Ankerite+ Albite
16: Ankerite+ Chlorite
17: F-Calcite+ Chlorite
18: F-Calcite+ Ankerite
19: Albite+Other
20: Fe-Calcite
21: Muscovite+ Albite+ Chlorite
22: Quartz+ Albite+ Calcite
23: F-Calcite
24: Fe-Calcite
25: F-Fe-Calcite
26: F-Fe-Calcite

Figure 2-5.3: Sample Newburn 5213.5m site 3 (SEM). Table 2-5A. Titania (9) fills dissolution voids in ankerite (14,15). Framboidal pyrite (5,8) fills dissolution voids in framework quartz grains and F-calcite.

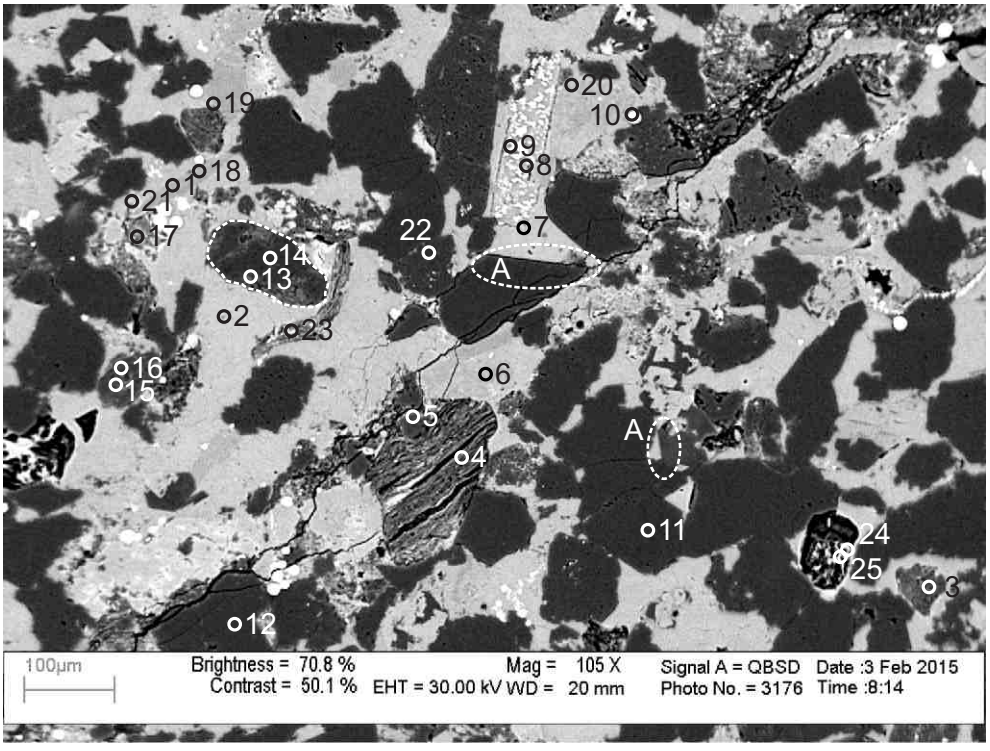

1: F-Calcite
2: F-Fe-Calcite
3: Albite
4: Chlorite+ Muscovite
5: Albite
6: F-Calcite
7: F-Fe-Calcite
8: F-Calcite+ Chlorite
9: Pyrite
10: Pyrite
11: Quartz
12: Quartz
13: Illite+ Quartz
14: Quartz
15: Muscovite+ Titania
16: Quartz+ Muscovite
17: Muscovite+ Chlorite+ Albite
18: F-Calcite
19: F-Calcite
20: F-Fe-Calcite
21: Chlorite
22: Albite
23: Chlorite+ Muscovite
24: Chlorite+ Muscovite
25: Chlorite+ Muscovite

Figure 2-5.4: Sample Newburn 5213.5m site 4 (SEM). Table 2-5A. Quartz overgrowths (positions A) appear to be corroded in contact with F-calcite. Granitoid lithic clast composed of quartz and muscovite (13,14). Partially chloritized muscovite (4) plastically deformed around quartz grain (5).

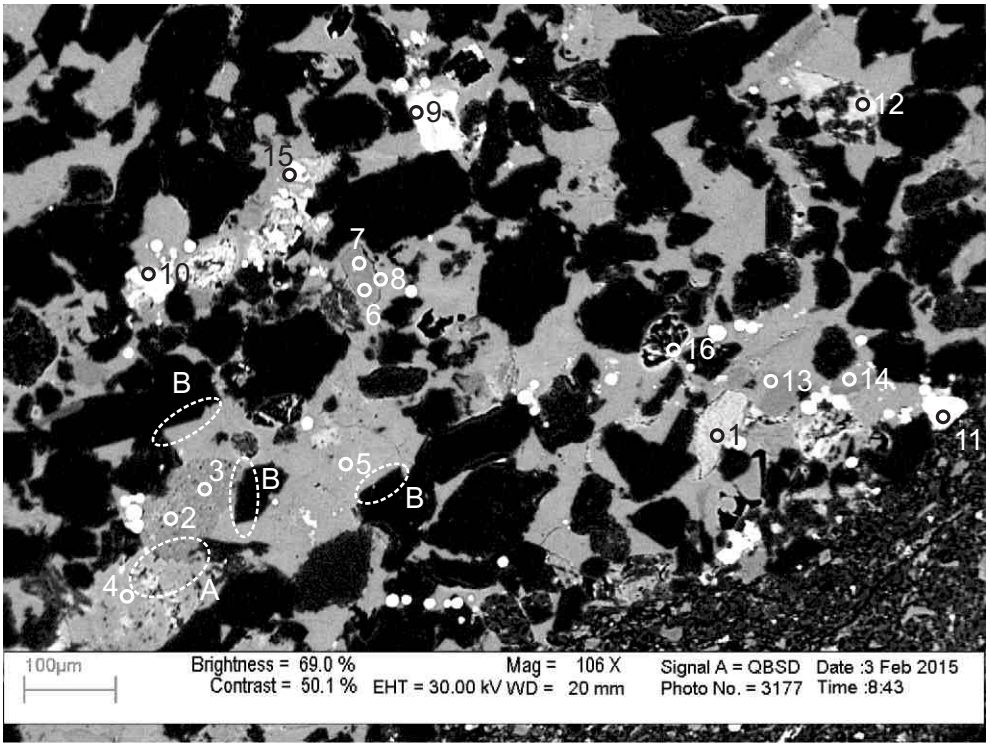

1: Chlorite
2: F-Calcite+ Chlorite
3: F-Calcite+ Chlorite
4: Ankerite
5: F-Fe-Calcite
6: F-Calcite
7: F-Calcite
8: F-Fe-Calcite
9: Titania
10: Titania
11: Zircon
12: Titania+ Chlorite
13: F-Calcite
14: F-Fe-Calcite
15: Titania
16: Chlorite

Figure 2-5.5: Sample Newburn 5213.5m site 5 (SEM). Table 2-5A. Chlorite (16) rims pore. Detrital subhedral zircon (11). High iron F-calcite (5,8,14) replaces low iron F-calcite (2,3,6,7,13). Chlorite cuts ankerite (4) and low iron F-calcite (2,3). Ankerite (4) is replaced by low iron F-calcite (2,3) and both were subsequently corroded forming secondary porosity (position A) and both postdate quartz overgrowth (positions B).

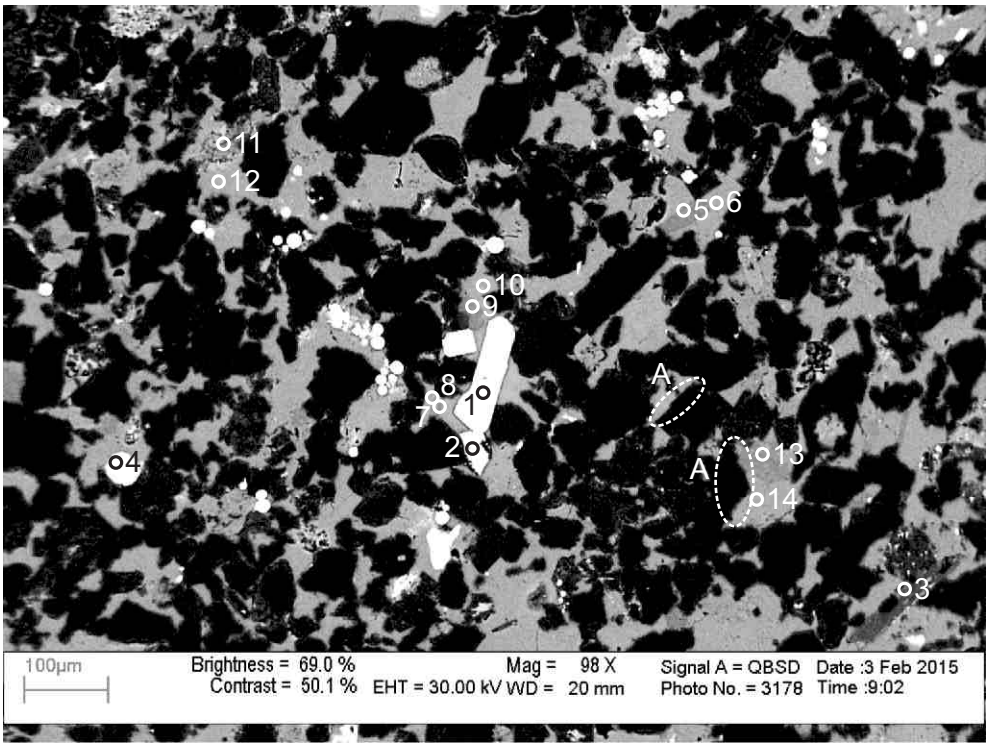

1: Zircon
2: Titania
3: Muscovite
4: Pyrite
5: F-Calcite
6: Fe-Calcite
7: F-Fe-Calcite
8: F-Calcite
9: F-Calcite
10: Fe-Calcite
11: Chlorite+ Calcite
12: Calcite
13: F-Calcite
14: Fe-Calcite

Figure 2-5.6: Sample Newburn 5213.5m site 6 (SEM). Table 2-5A. Diagenetic zircon (1) cuts framework grains and F-calcite (7-9). F-calcite (13) replaces and surrounds Fe-calcite (14). Quartz overgrowth (position A) appears corroded in contact with F-calcite. Pyrite (4) appears later than Fe-calcite.

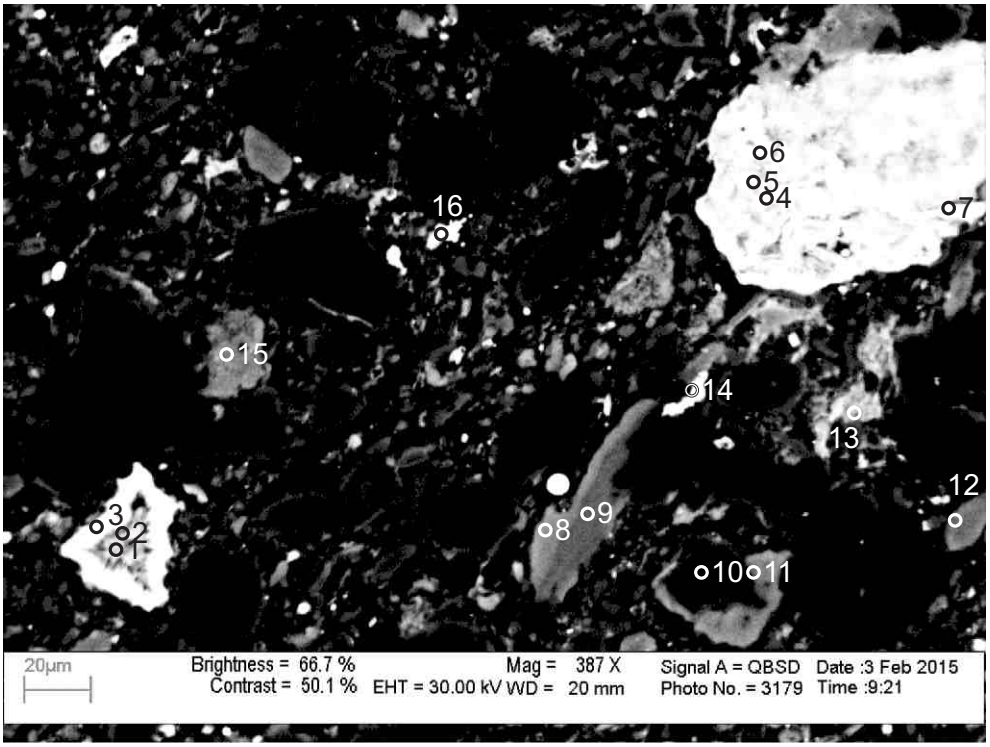

1: Chlorite+ Titania
2: Chlorite+ Titania
3: Titania+ Chlorite
4: Titania+ Chlorite
5: Titania+ Chlorite
6: Titania+ Chlorite
7: Titania+ Chlorite
8: F-Calcite
9: F-Calcite
10: Albite
11: F-Calcite+ Albite
12: F-Calcite+ Muscovite
13: Chlorite
14: Pyrite+ Calcite+ Chlorite
15: F-Calcite+ Chlorite
16: Pyrite+ Chlorite

Figure 2-5.7: Sample Newburn 5213.5m site 7 (SEM). Table 2-5A. Titania (3) rims pore filled with chlorite (1,2). Subhedral titania (4-7) appears to cut bedding.

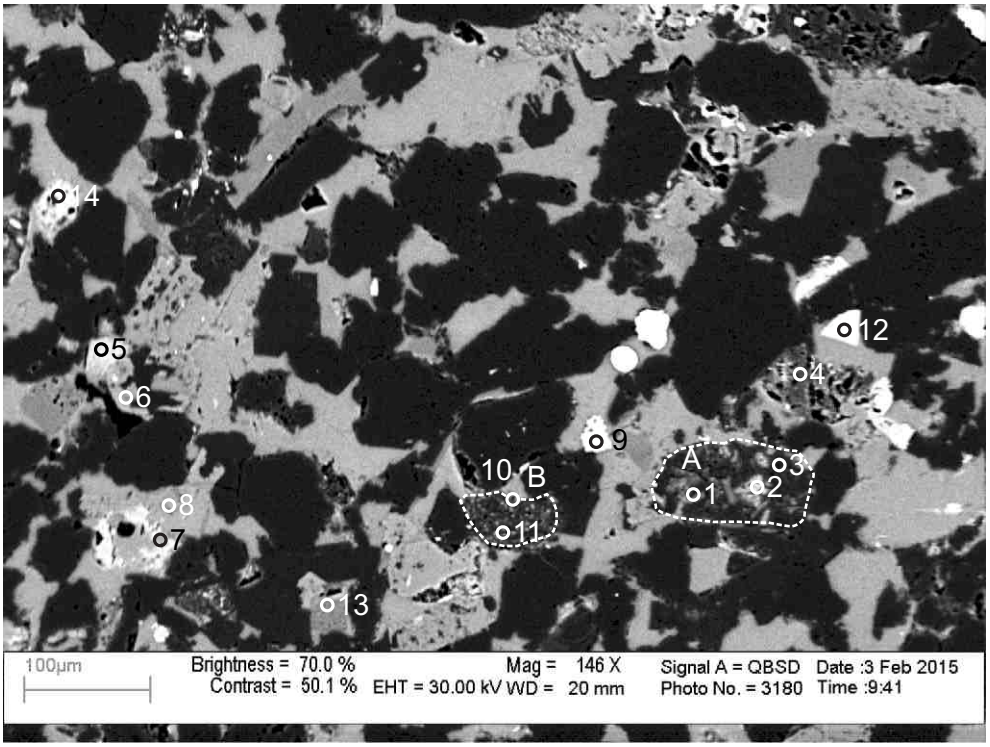

1: Muscovite+ Chlorite
2: Chlorite+ Albite
3: Albite+Illite
4: Albite+ Titania
5: Chlorite+ Titania
6: Ankerite+ Albite
7: F-Calcite+ Chlorite
8: Ankerite+ Chlorite
9: Titania
10: Albite
11: Albite+ Calcite
12:Fluorapatite
13: F-Calcite
14: Titania+ Chlorite

Figure 2-5.8: Sample Newburn 5213.5m site 8 (SEM). Table 2-5A. Titania engulfs partly dissolved albite (4). Diagenetic fluorapatite (12) engulfs framework grains and F-calcite. Granitoid lithic clast (position A) composed of albite, muscovite and chlorite (1-3). Trachytic lithic clast (position B).

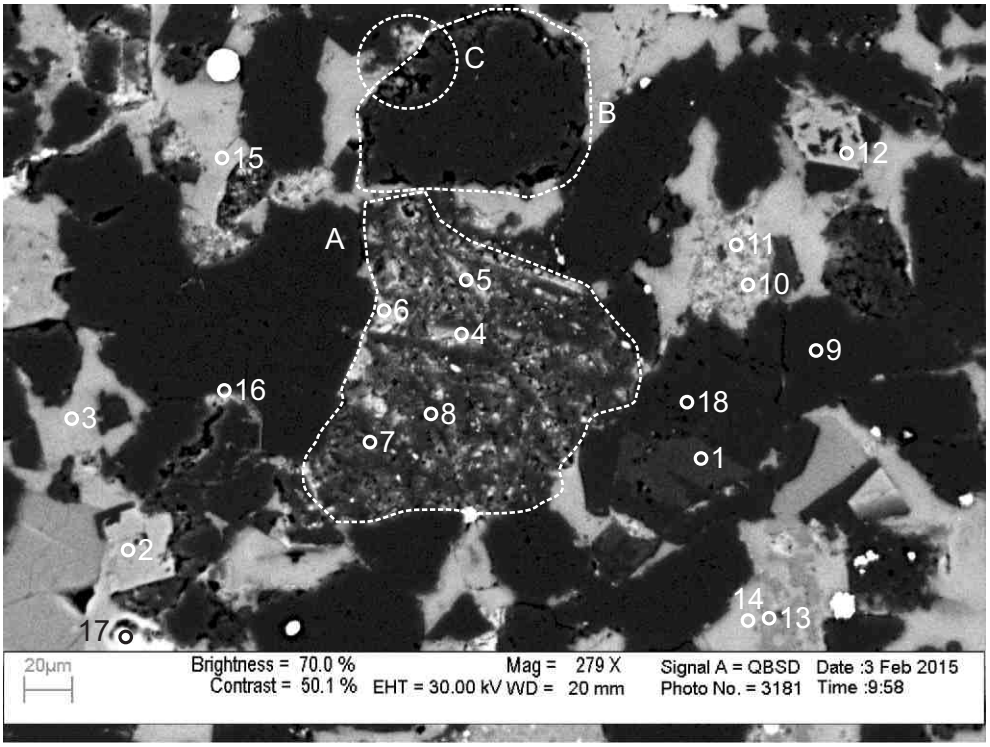

1: Albite
2: Ankerite
3: Fe-Calcite
4: Albite+ Chlorite
5: Albite+ Chlorite
6: Chlorite
7: Albite
8: Albite
9: Quartz
10: F-Calcite+ Chlorite
11: Chlorite+ Calcite
12: Ankerite+ Albite
13: F-Calcite+ Chlorite
14: F-Calcite+ Chlorite
15: Fe-Calcite
16: Quartz+ Chlorite+ Other
17: Spinel
18: Albite

Figure 2-5.9: Sample Newburn 5213.5m site 9 (SEM). Table 2-5A. Trachytic lithic clast (position A) with chlorite filling dissolution within albite (4-8). Dissolution of quartz grain along intergranular boundary shared with F-calcite (position B), and chlorite partially fills void (position C). Ankerite rhombohedron (12) engulfs albite (12) and is replaced by F-calcite/Fe-calcite. Detrital spinel grain (17) with dissolution void.

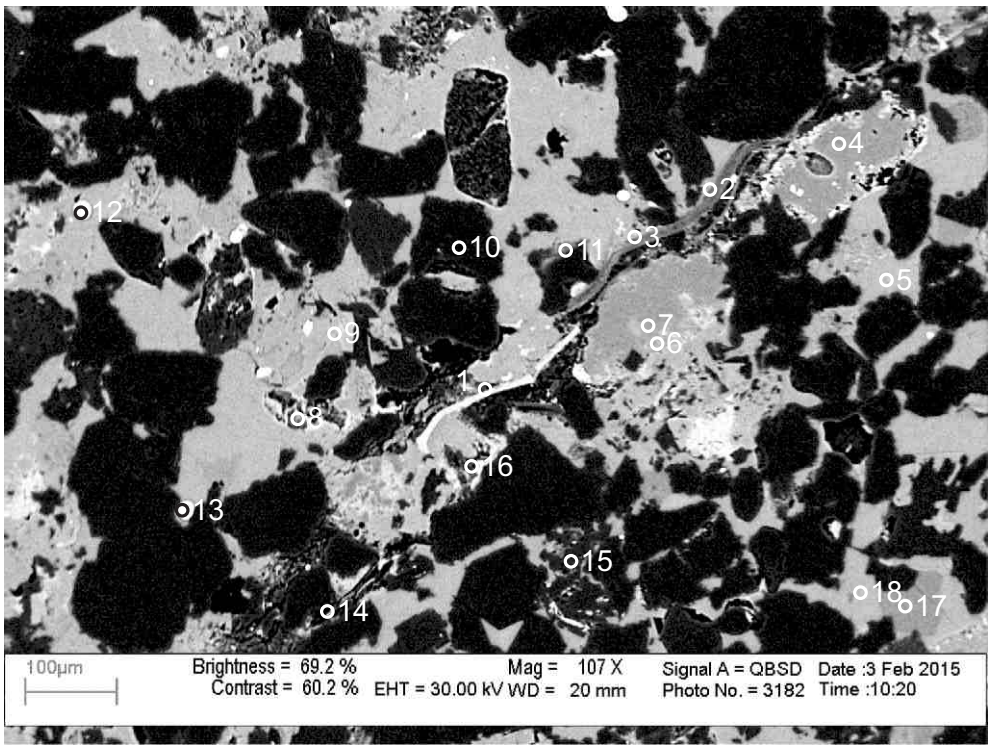

1: Chlorite+ Titania
2: Muscovite+ Chlorite
3: Muscovite+ Chlorite
4: F-Calcite
5: F-Fe-Calcite
6: F-Calcite+ Chlorite
7: F-Calcite
8: Albite+ Chlorite
9: F-Calcite+ Chlorite
10: Quartz
11: Quartz+ Fe-Calcite
12: Pyrite
13: Pyrite
14: Chlorite+ Muscovite
15: Albite+ Other
16: Albite+ Chlorite+ Muscovite+ Titania
17: F-Calcite
18: F-Fe-Calcite

Figure 2-5.10: Sample Newburn 5213.5m site 10 (SEM). Table 2-5A. Plastically deformed muscovite (2,3). F-calcite (17) is replaced by F-Fe-calcite (18).

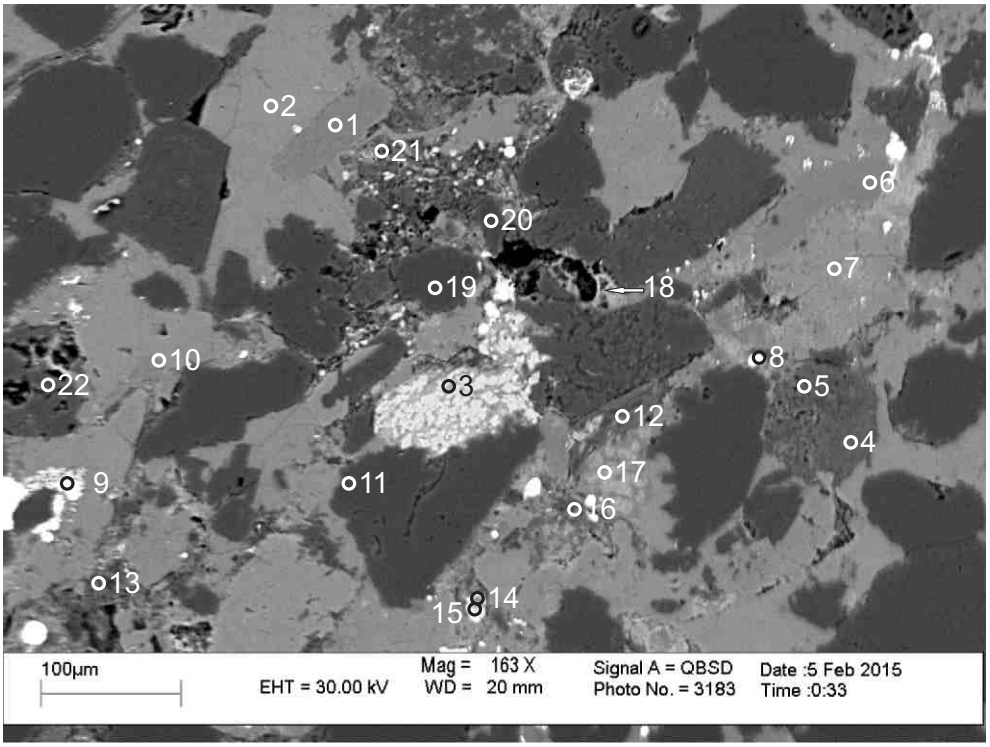

1: F-Calcite
2: Fe-Calcite
3: Chlorite
4: Albite
5: Albite
6: F-Calcite
7: F-Calcite+ Chlorite
8: Chlorite+ Pyrite
9: Pyrite+Other
10: F-Calcite
11: Quartz
12: Muscovite
13: Chlorite+ Muscovite
14: Pyrite+ Chlorite+ Calcite
15: Pyrite+ Albite+ Calcite
16: Chlorite+ Muscovite
17: Chlorite+ Ankerite
18: Chlorite
19: Quartz
20: Quartz
21: Muscovite+ Chlorite
22: Albite

Figure 2-5.11: Sample Newburn 5213.5m site 11 (SEM). Table 2-5A. Chlorite (18) surrounds pore and quartz grains. Partially dissolved albite (4,5,15,16,22) grains with dissolution voids are partially filled by chlorite.

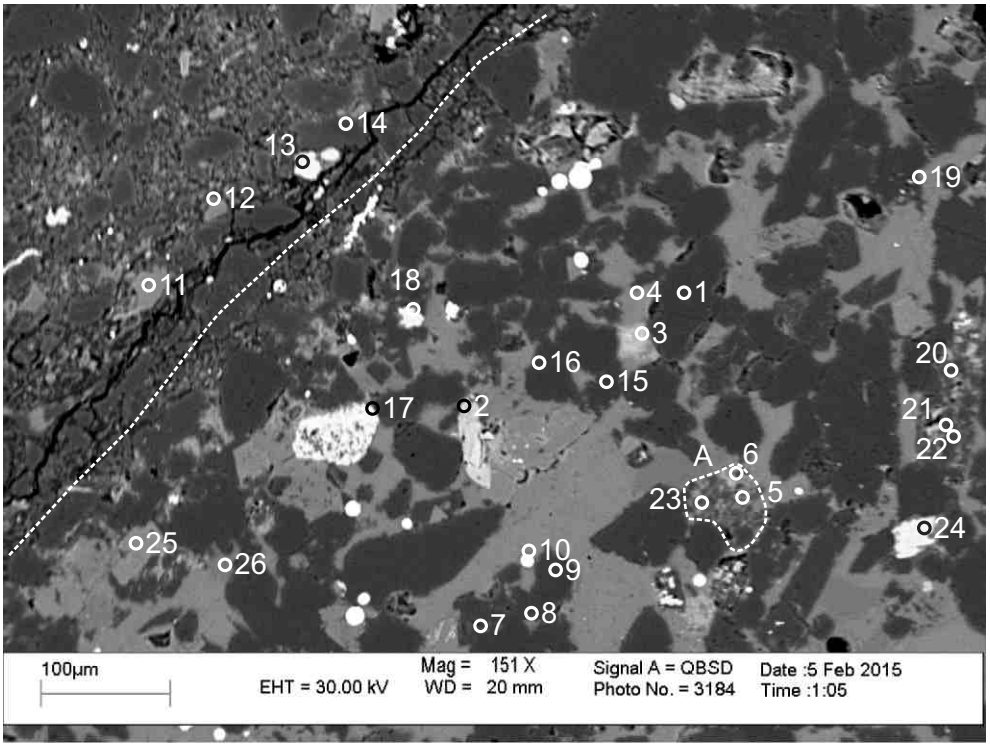

1: Quartz
2: Siderite+ Chlorite
3: Titania+ Chlorite
4: F-Fe-Calcite
5: Albite+ Muscovite+ Chlorite
6: Quartz+ Chlorite
7: Albite
8: Quartz+ Albite+ Calcite
9: Quartz
10: Calcite+ Pyrite
11: Fe-Calcite
12: Muscovite+ F-Calcite+ Chlorite
13: Titania+ Chlorite
14: Albite
15: Quartz
16: Quartz
17: Quartz+ Other
18: Quartz+ Titania+ Chlorite
19: F-Calcite+ Quartz
20: Albite
21: Albite
22: Albite
23: Muscovite+ Chlorite
24: Titania+Other
25: Ankerite
26: F-Calcite+ Quartz

Figure 2-5.12: Sample Newburn 5213.5m site 12 (SEM). Table 2-5A. Contact between sandy and silty bedding. Titania (24) engulfs quartz and F-calcite/Fe-calcite. Siderite (2) replaces quartz and F-calcite/Fe-calcite. Framboidal pyrite (10) fills dissolution voids in quartz and is surrounded by calcite. Granitoid lithic clast composed of quartz (6), albite (5) and muscovite (23) invaded by chlorite (5,6,23).

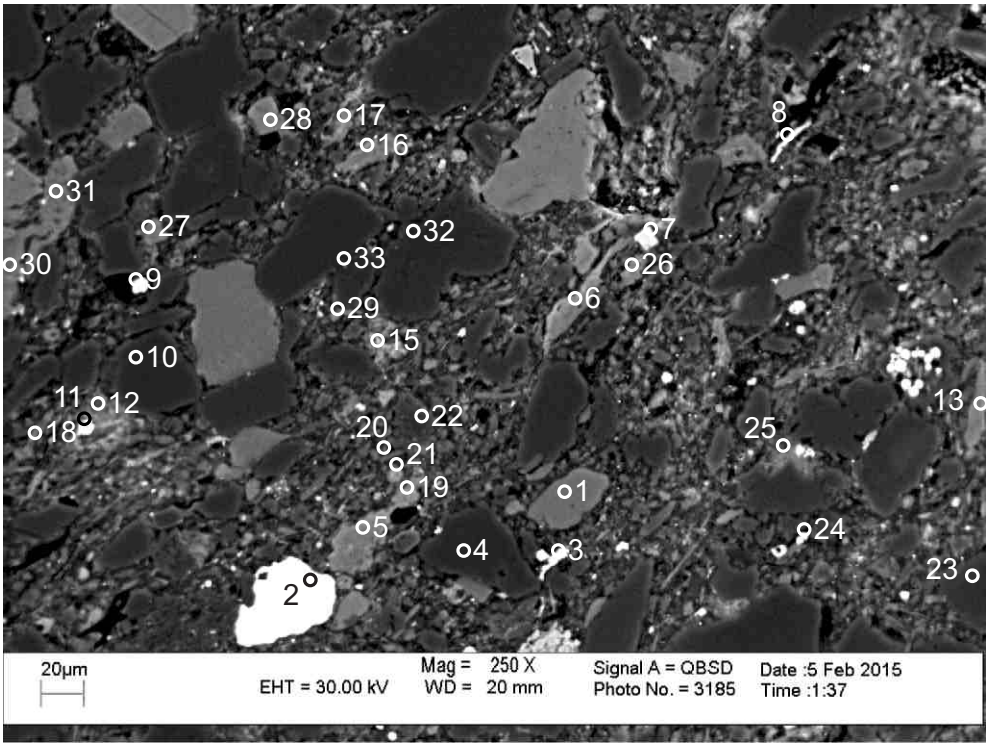

1: F-Calcite
2: Barite
3: Pyrite+Albite+ Muscovite
4: Quartz
5: F-Calcite+Chlorite
6: Calcite+Chlorite
7: Titania+Albite+ Ankerite
8: Pyrite+Muscovite+ Calcite
9: Pyrite+Albite
10: Quartz
11: Pyrite+Chlorite
12: Quartz+Chlorite
13: F-Calcite+ Muscovite
14: Quartz+Chlorite
15: Chlorite+Calcite
16: F-Calcite+Chlorite
17: F-Calcite+Chlorite
18: Muscovite+ Pyrite+Calcite
19: Calcite+Chlorite
20: Quartz+ Muscovite
21: Muscovite+Calcite
22: Quartz
23: Quartz
24: Mix
25: Quartz+Chlorite+ Calcite
26: F-Calcite+Chlorite
27: F-Calcite+Chlorite
28: F-Calcite+Chlorite
29: Albite+Quartz+ Calcite+Muscovite
30: F-Calcite+Quartz
31: F-Calcite+Chlorite
32: Quartz
33: Quartz+Other

Figure 2-5.13: Sample Newburn 5213.5m site 13 (SEM). Table 2-5A. Barite (2) fills porosity. Aligned framework grains and silty matrix of quartz (12,20,22), muscovite (3,20,22) and chlorite (25-28). Pyrite (3,8) may be pseudomorphing muscovite.

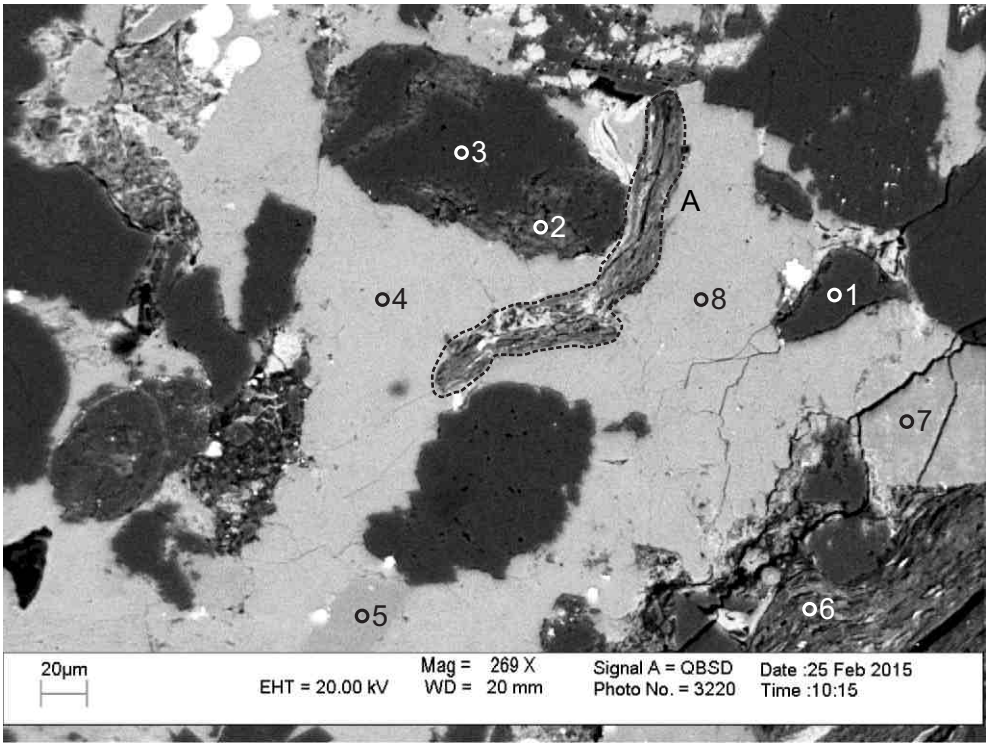

1:Quartz
2: Illite
3: Quartz
4: F-Fe-Calcite
5: F-Calcite
6: Chlorite+ Muscovite
7: F-Fe-Calcite
8: F-Fe-Calcite

Figure 2-5.14: Sample Newburn 5213.5m site 1 (SEM). Table 2-5B. Illite (2) fills dissolution in quartz (3). Chlorite replaces muscovite (6) along its cleavage planes. Plastically deformed chloritized muscovite (position A) surrounded and partially engulfed by F-Fe-calcite (4,8).

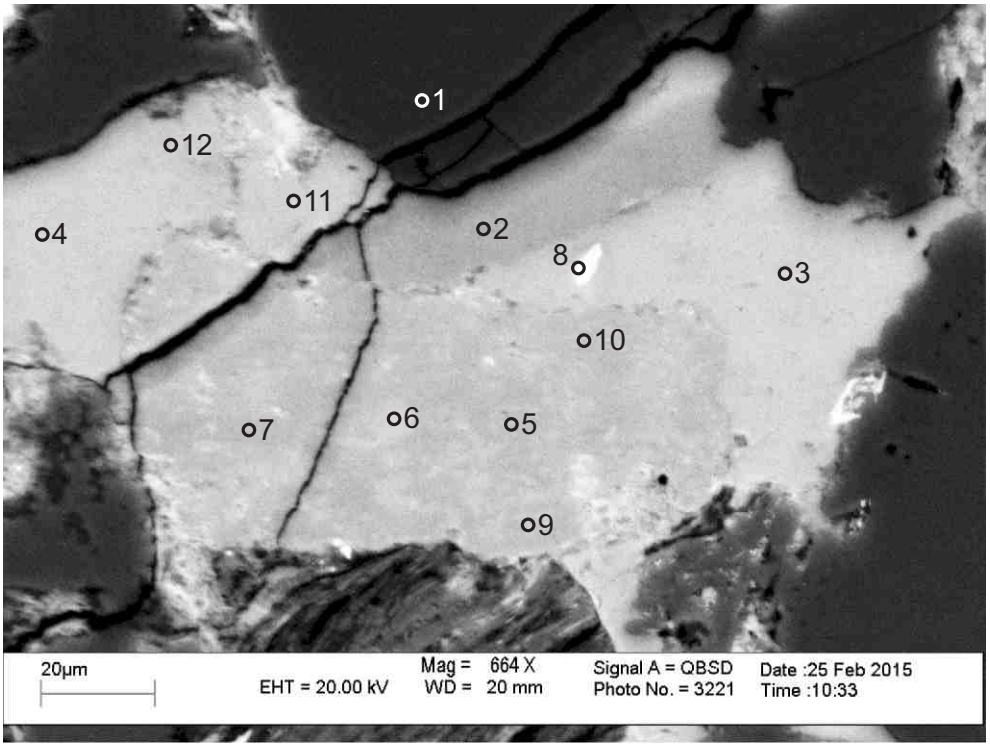

1:Quartz
2: F-Fe-Calcite
3: F-Fe-Calcite
4: F-Fe-Calcite
5: F-Fe-Calcite
6: F-Fe-Calcite
7: F-Calcite
8: Ankerite+ Chlorite
9. F-Fe-Calcite
10. F-Calcite
11. F-Calcite +Chlorite
12. Chlorite+ F-Calcite

Figure 2-5.15: Sample Newburn 5213.5m site 2 (SEM). Table 2-5B. Replacement of F-calcite (2,5,7,9) by F-Fe-calcite (3,4,6).

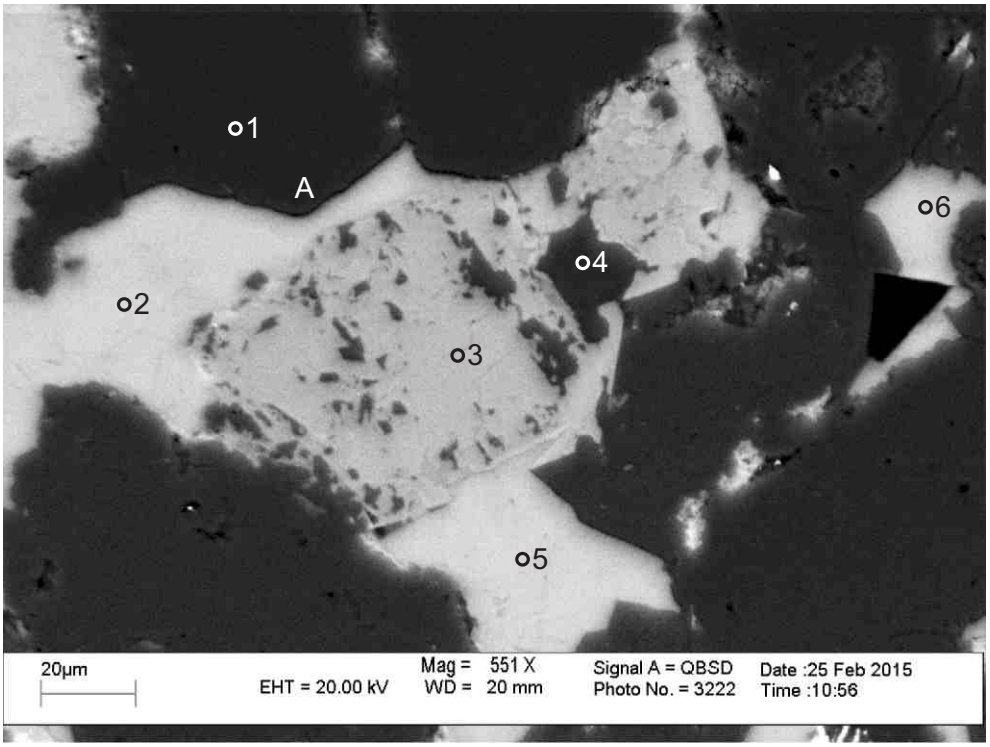

1. Quartz
2. F-Fe-Calcite
3. Ankerite
4. Albite
5. F-Fe-Calcite
6. F-Fe-Calcite

Figure 2-5.16: Sample Newburn 5213.5m site 3 (SEM). Table 2-5B. Ankerite (3) engulfs albite (4). F-Fe-calcite (2) surrounds and replaces ankerite (3) as well as quartz overgrowths (position A). F-Fe-calcite (6) forms along intergranular boundary.

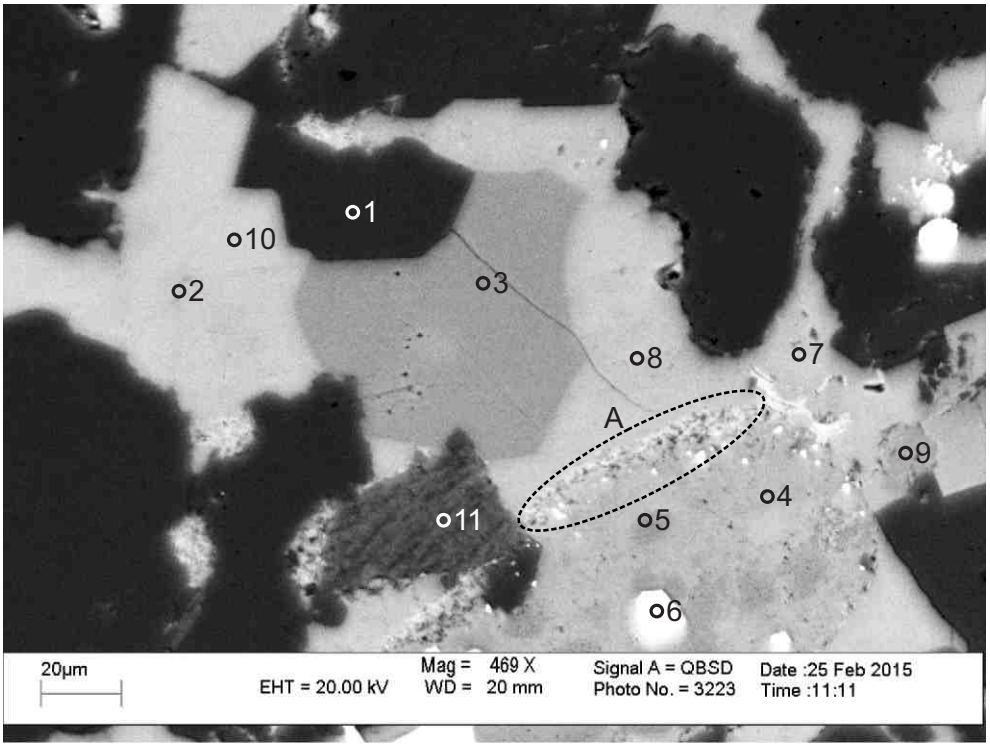

1. Albite
2. F-Calcite+ Quartz
3. F-Calcite
4. F-Fe-Calcite
5. F-Calcite
6. Pyrite
7. F-Fe-Calcite
8. F-Fe-Calcite
9. F-Calcite
10. F-Fe-Calcite
11. Illite

Figure 2-5.17: Sample Newburn 5213.5m site 4 (SEM). Table 2-5B. Dark patch of low iron F-calcite (3) being replaced by F-calcite (2,8) with higher iron levels. Pyrite (6) fills dissolution in F-calcite, and pyrite and chlorite (position A) also rim F-calcite which is surrounded by F-Fe-calcite.

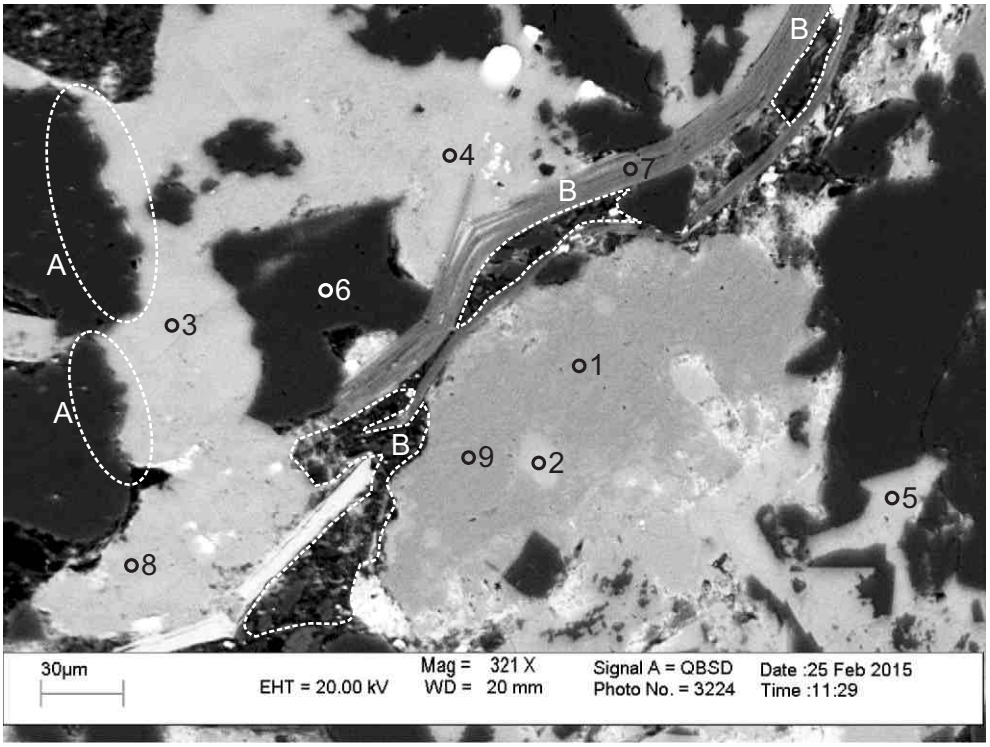

1. F-Calcite
2. F-Calcite+ Chlorite
3. F-Calcite+ Chlorite
4. F-Fe-Calcite
5. F-Fe-Calcite
6. Quartz
7. Muscovite
8. F-Fe-Calcite
9. F-Calcite

Figure 2-5.18: Sample Newburn 5213.5m site 5 (SEM). Table 2-5B. Plastically deformed muscovite (7). F-calcite (3) corrodes quartz overgrowths (positions A). Mechanically fractured quartz or felsic lithic clast (positions B) with voids partially filled by titania and chlorite.

Table 2-5A: Scaning Electron Microscope chemical analyses of sample 5213.5m from Newburn H-23 well.

Sample	Site	Position	Mineral	SiO_2	TiO_2	Al_2O_3	FeO	MnO	MgO	CaO	Na_2O	K_2O	P_2O_5	SO_3	F	Cl	Cr_2O_3	ZnO	SrO	ZrO_2	BaO	Ce_2O_3	HfO_2	Total	Actual Total
H-23 5213.5m	1	1	TiO_2	1.33	96.26	0.94	1.26			0.20														100	110
H-23 5213.5m	1	2	Fe-Cal				1.89	0.30	0.53	53.28														56	59
H-23 5213.5m	1	3	Qz+Other	73.42	1.27	13.26	4.04		1.29	3.41	1.17	2.13												100	118
H-23 5213.5m	1	4	Qz+Chl+Fe-Cal	82.42	0.45	7.78	6.32		1.19	1.08		0.73												100	149
H-23 5213.5m	1	5	Ab+Chl	53.29		21.64	14.05		2.57	0.74	7.71													100	134
H-23 5213.5m	1	6	Ank	0.72		0.57	15.65	0.72	9.82	28.53														56	77
H-23 5213.5m	1	7	Py	1.48		0.85	26.93		0.27	1.80	0.43			68.24										100	244
H-23 5213.5m	1	8	Ank	0.71			2.41	0.34	0.86	51.68														56	61
H-23 5213.5m	1	9	Qz	99.86			0.14																	100	127
H-23 5213.5m	1	10	Ab	61.37	0.42	19.54	5.83		0.66	0.76	10.50		0.92											100	119
H-23 5213.5m	1	11	TiO_2+Chl	3.06	88.26	3.40	4.30		0.41	0.57														100	134
H-23 5213.5m	1	12	Fe-Cal				2.21	0.26	0.55	52.98														56	72
H-23 5213.5m	1	13	Qz	99.49		0.51																		100	155
H-23 5213.5m	1	14	Qz	99.99																				100	125
H-23 5213.5m	1	15	Ab	62.19		19.65	5.25		0.85	0.88	10.46		0.73											100	117
H-23 5213.5m	1	16	Ms+Chl+Qz	74.40	0.92	15.66	2.87		1.81			4.35												100	136
H-23 5213.5m	1	17	Chl+Ab	44.58	1.03	34.79	8.80		6.82	1.46	2.53													100	124
H-23 5213.5m	1	18	Qz	98.23		0.72	1.04																	100	144
H-23 5213.5m	1	19	Ms+Chl+TiO_2	53.69	2.25	24.22	6.68		2.17	5.51	1.13	4.14				0.20								100	97
H-23 5213.5m	1	20	Chl	30.56		22.26	25.95		4.88	0.31	0.45	0.44				0.15								85	87
H-23 5213.5m	1	21	F-Cal+Ab	11.92		3.23	2.57	0.45	1.13	72.80	1.15	0.37			6.40									100	70
H-23 5213.5m	1	22	Ank+Py+Ap	2.67		0.81	24.08	1.17	15.95	47.64			4.40	3.27										100	74
H-23 5213.5m	1	23	Qz	99.99																				100	133
H-23 5213.5m	1	24	Qz+Other	92.97		2.42	2.19		0.63	1.80														100	126
H-23 5213.5m	1	25	Qz	99.99																				100	142
H-23 5213.5m	1	26	Qz	99.99																				100	146
H-23 5213.5m	1	27	Qz	99.99																				100	139
H-23 5213.5m	1	28	Qz	99.99																				100	137
H-23 5213.5m	1	29	Qz	99.99																				100	137
H-23 5213.5m	1	30	Ab+Chl	44.60	1.00	34.71	8.85		6.86	1.40	2.58													100	124
H-23 5213.5m	2	1	Py	0.19			27.00				1.09			71.72										100	242
H-23 5213.5m	2	2	Py	0.47		0.21	27.12				1.29			70.89										100	249
H-23 5213.5m	2	3	Py	0.28			26.91							72.81										100	249
H-23 5213.5m	2	4	Chl+Ap	20.79		13.85	20.29		4.76	20.60	0.46		19.25											100	113
H-23 5213.5m	2	5	F-Cal					0.31	1.32	51.44					2.93									56	63
H-23 5213.5m	2	6	F-Cal+Chl	2.10		1.64	0.35		4.81	77.73		0.22		1.60	11.59									100	73
H-23 5213.5m	2	7	Qz	98.64		1.17	0.18																	100	139
H-23 5213.5m	2	8	Ab	68.30		19.20				0.41	12.09													100	136
H-23 5213.5m	2	9	Qz	99.99																				100	135
H-23 5213.5m	2	10	Ab+Py+Cal	52.09		9.86	10.21		1.06	12.51	2.79	0.48		10.99										100	124
H-23 5213.5m	2	11	Ank+Qz	1.41			26.35	1.36	20.63	50.25														100	71
H-23 5213.5m	2	12	Ank+Chl	3.59		1.34	24.80	1.15	20.11	48.99														100	71

Table 2-5A: Scaning Electron Microscope chemical analyses of sample 5213.5m from Newburn H-23 well.

Sample	Site	Position	Mineral	SiO_2	TiO_2	Al_2O_3	FeO	MnO	MgO	CaO	Na_2O	K_2O	P_2O_5	SO_3	F	Cl	Cr_2O_3	ZnO	SrO	ZrO_2	BaO	Ce_2O_3	HfO_2	Total	Actual Total
H-23 5213.5m	2	13	Ms+Ank	52.99	0.98	22.09	6.47		2.42	9.53	0.82	3.69		0.80		0.20								100	103
H-23 5213.5m	2	14	F-Cal+Ms	28.47		14.34	4.08		2.35	42.30	0.86	1.83		2.17	3.59									100	99
H-23 5213.5m	2	15	Qz+Other	96.26		2.27	0.33			0.32	0.27	0.55												100	138
H-23 5213.5m	2	16	F-Cal+Qz	35.66		1.13	0.66		0.91	51.32		0.34			9.99									100	91
H-23 5213.5m	2	17	F-Cal	0.54		0.34	0.53		3.15	43.86				1.19	6.41									56	75
H-23 5213.5m	2	18	F-Cal+Qz	6.03			0.78		5.75	73.04				2.37	12.01									100	79
H-23 5213.5m	2	19	F-Fe-Cal	0.86	2.17	0.59	2.33	0.52	1.00	42.66					5.86									56	75
H-23 5213.5m	2	20	Ms+Chl	55.90	2.05	29.80	1.63		1.51	0.80	1.05	7.13				0.15								100	124
H-23 5213.5m	3	1	F-Cal						1.13	49.62					5.26									56	70
H-23 5213.5m	3	2	F-Cal+Chl	4.75		2.61	4.82		1.28	78.13					8.40									100	74
H-23 5213.5m	3	3	F-Cal						0.41	47.76				0.42	7.41									56	69
H-23 5213.5m	3	4	F-Cal+Chl	11.74		9.49	13.93		2.55	55.07					7.21									100	79
H-23 5213.5m	3	5	Py	0.21			26.69				0.24			65.27										92	242
H-23 5213.5m	3	6	Zrn	31.79																67.95			0.27	100	139
H-23 5213.5m	3	7	Qz+TiO_2	85.80	13.18		0.71			0.31														100	117
H-23 5213.5m	3	8	Py+Chl+Cal	7.02	0.27	5.65	28.30		1.46	3.81		0.19		53.31										100	187
H-23 5213.5m	3	9	TiO_2+Ilt	18.08	65.25	9.66	3.02		0.80	0.41		2.77												100	112
H-23 5213.5m	3	10	Qz	99.99																				100	132
H-23 5213.5m	3	11	Qz	97.27	0.28	1.72	0.28					0.43												100	129
H-23 5213.5m	3	12	Chl	26.04	0.26	19.00	30.77	0.24	5.48	1.55	0.85	0.61				0.20								85	89
H-23 5213.5m	3	13	F-Fe-Cal	0.66		0.35	2.09		0.51	50.06					2.33									56	59
H-23 5213.5m	3	14	Ank+Kln	3.55		1.21	23.77	1.14	18.99	51.35														100	64
H-23 5213.5m	3	15	Ank+Ab	7.72		2.61	21.81	1.14	16.95	48.06	1.71													100	69
H-23 5213.5m	3	16	Ank+Chl	3.08		1.00	23.34	0.98	19.75	51.87														100	66
H-23 5213.5m	3	17	F-Cal+Chl	7.06		5.39	7.85	0.37	1.86	70.02					7.44									100	72
H-23 5213.5m	3	18	F-Cal+Ank	1.20			3.91	0.59	1.16	86.95					6.20									100	75
H-23 5213.5m	3	19	Ab+Other	63.60		19.65	4.91		0.68	0.27	10.88													100	144
H-23 5213.5m	3	20	Fe-Cal				13.12	0.93	9.65	76.30														100	73
H-23 5213.5m	3	21	Ms+Ab+Chl	58.06	0.45	25.57	7.65		2.14		1.20	4.93												100	135
H-23 5213.5m	3	22	Qz+Ab+Cal	79.06	0.22	2.17	1.45			15.80	1.12	0.17												100	134
H-23 5213.5m	3	23	F-Cal						2.24	45.01				1.38	7.36									56	75
H-23 5213.5m	3	24	Fe-Cal				1.99	0.25	0.55	53.21														56	61
H-23 5213.5m	3	25	F-Fe-Cal				1.66	0.27	0.48	44.16					9.44									56	84
H-23 5213.5m	3	26	F-Fe-Cal				2.17	0.25	0.77	50.75					2.06									56	71
H-23 5213.5m	4	1	F-Cal				0.24		0.60	49.05				0.62	5.50									56	68
H-23 5213.5m	4	2	F-Fe-Cal				1.62		0.48	45.75					8.16									56	69
H-23 5213.5m	4	3	Ab	62.21		18.97	4.27		0.58	1.82	10.02	0.40	1.74											100	135
H-23 5213.5m	4	4	Chl+Ms	48.60	0.98	31.99	9.44		2.19		0.42	6.37												100	93
H-23 5213.5m	4	5	Ab	68.48		18.82	0.26			0.29	11.84	0.30												100	136
H-23 5213.5m	4	6	F-Cal			0.34	0.78		0.72	46.47				0.50	7.20									56	73
H-23 5213.5m	4	7	F-Fe-Cal	0.62		0.29	1.69	0.25	0.46	46.05					6.65									56	72
H-23 5213.5m	4	8	F-Cal+Chl	4.81		3.21	5.48	0.27		72.17		0.34		8.69	5.02									100	79
H-23 5213.5m	4	9	Py				26.00			3.18				70.82										100	239

Table 2-5A: Scaning Electron Microscope chemical analyses of sample 5213.5m from Newburn H-23 well.

Sample	Site	Position	Mineral	SiO_2	TiO_2	Al_2O_3	FeO	MnO	MgO	CaO	Na_2O	K_2O	P_2O_5	SO_3	F	Cl	Cr_2O_3	ZnO	SrO	ZrO_2	BaO	Ce_2O_3	HfO_2	Total	Actual Total
H-23 5213.5m	4	10	Py	0.45			27.00			0.78	0.82			70.97										100	256
H-23 5213.5m	4	11	Qz	99.99																				100	139
H-23 5213.5m	4	12	Qz	99.99																				100	129
H-23 5213.5m	4	13	Ilt+Qz	72.13		18.31	2.07		1.18		0.30	6.01												100	130
H-23 5213.5m	4	14	Qz	99.84			0.15																	100	132
H-23 5213.5m	4	15	Ms+TiO_2	62.02	4.22	24.73	1.45		0.73		0.47	6.37												100	122
H-23 5213.5m	4	16	Qz+Ms	93.78	0.75	3.97	0.39			0.18		0.93												100	125
H-23 5213.5m	4	17	Ms+Chl+Ab	46.29	0.40	25.28	19.70		4.05	0.57	1.90	1.53				0.29								100	105
H-23 5213.5m	4	18	F-Cal				0.22		0.83	48.44				0.50	6.00									56	69
H-23 5213.5m	4	19	F-Cal						0.68	46.72				0.53	8.08									56	72
H-23 5213.5m	4	20	F-Fe-Cal	0.54		0.45	1.58	0.18	1.51	45.09					6.64									56	75
H-23 5213.5m	4	21	Chl	31.07		21.82	24.88		4.45	1.52	0.42	0.70				0.14								85	101
H-23 5213.5m	4	22	Ab	74.19		15.38					10.42													100	145
H-23 5213.5m	4	23	Chl+Ms	35.13	0.55	26.43	30.70		5.12	0.74		1.17				0.18								100	95
H-23 5213.5m	4	24	Chl+Ms	42.18	0.43	27.40	22.64		4.73	0.71		1.70				0.20								100	120
H-23 5213.5m	4	25	Chl+Ms	41.24	0.77	26.79	23.68		4.11	0.56	0.81	1.81				0.21								100	105
H-23 5213.5m	5	1	Chl	28.17		21.89	29.31		4.88	0.25	0.52													85	112
H-23 5213.5m	5	2	F-Cal+Chl	3.59		1.81	2.25	0.30	2.85	74.45		0.26		1.37	13.10									100	73
H-23 5213.5m	5	3	F-Cal+Chl	2.74		1.44	2.75	0.30	2.59	74.54		0.22		2.60	12.83									100	74
H-23 5213.5m	5	4	Ank	0.58			14.61	0.70	10.97	29.15														56	65
H-23 5213.5m	5	5	F-Fe-Cal	0.50		0.32	1.84	0.25	0.66	46.49					5.95									56	70
H-23 5213.5m	5	6	F-Cal				0.43		0.82	47.39				0.78	6.58									56	73
H-23 5213.5m	5	7	F-Cal						0.67	46.59	0.39			0.67	7.68									56	74
H-23 5213.5m	5	8	F-Fe-Cal	0.53		0.38	2.26	0.32	0.55	48.28					3.68									56	68
H-23 5213.5m	5	9	TiO_2	0.71	98.32		0.63			0.36														100	116
H-23 5213.5m	5	10	TiO_2	0.77	96.78	0.49	0.49			1.47														100	112
H-23 5213.5m	5	11	Zrn	31.85																67.39			0.77	100	150
H-23 5213.5m	5	12	TiO_2+Chl	18.97	44.97	13.15	15.85		5.37	0.69	0.67	0.33												100	120
H-23 5213.5m	5	13	F-Cal	0.50		0.35	0.54		0.55	47.61					6.45									56	78
H-23 5213.5m	5	14	F-Fe-Cal	0.49			1.50	0.20	0.99	43.86				0.62	8.34									56	81
H-23 5213.5m	5	15	TiO_2	0.60	97.33	0.45	0.51			1.09														100	114
H-23 5213.5m	5	16	Chl	31.55		20.58	13.63		3.60	13.92	0.42	1.31												85	121
H-23 5213.5m	6	1	Zrn	31.45																67.88			0.67	100	139
H-23 5213.5m	6	2	TiO_2	1.22	96.78	0.76	0.85			0.36														100	117
H-23 5213.5m	6	3	Ms	47.15	0.93	33.39	2.47		0.57		1.31	9.18												95	132
H-23 5213.5m	6	4	Py				28.02			0.25				71.74										100	213
H-23 5213.5m	6	5	F-Cal						0.80	47.40	0.37			1.79	5.64									56	76
H-23 5213.5m	6	6	Fe-Cal				1.92	0.23	0.54	53.31														56	65
H-23 5213.5m	6	7	F-Fe-Cal				1.93	0.27	0.73	48.12					4.94									56	67
H-23 5213.5m	6	8	F-Cal	0.48					0.75	51.48					3.29									56	66
H-23 5213.5m	6	9	F-Cal				0.38	0.17	0.88	49.63				0.36	4.58									56	70
H-23 5213.5m	6	10	Fe-Cal				2.09	0.31	0.45	53.14														56	62

Table 2-5A: Scaning Electron Microscope chemical analyses of sample 5213.5m from Newburn H-23 well.

Sample	Site	Position	Mineral	SiO_2	TiO_2	Al_2O_3	FeO	MnO	MgO	CaO	Na_2O	K_2O	P_2O_5	SO_3	F	Cl	Cr_2O_3	ZnO	SrO	ZrO_2	BaO	Ce_2O_3	HfO_2	Total	Actual Total
H-23 5213.5m	6	11	Chl+Cal	28.71		23.66	29.29		5.99	12.37														100	86
H-23 5213.5m	6	12	Fe-Cal				2.49	0.58	0.72	52.21														56	58
H-23 5213.5m	6	13	F-Cal						1.72	51.40					2.88									56	70
H-23 5213.5m	6	14	Cal				2.28	0.28	0.44	53.00														56	64
H-23 5213.5m	7	1	Chl+TiO_2	31.17	6.92	25.83	29.87		6.20															100	109
H-23 5213.5m	7	2	Chl+TiO_2	30.53	8.77	25.26	29.13		6.10	0.22														100	111
H-23 5213.5m	7	3	TiO_2+Chl	2.91	92.93	2.08	1.39			0.50						0.18								100	102
H-23 5213.5m	7	4	TiO_2+Chl	3.62	89.07	2.93	3.41			0.43							0.54							100	107
H-23 5213.5m	7	5	TiO_2+Chl	2.18	93.49	1.34	1.93			0.43							0.60							100	105
H-23 5213.5m	7	6	TiO_2+Chl	1.71	93.64	1.93	1.63			0.42							0.69							100	107
H-23 5213.5m	7	7	TiO_2+Chl	3.42	92.46	2.34	1.24			0.32		0.23												100	115
H-23 5213.5m	7	8	F-Cal	0.79		0.35	0.73	0.18		51.51		0.08			2.36									56	63
H-23 5213.5m	7	9	F-Cal						0.59	48.96				0.53	5.91									56	68
H-23 5213.5m	7	10	Ab	68.73		18.97					12.30													100	140
H-23 5213.5m	7	11	F-Cal+Ab	17.99		5.97	2.61	0.27		63.17	3.56				6.42									100	77
H-23 5213.5m	7	12	F-Cal+Ms	5.01		1.36				85.94		0.22			7.48									100	69
H-23 5213.5m	7	13	Chl	33.20	0.26	21.34	24.74		4.67	0.31		0.49												85	109
H-23 5213.5m	7	14	Py+Cal+Chl	12.45		6.37	21.84		0.96	7.84	3.83	0.42		46.30										100	168
H-23 5213.5m	7	15	F-Cal+Chl	6.57		1.98	5.17	0.40	1.64	72.13					12.10									100	73
H-23 5213.5m	7	16	Py+Chl	11.17	0.97	6.27	25.43		1.86	1.09	0.70	0.54		51.99										100	180
H-23 5213.5m	8	1	Ms+Chl	54.70	0.32	28.72	3.24		1.72		1.86	9.42												100	135
H-23 5213.5m	8	2	Chl+Ab	47.94		22.73	21.29		3.58	0.31	4.13													100	108
H-23 5213.5m	8	3	Ab+Ilt	63.73		20.79	1.89		0.36	0.56	10.56	2.11												100	144
H-23 5213.5m	8	4	Ab+TiO_2	60.54	3.77	16.93	0.36			3.93	10.76	0.16	3.55											100	144
H-23 5213.5m	8	5	Chl+TiO_2	28.62	16.61	22.60	26.95		4.84	0.38														100	106
H-23 5213.5m	8	6	Ank+Ab	27.45		7.44	14.09	0.71	10.50	36.13	3.34	0.33												100	83
H-23 5213.5m	8	7	F-Cal+Chl	12.30		9.16	17.59	0.27	2.21	52.20		0.14			6.11									100	77
H-23 5213.5m	8	8	Ank+Chl	18.82		10.24	16.92	0.46	9.75	42.89	0.93													100	83
H-23 5213.5m	8	9	TiO_2	1.16	95.35		1.45			1.19				0.85										100	119
H-23 5213.5m	8	10	Ab	57.84	0.28	20.31	10.11		1.43	0.87	9.14													100	128
H-23 5213.5m	8	11	Ab+Cal	64.18		19.31	3.31		0.61	1.05	10.57	0.19	0.78											100	132
H-23 5213.5m	8	12	Fap				0.31			47.10			44.39		7.49	0.25						0.47		100	146
H-23 5213.5m	8	13	F-Cal						2.65	49.07				0.95	3.33									56	67
H-23 5213.5m	8	14	TiO_2+Chl	3.23	91.53	2.14	2.06			1.04														100	103
H-23 5213.5m	9	1	Ab	64.39		22.05				3.62	9.76	0.17												100	136
H-23 5213.5m	9	2	Ank	0.88			15.09	0.59	10.61	28.82														56	67
H-23 5213.5m	9	3	Fe-Cal				2.33	0.32	0.69	52.65														56	58
H-23 5213.5m	9	4	Ab+Chl	44.26		22.88	22.91		3.17		6.63	0.14												100	129
H-23 5213.5m	9	5	Ab+Chl	49.71		21.67	17.69		2.24		8.68													100	137
H-23 5213.5m	9	6	Chl	34.35		21.12	23.97		4.68	0.24	0.40	0.25												85	105
H-23 5213.5m	9	7	Ab	61.46		19.95	6.73		0.93	0.13	10.80													100	136
H-23 5213.5m	9	8	Ab	64.95		19.50	4.13		0.55		10.88													100	131

Table 2-5A: Scaning Electron Microscope chemical analyses of sample 5213.5m from Newburn H-23 well.

Sample	Site	Position	Mineral	SiO_2	TiO_2	Al_2O_3	FeO	MnO	MgO	CaO	Na_2O	K_2O	P_2O_5	SO_3	F	Cl	Cr_2O_3	ZnO	SrO	ZrO_2	BaO	Ce_2O_3	HfO_2	Total	Actual Total
H-23 5213.5m	9	9	Qz	99.99																				100	140
H-23 5213.5m	9	10	F-Cal+Chl	21.33		13.38	13.93		3.53	42.45		0.41		0.67	4.31									100	87
H-23 5213.5m	9	11	Chl+Cal	28.92		19.08	21.20		4.59	25.23		0.40		0.60										100	94
H-23 5213.5m	9	12	Ank+Ab	12.43		3.23	22.87	1.05	17.13	41.79	1.50													100	77
H-23 5213.5m	9	13	F-Cal +Chl	5.01		1.23	3.81		6.28	75.44				1.50	6.72									100	73
H-23 5213.5m	9	14	F-Cal +Chl	3.29		1.85	5.03	0.39	1.31	83.08					5.04									100	69
H-23 5213.5m	9	15	Fe-Cal	0.66			2.27	0.34	0.55	52.18														56	60
H-23 5213.5m	9	16	Qz+Chl+Other	58.61		16.48	19.22		3.18	0.83	0.61	1.07												100	124
H-23 5213.5m	9	17	Spl	1.90		36.00	14.96		10.65	1.57							34.09	0.86						100	111
H-23 5213.5m	9	18	Ab	68.80		18.88					12.34													100	139
H-23 5213.5m	10	1	Chl+TiO_2	41.29	4.00	19.80	23.53		8.29	2.42		0.67												100	120
H-23 5213.5m	10	2	Ms+Chl	45.61	1.02	29.10	2.77		0.68	10.37	0.77	9.67												100	127
H-23 5213.5m	10	3	Ms+Chl	37.14	0.90	26.38	3.49		0.83	20.71	0.55	7.25			2.76									100	121
H-23 5213.5m	10	4	F-Cal						0.34	48.28					7.38									56	80
H-23 5213.5m	10	5	F-Fe-Cal				1.70	0.22	0.58	45.03					8.46									56	79
H-23 5213.5m	10	6	F-Cal +Chl	5.48		3.85	8.98	0.48	2.97	66.80		0.24			11.21									100	80
H-23 5213.5m	10	7	F-Cal				0.20		1.74	43.93				1.50	8.64									56	81
H-23 5213.5m	10	8	Ab+Chl	52.58	0.28	21.79	14.38		2.27	0.52	7.52	0.45				0.20								100	120
H-23 5213.5m	10	9	F-Cal+Chl	17.33		9.81	23.76	0.48	8.79	33.76					6.08									100	82
H-23 5213.5m	10	10	Qz	99.30		0.49						0.20												100	139
H-23 5213.5m	10	11	Qz+Fe-Cal	61.44		0.91	1.80	0.23		35.64														100	117
H-23 5213.5m	10	12	Py	0.15			27.47			1.11				71.29										100	226
H-23 5213.5m	10	13	Py	0.26			27.76			0.22				71.77										100	231
H-23 5213.5m	10	14	Chl+Ms	52.41		30.29	11.68		2.16			3.48												100	103
H-23 5213.5m	10	15	Ab+Other	66.29		19.24	0.71			0.46	11.39	0.24		1.67										100	141
H-23 5213.5m	10	16	Ab+Chl+Ms+TiO_2	54.72	2.42	21.20	13.39		2.57	0.38	3.98	1.35												100	122
H-23 5213.5m	10	17	F-Cal						1.20	44.03	0.40			0.74	9.64									56	84
H-23 5213.5m	10	18	F-Fe-Cal				1.77	0.26	0.55	45.76					7.66									56	76
H-23 5213.5m	11	1	F-Cal						0.58	48.21					7.21									56	63
H-23 5213.5m	11	2	Fe-Cal				2.03	0.29	0.66	53.02														56	52
H-23 5213.5m	11	3	Chl	23.62		19.90	33.78	0.21	6.20	1.28														85	92
H-23 5213.5m	11	4	Ab	60.73		20.63	7.37		1.29	0.20	9.80													100	119
H-23 5213.5m	11	5	Ab	63.75		19.71	4.71		0.71		11.14													100	125
H-23 5213.5m	11	6	F-Cal				0.29		0.68	45.37					9.67									56	68
H-23 5213.5m	11	7	F-Cal +Chl	12.07		9.33	12.32	0.26	2.97	51.85					11.20									100	78
H-23 5213.5m	11	8	Chl+Py	55.43		8.13	8.81		0.95	4.27	3.61			18.80										100	122
H-23 5213.5m	11	9	Py+Other	2.14		0.76	26.95			1.69	0.50			67.97										100	166
H-23 5213.5m	11	10	F-Cal				1.43		0.40	46.35					7.82									56	58
H-23 5213.5m	11	11	Qz	99.86			0.14																	100	120
H-23 5213.5m	11	12	Ms	49.60	0.17	33.27	2.15		0.94		1.15	7.73												95	113
H-23 5213.5m	11	13	Chl+Ms	57.63	0.55	22.54	12.21		3.53	1.05		2.32				0.17								100	93
H-23 5213.5m	11	14	Py+Chl+Cal	15.44	0.35	8.56	17.46		1.06	15.57	1.12	1.07		39.38										100	109
H-23 5213.5m	11	15	Py+Ab+Cal	13.58		9.26	24.87		1.76	1.93	1.11	0.57		46.97										100	125

Table 2-5A: Scaning Electron Microscope chemical analyses of sample 5213.5m from Newburn H-23 well.

Sample	Site	Position	Mineral	SiO_2	TiO_2	Al_2O_3	FeO	MnO	MgO	CaO	Na_2O	K_2O	P_2O_5	SO_3	F	Cl	Cr_2O_3	ZnO	SrO	ZrO_2	BaO	Ce_2O_3	HfO_2	Total	Actual Total
H-23 5213.5m	11	16	Chl+Ms	46.91	0.63	24.28	15.62		3.52	6.11	0.65	2.11				0.18								100	93
H-23 5213.5m	11	17	Chl+Ank	33.48		24.90	26.17		5.79	8.58	0.58	0.31				0.19								100	95
H-23 5213.5m	11	18	Chl	30.78	0.20	24.12	23.77		5.01	0.29	0.59	0.24												85	96
H-23 5213.5m	11	19	Qz	99.79			0.21																	100	121
H-23 5213.5m	11	20	Qz	99.54			0.46																	100	121
H-23 5213.5m	11	21	Ms+Chl	53.50	0.68	23.43	12.92		2.72	3.22	0.69	2.69				0.18								100	93
H-23 5213.5m	11	22	Ab	66.94		18.82	0.41			0.99	12.43		0.41											100	119
H-23 5213.5m	12	1	Qz	99.99																				100	131
H-23 5213.5m	12	2	Sd+Chl	6.03		1.25	72.31	2.03	16.66	1.71														100	61
H-23 5213.5m	12	3	TiO_2+Chl	18.33	47.19	13.70	16.26		3.32	0.59	0.61													100	99
H-23 5213.5m	12	4	F-Fe-Cal				2.23	0.27	0.80	49.61					3.09									56	57
H-23 5213.5m	12	5	Ab+Ms+Chl	58.98		21.26	9.31		2.42	0.71	4.35	2.17	0.80											100	120
H-23 5213.5m	12	6	Qz+Chl	87.07		5.99	4.70		0.90	0.34	0.59	0.43												100	120
H-23 5213.5m	12	7	Ab	69.87		16.93	1.81			0.18	11.22													100	130
H-23 5213.5m	12	8	Qz+Ab+Cal	86.62		2.21	1.12			8.75	1.29													100	110
H-23 5213.5m	12	9	Qz	99.99																				100	126
H-23 5213.5m	12	10	Cal+Py				6.83	0.45	0.80	77.66				14.26										100	59
H-23 5213.5m	12	11	Fe-Cal				1.99	0.30	0.69	53.02														56	50
H-23 5213.5m	12	12	Ms+F-Cal+Chl	50.49	2.12	24.81	3.69		2.02	7.50	1.11	5.08		0.72	2.29	0.15								100	100
H-23 5213.5m	12	13	TiO_2+Chl	1.63	97.08	1.02	0.28																	100	98
H-23 5213.5m	12	14	Ab	67.88		19.22	0.19			0.34	12.26	0.12												100	130
H-23 5213.5m	12	15	Qz	99.88			0.12																	100	128
H-23 5213.5m	12	16	Qz	99.99																				100	128
H-23 5213.5m	12	17	Qz+Other	94.87	3.67	0.43	1.02																	100	108
H-23 5213.5m	12	18	Qz+TiO_2+Chl	74.08	18.02	2.31	2.32		0.40	2.90														100	116
H-23 5213.5m	12	19	F-Cal+Qz	24.32		0.60	3.91	0.40	1.23	65.57					3.97									100	72
H-23 5213.5m	12	20	Ab	67.58		19.27	0.71			0.28	12.16													100	137
H-23 5213.5m	12	21	Ab	66.74		18.91	0.54			0.90	12.07		0.85											100	139
H-23 5213.5m	12	22	Ab	62.27		18.48	2.64			2.42	11.66		2.54											100	135
H-23 5213.5m	12	23	Ms+Chl	74.57	0.23	14.68	4.97		1.97	0.31		3.25												100	119
H-23 5213.5m	12	24	TiO_2+Other	1.31	96.02		0.49			2.18														100	102
H-23 5213.5m	12	25	Ank				15.07	0.65	11.50	28.78														56	57
H-23 5213.5m	12	26	F-Cal+Qz	5.18			0.33		4.23	79.17	0.84			2.90	7.35									100	62
H-23 5213.5m	13	1	F-Cal						0.49	51.97				0.53	3.00									56	58
H-23 5213.5m	13	2	Brt											40.40					5.09		54.53			100	111
H-23 5213.5m	13	3	Py+Ab+Ms	6.46		4.31	25.22		0.81	0.70	0.84	0.25		61.40										100	177
H-23 5213.5m	13	4	Qz	99.71			0.14					0.14												100	121
H-23 5213.5m	13	5	F-Cal+Chl	5.56		4.86	7.42	0.35	3.10	68.71				0.90	9.12									100	64
H-23 5213.5m	13	6	Cal+Chl	6.40		5.48	4.08	0.34	3.32	80.16		0.23												100	59
H-23 5213.5m	13	7	TiO_2+Ab+Ank	25.73	49.51	10.05	5.29		1.38	5.27	2.26	0.49												100	98
H-23 5213.5m	13	8	Py+Ms+Cal	23.94	0.40	13.21	15.70		1.69	1.71	0.65	1.46	0.57	40.68										100	160
H-23 5213.5m	13	9	Py+Ab	3.49		1.81	23.85		0.35	0.38	1.67	0.20		68.24										100	197

Table 2-5A: Scaning Electron Microscope chemical analyses of sample 5213.5m from Newburn H-23 well.

Sample	Site	Position	Mineral	SiO_2	TiO_2	Al_2O_3	FeO	MnO	MgO	CaO	Na_2O	K_2O	P_2O_5	SO_3	F	Cl	Cr_2O_3	ZnO	SrO	ZrO_2	BaO	Ce_2O_3	HfO_2	Total	Actual Total
H-23 5213.5m	13	10	Qz	99.99																				100	120
H-23 5213.5m	13	11	Py+Chl	17.43		14.02	22.49		2.60	0.73	0.61	0.29		41.85										100	141
H-23 5213.5m	13	12	Qz+Chl	80.24		8.07	8.83		1.28	1.11		0.47												100	118
H-23 5213.5m	13	13	F-Cal+Ms	6.95		3.89	1.53		0.65	81.99		0.43			4.57									100	62
H-23 5213.5m	13	14	Qz+Chl	57.16		17.84	19.80		4.15	0.73		0.33												100	112
H-23 5213.5m	13	15	Chl+Cal	40.71		26.79	23.56		5.80	2.22		0.90												100	97
H-23 5213.5m	13	16	F-Cal+Chl	7.59		5.25	1.93		2.82	77.36		0.29		0.85	3.89									100	62
H-23 5213.5m	13	17	F-Cal+Chl	12.07		9.32	8.37	0.26	2.64	60.03		0.24			7.09									100	69
H-23 5213.5m	13	18	Ms+Py+Cal	50.10	0.55	25.24	8.77		3.61	4.59		4.48		2.65										100	92
H-23 5213.5m	13	19	Cal+Chl	17.95		12.21	13.87		3.95	51.07		0.28		0.70										100	68
H-23 5213.5m	13	20	Qz+Ms	85.65	0.22	8.69	1.67		0.68	0.99	0.46	1.63												100	116
H-23 5213.5m	13	21	Ms+Cal	54.34	1.02	21.28	3.55		1.79	12.35	1.08	3.66		0.77		0.16								100	92
H-23 5213.5m	13	22	Qz	98.12		1.15	0.49					0.23												100	119
H-23 5213.5m	13	23	Qz	99.99																				100	127
H-23 5213.5m	13	24	Mix	48.77	0.22	8.33	9.56		0.85	0.38	1.07	0.99		29.84										100	144
H-23 5213.5m	13	25	Qz+Chl+Cal	80.46		8.82	5.65		1.71	1.54	0.31	0.60		0.92										100	110
H-23 5213.5m	13	26	F-Cal+Chl	8.11		6.31	4.27		3.83	65.75		0.39		1.05	10.28									100	69
H-23 5213.5m	13	27	F-Cal+Chl	4.39		1.91	1.94		4.00	81.78		0.23		1.57	4.20									100	57
H-23 5213.5m	13	28	F-Cal+Chl	3.36		1.55	2.35	0.40	0.71	86.97		0.30			4.35									100	55
H-23 5213.5m	13	29	Ab+Qz+Cal+Ms	51.13	0.80	7.69	3.62	0.19	1.01	31.33	2.63	1.01		0.60										100	89
H-23 5213.5m	13	30	F-Cal+Qz	11.51	0.63	7.22	7.54		2.65	60.92		0.46		1.22	7.86									100	64
H-23 5213.5m	13	31	F-Cal+Chl	11.08		7.52	7.65	0.32	4.06	65.10		0.40			3.85									100	64
H-23 5213.5m	13	32	Qz	99.99																				100	120
H-23 5213.5m	13	33	Qz+Other	95.41	1.03	2.38	0.42					0.73												100	120

Table 2-5B: Scaning Electron Microscope chemical analyses of sample 5213.5m from Newburn H-23 well (re-annalysis of fluorine-calcite).

Sample	Site	Position	Mineral	SiO_2	Al_2O_3	FeO	MnO	MgO	CaO	Na_2O	K_2O	SO_3	F	Total	Actual Total
H-23 5213.5m	4	1	Ab	68.60	18.61				0.18	12.61				100	147
H-23 5213.5m	3	4	Ab	68.43	18.50	0.23			0.35	12.47				100	147
H-23 5213.5m	3	3	Ank	56.00										56	69
H-23 5213.5m	2	8	Ank+Chl	1.54	1.28	51.88	1.14	10.05	34.11					100	68
H-23 5213.5m	2	12	Chl+F-Cal	6.48	4.50	5.61		1.66	73.39		0.26		8.10	100	70
H-23 5213.5m	1	6	Chl+Ms	48.30	29.31	14.38		3.35		0.43	4.20			100	97
H-23 5213.5m	5	1	F-Cal			0.60		0.66	48.89			0.57	5.28	56	73
H-23 5213.5m	2	2	F-Cal			1.45		0.41	50.66				3.48	56	71
H-23 5213.5m	4	3	F-Cal	56.00										56	75
H-23 5213.5m	1	5	F-Cal					0.99	48.33				6.68	56	57
H-23 5213.5m	2	5	F-Cal			1.56	0.27	0.45	49.64				4.08	56	71
H-23 5213.5m	4	5	F-Cal	0.58	0.34	1.86	0.26	0.53	48.50				3.93	56	76
H-23 5213.5m	2	7	F-Cal		0.30	0.59		0.83	47.44			0.60	6.24	56	69
H-23 5213.5m	4	9	F-Cal			1.52	0.22	0.62	47.47				6.17	56	79
H-23 5213.5m	5	9	F-Cal			0.55		0.94	48.01			0.87	5.63	56	74
H-23 5213.5m	2	10	F-Cal	0.86	0.72	29.05	0.64	5.63	19.10					56	70
H-23 5213.5m	5	2	F-Cal+Chl	1.16	1.04	3.56		1.01	82.43				10.80	100	73
H-23 5213.5m	5	3	F-Cal+Chl	2.03	1.44	4.40		1.23	81.74				9.17	100	71
H-23 5213.5m	2	11	F-Cal+Chl	7.25	5.37	8.66		1.92	66.97				9.83	100	75
H-23 5213.5m	4	2	F-Cal+Qz	23.12		2.53		0.73	62.52				11.11	100	84
H-23 5213.5m	3	2	F-Fe-Cal	56.00										56	67
H-23 5213.5m	2	3	F-Fe-Cal			1.83	0.33	0.55	49.73				3.56	56	67
H-23 5213.5m	1	4	F-Fe-Cal			12.74	0.68	11.51	31.07					56	56

Table 2-5B: Scaning Electron Microscope chemical analyses of sample 5213.5m from Newburn H-23 well (re-annalysis of fluorine-calcite).

H-23 5213.5m	2	4	F-Fe-Cal	38.33	10.36	0.13			0.20	6.98				56	67
H-23 5213.5m	4	4	F-Fe-Cal			2.08	0.42	0.62	50.01				2.86	56	79
H-23 5213.5m	5	4	F-Fe-Cal			1.81	0.38	0.65	47.10				6.06	56	69
H-23 5213.5m	3	5	F-Fe-Cal	38.42	10.42				0.10	7.06				56	67
H-23 5213.5m	5	5	F-Fe-Cal	12.95		1.42		0.41	35.01				6.22	56	74
H-23 5213.5m	2	6	F-Fe-Cal					1.33	46.27	0.38		0.64	7.38	56	68
H-23 5213.5m	3	6	F-Fe-Cal	0.52	0.40	1.61	0.21	0.82	42.76				9.69	56	73
H-23 5213.5m	1	7	F-Fe-Cal			0.32		3.06	45.08			1.18	6.37	56	60
H-23 5213.5m	4	7	F-Fe-Cal			15.08			1.36			39.56		56	77
H-23 5213.5m	1	8	F-Fe-Cal	0.96	0.52	2.04	0.25	0.60	43.90				7.74	56	55
H-23 5213.5m	5	8	F-Fe-Cal			1.94	0.30	0.65	47.14				5.97	56	71
H-23 5213.5m	2	9	F-Fe-Cal	1.92	1.08	0.55		1.50	43.74			0.48	6.74	56	69
H-23 5213.5m	4	10	F-Fe-Cal			1.77	0.34	0.61	47.07				6.21	56	71
H-23 5213.5m	4	8	F-Cal+Ab+Ms	57.31	29.57	0.63			0.84	5.35	6.31			100	72
H-23 5213.5m	1	2	Ilt					0.77	78.23			0.56	10.45	90	105
H-23 5213.5m	4	11	Ilt	1.04	0.94	3.20		0.91	74.19				9.72	90	139
H-23 5213.5m	5	7	Ms	1.93	1.37	4.18		1.17	77.65				8.71	95	134
H-23 5213.5m	4	6	Py			26.93			2.43			70.64		100	241
H-23 5213.5m	1	1	Qz	99.99										100	126
H-23 5213.5m	2	1	Qz	99.99										100	143
H-23 5213.5m	3	1	Qz	99.99										100	143
H-23 5213.5m	1	3	Qz	99.99										100	120
H-23 5213.5m	5	6	Qz	99.75					0.24					100	142

Appendix 2-6: SEM-BSE images and EDS mineral analyses for sample Newburn H-23 5403.6m

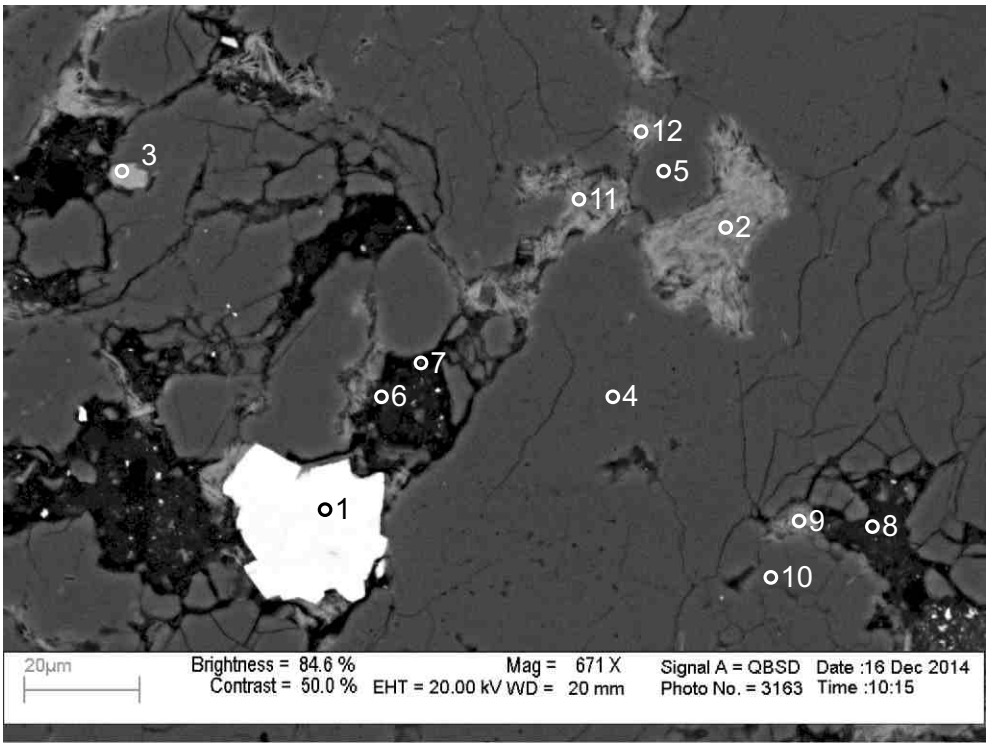

1: Pyrite
2: Chlorite
3:Fluorapatite +Other
4: Quartz
5: Quartz
6: DrillingMud +Other
7: DrillingMud +Other
8: DrillingMud +Other
9: Chlorite
10: Quartz
11: Chlorite
12: Chlorite+ Albite

Figure 2-6.1: Sample Newburn 5403.6m site 1 (SEM). Table 2-6A. Intergranular voids between quartz grains (4,5,10) filled with chlorite (2,9,11,12) as well as drilling mud (6-8). Diagenetic fluorapatite (3) engulfs quartz on edge of cavity. Euhedral pyrite (1) partially fills secondary porosity.

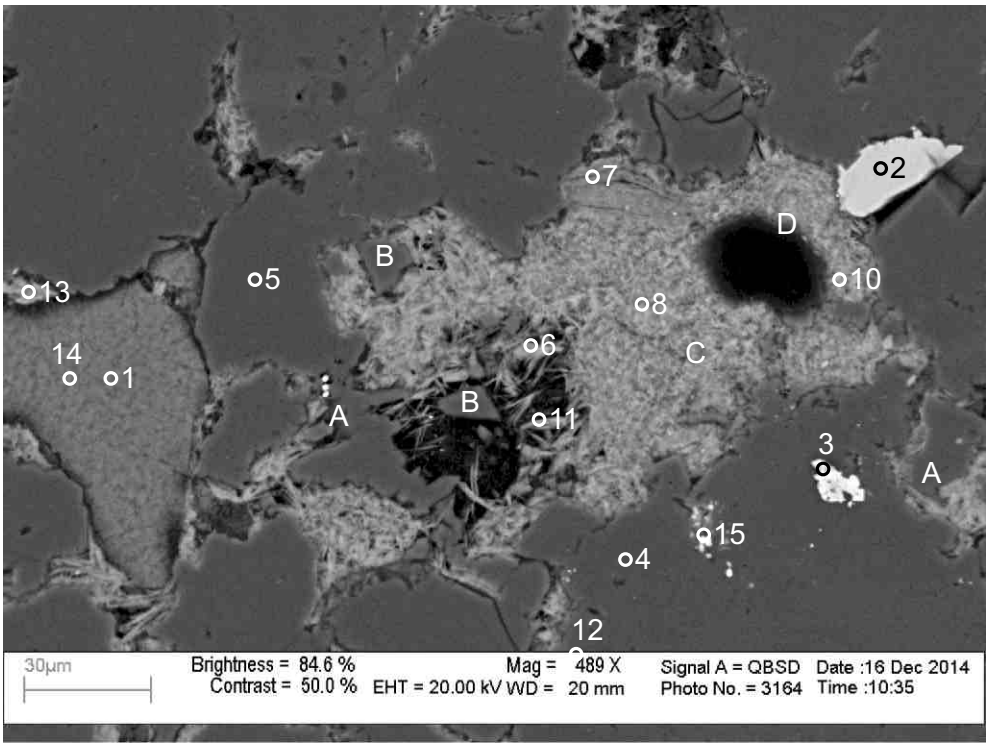

1: K-Feldspar
2: Titania
3: Pyrite +Other
4: Quartz
5: Quartz
6: Chlorite
7: Chlorite
8: Chlorite
9: Chlorite
10: Chlorite
11: Chlorite
12: Zircon +Albite
13: Chlorite
14: K-Feldspar +Chlorite
15: Zircon+ Other

Figure 2-6.2: Sample Newburn 5403.6m site 2 (SEM). Table 2-6A. Chlorite rims around quartz grains (position A). Detrital quartz (4) with zircon (15) inclusion. K-feldspar (1,14) with dissolution voids is partially filled by chlorite (14). Two small quartz grains (position B) are surrounded by fibrous chlorite (6,11). Remainder of large pore (position C) is filled with densely packed chlorite (7,8,10). Approximately 20 µm void (position D) may be residual or the result of later dissolution.

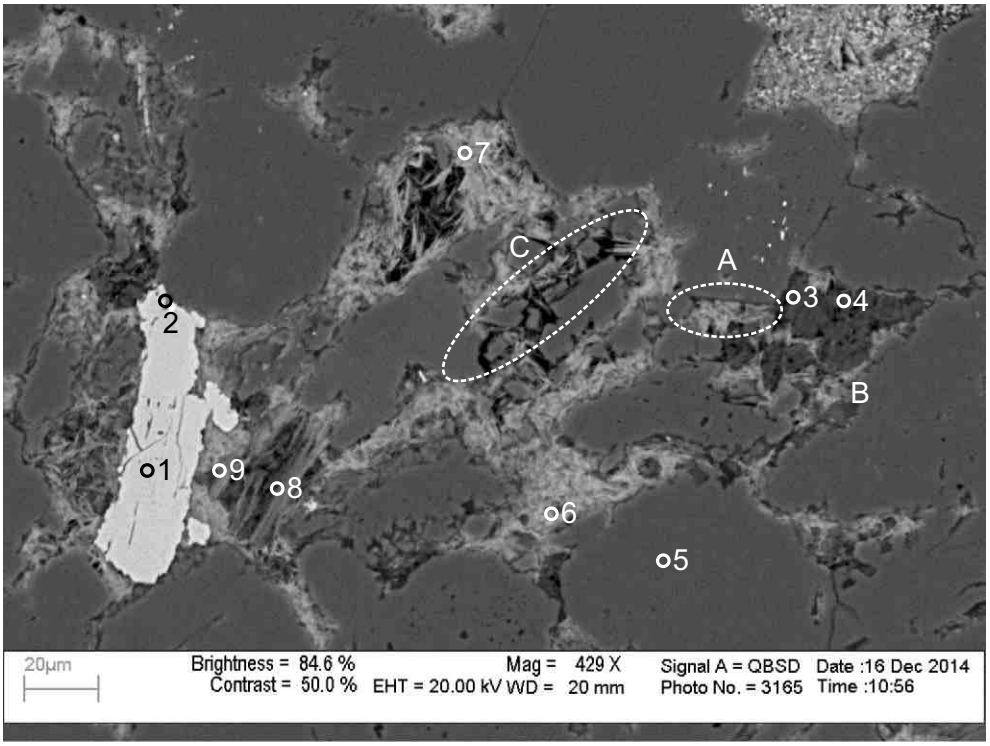

1: Titania
2: Mix
3: Kaolinite
4: Kaolinite
5: Quartz
6: Chlorite
7: Chlorite
8: Muscovite +Other
9: Muscovite

Figure 2-6.3: Sample Newburn 5403.6m site 3 (SEM).Table 2-6A. Kaolinite (3,4) fills porosity and is rimmed by chlorite (6, position B). Diagenetic titania (1). Quartz overgrowth (position A) predates chlorite. Fractured quartz with fibrous chlorite partially filling voids (position C).

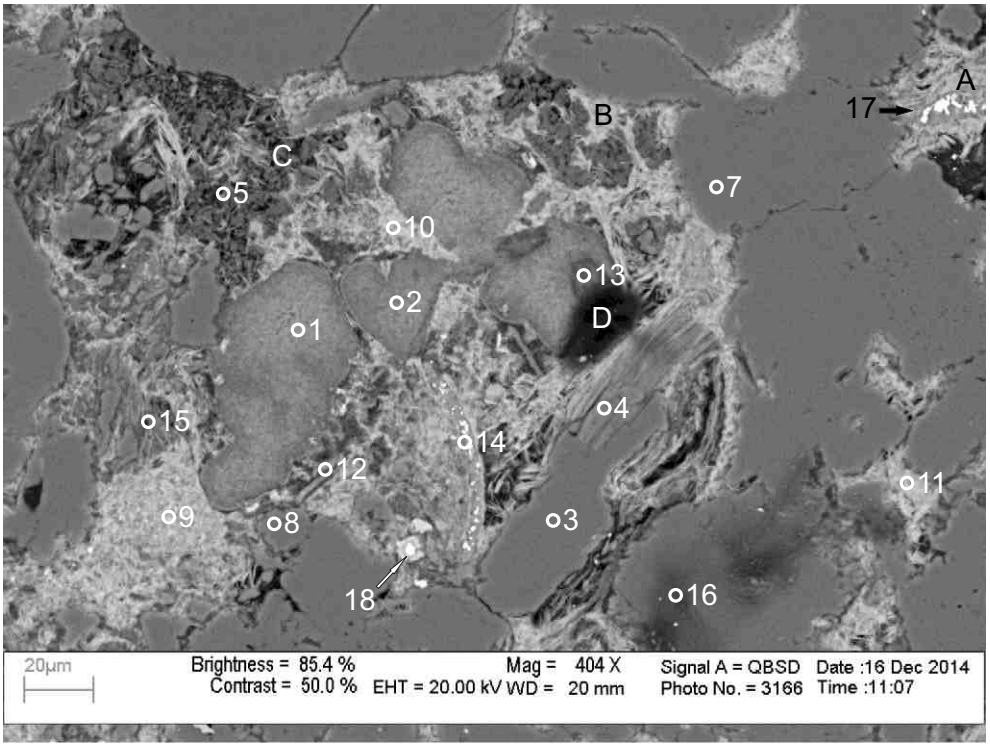

1: K-Feldspar+ Chlorite
2: K-Feldspar+ Chlorite
3: Quartz
6
4: Muscovite+ Albite
5: Chlorite
6: Albite
7: Quartz
8: Quartz
9: Chlorite
10: Chlorite
11: Chlorite
12: Muscovite
13: Muscovite
14: Pyrite+ F-Calcite+ Chlorite
15: Mix
16: Quartz
17: Pyrite+ F-Calcite
18: Siderite+ Pyrite+ Albite

Figure 2-6.4: Sample Newburn 5403.6m site 4 (SEM).Table 2-6A. Pyrite and calcite (17) fill a fracture in chlorite (position A). Chlorite (1,2) engulfs K-feldspar. Siderite rims pyrite (18). K-feldspar (1,2) with dissolution voids filled by chlorite. Kaolinite (5) fills pore in contact with quartz. Chlorite rims the kaolinite (position B) and crosscuts it (position C). Chlorite also fills voids between intergranular boundaries in quartz. Dissolution of K-feldspars generates secondary porosity filled by chlorite. Voids (position D) may be residual or the result of later dissolution.

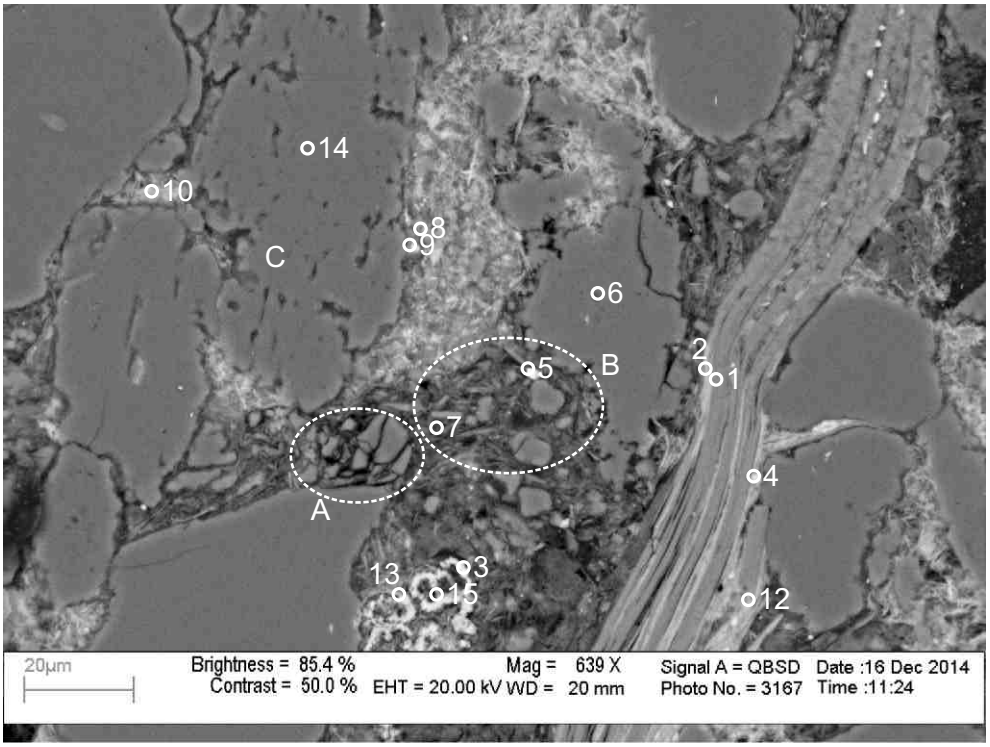

1: Muscovite
2: Muscovite
3: Siderite+ Muscovite
4: Chlorite+ Siderite+ Muscovite
5: Mix
6: Albite
7: Muscovite+ Other
8: Chlorite+ Fluorapatite
11
9: Fluorapatite +Albite+ Chlorite
10: Chlorite+ Other
11: Chlorite+ Albite
12: Chlorite
13: Siderite+ Chlorite
14: Quartz
15: Siderite+ Chlorite

Figure 2-6.5: Sample Newburn 5403.6m site 5 (SEM).Table 2-6A. Chlorite and siderite (4) form along the cleavage planes of plastically deformed muscovite (1,2). Mechanically fractured quartz (position A). Muddy matrix (position B) composed of muscovite, chlorite and quartz (5,7) with late siderite rims (3,13,15) surrounding part of this matrix. In places (position C) detrital quartz has a moderate amount of secondary porosity.

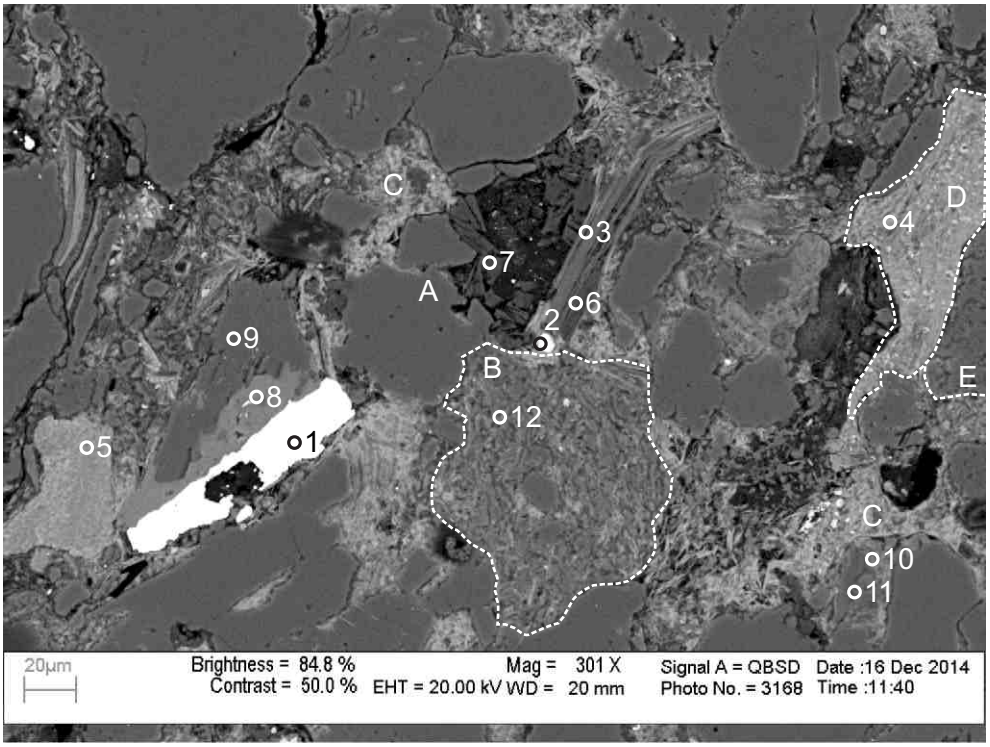

1: Barite
2: Pyrite
3: Muscovite
4: Chlorite
5: Chlorite
6: Kaolinite
7: Kaolinite
8: Albite+ Calcite
9: Albite
10: Illite
11: Albite+Illite
12: Chlorite+ K-Feldspar

Figure 2-6.6: Sample Newburn 5403.6m site 6 (SEM).Table 2-6A. Illite (10,11) engulfs albite (11). Albite (8,9) is engulfed by calcite (8), which appears to be engulfed by barite (1). Kaolinite (7) partly fills secondary porosity probably produced as a result of dissolution of quartz (position A). Lithic clast (position B) consists of chlorite and K-feldspar (12). Detrital muscovite (3) and lithic clast composed of chlorite (4) and siderite (position D) are plastically deformed. Trachytic lithic clast (position E) and chlorite rims (position C) are also present.

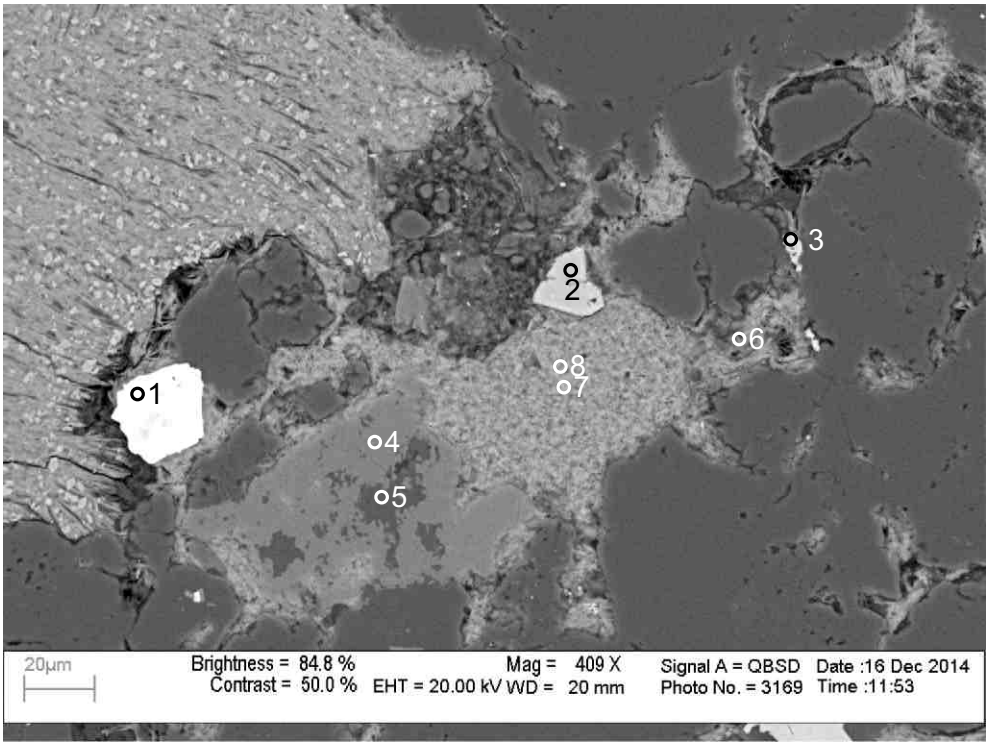

1: Pyrite+Other
2: Titania
3: Titania+ Other
4: Ankerite
5: Albite
6: Chlorite+ Other
7: Chlorite
8: Chlorite

Figure 2-6.7: Sample Newburn 5403.6m site 7 (SEM).Table 2-6A. Ankerite (4) is engulfing albite (5) and chlorite (7,8). Diagenetic titania (2) with euhedral crystal outline in contact with chlorite (7,8).

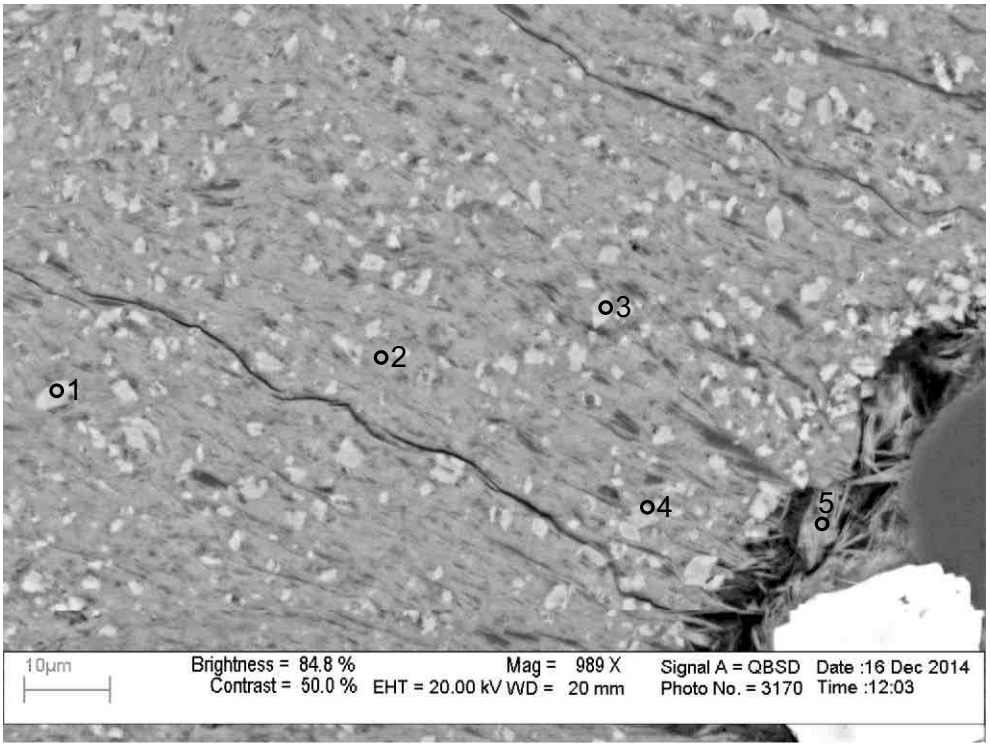

1: Siderite+ Chlorite
2: Chlorite
3: Siderite+ Chlorite
4: Siderite+ Other
5: Chlorite

Figure 2-6.8: Sample Newburn 5403.6m site 8 (SEM).Table 2-6A. Siderite (1,3,4) intermixed with chlorite (1,2,3,5) in a lithic clast or an intraclast.

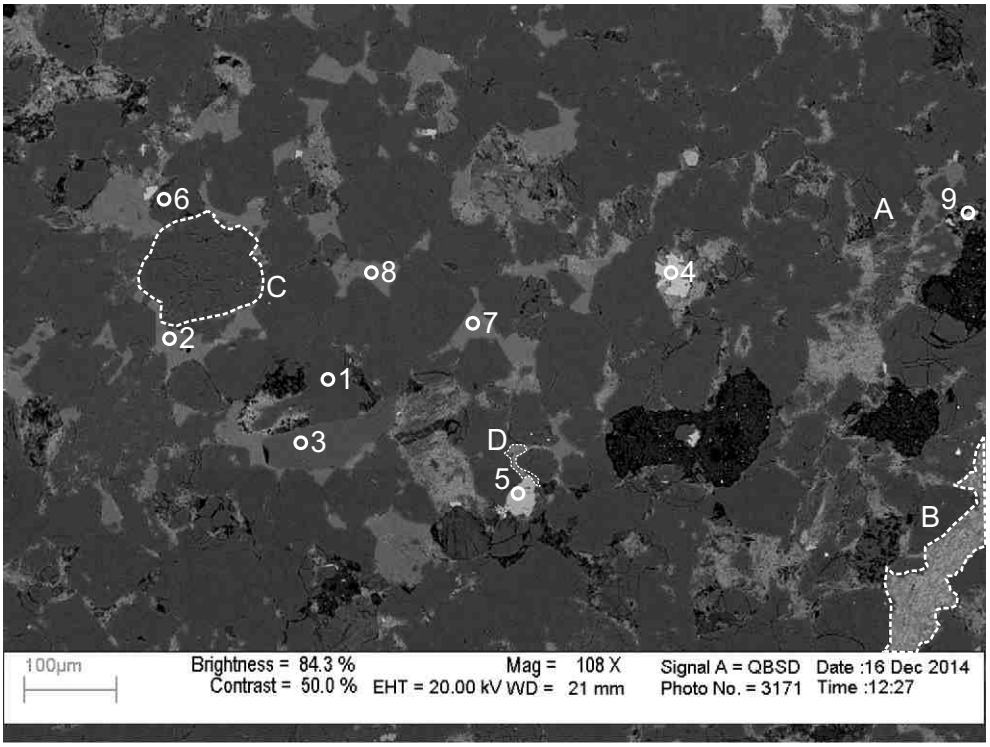

Figure 2-6.9: Sample Newburn 5403.6m site 9 (SEM).Table 2-6A. Kaolinite fills pore space against quartz without overgrowth (position A). F-calcite engulfs the kaolinite and fills secondary porosity (position A). Dissolution of detrital quartz (6) along intergranular boundaries. Trachytic lithic clast (postion C). Plastically deformed lithic clast composed of chlorite and siderite (position B). Titania (5) probably engulfs F-calcite (position D).

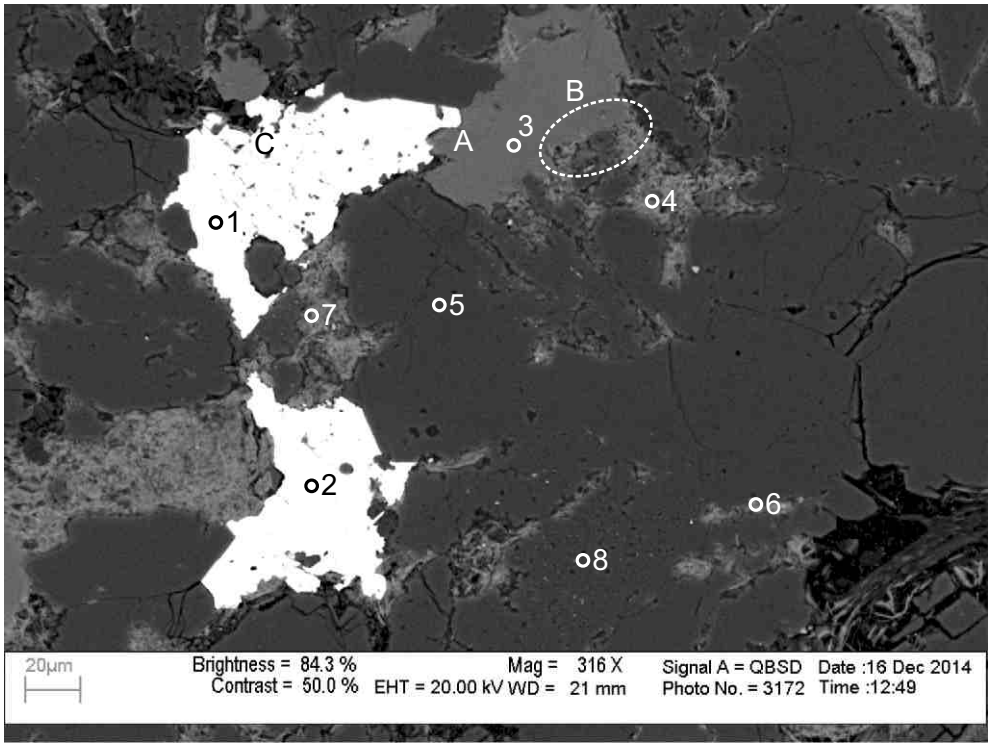

Figure 2-6.10: Sample Newburn 5403.6m site 10 (SEM).Table 2-6A. Diagenetic barite (1,2) engulfs quartz and F-calcite (3). F-calcite (3) is engulfing chlorite (4). F-calcite engulfs chlorite (position B). Barite engulfs F-calcite (position A) and chlorite (position C).

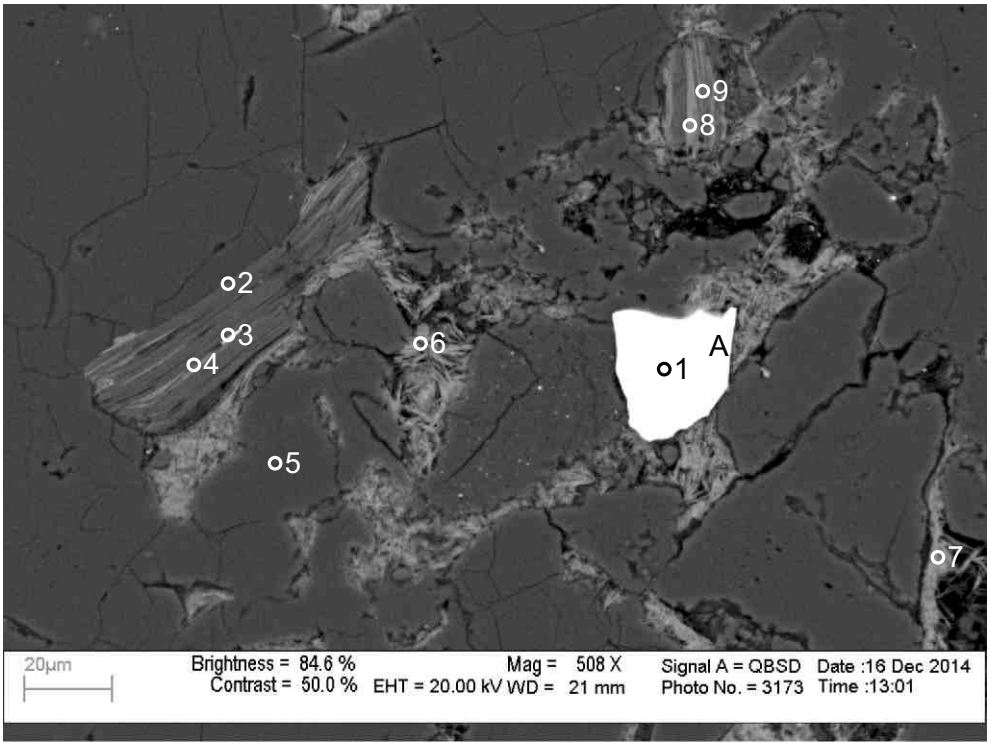

1: Zircon
2: Quartz+ Muscovite
3: Muscovite+ Sphalerite
4: Muscovite+ Chlorite
5: Quartz
6: Chlorite
7: Chlorite
8: Chlorite+ Muscovite
9: Chlorite+ Muscovite

Figure 2-6.11: Sample Newburn 5403.6m site 11 (SEM).Table 2-6A. Zircon (1) with straight crystal outlines towards chlorite (position A). Detrital muscovite (2-4) with diagenetic sphalerite (3) along its cleavage planes. Chlorite occupies secondary porosity between corroded quartz grains.

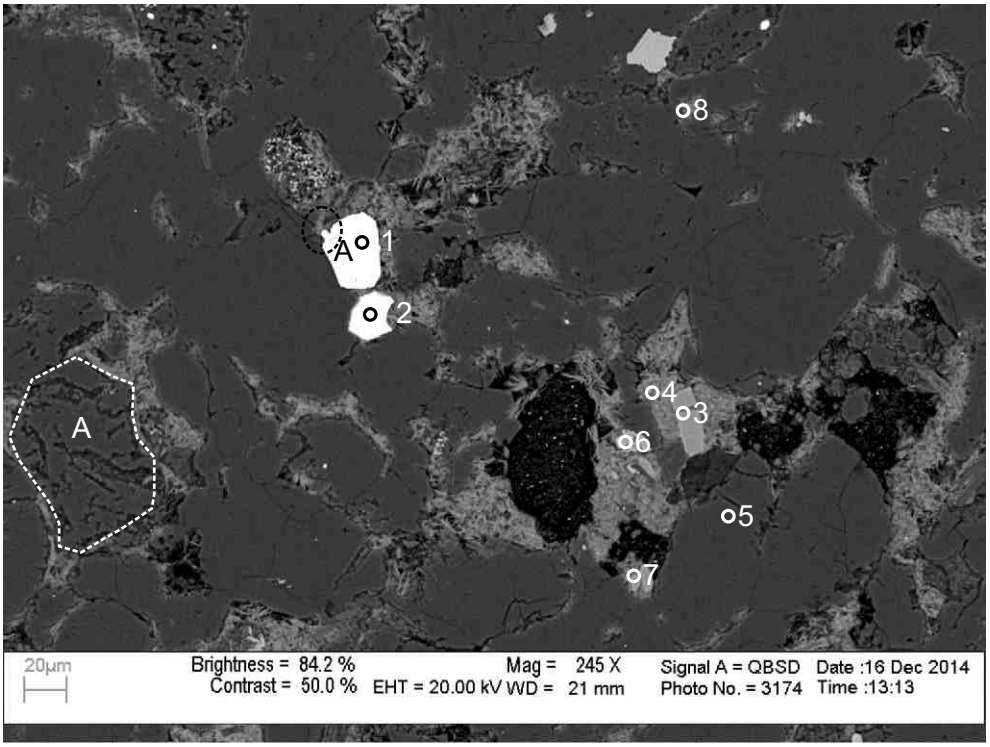

1: Zircon
2: Zircon
3: Fluorapatite
4: Chlorite+ Albite
5: Quartz
6: Titanai+ Other
7: Fluorapatite
8: Chlorite

Figure 2-6.12: Sample Newburn 5403.6m site 12 (SEM).Table 2-6A. Zircon (1,2) cuts quartz and probably engulfs chlorite (position A) and with euhedral crystal outlines towards both (1,2). Fluorapatite (3) cuts chlorite (4). Trachytic lithic clast (position A).

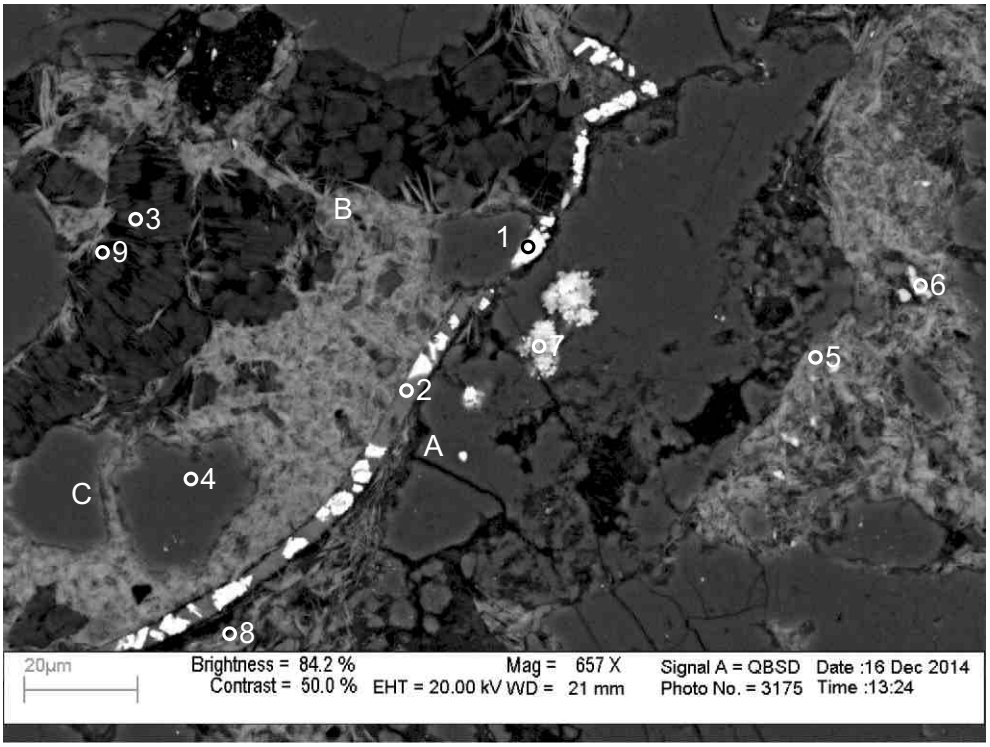

Figure 2-6.13: Sample Newburn 5403.6m site 13 (SEM).Table 2-6A. Vein filled with pyrite (1) and F-calcite (2) cutting through chlorite (position A). Chlorite cross-cuts porous kaolinite (3,9) (position B) and rims quartz (position C) grains (4).

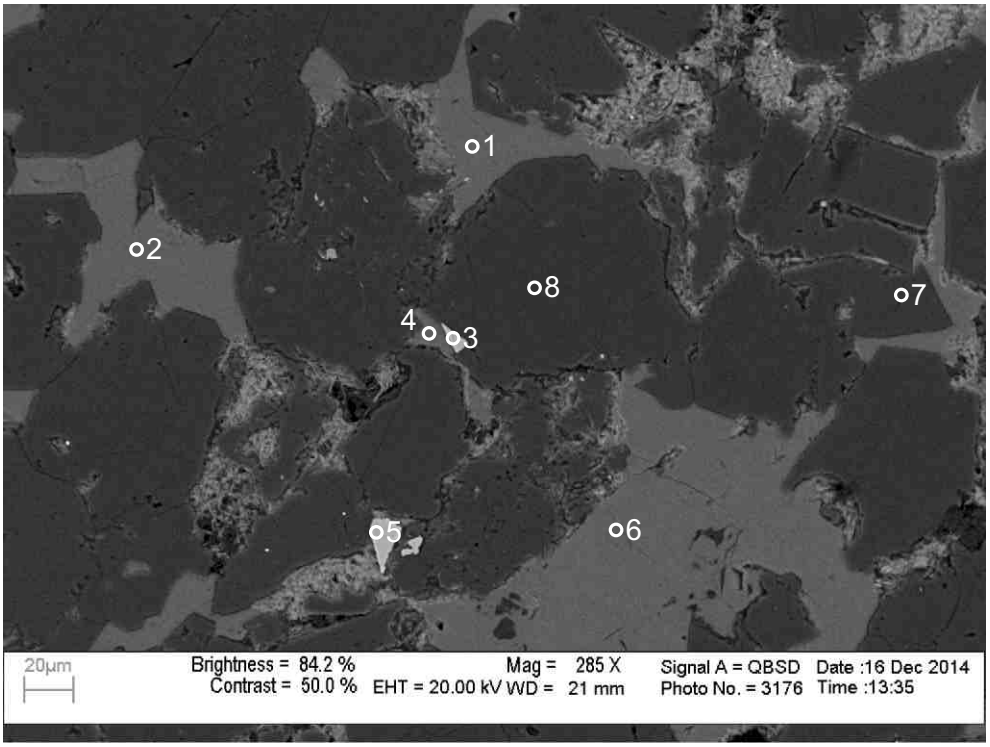

Figure 2-6.14: Sample Newburn 5403.6m site 14 (SEM).Table 2-6A. F-Fe-calcite (1,2,6) and F-calcite (4) bounded by quartz overgrowths. Titania (3) and F-calcite rim quartz (8).

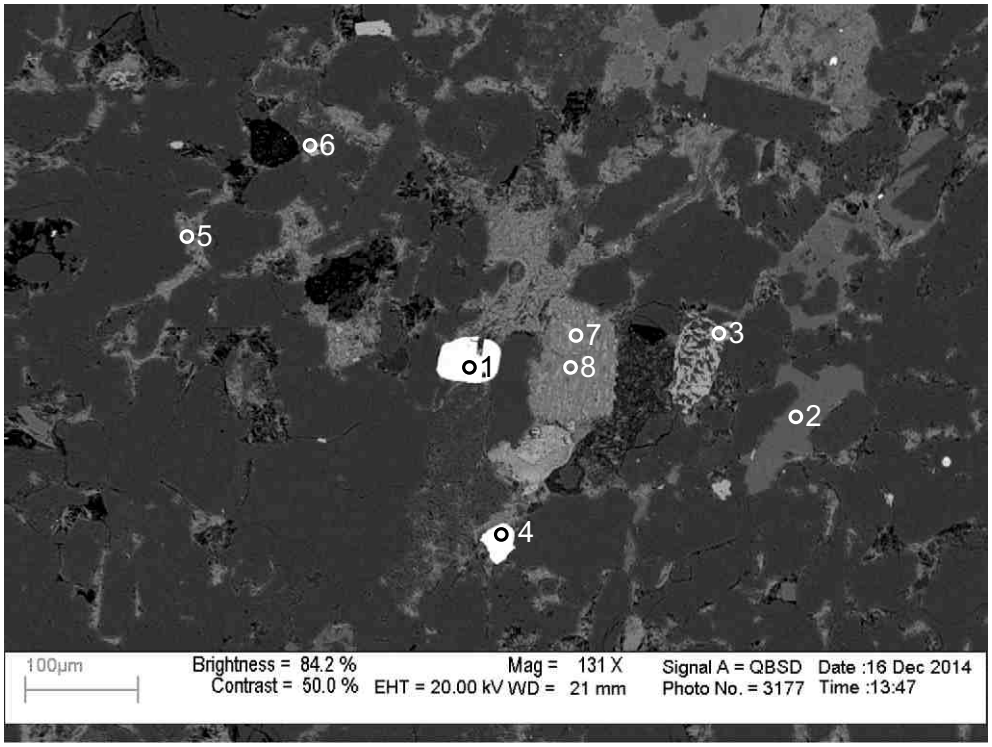

1: Zircon
2: F-Fe-Calcite
3: Titania+ K-Feldspar
4: Zircon
5: Chlorite
6: Titania+ Chlorite
7: Chlorite
8: Chlorite

Figure 2-6.15: Sample Newburn 5403.6m site 15 (SEM).Table 2-6A. Titania (3) engulfs K-feldspar (3). Diagenetic zircon (1) cuts quartz.

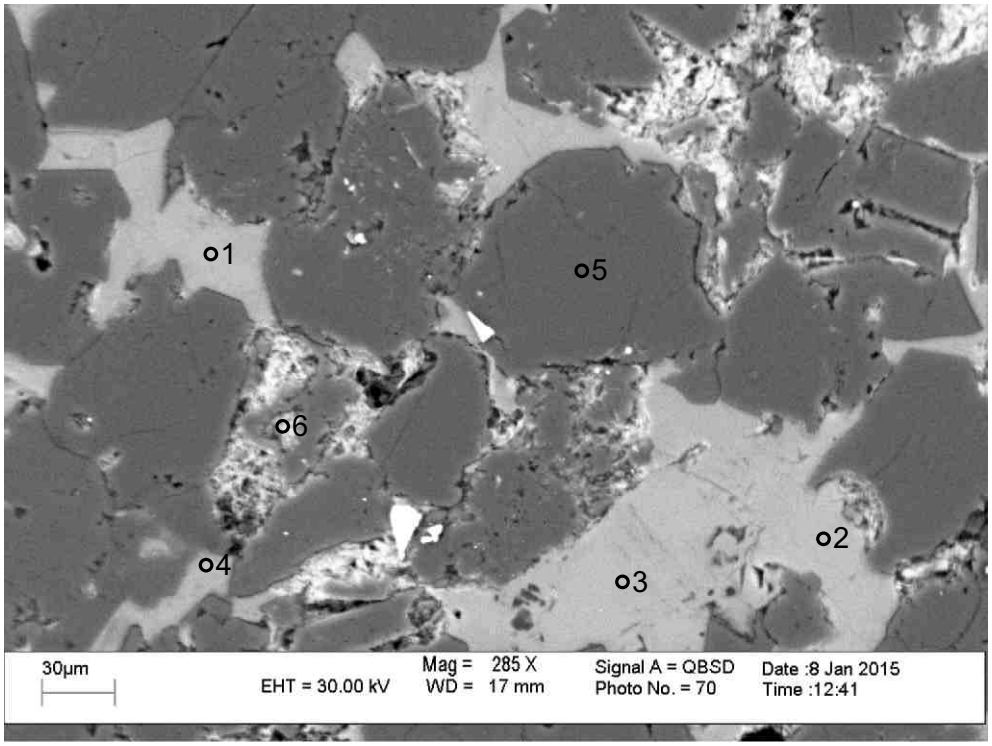

1. F-Calcite
2. F-Calcite
3. F-Calcite
4. F-Calcite
5. Quartz
6. Chlorite

Figure 2-6.16: Sample Newburn 5403.6m site 1 (SEM).Table 2-6B. Re-annalysis of Figure 2-6.14.

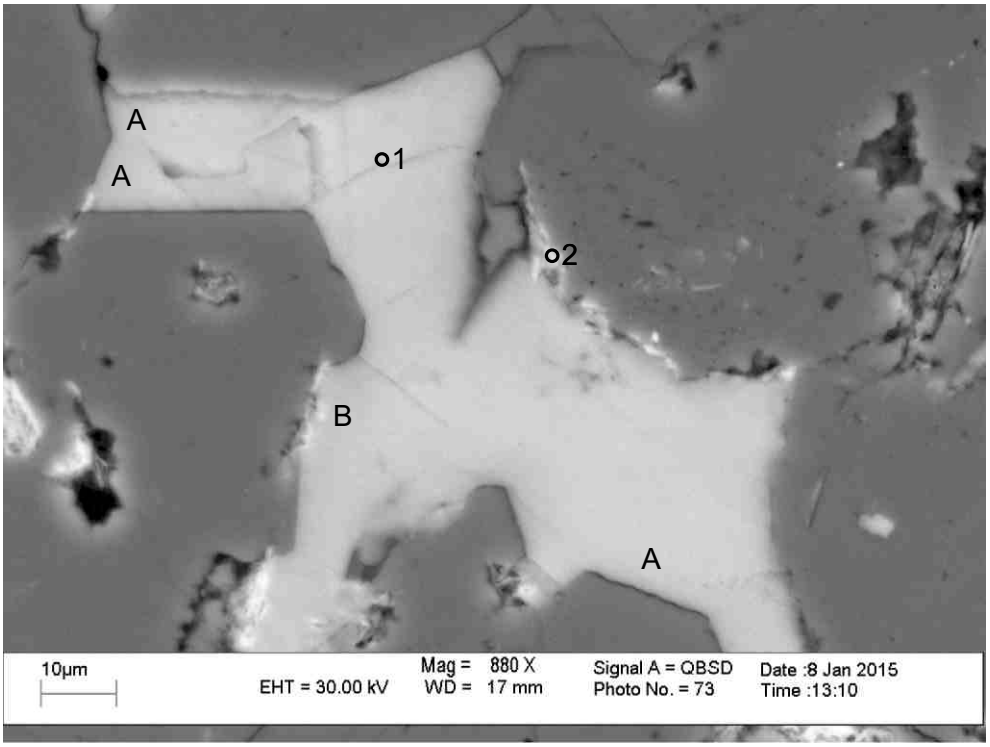

1. F-Calcite
2. Chlorite

Figure 2-6.17: Sample Newburn 5403.6m site 2 (SEM).Table 2-6B. Close up of position 2 Figure 2-6.14. F-calcite (1) in places bounded by euhedral quartz overgrowths (positions A). In other places (position B) the quartz overgrowths appear corroded.

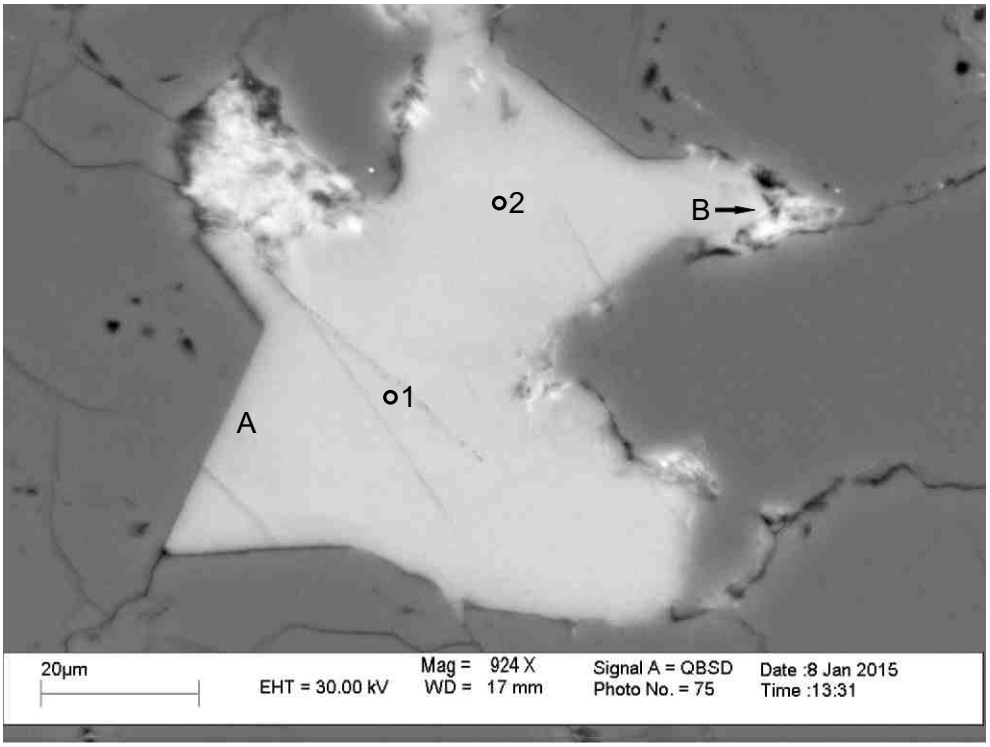

1. F-Calcite
2. F-Calcite

Figure 2-6.18: Sample Newburn 5403.6m site 3 (SEM).Table 2-6B. F-calcite (1,2) is in contact with quartz overgrowth (position A). Fibrous chlorite cuts F-calcite (position B).

Table 2-6A: Scanning Electron Microscope chemical analyses of sample 5403.6 from Newburn H-23 well.

Sample	Site	Position	Mineral	SiO_2	TiO_2	Al_2O_3	FeO	MnO	MgO	CaO	Na_2O	K_2O	P_2O_5	SO_3	F	Cl	Sc_2O_3	NiO	ZnO	As_2O_3	ZrO_2	BaO	Total	Actual Total
H-23 5403m	1	1	Py				27.93							72.07									100	200
H-23 5403m	1	2	Chl	29.37		23.98	26.21		4.97			0.47											85	85
H-23 5403m	1	3	Fap+Other	8.54		2.70	0.39		0.46	38.94	2.28		38.68	1.05	6.61	0.36							100	116
H-23 5403m	1	4	Qz	99.99																			100	111
H-23 5403m	1	5	Qz	99.99																			100	110
H-23 5403m	1	6	DM+Other	46.87		5.88	10.60		22.53	1.79	0.78	0.96		3.62	6.56	0.41							100	66
H-23 5403m	1	7	DM+Other	55.81		6.05	8.67		18.82	1.18	0.74	0.72		2.17	5.40	0.45							100	52
H-23 5403m	1	8	DM+Other	57.65	1.42	4.12	9.80		16.73	1.48	0.66	0.83		1.12	5.76	0.40							100	74
H-23 5403m	1	9	Chl	30.19		22.89	26.62		5.02			0.29											85	85
H-23 5403m	1	10	Qz	99.99																			100	111
H-23 5403m	1	11	Chl	27.27		22.69	30.47		4.56														85	78
H-23 5403m	1	12	Chl+Ab	37.97		24.73	30.85		5.37		1.07												100	94
H-23 5403m	2	1	Kfs	60.03		13.81	12.44		4.86			8.87											100	98
H-23 5403m	2	2	TiO_2		98.10		1.90																100	93
H-23 5403m	2	3	Py+Other	9.63		0.87	23.18				2.22	0.30		63.53						0.28			100	192
H-23 5403m	2	4	Qz	99.99																			100	113
H-23 5403m	2	5	Qz	99.99																			100	112
H-23 5403m	2	6	Chl	25.89		23.26	31.01		4.85														85	82
H-23 5403m	2	7	Chl	32.23		23.90	23.70		4.11			1.05											85	84
H-23 5403m	2	8	Chl	28.19		23.33	28.92		4.55														85	87
H-23 5403m	2	9	Chl	28.06		23.98	27.85		5.12														85	88
H-23 5403m	2	10	Chl	27.53		23.26	29.50		4.72														85	91
H-23 5403m	2	11	Chl	29.46		22.21	29.35		3.98														85	79
H-23 5403m	2	12	Zrn+Ab	50.81		8.54				0.64	5.61										34.40		100	107
H-23 5403m	2	13	Chl	28.31		22.96	28.91		4.48			0.34											85	85
H-23 5403m	2	14	Kfs+Chl	59.23		13.64	13.19		5.09			8.84											100	98
H-23 5403m	2	15	Zrn+Other	47.85	1.13	4.80	3.10			0.60	0.89						0.61				41.00		100	97
H-23 5403m	3	1	TiO_2		99.30		0.71																100	94
H-23 5403m	3	2	Mix	61.01	7.36	7.54	9.57		1.54			0.31									12.68		100	93
H-23 5403m	3	3	Kln	48.40		36.24									1.36								86	101
H-23 5403m	3	4	Kln	48.35		37.10	0.55																86	94
H-23 5403m	3	5	Qz	99.99																			100	114
H-23 5403m	3	6	Chl	27.93		22.96	29.06		4.30	0.35		0.40											85	85
H-23 5403m	3	7	Chl	28.85		23.57	27.74		4.84														85	92
H-23 5403m	3	8	Ms+Other	49.54		33.43	2.86		1.43		0.44	10.00			2.32								100	110
H-23 5403m	3	9	Ms	46.03	0.60	31.36	7.73		2.18			7.11											95	106
H-23 5403m	4	1	Kfs+Chl	59.58		11.72	12.36		6.55			9.80											100	95
H-23 5403m	4	2	Kfs+Chl	59.75	0.38	13.81	10.66		5.84			9.35				0.22							100	97

Table 2-6A: Scanning Electron Microscope chemical analyses of sample 5403.6 from Newburn H-23 well.

Sample	Site	Position	Mineral	SiO_2	TiO_2	Al_2O_3	FeO	MnO	MgO	CaO	Na_2O	K_2O	P_2O_5	SO_3	F	Cl	Sc_2O_3	NiO	ZnO	As_2O_3	ZrO_2	BaO	Total	Actual Total
H-23 5403m	4	3	Qz	99.99																			100	112
H-23 5403m	4	4	Ms+Ab	51.11		38.02	1.79				4.26	4.84											100	103
H-23 5403m	4	5	Chl	42.00		31.54	9.83		1.62														85	79
H-23 5403m	4	6	Ab	68.86		18.90					12.24												100	116
H-23 5403m	4	7	Qz	99.99																			100	115
H-23 5403m	4	8	Qz	99.99																			100	111
H-23 5403m	4	9	Chl	27.68		23.67	29.13		4.52														85	89
H-23 5403m	4	10	Chl	27.21		23.43	29.60		4.75														85	90
H-23 5403m	4	11	Chl	28.18		24.59	26.79		5.44														85	101
H-23 5403m	4	12	Ms	52.85		18.68	11.59		4.93			6.94											95	87
H-23 5403m	4	13	Ms	56.35		22.84	4.60		3.25			7.51				0.46							95	77
H-23 5403m	4	14	Py+F-Cal+Chl	4.68		3.95	11.82		1.76	49.20				21.62	6.96								100	78
H-23 5403m	4	15	Mix	53.74		35.28	4.08		1.28		1.55	4.10											100	91
H-23 5403m	4	16	Qz	98.00							0.62			1.37									100	96
H-23 5403m	4	17	Py+F-Cal	2.27		2.21	19.93		0.93	19.56				50.92	4.20								100	132
H-23 5403m	4	18	Sd+Py+Ab	3.42		2.87	60.89	0.66	8.17	5.95	1.70			16.36									100	68
H-23 5403m	5	1	Ms	47.89	1.22	31.45	3.93		0.81		0.64	9.06											95	98
H-23 5403m	5	2	Ms	44.72	1.12	29.84	9.78		1.87		0.73	6.95											95	100
H-23 5403m	5	3	Sd+Ms	26.48	4.60	13.70	42.36	0.92	5.27	4.58		2.08											100	65
H-23 5403m	5	4	Chl+Sd+Ms	20.94		14.98	51.46	1.10	7.94	2.59		1.00											100	73
H-23 5403m	5	5	Mix	38.14		32.10	9.24		2.24	1.02		3.01	13.18	1.05									100	74
H-23 5403m	5	6	Ab	68.75		18.82					12.42												100	117
H-23 5403m	5	7	Ms+Other	58.96	3.30	26.79	2.82		1.81		0.59	5.43				0.30							100	79
H-23 5403m	5	8	Chl+Fap	31.49		13.81	8.90		1.56	18.44	4.89		17.35		3.55								100	103
H-23 5403m	5	9	Fap+Ab+Chl	29.80		12.51	12.94		1.38	16.99	3.21		17.78		5.41								100	97
H-23 5403m	5	10	Chl+Other	37.76		27.66	27.90		4.59			0.84	0.99			0.24							100	89
H-23 5403m	5	11	Chl+Ab	36.28		25.96	31.03		4.64	0.31	1.77												100	92
H-23 5403m	5	12	Chl	30.01		23.82	25.13		5.64			0.41											85	95
H-23 5403m	5	13	Sd+Chl	8.28		7.35	68.17	1.60	7.35	7.28													100	55
H-23 5403m	5	14	Qz	99.99																			100	112
H-23 5403m	5	15	Sd+Chl	4.17		3.55	74.32	2.17	8.56	7.23													100	50
H-23 5403m	6	1	Brt											38.18								61.83	100	102
H-23 5403m	6	2	Py				26.77				0.50			72.32						0.42			100	214
H-23 5403m	6	3	Ms	49.74		36.17	1.41				1.62	6.06											95	94
H-23 5403m	6	4	Chl	32.18	0.64	24.45	23.85		3.88														85	88
H-23 5403m	6	5	Chl	27.64		22.48	30.09		4.20		0.59												85	82
H-23 5403m	6	6	Kln	48.72		36.97						0.31											86	93
H-23 5403m	6	7	Kln	46.55		36.14					0.33				2.98								86	94

Table 2-6A: Scanning Electron Microscope chemical analyses of sample 5403.6 from Newburn H-23 well.

Sample	Site	Position	Mineral	SiO_2	TiO_2	Al_2O_3	FeO	MnO	MgO	CaO	Na_2O	K_2O	P_2O_5	SO_3	F	Cl	Sc_2O_3	NiO	ZnO	As_2O_3	ZrO_2	BaO	Total	Actual Total
H-23 5403m	6	8	Ab+Cal	53.44		14.64				18.55	10.37	0.30			2.67								100	99
H-23 5403m	6	9	Ab	68.99		18.71					12.30												100	113
H-23 5403m	6	10	Ilt	55.06		20.96	3.97		2.61			7.41											90	108
H-23 5403m	6	11	Ab+Ilt	72.26		16.33	1.47		1.51		4.30	4.14											100	115
H-23 5403m	6	12	Chl+Kfs	46.81	0.33	29.08	14.16		3.63		0.51	5.50											100	109
H-23 5403m	7	1	Py+Other	0.26			27.36				1.35			71.04									100	201
H-23 5403m	7	2	TiO_2		100.00																		100	96
H-23 5403m	7	3	TiO_2+Other	5.69	91.76	0.60	1.94																100	98
H-23 5403m	7	4	Ank				14.23	0.90	10.82	30.05													56	54
H-23 5403m	7	5	Ab	68.63		18.71				0.43	12.23												100	113
H-23 5403m	7	6	Chl+Other	39.98	0.42	28.91	24.15		4.49		0.58	1.46											100	98
H-23 5403m	7	7	Chl	27.20		23.72	29.44		4.64														85	93
H-23 5403m	7	8	Chl	27.69		22.84	30.19		4.28														85	87
H-23 5403m	8	1	Sd+Chl	5.43		5.37	69.61	2.22	11.96	5.41													100	59
H-23 5403m	8	2	Chl	27.93		23.18	28.88		5.01														85	91
H-23 5403m	8	3	Sd+Chl	10.40		9.71	61.98	1.70	12.14	4.04													100	65
H-23 5403m	8	4	Sd+Other	12.94		10.88	59.91	1.55	11.76	2.95													100	66
H-23 5403m	8	5	Chl	28.93		24.38	26.64		4.58			0.47											85	95
H-23 5403m	9	1	Qz	99.99																			100	88
H-23 5403m	9	2	F-Fe-Cal				1.40	0.50		39.04					15.06								56	53
H-23 5403m	9	3	Chl+Ab	44.47	1.07	37.04	8.59		5.85		2.99												100	76
H-23 5403m	9	4	TiO_2+Other	2.67	91.41	2.68	2.47		0.78														100	83
H-23 5403m	9	5	TiO_2		99.17		0.82																100	77
H-23 5403m	9	6	Qz	99.99																			100	87
H-23 5403m	9	7	F-Fe-Cal				1.38	0.45	0.48	38.85					14.85								56	57
H-23 5403m	9	8	F-Fe-Cal				1.30	0.55	0.52	39.33					14.30								56	54
H-23 5403m	9	9	TiO_2	1.05	96.30	1.11	1.54																100	84
H-23 5403m	10	1	Brt											37.43								62.59	100	77
H-23 5403m	10	2	Brt											39.38								60.63	100	79
H-23 5403m	10	3	F-Cal				0.92			39.61					15.47								56	53
H-23 5403m	10	4	Ab+Chl	51.04		23.64	15.03		2.50		6.85	0.95											100	79
H-23 5403m	10	5	Qz	99.99																			100	86
H-23 5403m	10	6	Chl	37.51		17.48	24.70		4.22	0.37	0.71												85	74
H-23 5403m	10	7	Chl+Ab	43.15		24.17	27.27		3.52		1.90												100	63
H-23 5403m	10	8	Qz	99.99																			100	88
H-23 5403m	11	1	Zrn	31.06																	68.94		100	92
H-23 5403m	11	2	Qz+Ms	66.10		25.53	0.69				0.90	6.76											100	90
H-23 5403m	11	3	Ms+Sp	41.71	0.42	32.58	1.21					7.68		9.69					6.71				100	88

Table 2-6A: Scanning Electron Microscope chemical analyses of sample 5403.6 from Newburn H-23 well.

Sample	Site	Position	Mineral	SiO_2	TiO_2	Al_2O_3	FeO	MnO	MgO	CaO	Na_2O	K_2O	P_2O_5	SO_3	F	Cl	Sc_2O_3	NiO	ZnO	As_2O_3	ZrO_2	BaO	Total	Actual Total
H-23 5403m	11	4	Ms+Chl	40.26		32.61	19.73		3.13		0.59	3.69											100	78
H-23 5403m	11	5	Qz	99.99																			100	89
H-23 5403m	11	6	Chl	27.20		24.40	28.30		5.10														85	64
H-23 5403m	11	7	Chl	26.91		23.74	29.84		4.51														85	69
H-23 5403m	11	8	Chl+Ms	36.86		27.12	28.98		5.09			1.95											100	74
H-23 5403m	11	9	Chl+Ms	46.72		26.72	17.62		4.48			4.48											100	74
H-23 5403m	12	1	Zrn	30.63																	69.36		100	88
H-23 5403m	12	2	Zrn	30.91																	69.08		100	90
H-23 5403m	12	3	Fap	0.66			0.85			46.16			44.39		7.94								100	92
H-23 5403m	12	4	Chl+Ab	34.40		24.87	32.83		6.28	0.50	1.12												100	75
H-23 5403m	12	5	Qz	99.99																			100	92
H-23 5403m	12	6	TiO_2+Other	20.81	77.95	0.62	0.62																100	80
H-23 5403m	12	7	Fap	2.57		1.61	2.52			42.31			41.41		9.61								100	87
H-23 5403m	12	8	Chl	35.59		20.14	24.90		4.37														85	75
H-23 5403m	13	1	Py+Other	1.26			26.72			0.46	0.80			70.74									100	160
H-23 5403m	13	2	F-Fe-Cal	2.46		0.59	1.35		0.99	34.71		0.13		1.37	14.40								56	60
H-23 5403m	13	3	Kln	46.25		35.00	1.81								2.95								86	75
H-23 5403m	13	4	Qz	99.99																			100	89
H-23 5403m	13	5	Chl+Ab	35.06	1.15	24.92	32.91		4.61		1.35												100	69
H-23 5403m	13	6	TiO_2+Other	9.35	76.46	5.40	7.05		0.95		0.80												100	72
H-23 5403m	13	7	Py+Other	4.90			22.64				6.63			63.33				2.52					100	124
H-23 5403m	13	8	Chl+Other	35.02		27.27	30.28		5.36	0.42	1.05	0.59											100	66
H-23 5403m	13	9	Kln	46.03		35.04	2.23								2.70								86	74
H-23 5403m	14	1	F-Fe-Cal				1.33	0.54	0.55	39.86					13.71								56	53
H-23 5403m	14	2	F-Fe-Cal				1.53	0.54		39.80					14.13								56	51
H-23 5403m	14	3	TiO_2+Other	2.65	93.61	1.72	1.60			0.43													100	75
H-23 5403m	14	4	F-Cal				0.81			38.93					16.26								56	56
H-23 5403m	14	5	TiO_2+Other	1.07	96.25	0.72	1.97																100	72
H-23 5403m	14	6	F-Fe-Cal	1.66			1.47	0.47		39.02		0.30			13.09								56	54
H-23 5403m	14	7	Ab	68.37		19.25					12.36												100	93
H-23 5403m	14	8	Qz	99.99																			100	98
H-23 5403m	15	1	Zrn	30.98																	69.01		100	85
H-23 5403m	15	2	F-Fe-Cal				1.23			38.37					16.40								56	56
H-23 5403m	15	3	TiO_2+Kfs	25.18	73.93	0.59						0.29											100	82
H-23 5403m	15	4	Zrn	31.13																	68.86		100	85
H-23 5403m	15	5	Chl	27.25		24.39	29.38		3.98														85	61
H-23 5403m	15	6	TiO_2+Chl	8.21	78.13	5.67	6.27		1.09	0.63													100	68
H-23 5403m	15	7	Chl	27.90		22.24	27.67		7.19														85	72

Table 2-6A: Scanning Electron Microscope chemical analyses of sample 5403.6 from Newburn H-23 well.

Sample	Site	Position	Mineral	SiO_2	TiO_2	Al_2O_3	FeO	MnO	MgO	CaO	Na_2O	K_2O	P_2O_5	SO_3	F	Cl	Sc_2O_3	NiO	ZnO	As_2O_3	ZrO_2	BaO	Total	Actual Total
H-23 5403m	15	8	Chl	28.73		22.94	26.51		6.83														85	73

Table 2-6B: Scanning Electron Microscope chemical analyses of sample 5403.6m from Newburn H-23 well (re-annalysis of fluorine-calcite).

Sample	Site	Position	Mineral	SiO_2	Al_2O_3	FeO	MnO	MgO	CaO	Na_2O	K_2O	F	Y_2O_3	Total
H-23 5403.6m	1	1	F-Cal	0.18		0.80	0.29	0.20	40.77			13.50	0.27	56
H-23 5403.6m	1	2	F-Cal	0.13		1.48	0.49	0.49	38.29			15.04	0.08	56
H-23 5403.6m	1	3	F-Cal	0.13		1.57	0.53	0.39	41.06			12.08	0.24	56
H-23 5403.6m	1	4	F-Cal	0.41		1.24	0.44	0.26	39.05			14.35	0.25	56
H-23 5403.6m	1	5	Qz	99.99										100
H-23 5403.6m	1	6	Chl	43.19	25.60	25.54		3.98	0.22	1.46				100
H-23 5403.6m	2	1	F-Cal			1.22	0.46	0.37	36.28			17.67		56
H-23 5403.6m	2	2	Chl	57.52	16.04	18.77		3.18	4.09		0.39			100
H-23 5403.6m	3	1	F-Cal	0.11		1.43	0.45	0.41	39.79			13.69	0.13	56
H-23 5403.6m	3	2	F-Cal	0.13		0.48	0.22		40.16			14.81	0.19	56

Appendix 2-7: SEM-BSE images and EDS mineral analyses for sample Newburn H-23 5406.5m

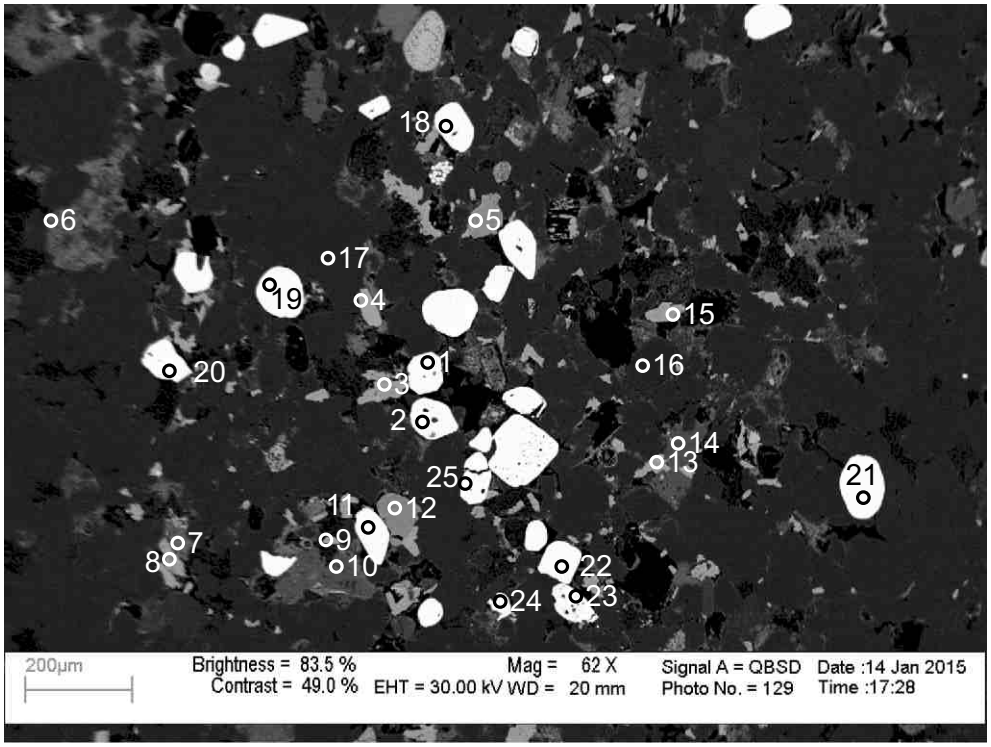

1: Zircon
2: Zircon
3: Titania
4: Spinel
5: Titania
6: Chlorite
7: Chlorite
8: Titania
9: Titania
10: Ankerite
11: Zircon
12: Spinel
13: Titania+ Chlorite
14: Ankerite
15: Titania
16: Quartz
17: Quartz
18: Zircon
19: Zircon
20: Zircon
21: Zircon
22: Zircon
23: Zircon
24: Zircon
25: Zircon

Figure 2-7.1: Sample Newburn 5406.5m site 1 (SEM). Large concentration of rounded detrital zircon (1,2,11,18-25), titania (3,8) and spinel (4,6,7,12) . Diagenetic titania (5,9,15) is also present with angular outlines and infilling pores. Other diagenetic minerals include chlorite (6,7,13) and ankerite (14).

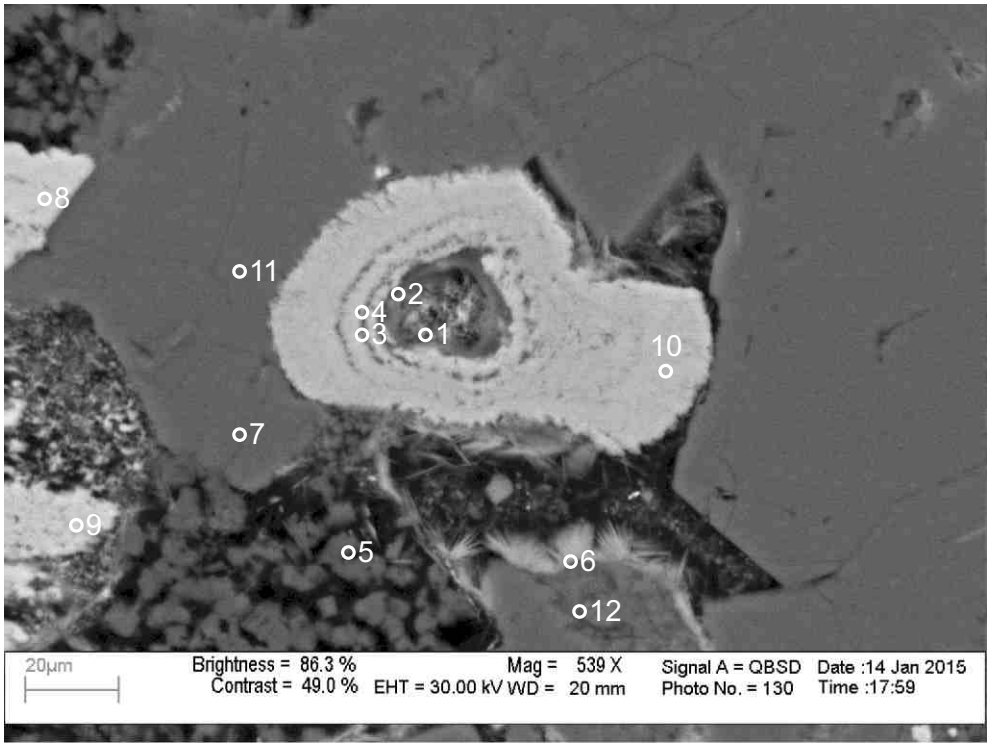

1: Hole
2: Hole
3: Siderite
4: Siderite
5: Kaolinite
6: Chlorite
7: Quartz
8: Titania
9: Titania
10: Siderite
11: Quartz
12: Quartz+ Illite

Figure 2-7.2: Sample Newburn 5406.5m site 2 (SEM). Siderite concretion (1-4) with a hole in the center. Fibrous chlorite (6) rims pore partially filled with kaolinite (5) booklets.

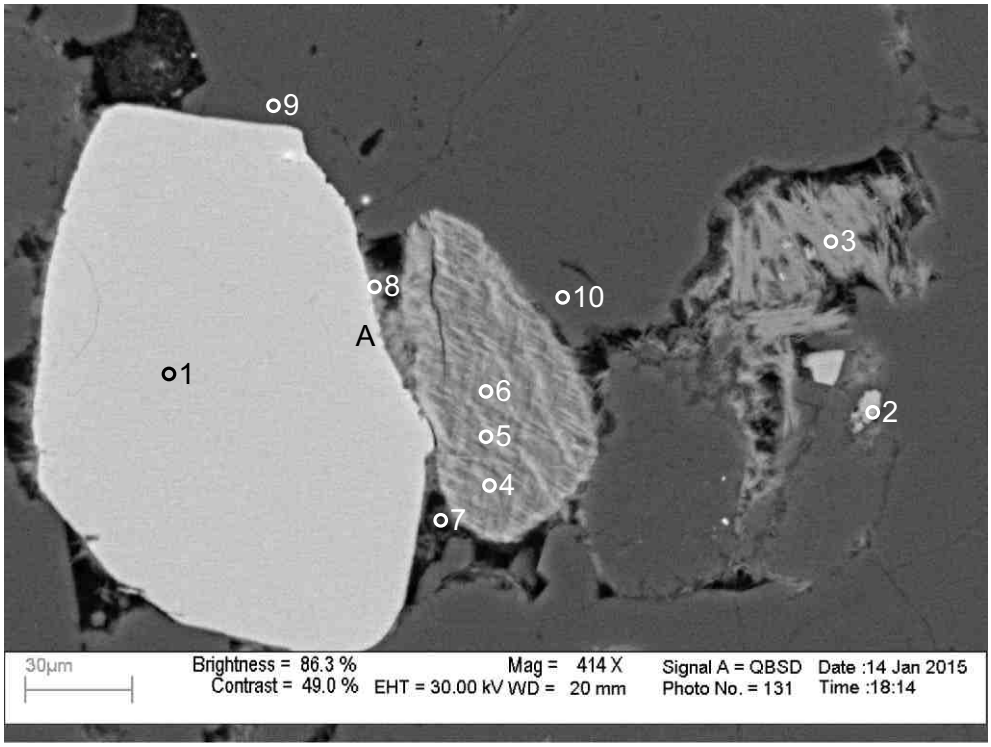

1: Spinel
2: Titania+ Quartz+ Other
3: Chlorite
4: Titania
5: Titania
6: Titania
7: Kaolinite+ Chlorite
8: Chlorite+ Spinel
9: Quartz
10: Quartz

Figure 2-7.3: Sample Newburn 5406.5m site 3 (SEM). Rounded detrital titania (4-6) grain. Detrital spinel (1) grain with straight crystal outline towards pore and towards adjacent quartz (9) grain, lining quartz overgrowth. Spinel grain is rimmed by fibrous of chlorite (8) in open pores which appear to have partly corroded it (position A). Fibrous chlorite (3) also fills porosity.

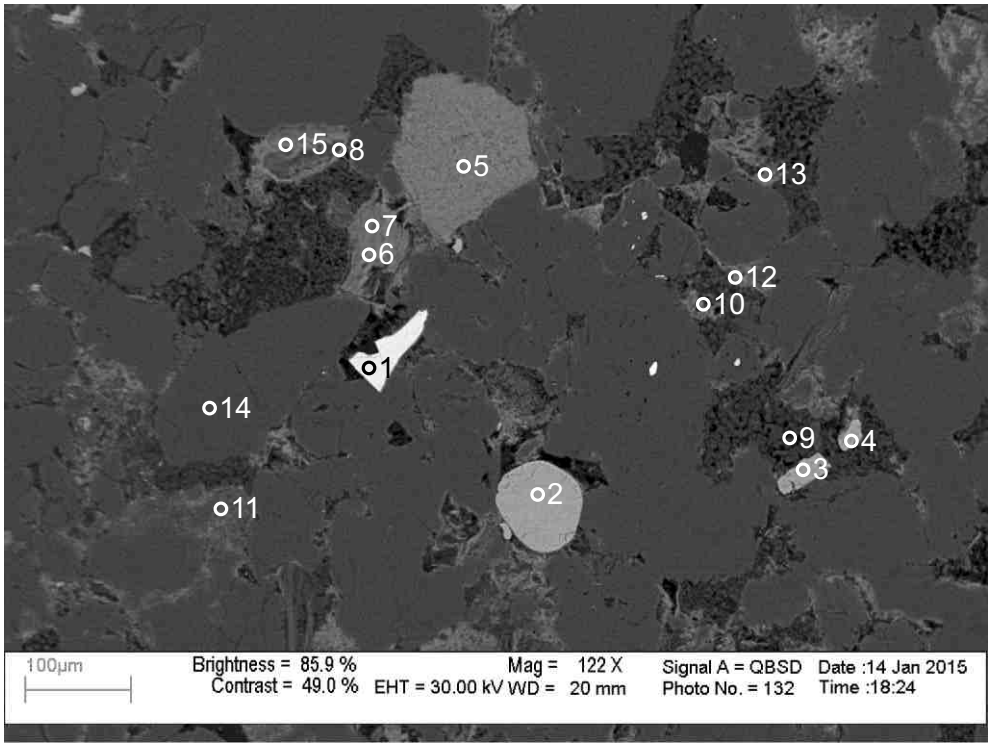

1: Zircon
2: Spinel
3: Titania
4: Titania+ Kaolinite
5: Chlorite
6: Chlorite
7: Chlorite
8: Chlorite
9: Kaolinite
10: Chlorite+ Quartz
11: Quartz+ Chlorite
12: Chlorite
13: Chlorite
14: Quartz
15: Chlorite

Figure 2-7.4: Sample Newburn 5406.5m site 4 (SEM). Diagenetic zircon (1) with straight crystal outlines, has partially cut quartz grains on two sides. Detrital spinel grain (2) limiting quartz overgrowth around its crystal outline. Chlorite (11) occupies voids between quartz crystal boundaries (11).

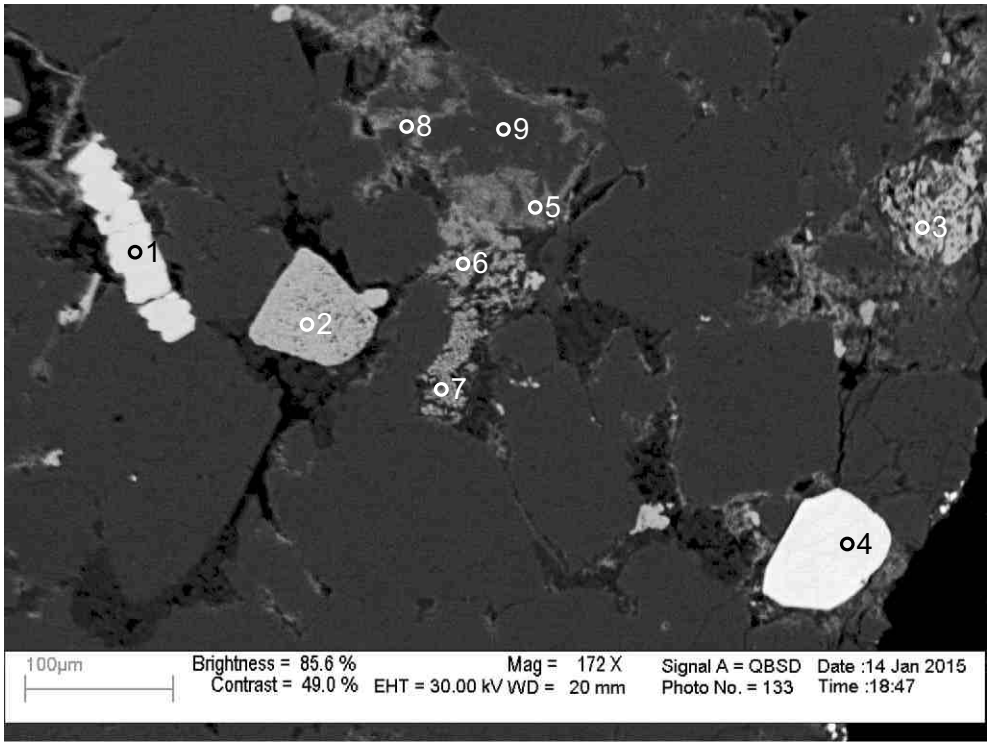

1: Pyrite
2: Titania+ Chlorite
3: Titania+ Quartz
4: Zircon
5: Chlorite
6: Titania
7: Titania
8: Quartz+ Chlorite
9: Quartz

Figure 2-7.5: Sample Newburn 5406.5m site 5 (SEM). Euhedral pyrite (1) grains form along crystal boundaries. Detrital titania (2) with dissolution voids infilled by chlorite (2). Sub-hedral detrital zircon (4).

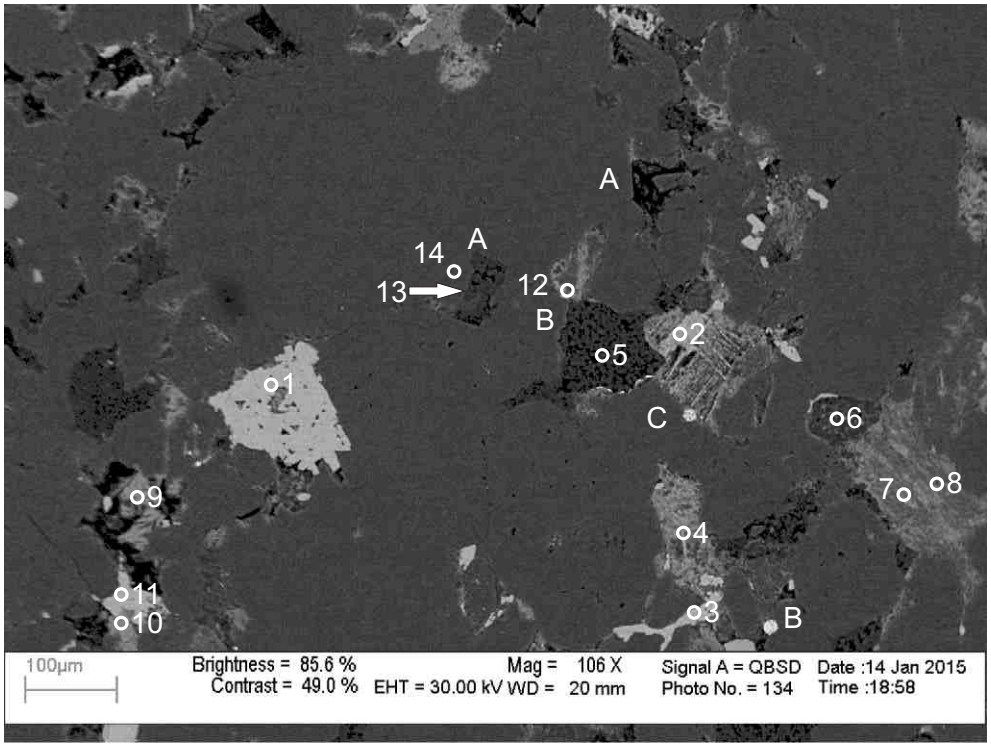

1: Titania
2: Titania
3: Titania
4: Chlorite+ Titania
5: Kaolinite
6:Muscovite+ Chlorite+ Titania
7:Muscovite+ Chlorite
8:Muscovite+ Chlorite+ Titania
9: Chlorite
10: Chlorite
11: Titania
12: Albite
13: Kaolinite
14: Quartz

Figure 2-7.6: Sample Newburn 5406.5m site 6 (SEM). Titania (3) filling voids between grain boundaries. Kaolinite fills pore after formation of quartz overgrowth (position A). Albite (12) is rimmed by chlorite. Framboidal pyrite (position C). Chlorite and pyrite rim pore filled with Kaolinite (5). Kaolinite shows irregular contact with quartz (position C). Subhedral titania (1) forms along intergranular boundary (or cuts framework grain), engulfs chlorite and cuts quartz. Fibrous chlorite (9) partly fills porosity.

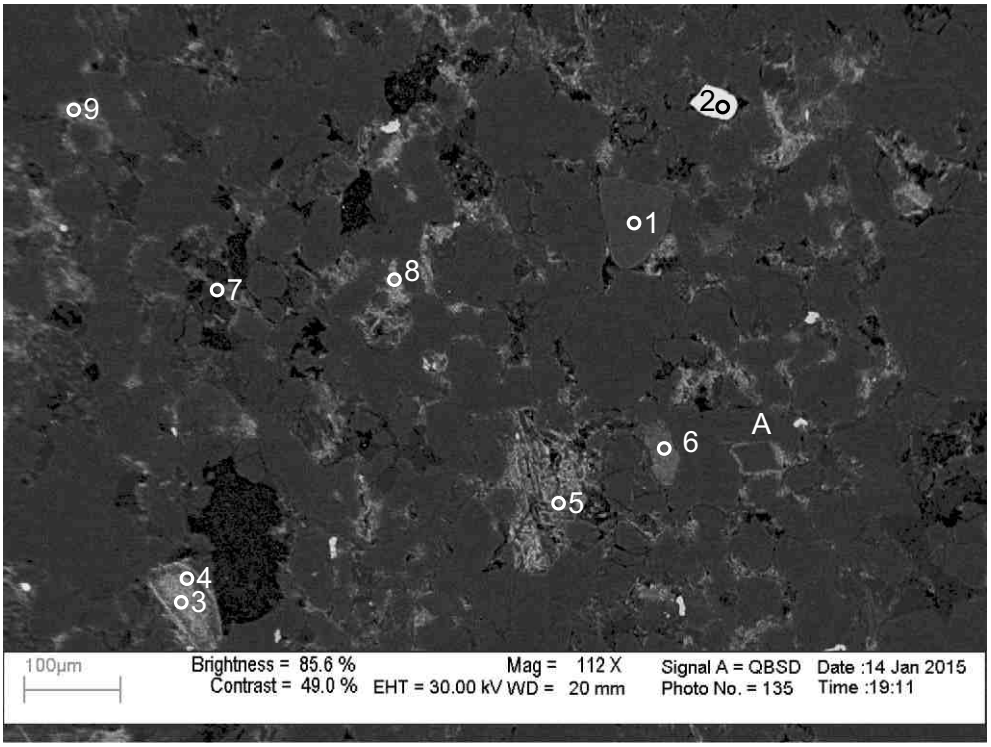

1:Tourmaline
2: Zircon
3: Titania
4: Titania
5: Chlorite
6:Glauconite +Quartz
7: Albite+ Chlorite
8: Chlorite
9: Chlorite

Figure 2-7.7: Sample Newburn 5406.5m site 7 (SEM). Glauconite (6) is a framework grain. Detrital tourmaline (1) inhibits quartz overgrowth. Chlorite rims quartz grain (position A). Fibrous chlorite (8) rims pore and crosscuts kaolinite.

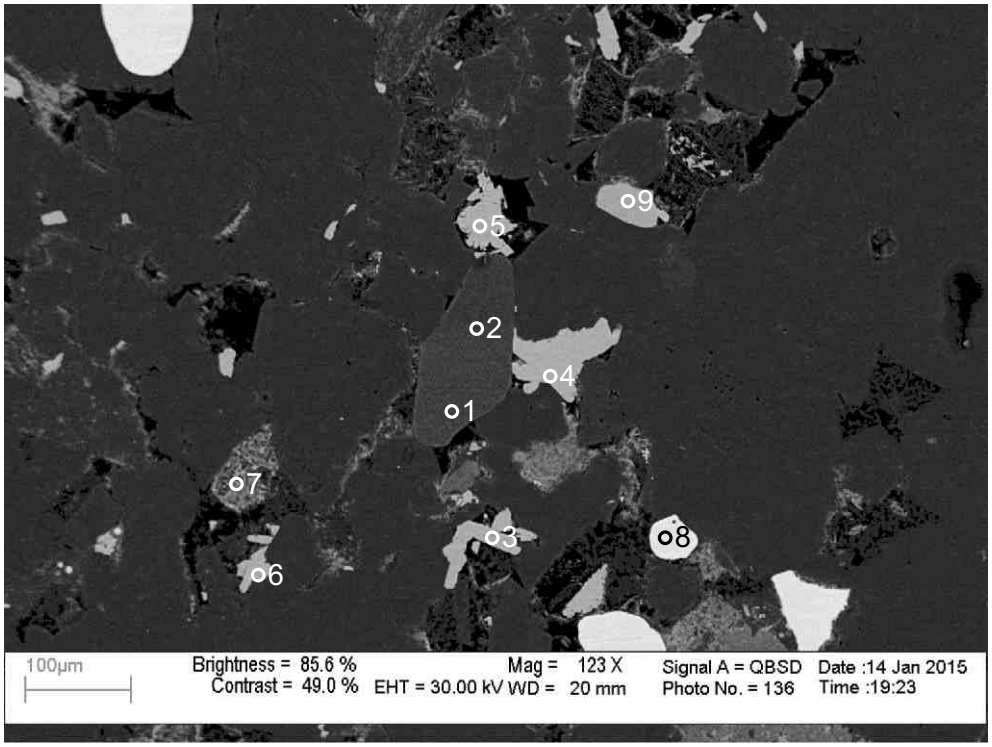

1:Tourmaline
2:Tourmaline
3: Titania
4: Titania
5: Titania
6: Titania
7:Muscovite+ Chlorite
8: Zircon
9: Titania

Figure 2-7.8: Sample Newburn 5406.5m site 8 (SEM). Chlorite (7) partially replaces muscovite (7). Detrital tourmaline grain (1,2) inhibits quartz overgrowth as well as the growth of titania (4,5). Diagenetic titania (5) with straight crystal outlines partially filling pore. Diagenetic titania (4,6,9) engulfs quartz. Diagenetic titania (3) partially fills pore with earlier kaolinite.

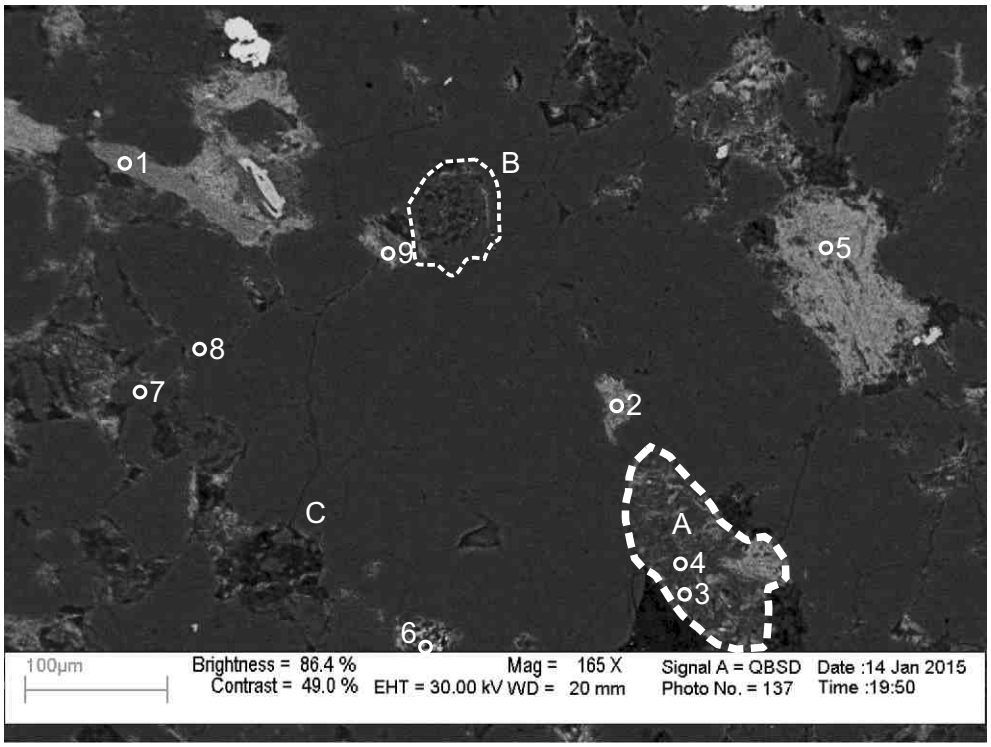

1: Chlorite
2: Chlorite
3: Chlorite+ Muscovite
4:Quartz +Muscovite +Chlorite
5: Chlorite
6: Titania
7: Quartz
8: Quartz
9: Chlorite

Figure 2-7.9: Sample Newburn 5406.5m site 9 (SEM). Shale clast comprised of quartz (4), muscovite and chlorite (3). Fully chloristized muscovite (1). Trachytic lithic clast (B). Kaolinite fills pore (position C) in contact with quartz displaying no overgrowths, and is cut by fibrous chlorite.

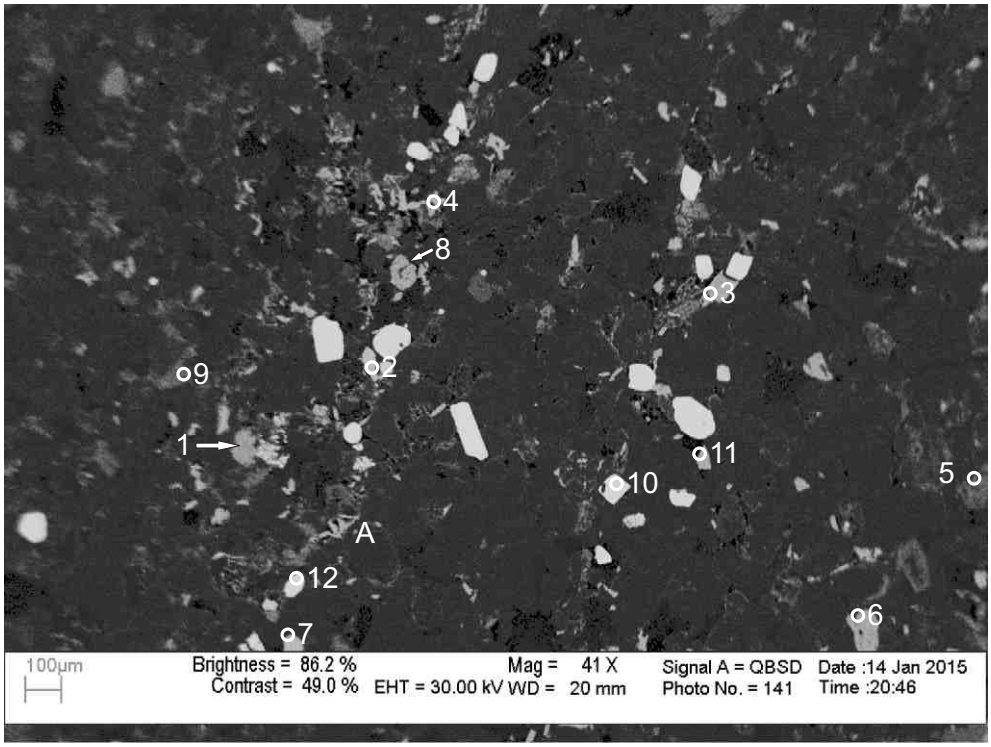

1: Siderite
2: Spinel
3: Titania
4: Titania
5: Chlorite
6: Titania
7: Spinel
8: Titania+ Chlorite
9: Chlorite
10: Zircon
11: Spinel
12: Zircon

Figure 2-7.10: Sample Newburn 5406.5m site 10 (SEM). Detrital zircon (10,12), titania (6), and spinel (2,7,11) in relatively straight lines, probably along original bedding picked out by heavy minerals. Euhedral diagenetic titania (3,4,8) fills pores and cuts quartz grains as well as chlorite previously filling pores (position A). Siderite (1) fills porosity.

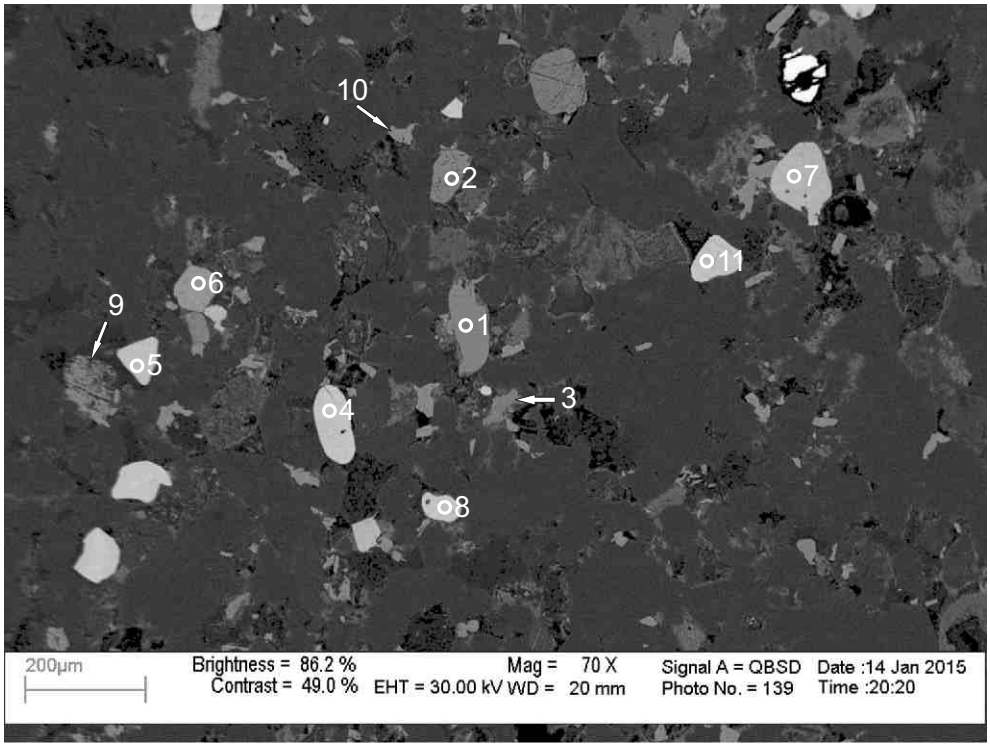

1: Titania
2: Spinel
3: Siderite+ Quartz
4: Zircon
5: Zircon
6: Spinel
7: Pyrite
8: Zircon
9: Titania
10: Titania
11: Zircon

Figure 2-7.11: Sample Newburn 5406.5m site 11 (SEM). Detrital zircon (4,5,8,11), spinel (2,6) and titania (1). Diagenetic titania fills pore replacing kaolinite and quartz (10) and forms between the cleavage planes of chloritized muscovite (9). Fractured spinel (2) inhibits quartz overgrowth. Siderite rhombohedron (3), probably represents late siderite.

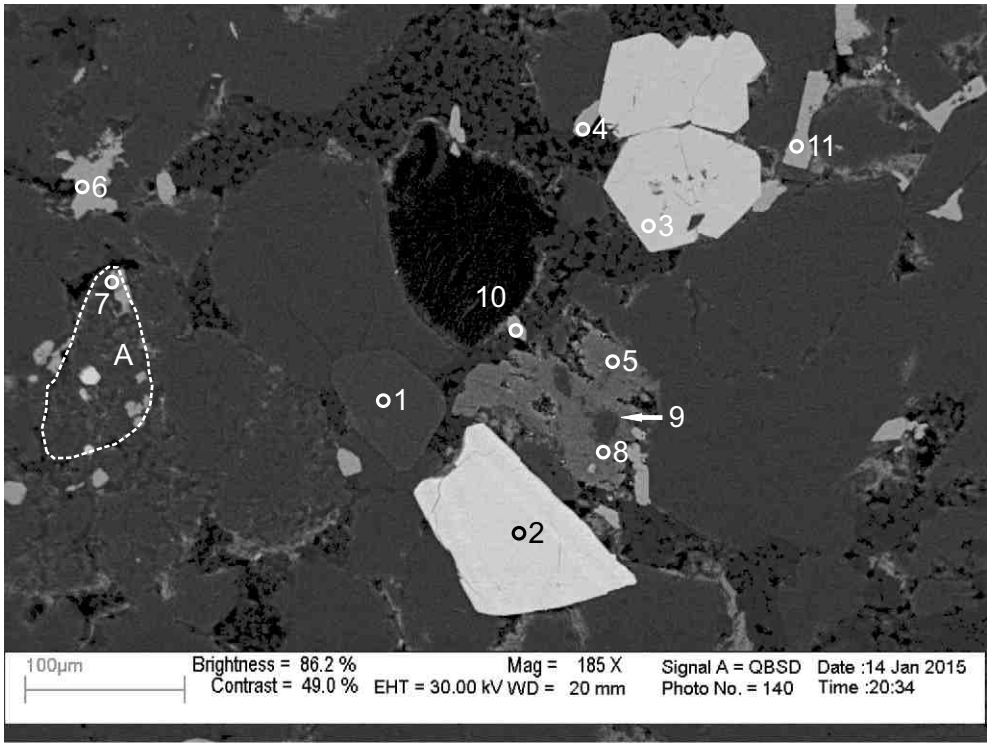

1:Tourmaline
2: Zircon
3: Pyrite
4: Titania
5: Ankerite
6: Titania
7: Titania+ Chlorite
8: Ankerite
9: Quartz
10: Titania
11: Titania

Figure 2-7.12: Sample Newburn 5406.5m site 12 (SEM). Ankerite (5,8) surrounds quartz (9) and engulfs kaolinite booklets. Euhedral diagenetic pyrite (3) engulfs quartz and is in contact with titania (4). Detrital tourmaline (1) inhibits quartz overgrowth. Trachytic lithic clast clast (position A). Diagenetic zircon (2) cuts framework grains.

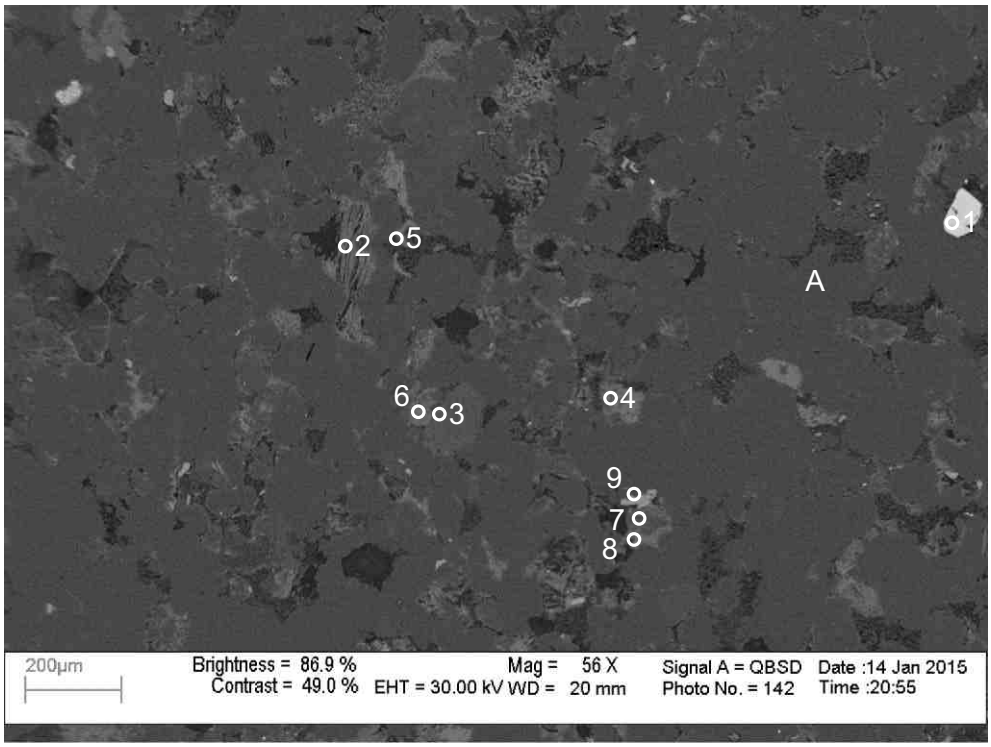

1: Zircon
2: Chlorite
3: Muscovite
4:Albite+ Chlorite
5: Chlorite
6: Chlorite
7: Quartz+ Other
8: Chlorite
9: Titania+ Quartz+ Other

Figure 2-7.13: Sample Newburn 5406.5m site 13 (SEM). Chloritized muscovite (2). Diagenetic zircon (1) with straight crystal outline towards voids. Kaolinite fills pore in contact with quartz overgrowth (position A).

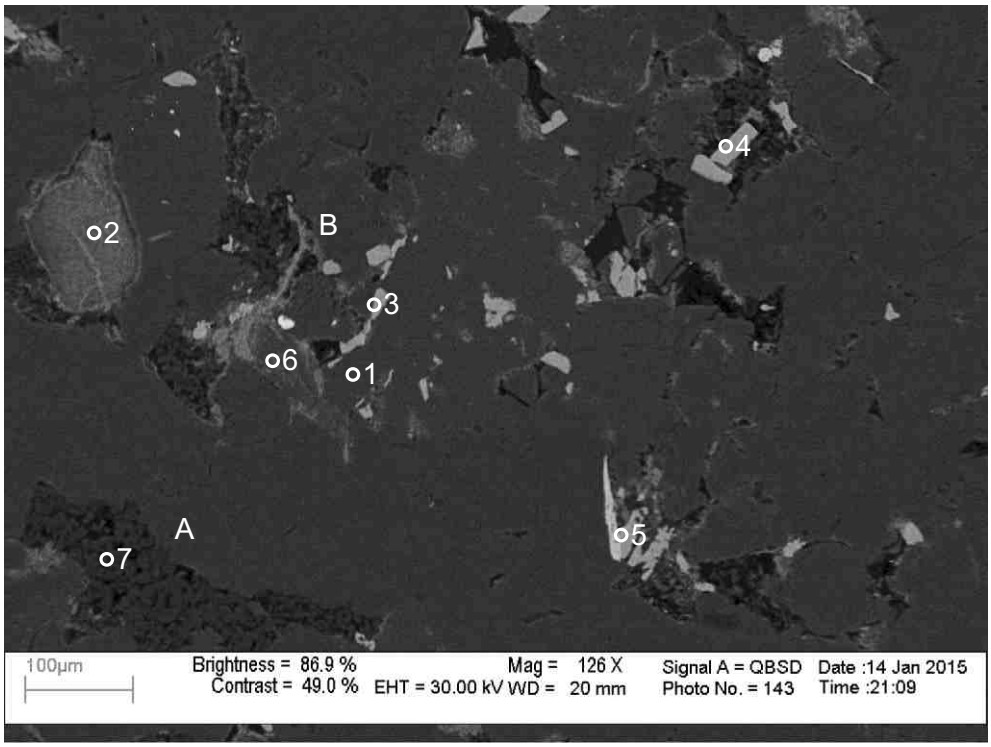

1: Albite
2: Chlorite
3: Titania
4: Titania
5: Titania+ Chlorite
6: Muscovite
7: Kaolinite

Figure 2-7.14: Sample Newburn 5406.5m site 14 (SEM). Titania (3) partially fills intergranular boundary. Detrital chlorite (2) with diagenetic chlorite rim. Kaolinite has irregular contact with quartz, appears to be corroding overgrowth (position A). Plastically deformed chloritized muscovite (position B).

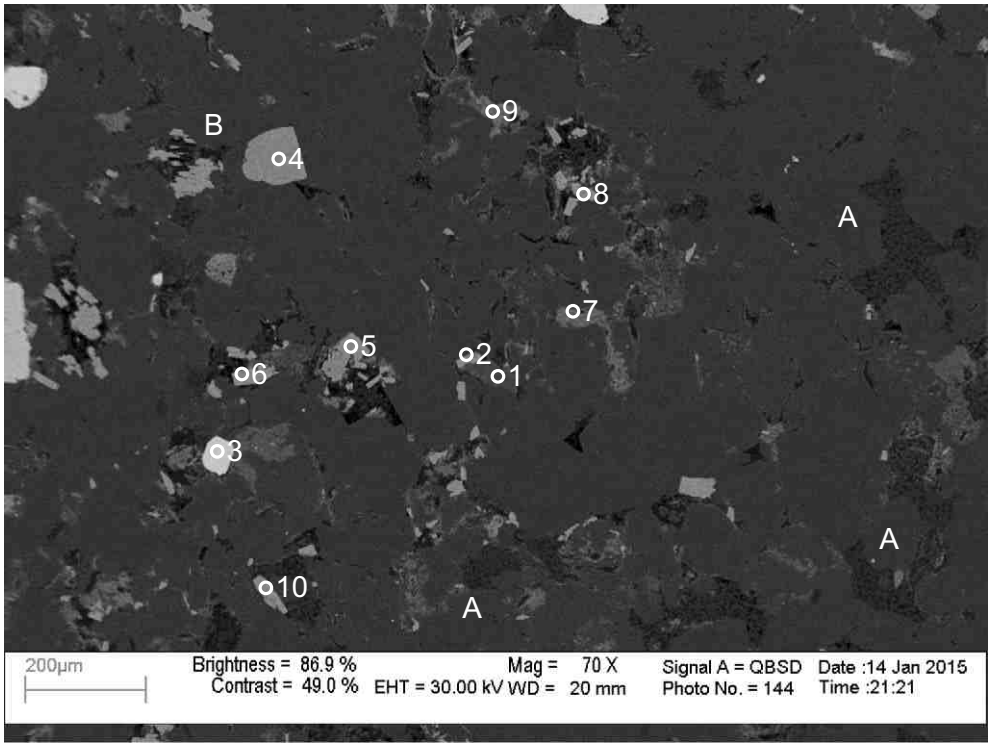

1: Albite+ Chlorite
2: Titania+ Quartz
3: Zircon
4: Spinel
5: Titania
6: Titania
7: Chlorite
8: Titania
9: Chlorite
10: Titania

Figure 2-7.15: Sample Newburn 5406.5m site 15 (SEM). Spinel (4) has euhedral crystal outline against quartz. Euhedral titania (5) partially fills pore and cuts quartz and chlorite. Chlorite (7) fills void along intergranular boundary. Irregular contact between kaolinite and quartz overgrowth (position A). Partly dissolved titania (position B)

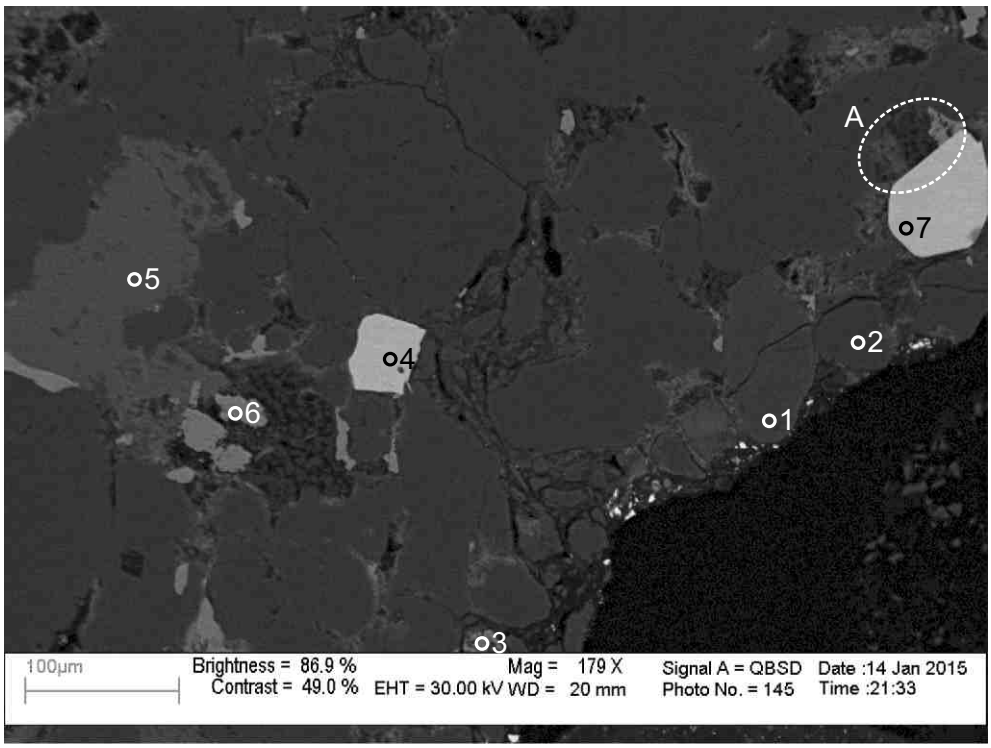

1:Tourmaline
2: Quartz
3: Titania+ Quartz
4: Zircon
5: Ankerite
6: Titania
7: Zircon

Figure 2-7.16: Sample Newburn 5406.5m site 16 (SEM). Ankerite (5) partially fills pore and surrounds quartz. Diagenetic zircon (4) with straight crystal outlines towards voids. Fractured detrital tourmaline (1). Diagenetic titania (6) cuts kaolinite booklets. Chlorite fills secondary porosity between quartz and zircon. Zircon recrystalization appears to post-date filling of pore (position A).

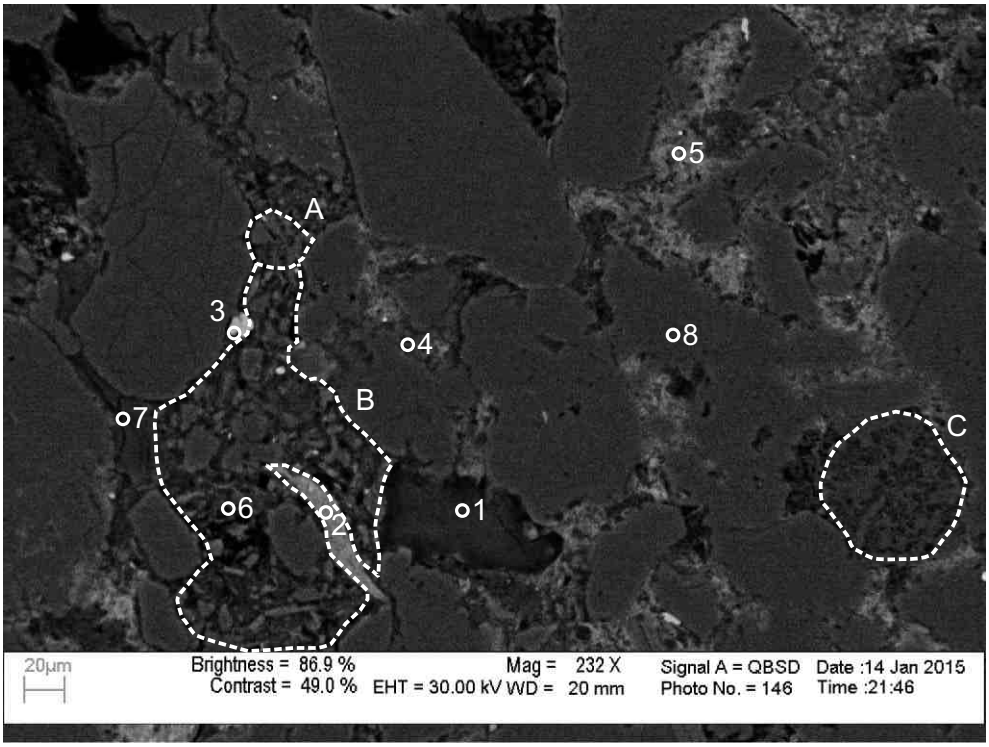

1:Muscovite+ Chlorite+ Other
2: Chlorite
3: Titania+ Chlorite
4: Quartz+ Other
5: Chlorite+ Pyrite
6: Illite+ Chlorite
7: Kaolinite
8: Quartz

Figure 2-7.17: Sample Newburn 5406.5m site 17 (SEM). Plastically deformed fully chloritized muscovite (2). Muscovite partially replaced by chlorite (1). A very small area of mechanically fractured quartz (position A) mixed with a muddy matrix of illite and chlorite (6)(position B). Trachytic lithic clast (position C).

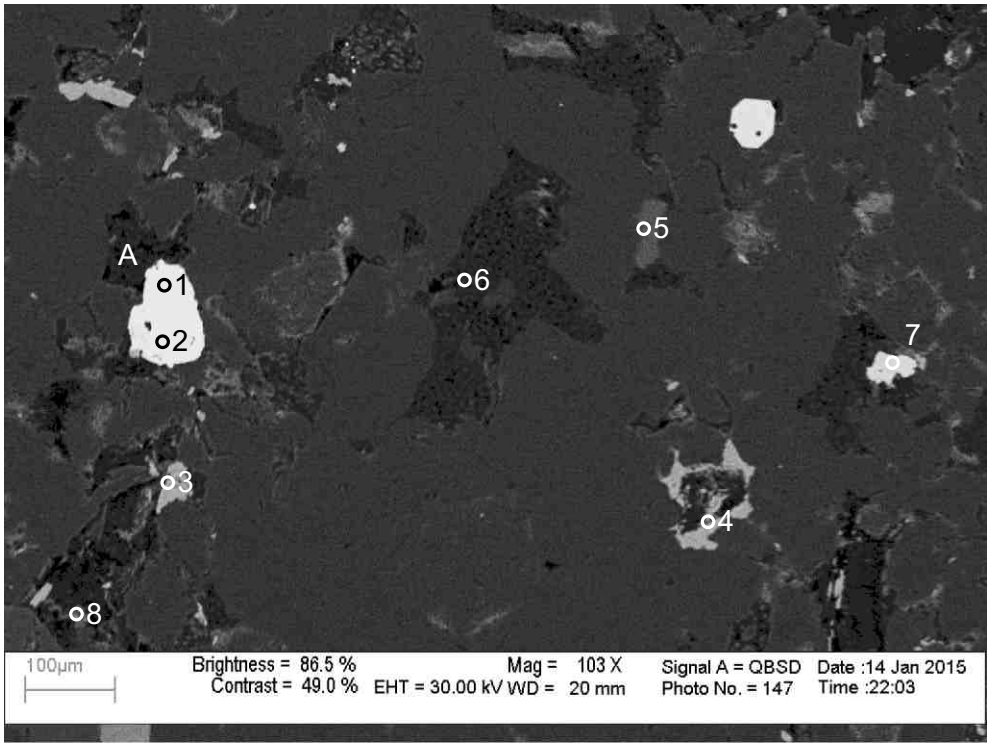

1: Xenotime
2: Xenotime
3: Titania+ Chlorite
4: Titania+ Chlorite
5: Calcite+ Other
6: Kaolinite
7: Pyrite
8: Chlorite+ Apatite

Figure 2-7.18: Sample Newburn 5406.5m site 18 (SEM). Titania and chlorite (4) fills void along quartz grain boundaries. Diagenetic xenotime (1,2) grain with dissolution voids and irregular contact with framework quartz. Xenotime engulfs kaolinite (position A). Calcite (5) rarely engulfs kaolinite and fills pore. Pyrite (7) engulfs kaolinite booklets and chlorite rim. Chlorite and apatite (8) crosscut kaolinite.

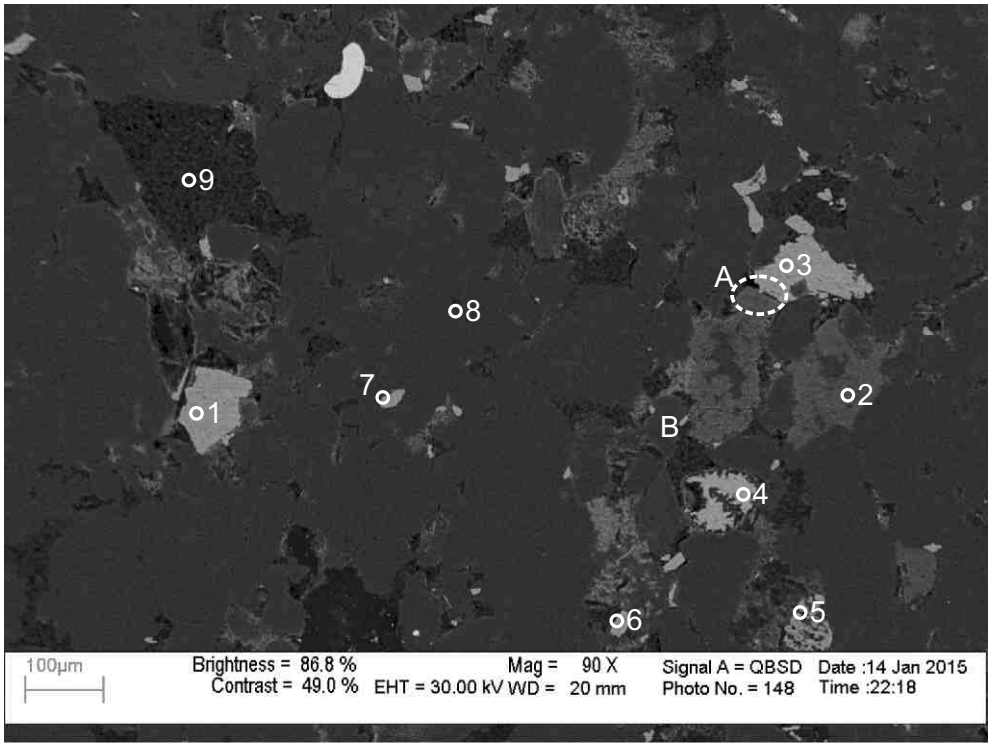

1: Spinel
2: Ankerite
3: Titania
4: Spinel
5: Muscovite+ Titania
6: Titania
7: Titania
8: Quartz
9: Kaolinite

Figure 2-7.19: Sample Newburn 5406.5m site 19 (SEM). Titania (5) engulfs muscovite (5) and forms along its cleavage planes. Partly dissolved spinel (4) rimmed by chlorite. Ankerite (2) engulfs quartz. Euhedral titania (3) surrounds quartz and cuts kaolinite booklets. Titania appears to cut corroded ankerite (position A). Ankerite engulfs kaolinite (position B).

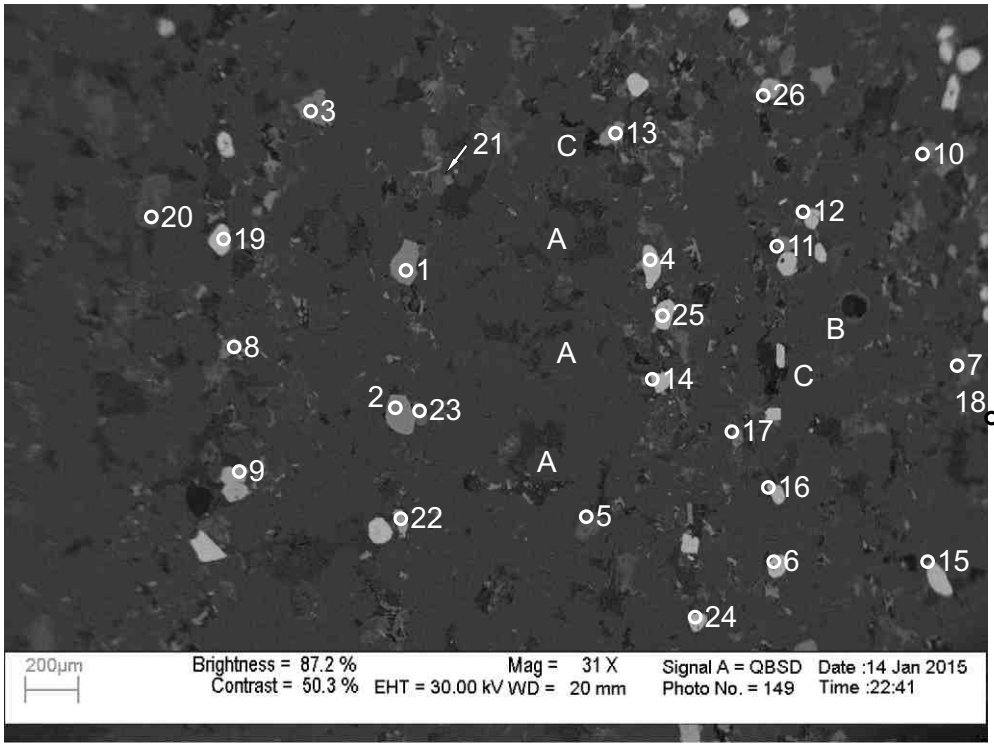

1: Spinel
2: Spinel
3: Titania+ Chlorite
4: Zircon
5: Chlorite
6: Zircon
7: Chlorite
8: Titania+ Chlorite
9: Pyrite
10: Titania+ Other
11: Spinel
12: Zircon
13: Spinel
14: Zircon
15: Zircon
16: Zircon
17: Titania
18: Pyrite
19: Zircon
20: Albite+ Ankerite
21:Fluorapatite
22: Pyrite
23: Titania
24: Zircon
25: Zircon
26: Pyrite

Figure 2-7.20: Sample Newburn 5406.5m site 20 (SEM). Detrital zircon (4,6,12,14,15,16,19,24,25), titania (23) and spinel (1,2,11) in relatively straight lines, probably along original bedding picked out by heavy minerals. Fluorapatite (21) appears to be corroded by kaolinite. Kaolinite has irregular contact with quartz overgrowth (position A). Circular void rimmed by chlorite (position B). Ankerite (20) engulfs albite. Large dissolution voids partly filled by euhedral titania (position C).

Table 2-7: Scanning Electron Microscope chemical analyses of sample 5406.5m from Newburn H-23 well.

Sample	Site	Position	Mineral	SiO_2	TiO_2	Al_2O_3	FeO	MnO	MgO	CaO	Na_2O	K_2O	P_2O_5	SO_3	F	Cl	Sc_2O_3	Cr_2O_3	CoO	Y_2O_3	ZrO_2	Nb_2O_5	Ce_2O_3	Gd_2O_3	Dy_2O_3	Yb_2O_3	HfO_2	Total	Actual Total
H-23 5406.5m	1	1	Zrn	31.72																	68.28							100	98
H-23 5406.5m	1	2	Zrn	31.55																	68.45							100	98
H-23 5406.5m	1	3	TiO_2 (D)		98.77		1.24																					100	79
H-23 5406.5m	1	4	Spl			24.85	18.77		10.53									45.85										100	81
H-23 5406.5m	1	5	TiO_2		98.70		1.03			0.27																		100	73
H-23 5406.5m	1	6	Chl	29.25		23.11	28.09		4.56																			85	64
H-23 5406.5m	1	7	Chl	28.23	0.38	23.19	28.72		4.47																			85	67
H-23 5406.5m	1	8	TiO_2 (D)	0.94	95.48	1.19	2.38																					100	67
H-23 5406.5m	1	9	TiO_2		98.63		1.38																					100	72
H-23 5406.5m	1	10	Ank	3.62		3.00	12.88	0.87	9.27	26.38																		56	47
H-23 5406.5m	1	11	Zrn	31.47																	68.53							100	91
H-23 5406.5m	1	12	Spl			37.60	13.32		14.09									34.99										100	80
H-23 5406.5m	1	13	TiO_2+Chl	2.10	95.00	1.08	1.45			0.38																		100	80
H-23 5406.5m	1	14	Ank				11.80	1.04	11.27	31.89																		56	48
H-23 5406.5m	1	15	TiO_2	0.71	95.95	1.55	1.80																					100	82
H-23 5406.5m	1	16	Qz	99.99																								100	99
H-23 5406.5m	1	17	Qz	99.99																								100	91
H-23 5406.5m	1	18	Zrn	31.42																	68.46						0.11	100	95
H-23 5406.5m	1	19	Zrn	31.72																	67.74						0.54	100	90
H-23 5406.5m	1	20	Zrn	31.64																	68.35							100	83
H-23 5406.5m	1	21	Zrn	31.60																	68.40							100	98
H-23 5406.5m	1	22	Zrn	31.94																	68.07							100	91
H-23 5406.5m	1	23	Zrn	32.37		2.10	1.11			1.20							0.98			2.67	58.22						1.36	100	58
H-23 5406.5m	1	24	Zrn	31.57																	68.12						0.29	100	87
H-23 5406.5m	1	25	Zrn	31.49																	67.54						0.98	100	89
H-23 5406.5m	2	1	Hole				47.35	2.78	0.73	2.75	2.14					0.25												56	27
H-23 5406.5m	2	2	Hole+Other	1.24		1.04	31.48	2.59	1.94	3.57	9.88	1.17				3.09												56	41
H-23 5406.5m	2	3	Sd				43.53	1.84	5.92	4.70																		56	36
H-23 5406.5m	2	4	Sd				45.58	1.44	3.86	5.11																		56	37
H-23 5406.5m	2	5	Kln	46.69	3.57	35.05	0.69																					86	53
H-23 5406.5m	2	6	Chl	30.85		24.28	25.05		3.57		0.71	0.54																85	68
H-23 5406.5m	2	7	Qz	99.99																								100	81
H-23 5406.5m	2	8	TiO_2	2.61	93.84	2.14	1.39																					100	67
H-23 5406.5m	2	9	TiO_2	1.05	96.10	0.74	2.12																					100	64
H-23 5406.5m	2	10	Sd				50.85	1.70		3.45																		56	36
H-23 5406.5m	2	11	Qz	99.99																								100	80
H-23 5406.5m	2	12	Qz+Ilt	74.08		20.39	1.30				0.75	3.47																100	73
H-23 5406.5m	3	1	Spl		0.38	17.86	24.39		10.51									46.86										100	67
H-23 5406.5m	3	2	TiO_2+Qz+Other	41.89	50.06	6.01	2.06																					100	59
H-23 5406.5m	3	3	Chl	28.55	0.38	22.32	28.19		5.57																			85	65
H-23 5406.5m	3	4	TiO_2 (D)	0.77	98.43		0.80																					100	54
H-23 5406.5m	3	5	TiO_2 (D)		100.00																							100	53
H-23 5406.5m	3	6	TiO_2 (D)	1.01	98.50		0.50																					100	53
H-23 5406.5m	3	7	Kln+Chl	47.25	4.04	36.26	10.20		1.29							0.37		0.58										100	41
H-23 5406.5m	3	8	Chl+Spl	23.87	1.25	22.66	32.55		4.49									15.19										100	46
H-23 5406.5m	3	9	Qz	99.99																								100	76
H-23 5406.5m	3	10	Qz	99.99																								100	76
H-23 5406.5m	4	1	Zrn	32.13																	67.36						0.50	100	73
H-23 5406.5m	4	2	Spl			21.94	15.28		10.91									51.89										100	65

Table 2-7: Scanning Electron Microscope chemical analyses of sample 5406.5m from Newburn H-23 well.

Sample	Site	Position	Mineral	SiO_2	TiO_2	Al_2O_3	FeO	MnO	MgO	CaO	Na_2O	K_2O	P_2O_5	SO_3	F	Cl	Sc_2O_3	Cr_2O_3	CoO	Y_2O_3	ZrO_2	Nb_2O_5	Ce_2O_3	Gd_2O_3	Dy_2O_3	Yb_2O_3	HfO_2	Total	Actual Total
H-23 5406.5m	4	3	TiO_2	0.98	95.60	1.70	1.71																					100	63
H-23 5406.5m	4	4	TiO_2+Kln	20.37	57.88	19.56	2.19																					100	68
H-23 5406.5m	4	5	Chl	27.91		22.82	29.15		5.12																			85	59
H-23 5406.5m	4	6	Chl	28.99		23.67	27.45		4.89																			85	60
H-23 5406.5m	4	7	Chl	31.01		23.79	25.11		4.54			0.55																85	56
H-23 5406.5m	4	8	Chl	29.56		24.99	25.11		5.34																			85	61
H-23 5406.5m	4	9	Kln	50.30		35.70																						86	57
H-23 5406.5m	4	10	Chl+Qz	50.68		33.14	12.74		2.04			0.95				0.47												100	34
H-23 5406.5m	4	11	Qz+Chl	74.68		11.24	10.33		3.02			0.72																100	64
H-23 5406.5m	4	12	Chl	30.61		23.63	25.73		4.54			0.49																85	56
H-23 5406.5m	4	13	Chl	31.80		24.11	24.96		3.73			0.39																85	56
H-23 5406.5m	4	14	Qz	99.99																								100	69
H-23 5406.5m	4	15	Chl	28.60		23.05	29.08		4.27																			85	51
H-23 5406.5m	5	1	Py				26.89							73.11														100	110
H-23 5406.5m	5	2	TiO_2+Chl (D)	3.19	93.76	2.14	0.55					0.35																100	52
H-23 5406.5m	5	3	TiO_2+Qz	43.90	51.06		1.79															3.26						100	65
H-23 5406.5m	5	4	Zrn	31.66																	68.34							100	67
H-23 5406.5m	5	5	Chl	33.84		21.04	20.67		8.91			0.54																85	52
H-23 5406.5m	5	6	TiO_2	1.39	94.63		3.98																					100	43
H-23 5406.5m	5	7	TiO_2	1.67	92.61	1.06	4.66																					100	41
H-23 5406.5m	5	8	Qz+Chl	40.99		27.91	16.71		14.41																			100	53
H-23 5406.5m	5	9	Qz	99.99																								100	68
H-23 5406.5m	6	1	TiO_2	1.43	95.36	1.59	1.62																					100	50
H-23 5406.5m	6	2	TiO_2	1.93	96.81		1.26																					100	54
H-23 5406.5m	6	3	TiO_2	2.27	94.35	1.78	1.61																					100	52
H-23 5406.5m	6	4	Chl+TiO_2	23.60	17.45	21.03	33.35		4.59																			100	43
H-23 5406.5m	6	5	Kln	48.86		37.14																						86	51
H-23 5406.5m	6	6	Ms+Chl+TiO_2	60.20	2.45	27.04	2.19		1.92			6.19																100	51
H-23 5406.5m	6	7	Ms+Chl	45.24	0.47	23.28	20.65		4.83		1.56	3.96																100	55
H-23 5406.5m	6	8	Ms+Chl+TiO_2	56.54	5.84	20.80	6.21		3.22		2.24	5.13																100	59
H-23 5406.5m	6	9	Chl	27.51		22.93	29.58		4.97																			85	45
H-23 5406.5m	6	10	Chl	27.22		23.60	29.33		4.86																			85	45
H-23 5406.5m	6	11	TiO_2	1.11	96.93		1.97																					100	46
H-23 5406.5m	6	12	Ab	60.82		20.67	7.94		0.96		9.61																	100	60
H-23 5406.5m	6	13	Kln	49.00		37.00																						86	23
H-23 5406.5m	6	14	Qz	99.99																								100	63
H-23 5406.5m	7	1	Tur	38.76		31.92	6.57		6.90	0.84	2.01																	87	53
H-23 5406.5m	7	2	Zrn	32.24																	67.76							100	64
H-23 5406.5m	7	3	TiO_2	2.44	91.24	2.02	2.05			0.45						0.69		1.11										100	37
H-23 5406.5m	7	4	TiO_2	1.82	92.46	1.66	1.75			0.48						0.74		1.10										100	33
H-23 5406.5m	7	5	Chl	29.90	2.03	24.30	23.85		4.39			0.52																85	45
H-23 5406.5m	7	6	Glt+Qz	61.97		8.50	12.66		7.38			9.48																100	54
H-23 5406.5m	7	7	Ab+Chl	52.30		24.09	14.50		2.52		5.99	0.59																100	50
H-23 5406.5m	7	8	Chl	26.42		18.47	32.62	0.43	5.93	1.13																		85	44
H-23 5406.5m	7	9	Chl	29.17		23.64	26.63		4.65					0.91														85	44
H-23 5406.5m	8	1	Tur	38.95		34.39	9.41		2.28		1.96																	87	49
H-23 5406.5m	8	2	Tur	38.64	0.46	33.58	8.67		3.57		2.08																	87	49
H-23 5406.5m	8	3	TiO_2	0.79	97.36		1.84																					100	48
H-23 5406.5m	8	4	TiO_2	2.03	95.51	1.06	1.39																					100	49

Table 2-7: Scanning Electron Microscope chemical analyses of sample 5406.5m from Newburn H-23 well.

Sample	Site	Position	Mineral	SiO_2	TiO_2	Al_2O_3	FeO	MnO	MgO	CaO	Na_2O	K_2O	P_2O_5	SO_3	F	Cl	Sc_2O_3	Cr_2O_3	CoO	Y_2O_3	ZrO_2	Nb_2O_5	Ce_2O_3	Gd_2O_3	Dy_2O_3	Yb_2O_3	HfO_2	Total	Actual Total
H-23 5406.5m	8	5	TiO_2	1.28	95.30	1.59	1.83																					100	49
H-23 5406.5m	8	6	TiO_2	0.86	96.85	1.00	1.31																					100	47
H-23 5406.5m	8	7	Ms+Chl	43.23	15.28	22.20	10.48		2.84			5.95																100	37
H-23 5406.5m	8	8	Zrn	31.17																	68.82							100	59
H-23 5406.5m	8	9	TiO_2		99.55		0.46																					100	50
H-23 5406.5m	9	1	Chl	30.88	1.05	21.46	25.51		6.10																			85	41
H-23 5406.5m	9	2	Chl	27.25		22.37	27.15		7.68	0.54																		85	45
H-23 5406.5m	9	3	Chl+Ms	57.20	0.78	22.96	10.47		6.43			2.17																100	55
H-23 5406.5m	9	4	Qz+Ms+Chl	65.82		24.60	3.47		0.80			5.32																100	50
H-23 5406.5m	9	5	Chl	29.54		23.34	27.78		3.92			0.42																85	44
H-23 5406.5m	9	6	TiO_2	2.82	91.13	1.53	4.52																					100	32
H-23 5406.5m	9	7	Qz	99.99																								100	53
H-23 5406.5m	9	8	Qz	99.99																								100	52
H-23 5406.5m	9	9	Chl	32.69		23.98	19.08	0.77	7.84			0.65																85	41
H-23 5406.5m	10	1	Sd	1.13			48.71	0.74	1.72	3.70																		56	23
H-23 5406.5m	10	2	Spl			18.99	26.53		10.31									44.17										100	45
H-23 5406.5m	10	3	TiO_2		98.57													1.43										100	51
H-23 5406.5m	10	4	TiO_2	1.48	96.91		1.62																					100	45
H-23 5406.5m	10	5	Chl	29.25		24.12	26.45		4.82							0.37												85	50
H-23 5406.5m	10	6	TiO_2		97.56		0.55							1.87														100	48
H-23 5406.5m	10	7	Spl			14.72	14.42	1.30	10.43									59.14										100	39
H-23 5406.5m	10	8	TiO_2+Chl	4.68	90.94	3.21	0.71					0.46																100	43
H-23 5406.5m	10	9	Chl	28.04		23.93	27.53		5.12	0.38																		85	36
H-23 5406.5m	10	10	Zrn	31.13																	68.86							100	56
H-23 5406.5m	10	11	Spl			28.14	21.79		13.95									36.12										100	51
H-23 5406.5m	10	12	Zrn	31.90																	66.66						1.44	100	49
H-23 5406.5m	11	1	TiO_2		98.98		1.02																					100	44
H-23 5406.5m	11	2	Spl	2.63	0.70	28.32	21.32		10.21									36.82										100	36
H-23 5406.5m	11	3	Sd+Qz	16.84		16.14	58.75	0.98	5.67	1.64																		100	35
H-23 5406.5m	11	4	Zrn	32.34																	67.65							100	50
H-23 5406.5m	11	5	Zrn	31.72																	68.28							100	47
H-23 5406.5m	11	6	Spl		1.97	20.75	33.33		6.45									37.51										100	40
H-23 5406.5m	11	7	Py				26.84							73.16														100	101
H-23 5406.5m	11	8	Zrn	31.49																	68.50							100	50
H-23 5406.5m	11	9	TiO_2	1.43	96.10	1.08	1.40																					100	37
H-23 5406.5m	11	10	TiO_2		98.80		1.20																					100	42
H-23 5406.5m	11	11	Zrn	29.59							5.27	1.06				2.03					62.06							100	60
H-23 5406.5m	12	1	Tur	38.90	0.61	33.65	5.13		6.19	0.37	2.16																	87	43
H-23 5406.5m	12	2	Zrn	31.23																	67.97						0.80	100	52
H-23 5406.5m	12	3	Py				27.04							72.96														100	92
H-23 5406.5m	12	4	TiO_2		99.02		0.99																					100	42
H-23 5406.5m	12	5	Ank				12.93	0.79	10.45	31.83																		56	25
H-23 5406.5m	12	6	TiO_2		98.23		1.76																					100	40
H-23 5406.5m	12	7	TiO_2+Chl	1.58	95.83	1.36	1.22																					100	40
H-23 5406.5m	12	8	Ank		3.42		12.03	0.77	10.31	29.47																		56	25
H-23 5406.5m	12	9	Qz	98.55	0.47		0.30			0.69																		100	51
H-23 5406.5m	12	10	TiO_2		96.91	1.61	1.48																					100	42
H-23 5406.5m	12	11	TiO_2	1.93	95.80		2.28																					100	42
H-23 5406.5m	13	1	Zrn	31.53																	68.47							100	59

Table 2-7: Scanning Electron Microscope chemical analyses of sample 5406.5m from Newburn H-23 well.

Sample	Site	Position	Mineral	SiO_2	TiO_2	Al_2O_3	FeO	MnO	MgO	CaO	Na_2O	K_2O	P_2O_5	SO_3	F	Cl	Sc_2O_3	Cr_2O_3	CoO	Y_2O_3	ZrO_2	Nb_2O_5	Ce_2O_3	Gd_2O_3	Dy_2O_3	Yb_2O_3	HfO_2	Total	Actual Total
H-23 5406.5m	13	2	Chl	33.18		24.73	22.05		4.07			0.97																85	37
H-23 5406.5m	13	3	Ms	48.16		34.44	1.67					10.72																95	46
H-23 5406.5m	13	4	Ab+Chl	46.98		25.21	21.47		3.85		2.49																	100	40
H-23 5406.5m	13	5	Chl	28.62		25.32	26.84		3.92							0.31												85	39
H-23 5406.5m	13	6	Chl	28.72		23.98	28.10		4.20																			85	39
H-23 5406.5m	13	7	Qz+Other	87.47	1.88	3.91	3.87		2.85																			100	50
H-23 5406.5m	13	8	Chl	32.23		22.04	21.83		8.89																			85	39
H-23 5406.5m	13	9	TiO_2+Qz+Other	24.39	71.76	1.87	1.97																					100	48
H-23 5406.5m	14	1	Ab	69.05		19.33					11.62																	100	48
H-23 5406.5m	14	2	Chl	30.46		24.07	25.39		4.72			0.37																85	36
H-23 5406.5m	14	3	TiO_2		98.08		1.92																					100	39
H-23 5406.5m	14	4	TiO_2		97.63		2.38																					100	42
H-23 5406.5m	14	5	TiO_2+Chl	1.24	95.30	1.44	2.03																					100	41
H-23 5406.5m	14	6	Ms	47.81	1.82	25.99	11.08		3.70			4.59																95	41
H-23 5406.5m	14	7	Kln	50.48		35.52																						86	33
H-23 5406.5m	15	1	Ab+Chl	43.70	0.78	37.26	12.80		2.89		2.55																	100	42
H-23 5406.5m	15	2	TiO_2+Qz	18.14	80.97		0.90																					100	46
H-23 5406.5m	15	3	Zrn	31.79																	68.22							100	44
H-23 5406.5m	15	4	Spl			30.18	14.82		11.44									43.56										100	40
H-23 5406.5m	15	5	TiO_2		98.08		1.92																					100	38
H-23 5406.5m	15	6	TiO_2	1.84	95.55	1.32	1.30																					100	37
H-23 5406.5m	15	7	Chl	27.04		24.86	28.60		4.50																			85	38
H-23 5406.5m	15	8	TiO_2	1.43	96.85		1.72																					100	41
H-23 5406.5m	15	9	Chl	27.97		23.41	29.14		4.48																			85	39
H-23 5406.5m	15	10	TiO_2	1.90	96.16		1.94																					100	35
H-23 5406.5m	16	1	Tur	39.16	1.55	29.78	5.69		7.49	0.82	2.52																	87	40
H-23 5406.5m	16	2	Qz	99.99																								100	48
H-23 5406.5m	16	3	TiO_2+Qz	9.73	90.26																							100	40
H-23 5406.5m	16	4	Zrn	31.45																	68.55							100	45
H-23 5406.5m	16	5	Ank				12.45	0.74	10.99	31.81																		56	22
H-23 5406.5m	16	6	TiO_2	1.11	97.36		1.53																					100	36
H-23 5406.5m	16	7	Zrn	31.49																	68.51							100	49
H-23 5406.5m	17	1	Ms+Chl+Other	57.42		25.98	3.87		1.72			6.01			4.51	0.50												100	35
H-23 5406.5m	17	2	Chl	29.60		18.79	22.71		4.68	4.16	1.11	0.35	3.60															85	36
H-23 5406.5m	17	3	TiO_2+Chl	8.96	86.42	3.17	1.44																					100	39
H-23 5406.5m	17	4	Qz+Other	94.04		3.14	2.07				0.74																	100	42
H-23 5406.5m	17	5	Chl+Py	40.75		25.45	25.97		4.84	0.60				2.37														100	35
H-23 5406.5m	17	6	Ilt+Chl	57.91	0.72	29.33	5.96		2.06			4.05																100	37
H-23 5406.5m	17	7	Kln	48.33	1.88	33.55	2.24																					86	38
H-23 5406.5m	17	8	Qz	99.99																								100	48
H-23 5406.5m	18	1	Xtm										42.14						1.55	44.95				2.10	4.41	4.85		100	38
H-23 5406.5m	18	2	Xtm										42.69						1.31	45.72					4.92	5.36		100	36
H-23 5406.5m	18	3	TiO_2+Chl	4.75	89.67	3.68	1.88																					100	35
H-23 5406.5m	18	4	TiO_2+Chl	2.91	93.49	1.53	2.08																					100	40
H-23 5406.5m	18	5	Cal+Other	1.88			3.31			94.82																		100	22
H-23 5406.5m	18	6	Kln	49.47		36.53																						86	37
H-23 5406.5m	18	7	Py				27.80							72.22														100	88
H-23 5406.5m	18	8	Chl+Ap	26.98		24.62	24.73		3.66	9.39			6.99	3.65														100	34
H-23 5406.5m	19	1	Spl			25.26	15.44		14.92									44.38										100	39

Table 2-7: Scanning Electron Microscope chemical analyses of sample 5406.5m from Newburn H-23 well.

Sample	Site	Position	Mineral	SiO_2	TiO_2	Al_2O_3	FeO	MnO	MgO	CaO	Na_2O	K_2O	P_2O_5	SO_3	F	Cl	Sc_2O_3	Cr_2O_3	CoO	Y_2O_3	ZrO_2	Nb_2O_5	Ce_2O_3	Gd_2O_3	Dy_2O_3	Yb_2O_3	HfO_2	Total	Actual Total
H-23 5406.5m	19	2	Ank	4.96		1.48	12.01	1.00	9.51	25.88	1.16																56	27
H-23 5406.5m	19	3	TiO_2		98.77		1.24																				100	40
H-23 5406.5m	19	4	Spl		0.77	27.68	27.76		8.01									35.80									100	40
H-23 5406.5m	19	5	Ms+TiO_2	46.46	24.77	22.15	0.86		0.99			4.73															100	29
H-23 5406.5m	19	6	TiO_2		96.48	1.68	1.85																				100	38
H-23 5406.5m	19	7	TiO_2	1.37	97.63		1.00																				100	37
H-23 5406.5m	19	8	Qz	99.99																							100	46
H-23 5406.5m	19	9	Kln	48.84		37.16																					86	34
H-23 5406.5m	20	1	Spl			11.22	15.45		13.95									59.39									100	39
H-23 5406.5m	20	2	Spl			18.93	23.70		10.99									46.38									100	37
H-23 5406.5m	20	3	TiO_2+Chl	18.31	45.30	14.34	18.78		3.25																		100	30
H-23 5406.5m	20	4	Zrn	30.70																	69.30						100	49
H-23 5406.5m	20	5	Chl	28.13		23.31	28.72		4.85																		85	34
H-23 5406.5m	20	6	Zrn	32.45																	67.54						100	48
H-23 5406.5m	20	7	Chl	28.88		23.06	28.75		4.31																		85	44
H-23 5406.5m	20	8	TiO_2+Chl	6.40	86.97	3.53	3.10																				100	31
H-23 5406.5m	20	9	Py				27.18							72.81													100	65
H-23 5406.5m	20	10	TiO_2+Other	1.54	96.38		2.08																				100	46
H-23 5406.5m	20	11	Spl			22.81	16.75		12.09									48.35									100	46
H-23 5406.5m	20	12	Zrn	32.58		5.67	5.90		1.14												54.72						100	50
H-23 5406.5m	20	13	Spl			10.09	21.43		5.90									62.59									100	40
H-23 5406.5m	20	14	Zrn	31.47																	68.53						100	50
H-23 5406.5m	20	15	Zrn	32.71																	67.30						100	51
H-23 5406.5m	20	16	Zrn	31.40																	68.59						100	49
H-23 5406.5m	20	17	TiO_2	0.79	99.22																						100	42
H-23 5406.5m	20	18	Py				26.45				2.82			70.24		0.50											100	96
H-23 5406.5m	20	19	Zrn	31.90																	68.11						100	37
H-23 5406.5m	20	20	Ab+Ank	30.16		10.11	13.33	1.03	9.63	29.76	5.97																100	25
H-23 5406.5m	20	21	Fap							47.15			44.71		6.46								1.69				100	41
H-23 5406.5m	20	22	Py	3.34			28.86							67.82													100	57
H-23 5406.5m	20	23	TiO_2		100.00																						100	28
H-23 5406.5m	20	24	Zrn	31.66																	68.34						100	44
H-23 5406.5m	20	25	Zrn	31.72																	68.28						100	49
H-23 5406.5m	20	26	Py	4.43		1.55	25.76				1.43			66.85													100	92

(D) = Detritral Mineral

Appendix 2-8: SEM-BSE images and EDS mineral analyses for sample Newburn H-23 5407m

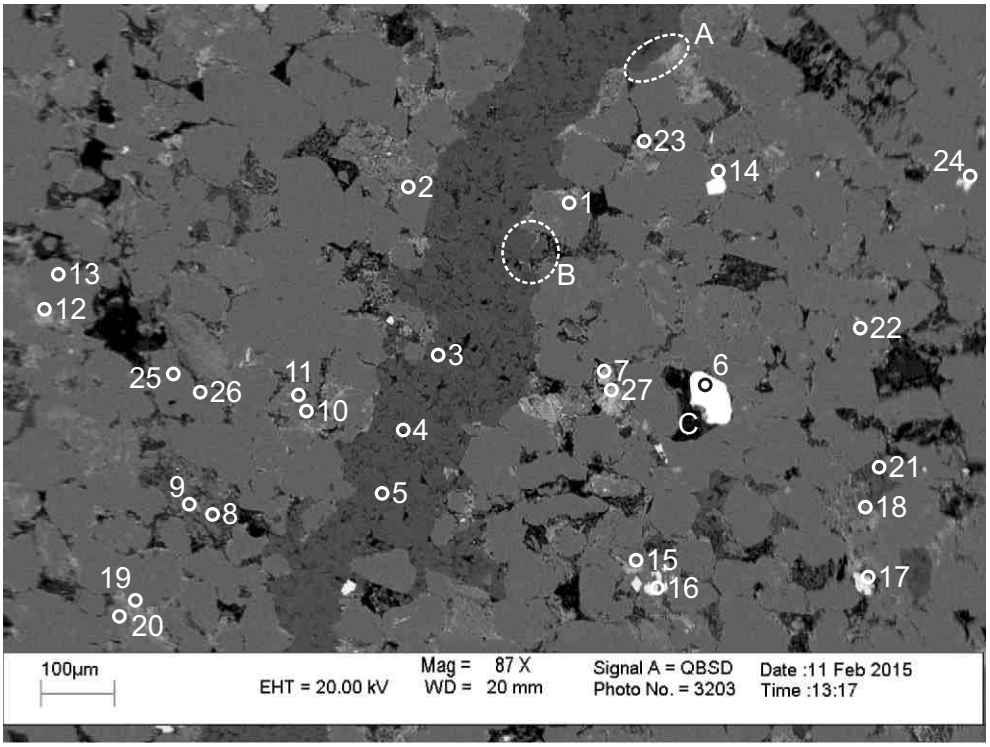

1: Albite
2: Quartz
3: Kaolinite
4: Kaolinite
5: Kaolinite
6: Zircon
7: Quartz+ Chlorite
8: Illite+ Chlorite
9: Illite+ Chlorite
10: Albite
11: Albite+ Chlorite
12: Quartz
13: Quartz
14: Quartz
15: Quartz
16: Albite+ Illite+ Chlorite
17: Quartz
18: Quartz
19: Quartz
20: Quartz
21: Quartz
22: Albite
23: Quartz
24: Quartz
25: Quartz
26: Quartz
27: Quartz

Figure 2-8.1: Sample Newburn 5407m site 1 (SEM). Table 2-8A. Kaolinite vein (3-5) fills fracture cutting framework quartz grains (position A). Chlorite cuts through kaolinite booklets in vein (position B). Diagenetic zircon (6) partially fills a pore with chlorite (position C). Chlorite and illite (16) fill dissolution voids in albite.

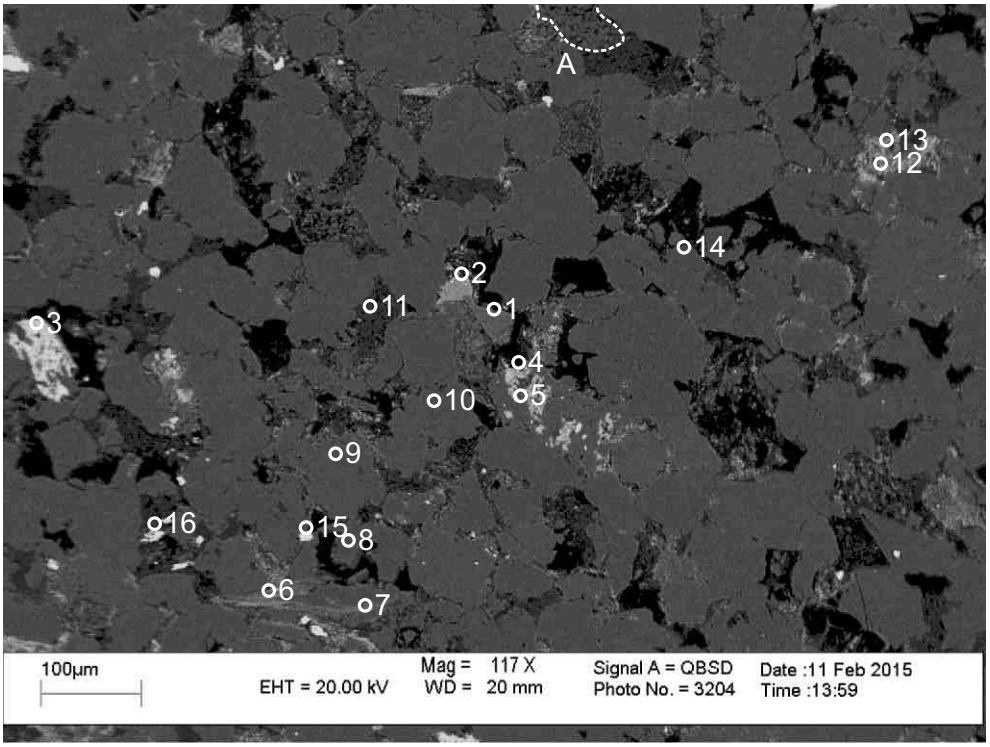

1: Kaolinite+ Other
2: F-Fe-Calcite
3: Titania+ Chlorite
4: Chlorite
5: Albite
6: Muscovite +Chlorite
7: Muscovite
8: Quartz
9: Albite
10: Albite
11: Kaolinite
12: Albite+ Chlorite
13: Chlorite
14: Quartz
15: Titania+ Quartz
16: Quartz+ Kaolinite

Figure 2-8.2: Sample Newburn 5407m site 2 (SEM). Table 2-8A. Chloritized muscovite (6,7). Chlorite (4) partially fills dissolution voids and engulfs albite (5). Titania (15) cuts quartz. Chlorite (12,13) engulfs kaolinite and fills pore. F-Fe-calcite (2) partially fills pore and engulfs kaolinite. Trachytic lithic clast (position B).

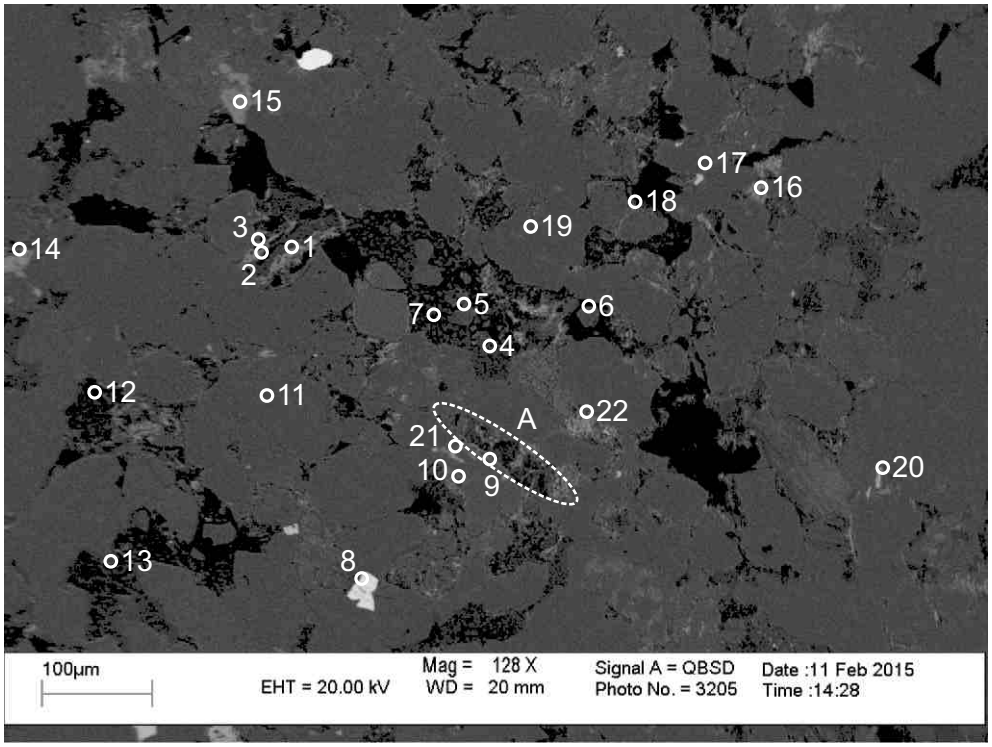

1: Chlorite
2: Muscovite+ Chlorite
3: Quartz+ Chlorite+ Pyrite
4: Kaolinite
5: Albite
6: Quartz
7: Kaolinite
8: Pyrite
9: Albite+ Chlorite
10: Albite
11: Quartz
12: Kaolinite+ Chlorite
13: Quartz+ Kaolinite
14: Chlorite
15: Ankerite+ Quartz
16: Chlorite
17: Quartz
18: Chlorite+ Albite+ Calcite
19: Quartz
20: Quartz
21: Albite
22: Quartz+ Chlorite

Figure 2-8.3: Sample Newburn 5407m site 3 (SEM). Table 2-8A. Chloritized muscovite (1-3). Chlorite (9) crosscuts kaolinite filling pore (position A). Ankerite (15) engulfs quartz. Pyrite (8) forms along intergranular boundary and engulfs quartz.

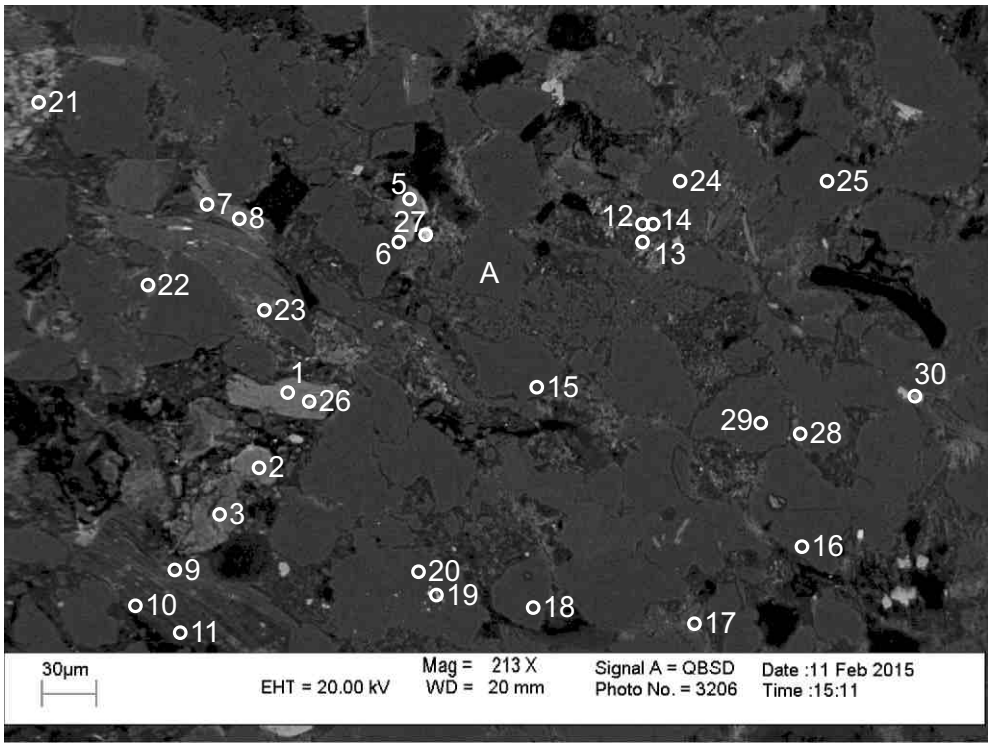

1: Chlorite
2: Chlorite+ Muscovite
3: Chlorite+ Muscovite
4: Titania
5: Chlorite+ Muscovite
6: Quartz
7: Chlorite
8: Chlorite
9: Albite+Chlorite
10: Kaolinite+ Chlorite
11: Kaolinite+ Chlorite
12: Chlorite+ Muscovite+ Calcite
13: Chlorite
14: Quartz
15: Quartz
16: Quartz
17: Chlorite+ Muscovite
18: Quartz
19: Zircon+ Albite+ Titania
20: Quartz
21: Siderite+ Chlorite
22: Chlorite
23: Quartz+ Chlorite
24: Albite
25: Quartz
26: Muscovite+ Chlorite
27: Pyrite
28: Albite
29: Quartz
30: Titania+ Quartz+ Other

Figure 2-8.4: Sample Newburn 5407m site 4 (SEM). Table 2-8A. Zircon (19) fills dissolution void in quartz (20). Trachytic lithic clast (position A). Siderite (21) engulfs kaolinite. Chlorite and kaolinite (9-11) replace muscovite along cleavage planes. Chloritized muscovite (1-3,5,7,8,12-14,23,26).

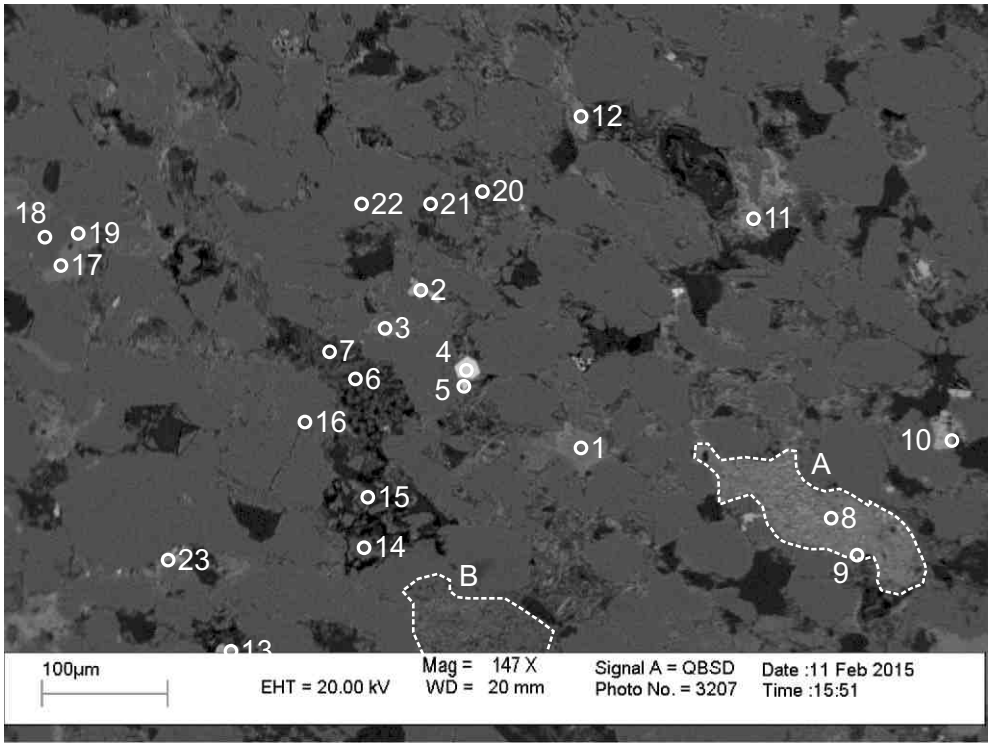

1: Chlorite
2: Titania+ Chlorite
3: Chlorite
4: Pyrite
5: Pyrite
6: Kaolinite
7: Muscovite+ Chlorite
8: Chlorite
9: Chlorite
10: Mix
11: Chlorite
12: Chlorite+ Muscovite
13: Titania+ Chlorite
14: Quartz
15: Kaolinite+ Other
16: Albite
17: F-Calcite
18: Albite
19: F-Calcite+ Other
20: Quartz
21: Quartz
22: Quartz
23: Albite

Figure 2-8.5: Sample Newburn 5407m site 5 (SEM). Table 2-8A. Subhedral pyrite (4,5) which fills porosity and cuts fibrous chlorite filling pore. Fine grained chlorite patch (position A). Kaolinite (6) replaces muscovite (7) and quartz and fills porosity. Trachytic lithic clast (position B).

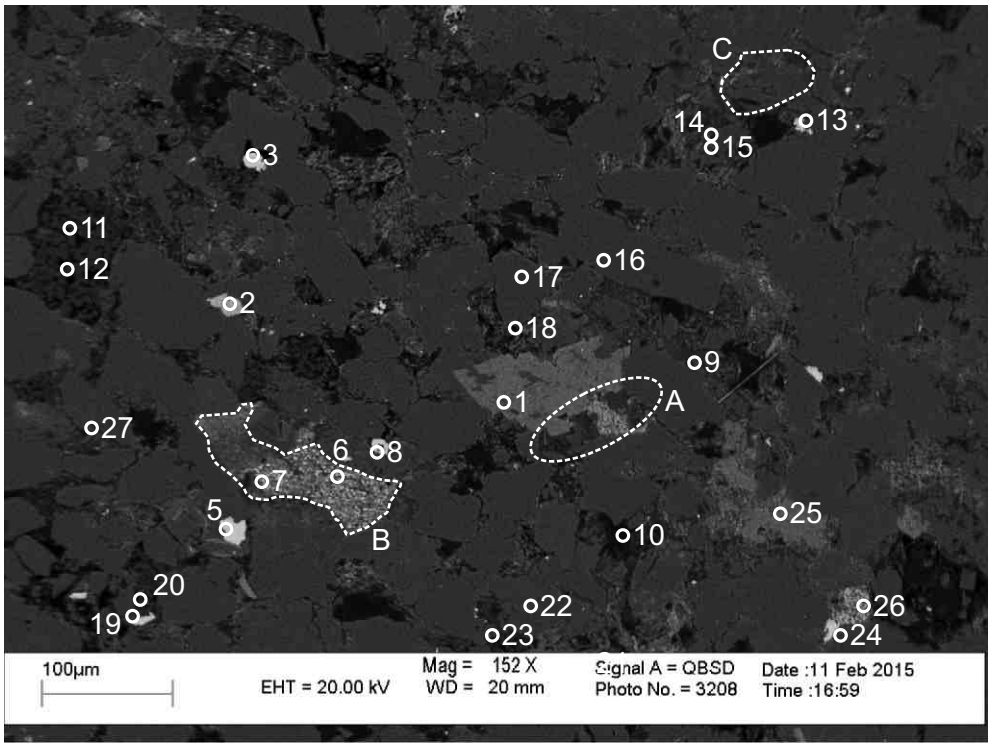

1: Albite+ Ankerite
2: Fluorapatite
3: Titania
4: Titania+ Kaolinite
5: Titania+ Chlorite
6: Chlorite+ Apatite
4
7: Chlorite+Other
8: Titania+Albite
9: Albite
10: Hole
11: Kaolinite
12: Kaolinite
13: Quartz
14: Kaolinite+ Chlorite
15: Albite+ Chlorite
16: Quartz
17: Quartz
18: Chlorite+ Quartz+ Titania
19: Titania+ Chlorite
20: Chlorite+ Illite+Pyrite
21: Pyrite
22: Albite
23: Albite+ Chlorite+ Kaolinite
24: Quartz
25: F-Calcite
26: Siderite+ Chlorite
27: Albite

Figure 2-8.6: Sample Newburn 5407m site 6 (SEM). Table 2-8A. Ankerite (1) engulfs albite. Kaolinite is engulfed by ankerite (1) and chlorite (position A). Apatite and chlorite (6,7) cement (position B). F-calcite (25) engulfs chlorite and fills pore.

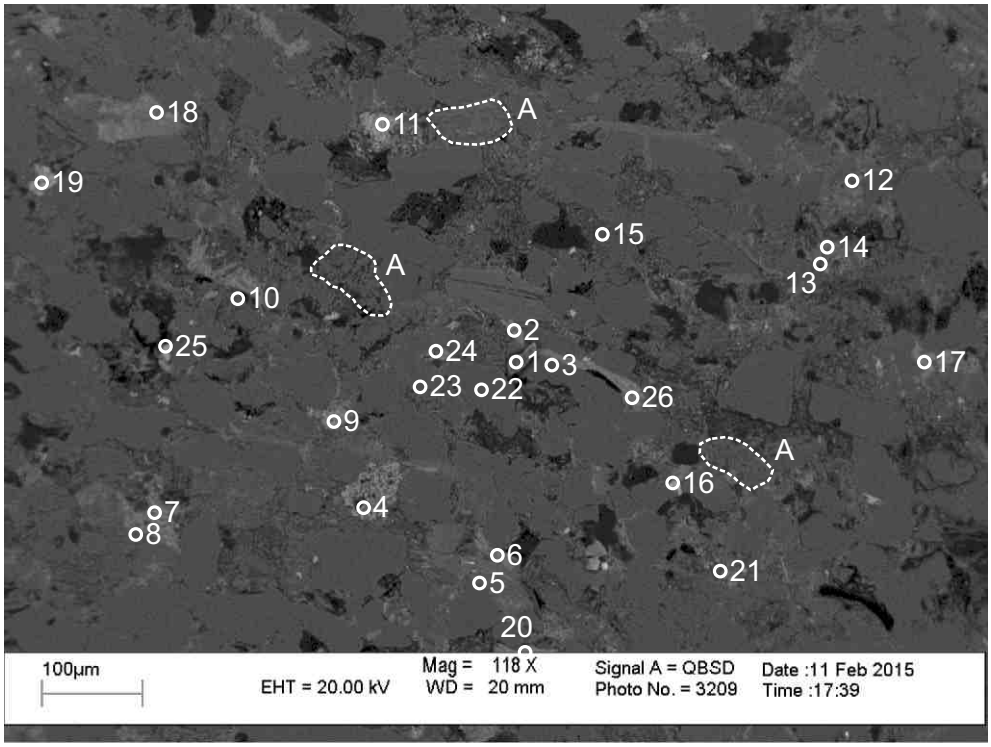

1: Glass (Slide)
2: Chlorite
3: Quartz
4: Mix
5: Muscovite
6: Chlorite
7: Chlorite
8: Albite
9: Siderite+ Chlorite
10: Quartz
11: Titania+ Other
12: Quartz+ Chlorite
13: Albite
14: Chlorite+ Other
15: Albite+ Pyrite
16: Titania+ Chlorite
17:Fluorapatite +Albite
18: Chlorite
19: Titania+ Chlorite+ Apatite
20: Chlorite+ Other
21: Chlorite+ Siderite
22: Quartz
23: Albite
24: Albite+ Chlorite
25: Titania+ Chlorite
26: Chlorite

Figure 2-8.7: Sample Newburn 5407m site 7 (SEM). Table 2-8A. Chlorite and siderite (21) fill porosity. Fluorapatite (17) fills dissolution voids in albite. Titania, chlorite and apatite (19) fill porosity. Trachytic lithic clast (position A).

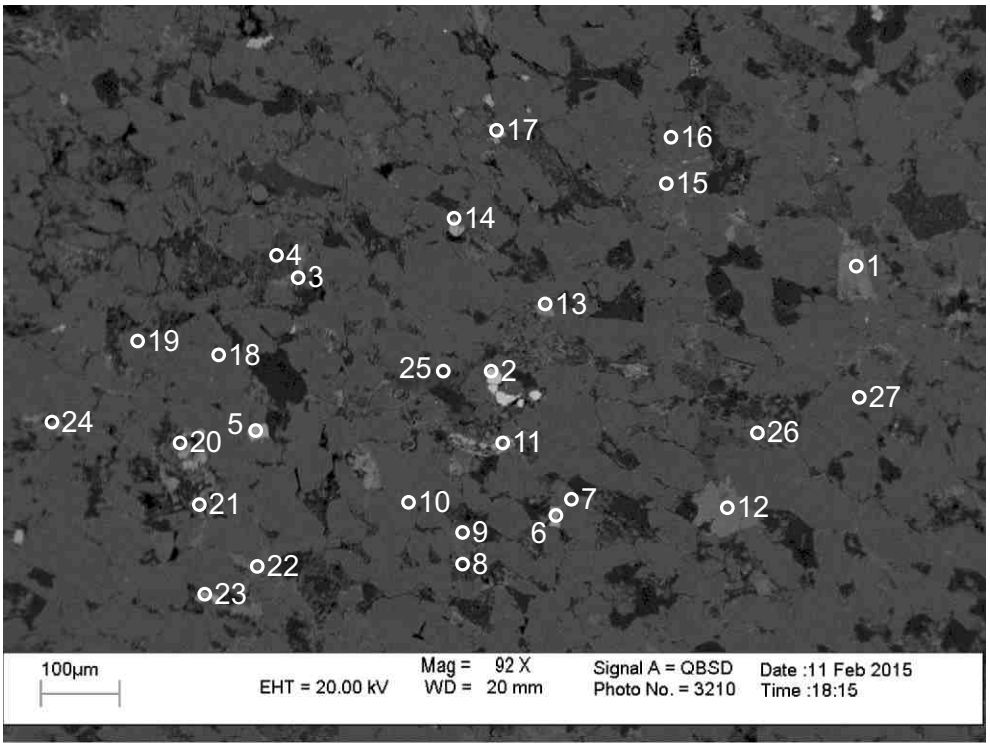

1: Chlorite
2: Pyrite
3: Chlorite
4: Kaolinite
5: Titania+ Chlorite
6: Quartz+ Other
7: Quartz
8: Chlorite
9: Quartz
10: Quartz
11: Titania
12: Ankerite+ Albite
13: Siderite+ Chlorite
14: Quartz
15: Albite+ Chlorite+ Apatite
16: Quartz
17: Quartz+ Muscovite+ Chlorite
18: Quartz
19: Quartz
20: Titania+ Chlorite
21: Chlorite
22: Chlorite
23: Titania+ Chlorite+ Quartz
24: Chlorite
25: Kaolinite
26: Chlorite
27: Quartz

Figure 2-8.8: Sample Newburn 5407m site 8 (SEM). Table 2-8A. Pyrite (2) fills dissolution void in quartz. Siderite (13) cuts chlorite and fills dissolution void. Ankerite (12) engulfs albite and kaolinite. Chlorite (3) partially rims pore filled by kaolinite.

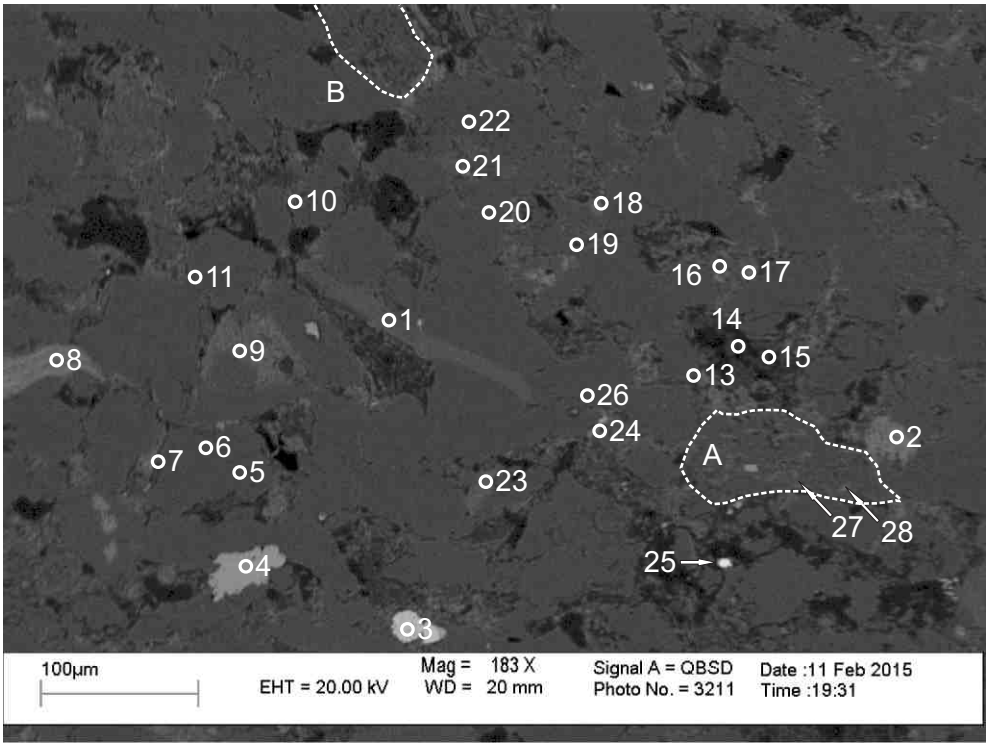

1: Muscovite
2: Chlorite
3: Pyrite
4: Titania+ Chlorite
5: Quartz
6: Quartz
7: Quartz+ Muscovite
8: Chlorite+ Calcite
9: Chlorite
10: Chlorite+Illite
11: Quartz
12: Muscovite+ Ankerite
13: Quartz+ Muscovite+ Chlorite
14: Kaolinite
15: Kaolinite+ Other
16: Albite
17: Chlorite
18: Quartz
19: Muscovite+ Chlorite
20: Albite
21: Albite
22: Quartz
23: Chlorite
24: Muscovite+ Chlorite
25: Quartz+ Sphalerite+ Kaolinite
26: Quartz
27: Quartz+Chlorite
28: Quartz+Chlorite

Figure 2-8.9: Sample Newburn 5407m site 9 (SEM). Table 2-8A. Plastically deformed muscovite (1). Chlorite laths (27,28) fill dissolution in quartz. Pyrite (3) cuts kaolinite and possibly quartz. Titania (4) cuts quartz grains and fills porosity. Sphalerite (25) partially fills pore. Granitoid lithic clast (position A) composed of quartz and chlorite (27,28). Trachytic lithic clast (position B).

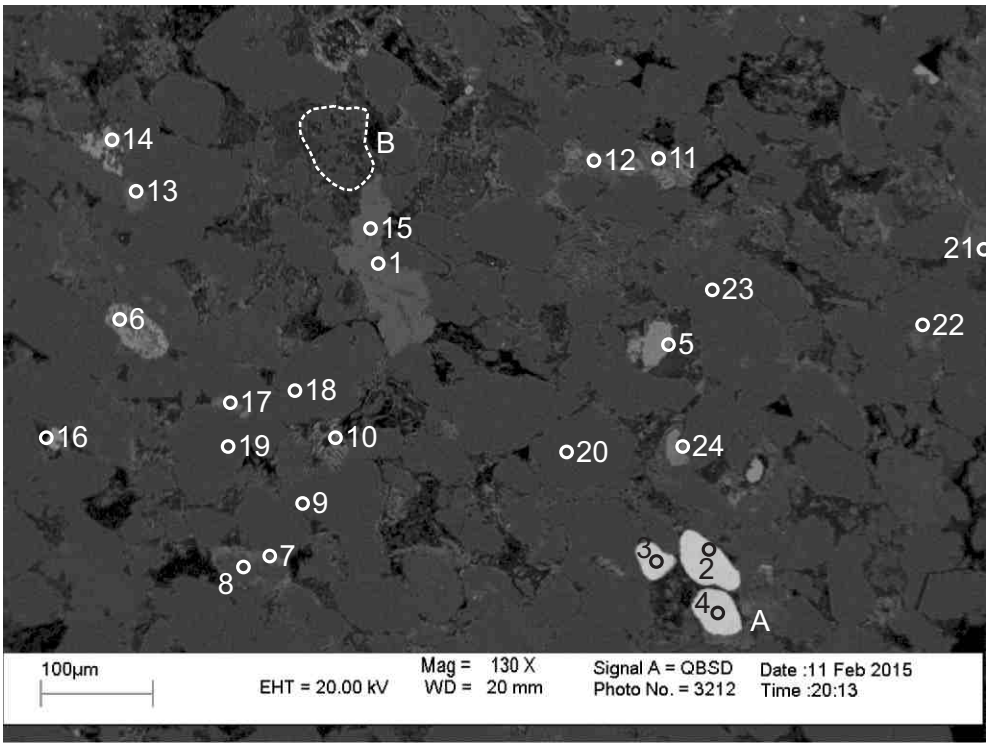

1: Ankerite
2: Zircon
3: Zircon
4: Zircon
5: Siderite
6: Titania+ Chlorite
7: Chlorite
8: Quartz
9: Quartz
10: Chlorite+ Titania+ Muscovite
11: Chlorite
12: Chlorite
13: Chlorite
14: Titania
15: Ankerite
16: Titania
17: Chlorite
18: Quartz
19: Quartz
20: Quartz
21: Muscovite+ Chlorite
22: Quartz+ Chlorite
23: Quartz
24: Mix

Figure 2-8.10: Sample Newburn 5407m site 10 (SEM). Table 2-8A. Zircon (2-4) is possibly detrital, rimmed by chlorite (position A) and inhibits quartz overgrowth. Siderite (5) engulfs kaolinite filling a pore. Ankerite (1,15) engulfs quartz and kaolinite. Chlorite (7) rims quartz (8) grain. Chlorite and titania (10) forms along the cleavage planes of muscovite. Trachytic lithic clast (position B).

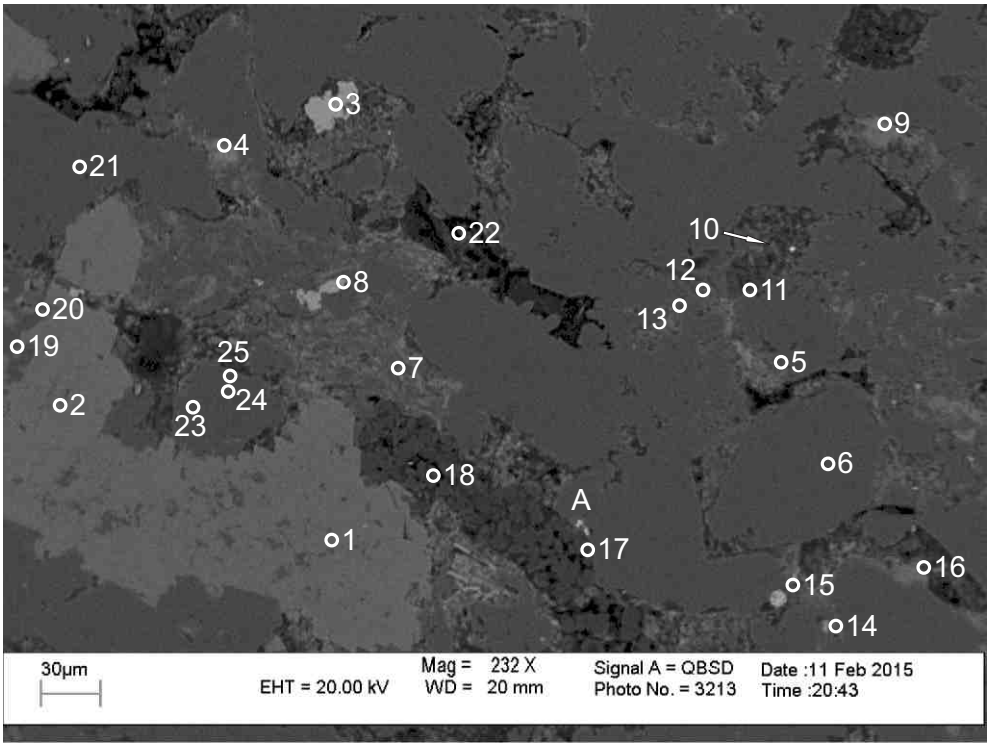

1: Ankerite
2: Ankerite
3: Titania+Other
4: Chlorite
5: Quartz+ Chlorite
6: Quartz
7: Illite+Chlorite
8: Titania+Other
9: Chlorite+ Apatite
10: Illite+Chlorite
11: Quartz+ Chlorite
12: Illite+Chlorite
13: Albite
14: Albite+Illite
15: Chlorite
16: Chlorite+ Calcite
17: Quartz
18: Kaolinite
19: Quartz+ Ankerite
20: Quartz
21: Quartz
22: Chlorite
23: Quartz
24: Quartz
25: Quartz

Figure 2-8.11: Sample Newburn 5407m site 11 (SEM). Table 2-8A. Kaolinite (18) vein (position A) fills fracture and is engulfed by ankerite (1), chlorite and illite (7). Chlorite and apatite (9) fills porosity. Fibrous chlorite (15) fills pore. Fibrous chlorite (10,11) cuts illite (10).

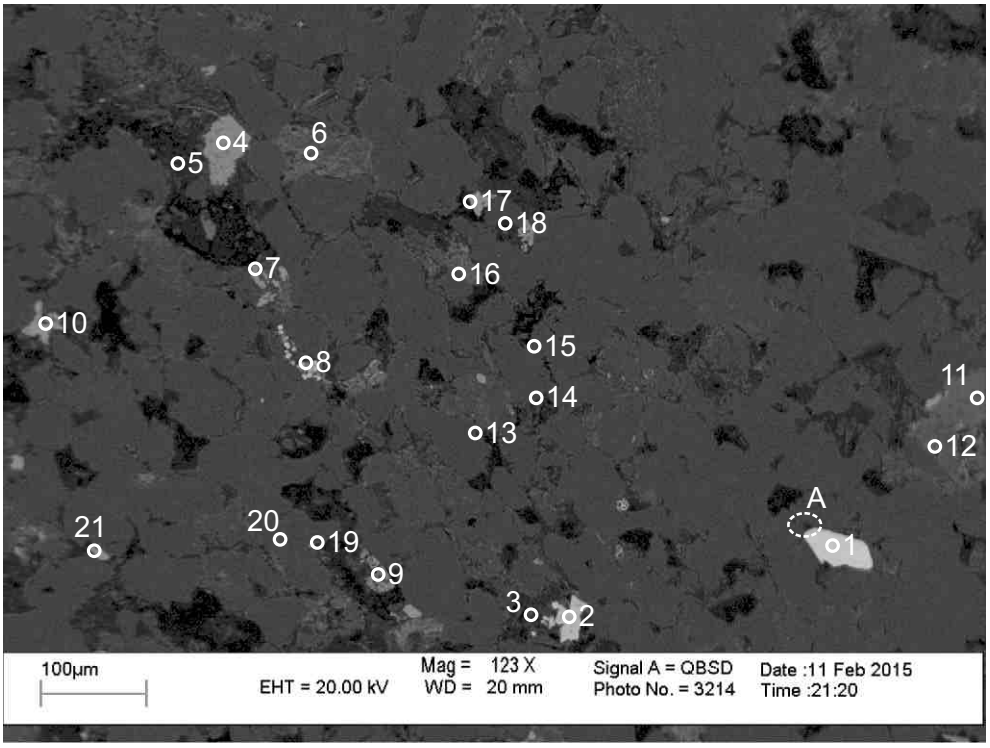

1: Zircon
2: Pyrite
3: Albite
4: Titania+Other
5: Kaolinite
6: Illite+ Chlorite+ Titania
7: Quartz+ Titania+ Other
8: Pyrite
9: Quartz+ Titania
10: Titania+ Kaolinite
11: Ankerite+ Albite
12: Muscovite+ Chlorite+ Titania
13: Quartz
14: Kaolinite+ Quartz
15: Quartz
16: Chlorite
17: Titania+ Chlorite
18: Quartz+ Chlorite+ Pyrite
19: Chlorite+ Muscovite
20: Albite
21: Tiania+ Chlorite

Figure 2-8.12: Sample Newburn 5407m site 12 (SEM). Table 2-8A. Diagenetic zircon (1) fills pore and cuts quartz. Chlorite (6) engulfs illite. Subhedral pyrite (2) cuts albite (3). Titania (10) engulfs kaolinite. Pyrite (8) forms along intergranular boundary. Quartz overgrowth (position A).

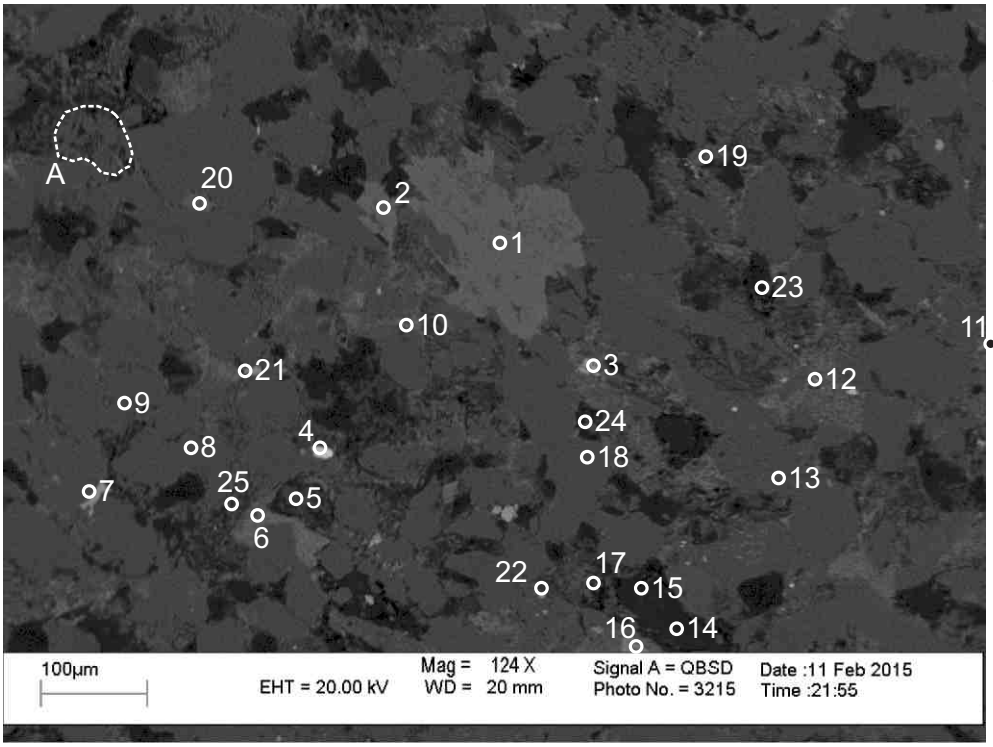

1: Ankerite
2: Ankerite
3: Pyrite
4: Zircon
5: Muscovite+ Kaolinite+ Ankerite
6: Chlorite+ Muscovite
7: Titania+Albite
8: Quartz
9: Quartz+ Other
10: Chlorite+ Apatite
11: Albite+ Chlorite+ Apatite
12: Pyrite+ Kaolinite
13: Albite
14: Drilling Mud
15: Drilling Mud
16: Siderite+ Chlorite
17: Albite
18: Quartz
19: Illite+Chlorite
20: Chlorite
21: Titania+ Quartz
22: Chlorite+ Titania+ Illite
23: Chlorite+Illite
24: Quartz+Other
25: Chlorite+ Albite

Figure 2-8.13: Sample Newburn 5407m site 13 (SEM). Table 2-8A. Ankerite (1,2) engulfs albite/quartz. Titania (21) cuts quartz. Trachytic lithic clast (position A).

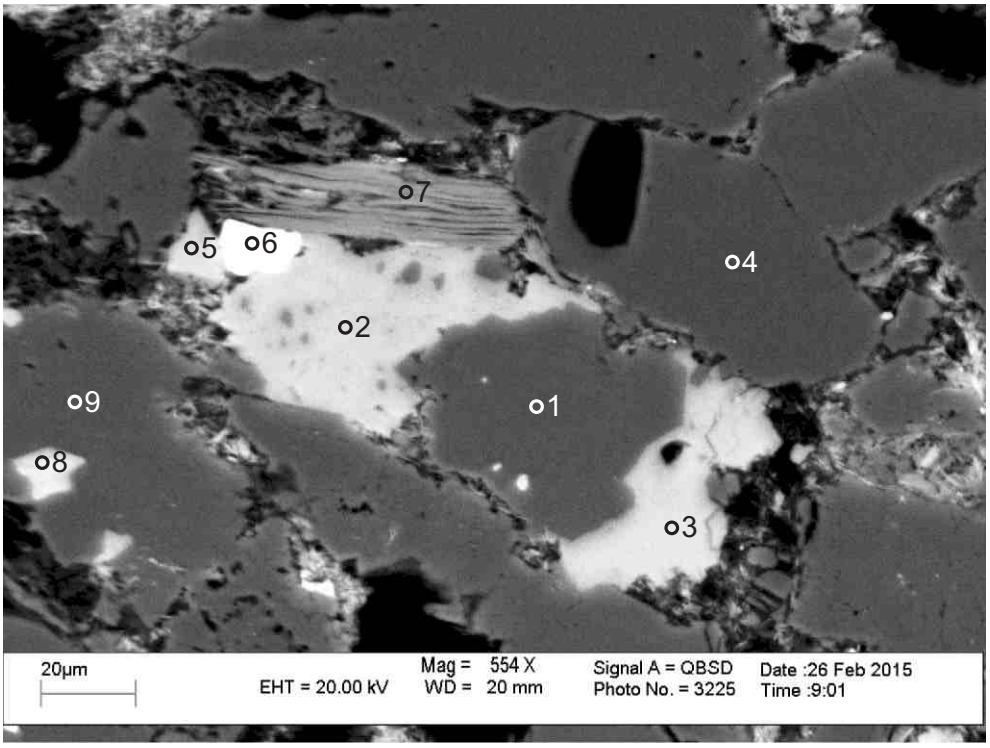

1. Albite
2. F-Calcite+ Other
3. F-Calcite
4. Quartz
5. F-Calcite+ Titania+ Quartz
6. Titania+ Chlorite
7. Muscovite +Chlorite
8. Chlorite
9. Albite

Figure 2-8.14: Sample Newburn 5407m site 1 (SEM). Table 2-8B. Chlorite (8) probably fills dissolution void in albite. F-calcite (2,3) engulfs albite (1). Titania (6) cuts F-calcite (2,5).

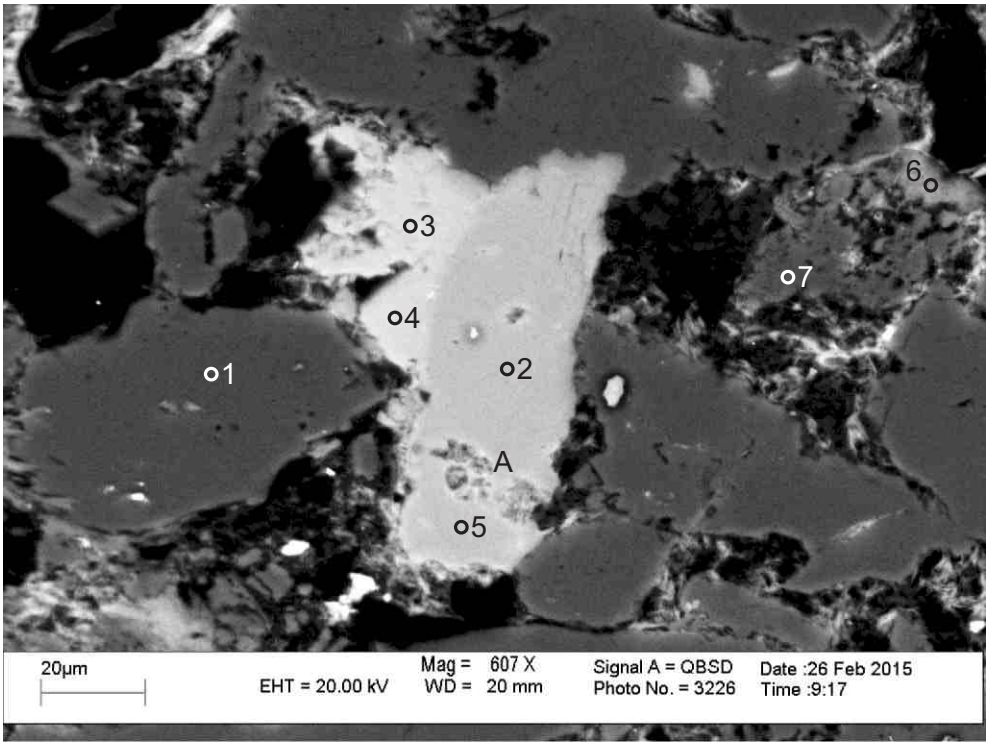

1. Quartz
2. F-Calcite+ Chlorite+ Pyrite
3. F-Fe-Calcite
4. F-Fe-Calcite
5. F-Calcite
6. Illite+ Chlorite
7. Albite

Figure 2-8.15: Sample Newburn 5407m site 2 (SEM). Table 2-8B. Illite (6) engulfs albite and is surrounded by chlorite. F-calcite (2,5) shows dissolution voids filled by fibrous chlorite (position A) and is replaced by F-Fe-calcite (3,4).

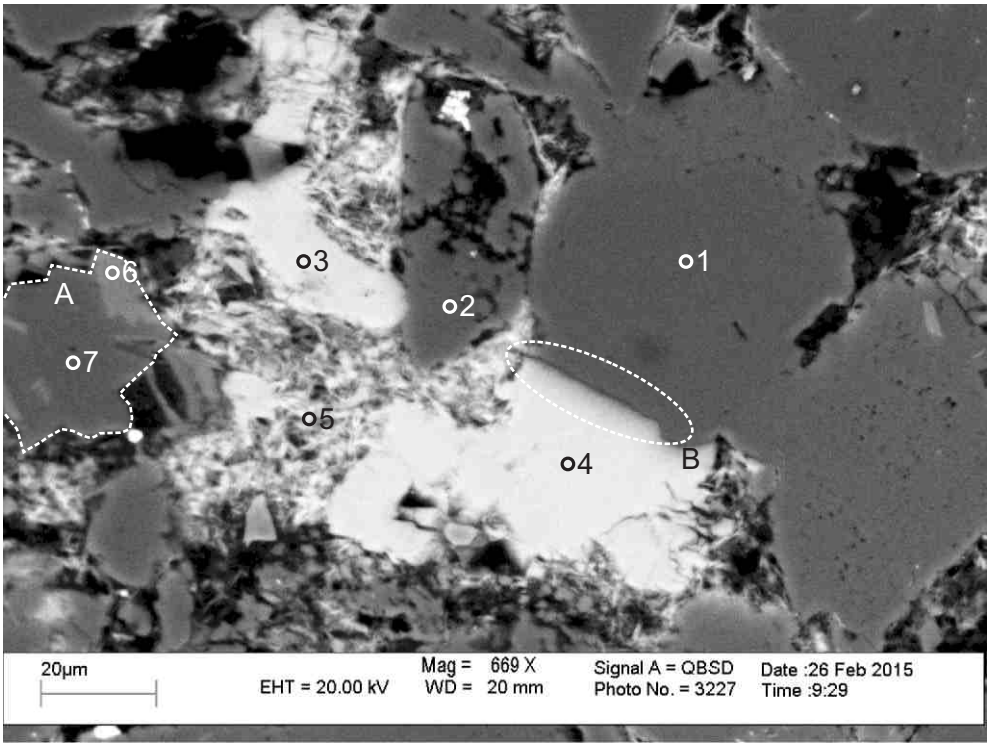

1. Quartz
2. Quartz
3. F-Calcite+ Ankerite
4. F-Calcite+ Ankerite
5. Chlorite+ Calcite
6. Muscovite
7. Quartz

Figure 2-8.16: Sample Newburn 5407m site 3 (SEM). Table 2-8B. Fibrous chlorite (5) engulfs F-calcite (3,4). Granitoid lithic clast (position A) composed of quartz (7) and muscovite (6). F-calcite (4) appears to corrode quartz (1) along quartz overgrowth (position B).

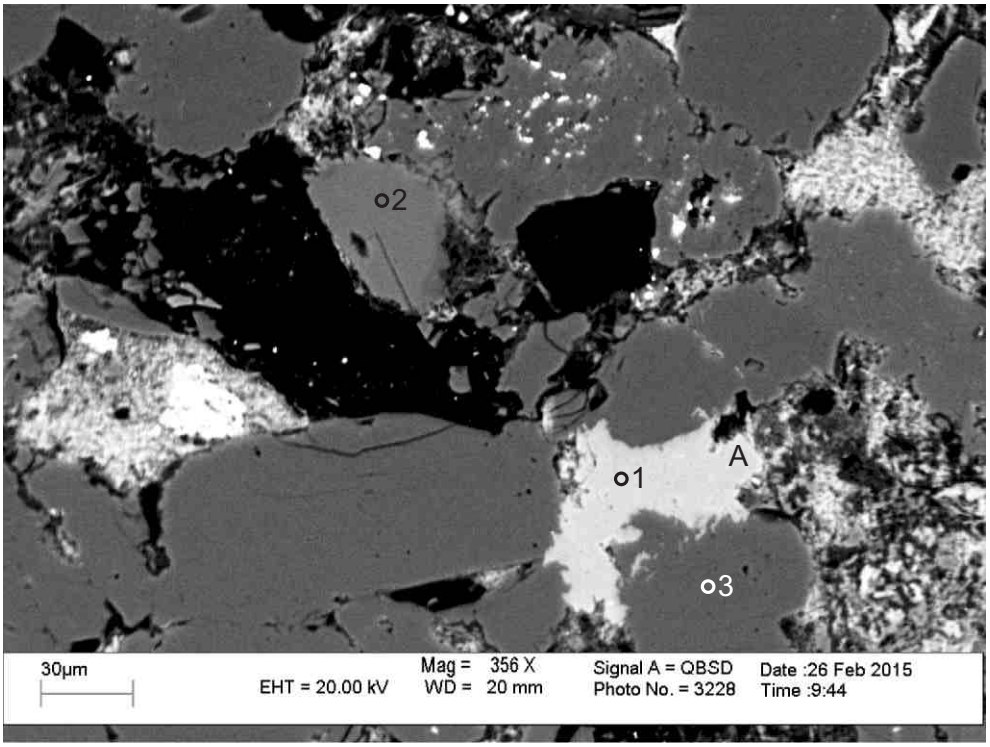

1. Ankerite+ Quartz
2. Oligoclase
3. Quartz

Figure 2-8.17: Sample Newburn 5407m site 4 (SEM). Table 2-8B. Ankerite (1) engulfs quartz (3) and chlorite (position A).

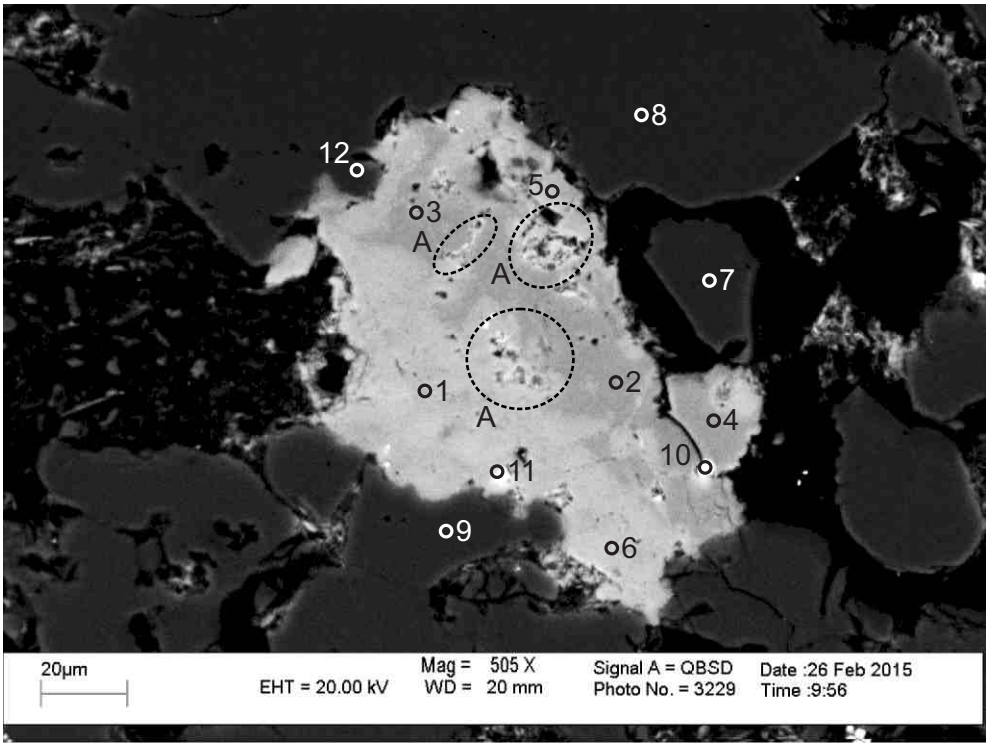

1. F-Fe-Calcite
2. F-Calcite
3. F-Calcite+ Chlorite
4. F-Calcite+ Chlorite
5. F-Calcite+ Chlorite
6. F-Fe-Calcite
7. Quartz
8. Quartz
9. Quartz
10. Pyrite+ F-Calcite +Chlorite
11. Pyrite+ F-Calcite +Chlorite
12. Quartz+ Chlorite+ Calcite

Figure 2-8.18: Sample Newburn 5407m site 5 (SEM). Table 2-8B. F-calcite (2,4) replaced by lighter F-Fe-calcite (1,6). Pyrite (10,11) fills dissolution in F-calcite (1-6,10,11). Chlorite (positions A) fills dissolution voids in F-calcite (5).

Table 2-8A: Scaning Electron Microscope chemical analyses of sample 5407m from Newburn H-23 well.

Sample	Site	Position	Mineral	SiO_2	TiO_2	Al_2O_3	FeO	MnO	MgO	CaO	Na_2O	K_2O	P_2O_5	SO_3	F	Cl	Sc_2O_3	ZnO	ZrO_2	WO_3	Total	Actual Total
H-23 5407m	1	1	Ab	75.68		14.64					9.41	0.26									100	104
H-23 5407m	1	2	Qz	99.32		0.68															100	95
H-23 5407m	1	3	Kln	48.15		36.24									1.61						86	77
H-23 5407m	1	4	Kln	48.90		36.81	0.28														86	74
H-23 5407m	1	5	Kln	48.09		36.68									1.24						86	75
H-23 5407m	1	6	Zrn	72.95															27.06		100	94
H-23 5407m	1	7	Qz+Chl	88.22		5.10	4.55		0.91	0.45				0.55		0.23					100	81
H-23 5407m	1	8	Ilt+Chl	73.03	0.95	17.44	1.85		1.74	0.66		3.96				0.35					100	63
H-23 5407m	1	9	Ilt+Chl	61.63	0.68	26.09	2.60		2.50		0.49	5.65				0.33					100	66
H-23 5407m	1	10	Ab	65.57		21.92	1.14				11.37										100	77
H-23 5407m	1	11	Ab+Chl	59.32		27.95	4.07		1.04		7.29					0.33					100	69
H-23 5407m	1	12	Qz	99.99																	100	73
H-23 5407m	1	13	Qz	99.99																	100	73
H-23 5407m	1	14	Qz	99.99																	100	85
H-23 5407m	1	15	Qz	99.99																	100	80
H-23 5407m	1	16	Ab+Ilt+Chl	80.97		10.94	2.29		0.86		3.87	1.07									100	76
H-23 5407m	1	17	Qz	99.99																	100	82
H-23 5407m	1	18	Qz	98.83		1.15															100	82
H-23 5407m	1	19	Qz	99.67			0.32														100	68
H-23 5407m	1	20	Qz	95.99	0.42	1.55	0.89		0.43	0.32		0.39									100	64
H-23 5407m	1	21	Qz	99.99																	100	81
H-23 5407m	1	22	Ab	67.45		19.25				0.31	13.00										100	85
H-23 5407m	1	23	Qz	99.99																	100	76
H-23 5407m	1	24	Qz	99.99																	100	80
H-23 5407m	1	25	Qz	99.99																	100	66
H-23 5407m	1	26	Qz	99.99																	100	67
H-23 5407m	1	27	Qz	99.73			0.27														100	75
H-23 5407m	2	1	Kln+Other	44.52	0.75	39.64	7.08		5.19	0.35	2.47										100	62
H-23 5407m	2	2	F-Fe-Cal				1.87		0.99	43.03					10.10						56	35
H-23 5407m	2	3	TiO_2+Chl	5.13	89.62	2.31	2.30		0.63												100	48
H-23 5407m	2	4	Chl	31.88		22.92	22.82		5.07	0.45	0.95			0.91							85	52
H-23 5407m	2	5	Ab	67.41		19.18	0.58				12.82										100	72
H-23 5407m	2	6	Ms+Chl	46.16	0.42	32.88	7.17		6.95		0.67	5.77									100	58
H-23 5407m	2	7	Ms	51.53	0.45	31.05	0.98		1.62		0.55	8.82									95	62
H-23 5407m	2	8	Qz	99.99																	100	63
H-23 5407m	2	9	Ab	67.51		19.20				0.32	12.97										100	68
H-23 5407m	2	10	Ab	68.09		18.73					13.20										100	68

Table 2-8A: Scaning Electron Microscope chemical analyses of sample 5407m from Newburn H-23 well.

Sample	Site	Position	Mineral	SiO_2	TiO_2	Al_2O_3	FeO	MnO	MgO	CaO	Na_2O	K_2O	P_2O_5	SO_3	F	Cl	Sc_2O_3	ZnO	ZrO_2	WO_3	Total	Actual Total
H-23 5407m	2	11	Kln	49.64		36.36															86	50
H-23 5407m	2	12	Ab+Chl	42.14		25.15	21.95		5.39	0.63	4.33					0.42					100	49
H-23 5407m	2	13	Chl	27.51		21.23	28.51	0.63	6.12	0.69						0.31					85	40
H-23 5407m	2	14	Qz	98.32		0.98	0.69														100	61
H-23 5407m	2	15	TiO_2+Qz	39.58	58.58											1.84					100	12
H-23 5407m	2	16	Qz+Kln	79.02	1.67	16.74	1.04			0.57		0.96									100	47
H-23 5407m	3	1	Chl	29.25		23.96	25.96		4.62	0.82						0.38					85	40
H-23 5407m	3	2	Ms+Chl	45.42		24.51	19.86		2.67	1.79		3.55		1.40		0.81					100	26
H-23 5407m	3	3	Qz+Chl+Py	66.74		12.89	15.14		2.70	0.53				1.62		0.37					100	35
H-23 5407m	3	4	Kln	48.64		37.13										0.22					86	48
H-23 5407m	3	5	Ab	67.96		18.84					13.20										100	64
H-23 5407m	3	6	Qz	99.99																	100	59
H-23 5407m	3	7	Kln	50.26		35.74															86	48
H-23 5407m	3	8	Py				24.69				0.65			74.66							100	95
H-23 5407m	3	9	Ab+Chl	45.33		24.17	19.48		2.93	1.13	5.76	0.67				0.52					100	41
H-23 5407m	3	10	Ab	65.61		20.10	1.43				12.66	0.19									100	64
H-23 5407m	3	11	Qz	99.99																	100	57
H-23 5407m	3	12	Kln+Chl	50.46		31.03	10.52		2.82	0.80	0.86			2.40		1.12					100	23
H-23 5407m	3	13	Qz+Kln	65.67		29.87	2.35		0.96	0.50						0.61					100	27
H-23 5407m	3	14	Chl	31.22		24.70	22.47		5.65	0.68						0.28					85	37
H-23 5407m	3	15	Ank+Qz	1.43			24.97	1.61	21.89	50.11											100	26
H-23 5407m	3	16	Chl	32.29		24.27	22.44		4.48	0.82		0.55				0.31		-0.16			85	44
H-23 5407m	3	17	Qz	99.62			0.37														100	61
H-23 5407m	3	18	Chl+Ab+Cal	43.70		23.20	21.01		3.50	1.11	1.19	0.69		4.37		1.26					100	20
H-23 5407m	3	19	Qz	99.99																	100	59
H-23 5407m	3	20	Qz	98.19		0.57	0.44			0.80											100	60
H-23 5407m	3	21	Ab	68.09		18.74					13.16										100	61
H-23 5407m	3	22	Qz+Chl	85.27		6.58	6.78		1.36												100	56
H-23 5407m	4	1	Chl	29.58	0.98	21.78	26.16		5.12	0.83	0.55										85	42
H-23 5407m	4	2	Chl+Ms	39.94		23.86	18.90		15.67			1.63									100	46
H-23 5407m	4	3	Chl+Ms	37.84	0.48	23.05	22.51		15.07			1.02									100	39
H-23 5407m	4	4	TiO_2		100.00																100	40
H-23 5407m	4	5	Chl+Ms	46.44		24.19	13.71		12.80			2.87									100	50
H-23 5407m	4	6	Qz	99.56			0.44														100	55
H-23 5407m	4	7	Chl	31.82		23.00	20.53		8.78	0.35	0.53										85	43
H-23 5407m	4	8	Chl	26.48		18.31	27.36	0.58	10.19	1.24	0.83										85	38
H-23 5407m	4	9	Ab+Chl	53.63	0.58	22.32	12.22		3.27		7.97										100	48

Table 2-8A: Scaning Electron Microscope chemical analyses of sample 5407m from Newburn H-23 well.

Sample	Site	Position	Mineral	SiO_2	TiO_2	Al_2O_3	FeO	MnO	MgO	CaO	Na_2O	K_2O	P_2O_5	SO_3	F	Cl	Sc_2O_3	ZnO	ZrO_2	WO_3	Total	Actual Total
H-23 5407m	4	10	Kln+Chl	52.17		39.13	6.93		1.77												100	43
H-23 5407m	4	11	Kln+Chl	52.26		38.89	6.99		1.86												100	37
H-23 5407m	4	12	Chl+Ms+Cal	33.37		20.41	33.11	0.70	8.54	2.04		1.32				0.52					100	35
H-23 5407m	4	13	Chl	27.36		20.38	27.82	0.44	6.17	1.16	0.66	0.66				0.34					85	35
H-23 5407m	4	14	Qz	97.87		1.91						0.23									100	55
H-23 5407m	4	15	Qz	99.99																	100	54
H-23 5407m	4	16	Qz	99.99																	100	55
H-23 5407m	4	17	Chl+Ms	42.14		24.17	20.42		10.28	0.55	0.80	1.66									100	39
H-23 5407m	4	18	Qz	99.99																	100	53
H-23 5407m	4	19	Zrn+Ab+TiO_2	50.63	4.45	4.95				0.60	3.06						0.51		35.80		100	50
H-23 5407m	4	20	Qz	99.99																	100	53
H-23 5407m	4	21	Sd+Chl	11.10		6.25	62.51	2.43	13.70	3.51						0.48					100	24
H-23 5407m	4	22	Chl	32.99		22.26	20.74		8.61			0.40									85	39
H-23 5407m	4	23	Qz+Chl	74.25		11.89	11.08		2.37			0.41									100	45
H-23 5407m	4	24	Ab	68.30		18.80					12.89										100	58
H-23 5407m	4	25	Qz	99.99																	100	55
H-23 5407m	4	26	Ms+Chl	53.93	0.47	26.38	8.79		6.20			4.23									100	44
H-23 5407m	4	27	Py	0.94		0.32	25.15		0.33		0.51			72.74							100	85
H-23 5407m	4	28	Ab	67.06		18.97	0.66				13.32										100	59
H-23 5407m	4	29	Qz	99.99																	100	54
H-23 5407m	4	30	TiO_2+Qz+Other	7.51	89.12	1.83	1.54														100	42
H-23 5407m	5	1	Chl	28.89		23.16	26.50		4.54	1.59						0.31					85	39
H-23 5407m	5	2	TiO_2+Chl	2.35	94.20	1.72	1.74														100	42
H-23 5407m	5	3	Chl	28.91		24.62	26.26		4.93							0.28					85	38
H-23 5407m	5	4	Py				25.59				0.43			73.99							100	90
H-23 5407m	5	5	Py	1.20		0.64	25.28		0.38		0.40			72.09							100	83
H-23 5407m	5	6	Kln	51.02		34.12	0.44									0.42					86	30
H-23 5407m	5	7	Ms+Chl	55.88		30.50	1.44		1.28	1.55		5.07			4.05	0.25					100	39
H-23 5407m	5	8	Chl	28.12		21.31	25.40		9.08	0.54	0.55										85	41
H-23 5407m	5	9	Chl	31.11		23.64	23.25		5.42	0.54	0.50	0.28				0.25					85	39
H-23 5407m	5	10	Mix	21.86	61.23	3.31	3.52		3.10	1.15	1.93			3.37		0.51					100	22
H-23 5407m	5	11	Chl	29.71		24.62	25.48		4.73	0.45											85	40
H-23 5407m	5	12	Chl+Ms	42.21		29.74	15.21		9.27			3.60									100	41
H-23 5407m	5	13	TiO_2+Chl	10.42	68.66	9.18	8.53		2.45		0.77										100	37
H-23 5407m	5	14	Qz	98.55		1.17						0.28									100	51
H-23 5407m	5	15	Kln+Other	55.53		33.46	7.11		1.87	0.42		1.34				0.25					100	38
H-23 5407m	5	16	Ab	64.92	0.65	19.39	1.69		0.53		12.43	0.39									100	51

Table 2-8A: Scaning Electron Microscope chemical analyses of sample 5407m from Newburn H-23 well.

Sample	Site	Position	Mineral	SiO_2	TiO_2	Al_2O_3	FeO	MnO	MgO	CaO	Na_2O	K_2O	P_2O_5	SO_3	F	Cl	Sc_2O_3	ZnO	ZrO_2	WO_3	Total	Actual Total
H-23 5407m	5	17	F-Cal				0.94			39.17					15.89						56	27
H-23 5407m	5	18	Ab	68.13		18.67					13.20										100	53
H-23 5407m	5	19	F-Cal+Other	3.14			1.36			67.68					27.80						100	28
H-23 5407m	5	20	Qz	99.99																	100	50
H-23 5407m	5	21	Qz	99.24		0.76															100	52
H-23 5407m	5	22	Qz	99.99																	100	52
H-23 5407m	5	23	Ab	65.93	1.22	18.91	1.87				12.07										100	49
H-23 5407m	6	1	Ab+Ank	45.01		12.89	8.65	0.71	5.41	17.42	9.92										100	41
H-23 5407m	6	2	Fap							44.69			45.46		7.95	0.32				1.59	100	49
H-23 5407m	6	3	TiO_2		99.28		0.71														100	38
H-23 5407m	6	4	TiO_2+Kln	8.15	83.02	7.78	1.07														100	43
H-23 5407m	6	5	TiO_2+Chl	2.52	92.69	2.32	2.47														100	35
H-23 5407m	6	6	Chl+Ap	21.26		15.19	41.49	1.10	7.74	6.67	0.90	0.70	4.93								100	29
H-23 5407m	6	7	Chl+Other	20.11		15.10	52.06	1.69	8.19	2.84											100	26
H-23 5407m	6	8	TiO_2+Ab	24.96	59.17	8.16	1.53				6.17										100	44
H-23 5407m	6	9	Ab	66.61		19.97	0.55				12.27	0.59									100	52
H-23 5407m	6	10	Hole	60.43		14.21	5.39		4.23	2.28	3.48			8.94		1.04					100	9
H-23 5407m	6	11	Kln	49.21		36.79															86	38
H-23 5407m	6	12	Kln	48.11		36.17									1.72						86	38
H-23 5407m	6	13	Qz	99.37		0.64															100	51
H-23 5407m	6	14	Kln+Chl	54.98		32.92	8.47		2.07	0.74		0.84									100	35
H-23 5407m	6	15	Ab+Chl	48.92	3.04	23.34	15.24		3.08		6.39										100	42
H-23 5407m	6	16	Qz	99.99																	100	49
H-23 5407m	6	17	Qz	99.99																	100	49
H-23 5407m	6	18	Chl+Qz+TiO_2	58.10	17.45	11.43	10.32		2.14							0.56					100	25
H-23 5407m	6	19	TiO_2+Chl	26.33	67.86	3.59	2.20														100	36
H-23 5407m	6	20	Chl+Ilt+Py	38.95		28.25	18.20		4.69	3.30		1.94		4.64							100	32
H-23 5407m	6	21	Py	0.83			24.96				0.58	0.22		72.79							99	68
H-23 5407m	6	22	Ab	67.90		18.82					13.28										100	51
H-23 5407m	6	23	Ab+Chl+Kln	57.22		35.52	3.86		0.75		2.26					0.38					100	25
H-23 5407m	6	24	Qz	99.99																	100	49
H-23 5407m	6	25	F-Cal				0.76			39.29					15.95						56	28
H-23 5407m	6	26	Sd+Chl	6.59		3.06	70.43	2.31	13.71	3.90											100	20
H-23 5407m	6	27	Ab	65.84	0.47	20.86	0.66				11.16	1.00									100	43
H-23 5407m	7	1	Glass (Slide)	72.58		1.27			4.76	6.79	13.93	0.66									100	51
H-23 5407m	7	2	Chl	28.87	0.76	21.74	24.20		8.74	0.69											85	38

Table 2-8A: Scaning Electron Microscope chemical analyses of sample 5407m from Newburn H-23 well.

Sample	Site	Position	Mineral	SiO_2	TiO_2	Al_2O_3	FeO	MnO	MgO	CaO	Na_2O	K_2O	P_2O_5	SO_3	F	Cl	Sc_2O_3	ZnO	ZrO_2	WO_3	Total	Actual Total
H-23 5407m	7	3	Qz	99.99																	100	50
H-23 5407m	7	4	Mix	11.59		6.99	61.26	2.44	12.44	3.58		1.04				0.68					100	22
H-23 5407m	7	5	Ms	58.34	0.66	27.00	1.02		1.03			6.95									95	46
H-23 5407m	7	6	Chl	28.82		19.41	25.30	0.48	10.09	0.89											85	34
H-23 5407m	7	7	Chl	29.33	0.79	21.28	26.53		6.57	0.50											85	34
H-23 5407m	7	8	Ab	66.76		19.08	1.83				12.32										100	45
H-23 5407m	7	9	Sd+Chl	4.71		2.70	73.09	1.98	13.13	4.41											100	20
H-23 5407m	7	10	Qz	99.99																	100	45
H-23 5407m	7	11	TiO_2+Other	1.03	98.30	0.68															100	33
H-23 5407m	7	12	Qz+Chl	90.38		4.16	4.16		0.99			0.33									100	47
H-23 5407m	7	13	Ab	67.30		19.03	0.99				12.69										100	53
H-23 5407m	7	14	Chl+Other	42.59	0.58	26.17	23.39		4.21	1.04	0.65	1.02				0.35					100	36
H-23 5407m	7	15	Ab+Py	66.53		18.22	0.75				13.17			1.37							100	52
H-23 5407m	7	16	TiO_2+Chl	4.90	85.91	4.67	4.53														100	37
H-23 5407m	7	17	Fap+Ab	28.39		10.92	5.49		0.80	20.46	4.87		24.72		4.34						100	51
H-23 5407m	7	18	Chl	31.88		19.75	21.29		9.96	1.12	0.59					0.41					85	33
H-23 5407m	7	19	TiO_2+Chl+Ap	9.41	50.43	8.43	7.81		1.54	10.17			11.89			0.30					100	32
H-23 5407m	7	20	Chl+Other	37.97	1.72	26.76	25.72		6.55	0.52	0.77										100	37
H-23 5407m	7	21	Chl+Sd	21.03		16.27	47.73	1.14	11.16	2.66											100	26
H-23 5407m	7	22	Qz	99.99																	100	48
H-23 5407m	7	23	Ab	64.77		21.13	0.85				11.63	1.63									100	49
H-23 5407m	7	24	Ab+Chl	62.12	0.58	20.46	4.88		1.18		10.76										100	43
H-23 5407m	7	25	TiO_2+Chl	3.59	93.06	1.55	1.79														100	33
H-23 5407m	7	26	Chl	29.50		23.63	25.36		5.65	0.60						0.26					85	35
H-23 5407m	8	1	Chl	33.29	0.40	22.89	21.25		6.34	0.47		0.37									85	42
H-23 5407m	8	2	Py				23.11							67.52							91	81
H-23 5407m	8	3	Chl	33.03		25.31	20.75		4.61	0.41		0.89									85	30
H-23 5407m	8	4	Kln	48.01		33.88	0.70							0.77	2.63						86	37
H-23 5407m	8	5	TiO_2+Chl	1.56	95.25	1.30	1.88														100	34
H-23 5407m	8	6	Qz+Other	93.06	1.05	3.80	1.04		0.46			0.59									100	46
H-23 5407m	8	7	Qz	99.04		0.51	0.45														100	48
H-23 5407m	8	8	Chl	33.89		23.11	21.30		5.22	0.93						0.54					85	17
H-23 5407m	8	9	Qz	99.11		0.64						0.24									100	47
H-23 5407m	8	10	Qz	99.49		0.51															100	46
H-23 5407m	8	11	TiO_2		96.33	0.76	2.92														100	33
H-23 5407m	8	12	Ank+Ab	12.98		3.50	20.92	1.41	18.97	40.83	1.39										100	25

Table 2-8A: Scaning Electron Microscope chemical analyses of sample 5407m from Newburn H-23 well.

Sample	Site	Position	Mineral	SiO_2	TiO_2	Al_2O_3	FeO	MnO	MgO	CaO	Na_2O	K_2O	P_2O_5	SO_3	F	Cl	Sc_2O_3	ZnO	ZrO_2	WO_3	Total	Actual Total
H-23 5407m	8	13	Sd+Chl	3.49		2.10	72.60	1.42	16.22	4.20											100	20
H-23 5407m	8	14	Qz	94.25		3.12	1.78		0.55			0.29									100	40
H-23 5407m	8	15	Ab+Chl+Ap	55.90		21.22	10.56		1.81	1.43	7.89		1.21								100	44
H-23 5407m	8	16	Qz	99.99																	100	50
H-23 5407m	8	17	Qz+Ms+Chl	82.53	0.65	11.47	2.43		0.98	0.43		1.51									100	41
H-23 5407m	8	18	Qz	99.99																	100	45
H-23 5407m	8	19	Qz	99.37		0.64															100	44
H-23 5407m	8	20	TiO_2+Chl	11.27	76.08	6.95	2.74		2.22			0.73									100	34
H-23 5407m	8	21	Chl	29.84		25.19	24.68		5.30												85	28
H-23 5407m	8	22	Chl	30.67		24.94	23.81		5.22	0.36											85	29
H-23 5407m	8	23	TiO_2+Chl+Qz	14.48	80.87	2.46	2.20														100	35
H-23 5407m	8	24	Chl	29.45		25.40	24.43		5.72												85	33
H-23 5407m	8	25	Kln	48.92		36.79						0.29									86	37
H-23 5407m	8	26	Chl	31.55	0.43	25.35	22.46		4.54	0.68											85	35
H-23 5407m	8	27	Qz	99.99																	100	52
H-23 5407m	9	1	Ms	49.55		32.48	1.75		1.13		0.47	9.63									95	46
H-23 5407m	9	2	Chl	29.14		23.25	27.72		4.33	0.56											85	37
H-23 5407m	9	3	Py	0.28			26.05				0.43			73.24							100	79
H-23 5407m	9	4	TiO_2+Chl	2.14	94.50	1.40	1.98														100	34
H-23 5407m	9	5	Qz	99.99																	100	46
H-23 5407m	9	6	Qz	99.99																	100	46
H-23 5407m	9	7	Qz+Ms	92.93	0.62	4.42	0.44		0.51			1.06									100	45
H-23 5407m	9	8	Chl+Cal	33.01	0.67	23.54	22.86		6.57	12.63		0.73									100	33
H-23 5407m	9	9	Chl	30.98		24.77	24.00		4.85			0.41									85	30
H-23 5407m	9	10	Chl+Ilt	41.76		27.44	23.49		4.89	0.57		1.02		0.82							100	30
H-23 5407m	9	11	Qz	99.99																	100	46
H-23 5407m	9	12	Ms+Ank	22.59		15.82	14.81	1.37	11.71	29.87		3.84									100	29
H-23 5407m	9	13	Qz+Ms+Chl	83.49		9.07	4.19		1.48	0.39		1.39									100	44
H-23 5407m	9	14	Kln	49.42		36.21	0.38														86	38
H-23 5407m	9	15	Kln+Other	57.31		37.53	2.07		1.41	0.73		0.47				0.48					100	23
H-23 5407m	9	16	Ab	68.28		18.86					12.85										100	51
H-23 5407m	9	17	Chl	31.95	1.19	24.17	22.86		4.02	0.39		0.42									85	32
H-23 5407m	9	18	Qz	99.64			0.35														100	48
H-23 5407m	9	19	Ms+Chl	58.87		22.07	12.30		3.18	0.60	0.57	2.06				0.33					100	34
H-23 5407m	9	20	Ab	77.18		13.32	0.36				9.14										100	48
H-23 5407m	9	21	Ab	68.33		18.63					13.05										100	50
H-23 5407m	9	22	Qz	99.99																	100	46

Table 2-8A: Scaning Electron Microscope chemical analyses of sample 5407m from Newburn H-23 well.

Sample	Site	Position	Mineral	SiO_2	TiO_2	Al_2O_3	FeO	MnO	MgO	CaO	Na_2O	K_2O	P_2O_5	SO_3	F	Cl	Sc_2O_3	ZnO	ZrO_2	WO_3	Total	Actual Total
H-23 5407m	9	23	Chl	33.87		20.14	16.59		12.10	0.84	0.80			0.65							85	32
H-23 5407m	9	24	Ms+Chl	48.56		30.35	13.30		3.42			4.37									100	37
H-23 5407m	9	25	Qz+Sp+Kln	58.08		17.31	1.70		0.81	0.34		0.55		12.54				8.68			100	34
H-23 5407m	9	26	Qz	99.99																	100	47
H-23 5407m	9	27	Qz+Chl	88.69		4.82	4.34		2.16												100	46
H-23 5407m	9	28	Qz+Chl	94.98		2.00	1.97		1.04												100	46
H-23 5407m	10	1	Ank				12.86	0.64	11.95	30.55											56	21
H-23 5407m	10	2	Zrn	30.74															69.27		100	49
H-23 5407m	10	3	Zrn	31.17															68.84		100	47
H-23 5407m	10	4	Zrn	30.76															69.23		100	49
H-23 5407m	10	5	Sd				51.96	2.45		1.59											56	19
H-23 5407m	10	6	TiO_2+Chl	8.56	83.00	3.44	4.34		0.66												100	33
H-23 5407m	10	7	Chl	31.12		20.56	23.97		8.88	0.47											85	34
H-23 5407m	10	8	Qz	98.51		0.85	0.63														100	44
H-23 5407m	10	9	Qz	99.99																	100	45
H-23 5407m	10	10	Chl+TiO_2+Ms	30.18	19.58	20.37	15.63		3.08	9.54		1.19				0.41					100	25
H-23 5407m	10	11	Chl	30.20		21.92	25.25		5.36	1.31		0.97									85	31
H-23 5407m	10	12	Chl	26.72		19.02	30.19		4.69	2.44	0.92	1.02									85	29
H-23 5407m	10	13	Chl	29.89		25.15	24.91		4.54	0.50											85	30
H-23 5407m	10	14	TiO_2		98.82		1.20														100	32
H-23 5407m	10	15	Ank				12.92	0.81	11.99	30.28											56	21
H-23 5407m	10	16	TiO_2		99.05		0.96														100	32
H-23 5407m	10	17	Chl	33.95		22.52	23.61		4.47	0.45											85	33
H-23 5407m	10	18	Qz	99.99																	100	44
H-23 5407m	10	19	Qz	99.99																	100	44
H-23 5407m	10	20	Qz	99.99																	100	46
H-23 5407m	10	21	Ms+Chl	54.49	0.65	27.10	4.79		2.98	1.41		7.87		0.72							100	43
H-23 5407m	10	22	Qz+Chl	84.90		6.10	6.34		2.35	0.29											100	44
H-23 5407m	10	23	Qz	99.99																	100	47
H-23 5407m	10	24	Mix	67.92		1.30	24.43	0.98	3.75	1.61											100	32
H-23 5407m	11	1	Ank	0.90			12.35	0.90	12.05	29.81											56	22
H-23 5407m	11	2	Ank				13.40	0.80	12.63	29.17											56	21
H-23 5407m	11	3	TiO_2+Other	0.83	96.25	0.76	2.17														100	35
H-23 5407m	11	4	Chl	31.53		21.88	24.21		6.53		0.63					0.23					85	36
H-23 5407m	11	5	Qz+Chl	95.13		1.91	2.44		0.51												100	46
H-23 5407m	11	6	Qz	99.99																	100	47
H-23 5407m	11	7	Ilt+Chl	61.03	0.72	23.05	6.34		3.50		0.62	4.75									100	43

Table 2-8A: Scaning Electron Microscope chemical analyses of sample 5407m from Newburn H-23 well.

Sample	Site	Position	Mineral	SiO_2	TiO_2	Al_2O_3	FeO	MnO	MgO	CaO	Na_2O	K_2O	P_2O_5	SO_3	F	Cl	Sc_2O_3	ZnO	ZrO_2	WO_3	Total	Actual Total
H-23 5407m	11	8	TiO_2+Other	30.21	63.52	3.25	2.64					0.40									100	36
H-23 5407m	11	9	Chl+Ap	35.25	1.60	21.41	26.09		9.87	2.78	0.63		2.36								100	38
H-23 5407m	11	10	Ilt+Chl	42.51		30.37	18.92		4.61	1.22		1.53				0.86					100	32
H-23 5407m	11	11	Qz+Chl	63.94		21.07	11.62		2.17	0.42		0.49				0.29					100	39
H-23 5407m	11	12	Ilt+Chl	49.91	0.48	24.81	17.75		3.43	1.25	0.65	1.30				0.41					100	33
H-23 5407m	11	13	Ab	67.68		18.76	0.36				13.20										100	51
H-23 5407m	11	14	Ab+Ilt	58.68	0.48	25.96	1.38		1.39		6.82	5.28									100	48
H-23 5407m	11	15	Chl	37.56		18.99	23.57		3.68					0.89		0.31					85	30
H-23 5407m	11	16	Chl+Cal	34.16		25.28	30.22		4.89	2.95		0.51		0.92		1.07					100	23
H-23 5407m	11	17	Qz	92.88		3.82	2.66		0.63												100	43
H-23 5407m	11	18	Kln	49.21		36.79															86	34
H-23 5407m	11	19	Qz+Ank	55.79		0.87	10.91	0.75	8.90	22.79											100	30
H-23 5407m	11	20	Qz	98.55					0.48	0.95											100	40
H-23 5407m	11	21	Qz	99.99																	100	44
H-23 5407m	11	22	Chl	33.15		25.38	19.36		4.48	0.84		0.84				0.95					85	29
H-23 5407m	11	23	Qz	99.99																	100	44
H-23 5407m	11	24	Qz	99.99																	100	45
H-23 5407m	11	25	Qz	99.99																	100	44
H-23 5407m	12	1	Zrn	30.61															69.39		100	49
H-23 5407m	12	2	Py				21.73		0.95					64.90							88	76
H-23 5407m	12	3	Ab	66.83		18.76	1.03				12.78			0.60							100	47
H-23 5407m	12	4	TiO_2+Other	1.90	96.56	1.53															100	34
H-23 5407m	12	5	Kln	48.57		36.58	0.85														86	32
H-23 5407m	12	6	Ilt+Chl+TiO_2	72.20	5.77	13.02	3.67		2.21			3.13									100	40
H-23 5407m	12	7	Qz+TiO_2+Other	55.15	39.57	4.08	1.21														100	31
H-23 5407m	12	8	Py	2.74		2.08	24.88				0.49			69.82							100	53
H-23 5407m	12	9	Qz+TiO_2	95.90	4.09																100	43
H-23 5407m	12	10	TiO_2+Kln	19.32	62.15	17.50	1.03														100	34
H-23 5407m	12	11	Ank+Ab	17.41		5.80	14.77	0.89	15.92	40.16	5.07										100	26
H-23 5407m	12	12	Ms+Chl+TiO_2	49.65	9.21	26.57	4.64		1.81			8.12									100	41
H-23 5407m	12	13	Qz	99.99																	100	46
H-23 5407m	12	14	Kln+Qz	69.10		30.89															100	28
H-23 5407m	12	15	Qz	99.99																	100	44
H-23 5407m	12	16	Chl	40.12		18.97	21.94		3.36	0.38						0.24					85	33
H-23 5407m	12	17	TiO_2+Chl	2.33	94.33	1.61	1.74														100	33
H-23 5407m	12	18	Qz+Chl+Py	88.69		1.63	2.35		1.67	0.60	0.81			4.25							100	35

Table 2-8A: Scaning Electron Microscope chemical analyses of sample 5407m from Newburn H-23 well.

Sample	Site	Position	Mineral	SiO_2	TiO_2	Al_2O_3	FeO	MnO	MgO	CaO	Na_2O	K_2O	P_2O_5	SO_3	F	Cl	Sc_2O_3	ZnO	ZrO_2	WO_3	Total	Actual Total
H-23 5407m	12	19	Chl+Ms	51.13		30.12	13.73		3.07			1.52				0.45					100	21
H-23 5407m	12	20	Ab	68.56		18.25					13.19										100	46
H-23 5407m	12	21	TiO_2+Chl	1.26	95.40	1.57	1.76														100	31
H-23 5407m	13	1	Ank				12.77	0.60	12.28	30.34											56	22
H-23 5407m	13	2	Ank				14.38	0.87	11.86	28.89											56	22
H-23 5407m	13	3	Py	1.80		0.68	25.61				0.55			71.37							100	68
H-23 5407m	13	4	Zrn	30.95	0.50														68.54		100	45
H-23 5407m	13	5	Ms+Kln+Ank	56.43	0.50	30.37	2.34		1.77	2.15	0.53	5.55				0.35					100	34
H-23 5407m	13	6	Chl+Ms	40.00		25.81	21.74		10.68	0.45		1.32									100	34
H-23 5407m	13	7	TiO_2+Ab	13.63	76.23	4.91	1.83				3.40										100	35
H-23 5407m	13	8	Qz	99.99																	100	43
H-23 5407m	13	9	Qz+Other	95.24		2.55	0.98		0.83			0.39									100	42
H-23 5407m	13	10	Chl+Ap	26.98		19.93	20.65		4.34	12.49	1.01		14.16			0.44					100	31
H-23 5407m	13	11	Ab+Chl+Ap	40.15		20.86	14.28		3.45	7.67	3.87		9.72								100	41
H-23 5407m	13	12	Py+Kln	14.05		11.38	29.33		2.65	0.97	0.74			40.88							100	40
H-23 5407m	13	13	Ab	68.20		18.90					12.90										100	50
H-23 5407m	13	14	DM	39.36		4.08	17.01		26.33	2.42	0.98	0.71			8.55	0.55					100	24
H-23 5407m	13	15	DM	40.56	0.68	3.14	4.05		32.09	8.47		1.16		0.92	8.38	0.54					100	25
H-23 5407m	13	16	Sd+Chl	2.22		2.02	71.67	1.65	18.29	4.14											100	20
H-23 5407m	13	17	Ab	68.67		13.98	5.31		1.06	0.81	9.21					0.97					100	21
H-23 5407m	13	18	Qz	99.99																	100	45
H-23 5407m	13	19	Ilt+Chl	40.37		29.89	23.32		4.78			1.04				0.59					100	30
H-23 5407m	13	20	Chl	30.55		24.23	24.80		4.68	0.43						0.31					85	30
H-23 5407m	13	21	TiO_2+Qz	16.69	83.30																100	35
H-23 5407m	13	22	Chl+TiO_2+Ilt	54.36	1.13	36.83	3.98		0.78			1.31		1.12		0.47					100	27
H-23 5407m	13	23	Chl+Ilt	46.46		30.04	15.36		3.95	0.59		1.64		1.45		0.50					100	29
H-23 5407m	13	24	Qz+Other	97.72			1.02		0.65					0.62							100	41
H-23 5407m	13	25	Chl+Ab	42.16		30.97	20.40		4.66		1.40					0.40					100	28

Table 2-8B: Scaning Electron Microscope chemical analyses of sample 5407m from Newburn H-23 well (re-annalysis of fluorine-calcite).

Sample	Site	Position	Mineral	SiO_2	TiO_2	Al_2O_3	FeO	MnO	MgO	CaO	Na_2O	K_2O	SO_3	F	Cl	Total	Actual Total
H-23 5407m	1	1	Ab	68.97		18.56					12.48					100	125
H-23 5407m	1	2	F-Cal+Other	3.29		1.1	2.01	0.89	0.53	71.58		0.53		20.08		100	72
H-23 5407m	1	3	F-Cal	0.37			0.91	0.31	0.38	41.54				12.48		56	71
H-23 5407m	1	4	Qz	99.99												100	124
H-23 5407m	1	5	F-Cal+TiO_2+Qz	1.26	1.8		1.84	0.41		71.07				23.63		100	71
H-23 5407m	1	6	TiO2+Chl	3.4	91.51	2.61	1.14			0.99		0.34				100	103
H-23 5407m	1	7	Ms+Chl	51.17	1.1	32.67	3.07		1.14		0.63	10.2				100	110
H-23 5407m	1	8	Chl	38.36		21.73	26.37		13.55							100	101
H-23 5407m	1	9	Ab	69.01		18.57					12.42					100	121
H-23 5407m	2	1	Qz	99.99												100	121
H-23 5407m	2	2	F-Cal+Chl+Py	4.21		2.93	4.31		1.11	64.89	0.5		2	20.05		100	73
H-23 5407m	2	3	F-Fe-Cal				1.38	0.59	0.52	40.95				12.55		56	71
H-23 5407m	2	4	F-Fe-Cal				1.48	0.50	0.53	40.92				12.57		56	70
H-23 5407m	2	5	F-Cal	0.67		0.44	0.81		0.51	40.78			1.10	11.68		56	73
H-23 5407m	2	6	Ilt+Chl	59.11		13.26	11.71		6.7		0.32	8.6			0.29	100	101
H-23 5407m	2	7	Ab	77.52		12.58	0.36				9.37	0.17				100	123
H-23 5407m	3	1	Qz	99.99												100	122
H-23 5407m	3	2	Qz	99.73			0.27									100	121
H-23 5407m	3	3	F-Fe-Cal				1.74	0.49	0.58	41.05				12.14		56	68
H-23 5407m	3	4	F-Cal				0.97	0.30	0.31	41.95				12.48		56	70
H-23 5407m	3	5	Chl+Cal	35.57		27.76	28.5		4.79	2.46		0.73			0.21	100	84
H-23 5407m	3	6	Ms	48.49		35.86	1.36		0.38		1.40	7.51				95	107
H-23 5407m	3	7	Qz	99.99												100	120
H-23 5407m	4	1	Ank+Chl	1.95		1.23	24.55	1.63	19.67	50.99						100	61
H-23 5407m	4	2	Oli	65.12		21.39				2.8	10.5	0.18				100	125
H-23 5407m	4	3	Qz	99.99												100	124
H-23 5407m	5	1	F-Fe-Cal				1.25	0.35	0.34	41.99				12.07		56	69
H-23 5407m	5	2	F-Cal						1.24	43.62			0.42	10.72		56	69
H-23 5407m	5	3	F-Cal+Chl	2.48		2.31	3.73		1.94	69.6			0.7	19.24		100	72
H-23 5407m	5	4	F-Cal+Chl	0.71		0.76	1.03		1.72	76.33			0.67	18.79		100	70

Table 2-8B: Scaning Electron Microscope chemical analyses of sample 5407m from Newburn H-23 well (re-annalysis of fluorine-calcite).

Sample	Site	Position	Mineral	SiO_2	TiO_2	Al_2O_3	FeO	MnO	MgO	CaO	Na_2O	K_2O	SO_3	F	Cl	Total	Actual Total
H-23 5407m	5	5	F-Cal+Chl	2.22		1.13	2.34	0.41	0.55	73.74				19.6		100	70
H-23 5407m	5	6	F-Fe-Cal				1.36	0.44		42.63				11.57		56	69
H-23 5407m	5	7	Qz	99.99												100	123
H-23 5407m	5	8	Qz	99.99												100	124
H-23 5407m	5	9	Qz	99.99												100	121
H-23 5407m	5	10	Py+F-Cal+Chl	4.75		4.38	24.53		1.13	10.4			51.31	3.48		100	148
H-23 5407m	5	11	Py+F-Cal+Chl	3.59		3.33	24.88		0.83	7			56.63	3.75		100	176
H-23 5407m	5	12	Qz+Chl+Cal	95.71		1.25	1.52			1.51						100	117

Appendix 2-9: SEM-BSE images and EDS mineral analyses for sample Newburn H-23 5408.5m

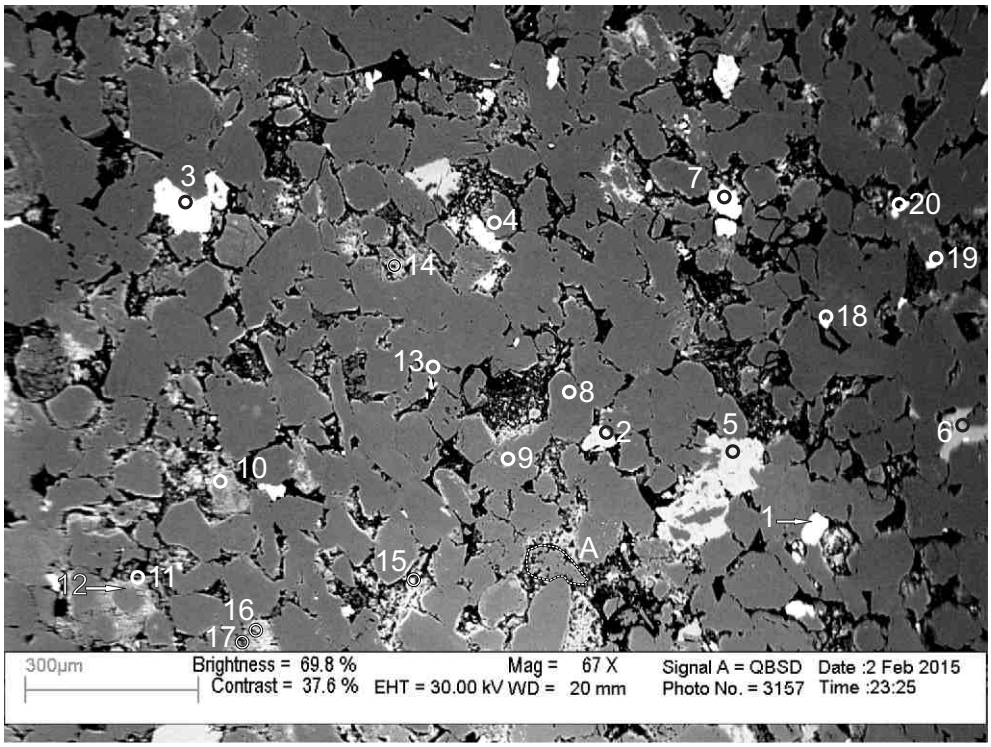

1: Zircon
2: Ankerite+ Chlorite
3: Barite
4: Quartz
5: Ankerite
6: F-Calcite+ Other
7: Pyrite
8: Quartz
9: Albite
10: Muscovite+ Chlorite
11: Quartz+ Chlorite
12: Chlorite+ F-Calcite
13: Quartz
14: Albite+ Chlorite+ Illite
15: Chlorite+ Quartz
16: Chlorite+ F-Calcite
17: Chlorite+ F-Calcite
18: Albite+ Titania
19: Albite
20: Albite+ Titania+ Chlorite

Figure 2-9.1: Sample Newburn 5408.5m site 1 (SEM). Table 2-9A. Diagenetic zircon (1) cuts quartz and partly fills pore. Diagenetic barite (3) engulfs quartz and fibrous chlorite filling pore. Pyrite (7) fills porosity and cuts fibrous chlorite. Ankerite (5) engulfs quartz. Chloritized muscovite (10). Chlorite fills porosity (15). Chlorite and calcite (12) rim quartz. Trachytic lithic clast (position A).

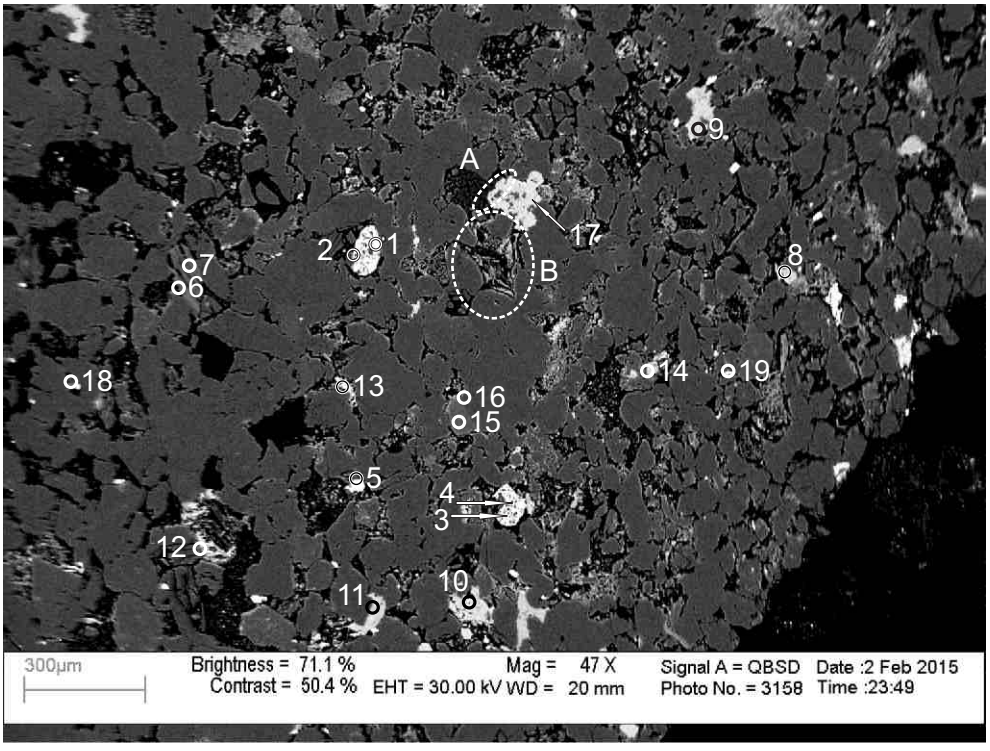

1: Titania+ Chlorite
2: Titania+ Chlorite
3: Titania+ Quartz+Illite
4: Titania+ Quartz
5: Pyrite+ Quartz
6: Muscovite
7: Muscovite
8: Ankerite+ Quartz
9: Ankerite
10: Ankerite
11: Ankerite
12: Chlorite
13: Chlorite
14: Ankerite+ Quartz
15: Oligoclase
16: Quartz
17: Ankerite+ Chlorite
18: Quartz+ Other
19: Titania+ Quartz+ Chlorite

Figure 2-9.2: Sample Newburn 5408.5m site 2 (SEM). Table 2-9A. Ankerite (17) engulfs quartz and kaolinite (position A). Fibrous chlorite fills pore (position B). Titania and chlorite (1,2) engulf quartz.

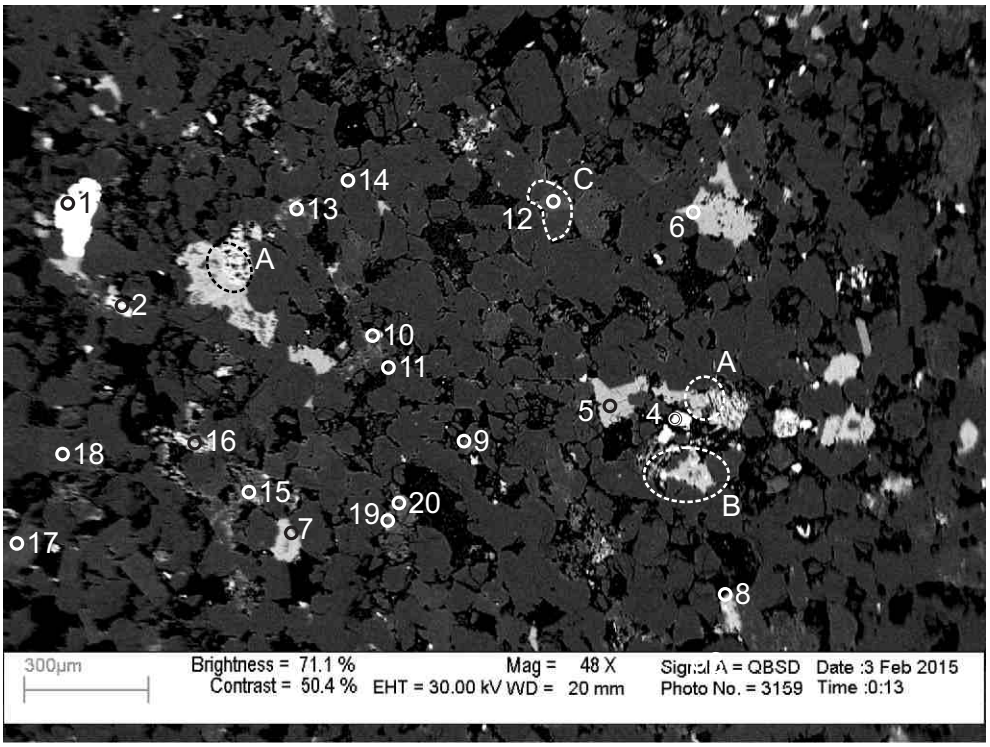

1: Barite
2: Titania+ Quartz+ Other
3: Pyrite
4: Titania
5: Fe-Calcite
6: Fe-Calcite
7: Chlorite+ Calcite+ Illite
8: Ankerite+ Albite
9: Muscovite
10: Chlorite+ Muscovite
11: Quartz
12: Oligoclase
13: Quartz+ Chlorite
14: Quartz
15: Albite+ Chlorite
16: Chlorite+ Calcite
17: Oligoclase
18: Albite
19: Muscovite
20: Albite+ Muscovite

Figure 2-9.3: Sample Newburn 5408.5m site 3 (SEM). Table 2-9A. Chlorite cuts calcite (16, positions A). Titania fills dissolution voids in Fe-calcite (position B). Granitoid lithic clast composed of quartz and oligoclase (12).

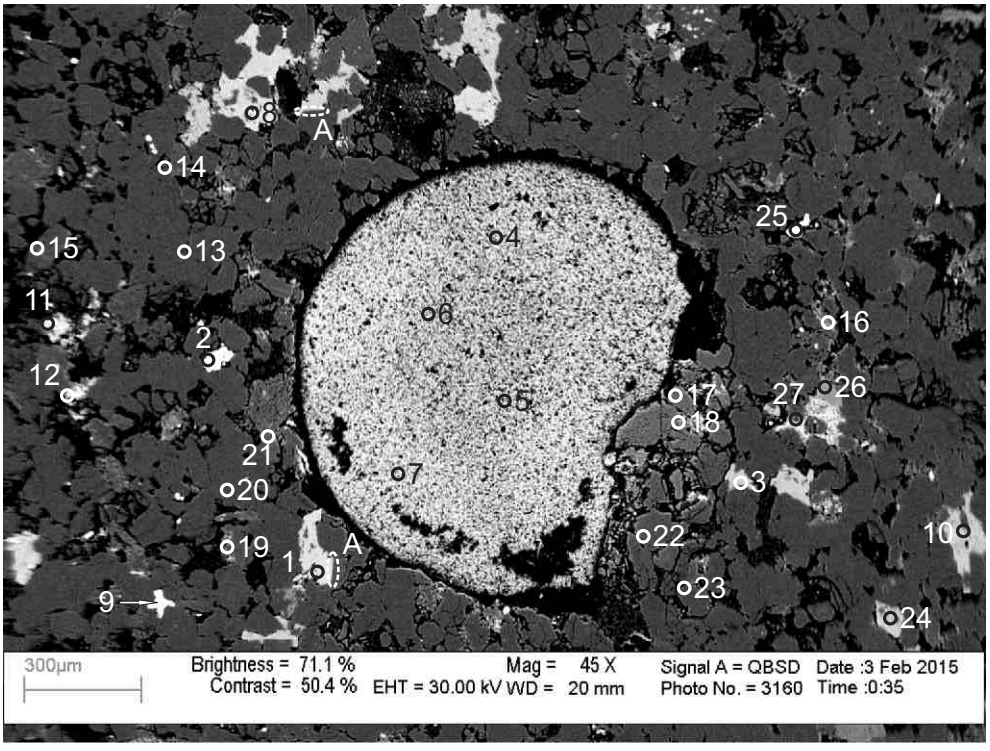

1: Ankerite
2: Pyrite
3: Calcite+ Chlorite
4: Glass (Slide)
5: Glass (Slide)
6: Glass (Slide)
7: Glass (Slide)
8: Ankerite
9: Barite
10: Calcite+ Chlorite
11: Chlorite
12: Chlorite
13: Quartz
14: Albite
15: Albite
16: Muscovite +Chlorite
17: Quartz
18: Quartz
19: Albite
20: Quartz
21: Chlorite
22: Quartz
23: Quartz+ Other
24: Calcite+ Chlorite
25: Pyrite
26: Muscovite
27: Quartz+ Chlorite

Figure 2-9.4: Sample Newburn 5408.5m site 4 (SEM). Table 2-9A. Large hole in thin section with exposed slide (4-7). Diagenetic barite (9) forms along intergranular boundary and engulfs quartz. Quartz overgrowths (positions A) abutting ankerite (1). Subhedral pyrite (2) fills pore and cuts quartz. Chlorite (27) rims quartz grain and replaces muscovite (26).

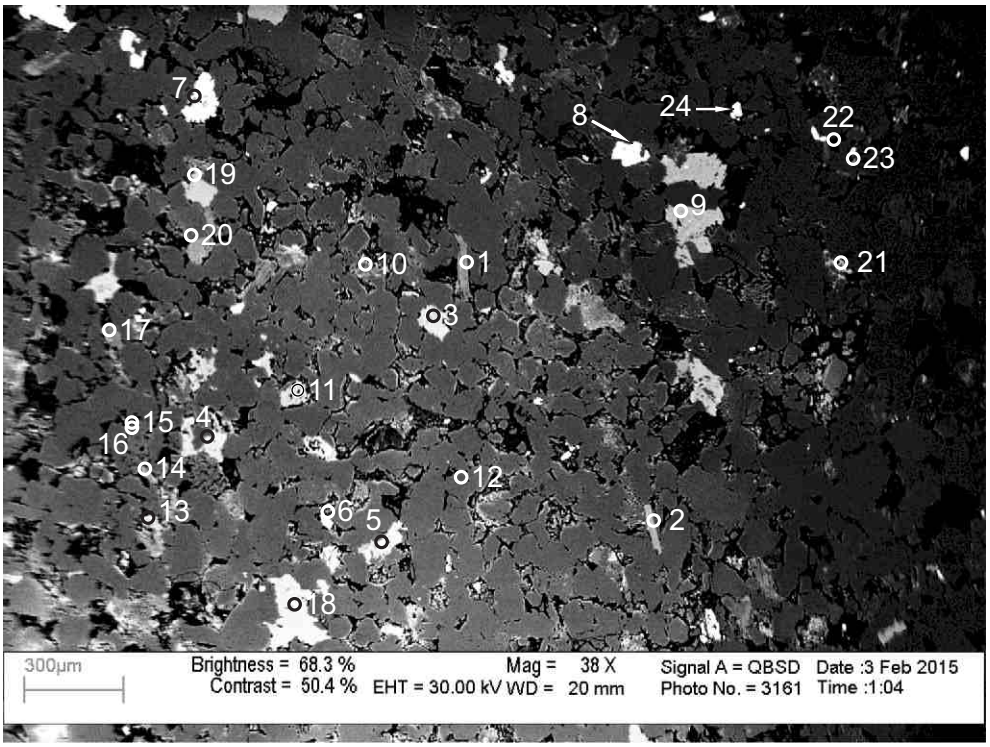

1: Quartz+ Muscovite
2: Quartz
3: Ankerite+ Chlorite
4: Fe-Calcite
5: Ankerite+ Chlorite
6: Quartz
7: Chlorite+Illite
8: Barite+Other
9: Ankerite+ Chlorite
10: Albite+ Chlorite
11: Calcite+ Chlorite
12: Quartz
13: Quartz
14: Quartz
15: Albite
16: Albite
17: Quartz
18: Fe-Calcite+ Chlorite
19: Quartz
20: Muscovite
21: Chlorite
22: Muscovite+ Albite
23: Albite
24: Zircon+Other

Figure 2-9.5: Sample Newburn 5408.5m site 5 (SEM). Table 2-9A. Diagenetic barite (8) forms along intergranular boundary and engulfs quartz. Diagenetic zircon (24) fills pore. Chlorite fills dissolution voids in ankerite (9) and calcite (11).

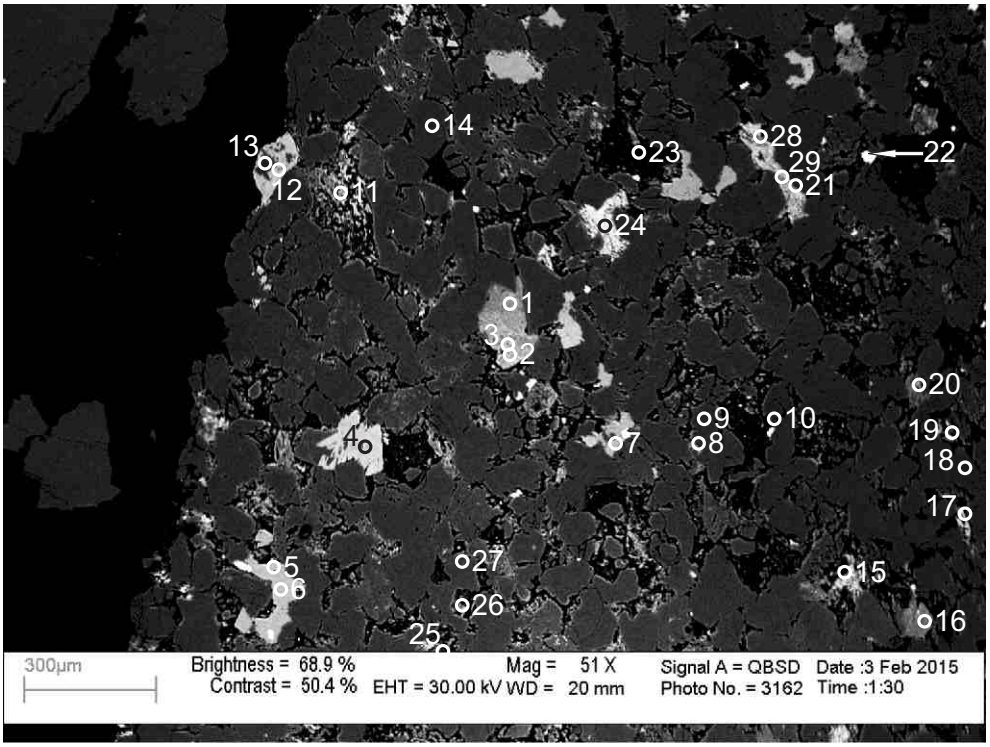

1: Chlorite
2: Chlorite
3: Chlorite
4: Ankerite+ Chlorite
5: Fe-Calcite+ Chlorite
6: Fe-Calcite
7: Fe-Calcite
8: Quartz+ Chlorite
9: Quartz
10: Quartz
11: Chlorite
12: Ankerite+ Albite
13: Albite
14: Quartz
15: Chlorite+ Other
16: Muscovite
17: Chlorite
18: Quartz
19: Muscovite+ Chlorite
20: Muscovite+ Chlorite
21: Quartz+ Chlorite
22: Titania+ Chlorite
23: Hole
24: Chlorite+ Ankerite
25: Chlorite
26: Quartz+ Other
27: Quartz
28: Chlorite+ Other
29: Chlorite+ Other

Figure 2-9.6: Sample Newburn 5408.5m site 6 (SEM). Table 2-9A. Chlorite cement (21,28,29). Chlorite (24) engulfs ankerite. Ankerite (12) engulfs albite (13). Titania (22) fills open porosity. Fibrous chlorite (11) fills pore.

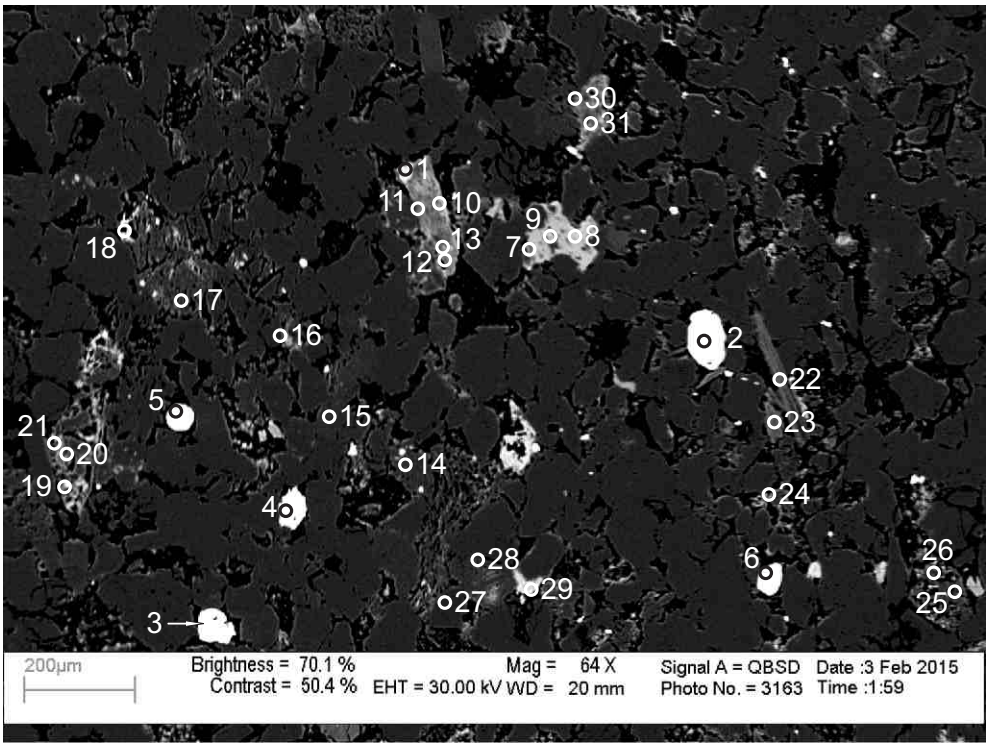

1: Chlorite+ Muscovite
2: Titania
3: Zircon
4: Titania+Other
5: Pyrite
6: V-Titania
7: Ankerite+ Quartz+Illite
8: Ankerite
9: Albite+Ankerite
10: Chlorite+ Muscovite
11: Muscovite+ Chlorite
12: Muscovite+ Chlorite
13: Muscovite+ Chlorite
14: Albite
15: Albite
16: Chlorite
17: Albite+Apatite
18: Chlorite+ Apatite
19: Chlorite+ Albite+Titania
20: Chlorite+ Albite+ Fluorite
21: Chlorite
22: Muscovite
23: Muscovite
24: Albite
25: Albite+Apatite
26: Albite+Apatite
27: Quartz
28: Albite
29: Quartz+ Chlorite+ Ankerite
30: Chlorite+ Muscovite
31: Chlorite+

Figure 2-9.7: Sample Newburn 5408.5m site 7 (SEM). Table 2-9A. Chloritized muscovite (1,10-13). Diagenetic Titania (2,4) fills open porosity and engulfs quartz. Diagenetic zircon (3) with dissolution void partly fills pore. Apatite fills dissolution voids in albite (25,26).

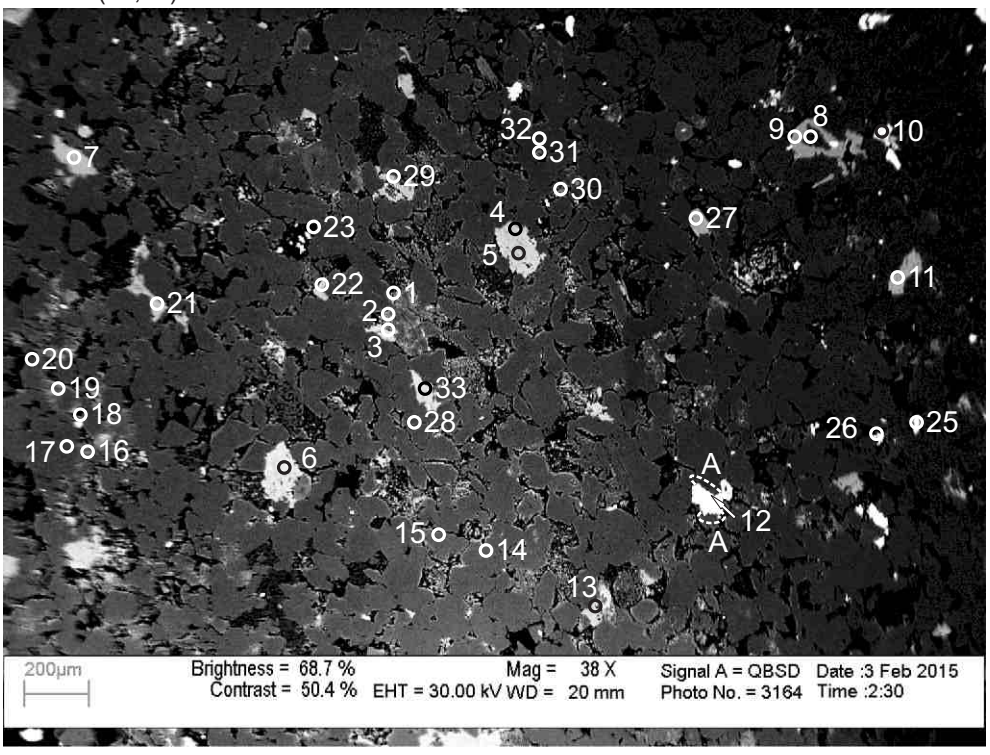

1: Chlorite+ Muscovite
2: Albite
3: Quartz+Chlorite
4: Quartz+Ankerite
5: Ankerite+Albite
6: Ankerite+ Titania+Chlorite
7: Fe-Calcite+ Quartz
8: Quartz+Chlorite
9: Fe-Calcite
10: Titania+ Quartz+Other
11: Ankerite+ Chlorite
12: Barite
13: F-Calcite+ Chlorite
14: Quartz
15: Quartz
16: Albite
17: Quartz
18: Quartz
19: Quartz+ Muscovite+ Chlorite
20: Quartz
21: Quartz
22: Albite
23: Quartz+Other
24: Pyrite
25: Quartz+ Titania+ Other
26: Pyrite
27: Calcite
28: Quartz
29: Quartz
30: Chlorite
31: Quartz
32: Quartz
33: Ankerite+Albite

Figure 2-9.8: Sample Newburn 5408.5m site 8 (SEM). Table 2-9A. Diagenetic barite (12) with straight crystal outline fills pore and engulfs quartz (position A). Ankerite (4,5) engulfs quartz (4) and albite (5). Fe-calcite (9) rims quartz (8). F-calcite (13) cuts chlorite.

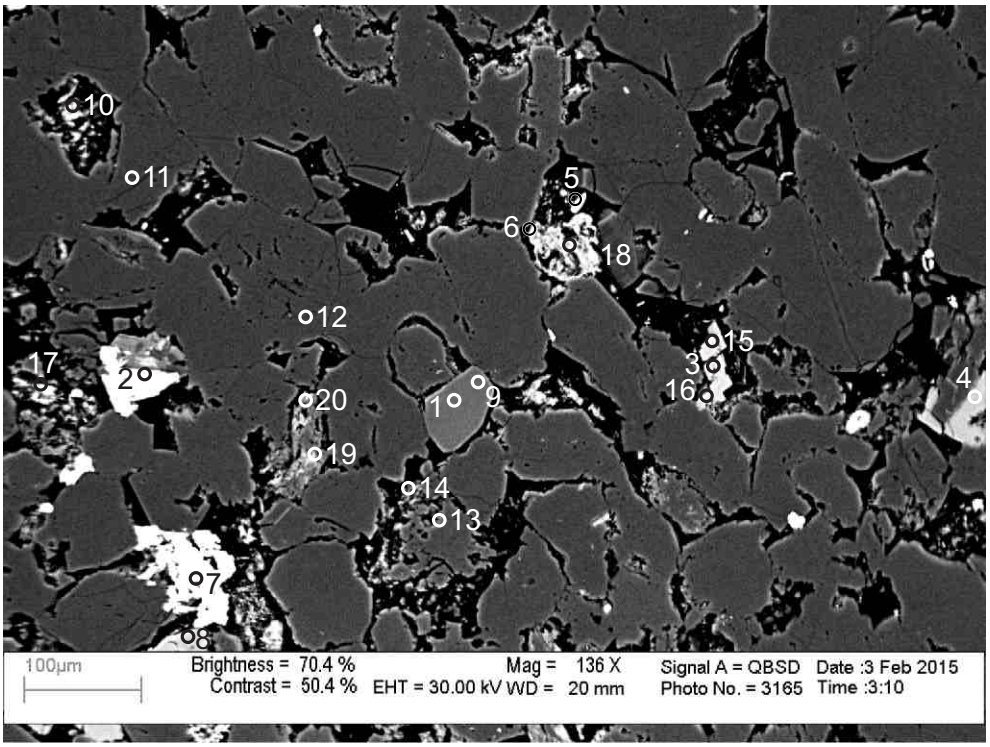

1: Tourmaline
2: Titania
3: Ankerite
4: Fe-Calcite
5: Titania+ Chlorite
6: Chlorite
7: Titania+ Chlorite
8: Fe-Calcite
9: Tourmaline
10: Chlorite
11: Quartz
12: Quartz
13: Quartz
14: Quartz+ Chlorite
15: Ankerite
16: Ankerite+ Chlorite
17: Titania+ Chlorite+ Other
18: Chlorite
19: Muscovite+ Chlorite
20: Quartz+ Muscovite

Figure 2-9.9: Sample Newburn 5408.5m site 9 (SEM). Table 2-9A. Detrital tourmaline (1,9). Chlorite (16) cuts ankerite (3,15) which fills pore. Fibrous chlorite (10) partly fills pore.

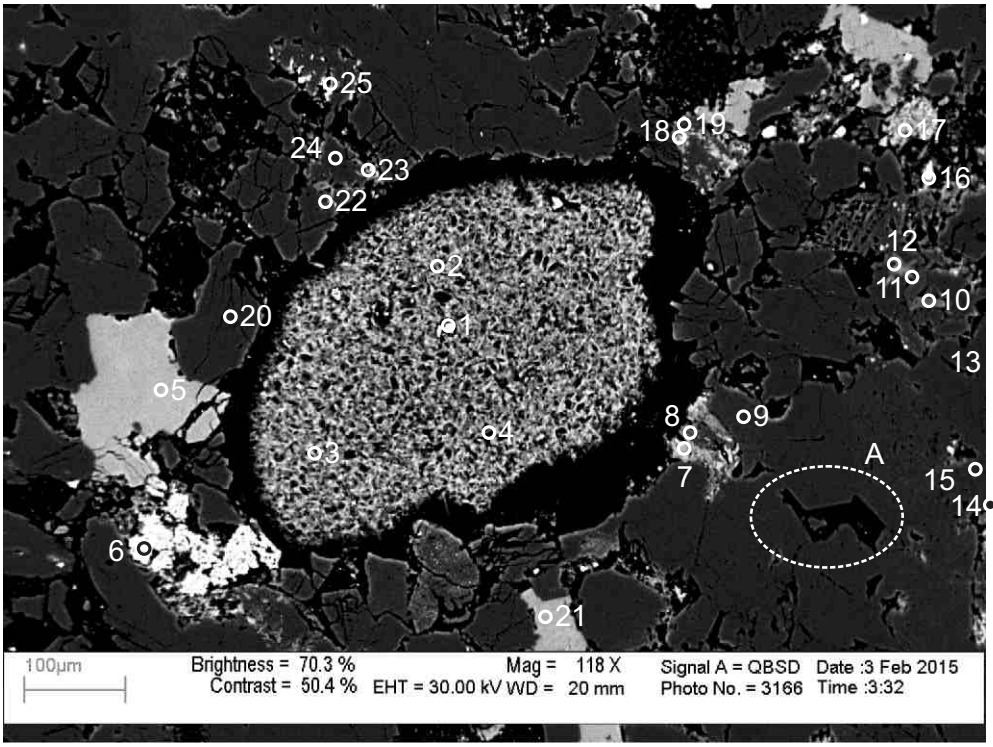

1: Halite+ Quartz+ Other
2: Glass(Slide)
3: Glass(Slide)
4: Glass(Slide)
5: Fe-Calcite
6: Siderite+ Apatite+ Chlorite
7: Muscovite+ Chlorite
8: Albite
9: Albite
10: Muscovite
11: Albite
12: Muscovite
13: Mix
14: Albite+ Chlorite
15: Quartz
16: Chlorite+ Other
17: Chlorite
18: Chlorite+ Apatite
19: Quartz+ Albite+ Chlorite
20: Quartz
21: Calcite
22: Illite+Albite+ Chlorite
23: Chlorite+Illite
24: Quartz
25: Albite

Figure 2-9.10: Sample Newburn 5408.5m site 10 (SEM). Table 2-9A. Large hole in thin section with exposed slide (2-4). Halite (1) in pore may be the result of contamination. Fe-calcite (5) engulfs quartz (20). Siderite engulfs apatite and chlorite, and fills pore (6). Quartz overgrowth (position A).

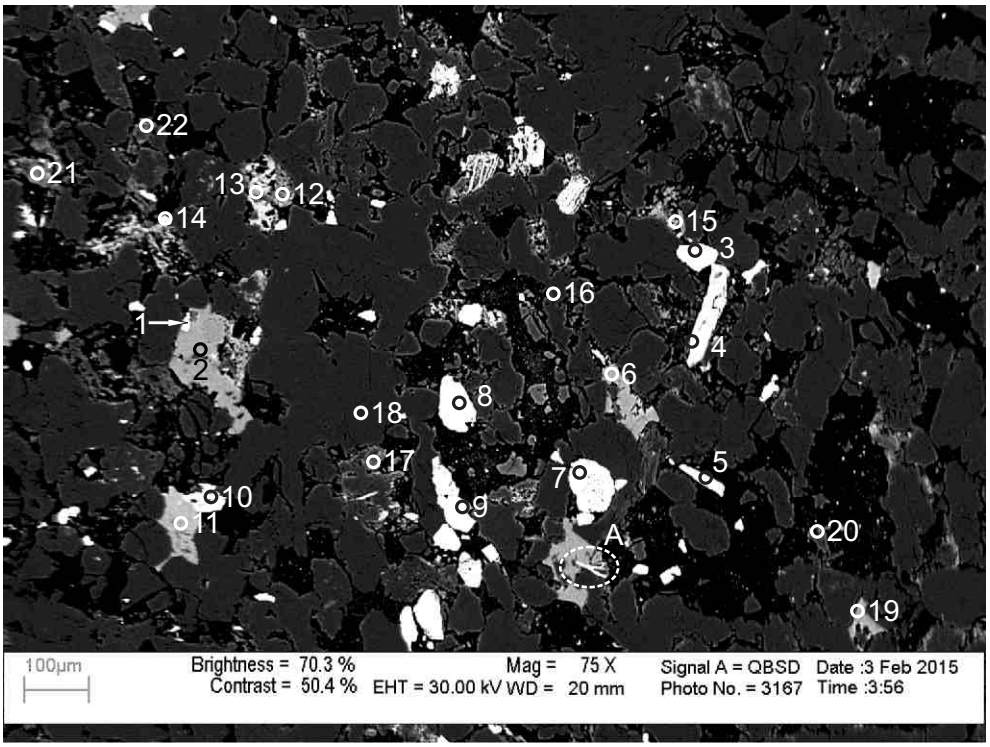

1: Titania+ Fe-Calcite
2: Fe-Calcite
3: Zircon
4: Titania+ Other
5: Fluorapatite
6: Fe-Calcite
7: Pyrite
8: Zircon
9: Zircon
10: Titania
11: Ankerite
12: Chlorite
13: Chlorite
14: Titania+ Quartz
15: Muscovite
16: Quartz
17: Quartz+ Muscovite+ Chlorite
18: Quartz
19: Fe-Calcite
20: Albite+ Chlorite
21: Quartz+ Titania
22: Muscovite+ Pyrite+ Other

Figure 2-9.11: Sample Newburn 5408.5m site 11 (SEM). Table 2-9A. Titania (1) forms along intergranular boundary between Fe-calcite (2) and quartz. Fibrous chlorite cuts Fe-calcite (position A). Diagenetic Titania (10) with straight crystal outlines engulfs ankerite (11). Diagenetic zircon (3,8,9) fills pore and engulfs quartz. Subhedral fluorapatite (5) partly fills pore.

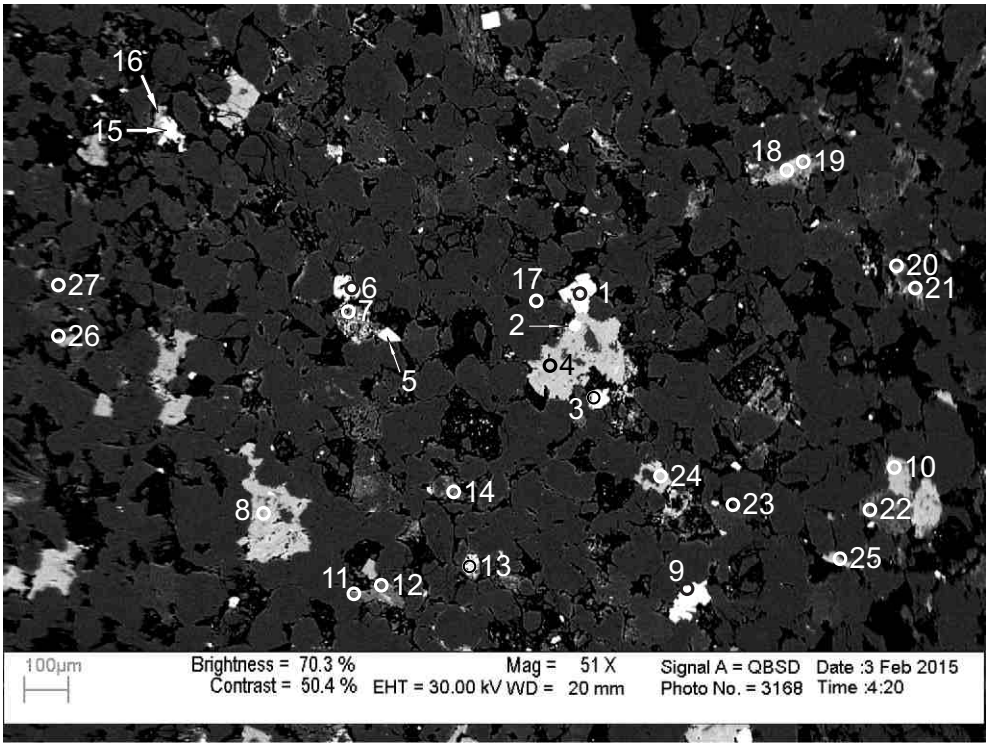

1: Titania
2: Zircon
3: Titania
4: Ankerite
5: Zircon
6: Titania
7: Titania
8: Ankerite+ Chlorite
9: Titania+Other
10: Ankerite
11: Muscovite
12: Muscovite
13: Titania+ Chlorite
14: Chlorite+ Muscovite
15: Titania+ Chlorite
16: Calcite+ Other
17: Quartz
18: Chlorite+ Ankerite
19: Chlorite
20: Muscovite+ Chlorite
21: Muscovite+ Chlorite
22: Quartz+Illite
23: Quartz
24: Ankerite
25: Quartz+ Ankerite
26: Albite+ Ankerite+ Chlorite
27: Quartz+ Other

Figure 2-9.12: Sample Newburn 5408.5m site 12 (SEM). Table 2-9A. Diagenetic zircon (5) and Titania (6) cut chlorite (7). Zircon (2) and Titania (1) engulf ankerite (4). Ankerite (24) rims quartz grain. Illite (22) engulfs quartz and is engulfed by ankerite (10). Calcite (16) isengulfed by Titania (15).

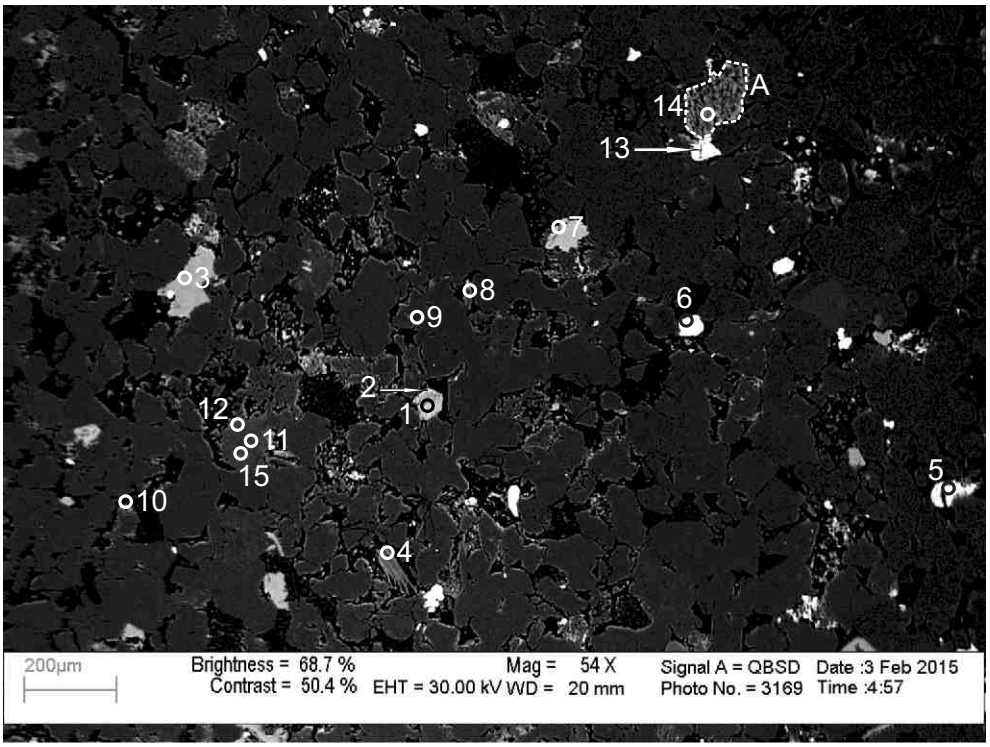

1: Chlorite
2: Chlorite
3: Fe-Calcite
4: Muscovite
5: Titania+ Chlorite
6: Zircon
7: Ankerite
8: Chlorite+ Muscovite
9: Quartz
10: Quartz+ Chlorite
11: Albite
12: Albite
13: Cr-Spinel
14: Chlorite
15: Albite

Figure 2-9.13: Sample Newburn 5408.5m site 13 (SEM). Table 2-9A. Schist lithic clast (position A). Detrital chromian spinel grain (13). Diagenetic Titania (5) cuts chlorite. Chlorite (1) replaces muscovite.

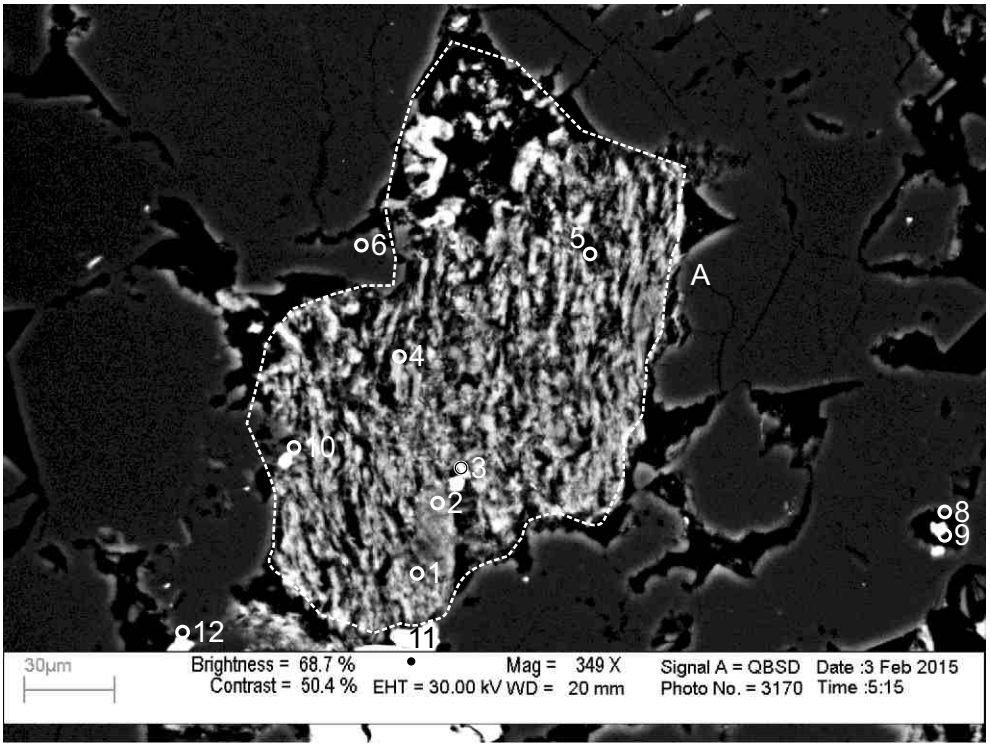

1: Chlorite+ Other
2: Albite+ Chlorite+ Illite
3: Titania+ Chlorite
7
4: Chlorite+ Other
5: Chlorite
6: Quartz
7: Quartz+ Titania+ Other
8: Quartz+ Titania+ Other
9: Quartz+ Titania+ Other
10: Chlorite+ Other
11: Cr-Spinel
12: Quartz+ Titania+ Illite

Figure 2-9.14: Sample Newburn 5408.5m site 14 (SEM). Table 2-9A. Schist lithic clast (position A) composed of quartz (6,7), albite (2), and chlorite (1,2,3,4,5). Titania (3,7) later fills dissolution voids in the clast.

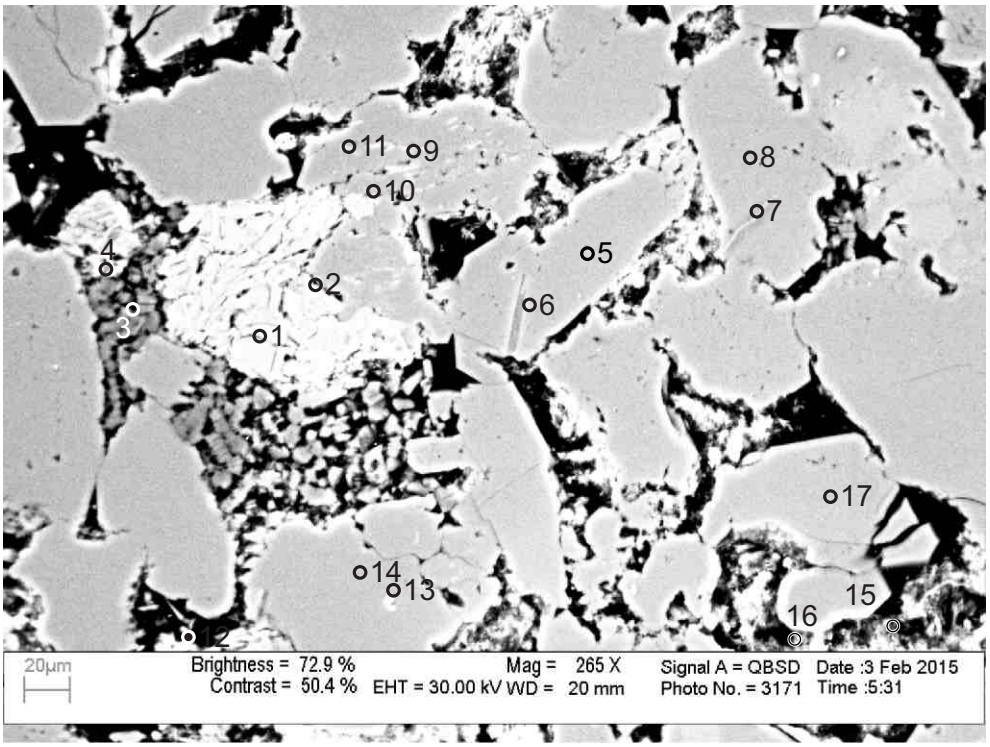

1: Muscovite
2: Albite+ Muscovite
3: Kaolinite
4: Quartz+ Muscovite+ Chlorite
5: Quartz
6: Quartz
7: Quartz
8: Quartz
9: Quartz
10: Quartz
11: Quartz
12: Chlorite+ Other
13: Quartz
14: Quartz
15: Chlorite+ Other
16: Chlorite+ Other
17: Quartz

Figure 2-9.15: Sample Newburn 5408.5m site 15 (SEM). Table 2-9A. Kaolinite (3) booklets fill pore, replace muscovite (1,2) and are engulfed by chlorite (4). Fibrous chlorite (15,16) fill pore.

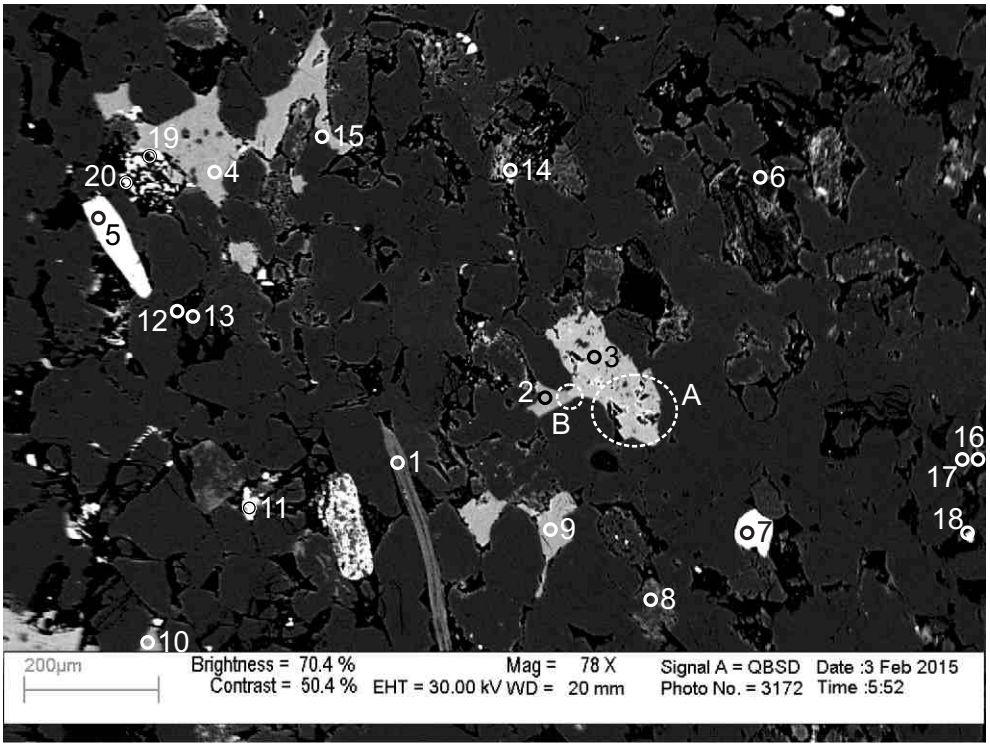

1: Muscovite+ Chlorite
2: Calcite
3: Ankerite+ Other
4: Fe-Calcite+ Other
5: Fluorapatite
6: Muscovite+ Quartz
7: Zircon
8: Muscovite+ Chlorite
9: Calcite
10: Calcite
11: Quartz+ Titania
12: Quartz+ Hole
13: Quartz
14: Quartz+ Chlorite+ Illite
15: Quartz+ Calcite
16: Mix
17: Quartz
18: Titania+ Chlorite
19: Titania+ Chlorite
20: Titania+ Chlorite

Figure 2-9.16: Sample Newburn 5408.5m site 16 (SEM). Table 2-9A. Fibrous chlorite (position A) fills dissolution voids in ankerite (3). Straight contact (position B) between calcite (2) and ankerite (3) gives an uncertain age relationship. Subhedral fluorapatite (5) cuts quartz grain and partly fills pore. Plastically deformed muscovite grain (1). Diagenetic zircon (7) partly fills pore and engulfs quartz.

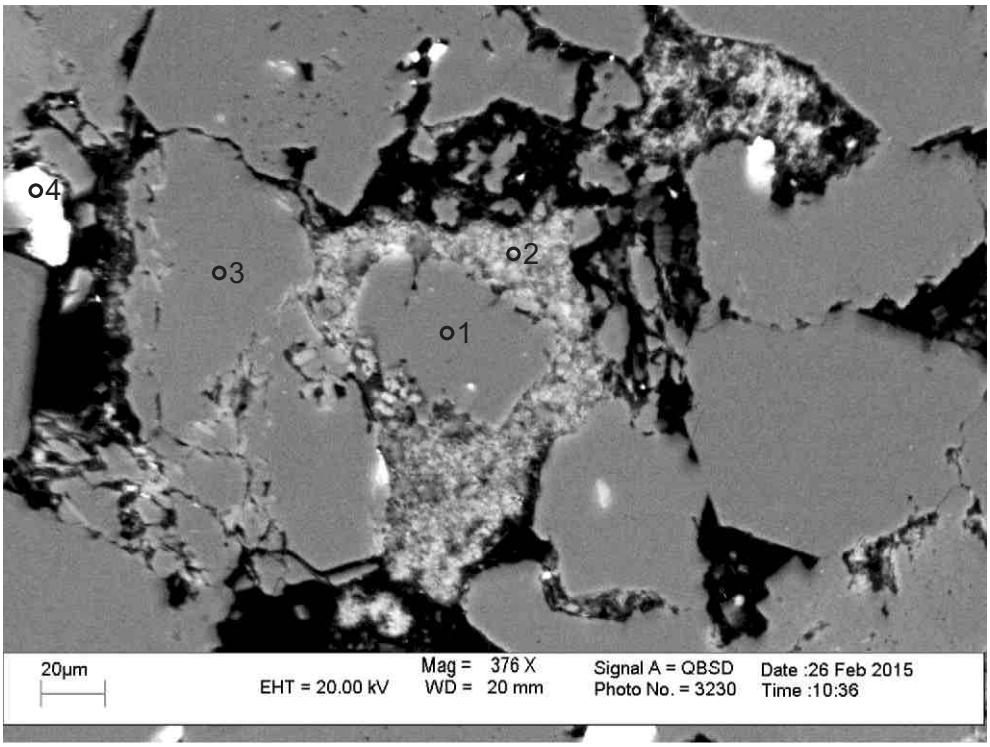

1. Quartz
2. Chlorite+ Fluorite
3. Quartz
4. Titania+ Illite

Figure 2-9.17: Sample Newburn 5408.5m site 1 (SEM). Table 2-9B. Chlorite and fluorite (2) rim quartz (1).

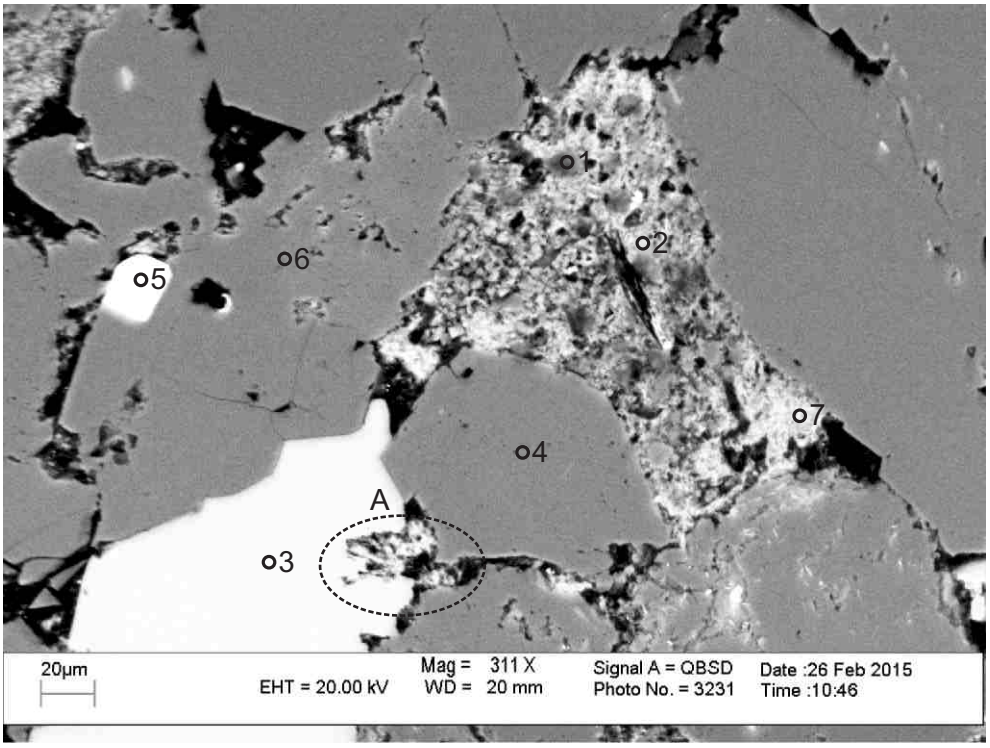

1. Chlorite+ Fluorite
2. Chlorite+ Fluorite
3. Fe-Calcite
4. Quartz
5. Titania
6. Albite
7. Chlorite

Figure 2-9.18: Sample Newburn 5408.5m site 2 (SEM). Table 2-9B. Chlorite and fluorite (1,2) fill pore and surround quartz. Fe-calcite (3) is engulfed by fibrous chlorite (position A).

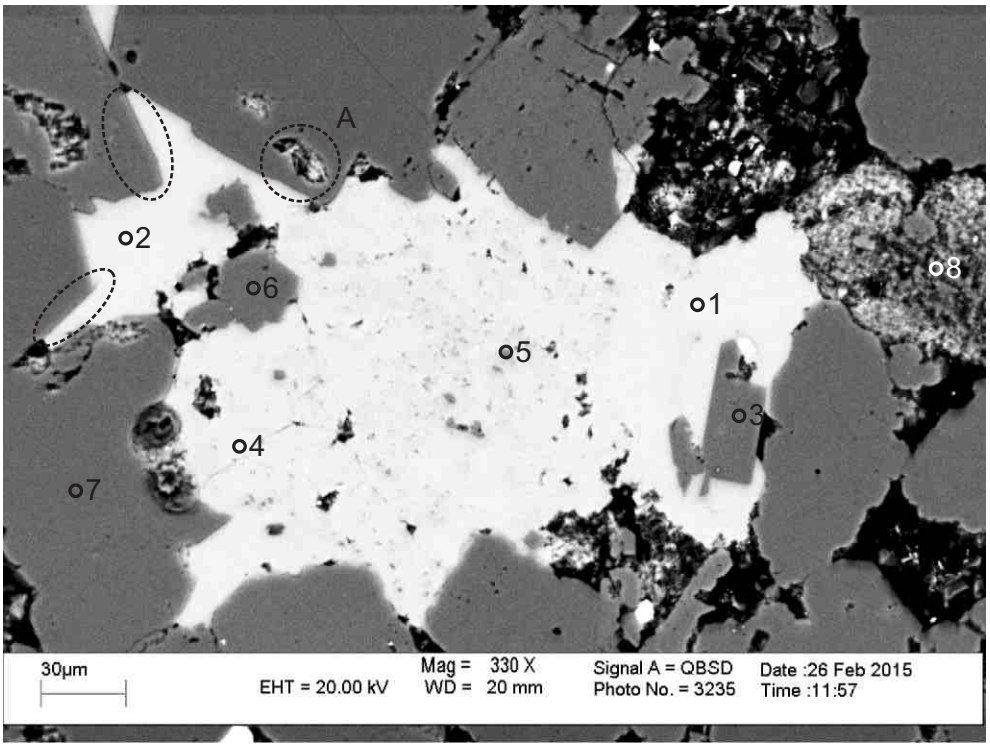

1. F-Fe-Calcite
2. F-Fe-Calcite
3. Albite
4. F-Fe-Calcite
5. Albite+ Illite+ F-Calcite
6. Albite
7. Quartz
8. Albite

Figure 2-9.19: Sample Newburn 5408.5m site 3 (SEM). Table 2-9B. Fibrous chlorite (position A) fills dissolution voids in quartz. F-calcite (4) engulfs albite and illite (5) F-Fe-calcite (1) seems to be at the rim.

Table 2-9B: Scaning Electron Microscope chemical analyses of sample 5408.5m from Newburn H-23 well (re-annalysis of fluorine-calcite).

Sample	Site	Position	Mineral	SiO_2	TiO_2	Al_2O_3	FeO	MnO	MgO	CaO	Na_2O	K_2O	SO_3	F	Cl	Total	Actual Total
H-23 5408.5m	1	1	Qz	99.69			0.31									100	121
H-23 5408.5m	1	2	Chl+Fl	29.78		24.75	30.26		4.64	3.18	0.43			5.28	1.66	100	76
H-23 5408.5m	1	3	Qz	99.99												100	115
H-23 5408.5m	1	4	TiO_2+Ilt	14.40	73.95	7.37	0.95		0.96	0.28		2.10				100	94
H-23 5408.5m	2	1	Chl+Fl	24.47	0.45	17.48	21.75		2.97	16.79	1.13	0.53		11.71	2.73	100	73
H-23 5408.5m	2	2	Chl+Fl	39.53	0.33	27.17	13.68		2.42	2.55	0.55	5.94		7.46	0.40	100	102
H-23 5408.5m	2	3	Fe-Cal				1.37	0.40	0.38	53.85						56	53
H-23 5408.5m	2	4	Qz	99.99												100	122
H-23 5408.5m	2	5	TiO_2	0.58	96.96	0.85	1.62									100	100
H-23 5408.5m	2	6	Ab	70.85		17.21					11.95					100	125
H-23 5408.5m	2	7	Chl	27.66		20.99	23.31		3.85	2.65	0.42	0.66		4.70	0.76	85	91
H-23 5408.5m	3	1	F-Fe-Cal				1.39	0.46	0.52	49.66				3.97		56	54
H-23 5408.5m	3	2	F-Fe-Cal				1.14			50.79				4.07		56	51
H-23 5408.5m	3	3	Ab	68.86		18.52					12.63					100	116
H-23 5408.5m	3	4	F-Fe-Cal	0.81			1.36	0.62	0.50	49.68				3.02		56	51
H-23 5408.5m	3	5	Ab+Ilt+F-Cal	52.97		14.74	0.58			18.58	8.93	2.34		1.88		100	97
H-23 5408.5m	3	6	Ab	68.56		18.63				0.22	12.59					100	110
H-23 5408.5m	3	7	Qz	99.99												100	107
H-23 5408.5m	3	8	Ab	63.58		19.35	4.53		0.68	0.88	10.72				0.26	100	98

Table 2-9A: Scanning Electron Microscope chemical analyses of 5408.5m from Newburn H-23 well.

Sample	Site	Position	Mineral	SiO_2	TiO_2	Al_2O_3	FeO	MnO	MgO	CaO	Na_2O	K_2O	P_2O_5	SO_3	F	Cl	V_2O_5	Cr_2O_3	CdO	As_2O_3	SrO	ZrO_2	BaO	Ce_2O_3	HfO_2	WO_3	B_2O_3	Total	Actual Total
H-23 5408.5m	1	1	Zrn	31.66																		67.65			0.70			100	147
H-23 5408.5m	1	2	Ank+Chl	2.91		1.34	24.53	1.72	21.21	48.29																		100	64
H-23 5408.5m	1	3	Brt											41.70									58.30					100	108
H-23 5408.5m	1	4	Qz	99.60																			0.40					100	139
H-23 5408.5m	1	5	Ank			0.64	14.04	0.85	11.89	28.57																		56	67
H-23 5408.5m	1	6	F-Cal+Other	1.30			1.71	0.59		90.56					5.83													100	66
H-23 5408.5m	1	7	Py	0.19			25.65							74.16														100	245
H-23 5408.5m	1	8	Qz	99.99																								100	138
H-23 5408.5m	1	9	Ab	67.71		18.95				0.25	13.09																	100	144
H-23 5408.5m	1	10	Ms+Chl	64.09	1.27	25.07	1.35		1.58			6.65																100	113
H-23 5408.5m	1	11	Qz+Chl	78.74		8.99	4.63		1.28	0.91		0.48			4.37	0.59												100	102
H-23 5408.5m	1	12	Chl+F-Cal	32.24		26.06	19.97		5.17	3.08	0.73				10.81	1.94												100	69
H-23 5408.5m	1	13	Qz	99.99																								100	132
H-23 5408.5m	1	14	Ab+Chl+Ilt	46.57		27.34	15.45		3.90	1.16	2.95	2.04				0.61												100	96
H-23 5408.5m	1	15	Chl+Qz	47.11		24.92	17.71		5.79	1.27	0.65	0.34	0.89	0.67		0.64												100	85
H-23 5408.5m	1	16	Chl+F-Cal	30.76	0.68	24.60	18.51		4.48	3.81	0.77	0.36			14.98	1.03												100	91
H-23 5408.5m	1	17	Chl+F-Cal	31.64	0.22	22.24	16.13		3.58	5.34	0.69	0.64			18.27	1.25												100	87
H-23 5408.5m	1	18	Ab+TiO_2	47.55	29.12	13.02	0.35				9.96																	100	147
H-23 5408.5m	1	19	Ab	68.37		18.82					12.81																	100	162
H-23 5408.5m	1	20	Ab+TiO_2+Chl	44.47	24.02	15.19	5.71		2.64	1.69	4.02	0.30		1.17		0.80												100	111
H-23 5408.5m	2	1	TiO_2+Chl	9.22	72.93	5.33	3.29		0.63	0.85	0.57	1.22			5.55	0.43												100	105
H-23 5408.5m	2	2	TiO_2+Chl	18.68	73.23	4.10	2.10		0.68	0.70		0.26				0.27												100	112
H-23 5408.5m	2	3	TiO_2+Qz+Ilt	21.76	66.21	7.80	1.52		0.70	0.35		1.53				0.16												100	110
H-23 5408.5m	2	4	TiO_2+Qz	10.78	86.99	0.96	1.26																					100	117
H-23 5408.5m	2	5	Py+Qz	22.25		1.02	21.06		0.28		0.28	0.08		55.01														100	200
H-23 5408.5m	2	6	Ms	48.20		36.14	0.61				1.62	8.43																95	113
H-23 5408.5m	2	7	Ms	49.24		36.19	0.44				1.62	7.52																95	113
H-23 5408.5m	2	8	Ank+Qz	19.02			21.74	1.37	13.80	44.07																		100	89
H-23 5408.5m	2	9	Ank				14.65	1.10	9.67	30.59																		56	76
H-23 5408.5m	2	10	Ank	0.43			14.94	1.02	10.12	29.49																		56	66
H-23 5408.5m	2	11	Ank				12.92	0.87	10.53	31.68																		56	62
H-23 5408.5m	2	12	Chl	29.33		22.53	27.03		4.06	1.40		0.31				0.33												85	86
H-23 5408.5m	2	13	Chl	30.80		22.26	26.30		4.35	0.84		0.24				0.20												85	96
H-23 5408.5m	2	14	Ank+Qz	18.57	0.62		24.60	1.33	13.70	41.21																		100	82
H-23 5408.5m	2	15	Oli	66.34		20.50	0.14			1.78	11.04	0.19																100	136
H-23 5408.5m	2	16	Qz	99.99																								100	138
H-23 5408.5m	2	17	Ank+Chl	10.10		9.01	26.96	1.20	13.76	38.97																		100	81
H-23 5408.5m	2	18	Qz+Other	97.70	1.37	0.47	0.45																					100	114
H-23 5408.5m	2	19	TiO_2+Qz+Chl	43.77	53.46	1.19	1.58																					100	152
H-23 5408.5m	3	1	Brt			0.49								21.62									38.02				39.88	100	161
H-23 5408.5m	3	2	TiO_2+Qz+Other	28.11	69.37	0.81	1.00			0.45						0.24												100	100
H-23 5408.5m	3	3	Py	0.39		0.25	25.01							63.88														90	231
H-23 5408.5m	3	4	TiO_2		100																							100	119
H-23 5408.5m	3	5	Fe-Cal				1.28	0.41		54.30																		56	61

Table 2-9A: Scanning Electron Microscope chemical analyses of 5408.5m from Newburn H-23 well.

Sample	Site	Position	Mineral	SiO_2	TiO_2	Al_2O_3	FeO	MnO	MgO	CaO	Na_2O	K_2O	P_2O_5	SO_3	F	Cl	V_2O_5	Cr_2O_3	CdO	As_2O_3	SrO	ZrO_2	BaO	Ce_2O_3	HfO_2	WO_3	B_2O_3	Total	Actual Total
H-23 5408.5m	3	6	Fe-Cal	1.48		0.48	1.43	0.53	0.42	51.37		0.29																56	68
H-23 5408.5m	3	7	Chl+Cal+Ilt	24.07	0.35	12.51	15.72	0.89	10.50	33.15		2.82																100	78
H-23 5408.5m	3	8	Ank+Ab	11.15		4.02	22.72	1.48	14.67	43.50	2.45																	100	79
H-23 5408.5m	3	9	Ms	51.65	0.38	31.92	0.98		0.90		0.48	8.68																95	119
H-23 5408.5m	3	10	Chl+Ms	60.00	0.18	16.51	10.88		9.25	0.53	0.34	2.17				0.13												100	120
H-23 5408.5m	3	11	Qz	99.99																								100	129
H-23 5408.5m	3	12	Oli	65.57		21.33				2.49	10.49	0.13																100	139
H-23 5408.5m	3	13	Qz+Chl	90.85		3.99	3.51		0.88			0.77																100	124
H-23 5408.5m	3	14	Qz	99.99																								100	129
H-23 5408.5m	3	15	Ab+Chl	45.76	0.88	24.07	19.31		3.50	0.78	5.31					0.38												100	91
H-23 5408.5m	3	16	Chl+Cal	32.90		27.08	32.69		5.39	1.39						0.55												100	78
H-23 5408.5m	3	17	Oli	65.97		20.96				2.08	10.99																	100	105
H-23 5408.5m	3	18	Ab	69.12		18.63					12.26																	100	110
H-23 5408.5m	3	19	Ms	53.06		24.79	5.81		2.85			8.13				0.35												95	92
H-23 5408.5m	3	20	Ab+Ms	63.51		21.28	2.75		0.61	0.53	9.56	1.76																100	126
H-23 5408.5m	4	1	Ank			0.44	15.52	1.05	9.98	29.01																		56	64
H-23 5408.5m	4	2	Py	0.17			25.20		0.43					66.17														92	222
H-23 5408.5m	4	3	Cal+Chl	2.72			2.15	0.63		94.50																		100	70
H-23 5408.5m	4	4	Glass (Slide)	74.12		1.23			4.28	7.46	11.92	0.55		0.42														100	110
H-23 5408.5m	4	5	Glass (Slide)	72.75		1.32			4.92	6.18	13.95	0.52		0.35														100	141
H-23 5408.5m	4	6	Glass (Slide)	73.03		1.25			4.92	6.21	14.01	0.58																100	141
H-23 5408.5m	4	7	Glass (Slide)	73.89		1.28			4.63	6.46	12.73	0.58		0.42														100	125
H-23 5408.5m	4	8	Ank	1.55		0.60	14.90	0.87	10.02	28.06																		56	67
H-23 5408.5m	4	9	Brt											38.90							0.88		60.24					100	109
H-23 5408.5m	4	10	Cal+Chl	3.23		1.04	2.78	0.98	1.04	90.19	0.73																	100	77
H-23 5408.5m	4	11	Chl	27.69		22.58	29.00		4.43	1.12						0.19												85	89
H-23 5408.5m	4	12	Chl	27.55		23.16	28.31		4.78	0.99						0.22												85	91
H-23 5408.5m	4	13	Qz	99.99																								100	129
H-23 5408.5m	4	14	Ab	66.61		18.33	0.22			1.36	11.95		1.51															100	128
H-23 5408.5m	4	15	Ab	67.43		20.35	0.31				11.07	0.83																100	120
H-23 5408.5m	4	16	Ms+Chl	51.34	0.28	25.62	12.65		4.54	0.41	0.49	4.65																100	138
H-23 5408.5m	4	17	Qz	99.99																								100	159
H-23 5408.5m	4	18	Qz	96.84		1.97	0.33					0.86																100	156
H-23 5408.5m	4	19	Ab	68.05		19.12	1.52				11.28																	100	117
H-23 5408.5m	4	20	Qz	99.99																								100	125
H-23 5408.5m	4	21	Chl	32.50	1.70	20.59	24.02		3.82	1.22		0.69				0.46												85	64
H-23 5408.5m	4	22	Qz	99.99																								100	149
H-23 5408.5m	4	23	Qz+Other	96.33		2.44	0.63		0.28			0.30																100	138
H-23 5408.5m	4	24	Cal+Chl	4.45		1.19	2.17	0.90	0.63	90.29		0.37																100	74
H-23 5408.5m	4	25	Py	0.19			24.75		0.51					63.35														89	275
H-23 5408.5m	4	26	Ms	48.19		30.32	3.88		1.97		0.32	10.32																95	146
H-23 5408.5m	4	27	Qz+Chl	95.39	0.38	1.25	2.03		0.80	0.17																		100	152
H-23 5408.5m	5	1	Qz+Ms	88.78	0.17	7.12	0.95		0.50	0.31		1.89				0.29												100	121
H-23 5408.5m	5	2	Qz	99.86			0.14																					100	140

Table 2-9A: Scanning Electron Microscope chemical analyses of 5408.5m from Newburn H-23 well.

Sample	Site	Position	Mineral	SiO_2	TiO_2	Al_2O_3	FeO	MnO	MgO	CaO	Na_2O	K_2O	P_2O_5	SO_3	F	Cl	V_2O_5	Cr_2O_3	CdO	As_2O_3	SrO	ZrO_2	BaO	Ce_2O_3	HfO_2	WO_3	B_2O_3	Total	Actual Total
H-23 5408.5m	5	3	Ank+Chl	10.27		1.23	20.75	1.28	19.93	46.55																		100	66
H-23 5408.5m	5	4	Fe-Cal				1.10	0.44		54.45																		56	41
H-23 5408.5m	5	5	Ank+Chl	11.83		8.73	20.42	1.19	14.81	43.03																		100	57
H-23 5408.5m	5	6	Qz	99.99																								100	122
H-23 5408.5m	5	7	Chl+Ilt	28.77		23.60	35.70	1.25	4.38	1.80	1.38	2.85				0.26												100	82
H-23 5408.5m	5	8	Brt+Other	9.01		1.11	0.60							36.56									52.73					100	144
H-23 5408.5m	5	9	Ank+Chl	2.67	0.50	0.98	19.77	1.46	18.64	50.79			4.51	0.65														100	79
H-23 5408.5m	5	10	Ab+Chl	61.89	0.52	19.56	3.98		5.12	0.27	8.17	0.51																100	119
H-23 5408.5m	5	11	Cal+Chl	8.56		1.72	2.24	0.70	0.91	85.88																		100	48
H-23 5408.5m	5	12	Qz	99.22		0.40	0.39																					100	129
H-23 5408.5m	5	13	Qz	99.86			0.13																					100	105
H-23 5408.5m	5	14	Qz	99.99																								100	107
H-23 5408.5m	5	15	Ab	64.67		19.63	2.20		0.45	0.15	12.90																	100	118
H-23 5408.5m	5	16	Ab	63.77		19.75	2.61		0.68	0.25	12.32			0.60														100	119
H-23 5408.5m	5	17	Qz	99.99																								100	112
H-23 5408.5m	5	18	Fe-Cal+Chl	5.35	3.29	3.65	9.15	0.94	9.77	67.57		0.29																100	50
H-23 5408.5m	5	19	Qz	99.19						0.81																		100	122
H-23 5408.5m	5	20	Ms	52.35		31.70	1.55		0.67		1.23	7.50																95	114
H-23 5408.5m	5	21	Chl	30.36		23.49	24.90		4.72	1.12						0.42												85	118
H-23 5408.5m	5	22	Ms+Ab	50.59	0.45	36.96	0.98		0.45		1.38	9.02				0.18												100	136
H-23 5408.5m	5	23	Ab	66.85		19.35	1.70			0.31	11.68	0.11																100	164
H-23 5408.5m	5	24	Zrn+Other	50.10		1.13	0.62			0.36												47.28			0.48			100	126
H-23 5408.5m	6	1	Chl	29.68		23.26	25.56		4.48	1.13						0.89												85	93
H-23 5408.5m	6	2	Chl	28.15		22.31	23.36		4.20	1.44					4.49	1.05												85	99
H-23 5408.5m	6	3	Chl	29.33		23.16	25.85		4.33	1.25						1.08												85	91
H-23 5408.5m	6	4	Ank+Chl	3.08		1.15	24.52	1.51	20.96	48.79																		100	64
H-23 5408.5m	6	5	Fe-Cal+Chl	5.24		4.06	4.66	0.46	1.13	71.44					13.00													100	65
H-23 5408.5m	6	6	Fe-Cal				1.23	0.43		54.35																		56	49
H-23 5408.5m	6	7	Fe-Cal	1.13		0.43	1.20	0.33		52.91																		56	61
H-23 5408.5m	6	8	Qz+Chl	91.84		3.91	2.55		0.99	0.21		0.37				0.13												100	138
H-23 5408.5m	6	9	Qz	99.99																								100	150
H-23 5408.5m	6	10	Qz	99.99																								100	159
H-23 5408.5m	6	11	Chl	28.06		22.34	27.67		4.11	2.01						0.82												85	78
H-23 5408.5m	6	12	Ank+Ab	9.97		2.89	22.86	1.37	17.59	43.66	1.66																	100	71
H-23 5408.5m	6	13	Ab	68.35		18.88	0.39				12.38																	100	138
H-23 5408.5m	6	14	Qz	99.99																								100	141
H-23 5408.5m	6	15	Chl+Other	42.87		31.90	13.64		2.98	1.46	0.69			0.82	4.86	0.78												100	113
H-23 5408.5m	6	16	Ms	50.15		30.03	2.18		1.62			8.83			2.06	0.12												95	143
H-23 5408.5m	6	17	Chl	31.42	0.36	23.42	23.17		4.13	1.49		0.49				0.52												85	112
H-23 5408.5m	6	18	Qz	99.99																								100	160
H-23 5408.5m	6	19	Ms+Chl	48.52	6.51	23.01	13.70		3.48	1.13	0.51	2.64				0.50												100	131
H-23 5408.5m	6	20	Ms+Chl	43.38	1.02	30.10	11.21		2.14	1.18		5.69			4.89	0.40												100	133
H-23 5408.5m	6	21	Qz+Chl	86.12		3.68	8.34		1.08	0.52						0.24												100	152
H-23 5408.5m	6	22	TiO_2+Chl	25.50	43.90	12.64	6.78		2.67	0.71	3.68	0.16			3.66	0.31												100	141

Table 2-9A: Scanning Electron Microscope chemical analyses of 5408.5m from Newburn H-23 well.

Sample	Site	Position	Mineral	SiO_2	TiO_2	Al_2O_3	FeO	MnO	MgO	CaO	Na_2O	K_2O	P_2O_5	SO_3	F	Cl	V_2O_5	Cr_2O_3	CdO	As_2O_3	SrO	ZrO_2	BaO	Ce_2O_3	HfO_2	WO_3	B_2O_3	Total	Actual Total
H-23 5408.5m	6	23	Hole	42.16	0.37	4.59	13.10		20.73	2.91	1.08	0.67		2.32	9.94	0.63			1.51									100	93
H-23 5408.5m	6	24	Chl+Ank	28.54	0.77	18.50	26.51		7.18	17.67				0.55		0.28												100	103
H-23 5408.5m	6	25	Chl	34.09		25.13	18.05		4.30	0.99		1.34				1.10												85	76
H-23 5408.5m	6	26	Qz+Other	93.53		4.16	1.14		0.70	0.20		0.14				0.13												100	112
H-23 5408.5m	6	27	Qz	99.99																								100	133
H-23 5408.5m	6	28	Chl+Other	45.14		16.50	25.99	0.19	5.29	1.92		0.23			4.11	0.65												100	115
H-23 5408.5m	6	29	Chl+Other	36.60		22.94	29.76		7.18	1.90	0.46	0.46				0.71												100	113
H-23 5408.5m	7	1	Chl+Ms	36.34		23.01	30.76	0.30	3.95	0.87		1.30				0.61						2.88						100	108
H-23 5408.5m	7	2	TiO_2	0.98	98.42	0.42	0.21																					100	132
H-23 5408.5m	7	3	Zrn	31.68																		68.01			0.32			100	131
H-23 5408.5m	7	4	TiO_2+Other	1.33	95.68	0.89	2.12																					100	111
H-23 5408.5m	7	5	Py	0.73		0.40	25.10							62.75														89	219
H-23 5408.5m	7	6	V-TiO_2	0.39	97.20												2.05	0.37										100	130
H-23 5408.5m	7	7	Ank+Qz+Ilt	25.84	1.17	18.84	19.52	0.71	10.13	21.41	0.65	1.75																100	107
H-23 5408.5m	7	8	Ank	0.59			15.48	1.05	10.13	28.75																		56	77
H-23 5408.5m	7	9	Ab+Ank	33.41		9.73	14.05	0.74	7.53	27.58	6.96																	100	107
H-23 5408.5m	7	10	Chl+Ms	39.34	0.57	28.38	22.82		3.45	0.81		4.35				0.29												100	96
H-23 5408.5m	7	11	Ms+Chl	50.01	1.43	32.41	5.67		1.53		0.39	8.40				0.16												100	123
H-23 5408.5m	7	12	Ms+Chl	46.61	1.12	31.42	10.65		2.17	0.60	0.36	6.82				0.24												100	124
H-23 5408.5m	7	13	Ms+Chl	46.89	4.80	29.78	9.10		1.97	0.60	0.32	6.23				0.28												100	126
H-23 5408.5m	7	14	Ab	68.75		19.25	0.30				11.69																	100	141
H-23 5408.5m	7	15	Ab	69.07		18.82					12.09																	100	140
H-23 5408.5m	7	16	Chl	31.15		21.13	27.52		3.82	0.92		0.17				0.30												85	97
H-23 5408.5m	7	17	Ab+Ap	66.87	0.47	18.33	0.18			1.23	11.62	0.14	1.15															100	143
H-23 5408.5m	7	18	Chl+Ap	16.94	5.39	13.64	25.91		2.65	23.59	0.85		8.18	0.85		2.00												100	35
H-23 5408.5m	7	19	Chl+Ab+TiO_2	40.37	8.49	19.97	17.43		2.50	1.71	4.22	0.17			4.52	0.62												100	94
H-23 5408.5m	7	20	Chl+Ab+Fl	36.73	1.08	23.45	24.66		3.63	2.32	3.28	0.43		0.52	3.03	0.84												100	94
H-23 5408.5m	7	21	Chl	29.02	0.41	22.53	26.60		4.06	1.56		0.30				0.53												85	89
H-23 5408.5m	7	22	Ms	47.71	0.60	34.53	1.02		0.65		1.06	9.43																95	145
H-23 5408.5m	7	23	Ms	49.18	0.40	32.65	0.72		1.50		0.66	9.89																95	144
H-23 5408.5m	7	24	Ab	65.80		19.25	2.75		0.35	0.15	11.70																	100	162
H-23 5408.5m	7	25	Ab+Ap	54.38	1.73	16.34	0.36			7.09	10.48	0.14	8.39		0.94	0.12												100	164
H-23 5408.5m	7	26	Ab+Ap	65.22	1.52	18.99	2.21		0.65	1.01	9.05	0.16	1.01			0.18												100	119
H-23 5408.5m	7	27	Qz	99.99																								100	139
H-23 5408.5m	7	28	Ab	68.54		19.10	0.30				12.07																	100	143
H-23 5408.5m	7	29	Qz+Chl+Ank	75.17		6.07	13.02		3.23	0.95		0.19		0.40		0.96												100	111
H-23 5408.5m	7	30	Chl+Ms	53.14	0.53	23.01	10.34		3.47	0.50	2.90	4.30			1.63	0.17												100	145
H-23 5408.5m	7	31	Chl+Ms	59.19	0.20	19.08	13.50		3.33	0.59	0.57	3.28				0.28												100	130
H-23 5408.5m	8	1	Chl+Ms	50.21	0.33	25.79	14.60		5.04	1.29	0.57	1.55				0.63												100	100
H-23 5408.5m	8	2	Ab	67.75		19.07	0.24				12.82	0.12																100	141
H-23 5408.5m	8	3	Qz+Chl	84.73		6.95	5.84		1.36	0.32		0.55				0.23												100	127
H-23 5408.5m	8	4	Qz+Ank	76.31			5.92	0.32	3.12	14.33																		100	114
H-23 5408.5m	8	5	Ank+Ab	9.28		4.01	21.48	1.23	18.47	43.85	1.66																	100	72
H-23 5408.5m	8	6	Ank+TiO_2+Chl	5.43	21.25	5.06	18.63	1.01	15.77	32.85																		100	59

Table 2-9A: Scanning Electron Microscope chemical analyses of 5408.5m from Newburn H-23 well.

Sample	Site	Position	Mineral	SiO_2	TiO_2	Al_2O_3	FeO	MnO	MgO	CaO	Na_2O	K_2O	P_2O_5	SO_3	F	Cl	V_2O_5	Cr_2O_3	CdO	As_2O_3	SrO	ZrO_2	BaO	Ce_2O_3	HfO_2	WO_3	B_2O_3	Total	Actual Total
H-23 5408.5m	8	7	Fe-Cal+Qz	1.71			2.07	0.71	1.26	94.25																		100	41
H-23 5408.5m	8	8	Qz+Chl	96.41		1.02	0.46			1.93		0.17																100	153
H-23 5408.5m	8	9	Fe-Cal				1.23	0.34		54.43																		56	66
H-23 5408.5m	8	10	TiO_2+Qz+Other	12.86	83.12	1.76	1.99			0.29																		100	135
H-23 5408.5m	8	11	Ank+Chl	2.35		1.28	25.31	1.61	19.58	49.87																		100	80
H-23 5408.5m	8	12	Brt											41.20									58.80					100	125
H-23 5408.5m	8	13	F-Cal+Chl	9.58		7.03	5.24	0.14	1.43	26.56		0.76			5.09	0.17												56	73
H-23 5408.5m	8	14	Qz	99.99																								100	122
H-23 5408.5m	8	15	Qz	99.15		0.70						0.14																100	123
H-23 5408.5m	8	16	Ab	61.46		20.44	4.84		1.19	0.36	11.51					0.19												100	100
H-23 5408.5m	8	17	Qz	98.17		0.87	0.15				0.80																	100	100
H-23 5408.5m	8	18	Qz	99.86			0.14																					100	104
H-23 5408.5m	8	19	Qz+Ms+Chl	73.07	0.23	15.87	3.87		3.13		0.66	3.14																100	100
H-23 5408.5m	8	20	Qz	99.75			0.26																					100	98
H-23 5408.5m	8	21	Qz	99.45						0.55																		100	110
H-23 5408.5m	8	22	Ab	70.44		15.44	0.35			2.07	11.69																	100	131
H-23 5408.5m	8	23	Qz+Other	95.88		2.19	0.71		0.66		0.38					0.16												100	136
H-23 5408.5m	8	24	Py	0.96		0.51	26.05				0.39			72.12														100	254
H-23 5408.5m	8	25	Qz+TiO_2+Other	86.00	8.42	3.61	1.00		0.35			0.59																100	153
H-23 5408.5m	8	26	Py	2.20		0.62	26.09			0.15	0.32			70.27						0.34								100	235
H-23 5408.5m	8	27	Cal				0.99	0.32		54.70																		56	60
H-23 5408.5m	8	28	Qz	98.53		0.83	0.64																					100	122
H-23 5408.5m	8	29	Qz	99.99																								100	129
H-23 5408.5m	8	30	Chl	27.51		21.12	23.54		4.61	2.26					4.90	1.05												85	81
H-23 5408.5m	8	31	Qz	99.99																								100	142
H-23 5408.5m	8	32	Qz	99.99																								100	142
H-23 5408.5m	8	33	Ank+Ab	15.44		5.25	14.88	1.07	13.63	39.23	4.57		5.91															100	75
H-23 5408.5m	9	1	Tur	38.46	0.77	33.77	5.12		6.10	0.88	1.91																	87	116
H-23 5408.5m	9	2	TiO_2	0.58	98.75		0.66																					100	104
H-23 5408.5m	9	3	Ank				13.81	0.96	11.09	30.14																		56	68
H-23 5408.5m	9	4	Fe-Cal				1.32	0.32	0.44	53.92																		56	62
H-23 5408.5m	9	5	TiO_2+Chl	4.81	87.26	3.74	2.77		0.90					0.55														100	115
H-23 5408.5m	9	6	Chl	32.56		21.77	24.77		4.26	1.36						0.28												85	106
H-23 5408.5m	9	7	TiO_2+Chl	2.25	93.86	1.47	2.43																					100	103
H-23 5408.5m	9	8	Fe-Cal				1.36	0.26		54.39																		56	53
H-23 5408.5m	9	9	Tur	39.00	0.71	33.76	5.11		5.97	0.56	1.90																	87	117
H-23 5408.5m	9	10	Chl	26.76	5.62	18.69	26.24		4.04	1.45	0.68	0.20		0.59		0.72												85	57
H-23 5408.5m	9	11	Qz	99.99																								100	128
H-23 5408.5m	9	12	Qz	99.99																								100	133
H-23 5408.5m	9	13	Qz	99.99																								100	136
H-23 5408.5m	9	14	Qz+Chl	89.42		6.01	2.44		1.38	0.38		0.37																100	145
H-23 5408.5m	9	15	Ank				14.44	1.00	10.02	30.54																		56	65
H-23 5408.5m	9	16	Ank+Chl	7.77		7.10	26.26	1.30	14.91	42.68																		100	73
H-23 5408.5m	9	17	TiO_2+Chl+Other	8.00	75.73	4.31	4.32		1.64	1.09					4.58	0.34												100	91

Table 2-9A: Scanning Electron Microscope chemical analyses of 5408.5m from Newburn H-23 well.

Sample	Site	Position	Mineral	SiO_2	TiO_2	Al_2O_3	FeO	MnO	MgO	CaO	Na_2O	K_2O	P_2O_5	SO_3	F	Cl	V_2O_5	Cr_2O_3	CdO	As_2O_3	SrO	ZrO_2	BaO	Ce_2O_3	HfO_2	WO_3	B_2O_3	Total	Actual Total
H-23 5408.5m	9	18	Chl	29.17		24.00	25.85		4.73	0.95						0.30												85	107
H-23 5408.5m	9	19	Ms+Chl	55.02	0.93	29.36	3.78		2.22		0.44	7.95				0.30												100	111
H-23 5408.5m	9	20	Qz+Ms	90.32	0.20	5.88	1.38		0.75			1.47																100	127
H-23 5408.5m	10	1	Hl+Qz+Other	19.72		0.53	0.12		0.99	1.78	43.99	0.19				32.68												100	150
H-23 5408.5m	10	2	Slide	72.95		1.32			5.01	6.58	13.59	0.55																100	142
H-23 5408.5m	10	3	Slide	74.51		1.27	0.17		4.34	7.01	11.72	0.63		0.37														100	121
H-23 5408.5m	10	4	Slide	73.61		1.42	0.13		5.04	5.99	13.29	0.52																100	144
H-23 5408.5m	10	5	Fe-Cal				1.10	0.29		54.61																		56	57
H-23 5408.5m	10	6	Sd+Ap+Chl	3.85		3.27	65.56	1.90	8.26	15.14			2.02															100	66
H-23 5408.5m	10	7	Ms+Chl	43.04		26.79	20.07		3.45	1.26		5.07				0.31												100	110
H-23 5408.5m	10	8	Ab	64.86		19.78	3.65		0.80		8.55	2.35																100	150
H-23 5408.5m	10	9	Ab	68.71		18.76					12.52																	100	146
H-23 5408.5m	10	10	Ms	51.12	0.31	31.50	1.26		0.86		0.92	9.01																95	137
H-23 5408.5m	10	11	Ab	67.11		19.84	0.66		0.41	0.94	10.77	0.28																100	152
H-23 5408.5m	10	12	Ms	54.77	0.88	23.28	4.24		2.82			9.01																95	134
H-23 5408.5m	10	13	Mix	24.43	56.98	1.44	4.08		10.74	1.51		0.45				0.38												100	85
H-23 5408.5m	10	14	Ab+Chl	50.96	0.25	19.46	14.20		1.43	3.43	8.41		1.70			0.18												100	123
H-23 5408.5m	10	15	Qz	99.07		0.40					0.53																	100	139
H-23 5408.5m	10	16	Chl+Other	34.25	0.73	19.50	34.26		6.30	2.69		1.05				1.19												100	62
H-23 5408.5m	10	17	Chl	26.42		19.85	29.86	0.21	5.83	2.39						0.43												85	99
H-23 5408.5m	10	18	Chl+Ap	36.60		17.18	19.52		7.88	8.16	2.09		8.57															100	123
H-23 5408.5m	10	19	Qz+Ab+Chl	89.40	0.38	3.44	4.62		0.75	0.39	1.02																	100	142
H-23 5408.5m	10	20	Qz	99.99																								100	134
H-23 5408.5m	10	21	Cal				1.11	0.38	0.41	54.10																		56	60
H-23 5408.5m	10	22	Ilt+Ab+Chl	57.99	0.47	25.85	3.02		2.69		2.43	7.54																100	129
H-23 5408.5m	10	23	Chl+Ilt	42.01		24.64	23.83		6.43	1.22		1.87																100	112
H-23 5408.5m	10	24	Qz	99.99																								100	137
H-23 5408.5m	10	25	Ab	66.61		18.71	0.73			1.18	11.99		0.76															100	148
H-23 5408.5m	11	1	TiO_2+Fe-Cal	0.41	79.22	0.36	1.29			18.74																		100	98
H-23 5408.5m	11	2	Fe-Cal				1.31	0.42		54.27																		56	55
H-23 5408.5m	11	3	Zrn	31.79																		67.68			0.54			100	145
H-23 5408.5m	11	4	TiO_2+Other	1.75	94.66	0.77	1.47			1.13						0.20												100	107
H-23 5408.5m	11	5	Fap	1.35			0.99		0.43	43.81			43.86		7.86	0.20										1.50		100	133
H-23 5408.5m	11	6	Fe-Cal	0.68		0.35	1.47	0.43	0.39	52.69																		56	65
H-23 5408.5m	11	7	Py	0.21			24.38			0.11				63.28														88	241
H-23 5408.5m	11	8	Zrn	29.29																		60.57			0.37			90	137
H-23 5408.5m	11	9	Zrn	31.49	0.78	0.57	1.45															65.04			0.68			100	121
H-23 5408.5m	11	10	TiO_2	0.86	98.73		0.44																					100	108
H-23 5408.5m	11	11	Ank	1.28			14.51	0.92	10.35	28.93																		56	62
H-23 5408.5m	11	12	Chl	27.98	0.65	22.19	27.11		4.17	1.93		0.22				0.74												85	88
H-23 5408.5m	11	13	Chl	28.27		21.99	28.73		4.11	1.28		0.20				0.42												85	95
H-23 5408.5m	11	14	TiO_2+Qz	11.42	86.07	0.43	1.20		0.60	0.27																		100	102
H-23 5408.5m	11	15	Ms	49.67	0.76	27.54	5.29		2.01			9.73																95	140
H-23 5408.5m	11	16	Qz	99.99																								100	141

Table 2-9A: Scanning Electron Microscope chemical analyses of 5408.5m from Newburn H-23 well.

Sample	Site	Position	Mineral	SiO_2	TiO_2	Al_2O_3	FeO	MnO	MgO	CaO	Na_2O	K_2O	P_2O_5	SO_3	F	Cl	V_2O_5	Cr_2O_3	CdO	As_2O_3	SrO	ZrO_2	BaO	Ce_2O_3	HfO_2	WO_3	B_2O_3	Total	Actual Total
H-23 5408.5m	11	17	Qz+Ms+Chl	77.74	0.22	12.24	4.19		2.24	0.32		3.05																100	111
H-23 5408.5m	11	18	Qz	99.99																								100	133
H-23 5408.5m	11	19	Fe-Cal				1.11	0.33		54.55																		56	64
H-23 5408.5m	11	20	Ab+Chl	60.28		19.14	6.48		1.09	1.27	10.46	0.13	0.89			0.25												100	120
H-23 5408.5m	11	21	Qz+TiO_2	89.95	9.89		0.17																					100	120
H-23 5408.5m	11	22	Ms+Py+Other	77.10	0.22	14.25	1.97		0.83			4.44		1.17														100	124
H-23 5408.5m	12	1	TiO_2	2.91	97.10																							100	117
H-23 5408.5m	12	2	Zrn	31.85																		67.66			0.48			100	145
H-23 5408.5m	12	3	TiO_2	0.79	98.90		0.30																					100	119
H-23 5408.5m	12	4	Ank				14.14	0.94	10.71	30.22																		56	71
H-23 5408.5m	12	5	Zrn	31.77																		67.90			0.33			100	136
H-23 5408.5m	12	6	TiO_2	1.50	97.26	0.76	0.21					0.26																100	113
H-23 5408.5m	12	7	Chl	38.27		25.57	28.17		5.02	1.20	1.54					0.22												100	104
H-23 5408.5m	12	8	Ank+Chl	4.32		3.53	24.74	1.47	17.96	47.99																		100	66
H-23 5408.5m	12	9	TiO_2+Other	0.94	97.33	0.70	1.04																					100	121
H-23 5408.5m	12	10	Ank	0.63		0.44	13.02	0.94	10.46	30.51																		56	79
H-23 5408.5m	12	11	Ms	47.62	0.29	35.60	1.03				0.45	10.02																95	111
H-23 5408.5m	12	12	Ms	48.88	0.29	32.29	1.54		1.20		0.34	10.47																95	115
H-23 5408.5m	12	13	TiO_2+Chl	12.98	64.35	8.37	10.00		3.27	0.45		0.25						0.35										100	106
H-23 5408.5m	12	14	Chl+Ms	69.20		12.55	11.84		4.00	0.66		1.58				0.17												100	116
H-23 5408.5m	12	15	TiO_2+Chl	3.38	92.89	1.34	1.42				0.94																	100	107
H-23 5408.5m	12	16	Cal+Other	1.86		1.25	2.55	0.62	0.78	92.93																		100	55
H-23 5408.5m	12	17	Qz	99.99																								100	143
H-23 5408.5m	12	18	Chl+Ank	28.86		17.95	29.38	0.44	7.69	14.87	0.54					0.24												100	107
H-23 5408.5m	12	19	Chl	28.53		19.52	27.74		6.64	1.48	0.55					0.55												85	104
H-23 5408.5m	12	20	Ms+Chl	53.22		20.65	14.29		7.16	0.71	0.46	3.28				0.23												100	130
H-23 5408.5m	12	21	Ms+Chl	61.39	0.50	17.71	11.80		4.23	0.70		3.48				0.20												100	138
H-23 5408.5m	12	22	Qz+Ilt	79.98		13.30	1.87		0.43			4.42																100	149
H-23 5408.5m	12	23	Qz	93.14		3.40	2.23		0.66		0.34	0.23																100	137
H-23 5408.5m	12	24	Ank				14.44	1.00	9.78	30.78																		56	72
H-23 5408.5m	12	25	Qz+Ank	45.99			13.46	0.85	8.80	30.89																		100	101
H-23 5408.5m	12	26	Ab+Ank+Chl	41.41		19.80	16.26		3.05	13.80	4.68	0.26				0.74												100	75
H-23 5408.5m	12	27	Qz+Other	98.00	0.17	1.32	0.37					0.13																100	116
H-23 5408.5m	13	1	Chl	32.22		18.14	18.87	0.31	14.75	0.71																		85	109
H-23 5408.5m	13	2	Chl	31.23		19.46	17.91	0.38	15.31	0.71																		85	106
H-23 5408.5m	13	3	Fe-Cal				1.00	0.25		54.75																		56	50
H-23 5408.5m	13	4	Ms	47.72	0.45	33.26	3.30		1.15		0.44	8.69																95	119
H-23 5408.5m	13	5	TiO_2+Chl	2.67	91.98	3.40	1.05		0.46	0.42																		100	123
H-23 5408.5m	13	6	Zrn	31.62																		68.05			0.33			100	151
H-23 5408.5m	13	7	Ank	0.49		0.44	14.99	1.01	10.71	28.35																		56	71
H-23 5408.5m	13	8	Chl+Ms	49.48		23.60	19.00		4.51	1.08		1.84				0.50												100	86
H-23 5408.5m	13	9	Qz	99.99																								100	137
H-23 5408.5m	13	10	Qz+Chl	72.86		16.80	7.15		2.06	0.50		0.30				0.32												100	93
H-23 5408.5m	13	11	Ab	67.11		19.54	0.28			0.64	12.27	0.16																100	132

Table 2-9A: Scanning Electron Microscope chemical analyses of 5408.5m from Newburn H-23 well.

Sample	Site	Position	Mineral	SiO_2	TiO_2	Al_2O_3	FeO	MnO	MgO	CaO	Na_2O	K_2O	P_2O_5	SO_3	F	Cl	V_2O_5	Cr_2O_3	CdO	As_2O_3	SrO	ZrO_2	BaO	Ce_2O_3	HfO_2	WO_3	B_2O_3	Total	Actual Total
H-23 5408.5m	13	12	Ab	66.46		20.22	0.58			1.05	11.68																	100	129
H-23 5408.5m	13	13	Cr-Spl		0.43	41.31	14.31		14.59									29.37										100	134
H-23 5408.5m	13	14	Chl	30.68	1.23	23.28	21.96		4.05	1.93		0.96				0.92												85	99
H-23 5408.5m	13	15	Ab	65.84		20.75	0.33			0.98	11.39	0.71																100	131
H-23 5408.5m	14	1	Chl+Other*	37.44		27.97	21.52		3.88	1.41	1.64	1.58			3.35	1.02		0.20										100	96
H-23 5408.5m	14	2	Ab+Chl+Ilt*	44.84	0.28	33.26	12.38		2.40	0.56	4.11	1.98				0.20												100	114
H-23 5408.5m	14	3	TiO_2+Chl*	24.96	33.44	18.20	18.17		2.64	0.94		0.98				0.66												100	91
H-23 5408.5m	14	4	Chl+Other*	37.91		28.78	23.54		3.85	1.96	0.65	2.05				1.27												100	89
H-23 5408.5m	14	5	Chl*	27.84		22.41	22.80		4.39	1.56	0.48	0.46			3.22	1.84												85	81
H-23 5408.5m	14	6	Qz*	98.10		0.57	1.34																					100	129
H-23 5408.5m	14	7	TiO_2+Qz+Other*	30.80	57.36	4.63	3.40		1.38	0.73						1.70												100	56
H-23 5408.5m	14	8	Qz+TiO_2+Other	59.79	21.58	6.18	4.88		1.54	3.95	0.86	0.17		0.55		0.50												100	105
H-23 5408.5m	14	9	Qz+TiO_2+Other	60.43	20.40	4.70	4.39		1.54	1.18	1.20	0.31	0.60	1.02	3.58	0.64												100	87
H-23 5408.5m	14	10	Chl+Other	36.84		27.06	23.14		3.32	1.87	2.49	0.79			3.43	1.03												100	88
H-23 5408.5m	14	11	Cr-Spl		0.70	40.64	14.40		13.58									30.70										100	116
H-23 5408.5m	14	12	Qz+TiO_2+Ilt	64.63	22.77	7.95	1.98		0.60	0.31		1.77																100	124
H-23 5408.5m	15	1	Ms	48.29	0.31	34.35	1.45		0.63		0.89	9.07																95	127
H-23 5408.5m	15	2	Ab+Ms	58.72		22.83	4.18		0.61	0.41	10.54	2.40				0.32												100	120
H-23 5408.5m	15	3	Kln	49.57		36.43																						86	108
H-23 5408.5m	15	4	Qz+Ms+Chl	82.32	0.18	10.32	3.67		1.31	0.36		1.63				0.21												100	119
H-23 5408.5m	15	5	Qz	99.99																								100	136
H-23 5408.5m	15	6	Qz	99.15		0.62						0.23																100	133
H-23 5408.5m	15	7	Qz	98.90											1.11													100	139
H-23 5408.5m	15	8	Qz	99.99																								100	137
H-23 5408.5m	15	9	Qz	94.38		3.51	0.41		0.46		0.62	0.61																100	131
H-23 5408.5m	15	10	Qz	95.04		3.33					1.33	0.30																100	134
H-23 5408.5m	15	11	Qz	96.03		2.48	0.66				0.63	0.22																100	128
H-23 5408.5m	15	12	Chl+Other	36.13		23.75	23.40		3.71	2.71		2.67		1.80		5.83												100	31
H-23 5408.5m	15	13	Qz	99.99																								100	130
H-23 5408.5m	15	14	Qz	99.99																								100	132
H-23 5408.5m	15	15	Chl+Other	42.78		29.40	16.25		5.14	1.50	1.67	0.31		1.05		1.89												100	61
H-23 5408.5m	15	16	Chl+Other	40.22		27.25	20.27		5.27	2.63		0.92		1.05		2.40												100	66
H-23 5408.5m	15	17	Qz	99.99																								100	137
H-23 5408.5m	16	1	Ms+Chl	48.39		35.22	4.61		1.01		0.38	10.25				0.15												100	114
H-23 5408.5m	16	2	Cal				0.56	0.23		55.21																		56	60
H-23 5408.5m	16	3	Ank+Other	3.42		0.93	25.41	1.69	17.99	50.58																		100	70
H-23 5408.5m	16	4	Fe-Cal+Other	3.76		1.11	2.89	1.02	0.96	89.76		0.48																100	60
H-23 5408.5m	16	5	Fap	1.30			0.45			46.59			43.45		6.98	0.14								1.07				100	121
H-23 5408.5m	16	6	Ms+Qz	75.86		15.19	3.80		0.96	0.38	0.43	3.23				0.15												100	135
H-23 5408.5m	16	7	Zrn	32.07			0.22															67.58			0.13			100	135
H-23 5408.5m	16	8	Ms+Chl	76.54		11.56	5.94		3.25			2.70																100	128
H-23 5408.5m	16	9	Fe-Cal				1.08	0.30	0.40	54.22																		56	59
H-23 5408.5m	16	10	Fe-Cal	0.54			1.33	0.35		53.78																		56	53
H-23 5408.5m	16	11	Qz+TiO_2	44.86	52.91	0.68	1.54																					100	111

Table 2-9A: Scanning Electron Microscope chemical analyses of 5408.5m from Newburn H-23 well.

Sample	Site	Position	Mineral	SiO_2	TiO_2	Al_2O_3	FeO	MnO	MgO	CaO	Na_2O	K_2O	P_2O_5	SO_3	F	Cl	V_2O_5	Cr_2O_3	CdO	As_2O_3	SrO	ZrO_2	BaO	Ce_2O_3	HfO_2	WO_3	B_2O_3	Total	Actual Total
H-23 5408.5m	16	12	Qz+hole	80.28		2.53	11.39		1.74	1.61	0.74	0.35				1.36												100	75
H-23 5408.5m	16	13	Qz	99.99																								100	126
H-23 5408.5m	16	14	Qz+Chl+Ilt	79.32	0.65	7.35	4.37		0.93	1.78		1.54		0.50	2.64	0.88												100	79
H-23 5408.5m	16	15	Qz+Cal	75.17			0.44			24.39																		100	108
H-23 5408.5m	16	16	Mix	42.10	5.14	25.34	7.38		2.27	8.42	0.54	6.91		0.67		1.21												100	74
H-23 5408.5m	16	17	Qz	99.58			0.27									0.16												100	134
H-23 5408.5m	16	18	TiO_2+Chl	6.80	85.72	2.55	4.17		0.56	0.21																		100	119
H-23 5408.5m	16	19	TiO_2+Chl	2.95	91.84	1.91	2.48			0.83																		100	104
H-23 5408.5m	16	20	TiO_2+Chl	2.57	90.63	2.06	3.99			0.46						0.31												100	72
* = Lithic Clast																													

Appendix 2-10: SEM-BSE images and EDS mineral analyses for sample Newburn H-23 5957.8m

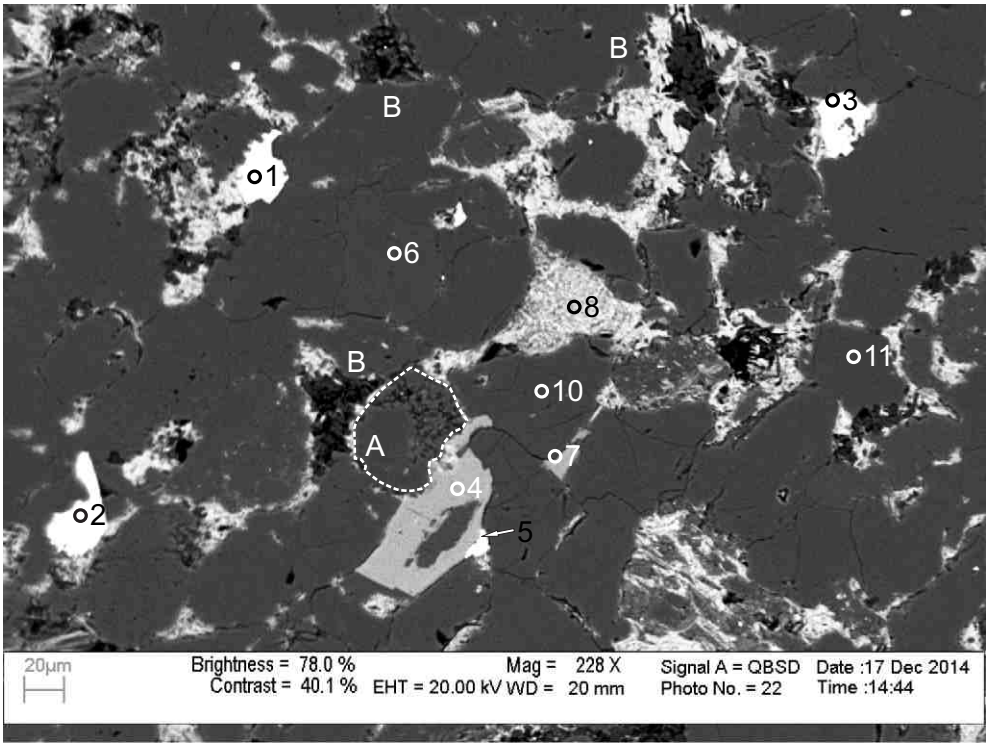

1: Titania
2: Titania
3: Titania
4: Ankerite
5: Titania+ Other
6: Albite
7: Ankerite+ Quartz
8: Chlorite
9: Chlorite+ Other
10: Quartz
11: Quartz

Figure 2-10.1: Sample Newburn 5957.8m site 1 (SEM). Ankerite (4) has an irregular contact with quartz. The quartz has abundant dissolution voids (position A). Titania (1) appears to have partly engulfed quartz and chlorite. Pores largely filled with kaolinite (position B) and rimmed by fibrous chlorite and rare chlorite fibers fill porosity between kaolinite booklets. Titania (5) appears to engulf ankerite (4).

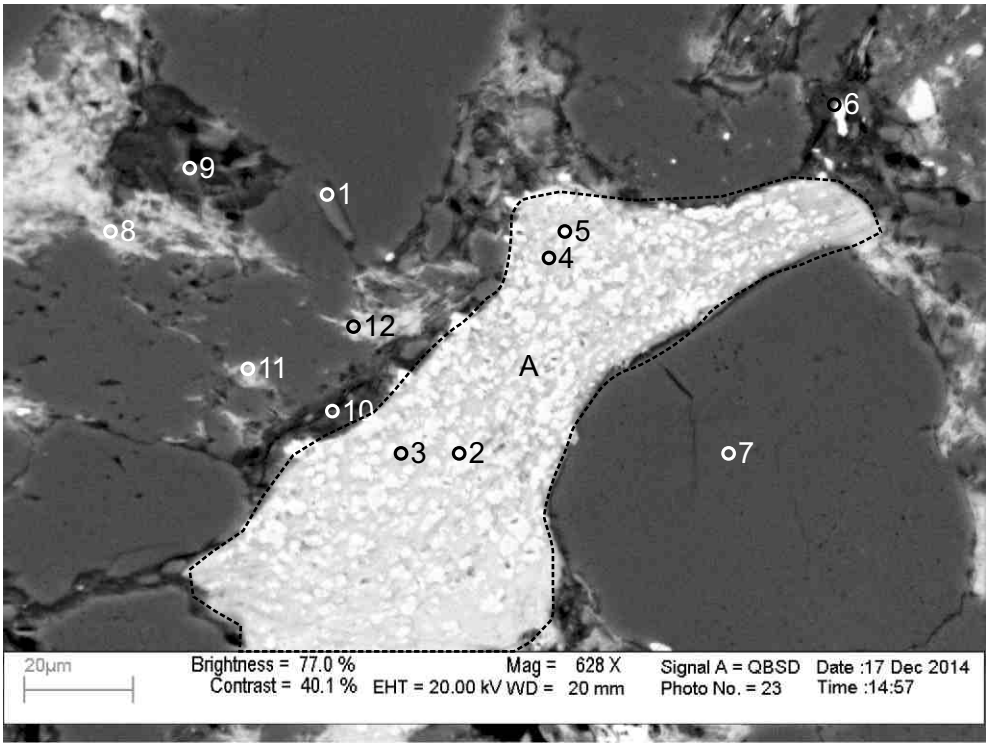

1: Quartz+Illite
2: Siderite+ Chlorite
3: Siderite+ Chlorite
4: Siderite+ Chlorite
5: Siderite+ Chlorite
6: Muscovite+ Titania
7: Quartz
8: Chlorite+ Albite
9: Kaolinite+ Illite
10: Kaolinite+ Illite
11: Chlorite+ Albite
12: Chlorite+ Albite

Figure 2-10.2: Sample Newburn 5957.8m site 2 (SEM). Mud intraclast (position A) comprised of chlorite cemented by siderite (2-5). Illite (1) forms in void between grain boundaries of quartz.

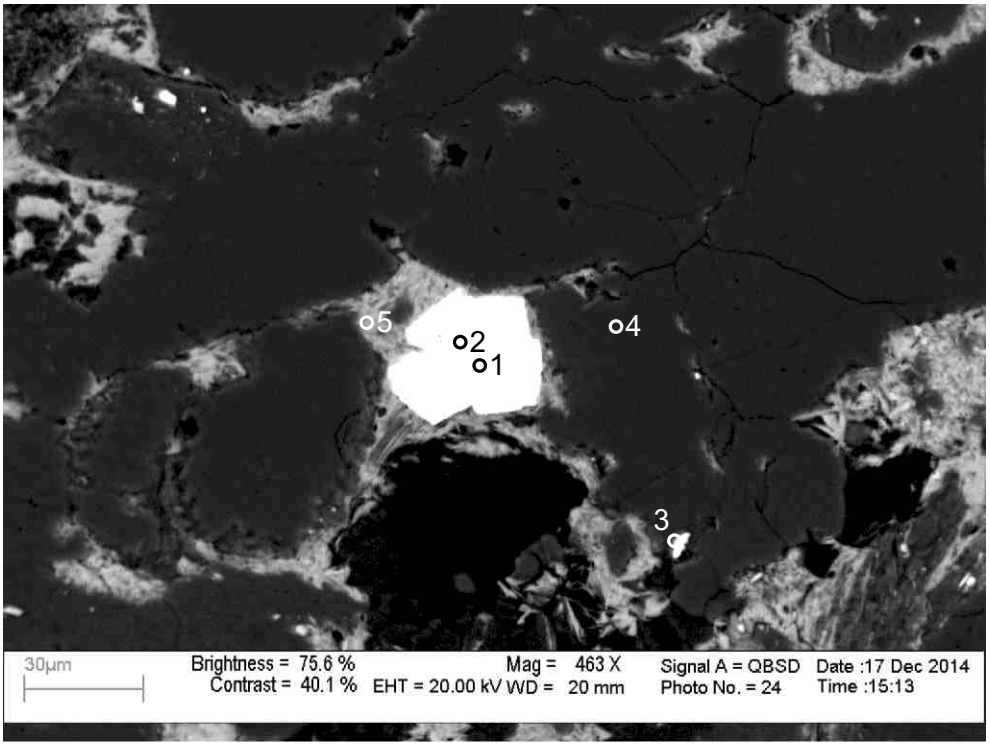

1: Pyrite
2: Pyrite
3: Quartz+ Chlorite
4: Quartz
5: Chlorite

Figure 2-10.3: Sample Newburn 5957.8m site 3 (SEM). Diagenetic euhedral pyrite (1,2) has partly cut chlorite (5).

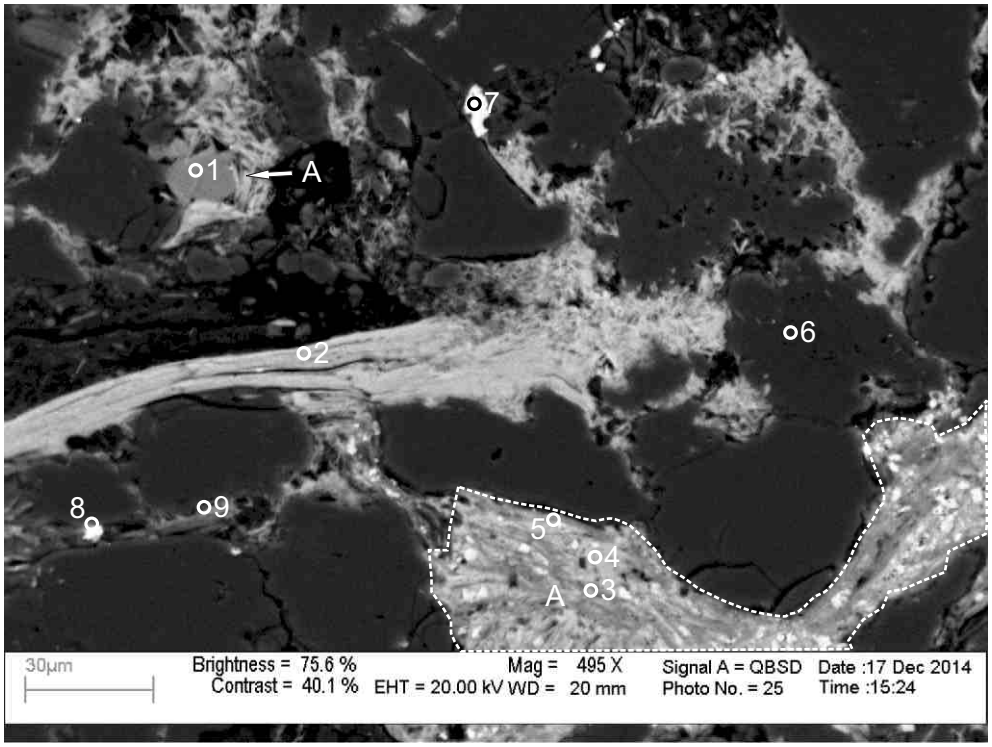

1: Calcite+ Chlorite
2: Chlorite+ Other
3: Chlorite
4: Chlorite
5: Chlorite
6: Quartz
7: Titania+Illite
8: Illite
9: Illite

Figure 2-10.4: Sample Newburn 5957.8m site 4 (SEM). Mud intraclast (position A) comprised of chlorite (3,4,5) plastically deformed around quartz grains. Fully chloritized muscovite (2). Illite (8,9) grows in voids along crystal boundaries between quartz grains. Calcite (1) appears to fill secondary porosity. Fibrous chlorite rims sparry calcite (1) grain (position A).

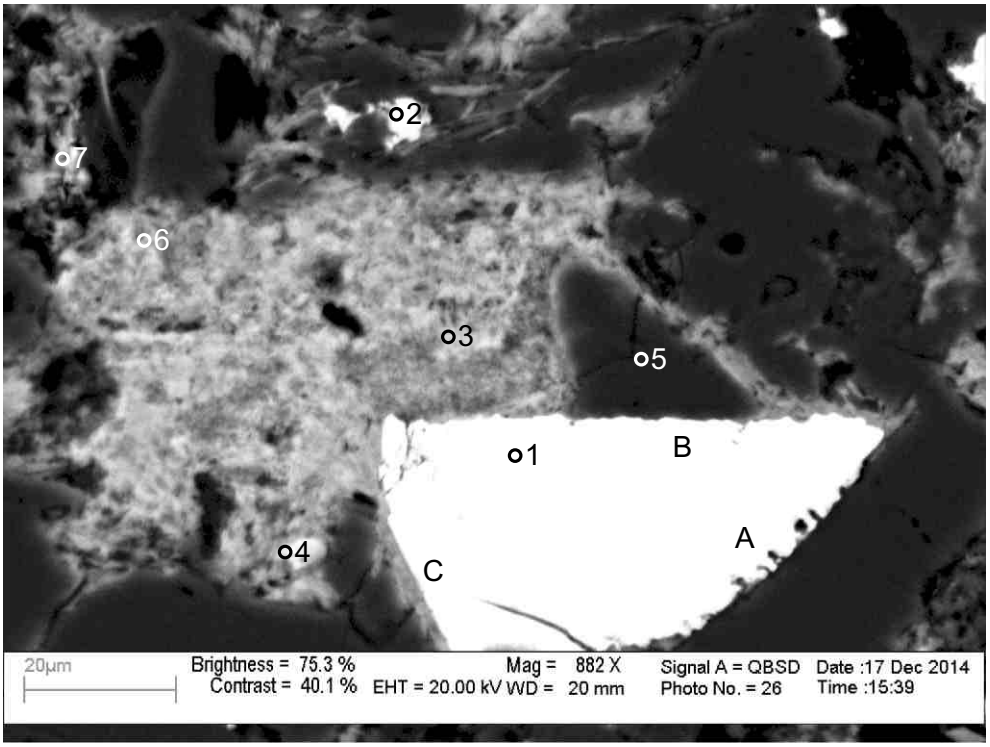

Figure 2-10.5: Sample Newburn 5957.8m site 5 (SEM). Chlorite fills pores and intergranular boundaries. Spinel (1) grain appears to possibly have cut quartz grain (position A,B) and then has been possibly corroded (position A,B). Straight euhedral edge is rimmed by chlorite (position C).

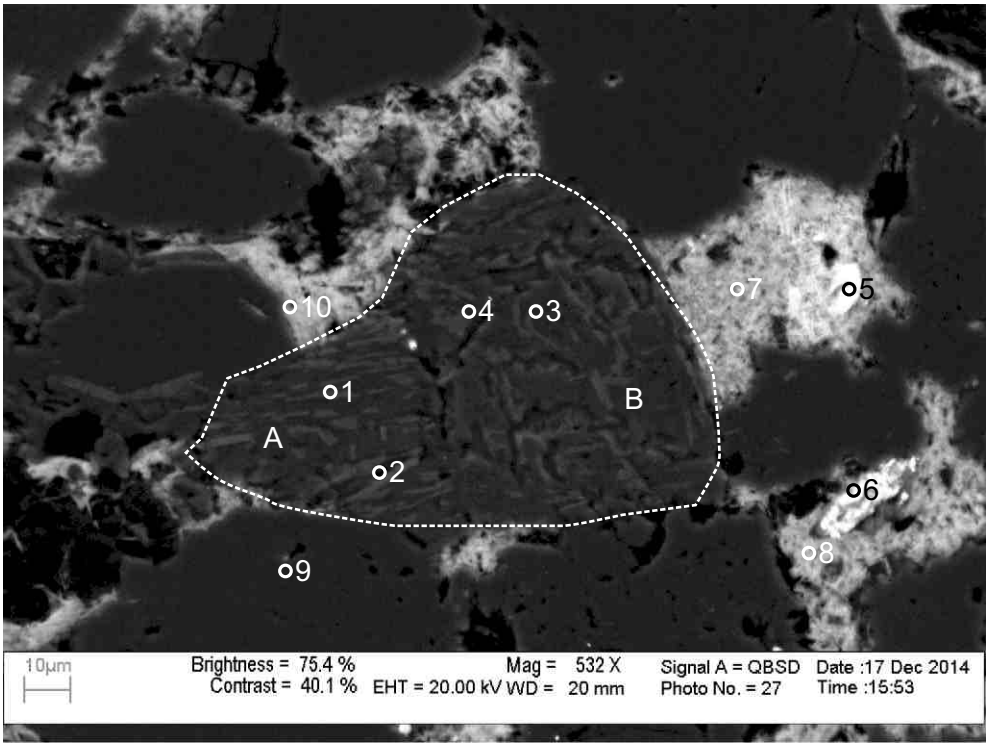

Figure 2-10.6: Sample Newburn 5957.8m site 6 (SEM). Trachytic lithic clast composed of albite (1-4) with dissolution voids filled by illite (1,2) with what appears to be a preferential orientation left to right (position A) and along crystal boundaries (position B). Titania is associated with chlorite (5,6).

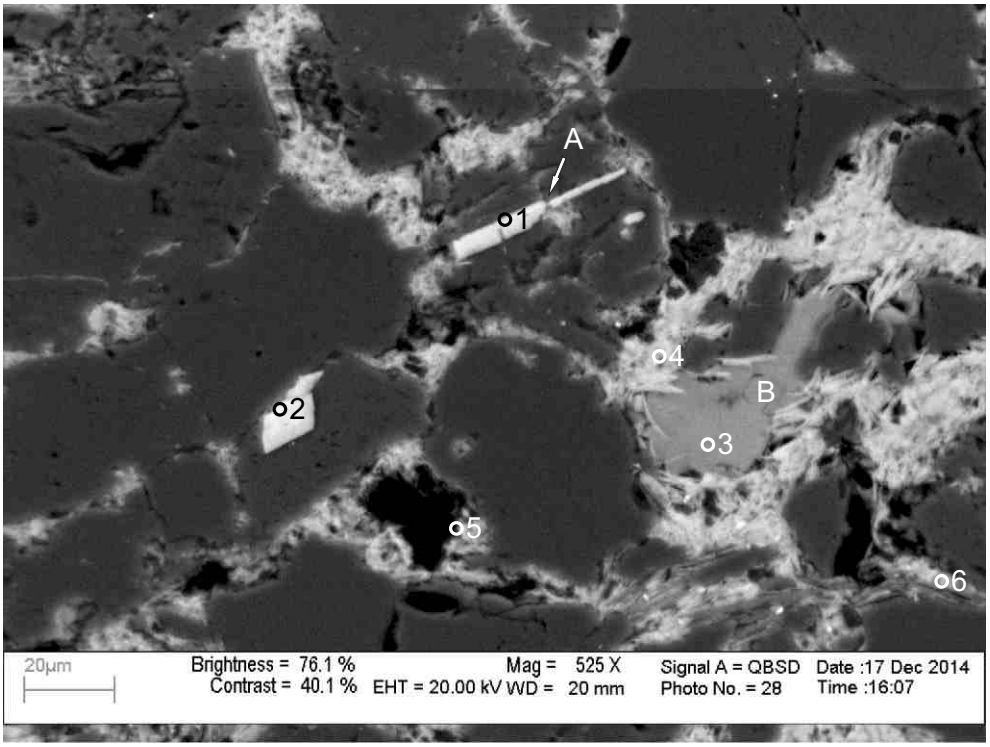

1: Fluorapatite +Albite
2: Siderite+ Chlorite
3: Fe-Calcite
4: Chlorite+ Other
5: Chlorite
6: Chlorite+ K-Feldspar

Figure 2-10.7: Sample Newburn 5957.8m site 7 (SEM). Euhedral fluorapatite (1) occurs within a fractured grain of albite and is then cut by chlorite in the fracture (position A). Calcite (3) engulfs chlorite fiber (4) and fills void bounded by chlorite (position B).

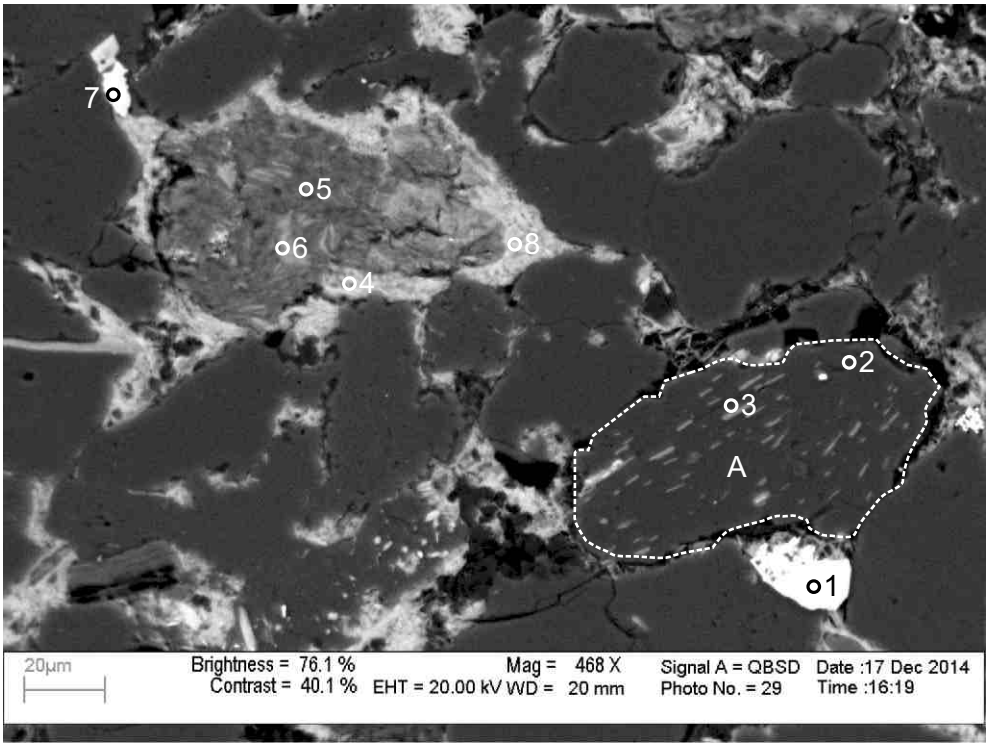

1: Titania
2: Quartz
3: Quartz+ Chlorite
4: Chlorite
5: Muscovite
6: Chlorite+ Muscovite
7: Titania+ Other
8: Chlorite

Figure 2-10.8: Sample Newburn 5957.8m site 8 (SEM). Chloritized muscovite (5) rimmed by chlorite (4). Lithic clast composed of quartz (2,3) and very minor chlorite laths (position A). Titania (1) engulfs chlorite and fills intergranular porosity (7).

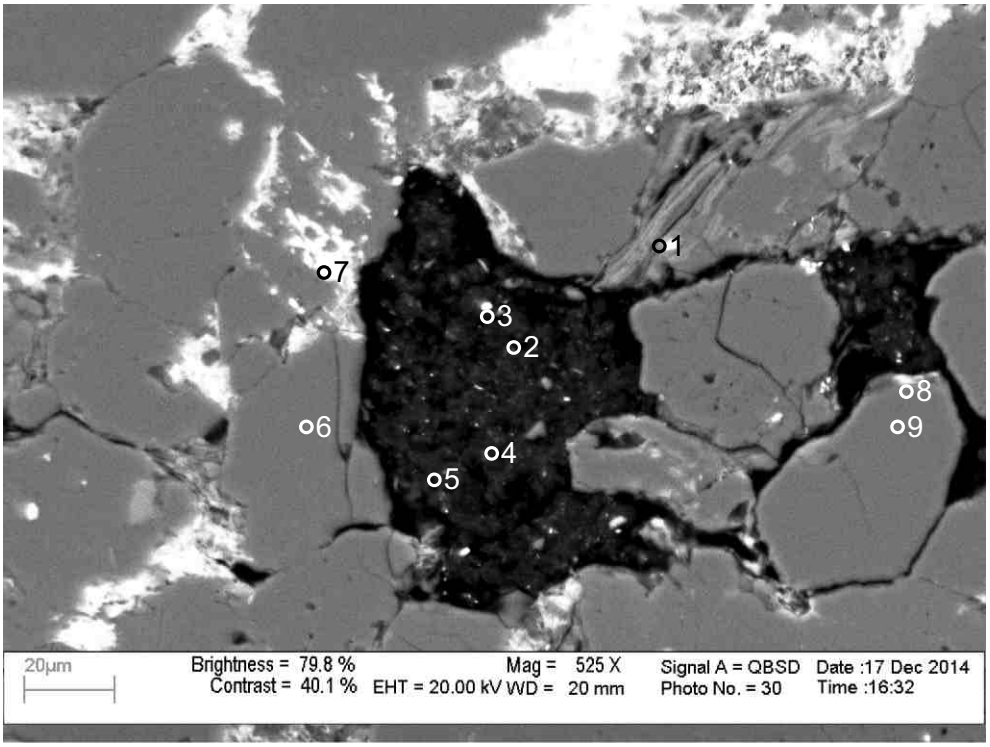

1: Muscovite+ Other
2: Drilling Mud +Fluorite
3: Siderite+ Quartz
4: Drilling Mud +Fluorite
5: Drilling Mud +Fluorite
6: Quartz
7: Chlorite+ Apatite
8: Quartz+ Chlorite
9: Quartz

Figure 2-10.9: Sample Newburn 5957.8m site 9 (SEM). Chlorite and apatite (7) fill intergranular boundaries. Drilling mud (2-5) fills pores. High secondary porosity.

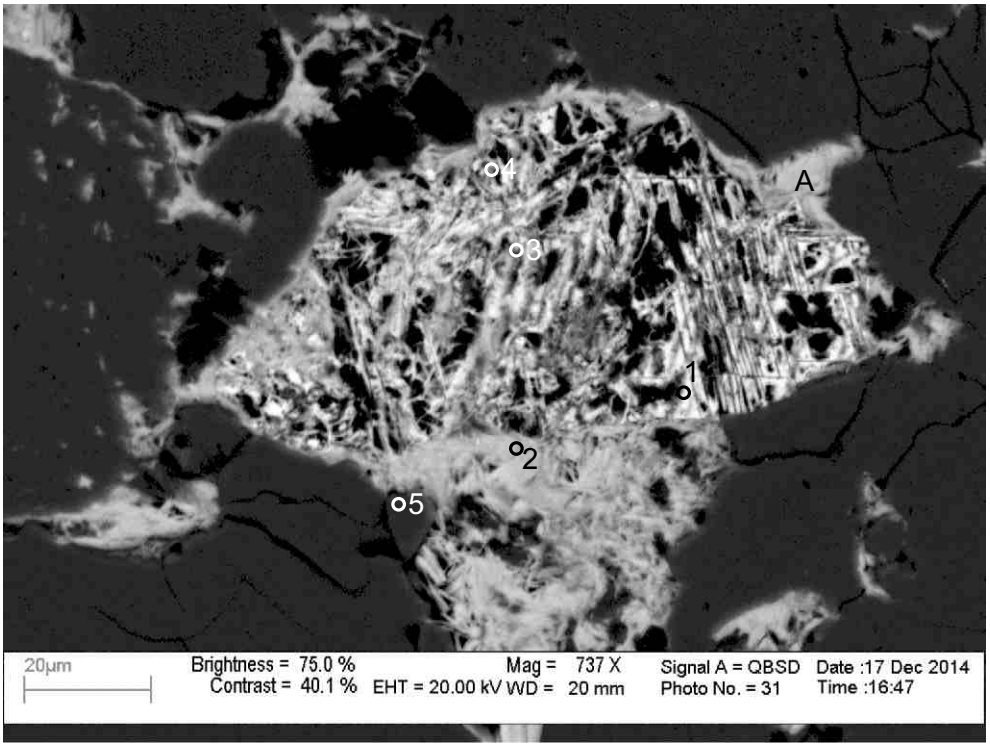

1: Titania+ Other
2: Chlorite+ Titania
3: Titania+ Chlorite
4: Titania+ Chlorite
5: Quartz

Figure 2-10.10: Sample Newburn 5957.8m site 10 (SEM). Chlorite rims (A) and cuts (3,4) detrital Titania (1) which has been partly dissolved. High secondary porosity.

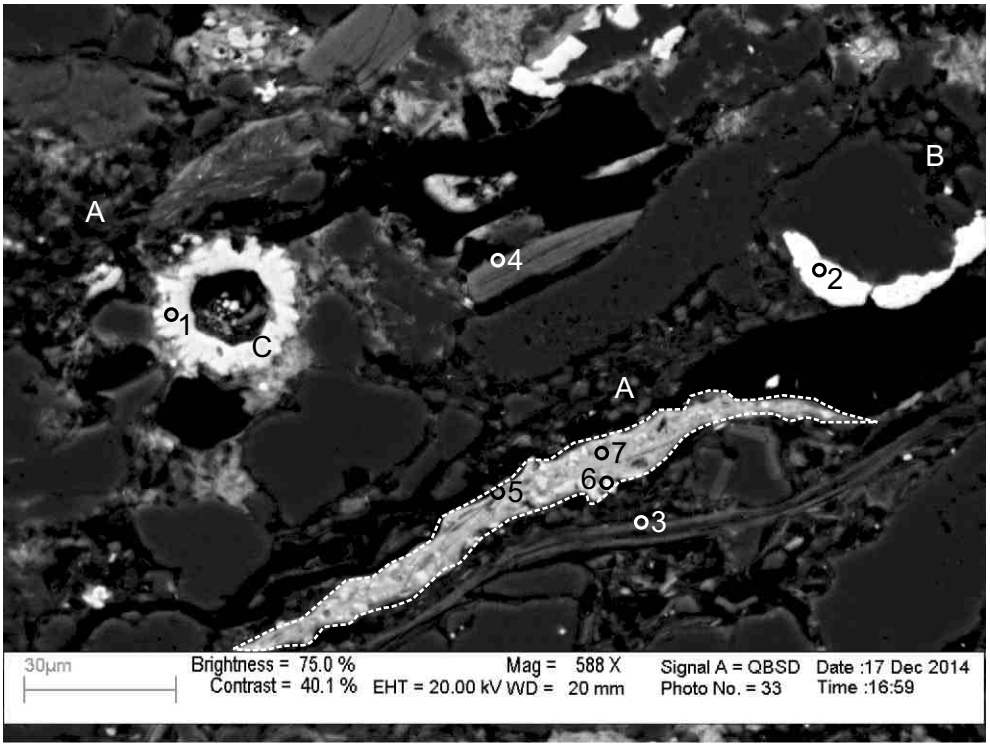

1: Siderite+ Other
2: Titania+ Other
3: Muscovite+ Other
4: Muscovite
5: Chlorite+ Other
6: Siderite+ Illite
7: Chlorite

Figure 2-10.11: Sample Newburn 5957.8m site 11 (SEM). Plastically deformed mud intraclast composed of chlorite(5,7) and illite (6) cemented by siderite (5,6). Diagenetic titania (2) rims quartz along intergranular boundary. Siderite (1) engulfs chlorite (position C), and rims a pore. Kaolinite fills porosity (position A) and is engulfed by titania (2, position B).

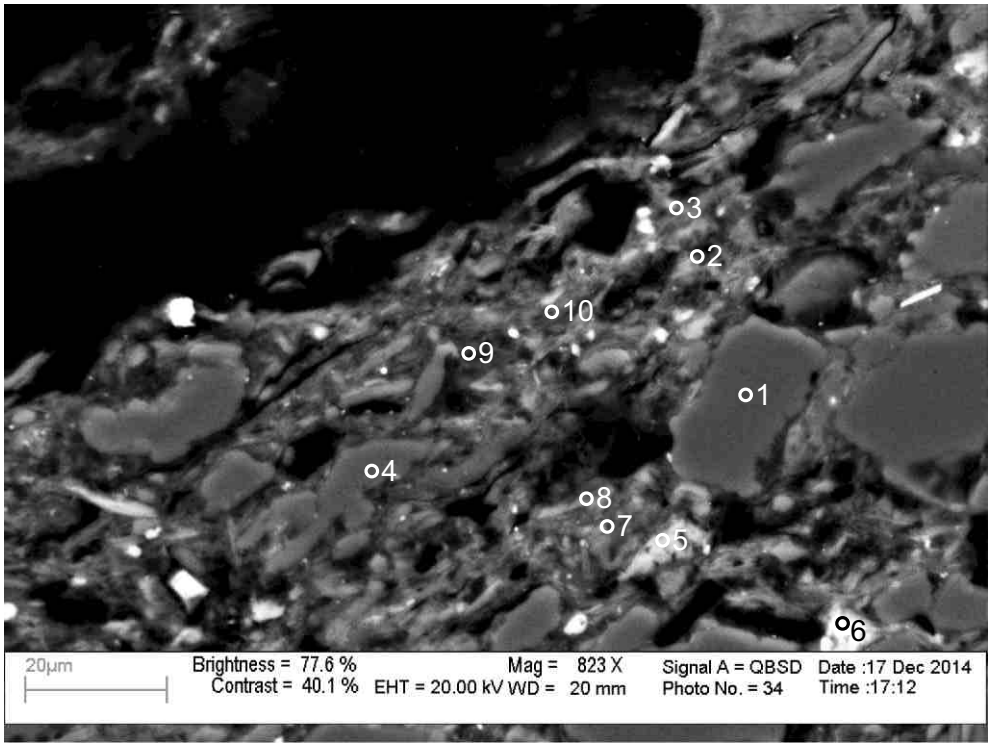

1: Quartz
2: Muscovite+ Chlorite
3: Muscovite+ Chlorite
4: Muscovite+ Chlorite
5: Chlorite+ Illite
6: Chlorite+ Siderite+ Apatite
7: Illite
8: Illite+ Kaolinite
9: Kaolinite+ Illite
10: Quartz+ Illite

Figure 2-10.12: Sample Newburn 5957.8m site 12 (SEM). Aligned grains of muscovite (2-4), illite (5,7-10), chlorite (2-6), quartz (1,10) and kaolinite (8,9) in muddy siltstone.

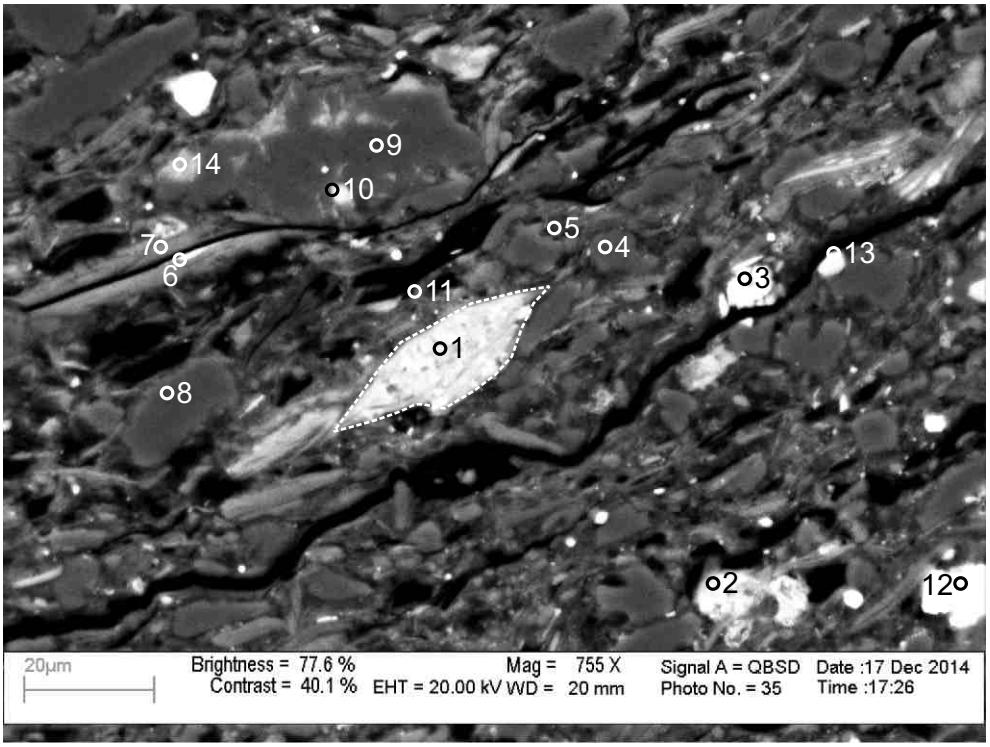

1: Chlorite+ Siderite
2: Titania+ Quartz+ Chlorite
3: Titania+ Quartz+ Chlorite
4: Albite
5: Illite+ Chlorite+ Kaolinite
6: Muscovite+ Chlorite
7: Muscovite+ Chlorite
8: Quartz
9: Albite
10:Fluorapatite +Albite
11: Muscovite+ Other
12: Zircon
13:Fluorapatite +Other
14: Chlorite+ Albite

Figure 2-10.13: Sample Newburn 5957.8m site 13 (SEM). Albite (9) with dissolution voids filled by fluorapatite (10) and chlorite (14). Mud intraclast composed of chlorite cemented by siderite (1).

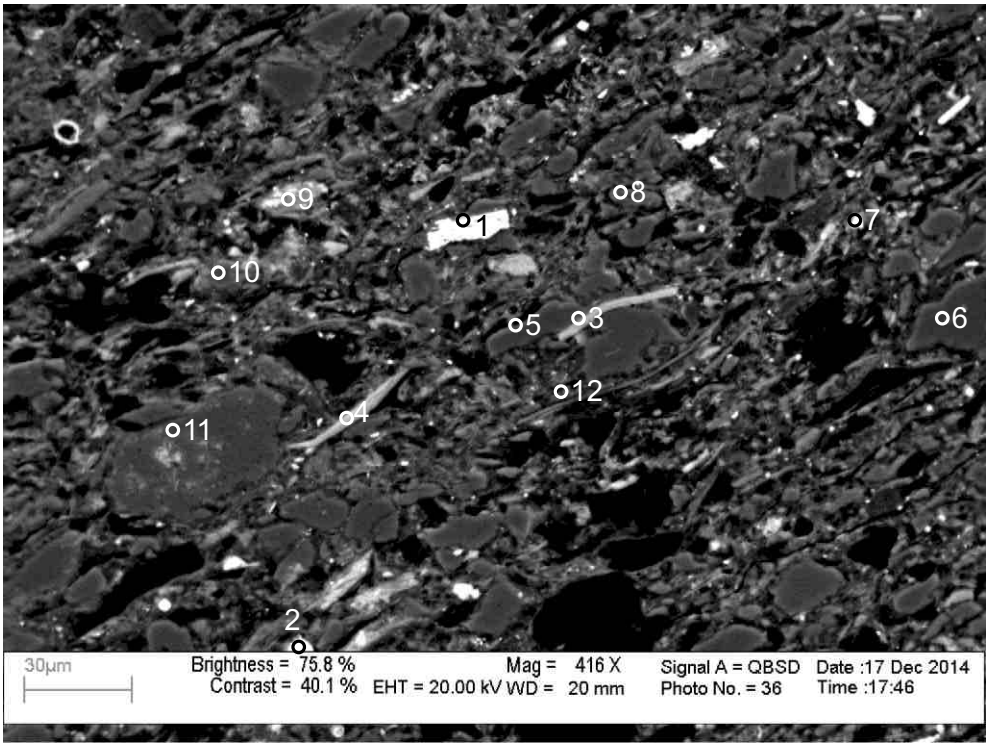

1: Titania+ Albite
2: Pyrite+ Chlorite
3: Chlorite+ Illite
4: Chlorite+ Illite
5: Quartz+ Other
6: Quartz
7: Zircon
8: Quartz+ Illite
9: Chlorite
10: Albite
11: Albite
12: Muscovite +Other

Figure 2-10.14: Sample Newburn 5957.8m site 14 (SEM). Muscovite altered to chlorite and illite (3,4). Titania (1) engulfs albite. Plastically deformed muscovite (12).

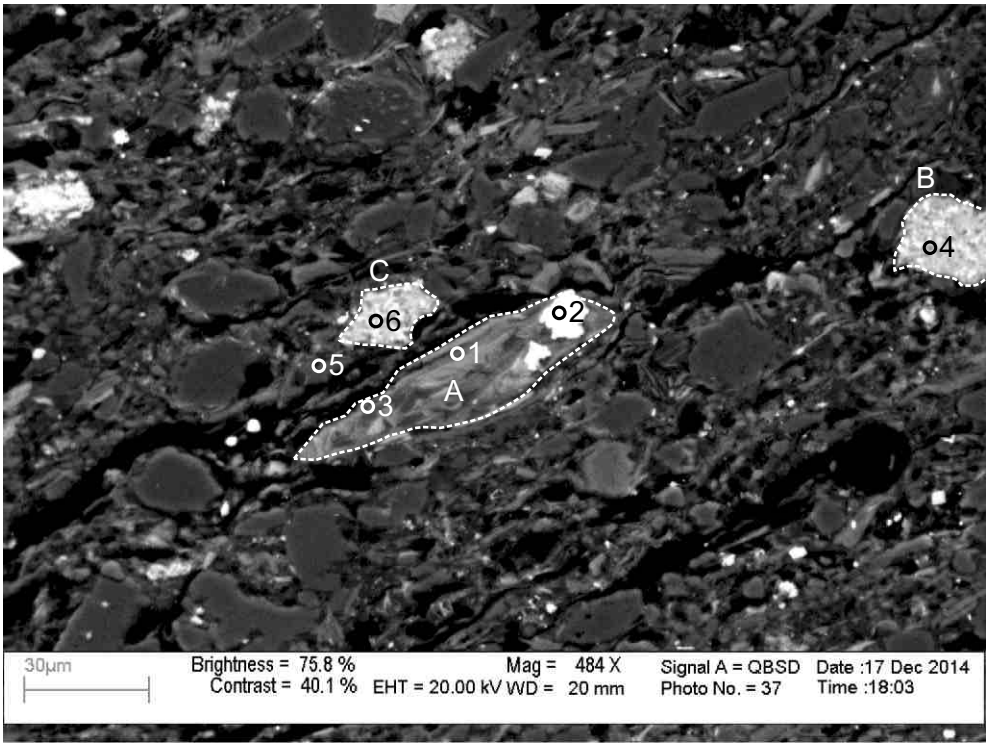

1: Chlorite+ Muscovite
2: Titania
3: Albite+ Other
4: Chlorite+ Siderite
5: Albite
6: Chlorite+ Siderite

Figure 2-10.15: Sample Newburn 5957.8m site 15 (SEM). Lithic clast (position A) originally composed of albite (3) and muscovite (1); the muscovite has been chloritized and the albite has been partially engulfed by titania (2). Mud intraclasts (positions B and C) composed of chlorite and cemented by siderite (4,6).

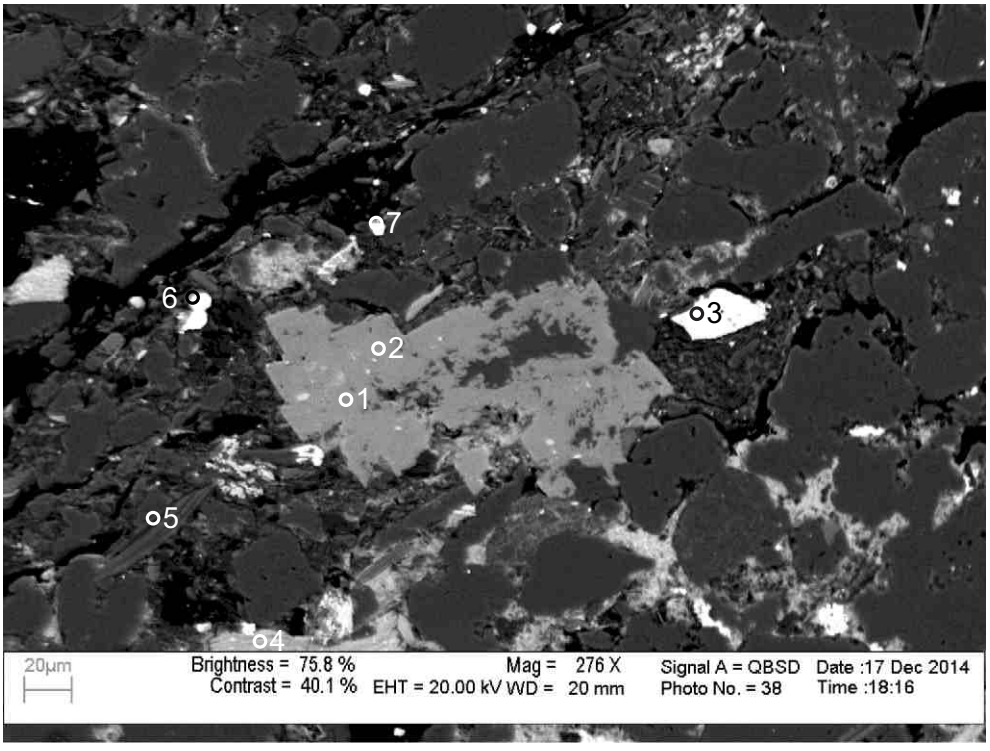

1: Ankerite
2: Ankerite+ Chlorite
3: Titania
4: Chlorite
5: Muscovite+ Other
6: Pyrite
7: Pyrite+ Chlorite

Figure 2-10.16: Sample Newburn 5957.8m site 16 (SEM). Euhedral ankerite (1,2) engulfs quartz and chlorite (2).

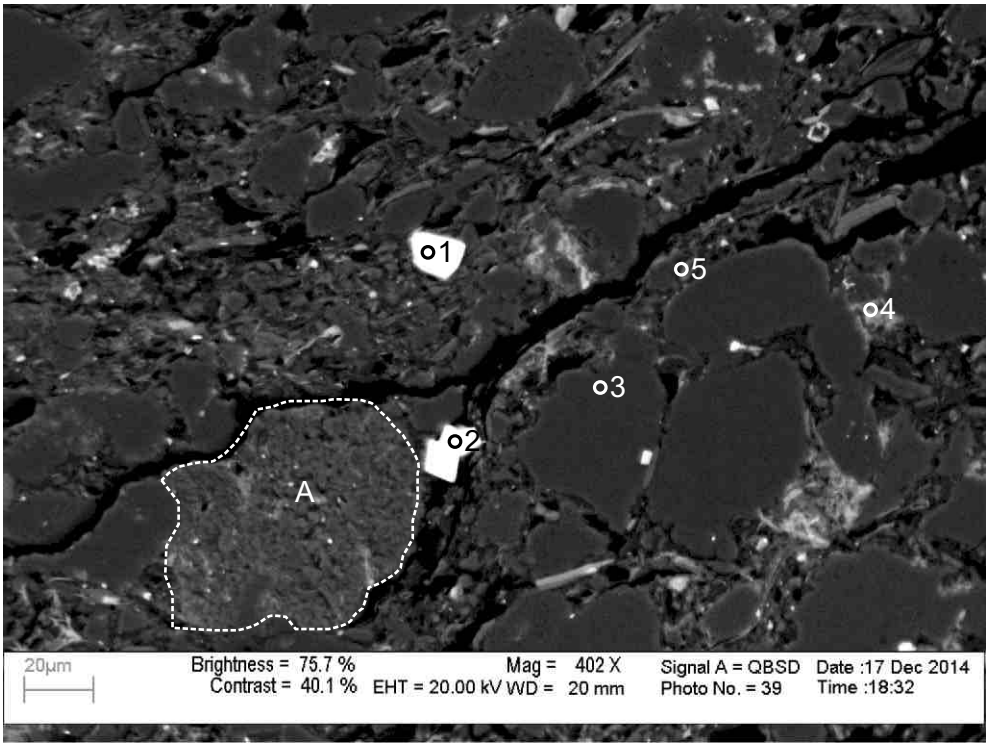

1: Zircon
2: Pyrite
3: Quartz
4: Chlorite+ K-Feldspar
5: Illite

Figure 2-10.17: Sample Newburn 5957.8m site 17 (SEM). Euhedral pyrite (2) grows in intergranular boundary. Lithic clast (position A). Zircon (1) cross cuts framework grains.

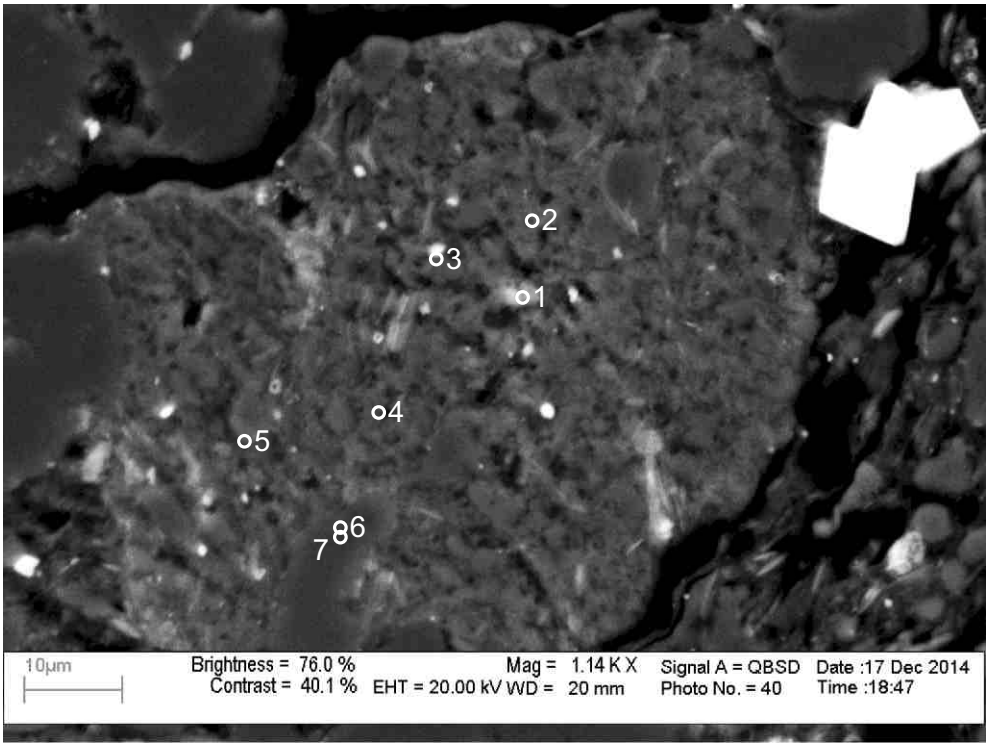

1: Chlorite+ Muscovite
2: Muscovite
3: Albite+Illite
4: Muscovite
5: Albite+Illite
6: Quartz+ Kaolinite
7: Albite

Figure 2-10.18: Sample Newburn 5957.8m site 18 (SEM). Close up of Figure 2-10.17 position A. Trachytic lithic clast composed of albite (3,5,7), quartz (6) and muscovite (1,2,4). The muscovite appears to have altered to produce chlorite (1) and illite (3,5).

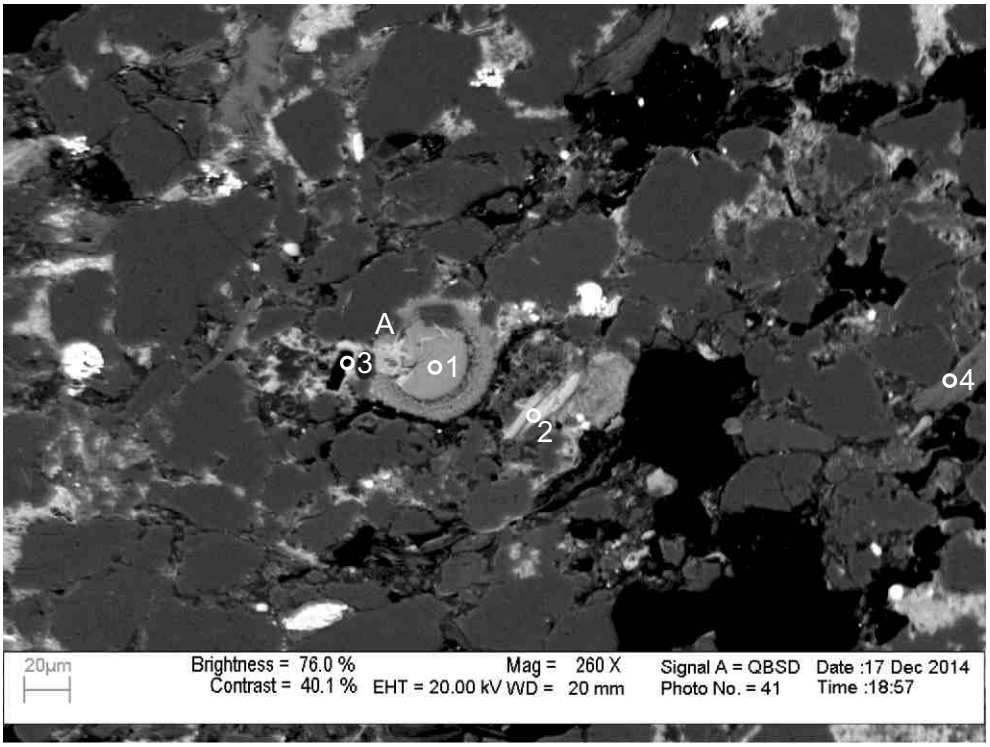

1: Fe-Calcite
2: Chlorite+ Albite
3: Chlorite
4: Muscovite

Figure 2-10.19: Sample Newburn 5957.8m site 19 (SEM). Possible coated grain of Fe-calcite (1) cut by chlorite (position A).

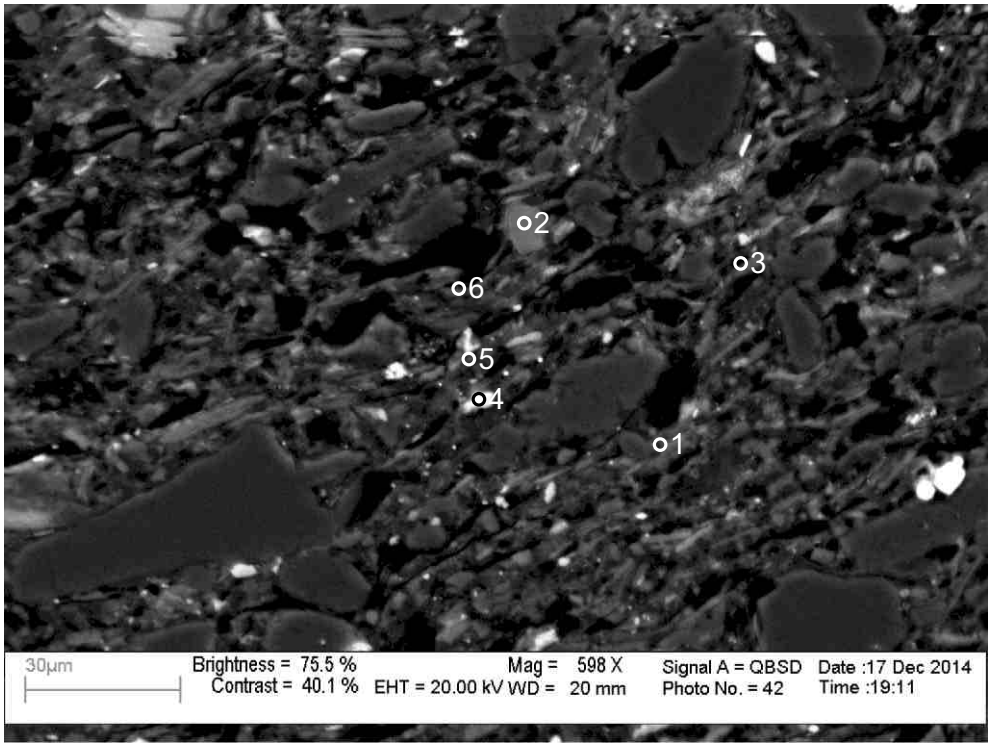

1: Muscovite
2: Calcite+ Other
3: Muscovite
4: Titania+ Other
5: Illite
6: Illite

Figure 2-10.20: Sample Newburn 5957.8m site 20 (SEM). Aligned grains of quartz, muscovite (1) and illite (5,6) in shale interval of sandstone.

Table 2-10: Scanning Electron Microscope chemical analyses of sample 5957.8m from Newburn H-23 well.

Sample	Site	Position	Mineral	SiO_2	TiO_2	Al_2O_3	FeO	MnO	MgO	CaO	Na_2O	K_2O	P_2O_5	SO_3	F	Cl	V_2O_5	Cr_2O_3	ZnO	ZrO_2	HfO_2	Total	Actual Total
H-23 5957m	1	1	TiO_2	1.41	95.76	0.91	1.93															100	105.75
H-23 5957m	1	2	TiO_2	1.33	95.91	0.87	1.90															100	103.6
H-23 5957m	1	3	TiO_2	1.20	97.78	0.57	0.45															100	115.05
H-23 5957m	1	4	Ank				16.15	1.07	9.35	29.43												56	62.65
H-23 5957m	1	5	TiO_2+Other	2.93	82.17	2.53	5.83		1.92	4.63												100	98.98
H-23 5957m	1	6	Ab	68.92		18.82					12.26											100	131.37
H-23 5957m	1	7	Ank+Qz	24.09			18.91	1.78	12.17	43.04												100	73.92
H-23 5957m	1	8	Chl	28.35		23.69	27.67		4.65		0.43	0.20										85	101.22
H-23 5957m	1	9	Chl+Other	33.29		26.57	30.97		7.06	1.11		0.23	0.78									100	109.42
H-23 5957m	1	10	Qz	99.99																		100	130.83
H-23 5957m	1	11	Qz	99.99																		100	136.99
H-23 5957m	2	1	Qz+Ilt	75.21	0.77	16.93	1.43		1.16		0.35	4.14										100	117.9
H-23 5957m	2	2	Sd+Chl	9.99		8.13	64.98	1.68	11.01	4.23												100	71.58
H-23 5957m	2	3	Sd+Chl	29.05	0.38	23.24	39.53	0.43	6.77	0.59												100	95.69
H-23 5957m	2	4	Sd+Chl	29.80	0.35	23.83	38.49	0.40	6.43	0.70												100	98.92
H-23 5957m	2	5	Sd+Chl	19.72		15.80	52.04	1.07	9.04	2.34												100	81.85
H-23 5957m	2	6	Ms+TiO_2	19.04	69.31	7.94	0.84		0.45	0.31	0.65	1.14				0.36						100	111.34
H-23 5957m	2	7	Qz	99.99																		100	129.89
H-23 5957m	2	8	Chl+Ab	36.28		27.91	29.82		4.58		1.12	0.30										100	101.55
H-23 5957m	2	9	Kln+Ilt	55.17		40.83	2.15		0.55			1.30										100	77.23
H-23 5957m	2	10	Kln+Ilt	58.76	0.63	32.86	3.68		0.85	0.32	0.69	2.20										100	107.05
H-23 5957m	2	11	Chl+Ab	48.73		23.17	18.49		2.95		6.65											100	117.46
H-23 5957m	2	12	Chl+Ab	42.42		24.70	24.49		3.81		4.57											100	110.39
H-23 5957m	3	1	Py				25.19				6.19			68.64								100	227.4
H-23 5957m	3	2	Py				27.18				3.33	0.18		69.29								100	225.19
H-23 5957m	3	3	Qz+Chl	74.04		2.48	1.92		0.35											21.22		100	130.3
H-23 5957m	3	4	Qz	99.99																		100	131.9
H-23 5957m	3	5	Chl	26.63		23.36	28.53		5.05		0.33	0.16		0.94								85	104.78
H-23 5957m	4	1	Cal+Chl	2.03		1.72	5.34	0.68	0.71	89.51												100	60.07
H-23 5957m	4	2	Chl+Other	35.57	3.85	23.62	28.23		8.29			0.42										100	105.7
H-23 5957m	4	3	Chl	30.61	0.43	20.95	22.42		10.60													85	107.16
H-23 5957m	4	4	Chl	26.47		23.88	29.59		5.06													85	106.43
H-23 5957m	4	5	Chl	25.92		15.83	30.19	0.69	9.64	1.30				0.76					0.66			85	96.22
H-23 5957m	4	6	Qz	99.99																		100	130.56
H-23 5957m	4	7	TiO_2+Ilt	3.44	94.53	1.25	0.49					0.30										100	110.92
H-23 5957m	4	8	Ilt	51.72	0.84	9.27	2.72		1.49			2.60								21.36		90	121.27
H-23 5957m	4	9	Ilt	52.71		21.70	10.11		1.59			3.89										90	115.68
H-23 5957m	5	1	Spl			17.36	19.97		9.80									52.89				100	111.78
H-23 5957m	5	2	TiO_2+Other	11.27	82.97	2.17	3.31					0.28										100	111.35
H-23 5957m	5	3	Chl	27.51		23.72	28.35		4.80									0.61				85	109.32
H-23 5957m	5	4	Fap+Chl	13.43		12.36	13.75		2.32	25.76			28.07		4.32							100	119.8

Table 2-10: Scanning Electron Microscope chemical analyses of sample 5957.8m from Newburn H-23 well.

Sample	Site	Position	Mineral	SiO_2	TiO_2	Al_2O_3	FeO	MnO	MgO	CaO	Na_2O	K_2O	P_2O_5	SO_3	F	Cl	V_2O_5	Cr_2O_3	ZnO	ZrO_2	HfO_2	Total	Actual Total
H-23 5957m	5	5	Qz	96.46		1.83	1.13					0.30						0.28				100	131.46
H-23 5957m	5	6	Chl	27.59		23.20	29.25		4.50	0.27		0.20										85	103.12
H-23 5957m	5	7	Chl	42.41		11.18	29.36		2.06													85	76.95
H-23 5957m	6	1	Ab+Ilt	59.21		28.19	0.26			0.66	6.62	5.06										100	126.28
H-23 5957m	6	2	Ab+Ilt	59.32		28.38	0.24			0.55	6.20	5.30										100	124.09
H-23 5957m	6	3	Ab	65.35		21.54				1.18	10.75	1.17										100	130.67
H-23 5957m	6	4	Ab	65.84		21.52	0.23			1.19	10.37	0.84										100	127.31
H-23 5957m	6	5	TiO_2+Chl	2.63	91.58	2.19	3.59															100	106.84
H-23 5957m	6	6	TiO_2+Chl	4.19	90.21	2.83	2.35			0.41												100	106.37
H-23 5957m	6	7	Chl	27.46		23.56	29.16		4.82													85	106.46
H-23 5957m	6	8	Chl	26.77		23.72	29.42		5.09													85	103.68
H-23 5957m	6	9	Qz	99.99																		100	127.39
H-23 5957m	6	10	Chl	26.44		23.35	30.29		4.92													85	98.82
H-23 5957m	7	1	Fap+Ab	15.83		4.33	0.44			34.28	2.31		36.09		6.74							100	133
H-23 5957m	7	2	Sd+Chl	2.85		0.74	74.19	4.26	14.84	3.12												100	64.74
H-23 5957m	7	3	Fe-Cal				1.64	0.45	0.52	53.39												56	58.56
H-23 5957m	7	4	Chl+Other	31.64		26.68	33.14		4.99	2.62	0.92											100	103.21
H-23 5957m	7	5	Chl	33.65	0.28	24.54	20.89		4.43		0.43	0.78										85	113.67
H-23 5957m	7	6	Chl+Kfs	45.18		26.79	20.27		4.48		0.62	2.65										100	112.09
H-23 5957m	8	1	TiO_2		99.55		0.45															100	110.79
H-23 5957m	8	2	Qz	99.77			0.23															100	130.75
H-23 5957m	8	3	Qz+Chl	85.16		5.03	5.92		3.88													100	128.86
H-23 5957m	8	4	Chl	29.75		24.62	25.35		4.52		0.36	0.40										85	108.77
H-23 5957m	8	5	Ms	51.03		29.18	2.75		2.68		0.26	9.10										95	114.19
H-23 5957m	8	6	Chl+Ms	35.06		25.89	23.93	0.32	13.56			1.25										100	108.23
H-23 5957m	8	7	TiO_2+Other	6.91	85.39	4.38	2.97					0.33										100	104.92
H-23 5957m	8	8	Chl	28.08		23.74	28.17		5.02													85	107.19
H-23 5957m	9	1	Ms+Other	60.39	7.29	23.26	1.49		1.43		0.39	5.75										100	117.1
H-23 5957m	9	2	DM+Fl	49.74	0.53	4.76	10.24		24.99	2.50	0.94	0.89		0.80	3.94	0.65						100	61.05
H-23 5957m	9	3	Sd+Qz	28.07		2.00	45.37	0.36	21.71	1.44	0.43	0.35				0.25						100	98
H-23 5957m	9	4	DM+Fl	50.25	0.63	4.97	9.88		26.91	2.71	0.66	0.86			2.42	0.70						100	63.39
H-23 5957m	9	5	DM+Fl	51.70	0.55	4.50	8.39		26.00	2.76	0.89	0.82			3.65	0.76						100	66.24
H-23 5957m	9	6	Qz	99.99																		100	128.33
H-23 5957m	9	7	Chl+Ap	32.69		24.38	30.57		4.24	3.50	1.38		3.28									100	106.72
H-23 5957m	9	8	Qz+Chl	78.44		8.92	8.95		3.30			0.40										100	122.81
H-23 5957m	9	9	Qz	99.99																		100	131.77
H-23 5957m	10	1	TiO_2+Other	2.61	94.38	2.02	0.99															100	91.97
H-23 5957m	10	2	Chl+TiO_2	30.50	2.80	27.29	33.14		5.80		0.46											100	102.23
H-23 5957m	10	3	TiO_2+Chl	5.50	87.34	4.16	2.38			0.32		0.30										100	86.72
H-23 5957m	10	4	TiO_2+Chl	10.23	67.37	9.64	10.94		1.84													100	87
H-23 5957m	10	5	Qz	99.47			0.51															100	130.24

Table 2-10: Scanning Electron Microscope chemical analyses of sample 5957.8m from Newburn H-23 well.

Sample	Site	Position	Mineral	SiO_2	TiO_2	Al_2O_3	FeO	MnO	MgO	CaO	Na_2O	K_2O	P_2O_5	SO_3	F	Cl	V_2O_5	Cr_2O_3	ZnO	ZrO_2	HfO_2	Total	Actual Total
H-23 5957m	11	1	Sd+Other	1.22			88.75	2.09	1.71	5.22			1.01									100	59.89
H-23 5957m	11	2	TiO_2+Other	1.75	95.86	0.76	1.62															100	108.88
H-23 5957m	11	3	Ms+Other	56.65	0.47	31.12	2.87		1.48		1.00	6.25				0.17						100	108.73
H-23 5957m	11	4	Ms	52.89		25.33	5.55		2.33			8.90										95	91.95
H-23 5957m	11	5	Chl+Other	39.64		25.89	26.96		5.65	0.57	0.66	0.61										100	108.75
H-23 5957m	11	6	Sd+Ilt	19.45	0.62	14.04	53.66	2.16	7.10	1.76		1.23										100	80.09
H-23 5957m	11	7	Chl	27.03	0.30	21.08	30.37		5.80	0.42												85	102.51
H-23 5957m	12	1	Qz	99.99																		100	130.47
H-23 5957m	12	2	Ms+Chl	56.88	0.53	28.32	4.37		1.86		1.93	6.08										100	115.26
H-23 5957m	12	3	Ms+Chl	62.51	3.92	22.50	4.37		2.17		0.69	3.83										100	133.89
H-23 5957m	12	4	Ms+Chl	64.71	0.47	22.11	1.05		0.68		8.88	2.11										100	120.71
H-23 5957m	12	5	Chl+Ilt	41.12	0.28	24.49	20.30		12.45			1.35										100	108.11
H-23 5957m	12	6	Chl+Sd+Ap	14.55		11.55	55.27	1.24	8.62	6.37		0.33	2.11									100	79.72
H-23 5957m	12	7	Ilt	51.79	0.95	28.87	1.58		1.42		0.32	5.09										90	114.2
H-23 5957m	12	8	Ilt+Kln	53.97	1.07	32.08	2.88		1.91		0.74	6.36	0.99									100	121.01
H-23 5957m	12	9	Kln+Ilt	56.07	2.00	35.47	1.74		1.14	0.38	0.57	2.63										100	90.9
H-23 5957m	12	10	Qz+Ilt	64.84	0.88	24.07	3.19		2.06		0.61	4.36										100	108.74
H-23 5957m	13	1	Chl+Sd	25.93		22.43	43.21	0.52	6.25	1.67												100	93.39
H-23 5957m	13	2	TiO_2+Qz+Chl	9.01	74.68	7.63	5.30		1.13	0.27		0.40					1.57					100	110.36
H-23 5957m	13	3	TiO_2+Qz+Chl	8.09	80.88	5.27	3.74		1.44			0.58										100	110.62
H-23 5957m	13	4	Ab	67.66		19.52	0.45			0.41	11.62	0.34										100	133.04
H-23 5957m	13	5	Ilt+Chl+Kln	56.39	0.37	31.08	5.54		1.53	0.50	1.36	3.24										100	110.62
H-23 5957m	13	6	Ms+Chl	50.57	0.33	24.77	13.60		3.13	0.90	0.51	6.20										100	107.25
H-23 5957m	13	7	Ms+Chl	52.92	0.25	25.81	11.06		3.08		0.53	6.32										100	108.16
H-23 5957m	13	8	Qz	99.99																		100	129.34
H-23 5957m	13	9	Ab	68.52		18.95	0.28				12.24											100	130.68
H-23 5957m	13	10	Fap+Ab	24.09		7.52	0.76			28.47	4.61		29.54		5.01							100	131.95
H-23 5957m	13	11	Ms+Other	55.47	1.00	28.89	4.86		2.30	0.95	1.16	5.35										100	104.87
H-23 5957m	13	12	Zrn	32.13		1.23	0.64			0.50										65.50		100	112.56
H-23 5957m	13	13	Fap+Other	12.32		5.37	0.69		0.38	36.88	1.82	0.61	36.18		5.72							100	133.38
H-23 5957m	13	14	Chl+Ab	39.81		22.66	27.75		6.43	0.43	2.41	0.49										100	111.74
H-23 5957m	14	1	TiO_2+Ab	17.26	70.46	5.52	1.76				4.79	0.19										100	123.75
H-23 5957m	14	2	Py+Chl	1.48		1.11	26.96				0.27	0.18		70.02								100	227.06
H-23 5957m	14	3	Chl+Ilt	69.67	0.75	14.11	8.04		3.63		2.40	1.39										100	129.32
H-23 5957m	14	4	Chl+Ilt	48.35	0.67	26.21	15.04		6.47	0.35	0.49	2.43										100	116.08
H-23 5957m	14	5	Qz+Other	94.98		3.38	0.57		0.27			0.82										100	118.5
H-23 5957m	14	6	Qz	98.40	0.85					0.74												100	134.47
H-23 5957m	14	7	Zrn	36.64		7.18	1.97		0.85			1.13								52.22		100	130.72
H-23 5957m	14	8	Qz+Ilt	75.66	0.27	18.20	0.69		0.53		0.54	4.11										100	126.59
H-23 5957m	14	9	Chl	31.11		20.43	21.87		10.37	0.88		0.34										85	103.33
H-23 5957m	14	10	Ab	67.47		19.37	0.63			0.28	11.50	0.73										100	133.42

Table 2-10: Scanning Electron Microscope chemical analyses of sample 5957.8m from Newburn H-23 well.

Sample	Site	Position	Mineral	SiO_2	TiO_2	Al_2O_3	FeO	MnO	MgO	CaO	Na_2O	K_2O	P_2O_5	SO_3	F	Cl	V_2O_5	Cr_2O_3	ZnO	ZrO_2	HfO_2	Total	Actual Total
H-23 5957m	14	11	Ab	67.38		19.05	1.47				11.95	0.14										100	130.45
H-23 5957m	14	12	Ms+Other	53.09	1.35	30.63	5.85		1.92		0.58	6.56										100	103.73
H-23 5957m	15	1	Chl+Ms	43.43		25.68	15.31		11.61			3.97										100	117.09
H-23 5957m	15	2	TiO_2	0.75	96.58	0.40	2.29															100	109.91
H-23 5957m	15	3	Ab+Other	64.07	0.53	20.86	2.16		1.72		8.67	1.99										100	134.09
H-23 5957m	15	4	Chl+Sd	25.01		21.96	44.91	0.61	6.05	1.47												100	94.76
H-23 5957m	15	5	Ab	65.72		21.22	0.93		0.41	0.29	10.42	1.00										100	129.79
H-23 5957m	15	6	Chl+Sd	24.39		21.01	46.36	0.50	5.85	1.87												100	89.8
H-23 5957m	16	1	Ank	0.41			14.87	1.33	9.52	29.87												56	62.5
H-23 5957m	16	2	Ank+Chl	1.18		1.04	26.82	2.76	17.54	50.65												100	63.42
H-23 5957m	16	3	TiO_2		99.68		0.31															100	111.73
H-23 5957m	16	4	Chl	29.83	0.55	20.98	25.72		7.73			0.20										85	102.98
H-23 5957m	16	5	Ms+Other	54.59	0.35	40.19	0.32				0.61	3.93										100	109.95
H-23 5957m	16	6	Py	1.05		0.62	27.14							71.19								100	236.64
H-23 5957m	16	7	Py+Chl	20.73		5.82	19.67		0.48	0.18		0.89		52.21								100	182.38
H-23 5957m	17	1	Zrn	30.93																67.85	1.23	100	133.71
H-23 5957m	17	2	Py	0.24			27.48							72.29								100	239.57
H-23 5957m	17	3	Qz	99.99																		100	131.5
H-23 5957m	17	4	Chl+Kfs	41.74		28.85	23.95		3.75	0.22		1.48										100	106.15
H-23 5957m	17	5	Ilt	56.23	0.65	22.13	3.73		2.02		0.50	4.76										90	123.44
H-23 5957m	18	1	Chl+Ms	47.73	0.42	27.63	13.38		5.24		0.47	5.14										100	109.55
H-23 5957m	18	2	Ms	53.46	0.54	26.24	3.96		2.60		1.14	7.06										95	117.45
H-23 5957m	18	3	Ab+Ilt	48.45	20.15	19.33	1.70		1.18		6.03	3.16										100	126.44
H-23 5957m	18	4	Ms	53.31	0.26	26.42	3.62		2.73		0.55	8.11										95	113
H-23 5957m	18	5	Ab+Ilt	59.43	0.43	23.51	4.75		1.28		7.59	3.00										100	129.92
H-23 5957m	18	6	Qz+Kln	81.16		18.84																100	0.32
H-23 5957m	18	7	Ab	66.94		19.59	1.13			0.31	11.45	0.58										100	131.19
H-23 5957m	19	1	Fe-Cal				2.27	0.57	0.68	52.49												56	57.34
H-23 5957m	19	2	Chl+Ab	33.46		27.12	31.51		6.17		1.77											100	106.78
H-23 5957m	19	3	Chl	34.35		27.63	18.72		3.92			0.39										85	101.13
H-23 5957m	19	4	Ms	49.90	0.74	30.86	1.59		1.59		0.64	9.68										95	121.93
H-23 5957m	20	1	Ms	52.47	1.06	27.83	3.17		2.61		0.67	7.18										95	114.9
H-23 5957m	20	2	Cal+Other	1.97		0.85	0.46		1.79	85.48		0.29		1.12	8.03							100	66.7
H-23 5957m	20	3	Ms	51.01	0.50	30.45	2.80		1.92		0.36	7.96										95	120.75
H-23 5957m	20	4	TiO_2+Other	13.11	75.18	9.92	0.76			0.27		0.77										100	114.15
H-23 5957m	20	5	Ilt	57.08	1.58	22.45	2.07		1.54	0.43	0.66	4.19										90	118
H-23 5957m	20	6	Ilt	60.54	0.48	19.57	3.00		1.47		1.39	3.55										90	111.7

Appendix 2-11: SEM-BSE images and EDS mineral analyses for sample Newburn H-23 5961.7m

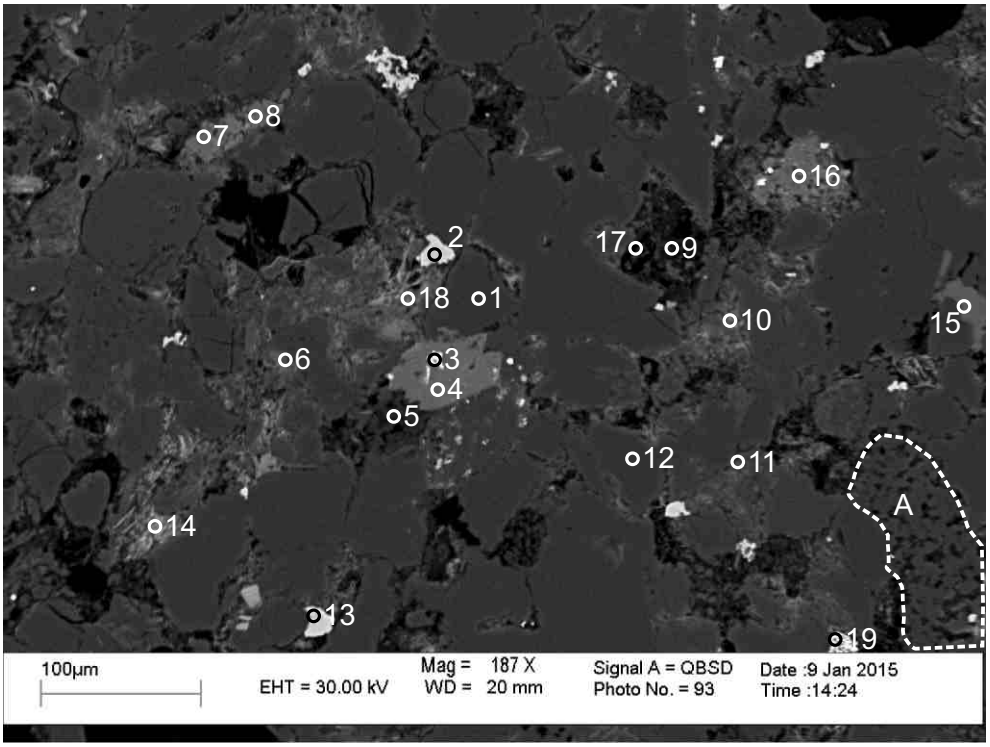

1: Quartz
2: Titania
3: Pyrite
4: Ankerite
5: Kaolinite
6: Albite
7: Fe-Calcite
8: Fe-Calcite
9: Chlorite+ Illite
10: Chlorite+ Albite
11: Albite
12: Quartz
13: Titania
14: Chlorite+ Apatite
15: Calcite+ Chlorite
16: Calcite+ Chlorite
17: Kaolinite+ Chlorite+ Other
18:Muscovite+ Chlorite
19: Pyrite

Figure 2-11.1: Sample Newburn 5961.7m site 1 (SEM). Ankerite (4) engulfs quartz (1) and kaolinite (5), pyrite (3) fills dissolution void. Fe-calcite (7,8) engulfs quartz and partially fills a pore. Titania (2) engulfs quartz. Trachytic lithic clast (position A). Calcite (16) is mixed with chlorite. Fibrous chlorite (9,17) fills pore.

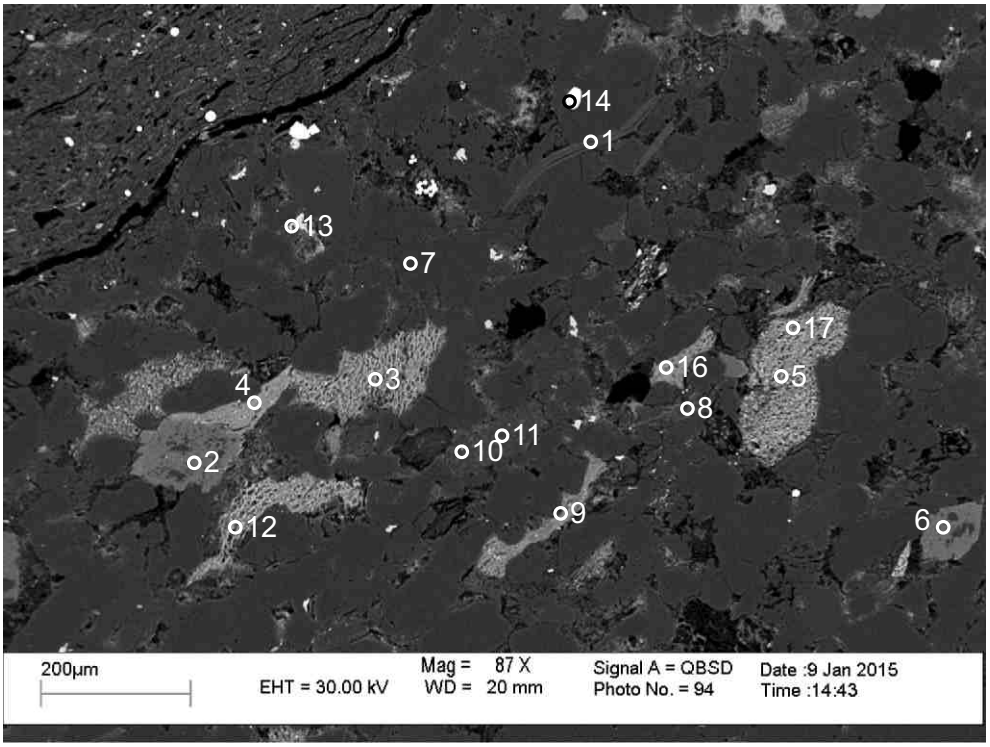

1: Muscovite
2: Ankerite
3: Chlorite
4: Chlorite
5: Fe-Chlorite
6: Ankerite
7: Quartz
•15
8: Ankerite+ Muscovite
9: Chlorite
10: Muscovite
11: Quartz+ Muscovite
12: Fe-Chlorite
13: Titania+ Quartz+ Chlorite
14: Zircon
15: Albite+ Muscovite +Chlorite
16: Chlorite
17: Fe-Chlorite

Figure 2-11.2: Sample Newburn 5961.7m site 2 (SEM). Probable pumice clasts which have altered, producing chlorite (3,4,5,9,12,17) and have later been deformed. Plastically deformed muscovite (1). Ankerite (2) engulfs quartz and chlorite (4).

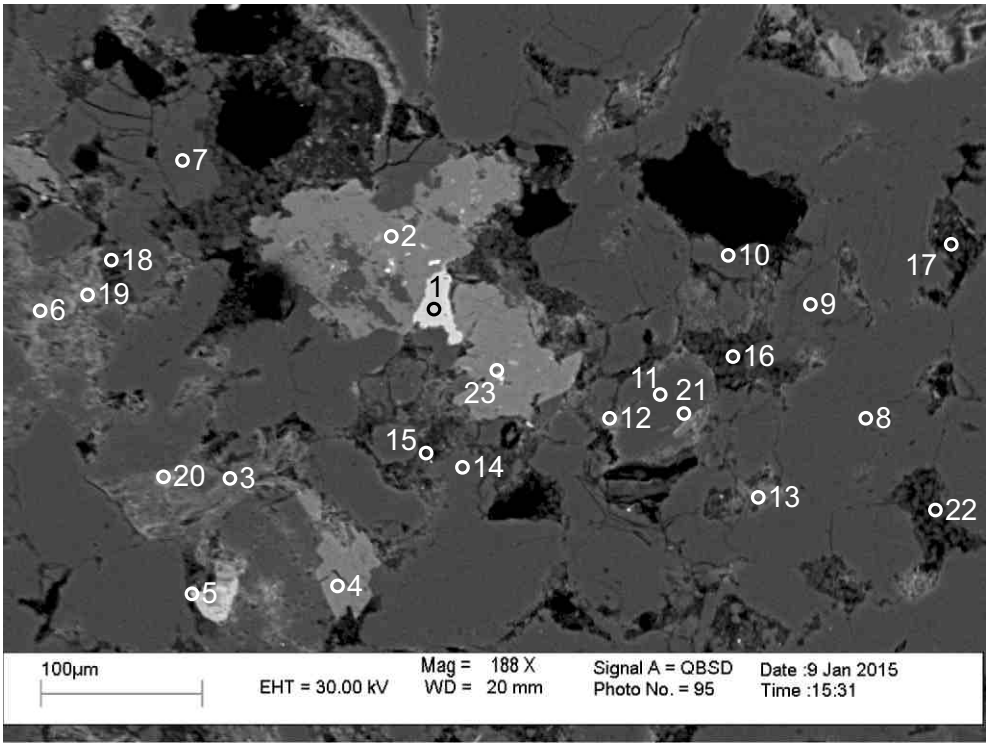

1: Titania
2: Ankerite
3: Muscovite
4: Ankerite
5: Titania+ Chlorite
6: Chlorite+Illite
7: Albite
8: Quartz
9: Quartz
10: Quartz
11: Quartz
12: Chlorite
13: Albite
14: Albite
15: Kaolinite+ Other
16: Kaolinite
17: Kaolinite+ Chlorite
18: Kaolinite+ Chlorite+ Albite
19: Chlorite
20: Chlorite
21: Quartz+ Fluorapatite+ Other
22: Kaolinite
23: Pyrite+ Calcite+ Chlorite

Figure 2-11.3: Sample Newburn 5961.7m site 3 (SEM). Chlorite (20) is partially replacing muscovite (3). Fluorapatite (21) cuts quartz. Ankerite (2) partially engulfs quartz. Titania (1) cuts ankerite. Pyrite (23) fills dissolution void in calcite. Chlorite (13) engulfs kaolinite filling pore. Ankerite (4) engulfs chlorite filling pore.

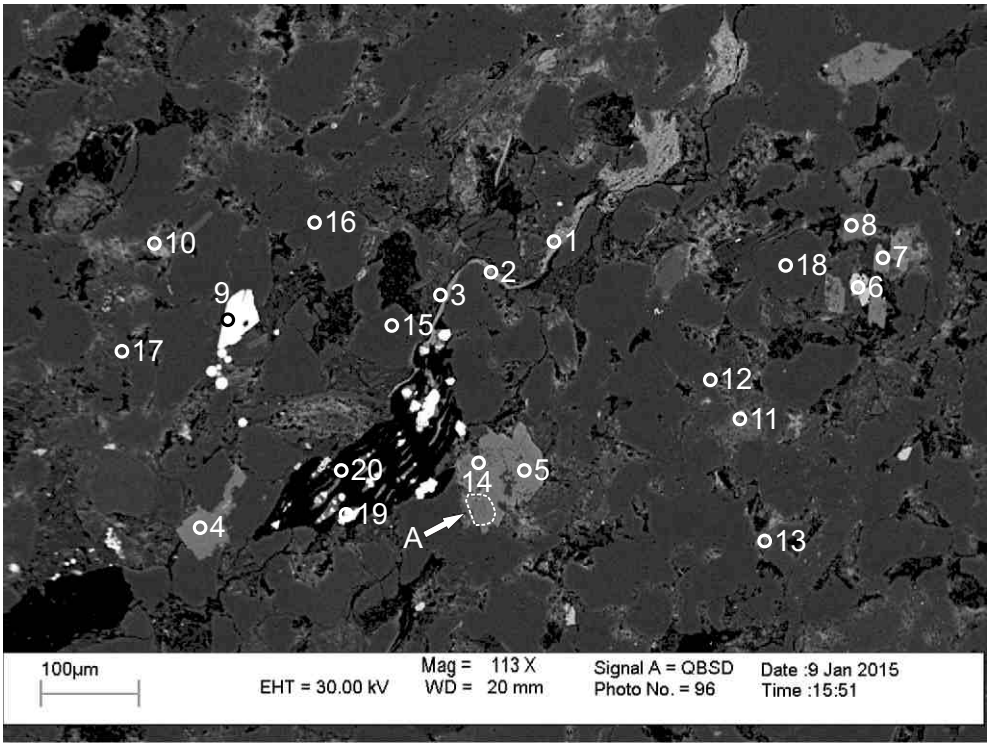

1: Chlorite
2: Chlorite
3: Chlorite
4: Ankerite
5: Ankerite
6: Titania
7: Ankerite+ Other
8: Fe-Calcite+ Albite
9: Zircon
10: Chlorite
11: Albite+ Chlorite
12: Albite+ Chlorite
13: Chlorite
14: Ankerite+ Quartz
15: Quartz
16: Quartz
17: Albite
18: Quartz
19: Pyrite
20: Hole

Figure 2-11.4: Sample Newburn 5961.7m site 4 (SEM). Probably a detrital zircon (9) with dissolution void and straight crystal outline in contact with kaolinite filling pore. Plastically deformed muscovite which has been completely chloritized (2,3). Chlorite pseudo-matrix (1). Ankerite (5,14) engulfs quartz with calcite either as replacement, relic, or filling dissolution void (position A). Pyrite (19) and chlorite form along cleavage planes of muscovite.

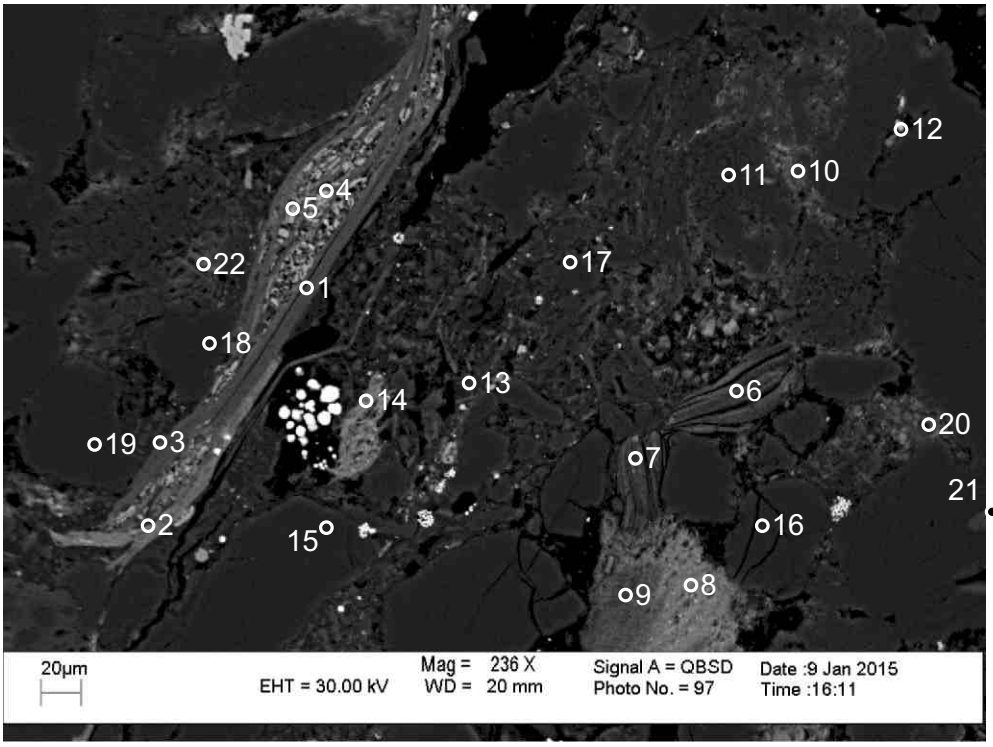

1: Chlorite
2: Chlorite
3: Chlorite
4: Chlorite
5: Siderite+ Chlorite
6: Muscovite+ Chlorite
7: Muscovite+ Chlorite
8: Chlorite
9: Titania+ Chlorite
10: Albite+ Chlorite
11: Albite+ Quartz
12:Muscovite+ Titania
13:Muscovite+ Other
14: Chlorite
15: Quartz
16: Quartz
17: Albite
18: Quartz
19: Quartz
20: Albite
21: Muscovite
22: Albite

Figure 2-11.5: Sample Newburn 5961.7m site 5 (SEM). Plastically deformed muscovite (6,7) is partially replaced by chlorite. Subhedral siderite (5) grows between cleavage planes in muscovite and expands the muscovite. Ragged detrital titania (9) has been engulfed by chlorite (8,9).

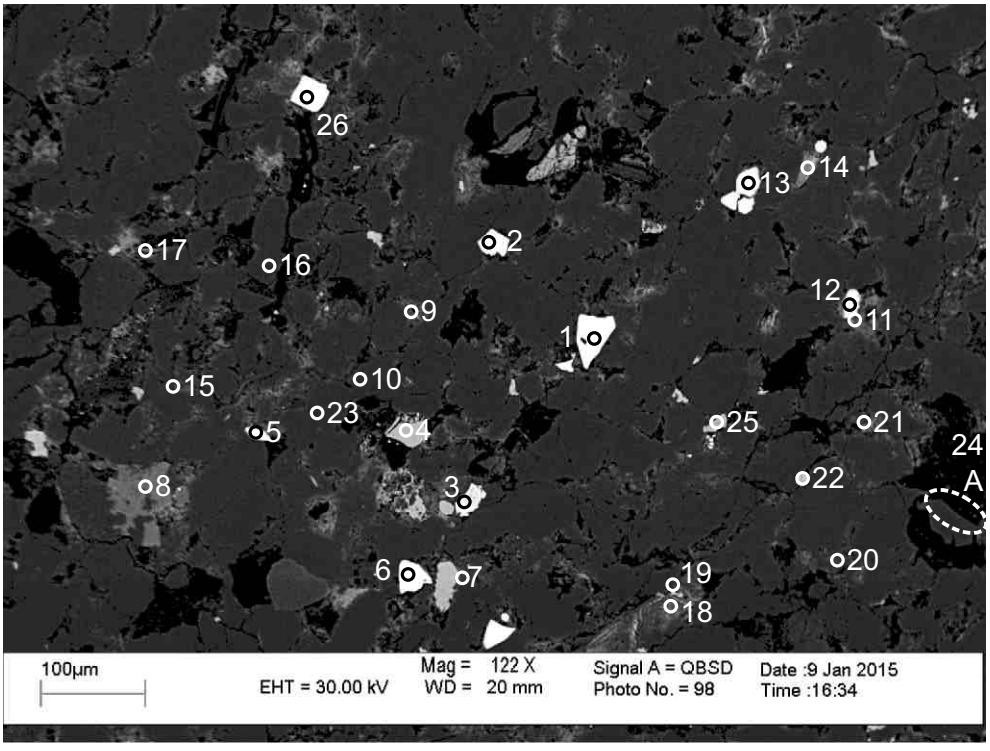

1: Zircon
2: Pyrite
3: Pyrite
4: Titania
5: Zircon
6: Zircon
7: Quartz
8: Ankerite
9: Albite+ Chlorite+Other
10: Quartz
11: Albite+ Muscovite+ Chlorite
12: Zircon+Other
13: Pyrite+Other
14: Chlorite+ Pyrite
15: Chlorite+ Albite+Illite
16: Quartz+ Other
17: Muscovite+ Chlorite
18: Quartz+ Titania+ Chlorite
19: Quartz+ Titania+ Chlorite
20: Albite
21: Chlorite
22: Titania+ Quartz
23: Quartz
24: Pyrite
25: Titania+Other
26: Zircon

Figure 2-11.6: Sample Newburn 5961.7m site 6 (SEM). Ankerite (8) is engulfing and replacing quartz. Diagenetic zircon (1,5,6,12,26) appears to be engulfing quartz and crossing intergranular boundaries (1,26). Chlorite and titania (18,19) engulf quartz. Quartz overgrowth (position A). Diagenetic zircon (26) cuts chlorite filling pore.

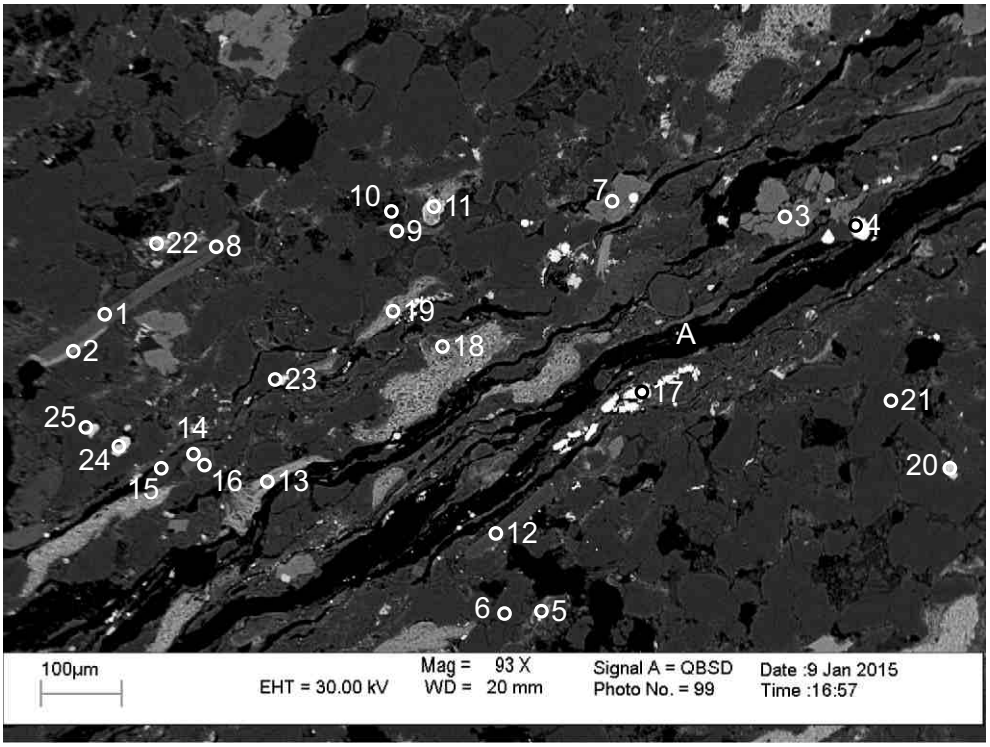

1: Muscovite
2: Muscovite+ Other
3: Ankerite
4: Pyrite
5: Quartz+ Chlorite+ Muscovite
6: Quartz
7: Ankerite
8: Muscovite
9: Muscovite
10: Kaolinite
11: Titania+ Muscovite
12: Muscovite
13: Chlorite
14: Albite+ Chlorite
15: Muscovite
16: Muscovite
17: Pyrite
18: Siderite+ Chlorite+ Albite
19: Chlorite
20: Titania
21: Quartz
22:Al-Phosphate
23: Pyrite+ Quartz
24: Titania
25: Titania

Figure 2-11.7: Sample Newburn 5961.7m site 7 (SEM). Probable altered pumice (13,18) plastically deformed around surrounding quartz. Fractured mudstone laminae (position A). Preserved bedding in the form of alligned muscovite (1,8), pseudomatrix, and mud laminae.

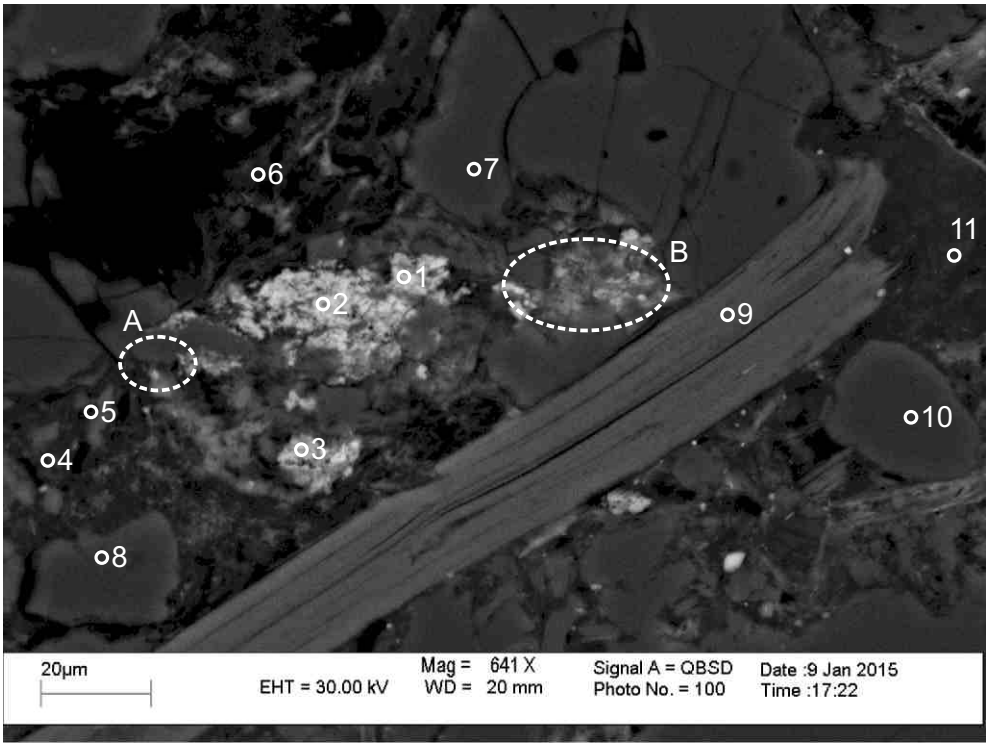

1:Al-Phosphate
2:Al-Phosphate
3:Al-Phosphate
4: Muscovite+ Other
5: Albite
6: Chlorite+ Muscovite
7: Quartz
8: Quartz
9: Muscovite
10: Quartz
11: Muscovite

Figure 2-11.8: Sample Newburn 5961.7m site 8 (SEM). Al-phosphate (1,2,3) appears to inhibit quartz overgrowth (position A) and to be cut by Chlorite (position B), however it may be contamination.

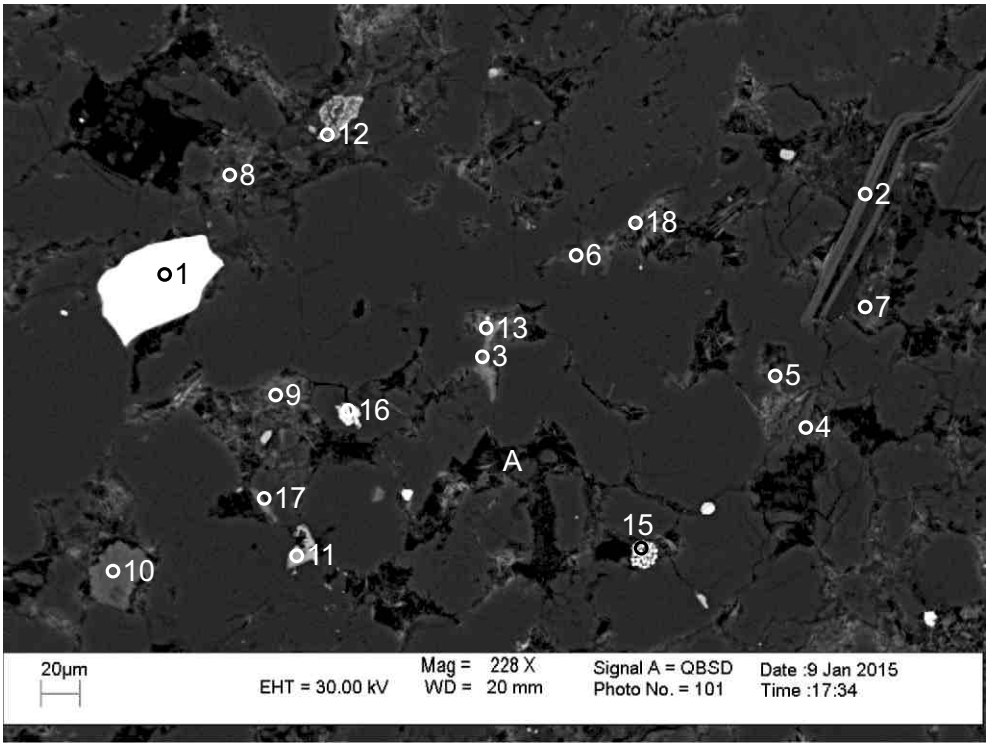

1: Zircon
2: Muscovite
3: Chlorite
4: Albite
5: Muscovite+ Chlorite
6: Muscovite
7: Muscovite+ Chlorite
8: Chlorite+ Muscovite
9: Chlorite
10: Calcite
11: Titania+ Other
12: Titania+ Quartz
13: Chlorite
14: Chlorite+ Muscovite
15: Pyrite+ Chlorite
16: Pyrite
17: Quartz+ Chlorite+ Albite
18: Chlorite+ Other

Figure 2-11.9: Sample Newburn 5961.7m site 9 (SEM). Framboidal pyrite (15). Zircon (1) appears to be diagenetic with straight crystal outlines in contact with quartz and pore. Fibrous chlorite partially fills pore (position A).

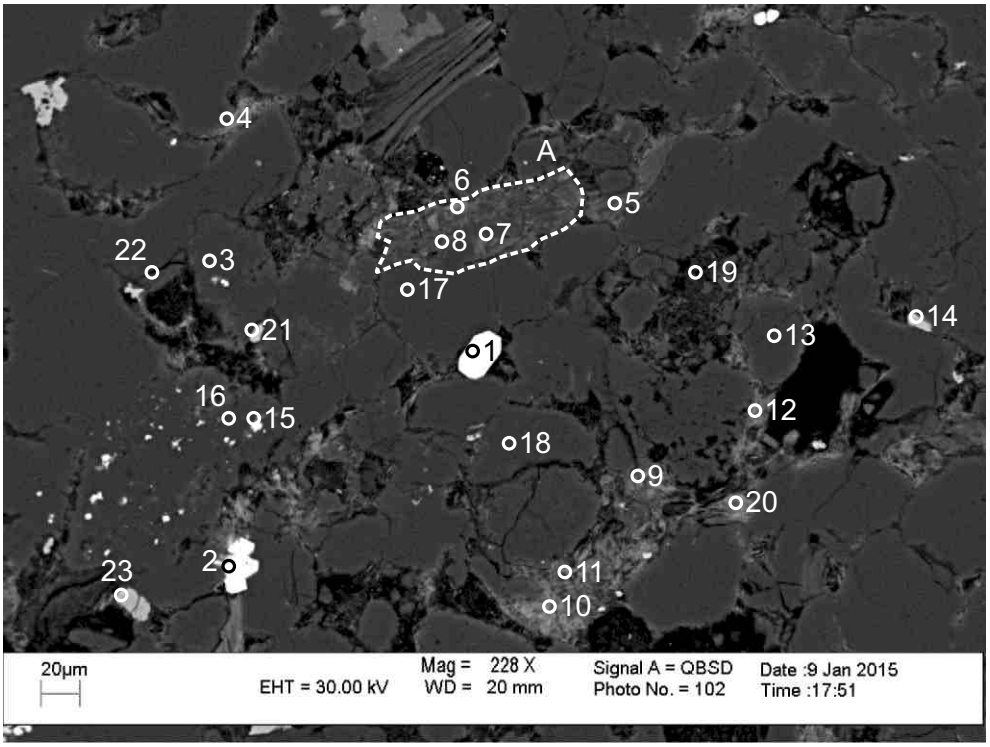

1: Zircon
2: Pyrite
3: Quartz+ Albite
4: Chlorite+ Quartz
5: Muscovite+ Chlorite
6: Chlorite+ Muscovite
7: Quartz+ Albite+ Muscovite
8: Muscovite+ Other
9: Chlorite
10: Chlorite
11: Chlorite
12: Chlorite
13: Quartz
14: Titania+ Quartz
15: Quartz+ Sphalerite
16: Quartz+ Other
17: Quartz
18: Quartz+ Other
19: Kaolinite+ Chlorite+ Muscovite
20: Chlorite
21: Titania+ Quartz+ Other
22: Quartz
23: Titania

Figure 2-11.10: Sample Newburn 5961.7m site 10 (SEM). Euhedral pyrite (2) grows in pore along an intergranular boundary. Sphalerite (15) fills dissolution voids in quartz. Granitoid ithic clast (position A) composed of quartz, albite and muscovite (6-8) with muscovite partially altered to chlorite (6). Titania (23) occurs in open porosity.

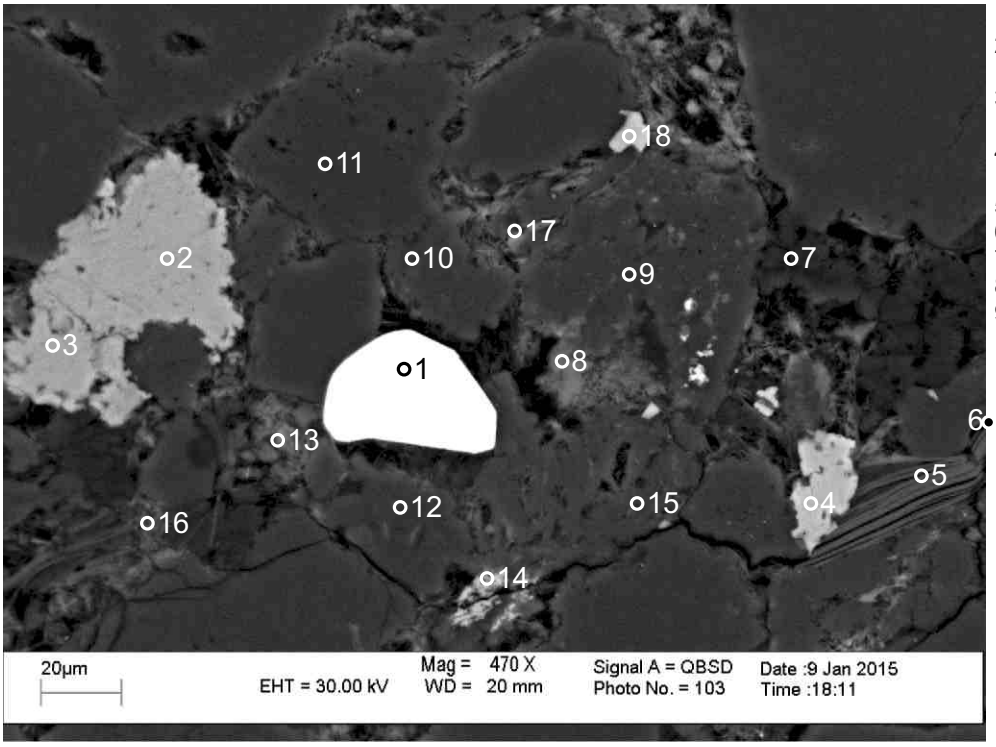

1: Zircon
2: Siderite+ Other
3: Siderite+ Other
4: Titania+ Other
5: Muscovite
6: Muscovite
7: Kaolinite
8: Chlorite
9: Quartz
10: Albite
11: Quartz
12: Quartz
13: Albite+ Chlorite
14: Titania+ Muscovite
15: Albite
16: Chlorite
17: Chlorite+ Other
18: Titania

Figure 2-11.11: Sample Newburn 5961.7m site 11 (SEM). Siderite (2,3) engulfs chlorite partially filling pore. Titania (14) engulfs muscovite. Kaolinite (7) partially fills pore, and is later surrounded by fibrous chlorite. Diagenetic Zircon (1) cuts chlorite and is euhedral against porosity.

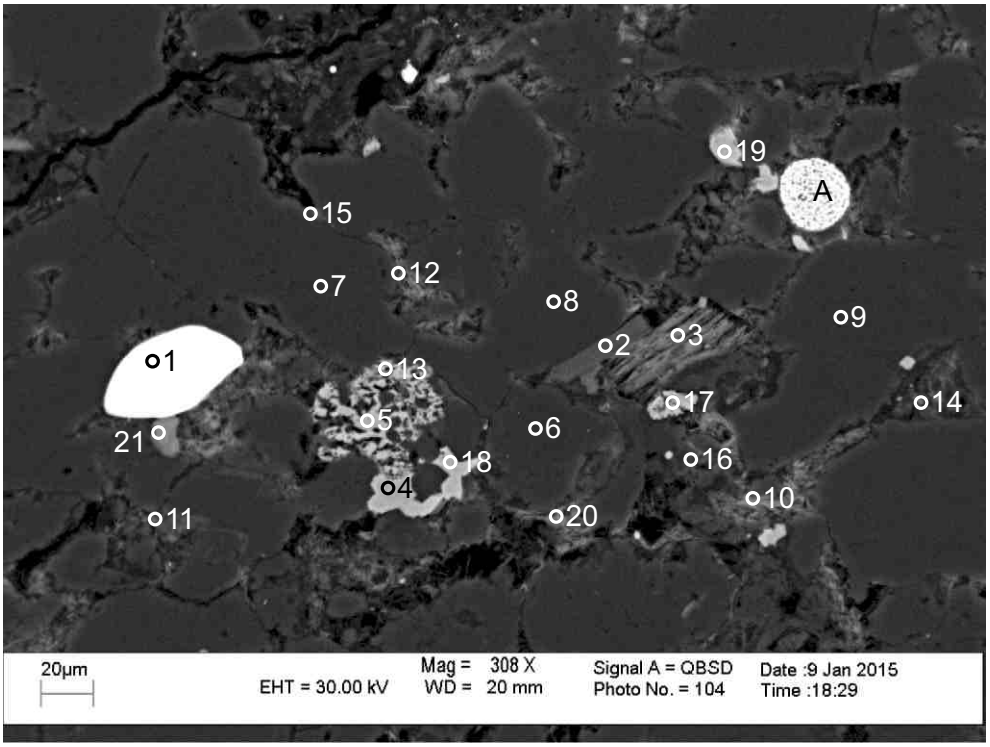

1: Zircon
2: Muscovite
3: Chlorite
4: Titania
5: Titania
6: Quartz
7: Quartz
8: Quartz
9: Quartz
10: Chlorite
11: Muscovite+ Chlorite
12: Chlorite
13: Titania+ Chlorite
14: Chlorite+ Illite
15: Illite+ Chlorite
16: Illite+ Chlorite
17: Titania+ Chlorite
18: Titania+ Chlorite
19: Titania+ Chlorite
20: Chlorite+ Albite
21:Fluorapatite +Chlorite

Figure 2-11.12: Sample Newburn 5961.7m site 12 (SEM). Titania (5,13) may be an altered framework grain or may fill dissolution voids in quartz. Titania (4,18) fills void along intergranular boundaries in quartz and appears to replace earlier titania (5,13). Fluorapatite (21) probably postdates chlorite. Framboidal pyrite (position A).

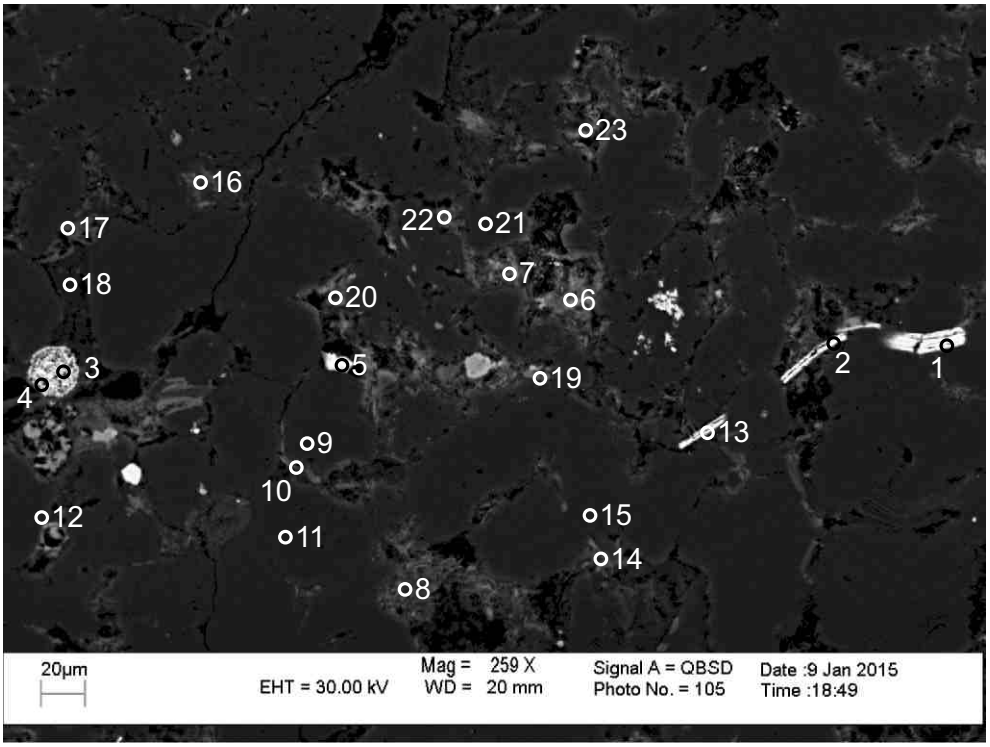

1: Pyrite
2: Pyrite
3: Pyrite
4: Pyrite
5: Zircon+ Other
6: Chlorite+ Other
7: Chlorite
8: Albite
9: Quartz
10: Chlorite+ Albite+ Illite
11: Quartz
12: Quartz+ Chlorite
13: Pyrite+ Chlorite
14: Quartz+ Chlorite
15: Quartz
16: Albite+ Chlorite
17: Muscovite
18: Muscovite +Chlorite
19: Albite+ Chlorite
20: Chlorite
21: Quartz+ Albite
22: Chlorite
23: Chlorite

Figure 2-11.13: Sample Newburn 5961.7m site 13 (SEM). Pyrite (1,2,13) appears to have pseudomorphed muscovite. Framboidal pyrite (3,4). Chlorite (8) surrounds kaolinite and partially fills pore.

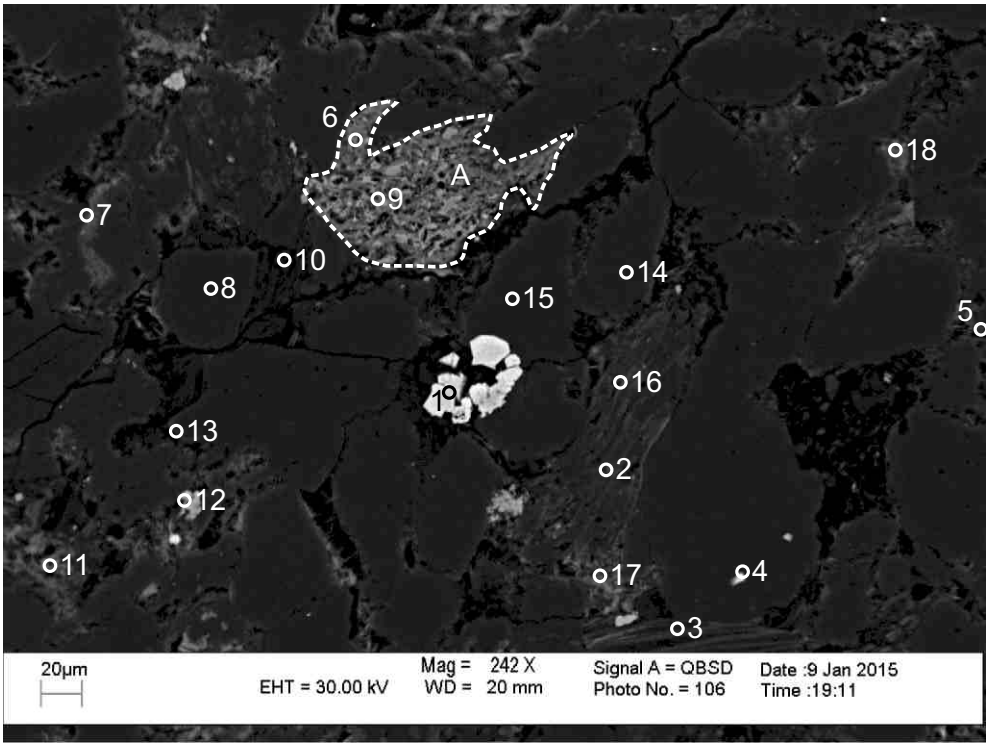

1: Pyrite
2: Muscovite+ Chlorite
3: Muscovite+ Chlorite
4: Quartz+ Titania
5: Albite+Other
6: Chlorite
7: Chlorite
8: Quartz
9: Chlorite+ Siderite+ Albite
10: Kaolinite+ Other
11: Chlorite
12: Titania+ Chlorite
13: Quartz
14: Albite
15: Quartz
16:Muscovite+ Chlorite
17: Chlorite
18: Chlorite+ Illite+ Albite

Figure 2-11.14: Sample Newburn 5961.7m site 14 (SEM). Probably an altered pumice clast (position A), comprised of chlorite and albite, and with later siderite (6,9) filling open preserved porosity. Pyrite (1) crystalites partially fill a pore.

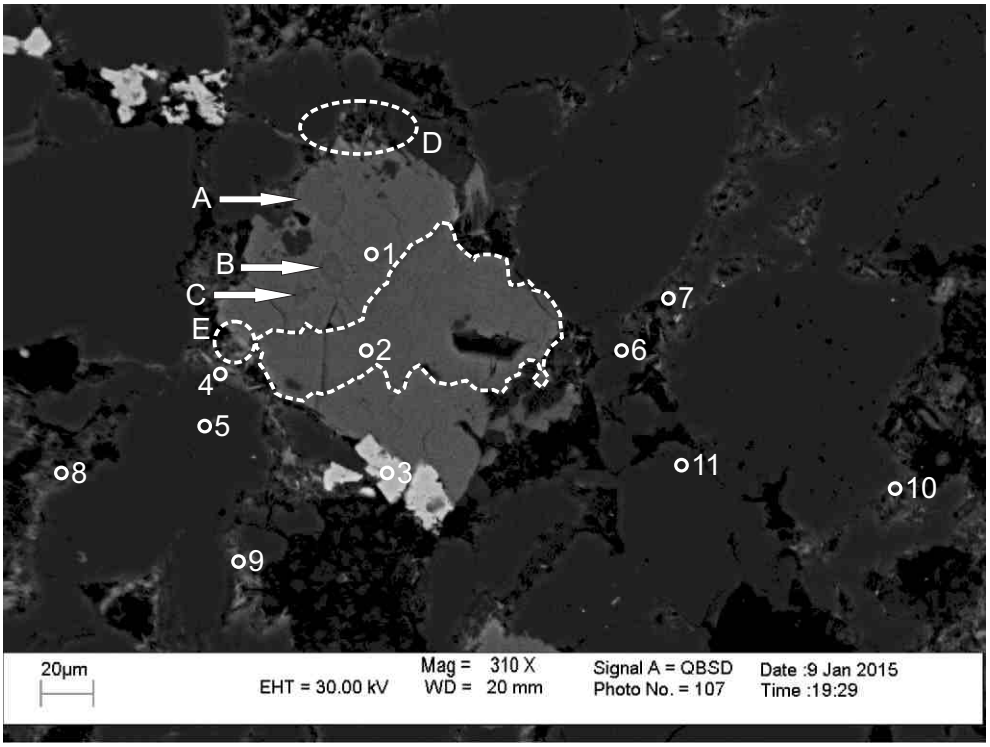

1: Ankerite
2: Fe-Calcite
3: Titania+ Other
4: Quartz+ Chlorite
5: Quartz
6: Albite
7: Albite+ Chlorite
8: Chlorite+ Other
9: Chlorite+ Illite
10: Chlorite
11: Quartz

Figure 2-11.15: Sample Newburn 5961.7m site 15 (SEM). Fe-calcite (positions A,B,C,2) in ankerite (1) with unclear age relationship. Titania (3) engulfs ankerite. Ankerite (1) engulfs kaolinite (position D) and chlorite (position E) filling pore.

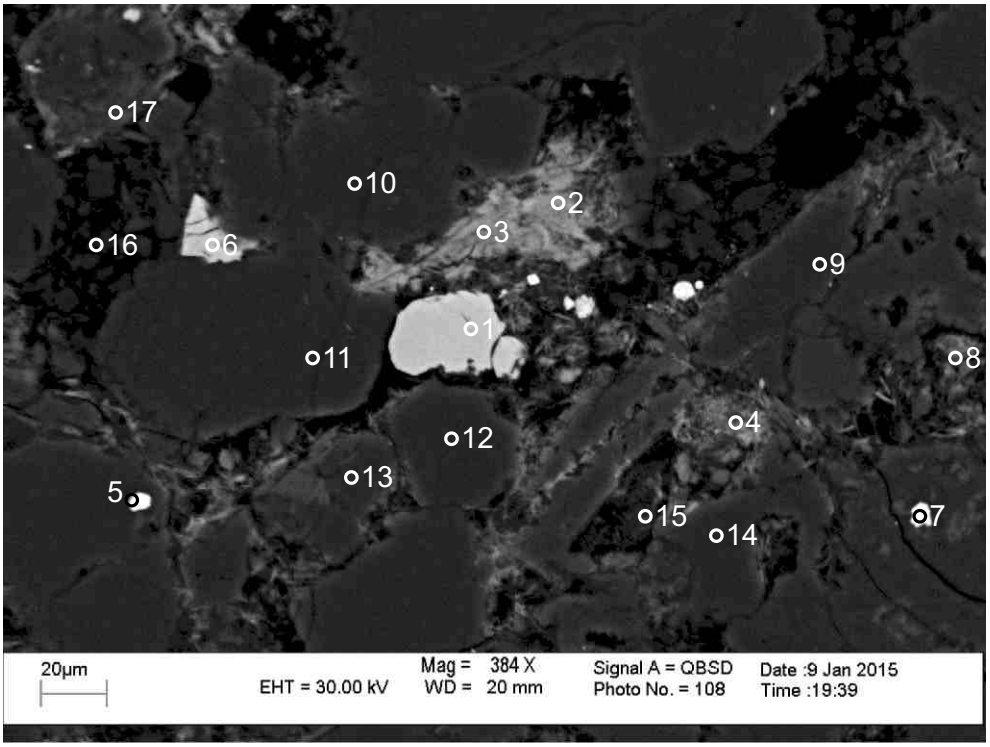

1: Titania
2: Chlorite
3: Chlorite
4: Chlorite
5: Sphalerite+ Quartz
6: Titania+ Chlorite
7: Sphalerite+ Quartz
8: Chlorite
9: Quartz+ Other
10: Quartz
11: Quartz
12: Quartz
13: Quartz
14: Quartz
15: Chlorite
16: Kaolinite
17:Muscovite+ Chlorite

Figure 2-11.16: Sample Newburn 5961.7m site 16 (SEM). Sphalerite (5,7) fills dissolution voids within quartz. Detrital Titania (1) with dissolution voids. Chlorite (2,3) engulfs kaolinite filling pore.

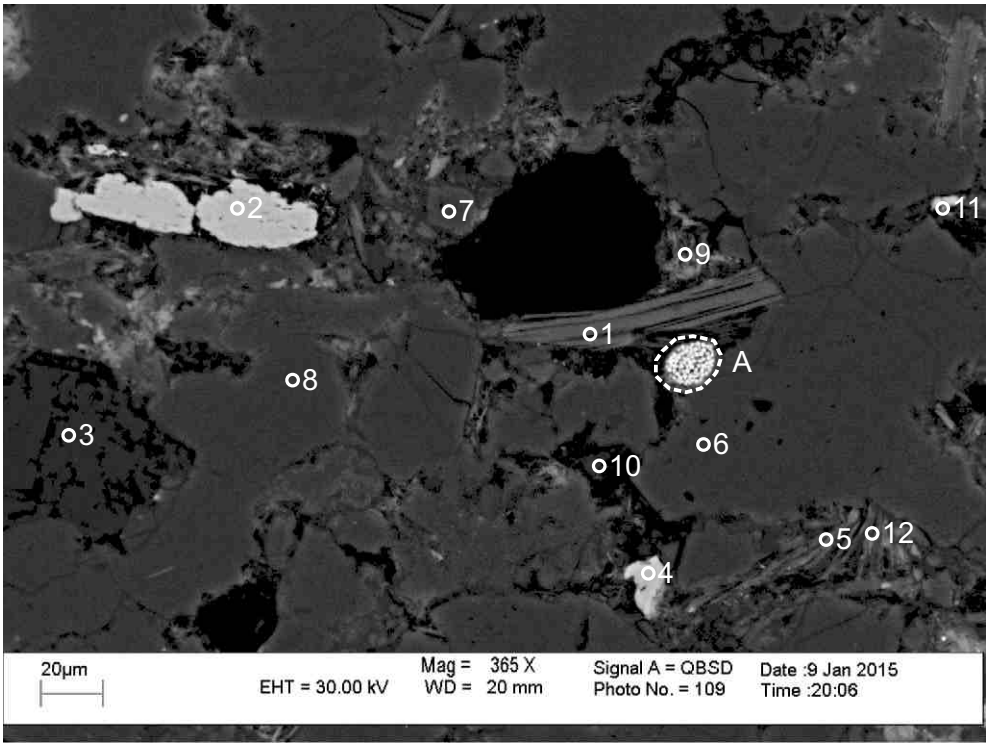

1: Muscovite+ Chlorite
2: Titania+ Other
3: Kaolinite
4: Titania
5: Muscovite
6: Quartz
7: Albite
8: Quartz
9: Chlorite
10: Quartz+ Muscovite +Other
11: Titania+ Quartz+ Other
12: Chlorite+ Muscovite +Apatite

Figure 2-11.17: Sample Newburn 5961.7m site 17 (SEM). Titania (2) possibly engulfs chlorite. Framboidal pyrite (position A) cuts quartz. Chlorite and apatite (12) replace muscovite (5).

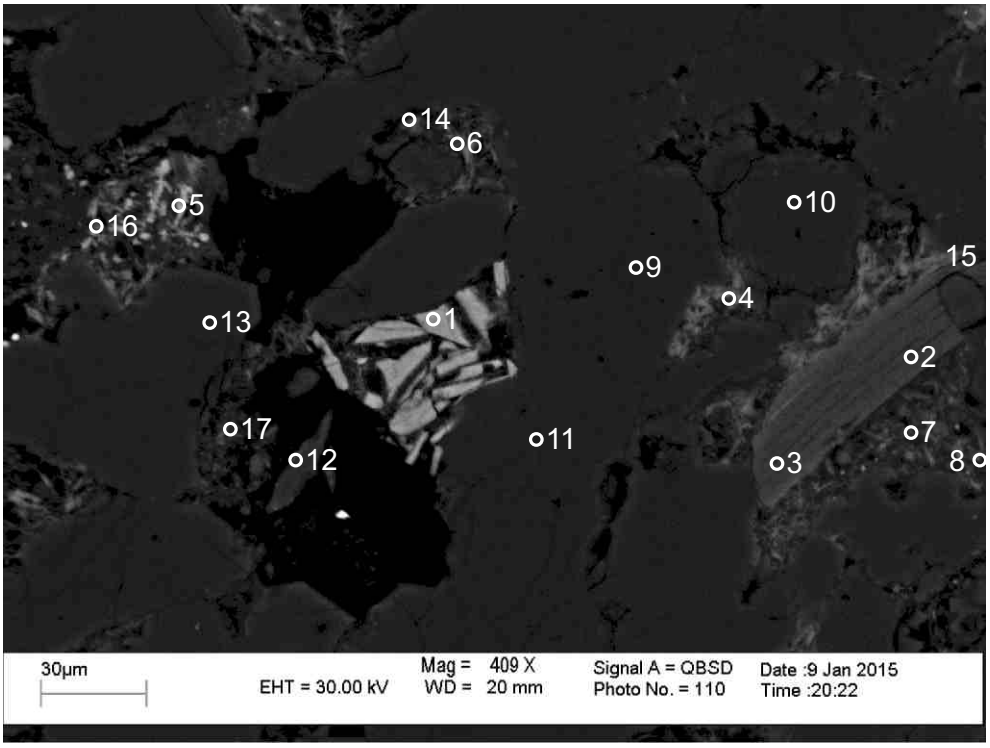

1: Titania+ Chlorite
2: Muscovite
3: Muscovite
4: Chlorite
5: Titania+ Albite+ Apatite
6: Chlorite
7: Muscovite+ Other
8: Muscovite+ Chlorite
9: Quartz
10: Quartz
11: Quartz
12: Quartz
13: Quartz
14: Ankerite+ Chlorite
15: Muscovite +Chlorite
16: Apatite+ Albite+ Other
17: Chlorite

Figure 2-11.18: Sample Newburn 5961.7m site 18 (SEM). Titania (1) appears to have been shattered by adjacent quartz grains (11,9). Apatite and titania (5,16) are cutting albite and quartz.

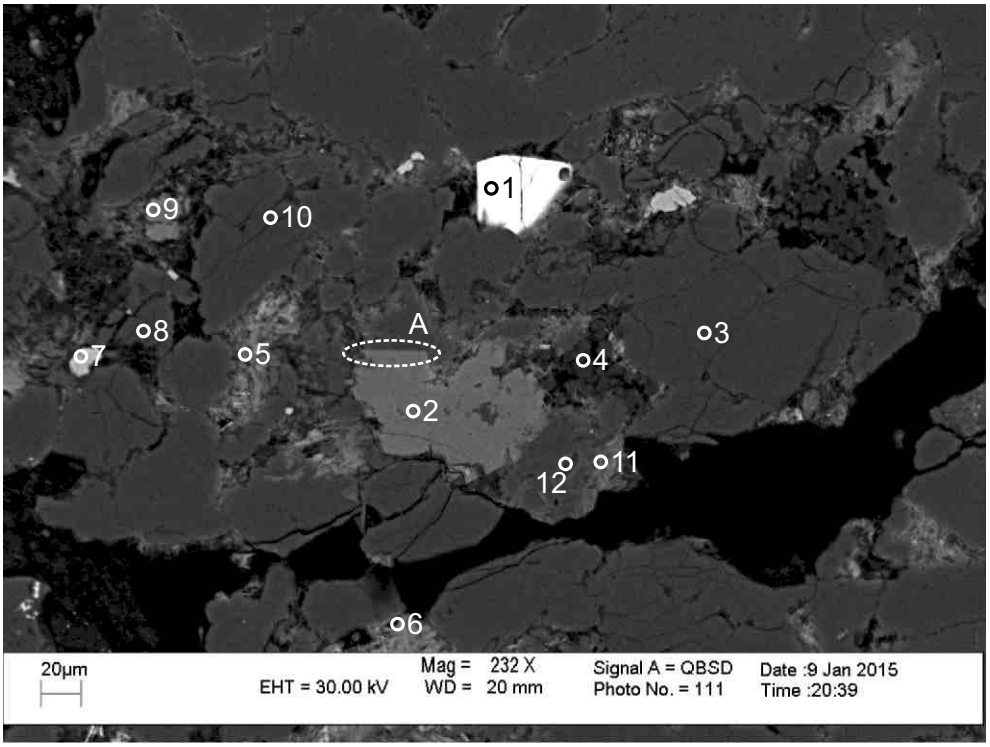

1: Zircon
2: Ankerite
3: Quartz
4: Kaolinite
5: Chlorite
6: Chlorite
7: Titania+ Chlorite
8: Quartz
9: Ankerite
10: Quartz
11: Chlorite+ Other
12: Quartz+ Muscovite +Chlorite

Figure 2-11.19: Sample Newburn 5961.7m site 19 (SEM). Diagenetic zircon (1) fills pore and engulfs quartz. Ankerite (2) is engulfing kaolinite (4) and quartz (position A).

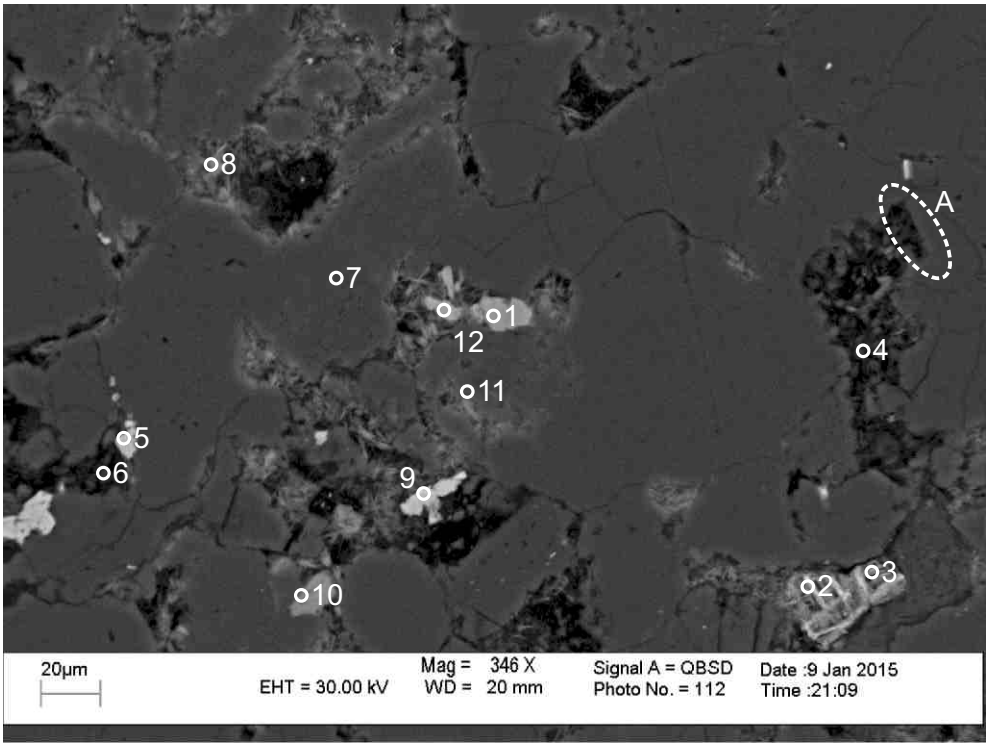

1: Fluorapatite
2: Titania+ Chlorite
3: Titania+ Chlorite
4: Kaolinite+ Chlorite+ Albite
5: Titania+ Chlorite
6: Kaolinite
7: Albite
8: Chlorite
9: Titania+ Chlorite
10: Chlorite
11: Albite+ Chlorite
12:Fluorapatite +Chlorite

Figure 2-11.20: Sample Newburn 5961.7m site 20 (SEM). Diagenetic titania (2,3) partially cuts chlorite. Fluorapatite (1,12) engulfs quartz and chlorite (12). Kaolinite fills pore with quartz overgrowth (position A). Titania (9) cuts fibrous chlorite.

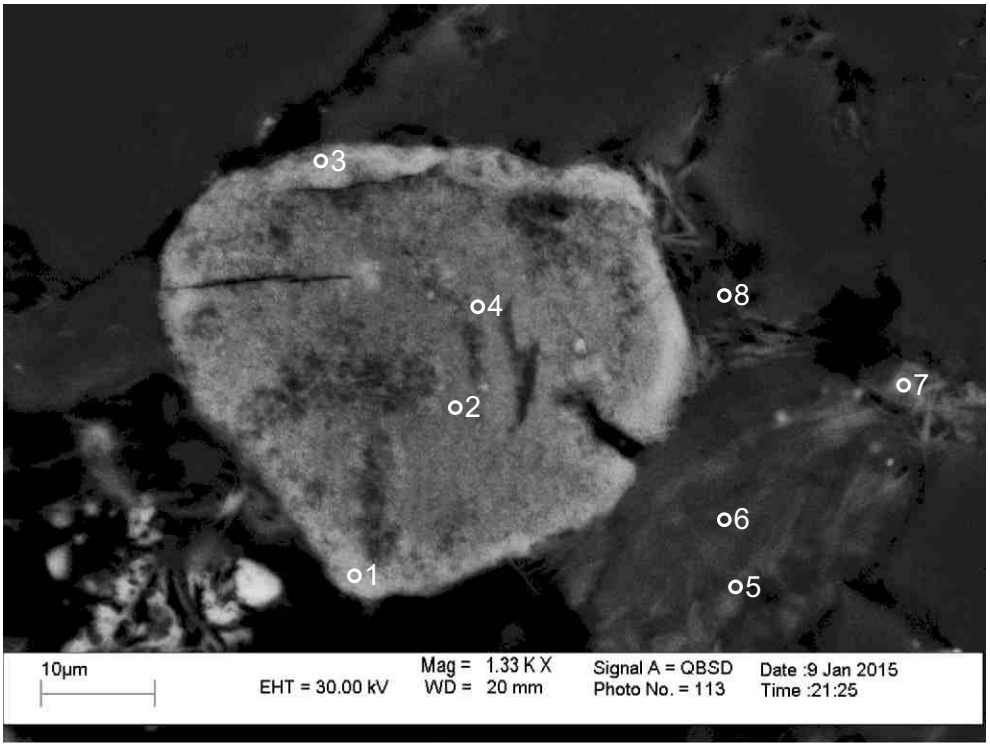

1: Titania+ Chlorite
2: Titania+ Chlorite
3: Titania+ Other
4: Titania+ Chlorite
5: Muscovite+ Chlorite
6: Muscovite+ Chlorite
7: Chlorite
8: Chlorite

Figure 2-11.21: Sample Newburn 5961.7m site 21 (SEM). Ragged detrital titania (1-4) partially dissolved and is rimmed by (1), and has dissolution voids filled by (2,4) later chlorite.

Table 2-11: Scanning Electron Microscope chemical analyses of sample 5961.7 from Newburn H-23 well.

Sample	Site	Position	Mineral	SiO_2	TiO_2	Al_2O_3	FeO	MnO	MgO	CaO	Na_2O	K_2O	P_2O_5	SO_3	F	Cl	Sc_2O_3	NiO	CuO	ZnO	As_2O_3	SrO	Y_2O_3	ZrO_2	La_2O_3	Ce_2O_3	Nd_2O_3	HfO_2	Total	Actual Total
H-23 5961.7m	1	1	Qz	99.99																									100	107
H-23 5961.7m	1	2	TiO_2	3.08	91.98	1.53	3.41																						100	82
H-23 5961.7m	1	3	Py	3.42	0.28	1.74	25.14	0.25	2.07	6.44		0.18		59.83				0.20			0.46								100	143
H-23 5961.7m	1	4	Ank		0.32		15.62	1.22	10.42	28.43																			56	54
H-23 5961.7m	1	5	Kln	49.23		36.77																							86	86
H-23 5961.7m	1	6	Ab	62.12		19.90	5.20		2.29		10.52																		100	105
H-23 5961.7m	1	7	Fe-Cal	1.05		0.81	2.11	0.57	0.76	50.70																			56	49
H-23 5961.7m	1	8	Fe-Cal	0.53			1.57	0.52	0.66	52.72																			56	47
H-23 5961.7m	1	9	Chl+Ilt	45.14	1.72	29.70	17.11		3.55			2.00				0.76													100	53
H-23 5961.7m	1	10	Chl+Ab	40.79		24.60	27.84		3.98	0.35	2.44																		100	82
H-23 5961.7m	1	11	Ab	59.19		20.41	9.73		1.11		9.56																		100	100
H-23 5961.7m	1	12	Qz	99.99																									100	107
H-23 5961.7m	1	13	TiO_2	1.84	97.86		0.30																						100	87
H-23 5961.7m	1	14	Chl+Ap	31.75		23.86	28.69		4.41	5.78	0.96	0.51	4.06																100	79
H-23 5961.7m	1	15	Cal+Chl	6.35		1.34	2.46	0.59		89.24																			100	49
H-23 5961.7m	1	16	Cal+Chl	8.45		5.82	8.76	0.92	1.69	72.79		0.66		0.90															100	58
H-23 5961.7m	1	17	Kln+Chl+Other	53.27	0.47	30.97	7.67		1.76		1.63	3.64				0.58													100	83
H-23 5961.7m	1	18	Ms+Chl	50.01	0.50	29.31	10.77		3.65			5.76																	100	98
H-23 5961.7m	1	19	Py	1.09		0.53	27.75		0.91		2.86			66.87															100	133
H-23 5961.7m	2	1	Ms	47.76	0.84	34.35	1.07		0.50		0.78	9.70																	95	103
H-23 5961.7m	2	2	Ank	0.77			14.47	1.48	9.72	29.55																			56	49
H-23 5961.7m	2	3	Chl	25.31	0.37	20.36	32.67	0.26	5.69	0.33																			85	73
H-23 5961.7m	2	4	Chl	28.53	0.94	20.63	25.32		6.41	1.22		0.30	1.66																85	81
H-23 5961.7m	2	5	Fe-Chl	27.53	0.37	22.20	40.16	0.58	7.49	0.84	0.82																		100	83
H-23 5961.7m	2	6	Ank	2.36		0.94	15.30	1.13	9.73	26.54																			56	60
H-23 5961.7m	2	7	Qz	99.99																									100	105
H-23 5961.7m	2	8	Ank+Ms	59.92		21.43	7.00		1.54	0.50	7.93	1.66																	100	99
H-23 5961.7m	2	9	Chl	30.92	1.29	19.49	26.17		6.16	0.24	0.54					0.19													85	84
H-23 5961.7m	2	10	Ms	59.43	0.41	24.40	2.51		1.18		0.42	6.65																	95	98
H-23 5961.7m	2	11	Qz+Ms	73.07	0.57	15.15	7.13		1.46			2.61																	100	101
H-23 5961.7m	2	12	Fe-Chl	28.17		22.22	40.05	0.70	7.06	0.94	0.88																		100	73
H-23 5961.7m	2	13	TiO_2+Qz+Chl	19.36	73.26	3.34	3.45		0.58																				100	95
H-23 5961.7m	2	14	Zrn	31.40						0.31														67.19				1.10	100	113
H-23 5961.7m	2	15	Ab+Ms+Chl	61.39	0.72	26.98	3.94		0.98		1.75	3.67				0.56													100	70
H-23 5961.7m	2	16	Chl	27.97		23.80	27.82		5.20	0.20																			85	88
H-23 5961.7m	2	17	Fe-Chl	25.71		20.18	40.60	0.59	7.28	2.57	1.04		1.79			0.25													100	78
H-23 5961.7m	3	1	TiO_2	2.18	92.31	1.97	2.96			0.59																			100	82
H-23 5961.7m	3	2	Ank				14.61	1.47	10.27	29.65																			56	49
H-23 5961.7m	3	3	Ms	50.31	0.98	26.34	7.14		3.31			6.93																	95	87
H-23 5961.7m	3	4	Ank				15.36	1.16	9.86	29.62																			56	49
H-23 5961.7m	3	5	TiO_2+Chl	4.60	89.96	4.12	1.31																						100	74
H-23 5961.7m	3	6	Chl+Ilt	39.58	0.67	27.19	25.67		4.31		0.75	1.83																	100	72
H-23 5961.7m	3	7	Ab	68.88		18.82					12.30																		100	98
H-23 5961.7m	3	8	Qz	99.99																									100	101
H-23 5961.7m	3	9	Qz	99.99																									100	101
H-23 5961.7m	3	10	Qz	99.99																									100	94
H-23 5961.7m	3	11	Qz	99.99																									100	101
H-23 5961.7m	3	12	Chl	31.11		23.60	25.31		4.78			0.20																	85	74
H-23 5961.7m	3	13	Ab	54.89		22.24	13.02		2.30		6.65	0.89																	100	93
H-23 5961.7m	3	14	Ab	68.73		18.99				0.20	12.09																		100	98
H-23 5961.7m	3	15	Kln+Other	53.05	0.33	35.26	5.29		1.04		1.08	3.10		0.85															100	72
H-23 5961.7m	3	16	Kln	50.27		34.80	0.93																						86	62
H-23 5961.7m	3	17	Kln+Chl	54.66		39.72	5.61																						100	76
H-23 5961.7m	3	18	Kln+Chl+Ab	49.86		31.31	13.77		2.59		2.48																		100	71

Table 2-11: Scanning Electron Microscope chemical analyses of sample 5961.7 from Newburn H-23 well.

Sample	Site	Position	Mineral	SiO_2	TiO_2	Al_2O_3	FeO	MnO	MgO	CaO	Na_2O	K_2O	P_2O_5	SO_3	F	Cl	Sc_2O_3	NiO	CuO	ZnO	As_2O_3	SrO	Y_2O_3	ZrO_2	La_2O_3	Ce_2O_3	Nd_2O_3	HfO_2	Total	Actual Total
H-23 5961.7m	3	19	Chl	30.86	3.21	23.17	21.92		4.54		0.75	0.35				0.21													85	76
H-23 5961.7m	3	20	Chl	30.84		19.18	27.65		7.33																				85	74
H-23 5961.7m	3	21	Qz+Fap+Other	62.55		5.05	0.78		0.53	10.14		1.54	15.70		3.70														100	106
H-23 5961.7m	3	22	Kln	50.59		35.41																							86	77
H-23 5961.7m	3	23	Py+Cal+Chl	3.23	0.87	1.06	23.74	1.05	2.92	15.43	0.65			49.89				0.50			0.67								100	106
H-23 5961.7m	4	1	Chl	28.72	0.59	20.57	27.33		7.43	0.35																			85	81
H-23 5961.7m	4	2	Chl	32.42	1.25	23.58	22.10		4.50			1.16																	85	78
H-23 5961.7m	4	3	Chl	34.99	0.66	23.80	19.12		4.48		1.19	0.75																	85	89
H-23 5961.7m	4	4	Ank	1.05			14.47	1.18	10.17	29.13																			56	46
H-23 5961.7m	4	5	Ank			0.71	15.72	1.14	9.55	28.88																			56	50
H-23 5961.7m	4	6	TiO_2	7.02	85.52	4.01	3.45																						100	84
H-23 5961.7m	4	7	Ank+Other	3.10	0.62	2.12	25.16	1.55	16.93	50.06		0.47																	100	54
H-23 5961.7m	4	8	Fe-Cal+Ab	5.80		2.25	2.51	0.90		86.51	2.02																		100	52
H-23 5961.7m	4	9	Zrn	31.98																				68.03					100	94
H-23 5961.7m	4	10	Chl	29.38		23.65	26.37		4.05	0.38	0.65	0.51																	85	73
H-23 5961.7m	4	11	Ab+Chl	54.85	0.30	21.37	13.44		1.82	0.20	8.02																		100	92
H-23 5961.7m	4	12	Ab+Chl	51.70	0.30	24.68	14.34		2.14		5.27	1.34				0.22													100	83
H-23 5961.7m	4	13	Chl	32.53	0.28	23.05	23.06		3.36	0.27	1.49	0.74				0.22													85	72
H-23 5961.7m	4	14	Ank+Qz	28.88		2.14	19.45	1.43	13.02	35.09																			100	56
H-23 5961.7m	4	15	Qz	99.99																									100	97
H-23 5961.7m	4	16	Qz	99.99																									100	96
H-23 5961.7m	4	17	Ab	72.73	0.25	16.29	0.53			0.32	8.93	0.94																	100	91
H-23 5961.7m	4	18	Qz	99.99																									100	104
H-23 5961.7m	4	19	Py				26.45				3.61			69.94															100	175
H-23 5961.7m	4	20	Hole	28.84		17.99	23.92							29.24															100	4
H-23 5961.7m	5	1	Chl	29.35		21.20	12.80	0.30	21.35																				85	83
H-23 5961.7m	5	2	Chl	31.06	0.32	23.45	23.20		4.84	1.32		0.82																	85	78
H-23 5961.7m	5	3	Chl	31.69		21.86	12.32	0.26	18.42			0.44																	85	85
H-23 5961.7m	5	4	Chl	24.13		19.16	30.28	0.56	10.19	0.68																			85	70
H-23 5961.7m	5	5	Sd+Chl	11.47		8.28	62.45	2.32	13.12	2.38																			100	53
H-23 5961.7m	5	6	Ms+Chl	52.77		28.06	9.22		4.16		0.69	4.85				0.24													100	82
H-23 5961.7m	5	7	Ms+Chl	48.52	0.52	27.27	13.06		6.50		0.58	3.55																	100	82
H-23 5961.7m	5	8	Chl	27.12	0.55	21.90	29.16		5.05	0.56			0.66																85	77
H-23 5961.7m	5	9	TiO_2+Chl	23.89	31.36	18.10	22.44		3.86							0.35													100	62
H-23 5961.7m	5	10	Ab+Chl	48.90		22.73	18.73		2.69	1.13	5.06		0.78																100	83
H-23 5961.7m	5	11	Ab+Qz	88.56		6.92	1.02				3.49																		100	96
H-23 5961.7m	5	12	Ms+TiO_2	54.91	9.91	23.79	4.72		1.23		0.73	4.44				0.26													100	63
H-23 5961.7m	5	13	Ms+Other	67.56	1.32	21.99	1.49		1.46	0.62	0.71	4.85																	100	94
H-23 5961.7m	5	14	Chl	28.06		21.66	28.10		6.61	0.32		0.25																	85	77
H-23 5961.7m	5	15	Qz	99.99																									100	95
H-23 5961.7m	5	16	Qz	99.02			0.73					0.24																	100	101
H-23 5961.7m	5	17	Ab	68.52		19.14	0.35				12.00																		100	100
H-23 5961.7m	5	18	Qz	99.79			0.21																						100	95
H-23 5961.7m	5	19	Qz	99.99																									100	93
H-23 5961.7m	5	20	Ab	61.97	0.25	20.26	6.54		1.03		9.25	0.71																	100	104
H-23 5961.7m	5	21	Ms	49.52	1.06	29.10	1.88		1.24		0.42	9.67			2.10														95	97
H-23 5961.7m	5	22	Ab	62.53		20.88	6.01		1.06		9.52																		100	91
H-23 5961.7m	6	1	Zrn	31.64																				67.38				0.99	100	102
H-23 5961.7m	6	2	Py				27.26				2.00			70.74															100	171
H-23 5961.7m	6	3	Py	0.34		0.30	26.22	0.27			1.69			71.19															100	170
H-23 5961.7m	6	4	TiO_2		100.00																								100	79
H-23 5961.7m	6	5	Zrn	31.79																				66.99				1.24	100	93
H-23 5961.7m	6	6	Zrn	31.45																				68.55					100	93
H-23 5961.7m	6	7	Qz	87.69	9.59	1.25	1.27					0.20																	100	98

Table 2-11: Scanning Electron Microscope chemical analyses of sample 5961.7 from Newburn H-23 well.

Sample	Site	Position	Mineral	SiO_2	TiO_2	Al_2O_3	FeO	MnO	MgO	CaO	Na_2O	K_2O	P_2O_5	SO_3	F	Cl	Sc_2O_3	NiO	CuO	ZnO	As_2O_3	SrO	Y_2O_3	ZrO_2	La_2O_3	Ce_2O_3	Nd_2O_3	HfO_2	Total	Actual Total
H-23 5961.7m	6	8	Ank	1.53			14.23	1.26	10.34	28.64																			56	45
H-23 5961.7m	6	9	Ab+Chl+Other	46.68		27.21	17.92		3.13		3.48	1.57																	100	77
H-23 5961.7m	6	10	Qz	99.09		0.59	0.32																						100	93
H-23 5961.7m	6	11	Ab+Ms+Chl	44.71	0.33	27.87	17.26		4.24	0.67	2.31	2.60																	100	76
H-23 5961.7m	6	12	Zrn+Other	42.98		1.59	1.04			0.38		0.31					0.34						1.79	49.61				1.95	100	100
H-23 5961.7m	6	13	Py+Other	0.28			27.45				1.07			71.19															100	177
H-23 5961.7m	6	14	Chl+Py	29.56		22.86	29.72	0.46	8.99	1.37	1.64			3.02						2.38									100	85
H-23 5961.7m	6	15	Chl+Ab+Ilt	65.93		18.16	11.26		2.16		0.69	1.81																	100	86
H-23 5961.7m	6	16	Qz+Other	96.03		2.51	0.32			0.34		0.78																	100	91
H-23 5961.7m	6	17	Ms+Chl	49.14	0.47	28.48	10.75		3.85		0.57	6.78																	100	79
H-23 5961.7m	6	18	Qz+TiO_2+Chl	38.89	16.70	18.14	15.61		10.18			0.47																	100	84
H-23 5961.7m	6	19	Qz+TiO_2+Chl	69.95	21.50	2.95	3.73		1.48	0.38																			100	88
H-23 5961.7m	6	20	Ab	65.01		19.63	4.22		0.58		10.38	0.18																	100	96
H-23 5961.7m	6	21	Chl	33.73		22.34	22.48		3.86		2.41					0.19													85	76
H-23 5961.7m	6	22	TiO_2+Qz	47.58	51.01	0.49	0.94																						100	74
H-23 5961.7m	6	23	Qz	99.99																									100	96
H-23 5961.7m	6	24	Py	0.28			27.27				1.95			70.49															100	174
H-23 5961.7m	6	25	TiO_2+Other	1.20	97.16	0.89	0.75																						100	80
H-23 5961.7m	6	26	Zrn	31.75																				68.26					100	92
H-23 5961.7m	7	1	Ms	47.32	0.55	31.49	3.42		1.34		0.58	10.30																	95	80
H-23 5961.7m	7	2	Ms+Other	59.98	0.73	24.94	5.44		3.71		1.02	4.14																	100	76
H-23 5961.7m	7	3	Ank	1.52		0.63	13.91	1.28	11.21	27.44																			56	52
H-23 5961.7m	7	4	Py				27.65				0.88			71.47															100	179
H-23 5961.7m	7	5	Qz+Chl+Ms	49.61	1.02	30.23	12.56		2.11		1.46	3.01																	100	78
H-23 5961.7m	7	6	Qz	98.87		0.91	0.22																						100	89
H-23 5961.7m	7	7	Ank	1.71		1.33	13.51	1.06	10.61	27.77																			56	50
H-23 5961.7m	7	8	Ms	47.85	0.48	31.63	3.16		1.31		0.48	10.09																	95	82
H-23 5961.7m	7	9	Ms	54.84	1.03	26.37	2.95		0.74			9.06																	95	88
H-23 5961.7m	7	10	Kln	48.92		34.62	0.88		0.71		0.54					0.33													86	60
H-23 5961.7m	7	11	TiO_2+Ms	12.47	77.66	7.22	0.64				0.88	1.12																	100	80
H-23 5961.7m	7	12	Ms	48.09		34.66	0.98		0.50		0.87	9.90																	95	86
H-23 5961.7m	7	13	Chl	29.84	0.96	19.10	28.89		6.21																				85	70
H-23 5961.7m	7	14	Ab+Chl	44.20		33.39	15.72		3.40		3.32																		100	73
H-23 5961.7m	7	15	Ms	52.77		31.99	2.52		0.96		0.91	5.85																	95	76
H-23 5961.7m	7	16	Ms	51.20	0.93	29.01	5.02		2.42		1.54	4.87																	95	63
H-23 5961.7m	7	17	Py	0.26			26.09	0.41	0.40		3.11			69.74															100	171
H-23 5961.7m	7	18	Sd+Chl+Ab	19.81	0.50	16.23	50.60	1.29	8.74	1.61	1.23																		100	58
H-23 5961.7m	7	19	Chl	29.71	0.68	21.62	26.53		5.71	0.42		0.34																	85	74
H-23 5961.7m	7	20	TiO_2	2.95	92.36	2.66	2.02																						100	88
H-23 5961.7m	7	21	Qz	99.99																									100	101
H-23 5961.7m	7	22	Al-Phosphate	30.03		28.82	1.70			0.62	4.30	0.76	19.20	1.67								3.31			2.65	5.34	1.57		100	73
H-23 5961.7m	7	23	Py+Qz	10.01		1.36	25.32							63.30															100	149
H-23 5961.7m	7	24	TiO_2	7.87	91.53		0.60																						100	80
H-23 5961.7m	7	25	TiO_2	2.40	97.23		0.39																						100	73
H-23 5961.7m	8	1	Al-Phosphate	13.58		34.03	3.34			0.83	0.71	1.10	26.97	2.37							0.95	4.44			3.67	6.16	1.82		100	80
H-23 5961.7m	8	2	Al-Phosphate	8.28		35.32	0.96			0.94		0.87	30.61	2.50							0.83	4.84			4.57	7.91	2.34		100	75
H-23 5961.7m	8	3	Al-Phosphate	28.54		29.38	3.32			0.52		1.35	22.91	1.67								3.13			2.62	4.97	1.59		100	70
H-23 5961.7m	8	4	Ms+Other	66.36	1.47	22.71	1.24		1.28		1.08	3.78			1.80	0.28													100	87
H-23 5961.7m	8	5	Ab	63.51	1.53	21.07	2.30				10.53	1.05																	100	96
H-23 5961.7m	8	6	Chl+Ms	53.46	3.80	28.57	6.59		2.04		0.80	4.31				0.43													100	58
H-23 5961.7m	8	7	Qz	99.99																									100	94
H-23 5961.7m	8	8	Qz	99.30		0.45	0.24																						100	92
H-23 5961.7m	8	9	Ms	48.56	0.43	31.06	3.03		1.32		0.55	10.05																	95	87

Table 2-11: Scanning Electron Microscope chemical analyses of sample 5961.7 from Newburn H-23 well.

Sample	Site	Position	Mineral	SiO_2	TiO_2	Al_2O_3	FeO	MnO	MgO	CaO	Na_2O	K_2O	P_2O_5	SO_3	F	Cl	Sc_2O_3	NiO	CuO	ZnO	As_2O_3	SrO	Y_2O_3	ZrO_2	La_2O_3	Ce_2O_3	Nd_2O_3	HfO_2	Total	Actual Total
H-23 5961.7m	8	10	Qz	99.99																									100	95
H-23 5961.7m	8	11	Ms	53.61	0.95	28.54	2.66		2.08		0.78	6.05				0.33													95	76
H-23 5961.7m	9	1	Zrn	32.11																				67.90					100	90
H-23 5961.7m	9	2	Ms	48.04	0.69	32.45	2.91		0.66		1.03	9.22																	95	90
H-23 5961.7m	9	3	Chl	34.82		19.58	26.76		3.53			0.31																	85	72
H-23 5961.7m	9	4	Ab	65.91		19.59	2.69				11.81																		100	96
H-23 5961.7m	9	5	Ms+Chl	59.85	0.45	25.13	4.63		2.06			7.85																	100	77
H-23 5961.7m	9	6	Ms	55.92		24.59	3.49		1.65		0.56	8.80																	95	86
H-23 5961.7m	9	7	Ms+Chl	53.80		35.75	2.51		1.03		1.21	5.71																	100	83
H-23 5961.7m	9	8	Chl+Ms	47.49	2.54	28.02	13.84		2.77	0.53	1.60	2.83				0.37													100	78
H-23 5961.7m	9	9	Chl	29.64		24.01	26.22		4.30			0.38				0.45													85	63
H-23 5961.7m	9	10	Fe-Cal				2.11	0.57		53.32																			56	39
H-23 5961.7m	9	11	TiO_2+Other	9.69	88.44	1.23	0.66																						100	74
H-23 5961.7m	9	12	TiO_2+Qz	23.47	73.11	2.00	0.78					0.65																	100	83
H-23 5961.7m	9	13	Chl	28.57		23.05	28.46		4.92																				85	75
H-23 5961.7m	9	14	Chl+Ms	40.39		29.46	22.82		4.49		1.07	1.45				0.33													100	79
H-23 5961.7m	9	15	Py+Chl	1.63		1.02	26.84							70.54															100	150
H-23 5961.7m	9	16	Py	13.67		1.06	21.82					0.22		62.85							0.38								100	135
H-23 5961.7m	9	17	Qz+Chl+Ab	71.64	0.38	11.38	12.07		2.79		1.28	0.46																	100	72
H-23 5961.7m	9	18	Chl+Other	44.84		24.15	24.97		4.43		0.90	0.48				0.22													100	77
H-23 5961.7m	10	1	Zrn	31.77																				67.15				1.10	100	94
H-23 5961.7m	10	2	Py				27.57				0.40			72.02															100	164
H-23 5961.7m	10	3	Qz+Ab	83.60		9.18				0.21	6.65	0.36																	100	96
H-23 5961.7m	10	4	Chl+Qz	51.68		19.84	24.35		4.13																				100	79
H-23 5961.7m	10	5	Ms+Chl	50.96		31.10	11.09		1.99			4.66				0.21													100	79
H-23 5961.7m	10	6	Chl+Ms	48.07		24.02	14.36		10.08			3.48																	100	81
H-23 5961.7m	10	7	Qz+Ab+Ms	82.21	0.88	9.47	1.93		0.81		2.97	1.73																	100	92
H-23 5961.7m	10	8	Ms+Other	62.06	0.33	24.15	4.63		2.22		0.54	6.07																	100	89
H-23 5961.7m	10	9	Chl	29.29		23.63	27.80		4.28																				85	59
H-23 5961.7m	10	10	Chl	27.46		23.61	29.24		4.69																				85	62
H-23 5961.7m	10	11	Chl	28.93		24.69	26.07		5.09							0.22													85	64
H-23 5961.7m	10	12	Chl	31.30		22.50	26.53		4.15			0.31				0.20													85	69
H-23 5961.7m	10	13	Qz	99.99																									100	93
H-23 5961.7m	10	14	TiO_2+Qz	36.22	63.79																								100	99
H-23 5961.7m	10	15	Qz+Sp	61.82		1.76	0.90					0.31		18.83						16.37									100	125
H-23 5961.7m	10	16	Qz+Other	97.78		1.30	0.42					0.47																	100	90
H-23 5961.7m	10	17	Qz	99.99																									100	93
H-23 5961.7m	10	18	Qz+Other	94.34		4.40						1.25																	100	92
H-23 5961.7m	10	19	Kln+Chl+Ms	55.45		37.64	5.39		0.58			0.93																	100	69
H-23 5961.7m	10	20	Chl	30.15		23.87	25.57		3.94	0.35	0.60	0.52																	85	76
H-23 5961.7m	10	21	TiO_2+Qz+Other	29.37	63.77	3.06	3.81																						100	85
H-23 5961.7m	10	22	Qz	99.99																									100	89
H-23 5961.7m	10	23	TiO_2	0.75	98.85		0.41																						100	75
H-23 5961.7m	11	1	Zrn	31.83																				68.17					100	91
H-23 5961.7m	11	2	Sd+Other	3.42		2.49	91.20	1.38		1.51																			100	44
H-23 5961.7m	11	3	Sd+Other	1.90			95.57	0.85		1.67																			100	43
H-23 5961.7m	11	4	TiO_2+Other	1.33	96.03	0.66	1.99																						100	78
H-23 5961.7m	11	5	Ms	52.11		28.24	3.87		2.27			8.51																	95	83
H-23 5961.7m	11	6	Ms	51.78		25.32	5.24		3.13			9.52																	95	81
H-23 5961.7m	11	7	Kln	48.42		36.34	1.25																						86	76
H-23 5961.7m	11	8	Chl	33.77	1.30	18.81	22.03		8.53			0.56																	85	67
H-23 5961.7m	11	9	Qz	94.06		1.78	3.50		0.41			0.24																	100	91
H-23 5961.7m	11	10	Ab	67.66		19.65	0.67				11.50	0.49																	100	92

Table 2-11: Scanning Electron Microscope chemical analyses of sample 5961.7 from Newburn H-23 well.

Sample	Site	Position	Mineral	SiO_2	TiO_2	Al_2O_3	FeO	MnO	MgO	CaO	Na_2O	K_2O	P_2O_5	SO_3	F	Cl	Sc_2O_3	NiO	CuO	ZnO	As_2O_3	SrO	Y_2O_3	ZrO_2	La_2O_3	Ce_2O_3	Nd_2O_3	HfO_2	Total	Actual Total
H-23 5961.7m	11	11	Qz	99.99																									100	90
H-23 5961.7m	11	12	Qz	97.61		1.13	0.91					0.34																	100	88
H-23 5961.7m	11	13	Ab+Chl	62.98		17.40	14.78		2.35		2.20	0.30																	100	79
H-23 5961.7m	11	14	TiO_2+Ms	17.43	72.76	7.09	0.78		0.83			1.11																	100	78
H-23 5961.7m	11	15	Ab	65.76		19.69	3.54				11.01																		100	85
H-23 5961.7m	11	16	Chl	32.10		23.50	23.18		3.73		1.58					0.91													85	65
H-23 5961.7m	11	17	Chl+Other	52.80		21.28	20.40		3.71		1.28	0.53																	100	85
H-23 5961.7m	11	18	TiO_2	7.10	90.33	0.79	1.78																						100	79
H-23 5961.7m	12	1	Zrn	31.79																				68.22					100	89
H-23 5961.7m	12	2	Ms	49.06	0.35	28.31	5.88		1.59			9.80																	95	81
H-23 5961.7m	12	3	Chl	27.36		22.28	28.51		5.50	1.36																			85	64
H-23 5961.7m	12	4	TiO_2	1.56	95.95	0.89	1.61																						100	75
H-23 5961.7m	12	5	TiO_2	2.05	96.26	0.91	0.77																						100	76
H-23 5961.7m	12	6	Qz	96.52		2.12					1.36																		100	84
H-23 5961.7m	12	7	Qz	99.99																									100	90
H-23 5961.7m	12	8	Qz	99.99																									100	91
H-23 5961.7m	12	9	Qz	99.99																									100	93
H-23 5961.7m	12	10	Chl	33.26		22.42	24.27		4.79			0.25																	85	75
H-23 5961.7m	12	11	Ms+Chl	52.32	0.30	28.83	9.69		3.25		0.63	4.96																	100	76
H-23 5961.7m	12	12	Chl	39.38		17.49	24.28		3.57							0.27													85	66
H-23 5961.7m	12	13	TiO_2+Chl	14.14	79.68	4.42	1.33					0.42																	100	76
H-23 5961.7m	12	14	Chl+Ilt	49.14	0.48	28.95	14.81		2.59		1.05	2.71				0.28													100	75
H-23 5961.7m	12	15	Ilt+Chl	69.67		16.61	7.35		1.89		0.59	3.89																	100	91
H-23 5961.7m	12	16	Ilt+Chl	71.68		16.31	7.87		1.94		0.74	1.43																	100	82
H-23 5961.7m	12	17	TiO_2+Chl	7.77	84.99	4.50	2.74																						100	63
H-23 5961.7m	12	18	TiO_2+Chl	3.55	93.01	1.81	1.62																						100	76
H-23 5961.7m	12	19	TiO_2+Chl	1.07	97.63	0.60	0.69																						100	78
H-23 5961.7m	12	20	Chl+Ab	37.07	0.30	26.68	29.00		5.34		1.29	0.31																	100	77
H-23 5961.7m	12	21	Fap+Chl	6.89		4.38	7.02			34.42		0.29	39.53		7.46														100	84
H-23 5961.7m	13	1	Py	4.19			25.10				0.69			67.97				1.77	0.30										100	147
H-23 5961.7m	13	2	Py	5.75		4.31	22.13							65.25				2.56											100	151
H-23 5961.7m	13	3	Py	2.48		1.02	25.27				0.54			70.69															100	151
H-23 5961.7m	13	4	Py	5.43		3.12	36.28					0.34		54.86															100	76
H-23 5961.7m	13	5	Zrn+Other	36.26		4.23	0.89			0.53							0.94						4.14	53.03					100	67
H-23 5961.7m	13	6	Chl+Other	43.83	0.35	27.44	22.04		4.86		0.98	0.49																	100	83
H-23 5961.7m	13	7	Chl	32.05		22.58	23.94		4.39	0.23	0.85	0.52				0.43													85	67
H-23 5961.7m	13	8	Ab	57.31		21.14	11.42		2.11		8.02																		100	77
H-23 5961.7m	13	9	Qz	99.99																									100	88
H-23 5961.7m	13	10	Chl+Ab+Ilt	56.22		25.15	12.49		2.95		1.09	1.88				0.23													100	73
H-23 5961.7m	13	11	Qz	99.99																									100	86
H-23 5961.7m	13	12	Qz+Chl	87.60	0.28	4.55	6.64		0.58			0.35																	100	84
H-23 5961.7m	13	13	Py+Chl	17.52		9.84	22.00		1.69		0.63	0.76		46.35				1.20											100	111
H-23 5961.7m	13	14	Qz+Chl	74.76		11.83	10.46		2.39			0.54																	100	85
H-23 5961.7m	13	15	Qz	99.99																									100	88
H-23 5961.7m	13	16	Ab+Chl	55.79	0.30	20.31	12.39		0.90		10.31																		100	85
H-23 5961.7m	13	17	Ms	53.20		26.07	3.98		1.87			9.88																	95	82
H-23 5961.7m	13	18	Ms+Chl	58.74	1.20	30.57	1.67		1.04		1.13	5.65																	100	67
H-23 5961.7m	13	19	Ab+Chl	46.08		25.06	21.09		3.61	0.22	3.56	0.39																	100	74
H-23 5961.7m	13	20	Chl	32.99		23.69	22.34		3.89		1.61	0.24				0.25													85	70
H-23 5961.7m	13	21	Qz+Ab	89.14		5.10	0.32				5.42																		100	98
H-23 5961.7m	13	22	Chl	30.71		22.98	25.85		3.83		0.66	0.57				0.40													85	61
H-23 5961.7m	13	23	Chl	33.27		20.27	27.00		4.45																				85	53
H-23 5961.7m	14	1	Py	0.51			29.99				1.54			67.95															100	125

Table 2-11: Scanning Electron Microscope chemical analyses of sample 5961.7 from Newburn H-23 well.

Sample	Site	Position	Mineral	SiO_2	TiO_2	Al_2O_3	FeO	MnO	MgO	CaO	Na_2O	K_2O	P_2O_5	SO_3	F	Cl	Sc_2O_3	NiO	CuO	ZnO	As_2O_3	SrO	Y_2O_3	ZrO_2	La_2O_3	Ce_2O_3	Nd_2O_3	HfO_2	Total	Actual Total
H-23 5961.7m	14	2	Ms+Chl	54.76	2.67	29.21	3.09		1.82			8.46																	100	81
H-23 5961.7m	14	3	Ms+Chl	52.03	0.58	38.75	0.71		0.66			7.25																	100	79
H-23 5961.7m	14	4	Qz+TiO_2	84.90	8.89		5.97	0.25																					100	82
H-23 5961.7m	14	5	Ab+Other	78.14		14.46	2.11		0.58		3.80	0.90																	100	79
H-23 5961.7m	14	6	Chl	28.70		22.09	26.94		5.64	0.51	1.13																		85	72
H-23 5961.7m	14	7	Chl	29.61		22.70	27.01		4.07		1.62																		85	66
H-23 5961.7m	14	8	Qz	99.99																									100	86
H-23 5961.7m	14	9	Chl+Sd+Ab	20.62		17.21	49.79	1.29	8.27	1.43	1.39																		100	59
H-23 5961.7m	14	10	Kln+Other	54.91		39.79	1.30				0.66	0.75			2.59														100	64
H-23 5961.7m	14	11	Chl	29.91		24.93	25.21		4.95																				85	65
H-23 5961.7m	14	12	TiO_2+Chl	8.51	77.61	7.58	5.04		1.24																				100	80
H-23 5961.7m	14	13	Qz	97.83		1.91	0.27																						100	89
H-23 5961.7m	14	14	Ab	69.03		18.82					12.16																		100	89
H-23 5961.7m	14	15	Qz	99.77			0.22																						100	89
H-23 5961.7m	14	16	Ms+Chl	62.61	0.30	22.77	6.09		1.97		0.61	5.64																	100	80
H-23 5961.7m	14	17	Chl	28.65		22.42	24.78		3.69	2.05	0.77	0.36	2.05			0.24													85	64
H-23 5961.7m	14	18	Chl+Ilt+Ab	49.33		23.88	18.29		5.72		1.08	1.70																	100	73
H-23 5961.7m	15	1	Ank				12.12	1.22	8.92	33.75																			56	42
H-23 5961.7m	15	2	Fe-Cal				1.74	0.48	0.69	53.09																			56	39
H-23 5961.7m	15	3	TiO_2+Other		97.60	0.62	1.21			0.56																			100	73
H-23 5961.7m	15	4	Qz+Chl	74.19		8.96	14.95		1.72			0.18																	100	86
H-23 5961.7m	15	5	Qz	99.37			0.62																						100	83
H-23 5961.7m	15	6	Ab	69.14		18.80	0.28				11.77																		100	89
H-23 5961.7m	15	7	Ab+Chl	57.12		22.01	12.22		2.34		5.88	0.22				0.22													100	79
H-23 5961.7m	15	8	Chl+Other	44.13		25.06	24.96		4.36		0.85	0.33				0.30													100	65
H-23 5961.7m	15	9	Chl+Ilt	53.61		24.02	16.15		2.57	0.50	0.77	2.37																	100	69
H-23 5961.7m	15	10	Chl	32.56		22.11	23.84		3.83		2.30					0.35													85	60
H-23 5961.7m	15	11	Qz	99.99																									100	87
H-23 5961.7m	16	1	TiO_2		100.00																								100	72
H-23 5961.7m	16	2	Chl	27.31		23.49	30.05		4.16																				85	66
H-23 5961.7m	16	3	Chl	26.89		23.22	30.06		4.82																				85	66
H-23 5961.7m	16	4	Chl	33.46	1.19	23.71	21.22		4.67			0.76																	85	64
H-23 5961.7m	16	5	Sph+Qz	25.24			0.80							40.90						33.08									100	141
H-23 5961.7m	16	6	TiO_2+Chl	7.83	89.51	1.10	1.58																						100	71
H-23 5961.7m	16	7	Sph+Qz	16.19		3.51	1.35					1.10		44.25						33.61									100	120
H-23 5961.7m	16	8	Chl	33.54		24.46	22.20		3.54			0.94				0.32													85	61
H-23 5961.7m	16	9	Qz+Other	97.44	0.37	1.04	0.82					0.34																	100	86
H-23 5961.7m	16	10	Qz	99.99																									100	85
H-23 5961.7m	16	11	Qz	99.99																									100	82
H-23 5961.7m	16	12	Qz	99.99																									100	85
H-23 5961.7m	16	13	Qz	97.48		1.13	0.49		0.36		0.53																		100	84
H-23 5961.7m	16	14	Qz	99.99																									100	86
H-23 5961.7m	16	15	Chl	31.42		23.32	23.93		5.87							0.45													85	57
H-23 5961.7m	16	16	Kln	50.00		36.00																							86	69
H-23 5961.7m	16	17	Ms+Chl	54.76		33.67	1.22		0.78		1.08	8.49																	100	77
H-23 5961.7m	17	1	Ms+Chl	50.49	0.53	35.15	2.43		0.56		1.00	9.84																	100	78
H-23 5961.7m	17	2	TiO_2+Other	0.58	97.46		1.97																						100	70
H-23 5961.7m	17	3	Kln	49.29		36.45	0.26																						86	69
H-23 5961.7m	17	4	TiO_2	0.75	98.83		0.42																						100	71
H-23 5961.7m	17	5	Ms	49.12		31.56	5.97		1.67		0.77	5.70				0.22													95	73
H-23 5961.7m	17	6	Qz	99.99																									100	86
H-23 5961.7m	17	7	Ab	68.56		18.99	0.21				12.26																		100	88
H-23 5961.7m	17	8	Qz	99.99																									100	83

Table 2-11: Scanning Electron Microscope chemical analyses of sample 5961.7 from Newburn H-23 well.

Sample	Site	Position	Mineral	SiO_2	TiO_2	Al_2O_3	FeO	MnO	MgO	CaO	Na_2O	K_2O	P_2O_5	SO_3	F	Cl	Sc_2O_3	NiO	CuO	ZnO	As_2O_3	SrO	Y_2O_3	ZrO_2	La_2O_3	Ce_2O_3	Nd_2O_3	HfO_2	Total	Actual Total
H-23 5961.7m	17	9	Chl	35.97	0.28	25.46	18.94		3.21			0.88				0.25													85	63
H-23 5961.7m	17	10	Qz+Ms+Other	76.20		18.93	0.48		0.75		0.67	2.66				0.31													100	63
H-23 5961.7m	17	11	TiO_2+Qz+Other	27.21	66.24	3.91	1.67		0.65			0.31																	100	78
H-23 5961.7m	17	12	Chl+Ms+Ap	48.62		34.52	8.75		1.61	1.72		3.12	1.37			0.30													100	61
H-23 5961.7m	18	1	TiO_2+Chl	1.84	96.01	0.81	1.33																						100	66
H-23 5961.7m	18	2	Ms	48.74	0.64	31.69	2.64		1.27		1.10	8.91																	95	78
H-23 5961.7m	18	3	Ms	48.18	0.65	32.42	2.48		0.71		1.17	9.39																	95	75
H-23 5961.7m	18	4	Chl	35.50		22.92	21.82		4.00			0.54				0.23													85	67
H-23 5961.7m	18	5	TiO_2+Ab+Ap	12.17	69.72	7.71	4.35		1.04	1.87	1.73		1.40																100	64
H-23 5961.7m	18	6	Chl	36.02		21.76	22.58		4.13			0.28				0.23													85	62
H-23 5961.7m	18	7	Ms+Other	51.21	0.68	27.59	8.21		2.59			5.77			3.95														100	70
H-23 5961.7m	18	8	Ms+Chl	55.47	1.83	26.76	7.17		2.17		0.85	5.47				0.28													100	71
H-23 5961.7m	18	9	Qz	99.99																									100	84
H-23 5961.7m	18	10	Qz	99.28		0.72																							100	84
H-23 5961.7m	18	11	Qz	99.26		0.51						0.24																	100	82
H-23 5961.7m	18	12	Qz	93.76		3.16	1.97		0.65			0.46																	100	80
H-23 5961.7m	18	13	Qz	99.99																									100	82
H-23 5961.7m	18	14	Ank+Chl	48.52		4.46	14.20	0.84	7.49	24.49																			100	60
H-23 5961.7m	18	15	Ms+Chl	49.54	0.72	35.26	2.71		0.70		1.21	9.87																	100	77
H-23 5961.7m	18	16	Ap+Ab+Other	16.19	9.69	10.37	4.19		1.04	27.23	1.25	0.88	29.15																100	71
H-23 5961.7m	18	17	Chl	38.15		24.06	17.05		4.00	0.29		1.21				0.24													85	56
H-23 5961.7m	19	1	Zrn	31.81																				68.19					100	84
H-23 5961.7m	19	2	Ank	1.81			14.09	1.38	9.41	29.30																			56	42
H-23 5961.7m	19	3	Qz	99.99																									100	84
H-23 5961.7m	19	4	Kln	49.19		36.37	0.44																						86	57
H-23 5961.7m	19	5	Chl	36.67		22.15	19.96		2.92		2.99	0.31																	85	55
H-23 5961.7m	19	6	Chl	32.51	1.08	21.61	20.25		9.34			0.20																	85	71
H-23 5961.7m	19	7	TiO_2+Chl	4.19	90.91	3.10	1.80																						100	65
H-23 5961.7m	19	8	Qz	99.99																									100	81
H-23 5961.7m	19	9	Ank				14.03	1.22	10.12	30.63																			56	40
H-23 5961.7m	19	10	Qz	99.99																									100	82
H-23 5961.7m	19	11	Chl+Other	40.26	3.99	25.13	25.78		3.57			1.29																	100	62
H-23 5961.7m	19	12	Qz+Ms+Chl	73.50		18.35	3.60		1.51			3.04																	100	77
H-23 5961.7m	20	1	Fap	1.16		0.49	0.84			46.82			43.90		6.59	0.20													100	82
H-23 5961.7m	20	2	TiO_2+Chl	9.88	68.66	8.99	10.65		1.84																				100	62
H-23 5961.7m	20	3	TiO_2+Chl	15.21	51.53	14.25	15.40		3.22							0.41													100	61
H-23 5961.7m	20	4	Kln+Chl+Ab	65.29		26.09	7.55				1.07																		100	59
H-23 5961.7m	20	5	TiO_2+Chl	6.27	91.93	1.38	0.42																						100	69
H-23 5961.7m	20	6	Kln	50.29		35.25	0.46																						86	63
H-23 5961.7m	20	7	Ab	68.84		18.86					12.31																		100	81
H-23 5961.7m	20	8	Chl	35.15		20.17	22.69		6.34			0.65																	85	66
H-23 5961.7m	20	9	TiO_2+Chl	3.68	90.71	3.06	2.56																						100	68
H-23 5961.7m	20	10	Chl	30.87		18.50	27.59		6.41		1.62																		85	68
H-23 5961.7m	20	11	Ab+Chl	60.00		21.41	8.47		1.94		8.18																		100	76
H-23 5961.7m	20	12	Fap+Chl	5.07		3.93	3.22		0.78	41.11			39.16		6.73														100	80
H-23 5961.7m	21	1	TiO_2+Chl	8.00	80.17	5.31	3.05		2.44	0.38		0.34				0.34													100	54
H-23 5961.7m	21	2	TiO_2+Chl	1.52	95.68	1.15	0.91			0.48						0.27													100	50
H-23 5961.7m	21	3	TiO_2+Other	5.78	87.61	3.40	1.14			0.43	1.29					0.35													100	56
H-23 5961.7m	21	4	TiO_2+Chl	1.75	95.01	1.45	1.00			0.43						0.36													100	50
H-23 5961.7m	21	5	Ms+Chl	49.82		29.48	9.62		6.18			4.88																	100	67
H-23 5961.7m	21	6	Ms+Chl	47.45	0.28	32.42	7.29		5.65		1.02	5.85																	100	74
H-23 5961.7m	21	7	Chl	36.02	0.54	23.36	19.96		3.72			1.09				0.31													85	62
H-23 5961.7m	21	8	Chl	36.25	2.51	22.42	19.53		4.00							0.29													85	54

Appendix 2-12: SEM-BSE images and EDS mineral analyses for sample Newburn H-23 5962m

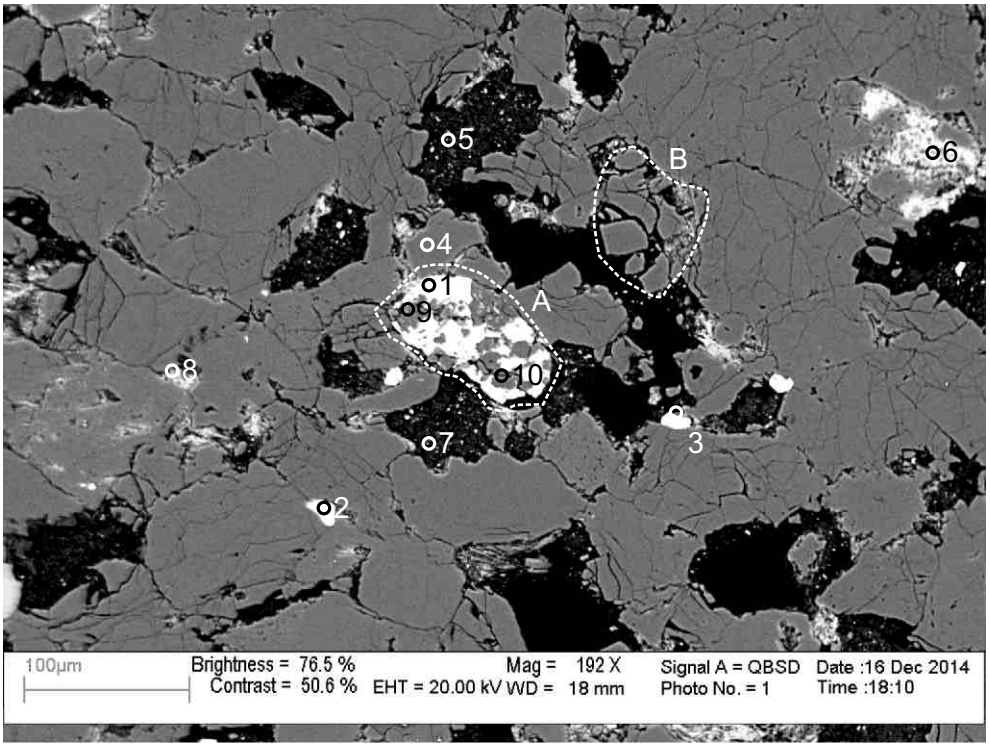

1: Titania
2: Titania
3: Chlorite+ Titania
4: Quartz
5: DrillingMud +Fluorite
6: Chlorite
7: DrillingMud +Fluorite
8: Chlorite
9: Quartz
10: Quartz+ Muscovite

Figure 2-12.1: Sample Newburn 5962m site 1 (SEM). Lithic clast (position A) composed of Quartz (9,10) muscovite (10) and titania (1). Chlorite (6) fills pore. Mechanically fractured quartz (position B) with chlorite filling pore.

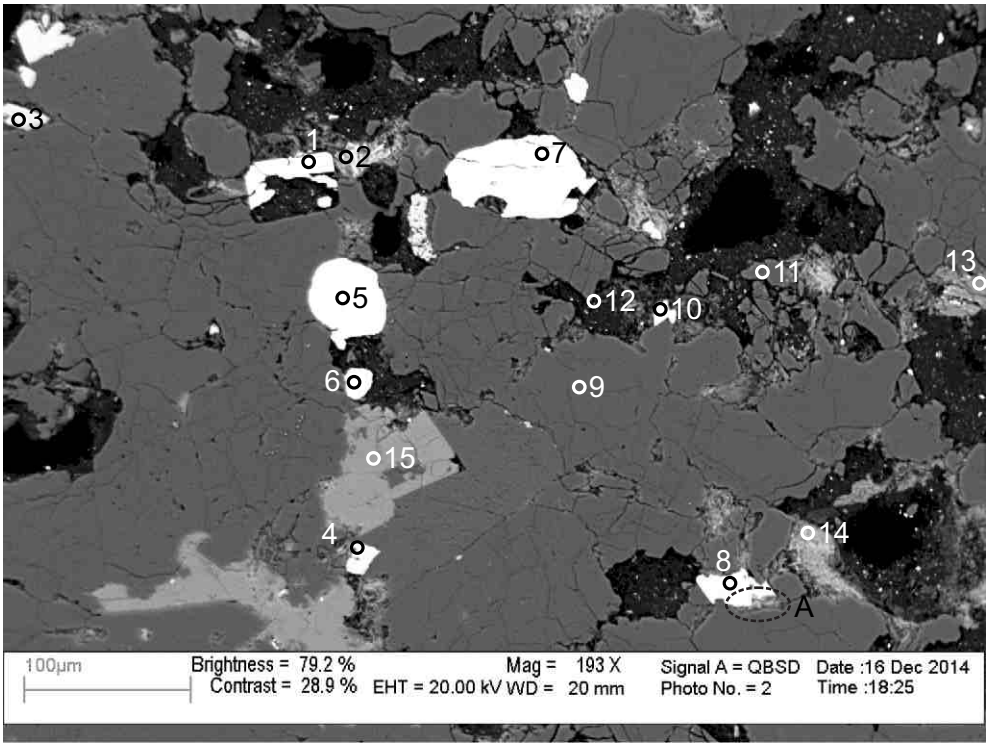

1: Zircon
2: Titania+ Chlorite
3: Titania+ Chlorite
4: Titania+ Other
5: Pyrite
6: Pyrite
7: Zircon
8: Titania
9: Quartz
10: Titania
11: Quartz
12: DrillingMud +Fluorite
13: Calcite+ Titania
14: Chlorite
15: Ankerite

Figure 2-12.2: Sample Newburn 5962m site 2 (SEM). Ankerite (15) engulfs quartz. Diagenetic zircon (1) and drilling mud fill porosity. Chlorite and illite (14) rim pore filled with drilling mud. Titania (8) engulfs chlorite filling pore (position A).

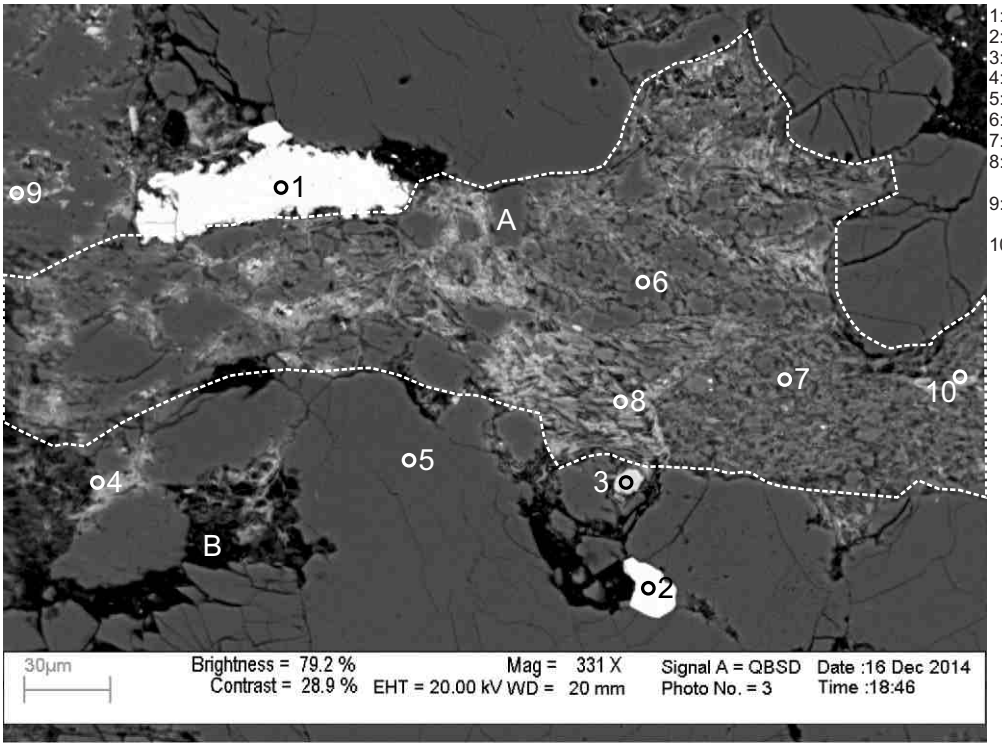

Figure 2-12.3: Sample Newburn 5962m site 3 (SEM). Schist lithic clast composed of albite (6,7), chlorite (8,10), and illite/muscovite (8,10) plastically deformed around framework quartz grains. Fluorapatite and chlorite (9) fill dissolution voids in quartz grain. Fibrous chlorite partially fills pore (position B).

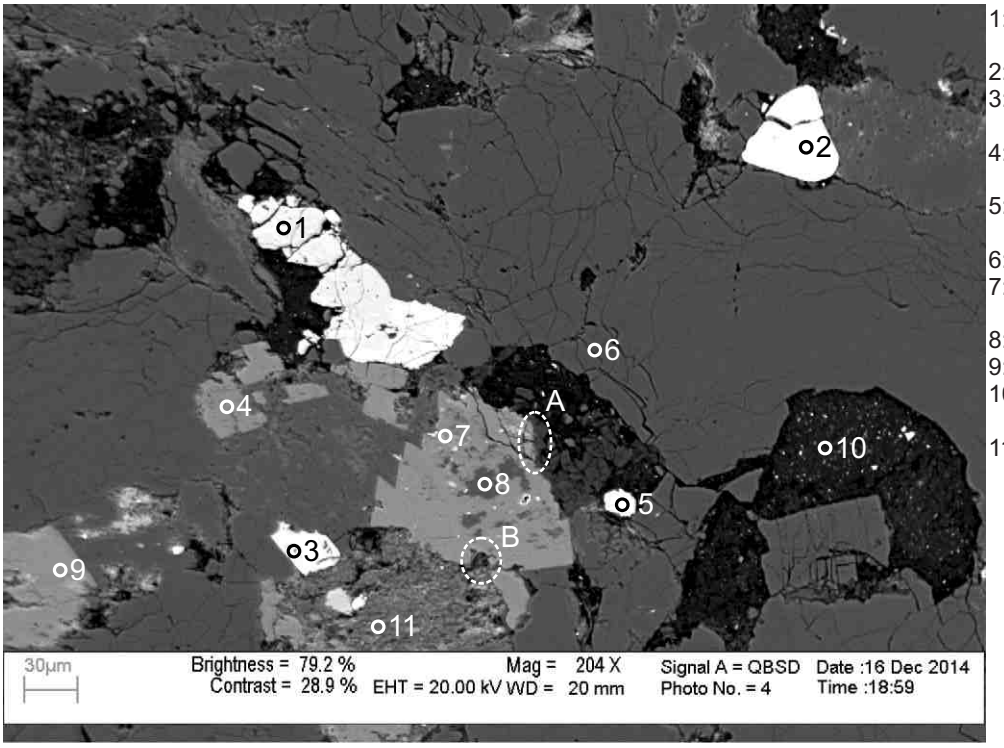

Figure 2-12.4: Sample Newburn 5962m site 4 (SEM). Fractured detrital zircon (2). Ankerite (7) engulfs albite (8). Chlorite and illite (11) are engulfed by ankerite (7,position B). Ankerite may also engulf kaolinite booklets (position A).

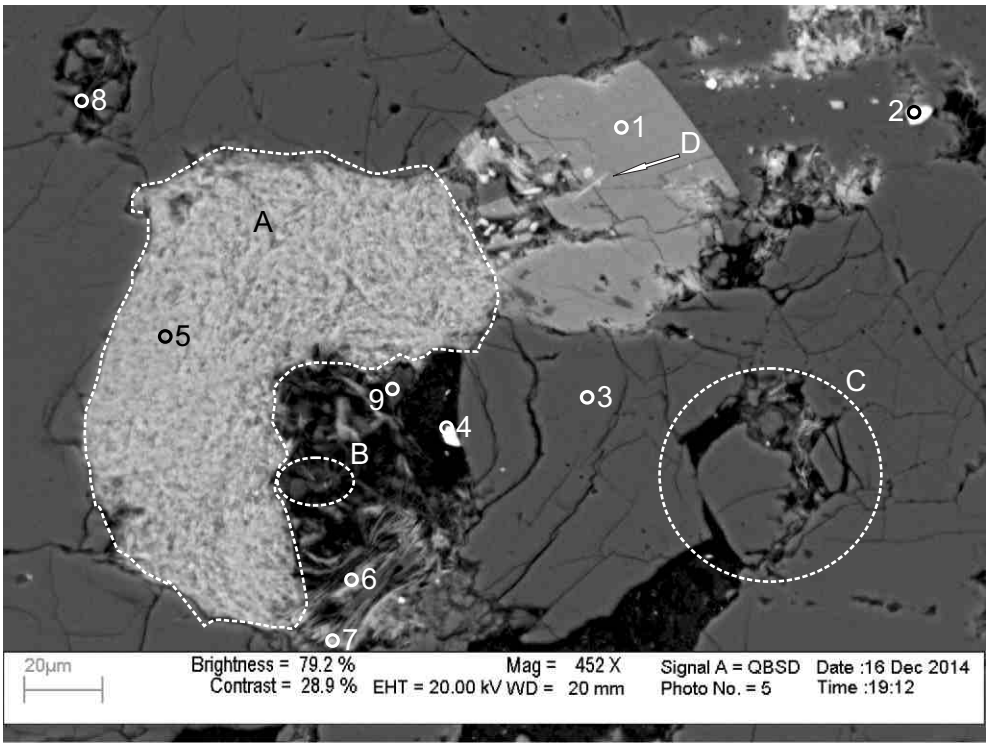

1: Ankerite
2: Titania+ Chlorite
3: Quartz
4: Fe-Hydroxide +Quartz
5: Chlorite
6: Chlorite+ Muscovite
7: Chlorite
8: Quartz+ Kaolinite+ Other
9: Kaolinite

Figure 2-12.5: Sample Newburn 5962m site 5 (SEM). Probable pumice clast (position A) which has altered to fibrous chlorite. Fe-Hydroxide (4) in void surrounded by drilling mud. Chlorite cuts kaolinite booklet (position B). Kaolinite (9) booklets occupy pore adjacent to the intraclast. Mechanically fractured quartz (position C). Fibrous chlorite fills pore generated after fracturing of quartz (position C). Fibrous chlorite cuts ankerite (1,position D).

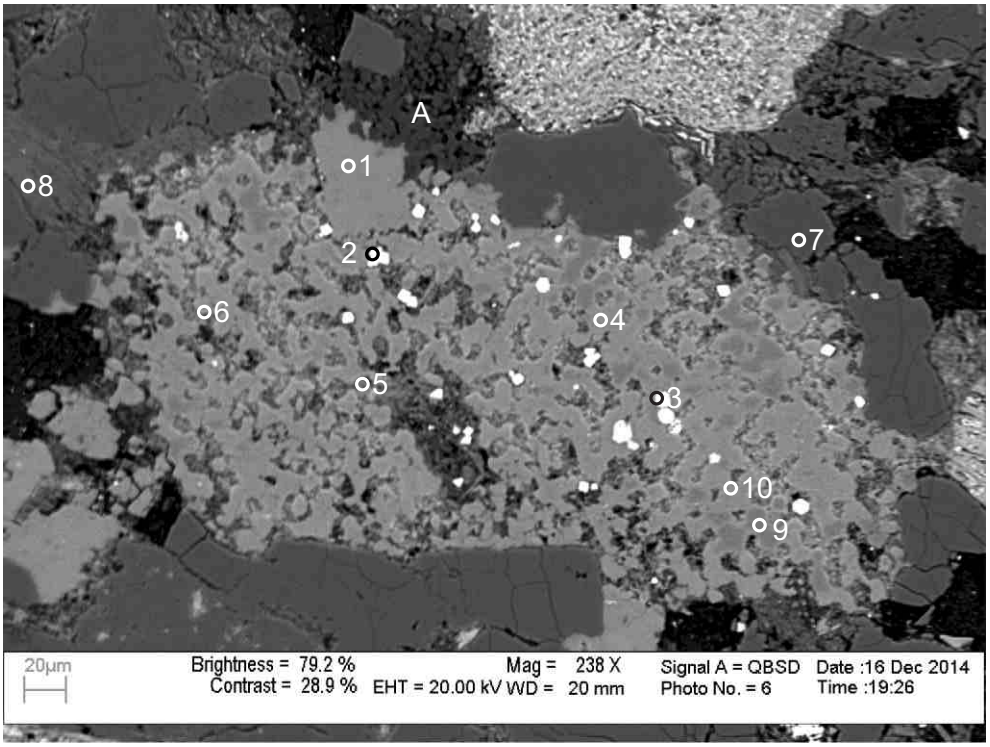

1: Fe-Calcite
2: Pyrite
3: Pyrite
4: Fe-Calcite
5: Chlorite+ Illite
6: Chlorite+ Illite
7: Quartz
8: Muscovite
9: Mg-Calcite+ Other
10: Calcite +Chlorite

Figure 2-12.6: Sample Newburn 5962m site 6 (SEM). Sparry calcite and Fe-calcite (1,4,9,10) engulfs chlorite and illite (5,6,10) as well as kaolinite (position A). Pyrite (2,3) fills dissolution in calcite. This may be an original pellet.

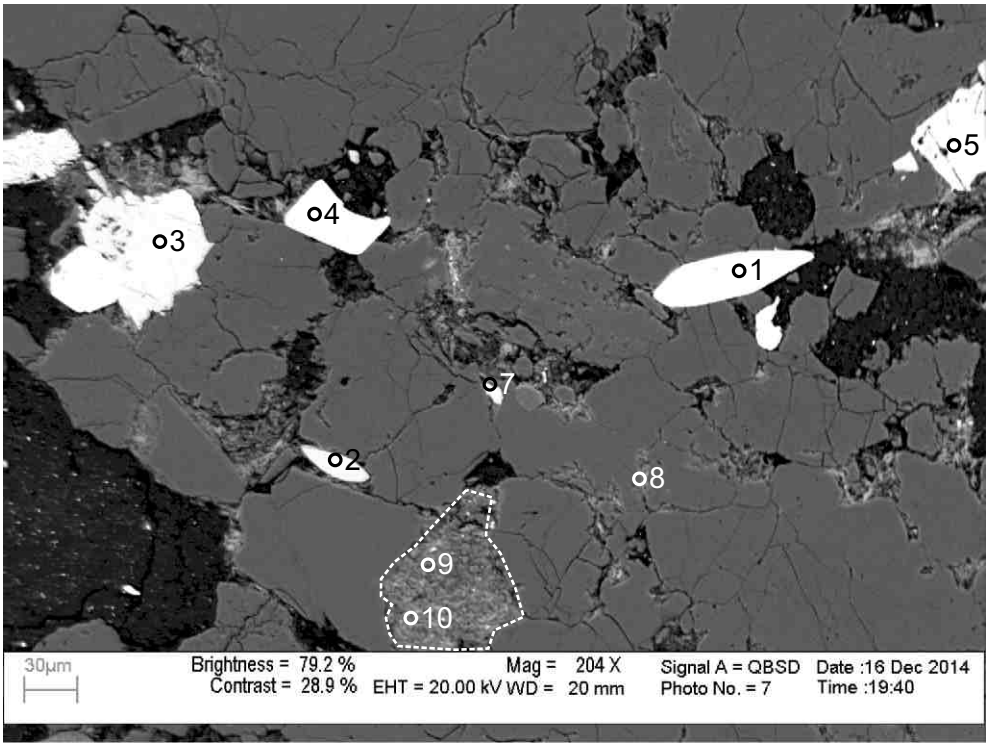

1: Zircon
2: Titania
3: Titania
4: Zircon
5: Spinel
6: Zircon
7: Titania+ Other
8: Albite
9: Quartz+Illite
10: Chlorite+ Feldspar+ Illite

Figure 2-12.7: Sample Newburn 5962m site 7 (SEM). Diagenetic zircon (4) with straight crystal outlines fills pore. Zircon (1) may be either detrital or diagenetic. Granitoid lithic clast composed of quartz and feldspar (9,10) with illite and chlorite filling dissolution voids.

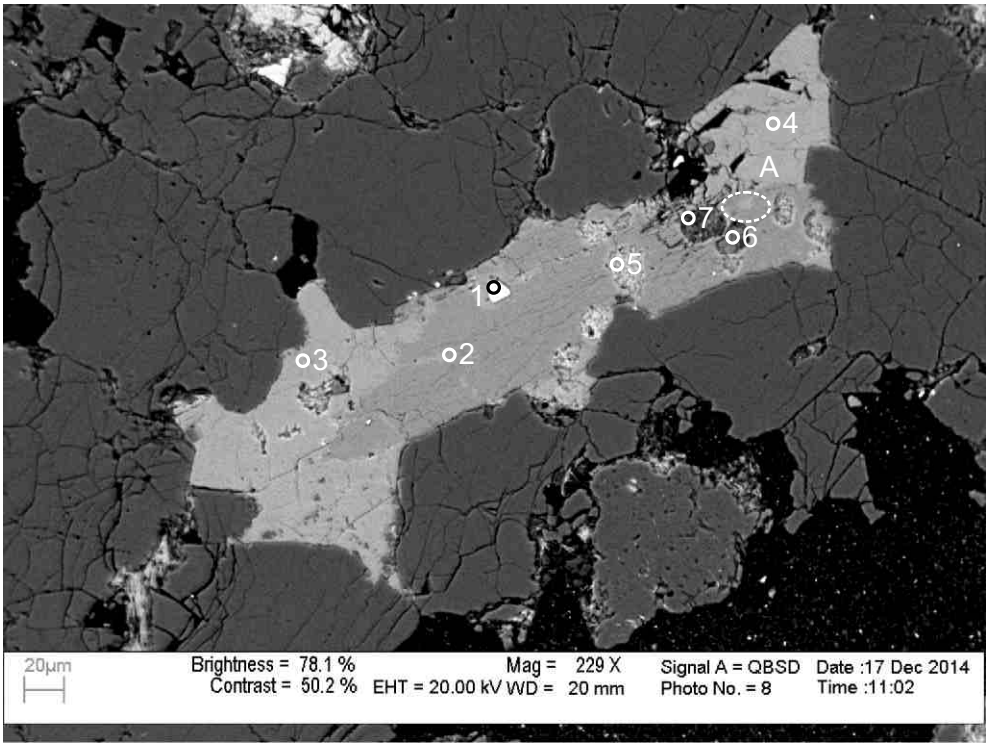

1: Pyrite
2: Fe-Calcite +Chlorite
3: Ankerite
4: Fe-Calcite
5: Chlorite
6: Chlorite+ Illite
7: Chlorite+ Illite

Figure 2-12.8: Sample Newburn 5962m site 8 (SEM). Ankerite (3) has been partially replaced by Fe-calcite (2) and contains dissolution voids. Fe-calcite surrounds dissolution voids filled with chlorite and illite (5,6,7) but relative age is unclear.

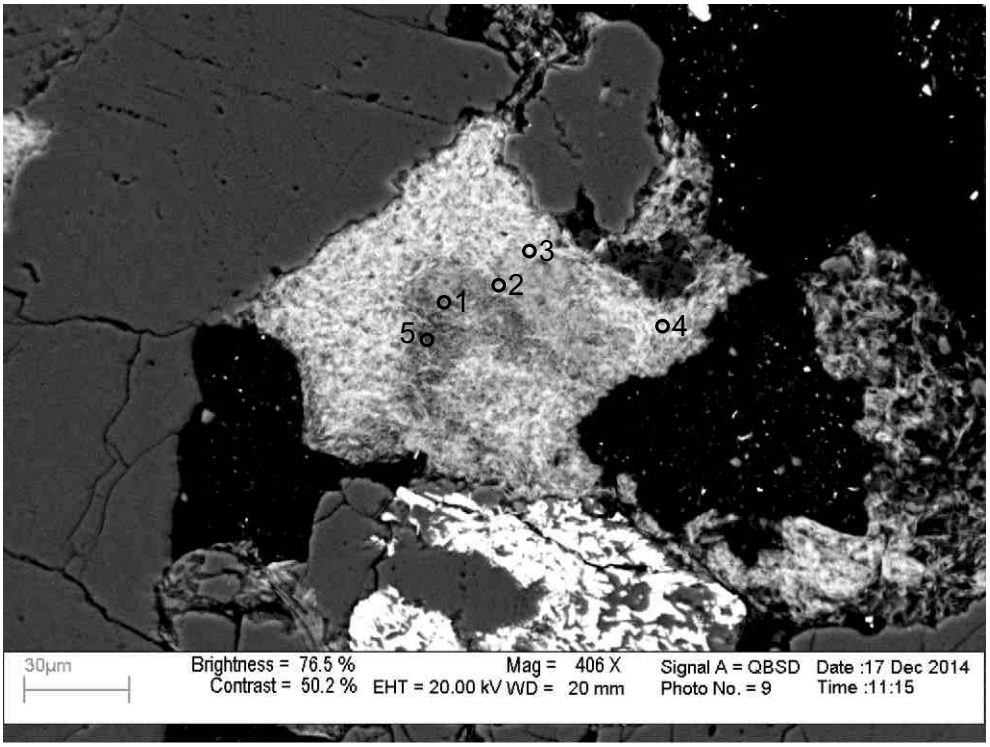

1: Chlorite
2: Chlorite
3: Chlorite
4: Chlorite
5: Chlorite

Figure 2-12.9: Sample Newburn 5962m site 9 (SEM). Compact fibrous chlorite (1-5) fills pore and is surrounded by secondary porosity filled with drilling mud.

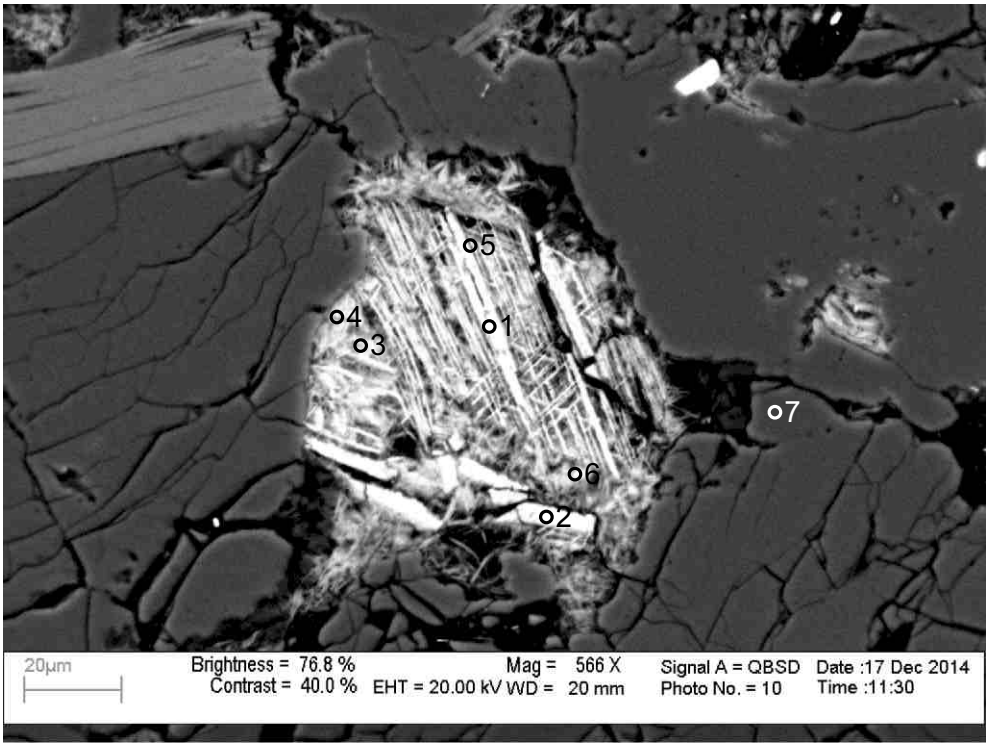

1: Titania+ Chlorite
2: Titania+ Chlorite
3: Titania+ Chlorite
4: Titania+ Chlorite
5: Titania+ Chlorite
6: Chlorite+ Titania
7: Quartz

Figure 2-12.10: Sample Newburn 5962m site 10 (SEM). Detrital Titania (1-6) with trellis structure surrounded by chlorite (1-6).

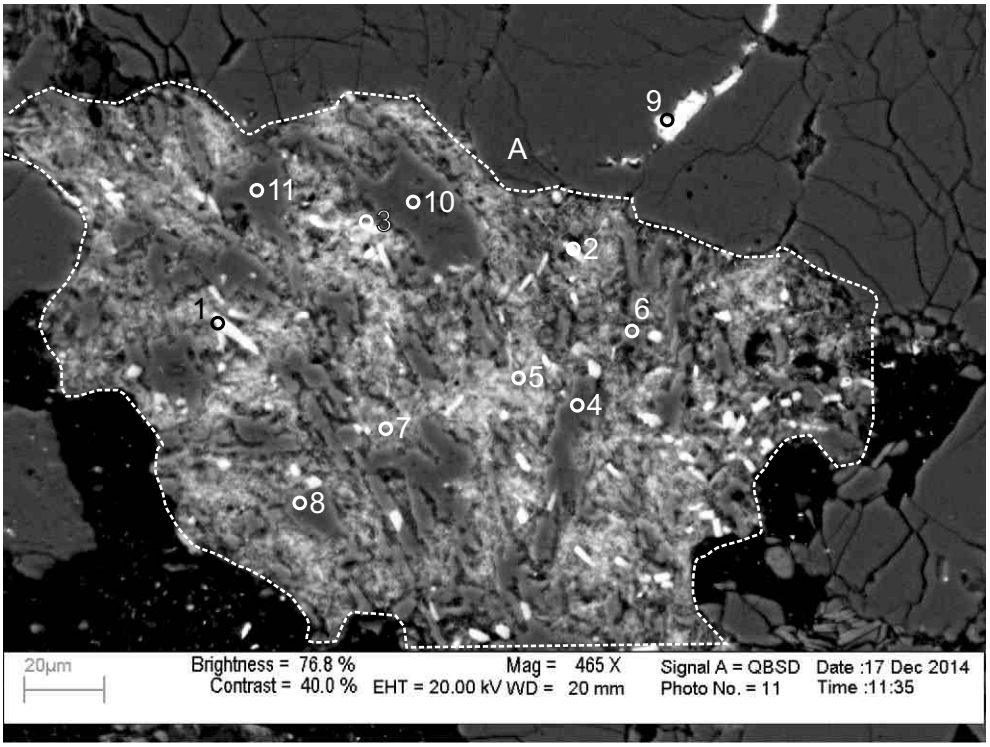

1: Fluorapatite +Chlorite
2: Fluorapatite +Chlorite
3: Chlorite+ Apatite
4: Albite
5: Albite+ Fluorapatite
6: Albite
7: Chlorite+ Albite
8: Albite
9: Kaolinite+ Monazite+ Other
10: Albite
11: Albite

Figure 2-12.11: Sample Newburn 5962m site 11 (SEM). Kaolinite (9) forms along an intergranular boundary and contains traces of monazite. Trachytic lithic clast (position A) is composed mostly of albite (4,8,10,11). Chlorite (1,2,3,7), fluorapatite (1,2,5) and apatite (3) fill dissolution voids in this clast. Apatite and fluorapatite cut chlorite (1,2,3).

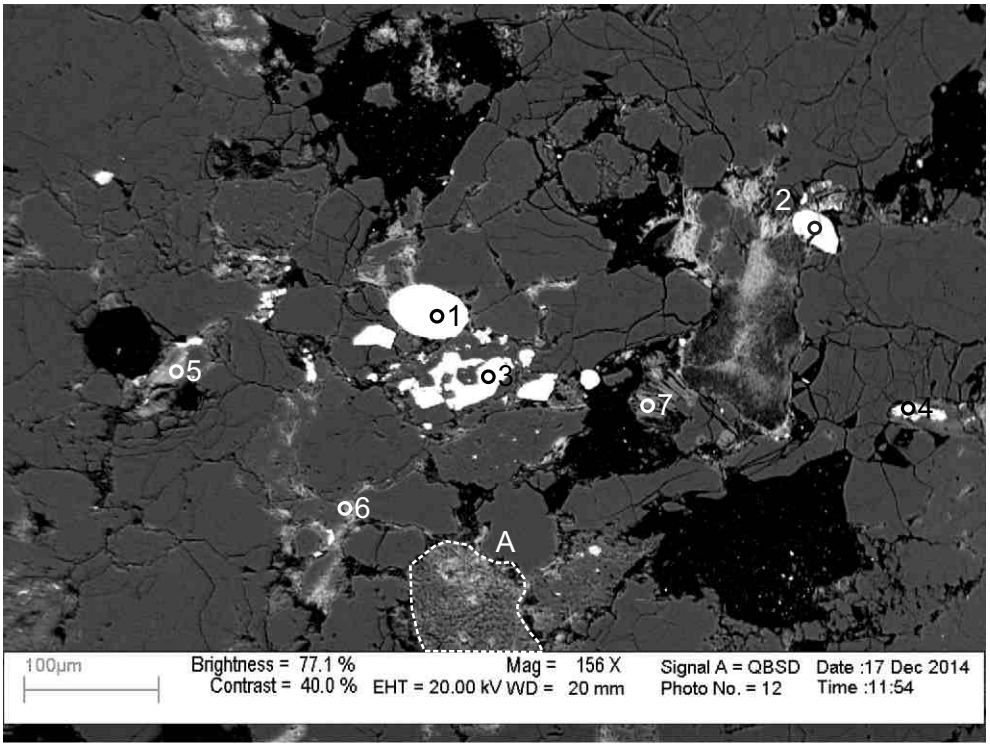

1: Zircon
2: Titania
3: Titania
4: Titania+ Chlorite
5: Chlorite
6: Chlorite
7: Muscovite+ Fluorite

Figure 2-12.12: Sample Newburn 5962m site 12 (SEM). Trachytic lithic clast (position A). Detrital titania (2) and zircon (1). Fluorite (7) forms along the cleavage planes of muscovite. Diagenetic titania (3) engulfs quartz.

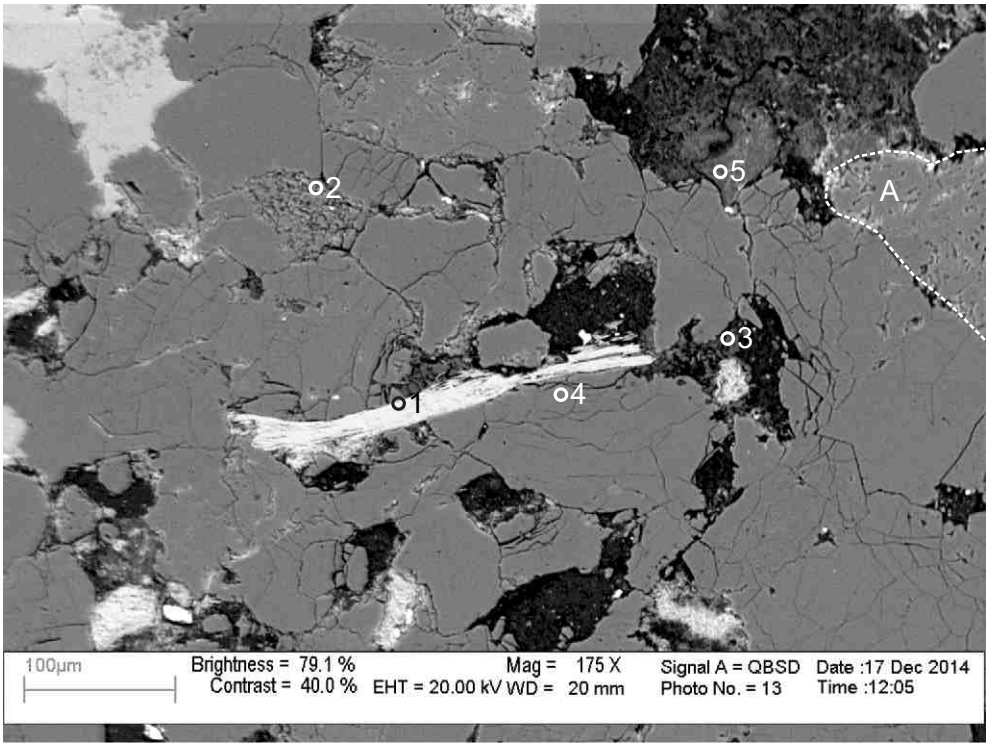

Figure 2-12.13: Sample Newburn 5962m site 13 (SEM). Chlorite replaces plastically deformed muscovite (1) and titania forms along its cleavage planes. Chlorite fills dissolution voids in trachytic lithic clast (position A).

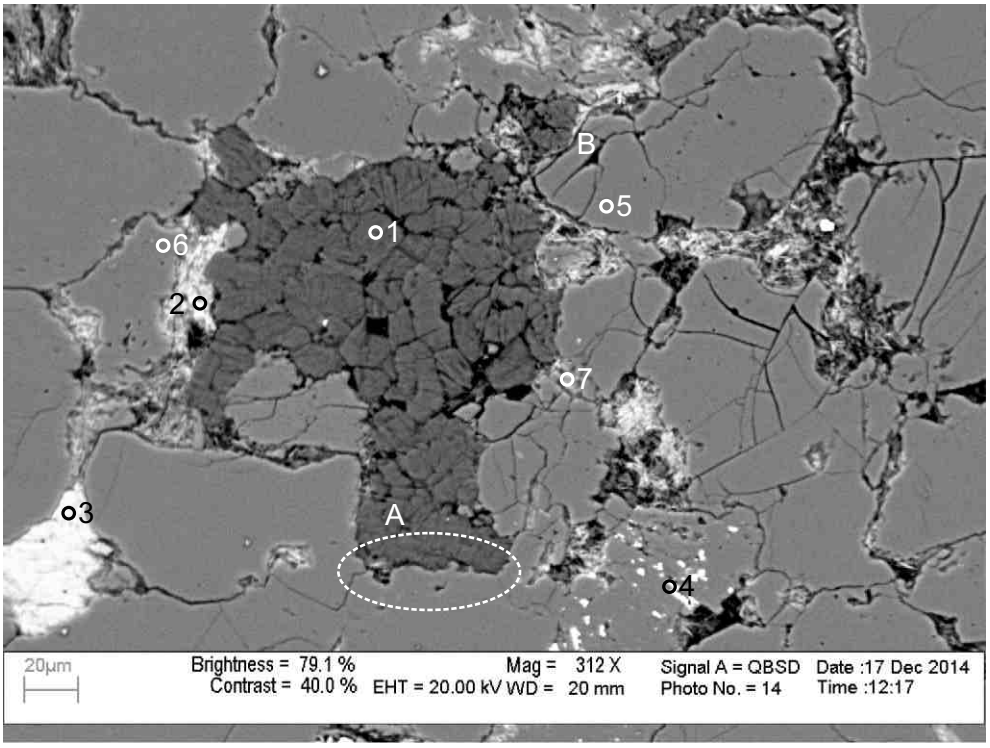

Figure 2-12.14: Sample Newburn 5962m site 14 (SEM). Kaolinite booklets (1) fill pore and engulf quartz (position A). Chlorite (2) surrounds (position B) and engulfs kaolinite filling pore.

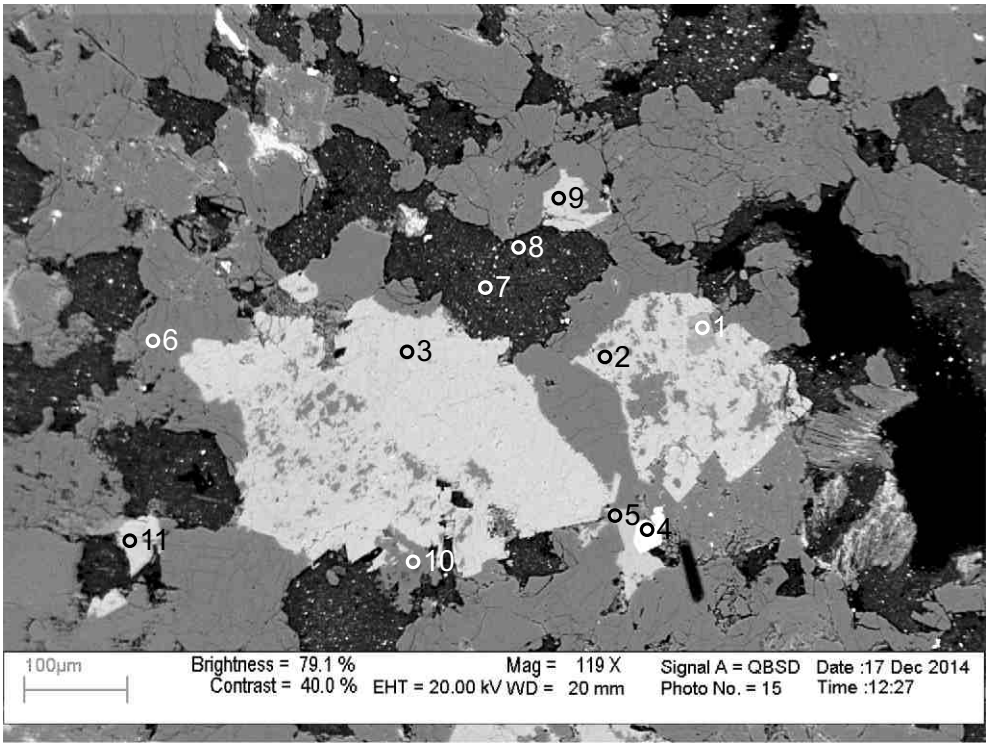

1: Muscovite
2: Ankerite
3: Ankerite
4: Titania
5: Fe-Calcite
6: Albite
7: Drilling Mud
8: Drilling Mud +Fluorite
9: Ankerite+ Albite
10: Quartz+ Kaolinite
11: Ankerite+ Kaolinite

Figure 2-12.15: Sample Newburn 5962m site 15 (SEM). Titania (4) cuts Fe-calcite (5). Ankerite (2,3) engulfs quartz (10) and muscovite (1).

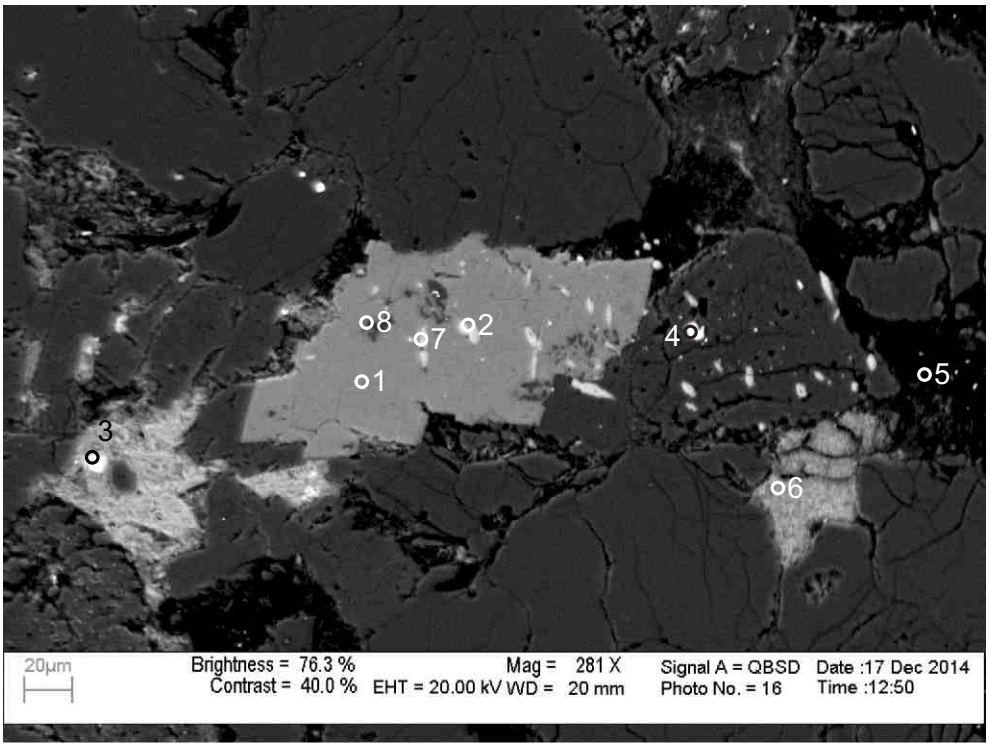

1: Ankerite
2: Fluorapatite +Other
3: Pyrite+ Chlorite
4: Pyrite+ Quartz
5: Drilling Mud +Fluorite
6: Chlorite
7: Fluorapatite +Other
8: Quartz+ Other

Figure 2-12.16: Sample Newburn 5962m site 16 (SEM). Fluorapatite (2,7) fills dissolution voids in ankerite (1). Pyrite (4) fills dissolution void in quartz.

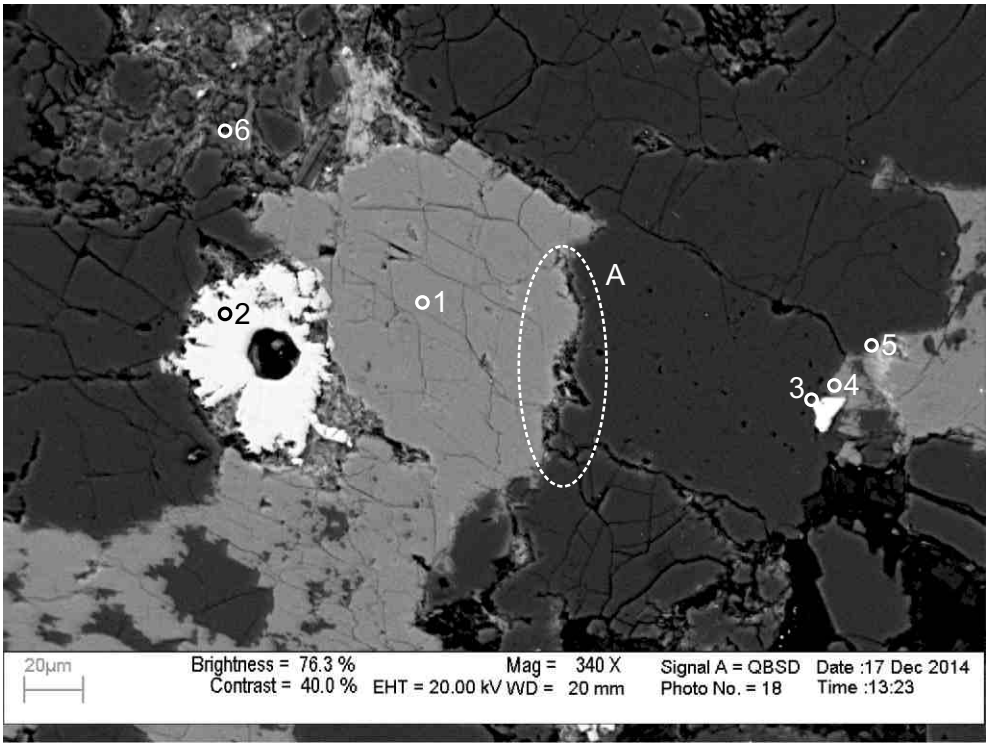

1: Ankerite
2: Siderite
3: Titania+ Other
4: Ankerite+ Quartz
5: Chlorite+ Other
6: Muscovite+ Other

Figure 2-12.17: Sample Newburn 5962m site 17 (SEM). Rosette of siderite has a central pore (2) and engulfs chlorite and ankerite (1). Chlorite (5) cuts Ankerite (4). Titania (3) cuts ankerite (4). Fibrous chlorite fills intergranular boundary between ankerite and quartz (position A).

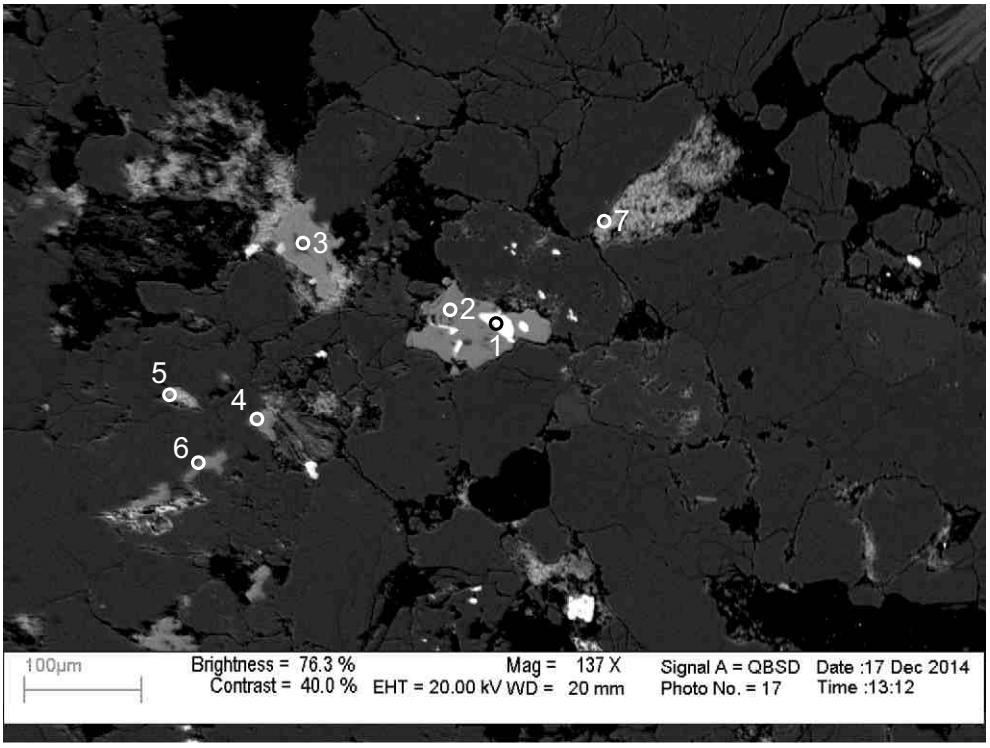

1: Barite
2: Fe-Calcite
3: Albite+ Ankerite
4: Fe-Calcite
5: Chlorite
6: Calcite+ Other
7: Chlorite

Figure 2-12.18: Sample Newburn 5962m site 18 (SEM). Barite (1) fills dissolution voids in Fe-calcite (2). Chlorite rims ankerite (3) which has engulfed albite.

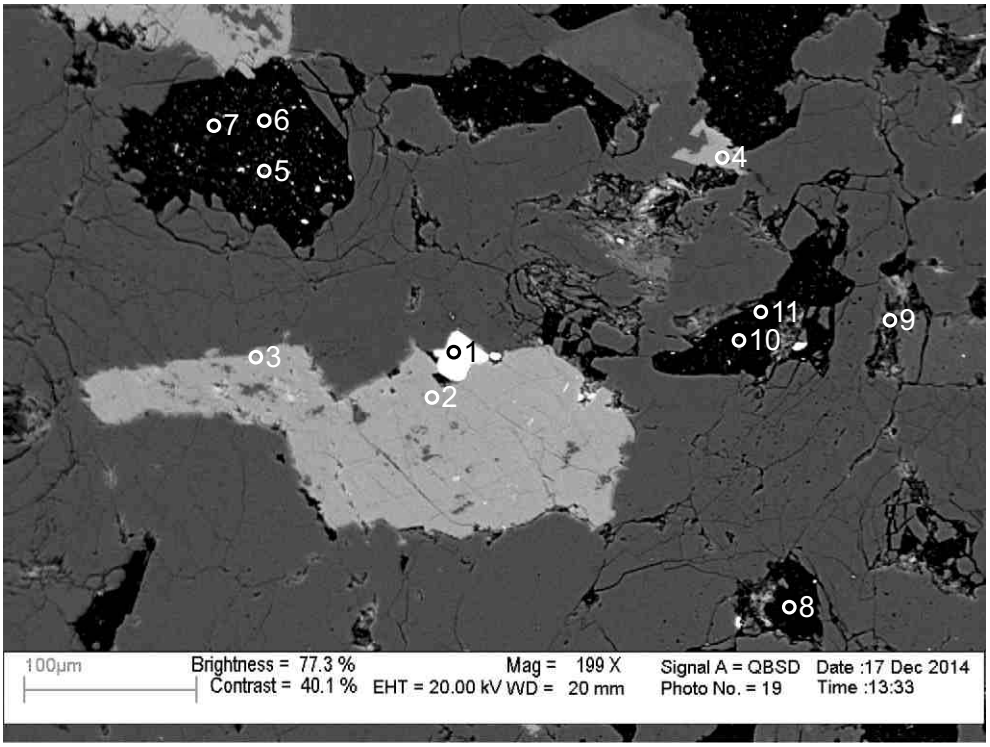

Figure 2-12.19: Sample Newburn 5962m site 19 (SEM). Titania (1) cuts ankerite (2). Ankerite (4) engulfs kaolinite filling pore. Abundant pores filled by drilling mud (5-8).

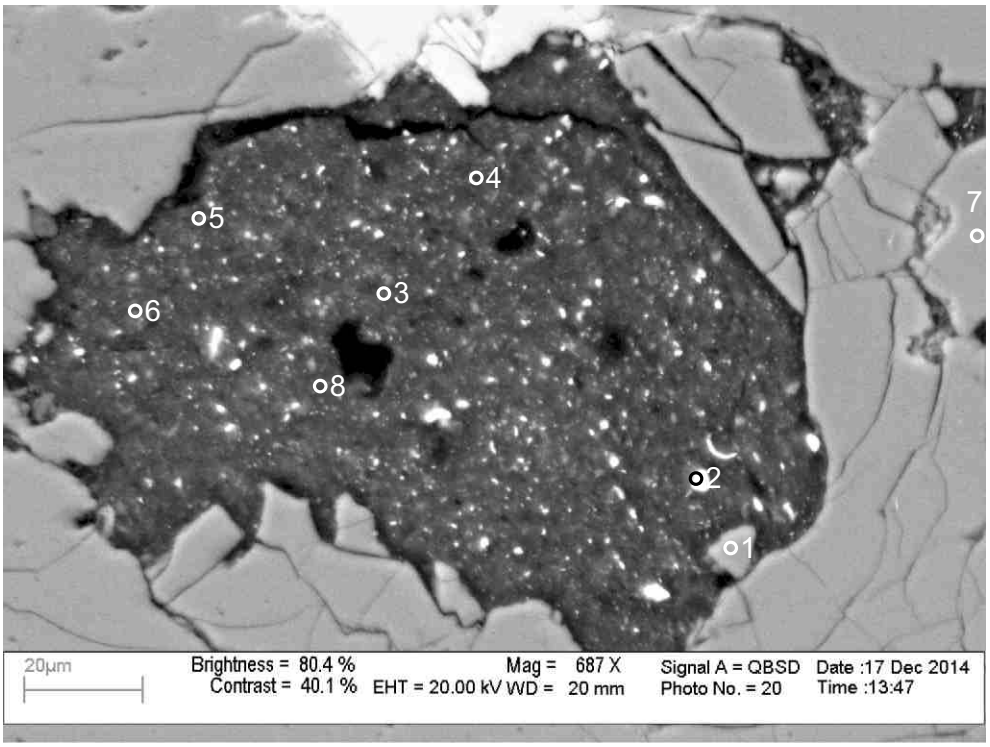

Figure 2-12.20: Sample Newburn 5962m site 20 (SEM). Drilling mud (2-6,8) fills pore.

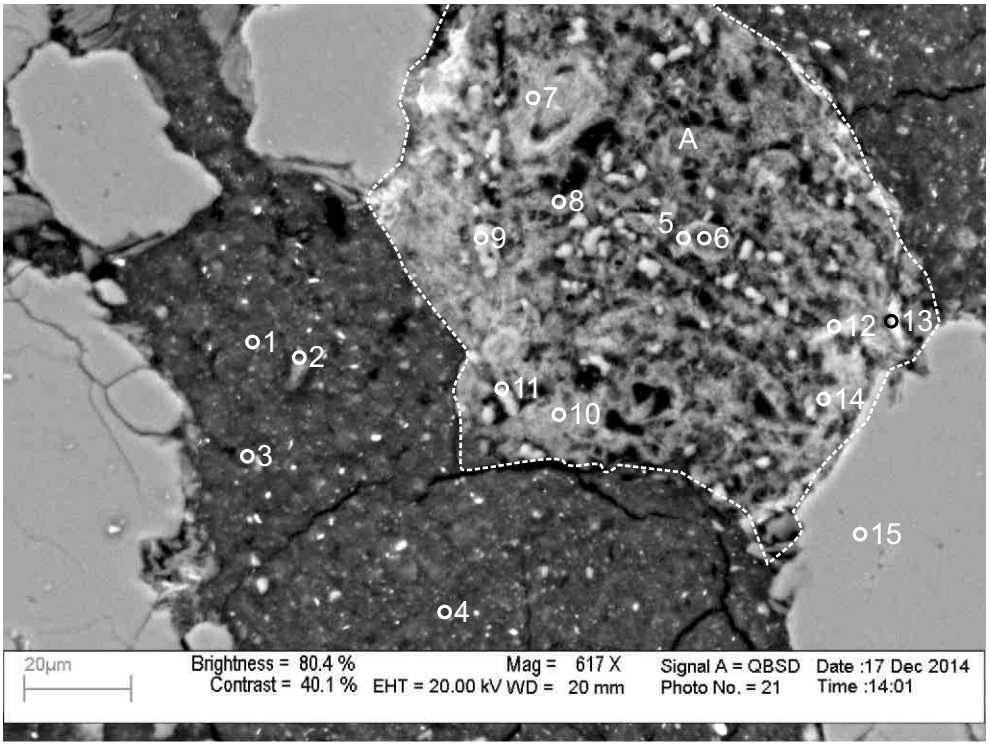

1: Drilling Mud+ Fluorite
2: Drilling Mud+ Fluorite
3: Drilling Mud+ Fluorite
4: Drilling Mud+ Fluorite
5: Muscovite+ Chlorite
6: Muscovite+ Chlorite
7: Muscovite+ Other
8: Muscovite+ Chlorite
9: Quartz
10: Muscovite+ Chlorite+ Other
11: Quartz
12: Muscovite+ Chlorite+ Other
13: Chlorite+ Muscovite
14: Muscovite+ Chlorite+ Other
15: Quartz

Figure 2-12.21: Sample Newburn 5962m site 21 (SEM). Slate clast (position A) composed of muscovite (5-8,12-14), quartz (9,11) and chlorite.

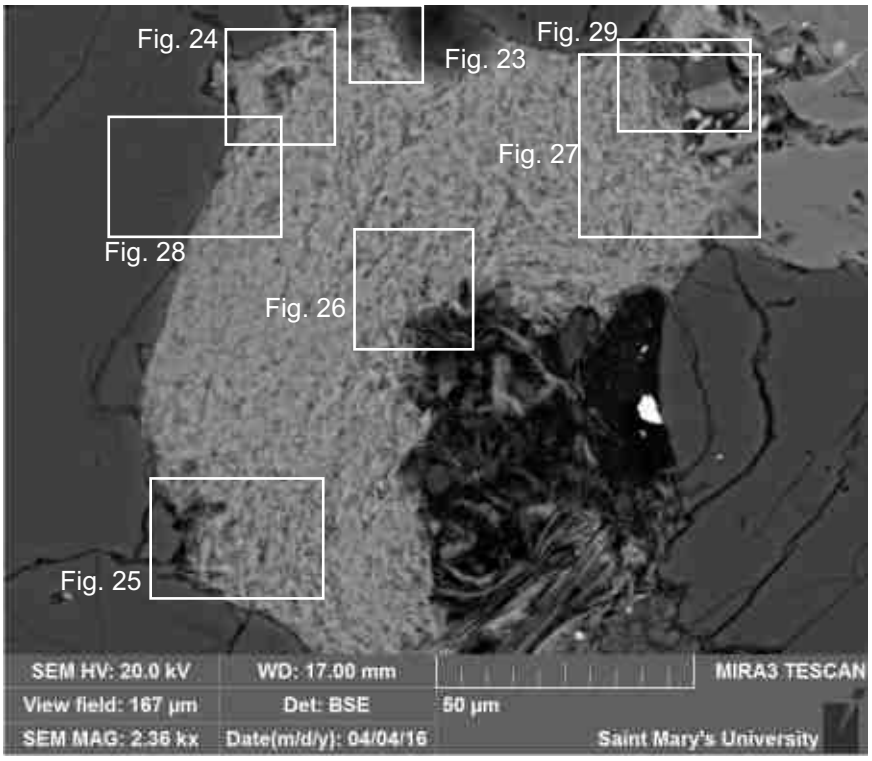

Figure 2-12.22: Sample Newburn 5962m (SEM). Second image of an altered pumice clast from site 5 (SEM) showing the location of high magnified images of the pumice clast.

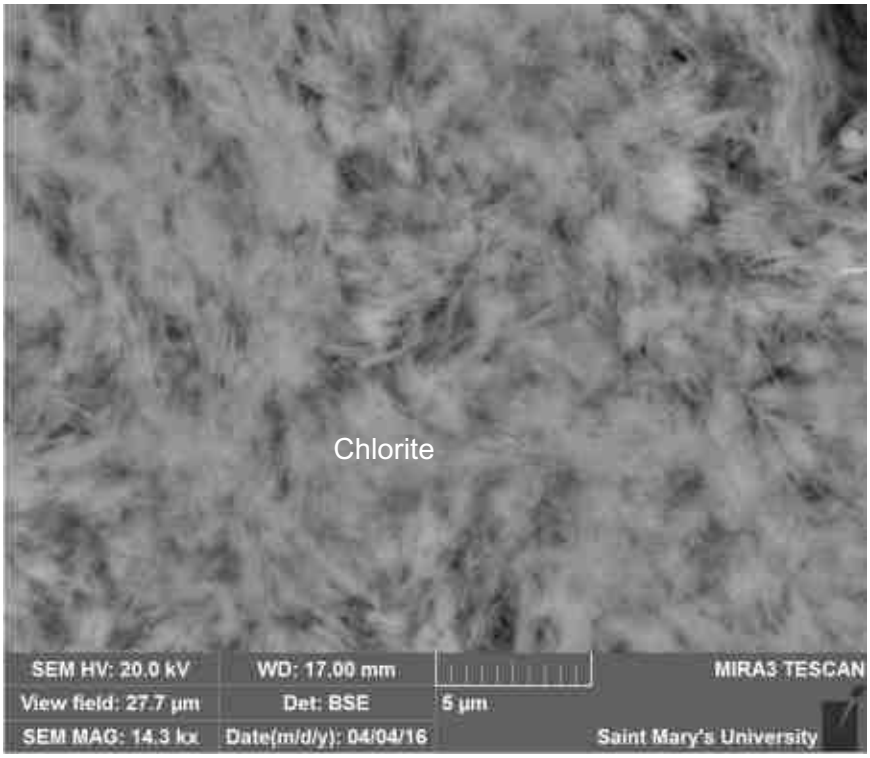

Figure 2-12.23: Sample Newburn 5962m (SEM). Fibrous chlorite appears to be from an altered pumice clast which was later compacted.

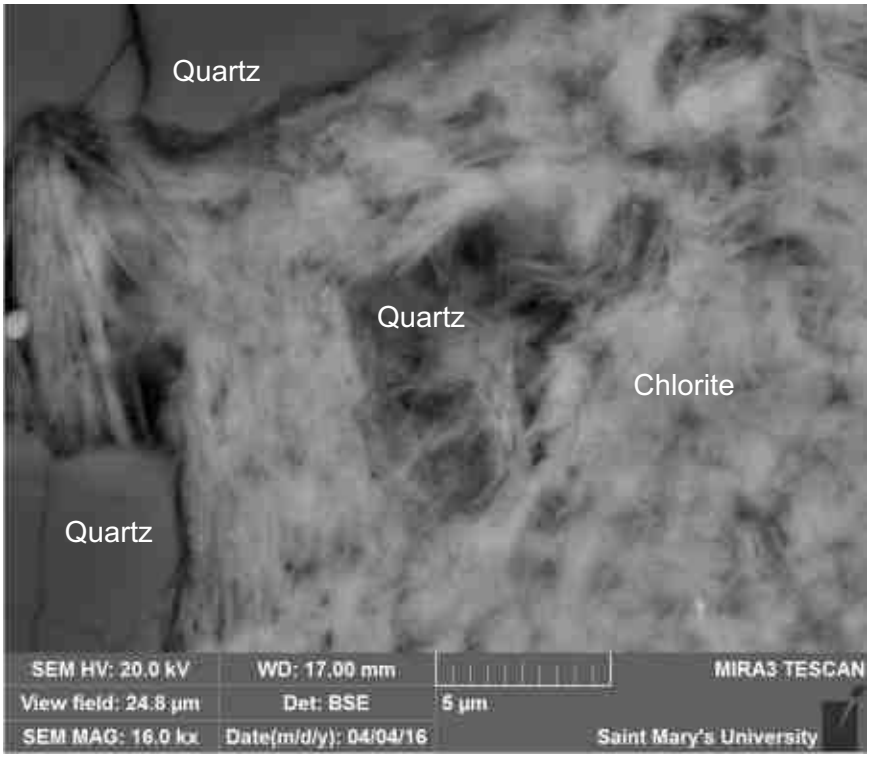

Figure 2-12.24: Sample Newburn 5962m (SEM). Fibrous chlorite from an altered pumice clast appears to engulf a fragment from the surrounding quartz grains.

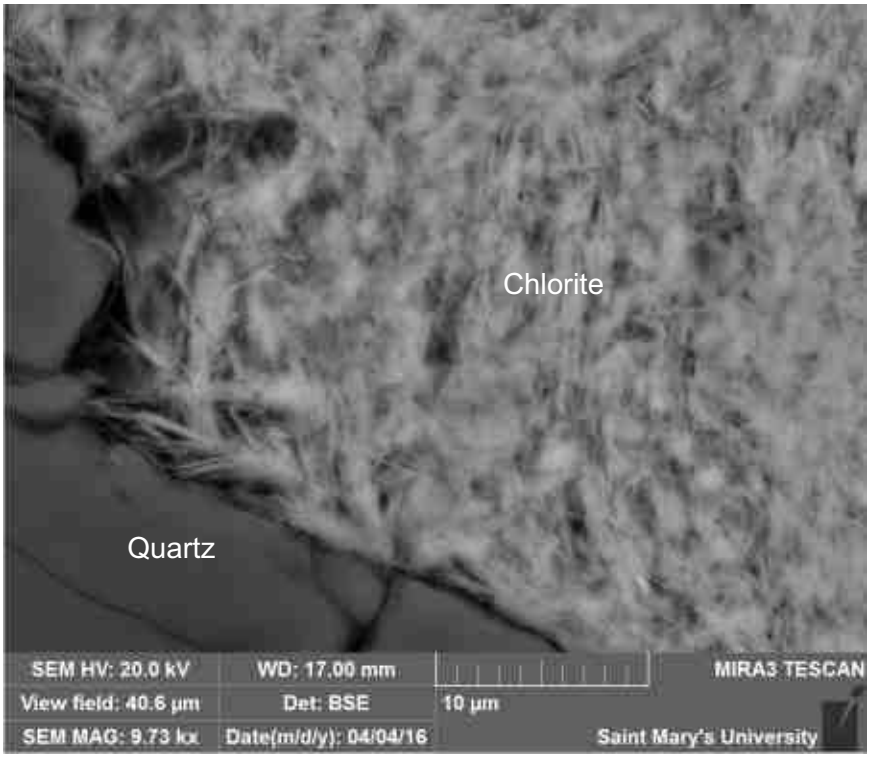

Figure 2-12.25: Sample Newburn 5962m (SEM). Fibrous chlorite appears to be from an altered pumice clast which was later compacted.

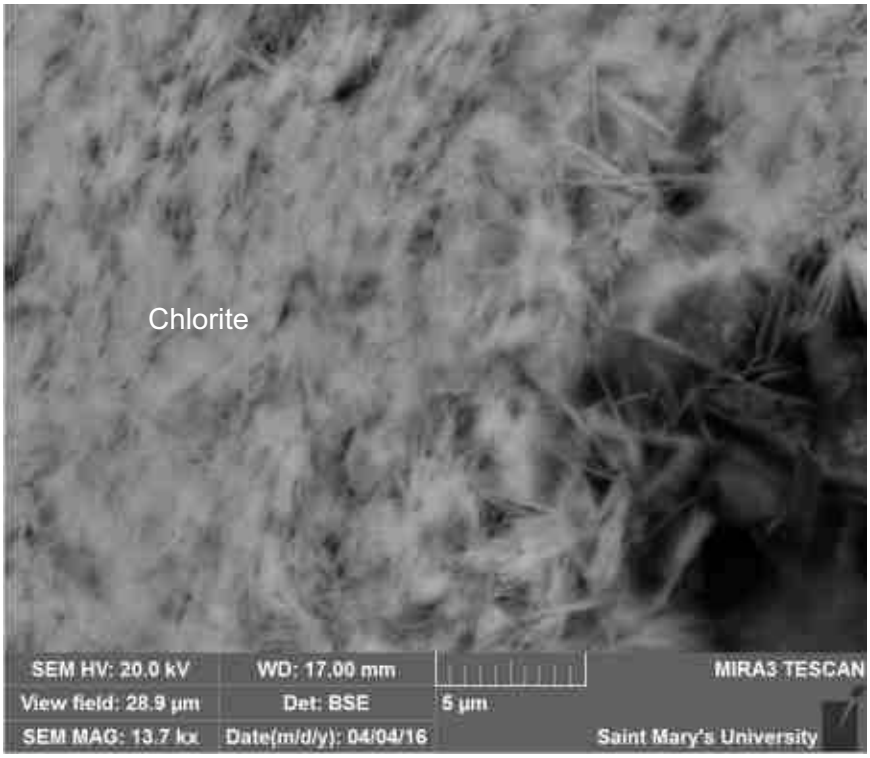

Figure 2-12.26: Sample Newburn 5962m (SEM). Fibrous chlorite probably from an altered pumice clast also forms into open porosity.

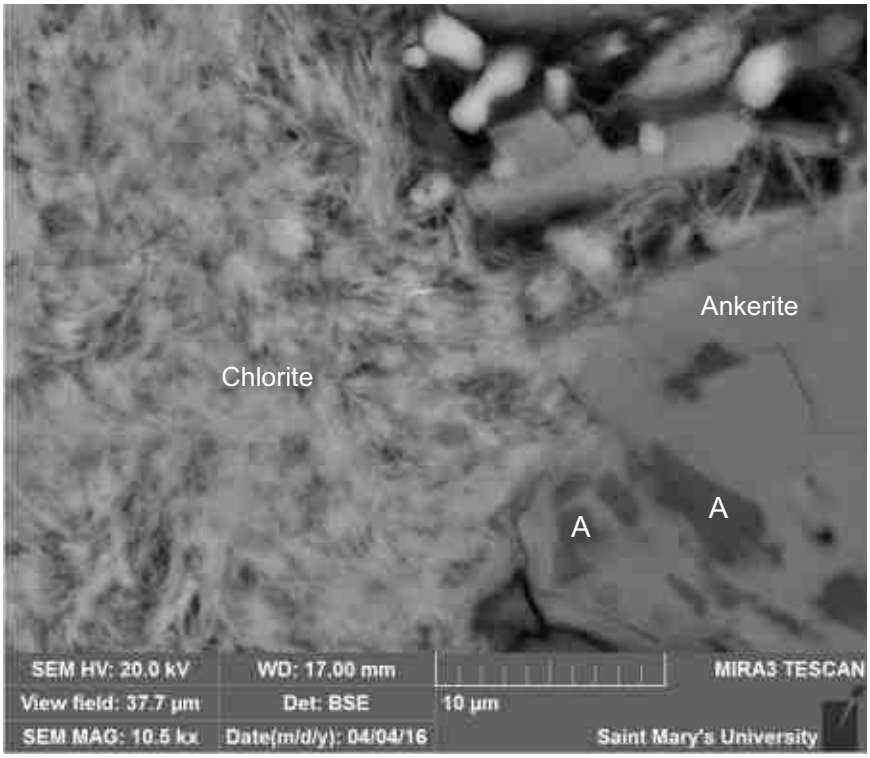

Figure 2-12.27: Sample Newburn 5962m (SEM). Fibrous chlorite surrounds ankerite. Ankerite engulfs albite (positions A).

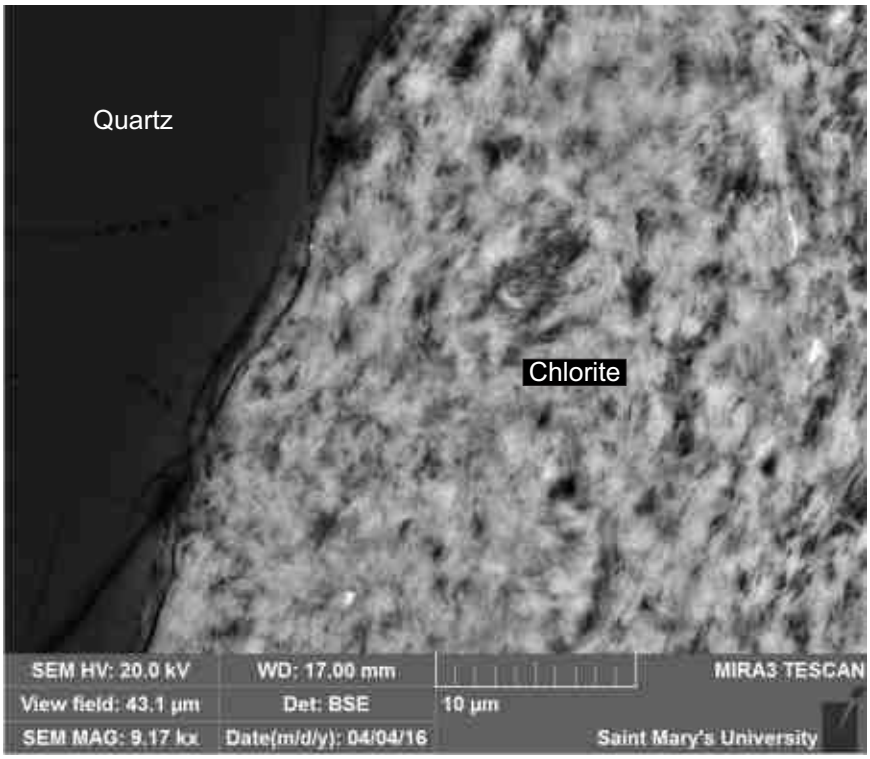

Figure 2-12.28: Sample Newburn 5962m (SEM). Fibrous chlorite appears to be from an altered pumice clast which was later compacted.

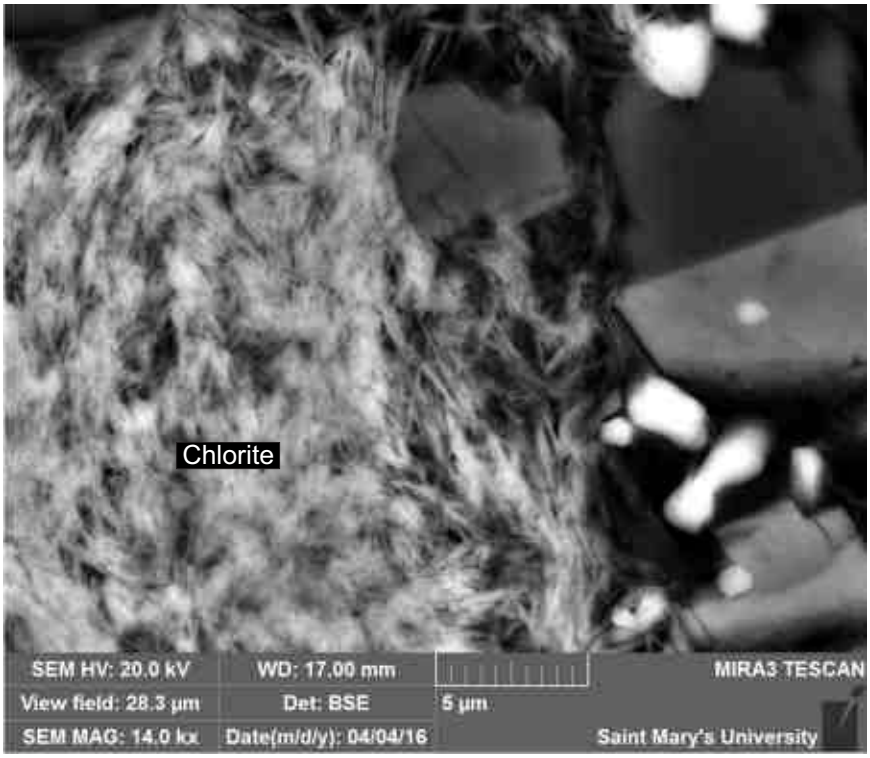

Figure 2-12.29: Sample Newburn 5962m (SEM). Fibrous chlorite probably from an altered pumice clast also forms into open porosity and surrounds framework grains.

Table 2-12: Scanning Electron Microscope chemical analyses of sample 5962m from Newburn H-23 well.

Sample	Site	Position	Mineral	SiO_2	TiO_2	Al_2O_3	FeO	MnO	MgO	CaO	Na_2O	K_2O	P_2O_5	SO_3	F	Cl	Cr_2O_3	CuO	ZnO	CdO	As_2O_3	ZrO_2	Nb_2O_5	BaO	La_2O_3	Ce_2O_3	Nd_2O_3	HfO_2	WO_3	Total	Actual Total
H-23 5962m	1	1	TiO_2	0.53	99.48																									100	107
H-23 5962m	1	2	TiO_2	0.77	96.96	1.06	1.21																							100	103
H-23 5962m	1	3	Chl+TiO_2	28.04	7.91	17.57	22.24		8.30	0.32		0.46				0.15														85	84
H-23 5962m	1	4	Qz	99.99																										100	124
H-23 5962m	1	5	DM+Fl	39.75		3.85	14.15		31.67	2.29	0.62	0.87		3.75	2.28	0.40	0.38													100	76
H-23 5962m	1	6	Chl	28.44		23.83	27.34		4.88			0.36				0.14														85	98
H-23 5962m	1	7	DM+Fl	45.42	0.40	4.27	12.41	0.31	28.29	1.41	0.47	0.99		2.20	2.98	0.49	0.37													100	73
H-23 5962m	1	8	Chl	29.77		23.09	26.26		5.07	0.20	0.36					0.25														85	84
H-23 5962m	1	9	Qz	95.28	4.70																									100	125
H-23 5962m	1	10	Qz+Ms	91.24	0.88	5.22	0.42		0.63			1.60																		100	117
H-23 5962m	2	1	Zrn	30.76																		69.23								100	84
H-23 5962m	2	2	TiO_2+Chl	3.25	76.63	2.87	5.24		0.78	0.28	0.94			7.02				3.00												100	67
H-23 5962m	2	3	TiO_2+Chl	2.31	96.53	1.15																								100	70
H-23 5962m	2	4	TiO_2+Other		97.56	1.15	1.27																							100	69
H-23 5962m	2	5	Py				27.83							72.17																100	152
H-23 5962m	2	6	Py	0.21			27.50							72.29																100	153
H-23 5962m	2	7	Zrn	31.23																		68.77								100	86
H-23 5962m	2	8	TiO_2	0.73	95.91	1.70	1.67																							100	72
H-23 5962m	2	9	Qz	99.99																										100	86
H-23 5962m	2	10	TiO_2	0.45	97.95	0.36	1.26																							100	73
H-23 5962m	2	11	Qz	99.99																										100	81
H-23 5962m	2	12	DM+Fl	44.41		4.31	10.94		31.36	1.33	0.74	0.78		2.20	3.47	0.48														100	54
H-23 5962m	2	13	Cal+TiO_2	0.71	21.25		2.88	0.96	0.80	73.42																				100	44
H-23 5962m	2	14	Chl	35.36		27.98	30.67		5.02	0.24		0.71																		100	70
H-23 5962m	2	15	Ank				15.30	0.95	10.53	29.22																				56	39
H-23 5962m	3	1	TiO_2+Other	0.86	96.63	0.77	1.72																							100	70
H-23 5962m	3	2	TiO_2		99.18		0.81																							100	71
H-23 5962m	3	3	Fap				0.27			46.22			43.90		8.32														1.30	100	88
H-23 5962m	3	4	Chl	31.82		22.08	25.48		4.71		0.70	0.20																		85	67
H-23 5962m	3	5	Qz	99.99																										100	85
H-23 5962m	3	6	Ab	66.76		19.08	2.38		0.50		10.95	0.31																		100	82
H-23 5962m	3	7	Ab	67.36		19.69	0.66			0.28	11.70	0.31																		100	88
H-23 5962m	3	8	Chl+Ilt/Ms	37.46		28.08	27.12		5.07		0.70	1.58																		100	70
H-23 5962m	3	9	Fap+Chl	25.78		15.19	14.13		2.04	17.13	2.26	0.71	19.20		3.56															100	72
H-23 5962m	3	10	Chl+Ilt/Ms	35.94	0.33	28.59	27.40		5.19	0.36	0.61	1.58																		100	71
H-23 5962m	4	1	TiO_2+Other	1.43	95.86	0.74	1.97																							100	69
H-23 5962m	4	2	Zrn	30.85																		69.15								100	89
H-23 5962m	4	3	TiO_2+Chl	2.12	94.20	1.51	1.89			0.28																				100	68
H-23 5962m	4	4	Ank+Other	4.56		2.89	25.99	1.83	16.35	47.73		0.66																		100	42
H-23 5962m	4	5	TiO_2+Chl	1.84	95.28	1.40	1.51																							100	70
H-23 5962m	4	6	Qz	99.99																										100	85
H-23 5962m	4	7	Ank+Other	8.21	9.51		20.78	2.10	15.11	44.30																				100	44
H-23 5962m	4	8	Ab	56.56		16.21	5.03	0.40	3.02	8.42	10.37																			100	76
H-23 5962m	4	9	Ank				15.79	1.11	9.56	29.54																				56	39
H-23 5962m	4	10	DM+Fl	41.12		6.71	8.68		26.38	1.30	1.74	1.28		1.95	9.54	1.02	0.29													100	58
H-23 5962m	4	11	Chl+Ilt	55.81	0.30	26.28	6.99		3.57		0.97	6.07																		100	74
H-23 5962m	5	1	Ank				15.53	1.34	9.75	29.37																				56	42
H-23 5962m	5	2	TiO_2+Chl	3.51	91.36	2.19	1.62		0.46		0.88																			100	75
H-23 5962m	5	3	Qz	99.99																										100	85
H-23 5962m	5	4	Hm+Qz	6.65			90.25		3.10																					100	62
H-23 5962m	5	5	Chl	31.19		26.55	36.47		5.12		0.69																			100	64
H-23 5962m	5	6	Chl+Ms	35.85		30.80	26.41		5.04		0.49	1.41																		100	65
H-23 5962m	5	7	Chl	33.39		25.68	19.75		3.71		0.50	1.97																		85	67
H-23 5962m	5	8	Qz+Kln+Other	66.96		23.00	5.58		0.71		0.86				2.62	0.27														100	59
H-23 5962m	5	9	Kln	48.46		35.20			0.54		0.34				1.45															86	77

Table 2-12: Scanning Electron Microscope chemical analyses of sample 5962m from Newburn H-23 well.

Sample	Site	Position	Mineral	SiO_2	TiO_2	Al_2O_3	FeO	MnO	MgO	CaO	Na_2O	K_2O	P_2O_5	SO_3	F	Cl	Cr_2O_3	CuO	ZnO	CdO	As_2O_3	ZrO_2	Nb_2O_5	BaO	La_2O_3	Ce_2O_3	Nd_2O_3	HfO_2	WO_3	Total	Actual Total
H-23 5962m	6	1	Fe-Cal				1.39	0.50		54.11																				56	38
H-23 5962m	6	2	Py	1.63		1.06	28.35		0.38	0.64	0.65			67.30																100	139
H-23 5962m	6	3	Py	0.66			28.73			1.05				69.57																100	143
H-23 5962m	6	4	Fe-Cal				1.66	0.67	0.43	53.24																				56	39
H-23 5962m	6	5	Chl+Ilt	38.31		27.17	22.68		3.90	5.22	0.73	1.71				0.28														100	63
H-23 5962m	6	6	Chl+Ilt	27.27		22.13	26.30		4.10	18.78	0.80	0.63																		100	56
H-23 5962m	6	7	Qz	99.99																										100	89
H-23 5962m	6	8	Ms	55.82		28.92	1.03		0.93		0.48	7.82																		95	76
H-23 5962m	6	9	Mg-Cal+Other				0.59		6.62	87.79				2.35	2.66															100	42
H-23 5962m	6	10	Cal+Chl	4.21		3.63	10.68	0.59	1.94	78.94																				100	42
H-23 5962m	7	1	Zrn	31.08																		68.92								100	87
H-23 5962m	7	2	TiO_2		99.22		0.78																							100	70
H-23 5962m	7	3	TiO_2		97.58		2.42																							100	69
H-23 5962m	7	4	Zrn	30.85																		69.15								100	84
H-23 5962m	7	5	Spl		0.45	23.30	28.88		5.75								41.64													100	75
H-23 5962m	7	6	Zrn	30.89																		69.11								100	86
H-23 5962m	7	7	TiO_2+Other	20.15	64.39	5.95	7.77		1.28		0.47																			100	71
H-23 5962m	7	8	Ab	64.11		19.73	5.12		0.68		10.19	0.18																		100	78
H-23 5962m	7	9	Qz+Ilt	79.15	0.27	13.26	3.07		0.95		0.34	2.98																		100	78
H-23 5962m	7	10	Chl+Feld+Ilt	53.80		23.79	14.79		2.97		2.71	1.95																		100	69
H-23 5962m	8	1	Py	0.19			27.66			1.39				70.77																100	250
H-23 5962m	8	2	Fe-Cal+Chl	1.73		1.47	7.09	0.61	1.53	87.58																				100	70
H-23 5962m	8	3	Ank				14.83	1.22	10.25	29.70																				56	72
H-23 5962m	8	4	Fe-Cal				1.00	0.50	0.38	54.11																				56	70
H-23 5962m	8	5	Chl	29.75		23.60	26.54		4.07	0.53		0.51																		85	121
H-23 5962m	8	6	Chl+Ilt	46.98		32.42	14.04		2.67	0.63	0.75	2.22				0.30														100	115
H-23 5962m	8	7	Chl+Ilt	40.30		28.65	23.05		4.01	0.87	0.78	1.88				0.48														100	95
H-23 5962m	9	1	Chl	27.90		23.87	28.40		4.84																					85	102
H-23 5962m	9	2	Chl	27.93		23.85	28.16		4.85			0.20																		85	113
H-23 5962m	9	3	Chl	28.73		24.09	27.23		4.95																					85	118
H-23 5962m	9	4	Chl	28.47	0.28	23.65	27.78		4.47			0.35																		85	120
H-23 5962m	9	5	Chl	27.78		24.75	27.36		4.90							0.20														85	96
H-23 5962m	10	1	TiO_2+Chl	1.88	92.63	1.49	1.70			0.24					2.08															100	130
H-23 5962m	10	2	TiO_2+Chl	3.49	89.11	2.87	3.64		0.70	0.22																				100	119
H-23 5962m	10	3	TiO_2+Chl	19.00	39.25	16.97	20.69		3.66		0.44																			100	124
H-23 5962m	10	4	TiO_2+Chl	20.94	40.75	15.06	19.19		3.03		1.04																			100	124
H-23 5962m	10	5	TiO_2+Chl	11.38	63.47	9.13	12.95		1.96		0.71					0.40														100	111
H-23 5962m	10	6	Chl+TiO_2	29.56	5.39	27.00	31.62		5.80		0.61																			100	125
H-23 5962m	10	7	Qz	99.99																										100	162
H-23 5962m	11	1	Fap+Chl	3.02		2.10	2.44		0.53	42.61			41.52		7.77															100	153
H-23 5962m	11	2	Fap+Chl	13.11		6.46	4.73		1.03	34.56	1.51		34.44		4.14															100	133
H-23 5962m	11	3	Chl+Ap	27.06		15.83	13.19		2.89	18.93	2.05		20.03																	100	146
H-23 5962m	11	4	Ab	68.07		18.82	0.49			0.35	12.27																			100	161
H-23 5962m	11	5	Ab+Fap	47.21		15.93	5.13		1.04	9.60	6.30		11.78		3.02															100	154
H-23 5962m	11	6	Ab	62.85		19.84	5.00		0.68	0.29	11.34																			100	157
H-23 5962m	11	7	Chl+Ab	36.75		26.55	29.73		4.88		1.79	0.30																		100	129
H-23 5962m	11	8	Ab	68.50		18.74	0.32				12.44																			100	163
H-23 5962m	11	9	Kln+Mzn+Other	25.29		29.08				1.82		0.29	27.31	3.57	0.30										3.39	6.98	1.96			100	130
H-23 5962m	11	10	Ab	68.86		18.97					12.17																			100	160
H-23 5962m	11	11	Ab	67.79		20.29	0.30				11.59																			100	159
H-23 5962m	12	1	Zrn	30.93																		68.16						0.90		100	162
H-23 5962m	12	2	TiO_2	0.45	95.53		0.98																3.05							100	141
H-23 5962m	12	3	TiO_2		99.53		0.46																							100	132
H-23 5962m	12	4	TiO_2+Chl	7.14	87.56	3.76	0.77					0.78																		100	141
H-23 5962m	12	5	Chl	36.57		18.46	17.17	0.37	12.03			0.39																		85	128

Table 2-12: Scanning Electron Microscope chemical analyses of sample 5962m from Newburn H-23 well.

Sample	Site	Position	Mineral	SiO_2	TiO_2	Al_2O_3	FeO	MnO	MgO	CaO	Na_2O	K_2O	P_2O_5	SO_3	F	Cl	Cr_2O_3	CuO	ZnO	CdO	As_2O_3	ZrO_2	Nb_2O_5	BaO	La_2O_3	Ce_2O_3	Nd_2O_3	HfO_2	WO_3	Total	Actual Total
H-23 5962m	12	6	Chl	29.91		24.25	25.23		4.31		0.76	0.54																		85	115
H-23 5962m	12	7	Ms+Fl	43.94	0.45	24.98	3.74		3.33	7.64	0.67	7.93			7.29															100	150
H-23 5962m	13	1	Chl+TiO_2	33.82	5.37	21.50	26.85		11.57		0.38	0.53																		100	129
H-23 5962m	13	2	Qz+Ms	91.58		4.44	0.41		0.38		0.28	1.32			1.56															100	150
H-23 5962m	13	3	Kln	49.00		36.69	0.31																							86	127
H-23 5962m	13	4	Qz	99.99																										100	159
H-23 5962m	13	5	Kln+Ms	54.08		32.24	2.51		0.90	0.63	1.97	4.77			2.61	0.31														100	143
H-23 5962m	14	1	Kln	47.74		36.87					0.24				1.14															86	135
H-23 5962m	14	2	Chl	29.21		24.38	25.76		4.16	0.71	0.60	0.19																		85	116
H-23 5962m	14	3	Chl	26.40		22.57	29.90		4.43	0.26	1.44																			85	121
H-23 5962m	14	4	Ab	51.49		11.53	1.14			0.39	7.73											27.70								100	139
H-23 5962m	14	5	Qz	99.99																										100	164
H-23 5962m	14	6	Qz	99.99																										100	156
H-23 5962m	14	7	Qz+Chl	75.30	0.30	10.92	10.82		1.84		0.39	0.42																		100	144
H-23 5962m	15	1	Ms	47.65	0.31	30.68	4.52		1.27			10.56																		95	153
H-23 5962m	15	2	Ank				15.10	1.13	10.74	29.04																				56	79
H-23 5962m	15	3	Ank				13.91	1.35	10.32	30.43																				56	76
H-23 5962m	15	4	TiO_2	0.53	96.75	0.72	1.72			0.28																				100	138
H-23 5962m	15	5	Fe-Cal				2.09	0.43	0.73	52.75																				56	72
H-23 5962m	15	6	Ab	68.05		18.76	0.87				12.31																			100	156
H-23 5962m	15	7	DM	45.48		4.42	16.85		28.80	1.39		0.58		1.52		0.45	0.53													100	98
H-23 5962m	15	8	DM+Fl	42.63		4.69	17.11		29.45	1.02		0.78		2.05	1.58	0.38	0.31													100	101
H-23 5962m	15	9	Ank+Ab	7.74		2.27	24.43	1.64	16.17	46.16	1.60																			100	86
H-23 5962m	15	10	Qz+Kln	85.05		14.93																								100	147
H-23 5962m	15	11	Ank+Kln	6.16		4.27	24.48	1.82	17.36	44.93		0.95																		100	78
H-23 5962m	16	1	Ank				15.32	1.13	10.37	29.19																				56	75
H-23 5962m	16	2	Fap+Other	1.11	2.77	0.93	6.30		3.57	46.01			34.37		4.97															100	130
H-23 5962m	16	3	Py+Chl	2.95		2.55	27.93		0.63		0.34			65.62																100	235
H-23 5962m	16	4	Py+Qz	14.29			22.93				0.40			61.53							0.86									100	257
H-23 5962m	16	5	DM+Fl	47.60	0.42	4.42	10.00		28.40	1.92	0.71	0.88		1.85	3.10	0.72														100	84
H-23 5962m	16	6	Chl	27.77		23.53	28.50		4.35		0.37	0.30				0.19														85	122
H-23 5962m	16	7	Fap+Other	0.71		0.43	6.83	0.36	3.88	48.17			33.87		5.74															100	123
H-23 5962m	16	8	Qz+Other	88.39		0.53	3.01		1.38	5.44	0.30			0.95																100	142
H-23 5962m	17	1	Ank				15.30	1.16	10.20	29.34																				56	78
H-23 5962m	17	2	Sd				53.11	0.84		1.15			0.90																	56	72
H-23 5962m	17	3	TiO_2+Other	4.11	91.59	2.65	1.38			0.28																				100	133
H-23 5962m	17	4	Ank+Qz	12.15			23.76	1.65	15.11	47.33																				100	83
H-23 5962m	17	5	Chl+Other	32.28		26.40	35.56		4.96		0.50	0.29																		100	121
H-23 5962m	17	6	Ms+Other	55.02	0.53	28.72	4.95		2.50		0.84	7.43																		100	147
H-23 5962m	18	1	Brt							0.67				37.78										61.55						100	147
H-23 5962m	18	2	Fe-Cal				1.93	0.80	0.80	52.47																				56	67
H-23 5962m	18	3	Ab+Ank	32.26		9.30	14.85	1.10	8.77	27.51	6.23																			100	103
H-23 5962m	18	4	Fe-Cal				1.92	0.59	0.72	52.77																				56	68
H-23 5962m	18	5	Chl	29.82		24.46	24.95		4.69		1.08																			85	117
H-23 5962m	18	6	Cal+Other	4.36		1.00	2.34	0.97	1.16	89.42	0.75																			100	69
H-23 5962m	18	7	Chl	29.85		23.63	25.81		4.09	0.59	0.62	0.42																		85	124
H-23 5962m	19	1	TiO_2		98.58		1.42																							100	129
H-23 5962m	19	2	Ank				15.06	1.11	10.51	29.32																				56	75
H-23 5962m	19	3	Ank+Kln	2.63		2.00	25.32	2.30	19.47	48.29																				100	77
H-23 5962m	19	4	Ank+Kln	7.66		6.50	25.58	1.63	14.69	43.96																				100	85
H-23 5962m	19	5	DM+Fl	40.47	0.38	4.16	13.01		32.35	2.98		0.87		2.35	2.97	0.47														100	88
H-23 5962m	19	6	DM+Fl	44.11		4.69	12.11		28.64	1.32	0.63	0.88		2.72	4.24	0.65														100	80
H-23 5962m	19	7	DM+Fl	47.19	0.50	5.56	9.02		28.80	1.29	1.33	0.88		2.17	2.80	0.47														100	90
H-23 5962m	19	8	DM+Fl	49.59	0.47	4.89	7.56		26.33	2.55	1.93	0.95		0.67	4.49	0.58														100	86
H-23 5962m	19	9	Kln	48.69		36.18	0.75				0.38																			86	122
H-23 5962m	19	10	DM+Fl	49.22	0.47	3.99	9.20		26.78	2.71	1.46	0.89			4.62	0.65														100	80

Table 2-12: Scanning Electron Microscope chemical analyses of sample 5962m from Newburn H-23 well.

Sample	Site	Position	Mineral	SiO_2	TiO_2	Al_2O_3	FeO	MnO	MgO	CaO	Na_2O	K_2O	P_2O_5	SO_3	F	Cl	Cr_2O_3	CuO	ZnO	CdO	As_2O_3	ZrO_2	Nb_2O_5	BaO	La_2O_3	Ce_2O_3	Nd_2O_3	HfO_2	WO_3	Total	Actual Total
H-23 5962m	19	11	DM+Fl	13.84	5.55	1.91	1.53		12.40	5.43				23.05	6.96	2.17			3.01	24.15											100	33
H-23 5962m	20	1	Qz	95.28			0.73		3.85			0.12																		100	146
H-23 5962m	20	2	DM+Hem	26.23		3.14	45.81		21.80	0.62	0.71	0.48		0.92		0.28														100	109
H-23 5962m	20	3	DM+Fl	47.43		5.63	8.79		30.39	1.22	0.86	0.76		1.67	2.75	0.50														100	90
H-23 5962m	20	4	DM	48.73		5.23	9.24		30.89	1.57		1.06		2.55		0.72														100	83
H-23 5962m	20	5	DM+Fl	45.46		4.42	12.29		29.45	1.13		0.90		1.87	4.02	0.48														100	87
H-23 5962m	20	6	DM+Fl	41.33		6.25	15.97		26.78	1.25	0.53	1.13		3.92	2.33	0.54														100	88
H-23 5962m	20	7	Qz	99.99																										100	155
H-23 5962m	20	8	DM	49.29		4.44	10.30		30.88	1.33	0.50	0.79		1.92		0.53														100	84
H-23 5962m	21	1	DM+Fl	48.32	0.55	3.80	8.37		27.33	4.30	0.98	0.98			4.96	0.44														100	78
H-23 5962m	21	2	DM+Fl	39.45	3.07	4.63	5.80		29.33	4.39	1.62	0.78		0.90	9.55	0.45														100	91
H-23 5962m	21	3	DM+Fl	49.07	0.45	3.36	7.69		31.44	2.35	0.51	0.77			3.92	0.45														100	87
H-23 5962m	21	4	DM+Fl	52.84	0.42	3.61	8.94		25.45	2.74	0.61	0.87		0.82	3.25	0.45														100	82
H-23 5962m	21	5	Ms+Chl	59.68		26.34	3.83		1.39		0.43	8.13				0.20														100	121
H-23 5962m	21	6	Ms+Chl	56.26	0.52	27.53	3.22		1.46		0.49	8.26				0.43						1.86								100	108
H-23 5962m	21	7	Ms+Other	54.06	0.32	29.08	2.47		1.29		0.44	8.46			3.88															100	128
H-23 5962m	21	8	Ms+Chl	59.23	0.50	26.98	3.06		1.38		0.58	7.91				0.34														100	109
H-23 5962m	21	9	Qz	98.08		1.66						0.26																		100	145
H-23 5962m	21	10	Ms+Chl+Other	56.03	0.42	28.31	2.86		1.66		0.42	8.08			1.97	0.28														100	114
H-23 5962m	21	11	Qz	96.48		2.95						0.57																		100	136
H-23 5962m	21	12	Ms+Chl+Other	55.70	0.30	28.06	2.80		1.49		0.58	7.90			2.96	0.20														100	136
H-23 5962m	21	13	Chl+Ms	39.85		30.61	22.59		4.79		0.43	1.49				0.24														100	127
H-23 5962m	21	14	Ms+Chl+Other	56.54		28.04	2.88		1.46		0.51	7.59			2.78	0.21														100	140
H-23 5962m	21	15	Qz	99.99																										100	158

DM = Drilling Mud

Appendix 3: SEM-BSE images, and Mineral Geochemical Analyses from Electron Microprobe (EM) Wavelength Dispersive Spectrometer (WDS).

Appendix 3-1: Representative SEM-BSE images and mineral analyses from EM-WDS of sample Newburn H-23 4353.5m.

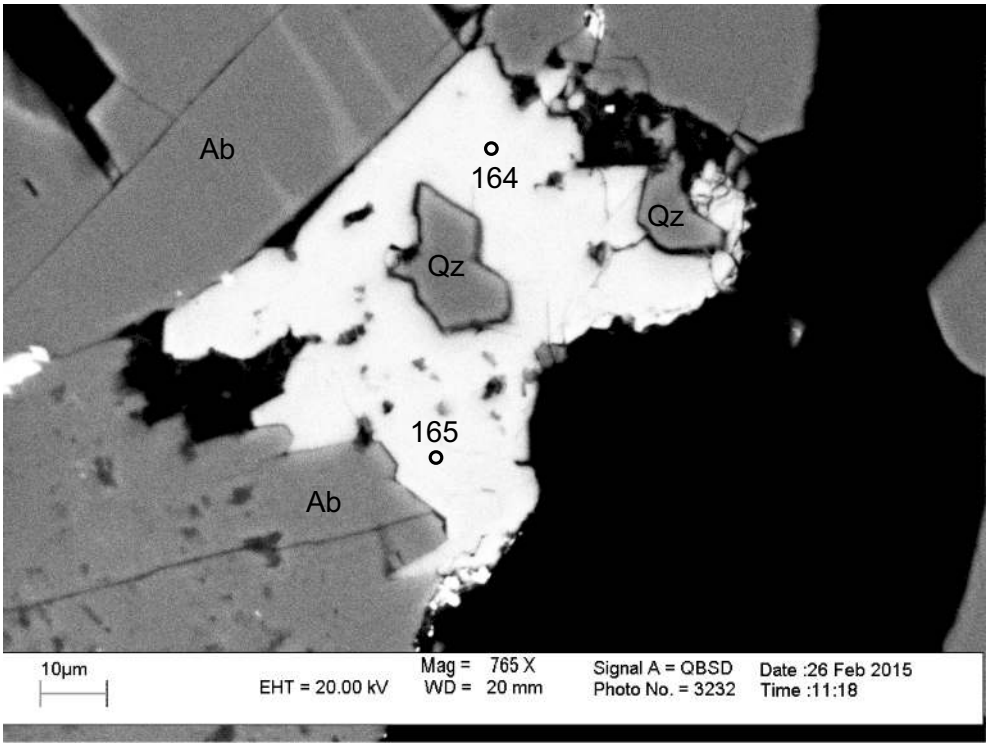

Figure 3-1.1: Sample Newburn H-23 4353.5m site 1 (probe). F-Fe-calcite (165) and Fe-calcite (164) engulf quartz.

No.	Mineral	SiO2	Al2O3	FeO	MnO	MgO	CaO	Na2O	K2O	F	SO3	Total
164	F-Fe-Cal	0.12		1.85	0.21	0.20	58.63	0.02	0.04	0.20		61.19
165	F-Fe-Cal	0.09	0.01	1.51	0.18	0.20	54.97	0.03	0.00	1.26	0.00	57.71

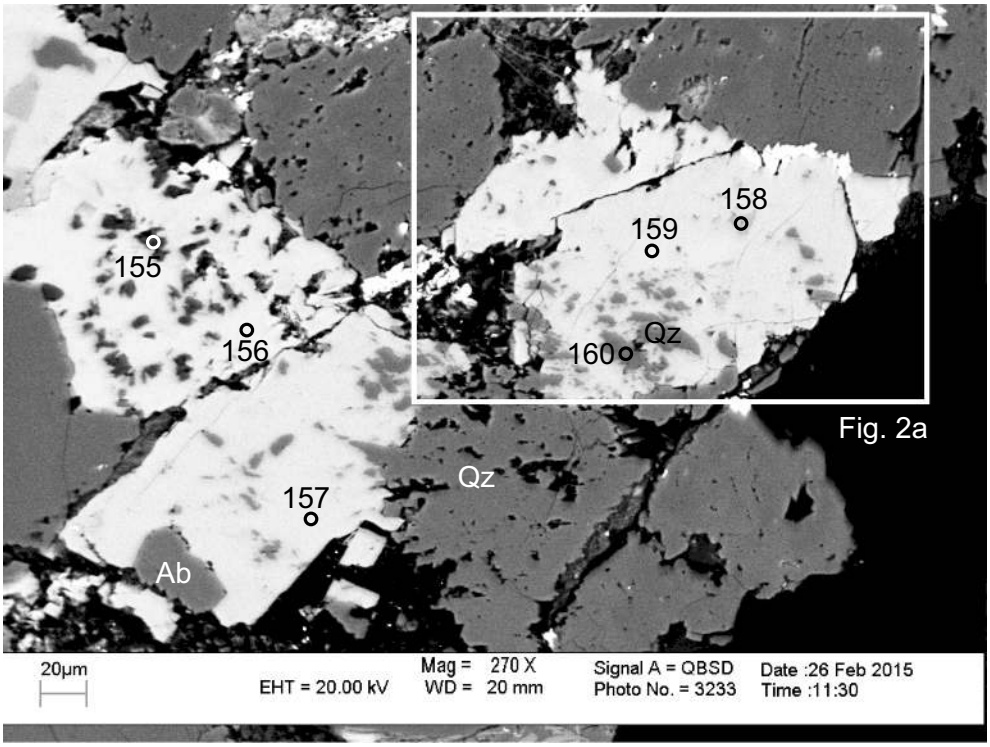

Figure 3-1.2: Sample Newburn H-23 4353.5m site 2 (probe). Fe-calcite (156,157,159) replaces albite (160), kaolinite (155), K-feldspar (158), and quartz.

No.	Mineral	SiO2	Al2O3	FeO	MnO	MgO	CaO	Na2O	K2O	F	SO3	Total
155	Kln+Cal	38.10	33.68	0.26	0.04	0.04	6.20	0.04	0.01		0.01	78.38
156	Fe-Cal	0.02	0.00	1.77	0.21	0.22	58.53	0.02	0.03		0.04	60.84
157	Fe-Cal	0.04	0.01	1.35	0.17	0.18	58.28	0.01				60.04
158	Kfs	67.07	18.87	0.07		0.01	0.47	0.62	15.88		0.02	103.00
159	Fe-Cal	0.02	0.02	1.76	0.20	0.29	59.64	0.02	0.00			61.94
160	Ab	70.84	20.94	0.01			0.32	11.88	0.06			104.05

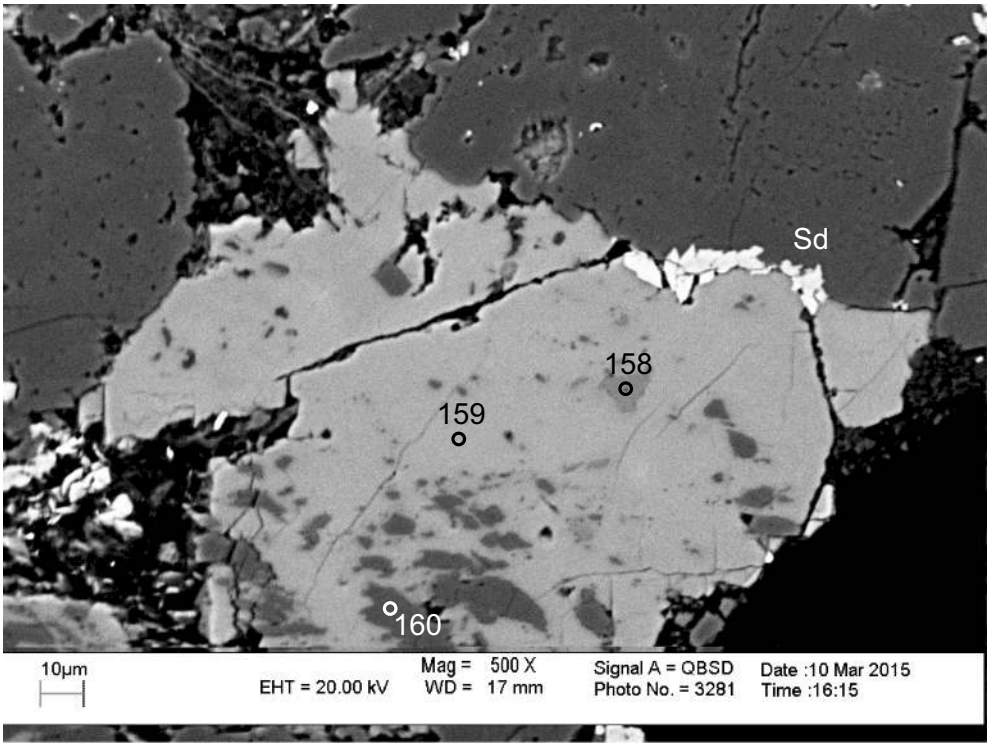

Figure 3-1.2a: Sample Newburn H-23 4353.5m site 2 (probe). Fe-Cal (159) replaces albite (160) and K-feldspar (158) and is replaced by siderite.

No.	Mineral	SiO2	Al2O3	FeO	MnO	MgO	CaO	Na2O	K2O	F	SO3	Total
158	Kfs	67.07	18.87	0.07		0.01	0.47	0.62	15.88		0.02	103.00
159	Fe-Cal	0.02	0.02	1.76	0.20	0.29	59.64	0.02	0.00			61.94
160	Ab	70.84	20.94	0.01			0.32	11.88	0.06			104.05

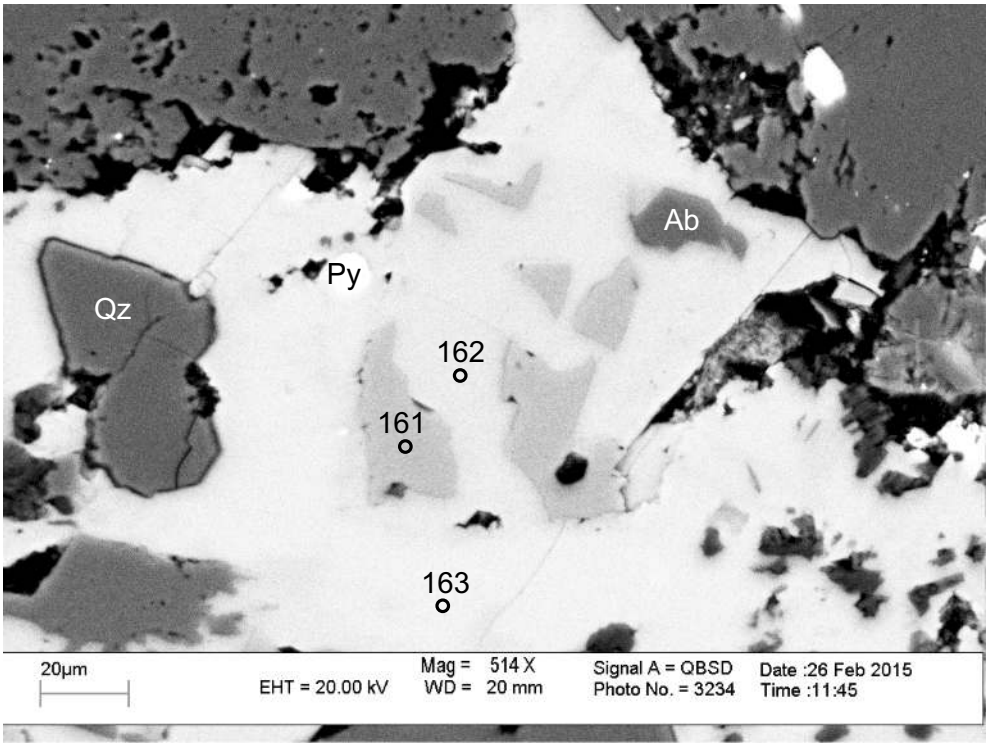

Figure 3-1.3: Sample Newburn H-23 4353.5m site 3 (probe). Fe-calcite (162,163) engulfs K-feldspar (161) and quartz. Pyrite (3) fills dissolution voids in Fe-calcite.

No.	Mineral	SiO2	Al2O3	FeO	MnO	MgO	CaO	Na2O	K2O	F	SO3	Total
161	Kfs	66.98	18.66	0.04	0.01	0.00	0.18	0.30	16.55		0.03	102.75
162	Fe-Cal	0.05	0.04	1.37	0.17	0.22	58.21	0.00	0.12			60.17
163	Fe-Cal	0.01	0.02	2.07	0.23	0.25	57.64	0.00	0.03		0.01	60.26

Appendix 3-2: Representative SEM-BSE images and mineral analyses from EM-WDS of sample Newburn H-23 5213.5m.

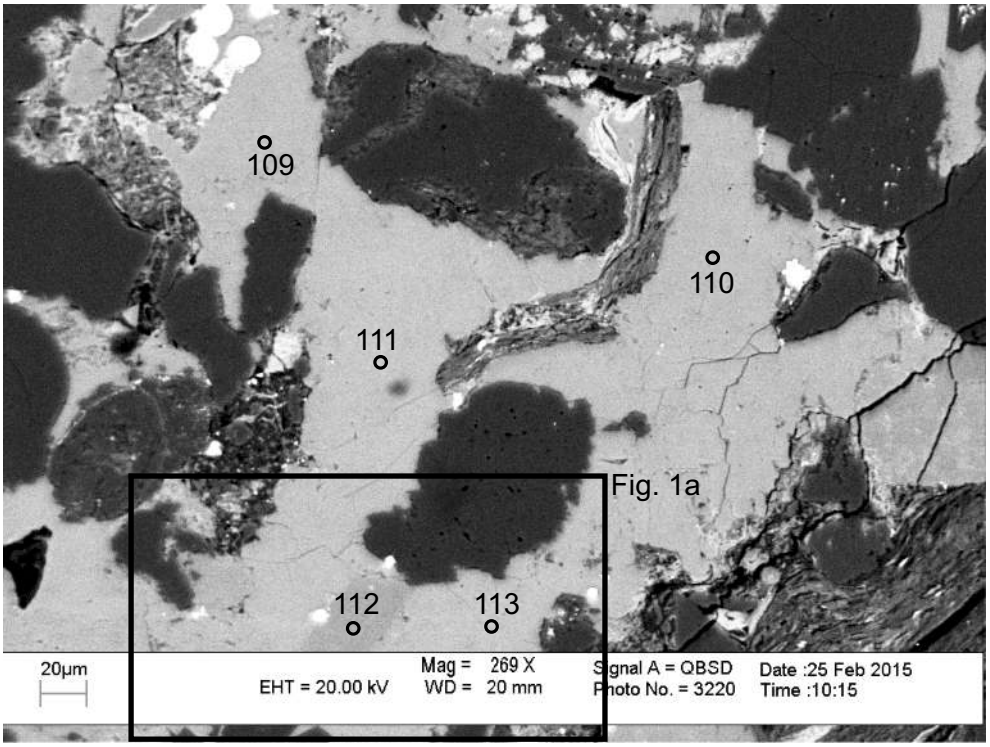

Figure 3-2.1: Sample Newburn H-23 5213.5m site 1 (probe). Fe-calcite (109-111,113) surrounds and replaces calcite (112).

No.	Mineral	SiO2	Al2O3	FeO	MnO	MgO	CaO	Na2O	K2O	F	SO3	Total
109	Fe-Cal	0.03	0.01	3.28	0.29	0.70	52.59	0.02	0.01		0.04	56.97
110	Fe-Cal	0.04	0.02	1.07	0.18	0.22	44.34	0.02	0.02			45.90
111	Fe-Cal	0.05		3.31	0.34	0.67	55.15	0.01	0.02		0.03	59.58
112	Cal	0.01	0.02	0.06	0.04	0.04	57.08	0.07			0.42	57.74
113	Fe-Cal	0.00	0.01	2.63	0.30	0.50	51.15	0.02	0.00		0.03	54.64

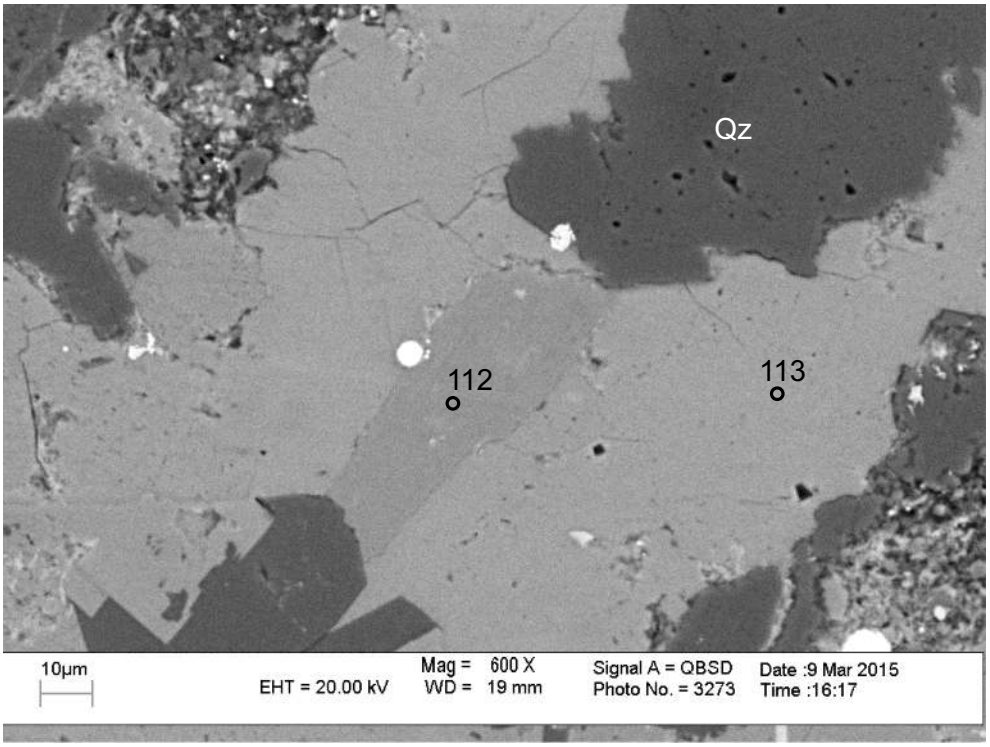

Figure 3-2.1a: Sample Newburn H-23 5213.5m site 1 (probe). Fe-calcite (113) replaces calcite (112). Fe-calcite (113) replaces quartz

No.	Mineral	SiO2	Al2O3	FeO	MnO	MgO	CaO	Na2O	K2O	F	SO3	Total
112	Cal	0.01	0.02	0.06	0.04	0.04	57.08	0.07			0.42	57.74
113	Fe-Cal	0.00	0.01	2.63	0.30	0.50	51.15	0.02	0.00		0.03	54.64

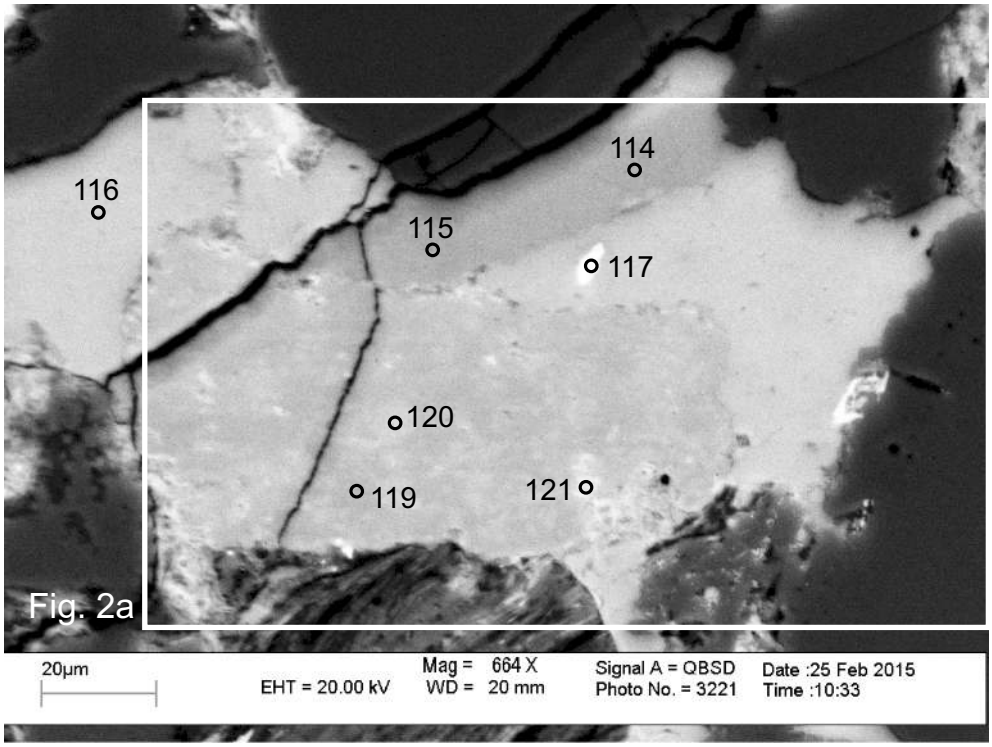

Figure 3-2.2: Sample Newburn H-23 5213.5m site 2 (probe). Fe-calcite (120) replaces Mg-calcite (115,119) and calcite (114). Siderite (117) fills a dissolution void in F-Fe-calcite (117). F-Fe-calcite (117) and Fe-calcite (116) surround and replace Mg-calcite.

No.	Mineral	SiO2	Al2O3	FeO	MnO	MgO	CaO	Na2O	K2O	F	SO3	Total
114	Cal	0.07	0.03	0.13	0.05	0.80	48.90	0.21	0.00		0.19	50.38
115	Mg-Cal	0.04	0.01	0.10	0.01	1.84	47.65	0.29			0.26	50.20
116	Fe-Cal	0.06	0.02	1.96	0.28	0.45	48.72		0.01		0.01	51.51
117	F-Fe-Cal+Sd	1.29	0.69	15.99	0.54	2.30	37.32	0.01	0.06	1.19	0.03	58.92
118	Cal	0.08	0.01	0.58	0.24	0.71	44.23	0.04	0.00		0.17	46.06
119	Mg-Cal			0.25		1.07	56.71		0.19		0.87	59.09
120	Fe-Cal	0.01		2.17	0.31	0.52	52.63				0.04	55.67
121	F-Cal+Chl	8.56	8.23	12.51	0.18	2.31	34.61	0.12	0.02	1.44	0.15	67.53

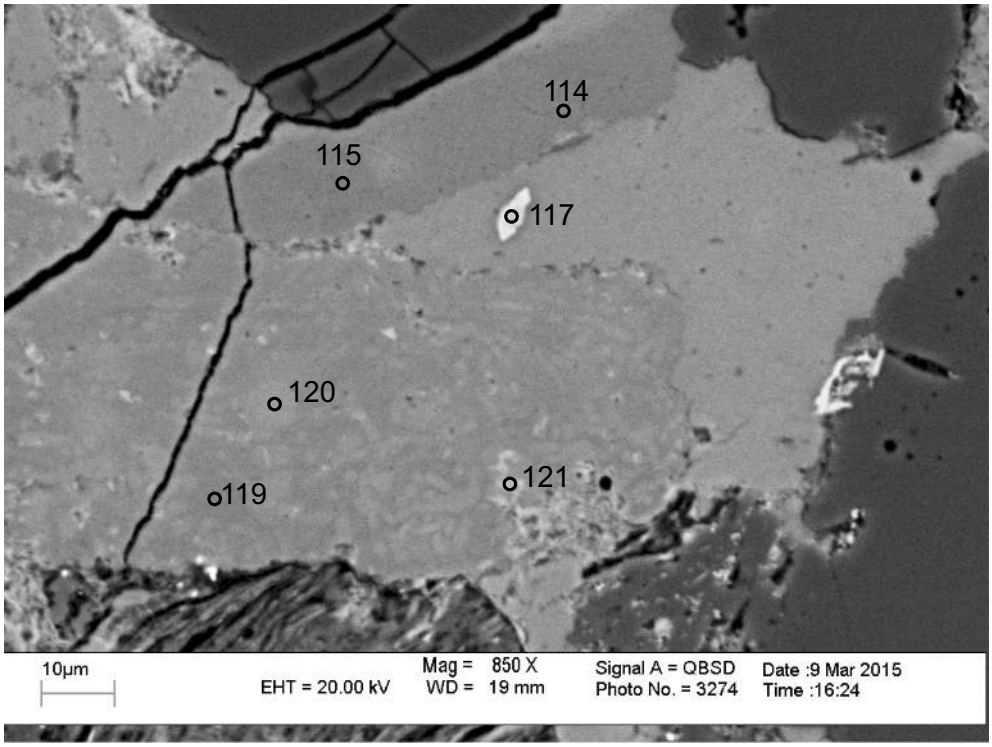

Figure 3-2.2a: Sample Newburn H-23 5213.5m site 2 (probe). Fe-calcite (120) replaces Mg-calcite (115,119) and calcite (114). Siderite (117) fills a dissolution void in F-Fe-calcite (117). F-Fe-calcite (117) appears to surround and replace Mg-calcite.

No.	Mineral	SiO2	Al2O3	FeO	MnO	MgO	CaO	Na2O	K2O	F	SO3	Total
114	Cal	0.07	0.03	0.13	0.05	0.80	48.90	0.21	0.00		0.19	50.38
115	Mg-Cal	0.04	0.01	0.10	0.01	1.84	47.65	0.29			0.26	50.20
117	Fe-F-Cal+Sd	1.29	0.69	15.99	0.54	2.30	37.32	0.01	0.06	1.19	0.03	58.92
119	Mg-Cal			0.25		1.07	56.71		0.19		0.87	59.09
120	Fe-Cal	0.01		2.17	0.31	0.52	52.63				0.04	55.67
121	F-Cal+Chl	8.56	8.23	12.51	0.18	2.31	34.61	0.12	0.02	1.44	0.15	67.53

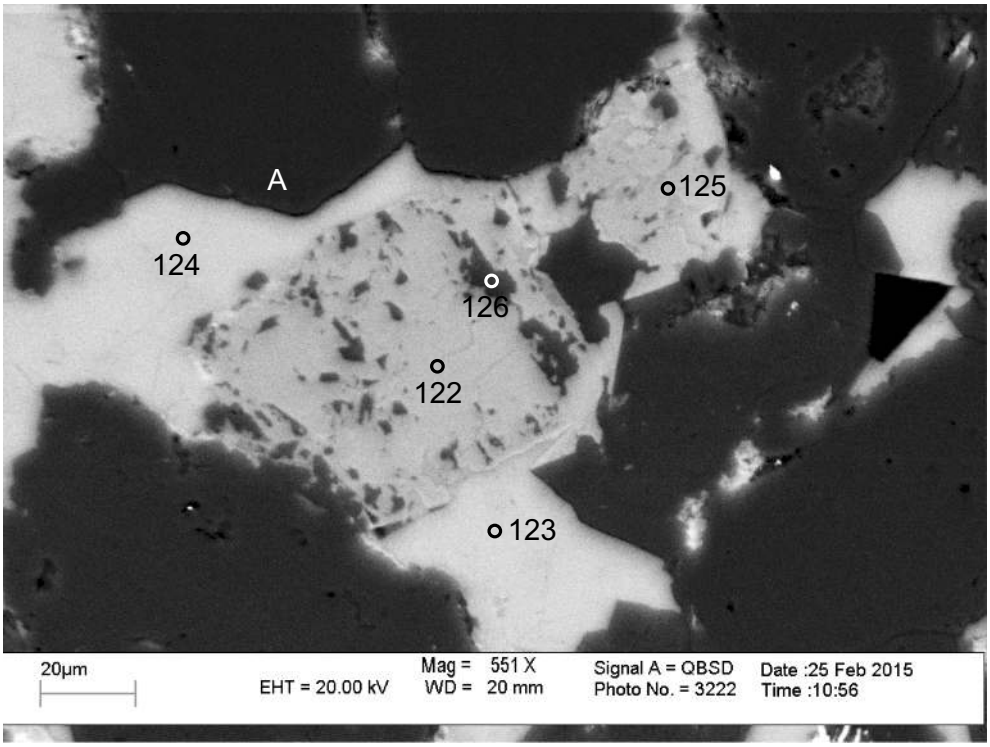

Figure 3-2.3: Sample Newburn H-23 5213.5m site 3 (probe). Ankerite (122,125) replaces and surrounds albite (126). Fe-calcite (123,124) surrounds and replaces ankerite (122,125) as well as quartz overgrowths (position A).

No.	Mineral	SiO2	Al2O3	FeO	MnO	MgO	CaO	Na2O	K2O	F	SO3	Total
122	Ank	0.05		12.16	0.58	9.23	27.79		0.01		0.02	49.83
123	Fe-Cal	0.06		2.66	0.32	0.62	51.01				0.01	54.67
124	Fe-Cal	0.06	0.01	3.20	0.35	0.73	54.43	0.00	0.01		0.01	58.80
125	Ank	0.12	0.06	9.29	0.44	6.82	35.53	0.01	0.01		0.02	52.29
126	Ab	69.57	20.41	0.28		0.04	0.25	12.06	0.00			102.61

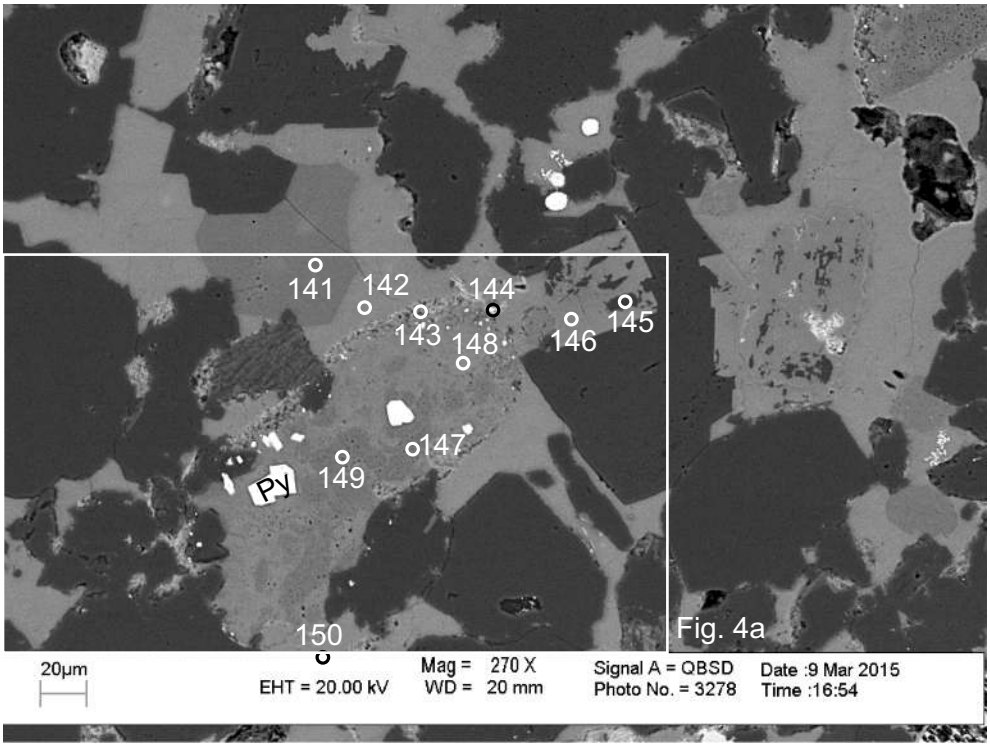

Figure 3-2.4: Sample Newburn H-23 5213.5m site 4 (probe).Mg-calcite (141,147,149) is replaced by Fe-calcite (142) and F-Fe-calcite (128). Pyrite (144) fills dissolution in F-Fe-calcite (148) and Mg-calcite and rims them. Ankerite (146) containing albite relics (145) is replaced by Fe-calcite.

No.	Mineral	SiO2	Al2O3	FeO	MnO	MgO	CaO	Na2O	K2O	F	SO3	Total
141	Mg-Cal		0.55	0.03	0.02	2.45	56.92	0.27	0.24		0.41	60.89
142	Fe-Cal	0.01	0.01	3.17	0.32	0.58	55.34		0.02		0.05	59.49
143	Chl	26.15	23.01	29.43	0.02	5.16	1.47	0.31	0.32	0.77	0.08	86.39
144	Chl+Py+Other	17.03	15.18	41.23	0.02	3.35	1.42	0.71	0.09	0.80	44.51	124.02
145	Ab	70.08	20.62	0.22	0.01	0.01	0.23	11.89	0.01		0.01	103.07
146	Ank	0.06		15.96	0.59	9.62	27.61	0.04				53.87
147	Mg-Cal	0.04	0.02	0.06	0.01	3.11	49.68	0.09	0.01		0.76	53.78
148	F-Fe-Cal	0.04	0.02	2.81	0.31	0.47	55.84	0.01	0.00	0.23	0.05	59.67
149	Mg-Cal	0.01	0.02	0.24	0.01	2.50	50.29	0.19	0.08		0.64	53.96
150	Fe-Cal	0.03	0.03	2.54	0.31	0.59	51.11	0.02	0.01		0.03	54.67

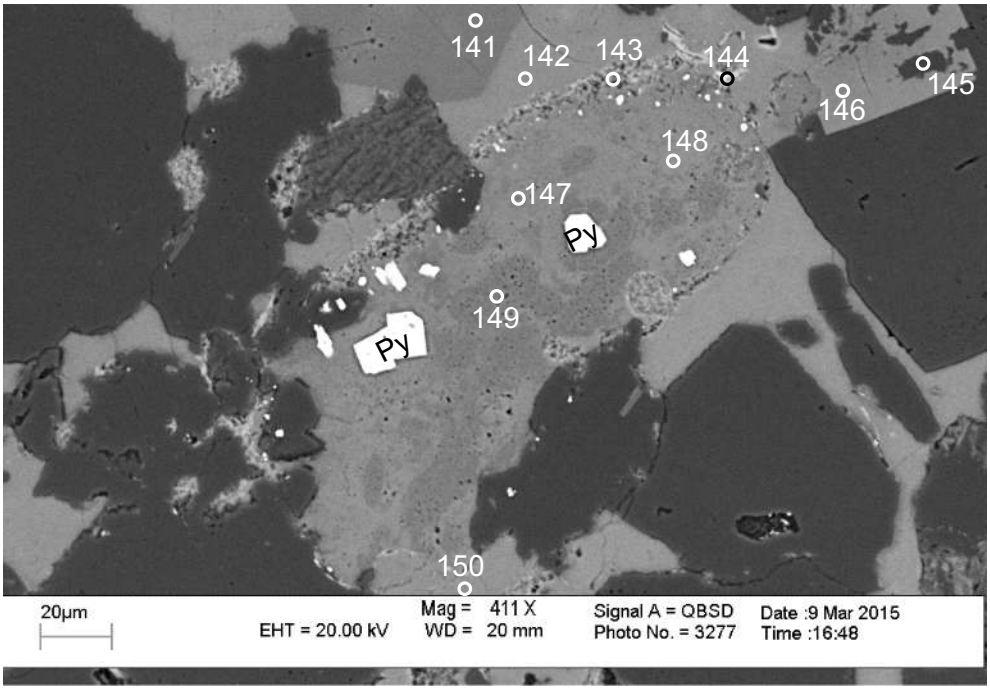

Figure 3-2.4a: Sample Newburn H-23 5213.5m site 4 (probe). Mg-calcite (141,147,149) is replaced by Fe-calcite (142) and F-Fe-calcite (128). Pyrite (144) fills dissolution in F-Fe-calcite (148) and Mg-calcite and rims them. Ankerite (146) containing albite relics (145) is replaced by Fe-calcite.

No.	Mineral	SiO2	Al2O3	FeO	MnO	MgO	CaO	Na2O	K2O	F	SO3	Total
141	Mg-Cal		0.55	0.03	0.02	2.45	56.92	0.27	0.24		0.41	60.89
142	Fe-Cal	0.01	0.01	3.17	0.32	0.58	55.34		0.02		0.05	59.49
143	Chl	26.15	23.01	29.43	0.02	5.16	1.47	0.31	0.32	0.77	0.08	86.39
144	Chl+Py+Other	17.03	15.18	41.23	0.02	3.35	1.42	0.71	0.09	0.80	44.51	124.02
145	Ab	70.08	20.62	0.22	0.01	0.01	0.23	11.89	0.01		0.01	103.07
146	Ank	0.06		15.96	0.59	9.62	27.61	0.04				53.87
147	Mg-Cal	0.04	0.02	0.06	0.01	3.11	49.68	0.09	0.01		0.76	53.78
148	Fe-F-Cal	0.04	0.02	2.81	0.31	0.47	55.84	0.01	0.00	0.23	0.05	59.67
149	Mg-Cal	0.01	0.02	0.24	0.01	2.50	50.29	0.19	0.08		0.64	53.96
150	Fe-Cal	0.03	0.03	2.54	0.31	0.59	51.11	0.02	0.01		0.03	54.67

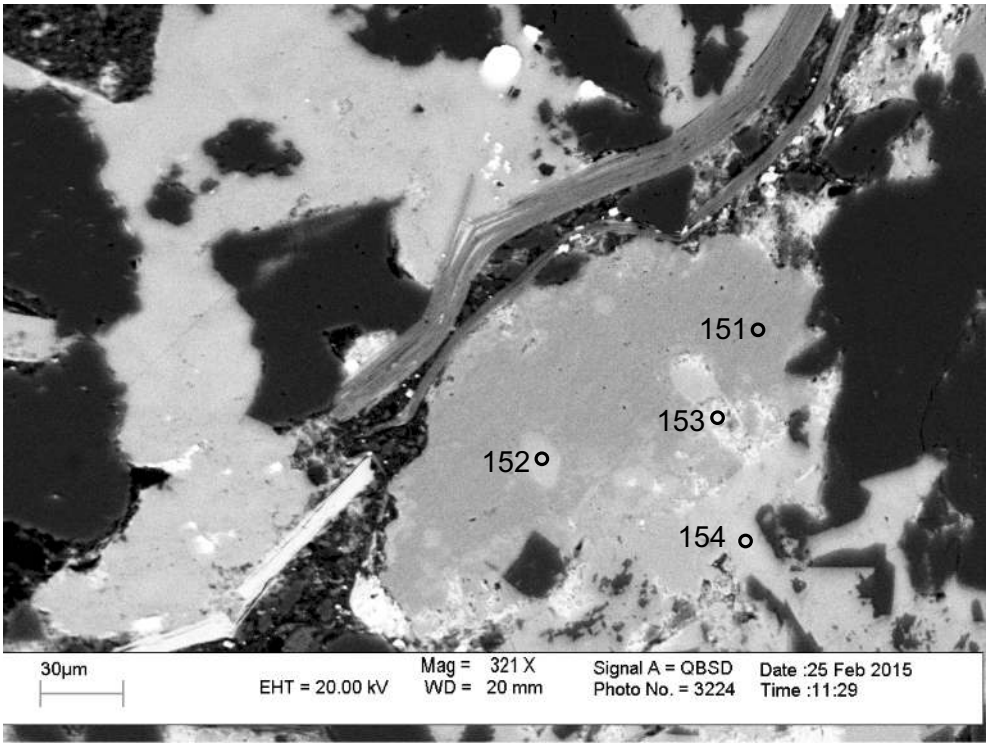

Figure 3-2.5: Sample Newburn H-23 5213.5m site 5 (probe). Calcite (151) is replaced by Fe-calcite (152,154) and both are cut by chlorite (153).

No.	Mineral	SiO2	Al2O3	FeO	MnO	MgO	CaO	Na2O	K2O	F	SO3	Total
151	Cal	0.05		0.07	0.01	0.81	55.55	0.29	0.02		0.34	57.13
152	Fe-Cal	0.02	0.01	1.99	0.26	0.42	50.46				0.04	53.20
153	Chl+Other	27.87	22.89	30.19	0.02	4.80	1.16	0.26	0.38	1.64	0.06	88.57
154	Fe-Cal	0.06	0.00	3.07	0.30	0.49	55.67	0.03		0.01	0.02	59.64

Appendix 3-3: Representative SEM-BSE images and mineral analyses from EM-WDS of sample Newburn H-23 5403.6m.

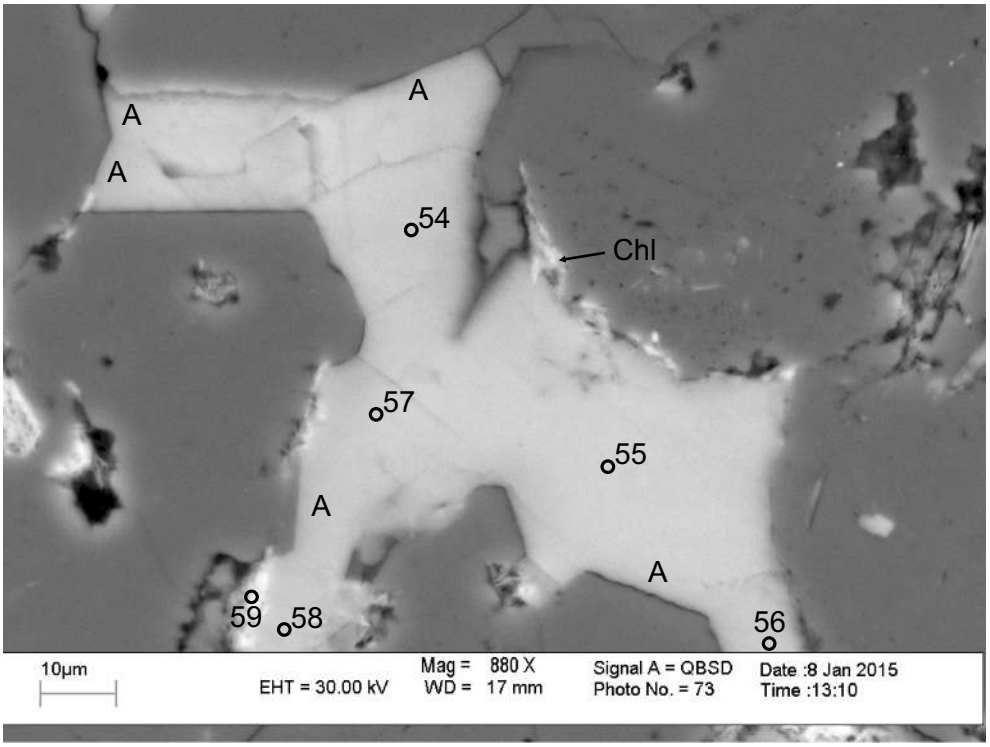

Figure 3-3.1: Sample Newburn H-23 5403.6m site 2 (probe). F-calcite (58,59), and F-Fe-calcite (54-57) are cut by chlorite and bounded by quartz overgrowths (positions A).

No.	Mineral	SiO2	Al2O3	FeO	MnO	MgO	CaO	Na2O	K2O	F	SO3	Total
54	F-Fe-Cal	0.17		2.78	0.77	0.41	55.89	0.03	0.01	0.77	0.02	60.52
55	F-Fe-Cal	0.11	0.00	2.86	0.77	0.39	56.16	0.02		0.80	0.02	60.78
56	F-Fe-Cal	0.23	0.02	2.96	0.75	0.37	53.57	0.03	0.02	1.24	0.01	58.69
57	F-Fe-Cal	0.16	0.01	2.35	0.70	0.43	56.28			1.82	0.02	61.01
58	Qz+F-Cal	35.43	0.13	1.25	0.42	0.26	32.77	0.12		2.31	0.06	71.78
59	Chl+F-Cal	12.00	10.92	15.73	0.33	2.14	29.92	0.22	0.08	3.28	0.00	73.26

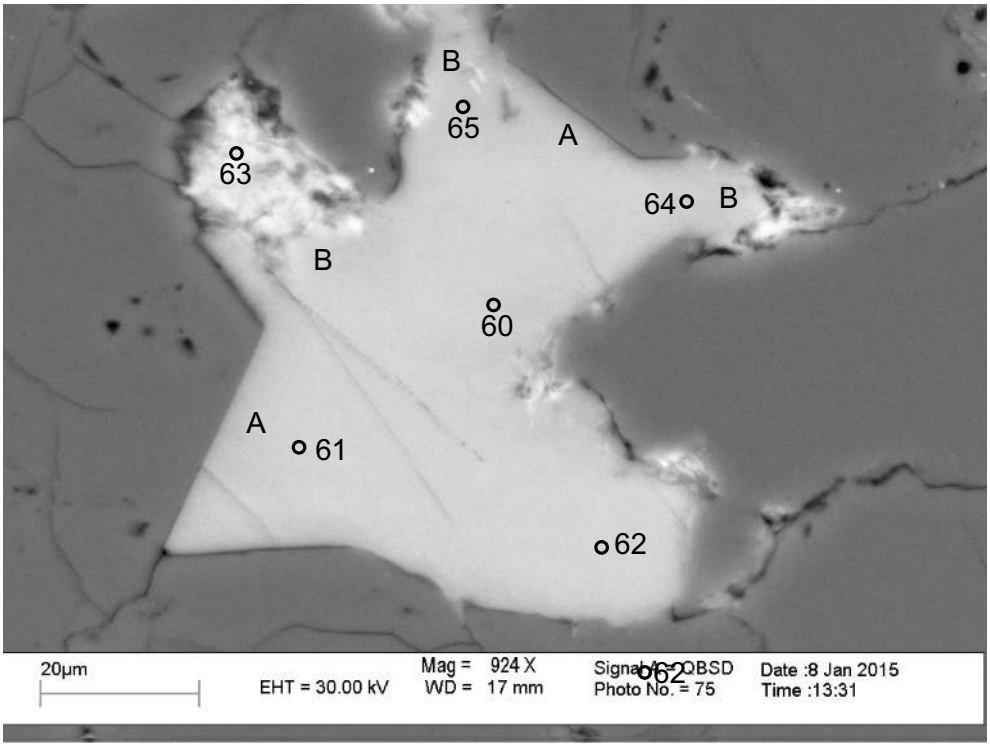

Figure 3-3.2: Sample Newburn H-23 5403.6m site 3 (probe). F-calcite (60) and F-Fe-cal (61,62,64,65) are in contact with quartz overgrowths (positions A). Fibrous chlorite cuts F-Fe-calcite (positions B).

No.	Mineral	SiO2	Al2O3	FeO	MnO	MgO	CaO	Na2O	K2O	F	SO3	Total
60	F-Cal	0.06	0.01	0.85	0.33	0.09	54.92	0.01	0.01	2.45		57.69
61	F-Fe-Cal	0.09		2.58	0.78	0.49	56.16	0.03	0.01	1.21		60.84
62	F-Fe-Cal	0.12	0.02	2.92	0.76	0.42	55.67			0.48	0.01	60.20
63	Chl	28.59	24.54	30.14	0.02	4.10	0.69	0.17	0.73	0.43	0.01	89.23
64	F-Fe-Cal	0.19	0.02	2.87	0.78	0.45	54.80			1.55	0.00	60.02
65	F-Fe-Cal	0.08	0.01	1.06	0.32	0.10	56.24	0.02		1.47	0.01	58.69

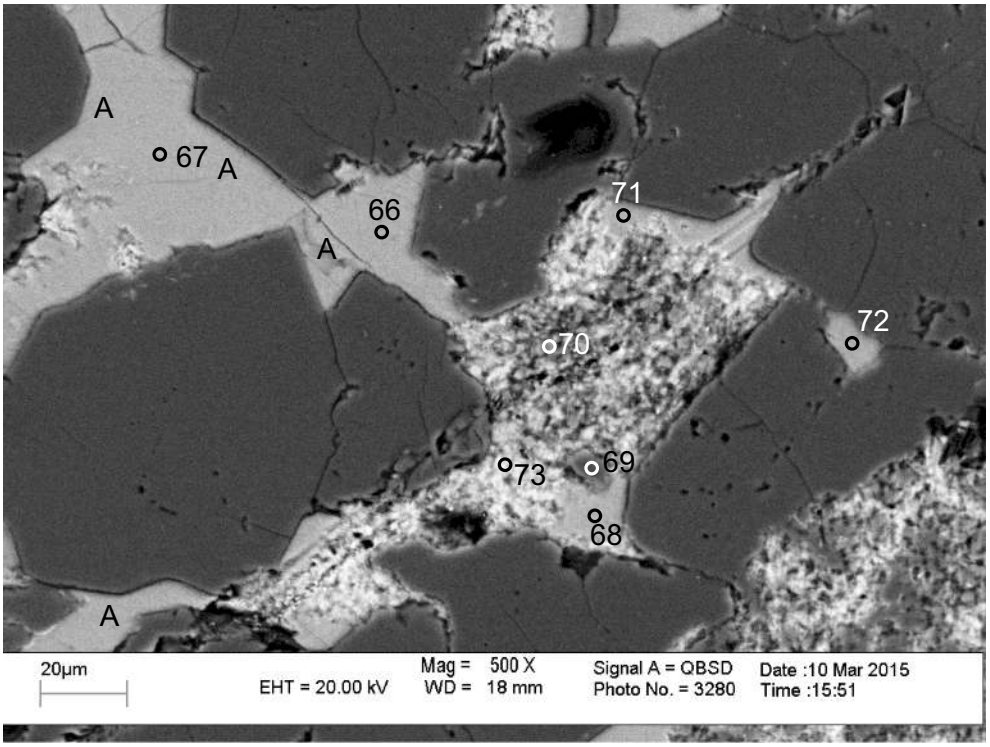

Figure 3-3.3: Sample Newburn H-23 5403.6m site 4 (probe). F-Fe-calcite (66-68,72) is bounded by quartz overgrowths (positions A). Chlorite (69-71,73) cuts F-Fe-cal.

No.	Mineral	SiO2	Al2O3	FeO	MnO	MgO	CaO	Na2O	K2O	F	SO3	Total
66	F-Fe-Cal	0.12	0.02	2.95	0.81	0.39	54.21	0.01		1.32		59.27
67	F-Fe-Cal	0.03	0.01	3.08	0.88	0.50	56.80	0.01	0.01	1.39	0.00	62.13
68	F-Fe-Cal	0.21	0.05	2.70	0.70	0.41	55.53	0.01		1.23		60.33
69	Chl+Other	37.93	15.19	24.99	0.02	2.70	3.23	0.20	0.30	1.82	0.28	85.90
70	Qz+Chl+Other	42.89	23.09	25.08	0.03	3.66	0.36	0.27	1.89	1.33	0.05	98.09
71	Chl+F-Cal	16.06	14.11	22.74	0.13	2.61	18.57	0.20	0.09	2.30	0.06	75.91
72	F-Fe-Cal	0.32		2.32	0.53	0.31	55.07	0.02		1.95		59.69
73	Chl+Other	24.66	20.09	31.80	0.02	3.96	0.45	0.39	0.24	3.04	0.09	83.46

Appendix 3-4: Representative SEM-BSE images and mineral analyses from EM-WDS of sample Newburn H-23 5407m.

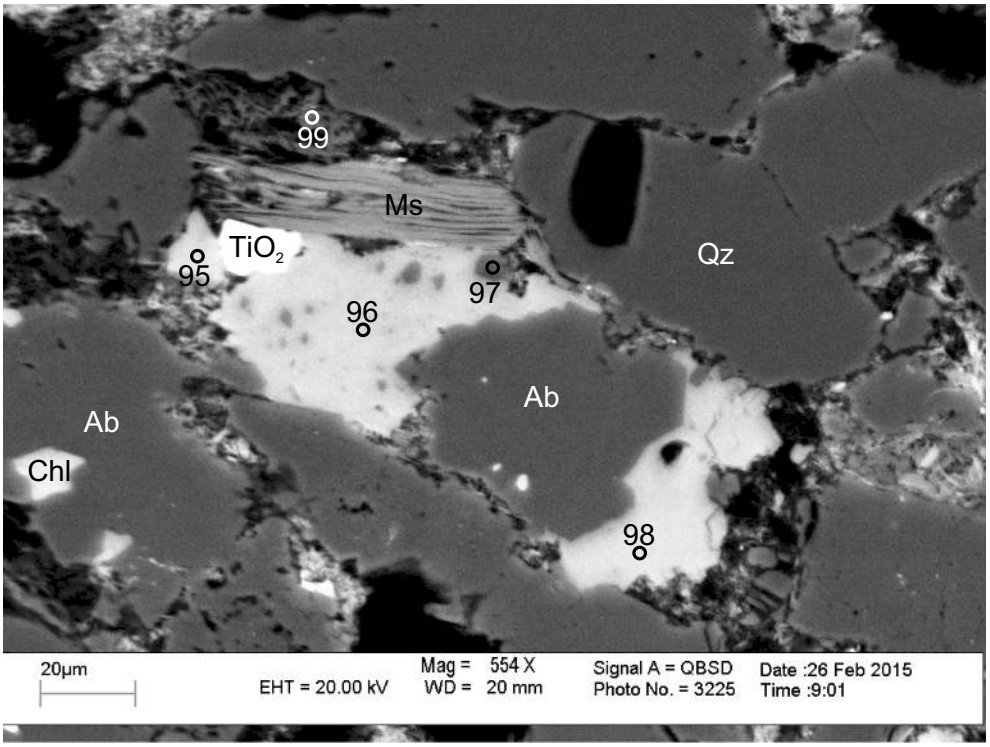

Figure 3-4.1: Sample Newburn H-23 5407m site 1 (probe). F-Fe-calcite (95,93,98) replaces and surrounds albite. Titania replaces F-Fe-calcite (95,96).

No.	Mineral	SiO2	Al2O3	FeO	MnO	MgO	CaO	Na2O	K2O	F	SO3	Total
95	F-Fe-Cal	0.16	0.02	2.12	0.39	0.34	57.21	0.02	0.03	1.01	0.01	60.89
96	F-Fe-Cal+Other	1.35	0.50	2.11	0.76	0.45	53.81	0.03	0.33	0.84	0.04	59.86
97	Ab	68.10	19.70	0.15	0.04	0.03	2.15	11.42	0.04	0.17	0.02	101.73
98	F-Fe-Cal	0.21	0.09	2.10	0.45	0.42	56.65	0.02	0.00	2.40		61.32
99	Ab	60.01	18.94	1.23	0.00	0.21	0.20	9.14	0.45	0.03	0.17	90.36

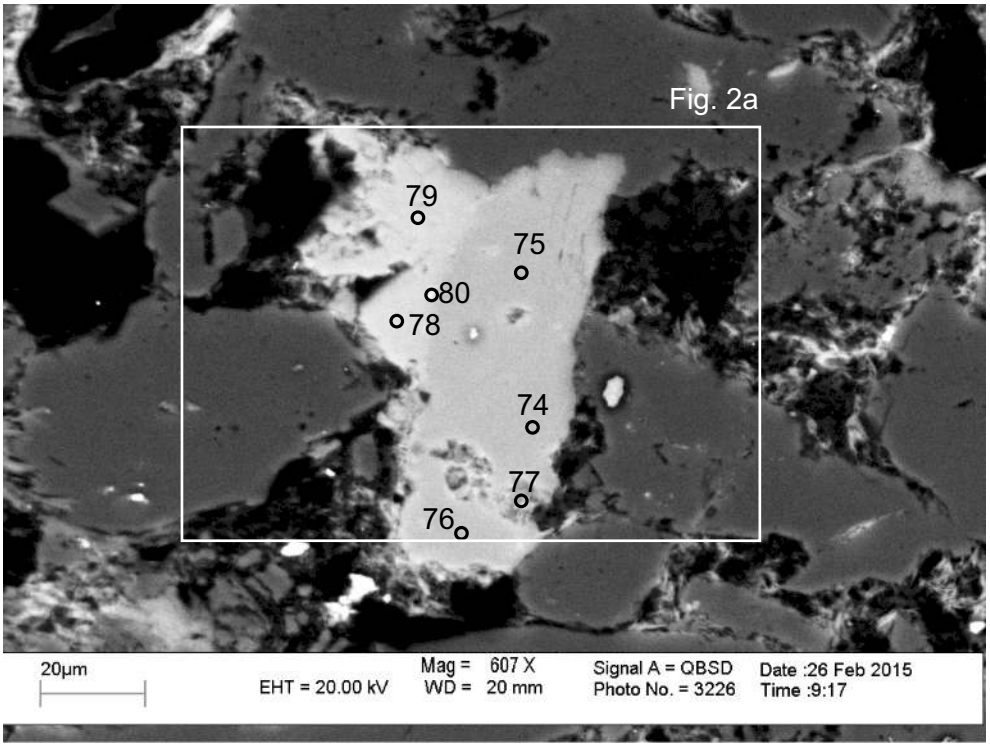

Figure 3-4.2: Sample Newburn H-23 5407m site 2 (probe). Calcite (74,76) and F-calcite (75) have dissolution voids filled by fibrous chlorite (77) and are replaced by F-Fe-calcite (78-80).

No.	Mineral	SiO2	Al2O3	FeO	MnO	MgO	CaO	Na2O	K2O	F	SO3	Total
74	Cal	0.03		0.16	0.04	0.45	61.19	0.14	0.04		0.94	62.98
75	F-Cal	0.03		0.11		0.48	55.23	0.20	0.03	0.38	1.02	57.32
76	Cal	0.03	0.01	0.26	0.01	0.51	54.00	0.16			0.94	55.92
77	Chl+Other	25.19	21.72	28.17	0.02	3.62	1.47	0.42	0.53	1.13	0.15	81.93
78	F-Fe-Cal	0.06	0.01	2.68	0.70	0.52	56.29	0.02	0.02	0.41	0.03	60.57
79	F-Fe-Cal	0.07	0.03	1.99	0.53	0.47	57.22	0.02	0.01	1.04	0.05	60.97
80	F-Fe-Cal+Other	1.06	0.56	3.16	0.24	0.60	51.60	0.16	0.00	2.14	0.64	59.24

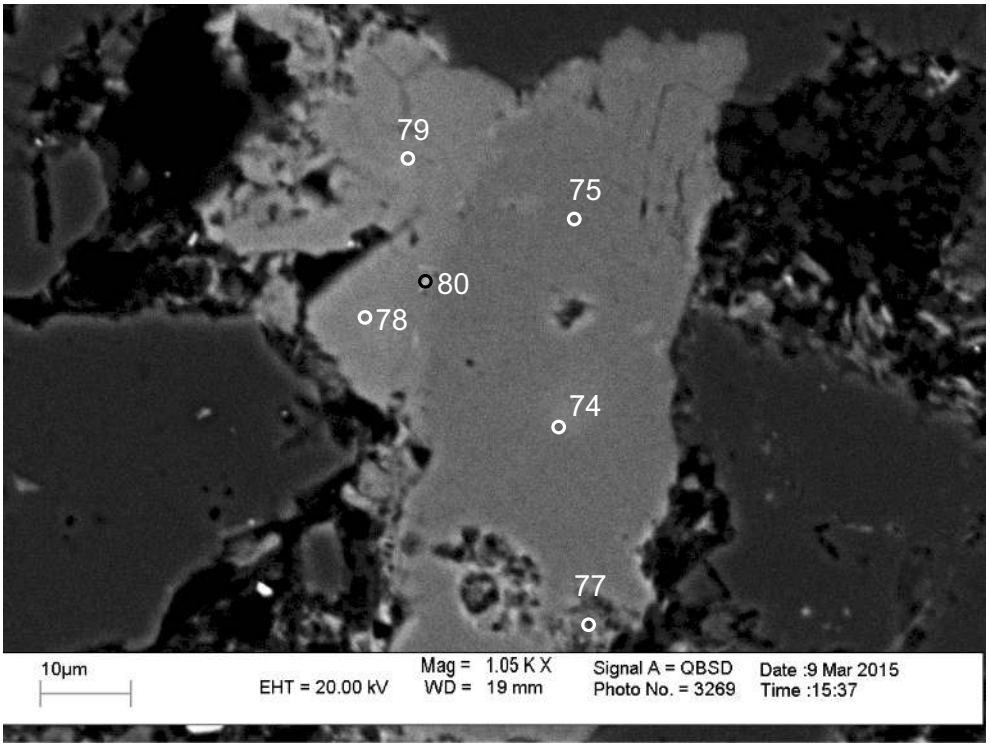

Figure 3-4.2a: Sample Newburn H-23 5407m site 2 (probe). Calcite (74,76) and F-calcite (75) have dissolution voids filled by fibrous chlorite (77) and are replaced by F-Fe-calcite (78-80).

No.	Mineral	SiO2	Al2O3	FeO	MnO	MgO	CaO	Na2O	K2O	F	SO3	Total
74	Cal	0.03		0.16	0.04	0.45	61.19	0.14	0.04		0.94	62.98
75	F-Cal	0.03		0.11		0.48	55.23	0.20	0.03	0.38	1.02	57.32
76	Cal	0.03	0.01	0.26	0.01	0.51	54.00	0.16			0.94	55.92
77	Chl+Other	25.19	21.72	28.17	0.02	3.62	1.47	0.42	0.53	1.13	0.15	81.93
78	F-Fe-Cal	0.06	0.01	2.68	0.70	0.52	56.29	0.02	0.02	0.41	0.03	60.57
79	F-Fe-Cal	0.07	0.03	1.99	0.53	0.47	57.22	0.02	0.01	1.04	0.05	60.97
80	F-Fe-Cal+Other	1.06	0.56	3.16	0.24	0.60	51.60	0.16	0.00	2.14	0.64	59.24

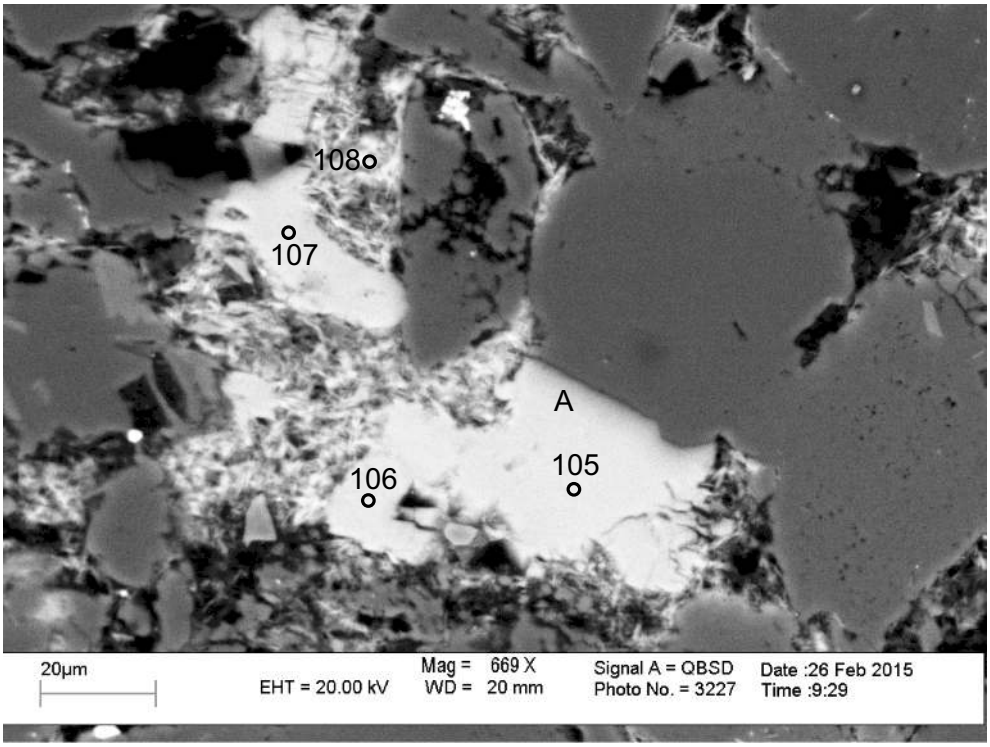

Figure 3-4.3: Sample Newburn H-23 5407m site 3 (probe). F-Fe-calcite (105-107) is cut by chlorite (108). F-Fe-calcite is cound be a quartz overgrowth (position A).

No.	Mineral	SiO2	Al2O3	FeO	MnO	MgO	CaO	Na2O	K2O	F	SO3	Total
105	F-Fe-Cal	0.06	0.03	2.05	0.48	0.36	56.78	0.01	0.01	1.07		60.40
106	F-Fe-Cal	0.10	0.02	1.60	0.36	0.25	57.80	0.02	0.02	1.40	0.02	61.00
107	F-Fe-Cal	0.09		2.92	0.88	0.43	55.29	0.01	0.03	0.54	0.00	59.97
108	Chl	27.08	23.93	25.03	0.05	3.43	0.62	0.15	0.46	0.53	0.09	81.14

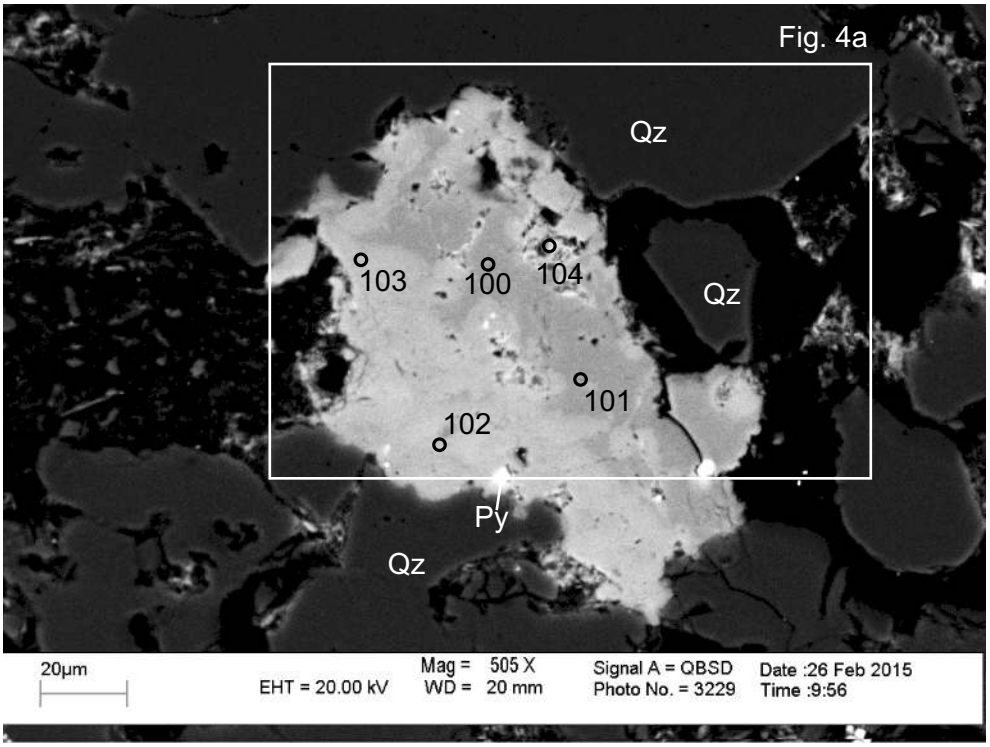

Figure 3-4.4: Sample Newburn H-23 5407m site 5 (probe). Mg-calcite (100,101) is replaced by F-Fe-calcite (102,103) and chlorite (104) fills dissolution voids in both.

No.	Mineral	SiO2	Al2O3	FeO	MnO	MgO	CaO	Na2O	K2O	F	SO3	Total
100	Mg-Cal	0.03	0.00	0.12	0.00	1.18	49.52	0.13			0.25	51.25
101	Mg-Cal	0.03		0.08		1.28	53.75	0.18	0.01		0.28	55.60
102	F-Fe-Cal	0.03	0.01	1.79	0.54	0.34	55.40	0.02		0.36	0.07	58.39
103	F-Fe-Cal	0.02	0.02	1.51	0.51	0.31	56.32	0.00		0.63	0.03	59.07
104	F-Cal+Chl	6.77	6.42	9.28	0.33	1.42	34.84	0.03	0.07	5.26	0.05	62.26

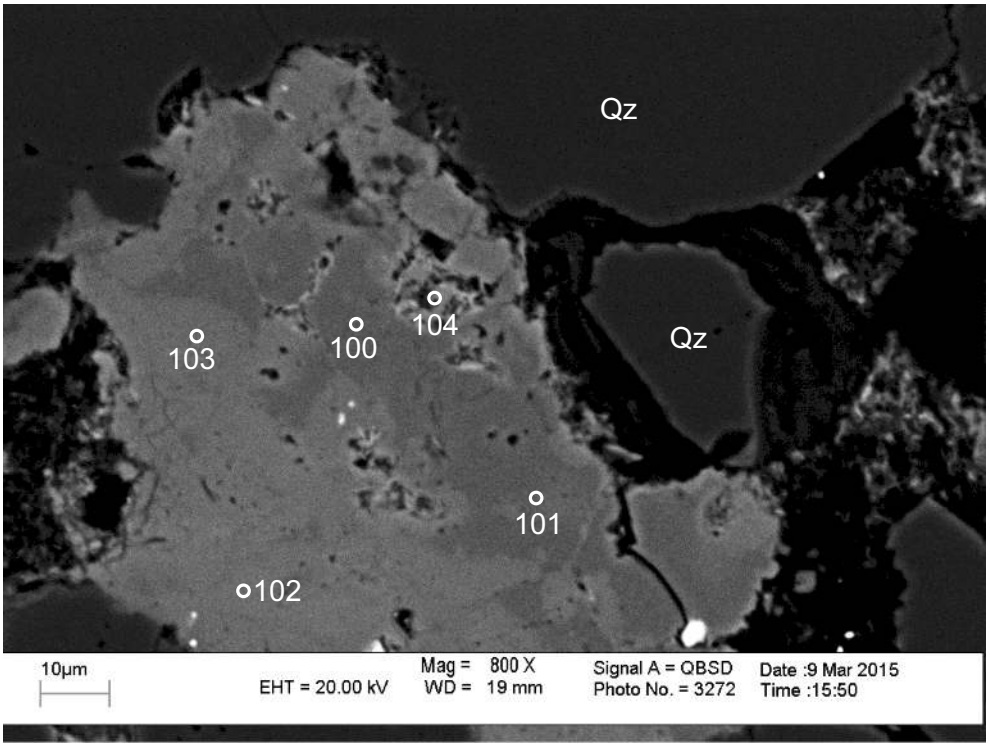

Figure 3-4.4a: Sample Newburn H-23 5407m site 5 (probe). Mg-calcite (100,101) is replaced by F-Fe-calcite (102,103) and chlorite (104) fills dissolution voids in both.

No.	Mineral	SiO2	Al2O3	FeO	MnO	MgO	CaO	Na2O	K2O	F	SO3	Total
100	Mg-Cal	0.03	0.00	0.12	0.00	1.18	49.52	0.13			0.25	51.25
101	Mg-Cal	0.03		0.08		1.28	53.75	0.18	0.01		0.28	55.60
102	F-Fe-Cal	0.03	0.01	1.79	0.54	0.34	55.40	0.02		0.36	0.07	58.39
103	F-Fe-Cal	0.02	0.02	1.51	0.51	0.31	56.32	0.00		0.63	0.03	59.07
104	F-Cal+Chl	6.77	6.42	9.28	0.33	1.42	34.84	0.03	0.07	5.26	0.05	62.26

Appendix 3-5: Representative SEM-BSE images and mineral analyses from EM-WDS of sample Newburn H-23 5408.5m.

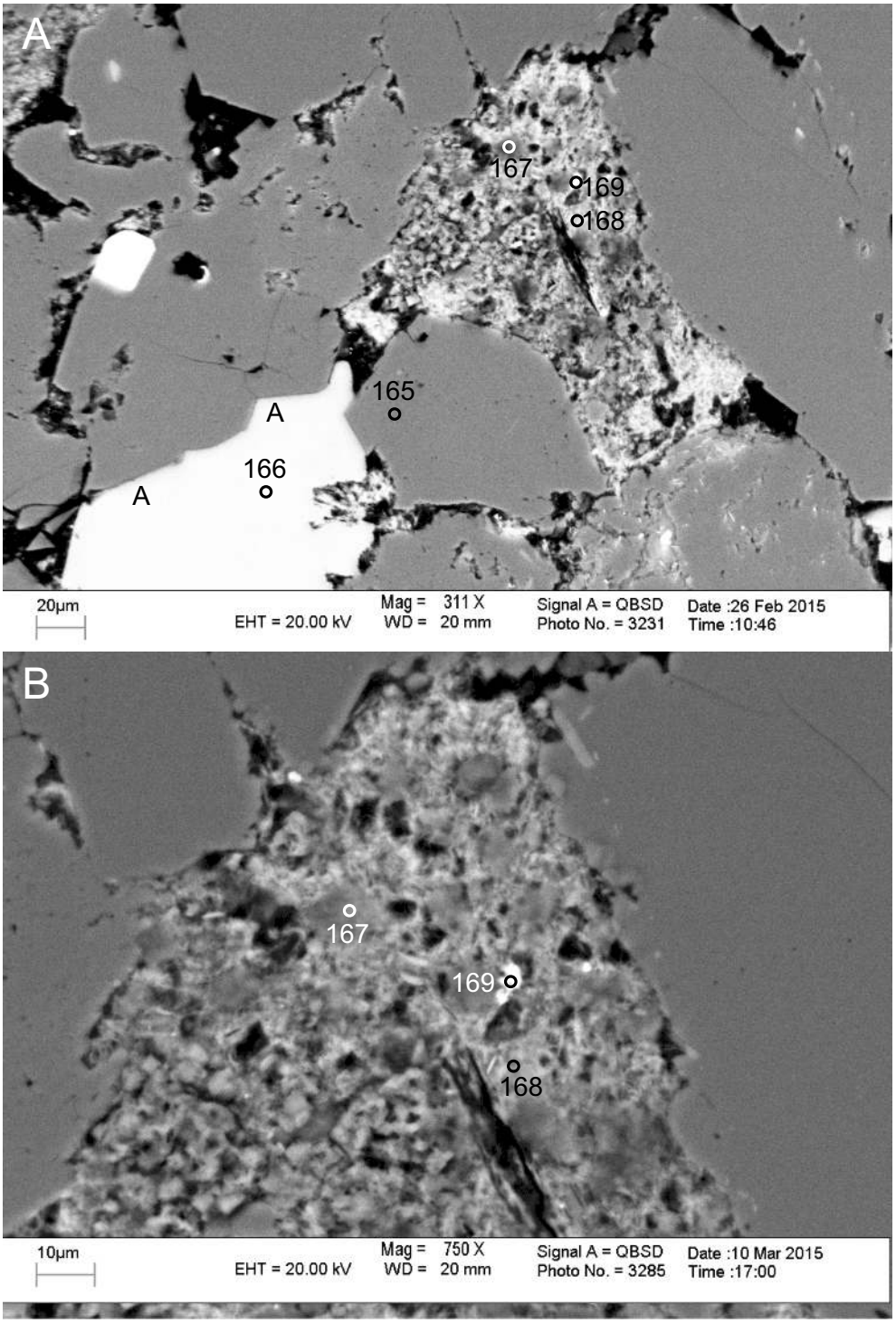

Figure 3-5.1: Sample Newburn H-23 5408.5 site 2 (probe). **A:** Fe-calcite (166) is bounded by quartz overgrowths (positions A). **B:** Possible clast composed of chlorite (168,169), titania (169), and possibly fluorite.

No.	Mineral	SiO2	Al2O3	FeO	MnO	MgO	CaO	Na2O	K2O	F	SO3	Total
166	Fe-Cal	0.04		2.16	0.48	0.35	57.37	0.02				60.42
167	F-Cal+Chl	7.21	6.00	6.99		1.10	22.43	1.03	0.23	5.86	0.29	48.67
168	Chl+Other	23.23	19.48	23.83	0.02	2.87	4.36	0.29	0.97	4.50	0.08	77.74
169	TiO2+Chl+Other	4.60	1.70	2.09		0.27	6.85	0.29	0.11	6.90	0.16	20.07

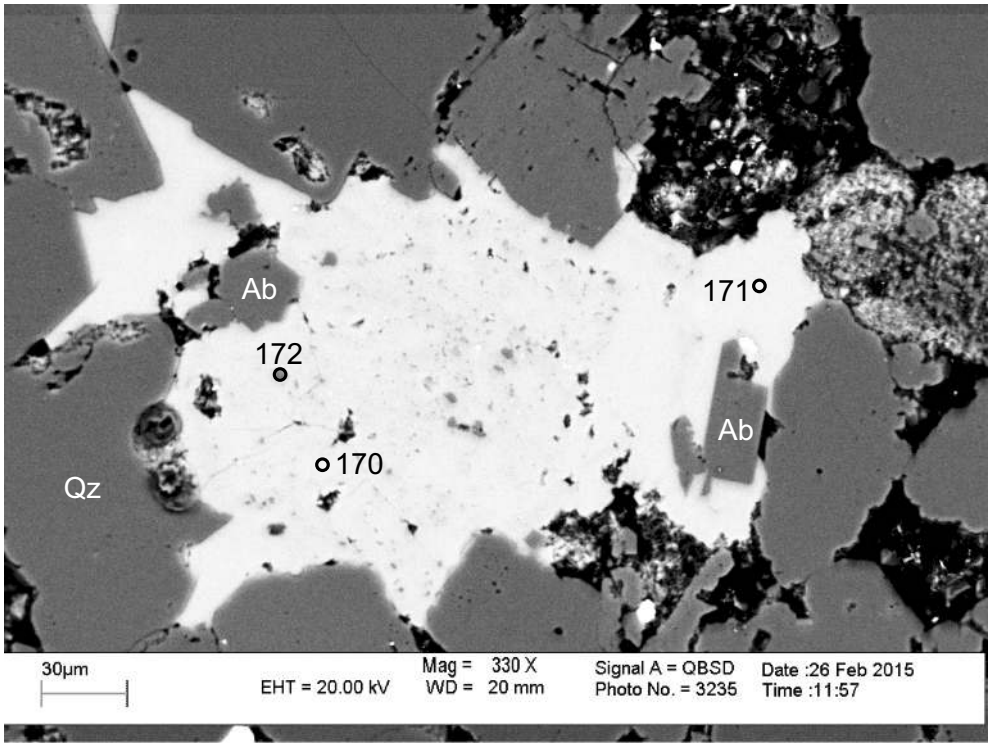

Figure 3-5.2: Sample Newburn H-23 5408.5m site 3 (probe). Fe-calcite (170,171) replaces albite and quartz.

No.	Mineral	SiO2	Al2O3	FeO	MnO	MgO	CaO	Na2O	K2O	F	SO3	Total
170	Fe-Cal	0.17	0.08	2.39	0.80	0.53	57.27	0.02				61.25
171	Fe-Cal	0.05	0.04	2.04	0.48	0.37	57.56	0.01		0.01		60.55
172	Qz+Cal	89.33	0.38	0.27	0.05	0.04	10.81	0.03	0.18		0.03	101.10

Table 3-1: EMP WDS chemical analyses of F-Fe-Calcite and other minerals from samples 4353.5m, 5213.5m, 5403.6m, 5407m, and 5408.5m.

Sample	Site	No.	Mineral	SiO2	Al2O3	FeO	MnO	MgO	CaO	Na2O	K2O	F	SO3	Total
H-23 5403.6m	2	54	Fe-F-Cal	0.17		2.784	0.769	0.406	55.885	0.028	0.007	0.767	0.024	60.517
H-23 5403.6m	2	55	Fe-F-Cal	0.112	0.003	2.857	0.769	0.386	56.155	0.015		0.798	0.021	60.78
H-23 5403.6m	2	56	Fe-F-Cal	0.228	0.017	2.964	0.753	0.372	53.571	0.028	0.018	1.243	0.014	58.685
H-23 5403.6m	2	57	Fe-F-Cal	0.155	0.012	2.351	0.699	0.433	56.284			1.819	0.019	61.006
H-23 5403.6m	2	58	Qz+F-Cal	35.434	0.133	1.249	0.416	0.262	32.768	0.123		2.308	0.059	71.78
H-23 5403.6m	2	59	Chl+F-Cal	12.003	10.924	15.734	0.331	2.135	29.924	0.223	0.083	3.275	0.004	73.257
H-23 5403.6m	3	60	F-Cal	0.064	0.007	0.848	0.332	0.09	54.916	0.007	0.01	2.446		57.69
H-23 5403.6m	3	61	Fe-F-Cal	0.094		2.581	0.778	0.489	56.159	0.025	0.012	1.211		60.839
H-23 5403.6m	3	62	Fe-F-Cal	0.119	0.02	2.917	0.763	0.42	55.667			0.483	0.009	60.195
H-23 5403.6m	3	63	Chl	28.591	24.535	30.141	0.018	4.101	0.691	0.166	0.728	0.434	0.008	89.23
H-23 5403.6m	3	64	Fe-F-Cal	0.192	0.017	2.867	0.781	0.453	54.803			1.553	0.003	60.015
H-23 5403.6m	3	65	Fe-F-Cal	0.077	0.01	1.056	0.321	0.104	56.243	0.016		1.471	0.009	58.688
H-23 5403.6m	4	66	Fe-F-Cal	0.118	0.017	2.952	0.807	0.394	54.209	0.01		1.318		59.27
H-23 5403.6m	4	67	Fe-F-Cal	0.03	0.006	3.082	0.878	0.504	56.801	0.012	0.005	1.391	0.003	62.126
H-23 5403.6m	4	68	Fe-F-Cal	0.208	0.049	2.703	0.702	0.414	55.53	0.005		1.233		60.325
H-23 5403.6m	4	69	Chl+Other	37.934	15.186	24.991	0.022	2.702	3.234	0.197	0.301	1.819	0.279	85.899
H-23 5403.6m	4	70	Qz+Chl+Other	42.889	23.092	25.078	0.032	3.66	0.358	0.265	1.892	1.329	0.051	98.086
H-23 5403.6m	4	71	Chl+F-Cal	16.058	14.112	22.744	0.127	2.608	18.565	0.204	0.094	2.299	0.062	75.905
H-23 5403.6m	4	72	Fe-F-Cal	0.322		2.315	0.526	0.306	55.072	0.021		1.953		59.693
H-23 5403.6m	4	73	Chl+Other	24.657	20.088	31.796	0.015	3.961	0.453	0.39	0.244	3.038	0.093	83.456
H-23 5407m	2	74	Cal	0.027		0.163	0.035	0.446	61.189	0.141	0.041		0.942	62.984
H-23 5407m	2	75	F-Cal	0.026		0.114		0.483	55.232	0.196	0.029	0.382	1.02	57.321
H-23 5407m	2	76	Cal	0.027	0.009	0.263	0.01	0.505	54	0.164			0.938	55.916
H-23 5407m	2	77	Chl+Other	25.187	21.721	28.171	0.015	3.616	1.468	0.423	0.528	1.13	0.147	81.93
H-23 5407m	2	78	Fe-F-Cal	0.063	0.013	2.684	0.695	0.516	56.294	0.019	0.017	0.414	0.028	60.569
H-23 5407m	2	79	Fe-F-Cal	0.065	0.025	1.987	0.532	0.465	57.215	0.018	0.005	1.039	0.051	60.965
H-23 5407m	2	80	Fe-F-Cal+Other	1.058	0.556	3.161	0.236	0.595	51.595	0.161	0.001	2.143	0.639	59.243
H-23 5407m	1	95	Fe-F-Cal	0.157	0.022	2.123	0.393	0.34	57.209	0.021	0.032	1.008	0.009	60.89
H-23 5407m	1	96	Fe-F-Cal+Other	1.348	0.5	2.114	0.757	0.445	53.809	0.029	0.327	0.841	0.043	59.859
H-23 5407m	1	97	Ab	68.098	19.7	0.146	0.042	0.026	2.147	11.417	0.038	0.17	0.017	101.729
H-23 5407m	1	98	Fe-F-Cal	0.212	0.093	2.1	0.446	0.415	56.646	0.016	0.003	2.4		61.32
H-23 5407m	1	99	Ab	60.008	18.939	1.225	0.003	0.212	0.2	9.137	0.446	0.033	0.174	90.363

Table 3-1: EMP WDS chemical analyses of F-Fe-Calcite and other minerals from samples 4353.5m, 5213.5m, 5403.6m, 5407m, and 5408.5m.

Sample	Site	No.	Mineral	SiO2	Al2O3	FeO	MnO	MgO	CaO	Na2O	K2O	F	SO3	Total
H-23 5407m	5	100	Mg-Cal	0.026	0.002	0.124	0.002	1.181	49.524	0.134			0.254	51.247
H-23 5407m	5	101	Mg-Cal	0.028		0.078		1.276	53.748	0.178	0.008		0.283	55.599
H-23 5407m	5	102	Fe-F-Cal	0.032	0.008	1.787	0.536	0.337	55.395	0.016		0.36	0.069	58.388
H-23 5407m	5	103	Fe-F-Cal	0.016	0.015	1.505	0.513	0.306	56.318	0.003		0.626	0.027	59.065
H-23 5407m	5	104	F-Cal+Chl	6.772	6.422	9.284	0.329	1.415	34.842	0.032	0.07	5.259	0.047	62.258
H-23 5407m	3	105	Fe-F-Cal	0.064	0.025	2.053	0.478	0.361	56.776	0.014	0.007	1.072		60.399
H-23 5407m	3	106	Fe-F-Cal	0.099	0.024	1.601	0.363	0.247	57.795	0.015	0.02	1.399	0.023	60.997
H-23 5407m	3	107	Fe-F-Cal	0.094		2.922	0.877	0.431	55.293	0.008	0.026	0.542	0.003	59.968
H-23 5407m	3	108	Chl	27.083	23.925	25.032	0.046	3.426	0.622	0.15	0.46	0.533	0.085	81.138
H-23 5213.5m	1	109	Fe-Cal	0.026	0.009	3.284	0.293	0.7	52.593	0.017	0.01		0.04	56.972
H-23 5213.5m	1	110	Fe-Cal	0.041	0.016	1.068	0.178	0.219	44.337	0.02	0.021			45.9
H-23 5213.5m	1	111	Fe-Cal	0.048		3.311	0.337	0.673	55.15	0.011	0.017		0.031	59.578
H-23 5213.5m	1	112	Cal	0.005	0.024	0.064	0.036	0.04	57.083	0.066			0.424	57.742
H-23 5213.5m	1	113	Fe-Cal	0.002	0.008	2.63	0.298	0.504	51.149	0.023	0.002		0.025	54.641
H-23 5213.5m	2	114	Cal	0.072	0.031	0.134	0.046	0.796	48.896	0.208	0.004		0.194	50.381
H-23 5213.5m	2	115	Mg-Cal	0.042	0.006	0.096	0.014	1.843	47.648	0.287			0.26	50.196
H-23 5213.5m	2	116	Fe-Cal	0.055	0.017	1.963	0.283	0.451	48.723		0.009		0.01	51.511
H-23 5213.5m	2	117	Fe-F-Cal+Sd	1.294	0.693	15.991	0.543	2.303	37.316	0.008	0.058	1.193	0.025	58.922
H-23 5213.5m	2	118	Cal	0.075	0.006	0.58	0.24	0.706	44.232	0.044	0.003		0.173	46.059
H-23 5213.5m	2	119	Mg-Cal			0.246		1.066	56.714		0.189		0.874	59.089
H-23 5213.5m	2	120	Fe-Cal	0.011		2.165	0.31	0.518	52.626				0.038	55.668
H-23 5213.5m	2	121	F-Cal+Chl	8.558	8.232	12.513	0.178	2.308	34.613	0.123	0.017	1.441	0.15	67.526
H-23 5213.5m	3	122	Ank	0.048		12.159	0.578	9.227	27.792		0.005		0.021	49.83
H-23 5213.5m	3	123	Fe-Cal	0.061		2.66	0.316	0.618	51.01				0.007	54.672
H-23 5213.5m	3	124	Fe-Cal	0.059	0.012	3.198	0.347	0.73	54.431	0.001	0.011		0.008	58.797
H-23 5213.5m	3	125	Ank	0.12	0.056	9.293	0.444	6.816	35.527	0.01	0.006		0.017	52.289
H-23 5213.5m	3	126	Ab	69.566	20.41	0.284		0.037	0.251	12.062	0.002			102.612
H-23 5213.5m	4	141	Mg-Cal		0.545	0.034	0.024	2.448	56.921	0.266	0.242		0.413	60.893
H-23 5213.5m	4	142	Fe-Cal	0.012	0.009	3.17	0.316	0.579	55.337		0.015		0.054	59.492
H-23 5213.5m	4	143	Chl	26.146	23.005	29.427	0.02	5.163	1.468	0.314	0.321	0.772	0.078	86.389
H-23 5213.5m	4	144	Chl+Py+Other	17.03	15.177	41.232	0.021	3.353	1.423	0.714	0.09	0.801	44.514	124.018
H-23 5213.5m	4	145	Ab	70.075	20.618	0.221	0.01	0.009	0.231	11.891	0.011		0.008	103.074

Table 3-1: EMP WDS chemical analyses of F-Fe-Calcite and other minerals from samples 4353.5m, 5213.5m, 5403.6m, 5407m, and 5408.5m.

Sample	Site	No.	Mineral	SiO2	Al2O3	FeO	MnO	MgO	CaO	Na2O	K2O	F	SO3	Total
H-23 5213.5m	4	146	Ank	0.055		15.96	0.586	9.619	27.608	0.044				53.872
H-23 5213.5m	4	147	Mg-Cal	0.044	0.018	0.064	0.005	3.106	49.683	0.086	0.013		0.756	53.775
H-23 5213.5m	4	148	Fe-F-Cal	0.041	0.017	2.806	0.307	0.466	55.84	0.013	0.004	0.227	0.047	59.672
H-23 5213.5m	4	149	Mg-Cal	0.013	0.016	0.235	0.012	2.495	50.29	0.188	0.076		0.638	53.963
H-23 5213.5m	4	150	Fe-Cal	0.034	0.032	2.537	0.309	0.592	51.106	0.02	0.007		0.028	54.665
H-23 5213.5m	5	151	Cal	0.049		0.066	0.014	0.807	55.552	0.289	0.02		0.335	57.132
H-23 5213.5m	5	152	Fe-Cal	0.018	0.012	1.985	0.263	0.423	50.462				0.038	53.201
H-23 5213.5m	5	153	Chl+Other	27.866	22.887	30.189	0.023	4.795	1.155	0.259	0.38	1.643	0.063	88.568
H-23 5213.5m	5	154	Fe-Cal	0.062	0.001	3.068	0.302	0.487	55.668	0.028		0.006	0.024	59.643
H-23 4353.5m	2	155	Kln+Cal	38.097	33.684	0.264	0.04	0.04	6.198	0.043	0.007		0.008	78.381
H-23 4353.5m	2	156	Fe-Cal	0.022	0.001	1.771	0.213	0.224	58.532	0.015	0.026		0.038	60.842
H-23 4353.5m	2	157	Fe-Cal	0.041	0.012	1.349	0.169	0.178	58.279	0.011				60.039
H-23 4353.5m	2	158	Kfs	67.07	18.868	0.066		0.013	0.466	0.621	15.881		0.016	103.001
H-23 4353.5m	2	159	Fe-Cal	0.015	0.017	1.764	0.201	0.291	59.636	0.015	0.002			61.941
H-23 4353.5m	2	160	Ab	70.838	20.939	0.013			0.322	11.883	0.055			104.05
H-23 4353.5m	3	161	Kfs	66.98	18.658	0.042	0.01	0.003	0.177	0.302	16.554		0.028	102.754
H-23 4353.5m	3	162	Fe-Cal	0.053	0.035	1.365	0.168	0.218	58.211	0.004	0.115			60.169
H-23 4353.5m	3	163	Fe-Cal	0.013	0.016	2.065	0.229	0.252	57.64	0.001	0.029		0.012	60.257
H-23 4353.5m	1	164	Fe-F-Cal	0.117		1.853	0.214	0.201	58.631	0.02	0.04	0.204		61.194
H-23 4353.5m	1	165	Fe-F-Cal	0.085	0.007	1.505	0.182	0.201	54.974	0.025	0.001	1.261	0.004	57.714
H-23 5408.5m	2	166	Fe-Cal	0.04		2.158	0.484	0.347	57.373	0.02				60.422
H-23 5408.5m	2	167	F-Cal+Chl	7.211	5.998	6.992		1.101	22.43	1.028	0.225	5.864	0.294	48.674
H-23 5408.5m	2	168	Chl+Other	23.229	19.48	23.832	0.022	2.871	4.363	0.29	0.966	4.497	0.083	77.74
H-23 5408.5m	2	169	TiO2+Chl+Other	4.596	1.701	2.09		0.271	6.854	0.292	0.113	6.901	0.16	20.072
H-23 5408.5m	3	170	Fe-Cal	0.172	0.081	2.387	0.798	0.531	57.267	0.016				61.252
H-23 5408.5m	3	171	Fe-Cal	0.052	0.036	2.035	0.482	0.368	57.564	0.012		0.008		60.554
H-23 5408.5m	3	172	Qz+Cal	89.327	0.382	0.268	0.049	0.035	10.805	0.025	0.184		0.028	101.103

Appendix 4: Selected EDS mineral analyses of muscovite, tourmaline, biotite, and spinel from the Newburn H-23 well for use in geochemical fingerprinting plots (Chapter 4.2).

Table 4-1: Selected muscovite analyses from the Newburn H-23 wells for use in Fig. 4.4.

Sample	Position	Site	SiO_2	TiO_2	Al_2O_3	FeO	MgO	CaO	Na_2O	K_2O	F	Total	Actual Total
H-23 4313.5m	8	9	55.73	0.84	28.7	1.61	1.24		0.88	6		95	102
H-23 4318.5m	2	5	48.57	0.68	35.74	0.56	0.41		1.03	8.02		95	83
H-23 4318.5m	9	18	53.47	0.36	30.86	1.41	1.45		0.71	6.74		95	61
H-23 4318.5m	12	8	62.29	0.26	23.84	1.27	0.84			6.51		95	48
H-23 4318.5m	4	1	45.83	0.41	36.64	0.63	0.44		1.22	9.84		95	105
H-23 4318.5m	4	2	46.11	0.41	37.04	0.57	0.43		1.11	9.33		95	102
H-23 4318.5m	14	7	45.93	1.12	33.72	0.83	1.08		0.28	12.04		95	81
H-23 4318.5m	14	8	45.35	1.24	33.79	0.77	0.96		0.41	12.49		95	86
H-23 4913.8m	4	2	57.43	0.45	25.83	1.93	0.67		1.48	7.21		95	109
H-23 4913.8m	4	3	54.9		29.92	0.48	0.67		0.77	6.5	1.75	95	121
H-23 4913.8m	8	2	49.35	0.3	37.4	0.55			1.69	5.7		95	117
H-23 4913.8m	9	4	49.06	0.45	35.68	0.61			1.65	7.55		95	103
H-23 4913.8m	14	1	48.88	0.52	35.48	0.66			1.78	7.69		95	100
H-23 4913.8m	15	2	53.36		31.37	0.85			1.88	7.53		95	92
H-23 5403m	6	3	49.74		36.17	1.41			1.62	6.06		95	94
H-23 5406.5m	13	3	48.16		34.44	1.67				10.72		95	46
H-23 5407m	2	7	51.53	0.45	31.05	0.98	1.62		0.55	8.82		95	62
H-23 5407m	3	6	48.49		35.86	1.36	0.38		1.4	7.51		95	107
H-23 5407m	7	5	58.34	0.66	27	1.02	1.03			6.95		95	46
H-23 5407m	9	1	49.55		32.48	1.75	1.13		0.47	9.63		95	46
H-23 5408.5m	2	6	48.2		36.14	0.61			1.62	8.43		95	113
H-23 5408.5m	2	7	49.24		36.19	0.44			1.62	7.52		95	113
H-23 5408.5m	3	9	51.65	0.38	31.92	0.98	0.9		0.48	8.68		95	119
H-23 5408.5m	5	20	52.35		31.7	1.55	0.67		1.23	7.5		95	114
H-23 5408.5m	7	22	47.71	0.6	34.53	1.02	0.65		1.06	9.43		95	145
H-23 5408.5m	7	23	49.18	0.4	32.65	0.72	1.5		0.66	9.89		95	144

Table 4-1: Selected muscovite analyses from the Newburn H-23 wells for use in Fig. 4.4.

Sample	Position	Site	SiO_2	TiO_2	Al_2O_3	FeO	MgO	CaO	Na_2O	K_2O	F	Total	Actual Total
H-23 5408.5m	10	10	51.12	0.31	31.5	1.26	0.86		0.92	9.01		95	137
H-23 5408.5m	12	11	47.62	0.29	35.6	1.03			0.45	10.02		95	111
H-23 5408.5m	12	12	48.88	0.29	32.29	1.54	1.2		0.34	10.47		95	115
H-23 5408.5m	15	1	48.29	0.31	34.35	1.45	0.63		0.89	9.07		95	127
H-23 5961.7m	2	1	47.76	0.84	34.35	1.07	0.5		0.78	9.7		95	103
H-23 5961.7m	7	12	48.09		34.66	0.98	0.5		0.87	9.9		95	86
H-23 5962m	6	8	55.82		28.92	1.03	0.93		0.48	7.82		95	76
H-23 5962m	12	11	48.94		36.25	1.2	0.39		0.67	7.54		95	117

Table 4-2: Selected tourmaline analyses from the Newburn H-23 wells for use in Fig. 4.6.

Sample	Position	Site	SiO_2	TiO_2	Al_2O_3	FeO	MnO	MgO	CaO	Na_2O	K_2O	F	Total	Actual Total
H-23 4300m	3	10	38.72	0.42	33.72	5.43		6.13	0.52	2.05			87	101
H-23 4300m	8	1	38.63	0.89	31.54	6.1		6.59	0.82	2.43			87	94
H-23 4300m	9	1	39.01	0.9	31.34	5.94		6.82	0.74	2.25			87	101
H-23 4300m	10	8	38.86	0.42	25.41	10.07		8.57	1.44	2.23			87	100
H-23 4300m	11	1	37.72	0.55	34.25	6.1		5.42	0.83	2.13			87	110
H-23 4300m	14	1	39.48		34.18	7.49		3.9		1.96			87	121
H-23 4300m	15	1	37.31	0.3	25.89	6.32		10.11	2.04	1.63		3.4	87	131
H-23 4300m	15	3	39.09	0.32	30.56	8.9		4.89		3.24			87	122
H-23 4300m	16	1	38.62	0.48	34.14	5.12		6.25	0.34	2.05			87	134
H-23 4300m	16	3	38.43	0.84	28.81	8.6		6.77	1.9	1.65			87	126
H-23 4300m	18	1	38.18	0.83	34.07	5.75		5.51	0.37	2.3			91	137
H-23 5406.5m	7	1	38.76		31.92	6.57		6.9	0.84	2.01			87	53
H-23 5406.5m	8	1	38.95		34.39	9.41		2.28		1.96			87	49
H-23 5406.5m	8	2	38.64	0.46	33.58	8.67		3.57		2.08			87	49
H-23 5406.5m	12	1	38.9	0.61	33.65	5.13		6.19	0.37	2.16			87	43
H-23 5406.5m	16	1	39.16	1.55	29.78	5.69		7.49	0.82	2.52			87	40
H-23 5408.5m	9	1	38.46	0.77	33.77	5.12		6.1	0.88	1.91			87	116
H-23 5408.5m	9	9	39	0.71	33.76	5.11		5.97	0.56	1.9			87	117
H-23 5965m	4	1	38.48	0.72	33.07	4.33		7.6	0.77	2.02			87	110
H-23 5975m	3	1	38.12	0.89	32.87	4.38		7.73	1.06	1.95			87	116

Table 4-3: Selected biotite analyses from the Newburn H-23 wells for use in Fig. 4.7.

Sample	Position	Site	SiO_2	TiO_2	Al_2O_3	FeO	MnO	MgO	Na_2O	K_2O	F	Total	Actual Total
H-23 4300m	8	6	37.64	4.87	11.09	5.9	0	18.23	1	6.84	10.43	96	120
H-23 5950m	6	1	39.86	2.35	17.76	12.9	0	13.88	0	9.24	0	96	120
H-23 5975m	6	1	46.87	4.27	19.39	12.52	0	3.51	0	9.43	0	96	106

Table 4-4: Selected spinel analyses from the Newburn H-23 wells for use in Figs. 4.8 and 4.9.

Sample	Position	Site	SiO_2	TiO_2	Al_2O_3	Cr_2O_3	FeO	MnO	MgO	Total
H-23 4300m	8	3			20.24	48.35	18.87		12.55	100
H-23 4300m	8	4			22.6	40.88	23.13		13.4	100
H-23 4300m	9	2			21.11	46.91	18.83		13.17	100
H-23 4300m	11	5			17.74	47.42	28.39		6.45	100
H-23 4318.5m	4	1		0.28	20.29	44.42	24.82		10.2	100
H-23 4318.5m	4	2			21.56	46.79	22.94		8.39	100
H-23 4353.5m	3	3			30.57	40.77	14.87		13.35	100
H-23 5406.5m	1	4			24.85	45.85	18.77		10.53	100
H-23 5406.5m	1	12			37.6	34.99	13.32		14.09	100
H-23 5406.5m	3	1		0.38	17.86	46.86	24.39		10.51	100
H-23 5406.5m	4	2			21.94	51.89	15.28		10.91	100
H-23 5406.5m	10	2			18.99	44.17	26.53		10.31	100
H-23 5406.5m	10	7			14.72	59.14	14.42	1.3	10.43	100
H-23 5406.5m	10	11			28.14	36.12	21.79		13.95	100
H-23 5406.5m	11	6		1.97	20.75	37.51	33.33		6.45	100
H-23 5406.5m	15	4			30.18	43.56	14.82		11.44	100
H-23 5406.5m	19	1			25.26	44.38	15.44		14.92	100
H-23 5406.5m	19	4		0.77	27.68	35.8	27.76		8.01	100
H-23 5406.5m	20	1			11.22	59.39	15.45		13.95	100
H-23 5406.5m	20	2			18.93	46.38	23.7		10.99	100
H-23 5406.5m	20	11			22.81	48.35	16.75		12.09	100
H-23 5406.5m	20	13			10.09	62.59	21.43		5.9	100
H-23 5408.5m	13	13		0.43	41.31	29.37	14.31		14.59	100
H-23 5408.5m	14	11		0.7	40.64	30.7	14.4		13.58	100
H-23 5957.8m	5	1			17.36	52.89	19.97		9.8	100
H-23 5962m	7	5		0.45	23.3	41.64	28.88		5.75	100